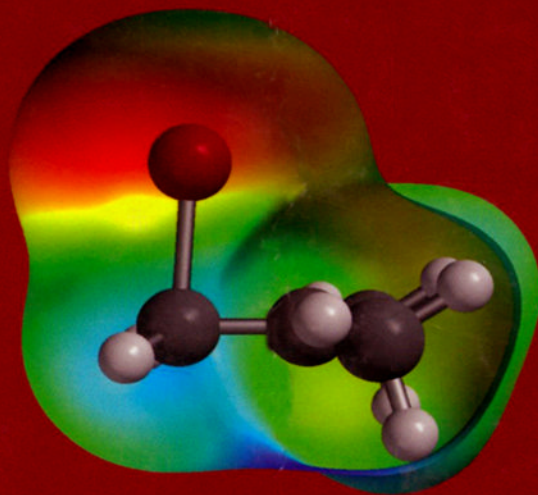


S E C O N D E D I T I O N

Perspectives on
Structure and
Mechanism
in Organic Chemistry



FELIX A. CARROLL

**PERSPECTIVES ON
STRUCTURE AND MECHANISM
IN ORGANIC CHEMISTRY**

PERSPECTIVES ON STRUCTURE AND MECHANISM IN ORGANIC CHEMISTRY

Second Edition

Felix A. Carroll
Davidson College



WILEY

A JOHN WILEY & SONS, INC., PUBLICATION

Copyright © 2010 by John Wiley & Sons, Inc. All rights reserved

Published by John Wiley & Sons, Inc., Hoboken, New Jersey
Published simultaneously in Canada

No part of this publication may be reproduced, stored in a retrieval system, or transmitted in any form or by any means, electronic, mechanical, photocopying, recording, scanning, or otherwise, except as permitted under Section 107 or 108 of the 1976 United States Copyright Act, without either the prior written permission of the Publisher, or authorization through payment of the appropriate per-copy fee to the Copyright Clearance Center, Inc., 222 Rosewood Drive, Danvers, MA 01923, (978) 750-8400, fax (978) 750-4470, or on the web at www.copyright.com. Requests to the Publisher for permission should be addressed to the Permissions Department, John Wiley & Sons, Inc., 111 River Street, Hoboken, NJ 07030, (201) 748-6011, fax (201) 748-6008, or online at <http://www.wiley.com/go/permissions>.

Limit of Liability/Disclaimer of Warranty: While the publisher and author have used their best efforts in preparing this book, they make no representations or warranties with respect to the accuracy or completeness of the contents of this book and specifically disclaim any implied warranties of merchantability or fitness for a particular purpose. No warranty may be created or extended by sales representatives or written sales materials. The advice and strategies contained herein may not be suitable for your situation. You should consult with a professional where appropriate. Neither the publisher nor author shall be liable for any loss of profit or any other commercial damages, including but not limited to special, incidental, consequential, or other damages.

For general information on our other products and services or for technical support, please contact our Customer Care Department within the United States at (800) 762-2974, outside the United States at (317) 572-3993 or fax (317) 572-4002.

Wiley also publishes its books in a variety of electronic formats. Some content that appears in print may not be available in electronic books. For more information about Wiley products, visit our web site at www.wiley.com.

Library of Congress Cataloging-in-Publication Data:

Carroll, Felix A.

Perspectives on structure and mechanism in organic chemistry / Felix A. Carroll.

p. cm.

Includes bibliographical references and index.

ISBN 978-0-470-27610-5 (cloth)

Printed in the United States of America

10 9 8 7 6 5 4 3 2

Contents

Preface xi

Acknowledgments xiii

Introduction xv

Chapter 1 | Fundamental Concepts of Organic Chemistry 1

- 1.1 Atoms and Molecules 1**
 - Fundamental Concepts 1
 - Molecular Dimensions 5
- 1.2 Heats of Formation and Reaction 8**
 - Experimental Determination of Heats of Formation 8
 - Bond Increment Calculation of Heats of Formation 10
 - Group Increment Calculation of Heats of Formation 12
 - Homolytic and Heterolytic Bond Dissociation Energies 16
- 1.3 Bonding Models 19**
 - Electronegativity and Bond Polarity 21
 - Complementary Theoretical Models of Bonding 24
 - Pictorial Representations of Bonding Concepts 28
 - The sp^3 Hybridization Model for Methane 29
 - Are There sp^3 Hybrid Orbitals in Methane? 31
 - Valence Shell Electron Pair Repulsion Theory 35
 - Variable Hybridization and Molecular Geometry 37
- 1.4 Complementary Descriptions of the Double Bond 42**
 - The σ, π Description of Ethene 42
 - The Bent Bond Description of Ethene 42
 - Predictions of Physical Properties with the Two Models 43
- 1.5 Choosing Models in Organic Chemistry 48**
 - Problems 48

Chapter 2 | Stereochemistry 53

- 2.1 Introduction 53**
- 2.2 Stereoisomerism 56**
 - Isomerism 56
 - Symmetric, Asymmetric, Dissymmetric, and Nondissymmetric Molecules 58
 - Designation of Molecular Configuration 67
 - Fischer Projections 72
 - Additional Stereochemical Nomenclature 76
- 2.3 Manifestations of Stereoisomerism 86**
 - Optical Activity 86

	Configuration and Optical Activity	90	
	Other Physical Properties of Stereoisomers	92	
2.4	Stereotopicity	94	
	Stereochemical Relationships of Substituents	94	
	Chirotopicity and Stereogenicity	98	
	Problems	101	
Chapter 3	 <i>Conformational Analysis and Molecular Mechanics</i>		113
3.1	Molecular Conformation	113	
3.2	Conformational Analysis	119	
	Torsional Strain	119	
	van der Waals Strain	120	
	Angle Strain and Baeyer Strain Theory	123	
	Application of Conformational Analysis to Cycloalkanes	124	
	Conformational Analysis of Substituted Cyclohexanes	128	
3.3	Molecular Mechanics	135	
3.4	Molecular Strain and Limits to Molecular Stability	155	
	Problems	169	
Chapter 4	 <i>Applications of Molecular Orbital Theory and Valence Bond Theory</i>		175
4.1	Introduction to Molecular Orbital Theory	175	
	Hückel Molecular Orbital Theory	175	
	Correlation of Physical Properties with Results of HMO Calculations	187	
	Other Parameters Generated Through HMO Theory	191	
	Properties of Odd Alternant Hydrocarbons	194	
	The Circle Mnemonic	198	
4.2	Aromaticity	199	
	Benzene	201	
	Aromaticity in Small Ring Systems	211	
	Larger Annulenes	215	
	Dewar Resonance Energy and Absolute Hardness	218	
4.3	Contemporary Computational Methods	220	
	Extended Hückel Theory	221	
	Perturbational Molecular Orbital Theory	226	
	Atoms in Molecules	232	
	Density Functional Theory	236	
4.4	Valence Bond Theory	237	
	Resonance Structures and Resonance Energies	237	
	Choosing a Computational Model	245	
	Problems	246	
Chapter 5	 <i>Reactive Intermediates</i>		253
5.1	Reaction Coordinate Diagrams	253	
5.2	Radicals	256	
	Early Evidence for the Existence of Radicals	257	
	Detection and Characterization of Radicals	258	

Structure and Bonding of Radicals	264
Thermochemical Data for Radicals	267
Generation of Radicals	269
Reactions of Radicals	270
5.3 Carbenes 278	
Structure and Geometry of Carbenes	278
Generation of Carbenes	282
Reactions of Carbenes	284
5.4 Carbocations 289	
Carbonium Ions and Carbenium Ions	289
Structure and Geometry of Carbocations	290
The Norbornyl Cation	300
Rearrangements of Carbocations	302
Radical Cations	305
5.5 Carbanions 310	
Structure and Geometry of Carbanions	310
Generation of Carbanions	315
Stability of Carbanions	317
Reactions of Carbanions	318
5.6 Choosing Models of Reactive Intermediates 320	
Problems	321
Chapter 6 <i>Methods of Studying Organic Reactions</i>	327
6.1 Molecular Change and Reaction Mechanisms 327	
6.2 Methods to Determine Reaction Mechanisms 327	
Identification of Reaction Products	327
Determination of Intermediates	328
Crossover Experiments	333
Isotopic Labeling	335
Stereochemical Studies	337
Solvent Effects	337
Computational Studies	339
6.3 Applications of Kinetics in Studying Reaction Mechanisms 341	
6.4 Arrhenius Theory and Transition-State Theory 348	
6.5 Reaction Barriers and Potential Energy Surfaces 360	
6.6 Kinetic Isotope Effects 370	
Primary Kinetic Isotope Effects	371
Secondary Kinetic Isotope Effects	380
Solvent Isotope Effects	384
6.7 Substituent Effects 385	
6.8 Linear Free Energy Relationships 389	
Problems	404
Chapter 7 <i>Acid and Base Catalysis of Organic Reactions</i>	413
7.1 Acidity and Basicity of Organic Compounds 413	
Acid–Base Measurements in Solution	413
Acid–Base Reactions in the Gas Phase	422
Comparison of Gas Phase and Solution Acidities	426
Acidity Functions	430

- 7.2 Acid and Base Catalysis of Chemical Reactions 433**
 Specific Acid Catalysis 434
 General Acid Catalysis 435
 Brønsted Catalysis Law 437
- 7.3 Acid and Base Catalysis of Reactions of Carbonyl Compounds and Carboxylic Acid Derivatives 439**
 Addition to the Carbonyl Group 439
 Enolization of Carbonyl Compounds 442
 Hydrolysis of Acetals 447
 Acid-Catalyzed Hydrolysis of Esters 449
 Alkaline Hydrolysis of Esters 452
 Hydrolysis of Amides 460
Problems 464

Chapter 8 | Substitution Reactions

469

- 8.1 Introduction 469**
- 8.2 Nucleophilic Aliphatic Substitution 472**
 Introduction 472
 The S_N1 Reaction 473
 The S_N2 Reaction 494
 Brønsted Correlations 504
 Hard–Soft Acid–Base Theory and Nucleophilicity 505
 Edwards Equations 506
 Swain–Scott Equation 507
 Mayr Equations 508
 The α Effect 511
 Leaving Group Effects in S_N2 Reactions 512
 Aliphatic Substitution and Single Electron Transfer 513
- 8.3 Electrophilic Aromatic Substitution 518**
 The S_EAr Reaction 518
 Quantitative Measurement of S_EAr Rate Constants: Partial Rate Factors 521
 Lewis Structures as Models of Reactivity in S_EAr Reactions 524
- 8.4 Nucleophilic Aromatic and Vinylic Substitution 527**
 Nucleophilic Aromatic Substitution 527
 Nucleophilic Vinylic Substitution 532
 Nucleophilic Substitution Involving Benzyne Intermediates 535
 Radical-Nucleophilic Substitution 541
Problems 545

Chapter 9 | Addition Reactions

551

- 9.1 Introduction 551**
- 9.2 Addition of Halogens to Alkenes 553**
 Electrophilic Addition of Bromine to Alkenes 553
 Addition of Other Halogens to Alkenes 575
- 9.3 Other Addition Reactions 585**
 Addition of Hydrogen Halides to Alkenes 585
 Hydration of Alkenes 592
 Oxymercuration 595

Hydroboration	600
Epoxidation	605
Electrophilic Addition to Alkynes and Cumulenes	609
Nucleophilic Addition to Alkenes and Alkynes	618
Nucleophilic Addition to Carbonyl Compounds	622
Problems	627

Chapter 10 | Elimination Reactions **633**

10.1 Introduction	633
10.2 Dehydrohalogenation and Related 1,2-Elimination Reactions	638
Potential Energy Surfaces for 1,2-Elimination	638
Competition Between Substitution and Elimination	645
Stereochemistry of 1,2-Elimination Reactions	647
Regiochemistry of 1,2-Elimination Reactions	654
10.3 Other 1,2-Elimination Reactions	665
Dehalogenation of Vicinal Dihalides	665
Dehydration of Alcohols	669
Deamination of Amines	677
Pyrolytic Eliminations	681
Problems	688

Chapter 11 | Pericyclic Reactions **697**

11.1 Introduction	697
11.2 Electrocyclic Transformations	702
Definitions and Selection Rules	702
MO Correlation Diagrams	707
State Correlation Diagrams	711
11.3 Sigmatropic Reactions	715
Definitions and Examples	715
Selection Rules for Sigmatropic Reactions	717
Further Examples of Sigmatropic Reactions	725
11.4 Cycloaddition Reactions	731
Introduction	731
Ethene Dimerization	731
The Diels–Alder Reaction	734
Selection Rules for Cycloaddition Reactions	739
11.5 Other Concerted Reactions	747
Cheletropic Reactions	747
Atom Transfer Reactions	749
Ene Reactions	750
11.6 A General Selection Rule for Pericyclic Reactions	753
11.7 Alternative Conceptual Models for Concerted Reactions	756
Frontier Molecular Orbital Theory	756
Hückel and Möbius Aromaticity of Transition Structures	763
Synchronous and Nonsynchronous Concerted Reactions	770
The Role of Reaction Dynamics in Rearrangements	773
Problems	778

Chapter 12 | Photochemistry**787**

- 12.1 Photophysical Processes 787**
 - Energy and Electronic States 787
 - Designation of Spectroscopic Transitions 790
 - Photophysical Processes 792
 - Selection Rules for Radiative Transitions 795
 - Fluorescence and Phosphorescence 798
 - Energy Transfer and Electron Transfer 801
- 12.2 Fundamentals of Photochemical Kinetics 804**
 - Actinometry and Quantum Yield Determinations 804
 - Rate Constants for Unimolecular Processes 805
 - Transient Detection and Monitoring 807
 - Bimolecular Decay of Excited States: Stern–Volmer Kinetics 809
- 12.3 Physical Properties of Excited States 810**
 - Acidity and Basicity in Excited States 811
 - Bond Angles and Dipole Moments of Excited State Molecules 815
- 12.4 Representative Photochemical Reactions 818**
 - Photochemical Reactions of Alkenes and Dienes 818
 - Photochemical Reactions of Carbonyl Compounds 832
 - Photochemical Reactions of α,β -Unsaturated Carbonyl Compounds 840
 - Photochemical Reactions of Aromatic Compounds 843
 - Photosubstitution Reactions 845
 - σ Bond Photodissociation Reactions 846
 - Singlet Oxygen and Organic Photochemistry 851
- 12.5 Some Applications of Organic Photochemistry 853**
 - Problems 862

References for Selected Problems 871

Permissions 883

Author Index 895

Subject Index 927

Preface

This book is the result of my experience teaching physical organic chemistry at Davidson College. During this time I felt a need for a text that not only presents concepts that are central to the understanding and practice of physical organic chemistry but that also teaches students to think about organic chemistry in new ways, particularly in terms of complementary conceptual models. Because of this approach, the first edition of *Perspectives on Structure and Mechanism in Organic Chemistry* attracted attention beyond the chemistry community and was even quoted in a philosophy dissertation.¹

Soon after the first edition appeared, I received a telephone call from a student of the philosophy of science, who asked how I came to write a book with this emphasis. I did not have a ready answer, but as we talked I realized that this was primarily due to the influences of George Hammond and Jacob Bronowski. I was a graduate student with George Hammond. Although I cannot recall ever discussing conceptual models with him, his views were nonetheless imprinted on me—but in such a subtle way that I did not fully recognize it at the time. Jacob Bronowski's impact was more distinct because it resulted from a single event—the film *Knowledge or Certainty* in a series titled *The Ascent of Man*. That film offers a powerful commentary on both the limits of human knowledge and the nature of science as “a tribute to what we can know although we are fallible.”^{2a} Perhaps a hybridization of their influences led me to emphasize that familiar conceptual models are only beginning points for describing structures and reactions and that using complementary models can provide a deeper understanding of organic chemistry than can using any one model alone.

As with the first edition, the first five chapters of this book consider structure and bonding of stable molecules and reactive intermediates. There is a chapter on methods organic chemists use to study reaction mechanisms, and then acid–base reactions, substitution reactions, addition reactions, elimination reactions, pericyclic reactions, and photochemical reactions are considered in subsequent chapters. In each case I have updated the content to reflect developments since publication of the first edition.

It is essential for an advanced text to provide complete references. The literature citations in this edition range from 1851 to 2009. They direct interested readers to further information about all of the topics and also acknowledge the researchers whose efforts produced the information summarized here. A teaching text must also provide a set of problems of varying

¹ Weisberg, M. *When Less is More: Tradeoffs and Idealization in Model Building*; Ph.D. Dissertation, Stanford University, 2003. See also Weisberg, M. *Philos. Sci.* **2004**, *71*, 1071.

² The quotations are from the book with the same title as the film series: Bronowski, J. *The Ascent of Man*; Little, Brown and Company, Boston, 1973; (a) p. 374; (b) p. 353.

difficulty. The nearly 400 problems in this edition do more than just allow students to test their understanding of the facts and concepts presented in a chapter. They also encourage readers to actively engage the chemical literature and to develop and defend their own ideas. Some problems represent straightforward applications of the information in the text, but other problems can best be answered by consulting the literature for background information before attempting a solution. Still other problems are open-ended, with no one "correct" answer. I have prepared a solutions manual giving answers for problems in the first two categories as well as comments about the open-ended problems.

In *Knowledge or Certainty*, Bronowski shows many portraits of the same human face and observes that "we are aware that these pictures do not so much fix the face as explore it. . . and that each line that is added strengthens the picture but never makes it final."^{2b} So it is with this book. It is not a photograph but is, instead, a portrait of physical organic chemistry. As with the human face, it is not possible to fix a continually changing science—we can only explore it. I hope that the lines added in this edition will better enable readers to develop a deeper and more complete understanding of physical organic chemistry.

FELIX A. CARROLL

Davidson College

Acknowledgments

I am grateful to the following colleagues for giving their time to read and to offer comments on portions of this edition.

Igor V. Alabugin, Florida State University
John E. Baldwin, Syracuse University
Christopher M. Hadad, Ohio State University
Richard P. Johnson, University of New Hampshire
Jeffrey I. Seeman, University of Richmond
Benjamin T. King, University of Nevada, Reno
Nancy S. Mills, Trinity University
Sason S. Shaik, Hebrew University, Jerusalem
Richard G. Weiss, Georgetown University
Frank H. Quina, University of São Paulo

I am also grateful to readers of the first edition who pointed out errors and made suggestions. In particular, I acknowledge Professor Robert G. Bergman of the University of California, Berkeley and his students for their helpful comments.

Sean Ohlinger of Wavefunction, Inc. helped to generate the cover image for this edition, and Kay Filar of Davidson College assisted in the preparation of the indices. I also thank Davidson students Chris Boswell, Will Crossland, Jon Huggins, Josh Knight, Jon Maner, Anna Nam, and Stephanie Scott for their thoughtful comments on an early draft of the book.

Finally, I thank the staff of John Wiley & Sons for bringing the manuscript into print, especially Senior Acquisitions Editor Anita Lekhwani, Editorial Program Coordinator Rebekah Amos, Senior Production Editor Rosalyn Farkas. I also thank Christina Della Bartolomea for copyediting the manuscript.

F. A. C

Introduction

Every organic chemist instantly recognizes the drawing in Figure 1 as benzene, or at least one of the Kekulé structures of benzene. Yet, it is not benzene. It is a geometric figure consisting of a regular hexagon enclosing three extra lines, prepared by marking white paper with black ink. When we look at the drawing, however, we *see* benzene. That is, we visualize a colorless liquid, and we recall a pattern of physical properties and chemical reactivity associated with benzene and with the concept of aromaticity. The drawing in Figure 1 is therefore only a macroscopic representation of a presumed submicroscopic entity. Even more, the drawing symbolizes the *concept* of benzene, particularly its structural features and patterns of reactivity.¹

That all organic chemists instantly recognize the drawing in Figure 1 as benzene is confirmation that they have been initiated into the chemical fraternity. The tie that binds the members of this fraternity is more than a collective interest. It is also a common way of viewing problems and their solutions. The educational process that initiates members into this fraternity, like other initiations, can lead to considerable conformity of thinking and of behavior.² Such conformity facilitates communication among members of the group, but it can limit independent behavior and action.

This common way of looking at problems was explored by T. S. Kuhn in *The Structure of Scientific Revolutions*.³ Kuhn described processes fundamental to all of the sciences, and he discussed two related meanings of the term *paradigm*:

On the one hand, it stands for the entire constellation of beliefs, values, techniques, and so on shared by the members of a given community. On the other it denotes one sort of element in that constellation, the concrete puzzle solutions which, employed as models or examples, can replace explicit rules as a basis for the solution of the remaining puzzles of normal science.^{3a,4}

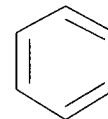


FIGURE 1.
A familiar drawing.

¹ For a discussion of "Representation in Chemistry," including the nature of drawings of benzene rings, see Hoffmann, R.; Laszlo, P. *Angew. Chem. Int. Ed. Engl.* **1991**, *30*, 1. For a discussion of the iconic nature of some chemical drawings, see Whitlock, H. W. *J. Org. Chem.* **1991**, *56*, 7297.

² Moreover, the interaction of these scientists with those who do not share their interests can be inhibited through what might be called a "sociological hydrophobic effect."

³ Kuhn, T. S. *The Structure of Scientific Revolutions*, 2nd ed.; The University of Chicago Press: Chicago, 1970; (a) p. 175; (b) p. 37.

⁴ The paradigm that we may think of chemistry only through paradigms may be an appropriate description of Western science only. For an interesting discussion of "Sushi Science and Hamburger Science," see Motokawa, T. *Perspect. Biol. Med.* **1989**, *32*, 489.

The parallel with a fraternity is more closely drawn by Kuhn's observation

...one of the things a scientific community acquires with a paradigm is a criterion for choosing problems that, while the paradigm is taken for granted, can be assumed to have solutions. To a great extent these are the only problems that the community will admit as scientific or encourage its members to undertake. Other problems... are rejected as metaphysical, as the concern of another discipline, or sometimes as just too problematic to be worth the time. A paradigm can, for that matter, even insulate the community from those socially important problems that are not reducible to the puzzle form, because they cannot be stated in terms of the conceptual and instrumental tools the paradigm supplies.^{3b,5,6}

The history of *phlogiston* illustrates how paradigms can dictate chemical thought. Phlogiston was said to be the "principle" of combustibility—a substance thought to be given off by burning matter.⁷ The phlogiston theory was widely accepted and was taught to students as established fact.⁸ As is the case with the ideas we accept, the phlogiston theory could rationalize observable phenomena (combustion) and could account for new observations (such as the death of animals confined in air-tight containers).⁹ As is also the case with contemporary theories, the phlogiston model could be modified to account for results that did not agree with its predictions. For example, experiments showed that some substances actually gained weight when they burned, rather than losing weight as might have been expected if a real substance had been lost by burning. Rather than abandoning the phlogiston theory, however, some of its advocates rationalized the results by proposing that phlogiston had negative weight.

As this example teaches us, once we have become accustomed to thinking about a problem in a certain way, it becomes quite difficult to think about it differently. Paradigms in science are therefore like the operating system of a computer: they dictate the input and output of information and control the operation of logical processes. Chamberlin stated the same idea with a human metaphor:

The moment one has offered an original explanation for a phenomenon which seems satisfactory, that moment affection for his intellectual child springs into existence. ... From an unduly favored child, it readily becomes master, and leads its author whithersoever it will.¹⁰

Recognizing that contemporary chemistry is based on widely (if perhaps not universally) accepted paradigms does not mean that we should resist using them. This point was made in 1929 in an address by Irving Langmuir, who was at that time president of the American Chemical Society.

⁵ See also the discussion of Sternberg, R. J. *Science* **1985**, 230, 1111.

⁶ The peer review process for grant proposals can be one way a scientific community limits the problems its members are allowed to undertake.

⁷ White, J. H. *The History of the Phlogiston Theory*; Edward Arnold & Co.: London, 1932.

⁸ Conant, J. B. *Science and Common Sense*; Yale University Press: New Haven, 1951; pp. 170–171.

⁹ Note the defense of phlogiston by Priestly cited by Pimentel, G. *Chem. Eng. News* **1989** (May 1), p. 53.

¹⁰ Chamberlin, T. C. *Science* **1965**, 148, 754; reprinted from *Science* (old series) **1890**, 15, 92. For further discussion of this view, see Bunnett, J. F. in Lewis, E. S., Ed. *Investigation of Rates and Mechanisms of Reactions*, 3rd ed., Part I; Wiley-Interscience: Hoboken, NJ, 1975; p. 478–479.

Skepticism in regard to an absolute meaning of words, concepts, models or mathematical theories should not prevent us from using all these abstractions in describing natural phenomena. The progress of physical chemistry was probably set back many years by the failure of the chemists to take full advantage of the atomic theory in describing the phenomena that they observed. The rejection of the atomic theory for this purpose was, I believe, based primarily upon a mistaken attempt to describe nature in some absolute manner. That is, it was thought that such concepts as energy, entropy, temperature, chemical potential, etc., represented something far more nearly absolute in character than the concept of atoms and molecules, so that nature should preferably be described in terms of the former rather than the latter. We must now recognize, however, that all of these concepts are human inventions and have no absolute independent existence in nature. Our choice, therefore, cannot lie between fact and hypothesis, but only between two concepts (or between two models) which enable us to give a better or worse description of natural phenomena.¹¹

Langmuir's conclusion is correct but, I think, incomplete. Saying that we often choose between two models does not mean that we must, from the time of that choice forward, use only the model that we accept. Instead, we must continually make selections, consciously or subconsciously, among many complementary models.¹² Our choice of models is usually shaped by the need to solve the problems at hand. For example, Lewis electron dot structures and resonance theory provide adequate descriptions of the structures and reactions of organic compounds for some purposes, but in other cases we need to use molecular orbital theory or valence bond theory. Frequently, therefore, we find ourselves alternating between these models. Furthermore, consciously using complementary models to think about organic chemistry reminds us that our models are only human constructs and are not windows into reality.

In each of the chapters of this text, we will explore the use of different models to explain and predict the structures and reactions of organic compounds. For example, we will consider alternative explanations for the hybridization of orbitals, the σ, π description of the carbon-carbon double bond, the effect of branching on the stability of alkanes, the electronic nature of substitution reactions, the acid-base properties of organic compounds, and the nature of concerted reactions. The complementary models presented in these discussions will give new perspectives on the structures and reactions of organic compounds.

¹¹ Langmuir, I. J. *Am. Chem. Soc.* **1929**, *51*, 2847.

¹² For other discussions of the role of models in chemistry, see (a) Hammond, G. S.; Osteryoung, J.; Crawford, T. H.; Gray, H. B. *Models in Chemical Science: An Introduction to General Chemistry*; W. A. Benjamin, Inc.: New York, 1971; pp. 2-7; (b) Sunko, D. E. *Pure Appl. Chem.* **1983**, *55*, 375; (c) Bent, H. A. *J. Chem. Educ.* **1984**, *61*, 774; (d) Goodfriend, P. L. *J. Chem. Educ.* **1976**, *53*, 74; (e) Morwick, J. J. *J. Chem. Educ.* **1978**, *55*, 662; (f) Matsen, F. A. *J. Chem. Educ.* **1985**, *62*, 365; (g) Dewar, M. J. S. *J. Phys. Chem.* **1985**, *89*, 2145.

Fundamental Concepts of Organic Chemistry

1.1 ATOMS AND MOLECULES

Fundamental Concepts

Organic chemists think of atoms and molecules as basic units of matter. We work with mental pictures of atoms and molecules, and we rotate, twist, disconnect, and reassemble physical models in our hands.^{1,2} Where do these mental images and physical models come from? It is useful to begin thinking about the fundamental concepts of organic chemistry by asking a simple question: What do we know about atoms and molecules, and how do we know it? As Kuhn pointed out,

Though many scientists talk easily and well about the particular individual hypotheses that underlie a concrete piece of current research, they are little better than laymen at characterizing the established bases of their field, its legitimate problems and methods.³

The majority of what we know in organic chemistry consists of what we have been taught. Underlying that teaching are observations that someone has made and someone has interpreted. The most fundamental observations are those that we can make directly with our senses. We note the physical state of a substance—solid, liquid, or gas. We see its color or lack of color. We observe whether it dissolves in a given solvent or whether it evaporates if exposed to the atmosphere. We might get some sense of its density by seeing it float or sink when added to an immiscible liquid. These are qualitative observations, but they provide an important foundation for further experimentation.

¹ For a detailed discussion of physical models in chemistry, see Walton, A. *Molecular and Crystal Structure Models*; Ellis Horwood: Chichester, England, 1978.

² For an interesting application of physical models to infer molecular properties, see Teets, D. E.; Andrews, D. H. *J. Chem. Phys.* **1935**, *3*, 175.

³ Kuhn, T. S. *The Structure of Scientific Revolutions*, 2nd ed.; The University of Chicago Press: Chicago, 1970; p. 47.

It is only a modest extension of direct observation to the use of some simple experimental apparatus for quantitative measurements. We use a heat source and a thermometer to determine melting and boiling ranges. We use other equipment to measure indices of refraction, densities, surface tensions, viscosities, and heats of reaction. Through classical elemental analysis, we determine what elements are present in a sample and what their mass ratios seem to be. Then we might determine a formula weight through melting point depression. In all of these experiments, *we use some equipment but still make the actual experimental observations by eye*. These limited experimental techniques can provide essential information nonetheless. For example, if we find that 159.8 grams of bromine will always be decolorized by 82.15 grams of cyclohexene, then we can observe the law of definite proportions. Such data are consistent with a model of matter in which submicroscopic particles combine with each other in characteristic patterns, just as the macroscopic samples before our eyes do. It is then only a matter of definition to call the submicroscopic particles atoms or molecules and to further study their properties. It is essential, however, to remember that our laboratory experiments are conducted with *materials*. While we may talk about the addition of bromine to cyclohexene in terms of individual molecules, we really can only infer that such a process occurs on the basis of experimental data collected with macroscopic samples of the reactants.

Modern instrumentation has opened the door to a variety of investigations, most unimaginable to early chemists, that expand the range of observations beyond those of the human senses. These instruments extend our eyes from seeing only a limited portion of the electromagnetic spectrum to practically the entire spectrum, from X-rays to radio waves, and they let us “see” light in other ways (e.g., in polarimetry). They allow us to use entirely new tools, such as electron or neutron beams, magnetic fields, and electrical potentials or current. They extend the range of conditions for studying matter from near atmospheric pressure to high vacuum and to high pressure. They effectively expand and compress the time scale of the observations, so we can study events that require eons or that occur in femtoseconds.^{4,5}

The unifying characteristic of modern instrumentation is that we no longer observe the chemical or physical change directly. Instead, we observe it only indirectly, such as through the change in illuminated pixels on a computer display. With such instruments, it is essential that we recognize the difficulty in freeing the observations from constraints imposed by our expectations. *To a layperson*, a UV–vis spectrum may not seem all that different from an upside-down infrared spectrum, and a capillary gas chromatogram of a complex mixture may appear to resemble a mass spectrum. But the chemist sees these traces not as lines on paper but as vibrating or rotating molecules, as electrons moving from one place to another, as substances separated from a mixture, or as fragments from molecular cleavage. Thus, implicit assumptions about the origins of experimental data both make the observations interpretable and influence the interpretation of the data.⁶

⁴ A femtosecond (fs) is 10^{-15} s. Rosker, M. J.; Dantus, M.; Zewail, A. H. *Science* **1988**, *241*, 1200 reported that the photodissociation of ICN to I and CN occurs in ca. 100 femtoseconds. See also Dantus, M.; Zewail, A. *Chem. Rev.* **2004**, *104*, 1717 and subsequent papers in this issue.

⁵ Baker, S.; Robinson, J. S.; Haworth, C. A.; Teng, H.; Smith, R. A.; Chirlă, C. C.; Lein, M.; Tisch, J. W. G.; Marangos, J. P. *Science* **2006**, *312*, 424; Osborne, I.; Yeston, J. *Science* **2007**, *317*, 765 and subsequent papers.

⁶ “Innocent, unbiased observation is a myth.”—P. Medawar, quoted in *Science* **1985**, *227*, 1188.

With that caveat, what do we know about molecules and how do we know it? We begin with the idea that organic compounds and all other substances are composed of atoms—indivisible particles which are the smallest units of that particular kind of matter that still retain all its properties. It is an idea whose origin can be traced to ancient Greek philosophers.⁷ Moreover, it is convenient to correlate our observation that substances combine only in certain proportions with the notion that these submicroscopic entities called atoms combine with each other only in certain ways.

Much of our fundamental information about molecules has been obtained from spectroscopy.⁸ For example, a 4000 V electron beam has a wavelength of 0.06 Å, so it is diffracted by objects larger than that size.⁹ Interaction of the electron beam with gaseous molecules produces characteristic circular patterns that can be interpreted in terms of molecular dimensions.¹⁰ We can also determine internuclear distance through infrared spectroscopy of diatomic molecules, and we can use X-ray or neutron scattering to calculate distances of atoms in crystals.

“Pictures” of atoms and molecules may be obtained through atomic force microscopy (AFM) and scanning tunneling microscopy (STM).^{11,12} For example, Custance and co-workers reported using atomic force microscopy to identify individual silicon, tin, and lead atoms on the surface of an alloy.¹³ Researchers using these techniques have reported the manipulation of individual molecules and atoms.¹⁴ There have been reports in which STM was used to dissociate an individual molecule and then examine the fragments,¹⁵ to observe the abstraction of a hydrogen atom from H₂S and from H₂O,¹⁶ and to reversibly break a single N–H bond.¹⁷ Such use of STM has been termed *angstromchemistry*.¹⁸ Moreover, it was proposed that scanning tunneling microscopy and atomic force microscopy could be used to image the lateral profiles of individual *sp*³ hybrid orbitals.¹⁹ Some investigators have

⁷ Asimov, I. *A Short History of Chemistry*; Anchor Books: Garden City, NY, 1965; pp. 8–14.

⁸ For a review of structure determination methods, see Gillespie, R. J.; Hargittai, I. *The VSEPR Model of Molecular Geometry*; Allyn and Bacon: Boston, 1991; pp. 25–39.

⁹ Moore, W. J. *Physical Chemistry*, 3rd ed.; Prentice-Hall: Englewood Cliffs, NJ, 1962; p. 575 ff.

¹⁰ For discussions of structure determination with gas phase electron diffraction, see Karle, J. in Maksić, Z. B.; Eckert-Maksić, M., Eds. *Molecules in Natural Science and Medicine*; Ellis Horwood: Chichester, England, 1991; pp. 17–27; Hedberg, K. *ibid.*; pp. 29–42.

¹¹ Hou, J. G.; Wang, K. *Pure Appl. Chem.* **2006**, *78*, 905.

¹² See Ottensmeyer, F. P.; Schmidt, E. E.; Olbrecht, A. J. *Science* **1973**, *179*, 175 and references therein; Robinson, A. L. *Science* **1985**, *230*, 304; *Chem. Eng. News* **1986** (Sept. 1), *4*; Hansma, P. K.; Elings, V. B.; Marti, O.; Bracker, C. E. *Science* **1988**, *242*, 209; Parkinson, B. A. *J. Am. Chem. Soc.* **1990**, *112*, 1030; Frommer, J. *Angew. Chem. Int. Ed. Engl.* **1992**, *31*, 1298.

¹³ Sugimoto, Y.; Pou, P.; Abe, M.; Jelinek, P.; Perez, R.; Morita, S.; Custance, O. *Nature (London)* **2007**, *446*, 64.

¹⁴ Weisenhorn, A. L.; MacDougall, J. E.; Gould, S. A. C.; Cox, S. D.; Wise, W. S.; Massie, J.; Maivald, P.; Elings, V. B.; Stucky, G. D.; Hansma, P. K. *Science* **1990**, *247*, 1330; Whitman, L. J.; Stroschio, J. A.; Dragoset, R. A.; Celotta, R. J. *Science* **1991**, *251*, 1206; Leung, O. M.; Goh, M. C. *Science* **1992**, *255*, 64.

¹⁵ Dujardin, G.; Walkup, R. E.; Avouris, P. *Science* **1992**, *255*, 1232.

¹⁶ Lauhon, L. J.; Ho, W. J. *Phys. Chem. B*, **2001**, *105*, 3987.

¹⁷ Katano, S.; Kim, Y.; Hori, M.; Trenary, M.; Kawai, M. *Science* **2007**, *316*, 1883.

¹⁸ For a review of the application of scanning tunneling microscopy to manipulation of bonds, see Ho, W. *Acc. Chem. Res.* **1998**, *31*, 567.

¹⁹ Chen, J. C. *Nanotechnology* **2006**, *17*, S195.

reported imaging single organic molecules in motion with a very different technique, transmission electron microscopy,²⁰ and others have reported studying electron transfer to single polymer molecules with single-molecule spectroelectrochemistry.²¹

Even though “seeing is believing,” we must keep in mind that in all such experiments we do not really see molecules; we see only computer graphics. Two examples illustrate this point: STM features that had been associated with DNA molecules were later assigned to the surface used to support the DNA,²² and an STM image of benzene molecules was reinterpreted as possibly showing groups of acetylene molecules instead.²³

Organic chemists also reach conclusions about molecular structure on the basis of logic. For example, the fact that one and only one substance has been found to have the molecular formula CH_3Cl is consistent with a structure in which three hydrogen atoms and one chlorine atom are attached to a carbon atom in a tetrahedral arrangement. If methane were a trigonal pyramid, then two different compounds with the formula CH_3Cl might be possible—one with chlorine at the apex of the pyramid and another with chlorine in the base of the pyramid. The existence of only one isomer of CH_3Cl does not require a tetrahedral arrangement, however, since we might also expect only one isomer if the four substituents to the carbon atom were arranged in a square pyramid with a carbon atom at the apex or in a square planar structure with a carbon atom at the center. Since we also find one and only one CH_2Cl_2 molecule, however, we can also rule out the latter two geometries. Therefore we infer that the parent compound, methane, is also tetrahedral. This view is reinforced by the existence of two different structures (enantiomers) with the formula CHClBrF . Similarly, we infer the flat, aromatic structure for benzene by noting that there are three and only three isomers of dibromobenzene.²⁴

Organic chemists do not think of molecules only in terms of atoms, however. We often envision molecules as collections of nuclei and electrons, and we consider the electrons to be constrained to certain regions of space (orbitals) around the nuclei. Thus, we interpret UV–vis absorption, emission, or scattering spectroscopy in terms of movement of electrons from one of these orbitals to another. These concepts resulted from the development of quantum mechanics. The Bohr model of the atom, the Heisenberg uncertainty principle, and the Schrödinger equation laid the foundation for our current ways of thinking about chemistry. There may be some truth in the statement that

The why? and how? as related to chemical bonding were in principle answered in 1927; the details have been worked out since that time.²⁵

We will see, however, that there are still uncharted frontiers of those details to explore in organic chemistry.

²⁰ Koshino, M.; Tanaka, T.; Solin, N.; Suenaga, K.; Isobe, H.; Nakamura, E. *Science*, **2007**, *316*, 853.

²¹ Palacios, R. E.; Fan, F.-R. F.; Bard, A. J.; Barbara, P. F. *J. Am. Chem. Soc.* **2006**, *128*, 9028.

²² Clemmer, C. R.; Beebe, T. P., Jr. *Science* **1991**, *251*, 640.

²³ Moler, J. L.; McCoy, J. R. *Chem. Eng. News* **1988** (Oct 24), 2.

²⁴ These examples were discussed in an analysis of “topological thinking” in organic chemistry by Turro, N. J. *Angew. Chem. Int. Ed. Engl.* **1986**, *25*, 882.

²⁵ Ballhausen, C. J. *J. Chem. Educ.* **1979**, *56*, 357.

TABLE 1.1 Bond Lengths and Bond Angles for Methyl Halides

Molecule	$r_{\text{C-H}}$ (Å)	$r_{\text{C-X}}$ (Å)	$\angle_{\text{H-C-H}}$	$\angle_{\text{H-C-X}}$
CH ₃ F	1.105	1.385	109°54'	109°2'
CH ₃ Cl	1.096	1.781	110°52'	108°0'
CH ₃ Br	1.10	1.939	111°38'	107°14'
CH ₃ I	1.096	2.139	111°50'	106°58'

Source: Reference 29.

Molecular Dimensions

Data from spectroscopy or from X-ray, electron, or neutron diffraction measurements allow us to determine the distance between atomic centers as well as to measure the angles between sets of atoms in covalently bonded molecules.²⁶ The most detailed information comes from microwave spectroscopy, although that technique is more useful for lower molecular weight than higher molecular weight molecules because the sample must be in the vapor phase.²⁷ Diffraction methods locate a center of electron density instead of a nucleus. The center of electron density is close to the nucleus for atoms that have electrons below the valence shell. For hydrogen, however, the electron density is shifted toward the atom to which it is bonded, and bonds to hydrogen are determined by diffraction methods to be shorter than are bond lengths determined with spectroscopy.²⁸ With solid samples, the possible effect of crystal packing forces must also be considered. Therefore, the various techniques give slightly different measures of molecular dimensions.

Table 1.1 shows data for the interatomic distances and angles of the methyl halides.²⁹ These distances and angles only provide geometric information about the location of nuclei (or local centers of electron density) as points in space. We infer that those points are connected by chemical bonds, so that the distance $r_{\text{C-H}}$ is the length of a C–H bond and the angle $\angle_{\text{H-C-H}}$ is the angle between two C–H bonds.

We may also define atomic dimensions, including the ionic radius (r_i), the covalent radius (r_c), and the van der Waals radius (r_{vdW}) of an atom.³⁰ The ionic radius is the apparent size of the electron cloud around an ion as deduced from the packing of ions into a crystal lattice.³¹ As might be expected, this value varies with the charge on the ion. The ionic radius for a C^{4+} ion is 0.15 Å, while that for a C^{4-} ion is 2.60 Å.³⁰ The van der Waals radius is the effective size of the atomic cloud around a covalently bonded atom as

²⁶ A tabulation of common bond length values was provided by Allen, F. H.; Kennard, O.; Watson, D. G.; Brammer, L.; Orpen, A. G.; Taylor, R. J. *Chem. Soc. Perkin Trans. 2* **1987**, S1.

²⁷ Wilson, E. B. *Chem. Soc. Rev.* **1972**, *1*, 293 and references therein; see also Harmony, M. D. *Acc. Chem. Res.* **1992**, *25*, 321.

²⁸ Clark, T. *A Handbook of Computational Chemistry*; John Wiley & Sons: New York, 1985; chapter 2.

²⁹ (a) Tabulations of bond length and bond angle measurements for specific molecules are available in *Tables of Interatomic Distances and Configuration in Molecules and Ions*; compiled by Bowen, H. J. M.; Donohue, J.; Jenkin, D. G.; Kennard, O.; Wheatley P. J.; Whiffen, D. H.; Special Publication No. 11, Chemical Society (London): Burlington House, W1, London, 1958. (b) See also the 1965 Supplement.

³⁰ Pauling, L. *Nature of the Chemical Bond*, 3rd ed.; Cornell University Press: Ithaca, NY, 1960.

³¹ For an extensive discussion of ionic radii, see Marcus, Y. *Ion Properties*; Marcel Dekker: New York, 1997.

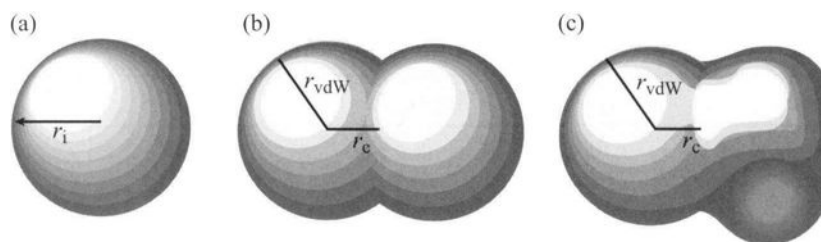


FIGURE 1.1
Radii values for chlorine.

perceived by another atom to which it is not bonded, and it also is determined from interatomic distances found in crystals. Note that the van der Waals radius is not the distance at which the repulsive interactions of the electrons on the two atoms outweigh the attractive forces between them, as is often assumed.^{32,33} Rather, it is a crystal packing measurement that gives a smaller value.^{32,33} The covalent radius of an atom indicates the size of an atom when it is part of a covalent bond, and this distance is much less than the van der Waals radius.³⁴ Figure 1.1 illustrates these radii for chlorine. The computer-drawn plots of electron density surfaces represent the following: (a) r_i for chloride ion; (b) r_c and r_{vdW} for chlorine in Cl_2 ; (c) r_c and r_{vdW} for chlorine in CH_3Cl .³⁵

Table 1.2 lists ionic and covalent radii values for several atoms. Note that the covalent radius for an atom depends on its bonding. A carbon atom with four single bonds has a covalent radius of 0.76 Å. The value is 0.73 Å for a carbon atom with one double bond, while the covalent radius for a triple-bonded carbon atom is 0.69 Å. The covalent radius of hydrogen varies considerably. The value of r_c for hydrogen is calculated to be 0.30 Å in H_2O and 0.32 Å in CH_4 .³⁰ We can also assign an r_{vdW} to a group of atoms. The value for a CH_3 or CH_2 group is 2.0 Å, while the van der Waals thickness of half the electron cloud in an aromatic ring is 1.85 Å.³⁰ Knowledge of van der Waals radii is important in calculations of molecular structure and reactivity, particularly with regard to proteins.³⁶

We may use the atomic radii to calculate the volume and the surface area of an atom. Then using the **principle of additivity** (meaning that the properties of a molecule can be predicted by summing the contributions of its component parts), we may calculate values for the volumes and surface areas of molecules. Such calculations were described by Bondi, and a selected set of atomic volume and surface areas is given in Table 1.3. For example, we estimate the molecular volume of propane by counting $2 \times 13.67 \text{ cm}^3/\text{mol}$ for the two methyl groups plus $10.23 \text{ cm}^3/\text{mol}$ for the methylene group, giving a total volume of $37.57 \text{ cm}^3/\text{mol}$. Similarly, we calculate that the volume of the atoms in hexane is $2 \times 13.67 \text{ cm}^3/\text{mol}$ for the two methyl groups plus $4 \times 10.23 \text{ cm}^3/\text{mol}$ for the four methylene groups, making a total volume of $68.26 \text{ cm}^3/\text{mol}$. The volume of one mole of liquid hexane at 20° is 130.5 mL,

³² Bondi, A. J. *Phys. Chem.* **1964**, *68*, 441.

³³ The difference is that distances between atoms in a crystal are determined by all of the forces acting on the molecules containing those atoms, not just the forces between those two atoms alone.

³⁴ Cordero, B.; Gómez, V.; Platero-Prats, A. E.; Revés, M.; Echeverría, J.; Cremades, E.; Barragán, F.; Alvarez, S. *Dalton Trans.* **2008**, 2832.

³⁵ The images were produced with a CAChe™ WorkSystem (CAChe Scientific).

³⁶ For example, see Proserpio, D. M.; Hoffmann, R.; Levine, R. D. *J. Am. Chem. Soc.* **1991**, *113*, 3217.

TABLE 1.2 Comparison of van der Waals, Ionic, and Covalent Radii for Selected Atoms (Å)

Atom	van der Waals Radius (r_{vdW}^a)	Ionic Radius		Covalent Radii (r_c)		
		Ion	r_i	Single Bonded ^b	Double Bonded	Triple Bonded
H	1.11 Å	H ⁻	2.08 Å	0.31 Å		
C	1.68	C ⁴⁻	2.60	0.76	0.73 ^b	0.69 ^b
N	1.53	N ³⁻	1.71	0.71		
O	1.50	O ²⁻	1.40	0.66		
F	1.51	F ⁻	1.36	0.57		
Cl	1.84	Cl ⁻	1.81	1.02	0.89	
Br	1.96	Br ⁻	1.95	1.20	1.04	
I	2.13	I ⁻	2.16	1.39	1.23	
P	1.85	P ³⁻	2.12	1.07	1.00	0.93
S	1.82	S ²⁻	1.64	1.05	0.94	0.87
Si	2.04	Si ⁴⁻	2.71	1.11	1.07	1.00

Source: Reference 30.

^aReference 37.

^bReference 34.

TABLE 1.3 Group Contributions to van der Waals Atomic Volume (V_W) and Surface Area (A_W)

Group	V_W (cm ³ / mole)	A_W (cm ² / mole $\times 10^9$)
Alkane, C bonded to four other carbon atoms	3.33	0
Alkane, CH bonded to three other carbon atoms	6.78	0.57
Alkane, CH ₂ bonded to two other carbon atoms	10.23	1.35
Alkane, CH ₃ bonded to one other carbon atom	13.67	2.12
CH ₄	17.12	2.90
F, bonded to a 1° carbon atom	5.72	1.10
F, bonded to a 2° or 3° carbon atom	6.20	1.18
Cl, bonded to a 1° carbon atom	11.62	1.80
Cl, bonded to a 2° or 3° carbon atom	12.24	1.82
Br, bonded to a 1° carbon atom	14.40	2.08
Br, bonded to a 2° or 3° carbon atom	14.60	2.09
I, bonded to a 1° carbon atom	19.18	2.48
I, bonded to a 2° or 3° carbon atom	20.35	2.54

Source: Reference 32.

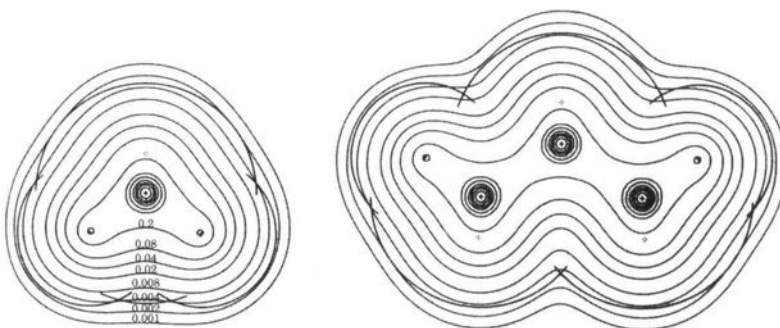
which means that nearly half of the volume occupied by liquid hexane corresponds to space that is outside the boundaries of the carbon and hydrogen atoms as defined above.

Increasingly, values for atomic and molecular volume are available from theoretical calculations. The calculated values vary somewhat, depending on

³⁷ Many sets of van der Waals radii are available in the literature. The data shown are values reported by Chauvin, R. *J. Phys. Chem.* **1992**, 96, 9194. These values correlate well with—but are sometimes slightly different from—values given by Pauling (reference 30), Bondi (reference 32), and O'Keefe, M.; Brese, N. E. *J. Am. Chem. Soc.* **1991**, 113, 3226. A set of van der Waals radii of atoms found in proteins was reported by Li, A.-J.; Nussinov, R. *Proteins* **1998**, 32, 111.

FIGURE 1.2

Contour maps and van der Waals radii arcs for methane (left) and propane (right). (Reproduced from reference 38.)

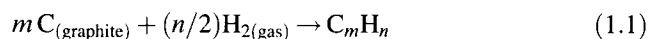


the definition of the surface of the atom or molecule. Usually the boundary of an atom is defined as a certain minimum value of electron density in units of au ($1.00 \text{ au} = 6.748 \text{ e}/\text{\AA}^3$). Bader and co-workers determined that the 0.001 au volumes of methane and ethane are 25.53 and 39.54 cm^3/mol , respectively, while the corresponding 0.002 au volumes are 19.58 and 31.10 cm^3/mol .³⁸ Thus, it appears that the 0.002 au values are closer to, but still somewhat larger than, those calculated empirically using the values in Table 1.3. The relationships between atomic volumes and van der Waals radii are illustrated for cross sections through methane and propane in Figure 1.2. The contour lines represent the electron density contours, and the intersecting arcs represent the van der Waals radii of the atoms.

1.2 HEATS OF FORMATION AND REACTION

Experimental Determination of Heats of Formation

Thermochemical measurements provide valuable insights into organic structures and reactions. The **heat of formation** (ΔH_f°) of a compound is defined as the difference in enthalpy between the compound and the starting elements in their standard states.³⁹ For a hydrocarbon with molecular formula (C_mH_n), we define ΔH_f° as the heat of reaction (ΔH_r°) for the reaction

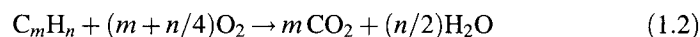


We usually determine the heat of formation of an organic compound indirectly by determining the heat of reaction of the compound to form other substances for which the heats of formation are known, and the heat of combustion ($\Delta H_{\text{combustion}}^\circ$) of a substance is often used for this purpose. Consider the combustion of a compound with the formula C_mH_n . The

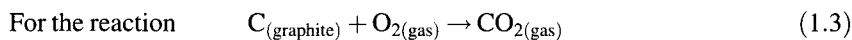
³⁸ Bader, R. F. W.; Carroll, M. T.; Cheeseman, J. R.; Chang, C. J. *Am. Chem. Soc.* **1987**, *109*, 7968. See the discussion of the theory of atoms in molecules in Chapter 4.

³⁹ Mortimer, C. T. *Reaction Heats and Bond Strengths*; Pergamon Press: New York, 1962; Clark, T.; McKervey, M. A. in Stoddart, J. F., Ed. *Comprehensive Organic Chemistry*, Vol. 1; Pergamon Press: Oxford, England, 1979; p. 66 ff. For a discussion of the experimental techniques involved in calorimetry experiments, see (a) Wiberg, K. in Liebman, J. F.; Greenberg, A., Eds. *Molecular Structure and Energetics*, Vol. 2; VCH Publishers: New York, 1987; p. 151; (b) Sturtevant, J. M. in Weissberger, A.; Rossiter, B. W., Eds. *Physical Methods of Chemistry*, Vol. I, Part V; Wiley-Interscience: New York, 1971; p. 347.

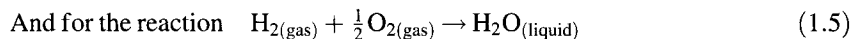
balanced chemical equation is



We know the heats of formation of CO₂ and H₂O:



$$\Delta H_r^\circ = \Delta H_f^\circ(CO_2) \quad (1.4)$$



$$\Delta H_r^\circ = \Delta H_f^\circ(H_2O) \quad (1.6)$$

Combining the above equations, we obtain

$$\Delta H_f^\circ(C_mH_n) = m \Delta H_f^\circ(CO_2) + (n/2)\Delta H_f^\circ(H_2O) - \Delta H_{\text{combustion}}^\circ(C_mH_n) \quad (1.7)$$

As an example, the heat of combustion of 1,3-cyclohexanedione was found to be -735.9 kcal/mol.^{40,41} Taking -94.05 kcal/mol and -68.32 kcal/mol as the standard heats of formation of CO₂ and H₂O, respectively, gives a standard heat of formation for crystalline 1,3-cyclohexanedione of $6(-94.05) + 4(-68.32) - (-735.9) = -101.68$ kcal/mol. It is sometimes necessary to correct heats of reaction for the heats associated with phase changes in the reactants or products. To convert from a condensed phase to the gas phase (e.g., for comparison with values calculated theoretically) the relevant terms are the heat of vaporization (ΔH_v°) of a liquid or heat of sublimation (ΔH_s°) of a solid.⁴²⁻⁴⁴ Correcting for the standard heat of sublimation of 1,3-cyclohexanedione, $+21.46$ kcal/mol, gives its standard heat of formation in the gas phase of -80.22 kcal/mol.

If we are interested only in the difference between the heats of formation of two compounds, we may be able to measure their relative enthalpies more accurately by measuring the heat of a less exothermic reaction. That is, we measure very accurately the ΔH of a reaction in which the two different reactants combine with identical reagents to give the same product(s). Figure 1.3 illustrates how the difference in enthalpy of reactants A and B can be calculated in this manner. If the reaction of A and C to give D has a ΔH_r of $-X$ kcal/mol, and if the reaction of B and C to give D has a ΔH_r of $-Y$ kcal/mol, then the difference in energy between A and B must be $(X - Y)$ kcal/mol. For example, Wiberg and Hao determined that ΔH_r values for the reaction of trifluoroacetic acid with 2-methyl-1-butene and with 2-methyl-2-butene were

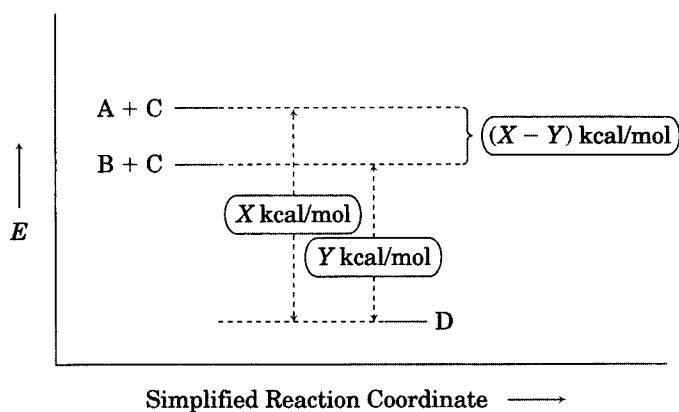
⁴⁰ Pilcher, G.; Parchment, O. G.; Hillier, I. H.; Heatley, F.; Fletcher, D.; Ribeiro da Silva, M. A. V.; Ferrão, M. L. C. C. H.; Monte, M. J. S.; Jiye, F. J. *Phys. Chem.* **1993**, *97*, 243.

⁴¹ The reported value (converted from kJ/mol) was -735.9 ± 0.2 kcal/mol. Experimental uncertainties will not be carried through this discussion because the emphasis is on the calculation procedure and not the precision of the experimental method.

⁴² Determination of heats of sublimation was discussed by Chickos, J. S. in Liebman, J. F.; Greenberg, A., Eds. *Molecular Structure and Energetics*, Vol. 2; VCH Publishers: New York, 1987; p. 67.

⁴³ The enthalpy associated with transformation of a solid to a liquid is the **heat of fusion**. For a discussion, see Chickos, J. S.; Braton, C. M.; Hesse, D. G.; Liebman, J. F. *J. Org. Chem.* **1991**, *56*, 927.

⁴⁴ Data for heat capacity can be used to correct ΔH values measured at one temperature to another temperature. See Orchin, M.; Kaplan, F.; Macomber, R. S.; Wilson, R. M.; Zimmer, H. *The Vocabulary of Organic Chemistry*; Wiley-Interscience: New York, 1980; pp. 255-256.

**FIGURE 1.3**

Calculation of the enthalpy difference of isomers.

-10.93 kcal/mol and -9.11 kcal/mol, respectively.⁴⁵ Therefore, the 2-alkene was judged to be 1.82 kcal/mol lower in energy than the 1-alkene. Heats of hydrogenation are also used to determine the difference in heats of formation of alkenes even though heats of combustion may be measured much more *precisely* than heats of hydrogenation. Because heats of hydrogenation are smaller in magnitude than are heats of combustion, small enthalpy differences between isomers may be determined more *accurately* by hydrogenation.⁴⁶

Bond Increment Calculation of Heats of Formation

Table 1.4 shows experimental ΔH_f° values for some linear alkanes.⁴⁷ There is a general trend in the data: each homolog higher than ethane has a ΔH_f° value about 5 kcal/mol more negative than the previous alkane. This observation suggests that it should be possible to use the principle of additivity (page 6) to predict the heat of formation of an organic compound by summing the contribution each component makes to ΔH_f° .⁴⁸ Extensive work in this area was done by Benson, who published tables of **bond increment contributions** to heats of formation and other thermodynamic properties.⁴⁸⁻⁵³ A portion of one such table is reproduced as Table 1.5.

The heats of formation of some linear alkanes calculated by the bond increment method are shown in Table 1.4. As an example of such calculations, let us determine the ΔH_f° values for methane and ethane. For methane, there

⁴⁵ Wiberg, K. B.; Hao, S. *J. Org. Chem.* **1991**, *56*, 5108.

⁴⁶ Davis, H. E.; Allinger, N. L.; Rogers, D. W. *J. Org. Chem.* **1985**, *50*, 3601.

⁴⁷ Experimental data for ΔH_f° at 298 K are from tabulations in Stull, D. R.; Westrum, E. F., Jr.; Sinke, G. C. *The Thermodynamics of Organic Compounds*; John Wiley & Sons: New York, 1969; pp. 243-245.

⁴⁸ Benson, S. W. *Thermochemical Kinetics*, 2nd ed.; Wiley-Interscience: New York, 1976; p. 24.

⁴⁹ Benson, S. W.; Buss, J. H. *J. Chem. Phys.* **1959**, *29*, 546.

⁵⁰ Benson, S. W.; Cruickshank, F. R.; Golden, D. M.; Haugen, G. R.; O'Neal, H. E.; Rodgers, A. S.; Shaw, R.; Walsh, R. *Chem. Rev.* **1969**, *69*, 279.

⁵¹ For a discussion of the development of bond increment and group increment calculations, see Schleyer, P. v. R.; Williams, J. E.; Blanchard, K. R. *J. Am. Chem. Soc.* **1970**, *92*, 2377.

⁵² Calculation of group increments to heats of formation of linear hydrocarbons was reported by Pitzer, K. S. *J. Chem. Phys.* **1940**, *8*, 711 and to nonlinear hydrocarbons by Franklin, J. L. *Ind. Eng. Chem.* **1949**, *41*, 1070.

⁵³ Cohen, N.; Benson, S. W. *Chem. Rev.* **1993**, *93*, 2419.

TABLE 1.4 Experimental and Calculated Heats of Formation of Linear Alkanes at 298 K

Compound	ΔH_f° (kcal/mol) obs.	ΔH_f° (kcal/mol) calc. ^a
Methane	-17.89	-15.32
Ethane	-20.24	-20.25
Propane	-24.82	-25.18
Butane	-30.15	-30.11

^aCalculations are based on bond increment values in Table 1.5.

are four C–H bonds, each contributing -3.83 kcal/mol, so the ΔH_f° value is -15.32 kcal/mol. For ethane, the ΔH_f° value is $6 \times (-3.83) + 1 \times (2.73)$ for the six C–H and one C–C bonds, respectively, and the total is -20.25 kcal/mol. As the chain is extended, each additional CH_2 group contributes $2 \times (-3.83) + 1 \times (2.73) = -4.93$ kcal/mol to the ΔH_f° value.

There is a problem with the ΔH_f° values obtained from the simple bond increment data in Table 1.5. The five isomers of hexane listed in Table 1.6 all have five C–C bonds and fourteen C–H bonds. Using the bond increment values in Table 1.5, we would predict each to have the same heat of formation (-39.97 kcal/mol). As shown in Table 1.6, however, the experimental heats of formation become more negative as the branching increases. Specifically, the structure with a quaternary carbon atom is more stable than an isomeric structure with two tertiary carbon atoms, and the structure with two tertiary

TABLE 1.5 Bond Increment Contributions to ΔH_f°

Bond	ΔH_f° (kcal/mol)	Bond	ΔH_f° (kcal/mol)
C–H	-3.83	N–H	-2.6
C–D	-4.73	S–H	-0.8
C–C	2.73	S–S	-6.0
C–F	-52.5	C–S	6.7
C–Cl	-7.4	C _d –C	6.7
C–Br	2.2	C _d –H	3.2
C–I	14.1	C _d –F	-39.0
C–O	-12.0	C _d –Cl	-5.0
O–H	-27.0	C _d –Br	9.7
O–D	-27.9	C _d –I	21.7
O–O	21.5	C _d –C _d	7.5

Source: Reference 48.

TABLE 1.6 Heats of Formation (kcal/mol) of Isomeric C₆H₁₄ Structures

Compound	ΔH_f° , obs. ^a	ΔH_f° , calc. ^b	ΔH_f° , corr. ^c
Hexane	-39.96	-39.96	-39.96
2-Methylpentane	-41.66	-42.04	-41.24
3-Methylpentane	-41.02	-42.04	-41.24
2,2-Dimethylbutane	-44.35	-44.77	-43.16
2,3-Dimethylbutane	-42.49	-44.12	-42.52

^aExperimental data for ΔH_f° at 298 K are from reference 47, pp. 247–249.

^bCalculated from group increments in Table 1.7 without correcting for gauche interactions.

^cData from the previous column corrected for gauche interactions. See Table 1.7 and Figure 1.4.

carbon atoms is more stable than structures with only one tertiary carbon atom, even though all isomers have the same number of C–C and C–H bonds. Thus, we must conclude that the heat of formation of a compound depends not only on the number of carbon–carbon bonds, but also on the nature of the carbon–carbon bonds.

One way to describe the extent to which heats of formation depend on bonding patterns is to consider an **isodesmic reaction**—a reaction in which both the reactants and the products have the same number of bonds of a given type, even though there may be changes in the relationship of one bond to another.^{54,55} For example, consider the hypothetical conversion of *n*-hexane to 2,2-dimethylbutane. Both the reactant and the product have five C–C and fourteen C–H bonds. The simple bond increment approach would calculate that the heat of the reaction should be 0, but the data in Table 1.6 indicate that the heat of the reaction should be –4.4 kcal/mol. Therefore, the heat of an isodesmic reaction is an indication of deviation from the additivity of bond energies.^{54,56}

Group Increment Calculation of Heats of Formation

An alternative to the bond increment method is the **group increment** approach, which allows calculation of enthalpy differences that result from different arrangements of bonds within molecules. We consider not the bonds holding atoms together but the groups that result from these bonds. Table 1.7 lists the group increment values for a series of organic functional groups.⁵⁰ Using these data, we can closely approximate the heats of formation of the isomeric hexanes. Consider 2-methylpentane. Three methyl groups [C–(H)₃(C) in the table] contribute –10.08 kcal/mol each to the heat of formation, two methylene units [C–C(H)₂(C)₂] contribute –4.95 kcal/mol each, and one methine unit [C–(H)(C)₃] contributes –1.90 kcal/mol. Thus, estimated heat of formation is

$$\Delta H_f^\circ = 3 \times (-10.08) + 2 \times (-4.95) + 1 \times (-1.90) = -42.04 \text{ kcal/mol} \quad (1.8)$$

The experimental value is (–41.66 kcal/mol).⁴⁷

Note that the estimated heats of formation calculated in this way assign the same contribution to each group without regard to its position in the molecule and without regard to strain. In branched acyclic alkanes, the major form of strain to consider is van der Waals repulsion due to *unavoidable* butane gauche interactions, which may be assigned 0.8 kcal/mol each.⁵⁷ Figure 1.4 shows a Newman projection and gives the number of

⁵⁴ Hehre, W. J.; Ditchfield, R.; Radom, L.; Pople, J. A. *J. Am. Chem. Soc.* **1970**, *92*, 4796. See also Ponomarev, D. A.; Takhistov, V. V. *J. Chem. Educ.* **1997**, *74*, 201.

⁵⁵ A **homodesmotic reaction** is a reaction in which not only are the number of bonds of each type conserved, but the number of carbon atoms with zero, one, two, or three hydrogen atoms is also conserved. For details, see George, P.; Trachtman, M.; Bock, C. W.; Brett, A. M. *Tetrahedron* **1976**, *32*, 317. Isomers interconverted by homodesmotic reactions are termed **isologous** (cf. Engler, E. M.; Andose, J. D.; Schleyer, P. v. R. *J. Am. Chem. Soc.* **1973**, *95*, 8005).

⁵⁶ Isodesmic reactions are widely used in theoretical studies because errors in the energies of reactants and products are more likely to cancel, thereby allowing simple computational approaches to give accurate estimates of heats of reactions. For a discussion, see Hehre, W. J.; Radom, L.; Schleyer, P. v. R.; Pople, J. A. *Ab initio Molecular Orbital Theory*; Wiley-Interscience: New York, 1986.

⁵⁷ Molecular conformation and van der Waals strain will be discussed in Chapter 3.

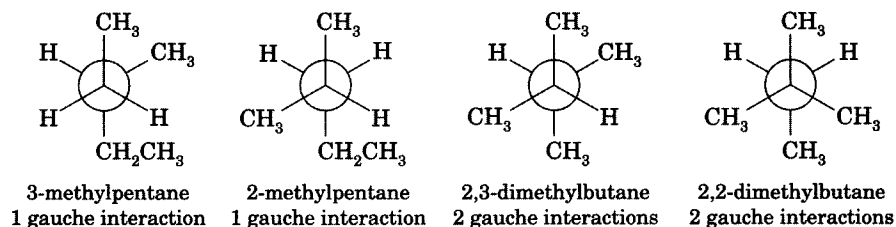
TABLE 1.7 Group Increment Contributions to Heats of Formation

Group	$\Delta H_{f,298}^{\circ}$ (kcal/mol)	Group	$\Delta H_{f,298}^{\circ}$ (kcal/mol)
C-(H) ₃ (C)	-10.08	C _d -(C _B)(C)	8.64
C-(H) ₂ (C) ₂	-4.95	C-(C _B)(C)(H) ₂	-4.86
C-(H)(C) ₃	-1.90	C-(C _B)(C) ₂ (H)	-0.98
C-(C) ₄	0.50	C _t -(H)	26.93
C _d -(H) ₂	6.26	C _t -(C)	27.55
C _d -(H)(C)	8.59	C _t -(C _d)	29.20
C _d -(C) ₂	10.34	C _B -(H)	3.30
C _d -(C _d)(H)	6.78	C _B -(C)	5.51
C _d -(C _d)(C)	8.88	C _B -(C _d)	5.68
[C _d -(C _B)(H)]	6.78		

Source: Reference 50.

gauche interactions for each of the isomers of hexane. Correcting the initial ΔH_f° of 2-methylpentane for one such interaction gives -41.24 kcal/mol, which is closer to the experimental value. Angle strain corrections must be applied for ring compounds. For example, cyclopropane, cyclobutane, and cyclopentane rings add 27.6, 26.2, and 6.3 kcal/mol, respectively, to a heat of formation calculated from the data in Table 1.7.^{50,58}

The origin of the increased stability of branched alkanes relative to nonbranched isomers has been the subject of some debate. Benson and Luria proposed that alkanes have polarized $C^{\delta-}-H^{\delta+}$ bonds and that the sum of the electrostatic interactions of a branched compound is lower in energy than the sum of electrostatic interactions in a linear structure.⁵⁹ Laidig calculated that branched hydrocarbons have overall smaller distances between atoms than do linear isomers and that the resulting increase in nucleus–electron attraction in a branched compound outweighs the increase in nuclear–nuclear and electron–electron repulsion.⁶⁰ More recently, the stabilization of branched alkanes has been attributed to attractive interactions involving alkyl groups bonded to the same carbon atom.⁶¹

**FIGURE 1.4**

Gauche interactions in hexane isomers.

⁵⁸ These examples only hint at the analysis of heats of formation of organic compounds that is possible. Benson and co-workers summarized the methods and data for calculations for the major functional groups in organic chemistry.^{48,50} In addition, the data allow calculation of heat capacities and entropies of these compounds in the same manner in which heats of formation are determined. Heats of formation are valuable reference points in discussing the stabilities of various isomers or products of reactions, whether they are calculated by bond increments or group increments or are derived as part of a theoretical calculation.

⁵⁹ Benson, S. W.; Luria, M. J. *Am. Chem. Soc.* **1975**, *97*, 704.

⁶⁰ Laidig, K. E. J. *Phys. Chem.* **1991**, *95*, 7709.

⁶¹ Schreiner, P. R. *Angew. Chem. Int. Ed.* **2007**, *46*, 4217.

TABLE 1.8 Calculation of Gas Phase ΔH_f° Values^a of Alkanes Assuming Geminal Interactions Are Repulsive

Compound	n_{C-C}	n_{C-H}	n_{H-C-H}	n_{H-C-C}	n_{C-C-C}	n_C	n_H	ΔH_f (calculated)	ΔH_f (literature)
Methane	0	4	6	0	0	1	4	-17.2	-17.9
Ethane	1	6	6	6	0	2	6	-20.4	-20.0
Propane	2	8	7	10	1	3	8	-25.3	-25.0
Butane	3	10	8	14	2	4	10	-30.2	-30.4
2-Methylpropane	3	10	9	12	3	4	10	-31.9	-32.1
<i>n</i> -Pentane	4	12	9	18	3	5	12	-35.1	-35.1
2-Methylbutane	4	12	10	16	4	5	12	-36.8	-36.7
2,2-Dimethylpropane	4	12	12	12	6	5	12	-40.3	-40.1
Hexane	5	14	10	22	4	6	14	-40.0	-40.0
Cyclohexane	6	12	6	24	6	6	12	-29.4	-29.4
	E_{C-C}	E_{C-H}	E_{H-C-H}	E_{H-C-C}	E_{C-C-C}	E_C	E_H		
	-146.00	-124.20	6.64	9.29	10.20	60.70	52.10		

Source: Reference 62.

^a Energies are in kcal/mol.

Gronert proposed a very different explanation.⁶² He noted that van der Waals interactions between nonbonded groups that are closer than the sum of their van der Waals radii, such as C1 and C4 in the gauche conformation of butane, are known to be repulsive. Since C1 and C3 in neopentane are even closer to each other than are C1 and C4 in gauche butane, he argued that their interaction should be repulsive as well. Moreover, the interactions between two hydrogen atoms bonded to the same carbon as well as those between hydrogen and carbon atoms bonded to the same carbon were also said to be repulsive. The effect of branching (e.g., conversion of butane to isobutane) is to reduce the number of H-C-C interactions while increasing the number of H-C-H and C-C-C interactions. Gronert proposed that the steric energy of an H-C-C interaction is less than the average of those for the H-C-H and C-C-C interactions, so the effect of the branching is to decrease overall intramolecular repulsion and produce a more stable isomer. Using equations 1.9 and 1.10, along with the interaction values (E) for C-H and C-C bonding and specific values for repulsive 1,3 interactions shown in Table 1.8, Gronert was able to reproduce the observed gas phase ΔH_f° values of a series of alkanes. For example, the ΔH_f° of *n*-pentane in kcal/mol is calculated as shown in equation 1.11.

$$\Delta H_f = n_{C-C}E_{C-C} + n_{C-H}E_{C-H} + n_{C-C-C}E_{C-C-C} + n_{C-C-H}E_{C-C-H} + n_{H-C-H}E_{H-C-H} + f(C, H) \quad (1.9)$$

where

$$f(C, H) = (170.6 + E_C)n_C + 52.1 n_H \quad (1.10)$$

$$\begin{aligned} \Delta H_f &= 4(-146) + 12(-124.2) + 9(6.64) + 18(9.29) + 3(10.2) \\ &\quad + 5(231.3) + 12(52.1) = -35.1 \text{ kcal/mol} \end{aligned} \quad (1.11)$$

⁶² Gronert, S. *J. Org. Chem.* **2006**, *71*, 1209; 9560. The literature values in Table 1.8 are from this source. The values of the E parameters at the bottom of the table are shown to two decimal places, while those in the sources cited here were reported to one decimal place.

TABLE 1.9 Calculation of Gas Phase ΔH_f° Values^a of Alkanes Assuming Geminal Methyl Interactions Are Stabilizing

Alkane	n_{CH_2}	$n_{\text{primary branches}}$	$n_{\text{tertiary branches}}$	$n_{\text{quaternary branches}}$	ΔH_f° (calculated)	ΔH_f° (literature)
Methane	0	0	0	0	-17.89	-17.89
Ethane	1	0	0	0	-20.04	-20.04
Propane	2	1	0	0	-25.02	-25.02
Butane	3	2	0	0	-30.00	-32.07
Isobutane	3	0	1	0	-32.08	-2.07
Pentane	4	3	0	0	-34.98	-35.08
Isopentane	4	1	1	0	-37.06	-36.73
Neopentane	4	0	0	1	-39.98	-40.14
Hexane	5	4	0	0	-39.96	-39.96

Source: Reference 64.

^aEnergies are in kcal/mol.

Gronert's explanation for the stability of branched alkanes was supported by some investigators, but disputed by others.⁶³ In particular, Wodrich and Schleyer pointed out that comparable results could be obtained by assuming that the interactions of geminal methyl groups are stabilizing (equation 1.12).^{64,65} Here n_{CH_2} is the number of methylene units conceptually added to methane to form the alkane, $n_{\text{primary branches}}$ is the number of C-CH₂-C units, $n_{\text{tertiary branches}}$ is the number of 3° carbon units, and $n_{\text{quaternary branches}}$ is the number of 4° carbons in the structure. Some results obtained with this approach are shown in Table 1.9, and a calculation of ΔH_f° for *n*-pentane is shown in equation 1.13.

$$\Delta H_f = -17.89 - 2.15 n_{\text{CH}_2} - 2.83 n_{\text{primary branches}} - 7.74 n_{\text{tertiary branches}} - 13.49 n_{\text{quaternary branches}} \quad (1.12)$$

$$\Delta H_f = -17.89 + 4(-2.15) + 3(-2.83) + 0(-7.74) + 0(-13.49) = -35 \text{ kcal/mol} \quad (1.13)$$

We will explore the nature of geminal interactions more fully in the context of radical stabilities (Chapter 5). The points to be made here are (i) two very different models can be used to predict the heats of formation of alkanes, and (ii) a good correlation does not necessarily establish a cause and effect relationship. As Wodrich and Schleyer noted, the fact that the number of births in some European countries correlates with the number of storks in those countries does not demonstrate that babies are delivered by storks. It

⁶³ Mitoraj, M.; Zhu, H.; Michalak, A.; Ziegler, T. *J. Org. Chem.* **2006**, *71*, 9208.

⁶⁴ Wodrich, M. D.; Schleyer, P. v. R. *Org. Lett.* **2006**, *8*, 2135.

⁶⁵ Wodrich, M. D.; Wannere, C. S.; Mo, Y.; Jarowski, P. D.; Houk, K. N.; Schleyer, P. v. R. *Chem. Eur. J.* **2007**, *13*, 7731 proposed the concept of *protobranching* to explain the energy-lowering effect of geminal interactions.

TABLE 1.10 DH° Values (kcal/mol) for Bonds to Hydrogen

Compound	DH° (kcal/mol)	Compound	DH° (kcal/mol)
H-H	104.2	H-F	136.3
H-CN	126.3	H-Cl	103.2
H-NH ₂	107.6	H-Br	87.5
HO-H	118.8	H-I	71.3
H-CH ₂ OH	96.1	HS-H	91.2
CH ₃ O-H	104.6	H-ONO ₂	101.7
CH ₃ S-H	87.4	CH ₃ CH ₂ O-H	104.7
H-CH ₂ SH	94	(CH ₃) ₂ CHO-H	105.7
HOO-H	87.8	(CH ₃) ₃ CO-H	106.3
CH ₃ OO-H	88	C ₆ H ₅ O-H	90
H-CHO	88.1	CH ₃ CH ₂ OO-H	85
CH ₃ C(O)-H	89.4	(CH ₃) ₃ COO-H	84
HCOO-H	112	CH ₃ COO-H	112
H-COOH	>96	C ₆ H ₅ COO-H	111

Source: Reference 69.

will be useful to remember this comment as we consider explanations for other chemical phenomena in later chapters.⁶⁶

Homolytic and Heterolytic Bond Dissociation Energies

Heats of reaction are important values for processes that involve reactive intermediates. For example, the **standard homolytic bond dissociation enthalpy** of compound A-B, denoted $DH^\circ(A-B)$ or $DH_{298}(A-B)$, is the heat of reaction (ΔH_r°) at 298 K for the gas phase dissociation reaction in equation 1.14.



$DH^\circ(A-B)$ values can be calculated from the relationship^{67,68}

$$DH^\circ(A-B) = \Delta H_{r(\text{equation 1.14})}^\circ = \Delta H_f^\circ(A^\bullet) + \Delta H_f^\circ(B^\bullet) - \Delta H_f^\circ(A-B) \quad (1.15)$$

Here $\Delta H_f^\circ(A^\bullet)$ is the heat of formation of radical A^\bullet , $\Delta H_f^\circ(B^\bullet)$ is the heat of formation of radical B^\bullet , and $\Delta H_f^\circ(A-B)$ is the heat of formation of A-B. $DH^\circ(A-B)$ is also called the **bond dissociation energy** of A-B. Table 1.10 gives a list of standard bond dissociation enthalpies for bonds involving hydrogen atoms, and Table 1.11 gives a list of DH° values for bonds between carbon atoms in various alkyl groups and a number of common organic substituents.⁶⁹

⁶⁶ See also Stanger, A. *Eur. J. Org. Chem.* **2007**, 5717.

⁶⁷ Benson, S. W. *J. Chem. Educ.* **1965**, 42, 502.

⁶⁸ A standard bond dissociation energy is different from an **average** bond dissociation energy. The latter is just the value obtained by calculating the heat of atomization of a compound (the enthalpy change on converting the molecule to individual atoms) divided by the number of bonds from one atom to another in the molecule. For more details on this distinction, see reference 67.

⁶⁹ Blanksby, S. J.; Ellison, G. B. *Acc. Chem. Res.*, **2003**, 36, 255. This reference provides the uncertainties for the values in Tables 1.10 and 1.11.

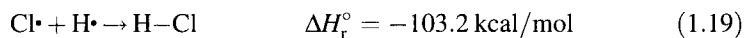
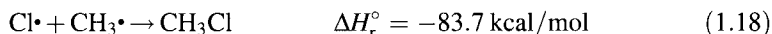
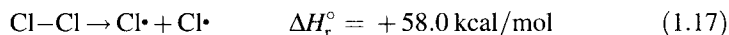
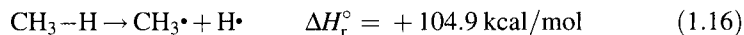
TABLE 1.11 DH° Values (kcal/mol) for Selected Bonds to Alkyl Groups

Substituent \ R	CH ₃	CH ₃ CH ₂	(CH ₃) ₂ CH	(CH ₃) ₃ C	CH ₂ =CH	CH ₂ =CHCH ₂	C ₆ H ₅	C ₆ H ₅ CH ₂	CH ₃ O	HC(O)	CH ₃ CH(O)
H	104.9	101.1	98.6	96.5	110.7	88.8	112.9	89.7	104.6	88.1	89.4
F	115	—	110.6	—	123.3	—	127.2	98.7	—	—	122.2
Cl	83.7	84.8	85.2	84.9	91.2	—	97.1	74	—	—	84.7
Br	72.1	72.4	73.9	72.6	80.8	59	84	63	—	—	71.7
I	57.6	56.9	57	55.6	—	45.6	67	51	—	—	53.8
HO	92.1	94.0	95.5	95.8	—	80.1	112.4	82.6	—	109.5	109.9
CH ₃ O	83.2	85	85.8	84	—	—	101	—	38	99.6	100
NH ₂	85.2	84.8	86.0	85.7	—	—	104.2	71.7	—	—	99.1
CN	122.4	121.6	120.9	117.8	133	108.7	134	—	—	—	—
NO ₂	61.0	61.6	62.9	62.8	—	—	72.5	50.5	42	—	—
CH ₃	90.1	89.0	88.6	87.5	101.4	76.5	103.5	77.6	*	84.8	84.5
CH ₃ CH ₂	*	87.9	87.1	85.6	100.0	75.4	102.2	76.7	*	83.3	83.5
(CH ₃) ₂ CH	*	*	85.6	82.7	99.2	75.2	101.0	76.4	*	83.1	81.9
(CH ₃) ₃ C	*	*	*	78.6	97.8	73.2	98.3	—	*	—	79.4
CH ₂ =CH	*	*	*	*	116	87.3	116	—	—	—	41
CH ₂ CHCH ₂	*	*	*	*	*	62.7	—	—	—	—	—
HC≡C	126.5	125.1	124.5	122.3	—	—	—	—	—	—	—
HC≡CCH ₂	78	77	—	—	—	—	—	—	—	—	—
C ₆ H ₅	*	*	*	*	*	—	118	*	*	99.3	98.8
C ₆ H ₅ CH ₂	*	*	*	—	—	—	97	65.2	—	—	71.4

Note: * Means a redundant entry. — Means not available.

Source: Reference 69.

Values of ΔH_r° for dissociation reactions can be combined to allow prediction of heats of reaction. A familiar example is the calculation of ΔH_r° for the reaction of chlorine with methane to produce HCl plus methyl chloride. Using Table 1.11 and the bond dissociation enthalpies of Cl_2 and HCl,⁷⁰ we can write the following reactions:



Summing these four equations and canceling the radicals that appear on both sides gives



Note that the calculation of ΔH_r° does not presume that the reaction takes place by a radical pathway. Rather, according to Hess' law, the difference in enthalpy between reactants and products is independent of the path of the reaction.⁴⁶

If a bond dissociation occurs so that one of the species becomes a cation and the other becomes an anion, then the energy of the reaction is termed a **standard heterolytic bond dissociation energy**:



Therefore,

$$DH(\text{A}^+, \text{B}^-) = \Delta H_{\text{het}}^\circ = \Delta H_f^\circ(\text{A}^+) + \Delta H_f^\circ(\text{B}^-) - \Delta H_f^\circ(\text{A-B}) \quad (1.22)$$

As will be discussed in Chapter 7, it is possible to relate homolytic and heterolytic reaction enthalpies by using data for ionization potential (the energy required to remove an electron from a species) and electron affinity (the energy gained by adding an electron to a species).⁷¹

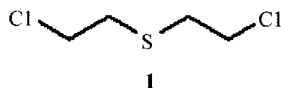
In the gas phase, heterolytic bond dissociation enthalpies are much higher than homolytic bond dissociation enthalpies because energy input is needed to separate the two ions as well as to break the bond. For example, the heterolytic bond dissociation energy of HCl in the gas phase is 333.4 kcal/mol, which is more than three times the 103.2 kcal/mol homolytic bond dissociation energy.⁷² Solvation of the ions can reduce the value of $\Delta H_{\text{het}}^\circ$ dramatically, however, and HCl readily ionizes in aqueous solution. Similarly, the calculated homolytic dissociation energy of a C-Cl bond in 2,2'-dichlorodiethyl sulfide (**1**) decreases only slightly from the gas phase to a solvent with $\epsilon = 5.9$, while the heterolytic dissociation energy of that bond decreases from

⁷⁰ Lide, D. R., Jr. *CRC Handbook of Chemistry and Physics*, 84th ed.; CRC Press: Boca Raton, FL, 2003, Section 9.

⁷¹ Arnett, E. M.; Flowers, R. A. II *Chem. Soc. Rev.* **1993**, 22, 9.

⁷² Berkowitz, J.; Ellison, G. B.; Gutman, D. J. *Phys. Chem.* **1994**, 98, 2744.

154.8 kcal/mol in the gas phase to 138.5 kcal/mol in the same solvent.^{73–75} Even carbon–carbon σ bonds can dissociate heterolytically. One hydrocarbon was reported to exist as a covalently bonded compound in benzene, as a mixture of molecules and ions in acetonitrile, and as an ionic species in dimethyl sulfoxide.⁷⁶



1.3 BONDING MODELS

The preceding discussion implicitly assumed the simple view of chemical bonding developed by G. N. Lewis.⁷⁷ Atoms are represented by element symbols with dots around them to indicate the number of electrons in the valence shell of the atom. Covalent bonds are formed by the sharing of one or more pairs of electrons between atoms so that both atoms achieve an electron configuration corresponding to a filled outer shell.⁷⁸ For example, combination of two chlorine atoms can produce a chlorine molecule, as shown in Figure 1.5.

This elementary description of bonding assumes some knowledge of electron shells of the atoms, but it does not presume a detailed knowledge of the results of quantum mechanics. The representation of Cl_2 does not specify what orbitals are populated, the geometric shapes of these orbitals, or the distribution of electrons in the final molecule of chlorine. This approach to describing chemical bonding might be adequate for some purposes, but it leaves many questions unanswered. In particular, this bonding description is purely qualitative. It would be desirable to have a mathematical description of bonding so that quantitative predictions about bonding can be compared with experimental observations.

It is helpful to distinguish here two types of information that we wish to acquire about organic molecules. The first type is physically *observable* data

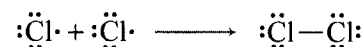


FIGURE 1.5

A representation of bonding in Cl_2 .

⁷³ Politzer, P.; Habibollahzadeh, D. J. *Phys. Chem.* **1994**, *98*, 1576.

⁷⁴ The effects of solvent are thought to be negligible when carbon-centered radicals are formed, but solvent effects can be significant in the case of oxygen-centered radicals. Borges dos Santos, R. M.; Cabral, B. J. C.; Martinho Simões, J. A. *Pure Appl. Chem.* **2007**, *79*, 1369.

⁷⁵ In one case merely adding ether to a pentane solution of a compound was seen to produce heterolytic dissociation: Arnett, E. M.; Amarnath, K.; Harvey, N. G.; Cheng, J.-P. *Science* **1990**, *247*, 423.

⁷⁶ Kitagawa, T.; Takeuchi, K. *J. Phys. Org. Chem.* **1998**, *11*, 157.

⁷⁷ The Lewis concept has been called “the most widely used model in contemporary chemistry.” Frenking, G.; Shaik, S. J. *Comput. Chem.* **2007**, *28*, 1.

⁷⁸ Lewis, G. N. *J. Am. Chem. Soc.* **1916**, *38*, 762. It is interesting to note that Lewis proposed a model for bonding in which electrons were positioned at the corners of a cube, so an octet meant an electron at every corner. Single bonds were constructed by allowing two cubes to share one edge (and thus one pair of electrons). In the case of a double bond, the two cubes shared a face (and therefore two pairs of electrons). The cubical model offered no simple representation for triple bonds, but a model based on tetrahedral arrangement of carbon valences was able to do so. For a discussion of the role of G. N. Lewis in the development of structural theory in organic chemistry, see Calvin, M. J. *Chem. Educ.* **1984**, *61*, 14; Zandler, M. E.; Talaty, E. R. J. *Chem. Educ.* **1984**, *61*, 124; Saltzman, M. D. J. *Chem. Educ.* **1984**, *61*, 119; Stranges, A. N. J. *Chem. Educ.* **1984**, *61*, 185; Pauling, L. J. *Chem. Educ.* **1984**, *61*, 201; Shaik, S. J. *Comput. Chem.* **2007**, *28*, 51.

that are characteristic of entire molecules or samples of molecules. A molecular dipole moment belongs to this category. The second kind of information includes those *nonobservable* constituent properties of a structure that, taken together, give rise to the overall molecular properties. Partial atomic charges and bond dipole moments belong to this category.

A dipole moment is a vector quantity that measures the separation of electrical charge. Dipole moments have units of electrical charge (a full plus or minus charge corresponding to 4.80×10^{-10} esu) times distance, and they are usually expressed in units of debye (D), with $1 \text{ D} = 10^{-18} \text{ esu cm}$.^{79,80} Thus, a system consisting of two atoms, one with a partial charge of $+0.1$ and the other a partial charge of -0.1 , located 1.5 \AA apart would have a dipole moment of

$$0.1 \times (4.8 \times 10^{-10} \text{ esu}) \times (1.5 \times 10^{-8} \text{ cm}) = 0.72 \times 10^{-18} \text{ esu} \cdot \text{cm} = 0.72 \text{ D} \quad (1.23)$$

Molecular dipole moments can be measured by several techniques, including the determination of the dielectric constant of a substance as a gas or in a nonpolar solution and the study of the effect of electrical fields on molecular spectra (Stark effect).

Molecular dipole moments are useful to us primarily as a source of information about molecular structure and bonding. While the center of charge need not coincide with the center of an atom, that is a convenient first approximation. For example, the dipole moment of CH_3F is 1.81 D .^{81,82} We associate the charge separation with the bonding between C and F. Since those atoms are 1.385 \AA apart (Table 1.1), the partial charge can be calculated to be $+0.27$ on one of the atoms and -0.27 on the other.

If there is more than one bond dipole moment in a molecule, then the molecular dipole moment is the vector sum of the individual moments. This idea can be useful in determining the structures and bonding of molecules. For example, Smyth determined that the three isomers of dichlorobenzene have dipole moments of 2.30 , 1.55 , and 0 D .⁸³ The dipole moment of chlorobenzene was known to be 1.61 D . Smyth reasoned that two C–Cl bond dipole moments add to each other in one isomer of dichlorobenzene, that they cancel each other partially in a second isomer, and that they cancel each other completely in the third isomer. Using the relationship

$$\mu = 2 \times 1.61 \times 10^{-18} \times \cos(0.5A) \quad (1.24)$$

where A is the angle between the two bond dipole moments, Smyth calculated that the three isomers of dichlorobenzene had A values of 89° , 122° , and 180° and that these values corresponded to the ortho, meta, and para isomers of dichlorobenzene, respectively. The expected angle for

⁷⁹ For background on the theory and measurement of dipole moments, see Minkin, V. I.; Osipov, O. A.; Zhdanov, Y. A. in Hazzard, B. J., trans. *Dipole Moments in Organic Chemistry*; Vaughan, W. E.; Plenum Press: New York, 1970.

⁸⁰ Smyth, C. P. in Weissberger, A.; Rossiter, B. W., Eds. *Physical Methods of Chemistry*, Vol. 1, Part IV; Wiley-Interscience: New York, 1972; pp. 397–429.

⁸¹ McClellan, A. L. *Tables of Experimental Dipole Moments*, Vol. 2; Raha Enterprises: El Cerrito, CA, 1974; p. 167.

⁸² A value of 1.857 D is given in reference 29b. That is a more recent value and may be more accurate than the number used here. The values for the other methyl fluorides there are very similar to those given in reference 81.

⁸³ Smyth, C. P.; Morgan, S. O. *J. Am. Chem. Soc.* **1927**, *49*, 1030.

o-dichlorobenzene is 60°, but Smyth argued that the apparent angle is larger because repulsion of the two adjacent chlorines enlarges the angle between the dipoles but does not appreciably alter the geometry of the benzene ring.⁸⁴

To account for the dipole moment associated with a covalent bond, we say that the electrons in the bond are not shared equally between the two atoms. One atom must have a greater ability to attract the pair of shared electrons than the other. As a result, a bond can be described as having a mixture of both ionic and covalent bonding. It is useful to define a weighting parameter, λ , to indicate how much ionic character is mixed into the covalent bond. Thus, we may write

$$\text{Polar Bond} = [\text{Covalent Bond}] + \lambda[\text{Ionic Bond}] \quad (1.25)$$

The percentage ionic character⁸⁵ in the bond is related to λ by equation 1.26:

$$\% \text{ Ionic Character} = \frac{\lambda^2}{(1 + \lambda^2)} \times 100 \% \quad (1.26)$$

In an HCl molecule with partial charges of +0.17 on the hydrogen atom and -0.17 on the chlorine atom, the value of λ is 0.45.

Electronegativity and Bond Polarity

The polarity of covalent bonds is attributed to **electronegativity**, which Pauling defined as “the power of an atom in a molecule to attract electrons to itself.”⁸⁶ It is generally the case that the bond dissociation energy of a polar diatomic molecule A–B is greater than one-half of the sum of the bond dissociation energies of A–A and B–B.⁸⁷ For example, the average of the bond strengths of H₂ and Cl₂ is 81.1 kcal/mol, but the homolytic dissociation energy of H–Cl is 103.2 kcal/mol.^{88,89} We ascribe the increased bond dissociation energy to the ionic character of the polar bond because the bond dissociation must overcome Coulombic effects in addition to the covalent bonding interaction. Pauling obtained a set of electronegativity values (χ_P) by correlating standard bond dissociation energies between different atoms (A–B) with the average of the standard bond dissociation energies of identical atoms (A–A and B–B) as shown in equation 1.27, where $\Delta\chi$ is the difference in χ values of A and B.⁸⁶ The electronegativity of fluorine was

⁸⁴ Not only did this study identify which isomer of dichlorobenzene was which, but it also reinforced the view that benzene is a planar molecule. Alternative structures, such as Baeyer, Körner, or Ladenburg benzene, would have given different molecular dipole moments.

⁸⁵ Coulson, C. A. *Valence*; Clarendon Press: Oxford, England, 1952; p. 128.

⁸⁶ Pauling, L. J. *Am. Chem. Soc.* **1932**, *54*, 3570.

⁸⁷ This idea was called the “postulate of the additivity of normal covalent bonds” by Pauling (reference 30).

⁸⁸ The premise that covalent bonds between atoms with different electronegativity values are stronger than the corresponding bonds between identical atoms is not always found to be true. Benson (reference 67) pointed out that the reaction of Hg₂ with Cl₂ to produce 2 HgCl, is endothermic by at least 10 kcal/mol.

⁸⁹ Reddy, R. R.; Rao, T. V. R.; Viswanath, R. *J. Am. Chem. Soc.* **1989**, *111*, 2914.

TABLE 1.12 Comparison of Electronegativity Values^a

Atom	χ_P	χ_M	χ_{spec}	χ_α	V_x
H	2.20	3.059	2.300	2.27	2.70
Li	0.91	1.282	0.912	0.94	0.75
Be	1.57	1.987	1.576	1.55	2.08
B	2.04	1.828	2.051	2.02	3.66
C	2.55	2.671	2.544	2.56	5.19
N	3.04	3.083	3.066	3.12	6.67
O	3.44	3.215	3.610	3.62	8.11
F	3.98	4.438	4.193	4.23	9.915
Na	0.93	1.212	0.869	0.95	0.65
Mg	1.31	1.630	1.293	1.32	1.54
Al	1.61	1.373	1.613	1.55	2.40
Si	1.90	2.033	1.916	1.87	3.41
P	2.19	2.394	2.253	2.22	4.55
S	2.58	2.651	2.589	2.49	5.77
Cl	3.16	3.535	2.869	2.82	7.04
K	0.82	1.032	0.734	0.84	0.51
Ca	1.00	1.303	1.034	1.11	1.15
Br	2.96	3.236	2.685	2.56	6.13
I	2.66	2.880	2.359	2.27	5.25

^a Values for χ_P , χ_M , and χ_{spec} are taken from the compilation of Allen (reference 95). Values for χ_α are taken from reference 94. Values of V_x are from reference 100.

arbitrarily set to 4.0, and the electronegativities of other atoms were then determined (Table 1.12).

$$D_{A-B} = \sqrt{D_{A-A}D_{B-B}} + 30 (\Delta\chi)^2 \quad (1.27)$$

On the one hand, the concept of electronegativity has been called “perhaps the most popular intuitive concept in chemistry.”⁹⁰ On the other hand, it is difficult to determine precise values for electronegativity because a set of electronegativity values amounts to “a chemical pattern recognition scheme which is not amenable to direct physical measurement.”⁹¹ Therefore, a great variety of other approaches have been taken in describing and quantifying electronegativity.

The Pauling electronegativity scale is inherently dependent on measurements made on molecules, but there have been many attempts to define electronegativity as an atomic property. Sanderson’s definition of electronegativity as “the effectiveness of the nuclear charge as sensed within an outer orbital vacancy” of an atom suggests that some atomic properties should be related to electronegativity.⁹² Mulliken introduced an electronegativity scale (χ_M) based on the average of the ionization potential (I) and electron affinity (A) of atoms; that is, $\chi = (I + A)/2$.⁹³ (A greater electron affinity means a greater attraction of an atom for an electron from outside the atom; a greater

⁹⁰ Sen, K. D. in the Editor’s Note to reference 97.

⁹¹ Allen, L. C.; Egnolf, D. A.; Knight, E. T.; Liang, C. J. *Phys. Chem.* **1990**, *94*, 5602 (quotation from p. 5605).

⁹² Sanderson, R. T. J. *Chem. Educ.* **1988**, *65*, 112, 227. See also Pauling, L. J. *Chem. Educ.* **1988**, *65*, 375.

⁹³ Mulliken, R. S. *J. Chem. Phys.* **1934**, *2*, 782; **1935**, *3*, 573.

ionization potential means a greater affinity of an atom for a nonbonded electron localized on the atom.) Nagle introduced an electronegativity value based on atomic polarizability.⁹⁴ Allen proposed electronegativity values based on the average ionization potential of all of the *p* and *s* electrons on an atom.⁹⁵⁻⁹⁷ Domenicano and co-workers developed a set of group electronegativities based on the effect of a substituent on a benzene ring.⁹⁸ Building on a suggestion of Yuan,⁹⁹ Benson proposed another measure of electronegativity, V_x , which is calculated by dividing the number of valence electrons about an atom by its covalent radius.¹⁰⁰ Thus, seven electrons in the valence shell of a fluorine atom, divided by 0.706 Å, gives a V_x value of 9.915 for fluorine. Values of V_x correlate well with a number of physical properties.¹⁰⁰

Table 1.12 compares the electronegativity values reported by Pauling (χ_P), Mulliken (χ_M), Allen (χ_{spec}), Nagle (χ_α), and Benson (V_x).¹⁰¹ The Pauling, Allen, and Nagle values are usually quite similar, suggesting that the properties of atoms in molecules may indeed be related to the properties of isolated atoms. However, while the Mulliken values are similar to the other values, there are some differences, particularly for hydrogen. The Benson values are likewise larger in magnitude, but (except for hydrogen) they generally correlate well with the Pauling values.

Theoretical studies have offered additional perspectives on electronegativity. Parr and co-workers¹⁰² defined a quantity, μ , as the “electronic chemical potential,” which measures “the escaping tendency” of the electrons in the system.¹⁰³ The value of μ is approximately the same as $(I + A)/2$, the Mulliken electronegativity, so the value χ_M has been termed *absolute* electronegativity.¹⁰³ Closely related to the concept of electronegativity is the concept of **chemical potential**, which is also given the symbol μ and which is defined as $\partial E/\partial N$, where E is the energy of the system and N is the number of

⁹⁴ Nagle, J. K. *J. Am. Chem. Soc.* **1990**, *112*, 4741.

⁹⁵ Allen, L. C. *J. Am. Chem. Soc.* **1989**, *111*, 9003. Allen called this definition of electronegativity “the third dimension of the periodic table.” For a summary, see Borman, S. A. *Chem. Eng. News* **1990** (Jan 1), 18. Also see Politzer, P.; Murray, J. S.; Grice, M. E. *Collect. Czech. Chem. Commun.* **2005**, *70*, 550; Murphy, L. R.; Meek, T. L.; Allred, A. L.; Allen, L. C. *J. Phys. Chem. A* **2000**, *104*, 5867.

⁹⁶ For other treatments of electronegativity, see Boyd, R. J.; Edgecombe, K. E. *J. Am. Chem. Soc.* **1988**, *110*, 4182; Bratsch, S. G. *J. Chem. Educ.* **1988**, *65*, 223; Li, K.; Wang, X.; Xue, D. *J. Phys. Chem. A* **2008**, *112*, 7894.

⁹⁷ For a summary of these electronegativity scales, see Mullay, J. in Sen, K. D.; Jorgensen, C. K., Eds. *Electronegativity*; Springer-Verlag: Berlin, 1987.

⁹⁸ Campanelli, A. R.; Domenicano, A.; Ramondo, F.; Hargittai, I. *J. Phys. Chem. A* **2004**, *108*, 4940.

⁹⁹ Yuan, H. C. *Acta Chim. Sin.* **1964**, *30*, 341; cf. reference 100; *Chem. Abstr.* **1965**, *62*, 2253h.

¹⁰⁰ Luo, Y.-R.; Benson, S. W. *J. Phys. Chem.* **1988**, *92*, 5255; *J. Am. Chem. Soc.* **1989**, *111*, 2480; *J. Phys. Chem.* **1989**, *93*, 3304. See also Luo, Y.-R.; Pacey, P. D. *J. Am. Chem. Soc.* **1991**, *113*, 1465 and references therein; Luo, Y.-R.; Benson, S. W. *Acc. Chem. Res.* **1992**, *25*, 375.

¹⁰¹ Table 1.12 lists χ values for atoms only, but it is also possible to calculate “group electronegativities” to take into account the net effect of a group of atoms. For a tabulation of group electronegativities calculated by a variety of methods, see Bratsch, S. G. *J. Chem. Educ.* **1985**, *62*, 101. As an example, the group electronegativity of the CH₃ group is about 2.3, while that for CF₃ is about 3.5.

¹⁰² Parr, R. G.; Donnelly, R. A.; Levy, M.; Palke, W. E. *J. Chem. Phys.* **1978**, *68*, 3801.

¹⁰³ Pearson, R. G. *Acc. Chem. Res.* **1990**, *23*, 1.

electrons.^{104–106} Parr and co-workers defined

$$\chi = -\mu = -\delta E/\delta\rho \quad (1.28)$$

where the energy is related to a theoretical treatment of electron density.¹⁰⁷

As a result of the many theoretical treatments, chemists now find themselves using one term to mean different things, since “the electronic chemical potential, μ , . . . is an entirely different chemical quantity” from the concept of electronegativity as the origin of bond polarity.¹⁰⁶ As Pearson noted:

The fact that there are two different measures both called (electronegativity) scales creates considerable opportunity for confusion and misunderstanding. Since the applications are so different, it is not a meaningful question to ask which scale is more correct. Each scale is more correct in its own area of use.¹⁰³

Usually we will use the term *electronegativity* in the sense originally proposed by Pauling, but we must recognize the alternative meanings in the literature. Moreover, we see that a simple idea that is intuitively useful in understanding some problems of structure and bonding (e.g., dipole moments) may become more difficult to use as we attempt to make it more precise. The next section will further illustrate this theme.

Complementary Theoretical Models of Bonding

The Lewis model for forming a chemical bond by sharing an electron pair leads to a theoretical description of bonding known as **valence bond theory (VB theory)**.¹⁰⁸ The key to VB theory is that we consider a structure to be formed by bringing together complete atoms and then allowing them to interact to form bonds. In **molecular orbital theory (MO theory)**, on the other hand, we consider molecules to be constructed by bringing together nuclei (or nuclei and filled inner shells) and then placing electrons in orbitals calculated for the entire array of nuclei.⁸⁵ Therefore, MO theory does not generate discrete chemical bonds. Rather, it generates a set of orbitals that allow electrons to roam over many nuclei, perhaps an entire molecule, so it does not restrict them to any particular pair of nuclei.

Both VB and MO theories utilize mathematical expressions that can rapidly become complex, even for simple organic molecules. Moreover, VB theory and MO theory are usually described with different symbols, so it can be difficult to distinguish the similarities among and differences between them. Therefore, it may be useful to consider first a very simple bonding problem, the formation of a hydrogen molecule from two hydrogen atoms. The principles will be the same as for larger molecules, but the comparison of the two approaches will be more apparent in the case of H₂.

The discussion that follows has been adapted from several introductory texts on bonding, which may be consulted for more

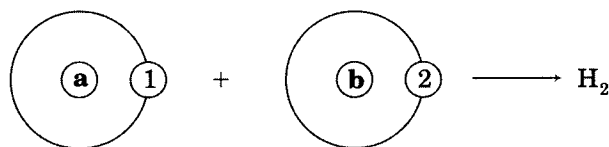
¹⁰⁴ Pritchard, H. O.; Sumner, F. H. *Proc. R. Soc. (London)* **1956**, A235, 136.

¹⁰⁵ Iczkowski, R. P.; Margrave, J. L. *J. Am. Chem. Soc.* **1961**, 83, 3547.

¹⁰⁶ Allen, L. C. *Acc. Chem. Res.* **1990**, 23, 175.

¹⁰⁷ Here ρ is actually a functional, and the approach is known as density functional theory. For an introduction, see (a) Parr, R. G.; Yang, W. *Density-Functional Theory of Atoms and Molecules*; Oxford University Press: New York, 1989; (b) March, N. H. *Electron Density Theory of Atoms and Molecules*; Academic Press: New York, 1991.

¹⁰⁸ A summary of the development of VB theory and a discussion of the merits of VB and MO theories was given by Klein, D. J.; Trinajstić, N. *J. Chem. Educ.* **1990**, 67, 633.

**FIGURE 1.6**

Formation of a hydrogen molecule from two hydrogen atoms.

details.¹⁰⁹ We begin with two isolated hydrogen atoms, as shown in Figure 1.6. Each atom has one electron in a 1s orbital. We can write a wave equation for the 1s orbital, since the hydrogen atom can be solved exactly in quantum mechanics. Electron 1 is initially associated with hydrogen nucleus a , and electron 2 is associated with hydrogen nucleus b . Bringing the two atoms together allows bonding to occur, as shown in Figure 1.6.

Now we want to write a wave equation that will mathematically describe the electron distribution in the hydrogen molecule. The valence bond method initially used by Heitler and London described one possible wave function as¹¹⁰

$$\Psi_1 = ca(1)b(2) \quad (1.29)$$

in which c is a constant, $a(1)$ is the wave function for electron 1 in a 1s orbital on hydrogen nucleus a , and $b(2)$ is the wave function for electron 2 in a 1s orbital on hydrogen nucleus b . Since the electrons are indistinguishable, it should be equally acceptable to write

$$\Psi_2 = ca(2)b(1) \quad (1.30)$$

Both descriptions are possible, so both need to be included in the wave function for the molecule. Therefore, Heitler and London wrote that

$$\Psi_{\text{VB}} = ca(1)b(2) + ca(2)b(1) \quad (1.31)$$

In this case the constants are chosen so that the overall wave function is properly normalized and made antisymmetric with respect to spin.

The molecular orbital approach to describing hydrogen also starts with two hydrogen nuclei (a and b) and two electrons (1 and 2), but we make no initial assumption about the location of the two electrons.¹⁰⁹ We solve (at least in principle) the Schrödinger equation for the molecular orbitals around the pair of nuclei, and we then write a wave equation for one electron in a resulting MO:

$$\Psi_1 = c_1a(1) + c_2b(1) \quad (1.32)$$

Note that electron 1 is associated with both nuclei. Similarly,

$$\Psi_2 = c_1a(2) + c_2b(2) \quad (1.33)$$

The combined MO wave function, then, is the product of the two one-electron wave functions:

$$\Psi_{\text{MO}} = \Psi_1 \Psi_2 = c_1^2a(1)a(2) + c_2^2b(1)b(2) + c_1c_2[a(1)b(2) + a(2)b(1)] \quad (1.34)$$

¹⁰⁹ For examples, see reference 9, p. 517 ff; Eyring, H.; Walter, J.; Kimball, G. E. *Quantum Chemistry*; John Wiley & Sons: New York, 1944; p. 212 ff. The mathematics is described in some detail in Slater, J. C. *Quantum Theory of Molecules and Solids, Vol. I. Electronic Structure of Molecules*; McGraw-Hill: New York, 1963.

¹¹⁰ Heitler, W.; London, F. Z. *Physik* **1927**, *44*, 455.

We see that Ψ_{MO} is more complex than Ψ_{VB} , and that, in fact, Ψ_{VB} is incorporated into Ψ_{MO} . Specifically, the third term of Ψ_{MO} is the same as Ψ_{VB} if the constants are made the same. What is the physical significance of the differences in Ψ_{VB} and Ψ_{MO} ? Ψ_{MO} includes two terms that Ψ_{VB} does not: $a(1)a(2)$ and $b(1)b(2)$. Each of these terms represents a **configuration** (arrangement of electrons in orbitals) in which *both* electrons are formally localized in what had been a 1s orbital on *one* of the hydrogen atoms. Therefore, these terms describe ionic structures. In other words, $a(1)a(2)$ represents a^-b^+ , and $b(1)b(2)$ represents a^+b^- . We now see that the MO treatment appears to give large weight to terms that represent electronic configurations in which both electrons are on one nucleus, while the VB treatment ignores these terms.

Which approach is correct? Usually our measure of the “correctness” of any calculation is how accurately it reproduces a known physical property. In the case of H_2 , a relevant property is the homolytic bond dissociation energy. The simple VB calculation described here gives a value of 3.14 eV (72.4 kcal/mol) for H_2 dissociation.¹⁰⁹ The simple MO calculation gives a value of 2.70 eV (62.3 kcal/mol). The experimental value is 4.75 eV (109.5 kcal/mol).¹⁰⁹ Obviously, neither calculation is correct unless one takes order of magnitude agreement as satisfactory; in that case, both calculations are correct.

It may seem reasonable that the MO method gives a result that underestimates the bond dissociation energy because the wave equation includes patterns of electron density that resemble ionic species such as a^+b^- . But why is the VB result also in error? The answer seems to be that, while the MO approach places too much emphasis on these ionic electron distributions, the VB approach underutilizes them. A strong bond apparently requires that both electrons spend a lot of time in the region of space between the two protons. Doing so must make it more likely that the two electrons will, at some instant, be on the same atom.¹¹¹ Thus, we might improve the accuracy of the VB calculation if we add some terms that keep the electrons closer together between the nuclei.

Similarly, we could improve the MO calculation by adding some terms that would decrease the ionic character of the bonding orbital. If we include a description of the hydrogen atoms in which the electron in each case has some probability of being in an orbital higher than the 1s orbital, then excessively repulsive interactions will become less significant in the final molecular orbital.¹¹² There are other changes we can make as well. Table 1.13 shows how the calculated stability of H_2 varies according to the complexity of the MO calculation.^{113,114} Including 13 terms makes a major improvement. From that point on almost any change decreases the stability of the calculated structure almost as much as it increases it, but small gains can be won. An MO

¹¹¹ Colloquial terminology is used here to be consistent with the level of presentation of the theory.

¹¹² This procedure is called *configuration interaction*; cf. Coffey, P.; Jug, K. *J. Chem. Educ.* **1974**, *51*, 252. See also Coulson, C. A.; Fischer, I. *Philos. Mag.* **1949**, *40*, 386.

¹¹³ (a) Data from McWeeny, R. *Coulson's Valence*, 3rd ed.; Oxford University Press: Oxford, England, 1979; p. 120 and references therein. (b) See also Davis, J. C., Jr. *Advanced Physical Chemistry*; Ronald Press: New York, 1965; p. 426.

¹¹⁴ For additional references, see King, G. W. *Spectroscopy and Molecular Structure*; Holt, Rinehart and Winston: New York, 1964; p. 149.

TABLE 1.13 Calculated Values for H₂ Stability

Calculation Method	DE (calc.)
Simple valence bond theory	3.14 eV
Simple molecular orbital theory	2.70 eV
James–Cooledge (13 parameters)	4.72 eV
Kolos–Wolniewicz (100 terms)	4.7467 eV
Experimental value	4.7467 eV

Source: Reference 113.

equation with 50 terms does quite well. Similarly, a VB calculation with a large number of terms can also produce an answer that is within experimental error of the measured value. If enough terms are included, therefore, the two methods can produce equivalent results.^{85,115}

There are several conclusions to be drawn from this analysis:

1. Neither *simple* VB theory nor *simple* MO theory produces a value for the dissociation energy (DE) that is very close to the experimental value.
2. Both VB and MO theories can be modified to produce more accurate results. Even for a simple molecule such as H₂, however, many terms may be required to produce an acceptable value for the property of interest.

More important for our purposes here are the following conclusions:

3. As both simple VB theory and simple MO theory are modified to give a more accurate result, they must necessarily produce more nearly equivalent results. In that sense they must become more like each other, and the modifications may make their theoretical bases more nearly equivalent as well.
4. Both simple VB theory and simple MO theory should be regarded only as *approaches* for the calculation of molecular properties, not as final answers. They should be viewed as complementary initial models for computational chemistry, not as depictions of reality.

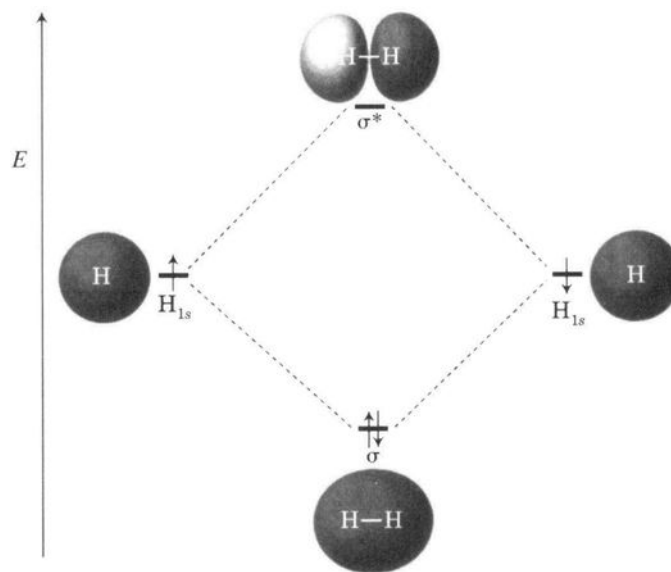
This last point was emphasized by Shaik and Hiberty:

A modern chemist should know that there are two ways of describing electronic structure. . . [that are] not two contrasting theories, but rather two representations or two guises of the same reality. Their capabilities and insights into chemical problems are complementary. . .¹¹⁶

Why then don't we just talk about high level theoretical calculations and ignore the simple theories? The elementary theories are useful to us because they provide good conceptual models for the computational process. We can visualize the interactions represented by equation 1.34, as well as the physical situation suggested by equation 1.31. It is much more difficult for us to envision the interactions involved in a 50- or 100-term wave function, however. As the accuracy of the model is increased, its simplicity is decreased.

¹¹⁵ Kolos, W.; Wolniewicz, L. *J. Chem. Phys.* **1968**, *49*, 404.

¹¹⁶ Shaik, S.; Hiberty, P. C. *Helv. Chim. Acta* **2003**, *86*, 1063.

**FIGURE 1.7**

Combination of atomic hydrogen orbitals to produce molecular hydrogen.

We must choose the model that is sufficiently accurate for our computational purposes, yet still simple enough that we have some understanding of what the model describes. Otherwise the model is a black box, and we have no understanding of what it does. Perhaps we do not even know whether the answers it produces are physically reasonable.

Pictorial Representations of Bonding Concepts

The MO and VB methods described above illustrate the use of mathematical models in chemistry. Chemists often use other, nonmathematical models to depict the results of calculations in schematic or pictorial form. Continuing the example of H_2 , we represent the combination of two atomic hydrogen $1s$ orbitals to make two new molecular orbitals, the familiar σ and σ^* orbitals (Figure 1.7). The vertical arrow on the left in Figure 1.7 indicates that the σ and σ^* orbitals differ in energy, the σ MO being lower in energy than the original hydrogen $1s$ orbitals, and the σ^* orbital being higher in energy.¹¹⁷ The σ orbital is a bonding orbital, and population of the σ MO with two electrons produces a stable H_2 molecule. On the other hand, σ^* is an antibonding orbital, and population of this orbital with an electron destabilizes the molecule.

Let us apply this pictorial representation of bonding to one of the fundamental concepts in organic chemistry—the bonding of methane. We usually begin with the atomic orbitals of the carbon atom and then consider

¹¹⁷ This figure is somewhat stylized, since it shows the σ and σ^* orbitals symmetrically displaced above and below the energy of the initial hydrogen $1s$ orbitals. In fact, the σ^* should be more antibonding than the σ orbital is bonding. For details, see Albright, T. A.; Burdett, J. K.; Whangbo, M.-H. *Orbital Interactions in Chemistry*; Wiley-Interscience: New York, 1985; p. 12 ff. In addition, Willis, C. J. *J. Chem. Educ.* **1988**, *65*, 418 calculated that the H–H bond energy is only about 19% of the energy gained by moving two electrons from hydrogen $1s$ orbitals to the H_2 σ bonding orbital. The other 81% of that energy is consumed in offsetting electrical repulsion within the molecule.

the four hydrogen atoms. We represent the energies of the orbitals of atomic carbon as shown in Figure 1.8. Each horizontal line represents the energy associated with a particular atomic wave function calculated from quantum mechanics. The small arrows represent electrons, and the direction of each arrow indicates the spin quantum number of the electron it represents. We know that we may put no more than two arrows on each horizontal line (i.e., two electrons in the same atomic orbital), and then only if the arrows point in opposite directions (meaning that the two electrons have paired spins).

If we combine the energy level diagram for carbon with the bonding model shown schematically in Figure 1.7, we can construct a representation of a one-carbon hydrocarbon in which each unpaired electron in a $2p$ orbital on carbon is paired with an electron from a hydrogen atom to form a C–H bond (Figure 1.9). While this result is the logical extension of the bonding model illustrated in Figure 1.8, it clearly is not correct. There is abundant experimental data indicating that methane has the molecular formula CH_4 , not CH_2 .

The sp^3 Hybridization Model for Methane

Once a model is fixed in our minds, we find it almost impossible to discard or ignore it unless another model is available to take its place. Instead, models are almost always modified to fit new data—and that is what we do here. We use the concept of **hybridization** to change our mental picture of the atomic orbitals of carbon to a more useful one. The procedure was described by Pauling and has been discussed by a number of authors.^{118–121}

Beginning with the unhybridized carbon orbitals in Figure 1.10(a), we promote an electron from a $2s$ orbital to a $2p$ orbital, as shown in Figure 1.10(b). Then we combine the s and p orbitals to produce four sp^3 hybrid orbitals that are equal in energy, as shown in Figure 1.10(c).^{122–124} Promotion of the electron requires about 96 kcal/mol, but this is more than offset by the additional stabilization (about 200 kcal/mol) gained by forming two additional C–H bonds.¹²⁵ The wave functions of the hybrid orbitals (where C_{2s} represents the wave function for a $2s$ orbital on carbon, etc.) are shown in equations 1.35–1.38.¹²⁶

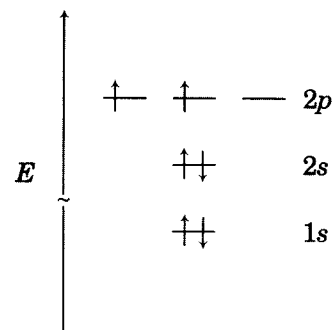


FIGURE 1.8

Energy levels of atomic carbon orbitals.

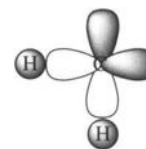


FIGURE 1.9

A bonding model of “methane” as CH_2 .

¹¹⁸ (a) Pauling, L. *J. Am. Chem. Soc.* **1931**, 53, 1367; reference 30, p. 118; (b) See also Slater, J. C. *Phys. Rev.* **1931**, 37, 481.

¹¹⁹ Compare Hsu, C.-Y.; Orchin, M. *J. Chem. Educ.* **1973**, 50, 114.

¹²⁰ Root, D. M.; Landis, C. R.; Cleveland, T. J. *Am. Chem. Soc.* **1993**, 115, 4201.

¹²¹ For a reconsideration of the concept of hybridization, see Magnusson, E. J. *Am. Chem. Soc.* **1984**, 106, 1177.

¹²² Matteson, D. S. *Organometallic Reaction Mechanisms of the Nontransition Elements*; Academic Press: New York, 1974; p. 5.

¹²³ Ogilvie, J. F. *J. Chem. Educ.* **1990**, 67, 280.

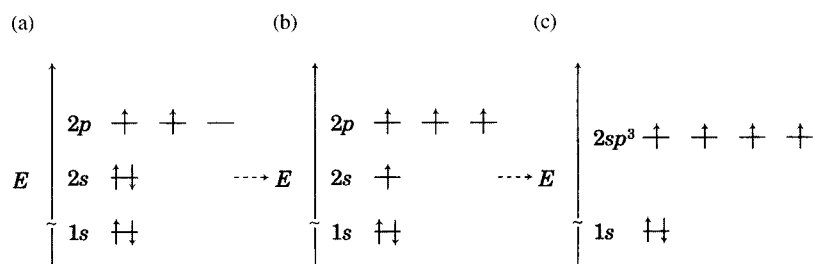
¹²⁴ Strictly speaking, there are hybridized *orbitals* but not hybridized *atoms*. However, organic chemists frequently use the term “ sp^3 -hybridized carbon” to refer to a carbon atom with sp^3 hybrid orbitals.

¹²⁵ See the discussion in Hameka, H. F. *Quantum Theory of the Chemical Bond*; Hafner Press: New York, 1975; p. 216 ff.

¹²⁶ Bennett, W. A. *J. Chem. Educ.* **1969**, 46, 746.

FIGURE 1.10

Hybridization of carbon orbitals to produce sp^3 hybridized orbitals.



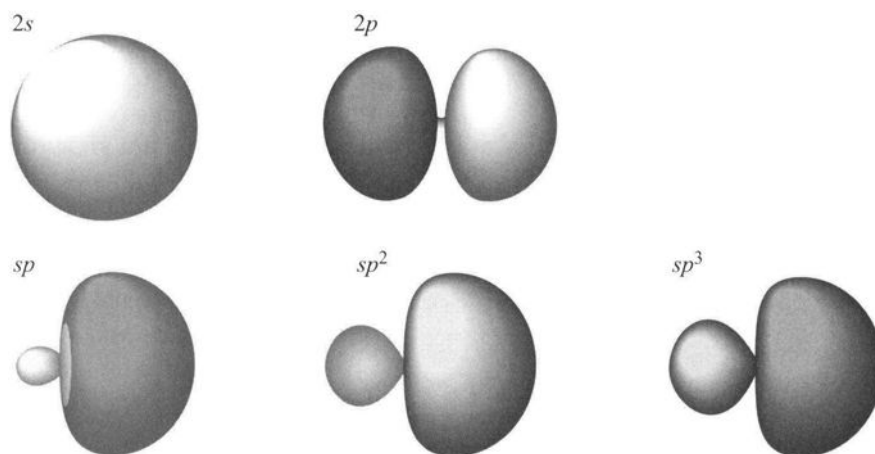
$$\phi_{sp^3_{(1)}} = \frac{1}{2}(C_{2s} + C_{2p_x} + C_{2p_y} + C_{2p_z}) \quad (1.35)$$

$$\phi_{sp^3_{(2)}} = \frac{1}{2}(C_{2s} + C_{2p_x} - C_{2p_y} - C_{2p_z}) \quad (1.36)$$

$$\phi_{sp^3_{(3)}} = \frac{1}{2}(C_{2s} - C_{2p_x} + C_{2p_y} - C_{2p_z}) \quad (1.37)$$

$$\phi_{sp^3_{(4)}} = \frac{1}{2}(C_{2s} - C_{2p_x} - C_{2p_y} + C_{2p_z}) \quad (1.38)$$

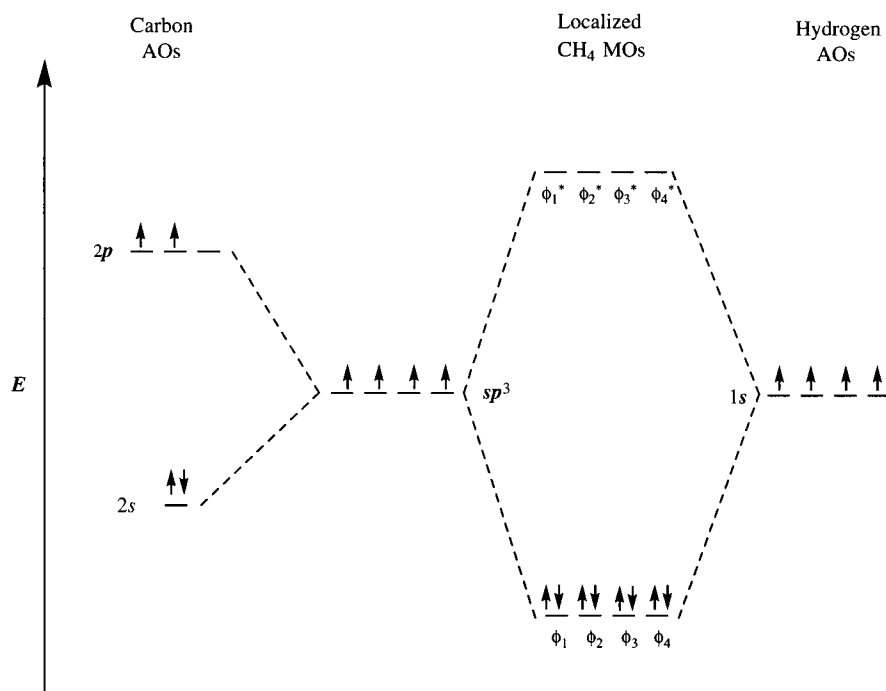
Figure 1.11 shows the contours of one of the sp^3 orbitals as well as those of carbon 2s, 2p, sp , and sp^2 hybrids.¹²⁷ Each of the sp^3 orbitals in equations 1.35–1.38 has a large lobe and a small lobe. The two lobes have a different mathematical sign, and the four large lobes point toward the corners of a regular tetrahedron.¹²⁸ Now we can describe methane as CH_4 by combining each of the four carbon sp^3 hybrid orbitals with a 1s orbital on hydrogen. A qualitative energy diagram for the process is shown in Figure 1.12. The four

**FIGURE 1.11**

Sizes and shapes of carbon atomic and hybrid orbitals.

¹²⁷ The orbital contours were generated with CAChe™ visualization software.

¹²⁸ The shapes of these orbitals are quite different from the representations shown in many chemistry textbooks. Compare Allendoerfer, R. D. J. *Chem. Educ.* **1990**, 67, 37.

**FIGURE 1.12**

Mixing of hydrogen 1s and carbon sp^3 orbitals to make localized MOs of methane. (Adapted from reference 138.)

sp^3 hybrid orbitals point to the corners of a tetrahedron, which is consistent with CH_4 having tetrahedral geometry (Figure 1.13).^{29,129}

It is important to note in this discussion that we hybridize the atomic orbitals to produce a different model. As Ogilvie noted,

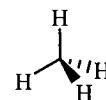
According to *Coulson's Valence*, "hybridization is not a physical effect but merely a feature of [a] theoretical description". . . . Despite the fact that many authors of textbooks of general chemistry have written that CH_4 has a tetrahedral structure because of sp^3 hybridization, there neither exists now, nor has ever existed, any quantitative experimental or theoretical justification of such a statement.^{123,130}

In addition, Matteson noted that

Hybridization is not something that atoms do or have done to them. It is purely a mental process gone through by the chemist, who wants to group atomic orbitals according to their symmetry properties so he can talk about one localized bond and ignore the rest. Hybridization does not change the shape of the electron distribution in any atom.¹²²

Are There sp^3 Hybrid Orbitals in Methane?

The hybridization concept is so ingrained in organic chemistry that we often use the concepts of sp^3 hybridization and tetrahedral geometry interchangeably.¹²⁰ We will now discuss one important experimental technique that will cause us to rethink what we have said about methane. The technique



$$l_{\text{C-H}} = 1.091 \text{ \AA}$$

FIGURE 1.13

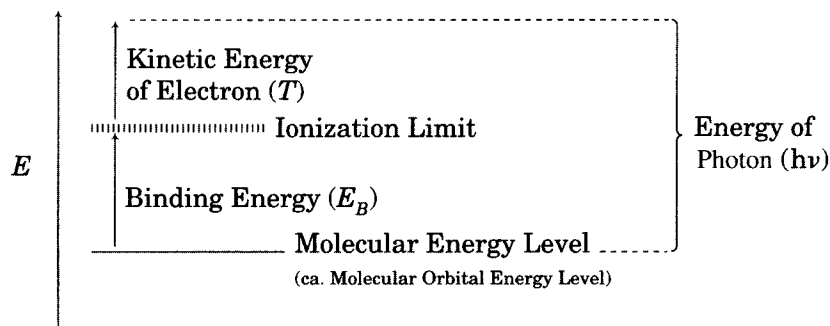
Experimental geometry of methane.

¹²⁹ We usually write the bond angle as 109.5° . Mathematically, it is $109^\circ 28'$, which corresponds to 109.47° . A method for the calculation of sp , sp^2 , and sp^3 interorbital angles was given by Duffey, G. H. *J. Chem. Educ.* **1992**, *69*, 171.

¹³⁰ For a rebuttal of this view, see Pauling, L. *J. Chem. Educ.* **1992**, *69*, 519.

FIGURE 1.14

Energy relationships in photoelectron spectroscopy.



is **photoelectron spectroscopy** (PES), which is used to probe the energy levels that electrons occupy within molecules.^{131,132} The essence of PES is the measurement of the energies of electrons that have been ejected from molecules or atoms by high energy photons (light). As shown in Figure 1.14, the difference between the energies of the electrons (energy out) and the energy of the photons causing the displacement (energy in) is taken to be a measure of the binding energy holding the electrons in the molecule or atom. The higher the energy level from which an electron is removed, the less is its binding energy, and the greater will be its kinetic energy. This relationship is shown in equation 1.39, where $h\nu$ is the energy of the photon, T is the kinetic energy of the electron ejected from the molecule, and E_B is the binding energy of the electron in the molecule. Based on Koopmans' theorem, we associate the number and position of binding energy levels in a structure with the energies of its atomic or molecular orbitals.¹³³

$$h\nu = T + E_B \quad (1.39)$$

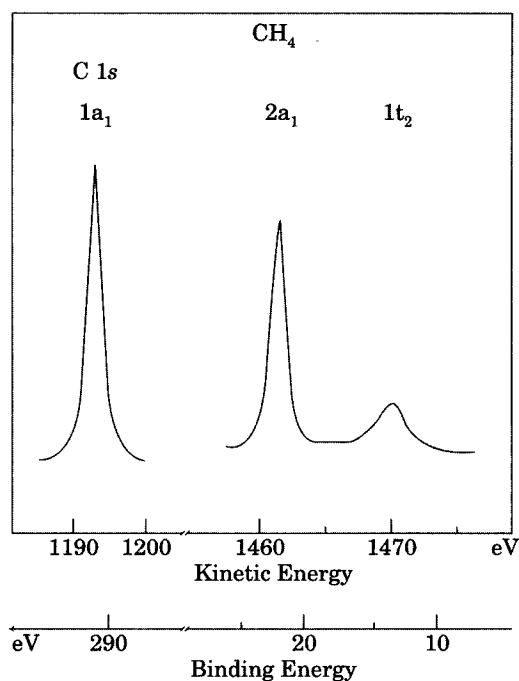
Figure 1.15 shows a PES spectrum of methane.¹³⁴ One peak at very high binding energy (>290 eV) is characteristic of molecules with electrons in carbon $1s$ orbitals. However, there are two peaks at lower energy: one at 23.0 eV and one at 12.7 eV. Therefore, we are led to the conclusion that the electrons in methane are in three different energy levels, one energy level corresponding to the carbon $1s$ electrons, and two different energy levels corresponding to the other electrons in the molecule. It is somewhat difficult to reconcile this experimental result with an intuitive bonding model in which methane is constructed of four equivalent $C(sp^3)-H(1s)$ bonds produced by overlap of four equivalent sp^3 hybrid orbitals on a carbon atom with four hydrogen $1s$ orbitals (Figure 1.12).

¹³¹ A related procedure is called electron spectroscopy for chemical analysis (ESCA). For a discussion of PES, ESCA, and similar techniques, see Baker, A. D.; Brundle, C. R.; Thompson, M. *Chem. Soc. Rev.* **1972**, *1*, 355; Baker, A. D. *Acc. Chem. Res.* **1970**, *3*, 17. Another technique, Auger spectroscopy, is discussed in reference 133.

¹³² Bock, H.; Mollère, P. D. *J. Chem. Educ.* **1974**, *51*, 506; Baker, A. D. *Acc. Chem. Res.* **1970**, *3*, 17; Ballard, R. E. *Photoelectron Spectroscopy and Molecular Orbital Theory*; John Wiley & Sons: New York, 1978.

¹³³ For a discussion of the application of Koopmans' theorem in PES, see Albridge, R. G. in Weissberger, A.; Rossiter, B. W., Eds. *Physical Methods of Chemistry*, Vol. I, Part IIID; Wiley-Interscience: New York, 1972; p. 307.

¹³⁴ Hamrin, K.; Johansson, G.; Gelius, U.; Fahlman, A.; Nordling, C.; Siegbahn, K. *Chem. Phys. Lett.* **1968**, *1*, 613.

**FIGURE 1.15**

PES spectrum of methane.
(Adapted from reference 134.)

One important aspect of MO theory—the concept of **symmetry-correct molecular orbitals**—not only makes it possible to explain this experimental result but, in fact, requires it. A fundamental property of molecular orbitals is that they have the full symmetry of the basis set of atomic orbitals used to generate the molecular orbitals.¹³⁵ This means that the molecular orbitals must be either symmetric or antisymmetric with respect to the symmetry operations provided for by the symmetry group of the atomic orbitals.¹³⁶ If we consider each C–H σ bond formed by overlap of an sp^3 orbital on a carbon atom with a 1s orbital on a hydrogen atom to be an MO, then clearly each of these MOs lacks the full symmetry of the basis set of s and p atomic orbitals.

There are two ways to correct our treatment of methane by inclusion of symmetry-correct MOs. The first approach is to consider the descriptions of C–H bonds to be **localized molecular orbitals (LMOs)**—that is, molecular orbitals that have electron density on only a portion of a molecule. We can then consider these LMOs to be the basis set of orbitals for a new MO calculation to determine the symmetry-correct, **delocalized MOs** for the

¹³⁵ The term *basis set* refers to the set of atomic orbitals used to construct the molecular orbitals.

¹³⁶ The terms *symmetric* and *antisymmetric* mean that the result of any symmetry operation will be an orbital of the same type and in the same location as before the transformation. If the orbital is symmetric with respect to that transformation, then the orbital produced will also have + and – lobes in the same locations as before; if the orbital is antisymmetric, then the resulting orbital will have + lobes where – lobes were, and vice versa. All MOs must be either symmetric or antisymmetric. If a symmetry operation that corresponds to an element of symmetry of the basis set of atomic orbitals transforms a lobe to a position in space in which there was not a lobe beforehand, that MO is said to be **asymmetric** (without symmetry) and is not allowable as a symmetry-correct MO for the molecule. These topics will be discussed in more detail in Chapters 4 and 11.

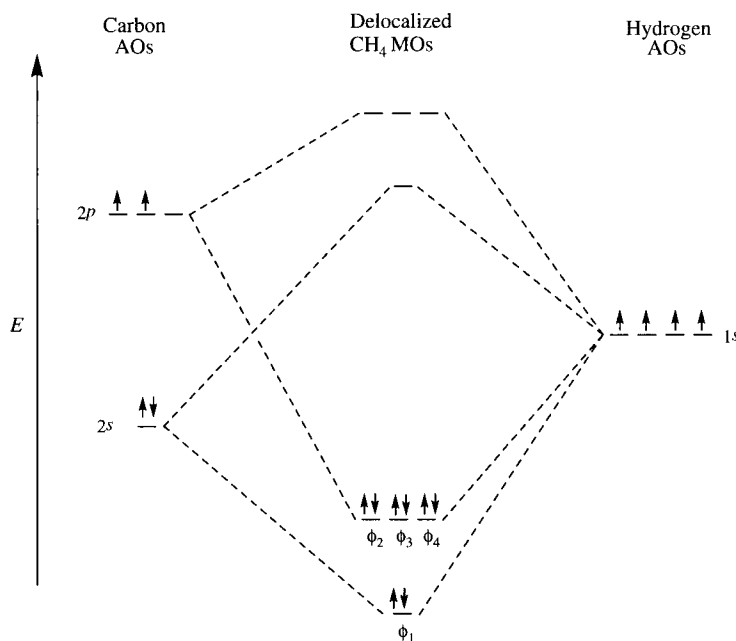


FIGURE 1.16

Mixing of atomic orbitals on carbon with hydrogen 1s orbitals to make molecular orbitals of methane. (Adapted from reference 138.)

molecule.^{126,137–139} The second, more direct approach is to calculate delocalized methane molecular orbitals directly from the unhybridized orbitals: a carbon 2s orbital, three carbon 2p orbitals, and four hydrogen 1s orbitals. Both procedures produce four delocalized molecular orbitals, each of which has the full symmetry of the original basis set of tetrahedral methane.¹⁴⁰

The resulting molecular orbitals for methane are listed in equations 1.40–1.43, where H_1 is the hydrogen 1s orbital on hydrogen 1, and so on.¹²⁶ Figure 1.16 shows a qualitative MO energy level diagram, and Figure 1.17 represents the three-dimensional electron contour plot for the orbitals.¹⁴¹ We see that one MO (ϕ_1) represents a bonding interaction of the carbon 2s orbital with all four of the hydrogen 1s orbitals, while the other orbitals each have both bonding and some antibonding interactions. Therefore, ϕ_1 is lower in energy than the other three. These figures make clear that there are two different energy levels for the bonding electrons, so two PES bands would be predicted. We conclude, therefore, that the customary view of sp^3 hybridization, while useful for predicting geometries, does not provide the most direct explanation for the PES results.

¹³⁷ Flurry, R. L., Jr. *J. Chem. Educ.* **1976**, 53, 554; Cohen, I.; Del Bene, J. J. *J. Chem. Educ.* **1969**, 46, 487.

¹³⁸ Hoffman, D. K.; Ruedenberg, K.; Verkade, J. G. *J. Chem. Educ.* **1977**, 54, 590.

¹³⁹ Dewar, M. J. S.; Dougherty, R. C. *The PMO Theory of Organic Chemistry*; Plenum Press: New York, 1975; p. 21 ff.

¹⁴⁰ Note that the four molecular orbitals are not tetrahedral in shape. Rather, each is either symmetric or antisymmetric with respect to the symmetry operations of the T_d point group.

¹⁴¹ Graphics with semiempirical MO calculations using a CAChe™ WorkSystem. For a more complete discussion of the molecular orbitals of methane, see Jorgensen, W. L.; Salem, L. *The Organic Chemist's Book of Orbitals*; Academic Press: New York, 1973; p. 68.

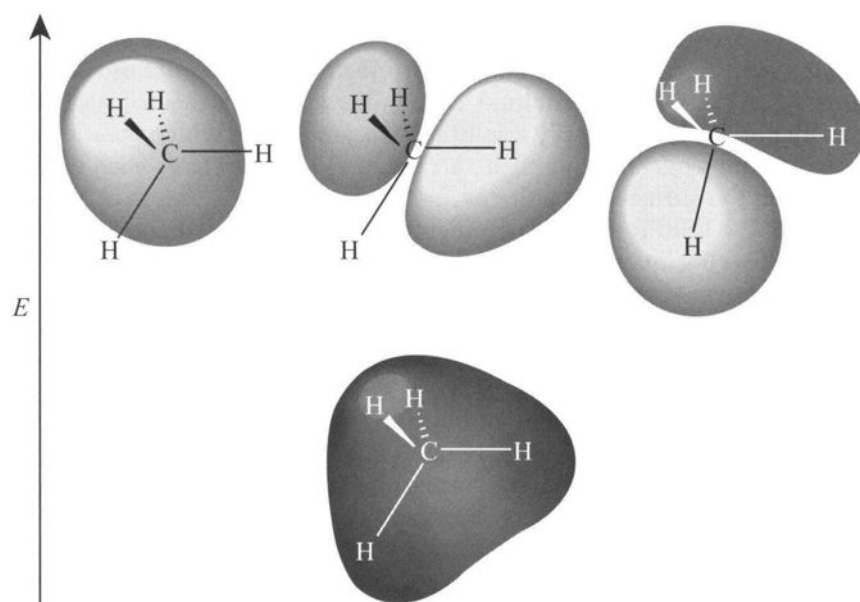


FIGURE 1.17
Bonding MOs for methane.

$$\phi_1 = 0.545 C_{2s} + 0.272(H_1 + H_2 + H_3 + H_4) \quad (1.40)$$

$$\phi_2 = 0.545 C_{2p_x} + 0.272 (H_1 + H_2 - H_3 - H_4) \quad (1.41)$$

$$\phi_3 = 0.545 C_{2p_y} + 0.272(H_1 - H_2 + H_3 - H_4) \quad (1.42)$$

$$\phi_4 = 0.545 C_{2p_z} + 0.272(H_1 - H_2 - H_3 + H_4) \quad (1.43)$$

We must now address a fundamental question. Are there C–H bonds in methane? The answer from MO theory is clearly no. Population of the four bonding molecular orbitals with four pairs of electrons leads to a bonding interaction *among* the carbon atom and all of the hydrogen atoms (not just *between* carbon and the individual hydrogens). Thus, we should say that there is *bonding* in MO theory, but there are not distinct *bonds* formed by separate electron pairs localized between two atoms.

It is important to recognize that this conclusion is not a repudiation of valence bond theory.¹⁴² As Shaik and Hiberty pointed out, a correct valence bond theory description of the bonding in methane produces a result that is entirely consistent with the PES result.¹¹⁶ Rather, the PES result is a reminder that illustrations of C–H bonds formed by overlap of hydrogen 1s and carbon sp^3 orbitals should not be considered pictures of reality.

Valence Shell Electron Pair Repulsion Theory

We have seen that the tetrahedral shape of methane is consistent with a bonding model based on sp^3 hybrid orbitals on carbon. We should not conclude, however, that the geometry is a result of sp^3 hybridization. We

¹⁴² Pauling argued that the photoelectron spectrum of methane is consistent with sp^3 hybridization for methane. Pauling, L. J. *Chem. Educ.* **1992**, 69, 519. See also the discussion by Simons, J. J. *Chem. Educ.* **1992**, 69, 522.

could have predicted the geometry just as well from the Lewis structure of methane simply by using **valence shell electron pair repulsion (VSEPR) theory**.^{143–145} The VSEPR method does not require the use of atomic or molecular orbitals; it is simply a solution to a problem in which the mutually repulsive points (electron pairs) are arranged as far apart from each other as possible on the surface of a sphere.¹⁴⁶

To use the VSEPR theory to predict the geometry of methane, we simply ask the following question: What is the most stable arrangement for four pairs of electrons bonded to a central atom? The tetrahedral arrangement provides for the maximum distance between each electron pair and the other three electron pairs, so we expect this arrangement to be the most stable.¹⁴⁷ A simple method to calculate the bond angles of the resulting regular tetrahedron was pointed out by Ferreira.¹⁴⁸ Methane does not have a molecular dipole moment, even though each C–H bond might be slightly polar. Any bond dipole moment corresponding to one C–H bond aligned with the *x*-axis must therefore be canceled by the vector sum of the projections of the other three C–H bond dipole moments along the *x*-axis. Thus, the cosine of an H–C–H bond angle must be $1/3$, so the bond angle must be $109^{\circ}28'$.

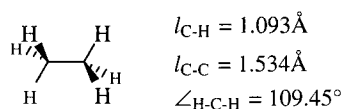


FIGURE 1.18

Experimental geometry of ethane.

The VSEPR approach can easily be extended to ethane. Since each carbon atom has four substituents and since the electronegativity of carbon is close to that of hydrogen, we would predict the local geometry about each carbon atom to be tetrahedral as in methane. The H–C–H bond angles at each carbon atom should remain 109.5° , as should the H–C–C bond angles. The C–C bond would be longer than the C–H bonds because the covalent radius of a carbon atom is greater than that of a hydrogen atom. This prediction is consistent with the experimental geometry reported for ethane, as shown in Figure 1.18.²⁹

Now let us consider methyl chloride. The covalent radius of chlorine (Table 1.2) is about 0.22 \AA greater than that of carbon, so the C–Cl bond distance should be about 1.76 \AA . Thus, we predict the molecular geometry of methyl chloride to be as shown in Figure 1.19(a). Spectroscopic data suggest, however, that the structure is like that shown in Figure 1.19(b).^{29,149} While the C–Cl bond length is reasonable, the H–C–H bond angle is greater than 109.5° , and the H–C–Cl angle is smaller than 109.5° .

We can rationalize the difference between prediction and experiment with VSEPR theory by noting that the electronegativity of chlorine is greater than that of carbon (Table 1.12). In a methane C–H bond, the carbon atom and the hydrogen atom attract the electron pair approximately equally. In CH_3Cl , however, the electrons in the C–Cl bond will be pulled toward the

¹⁴³ For a discussion of VSEPR, see Gillespie, R. J. *J. Chem. Educ.* **1963**, *40*, 295; Bent, H. A. *Chem. Rev.* **1961**, *61*, 275; Burdett, J. K. *Chem. Soc. Rev.* **1978**, *7*, 507. See also reference 8.

¹⁴⁴ Gillespie, R. J. *Chem. Soc. Rev.* **1992**, *21*, 59.

¹⁴⁵ Hall, M. B. *J. Am. Chem. Soc.* **1978**, *100*, 6333.

¹⁴⁶ The model may be more intuitively useful if we visualize the electron points as three-dimensional objects with shapes similar to those calculated for hybrid atomic orbitals. See Gillespie, R. J. *J. Chem. Educ.* **1963**, *40*, 295.

¹⁴⁷ The origin of the repulsion is thought to result from the Pauli exclusion principle and not from Coulombic repulsion of the electron pairs. For a discussion, see Allen, L. C. *Theor. Chim. Acta (Berlin)* **1972**, *24*, 117.

¹⁴⁸ Ferreira, R. J. *Chem. Educ.* **1998**, *75*, 1087.

¹⁴⁹ See also Wiberg, K. B. *J. Am. Chem. Soc.* **1979**, *101*, 1718 and references therein.

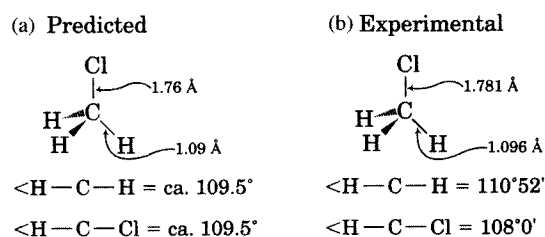


FIGURE 1.19

(a) Qualitative prediction of CH_3Cl geometry. (b) Experimental data.

chlorine atom and away from the carbon atom. In terms of VSEPR theory, points on a sphere representing pairs of electrons used for bonding to electronegative groups can be considered less repulsive to other points (electron pairs) than are points corresponding to bonds to less electronegative atoms.¹⁴⁴ This should decrease the Cl-C-H bond angle, as is observed. In turn, the carbon atom will pull electron density from the hydrogen atoms attached to it. Since electron density associated with the C-H bonds has been increased near the carbon nucleus, the repulsion between pairs of C-H bonds is now increased, at least by comparison with C-H bond repulsion by the C-Cl bond. Therefore, the H-C-H bond angle is expanded relative to that of methane.

Variable Hybridization and Molecular Geometry

The qualitative VSEPR explanation of the geometry of methyl chloride can be made quantitative by a modification of the concept of hybridized atomic orbitals (Figure 1.20). Because methyl chloride is less symmetric than methane, we envision the hybrid orbitals on carbon to be different in energy.¹⁵⁰ Carbon $2p$ orbitals are higher in energy than $2s$ orbitals (Figure 1.8) because electrons in a $2p$ orbital are further from the carbon nucleus than electrons in a $2s$ orbital. Because the chlorine will pull some electron density away from the less electronegative carbon atom, these electrons will be further from the carbon nucleus and will best be described as being in an orbital having less s character and more p character than sp^3 .¹⁵¹⁻¹⁵³ As a result, there must be more s character in the carbon orbitals used for the three C-H bonds, so the H-C-H bond angles are expanded from 109.5° to 110.5° .

To make this bonding description quantitative, it is useful to describe an sp^n orbital in terms of its **hybridization index**, n , and its **hybridization parameter**, λ , defined as $\lambda^2 = n$. Now the fractional s character of the i th orbital is given by the expression $1/(1 + \lambda_i^2)$.^{154,155} For example, the fraction of

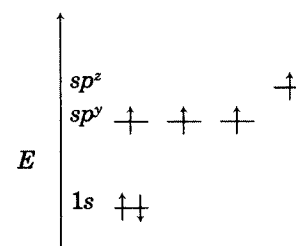


FIGURE 1.20

Hybridization of carbon proposed for CH_3Cl .

¹⁵⁰ For further reading, see (a) Breslow, R. *Organic Reaction Mechanisms*, 2nd ed.; W. A. Benjamin: Menlo Park, CA, 1969; p. 3; (b) Coulson, C. A.; Stewart, E. T. in Patai, S., Ed. *The Chemistry of Alkenes*, Vol. 1; Wiley-Interscience: London, 1964; p. 98 ff.

¹⁵¹ The fundamental principle is that the more s character in a carbon orbital, the more electronegative is that orbital: Walsh, A. D. *Discuss. Faraday Soc.* **1947**, 2, 18; *J. Chem. Soc.* **1948**, 398.

¹⁵² Bent, H. A. *Chem. Rev.* **1961**, 61, 275.

¹⁵³ The lower energy of s orbitals results because their average distance from the nucleus is less than is the average distance from the nucleus for p orbitals of the same principal quantum number. See reference 118a.

¹⁵⁴ Coulson, C. A. *J. Chem. Soc.* **1955**, 2069.

¹⁵⁵ (a) Mislow, K. *Introduction to Stereochemistry*; W. A. Benjamin: New York, 1966; pp. 13-23; (b) reference 113a, p. 195 ff.

s character of an sp^3 hybrid orbital is $1/(1+3)=1/4$. Since the total s character of all the hybrid orbitals must sum to 1, equation 1.44 holds:

$$\sum_i \frac{1}{1+\lambda_i^2} = 1 \quad (1.44)$$

Similarly, the total p character of the hybrid orbitals must equal the number of p orbitals involved in the hybridization. For an sp^3 -hybridized carbon, equation 1.45 applies, where $\lambda_i^2/(1+\lambda_i^2)$ is the fractional p character of the i th hybrid orbital.

$$\sum_i \frac{\lambda_i^2}{1+\lambda_i^2} = 3 \quad (1.45)$$

Hybridization parameters can be related to molecular geometry. The interorbital angle θ_{ab} between hybrid orbitals from carbon to atom a and to atom b can be determined from equation 1.46.¹⁵⁶ If atoms a and b are identical, then equation 1.47 applies.

$$1 + \lambda_a \lambda_b \cos \theta_{ab} = 0 \quad (1.46)$$

$$1 + \lambda_a^2 \cos \theta_{aa} = 0 \quad (1.47)$$

Note that these equations predict that the interorbital angle will increase with greater s character, which is consistent with the increase in bond angle from 109.5° to 120° to 180° as the hybridization changes from sp^3 to sp^2 to sp , respectively.

For a monosubstituted methane such as methyl chloride, denoted here as CA_3B , there are only two different bond angles: θ_{aa} and θ_{ab} . They are related by the expression¹⁵⁷

$$3\sin^2\theta_{ab} = 2(1 - \cos\theta_{aa}) \quad (1.48)$$

so knowledge of only one of these bond angles is sufficient to calculate the other. In the case of methyl chloride, the H–C–Cl bond angle is 108° , so we can calculate the H–C–H bond angle.

$$\cos\theta_{aa} = 1 - \frac{3\sin^2\theta_{ab}}{2} \quad (1.49)$$

We find that $\theta_{aa} = 110.5^\circ$. The value of λ_a^2 can now be calculated from the formula

$$\lambda_a^2 = -\frac{1}{\cos\theta_{aa}} = 2.80 \quad (1.50)$$

¹⁵⁶ For strained molecules, such as those with small rings, the interorbital bond angle may not be the same as that of the internuclear bond angle. See the discussions of bent bonds later in this chapter.

¹⁵⁷ If there are two sets of identical ligands, CA_2B_2 , there will be three bond angles: θ_{aa} , θ_{ab} , and θ_{bb} . They are related by the formula $\cos\theta_{ab} = -\cos 2\theta_{aa} \cos 2\theta_{bb}$. For further details and examples, see reference 155a.

Thus, the orbitals used to bond hydrogen to carbon in methyl chloride are $sp^{2.80}$. Since the total s character in all four orbitals to carbon must sum to 1.00, equation 1.51 holds.

$$3\left(\frac{1}{1+2.80}\right) + \frac{1}{1+\lambda_b^2} = 1 \quad (1.51)$$

Rearranging equation 1.51 and solving for λ_b^2 gives a value of 3.75. Therefore, the C–Cl bond uses a $sp^{3.75}$ hybrid orbital on carbon.

The association of tetravalent carbon with sp^3 hybridization is so entrenched in organic chemistry that it may be surprising that C–C–C bond angles are 109.47° only for carbon atoms with four identical substituents. The C–C–C angle of propane is 112.4° ,¹⁵⁸ and the C–C–C angles in pentane, hexane, and heptane are similar.¹⁵⁹ A survey of 3431 X-ray crystallography measurements by Boese, Schleyer, and their co-workers revealed a range of C–C–C bond angles from 74.88° to 159.66° , with the mean being $113.5^\circ \pm 4.5^\circ$.¹⁶⁰ These researchers also demonstrated that the mean angle C–C–X in a series of ethyl derivatives varies with the electronegativity of the group X, with compounds having a more electronegative X (e.g., F, OH) having smaller C–C–X angles than compounds with less electronegative X groups (e.g., Na, Li).¹⁶¹

Now let us consider CH_2Cl_2 . Myers and Gwinn determined from the microwave spectra of isotopically substituted methylene chloride that the C–Cl distance is 1.772 Å and the C–H distance is 1.082 Å. The Cl–C–Cl angle was determined to be $111^\circ 47'$, while the H–C–H angle was found to be $112^\circ 0'$.¹⁶² Using equation 1.50, we calculate λ_{Cl}^2 to be 2.69, so the C–Cl bonding uses a carbon orbital that is an $sp^{2.69}$ hybrid. Using equation 1.44, we calculate λ_{H}^2 to be 3.37. That corresponds to an H–C–H angle of 107° , but the experimental value is 112° . Clearly, there is an inconsistency between the experimental values and our expectation based on the principles of variable hybridization.

One approach to this problem is to reexamine our intuitive model of a covalent bond as a straight line between two atoms. We must consider the possibility that the C–Cl or C–H bonds (or both) may actually be curved.¹⁶³ Figure 1.21 shows the proposed curved bond structure for CH_2Cl_2 . We can reconcile the apparent conflict between geometry and hybridization parameters if we define the **internuclear bond angle** to be the angle measured by the shortest distance between pairs of nuclei and define the **interorbital bond angle** to be the angle the hybrid orbitals make as they leave the carbon atom. The experimental geometry provides internuclear bond angles, while the

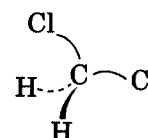


FIGURE 1.21
Curved bond representation of CH_2Cl_2 .

¹⁵⁸ Lide, D. R., Jr. *J. Chem. Phys.* **1960**, *33*, 1514.

¹⁵⁹ Bonham, R. A.; Bartell, L. S.; Kohl, D. A. *J. Am. Chem. Soc.* **1959**, *81*, 4765.

¹⁶⁰ Boese, R.; Bläser, D.; Niederprüm, N.; Nüsse, M.; Brett, W. A.; Schleyer, P. v. R.; Bühl, M.; Hommes, N. J. R. v. E. *Angew. Chem. Int. Ed. Engl.* **1992**, *31*, 314.

¹⁶¹ Because the C–C–X bond angle also varied with rotation about the C–X bond, electronegativity was judged not to be the only determinant of bond angles. A role was also described for hyperconjugation, a concept that will be discussed in later chapters.

¹⁶² Myers, R. J.; Gwinn, W. D. *J. Chem. Phys.* **1952**, *20*, 1420.

¹⁶³ An alternative possibility is that the hybrid orbitals in CH_2Cl_2 involve some d orbital character, but Myers and Gwinn (reference 162) discounted this possibility because of the much higher energy of d orbitals.

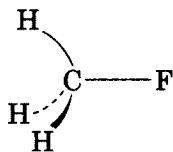


FIGURE 1.22
Curved bond paths suggested for CH_3F . (Reproduced from reference 167.)

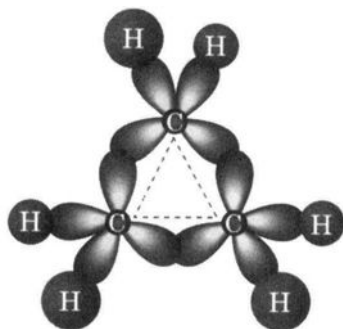


FIGURE 1.23
Relationship between internuclear and interorbital angles in cyclopropane. (Adapted from reference 150a.)

variable hybridization analysis considers interorbital bond angles. Thus, the H–C–H and Cl–C–Cl internuclear angles could both be greater than 109° , but the interorbital angles could still be 107° .

Curved bonds have also been proposed for CH_3F . Because of the greater electronegativity of fluorine than chlorine, we might expect the C–F bond to utilize even more p character on carbon than does the C–Cl bond in CH_3Cl . This should decrease the H–C–F bond angle even more than the H–C–Cl angle in CH_3Cl . However, the H–C–F bond angle in CH_3F is found to be 108.9° .¹⁶⁴ Wiberg and co-workers have explained this apparent anomaly by suggesting that there is considerable curvature in the C–H bonds, as shown in Figure 1.22.^{165,166} The H–C–F angle made by the C–F bond path and by one of the C–H bond paths as they leave the carbon atom is estimated to be 106.7° , which is, as expected, smaller than the H–C–Cl bond angle in methyl chloride.^{167,168}

The idea of curved bonds in methylene chloride and methyl fluoride may seem unfamiliar, but this explanation has long been invoked to describe bonding in cyclopropane.¹⁶⁹ The experimental values for the C–C and C–H bond lengths are 1.510 \AA and 1.089 \AA , respectively, and the H–C–H angle is 115.1° .¹⁷⁰ The hybridization of the orbital on carbon used for C–H bonding is computed to be $sp^{2.36}$, making the hybridization used for C–C bonds $sp^{2.69}$. In turn, that value predicts a C–C–C interorbital value of 111.8° .¹⁷¹ Since this is considerably larger than the 60° internuclear angle required for an equilateral triangle, we conclude that the orbitals used for C–C bonding overlap considerably outside the internuclear lines (the dashed lines in Figure 1.23).

The hybridization parameter is useful as a tool to describe molecular bonding, but it is not a parameter that can be measured directly. It can be determined indirectly, however, through the study of physically observable values that correlate with it.¹⁷² It is generally accepted that NMR coupling constants involving hydrogen depend on the close approach of an electron to the nucleus and so provide a measure of the density of bonding electrons at the nucleus.¹⁷³ Since s orbitals but not p orbitals have electron density at the nucleus, the coupling constant is a probe of the s character of the bond at the two nuclei in the C–H bond. Equation 1.52 shows a useful empirical relation-

¹⁶⁴ Clark, W. W.; De Lucia, F. C. *J. Mol. Struct.* **1976**, 32, 29.

¹⁶⁵ The curved bond line follows the path of maximum electron density from one atom to another and is known as a **bond path**. See Runtz, G. R.; Bader, R. F. W.; Messer, R. R. *Can. J. Chem.* **1977**, 55, 3040. For a discussion, see Krug, J. P.; Popelier, P. L. A.; Bader, R. F. W. *J. Phys. Chem.* **1992**, 96, 7604.

¹⁶⁶ Wiberg, K. B. *Acc. Chem. Res.* **1996**, 29, 229.

¹⁶⁷ Wiberg, K. B.; Hadad, C. M.; Breneman, C. M.; Laidig, K. E.; Murcko, M. A.; LePage, T. J. *Science* **1992**, 252, 1266.

¹⁶⁸ For a discussion of theories concerning the stability and geometry of carbon atoms with two, three, or four fluorine substituents, see Wiberg, K. B.; Rablen, P. R. *J. Am. Chem. Soc.* **1993**, 115, 614.

¹⁶⁹ For a leading reference to some theoretical treatments for the bonding in cyclopropane, see Hamilton, J. G.; Palke, W. E. *J. Am. Chem. Soc.* **1993**, 115, 4159.

¹⁷⁰ Bastiansen, O.; Fritsch, F. N.; Hedberg, K. *Acta Crystallogr.* **1964**, 17, 538.

¹⁷¹ The bond path angle for the C–C–C bonds in cyclopropane was determined to be 78° on the basis of the theory of atoms in molecules (reference 38).

¹⁷² For a discussion and references, see Ferguson, L. N. *Highlights of Alicyclic Chemistry*, Part 1; Franklin Publishing Company: Palisade, NJ, 1973; p. 52 ff.

¹⁷³ Crăciun, L.; Jackson, J. E. *J. Phys. Chem. A* **1998**, 102, 3738.

TABLE 1.14 Correlation of Rate Constants of Proton Exchange with $J_{13\text{C-H}}$

Compound	Relative Rate ^a	$J_{13\text{C-H}}$
Cyclopropane	7.0×10^4	161
Cyclobutane	28.0	134
Cyclopentane	5.7	128
Cyclohexane	1.00	123, 124
Cycloheptane	0.76	123
Cyclooctane	0.64	122

^aSee reference 172.

ship between the NMR coupling constant for ^{13}C and H ($J_{13\text{C-H}}$) and the hybridization parameter.^{155,174,175}

$$J_{13\text{C-H}}(\text{cps}) = \frac{500}{1 + \lambda_a^2} \quad (1.52)$$

We expect electron density at hydrogen to be related to the acidity of a C–H bond, and Streitwieser and co-workers demonstrated a correlation between $J_{13\text{C-H}}$ and the kinetic acidities (the rates of exchange of C–H protons for tritium catalyzed by cesium cyclohexylamide). The data in Table 1.14 show a good correlation of $\log k_{\text{rel}}$ (rate constant relative to that of cyclohexane) with $J_{13\text{C-H}}$ as shown in equation 1.53.¹⁷²

$$\log k_{\text{rel}} = 0.129 J_{13\text{C-H}} - 15.9 \quad (1.53)$$

An explanation for the correlation of acidity with $J_{13\text{C-H}}$ is that both are related to the hybridization of the carbon orbital used for C–H bonding. Because s orbitals are lower in energy than p orbitals, a hybrid orbital with more s character will be lower in energy and thus have electron density closer to the nucleus than will a hybrid with less s character. This lower energy orbital will be more electronegative and will be better able to stabilize a negative charge when a proton is removed in an acid–base reaction.¹⁵²

It must be reemphasized that hybridization is only a conceptual and a mathematical model that allows us to calculate molecular parameters. Changing hybridization is simply modifying that original model to suit a current need, just as the concept of hybridization represents only a change to the model of atomic energy levels. Variable hybridization should not be considered more fundamental than the VSEPR model, just more mathematical. The ability to make quantitative predictions of molecular geometry and physical properties makes the variable hybridization model quite useful for some problems. On the other hand, the VSEPR model is also valuable as an intuitive basis for qualitatively correct predictions. As is so often the case, we need not decide which of two complementary models to adopt for all situations; we need only to determine which best serves our purposes in a particular case.

¹⁷⁴ Muller, N.; Pritchard, D. E. *J. Chem. Phys.* **1959**, *31*, 1471 found that better correlations were obtained when calculated atomic charges were included in the equation.

¹⁷⁵ Liberles, A. *J. Chem. Educ.* **1977**, *54*, 479 used hybridization parameters to show that lone pairs in sp hybrid orbitals have a greater local dipole moment than do lone pairs in any other hybrids.

1.4 COMPLEMENTARY DESCRIPTIONS OF THE DOUBLE BOND

The σ, π Description of Ethene

Let us next consider alternative descriptions of the carbon–carbon double bond. Nearly all introductory organic chemistry textbooks describe the double bond in terms of the σ, π formulation.¹⁷⁶ The simplest example of such bonding is ethene, in which one of the two carbon–carbon bonds is said to be a σ bond formed through overlap of an sp^2 hybrid orbital (Figure 1.24) on each of the carbon atoms, while the second carbon–carbon bond is described as a π bond, made by overlap of two parallel $2p$ orbitals on the carbon atoms (Figure 1.25). To be more complete, we say that overlap of the two sp^2 hybrids produces both a σ bonding and a σ^* antibonding orbital. Similarly, overlap of the two p orbitals produces both a π bonding and a π^* antibonding orbital. A pictorial representation of the carbon–carbon σ and π bonds is shown in Figure 1.26. This description of the carbon–carbon double bond is very familiar, but is it correct? Frenking and Krapp described π bonding as one of the “unicorns in the world of chemical bonding models.”¹⁷⁷ By that they mean that everyone knows what a unicorn looks like even though no one has ever seen one.

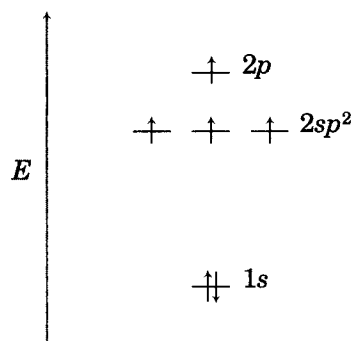


FIGURE 1.24
Depiction of carbon with sp^2 hybridization.

The σ, π model does have qualitative utility because it correctly predicts the carbon–carbon bond length of ethene to be shorter than the carbon–carbon bond length of ethane. The reason is that the overlap of sp^2 orbitals (which have more s character and are therefore closer to the carbon nucleus than are sp^3 hybrids) makes a shorter bond, and the two atoms should be pulled even closer by the π bond. On the other hand, the interorbital angle between two sp^2 hybrid orbitals on the same carbon atom is 120° , so the simple σ, π model predicts the H–C–H and H–C–C bond angles to be 120° (Figure 1.27). Figure 1.28 shows the geometry of ethene determined from spectroscopic measurements, and the H–C–H bond angles are 117° , not 120° .²⁹ Most organic chemists are not bothered by this discrepancy between prediction and experiment. We usually argue that the geometry of ethene is an anomaly and that other alkenes would obey our predicted bond angles. We will return to the ethene geometry shortly, but first let us consider another model for the bonding of ethene.

The Bent Bond Description of Ethene

A much older description of ethene is known as the bent bond formulation.¹⁷⁸ The double bond is described as the result of overlap of two sp^3 hybrid orbitals on *each* of the two carbon atoms, as shown in Figure 1.29. This model also predicts that ethene should be a planar molecule, but it predicts H–C–H bond angles of 109.5° —which is even further from the observed 117° than was the prediction based on sp^2 hybridization. Furthermore, except for cyclopropane, we feel uncomfortable about drawing molecular pictures with bonds that

¹⁷⁶ One text that presented the bent bond formulation was Roberts, J. D.; Stewart, R.; Caserio, M. C. *Organic Chemistry*; W. A. Benjamin: Menlo Park, CA, 1971.

¹⁷⁷ Frenking, G.; Krapp, A. J. *Comput. Chem.* **2007**, *28*, 15.

¹⁷⁸ Bent bonds are also known as banana bonds or τ (tau) bonds. For a discussion of the utility of this model in explaining molecular conformation and reactivity, see Wintner, C. E. J. *Chem. Educ.* **1987**, *64*, 587 and references therein.

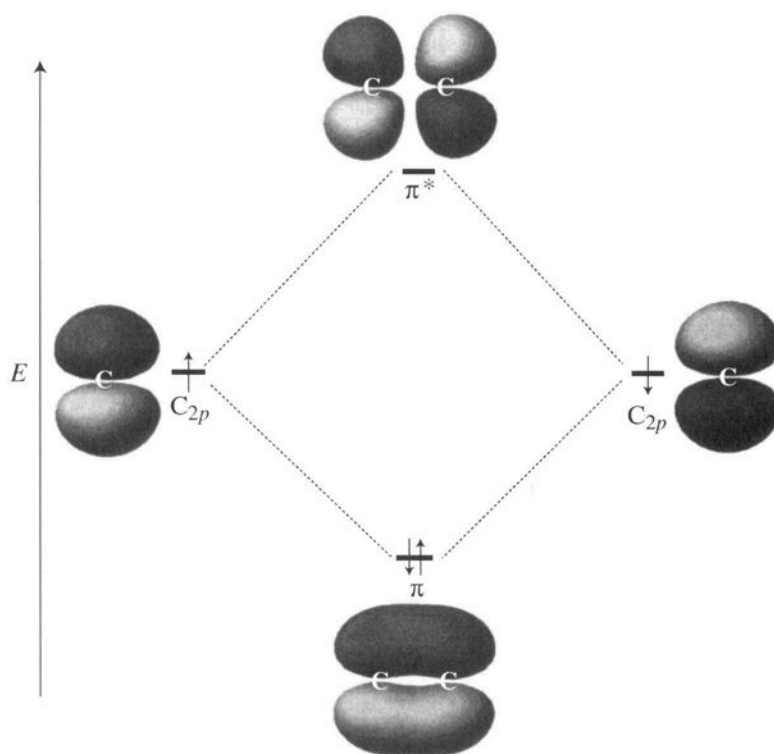


FIGURE 1.25

Energies of ethene π and π^* orbitals.

curve in space as do those in Figure 1.29. Nevertheless, one advocate of the bent bond description was Linus Pauling, who wrote:

There may be chemists who would contend that one innovation of great significance has been made—the introduction of the σ, π description of the double bond and the triple bond and of conjugated systems, in place of the bent bond description. I contend that the σ, π description is less satisfactory than the bent bond description, that this innovation is only ephemeral, and that the use of the σ, π description will die out before long. ...¹⁷⁹

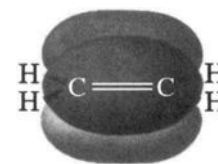


FIGURE 1.26

The σ, π formulation for ethene.

Predictions of Physical Properties with the Two Models

Geometry of Alkenes

Although Pauling's prediction has not yet come true, there are advantages in using the bent bond formulation. One advantage is conceptual simplicity. If the sp^3 hybridization model can give the correct answer, why use a whole family of explanations (sp^3 , sp^2 , and sp) for bonding questions? A practical advantage is the ease of construction of physical models. Some molecular model kits designed for introductory organic chemistry courses use bent bonds as the physical model of the double bond. Such models give acceptable structural geometries, require fewer parts in the model set, and are easier for novices to use than are model kits that attempt to represent π bonds. Still another advantage is that the bent bond formulation seems to provide more quantitative answers than does the σ, π formulation. Consider the measure-

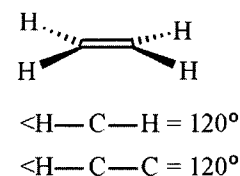
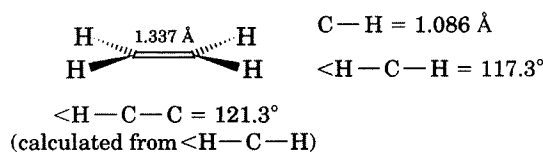


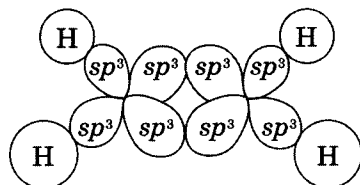
FIGURE 1.27

Predicted geometry of ethene.

¹⁷⁹ Pauling, L. in *Theoretical Organic Chemistry, The Kekulé Symposium*; Butterworths Scientific Publications: London, 1959; p. 1.

**FIGURE 1.28**

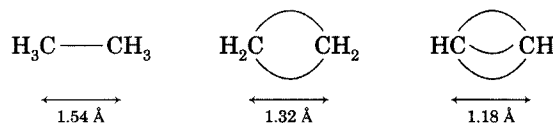
Experimental geometry of ethene.

**FIGURE 1.29**Overlap of sp^3 hybrid orbitals in the bent bond description of ethene.

ment of the carbon-carbon distances illustrated in Figure 1.30. Taking the C-C bond length of ethane, 1.54 Å, as the length of an arc formed by overlap of sp^3 orbitals outside the internuclear line, Pauling calculated that ethene should have an internuclear distance of 1.32 Å, quite close to the experimental value.³⁰ Similarly, three bent bonds arranged as 1.54 Å arcs directed 109.47° apart produce a C-C internuclear distance of 1.18 Å for ethyne, which is essentially the same as the experimental value.¹⁸⁰ The σ, π formulation makes no quantitative prediction about the length of the double or triple bond.

FIGURE 1.30

Quantitative predictions of the bent bond formulation.



Acidities of Hydrocarbons

The alkanes, alkenes, and alkynes are not usually considered to be acidic, but it is possible to measure rates and equilibria of proton removal in solution and in the gas phase (Chapter 7). Table 1.15 shows some experimental data for acidities as indicated by $\Delta H_{\text{acid}}^\circ$, the enthalpy change for detachment of a proton from the hydrocarbon in the gas phase, showing that the ethyne is more acidic than ethene, which in turn is more acidic than ethane.

We explain these results by considering the relative stabilities of the carbanions formed by removal of a proton from each structure. In the σ, π formulation, the hybridization of the carbon orbital with the nonbonded electron pair changes from sp^3 to sp^2 to sp as a proton is removed ethane to ethene to ethyne, respectively (Figure 1.31). Again, the more s character in an

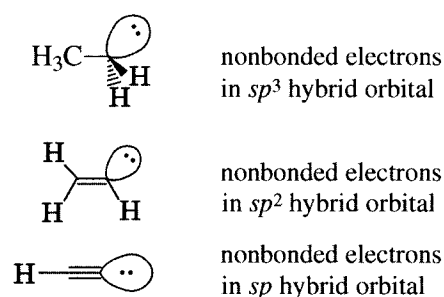
TABLE 1.15 Gas Phase Acidities of C_2 Hydrocarbons

Compound	$\Delta H_{\text{acid}}^\circ$ (kcal/mol)
Ethane	420.1 ± 2.0
Ethene	409.4 ± 0.6
Ethyne	378.5 ± 0.2

Source: Reference 181.

¹⁸⁰ Robinson, E. A.; Gillespie, R. J. *J. Chem. Educ.* **1980**, *57*, 329 described these calculations as well as the use of molecular models with bent bonds to measure the internuclear distances.

¹⁸¹ Data from the compilation by Bartmess, J. E. in Mallard, W. G.; Linstrom, P. J., Eds. *NIST Webbook, NIST Standard Reference Database Number 69*; National Institute of Standards and Technology: Gaithersburg, MD (<http://webbook.nist.gov>).

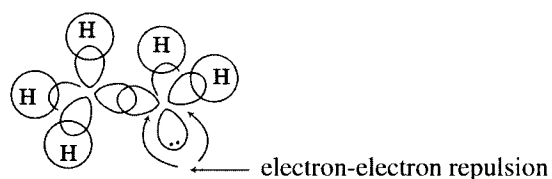
**FIGURE 1.31**

σ, π rationalization of carbanion stabilities. (Charges are not shown.)

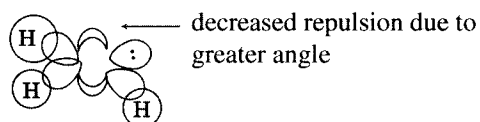
atomic orbital, the greater is the electron attracting power of that orbital, and the more stable should be an anion produced by removing a proton and leaving a nonbonded pair of electrons in that orbital.¹⁵² Thus, the order of carbanion stability should be $(sp)\text{C}^- > (sp^2)\text{C}^- > (sp^3)\text{C}^-$, which is the same as the ranking of hydrocarbon acidities: $(sp)\text{C-H} > (sp^2)\text{C-H} > (sp^3)\text{C-H}$.

The same phenomena can be rationalized with the bent bond formulation by noting the effect of curved C–C bonds on the electron pair repulsions around each carbon atom. As Figure 1.32 shows, formation of bent bonds in ethene pulls the electrons closer to the center of the C–C internuclear line; in turn, this decreases the repulsion between the electron pair comprising the C–H bond in question and the electron pairs comprising the bent C–C bonds. That means that the C–H electrons see a less shielded carbon nucleus, so they are attracted more strongly to the carbon nucleus. An unshared pair of electrons left behind by removal of a proton from ethene, as shown in Figure 1.32(b), is much more stable than is a pair of electrons left behind by removal of a proton from ethane, as shown in Figure 1.32(a). For the same reason, a nonbonded pair of electrons is more stable on a triple bonded carbon, as shown in Figure 1.32(c), than on a double bonded carbon. Thus, the bent bond formulation can rationalize these experimental observations, at least qualitatively, as well as can the σ, π description.

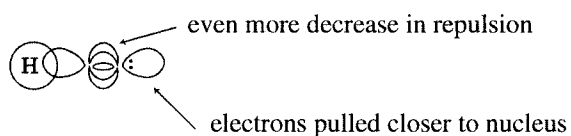
(a) Ethane



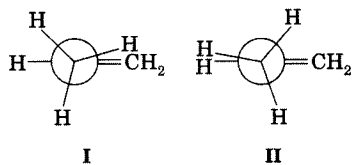
(b) Ethene



(c) Ethyne

**FIGURE 1.32**

Bent bond rationalization of acidities. (Charges are not shown.)

**FIGURE 1.33**

Conformations of propene: σ, π description. (Adapted from reference 182.)

Conformations of Propene

Let us now consider which bonding model is more amenable to qualitative predictions of molecular conformation. Specifically, what should be the preferred conformation of propene? Walters noted that two conformers of propene (designated as I and II) can be visualized as Newman projections observed by sighting down the C3–C2 bond (Figure 1.33).^{182,183} In conformer I, a C–H bond eclipses a carbon–carbon double bond. In conformer II, a C–H bond eclipses a C–H bond. Assuming that there is greater electron density in a double bond than in a C–H single bond, we would expect conformer II to be more stable. Experimentally, however, conformer I was found to be more stable by about 2 kcal/mol.¹⁸⁴

If we depict the same Newman projections with bent bonds, as shown in Figure 1.34, we see that conformer II now represents essentially an all-eclipsed conformation. Thus, it is easily predicted to be less stable than I, which is an all-staggered arrangement. If utility is the main criterion for adopting conceptual models, then this result would seem to argue persuasively for using the bent bond formulation.^{185,186} The bent bond model leads directly to a correct prediction of conformational stability, but the σ, π model does not.¹⁸⁷

Pauling's prediction that the use of the σ, π description will wane may yet come true. In recent years some theoreticians have determined that calculations of molecular structure are in better agreement with the bent bond description than with the σ, π description. Figure 1.35(a) shows calculated contour lines of a carbon orbital in a plane that is perpendicular to the molecular plane of ethene, and Figure 1.35(b) shows contour lines for an orbital in a plane containing the carbon atoms of cyclopropane. Clearly, much of the orbital lies outside the internuclear bond line in each case. It is generally agreed that the bonds in cyclopropane are bent; the picture from this theoretical calculation reinforces the view that they are bent in ethene also.

This conclusion was reinforced by a number of investigations. The title of one publication was "Double Bonds Are Bent Equivalent Hybrid (Banana) Bonds."¹⁸⁸ Another study concluded that "the GVB description of the double bond in (C₂F₄) is *not* the traditional picture of σ and π bonds but rather a representation in terms of two bent bonds."¹⁸⁹ Still another paper comparing

¹⁸² Walters, E. A. *J. Chem. Educ.* **1966**, *43*, 134.

¹⁸³ Newman projections and other stereochemical representations will be discussed in Chapter 2.

¹⁸⁴ Herschbach, D. R.; Krisher, L. C. *J. Chem. Phys.* **1958**, *28*, 728.

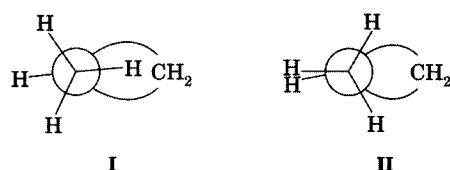
¹⁸⁵ The emphasis in the present discussion is on the application of two very simple conceptual models to a particular problem. High level calculations provide a much deeper analysis of the conformations of propene and other molecules. For a discussion, see Bond, D.; Schleyer, P. v. R. *J. Org. Chem.* **1990**, *55*, 1003.

¹⁸⁶ Proponents of the σ, π formulation could argue that taking additional factors into account would correct the initial prediction that conformer II is more stable. When faced with discrepancies between prediction and experiment, the proponents of a particular conceptual model often take the position that consideration of additional factors would favor their model.

¹⁸⁷ This discussion implicitly treats the methyl group as interacting with the vinyl group only through steric interactions. This assumption ignores the electronic interactions inherent in any molecular entity. See, for example, Mo, Y.; Peyerimhoff, S. D. *J. Chem. Phys.* **1998**, *109*, 1687.

¹⁸⁸ Palke, W. E. *J. Am. Chem. Soc.* **1986**, *108*, 6543.

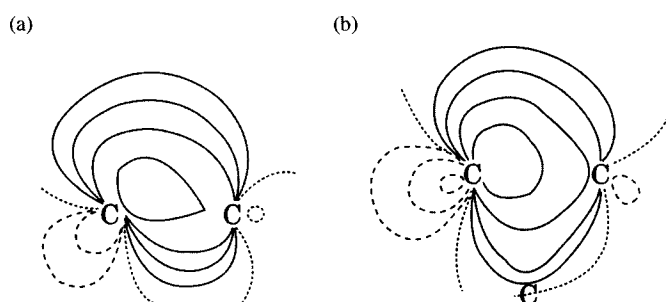
¹⁸⁹ GVB is a type of theoretical calculation. Schultz, P. A.; Messmer, R. P. *J. Am. Chem. Soc.* **1988**, *110*, 8258.

**FIGURE 1.34**

Conformations of propene: bent bond formulation. (Adapted from reference 182.)

the bent bond and σ,π models concluded that "... from an energetical point of view, both constructions provide an equally good starting point for the treatment of correlation effects beyond the one-electron configuration."¹⁹⁰ Another study concluded that "our results yield bent bonds as the favored bonding description, showing that the σ,π bond descriptions of multiple bonds are artifacts of approximations to the full independent-particle equations."¹⁹¹ For systems that exhibit resonance, such as benzene and the allyl radical, these authors stated the conclusion even more succinctly: "bent bonds are better."^{192,193}

The distinction between the bent bond and σ,π formulations of the double bond is not as clear-cut as the discussion above might suggest. Although the results depend on the level of theory used, the two models predict essentially the same result at higher levels of analysis.¹⁹⁴ As Schultz and Messmer put it, "no experiment can possibly distinguish between a σ,π double bond and double bent bonds in any system, and therefore neither can be proven to be 'right' in an absolute sense; both are approximate descriptions."¹⁹¹ The σ,π model for the double bond and the bent bond description should each be taken as viable *starting points* to describe molecular structure but not as complete descriptions.^{30,195} Each approach has its advantages and disadvantages. It is important that we consider both methods and that we know why we choose one over the other when we talk about organic chemistry.

**FIGURE 1.35**

Contour lines for a bonding orbital on one carbon in (a) ethene and (b) cyclopropane. (Adapted from reference 169.)

¹⁹⁰ Karadakov, P. B.; Gerratt, J.; Cooper, D. L.; Raimondi, M. *J. Am. Chem. Soc.* **1993**, *115*, 6863.

¹⁹¹ Schultz, P. A.; Messmer, R. P. *J. Am. Chem. Soc.* **1993**, *115*, 10925.

¹⁹² Schultz, P. A.; Messmer, R. P. *J. Am. Chem. Soc.* **1993**, *115*, 10943.

¹⁹³ For a different view, see Carter, E. A.; Goddard W. A. III. *J. Am. Chem. Soc.* **1988**, *110*, 4077.

¹⁹⁴ Gallup, G. A. *J. Chem. Educ.* **1988**, *65*, 671 and references therein.

¹⁹⁵ England, W. J. *J. Chem. Educ.* **1975**, *52*, 427; Palke, W. E. *J. Am. Chem. Soc.* **1986**, *108*, 6543.

1.5 CHOOSING MODELS IN ORGANIC CHEMISTRY

Conceptual, mathematical, and physical models are essential tools in organic chemistry because they help rationalize the results of experiments (observables) with theory (nonobservables). Yet the paradox is that these models may be most useful to us when they are oversimplified to the point of being incorrect in some way. Without a straight line or pair of dots to represent a chemical bond, we would find it difficult to describe chemistry in a practical way. Yet in some cases we find it advantageous to draw those lines curved instead of straight, and sp^3 hybrid orbitals cannot be relied on even to predict all of the properties of methane. A more detailed description of that line and of those orbitals can be made only with the help of computers and high level mathematics.

If any one of our models is asked to give a more correct answer to a problem, it quickly becomes more complex. Electronegativity is useful in a qualitative sense, but attempts to make it more quantitative lead to different conclusions about what it means and how it should be determined. Elementary VB theory and MO theory are intuitively reasonable, but further development obscures the simple mental pictures each provides. We feel a need to retain these simple pictures, therefore, even when we know that they cannot be totally accurate.

One solution to the use of oversimplified models in organic chemistry is to hybridize complementary conceptual models, just as we hybridize the two Kekulé structures for benzene in our minds in order to understand and describe aromaticity. The σ, π and bent bond descriptions represent a pair of models that serve as useful beginning points or approaches to the description of the double bond. Visualizing a hybrid of these two mental pictures may be more nearly correct than is thinking in terms of either model alone.

Perhaps another metaphor may be useful. In the end, our models must be described in a language of some kind, but having *a* language to describe something does not necessarily make that explanation complete.¹⁹⁶ If we view complementary models as different languages to describe chemistry, we find it better to be multilingual—to be able to converse in many languages, to translate from one language to another, and to think in more than one language. If we have only one approach, then we are only computers doing what we have been programmed to do. Progress in chemistry requires the ability to see relationships in a new way, and that requires education, not just training.¹⁹⁷

Problems

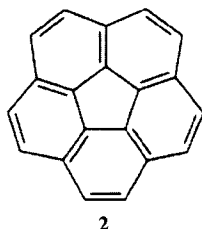
- 1.1. Kuhn (reference 3) wrote that scientists “are little better than laymen at characterizing the established bases of their field.” Briefly summarize the physical phenomena that support your belief in atomic and molecular theory.

¹⁹⁶ For provocative comments on language and models, see Bent, H. A. *J. Chem. Educ.* **1984**, *61*, 774. In particular, Bent noted that “indeed, to be useful, *a model must be wrong, in some respects—else it would be the thing itself.* The trick is to see—with the help of a teacher—*where it’s right.*”

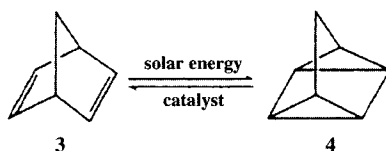
¹⁹⁷ One aspect of this idea is what Turro (reference 24) called “organic thinking,” which is one of the ways that the study of organic chemistry transfers to other areas:

An important value of learning organic chemistry is the mastering of “organic thinking,” an approach to intellectual processing whereby the “sameness” of many families of structures and reactions is revealed.

- 1.2. Find a popular or scientific article that refers to observations of a single atom or atoms.
- What is the nature of the experiment?
 - What observations are made directly with the human senses?
- 1.3. **a.** Consider two geometries for methane other than the regular tetrahedron. Show how each alternative geometry is inconsistent with the known number of isomers of some derivative of methane.
- b.** Consider at least four structures with the molecular formula C_6H_6 and show how each is inconsistent with the known number of isomers of benzene substitution products having a given molecular formula.
- c.** In parts a and b of this problem, you assumed that the structure of a derivative (e.g., bromobenzene) is essentially the same as that of the parent structure (e.g., benzene). Is that assumption valid? For example, how can we know that methane is not planar, even though chloromethane is roughly tetrahedral?
- 1.4. Use the values in Table 1.3 to determine the van der Waals volume and surface area for each of the pentanes. Verify that for *n*-pentane the values are correctly predicted by the formulas $V_W = 6.88 + 10.23 N_C$ and $A_W = 1.54 + 1.35 N_C$, where N_C is the number of carbon atoms in the molecule.
- 1.5. The heat of formation of corannulene (**2**) in the crystal state is 81.81 kcal/mol. Its heat of sublimation has been calculated to be 29.01 kcal/mol. What is the ΔH_f° of **2** in the vapor phase?



- 1.6. A proposed system for the conversion and storage of solar energy was based on the photochemical isomerization of norbornadiene (**3**) to quadricyclane (**4**) during sunny periods, with catalytic conversion of **4** to **3** and release of energy at a later time. The heats of hydrogenation of **3** and **4** (both in the liquid phase) to norbornane are -68.0 kcal/mol and -92.0 kcal/mol, respectively. What is the potential for energy storage, in kcal/mol, for the photochemical conversion of **3** to **4**?



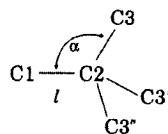
- 1.7. The standard heat of combustion of 4,4-dimethyl-1,3-cyclohexanedione was determined to be -1042.90 kcal/mol. Its standard heat of sublimation is $+23.71$ kcal/mol. What is the ΔH_f° (gas phase) of this compound?
- 1.8. The heat of hydrogenation of phenylethyne was found to be -66.12 kcal/mol, and the heat of formation of phenylethane is 7.15 kcal/mol. What is the ΔH_f° of phenylethyne?
- 1.9. **a.** The heat of formation of 2,5-thiophenedicarboxylic acid at 298.15 K is -772.4 2.2 kJ/mol. Its heat of sublimation is 139.8 ± 0.4 kJ/mol. What is the ΔH_f° of the compound in the gas phase?
- b.** The heat of formation of liquid 2-acetylthiophene at 298.15 K is -118.0 ± 1.7 kJ/mol, while that of crystalline 3-acetylthiophene is -129.1 ± 1.4 kJ/mol.

The heat of vaporization of 2-acetylthiophene at 298.15 K is 58.8 ± 1.2 kJ/mol, and the heat of sublimation of 3-acetylthiophene at 298.15 K is 74.6 ± 1.1 kJ/mol. What is the difference in the gas phase heats of formation of these two compounds?

- 1.10. *cis*-3-Methyl-2-pentene has a ΔH_f° that is 1.65 kcal/mol more negative than that of 2-ethyl-1-butene. The ΔH_r of 2-ethyl-1-butene with trifluoroacetic acid is -10.66 kcal/mol. Predict the heat of reaction of *cis*-3-methyl-2-pentene with trifluoroacetic acid under the same conditions.
- 1.11. The heat of hydrogenation of *cis*-1,3,5-hexatriene to hexane is -81 kcal/mol, while that of the *trans* isomer is -80.0 kcal/mol. Under the same conditions the heat of hydrogenation of 1,5-hexadiene is -60.3 kcal/mol. What would be the heat of hydrogenation for just the middle double bond of the *cis* and *trans* isomers of 1,3,5-hexatriene?
- 1.12. Calculate ΔH_f° for heptane using both equations 1.9 and 1.12. How do these predictions compare with literature values?
- 1.13. The dipole moments of CH_3F , CH_3Cl , CH_3Br , and CH_3I are reported to be 1.81, 1.87, 1.80, and 1.64 D, respectively.⁶⁹
- Calculate the partial charge on the halogen in each of the methyl halides (assuming that the halogen bears the partial negative charge and that the partial positive charge is centered on the carbon atom) using the C–X bond lengths listed in Table 1.1.
 - What trend, if any, do you see in the dipole moments of the methyl halides? How do you rationalize this result?
- 1.14. For what category of atoms could Allen or Nagle but not Pauling electronegativity values be determined?
- 1.15. The C–C–C bond angle of propane is reported to be 112.4° . What is the hybridization of the orbitals on C2 used for C–C and C–H bonding?
- 1.16. Both experimental and theoretical studies indicate that the C1–C2 bond length (l) and the C1–C2–C3 bond angle (α) in molecules having the following general structure are strongly correlated. (The C1–C2–C3' and the C1–C2–C3'' bond angles are also α .) One study found that they could be related by the equation

$$l = 2.0822 - 0.0049 \alpha \quad (1.54)$$

where distances are in Å and angles are in degrees.



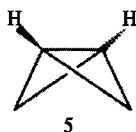
- What does this equation indicate about the change in bond length expected when the adjacent angle changes to a value greater than or less than 109.5° ?
 - Rationalize the form of equation 1.54 in terms of both variable hybridization theory and VSEPR theory.
- 1.17. a. Arrange the following compounds in order of increasing length of C–H bonds and rationalize your answer: ethane, ethene, ethyne, cyclopropane, and cyclobutane.
- b. Arrange these compounds in order of increasing length of C–C single bonds and explain your answer: ethane, 2-methylpropane, 2-methylpropene, 1,3-butadiene, 1,3-butadiyne, 1-butene-3-yne.

- 1.18. a. Use the bent bond description of double bonds to rationalize that the H–C–H bond angles in ethene are 117° and not 109.5°.
 b. Modify your explanation to predict the H–C–H angle of formaldehyde. Specifically, should it be larger or smaller than the H–C–H angle of ethene?
- 1.19. Consider again ethene and formaldehyde, this time analyzing the double bond in each as a two-membered ring. Calculate the fractional *s* character and hybridization parameter for the C–H bond in each.
- 1.20. a. Consider the formula $J_{13\text{C-H}} = 5.7 \times (\% s) - 18.4 \text{ Hz}$. Determine whether this formula is equivalent to that in equation 1.52, and explain your reasoning.
 b. Muller and Pritchard (reference 174) determined that the lengths of C–H bonds correlate with values of $J_{13\text{C-H}}$ according to equation 1.55:

$$r_{\text{C-H}} = 1.1597 - 4.17 \times 10^{-4} J_{13\text{C-H}} \quad (1.55)$$

Use equations 1.52 and 1.55 to relate the length of a C–H bond directly to λ^2 .

- 1.21. Analyze cyclopropane, cyclobutane, and cyclopentane according to both the bent bond (using sp^3 hybrid orbitals) and variable hybridization descriptions.
- a. For each compound, use the literature value for the H–C–H bond angle to calculate the fractional *s* and *p* character of the carbon orbitals used for C–H bonds, then use the result to calculate the interorbital C–C–C bond angle. How do the calculated values differ from the literature values of the internuclear bond angles? What does that tell you about the nature of the strain in the molecule? What does that suggest to you about the chemical properties of cyclobutane (e.g., reaction with electrophiles).
- b. What does each model suggest to you about the acidities of the C–H bonds? How do the literature data for the acidity of cyclopropane agree with the predictions?
- 1.22. McNelis and Blandino noted that the sum of the six bond angles (109.5° degrees each) around a tetrahedral carbon atom is 657° and postulated that the bond angles in other tetraligant species should sum to that same value.¹⁹⁸ For example, the H–C–F bond angle in fluoromethane was reported to be 109° 2' (Table 1.1). Since there are three H–C–F and three H–C–H angles, the “657” method predicts the H–C–H bond angle to be $\frac{1}{3}(657^\circ - 3 \times 109.03^\circ) = 110^\circ$.
- a. How does this result compare with an experimental value?
- b. Does the predictive ability of the “657” method depend on the extent to which the geometry at a carbon atom is nearly tetrahedral? If so, determine the range of $\angle_{\text{H-C-F}}$ values for which the “657” method produces a predicted H–C–H angle that is less than 10° different from the value calculated using the trigonometric relationships.
- 1.23. The C–H coupling constants for ethane, ethene, and ethyne are 125.2, 156, and 249 Hz, respectively. Do these values correlate with the gas phase acidity values in Table 1.15? If so, use the correlation to estimate the gas phase acidity of cyclopropane ($J_{13\text{C-H}} = 161$).
- 1.24. In bicyclo[1.1.0]butane (5), the $^{13}\text{C} - ^1\text{H}$ coupling constant for the bridgehead C–H groups is 202 Hz. Calculate the % *s* character in the bond from carbon to hydrogen at this position. Would you expect the acidity of the bridgehead protons to be greater or less than that of the protons in acetylene?



¹⁹⁸ McNelis, E.; Blandino, M. *New J. Chem.* **2001**, 25, 772. More precisely, $6 \times 109.47^\circ = 656.82^\circ$.

- 1.25. If λ is a function of molecular geometry and $J_{13\text{C-H}}$ is also a function of λ , then is not $J_{13\text{C-H}}$ really a function of geometry? Is λ an observable? If not, do we need to define λ at all?
- 1.26. On page 32 we saw experimental evidence that some familiar views of hybridization are at best oversimplified. In view of this result, can you justify the continued use of hybridized orbitals as a conceptual model in organic chemistry?
- 1.27. Greenberg and Liebman have stated that “we believe organic chemistry is essentially a pictorial and not a mathematical science.”¹⁹⁹ Do you agree with this statement? Do you think organic chemistry should be a mathematical science? Do you believe it will become so in the future?
- 1.28. Respond to Coulson’s observation about the nature of theory in chemistry:

Sometimes it seems to me that a bond between two atoms has become so real, so tangible, so friendly that I can almost see it. And then I awake with a little shock: for a chemical bond is not a real thing: it does not exist: no one has ever seen it, no-one ever can. It is a figment of our own imagination. . . . Here is a strange situation. The tangible, the real, the solid, is explained by the intangible, the unreal, the purely mental.¹⁵⁴

- 1.29. Respond to Roald Hoffmann’s statement that

. . . much that goes into the acceptance of theories has little to do with rationalization and prediction. Instead, I will claim, what matters is a heady mix of factors in which psychological attitudes figure prominently.²⁰⁰

Hoffmann also wrote that

. . . explanations are almost always stories. Indeed, moralistic and deterministic stories. For to be satisfying they don’t just say $A \rightarrow B \rightarrow C \rightarrow D$, but $A \rightarrow B \rightarrow C \rightarrow D$ *because* of such and such properties of A, B and C. The implicit strong conviction of causality, justified by seemingly irrefutable reason, may be dangerously intoxicating. This is one reason why I wouldn’t like scientists and engineers to run this world.²⁰⁰

Do you think scientists who understand the limitations of human knowledge discussed in this chapter would be better able to run the world than Hoffmann imagines?

- 1.30. Weisberg argues that there is a trade-off between precision and generality in the models that scientists use and that “sacrificing precision in model descriptions can often add explanatory depth to the models picked out by these descriptions.”²⁰¹ Cite examples from this chapter that are consistent with Weisberg’s statement. Are any examples inconsistent with Weisberg’s conclusion?

¹⁹⁹ Greenberg, A.; Liebman, J. F. *Strained Organic Molecules*; Academic Press: New York, 1978; p. 37.

²⁰⁰ Hoffmann, R. *Am. Sci.* **2003**, *91*, 9.

²⁰¹ Weisberg, M. *Philos. Sci.* **2004**, *71*, 1071

Stereochemistry

2.1 INTRODUCTION

The term **stereochemistry** refers to the three-dimensional nature of molecules and to their space-filling properties.^{1,2} Many computer models can give a perception of three dimensions, but printed and hand-drawn representations of molecules are two-dimensional images that are meaningful only to those who understand implicit rules for visualizing the third dimension.³ Furthermore, such drawings have meanings on many levels.

- Structure drawings are not always meant to be taken “literally.” For example, a Kekulé structure of benzene does not mean a deformed 1,3,5-cyclohexatriene molecule.
- Often drawings are not designed to show all aspects of structure, only those that are to be emphasized to the viewer. A Kekulé structure for benzene may not show the hydrogen atom bonded to each carbon atom, since the point of emphasis is the aromatic ring.
- A drawing may imply as much about the conceptual model used to analyze a problem as it tells about the chemical substance under consideration. A representation of a carbon–carbon double bond may use the σ, π formulation or the bent bond formulation.

Let us look more closely at some specific types of structural representations and categorize the information they are intended to convey. Some drawings represent only the **constitution** of a molecule—the order in which the atoms are bonded—without indicating anything about the spatial orientation of the atoms. One way to do that is by representing the molecule as a line

¹ Eliel, E. L.; Wilen, S. H.; Doyle, M. P. *Basic Organic Stereochemistry*; John Wiley & Sons: New York, 2001.

² Eliel, E. L.; Wilen, S. H. *Stereochemistry of Organic Compounds*; John Wiley & Sons: New York, 1994.

³ Hoffmann and Laszlo presented an analysis of the way chemists use drawings to convey information: Hoffmann, R.; Laszlo, P. *Angew. Chem. Int. Ed. Engl.* **1991**, *30*, 1.

of element symbols and number notations (a kind of word structure). For example, pentane could be shown as $\text{CH}_3\text{CH}_2\text{CH}_2\text{CH}_2\text{CH}_3$. We may also show the bonds connecting the carbon atoms, as in $\text{CH}_3\text{-CH}_2\text{-CH}_2\text{-CH}_2\text{-CH}_3$, but that is not necessary because covalent bonds are implicit in molecular representations. With the understanding that a methylene group can be considered as a unit, we could also write pentane as $\text{CH}_3(\text{CH}_2)_3\text{CH}_3$.

Organic chemists find it increasingly necessary to represent molecular structures in a format that is easily stored and retrieved electronically. A number of such methods have been proposed, but two formats are becoming widely used. One is the International Chemical Identifier (InChI) system developed by IUPAC.⁴ Some software drawing programs are able to write InChI terms, and a web site allows one to generate an InChI designation for a structure drawn using a graphical user interface.⁵ The InChI string for pentane is `InChI=1/C5H12/c1-3-5-4-2/h3-5H2, 1-2H3`, while that for cholesterol is `InChI=1/C27H46O/c1-18(2)7-6-8-19(3)23-11-12-24-22-10-9-20-17-21(28)13-15-26(20,4)25(22)14-16-27(23,24)5/h9,18-19, 21-25,28H,6-8,10-17H2,1-5H3/t19-,21+,22+,23-,24+,25+,26+,27-/m1/s1`. The Simplified Molecular Input Line Entry System (SMILES) formalism, which was reported by Weininger and others, produces a more compact string.⁶ The SMILES notation for pentane is `CCCCC`, while that for cholesterol is

```
[H][C@@]1(CC[C@@]2([H])[C@]3([H])CC=C4C[C@@H](O)CC[C@]4(C)[C@@]3([H])CC[C@]12C)[C@H](C)CCCC(C)C.
```

These alphanumeric representations are precise, but they are of limited utility unless they are interpreted with a computer. Most organic chemists prefer to work with graphical representations of chemical structures. The common convention in such drawings is that a line represents a chemical bond, that there is a carbon atom at each intersection and at each terminus of a line unless another atom is indicated, and that each carbon atom has sufficient hydrogens as substituents to satisfy normal valency requirements. With this system pentane is the jagged line **1** (Figure 2.1). That drawing is not much better than $\text{CH}_3\text{CH}_2\text{CH}_2\text{CH}_2\text{CH}_3$ for pentane, but such representations become more useful as the molecules to be depicted become larger as, for example, cholesterol (**2**).

Cholesterol not only has more atoms and more connectivity than does pentane, but it differs in another important way. Physical models tell us that all of the carbon atoms of pentane *could* lie in one plane, but those of cholesterol cannot. Therefore, our drawing for cholesterol must have some way to indicate not only connectivity but also the orientation of the various parts of the molecule. We view the drawing as a projection (a shadow, in effect) of a real object, and we often use angles and line thicknesses to convey three-dimensional information.⁷ Objects in the distance (behind the plane of the main scene) are reduced in size and/or angled to give an effect of distance, while objects in the front of the main scene are large and bold.

⁴ Royner, S. L. *Chem. Eng. News* **2005** (Aug 22), 39.

⁵ <http://pubchem.ncbi.nlm.nih.gov/edit/>.

⁶ Weininger, D. J. *Chem. Inf. Comp. Sci.* **1988**, *28*, 31 and succeeding papers in that issue.

⁷ In a Fischer projection (page 72) the three-dimensional information is conveyed both by the figure itself and by a set of rules for the interpretation of the figure.

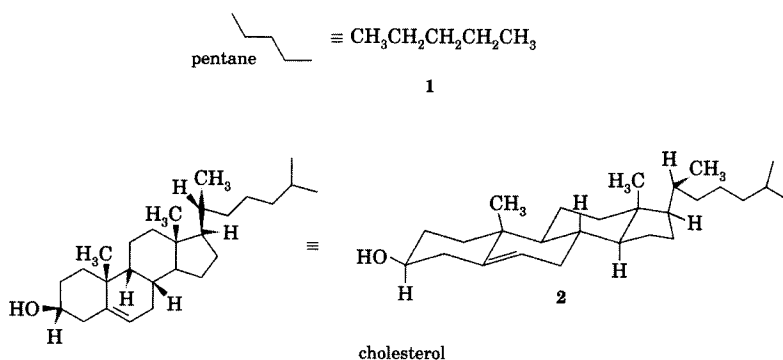


FIGURE 2.1
Representations of pentane (1) and cholesterol (2).

Consider the several drawings of 2-chlorobutane (3) in Figure 2.2. In representations **3a** and **3b**, a bold wedge suggests a bond projecting toward the viewer. A hashed line suggests a bond projecting away from the viewer. Solid lines that do not change in size suggest bonds in a central plane. Another way to represent the same molecule is to let all bonds be represented by straight lines with a type of drawing usually called a sawhorse representation because of its similarity to a carpenter's device with the same name (**3c**). The stereochemical relationships in such a figure can be made more apparent by the use of hashed or bold wedges, as in **3d**.

An important part of stereochemical drawings is the clear representation of **conformations**, which are different spatial relationships that are interconvertible by rotation about single bonds.⁸ In a Newman projection we represent the view from sighting down a particular bond in such a way that one atom totally eclipses another one.⁹ As illustrated in Figure 2.2 for one conformation of 2-chlorobutane (**3e**), we see three substituents on the carbon atom nearer our eyes, and we stylistically show their bonds meeting at the center of a circle. The fourth substituent to the front carbon atom is the other (eclipsed) carbon atom. We can see three substituents attached to the second carbon atom, but the lines representing bonds to these substituents are visible only to the edge of the circle representing the second carbon atom.

Bold and hashed wedges are commonly used in complex molecules, but an additional convention is required. For example, in the representation of paclitaxel (**4**),¹⁰ it cannot be true that all of the bold wedges project toward the viewer to the same plane in space, nor can it be true that all of the dashed wedges project to the same plane behind the page. Rather, each wedge is a local descriptor only, and the sense of depth of the viewer is to be reset at the origin of each wedge.

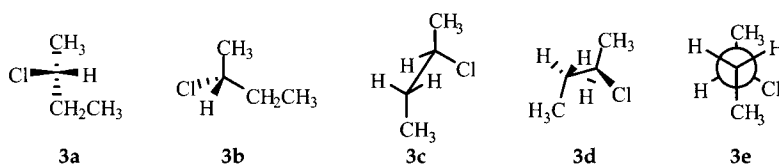
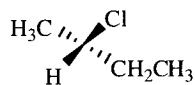


FIGURE 2.2
Representations of 2-chlorobutane (3).

⁸ See the discussion in Chapter 3.

⁹ Newman, M. S. *J. Chem. Educ.* **1955**, 32, 344.

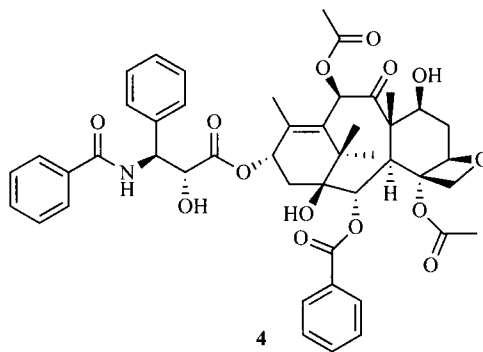
¹⁰ Guénard, D.; Guéritte-Voegelein, F.; Potier, P. *Acc. Chem. Res.* **1993**, 26, 160.



not acceptable

FIGURE 2.3

An unacceptable representation (3f) of 2-chlorobutane.



Unambiguous, accurate graphical representation of the stereochemistry of chemical structures is essential. To this end, a task group in the IUPAC Chemical Nomenclature and Structure Representation Division prepared a document that specifies preferred, acceptable, and not acceptable graphical representations for a wide variety of structures.¹¹ In Figure 2.2, representation 3a is considered acceptable, but 3b is preferred. However, structure 3f (Figure 2.3) is considered not acceptable.

A widely used representation for crystallographic data is the ORTEP (Oak Ridge Thermal Ellipsoid Program) plot, as in the example of cyclobutane (Figure 2.4). The ellipsoids provide a measure of the averaged displacements of the atoms in the crystal.¹²

2.2 STEREOISOMERISM

Isomerism

Isomers are different chemical compounds that have the same molecular formula. Whether two compounds are considered different depends in part

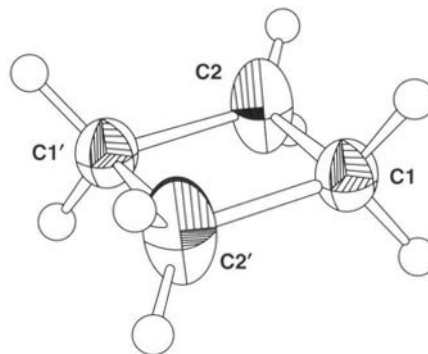


FIGURE 2.4

ORTEP plot for cyclobutane.
(Reproduced from reference 13.)

¹¹ Brecher, J. *Pure Appl. Chem.* **2008**, *80*, 277.

¹² Burnett, M. N.; Johnson, C. K. *ORTEP III: Oak Ridge Thermal Ellipsoid Plot Program for Crystal Structure Illustrations*. Oak Ridge National Laboratory Report ORNL-6895, 1996.

¹³ Stein, A.; Lehmann, C. W.; Luger, P. J. *Am. Chem. Soc.* **1992**, *114*, 7684.

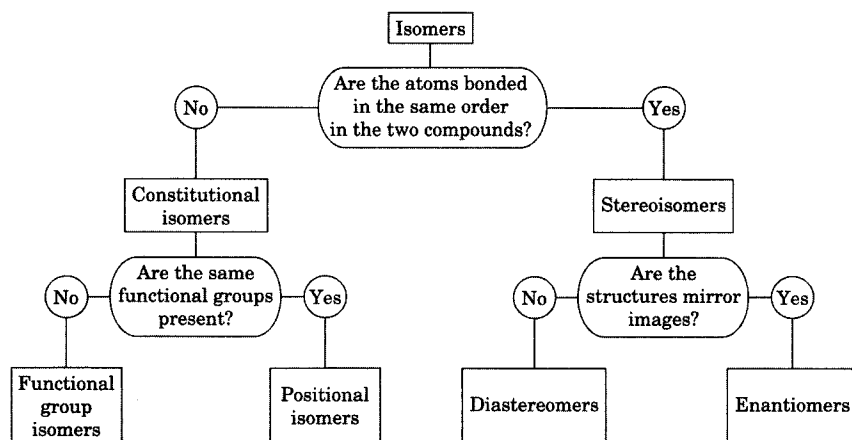


FIGURE 2.5
Relationships among isomers.

on how rapidly they are interconverted under given conditions. As an example, the interconversion of the axial and equatorial conformations of methylcyclohexane has a ΔG^\ddagger of only about 11 kcal/mol at 25°. ^{14–16} Thus, we do not consider them to be isomers because they rapidly interconvert at room temperature. Typically, the ΔG^\ddagger for an isomerization reaction must be greater than about 23 kcal/mol in order for us to be able to isolate two species in equilibrium. ¹⁷

We may describe isomers as being either **constitutional isomers**, ¹⁸ which are pairs of compounds that have the same atoms connected in different ways, or as **stereoisomers**, which are molecules with the same order of bonding but with different spatial relationships among the atoms (Figure 2.5). ^{19,20} We may further divide constitutional isomers into **functional group isomers**, in which the same atoms are used to form different functional groups, and **positional isomers**, in which the same functional groups are present but are located in different positions in the two structures. Ethanol and dimethyl ether are functional group isomers, while 1-chloropropane and 2-chloropropane are positional isomers.

Enantiomers are stereoisomers that are nonsuperimposable mirror images. Such structures are said to be **chiral**, that is, “handed,” and to possess

¹⁴ Piercy, J. E.; Subrahmanyam, S. V. *J. Chem. Phys.* **1965**, *42*, 4011; Aliev, A. E.; Harris, K. D. M. *J. Am. Chem. Soc.* **1993**, *115*, 6369; Fernández-Alonso, M. C.; Cañada, J.; Jiménez-Barbero, J.; Cuevas, G. *ChemPhysChem* **2005**, *6*, 671.

¹⁵ Conformational terms are discussed in Chapter 3. For a discussion of the concept of isomerism, see Eliel, E. L. *Isr. J. Chem.* **1976/77**, *15*, 7 and reference 2.

¹⁶ At much lower temperatures, conformational change is slowed. For example, Jensen, F. R.; Bushweller, C. H. *J. Am. Chem. Soc.* **1966**, *88*, 4279 studied pure equatorial chlorocyclohexane by NMR at -151°C.

¹⁷ Kalinowski, H.-O.; Kessler, H. *Top. Stereochem.* **1973**, *7*, 295.

¹⁸ Constitutional isomers are sometimes called *structural isomers*, but that term has been criticized because stereoisomerism may be considered to be a component of the structure of a molecule. In the 1974 IUPAC nomenclature rules (reference 84), the term *structural* is “abandoned as insufficiently specific.”

¹⁹ For a discussion of stereochemical nomenclature, see Eliel, E. L. *J. Chem. Educ.* **1971**, *48*, 163.

²⁰ A more detailed flow chart of isomeric relationships was given by Black, K. A. *J. Chem. Educ.* **1990**, *67*, 141.

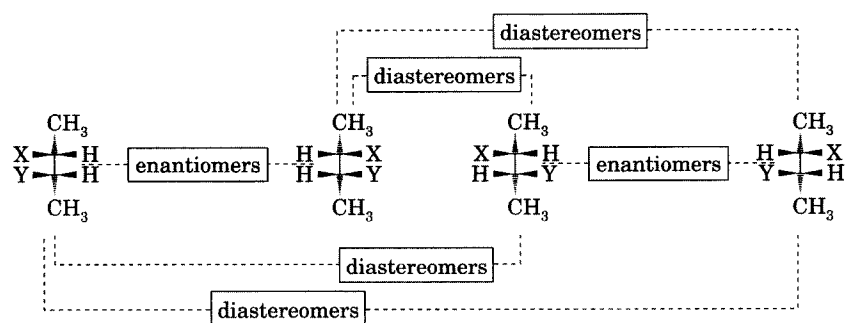
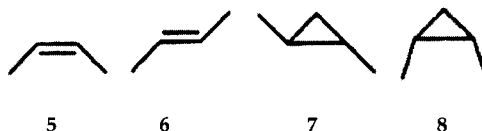


FIGURE 2.6
Stereoisomeric relationships
among 2,3-disubstituted butanes.

the property of **chirality**.^{21,22} **Diastereomers** are stereoisomers that are not mirror images. These terms are illustrated in Figure 2.6 for a 2,3-disubstituted butane. Note that a structure can have only one enantiomer, but it may have more than one diastereomer. The term diastereomers also includes stereoisomers called **cis,trans isomers** (formerly **geometric isomers**) such as *cis*- and *trans*-2-butene (5 and 6) and *cis*- and *trans*-1,2-dimethylcyclopropane (7 and 8). In each case there is no interconversion of the two isomers at room temperature because a structural feature such as a double bond or a ring prevents rotation about a carbon-carbon bond.



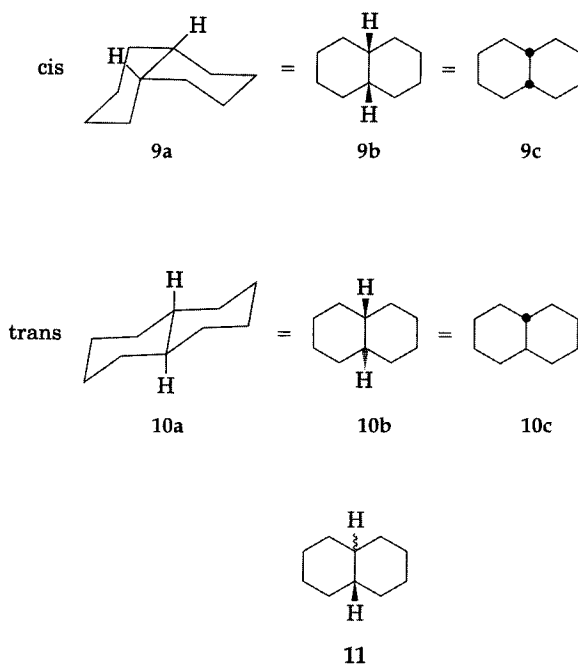
The representation of stereoisomerism in large structures can be cumbersome. For example, the *cis* and *trans* isomers of decalin (decahydronaphthalene) could be represented by the line drawings on the left (9a and 10a, respectively) in Figure 2.7. We could show them more compactly as structures 9b and 10b. These drawings convey the same information about the ring fusion but do not explicitly show the conformations of each six-membered ring. To make the drawings even simpler, we adopt the convention that a solid dot represents a hydrogen atom coming out of the plane of the molecule toward the viewer, as shown by 9c and 10c. The price of representational simplicity is a greater necessity to understand the implicit meaning of such drawings. Otherwise, important stereochemical features may be unrecognized. If the stereochemistry at a particular atom is not known, then we may represent the bond to a substituent with a wavy line, denoted a ξ -bond (pronounced “xi-bond”), as in 11.

Symmetric, Asymmetric, Dissymmetric, and Nondissymmetric Molecules

Before continuing the discussion of molecular structures that exhibit enantiomerism, it will be useful to review some designations of molecular

²¹ The word *chirality* is attributed to Lord Kelvin (reference 42).

²² Mezey, P. G., Ed. *New Developments in Molecular Chirality*; Kluwer Academic Publishers: Dordrecht, Netherlands, 1991.

**FIGURE 2.7**

Representations of decalin isomers.

symmetry.^{23–26} A **symmetry element** corresponds to a plane, point, or line about which we could (at least in principle) carry out a **symmetry operation** on a structure, the result of which would be a structure equivalent to the original one. Four types of symmetry operations (with their associated symmetry elements indicated in parentheses) need to be considered:²³

1. reflection in a plane of symmetry (σ)
2. inversion of all atoms through a center of symmetry (center of inversion, i)
3. rotation about a proper axis (C_n)
4. rotation about an improper axis (S_n , corresponding to rotation about an axis followed by reflection through a plane perpendicular to that axis)

A C_n symmetry element means that there is an axis through the structure such that a $360^\circ/n$ rotation about the axis produces a structure that appears identical to the original. A C_2 axis (also termed a twofold rotation axis) means that a 180° rotation produces a structure identical to the original structure. *cis*-2-Butene (Figure 2.8) has a C_2 rotation axis. It also has two planes of symmetry, and both are denoted vertical planes of symmetry (σ_v) because they include the C_2 rotation axis. To distinguish between them, one is denoted as σ_v and the

²³ Cotton, F. A. *Chemical Applications of Group Theory*, 2nd ed.; Wiley-Interscience: New York, 1971.

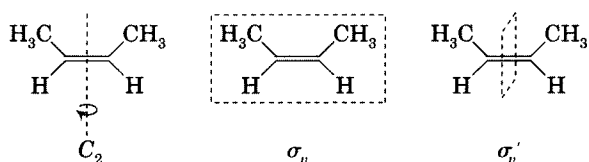
²⁴ Orchin, M.; Jaffé, H. H. *Symmetry, Orbitals and Spectra* (S. O. S.); Wiley-Interscience: New York, 1971; pp. 91–136.

²⁵ Juaristi, E. *Introduction to Stereochemistry and Conformational Analysis*; Wiley-Interscience: New York, 1991.

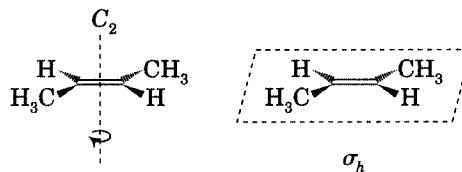
²⁶ Heilbronner, E.; Dunitz, J. D. (Pfalzberger, R., illus.) *Reflections on Symmetry*; Verlag Helvetica Chimica Acta: Basel, 1993.

FIGURE 2.8

C_2 (left), σ_v (center), and σ_v' (right) symmetry elements in *cis*-2-butene.

**FIGURE 2.9**

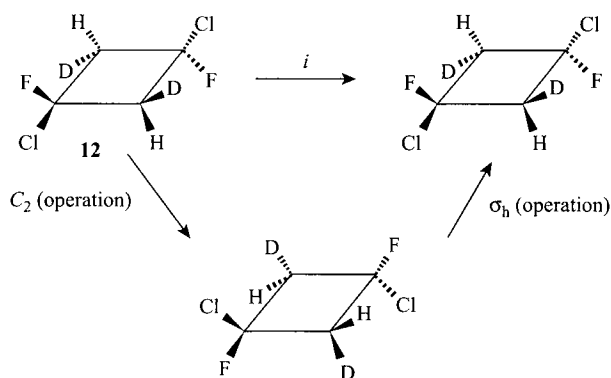
C_2 (left) and σ_h (right) symmetry elements in *trans*-2-butene.



other one is designated σ_v' . *trans*-2-Butene (Figure 2.9) has a C_2 rotation axis and a plane of symmetry that is denoted a horizontal plane of symmetry (σ_h) because it is perpendicular to the C_2 rotation axis.

If a center of inversion (i) is present, reflecting each atom through the center of the molecule produces a structure equivalent to the starting structure.²⁷ This process is illustrated in the top portion of Figure 2.10 for a cyclobutane derivative (12).

A C_n axis is said to be a **proper** rotation axis. An **improper axis**, S_n , exists when equivalency is restored by carrying out two operations consecutively: a rotation about a proper axis, C_n , followed by reflection through a plane perpendicular to that axis. In the cyclobutane shown in Figure 2.10, for example, a C_2 rotation about an axis perpendicular to the plane of the four carbon atoms, followed by a reflection through the plane containing the four carbon atoms, produces a structure identical to the starting structure.²⁸ Note that neither the C_2 rotation axis nor the σ_h reflection symmetry element is

**FIGURE 2.10**

Examples of symmetry operations on a cyclobutane derivative.

²⁷ More precisely, the process of inversion through a point with coordinates of (0,0,0) moves each atom at point (x, y, z) to point ($-x, -y, -z$); see reference 23.

²⁸ As we will discuss in Chapter 3, cyclobutane is slightly puckered. However, the planar form is taken to represent the time average of the accessible conformations, so this representation of the structure is used for symmetry analysis.

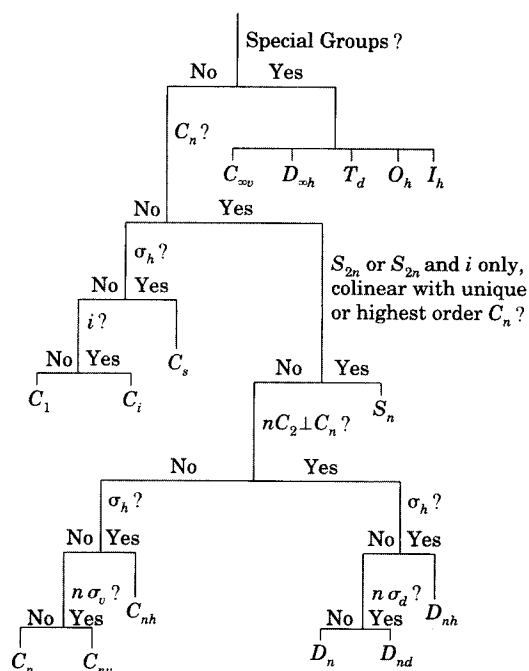


FIGURE 2.11
Point group classification scheme.
(Adapted from reference 31.)

individually present in **12**.²⁹ It is only the combination of the C_2 and σ_h operations that produces a structure equivalent to the original.

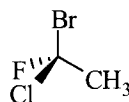
We commonly describe the symmetry of a structure in terms of a **point group**, which is a symmetry designator determined by the number and kind of symmetry elements present in that structure. Structure **12** belongs to the point group C_i . The point group D_n includes structures that contain a C_n plus n C_2 elements perpendicular to the C_n axis. The point group D_{nh} includes structures that contain a C_n , n C_2 elements perpendicular to the C_n axis, and a σ_h . For the sake of completeness, we define an identity operator, E , that does not move any part of the structure.³⁰ It is convenient to think of a structure that has only the E element as belonging to point group C_1 , since the only operation that restores the original structure is a 360° rotation. Details about the designation of point groups are provided in references 23 and 24, and a classification scheme for point group designations is reproduced in Figure 2.11.³¹ In this scheme, each vertical line represents a question. (For example, the notation " C_n ?" means "Is there a C_n axis?") If the answer to the question is yes, the scheme moves along the right line below that question. If the answer is no, the scheme moves along the left line below the question.

²⁹ We may carry out any symmetry operation on any structure, whether or not the corresponding symmetry element is present in the structure. If the symmetry element is present, then the operation produces a structure in which every point is oriented the same as an equivalent point in the starting structure. If the symmetry element is not present, then the result of carrying out the symmetry operation is a structure that is *not* equivalent to the starting structure.

³⁰ The E operator is also called I (reference 24).

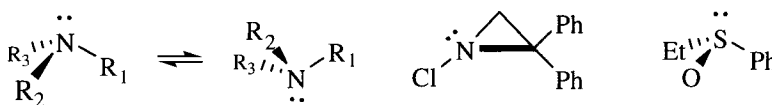
³¹ Carter, R. L. *J. Chem. Educ.* **1968**, *45*, 44.

Point group designations facilitate discussions of chirality. We usually think first of molecules that show enantiomerism as being **asymmetric**³² (without symmetry) due to the presence of a carbon atom with four different substituents, as illustrated by the 1-bromo-1-chloro-1-fluoroethane isomer **13**. More generally, asymmetric structures have three or more nonequivalent substituents bonded to a central atom in such a way that the central atom and the substituents do not all lie in the same plane.³³ Such structures are said to exhibit enantiomerism due to asymmetry about a point and belong to point group C_1 .³⁴



13

A nitrogen atom with three different substituents meets the formal requirement for asymmetry stated above if the nonbonded pair of electrons is considered to be a fourth substituent. Ordinarily, however, trialkylamines are not optically active, because rapid inversion produces a mirror image structure (**14**).³⁵ Inversion can be slowed by incorporating the nitrogen into a three-membered ring and by substituting halogen for hydrogen on the nitrogen atom. As a result, the barrier to inversion of *N*-chloroaziridines is about 25 kcal/mol.³⁶ For example, 1-chloro-2,2-diphenylaziridine (**15**) has been isolated as a single enantiomer.³⁷ Similarly, the phenyl ethyl sulfoxide **16** can be resolved due to slow inversion at the sulfur.³⁸



14

15

16

³² It is a common mistake to misspell this word "assymmetric."

³³ In some cases, the central atom may have more than four substituents. In particular, metal complexes may be chiral due to the pattern of ligands about the central atom.

³⁴ Structures that belong to point group C_1 are chiral, whether or not there are four different groups bonded to a central atom. For example, Hamill, H.; McKerverey, M. A. *Chem. Commun.* **1969**, 864 reported the synthesis of a chiral structure, 3-methyl-5-bromoadamantanecarboxylic acid, in which the center of chirality is a point in the center of the adamantane skeleton.

³⁵ For reviews, see Binsch, G. *Top. Stereochem.* **1968**, 3, 97; Lambert, J. B. *Top. Stereochem.* **1971**, 6, 19.

³⁶ Shustov, G. V.; Kachanov, A. V.; Korneev, V. A.; Kostyanovsky, R. G.; Rauk, A. J. *Am. Chem. Soc.* **1993**, 115, 10267.

³⁷ Brückner, S.; Forni, A.; Moretti, I.; Torre, G. J. *Chem. Soc., Chem. Commun.* **1982**, 1218. Diaziridines can also be optically active: Dyachenko, O. A.; Atovmyan, L. O.; Aldoshin, S. M.; Polyakov A. E.; Kostyanovskii, R. G. *J. Chem. Soc., Chem. Commun.* **1976**, 50 and references therein.

³⁸ Kobayashi, M.; Kamiyama, K.; Minato, H.; Oishi, Y.; Takada, Y.; Hattori, Y. *J. Chem. Soc. D Chem. Commun.* **1971**, 1577.

In addition to molecules belonging to point group C_1 , there are structures that exhibit enantiomerism but which do have some symmetry.³⁹ Therefore, the more precise statement of the requirement for enantiomerism is *dissymmetry*. That is the Anglicized form of *dissymmetrie*, a word coined by Pasteur to describe a structure that is not superimposable on its mirror image.^{40–42} Thus, all chiral molecules are **dissymmetric**.⁴³ Not all dissymmetric molecules are asymmetric, however. Any structure is chiral if it does not have an improper rotation axis (S_n)—that is, if it belongs to point group C_n or D_n .⁴⁴ Structures belonging to point group C_1 are both asymmetric and dissymmetric, while structures belonging to other C_n point groups are dissymmetric but not asymmetric. Some examples of chiral C_n structures are compounds **17**⁴⁵ (C_2) and **18**⁴⁶ (C_6). Chiral structures with D_n symmetry include **19**⁴⁷ and **20**⁴⁸, which have D_2 symmetry, as well as **21**,⁴⁹ which has D_3 symmetry.^{50,51}

³⁹ For a compilation of chiral structures, including structures categorized according to point groups, see Klyne, W.; Buckingham, J. *Atlas of Stereochemistry*, 2nd ed.; Oxford University Press: New York, 1978.

⁴⁰ Pasteur, L. *Researches on the Molecular Asymmetry of Natural Organic Products*; Alembic Club Reprint No. 14, William F. Clay: Edinburgh, 1897. See also Shallenberger, R. S.; Wienen, W. J. *J. Chem. Educ.* **1989**, *66*, 67.

⁴² Barron, L. D. *J. Am. Chem. Soc.* **1986**, *108*, 5539 noted that there is a difference between the words *dissymmetry* and *chirality*, since dissymmetry is the *absence* of certain symmetry elements, while chirality is the *presence* of the attribute of handedness. However, Mislow defined chirality as the “absence of reflection symmetry” and investigated the quantification of chirality: Buda, A. B.; Auf der Heyde, T.; Mislow, K. *Angew. Chem. Int. Ed. Engl.* **1992**, *31*, 989. Zabrodsky, H.; Peleg, S.; Avnir, D. *J. Am. Chem. Soc.* **1993**, *115*, 8278 treated symmetry as a continuous and quantifiable property rather than as a “yes or no” condition. Zabrodsky, H.; Avnir, D. *J. Am. Chem. Soc.* **1995**, *117*, 462 gave a quantitative definition of chirality. See also the discussion in reference 22, pp. 241–256.

⁴³ The terms *dissymmetric* and *chiral* are synonymous. *Nondissymmetric* and *achiral* are also synonyms.

⁴⁴ For a more detailed discussion and a proof of this statement, see reference 23.

⁴⁵ Banks, R. B.; Walborsky, H. M. *J. Am. Chem. Soc.* **1976**, *98*, 3732.

⁴⁶ Farina, M.; Morandi, C. *Tetrahedron* **1974**, *30*, 1819 presented a general discussion of chiral molecules with high symmetry.

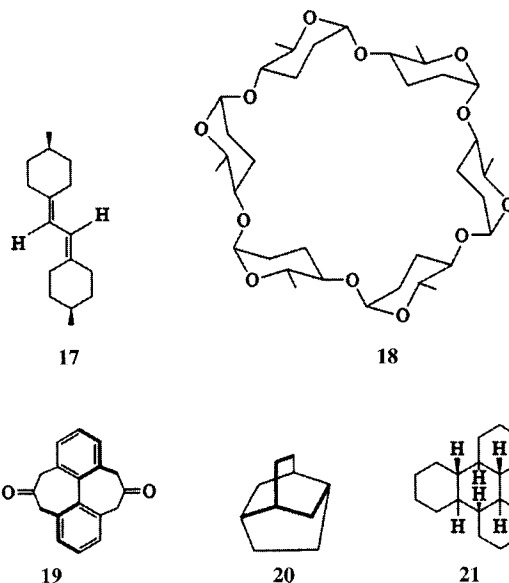
⁴⁷ Mislow, K.; Glass, M. A. W.; Hopps, H. B.; Simon, E.; Wahl, G. H., Jr. *J. Am. Chem. Soc.* **1964**, *86*, 1710.

⁴⁸ Tichý, M. *Collect. Czech. Chem. Commun.* **1974**, *39*, 2673.

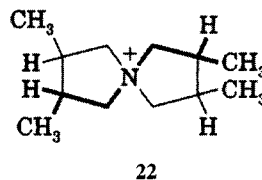
⁴⁹ Farina, M.; Audisio, G. *Tetrahedron* **1970**, *26*, 1827, 1839.

⁵⁰ Chiral cage-shaped molecules with high symmetry were reviewed by Naemura, K. in Osawa, E.; Yonemitsu, O., Eds. *Carbocyclic Cage Compounds: Chemistry and Applications*; VCH Publishers: New York, 1992; pp. 61–90.

⁵¹ A particularly interesting D_3 structure is that reported for an isomer of the fullerene C_{78} , a chiral structure composed only of carbon atoms: Diederich, F.; Whetten, R. L.; Thilgen, C.; Ettl, R.; Chao, I.; Alvarez, M. M. *Science* **1991**, *254*, 1768. The C_{76} fullerene was isolated in enantiomeric form by kinetic resolution: Hawkins, J. M.; Meyer, A. *Science* **1993**, *260*, 1918.



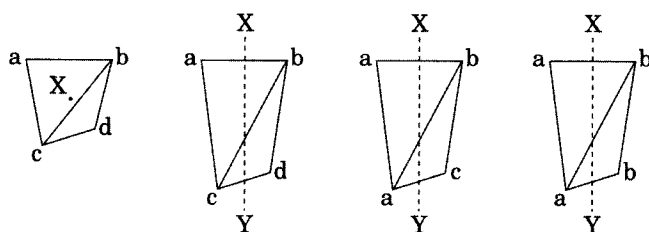
A structure with C_i , C_s , C_{nv} , C_{nh} , D_{nd} , D_{nh} , T_d , O_h , or S_n symmetry is **achiral**, that is, **nondissymmetric**.⁵² Of particular interest are structures with S_n symmetry. As shown in Figure 2.10, the S_2 operation is identical to inversion (i). The S_1 operation is identical to σ . It is frequently said that structures having a σ or i symmetry element are achiral, but this statement is incomplete. Any structure belonging to an S_n point group is nondissymmetric, whether or not it contains a mirror plane or a center of inversion. An example is the achiral 3,4,3',4'-tetramethylspiro(1,1')bipyrrolidinium ion **22**, which has S_4 symmetry.⁵³



Some structures are said to have chirality about an axis, which can be considered to be one of the rotational axes in a more symmetric structure that no longer exists because substituents have been moved due to "stretching" of

⁵² For further discussions of the relationship of point groups to chirality, see Mislow, K. *Introduction to Stereochemistry*; W. A. Benjamin: New York, 1966; p. 33; reference 41; reference 178; Harris, D. C.; Bertolucci, M. D. *Symmetry and Spectroscopy*; Oxford University Press: New York, 1978; p. 9.

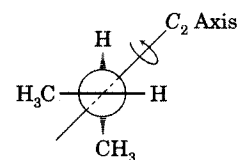
⁵³ McCasland, G. E.; Proskow, S. *J. Am. Chem. Soc.* **1955**, *77*, 4688; **1956**, *78*, 5646. It is interesting to note that **22** was reported to be "optically inactive within experimental error." The observed specific rotation of **22** was found to be $[\alpha]_D^{30} + 0.012^\circ$ (water, c 5, l 0.5) when prepared from one precursor and $[\alpha]_D^{30} - 0.027^\circ$ when prepared from the enantiomeric precursor. The small optical activities apparently resulted from trace impurities in the final products.

**FIGURE 2.12**

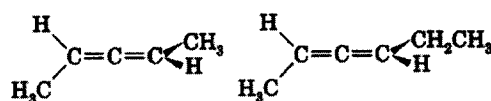
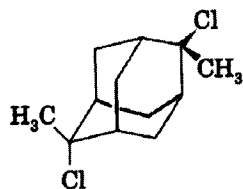
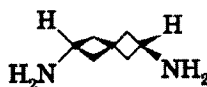
Stretching a structure with chirality about a point to produce structures with chirality about an axis. (Adapted from reference 55.)

the axis.^{54,55} The structure on the left in Figure 2.12 is chiral about a point (near the letter X). Stretching the figure as indicated involves motion in a direction along the line XY, which is the axis of chirality. It should be stressed that the four substituents no longer have to be different to produce chirality. Indeed, all three of the elongated structures are chiral.

Chirality about an axis is exemplified by allenes, such as the 2,3-pentadiene enantiomer **23**.^{56,57} In **23** the methyl and hydrogen substituents on C2 lie in a plane (in the page) that is perpendicular to the plane containing the methyl and hydrogen substituents on C4. Here the axis of chirality is coincident with the C2–C3–C4 bond axis. The structure has a C_2 symmetry element, so it is dissymmetric, not asymmetric. The C_2 rotation axis is perpendicular to the axis of chirality, as illustrated in Figure 2.13.⁵⁸ It must be emphasized that not all structures that are chiral about an axis have a C_2 rotation axis. For example, the 2,3-hexadiene enantiomer **24** also has an axis of chirality coincident with the C2–C3–C4 bond axis, but it does not have a C_2 rotation axis. The adamantane **25** and appropriately substituted spiro compounds, such as **26**, are also chiral about an axis.⁵⁹

**FIGURE 2.13**

C_2 axis in **23**.

**23****24****25****26**

⁵⁴ For illustrations and examples of both an axis of chirality and a plane of chirality, see Prelog, V. (with Cahn, R. S.) *Chem. Brit.* **1968**, 4, 382. See also Prelog, V. *Science* **1976**, 193, 17.

⁵⁵ Cahn, R. S. *J. Chem. Educ.* **1964**, 41, 116.

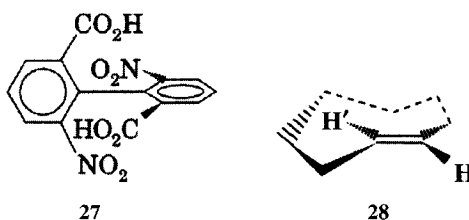
⁵⁶ Jones, W. M.; Walbrick, J. M. *Tetrahedron Lett.* **1968**, 5229; Waters, W. L.; Caserio, M. C. *Tetrahedron Lett.* **1968**, 5233.

⁵⁷ For a review of the chirality of allenes, see Runge, W. in Patai, S., Ed. *The Chemistry of Ketenes, Allenes and Related Compounds*, Part 1; Wiley-Interscience: Chichester, England, 1980; pp. 99–154.

⁵⁸ For a discussion of the C_2 axis and the axis of chirality in such systems, see Bassindale, A. *The Third Dimension in Organic Chemistry*; John Wiley & Sons: Chichester, England, 1984; pp. 34, 104.

⁵⁹ Hulshof, L. A.; Wynberg, H.; van Dijk, B.; de Boer, J. L. *J. Am. Chem. Soc.* **1976**, 98, 2733.

In examples 23–26, chirality about an axis was enforced by rings or double bonds. Some molecules may be dissymmetric due to restricted rotation about a carbon–carbon single bond. Compounds such as the biphenyl 27⁶⁰ are called **atropisomers**, since they are resolvable only because the activation energy for rotating about the biphenyl single bond is large due to steric hindrance of the pairs of ortho substituents.⁶¹ Although there can be some variation in the angle that the plane of one phenyl group makes with respect to the plane of the other phenyl, any particular conformation of 27 has a C_2 rotation axis and is dissymmetric. As noted in the case of allenes, a C_2 rotation axis *may* be present in a molecule that is chiral about an axis, but it is not required. Replacing one of the CO_2H groups of 27 with a CH_2OH group would remove the C_2 rotation axis, but the structure would still be chiral about an axis.



We may consider a plane to be an element of chirality if part of a structure lies in the plane but other parts of the structure leave the plane so as to produce chirality. An example is *trans*-cyclooctene (28), which is chiral with respect to a plane that includes the two double-bonded carbon atoms and *one* of the carbon atoms adjacent to the double bond.^{62,63} More than one chain can pass through the double bond, as illustrated by “[8.10]-betweenanene” (29).^{64,65} Another example is the [6]paracyclophane 30, in which the plane of chirality can be defined by the three positions marked with an asterisk.⁶⁶ In many cases we may consider the chiral element to be either an axis or a plane, and Schlögl has noted the difficulty in defining a plane of chirality.⁶⁶ Helical (threaded) structures can also be considered chiral with

⁶⁰ Newman, P.; Rutkin, P.; Mislow, K. J. *Am. Chem. Soc.* **1958**, *80*, 465.

⁶¹ (a) Ōki, M. *Top. Stereochem.* **1983**, *14*, 1 and references therein; (b) Ōki, M. *The Chemistry of Rotational Isomers*; Springer-Verlag: Berlin, 1993.

⁶² The (+) enantiomer had $[\alpha]_D^{25} + 414^\circ$ (c 0.55, methylene chloride). Cope, A. C.; Ganellin, C. R.; Johnson, H. W. Jr.; Van Auken, T. V.; Winkler, H. J. S. *J. Am. Chem. Soc.* **1963**, *85*, 3276.

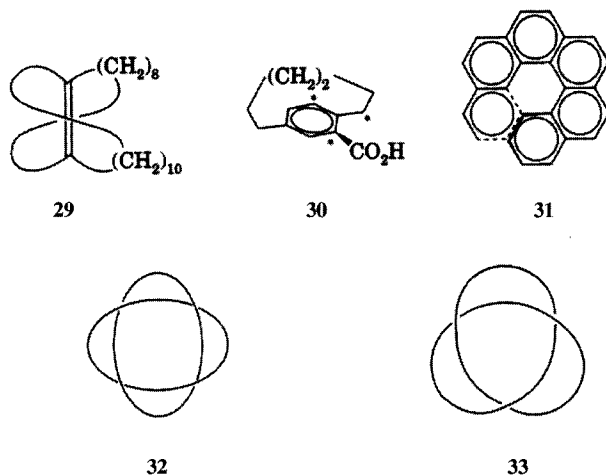
⁶³ In an X-ray crystal study, (–)-*trans*-cyclooctene was found to have the *R* configuration, and the twist angle of the carbon–carbon double bond was estimated to be 43.5° . Manor, P. C.; Shoemaker, D. P.; Parkes, A. S. *J. Am. Chem. Soc.* **1970**, *92*, 5260.

⁶⁴ Marshall, J. A. *Acc. Chem. Res.* **1980**, *13*, 213 and references therein.

⁶⁵ For a discussion of the stereochemistry of these and other structures with twisted double bonds, see Nakazaki, M.; Yamamoto, K.; Naemura, K. *Top. Curr. Chem.* **1984**, *125*, 1.

⁶⁶ Schlögl, K. *Top. Curr. Chem.* **1984**, *125*, 27. (This example is adapted from the discussion on pp. 30–31.)

respect to either an axis or a plane, as in the case of hexahelicene (**31**).^{67–70} Catenanes (structures formed by interlocking rings) can be chiral, as exemplified by the doubly interlocked **32**.⁷¹ Structure **33**, a trefoil knot, is also chiral.^{72–74} Schill and Sauvage provided a detailed account of the occurrence, synthesis, and chirality of these and other novel molecular structures.^{75,76}



Designation of Molecular Configuration

Chirality About a Point

The goal of organic nomenclature is to provide concise and unambiguous identification of the structures of organic compounds. An important aspect of structure is **configuration**—the three-dimensional arrangement of atoms that characterizes a particular stereoisomer. The most generally used system for specifying configuration is the *R* (for *rectus*) and *S* (for *sinister*) system, which

⁶⁷ Resolution of racemic **31** through formation of diastereotopic charge transfer complexes with optically active 2-(2,4,5,7-tetranitro-9-fluorenylideneaminoxy)propionic acid produced (–)-**31** with $[\alpha]_D^{24} -3640^\circ$ (CHCl₃). Newman, M. S.; Lutz, W. B.; Lednicer, D. *J. Am. Chem. Soc.* **1955**, *77*, 3420.

⁶⁸ Newman, M. S.; Lednicer, D. *J. Am. Chem. Soc.* **1956**, *78*, 4765.

⁶⁹ For leading references to the racemization of chiral hexahelicene derivatives, see Prinsen, W. J. C.; Hajee, C. A. J.; Laarhoven, W. H. *Polycyclic Aromatic Compounds* **1990**, *1*, 21.

⁷⁰ An X-ray crystal structure confirmed the helical structure of the molecule: Mackay, I. R.; Robertson, J. M.; Sime, J. G. *J. Chem. Soc. D Chem. Commun.* **1969**, 1470.

⁷¹ For a discussion and a report of the synthesis of a doubly interlocked catenane, see Nierengardt, J.-F.; Dietrich-Buchecker, C. O.; Sauvage, J.-P. *J. Am. Chem. Soc.* **1994**, *116*, 375. For a discussion of knots in proteins, see Liang, C.; Mislow, K. *J. Am. Chem. Soc.* **1994**, *116*, 11189.

⁷² Krow, G. *Top. Stereochem.* **1970**, *5*, 59 ff.

⁷³ Boeckmann, J.; Schill, G. *Tetrahedron* **1974**, *30*, 1945.

⁷⁴ For assignment of *R* or *S* designations to molecular knots, see Mezey, P. G. *J. Am. Chem. Soc.* **1986**, *108*, 3976.

⁷⁵ Schill, G. in Boeckmann, J., trans. *Catenanes, Rotaxanes and Knots*; Academic Press: New York, 1971.

⁷⁶ See also Sauvage, J.-P. *Acc. Chem. Res.* **1990**, *23*, 319.

was introduced by Cahn, Ingold, and Prelog (CIP).⁷⁷⁻⁷⁹ For a chiral molecule with four different substituents bonded to a tetrahedral carbon atom, one begins by assigning priorities to the substituents.⁸⁰ Next, one views the structure (i.e., a drawing or a model of it) in such a way that the substituent with the lowest priority is held away from one's eye. One then considers the other three substituents. If one's eye traces a clockwise ("to the right") pattern while looking from the highest priority substituent to the second highest and then to the third highest, the configuration is said to be *R*. If, however, the substituents are arranged such that looking from highest priority to second priority to third priority traces a counterclockwise pattern, the configuration is *S*. The *R* and *S* designations therefore indicate **absolute configuration**—the arrangement of atoms in space that distinguishes a structure from its enantiomer.²

The priorities of substituents are determined according to a detailed set of criteria, some of which are presented here.⁸¹ The highest priority substituent is the one with the highest atomic number. If the chiral center has two identical atoms bonded to it, then one considers the substituents for each of them and assigns priority to the atom that has the higher priority substituent.⁸² Thus, $-\text{CH}_2\text{Br}$ takes priority over $-\text{CH}_2\text{Cl}$ because the atomic number of bromine is greater than that of chlorine. Similarly, $-\text{CH}_2\text{CH}_2\text{Cl}$ is higher in priority than $-\text{CH}_2\text{CH}_2\text{F}$. Priority is determined at the point of first difference between substituents, so the group $-\text{CH}_2\text{CHFCH}_3$ is higher in priority than the group $-\text{CH}_2\text{CH}_2\text{CH}_2\text{Cl}$.

C2 of 1,1,3-trichloro-2-methylpropane (**34**) has two substituents on which chlorine is the highest atomic number atom. Priority between them cannot be assigned on the basis of atomic number, since both carbon atoms have a chlorine as the substituent with the highest atomic number. In that case we count the number of substituents with the highest atomic number. Thus, the group $-\text{CHCl}_2$ has priority over $-\text{CH}_2\text{Cl}$, since there are two chlorine atoms on $-\text{CHCl}_2$. This counting is used only in the case of ties based on atomic number. The $-\text{CH}_2\text{Br}$ substituent in 3-bromo-1,1-dichloro-2-methylpropane (**35**) has higher priority than the $-\text{CHCl}_2$ group because bromine has a higher atomic number than chlorine. The fact that there are two chlorine atoms in the $-\text{CHCl}_2$ group does not matter.

⁷⁷ Cahn, R. S.; Ingold, C. K.; Prelog, V. *Experientia* **1956**, *12*, 81; *Angew. Chem. Int. Ed. Engl.* **1966**, *5*, 385.

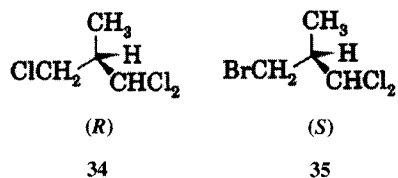
⁷⁸ For proposed modifications of the Cahn-Ingold-Prelog system, see Dodziuk, H.; Mirowicz, M. *Tetrahedron: Asymmetry* **1990**, *1*, 171; Dodziuk, H. *Tetrahedron: Asymmetry* **1992**, *3*, 43; Mata, P.; Lobo, A. M.; Marshall, C.; Johnson, A. P. *Tetrahedron: Asymmetry* **1993**, *4*, 657.

⁷⁹ In this context, the Latin word *rectus* is often said to mean "right." As Todd and Koga noted, *rectus* means "straight" or "proper" and *dexter* means "right." The word *sinister* does mean "left." Compare Todd, D. J. *Chem. Educ.* **1987**, *64*, 732; Koga, G. *Chem. Eng. News* **1988** (Apr 4), 3.

⁸⁰ Priorities are often indicated numerically. Some authors use the numbers 1-4 (or I-IV) with 4 (IV) being highest priority, but others use the same numbers with 1 (I) being highest priority. To avoid confusion, we will use the letters A-D, with A being highest priority.

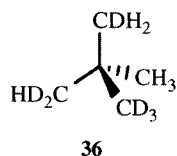
⁸¹ Additional criteria apply to situations not considered in the present discussion. Details are provided in reference 77.

⁸² The term *chirality center* is also used. For a discussion of stereochemical nomenclature, see Wade, L. G., Jr. *J. Chem. Educ.* **2006**, *83*, 1793. Also see the discussion by Mislow, K. *Chirality* **2002**, *14*, 126.

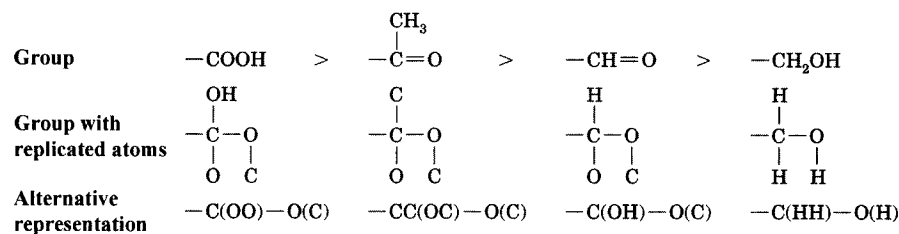


Counting the number of substituents with a given atomic number is also important when substituents have double or triple bonds. In such a case, the multiple-bonded atoms are considered to be replicated. For example, Figure 2.14 shows that $-\text{CO}_2\text{H}$ is considered to be $-\text{C}(\text{OO})-\text{O}(\text{C})$, so it has priority over $-\text{COCH}_3$, which in turn is higher in priority than $-\text{CHO}$.

If two substituents are identical except for isotopic substitution, then the substituent having an isotope with the greater atomic mass takes priority over the substituent with the isotope of lower atomic mass. Therefore, the group $-\text{CH}_2\text{D}$ is higher in priority than the group $-\text{CH}_3$, and the group $-\text{CH}_2-\text{CH}_2-^{13}\text{CH}_3$ is higher in priority than the group $-\text{CH}_2-\text{CH}_2-\text{CH}_3$. As an example, the deuterated neopentane **36** has the *R* configuration because the priorities are $\text{CD}_3 > \text{CHD}_2 > \text{CH}_2\text{D} > \text{CH}_3$.⁸³ Note that isotopic substitution is considered only when no other criteria apply. For example, the group $-\text{CH}_2-\text{CH}_2-\text{F}$ takes priority over the group $-\text{CD}_2-\text{CH}_3$. A more detailed discussion of priorities appears in the IUPAC nomenclature rules,⁸⁴ and a listing of groups in order of priority was given by Klyne and Buckingham.³⁹



The *R* and *S* nomenclature system is very useful in naming biological products such as α -tocopherol. Natural vitamin E is $(2R,4'R,8'R)$ - α -tocopherol (**37**), but commercial vitamin capsules contain the acetates of both the natural vitamin and of $(2S,4'R,8'R)$ - α -tocopherol. Both acetates are hydrolyzed to the phenol in the intestine before absorption into the body, but the acetate of natural vitamin E is hydrolyzed more rapidly.⁸⁵

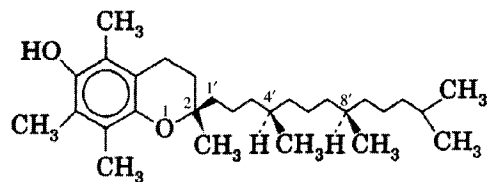
**FIGURE 2.14**

Priorities for carbon atoms with double bonds to oxygen. (Adapted from reference 55.)

⁸³ Haesler, J.; Schindelholz, I.; Riguët, E.; Bochet, C. G.; Hug, W. *Nature* **2007**, *446*, 526.

⁸⁴ Rigaudy, J.; Klesney, S. P. *Nomenclature of Organic Chemistry*; Pergamon Press: Oxford, England, 1979; pp. 486–490.

⁸⁵ Ingold, K. U. *Aldrichim. Acta* **1989**, *22*, 69.



37

Chirality About an Axis or a Plane

The *R* and *S* nomenclature system can also be used for structures with an axis or plane of chirality if we apply the additional rule that substituents on the end of an axis or on the surface of a plane nearer the observer are arbitrarily given higher priority than those further away. Some authors augment the *R* and *S* labels in order to specify that the designation applies to axial or planar chirality, so the terms *R_a* and *S_a* (or *aR* and *aS*) for axial chirality and *R_p* and *S_p* (or *pR* and *pS*) for planar chirality also appear in the literature.^{11,86}

As an example, let us consider the enantiomer of glutinic acid **38a** (Figure 2.15).⁸⁷ Viewing the structure along the C=C=C axis from the right of the drawing (as indicated by the "eye" symbol) would produce the image **38b**. Using the rule that near groups precede far groups in priority, we first assign highest priority (A) to the CO₂H group and second priority (B) to the hydrogen substituent on the near carbon atom. The CO₂H group on the far carbon atom is third priority (C), and the hydrogen substituent on that carbon atom is lowest in priority (D). Now we determine the configuration as we would for a chiral carbon having the same substituents with priorities A, B, C, and D bonded to it. Thus, the structure is determined to be *R*.

As another example, consider the biphenyl **27** shown in Figure 2.16(a).⁶⁰ Viewing the three-dimensional representation from the perspective indicated by the top eye symbol would produce the image in Figure 2.16(b).⁸⁸ Again, assigning the two "near" groups higher priority than the two far ones, the structure is found to be *S*. It may not be immediately obvious, but choice of perspective of the original structure does not affect the designation. Viewing

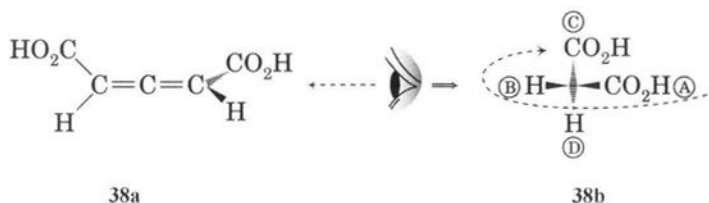


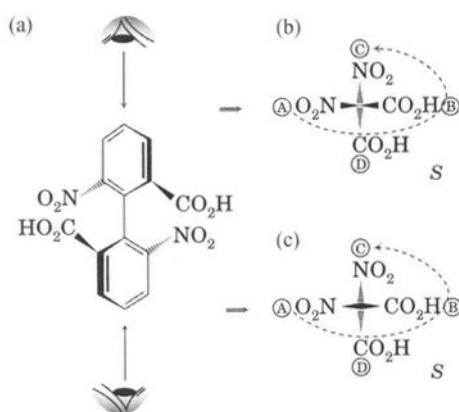
FIGURE 2.15

Determination of configuration of **38**.

⁸⁶ For a discussion of the designation of axial and planar chirality, see Nader, N.-P. *Chem. Educ. J.* **2006**, *9*, 6.

⁸⁷ Agosta, W. C. *J. Am. Chem. Soc.* **1964**, *86*, 2638.

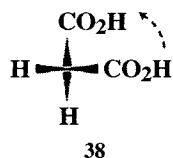
⁸⁸ Note that viewing **27** so that the NO₂ and CO₂H groups are horizontal on the near phenyl ring and vertical on the far phenyl ring requires a slight rotation of the entire structure about the bond connecting the two benzene rings.

**FIGURE 2.16**

Determination of *R* or *S* designation for an atropisomer of **27**.

27 from the angle shown by the bottom eye produces Figure 2.16(c), which is also *S*.

Frequently, designation of helical molecules is done not with *R* and *S* but instead with *P* (for plus) and *M* (for minus).⁸⁹ Hexahelicene **31** (page 67) is said to be "left-handed," since the helix makes a left-handed or counterclockwise turn as it proceeds *away* from the observer. Therefore, **31** is an *M* helix, which corresponds to the *R* designation. (Viewing the helix from the other end would not change this designation.) Similarly, **38** can be considered an *M* helical structure in which the CO₂H groups move counterclockwise as they proceed away from the observer. Conversion of *M* to *R* and *P* to *S* is easy, since the relative order of the letters *M* and *P* corresponds to the relative order of the letters *R* and *S* in the alphabet.⁷²



The *R* or *S* designation of *trans*-cyclooctene (**28**, Figure 2.17) can most easily be determined by considering the structure to have chirality about an axis. Viewing **28** as indicated by the eye symbol reveals it to have the *R* configuration. Krow detailed the application of the rules for planar chirality to

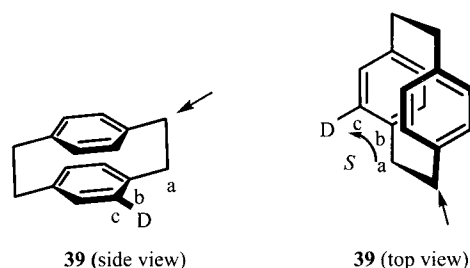
**FIGURE 2.17**

Determination of the configuration of **28**.

⁸⁹ Although the symbols *M* and *P* are not derived from words of foreign origin, they are nonetheless italicized: Dodd, J. S., Ed. *The ACS Style Guide*; American Chemical Society: Washington, DC, 1986; p. 75.

FIGURE 2.18

Determination of the configuration of **39**. The straight arrows designate the pilot atom. The curved arrow identifies the configuration of the structure.



28 and other molecules,⁷² and Hirschmann and Hanson described approaches to factoring chirality and stereoisomerism.⁹⁰

Determining the *R* or *S* configuration of a structure that is chiral about a plane is not as straightforward as is determining the configuration of a structure chiral about a point or an axis.¹ First, the chiral plane is chosen so as to contain as many of the atoms as possible.⁹¹ In the deuterated paracyclophane **39**, the chiral plane consists of the benzene ring containing the deuterium atom and the two methylene groups attached to this ring (Figure 2.18). Next, one identifies an atom that is not in the plane but which is as close to the plane as possible; this atom is designated the “pilot atom” and is denoted by an arrow. In **39** there are two methylene carbons bonded to the upper benzene ring that are each one atom removed from the lower, chiral plane. In such cases, one chooses as the pilot atom the atom that is closer to a group (in this case the D atom) that is higher in priority according to the sequence rules. Then if the three atoms in the chiral plane that are bonded to the pilot atom are arranged in a clockwise pattern in the chiral plane *as viewed from the pilot atom*, the chirality is designated *R* (*pR*). In the case of **39**, the pattern from a to b to c is counterclockwise, so **39** is designated *S*.⁹² If one considers the pilot atom and atoms a, b, and c to be four atoms of a helical structure, then **39** is designated *M*. Thus, *pR* corresponds to *P* and *pS* to *M*, which is the opposite of the correlation of the *axial* chirality descriptors *aR* and *aS*, which correspond to *M* and *P*, respectively.¹

Fischer Projections

The *R* and *S* system is useful in discussing the Fischer projection, which is one of the most important two-dimensional representations of chiral molecules.⁹³ This type of drawing was initially developed to display the stereochemical relationships among carbohydrates with several chiral centers,⁹⁴ but it is also useful in many other applications. In a Fischer projection, molecules are represented by crossing vertical and horizontal lines, with each intersection representing a carbon atom. Horizontal lines represent bonds that would project forward in space if we drew the molecule using perspective notation

⁹⁰ Hirschmann, H.; Hanson, K. R. *Top. Stereochem.* **1983**, *14*, 183.

⁹¹ It cannot be that all of the atoms lie in the plane. If that were the case, the structure would not be chiral.

⁹² Hoffman, P. H.; Ong, E. C.; Weigang, O. E., Jr.; Nugent, M. J. *J. Am. Chem. Soc.* **1974**, *96*, 2620.

⁹³ The Fischer projection is also called the Fischer–Tollens projection (reference 11).

⁹⁴ Lichtenthaler, F. W. *Angew. Chem. Int. Ed. Engl.* **1992**, *31*, 1541. Also see Maehr, H. *Tetrahedron: Asymmetry* **1992**, *3*, 735.

for the chemical bonds. Vertical lines represent bonds that would project back from the carbon atom at the point of intersection. For example, the stereoisomer of 2-chlorobutane represented in many different ways in Figure 2.2 would be shown as the Fischer projection 3g.

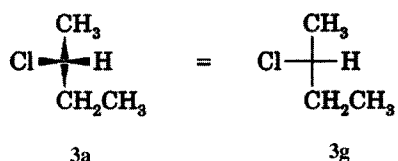


Figure 2.19 shows three stereochemical representations for (2*S*,3*S*)-2-chloro-3-pentanol (**40**). One can interconvert these representations by imagining the view to be had from various perspectives. For example, viewing **40a** from the perspective indicated by the eye would produce the bold/dashed wedge figure **40b**, which is properly oriented (substituents on a horizontal line project *toward* the viewer) to simply draw the Fischer projection, **40c**. Note that a Fischer projection shows an eclipsed conformation of the structure, so ordinarily it does not represent the most stable conformation.

As we have noted, a two-dimensional figure can represent a three-dimensional structure only if we accept implicit rules for drawing and changing it. Therefore, some operations on a Fischer projection are “allowed,” and some are “forbidden.” Rotation of an entire Fischer projection 180° about an axis perpendicular to the page and through the center of the carbon skeleton (Figure 2.20) preserves the configuration of the structure, as does the cyclic rotation of any three substituents to a chiral center while holding the fourth substituent fixed (Figure 2.21). Therefore, these two processes are allowed operations on Fischer projections.

In contrast, flipping a Fischer projection, as shown by the conversion of **40a** to **41** in Figure 2.22, gives the enantiomer of the original structure, while exchanging any two groups, as shown by the conversion of **40a** to **42** in Figure 2.23, gives the diastereomer of the original chiral center. Therefore, these procedures are forbidden operations for Fischer projections.

A stereochemical drawing, once committed to paper, represents a specific stereoisomer. That is, the image defines the chirality sense of the object it depicts. Sometimes, chemists must convey information about structures whose absolute configurations may be unknown. For example, suppose we

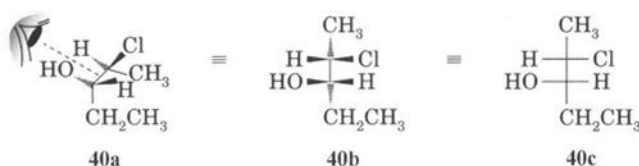


FIGURE 2.19
Representations of (2*S*,3*S*)-2-chloro-3-pentanol.

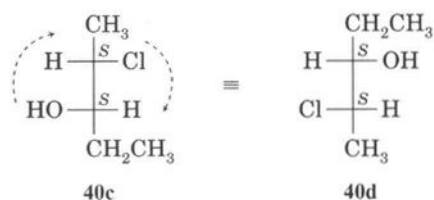
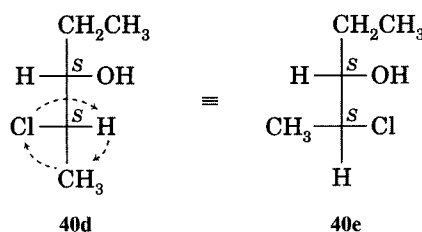


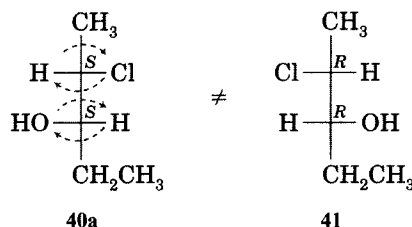
FIGURE 2.20
Effect of rotating the Fischer projection of **40c** 180° about an axis perpendicular to the midpoint of the C2–C3 bond.

FIGURE 2.21

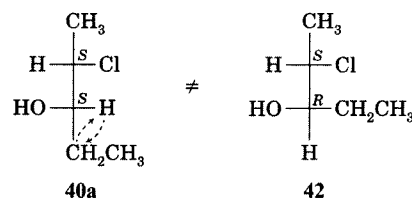
Conversion of the Fischer projection **40d** into **40e** as the result of a 120° rotation about the C2–C3 bond.

**FIGURE 2.22**

Effect of flipping a Fischer projection.

**FIGURE 2.23**

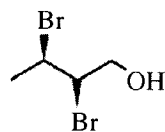
Effect of interchanging two groups attached to one chiral center in a Fischer projection.



are seeking to identify an unknown substance and have determined from atom connectivities that it is 2-chloro-3-hydroxypentane. Suppose also that we have determined the relative configurations of the two chiral centers and know that the substance being studied is either the (*R,R*) or the (*S,S*) isomer. We might represent the compound with a drawing such as **40a**, but we would have to verbally augment the figure by stating that the compound under investigation is either the structure drawn or its mirror image. Similarly, we cannot represent a mixture of enantiomers with just one stereodrawing unless there is an accompanying explanation.

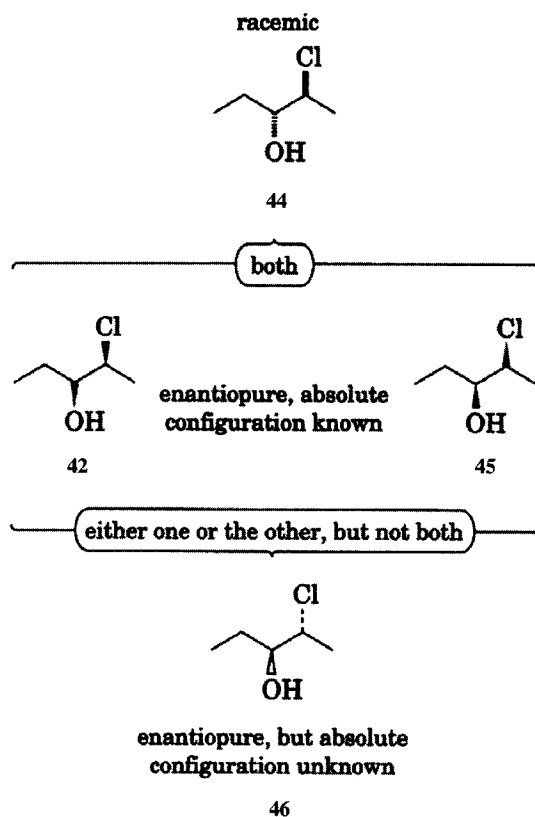
To provide a more complete but still compact stereodescription of molecular entities, Maehr suggested a convention based on a redeployment of some commonly used notations for the placement of bonds in space as follows:⁹⁵

1. *Solid* and *broken wedges* were defined as descriptors of *topography* that denote the *absolute configuration* of a chiral structure. Thus, (*2S,3R*)-2,3-dibromobutanol was represented by Maehr as **43**.

**43**

⁹⁵ Maehr, H. J. *Chem. Educ.* **1985**, 62, 114; *J. Chem. Inf. Comp. Sci.* **2002**, 42, 894.

2. *Solid and broken bold lines* were designated as descriptors of *geometry*. Employed within a stereostructure, they portray the stereochemical relationship among similarly represented stereocenters within a molecule, but they also imply that a molecule is *racemic*. Therefore, **44** represents both the structure obtained by replacing the bold line by a solid wedge and the dashed line by a broken wedge (**42**) and the enantiomer of that structure (**45**).



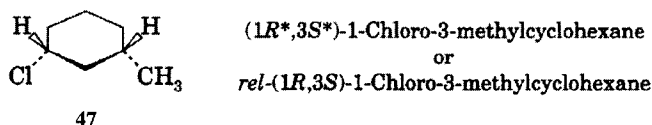
3. *Wedge outlines and dotted (broken) lines* were also defined as descriptors of geometry, but they portray only the stereochemical *relationship* among similarly represented stereocenters. They inform the viewer that the compound is a single enantiomer, but they do not indicate the absolute configuration of the chiral centers. Thus, **46** is either **42** or **45**, but not both.

The stereochemical information for some molecules with several stereocenters may be limited, as, for example, during the structure elucidation of a new natural product. The absolute configuration may be established for the stereocenters in one part of the molecule, while in another part of the molecule only relative configurations may be known. In such a case, the Maehr convention allows the unambiguous representation of the stereochemical knowledge about the compound with a single diagram incorporating descriptors of type (1) and (3), respectively. A single diagram using type (1) and type (2) descriptors could represent the product obtained by esterifying a racemic carboxylic acid with an optically active alcohol. The Maehr conven-

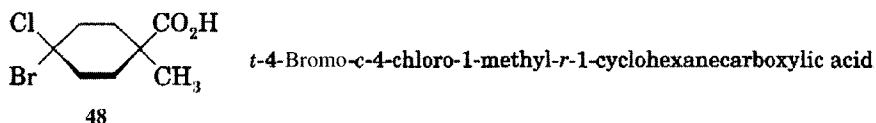
tion found some acceptance,⁹⁶ but a contemporary author cannot assume that readers will be familiar with it. Current IUPAC recommendations state that, in order to avoid ambiguity, it is safest to accompany structural drawings with additional descriptive text so that the stereochemical meaning of the drawings is entirely clear.¹¹

Additional Stereochemical Nomenclature

There is also an extension of the *R* or *S* system that is useful for situations in which we know the relative configuration of the chiral centers in a molecule but not the actual three-dimensional structure. For example, the drawing of compound **47** uses the Maehr notation to indicate that the relationship of the methyl and chloro substituents is *cis* but that we do not know whether the structure has the configuration shown or its mirror image. In one system of nomenclature, the first-named substituent is arbitrarily assumed to be on an *R* chiral center, and that center is denoted as *R**.⁹⁷ The configuration of the chiral center bearing the second-named substituent is then determined to be either *R** or *S** according to this arbitrary assumption. Another way to treat the same problem is to use the prefix *rel* (for relative) to indicate that the actual configuration is not known. Thus, **47** could be named either as (1*R**,3*S**)-1-chloro-3-methylcyclohexane or as *rel*-(1*R*,3*S*)-1-chloro-3-methylcyclohexane.



The *r* (for “reference”) system was developed to serve as the reference for the stereochemical placement of substituents and is particularly useful for diastereomers.⁹⁸ In the case of **48**, for example, the carboxylic acid function is taken as the reference, and the other substituents are indicated as being either *cis* (*c*) or *trans* (*t*) to it.



The CIP priority rules have also been adapted for naming geometric isomers in which the designations *cis* and *trans* are ambiguous. Assigning priorities A or B to the two substituents on each carbon atom of an alkene results in one or the other of two possible results, as shown at the top of Figure 2.24. We designate as *Z* (an abbreviation of the German word *zusammen*, meaning “together”) the isomer in which the two higher priority

⁹⁶ Compare Kende, A. S., Ed. *Org. Synth.* **1986**, 64, p. x.

⁹⁷ Fletcher, J. H.; Dermer, O. C.; Fox, R. B. *Nomenclature of Organic Compounds*, *Adv. Chem. Ser.* 126, American Chemical Society: Washington, DC, 1974; p. 108.

⁹⁸ For further discussion of the *r* notation, see (a) reference 97, p. 112 ff; (b) Orchin, M.; Kaplan, F.; Macomber, R. S.; Wilson, R. M.; Zimmer, H. *The Vocabulary of Organic Chemistry*; John Wiley & Sons: New York, 1980; p. 139.

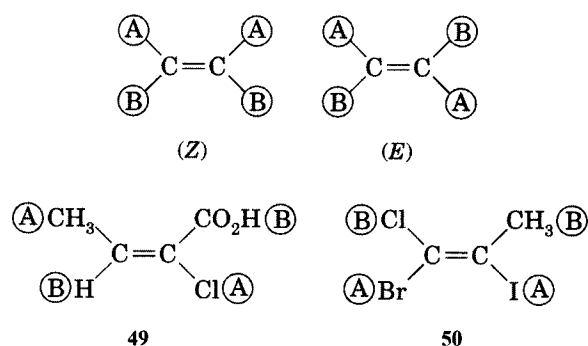
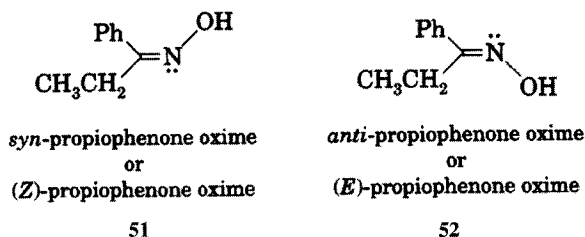


FIGURE 2.24
Examples of *E* and *Z* nomenclature of alkenes.

substituents (A) are cis to each other. We designate as *E* (German, *entgegen*, “opposite”) the isomer in which the two higher priority substituents are trans.⁹⁹ *Z* is often equivalent to cis, and *E* is often equivalent to trans, but that is not always the case. In the 2-butenes, the *Z* isomer is the cis isomer, while the *E* isomer is trans. In compound 49, however, the parent chain passes through the double bond in a cis fashion, but the designation is *E* because of the priorities of the substituents. There is not a parent chain passing through the double bond in structure 50, but the *E* and *Z* system names this compound simply and unambiguously as (*Z*)-1-bromo-1-chloro-2-iodopropene.

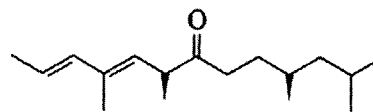
The *E* or *Z* nomenclature can also replace the older *syn-anti* terminology. Compound 51 has been called *syn*-propiophenone oxime because the OH and the phenyl are on the same side of the double bond, while 52 has been called the *anti* isomer because these two larger groups are on opposite sides. The distinction between *syn* and *anti* depends on the size or complexity of the substituents, and that may not always be unambiguous. Moreover, many authors reserve the terms *syn* and *anti* to describe the stereochemical pathway of a reaction, not the stereochemistry of molecules. With the *E* or *Z* system, 51 is unambiguously the *Z* isomer, while 52 is the *E* oxime.



The *R* or *S* and the *E* or *Z* nomenclature systems can be combined as needed to name specific compounds. For example, the IUPAC name of (–)-matsuone (53), the primary sex attractant pheromone of a red pine scale, is (2*E*,4*E*,6*R*,10*R*)-4,6,10,12-tetramethyl-2,4-tridecadien-7-one.¹⁰⁰

⁹⁹ Blackwood, J. E.; Gladys, C. L.; Loening, K. L.; Petrarca, A. E.; Rush, J. E. *J. Am. Chem. Soc.* **1968**, *90*, 509.

¹⁰⁰ The synthesis of (–)-matsuone was described by Cywin, C. L.; Webster, F. X.; Kallmerten, J. J. *Org. Chem.* **1991**, *56*, 2953.



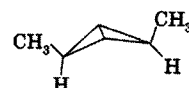
Matsuone

53

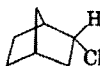
The terms **endo** and **exo** are useful in naming bicyclic systems. The **endo** substituent is held toward the inside of a carbon skeleton envelope, while the **exo** substituent is toward the outside. The nomenclature is exemplified by the 2,4-dimethylbicyclobutanes **54** and **55** and by the 2-chloronorbornanes **56** and **57**. In the 2-chloronorbornanes, the chlorine sees two envelopes, one due to a six-membered ring and one due to a five-membered ring. The *exo*, *endo* convention refers to the envelope determined by the larger bridge, so **57** is the *exo* isomer. A more complicated example is that of 6-*exo*-(acetyloxy)-8-azabicyclo[3.2.1]octan-2-*exo*-ol (**58**), an alkaloid isolated from a Chinese herb.¹⁰¹ If there is a substituent on a smaller ring as well as on a larger ring, then the *endo*, *exo* and *syn*, *anti* designations may both apply.¹⁰² Thus, **59** is 2-*endo*-bromo-7-*syn*-chlorobicyclo[2.2.1]heptane.

*exo*, *endo*-2,4-dimethylbicyclobutane

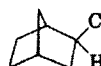
54

*exo*, *exo*-2,4-dimethylbicyclobutane

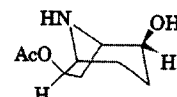
55

*endo*-2-chloronorbornane

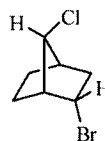
56

*exo*-2-chloronorbornane

57

6-*exo*-(acetyloxy)-8-azabicyclo-
[3.2.1]octan-2-*exo*-ol

58



59

The *R* and *S* system is widely accepted for most organic compounds, but for historical reasons we often use the *D* and *L* system for carbohydrates and amino acids. By convention, a Fischer projection is drawn vertically with the

¹⁰¹ Jung, M. E.; Longmei, Z.; Tangsheng, P.; Huiyan, Z.; Yan, L.; Jingyu, S. *J. Org. Chem.* **1992**, *57*, 3528.

¹⁰² Moss, G. P. *Pure Appl. Chem.* **1996**, *68*, 2193.

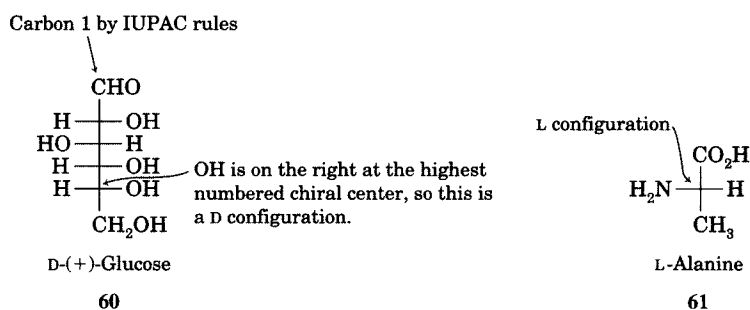


FIGURE 2.25
Examples of D and L nomenclature.

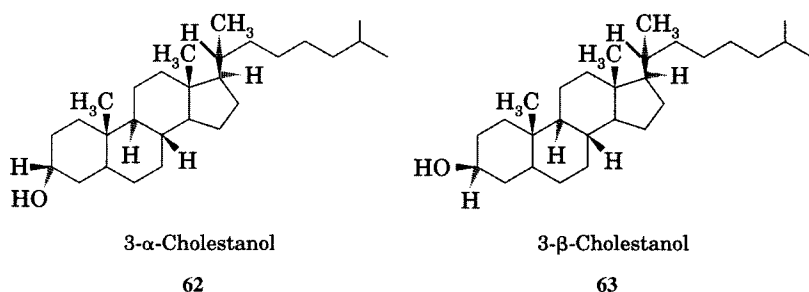


FIGURE 2.26
Examples of α and β nomenclature.

(IUPAC) atom numbers increasing from top to bottom.¹⁰³ The *highest numbered* chiral center will have two "horizontal" substituents, normally either H and OH (for carbohydrates) or H and NH₂ (for α -amino acids). If the OH or NH₂ is on the right, the structure is D (as in D-(+)-glucose, **60**) (Figure 2.25). If the OH or NH₂ is on the left, the structure is L (as in L-alanine, **61**).

The terms α and β are useful in describing the stereochemistry of steroid and carbohydrate systems. For steroid systems such as the isomers of 3-cholestanol in Figure 2.26, an α hydroxyl group is one that lies beneath the approximate molecular "plane."^{104,105} Thus, **62** is 3- α -cholestanol. On the other hand, a β substituent lies above the approximate plane of the molecule, as shown by the structure of 3- β -cholestanol (**63**).¹⁰⁶

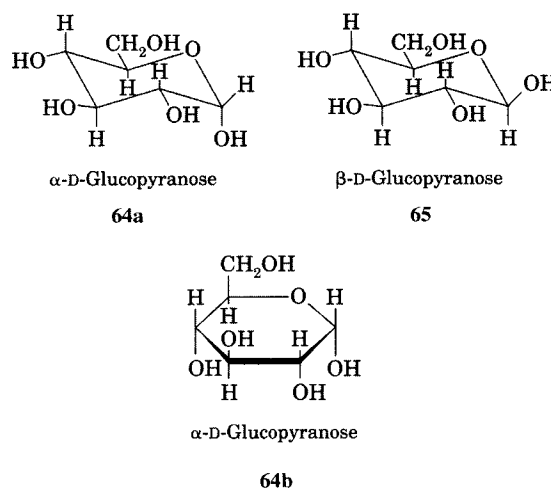
Similarly, **64**, the cyclic form of D-glucose having the hemiacetal hydroxyl group down, would be called α -D-glucopyranose, and β -D-glucopyranose is

¹⁰³ An alternative definition specifies that the more highly oxidized terminal carbon atom be at the top of the Fischer projection. For carbohydrates and amino acids, there is ordinarily no conflict between these two definitions. For historical notes and an elaboration of the D and L nomenclature system, see Slocum, D. W.; Sugarman, D.; Tucker, S. P. *J. Chem. Educ.* **1971**, *48*, 597; reference 140a, pp. 88–92.

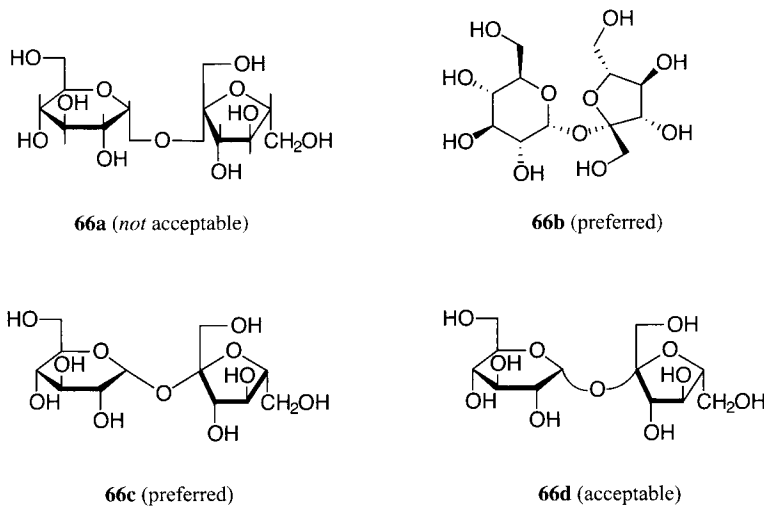
¹⁰⁴ The rules for conformation nomenclature in cyclic monosaccharides have been summarized by Schwarz, J. C. P. *J. Chem. Soc. Chem. Commun.* **1973**, 505.

¹⁰⁵ For a discussion of the stereochemical designations of steroids, see Fieser, L. F.; Fieser, M. *Steroids*; Reinhold Publishing Corporation: New York, 1959; pp. 2–3 and p. 330 ff.

¹⁰⁶ The designation of substituents as α or β in carbohydrates is not as straightforward as it is with steroids. For D sugars, as proposed by Hudson, the more dextrorotary of each α,β pair is the α anomer. For L sugars, the more levorotary of each α,β pair is the α anomer. See Hudson, C. S. *J. Am. Chem. Soc.* **1909**, *31*, 66. For a discussion, see Pigman, W. *The Carbohydrates*; Academic Press: New York, 1953; pp. 42–43.

**FIGURE 2.27**

Representations of α and β nomenclature in D-glucopyranose.

**FIGURE 2.28**

Representations of sucrose.

65 (Figure 2.27).¹⁰⁷ In these drawings the cyclic hemiacetal form of the carbohydrate is shown as a six-membered ring in the chair conformation. An older representation of carbohydrates that represents structures with planar six-membered rings is the Haworth drawing **64b**.⁸

When monosaccharides (individual carbohydrate units such as glucose) are joined together to form disaccharides and polysaccharides by converting hemiacetal groups into acetal linkages, the problem of depicting the stereochemistry can become even more complex. Figure 2.28 shows four representations for sucrose (**66**). Drawings such as **66a** are widely used, but current IUPAC recommendations label them as not acceptable.¹¹ The vertical straight

¹⁰⁷ The name glucopyranose is derived from the systematic nomenclature of carbohydrates: *gluco* refers to glucose, *pyran* means that the compound is in the hemiacetal form so that there is a six-membered ring containing oxygen, and *ose* is the usual suffix for carbohydrates. A furanose ring would be a five-membered carbohydrate ring containing one oxygen atom.

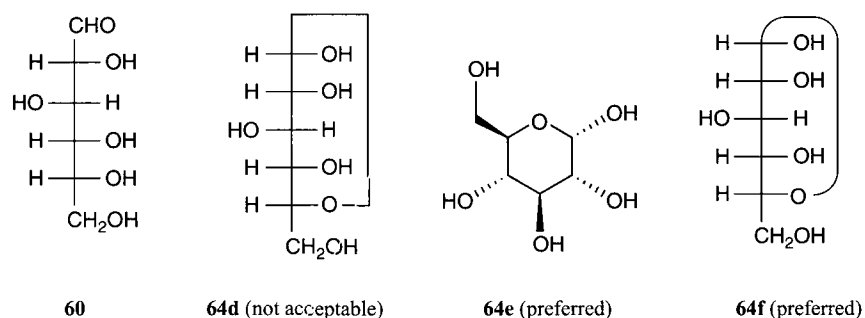
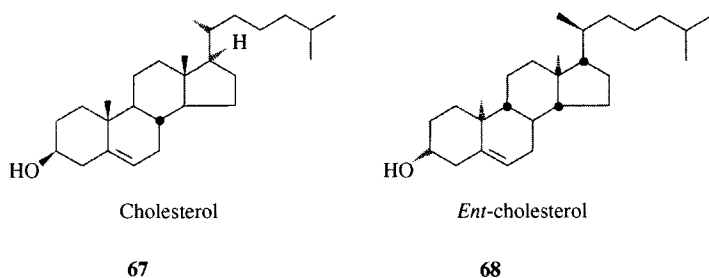


FIGURE 2.29
Representation of D-glucose (**60**)
and α -D-glucopyranose (**64**).

lines from the rings are intended to represent bonds to hydrogen atoms, but this use is not consistent with the formalism that a straight line represents a bond to carbon unless a different atom label terminates the line. Moreover, the "bent bond" connections for the glycosidic linkages in the center of that figure are indistinguishable from the methylene group of the $-\text{CH}_2\text{OH}$ substituents on the rings. To avoid these ambiguities, IUPAC recommends drawings such as **66b** and **66c**. To avoid the appearance of a 180° O-C-O bond angle in **66c**, the IUPAC recommendations consider **66d**, with its curved glycosidic bond lines, to be acceptable.

Fischer projections are especially useful for the acyclic forms of monosaccharides (e.g., D-glucose, **60**) and have been adapted to display their cyclic hemiacetal or hemiketal forms as shown with **64d** (Figure 2.29). Again, the right angles in **64d** present the same issues as those in **66a**. To avoid these problems, current IUPAC recommendations recommend the use of figures such as **64e** and **64f**.¹¹

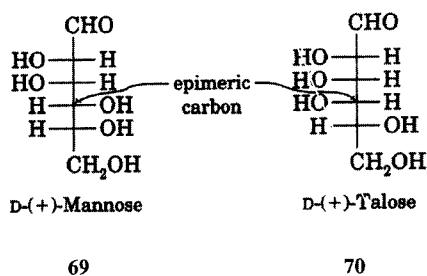
In some cases, particularly natural products with many chiral centers, it is convenient to name the mirror image of a substance having a trivial or common name by simply indicating that the structure is the enantiomer (*ent*-) of the natural compound. The enantiomer of cholesterol (**67**) is therefore *ent*-cholesterol (**68**).¹⁰⁸



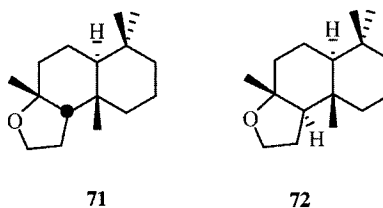
Several stereochemical labels have been developed for diastereomers. **Epimers** are diastereomers that differ in configuration at only one of several chiral centers. The chiral center at which the difference in configuration occurs is said to be the **epimeric center**. Structures **69** and **70** are epimeric at C4. **Anomers** are epimers in the carbohydrate series that differ only at the

¹⁰⁸ Rychnovsky, S. D.; Mickus, D. E. *J. Org. Chem.* **1992**, *57*, 2732.

hemiacetal carbon atom. Examples are the α and β forms of D-(+)-glucopyranose (**64** and **65**, Figure 2.27).



The prefix **epi** is a convenient way to name chiral structures that are epimers of molecules with nonsystematic names. For example, ambrox (**71**) is a substance in ambergris, a whale product that was used in perfumes for hundreds of years.¹⁰⁹ Researchers identified a synthetic isomer of ambrox that is epimeric at the 9 position and which offers even greater potential for use in perfume. This compound was named 9-*epi*-ambrox (**72**), a designation that compactly specifies its structure in the context of the known parent compound.¹¹⁰



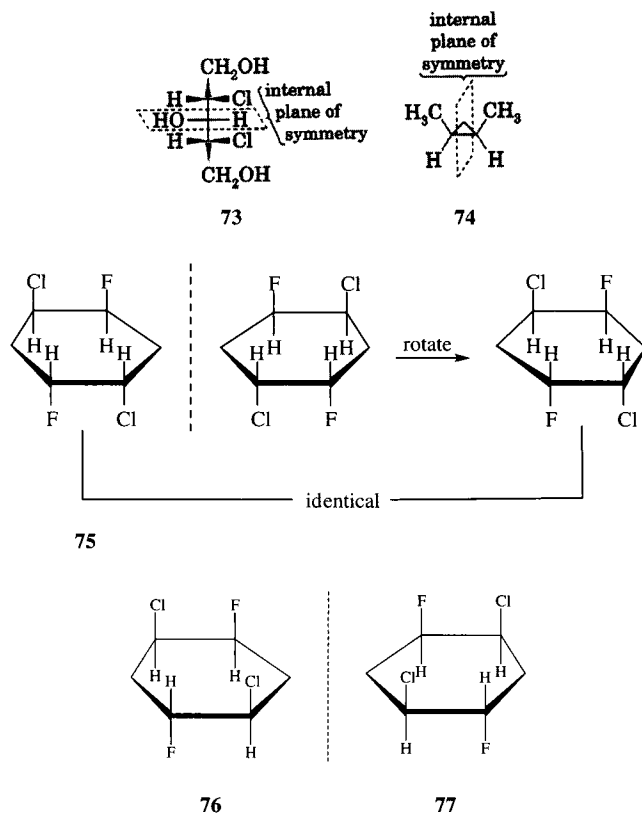
The term **meso** is commonly used to designate an achiral structure that is a diastereomer of one or more chiral structures.¹¹¹ A meso compound contains chiral substructures but is not itself chiral because of overall molecular symmetry. Such structures often—but not always—have a plane of symmetry in at least one conformation, as is illustrated for **73** and **74**. These structures are said to be *internally compensated*.¹¹² An example of a meso structure that does not have a plane of symmetry is the 1,4-dichloro-2,5-difluorocyclohexane **75**, which is achiral because it has a center of symmetry. Structure **75** is a diastereomer of the enantiomeric pair **76** and **77**.

¹⁰⁹ Budavari, S., Ed. *The Merck Index*, 11th ed.; Merck & Co.: Rahway, NJ, 1989; p. 62.

¹¹⁰ Paquette, L. A.; Maleczka, R. E., Jr. *J. Org. Chem.* **1991**, *56*, 912.

¹¹¹ Ault recommended using *meso* to define an optical activity relationship and not a structural feature (i.e., a macroscopic and not a molecular distinction). By this definition, meso refers to "an optically inactive member of a set of stereoisomers, at least two of which are optically active." Ault, A. J. *Chem. Educ.* **2008**, *85*, 441.

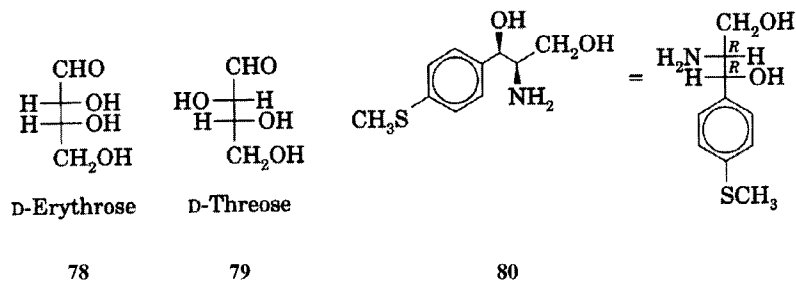
¹¹² Effectively, a compound such as **73** is a one-molecule racemate.



Two other stereochemical designations that are most easily determined from Fischer projections are **erythro** and **threo**. These terms derive from the structures of the carbohydrates erythrose, 78, and threose, 79. If the two carbohydrates are drawn as Fischer projections, it is seen that erythrose has two identical substituents (OH groups) on adjacent chiral centers and on the same side of the Fischer projection. By analogy, other structures which have identical (or similar) substituents on adjacent chiral centers and on the same side of the Fischer projection are also called erythro. In the case of threose, the two identical substituents on adjacent chiral centers are on opposite sides of the Fischer projection when the main chain is drawn vertically. By analogy, other structures having similar stereochemical character are termed threo.¹¹³ For example, the precursor for the synthesis of the antibiotic Thiamphenicol is *threo*-(1*R*,2*R*)-2-amino-1-[4-methylthio]phenyl]-1,3-propanediol, 80.¹¹⁴ Here the *threo* modifier is redundant but is nevertheless useful in visualizing the three-dimensional structure of the compound.

¹¹³ The terms *erythro* and *threo* may be defined in a different fashion using the *R* and *S* priority designations and Newman projections: reference 95; reference 117. See also Seebach, D.; Prelog, V. *Angew. Chem. Int. Ed. Engl.* **1982**, *21*, 654; Gielen, M. *J. Chem. Educ.* **1977**, *54*, 673.

¹¹⁴ The conversion of the (1*S*,2*S*) isomer into the (1*R*,2*R*) enantiomer was described: Giordano, C.; Cavicchioli, S.; Levi, S.; Villa, M. *J. Org. Chem.* **1991**, *56*, 6114.



The terms erythro and threo still find wide use, but some extensions of those terms have resulted in ambiguous designations.^{115,116} Therefore, several authors reported alternative stereochemical descriptors for structures of known stereochemistry. Carey and Kuehne proposed the pref-parf system, where pref is an abbreviation for "preference reflective" and parf is an abbreviation for "preference antireflective."¹¹⁷ Consider a structure having substituents with priorities A, B, and C on one chiral center and substituents with priorities A', B', and C' on the other chiral center. If we view a sawhorse representation of the structure in such a way that the priority sequences (though not the actual substituents) are mirror images, as shown in Figure 2.30(a), then the structure is pref. If the CIP priority sequences are not mirror images, as shown in Figure 2.30(b), then the structure is parf. Thus, D-erythrose is the pref diastereomer, while D-threose is the parf diastereomer.

Prelog and Helmchen proposed the *lu* notation, where *l* represents *like*, and *u* stands for *unlike*.¹¹⁸ If a structure has two chiral centers and both are *R*, the structure is *l*. If one is *R* and the other is *S*, however, then it is designated *u*. Thus, D-erythrose, (2*R*,3*R*)-2,3,4-trihydroxypropanal, is the *l* diastereomer, while D-threose, (2*S*,3*R*)-2,3,4-trihydroxypropanal, is the *u* diastereomer.^{119,120}

One stereochemical term that appeared with some regularity in the literature is **homochiral**. Unfortunately, this term has had different meanings and thus was the subject of some debate. Damewood noted that the term as defined by Kelvin meant two species with the same handedness and cited elaboration of this meaning by Anet and Mislow, but that the term also had been used to mean a sample in which one enantiomer exists in pure form or is present in greater concentration than its mirror image.¹²¹⁻¹²⁴ Several authors

¹¹⁵ Noyori, R.; Nishida, I.; Sakata, J. *J. Am. Chem. Soc.* **1981**, *103*, 2106.

¹¹⁶ See also the discussion of Tavernier, D. *J. Chem. Educ.* **1986**, *63*, 511.

¹¹⁷ Carey, F. A.; Kuehne, M. E. *J. Org. Chem.* **1982**, *47*, 3811.

¹¹⁸ Prelog, V.; Helmchen, G. *Angew. Chem. Int. Ed. Engl.* **1982**, *21*, 567; Seebach, D.; Prelog, V. *Angew. Chem. Int. Ed. Engl.* **1982**, *21*, 654.

¹¹⁹ See also Brewster, J. H. *J. Org. Chem.* **1986**, *51*, 4751.

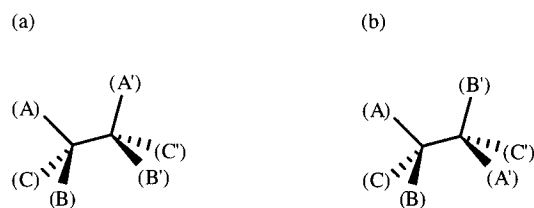
¹²⁰ The *l* and *u* designations are not the same as the *lk* (like) and *ul* (unlike) designations for the topicity of approach of two reactants in asymmetric synthesis. The terms *l* and *u* refer to products, while the terms *lk* and *ul* refer to the steric course of reactions: Seebach, D.; Prelog, V. *Angew. Chem. Int. Ed. Engl.* **1982**, *21*, 654.

¹²¹ Lord Kelvin. *Baltimore Lectures on Molecular Dynamics and the Wave Theory of Light*; Clay: London, 1904; p. 618.

¹²² Anet, F. A. L.; Miura, S. S.; Siegel, J.; Mislow, K. *J. Am. Chem. Soc.* **1983**, *105*, 1419.

¹²³ Mislow, K.; Bickart, P. *Isr. J. Chem.* **1976/77**, *15*, 1.

¹²⁴ Damewood, J. R., Jr. *Chem. Eng. News* **1985** (Nov 4), 5.

**FIGURE 2.30**

Pref (a) and parf (b) relationships.

proposed and discussed possible alternative terms for enantiomerically pure or enriched substances. Among the suggestions were *enantiopure*, *scalemic*, *unichiral*, *monochiral*, and *aracemic*.¹²⁵ A member of the IUPAC commission preparing a *Glossary of Stereochemical Terms* reported that the committee favored the terms *enantiomerically pure* or *enantiomerically enriched* and specifically discouraged the use of the term *homochiral*.^{11,126} As a result, readers of the chemical literature, especially the older literature, will need to consider carefully how the word *homochiral* is used in each paper.

Another source of uncertainty in the use of stereochemical terminology concerns the terms **stereospecific** and **stereoselective**, which were proposed by Zimmerman and co-workers.¹²⁷ Adams reviewed the varied definitions of these terms and recommended that they be used as follows:¹²⁸

- *Stereoselective Reaction*: A reaction in which one stereoisomer (or pair of enantiomers) is formed or destroyed at a greater rate or to a greater extent (at equilibrium) than other possible stereoisomers.
- *Stereospecific Reaction*: A reaction in which stereoisomerically different reactants yield stereoisomerically different products.

A familiar example of a stereoselective reaction would be the formation of a higher yield of *trans*-2-butene than *cis*-2-butene in an E2 reaction, no matter whether the starting material is (*R*)- or (*S*)-2-bromobutane. The addition of bromine to *trans*-2-butene to produce *meso*-2,3-dibromobutane or the addition of bromine to the *cis* isomer to produce an equimolar mixture of the two enantiomers of 2,3-dibromobutane is a stereospecific reaction. Note that a reaction that gives only one of a pair of enantiomers is not necessarily stereospecific. A yeast-mediated reduction of 3-chloropropiophenone gives (*S*)-3-chloro-1-phenylpropan-1-ol, with no evidence for formation of the *R* enantiomer.¹²⁹ Because the reactant cannot exist as stereoisomers, it is not possible for stereoisomerically different reactants to give stereoisomerically different products, and the reaction can only be considered stereoselective, not stereospecific.

Part of the confusion about the terms *stereoselective* and *stereospecific* comes from the use of other terms that sound similar but in which the

¹²⁵ Eliel, E. L.; Wilen, S. H. *Chem. Eng. News* **1990** (Sept 10), 2; Heathcock, C. H. *Chem. Eng. News* **1991** (Feb 4), 3; Gal, J. *Chem. Eng. News* **1991** (May 20), 42; Castrillón, J. *Chem. Eng. News* **1991** (June 24), 94; Eliel, E. L.; Wilen, S. H. *Chem. Eng. News* **1991** (July 22), 3; Brewster, J. H. *Chem. Eng. News* **1992** (May 18), 3.

¹²⁶ Halevi, E. A. *Chem. Eng. News* **1992** (Oct 26), 2.

¹²⁷ Zimmerman, H. E.; Singer, L.; Thyagarajan, B. S. *J. Am. Chem. Soc.* **1959**, *81*, 108. The definitions are in footnote 16, p. 110.

¹²⁸ Adams, D. L. *J. Chem. Educ.* **1992**, *69*, 451.

¹²⁹ Fronza, G.; Fuganti, C.; Grasselli, P.; Mele, A. *J. Org. Chem.* **1991**, *56*, 6019.

suffixes *-selective* and *-specific* do not mean the same relationship as they do in stereospecific and stereoselective. The term **regioselective** refers to reactions that lead to the formation of one positional isomer in greater yield than another.^{98b} An example would be the formation of more 2-alkene than the isomeric 1-alkene in the E2 reaction of an alkyl halide. The term **regio-specific** means "completely regioselective," so its meaning is not parallel with *stereospecific*. Because of this difficulty, Adams recommended that the term *regiospecific* not be used.¹²⁸

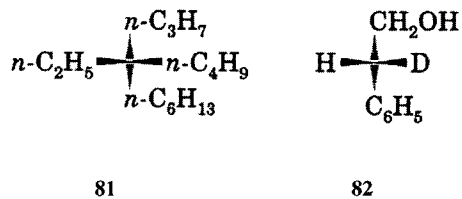
2.3 MANIFESTATIONS OF STEREOISOMERISM

Optical Activity

Rotation of Plane-Polarized Light

The physical phenomenon that led to the study of enantiomers is optical activity—the rotation of plane-polarized light. We indicate the experimental results by saying that the rotation is clockwise—also denoted as (+), (*d*), or *dextrorotatory*—or counterclockwise—also indicated as (–), (*l*), or *levorotatory*. Because of the similarity of *d* and *l* with D and L, the use of (+) and (–) to indicate the direction of rotation of the plane of polarization is now favored.⁸⁴

It is important to recognize that chirality is a *molecular designation*, but optical activity is a *macroscopic observation*. It is possible for a carbon atom to have four different substituents and yet a sample of the substance not appear to rotate the plane of polarized light. This can happen most easily if the four substituents are so similar that rotation of light is too small to be observed. For example, optical activity could not be detected in butylethylhexylpropylmethane (5-ethyl-5-propylundecane, **81**).¹³⁰ A substance having both deuterium and hydrogen at a chiral center can produce measurable optical activity, however, as shown by **82**. Here the (–) enantiomer was found to have a specific rotation of $-3.006 \pm 0.004^\circ$.¹³¹



Optical activity is reported as **specific rotation**, $[\alpha]$, calculated as shown in equation 2.1.

¹³⁰ Wynberg, H.; Hekkert, G. L.; Houbiers, J. P. M.; Bosch, H. W. *J. Am. Chem. Soc.* **1965**, *87*, 2635. Such a structure may be termed *cryptochiral*: Mislow, K.; Bickart, P. *Isr. J. Chem.* **1976/77**, *15*, 1. Precursors to **81** were chiral structures with significant optical activity, so failure to observe optical activity with **81** was not due to racemization or low optical purity. See also Wynberg, H.; Hulshof, L. A. *Tetrahedron* **1974**, *30*, 1775.

¹³¹ Streitwieser, A., Jr.; Wolfe, J. R., Jr.; Schaeffer, W. D. *Tetrahedron* **1959**, *6*, 338. For a review of chirality resulting from isotopic substitution, see Arigoni, D.; Eliel, E. L. *Top. Stereochem.* **1969**, *4*, 127.

$$[\alpha]_{\lambda}^T = \frac{\theta}{lc} \quad (2.1)$$

Here θ is the observed rotation, l is the path length of the sample, and c is the sample concentration. The wavelength at which the measurement is made is denoted by λ , and T is the temperature (in °C). The sodium emission D line at 589 nm is a bright, sharp spectral line that can easily be produced, and it is often used for polarimetry measurements. Because one needs a longer path length to measure optical rotation precisely than typically is needed for UV-vis spectroscopy, the standard sample length is 1 decimeter (dm), which is 10 cm. In many cases the molecular weight of the substance to be tested is not known, so the concentration is reported as g/mL (i.e., the density for a pure liquid or the concentration for a solution), as opposed to moles/liter. Thus, an experimental measurement at 25° in which a pure sample with density 0.8 g/mL gave a rotation of the sodium D line of +36° in a 10 cm cell would give a specific rotation $[\alpha]_{\text{D}}^{36} = 45^{\circ} \text{ mL g}^{-1} \text{ dm}^{-1}$.¹³²

For solutions it is necessary to specify the solvent, since solvent–solute interactions can affect not only the magnitude of optical activity, but perhaps the direction of the rotation as well.^{140a} For example, the specific rotation of (–)- α -methylbenzylamine was found to be –31.86° in benzene and –52.29° in CCl₄.¹³³ Specific rotations are usually reported in an abbreviated format. The specific rotation of cholesterol is given as $[\alpha]_{\text{D}}^{20} -31.5^{\circ}$ ($c=2$ in ether); $[\alpha]_{\text{D}}^{20} -39.5^{\circ}$ ($c=2$ in chloroform).¹⁰⁹ Note that in this format, the concentration of a solution is usually taken to mean grams per 100 mL.¹⁰⁹ It is also possible to define a molecular rotation (Φ) when molecular weight is known, as shown in equation 2.2. Calculating molecular rotation makes it easier to determine the effect of the same chromophore in different molecules.¹³⁴

$$[\Phi] = 0.01 \times [\alpha] \times (\text{Molecular weight}) \quad (2.2)$$

Our discussion to this point has assumed that we can obtain pure enantiomers. In many cases we can obtain one pure enantiomer from a natural source, but often we find that enantiomeric species are formed as a **racemate**—an equimolar mixture of the two enantiomers.¹³⁵ Racemates (frequently termed *racemic mixtures*) are denoted with the prefixes (±)-, *rac*-, *RS*-, or *SR*-. We may try to **resolve** a racemate (separate it into enantiomers) by any of a variety of chemical or biological means.¹³⁶ If we are nevertheless unable to obtain one pure enantiomer, we may be forced to use a mixture in which there is more of one enantiomer than its mirror image. In such cases we would like to know the **optical purity** of the sample, which is defined as the percentage of $[\alpha]$ of the pure enantiomer exhibited by the mixture. For example, the specific rotation of (+)-glyceraldehyde is +14°. A mixture of 95% (+)-glyceraldehyde and 5% (–)-glyceraldehyde is said to be 90% optically pure because the rotation of the sample is 12.6°, which is 90% of

¹³² While specific rotation is ordinarily reported only as degrees, it is helpful to carry units through calculations to ensure that correct path length and concentration units are used.

¹³³ Fischer, A. T.; Compton, R. N.; Pagni, R. M. *J. Phys. Chem. A* **2006**, *110*, 7067.

¹³⁴ Crabbé, P. in reference 146a, p. 1.

¹³⁵ A term formerly used for a racemate is *racemic modification*.

¹³⁶ For a review, see Wilen, S. H. *Top. Stereochem.* **1971**, *6*, 107.

the rotation that would be observed if all of the molecules were (+)-glyceraldehyde. The **enantiomeric excess** (*ee*), which is defined as the percent of the major enantiomer minus the percent of the minor enantiomer, is numerically identical to the optical purity of a substance.¹³⁷

$$ee = (\text{Fraction major enantiomer} - \text{Fraction minor enantiomer}) \times 100\% \quad (2.3)$$

Optical Rotary Dispersion and Circular Dichroism

The sodium D line is often chosen for optical activity measurements, but optical activity can be measured at any wavelength. In the technique of **optical rotary dispersion (ORD)**, the value of $[\Phi]$ is determined over the entire near-UV–vis spectrum. Optical activity is usually greater at shorter wavelengths than at longer wavelengths, so a (+) compound will generally show a curve that is more dextrorotatory at short wavelengths than at long wavelengths, while a (–) compound will be more levorotatory at shorter wavelengths.

Any optically active compound will have an ORD curve. If the graph of $[\Phi]$ versus λ does not show a maximum or minimum but simply increases in magnitude from longer to shorter wavelengths, the curve is called a **plain curve**. In some cases the ORD curve exhibits a maximum or minimum (or both), which is called a **Cotton effect**. Cotton effects occur at wavelengths near a UV–vis absorption band of the optically active compound. Figure 2.31 shows the ORD curve for 2 α -bromocholestan-3-one.¹³⁸ The ORD exhibits a **positive Cotton effect**, meaning that the magnitude of the observed optical activity increases from 400 nm to about 310 nm, then it decreases and actually becomes negative at wavelengths shorter than 300 nm. The midpoint between the extrema (most positive value and most negative value) of the Cotton effect is 293 nm, which is close to the UV–vis absorption maximum at 286 nm. It is important to note that optical rotary dispersion is highly dependent on solvent. One theoretical study found that in benzene the dissymmetric solvent shell around (S)-1,2-epoxypropane, and not the chiral structure itself, is primarily responsible for the observed ORD.¹³⁹

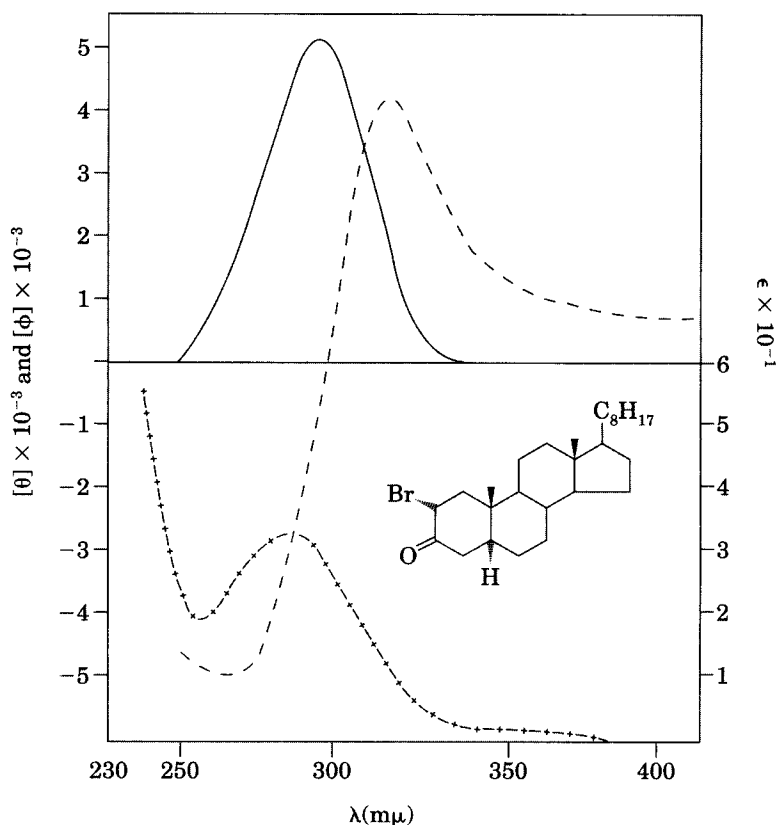
Plane-polarized light has the electric vectors of all of the photons in one plane, which is physically identical to taking the vector sum of two different circular polarizations of light, one clockwise and one counterclockwise.¹⁴⁰ Optical activity therefore results from the different indices of refraction that a medium has for left and right circularly polarized light. This means that the speed of the light through the medium is different for the two polarizations, a phenomenon known as **circular birefringence**. Not only are the two circular polarizations refracted differently, but they are also absorbed differently by an optically active material. The light passing through the sample is said to be

¹³⁷ For a review of the determination of enantiomeric purity (a) by NMR, see Parker, D. *Chem. Rev.* **1991**, *91*, 1441; (b) for other methods, see Raban, M.; Mislow, K. *Top. Stereochem.* **1967**, *2*, 199.

¹³⁸ Djerassi, C.; Wolf, H.; Bunnenberg, E. *J. Am. Chem. Soc.* **1963**, *85*, 324.

¹³⁹ Mukhopadhyay, P.; Zuber, G.; Wipf, P.; Beratan, D. N. *Angew. Chem. Int. Ed.* **2007**, *46*, 6450.

¹⁴⁰ For a discussion of optical activity and circularly polarized light, see (a) Eliel, E. L. *Stereochemistry of Carbon Compounds*; McGraw-Hill: New York, 1962; chapter 14; (b) reference 2; pp. 992–999; (c) Hill, R. R.; Whatley, B. G. *J. Chem. Educ.* **1980**, *57*, 306; (d) Brewster, J. H. *Top. Stereochem.* **1967**, *2*, 1.

**FIGURE 2.31**

ORD (- - -), CD (---), and UV-vis (+--+) spectra of 2 α -bromocholestan-3-one in dioxane solution. (Adapted from reference 138.)

elliptically polarized, and the phenomenon of differential absorption is known as **circular dichroism (CD)**.¹⁴¹ The sample will thus have a different extinction coefficient for left circularly polarized light (ϵ_L) from that for right circularly polarized light (ϵ_R). With instrumentation to measure the absorption spectrum with both circular polarizations, one can determine the differential dichroic absorption ($\Delta\epsilon$) and molecular ellipticity ($[\Theta]$) of the sample:

$$\Delta\epsilon = \epsilon_L - \epsilon_R \quad (2.4)$$

$$[\Theta] = 3300\Delta\epsilon \quad (2.5)$$

Figure 2.31 also shows the CD curve for 2 α -bromocholestan-3-one. The maximum corresponds closely to the λ_{\max} of the first absorption peak in the UV-vis spectrum of the compound.¹⁴² In some cases CD curves can be helpful in locating UV-vis spectra that are too weak to be seen clearly in a normal absorption spectrum.¹³⁸

¹⁴¹ Berova, N.; Nakanishi, K.; Woody, R. W., Eds. *Circular Dichroism: Principles and Applications*, 2nd ed.; Wiley-VCH: New York, 2000.

¹⁴² Because ORD and CD curves are both determined by the absorption spectrum of the compound, they are related to each other. Tinoco presented an analysis of the relationship of UV, CD, and ORD curves for helices, such as those formed by polynucleic acids: Tinoco, I., Jr. *J. Am. Chem. Soc.* **1964**, *86*, 297.

ORD and CD curves play an important role in determining the structures and stereochemistry of organic compounds. Based on the spectra of compounds of known structure and absolute stereochemistry, empirical rules have been developed to predict ORD and CD spectra for similar compounds. One of the better known such rules is the **octant rule** for correlating the sign and magnitude of the Cotton effect with the structure of saturated ketones.¹⁴³ The center of the carbon–oxygen double bond is taken as the origin for x , y , and z axes, so that the xy , xz , and yz planes divide space near the carbonyl group into eight regions or *octants*. A substituent in a particular octant contributes to a positive or negative Cotton effect according to the product of its x , y , and z coordinates. This system has been particularly useful in determining the structures of steroids. Additional sources of information about circular dichroism and optical rotary dispersion can be found in papers and monographs by Mason,¹⁴⁴ Snatzke,¹⁴⁵ Crabbé,¹⁴⁶ Djerassi,¹⁴⁷ and Eliel.^{140a} The discussion here has emphasized UV–vis spectroscopy, but infrared radiation may also be used to study vibrational circular dichroism and Raman optical activity.^{148–150}

Configuration and Optical Activity

The designators D and L , R and S , and erythro and threo are molecular notations of configuration, but the $(+)$ and $(-)$ designators result from macroscopic observations made on a bulk sample of material. How can we know the configuration of a compound that has a particular optical activity? For much of the early period in the development of stereochemical theory, that information was not attainable, and there was no way of knowing whether it would ever be obtained. The usual methods for determining the structure of molecules, such as ordinary X-ray diffraction, do not distinguish between enantiomers. Nevertheless, there still needed to be some systematic method for discussing the configurations and optical activities of organic compounds, so Fischer arbitrarily proposed that $(+)$ -tartaric acid had the configuration shown in **83**.¹⁵¹ Later, Bijvoet and co-workers were able to study sodium rubidium tartrate with a type of X-ray diffraction in which the X-rays are not only diffracted but are also absorbed by the rubidium.¹⁵¹ The results allowed

¹⁴³ Moffitt, W.; Woodward, R. B.; Moscowitz, A.; Klyne, W.; Djerassi, C. *J. Am. Chem. Soc.* **1961**, *83*, 4013.

¹⁴⁴ Mason, S. F. *Q. Rev. Chem. Soc.* **1963**, *17*, 20.

¹⁴⁵ Snatzke, G., Ed. *Optical Rotary Dispersion and Circular Dichroism in Organic Chemistry*; Heyden and Son: London, 1967.

¹⁴⁶ (a) Crabbé, P. *Optical Rotary Dispersion and Circular Dichroism in Organic Chemistry*; Holden-Day: San Francisco, 1965; (b) Crabbé, P. *Top. Stereochem.* **1967**, *1*, 93.

¹⁴⁷ Djerassi, C. *Optical Rotary Dispersion: Applications to Organic Chemistry*; McGraw-Hill: New York, 1960.

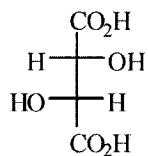
¹⁴⁸ Freedman, T. B.; Nafie, L. A. *Top. Stereochem.* **1987**, *17*, 113.

¹⁴⁹ Holzwarth, G.; Hsu, E. C.; Mosher, H. S.; Faulkner, T. R.; Moscowitz, A. *J. Am. Chem. Soc.* **1974**, *96*, 251.

¹⁵⁰ Barron, L. D.; Bogaard, M. P.; Buckingham, A. D. *J. Am. Chem. Soc.* **1973**, *95*, 603.

¹⁵¹ Bijvoet, J. M.; Peerdeman, A. F.; van Bommel, A. J. *Nature* **1951**, *168*, 271.

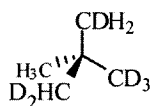
Bijvoet to confirm Fischer's assignment.¹⁵² Bijvoet's pioneering work introduced a system for the determination of the absolute configuration of other molecules,¹⁵³ and many absolute configurations have been cataloged.^{39,154}



(+)-tartaric acid

83

The accumulation of extensive experimental data relating absolute configuration to optical activity made it possible for absolute configuration to be predicted by computation. Brewster proposed that the sign of $[\alpha]$ can be predicted by analyzing the polarizabilities of the substituents arranged around a chiral center.¹⁵⁵ If the polarizabilities of the substituents shown in Figure 2.32 are $A > B > C > D$, then the corresponding compound would be expected to be dextrorotatory. For the example in which the substituents (and their polarizabilities) are Br (8.7), C_6H_5 (3.4), CH_3 (2.6), and H (1.0), the specific rotation is $+178^\circ$. As another example, Haesler and co-workers combined *ab initio* calculations with Raman optical activity measurements to determine that a sample of the selectively deuterated neopentane **36** has the *R* configuration.¹⁵⁶



36

It is also possible to determine the absolute configuration of a compound indirectly by relating its configuration to that of another structure for which the absolute configuration has been determined directly. In other words, if we know the **relative configuration** of two compounds and if we also know the absolute configuration of one of them, then we can deduce the absolute configuration of the other.¹⁵⁷ For example, the absolute configuration of (–)-serine, **84** (Figure 2.33), was determined to be *S* by absolute X-ray structure determination.¹⁵⁸ A reaction carried out on **84** that does not involve breaking

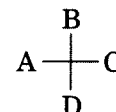


FIGURE 2.32

Chiral structure expected to be dextrorotatory if polarizabilities are $A > B > C > D$.

¹⁵² It is worthwhile to read Bijvoet's original paper, because it reinforces some ideas that are carried through this text. Bijvoet pointed out that "Fischer's convention ... appears to answer to reality" (emphasis in the original paper), and he explicitly referred to the assignment of stereochemistry as a model.

¹⁵³ For a discussion of the determination of absolute configuration from crystals and for an explanation of Bijvoet's method, see Addadi, L.; Berkovitch-Yellin, Z.; Weissbuch, I.; Lahav, M.; Leiserowitz, L. *Top. Stereochem.* **1986**, *16*, 1.

¹⁵⁴ For further discussion of the correlation of configurations, see Mills, J. A.; Klyne, W. *Prog. Stereochem.* **1954**, *1*, 177.

¹⁵⁵ Brewster, J. H. *J. Am. Chem. Soc.* **1959**, *81*, 5475 and succeeding papers in that volume.

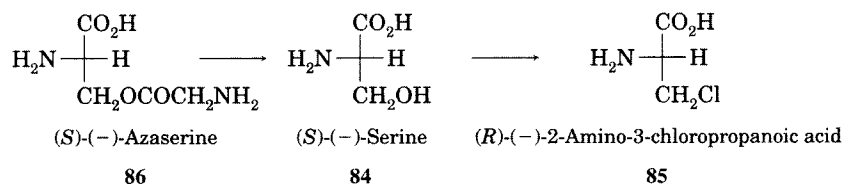
¹⁵⁶ Reference 83; see also the commentary by Barron, L. D. *Nature* **2007**, *446*, 505. Because of insufficient sample, the specific rotation of polarized light could not be measured, so it was not determined whether **36** is (+) or (–).

¹⁵⁷ For a description of the method used to relate absolute configuration to optical activity for tartaric acid, see reference 140a, p. 95 ff; reference 2, pp. 113–114.

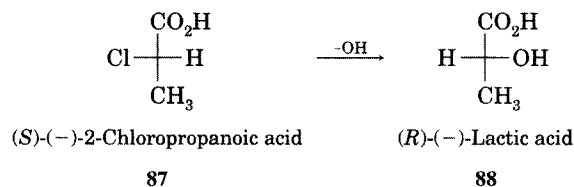
¹⁵⁸ Zalkin, A.; Forrester, J. D.; Templeton, D. H. *Science* **1964**, *146*, 261.

FIGURE 2.33

Reactions proceeding with retention of configuration.

**FIGURE 2.34**

Reaction proceeding with inversion of configuration.



any bonds to the chiral center (i.e., a reaction that proceeds with **retention of configuration**) must give a product with the same relative configuration as **84**. Therefore, the substitution of Cl for OH on C3 by a mechanism not involving breaking any bonds to C2 produces (–)-2-amino-3-chloropropanoic acid with the absolute configuration shown in **85** (Figure 2.33).¹⁵⁹ Similarly, hydrolysis of (–)-azaserine, **86**, produces (S)-(-)-serine by a mechanism that does not involve breaking any bond to the chiral center. This reaction thus proceeds with retention of configuration, so **86** must have the *S* configuration.¹⁶⁰

Note that **85**, which is an *R* configuration, was formed from a structure (**84**) having the *S* configuration by a pathway in which the configuration of the reactant was retained. This example illustrates that the *R* or *S* designation for a chiral center can change if a reaction alters the priorities of substituent atoms attached to the chiral center, even if the configuration of the chiral center is retained.

We may also determine the relative configuration of chiral structures even though bonds are broken to the chiral center if we are able to determine whether the reaction proceeds with retention or with inversion of configuration. The S_N2 reaction of (S)-(-)-2-chloropropanoic acid (**87**) with hydroxide ion produces (–)-lactic acid, which must have the *R* configuration (**88**, Figure 2.34).¹⁶¹ Note that in this case the direction of rotation of plane-polarized light stays the same, even though there *has* been an inversion of the substituents at the chiral center.

Other Physical Properties of Stereoisomers

A sample composed only of one enantiomer has physical properties that are identical to the properties of a sample composed only of the other enantiomer if all measurements are made with nonpolarized light and without the use of chiral reagents. Thus, enantiomers have the same melting point, boiling point, index of refraction, and so on. Mixtures of enantiomers may have different physical properties from those of either enantiomer alone, however. In

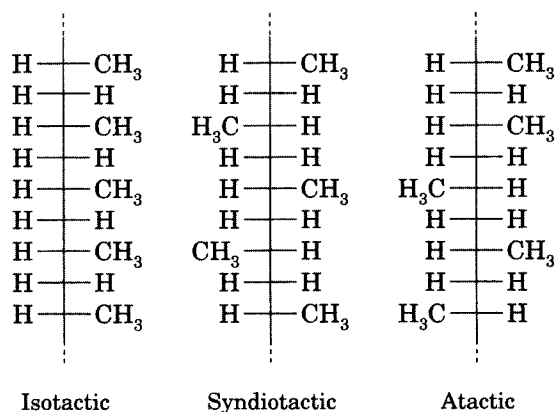
¹⁵⁹ Fischer, E.; Raske, K. *Ber. Dtsch. Chem. Ges.* **1907**, *40*, 3717.

¹⁶⁰ Fusari, S. A.; Haskell, T. H.; Frohardt R. P.; Bartz, Q. R. *J. Am. Chem. Soc.* **1954**, *76*, 2881.

¹⁶¹ Brewster, P.; Hughes, E. D.; Ingold, C. K.; Rao, P. A. D. S. *Nature* **1950**, *166*, 178.

TABLE 2.1 Physical Properties of Tartaric Acids

Isomer	Melting Point
(+) or (-)	171–174°
(±)	206°
meso	146–148°

**FIGURE 2.35**

Fischer projections of isotactic, syndiotactic, and atactic polypropylene segments.

particular, a racemate usually has different properties from those of the pure enantiomers. Table 2.1 shows the physical properties of (+)-, (-)-, (±)-, and *meso*-tartaric acid.¹⁶²

Stereochemical relationships play an especially important role in the properties of polymers.¹⁶³ Consider the three polypropylene segments illustrated as Fischer projections in Figure 2.35. In the *isotactic* polymer, all of the methyl-substituted carbon atoms have the same configuration. In the *syndiotactic* polymer, the methyl-substituted carbon atoms have alternating configurations. In the *atactic* polymer there is a random pattern of configurations at the methyl-substituted carbon atoms. As with smaller molecules, the physical properties of diastereomeric polymers differ. Table 2.2 shows the relationship between tacticity and properties of polypropene.^{164,165}

¹⁶² Data from Lide, D. R., Ed. *CRC Handbook of Chemistry and Physics*, 71st ed.; CRC Press: Boca Raton, FL, 1990; p. 3-475.

¹⁶³ Goodman, M. *Top. Stereochem.* **1967**, 2, 73; Jenkins, A. D. *Pure Appl. Chem.* **1981**, 53, 733.

¹⁶⁴ These data are from the compilation by Quirk, R. P. *J. Chem. Educ.* **1981**, 58, 540.

¹⁶⁵ For reviews, see Bawn, C. E. H.; Ledwith, A. *Q. Rev. Chem. Soc.* **1962**, 16, 361; Farina, M. *Top. Stereochem.* **1987**, 17, 1. Also see Coates, G. W.; Waymouth, R. M. *Science* **1995**, 267, 217.

TABLE 2.2 Tacticity and Physical Properties of Polypropene

Tacticity	Density (g/cm ³)	Phase Transition Temperature (°C)	Solubility in <i>n</i> -Heptane
Atactic	0.86	-35	Soluble
Syndiotactic	0.91	138	Soluble
Isotactic	0.94	171	Insoluble

Source: Reference 164.

2.4 STEREOTOPICITY

Stereochemical Relationships of Substituents

The emphasis to this point has been on the stereochemical relationship of one structure to another. However, the principles developed so far are also relevant to the consideration of symmetry relationships within a single molecule. Many of the labels for these relationships are based on the suffix *-topic*, from the Greek for "place."¹⁶⁶ Terms incorporating this suffix apply both to atoms and to spaces in a molecule, although we usually think of them in terms of atoms. Identical atoms that occupy equivalent environments (both in terms of chemical properties and local or molecular symmetry) are said to be **homotopic** (i.e., to have the same place).¹⁶⁷ Identical atoms in nonequivalent environments are said to be **heterotopic** (for different place). Heterotopic substituents can be either **constitutionally heterotopic** or **stereo-heterotopic**. Stereoheterotopic substituents can be either **enantiotopic** or **diastereotopic**.¹⁶⁸

Consider the examples in Figures 2.36–2.39. Any proton on either CH₃ group of propane (**89**) is homotopic with any other methyl proton, since the product of replacing any one proton by another substituent (shown as an X in **90**) is the same as that produced by replacing any other methyl proton (Figure 2.36). If necessary, the products can be seen to be identical by rotating the entire molecule, by rotation of one part of the molecule about an internal bond, or both. The two methylene protons on C2 of propane are also homotopic.

Any one of the methyl protons and any one of the methylene protons of butane (**91**) are constitutionally heterotopic because the replacements produce the constitutional isomers **92** and **93**, respectively (Figure 2.37). The two protons on either one of the methylene groups of butane are enantiotopic, however, since the product of replacing one methylene hydrogen by X (**94a**) is the enantiomer of the product formed by replacing the other hydrogen (on the *same* methylene) by X (**94b**, Figure 2.38). Similarly, the two methylene

¹⁶⁶ For more details of stereoisomeric relationships of substituents, see Mislow, K.; Raban, M. *Top. Stereochem.* **1967**, 1, 1.

¹⁶⁷ More precisely, homotopic atoms or groups in a molecule are related by a *n*-fold rotation axis (reference 11).

¹⁶⁸ Structures that differ only in isotopic composition, such as CH₄ and CH₃D, are termed **isotopologues**. Structures that have identical composition but differ in the location of isotopic groups, such as CH₃CH₂CH₂D and CH₃CHDCH₃, are termed **isotopomers** (a shortened form of *isotopic isomers*). Muller, P. *Pure Appl. Chem.* **1994**, 66, 1077. See also Stoll, S. *Chem. Educ.* **2007**, 12, 240.

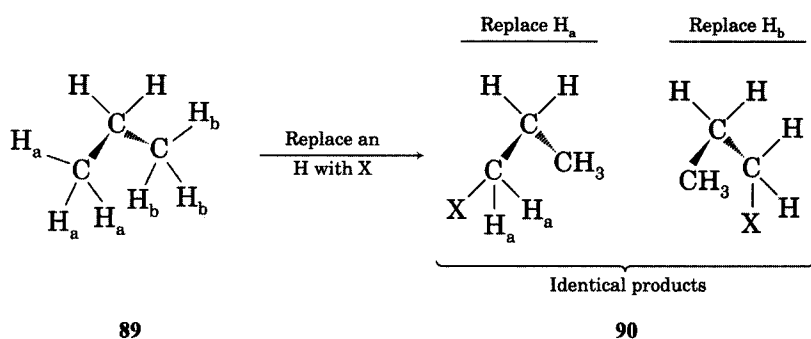


FIGURE 2.36
Examples of homotopic relationships.

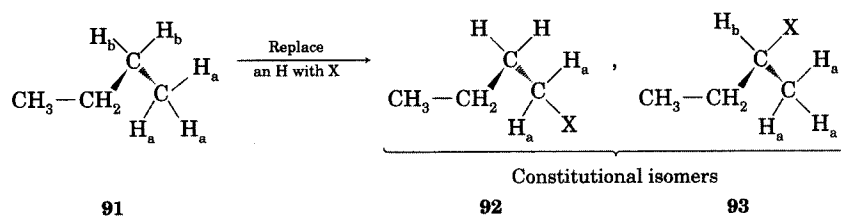


FIGURE 2.37
Example of constitutionally heterotopic relationship.

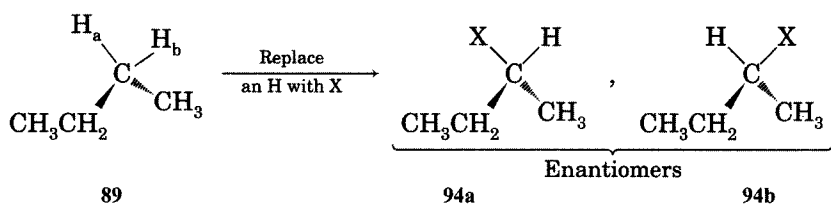


FIGURE 2.38
Example of enantiotopic relationship.

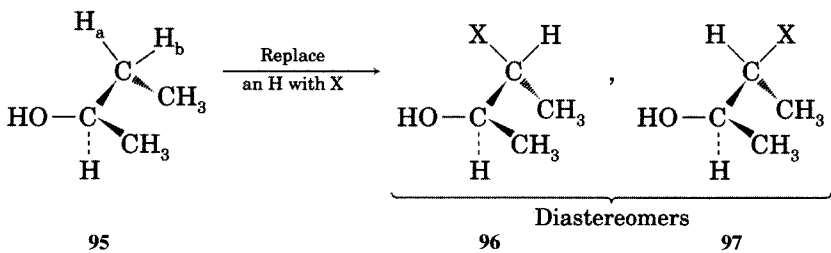
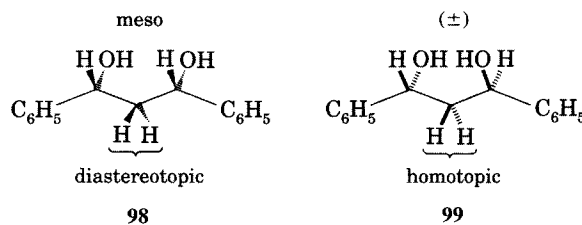


FIGURE 2.39
Example of diastereotopic relationship.

hydrogen atoms on C3 of (*R*)-2-butanol (**95**) are diastereotopic, since replacement of one by X generates a product, **96**, that is the diastereomer of the product (**97**, Figure 2.39) obtained by replacing the other one.

Understanding enantiotopic and diastereotopic relationships is essential in the interpretation of NMR spectra. Enantiotopic protons are equivalent in

FIGURE 2.40
Diastereotopic and homotopic
relationship in methylene protons
of stereoisomers.



typical NMR spectroscopy experiments, but diastereotopic protons are nonequivalent.^{169,170} Groups with identical chemical shift are said to be **isochronous**, while groups with nonequivalent chemical shifts are **anisochronous**.¹⁷¹ Not only may two diastereotopic protons on the same carbon atom have different chemical shifts, but they will also split each other, resulting in a complex spectrum.¹⁷² Consider the diastereomers of 1,3-diphenyl-1,3-propanediol shown in Figure 2.40.¹⁷³ In the meso structure, **98**, the two hydrogens on C2 are diastereotopic, so they have different chemical shifts and split each other. In the chiral diastereomer, **99**, however, the two central methylene hydrogens are homotopic. They have identical chemical shifts, and they do not split each other.

Two examples discussed by Jennings further illustrate the principles.^{171b} In *cis*- and *trans*-1,3-dimethylindane (Figure 2.41), the two methylene protons are diastereotopic in the meso structure, **100**, so they have different chemical shifts and split each other. In the chiral *trans* isomer, **101**, they are isochronous, so they have the same chemical shift and do not split each other. In contrast, the benzyl methylene protons in *N*-benzyl-2,6-dimethylpiperidine are enantiotopic in the *cis* isomer (**102**), but they are diastereotopic in the *trans* isomer (**103**).

Structures that are achiral but which can be made chiral by substitution are said to be **prochiral**.¹⁷⁴ In the example of butane, replacement of one of the hydrogen atoms on C2 by a deuterium atom as shown on the top of Figure 2.42 gives (*R*)-2-deuteriobutane, (*R*)-**104**. Therefore, that hydrogen is said to be the pro-(*R*) substituent and is indicated by the symbol H_R.^{175,176} Replacement of

¹⁶⁹ If we use a chiral solvent for NMR spectroscopy, then chemical shifts induced by solute-solvent interactions may be different for enantiotopic protons, and the spectrum may show differences between them. Moreover, chiral shift reagents can also make them distinguishable.¹⁶⁶

¹⁷⁰ Ault, A. J. *Chem. Educ.* **1974**, *51*, 729. For the theoretical basis of chemical shift nonequivalence, see Stiles, P. J. *Chem. Phys. Lett.* **1976**, *43*, 23. Note that the term magnetic nonequivalence is no longer favored (reference 171b).

¹⁷¹ (a) Compare Binsch, G.; Eliel, E. L.; Kessler, H. *Angew. Chem. Int. Ed. Engl.* **1971**, *10*, 570; (b) Jennings, W. B. *Chem. Rev.* **1975**, *75*, 307 and references therein.

¹⁷² Compare Waugh, J. S.; Cotton, F. A. *J. Phys. Chem.* **1961**, *65*, 562.

¹⁷³ For a discussion of the NMR spectra, see Deprés, J.-P.; Morat, C. *J. Chem. Educ.* **1992**, *69*, A232.

¹⁷⁴ Prochiral molecules can also be made chiral by other types of reactions, such as the addition of HCl to 2-butene.

¹⁷⁵ In the example of 2,2-dichlorobutane, replacement of one chlorine with a higher atomic mass isotope would serve to distinguish between the two stereoheterotopic positions. Clearly, this analysis is artificial, since Cl atoms occur naturally as different isotopes. Our designation of pro-(*R*) or pro-(*S*) is based on a definition of stereotopicity, not on an isotopic substitution that we are likely to carry out.

¹⁷⁶ The terms pro-(*R*), pro-(*S*), *re*, and *si* were defined by Hanson, K. R. *J. Am. Chem. Soc.* **1966**, *88*, 2731.

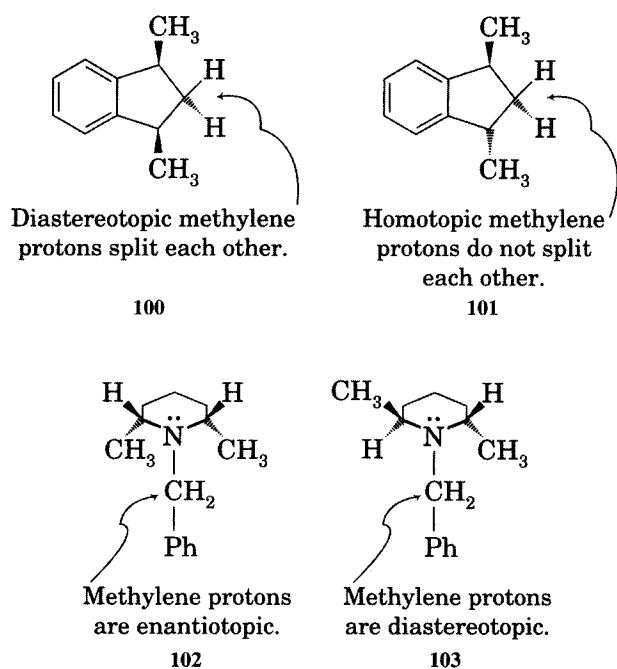


FIGURE 2.41
NMR consequences of stereochemical relationships.

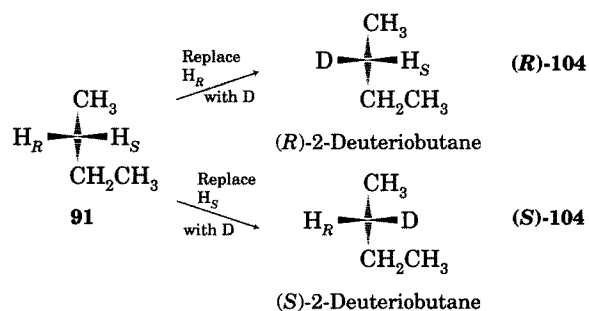


FIGURE 2.42
Prochiral relationships.

the other hydrogen by deuterium gives (*S*)-2-deuteriobutane, (*S*)-104, so that hydrogen is the pro-*S* substituent and is designated H_S .¹⁷⁷ Identification of diastereotopic and enantiotopic substituents is particularly important in biochemistry, because enzymes may distinguish between prochiral groups.

Since topicity is a property of atoms in *and spaces near* a molecule, *spaces around an achiral molecule* can also be considered prochiral. For example, reduction of acetophenone (**105**) by lithium aluminum hydride gives either (*R*)- or (*S*)-1-phenylethanol (**106**), depending on the pathway of the reaction (Figure 2.43). In talking about the reaction pathway, it is useful to differentiate

¹⁷⁷ Eliel noted some formal statements of pro-*R* and pro-*S* determinations. One easy rule to use is that one arranges the substituents according to normal rules of priority. Then one arbitrarily assigns one of the two identical groups a higher priority than the other one of them. If this arbitrary assignment gives a formal *R* configuration, then the group assigned higher priority is the pro-*R* group. If the arbitrary assignment of higher priority makes the configuration *S*, then the group assigned higher priority is the pro-*S* substituent. Eliel, E. L. *J. Chem. Educ.* **1971**, *48*, 163.

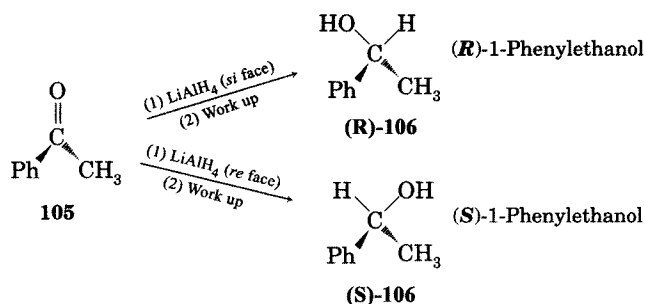


FIGURE 2.43

Stereochemical consequences of a ketone reduction.

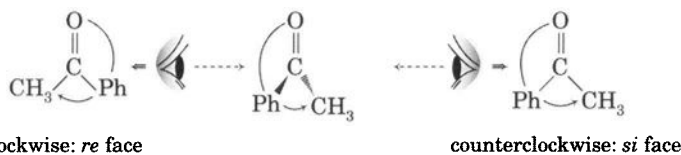


FIGURE 2.44

Prochiral faces of molecules.

the faces of the molecule as the *re* face (from the Latin *rectus*) or as the *si* face (from the Latin *sinister*),⁷⁹ just by applying the CIP sequence rules to the three substituents in the planar molecule as viewed from each face (Figure 2.44).¹⁷⁶

Chirotopicity and Stereogenicity

Mislow and Siegel pointed out that the local geometry of a molecule and its stereoisomerism are two distinctly different properties. Furthermore, they distinguished between **chirotopicity** and **stereogenicity** as follows:¹⁷⁸

- *Chirotopicity* is a local geometry that produces chirality. Not only are the atoms in a chiral environment said to be *chirotopic*, but the spaces around atoms in a chiral environment are also considered chirotopic. Atoms (or spaces) in an achiral environment are said to be *achirotopic*.
- *Stereogenicity* is the property of producing a new stereoisomer by the interchange of two bonded atoms in a structure. An atom that displays stereogenicity is said to be *stereogenic*, that is, it is a stereocenter. (A space cannot be a stereocenter, since atoms cannot be interchanged about it by breaking bonds to it.)

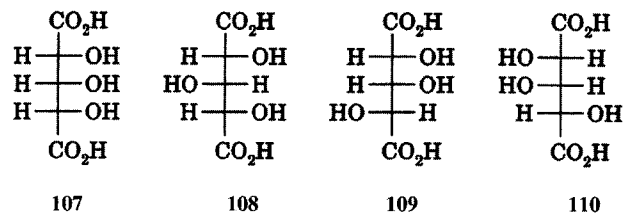
Mislow and Siegel gave as an example the set of isomers of 2,3,4-trihydroxyglutaric acid, **107–110**. Neither **107** nor **108** is chiral because both are meso structures. In both structures, C3 has been labeled “undoubtedly an ‘asymmetric’ carbon atom.”^{179,180} According to Mislow and Siegel, however, C3 is stereogenic and achirotopic in **107** and **108**.¹⁸¹ On the other hand, C3 is nonstereogenic and chirotopic in compounds **109** and **110**.

¹⁷⁸ Mislow, K.; Siegel, J. J. *Am. Chem. Soc.* **1984**, *106*, 3319. For a summary of this paper, see (a) Maugh, T. H. II. *Science* **1984**, *225*, 915; (b) Dagani, R. *Chem. Eng. News* **1984** (June 11), 21.

¹⁷⁹ Jaeger, F. M., cited in reference 178.

¹⁸⁰ An alternative term for C3 of **107** is *pseudoasymmetric* (reference 11).

¹⁸¹ It is important to recognize that the definition of stereogenicity calls for interchange of two groups to produce a *stereoisomer*, not necessarily an *enantiomer*. In this case the interchange produces a diastereomer.



Mislow and Siegel introduced new definitions to clarify some ambiguous stereochemical nomenclature, and they restated some topicity definitions to make them consistent with the stereochemical terms. The flow chart in Figure 2.45 shows their classification for the kinds of substituents within a molecule.¹⁷⁸ The classification system is based on the answer to three questions:

1. Are the atoms related by a symmetry operation of the molecule?
2. Are they related by a symmetry operation of the first kind?¹⁸²
3. Do they have the same bonding connectivity (constitutions)?

In each case, a yes answer causes branching along the bold line, a no answer causes branching along the lighter line.

Mislow and Siegel also extended the definition of the term *prochiral* as follows:

We define as **(pro)^p-chiral** ($p > 0$) any finite, achiral object that can be desymmetrized into a chiral object by *at most* p stepwise replacements of a point by a differently labeled one and as **(pro)^p-chirality** the corresponding property of an achiral object.^{183,184}

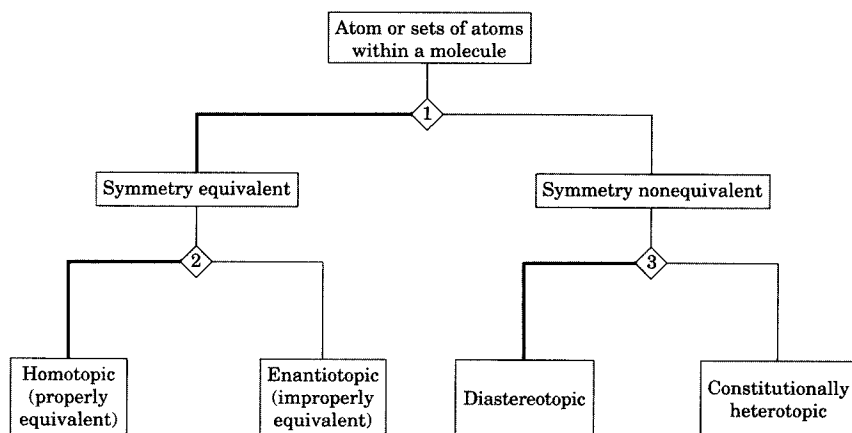


FIGURE 2.45
Topic relationships. (Reproduced from reference 178.)

¹⁸² A symmetry operation of the first kind is a proper rotation (C_n), as opposed to an improper rotation (S_n).

¹⁸³ Note that each subsequent replacement reduces the symmetry of the previous structure from (pro)⁽ⁿ⁺¹⁾-chiral to (pro)ⁿ-chiral, where n is an integer greater than 1.

¹⁸⁴ The emphasis in the definition is added.

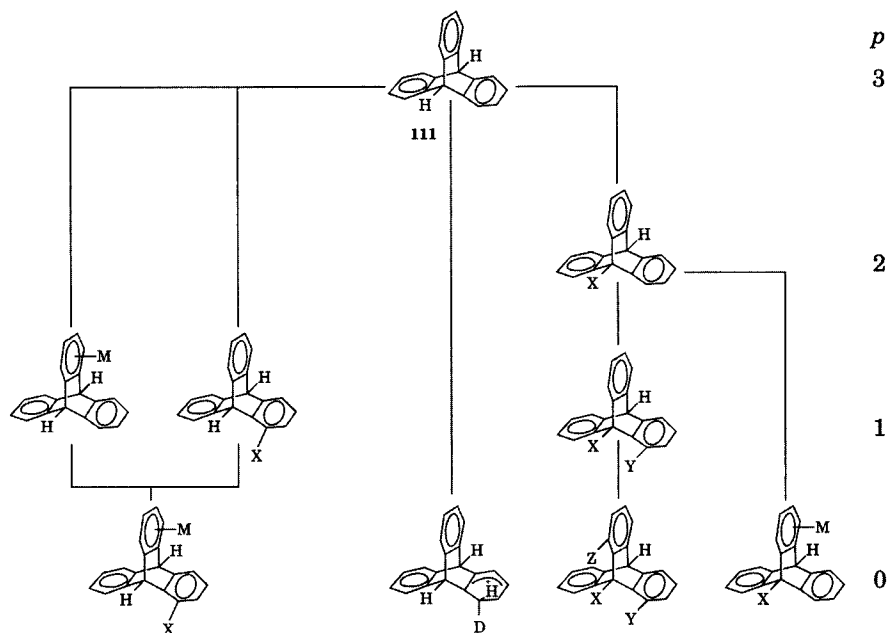


FIGURE 2.46
Prochirality determination of triptycene. (Reproduced from reference 178.)

Note that (pro)^p-chirality is a property of the entire molecule, not just a particular atom within the molecule. Consider the example of triptycene, **111**, in Figure 2.46. The structure can be desymmetrized by several pathways, one of which will produce a chiral structure in only one step. However, the desymmetrization can be accomplished in *at most* three steps if each step involves a different symmetry element, so it is said to be (pro)³-chiral.¹⁸⁵ Table 2.3 lists the (pro)^p-chirality of molecules as a function of their symmetry.¹⁸⁶

TABLE 2.3 Prochirality and Molecular Symmetry

Desymmetrization Index <i>p</i>	0	1	2	3
Description of molecule (segment)	chiral (chirotopic)	(pro) ¹ -chiral ((pro) ¹ -chirotopic)	(pro) ² -chiral ((pro) ² -chirotopic)	(pro) ³ -chiral ((pro) ³ -chirotopic)
Molecular or local symmetry	<i>C_{nv}</i> , <i>D_{nv}</i> , <i>T</i> , <i>O</i> , <i>I</i>	<i>C_s</i> , <i>C_i</i> , <i>S_{2n}</i>	<i>C_{nv'}</i> , <i>C_{nh}</i>	<i>D_{nd'}</i> , <i>D_{nh'}</i> , <i>T_{d'}</i> , <i>T_{h'}</i> , <i>O_{h'}</i> , <i>I_{h'}</i> , <i>K_{h'}</i>
Invariant achirotopic subspace ^a	None	A plane or the central point	An axis or the central point	The central point

Source: Reference 178.

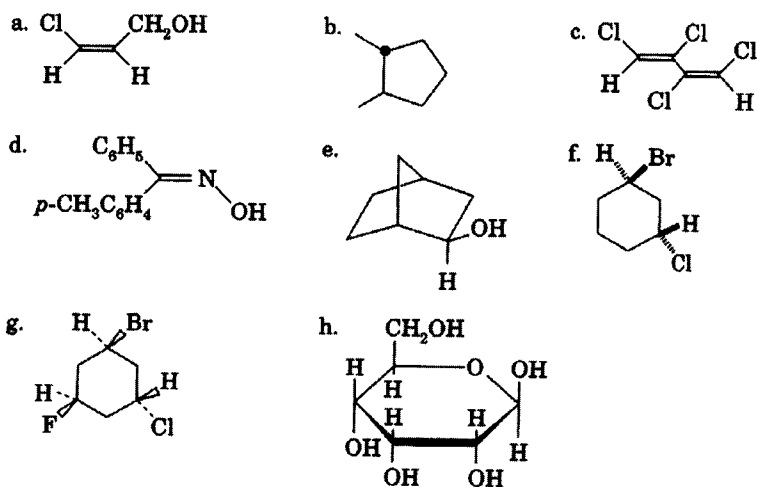
^aA set of points that remain stationary under every improper rotation of the point group.

¹⁸⁵ A desymmetrization step removes the smallest number of symmetry elements possible in one step (reference 11).

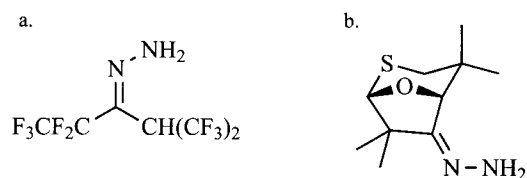
¹⁸⁶ Prochirality was discussed in terms of group theory by Fujita, *S. J. Am. Chem. Soc.* **1990**, *112*, 3390; *Tetrahedron* **1990**, *46*, 5943; **1991**, *47*, 31.

Problems

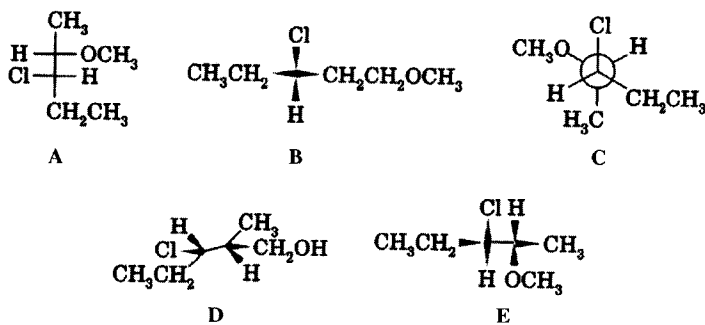
- 2.1. Designate one or more appropriate stereochemical labels (such as *syn*, *anti*, *E*, *Z*, *R*, *S*, *endo*, *exo*, α , β , *rel*, *R*^{*}, or *S*^{*}) for each of the following structures. Note that parts f and g use the Maehr notation discussed on page 74.



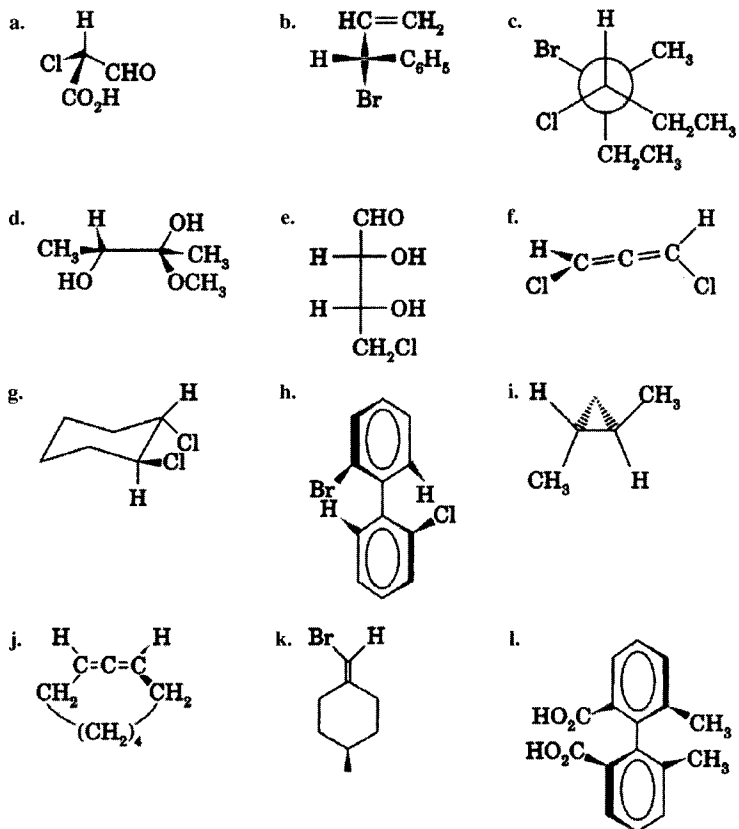
- 2.2. Label the double bonds in the following compounds as *E* or *Z*.



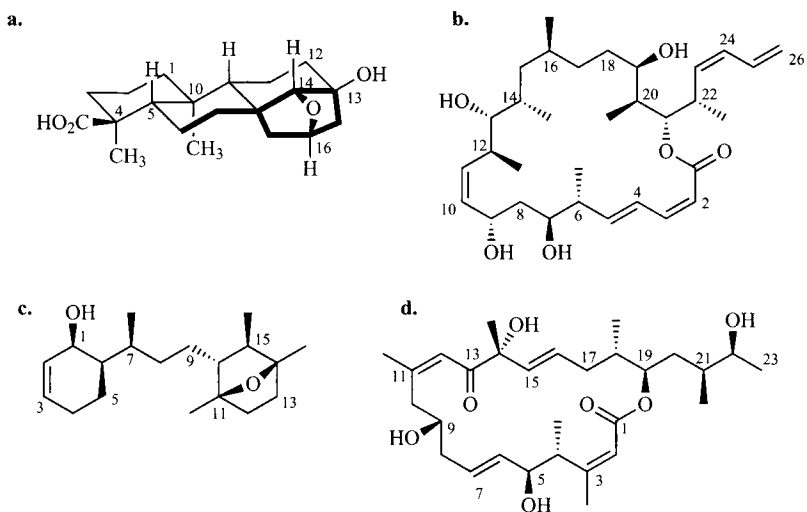
- 2.3. Consider the relationship of structure A with each of the structures B, C, D, and E. (Some structures are deliberately drawn in nonstandard representations.) Determine whether A and each of the other structures comprise a pair of identical compounds, positional isomers, functional group isomers, enantiomers, diastereomers, or nonisomeric compounds (i.e., compounds with different molecular formulas).

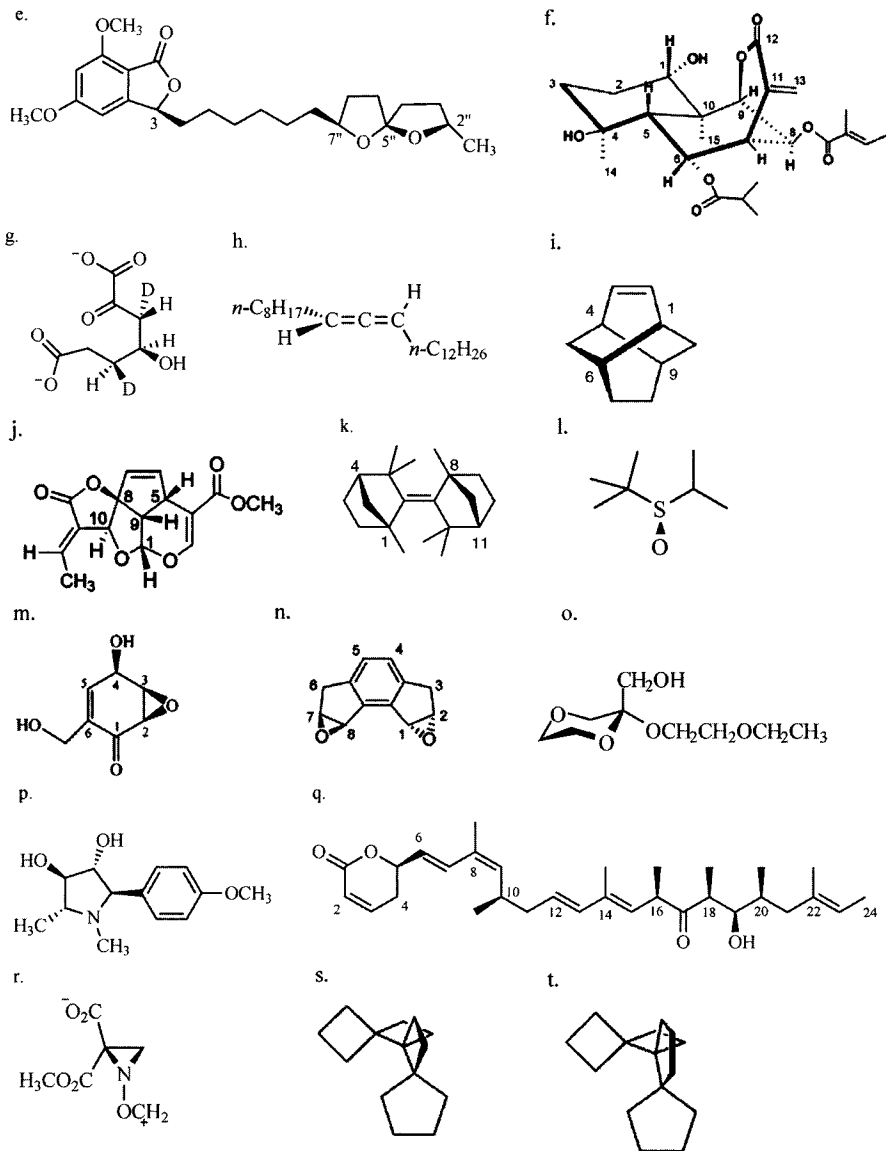


2.4. Name each of the following structures, using *R*, *S*, *M*, or *P* designations.

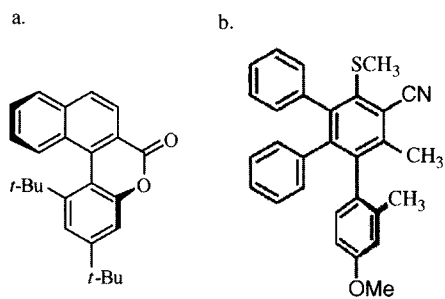


2.5. Assign the *R* or *S* designation to each element of chirality in the following structures

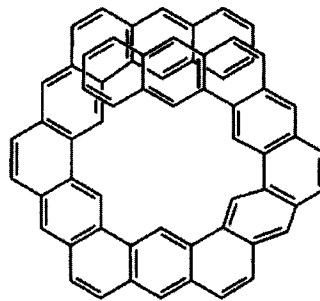




2.6. Assign the *M* or *P* designation to the following structures:

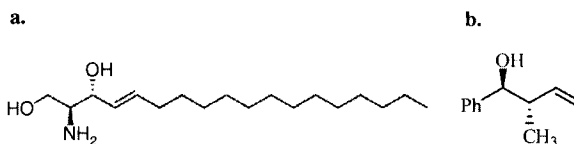


2.7. Assign both the *R* or *S* and the *M* or *P* designation to the helicene 112.

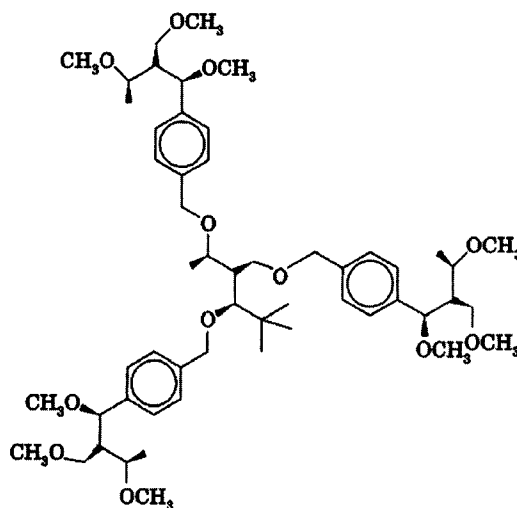


112

2.8. Label the following compounds as *erythro* or *threo*.



2.9. How many stereoisomers are possible for the dendrimer 113?

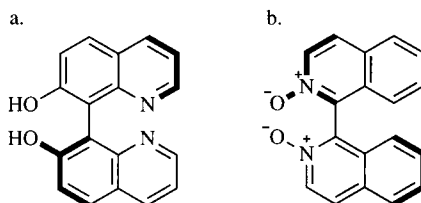


113

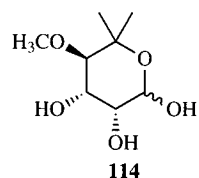
- 2.10. Demonstrate that structure 12 (page 60) is achiral by showing that it can be superimposed on its mirror image.
- 2.11. How many stereoisomers are possible for the propionic acid ester of 3,7,11-trimethyl-2-tridecanol?
- 2.12. Draw a clear three-dimensional representation for each of the following compounds:
- (*2E,4E,6R,10R*)-4,6,10,12-tetramethyl-2,4-tridecadien-7-one
 - (*2S,4'R,8'R*)- α -tocopheryl acetate

- c. (2*R*,4*R*)-1,2:4,5-diepoxy-pentane
 d. (*S*,*S*)-cyclopropane-1, 2-²H₂
 e. (*S*)-3-butene-1,2-diol
 f. (*R*)-3-hydroxy-3-phenylpropanoic acid
 g. (*Z*,*Z*)-deca-,3,7-diene-1,5,9-tri-yne
 h. (2*R*,6*S*,10*S*)-6,10,14-trimethylpentadecan-2-ol
 i. (*R*)-(-)-(4-methylcyclohexylidene)acetic acid
 j. (*S*)-2,2'-dihydroxy-4,5,6,4',5',6'-hexamethoxybiphenyl
 k. (2*S*, 3*S*)-cyclopropane-1-¹³C, ²H-2, 3-²H₂
 l. (*S*)-[2-(phenylmethoxy)ethyl]oxirane
 m. (±)-*threo*-1,2-dihydroxybutyric acid
 n. *r*-1,*cis*-3-dimethoxy-*trans*-5-methylcyclohexane
 o. (*S*,*S*)-(-)-1,6-bis(*o*-chlorophenyl)-1,6-diphenylhexa-2,4-diyne-1,6-diol
- 2.13. Draw a clear representation of the three-dimensional structure of each of the following compounds:
- a. (3*S*,4*S*)-*d*₆-cyclopentene
 b. (3*R*,4*S*,5*R*,6*S*)-3,4,5,6-tetrahydrocyclohex-1-enecarboxylic acid
 c. (2*E*,6*E*,11*S*,12*R*)-3,7,11,15-tetramethylhexadeca-2,6,14-triene-1,12-diol
 d. (4*S*,6*R*,8*R*,10*S*,16*R*,18*S*)-4,6,8,10,16,18-hexamethyldocosane
 e. (6*Z*,9*Z*,4*S*,5*S*)-4,5-epoxynonadeca-6,9-diene
 f. (1*R*,5*R*)-2,6-diphenylbicyclo[3.3.1]nona-2,6-diene
 g. *l*-*threo*-3-fluoroglutamic acid
 h. *r*-1,*c*-2,*c*-3,*t*-4-tetrachlorotetralin
 i. (*R*)-1-chloro-2,2-dimethylaziridine
 j. (8*S*,9*S*,10*S*)-8,10-dimethyl-1-octalin
 k. (3*R*,9*R*,10*R*)-heptadec-1-ene-4,6-diyne-3,9,10-triol
 l. (*R*)-dibenzyl (¹²CH₂, ¹³CH₂) sulfoxide (Ph¹²CH₂SO¹³CH₂Ph)
 m. (*Z*,*Z*)-2,8-dimethyl-1,7-dioxaspiro[5.5]undecane
 n. (2*R*,3*R*,5*E*)-2-hydroxy-3-methyl-5-heptenal
 o. (2*S*,3*S*)-octane-2,3-diol
 p. (1*R*,2*R*,3*R*,4*R*,5*S*)-1-(methylthio)-2,3,4-trihydroxy-5-aminocyclopentane
- 2.14. Indicate whether each of the following reactions proceeds with inversion of configuration or retention of configuration at each chiral center:
- a. (*R*)-(+)-1,2-epoxybutane → (*R*)-(-)-3-hexanol (upon treatment with ethyllithium)
 b. (*S*)-(+)-2,2-dimethylcyclopropanecarboxamide → (*S*)-(-)-2,2-dimethylcyclopropylamine (Hofmann conditions)
 c. (*S*)-ethanol-1-*d* → (*S*)-[1-²H, 1-³H]ethane (reagents: (i) TsCl, Et₃N; (ii) LiEt₃B³H)
 d. (*S*)-[1-²H, 1-³H]ethane → (*R*)-[1-²H, 1-³H]ethanol (by action of methane monooxygenase)
 e. (*S*)-(+)-1-bromo-1-methyl-2,2-diphenylcyclopropane → (*R*)-(-)-2-methyl-1,1-diphenylcyclopropane
 f. (2*R*,3*S*)-(+)-3-bromobutan-2-ol → (2*S*,3*S*)-(-)-2,3-dibromobutane
 g. *D*-(+)-1-buten-3-ol → *D*-(-)-3-methoxy-1-butene
 h. reduction of (1*R*,2*R*,3*R*)-1-phenyl-2-methyl-1,3-butanediol to (2*R*,3*R*)-3-methyl-4-phenyl-2-butanol
 i. ring-opening hydrogenolysis of the C_{benzylic}-N bond of methyl (2*S*,3*R*)-3-methyl-3-phenylaziridine-2-carboxylate to methyl (2*S*,3*R*)-2-amino-3-methyl-3-phenylpropionate

2.15. Label the following structures as aR or aS.

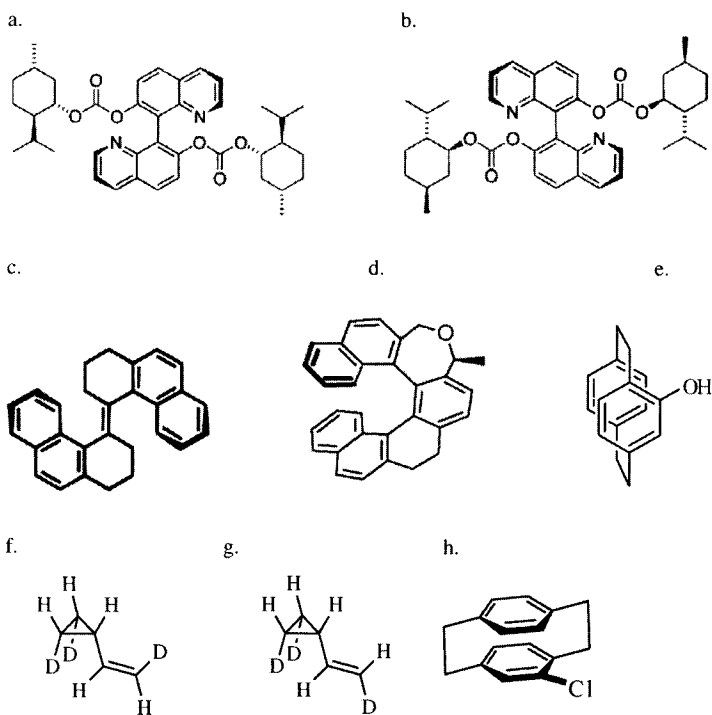


2.16. Characterize structure **114** as D or L.

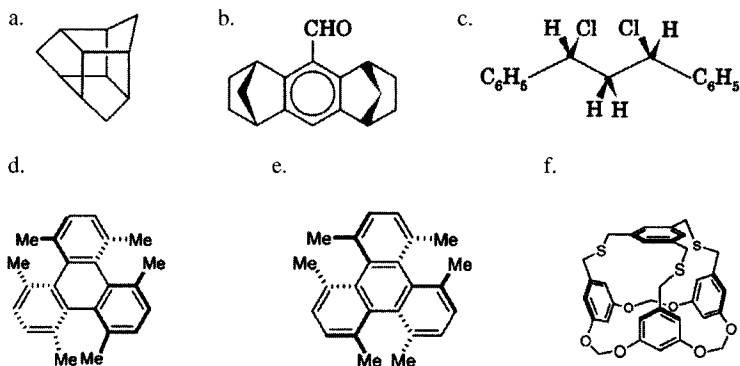


2.17. Show a Fischer projection for each of the four possible stereoisomers of 2-methylbutane-1,2,3,4-tetraol. Label each chiral center as R or S and label each structure with the D or L and the *erythro* or *threo* notation.

2.18. Provide appropriate stereochemical designations for each stereocenter in the structures below. What is the relationship of structures a and b?

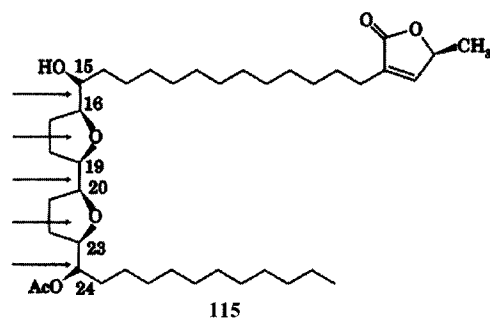


2.19. Assign the point group for each of the following compounds and indicate whether each is chiral:

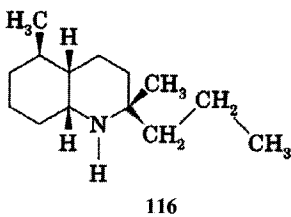


2.20. a. Assign an appropriate stereochemical designator (*threo*, *erythro*, *E*, *Z*, etc.) to each of the positions marked with an arrow in (+)-Uvaricin (**115**).

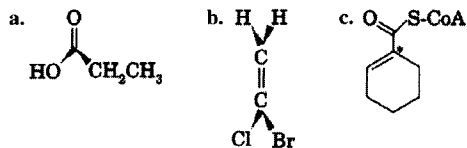
b. Draw the structure of (15,16,19,20,23,24)-*hexaepi*-Uvaricin and give a stereochemical designator for each of the corresponding positions in this compound.



2.21. The decahydroquinoline alkaloid **116** was labeled 195A. Draw a clear three-dimensional representation of 2-*epi*-195A.

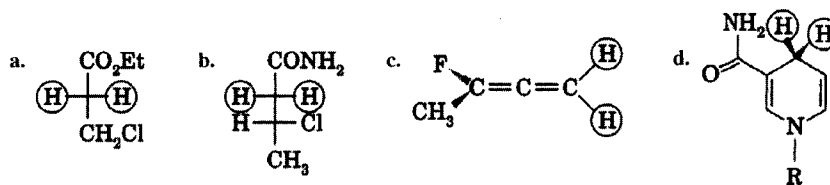


2.22. Indicate the *re* and *si* faces for the following structures. In part c indicate the prochirality about the atom marked with the asterisk. (CoA is an abbreviation for coenzyme A.)

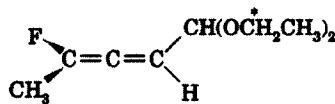


2.23. In each of the following structures indicate whether the circled groups are

- (i) homotopic or heterotopic;
- (ii) if heterotopic, whether they are constitutionally heterotopic or stereoheterotopic;
- (iii) if stereoheterotopic, whether they are enantiotopic or diastereo-topic;
- (iv) if enantiotopic or diastereotopic, indicate which is pro-(*R*) and which is pro-(*S*).

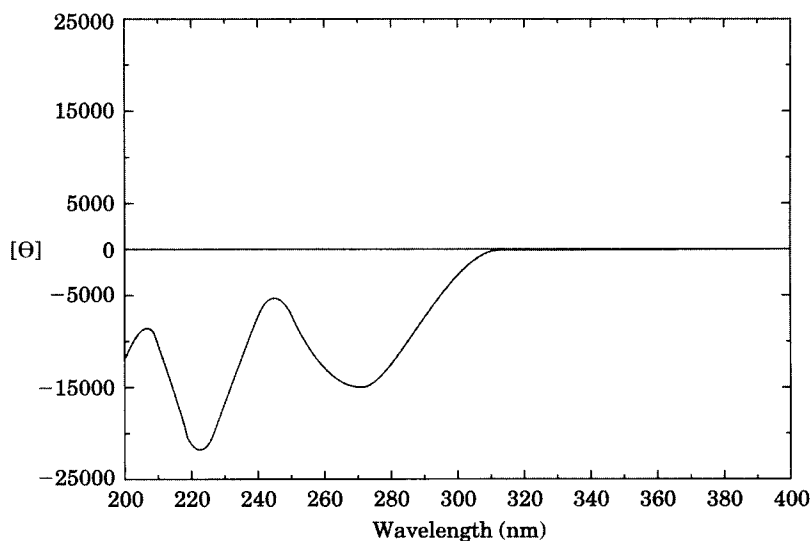


2.24. How many NMR signals would you expect from the protons on the methylene groups marked with the asterisk in 117?



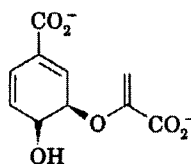
117

- 2.25. Mislow and Siegel noted that C3 in both compounds 109 and 110 is nonstereogenic *and* chirotopic. Use the definitions of these terms and the properties of the molecules to demonstrate that this statement is correct.
- 2.26. Use the Mislow and Siegel definition of (pro)^p-chirality to determine the order of prochirality of the following structures:
- a. barrelene
 - b. cubane
 - c. bicyclo[1.1.0]butane
 - d. bicyclo[2.2.2]octane
- 2.27. The ¹H NMR spectrum of the methylene group of 2-phenyl-3-methylbutylmagnesium chloride in THF solution indicates that the two protons are magnetically nonequivalent at 66° but are magnetically equivalent at 120°. Propose an explanation for the effect of temperature on the spectrum of this compound.
- 2.28. The specific rotation of (–)-2-bromobutane was reported to be –23.13°. A sample prepared by nucleophilic attack of bromide ion on the tosylate of partially resolved 2-butanol had a measured specific rotation of –16.19°. What is the mole fraction of each enantiomer in this sample of 2-bromobutane?

**FIGURE 2.47**

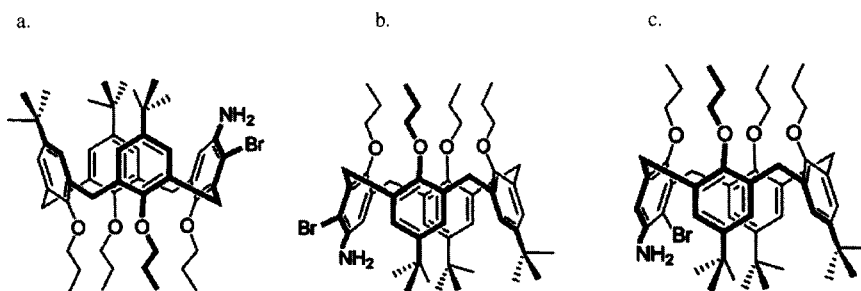
Circular dichroism spectrum of (-)-chorismate. (Adapted from reference 187.)

- 2.29. Reaction of acetaldehyde with a chiral, partially deuterated reducing agent produced ethanol-1-*d* with $[\alpha]_D = -0.123 \pm 0.025^\circ$. This product was calculated to be $44 \pm 9\%$ optically pure. The ethanol-1-*d* was converted to the *p*-nitrobenzenesulfonate, which was then used in an acetoacetic ester synthesis with methyl acetoacetate and sodium methoxide. The product of that reaction was hydrolyzed and decarboxylated to give 2-pentanone-4-*d* having $[\alpha]_D + 0.25 \pm 0.03^\circ$. Clemmensen reduction of that compound produced pentane-2-*d* having $[\alpha]_D + 0.19 \pm 0.06^\circ$. The compound (-)-pentane-2-*d* was reported to have the (*S*) configuration.
- If the initially formed ethanol-1-*d* is 44% optically pure, what would be the specific rotation of optically pure ethanol-1-*d*?
 - What is the absolute configuration of the ethanol-1-*d* formed in the reduction reaction?
- 2.30. The biologically important compound (-)-chorismate (**118**) exhibits the circular dichroism spectrum shown in Figure 2.47.
- Draw a clear three-dimensional representation of (+)-chorismate.
 - Sketch the CD spectrum expected for (+)-chorismate.

**118**

¹⁸⁷ Hilvert, D.; Nared, K. D. *J. Am. Chem. Soc.* **1988**, *110*, 5593.

- 2.31. The circular dichroism spectrum of structure a is shown in Figure 2.48. Modify the figure to show the CD spectrum expected for structure b and then do the same for structure c.



- 2.32. A study of the mechanism of the Wurtz reaction required knowing the configuration of (–)-3-methylnonane produced in the reaction. The researchers treated (R)-(–)-2-bromooctane with the product formed by adding sodium and diethyl malonate to ethanol. The levorotatory product was then hydrolyzed and heated until 1 mole of CO₂ was lost per mole of product, producing a levorotatory monocarboxylic acid. Treatment of the product with LiAlH₄, then PBr₃, and then with LiAlH₄ again produced (–)-3-methylnonane. Show the mechanism of each of the reactions in this sequence and tell whether the product (–)-3-methylnonane has the same configuration as the reactant (R)-(–)-2-bromobutane.
- 2.33. *Alcaligenes bronchisepticus* KU 1201 decarboxylates α-methyl-α-phenylmalonic acid to form (R)-α-phenylpropanoic acid.
- In the absence of an isotopic label, is the parent reaction stereoselective or stereospecific?
 - In separate experiments, each of the carboxyl carbon atoms was labeled with ¹³C. When the reactant was (S)-(–)-[1-¹³C]-α-methyl-α-phenylmalonic acid, the product was (R)-[1-¹³C]-α-phenylpropanoic acid. When the (R)-(+)-enantiomer of the starting material was used, the product was (R)-(–)-α-phenylpropanoic acid (without the ¹³C label).

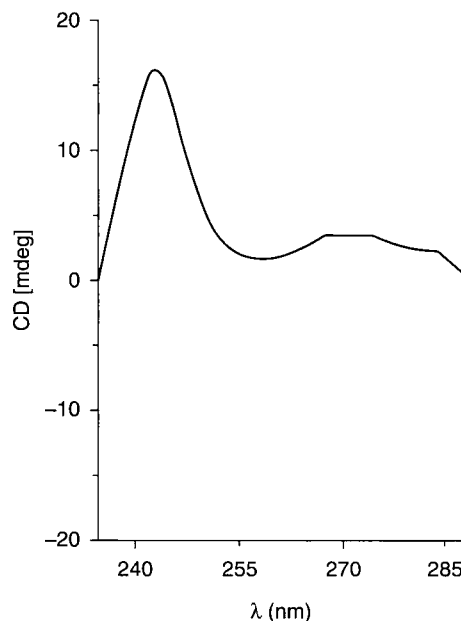


FIGURE 2.48
CD spectrum of structure a.

- i. Which carboxyl group (pro-*R* or pro-*S*) is removed in the decarboxylation?
- ii. Does the decarboxylation take place with retention or inversion of configuration?
- 2.34. *cis*-3,7-Dimethyl-1,5-cyclooctanedione underwent two successive Baeyer–Villiger rearrangements to give two products, both with the molecular formula $C_{10}H_{16}O_4$. When one of these products was reduced with $LiAlH_4$, two achiral diols were obtained. When the other was reduced, the product was the racemate of a chiral diol. What are the structures of the products obtained in each of the $LiAlH_4$ reductions?
- 2.35. Figure 2.49 shows a segment of a threodiisotactic polymer. Draw a corresponding segment of an erythrodiisotactic polymer having the same R_1 and R_2 substituents.
- 2.36. Are either or both of these two paracyclophanes chiral?

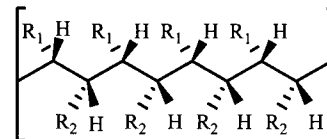
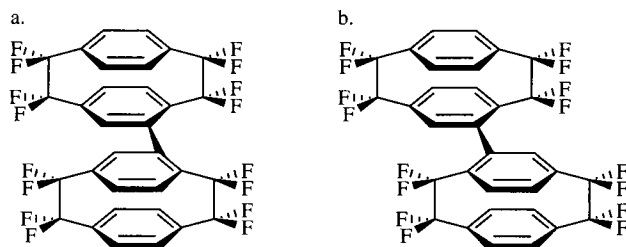


FIGURE 2.49



Conformational Analysis and Molecular Mechanics

3.1 MOLECULAR CONFORMATION

The discussion of stereochemistry in Chapter 2 implicitly assumed that molecules are as rigid as the physical models or two-dimensional pictorial representations that we use to study them. Our current understanding of quantum mechanics, thermodynamics, and spectroscopy tells us that molecules are in constant motion, however. At room temperature they vibrate and (in the liquid or gas phase) rotate. Not only may the entire molecule rotate, but bond rotations within a structure can change intramolecular spatial relationships.

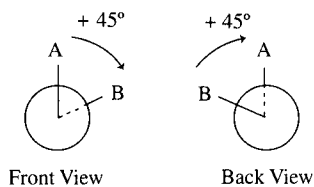
The term **conformation** generally refers to one of the spatial arrangements that a molecule can achieve by rotation about single bonds.^{1,2} If a molecule has several bonds about which rotation can occur, then the shape of the molecule can change significantly. Even though they ordinarily cannot be isolated, conformations that correspond to energy minima are known as **conformers**, a contraction of *conformational isomers*. Occasionally they are called **rotamers**, a shortened form of *rotational isomers*.

A conformation can be identified by a **dihedral angle**, which is the angle made by two bonds on adjacent atoms when the adjacent atoms are eclipsed in a Newman projection.³ Consider a C–C unit with substituent A on one carbon atom and substituent B on the other. The dihedral angle is the angle between the lines A–C and C–B in the Newman projection. The angle is considered positive if the arrow drawn from the near bond line curves clockwise toward the second bond line and negative if the arrow curves counterclockwise.

¹ The origin of the term *conformation* is ascribed to Haworth, W. N. *The Constitution of Sugars*; E. Arnold and Co.: London, 1929; p. 90 ff. See also Barton, D. H. R.; Cookson, R. C. *Q. Rev. Chem. Soc.* **1956**, *10*, 44.

² Eliel noted the difficulties in precisely defining the term *conformation*: (a) Eliel, E. L.; Allinger, N. L.; Angyal, S. J.; Morrison, G. A. *Conformational Analysis*; Wiley-Interscience: New York, 1965; p. 1; (b) Eliel, E. L. *J. Chem. Educ.* **1975**, *52*, 762.

³ Alternatively, it may be considered the angle made by the intersection of two planes, one defined by the two carbon atoms and atom A, the other defined by the two carbon atoms and atom B.

**FIGURE 3.1**

Determination of dihedral angle for A–C–C–B bonds.

As shown in Figure 3.1, the dihedral angle is the same no matter which way the Newman projection is viewed.

Several important conformational terms are best described with Newman projections. Consider the set of conformations of the structure A–CH₂–CH₂–B (1) in Figure 3.2. In Figure 3.2(a) the A–C and C–B bonds are eclipsed. Rotating about the C–C bond so that the substituents on the front carbon atom stay fixed but the substituents on the back carbon atom rotate 60° clockwise, we produce a **staggered** conformation, which is a general term for conformations with 60°, 180°, or 300° dihedral angles. The 60° conformation in Figure 3.2(b) is called **gauche** (sometimes termed **skew** or **syn**).

Rotation of the substituents on the back carbon atom an additional 60° produces another eclipsed conformation, Figure 3.2(c), this time with the C–A bond eclipsing a C–H bond on the back carbon atom, and the C–B bond eclipsing a C–H bond on the front carbon atom. Rotation another 60° produces the **anti** conformation, Figure 3.2(d). A further 60° rotation of the

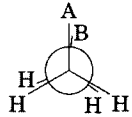
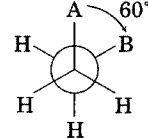
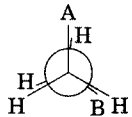
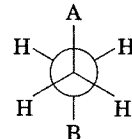
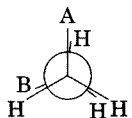
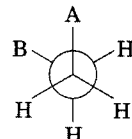
Newman Projection	Dihedral Angle	Conformation Description
(a) 	0°	eclipsed
(b) 	60°	gauche (skew) (syn) (staggered)
(c) 	120°	eclipsed
(d) 	180°	anti (trans) (staggered)
(e) 	240°	eclipsed
(f) 	300°	gauche (skew) (syn) (staggered)

FIGURE 3.2

Conformations of A–CH₂–CH₂–B (1). (Adapted from reference 5.)

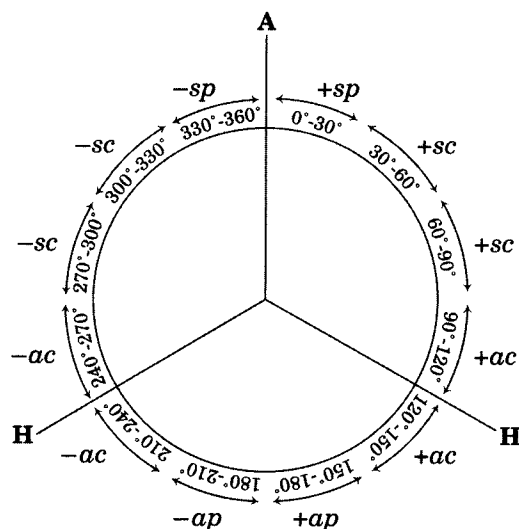


FIGURE 3.3
Conformational descriptors.

back carbon atom produces another eclipsed conformation, Figure 3.2(e), and one more 60° rotation leads to yet another gauche conformation, Figure 3.2(f).

The terms eclipsed, gauche, and anti define dihedral angles in 60° increments. In order to categorize conformations with other dihedral angles, Prelog and Klyne developed the alternative notation for conformations illustrated in Figure 3.3.⁴⁻⁶ If the dihedral angles are within 30° of either 0° or 180° , then the substituents A and B are approximately coplanar or **periplanar**. If the major substituents of interest on adjacent carbon atoms are in a conformation with dihedral angle between -30° and 0° , the conformation is *-syn-periplanar* (*-sp*), where the prefix *syn* indicates that the substituents are located on the same side and the minus sign indicates a negative dihedral. If the dihedral angle is between 0° and $+30^\circ$, then the conformation is *+syn-periplanar* (*+sp*). Similarly, if the dihedral angle is between 150° and 180° , the conformation is *+anti-periplanar* (*+ap*), and a conformation with dihedral angle between 180° and 210° is *-anti-periplanar* (*-ap*). Exactly 180° would be *ap* (without a sign), and exactly 0° would be *sp*.

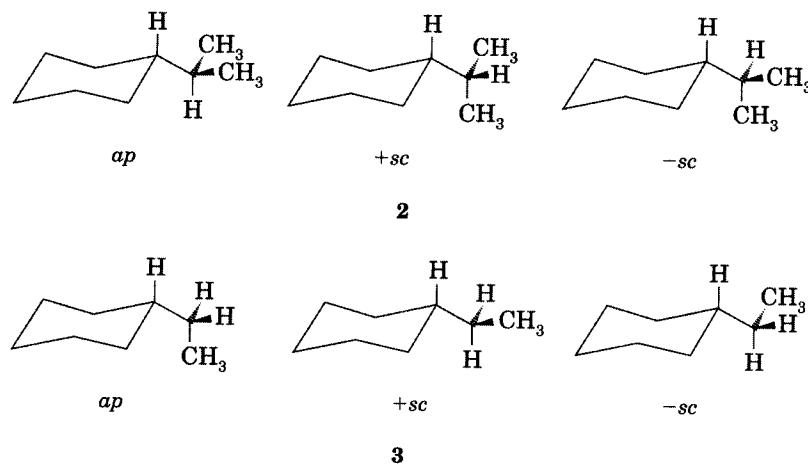
If the dihedral angle A-C-C-B is near 60° , near 120° , near 240° or near 300° , then one of the substituents is said to be *clinal* (inclined or slanted) with respect to the other. The notation for conformations with dihedral angles of 30° to 90° is *+syn-clinal* (*+sc*); 90° to 150° is *+anti-clinal* (*+ac*); 210° to 270° is *-anti-clinal* (*-ac*); and 270° to 330° is *-syn-clinal* (*-sc*).

When applying this conformational nomenclature, it is essential to identify the substituents on the two carbon atoms that determine the conformational designation.

⁴ Klyne, W.; Prelog, V. *Experientia* **1960**, *16*, 521.

⁵ See also the discussion of this system by Hanack, M. in Neumann, H. C., trans. *Conformation Theory*; Academic Press: New York, 1965; pp. 68-69.

⁶ IUPAC Organic Chemistry Division Commission on Nomenclature of Organic Chemistry, Rigaudy, J.; Klesney, S. P., Eds. *Nomenclature of Organic Chemistry, Sections A, B, C, D, E, F, and H*; Pergamon Press: Oxford, England, 1979; Section E-5.6, p. 484.

**FIGURE 3.4**

Conformational designs of isopropylcyclohexane (2) and ethylcyclohexane (3).

1. If there are three different substituents on a carbon atom, then the defining group is that which has highest priority according to the Cahn–Ingold–Prelog (CIP) sequence rules.⁷
2. If the three substituents on a carbon atom are identical, then the one that gives the smallest dihedral angle with the determining substituent on the other carbon atom is chosen.
3. If a carbon atom has two substituents that are identical, then it is the third substituent that determines the classification.

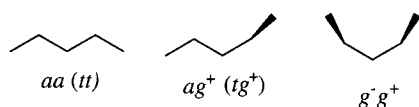
As an example of the last criterion, consider isopropylcyclohexane (2) and ethylcyclohexane (3, Figure 3.4). In 2 we are concerned with conformations about the bond from the ring carbon to C2 of the isopropyl group. Each of the carbons has one hydrogen and two other substituents that are identical to each other. Therefore, the H–C–C–H dihedral angle determines the conformational classification, and the three conformations shown are the *ap*, *+sc*, and *-sc* conformations. In 3, however, the unique atoms are the hydrogen on the cyclohexane ring and the methyl on C1 of the substituent group.⁸

A gauche conformation with a positive dihedral angle of $+60^\circ$ can be denoted g^+ , while a gauche conformation with a dihedral angle of -60° (i.e., $+300^\circ$) can be denoted g^- . The anti conformer can be denoted a . The anti conformer may also be denoted t , because the 180° dihedral angle conformation is often called “trans” in the physical chemistry literature.⁹ Organic chemists usually reserve the term trans for cis, trans isomers, however. This compact notation is particularly useful for representing several consecutive conformations in concise fashion. For example, three conformations of

⁷ Cahn, R. S.; Ingold, C. K.; Prelog, V. *Experientia* **1956**, *12*, 81; *Angew. Chem. Int. Ed. Engl.* **1966**, *5*, 385.

⁸ These conformations are discussed in Golan, O.; Goren, Z.; Biali, S. E. *J. Am. Chem. Soc.* **1990**, *112*, 9300.

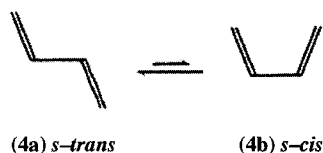
⁹ Hoffmann, R. W. *Angew Chem. Int. Ed.* **2000**, *39*, 2054.

**FIGURE 3.5**

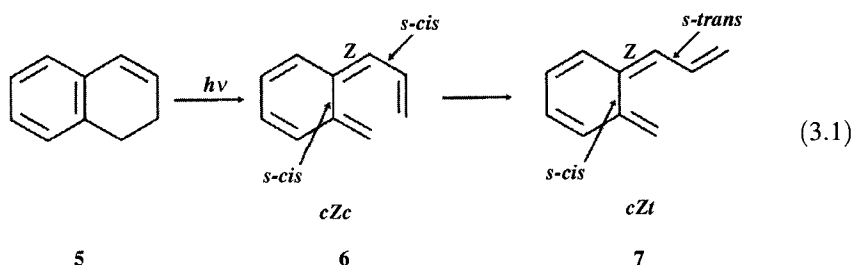
Compact conformational notation.

n-pentane about the C2–C3 and C3–C4 bonds could be represented as in Figure 3.5.^{10,11}

Another notation for conformers has been developed to describe the geometry about the single bond of 1,3-butadiene (**4**). We will see in Chapter 4 that theory predicts some double bond character for the C2–C3 bond, so there are two conformational energy minima separated by an energy maximum associated with rotation about the C2–C3 bond. We describe **4a** as *s-trans*-1,3-butadiene, since the two double bond units are *trans* to each other across the formally single bond. Similarly, **4b** is the *s-cis* conformer.¹² With the advent of the (*E*) and (*Z*) nomenclature system, the notations *s-(Z)* and *s-(E)* have begun to replace *s-cis* and *s-trans*.



It is useful to combine the (*E*) and (*Z*) nomenclature system with the *s-cis*, *s-trans* system when designating the stereochemistry and conformation of polyenes. In such cases *s-cis* may be abbreviated as *c* and *s-trans* as *t*. For example, the photochemical reaction of 1,2-dihydronaphthalene (**5**) first forms the *cZc* conformer **6**, which then rotates about the single bond to form the *cZt* conformer **7** (equation 3.1).¹³



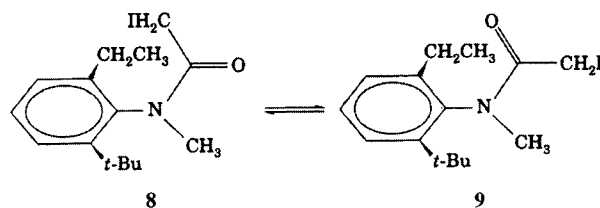
¹⁰ Klauda, J. B.; Brooks, B. R.; MacKerell, A. D., Jr.; Venable, R. M.; Pastor, R. W. *J. Phys. Chem. B* **2005**, *109*, 5300.

¹¹ There are six other conformations of *n*-pentane: ag^- , g^+a , g^-a , g^+g^+ , g^-g^- , and g^+g^- . For a discussion, see Senderowitz, H.; Guarnieri, F.; Still, W. C. *J. Am. Chem. Soc.* **1995**, *117*, 8211.

¹² The two double bonds are not entirely coplanar in the *s-cis* conformation. Both theoretical studies and experimental data suggest that the two double bonds might be nonplanar by about 25° to 35°, making the term *s-gauche* a better descriptor for the less stable conformer for 1,3-butadiene: Wiberg, K. B.; Rosenberg, R. E. *J. Am. Chem. Soc.* **1990**, *112*, 1509.

¹³ Keijzer, F.; Stolte, S.; Woning, J.; Laarhoven, W. H. *J. Photochem. Photobiol. A: Chem.* **1990**, *50*, 401 and references therein.

Ordinarily conformational isomers cannot be separated from each other. However, the C(O)–N bond of an amide also shows appreciable double bond character and thus restricted rotation. Chupp and Olin found a series of 2',6'-dialkyl-2-halo-N-methylacetanilides in which the barrier to rotation was so high that conformational isomers could be separated, purified, and characterized. For example, the melting points of the conformers **8** and **9** are 64–65°C and 105–106°C, respectively.^{14,15}



Molecular conformations are determined by a wide variety of experimental techniques.¹ Conformations of molecules in crystals may be determined by X-ray diffraction,¹⁶ and molecules in the gas phase may be investigated by electron diffraction¹⁷ and microwave spectroscopy.¹⁸ NMR,¹⁹ vibrational spectroscopy,²⁰ UV spectroscopy,²¹ and circular dichroism studies are also useful.²² Other techniques include calorimetry¹ and the determination of physical properties such as pK values²³ and dipole moments.²⁴ In addition, conformation may be inferred from kinetics of reactions of functional groups that may be in different conformational environments.¹

¹⁴ Chupp, J. P.; Olin, J. F. *J. Org. Chem.* **1967**, *32*, 2297.

¹⁵ (a) Two separable isomers were identified for triacetone triperoxide: Denekamp, C.; Gottlieb, L.; Tamiri, T.; Tsoglin, A.; Shilav, R.; Kapon, M. *Org. Lett.* **2005**, *7*, 2461. (b) The equatorial conformers of bromo- and chlorocyclohexane were isolated as inclusion complexes: Hirano, S.; Toyota, S.; Toda, F. *Chem. Commun.* **2004**, 2354.

¹⁶ Lipscomb, W. N.; Jacobson, R. A. in Weissberger, A.; Rossiter, B. W., Eds. *Techniques of Chemistry, Vol. I. Physical Methods of Chemistry. Part III D*; Wiley-Interscience: New York, 1972; pp. 1–123; Cameron, A. F. in Bentley, K. W.; Kirby, G. W., Eds. *Techniques of Chemistry. Volume IV. Part I*, 2nd ed.; Wiley-Interscience: New York, 1972; pp. 481–513.

¹⁷ Bartell, L. S. in Weissberger, A.; Rossiter, B. W., Eds. *Techniques of Chemistry. Volume I. Physical Methods of Chemistry. Part III D*; Wiley-Interscience: New York, 1972; pp. 125–158.

¹⁸ Flygare, W. H. in Weissberger, A.; Rossiter, B. W., Eds. *Techniques of Chemistry. Volume I. Physical Methods of Chemistry. Part III A*; Wiley-Interscience: New York, 1972; pp. 439–497.

¹⁹ McFarlane, W. in Bentley, K. W.; Kirby, G. W., Eds. *Techniques of Chemistry. Volume IV. Part I*, 2nd ed.; Wiley-Interscience: New York, 1972; pp. 225–322; Phillips, L. in Bentley, K. W.; Kirby, G. W., Eds. *Techniques of Chemistry. Volume IV. Part I*, 2nd ed.; Wiley-Interscience: New York, 1972; pp. 323–353.

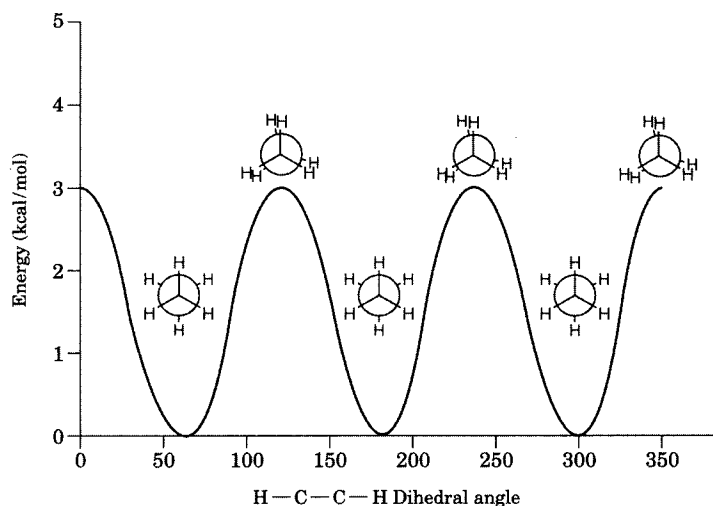
²⁰ Devlin, J. P.; Cooney, R. P. J. in Bentley, K. W.; Kirby, G. W., Eds. *Techniques of Chemistry. Volume IV. Part I*, 2nd ed.; Wiley-Interscience: New York, 1972; pp. 121–224.

²¹ Timmons, C. J. in Bentley, K. W.; Kirby, G. W., Eds. *Techniques of Chemistry. Volume IV. Part I*, 2nd ed.; Wiley-Interscience: New York, 1972; pp. 58–119.

²² Barrett, G. C. in Bentley, K. W.; Kirby, G. W., Eds. *Techniques of Chemistry. Volume IV. Part I*, 2nd ed.; Wiley-Interscience: New York, 1972; pp. 515–610.

²³ Barlin, G. B.; Perrin, D. D. in Bentley, K. W.; Kirby, G. W., Eds. *Techniques of Chemistry. Volume IV. Part I*, 2nd ed.; Wiley-Interscience: New York, 1972; pp. 611–676.

²⁴ Smyth, C. P. in Weissberger, A.; Rossiter, B. W., Eds. *Techniques of Chemistry. Volume I. Physical Methods of Chemistry. Part IV*; Wiley-Interscience: New York, 1972; pp. 397–429.

**FIGURE 3.6**

Torsional energy due to conformation changes in ethane.

3.2 CONFORMATIONAL ANALYSIS

Usually we are not as interested in describing all possible spatial arrangements that result from rotation about bonds within a molecule as in describing the relative stabilities of the energy minima. We also want to know the energetic barriers to rotations that lead to the interconversion of conformational minima.²⁵ The energy of any molecular conformation is determined by all of the stabilizing and destabilizing forces that act on the atoms at that instant.²⁶ The search for knowledge of this kind comprises an important part of the field of *conformational analysis*, which attributes conformational energies to the presence or absence of specific types of strain present in the different conformations. The three types of strain that are usually most useful in this regard are torsional strain, van der Waals strain, and angle strain.

Torsional Strain

Torsional strain results from deviations from staggered conformations. The usual way to analyze torsional energies is to compare energies of conformations with different dihedral angles (as represented with Newman projections) on an energy level diagram. Figure 3.6 shows that the potential energy of ethane varies in a sinusoidal fashion with the angle of rotation. Pitzer determined that the eclipsed conformation of ethane is about 3 kcal/mol

²⁵ The principles of conformational analysis were established by Barton, D. H. R. *Experientia* **1950**, *6*, 316. For general references, see reference 2a and Dauben, W. G.; Pitzer, K. S. in Newman, M. S., Ed. *Steric Effects in Organic Chemistry*; John Wiley & Sons: New York, 1956; pp. 1–60.

²⁶ Except for explicit references to free energy, in this discussion we will use the word *energy* to mean enthalpy.

higher in energy than the staggered conformation.^{27,28} Based on the microwave spectrum of CH_3CHD_2 , Hirota and co-workers concluded that the rotational barrier of ethane is 2.90 ± 0.03 kcal/mol.²⁹ This barrier is low enough that the methyl groups of ethane are said to exhibit “free rotation.”³⁰

The origin of the rotational barrier in ethane has been the subject of considerable debate. For much of the recent history of organic chemistry, the barrier was attributed to a steric interaction of the C–H bonds on one end of the molecule with those on the other end. The term *steric interaction* is an oversimplification because it is used to describe two closely related but different effects. One of these is a Coulombic interaction resulting from the repulsion of negatively charged electrons located near each other in space. The other is a quantum mechanical effect that arises when two doubly occupied orbitals are pushed together. In order to avoid a violation of the Pauli exclusion principle, the orbitals are forced to adopt high energy configurations to ensure their orthogonality.³¹ It is the second effect that was thought to be primarily responsible for the torsional barrier in ethane.³² This explanation was not universally accepted, however. In particular, Eliel and Wilen argued against a steric basis for the torsional barrier because the distance between hydrogen atoms on C1 and those on C2 in the eclipsed conformation is barely less than the sum of their van der Waals radii.³³

A very different explanation was put forward by Pophristic and Goodman.³⁴ They proposed that the rotational barrier in ethane results not from steric *destabilization* of the eclipsed conformation but, instead, from *stabilization* of the staggered conformation arising from delocalization of the σ bonding electrons. We will discuss the mechanism of this proposed stabilization in Chapter 4, but there is one point to be made here. When observable physical properties such as torsional energy are attributed to *nonobservables*—that is, to concepts such as steric effects that are inherently associated with other nonobservables such as molecular orbitals—it is difficult to establish the origin of the physical property.³⁵

van der Waals Strain

Figure 3.7 shows a potential energy curve for rotation about the C2–C3 bond of butane in the gas phase.³⁶ Although the gauche and anti conformations are

²⁷ Kemp, J. D.; Pitzer, K. S. *J. Am. Chem. Soc.* **1937**, *59*, 276. Torsional strain is often called **Pitzer strain**.

²⁸ Weiss, S.; Leroi, G. E. *J. Chem. Phys.* **1968**, *48*, 962.

²⁹ Hirota, E.; Saito, S.; Endo, Y. *J. Chem. Phys.* **1979**, *71*, 1183.

³⁰ Zheng, J.; Kwak, K.; Xie, J.; Fayer, M. D. *Science* **2006**, *313*, 1951 determined that the rate constant for a 120° rotation from staggered to eclipsed to staggered ethane is about $8.3 \times 10^{10} \text{ s}^{-1}$.

³¹ Weinhold, F. *Nature* **2001**, *411*, 539.

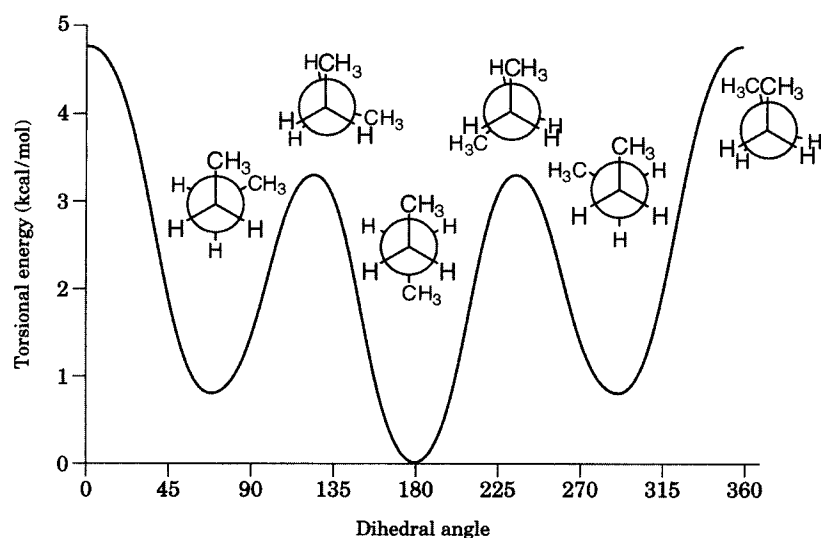
³² Sovers, O. J.; Kern, C. W.; Pitzer, R. M.; Karplus, M. *J. Chem. Phys.* **1968**, *49*, 2592.

³³ Eliel, E. L.; Wilen, S. H. *Stereochemistry of Organic Compounds*; John Wiley & Sons: New York, 1994.

³⁴ Pophristic, V.; Goodman, L. *Nature* **2001**, *411*, 565.

³⁵ See also Pendás, A. M.; Blanco, M. A.; Francisco, E. *J. Comput. Chem.* **2008**, *30*, 98.

³⁶ This figure is modified from a figure in reference 41. The curve was calculated from equation 3.8 on page 139 with $V_1 = 1.522$ kcal/mol, $V_2 = -0.315$ kcal/mol, and $V_3 = 3.207$ kcal/mol (as reported in reference 41).

**FIGURE 3.7**

Energy changes due to rotation about the C2–C3 bond of butane in the gas phase.

both staggered, the anti conformation is more stable by 0.8 kcal/mol.^{37–39} This energy difference is usually attributed to van der Waals strain, a repulsion of nonbonded atoms when they are closer than the sum of their van der Waals radii, as is the case of the two methyl groups in the gauche conformation of butane. The eclipsed conformations also differ in energy. Two of the energy maxima have two methyl–hydrogen and one hydrogen–hydrogen eclipsed arrangements. The higher energy eclipsed conformation has two hydrogen–hydrogen and one methyl–methyl eclipsed arrangements. Both kinds of eclipsed conformation are higher in energy than are the eclipsed conformations in ethane. Evidently the eclipsed conformations include not only torsional strain but also some van der Waals strain. This explanation also rationalizes the higher energy when the two methyl groups are eclipsed, since two methyls should interact more strongly than a methyl and a hydrogen.⁴⁰

It is interesting to ask what these energy differences mean in terms of the distribution of conformations in a sample of butane molecules. The solid line in Figure 3.8 shows the population distributions calculated for butane in the gas phase at 25°.⁴¹ It is evident that some structures are in conformations near, but not exactly at, the energy minima. There is a large distribution of conformations about the 180° (anti) angle and smaller distributions about

³⁷ Pitzer, K. S. *J. Chem. Phys.* **1940**, *8*, 711. The exact value depends on the theoretical technique used for measurement and the phase (gas or liquid; potentials are somewhat higher in the gas phase). A value of 0.97 kcal/mol was measured by Verma, A. L.; Murphy, W. F.; Bernstein, H. J. *J. Chem. Phys.* **1974**, *60*, 1540.

³⁸ Wiberg, K. B.; Murcko, M. A. *J. Am. Chem. Soc.* **1988**, *110*, 8029.

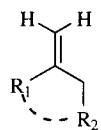
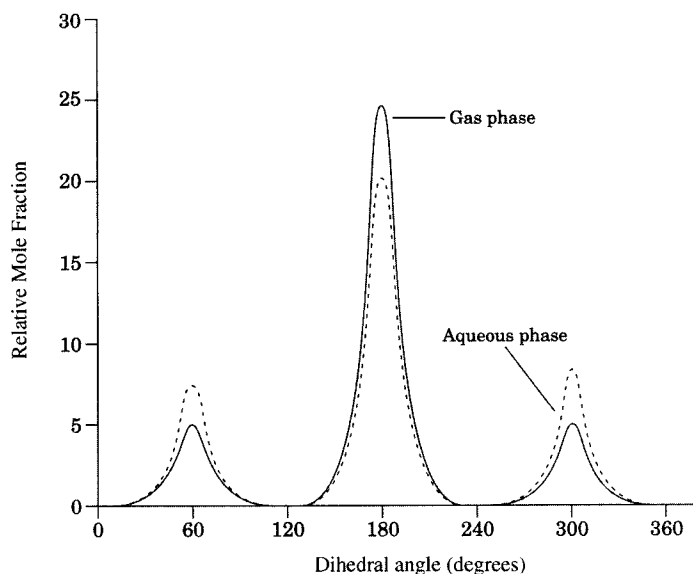
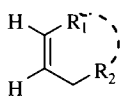
³⁹ Although it may not be evident from Figure 3.7, the dihedral angle of the gauche conformation is 65°. See the discussion on page 146.

⁴⁰ The *syn* rotational barrier shown is quite close to the value of 4.89 kcal/mol calculated by Allinger, N. L.; Grev, R. S.; Yates B. F.; Schaefer, H. F. III. *J. Am. Chem. Soc.* **1990**, *112*, 114.

⁴¹ Jorgensen, W. L.; Buckner, J. K. *J. Phys. Chem.* **1987**, *91*, 6083.

FIGURE 3.8

Population distributions for butane conformers in the gas phase (solid line) and in water (dashed line) at 25°. The units of the vertical axis are relative mole fraction per degree of rotation. (Adapted from reference 41.)

A^(1,2) StrainA^(1,3) Strain**FIGURE 3.9**

Examples of A^(1,2) and A^(1,3) strain. The dashed lines show the stereochemical interactions.

the 60° and 300° (gauche) dihedral angles. The calculations agree well with experiment: about 62% of the molecules were found to be in the most stable (anti) conformation in a gas phase measurement.⁴² The distribution of butane conformations is very similar to the distribution of conformer populations about internal CH₂–CH₂ segments in other alkanes.⁴³ In butane both the energy of the gauche conformation and the barrier to rotation are lower in solution. The dashed line in Figure 3.8 shows the population distribution for butane in water at 25°, indicating that conformational distributions are to some extent dependent on the environment.

Another manifestation of van der Waals strain is evident in allylic compounds (Figure 3.9).⁴⁴ A^(1,2) strain results when two substituents, one on the allylic carbon and the other on the first carbon of the vinyl group to which it is attached, are brought into close proximity. A^(1,3) strain occurs when substituents on C1 and C3 of an allylic system are in close proximity (Figure 3.9). Such interactions have important consequences in stereoselective reactions.⁴⁵ Understanding the principles of conformational analysis, including A strain, is particularly useful in correlating the function of natural products with patterns of alkyl substitution and in the design of synthetic compounds with biological activity. Hoffmann noted that conformations having A^(1,3) strain or *syn*-pentane interactions (which are essentially the same as cyclohexane 1,3-diaxial interactions, as shown in Figure 3.10) are higher in energy than are conformations that avoid these interactions. Therefore, methyl substituents in some natural products give the compounds a

⁴² Murphy, W. F.; Fernández-Sánchez, J. M.; Raghavachari, K. *J. Phys. Chem.* **1991**, *95*, 1124.

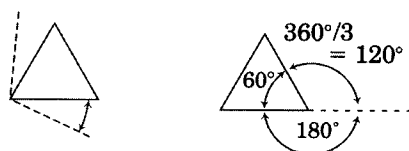
⁴³ Lahtela, M.; Pakkanen, T. A.; Nissfolk, F. *J. Phys. Chem. A* **1997**, *101*, 5949.

⁴⁴ Johnson, F. *Chem. Rev.* **1968**, *68*, 375.

⁴⁵ Hoffmann, R. W. *Chem. Rev.* **1989**, *89*, 1841.

**FIGURE 3.10**

Similarity of *syn*-pentane interactions (left) to 1,3-diaxial interactions in cyclohexane (right).



$$\begin{aligned} \text{Angle strain} &= \\ &= (1/2) (109.5^\circ - 60^\circ) \\ &= 24.75^\circ \end{aligned}$$

FIGURE 3.11

Calculation of angle strain for cyclopropane.

“predisposition to adopt the conformation necessary for biological function.”⁴⁶

Angle Strain and Baeyer Strain Theory

Strain that results from deviation from standard bond angles is called **angle strain** or **Baeyer strain**. Baeyer proposed that all rings are inherently strained because their bond angles cannot be exactly 109.5° .⁴⁷ Because three points define a plane, the three carbon atoms in cyclopropane are required to be planar. By symmetry, all three carbon atoms in cyclopropane are equivalent, so all must have the same bond angles. Representing the carbon atoms in cyclopropane as an equilateral triangle, we see immediately that the C–C–C bond angles must be 60° . Subtracting 60° from the 109.5° bond angle expected for sp^3 -hybridized carbon gives a 49.5° difference. That difference is the sum of two angle deviations, so we calculate that there is 24.75° of angle strain at each carbon atom (Figure 3.11).⁴⁸

A method for calculating the C–C–C internuclear bond angle of any *planar* cycloalkane is illustrated for cyclopropane in Figure 3.11. Extending any one bond line produces an external angle of 180° at a carbon atom. The angle between that extended bond line and an adjacent bond line is equal to 360° divided by the number of carbons in the cycloalkane. Subtracting that value from 180° then gives the internal bond angle for the cycloalkane. For planar cyclobutane, the deviation at each carbon atom is 9.5° ; for cyclopentane it is less than 1° ; and for planar cyclohexane it is -5° . Multiplying the angle strain for each carbon atom by the number of carbon atoms in each molecule produces the calculated angle strain for each compound shown in Table 3.1.

⁴⁶ Hoffmann, R. W. *Angew. Chem. Int. Ed.* **2000**, 39, 2054.

⁴⁷ Baeyer, A. *Chem. Ber.* **1885**, 18, 2269.

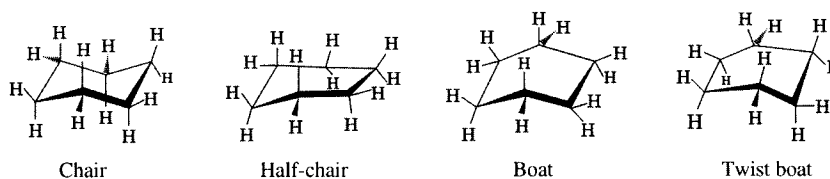
⁴⁸ In this discussion angle strain is expressed in degrees, not in kcal/mol.

TABLE 3.1 Calculated and Experimental Angle Strain

Compound	Angle Strain/CH ₂	Total Angle Strain	Experimental Strain/CH ₂ (kcal/mol)
Cyclopropane	24°44'	74°12'	9.2
Cyclobutane	9°44'	38°56'	6.55
Cyclopentane	0°44'	3°40'	1.3
Cyclohexane	-5°16'	-31°36'	0.0
Cyclodecane	-17°16'	-172°42'	1.2

Source: Reference 49.

FIGURE 3.12
Major conformations
of cyclohexane.



Application of Conformational Analysis to Cycloalkanes

The experimental data in Table 3.1 show that the calculated values of total angle strain are approximately correct only for cyclopropane, cyclobutane, and cyclopentane.^{49,50} Cyclohexane is definitely not the strained compound Baeyer's theory predicts, and the larger ring compounds are also not very strained. Any chemist today can explain the discrepancy between these calculated and experimental values of strain energy: cyclohexane is not planar. In either the chair or boat conformations (Figure 3.12), all bond angles can be approximately 109.5°. In the chair conformation of cyclohexane, all bonds are staggered, and there are no apparent van der Waals repulsions in the molecule.⁵¹

The boat conformation of cyclohexane is an energy maximum, but a similar conformation called the twist boat is an energy minimum.⁵² Although the twist boat has more *angle* strain than the boat, decreased *torsional* strain produces an overall lower energy. The two hydrogen atoms labeled H_f in the boat and twist boat conformations shown in Figure 3.12 are termed "flagpole" hydrogens, while the hydrogen atoms labeled H_b are termed "bowsprit"

⁴⁹ Eliel, E. L. *Stereochemistry of Carbon Compounds*; McGraw-Hill: New York, 1962; p. 189.

⁵⁰ Cremer and Gauss emphasized that the total "conventional ring strain energies" of cyclopropane and cyclobutane are essentially the same and that calculating strain/CH₂ disguises an important question: Is cyclopropane more stable than one would expect from typical conformational analysis considerations or is cyclobutane more strained than we expect? For a discussion of this point and leading references, see Cremer, D.; Gauss, J. *J. Am. Chem. Soc.* **1986**, *108*, 7467.

⁵¹ Electron diffraction measurements suggest that the preferred conformation of cyclohexane is a somewhat flattened chair, with C-C-C bond angles of 111° and torsional angles of 55.9°. For a review of cyclohexane data, see Ōsawa, E.; Collins J. B.; Schleyer, P. v. R. *Tetrahedron* **1977**, *33*, 2667. See also Dommen, J.; Brupbacher, T.; Grassi, G.; Bauder, A. *J. Am. Chem. Soc.* **1990**, *112*, 953. For a theoretical analysis, see reference 38.

⁵² Johnson, W. S.; Bauer, V. J.; Margrave, J. L.; Frisch, M. A.; Dreger, L. H.; Hubbard, W. N. *J. Am. Chem. Soc.* **1961**, *83*, 606.

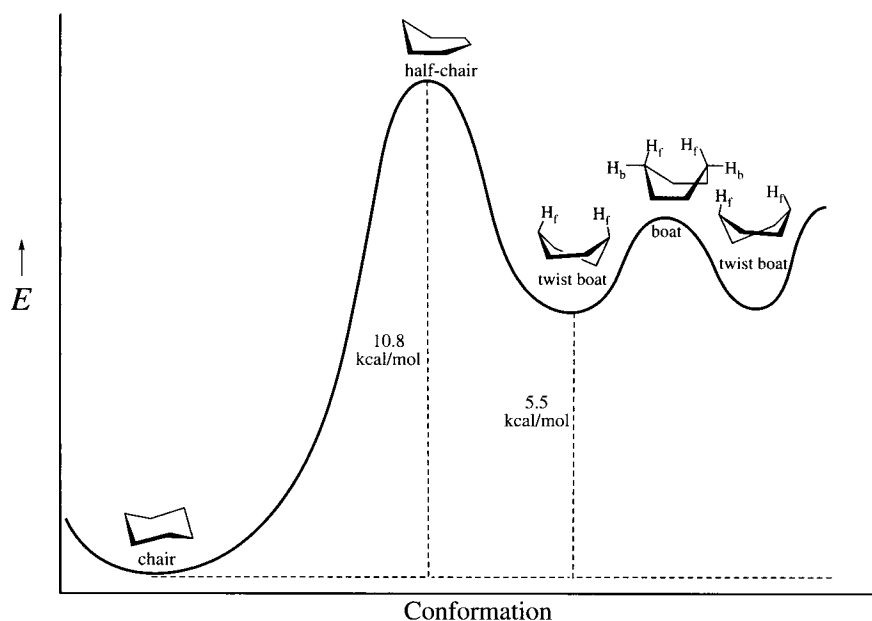


FIGURE 3.13
Relative energies of cyclohexane conformations.

hydrogens. van der Waals repulsion of the flagpole hydrogens is often cited as an additional component of the strain energy in the boat conformation, but the magnitude of this effect has been questioned.⁵³ The twist boat has been observed spectroscopically by rapidly condensing hot cyclohexane vapor into an argon matrix at 20 K. The activation energy required to convert from the twist boat to a chair conformation was determined to be 5.3 kcal/mol, with the twist boat being 5.5 kcal/mol higher in energy than the chair conformation.^{54,55} The energies of the various conformations are shown in Figure 3.13.

Why did Baeyer not consider the possibility that cyclohexane and larger molecules are nonplanar?⁵⁶ According to Ramsay, Baeyer used a set of Kekulé tetrahedral molecular models in which half-bonds were joined with spring connectors to make bonds between atoms. This model set allowed—indeed, required—one to construct a planar representation of a cyclic molecule and then to measure angle strain by the deviation of the bonds from the straight lines between atoms.⁵⁷ Thus, cyclohexane would be represented by the model in Figure 3.14. As is so often the case, ideas that become firmly planted in the minds of scientists are difficult to displace. Bassindale noted that by 1890, only

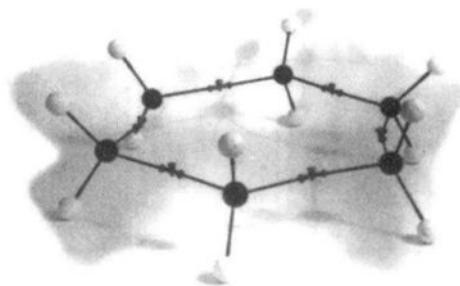
⁵³ Sauers, R. R. *J. Chem. Educ.* **2000**, *77*, 332 reported a density functional calculation indicating that those hydrogens are about 2.5 Å apart and thus contribute only minimally to the twist boat–boat–twist boat barrier.

⁵⁴ Squillacote, M.; Sheridan, R. S.; Chapman, O. L.; Anet, F. A. L. *J. Am. Chem. Soc.* **1975**, *97*, 3244.

⁵⁵ The activation barrier for the conversion of chair cyclohexane to the twist boat was found to be $\Delta G^\ddagger = 10.3$ kcal/mol, with $\Delta H^\ddagger = 10.8$ kcal/mol and $\Delta S^\ddagger = 2.8$ eu; Anet, F. A. L.; Bourn, A. J. R. *J. Am. Chem. Soc.* **1967**, *89*, 760.

⁵⁶ Baeyer's theory should not be viewed with condescension. It was experimentally observable that rings larger or smaller than cyclopentane and cyclohexane were difficult to synthesize. Small rings do have appreciable angle strain. The larger rings can also be difficult to synthesize because of the unfavorable entropy involved in bringing two ends of a long, linear molecule together to make a bond.

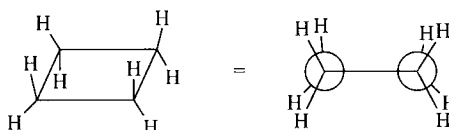
⁵⁷ Ramsay, O. B. *J. Chem. Educ.* **1977**, *54*, 563.

**FIGURE 3.14**

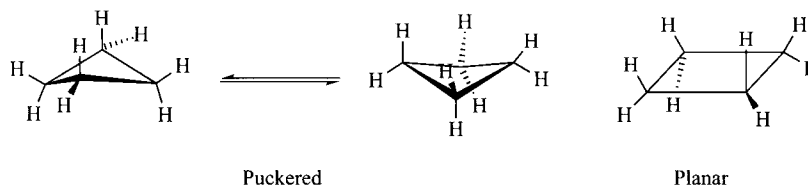
Kekulé–Baeyer model of cyclohexane. (Adapted from reference 57.)

FIGURE 3.15

Hypothetical planar conformation of cyclobutane.

**FIGURE 3.16**

Puckered conformation of cyclobutane.



five years after the proposal of angle strain theory by Baeyer, Sachse pointed out that the angle strain could be relieved by nonplanar conformations of the rings, and the idea was proposed again in 1918 by Mohr. Nevertheless, it was only in the 1950s that the idea of nonplanar cyclohexane became widely accepted.⁵⁸

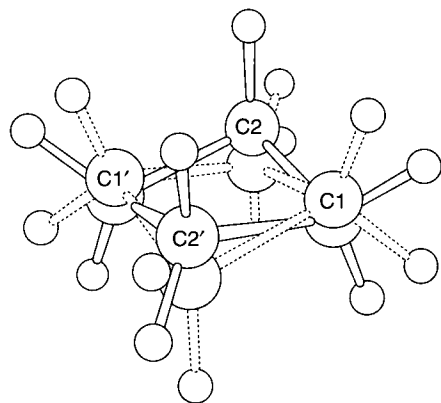
In the preceding discussion, we implicitly assumed that the strain in cyclobutane and cyclopropane was due to angle strain only. However, a Newman projection of planar cyclobutane (Figure 3.15) shows that all of the C–H bonds are eclipsed, suggesting that there is considerable torsional strain in the planar conformation. Distortion from planarity can relieve some of the torsional strain, but that necessarily increases the angle strain by making the C–C–C bond angles less than 90° .⁵⁹ Yet, theoretical calculations indicated that cyclobutane is puckered by about 30° , as shown in Figure 3.16, with an inversion barrier for conversion of one puckered form to the other of 1.38 kcal/mol.^{60,61} The puckered structure was reported to

⁵⁸ Bassindale, A. *The Third Dimension in Organic Chemistry*; John Wiley & Sons: Chichester, England, 1984; p.81.

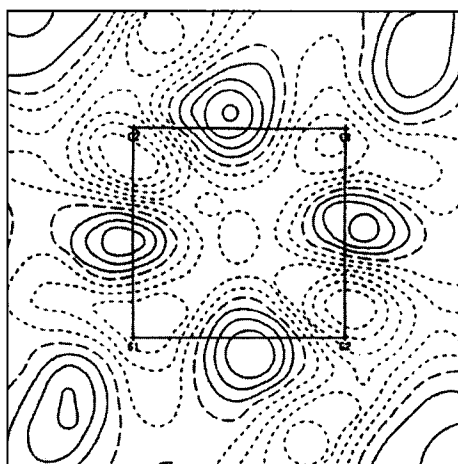
⁵⁹ The term *planar* in discussions of cycloalkane conformations refers only to the carbon atoms.

⁶⁰ Glendening, E. D.; Halpern, A. M. *J. Phys. Chem. A* **2005**, *109*, 635 concluded that hyperconjugative stabilization has an additional stabilizing effect on the puckered conformation.

⁶¹ For a compilation of experimental data, see Legon, A. C. *Chem. Rev.* **1980**, *80*, 231.

**FIGURE 3.17**

Disordered view of cyclobutane from X-ray crystallography. (Reproduced from reference 63.)

**FIGURE 3.18**

Electron density contours of cyclobutane calculated from X-ray diffraction data. (Reproduced from reference 63.)

have $l_{C-C} = 1.5549 \text{ \AA}$, $l_{C-H(\text{axial})} = 1.0934 \text{ \AA}$, $l_{C-H(\text{equatorial})} = 1.0910 \text{ \AA}$, $\angle_{\text{HCH}} = 109.33^\circ$, and $\angle_{\text{CCC}} = 88.23^\circ$.⁶²

Figure 3.17 shows the structure of cyclobutane determined through X-ray crystallography of a single crystal at 117 K.⁶³ The X-ray data were most consistent with a disordered array (represented by solid and dotted lines) of puckered cyclobutane molecules in the crystal. The calculated value of the dihedral angle for the ring carbon atoms in the crystal was 31° . Experimental gas phase studies confirmed that the barrier to puckering is less than 1.5 kcal/mol.⁶⁴

One interesting aspect of the X-ray data is the representation of electron density around the cyclobutane ring. Figure 3.18 shows electron density contours superimposed on a square with a carbon atom at each corner, representing the time-average position of the atoms in the ring. Note that the greatest value of electron density is actually outside the lines of the square formed by shortest path internuclear bonds, suggesting that cyclobutane has

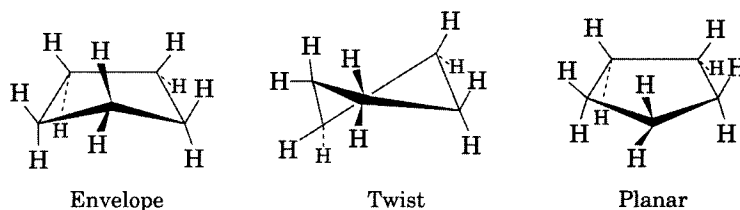
⁶² Kummli, D. S.; Frey, H. M.; Leutwyler, S. J. *Phys. Chem. A* **2007**, *111*, 11936 and references therein.

⁶³ Stein, A.; Lehmann, C. W.; Luger, P. J. *Am. Chem. Soc.* **1992**, *114*, 7684.

⁶⁴ Cremer, D. J. *Am. Chem. Soc.* **1977**, *99*, 1307.

FIGURE 3.19

Envelope, twist, and (hypothetical) planar conformations of cyclopentane.



curved bonds.⁶⁵ That bond curvature relieves additional torsional strain but does not bring the two “axial” hydrogens so close that repulsion becomes a problem.⁶⁴

Distortion from planarity to relieve torsional strain also applies to cyclopentane (Figure 3.19).⁶⁶ Experimental evidence indicates that the molecule exhibits ten different envelope conformations in which one carbon atom at a time is above or below the plane defined by the other four, as well as ten twist or half-chair conformations in which three carbon atoms at a time define a plane, with the fourth carbon atom above this plane and the fifth below it. The molecule is continually changing its conformation, however, so that each carbon atom is 0.458 Å above the molecular plane one-fifth of the time, with the barrier to planarity of 5.16 kcal/mol.⁶⁷ In the absence of isotopic labeling, the effect of this shifting permutation is indistinguishable from a rotation of the molecule about an axis through its center. For that reason, the process is called **pseudorotation**.⁶⁸ The energy barrier for pseudorotation is so small that the process is described as essentially barrierless.⁶⁹

Conformational Analysis of Substituted Cyclohexanes

Figure 3.20 shows that there are essentially two kinds of positions for substituents in the chair conformation of cyclohexane. Each carbon atom has one substituent that is approximately in the plane of the carbon atoms and another substituent that is perpendicular to this plane. The substituent lying approximately in the plane is called the **equatorial** substituent, while the one perpendicular to the plane is called the **axial** substituent.⁷⁰ Of course,

⁶⁵ Such bonds had been suggested by Bartell, L. S.; Andersen, B. J. *Chem. Soc. Chem. Commun.* **1973**, 786, who also noted that the CH₂ groups should tilt inward toward each other.

⁶⁶ Kilpatrick, J. E.; Pitzer, K. S.; Spitzer, R. J. *Am. Chem. Soc.* **1947**, 69, 2483.

⁶⁷ Bauman, L. E.; Laane, J. J. *Phys. Chem.* **1988**, 92, 1040.

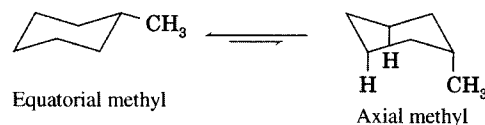
⁶⁸ This type of pseudorotation is not to be confused with a different use of the term in inorganic chemistry. There the term refers to ligand exchange around a central atom; cf. Berry, R. S. *J. Chem. Phys.* **1960**, 32, 933.

⁶⁹ Variyar, J. E.; MacPhail, R. A. *J. Phys. Chem.* **1992**, 96, 576; see also MacPhail, R. A.; Variyar, J. E. *Chem. Phys. Lett.* **1989**, 161, 239. For a detailed analysis of the conformational dynamics of cyclopentane, see Wu, A.; Cremer, D.; Auer, A. A.; Gauss, J. J. *Phys. Chem. A* **2002**, 106, 657.

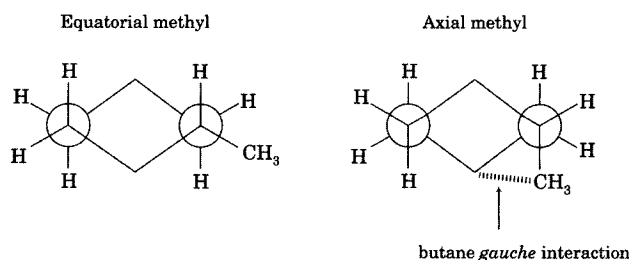
⁷⁰ The classification of hydrogens into what we now call axial and equatorial was by Hassel, O. *Tids. Kjem., Bergvesen Met.* **1943**, 3, 32. A translation of this paper by Hedberg, K. appeared in *Top. Stereochem.* **1971**, 6, 11. Hassel termed the hydrogens ϵ (from the Greek $\epsilon\sigma\tau\eta\kappa\acute{o}\varsigma$, “standing”) and κ (from the Greek, $\kappa\acute{\alpha}\iota\mu\epsilon\nu\omicron\varsigma$, “reclining”). Pitzer (reference 74) termed the hydrogens *polar* and *equatorial*. Later, Barton, D. H. R.; Hassel, O.; Pitzer, K. S.; Prelog, V. *Science* **1954**, 119, 49 suggested that the term *axial* be used instead of polar to distinguish conformations from dipolar properties. The field of conformational analysis was established primarily through the work of Hassel and of Barton, who shared the 1969 Nobel Prize in chemistry. A seminal paper by Barton (reference 25) is also reprinted in *Top. Stereochem.* **1971**, 6, 1.

**FIGURE 3.20**

Interchange of axial and equatorial positions of substituents in cyclohexane conformers.

**FIGURE 3.21**

Axial and equatorial conformations of a methyl substituent on cyclohexane.

**FIGURE 3.22**

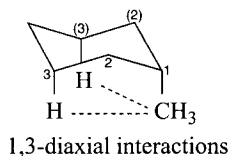
Newman projections of mono-substituted cyclohexane conformations.

cyclohexane is not entirely planar. Three of the carbon atoms are relatively higher than the two carbons on either side of them, while the other three carbon atoms are relatively lower than those on either side of them. Each carbon atom that is relatively higher has an axial substituent that points upward, while each carbon that is relatively lower has an axial carbon that is directed downward. Chair–chair interconversion in cyclohexane switches the relative position of the carbon atoms and also changes axial hydrogens into equatorial hydrogens, and vice versa.

The two chair conformations shown in Figure 3.20 have the same energy when all of the substituents are hydrogens. Let us now consider the conformations of methylcyclohexane. In one chair conformation the methyl group is equatorial, while in the other conformation it is axial (Figure 3.21). We do not expect either conformation to show appreciable angle strain, nor should there be torsional strain if the methyl carbon–ring carbon bond is staggered. Nevertheless, the equatorial conformation is more stable by about 1.8 kcal/mol, a difference we attribute to van der Waals strain.

If we use a Newman projection that lets us view down two carbon–carbon bonds at the same time to compare the two conformations of methylcyclohexane (Figure 3.22), we see that the axial methyl and a carbon–carbon bond on an adjacent carbon atom are gauche with respect to each other.⁷¹ We can also describe the interaction of the axial methyl with the third carbon atom away from the point of attachment of the methyl group in a different way.

⁷¹ Viewing the molecule from another orientation would show that there is one more such interaction.

**FIGURE 3.23**

Two 1,3-diaxial interactions in axial methylcyclohexane.

Since the methyl group and the axial hydrogen on the third carbon atom are closer than the sum of their van der Waals radii, we assume that there is a van der Waals repulsion, and we term the interaction a **1,3-diaxial interaction** (Figure 3.23). It is important to recognize that this is the same as a butane gauche interaction; it is just described in a slightly different way. Figure 3.23 also makes it easier to recognize that there are two 1,3-diaxial (butane gauche) interactions in axial methylcyclohexane.

This familiar explanation of the equatorial preference of a methyl group on cyclohexane is so firmly established in organic chemistry that it may be surprising to find that some evidence contradicts it. Wiberg and co-workers carried out a study of the alkylcyclohexanes using a variety of theoretical methods.⁷² They found that the higher energy of the axial conformation of methylcyclohexane was not associated with any deformation in the C2–C3–H bond angle, which might have been expected if “1,3-diaxial” repulsions are responsible for the greater enthalpy of the axial conformer. They did identify perturbations in the bond angles around C1, however. They concluded that “the data indicate that repulsive steric interaction between an axial methyl group and the ring carbons, including the gauche torsional interaction, is the major component responsible for destabilization of the axial methyl group.” Similar results were obtained in a computational study of dihalocyclohexanes.⁷³ It will be difficult for organic chemists to put aside long-held beliefs about 1,3-diaxial interactions, and we will continue to use that term in these discussions. Nonetheless, we should recognize that even firmly established explanations may be subject to revision.

Since there are two 1,3-diaxial interactions for each axial methyl, we predict the axial conformation to be less stable than the equatorial conformation by about 1.8 kcal/mol,⁷⁴ which is close to the experimental value of 1.74 kcal/mol.⁷⁵ Thus, 1.74 kcal/mol is the **equatorial preference** or **Avalue** for a methyl substituent.⁷⁶ If we treat the distribution of a molecule between two conformations as a chemical equilibrium, we can use equation 3.2 to calculate that 6% of the methyl groups will be axial and 94% will be equatorial at 25°.

$$\Delta G^\circ = -RT \ln K \quad (3.2)$$

For substituents larger than a methyl substituent, we expect the impact of the 1,3-diaxial or butane gauche interaction to be greater. Table 3.2 provides values of the equatorial preference of other substituent groups as compiled by Hirsch.⁷⁷

⁷² Wiberg, K. B.; Hammer, J. D.; Castejon, H.; Bailey, W. F.; DeLeon, E. L.; Jarret, R. M. *J. Org. Chem.* **1999**, *64*, 2085.

⁷³ Wiberg, K. B. *J. Org. Chem.* **1999**, *64*, 6387.

⁷⁴ A butane gauche interaction was calculated to be 0.8 kcal/mol, but a value of 0.9 kcal/mol gave the best fit between calculated and observed values for a series of disubstituted cycloalkanes. Beckett, C. W.; Pitzer, K. S.; Spitzer, R. *J. Am. Chem. Soc.* **1947**, *69*, 2488.

⁷⁵ Booth, H.; Everett, J. R. *J. Chem. Soc. Chem. Commun.* **1976**, 278; *J. Chem. Soc. Perkin Trans. 2* **1980**, 255. See also reference 72.

⁷⁶ Winstein, S.; Holness, N. J. *J. Am. Chem. Soc.* **1955**, *77*, 5562. A values are discussed on p. 5574 of this paper.

⁷⁷ Hirsch, J. A. *Top. Stereochem.* **1967**, *1*, 199.

TABLE 3.2 Conformational Preferences of Substituted Cyclohexanes

Substituent	A Values (kcal/mol, at 25°)	Substituent	A Values (kcal/mol, at 25°)
-F	0.15	-C ₂ F ₅	2.67 ^d
-Cl	0.43	-OCF ₃	0.79 ^d
-Br	0.38	-SCF ₃	1.18 ^d
-I	0.43	-CO ₂ H	1.35
-CN	0.17	-CO ₂ ⁻	1.92
-CH ₃	1.74 ^a	-CO ₂ CH ₃	1.27
-CH ₂ CH ₃	1.79 ^a	-OH	0.52 (aprotic solvent)
-CH(CH ₃) ₂	2.21 ^a		0.87 (protic solvent)
-C(CH ₃) ₃	>5.4 ^b	-OCH ₃	0.60
-C ₆ H ₁₁	2.15	-NH ₂	1.20 (aprotic solvent)
-D	0.0063 ± 0.0015 ^c		1.60 (protic solvent)
-CH ₂ F	1.59 ^d	-NH(CH ₃)	1.0 (aprotic solvent)
-CF ₂ H	1.85 ^d	-N(CH ₃) ₂	2.1 (protic solvent)

Source: Except as noted, data are from reference 77.

^a Reference 75.

^b Reference 76.

^c Reference 78.

^d Reference 79.

It is important to note that *A* values are free energy values, not enthalpy terms, and that entropy contributions can also play an important role in determining *A* values.⁸⁰ Booth and Everett used variable temperature ¹³C NMR to determine ΔG° , ΔH° , and ΔS° for the axial to equatorial change of alkylcyclohexanes in CFCl₃-CDCl₃ solution.⁷⁵ The values of ΔH° for methyl, ethyl, and isopropyl substituents were -1.75, -1.60, and -1.52 kcal/mol, respectively.⁸¹ That is, the enthalpy of axial to equatorial change was more favorable for methyl than for isopropyl. This trend results from the *difference* between the total number of butane gauche interactions for an axial conformer and the total number of butane gauche interactions for the equatorial conformer of each compound. For example, methylcyclohexane has two butane gauche (1,3-diaxial) interactions in the axial conformation but none in the equatorial conformation. Axial ethylcyclohexane has two low energy conformations, each of which has three butane gauche interactions. Equatorial ethylcyclohexane has three accessible conformations, two of which have one butane gauche interaction and one of which has two butane gauche interactions. The enthalpy difference between the axial and equatorial

⁷⁸ Anet, F. A. L.; Kopelevich, M. J. *Am. Chem. Soc.* **1986**, *108*, 1355. The *A* value was determined to be 0.0083 ± 0.0015 at -95°C. Anet, F. A. L.; O'Leary, D. J. *Tetrahedron Lett.* **1989**, *30*, 1059.

⁷⁹ Carcenac, Y.; Tordeux, M.; Wakselman, C.; Diter, P. *New J. Chem.* **2006**, *30*, 447.

⁸⁰ Squillacote, M. E. *J. Chem. Soc. Chem. Commun.* **1986**, 1406.

⁸¹ The ΔG° , ΔH° , and ΔS° values for the axial to equatorial change of the benzyl group were found to be -1.76 kcal/mol, -1.52 kcal/mol, and +0.81 eu, respectively. Juaristi, E.; Labastida, V.; Antúnez, S. J. *Org. Chem.* **1991**, *56*, 4802.

conformations is thus greater than one but smaller than two butane gauche interactions. This means that the enthalpy difference between the two conformers of ethylcyclohexane should be less than the difference in enthalpy of the methylcyclohexane conformers. Similarly, the ΔS° values for the methyl, ethyl, and isopropyl substituents, -0.03 , $+0.64$, and $+2.31$ eu, respectively, can be rationalized on the basis of the different number of rotamers possible for each group in the axial and equatorial positions.⁷⁵ The overall ΔG° values calculated at 300 K for methyl, ethyl, and isopropyl were 1.74, 1.79, and 2.21 kcal/mol, respectively. At room temperature, therefore, the entropy term actually determines the trend in the A values of these three substituents.

The conformational preference of disubstituted cyclohexanes can be computed from the A values of the two substituents individually if the two substituents do not directly interact with each other. For *cis*-1-methyl-4-phenylcyclohexane, ΔG for axial phenyl to equatorial phenyl is -1.13 kcal/mol. Using 1.74 kcal/mol as the A value for methyl and assuming that the effects of the two substituents on the 1 and 4 positions are independent of each other, then the A value for phenyl is 2.87 kcal/mol.⁸² With an A value of at least 5.4 kcal/mol for the *t*-butyl group, *t*-butylcyclohexane is predicted to exist in solution at 25° with only about 0.01% of the *t*-butyl groups in the axial position. This strong preference is the basis for the use of *t*-butyl as a "locking group" in studies of chemical reactions at axial or equatorial positions. Thus, *trans*-4-*t*-butylcyclohexanol can be used to study reactions of an equatorial alcohol, while the *cis* isomer can be used to study the reactions of an axial hydroxyl group.⁷⁶

Most natural products having cyclohexane rings exhibit chair conformations, but a class of compounds found in hops has been found to exhibit a (twist) boat conformation in one of four six-membered rings.⁸³ The results of a molecular mechanics study indicated that *cis,trans,cis*-1,2-diisopropyl-3,4-dimethylcyclohexane is the smallest monocyclic cyclohexane that is expected to exhibit a twist boat as its lowest energy conformation.⁸⁴ If a *cis* substituent at C4 of a *t*-butylcyclohexane derivative is very large, that substituent may not be axial because the cyclohexane may not be in the chair conformation. Noe and co-workers were able to detect both the twist boat and chair conformations (Figure 3.24) of *cis*-1,4-di-*t*-butylcyclohexane with low temperature ¹³C NMR.⁸⁵ The twist boat was found to be more stable than the chair by 0.47 kcal/mol at 129 K.

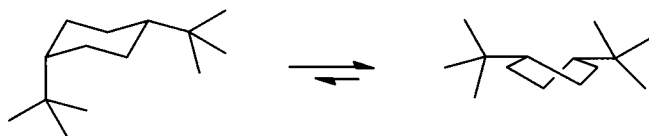
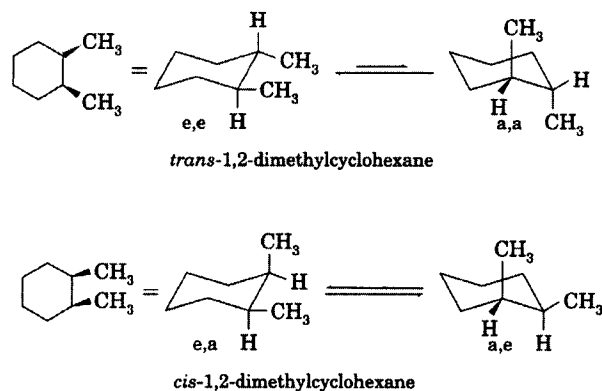
For the 1,2-dimethylcyclohexanes, we must not only worry about 1,3-diaxial interactions of the substituents with the ring hydrogens, but we must also consider possible interactions of the substituents with each other.¹ Shown in Figure 3.25 are the two chair conformations of *cis*-1,2-dimethylcyclohexane

⁸² Eliel, E. L.; Manoharan, M. *J. Org. Chem.* **1981**, *46*, 1959. A value of $\Delta G = -0.32$ kcal/mol was determined for axial phenyl to equatorial phenyl in 1-methyl-1-phenylcyclohexane. Here the A values are not additive on the same carbon atom because the presence of the methyl keeps the phenyl from adopting the most stable orientation.

⁸³ Dasgupta, S.; Tang, Y.; Moldowan, J. M.; Carlson, R. M. K.; Goddard, W. A. III. *J. Am. Chem. Soc.* **1995**, *117*, 6532.

⁸⁴ Weiser, J.; Golan, O.; Fitjer, L.; Biali, S. E. *J. Org. Chem.* **1996**, *61*, 8277.

⁸⁵ Gill, G.; Pawar, D. M.; Noe, E. A. *J. Org. Chem.* **2005**, *70*, 10726.

**FIGURE 3.24**Conformations of *cis*-1,4-di-*t*-butylcyclohexane.**FIGURE 3.25**Conformations of *trans*- and *cis*-1,2-dimethylcyclohexanes.

as well as the two corresponding conformations for the *trans* isomer.⁸⁶ We first determine that the diequatorial (*e,e*) conformation of the *trans* isomer should be about 2.7 kcal/mol more stable than the diaxial (*a,a*) conformation. The equilibrium mixture of *trans*-1,2-dimethylcyclohexane conformers at room temperature therefore should be composed almost exclusively of molecules in the *e,e* conformation. As a result, the energy of the *e,e* conformation can be used to approximate the energy of the *trans* isomer.

For the *cis* isomer of 1,2-dimethylcyclohexane, both conformations have one axial and one equatorial methyl, so the *e,a* and *a,e* conformations are equivalent in energy. Thus, we conclude that the *cis* isomer has two 1,3-diaxial methyl–hydrogen interactions for the axial methyl group, plus one additional gauche interaction between the two methyls.⁸⁷ The *trans* isomer has only the butane gauche interaction between the two methyls in the *e,e* conformation (which represents the great majority of molecules), so we predict that the *trans* isomer should be more stable than the *cis* isomer by two methyl 1,3-diaxial interactions or 1.8 kcal/mol. The literature value (Table 3.3) is 1.87 kcal/mol. One can similarly analyze other dimethylcyclohexanes and compare the

⁸⁶ Numerous articles in *J. Chem. Educ.* have addressed the problem of recognizing *cis* and *trans* isomers of cyclohexanes. For example, see Richardson, W. S. *J. Chem. Educ.* **1989**, *66*, 478. A useful technique is to say that each carbon atom has two substituent positions, one “more up than down” and one “more down than up.” If two substituents are both “more up” or are both “more down,” then they are *cis* to each other. If one is “more up” and the other is “more down,” then they are *trans*.

⁸⁷ Although a 1,3-diaxial interaction between a methyl and a hydrogen is often presumed to be exactly equal to a butane gauche interaction, this is not necessarily the case. The gauche butane can adopt a conformation in which the C–C–C dihedral angle is more than 60° (see the sample MM2 calculation beginning on page 140) to minimize some van der Waals repulsion, although at the cost of introducing some other strain. In cyclohexane some flattening of the ring can lead to decreased van der Waals repulsion, although again at the cost of other kinds of strain. The data suggest that the *A* value of methylcyclohexane is more than twice as much as two gauche interactions in butane. For a discussion, see Hendrickson, J. B. *J. Am. Chem. Soc.* **1967**, *89*, 7043.

TABLE 3.3 Conformational Preference of Dimethylcyclohexanes

Substitution	More Stable Isomer	ΔH (kcal/mol)
1,2	trans	1.87
1,3	cis	1.96
1,4	trans	1.90

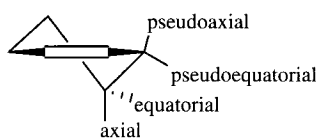
Source: Reference 49.

results with those shown in Table 3.3. In the 1,3 and 1,4 isomers, there are no gauche interactions between the two methyls, so only the number of 1,3-diaxial interactions in each isomer need be considered.

We should not assume that all alkyl substituents prefer the equatorial conformation. Goren and Biali reported that the preferred conformation of all-*trans*-1,2,3,4,5,6-hexaisopropylcyclohexane has all six isopropyl groups axial rather than equatorial.⁸⁸ They concluded that severe torsional and steric interactions between the equatorial isopropyl groups are responsible for the surprising conformational preference. Moreover, Biali determined that, with an appropriately shaped substituent, it might be possible for a *monoalkylcyclohexane* to be more stable with the substituent in the axial rather than in the equatorial position.⁸⁹

The relative energies of the dialkylcyclohexanes are not affected significantly by dipole-dipole interactions, but that factor is much more important in the conformational equilibria of molecules that have polar groups.^{5,49} With *trans*-1,2-dichlorocyclohexane, for example, about 25% of the molecules are in the diaxial conformation in benzene solution at room temperature. This arrangement minimizes the unfavorable dipole-dipole interaction present in the diequatorial conformation. With *trans*-1,2-dibromocyclohexane, the population of diaxial conformer is more than 50% under the same conditions. There is van der Waals repulsion as well as a dipole-dipole interaction in the diequatorial conformation.⁹⁰ The *trans* isomer of 1,4-dibromocyclohexane also exhibits a greater population of diaxial than diequatorial conformation in solution, although the diequatorial conformation is favored in the solid state.⁹¹ With polar substituents capable of hydrogen bonding, still another factor comes into play. The diequatorial conformer of *trans*-1,2-cyclohexane-diol is favored due to hydrogen bonding, since intramolecular hydrogen bonding is not feasible in the diaxial conformation.⁹²

The discussion to this point has concerned only cycloalkanes. Additional considerations come into play with cycloalkenes. For example, cyclohexene is said to adopt a half-chair conformation having methylene hydrogen atoms in four different environments.⁹³ The hydrogen atoms are considered to be in axial or equatorial positions on C4 and C5, but those on C3 and C6 are said to be **pseudoaxial** and **pseudoequatorial** (Figure 3.26).

**FIGURE 3.26**

Conformational designations for methylene hydrogens in cyclohexene.

⁸⁸ Goren, Z.; Biali, S. E. *J. Am. Chem. Soc.* **1990**, *112*, 893; see also reference 8.

⁸⁹ Biali, S. E. *J. Org. Chem.* **1992**, *57*, 2979.

⁹⁰ Bender, P.; Flowers, D. L.; Goering, H. L. *J. Am. Chem. Soc.* **1955**, *77*, 3463.

⁹¹ Kozima, K.; Yoshino, T. *J. Am. Chem. Soc.* **1953**, *75*, 166.

⁹² Kuhn, L. P. *J. Am. Chem. Soc.* **1958**, *80*, 5950.

⁹³ Barton, D. H. R.; Cookson, R. C.; Klyne, W.; Shoppee, C. W. *Chem. Ind. (London)* **1954**, 21.

3.3 MOLECULAR MECHANICS

One of the limitations of conformational analysis is that it uses a limited set of interactions to predict the energy of a conformation. That is, a cyclohexane substituent is said to be either axial or equatorial; a dihedral angle is either staggered or eclipsed; a staggered conformation is either anti or gauche. Furthermore, it requires data for rather specific reference compounds for each type of comparison we make. For example, if there is a 1,3-diaxial interaction involving a methyl and a carbomethoxy group, we would be hard pressed to estimate the resulting strain from the *A* values of the two substituents alone. If there is a van der Waals repulsion between those same two groups on a different molecular framework, the *A* values for cyclohexane would be of limited value. Therefore, it would be advantageous to be able to calculate conformational energies from equations in which energy is a function of a structural parameter (bond length, bond angle, etc.) and not a particular molecular skeleton. This approach has given rise to a field of computational chemistry known as **molecular mechanics**.

The term *molecular mechanics* distinguishes this approach from quantum mechanics because the method uses a classical mechanics (mass and spring) approach to ascribe the energy of a particular conformation to specific bonding parameters. Molecular mechanics has also been called the Westheimer method because equations for calculating steric strain were used by Westheimer in a study of racemization of optically active biphenyls.^{94,95} Other terms include *quantitative conformational analysis*⁹⁶ and (more generally) the *force field method*. A force field is defined as a set of equations and constants that relate energy to internal coordinates.⁹⁷ Both the equations and the constants are important. A reliable force field must have a correct analytic form (the equations) and a valid parameterization (the specific constants for each type of interaction).⁹⁸⁻¹⁰⁰ Molecular geometries and energies can also be obtained from molecular orbital calculations (Chapter 4), but molecular

⁹⁴ For example, see Allinger, N. L.; Hirsch, J. A.; Miller, M. A.; Tyminski, I. J.; Van-Catledge, F. A. *J. Am. Chem. Soc.* **1968**, *90*, 1199.

⁹⁵ See Westheimer, F. H. in Newman, M. S., Ed. *Steric Effects in Organic Chemistry*; John Wiley & Sons: New York, 1956; p. 523 ff; Westheimer, F. H.; Mayer, J. E. *J. Chem. Phys.* **1946**, *14*, 733; Westheimer, F. H. *J. Chem. Phys.* **1947**, *15*, 252. Similar ideas were developed independently by Hill, T. L. *J. Chem. Phys.* **1946**, *14*, 465.

⁹⁶ Williams, J. E.; Stang, P. J.; Schleyer, P. v. R. *Annu. Rev. Phys. Chem.* **1968**, *19*, 531.

⁹⁷ This definition is revised slightly from that given by Hagler, A. T.; Stern, P. S.; Lifson, S.; Ariel, S. *J. Am. Chem. Soc.* **1979**, *101*, 813.

⁹⁸ In order to carry out a molecular mechanics calculation, all the force constants for each type of atom under consideration must be known. In the case of MM2, only some atom types were included at the time of development of the procedure. Others were added later, in some cases by other researchers. Lipkowitz has provided a summary of parameter sources: Lipkowitz, K. B. *QCPE Bulletin* **1992**, *12*, 6.

⁹⁹ The parameters are based on diverse experimental data and must be optimized so that the force field produces reliable results. For a discussion, see Pearlman, D. A.; Kollman, P. A. *J. Am. Chem. Soc.* **1991**, *113*, 7167.

¹⁰⁰ Parameterization has been called an art and a science. Bowen, J. P.; Allinger, N. L. in Lipkowitz, K. B.; Boyd, D. B., Eds. *Reviews in Computational Chemistry II*; VCH Publishers: New York, 1991; pp. 81-97.

mechanics calculations are much faster because the time required for a molecular mechanics calculation varies with the *square* of the number of *atoms*, while the computation time for an ab initio calculation varies with the *fourth* power of the number of *orbitals*.¹⁰¹ In addition, molecular mechanics calculations can be quite accurate for structures that have intramolecular interactions similar to those in the reference compounds used to develop the molecular mechanics program.¹⁰²

Among the more widely used molecular mechanics methods are those developed by Allinger and co-workers. The original formulation, MM1, was reported in 1973.¹⁰¹ A modification published in 1977 was named MM2 and is frequently cited as MM2(77).¹⁰³ MM3 was released in 1989,¹⁰⁴ and MM4 was released in 1996.¹⁰⁵ Alternative approaches were reported by Schleyer,¹⁰⁶ Bartell,¹⁰⁷ Goddard,¹⁰⁸ and Rappé.^{109,110} Among other widely cited force fields are AMBER¹¹¹ and CHARMM.¹¹² For further discussion about molecular mechanics, see the reviews by Schleyer^{96,106} and by Allinger¹⁰² and the monograph of Burkert and Allinger.¹¹³

Unlike conformational analysis, in which relative energies are compared by assigning fixed amounts of strain to specific interactions (such as butane gauche interactions), molecular mechanics determines the energy of a conformation by computing the value of a mathematical function. An equation such as equation 3.3 can be used to calculate the total **steric energy** of the molecule as the sum of a number of different kinds of interactions.^{113,114} Most molecular mechanics methods include as a

¹⁰¹ Allinger, N. L. *Adv. Phys. Org. Chem.* **1976**, *13*, 1.

¹⁰² For example, the MM3 calculation of the heat of formation of C₆₀ was much closer to the experimental value than were the values calculated by the molecular orbital methods to be discussed in Chapter 4. Beckhaus, H.-D.; Rüchardt, C.; Kao, M.; Diederich, F.; Foote, C. S. *Angew. Chem. Int. Ed. Engl.* **1992**, *31*, 63.

¹⁰³ Allinger, N. L. *J. Am. Chem. Soc.* **1977**, *99*, 8127.

¹⁰⁴ (a) Allinger, N. L.; Yuh, Y. H.; Lii, J.-H. *J. Am. Chem. Soc.* **1989**, *111*, 8551; (b) Lii, J.-H.; Allinger, N. L. *J. Am. Chem. Soc.* **1989**, *111*, 8566; (c) Lii, J.-H.; Allinger, N. L. *J. Am. Chem. Soc.* **1989**, *111*, 8576.

¹⁰⁵ Allinger, N. L.; Chen, K.-H.; Lii, J.-H. *J. Comput. Chem.* **1996**, *17*, 642.

¹⁰⁶ Engler, E. M.; Andose, J. D.; Schleyer, P. v. R. *J. Am. Chem. Soc.* **1973**, *95*, 8005.

¹⁰⁷ Fitzwater, S.; Bartell, L. S. *J. Am. Chem. Soc.* **1976**, *98*, 5107.

¹⁰⁸ Mayo, S. L.; Olafson, B. D.; Goddard, W. A. III. *J. Phys. Chem.* **1990**, *94*, 8897.

¹⁰⁹ Rappé, A. K.; Casewit, C. J.; Colwell, K. S.; Goddard, W. A. III. Skiff, W. M. *J. Am. Chem. Soc.* **1992**, *114*, 10024.

¹¹⁰ Casewit, C. J.; Colwell, K. S.; Rappé, A. K. *J. Am. Chem. Soc.* **1992**, *114*, 10035, 10046.

¹¹¹ Weiner, S. J.; Kollman, P. A.; Nguyen, D. T.; Case, D. A. *J. Comput. Chem.* **1986**, *7*, 230.

¹¹² Nilsson, L.; Karplus, M. *J. Comput. Chem.* **1986**, *7*, 591. Also see Smith, J. C.; Karplus, M. *J. Am. Chem. Soc.* **1992**, *114*, 801.

¹¹³ Burkert, U.; Allinger, N. L. *Molecular Mechanics*, ACS Monograph 177; American Chemical Society: Washington, DC, 1982.

¹¹⁴ The discussion here is a simplified presentation of the principles of molecular mechanics calculations in MM2. The treatment in MM3 is more complex.¹⁰⁴

minimum the components in equation (3.3), and frequently other terms are also included.¹¹⁵⁻¹¹⁷

$$E_{\text{steric}} = E(r) + E(\theta) + E(\Phi) + E(d) \quad (3.3)$$

$E(r)$ is the energy of stretching or compressing an individual bond,
 $E(\theta)$ is the energy of distorting a bond angle from the ideal,
 $E(\Phi)$ is the torsional strain (due to nonstaggered bonds), and
 $E(d)$ is the energy of nonbonded interactions arising from van der Waals forces, which may be stabilizing or destabilizing.¹¹⁸

The magnitude of $E(r)$ for each bond is a function of the extent of stretching or compression of the bond and is given by the formula

$$E(r) = 0.5k_r \times (\Delta r)^2 \times (1 + CS \times \Delta r) \quad (3.4)$$

where k_r is the force constant associated with the deformation, Δr is the deformation of the bond length from the minimum energy length, and CS is a cubic stretching constant. Note that the energy increases with the square of the deformation (although a negative value for CS allows the bond to weaken somewhat at large deformations). Apparently the resistance to deformation is quite strong; stretching or compressing a carbon-carbon single bond by 0.1 Å is endothermic by about 2.5 kcal/mol (Table 3.4). As a result, carbon-carbon bond lengths usually vary only slightly over a wide variety of strained and unstrained compounds.^{119,120} For example, the minimum energy geometry calculated for cyclohexane has a C-C bond length of 1.5356 Å, which is a bond length deformation of 0.0126 Å, and that is calculated to give a stretching energy for each C-C bond of 0.0487 kcal/mol.¹²¹

The magnitude of $E(\theta)$ is determined from the formula

$$E(\theta) = 0.5k_\theta \times (\Delta\theta)^2 \times (1 + SF \times \Delta\theta^4) \quad (3.5)$$

¹¹⁵ There may also be an energy associated with "out of plane deformation" for some molecules. For a discussion of the forces included in a MM calculation, see Susnow, R.; Nachbar, R. B., Jr.; Schutt, C.; Rabitz, H. J. *Phys. Chem.* **1991**, *95*, 8585.

¹¹⁶ For a discussion of the components of a force field and the use of ab initio methods in force field development, see Dinur, U.; Hagler, A. T. in Lipkowitz, K. B.; Boyd, D. B., Eds. *Reviews in Computational Chemistry II*; VCH Publishers: New York, 1991; pp. 99-164; Hwang, M. J.; Stockfisch, T. P.; Hagler, A. T. *J. Am. Chem. Soc.* **1994**, *116*, 2515.

¹¹⁷ In addition to the terms in equation 3.3, other types of interactions may be important. These include dipole-dipole forces (which may be stabilizing or destabilizing), as well as hydrogen bonding, electrostatic effects, donor-acceptor interactions, and solvation effects. Understanding these interactions can be vital to calculating the conformation of molecules more complex than the simple hydrocarbons discussed here. For discussions, see (a) Kingsbury, C. A. *J. Chem. Educ.* **1979**, *56*, 431; (b) Liberles, A.; Greenberg, A.; Eilers, J. E. *J. Chem. Educ.* **1973**, *50*, 676; (c) Juaristi, E. *J. Chem. Educ.* **1979**, *56*, 438; (d) reference 113.

¹¹⁸ The kinds of noncovalent interactions that give rise to van der Waals forces are particularly important in determining the structures and properties of molecular complexes. Hobza, P.; Zahradnik, R.; Müller-Dethlefs, K. *Collect. Czech. Chem. Commun.* **2006**, *71*, 443.

¹¹⁹ Clark, T.; McKervey, M. A. in Stoddart, J. F., Ed. *Comprehensive Organic Chemistry*, Vol. 1; Pergamon Press: Oxford, England, 1979; p. 37.

¹²⁰ Liebman, J. F.; Greenberg, A. *Chem. Rev.* **1976**, *76*, 311.

¹²¹ Calculated with QCMP010 from the Quantum Chemistry Program Exchange, Bloomington, IN, 1985. The program was written by Allinger, N. L.; Yuh, Y. H. and was modified by Petillo, P. A.

TABLE 3.4 Dependence of Carbon–Carbon Bond Deformation Energy on Δr

Δr (Å)	Strain Energy ^a (kcal/mol)
0.001	3.2×10^{-4}
0.002	1.3×10^{-3}
0.005	7.8×10^{-3}
0.01	3.1×10^{-2}
0.05	7.1×10^{-1}
0.10	2.53

^a Calculations based on equations and data from reference 121.

TABLE 3.5 Dependence of Strain Energy on C–C–C Angle Deviation

$\Delta\theta$ (deg)	Angle Strain (kcal/mol)
0.1	9.8×10^{-5}
0.5	2.5×10^{-3}
1.0	9.8×10^{-3}
3.0	8.4×10^{-2}
5.0	2.1×10^{-1}

where $\Delta\theta$ is the deviation from ideal bond angles (e.g., 109.5° for sp^3 hybrid orbitals) and SF is a constant. Note that there is again a dependence of the energy on the square of the magnitude of the deformation, although there is a minor dependence on the sixth power as well.¹²² In this case, however, the energy penalty for deformation of a bond angle is much smaller than the penalty for deformation of a bond length. A 5° deviation from 109.5° raises the energy of a structure only about 0.2 kcal/mol. Table 3.5 shows the energies calculated for C–C–C angle deviations from 109.5° using equation 3.5. The expected bond angle of 109.5° for tetrasubstituted organic compounds is actually observed for only methane and a few other symmetrically substituted carbon atoms. In other cases the C–C–C bond angles are found to vary from 111° to 113° for acyclic alkanes.

In addition to the pure bending strain given in equation 3.5, it is also useful to calculate a stretch–bending strain energy, E_{SB} , which incorporates both bond angle and bond length deformations. The rationale for this parameter is that the energy of an angle deformation is affected by stretching of the bonds that make that angle.¹²³ The energy for this term is given by the equation

$$E_{SB} = k_{SB} \times \Delta\theta_{abc} \times (\Delta r_{a-b} + \Delta r_{b-c}) \quad (3.6)$$

¹²² In the example on page 145, the value of SF is 0.7×10^{-7} .

¹²³ Because coordinates for bond lengths, bond angles, and other easily visualized sources of strain are interrelated, the types of strain are not totally separate (reference 96). Therefore, it may be necessary to add some cross terms to achieve a better calculation. The choice of such cross terms depends on the model used. The MUB-2 force field included a stretch–torsion term (reference 107).

In the example of cyclohexane, the C1–C2–C3 bond angle is calculated to be 110.88°, which differs by 1.41° from the ideal bond angle of 109.47°. The resulting contribution to $E(\theta)$ (for one C–C–C unit) is calculated to be 0.01 kcal/mol. By comparison, the value of E_{SB} for this same C–C–C unit is determined to be 0.02 kcal/mol, based on a carbon–carbon bond length deformation of 0.0126 Å.

The torsional strain equation for a pair of tetrasubstituted carbon atoms, each bearing three *identical* substituents, has the form

$$E(\Phi) = 0.5 V_0 \times (1 + \cos 3\Phi) \quad (3.7)$$

where V_0 is the rotational energy barrier and Φ is the torsional (dihedral) angle. If the three substituents on each carbon are not identical, then a more general equation applies:¹²¹

$$E(\Phi) = 0.5V_1 \times (1 + \cos \Phi) + 0.5V_2 \times (1 - \cos 2\Phi) + 0.5V_3 \times (1 + \cos 3\Phi) \quad (3.8)$$

where the values of V_1 , V_2 , and V_3 vary with the particular atom types. In this formulation positive values for V_1 and V_3 destabilize eclipsed forms, while a positive value for V_2 destabilizes 90° arrangements.

The van der Waals strain energy, included in $E(d)$, depends on the extent and pattern of substitution within the structure. The interaction of atoms that are not bonded to each other is very weak at long distances but initially becomes slightly attractive due to London dispersion forces when the atoms begin to come close. If the two atoms are pushed too close together, however, the interaction very quickly becomes quite repulsive. Different force fields use different values for van der Waals radii and different equations for the change in energy with distance between the nonbonded atoms. The effect of internuclear distance on the van der Waals energy of two nonbonded hydrogen atoms, calculated from the equation on page 143, is shown in Figure 3.27.¹²⁴

Let us examine the molecular mechanics approach by carrying out a very simple calculation—the optimization of the *gauche* conformation of butane. We start with an initial conformation in which the C–C–C–C dihedral angle (atoms 1–2–3–4 in Figure 3.28) is 60°. ¹²⁵ The following lines show part of the input file for the *gauche* conformation of butane in a format used by one molecular mechanics program.¹²⁶ The input file includes the name of the compound, any constraints on the program, and information about the connectivity of the atoms. There is a connected atoms list (1 2 3 4 in the third line), and an attached atoms list (1 5 1 6, etc. in the next line, meaning that atom 5 is bonded to atom 1, and so on.) Then come the x , y , and z coordinates of each

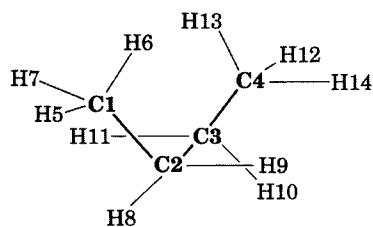
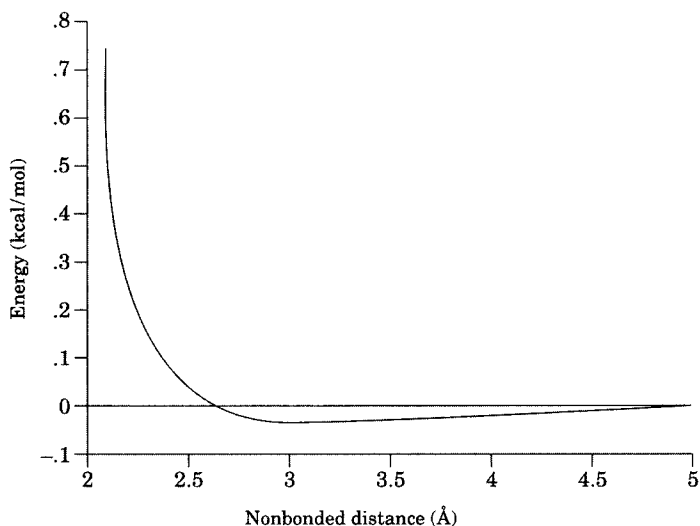
¹²⁴ For a discussion of different formulations of the van der Waals interaction, see Halgren, T. A. *J. Am. Chem. Soc.* **1992**, *114*, 7827. van der Waals force field parameters can be obtained from theoretical calculations. Compare Bordner, A. J.; Cavasotto, C. N.; Abagyan, R. A. *J. Phys. Chem. B* **2003**, *107*, 9601.

¹²⁵ The initial geometry was determined by carrying out a molecular mechanics calculation on a structure in which the C–C–C–C dihedral angle was fixed at 60°.

¹²⁶ The input file was written with the program PCMODEL (Serena Software, Bloomington, IN). The force field used in PCMODEL is known as MMX. For a discussion, see Gajewski, J. J.; Gilbert, K. E.; McKelvey, J. in Liotta, D., Ed. *Advances in Molecular Modeling*, Vol. 2; JAI Press: Greenwich, CT, 1990; pp. 65–92. Some portions of the input file, as well as some portions of the molecular mechanics output, have been omitted for clarity.

FIGURE 3.27

van der Waals energy of non-bonded hydrogen atom interactions.

**FIGURE 3.28**

Initial butane gauche conformation with 60° dihedral angle.

atom and the atom type. Type 1 is a tetravalent carbon; type 5 is a hydrogen.¹²⁷

Input File

```
gauche BUTANE
  1  2    3  4    0  0    0  0    0  0    0  0    0  0    0  0
  1  5    1  6    1  7    2  8    2  9    3 10    3 11    4 12
  4 13    4 14
-0.99450  0.36461  1.25785  1   -0.19237 -0.79026  0.64416  1
  0.16751 -0.57567 -0.83551  1    1.02035  0.67436 -1.08807  1
-1.22001  0.14650  2.32252  5   -0.40988  1.30620  1.19903  5
-1.94901  0.49837  0.70753  5   -0.76482 -1.73514  0.75297  5
  0.73596 -0.94743  1.23223  5    0.70118 -1.46973 -1.22046  5
-0.76285 -0.51485 -1.43806  5    1.24327  0.76931 -2.17124  5
  0.47470  1.58046 -0.75181  5    1.97614  0.60119 -0.52865  5
```

The molecular mechanics program reads the input file and uses the atom coordinates and bonding information to compute the steric energy of the initial conformation of the structure.

Initial Calculation of Coordinates and Energy

```
gauche BUTANE
GEOMETRY AND STERIC ENERGY OF INITIAL CONFORMATION.
CONNECTED ATOMS
  1- 2- 3- 4-
ATTACHED ATOMS
  1- 5, 1- 6, 1- 7, 2- 8, 2- 9, 3-10, 3-11, 4-12,
  4-13, 4-14,
INITIAL ATOMIC COORDINATES
ATOM      X      Y      Z      TYPE
C ( 1)   -0.99450  .36461  1.25785  ( 1)
C ( 2)   -0.19237  -0.79026  .64416  ( 1)
C ( 3)    .16751  -0.57567  -0.83551  ( 1)
```

¹²⁷ For a discussion and more extensive examples, see the monograph by Clark, T. *A Handbook of Computational Chemistry*; John Wiley & Sons: New York, 1985.

C (4)	1.02035	.67436	-1.08807	(1)
H (5)	-1.22001	.14650	2.32252	(5)
H (6)	-.40988	1.30620	1.19903	(5)
H (7)	-1.94901	.49837	.70753	(5)
H (8)	-.76482	-1.73514	.75297	(5)
H (9)	.73596	-.94743	1.23223	(5)
H(10)	.70118	-1.46973	-1.22046	(5)
H(11)	-.76285	-.51485	-1.43806	(5)
H(12)	1.24327	.76931	-2.17124	(5)
H(13)	.47470	1.58046	-.75181	(5)
H(14)	1.97614	.60119	-.52865	(5)

INITIAL STERIC ENERGY IS 3.6711 KCAL.

COMPRESSION	.1756
BENDING	.6224
STRETCH-BEND	.0670
VANDERWAALS	
1,4 ENERGY	2.2947
OTHER	.1294
TORSIONAL	.3820

The molecular mechanics calculation thus indicates that the steric energy of the initial 60° conformer is 3.67 kcal/mol and that this energy is made up mostly of van der Waals repulsion but also has significant bending and torsion contributions.

The next step is to vary the location of the atoms in a systematic way to achieve a more stable conformation. This process is repeated until the change in steric energy from one such procedure to the next is less than some predetermined value, at which time the energy of the structure is said to be "minimized." Initially, the hydrogens attached to carbon atoms are moved with the carbon atoms, but later the hydrogens are moved independently.

Iterative Minimization of Total Steric Energy

gauche BUTANE

ENERGY MINIMIZATION
INITIAL ENERGY

TOTAL ENERGY IS	3.6711	KCAL.		
COMPRESS	.1756	VANDERWAALS	TORSION	.3820
BENDING	.6224	1,4	2.2947	
STRBEND	.0670	OTHER	.1294	DIPL/CHG .0000

***** CYCLE 1 *****

(CH)MOVEMENT = 1

ITERATION 1	AVG. MOVEMENT =	.01320	A
ITERATION 2	AVG. MOVEMENT =	.00616	A
ITERATION 3	AVG. MOVEMENT =	.00390	A
ITERATION 4	AVG. MOVEMENT =	.00237	A
ITERATION 5	AVG. MOVEMENT =	.00153	A
TOTAL ENERGY IS	3.0383	KCAL.	
COMPRESS	.1695	VANDERWAALS	TORSION .4315
BENDING	.6027	1,4	2.1050
STR-BEND	.0752	OTHER .3457	DIPL/CHG .0000
ITERATION 6	AVG. MOVEMENT =	.00097	A
ITERATION 7	AVG. MOVEMENT =	.00062	A
ITERATION 8	AVG. MOVEMENT =	.00040	A

```

ITERATION 9  AVG. MOVEMENT = .00025 A
ITERATION 10 AVG. MOVEMENT = .00017 A

TOTAL ENERGY IS 3.0349 KCAL.
COMPRESS .1670  VANDERWAALS      TORSION .4490
BENDING .5937  1,4      2.1112
STRBEND .0742  OTHER .3603  DIPL/CHG .0000

ITERATION 11  AVG. MOVEMENT = .00011 A
ITERATION 12  AVG. MOVEMENT = .00008 A
ITERATION 13  AVG. MOVEMENT = .00006 A
ITERATION 14  AVG. MOVEMENT = .00005 A
ITERATION 15  AVG. MOVEMENT = .00004 A

```

```

TOTAL ENERGY IS 3.0348 KCAL.
COMPRESS .1667  VANDERWAALS      TORSION .4509
BENDING .5930  1,4      2.1121
STRBEND .0741  OTHER .3620  DIPL/CHG .0000

```

***** CYCLE 2 *****

(CH)MOVEMENT = 0

```

ITERATION 16  AVG. MOVEMENT = .00003 A

TOTAL ENERGY IS 3.0348 KCAL.
COMPRESS .1667  VANDERWAALS      TORSION .4510
BENDING .5930  1,4      2.1122
STRBEND .0741  OTHER .3621  DIPL/CHG .0000

```

***** ENERGY IS MINIMIZED WITHIN .0011 KCAL *****
***** ENERGY IS 3.0348 KCAL *****

Then the program writes the final coordinates of all atoms and computes the contribution of all interactions to the overall steric energy of the molecule.

Final Coordinates and Energy

```

gauche BUTANE
GEOMETRY AND STERIC ENERGY OF FINAL CONFORMATION.
CONNECTED ATOMS
1- 2- 3- 4-

ATTACHED ATOMS
1- 5, 1- 6, 1- 7, 2- 8, 2- 9, 3-10, 3-11, 4-12,
4-13, 4-14,

FINAL ATOMIC COORDINATES AND BONDED ATOM TABLE
ATOM      X      Y      Z      TYPE  BOUND TO ATOMS
C( 1)  -1.02860  .32977  1.27109  ( 1)  2, 5, 6, 7
C( 2)   -.17615 - .78428  .64958  ( 1)  1, 3, 8, 9
C( 3)   .13702 - .55745 - .83879  ( 1)  2, 4, 10, 11
C( 4)   1.01904  .67110 -1.09710  ( 1)  3, 12, 13, 14
H( 5)  -1.29907  .08253  2.32393  ( 5)  1,
H( 6)   -.48525  1.30158  1.29228  ( 5)  1,
H( 7)  -1.97660  .47462  .70367  ( 5)  1,

```

H(8)	-.72460	-1.75130	.75768	(5)	2,
H(9)	.77684	-.88816	1.22141	(5)	2,
H(10)	.66177	-1.45957	-1.23684	(5)	3,
H(11)	-.81609	-.45968	-1.41149	(5)	3,
H(12)	1.28620	.74842	-2.17665	(5)	4,
H(13)	.50045	1.61672	-.81973	(5)	4,
H(14)	1.96872	.61329	-.51708	(5)	4,

BOND LENGTHS AND STRETCHING ENERGY (13 BONDS)

ENERGY = 71.94 (KS) (DR) (DR) (1+ (CS) (DR))

DR = R-RO

CS = -2.000

BOND	LENGTH	R(0)	K(S)	ENERGY
C(1)-C(2)	1.5343	1.5230	4.4000	.0395
C(1)-H(5)	1.1148	1.1130	4.6000	.0011
C(1)-H(6)	1.1136	1.1130	4.6000	.0001
C(1)-H(7)	1.1143	1.1130	4.6000	.0006
C(2)-C(3)	1.5378	1.5230	4.4000	.0671
C(2)-H(8)	1.1170	1.1130	4.6000	.0052
C(2)-H(9)	1.1162	1.1130	4.6000	.0034
C(3)-C(4)	1.5343	1.5230	4.4000	.0394
C(3)-H(10)	1.1170	1.1130	4.6000	.0052
C(3)-H(11)	1.1162	1.1130	4.6000	.0034
C(4)-H(12)	1.1148	1.1130	4.6000	.0011
C(4)-H(13)	1.1136	1.1130	4.6000	.0001
C(4)-H(14)	1.1143	1.1130	4.6000	.0006

NON-BONDED DISTANCES, VAN DER WAALS ENERGY

54 VDW INTERACTIONS (1, 3 EXCLUDED)

ENERGY = KV*(2.90(10**5)EXP(-12.50/P) - 2.25(P**6))

RV = RVDW(I) + RVDW(K)

KV = SQRT(EPS(I)*EPS(K))

P = (RV/R) OR (RV/R#)

(IF P.GT.3.311, ENERGY = KV(336.176)(P**2))

IN THE VDW CALCULATIONS THE HYDROGEN ATOMS ARE RELOCATED
SO THAT THE ATTACHED HYDROGEN DISTANCE IS REDUCED BY .915

ATOM PAIR	R	R#	RV	KV	ENERGY	(1,4)
C(1), C(3)	2.5685					
C(1), C(4)	3.1492		3.800	.0440	.0989	*
C(1), H(8)	2.1649					
C(1), H(9)	2.1784					
C(1), H(10)	3.5141	3.4297	3.340	.0460	-.0527	*
C(1), H(11)	2.8044	2.7677	3.340	.0460	.1037	*
C(1), H(12)	4.1738	4.0849	3.340	.0460	-.0279	
C(1), H(13)	2.8924	2.8985	3.340	.0460	.0172	
C(1), H(14)	3.5017	3.4592	3.340	.0460	-.0520	
C(2), C(4)	2.5686					
C(2), H(5)	2.1945					
C(2), H(6)	2.2044					
C(2), H(7)	2.1976					
C(2), H(10)	2.1718					
C(2), H(11)	2.1824					
C(2), H(12)	3.5320	3.4466	3.340	.0460	-.0524	*
C(2), H(13)	2.8951	2.8519	3.340	.0460	.0418	*
C(2), H(14)	2.8133	2.7760	3.340	.0460	.0964	*

C (3), H (5)	3.5320	3.4465	3.340	.0460	-.0524	*
C (3), H (6)	2.8956	2.8524	3.340	.0460	.0415	*
C (3), H (7)	2.8128	2.7755	3.340	.0460	.0968	*
C (3), H (8)	2.1717					
C (3), H (9)	2.1825					
C (3), H(12)	2.1945					
C (3), H(13)	2.2044					
C (3), H(14)	2.1976					
C (4), H (5)	4.1742	4.0852	3.340	.0460	-.0279	
C (4), H (6)	2.8930	2.8991	3.340	.0460	.0169	
C (4), H (7)	3.5008	3.4583	3.340	.0460	-.0521	
C (4), H (8)	3.5141	3.4297	3.340	.0460	-.0527	*
C (4), H (9)	2.8045	2.7678	3.340	.0460	.1035	*
C (4), H(10)	2.1649					
C (4), H(11)	2.1784					
H (5), H (6)	1.7924					
H (5), H (7)	1.7995					
H (5), H (8)	2.4791	2.3892	3.000	.0470	.2329	*
H (5), H (9)	2.5431	2.4457	3.000	.0470	.1512	*
H (5), H(10)	4.3477	4.1964	3.000	.0470	-.0138	
H (5), H(11)	3.8053	3.6823	3.000	.0470	-.0280	
H (5), H(12)	5.2328	5.0511	3.000	.0470	-.0046	
H (5), H(13)	3.9338	3.8523	3.000	.0470	-.0221	
H (5), H(14)	4.3625	4.2569	3.000	.0470	-.0127	
H (6), H (7)	1.8040					
H (6), H (8)	3.1086	2.9421	3.000	.0470	-.0542	*
H (6), H (9)	2.5284	2.4337	3.000	.0470	.1667	*
H (6), H(10)	3.9161	3.7824	3.000	.0470	-.0244	
H (6), H(11)	3.2437	3.1508	3.000	.0470	-.0517	
H (6), H(12)	3.9341	3.8526	3.000	.0470	-.0221	
H (6), H(13)	2.3519	2.4107	3.000	.0470	.1990	
H (6), H(14)	3.1256	3.1085	3.000	.0470	-.0531	
H (7), H (8)	2.5544	2.4549	3.000	.0470	.1401	*
H (7), H (9)	3.1156	2.9487	3.000	.0470	-.0544	*
H (7), H(10)	3.8036	3.6800	3.000	.0470	-.0281	
H (7), H(11)	2.5872	2.5856	3.000	.0470	.0276	
H (7), H(12)	4.3609	4.2554	3.000	.0470	-.0127	
H (7), H(13)	3.1243	3.1072	3.000	.0470	-.0532	
H (7), H(14)	4.1322	4.0101	3.000	.0470	-.0178	
H (8), H (9)	1.7929					
H (8), H(10)	2.4465	2.3596	3.000	.0470	.2856	*
H (8), H(11)	2.5263	2.4297	3.000	.0470	.1720	*
H (8), H(12)	4.3477	4.1964	3.000	.0470	-.0138	
H (8), H(13)	3.9157	3.7820	3.000	.0470	-.0244	
H (8), H(14)	3.8040	3.6803	3.000	.0470	-.0280	
H (9), H(10)	2.5264	2.4299	3.000	.0470	.1718	*
H (9), H(11)	3.1070	2.9404	3.000	.0470	-.0542	*
H (9), H(12)	3.8059	3.6828	3.000	.0470	-.0279	
H (9), H(13)	3.2430	3.1501	3.000	.0470	-.0517	
H (9), H(14)	2.5879	2.5862	3.000	.0470	.0272	
H(10), H(11)	1.7929					
H(10), H(12)	2.4796	2.3895	3.000	.0470	.2322	*
H(10), H(13)	3.1086	2.9422	3.000	.0470	-.0542	*
H(10), H(14)	2.5540	2.4545	3.000	.0470	.1405	*
H(11), H(12)	2.5426	2.4453	3.000	.0470	.1518	*
H(11), H(13)	2.5288	2.4341	3.000	.0470	.1662	*
H(11), H(14)	3.1155	2.9487	3.000	.0470	-.0544	*

H(12), H(13) 1.7924
 H(12), H(14) 1.7995
 H(13), H(14) 1.8040

BOND ANGLES, BENDING AND STRETCH-BEND ENERGIES (24 ANGLES)

$$EB = 0.021914 (KB) (DT) (DT) (1+SF*DT**4)$$

$$DT = THETA - TZERO$$

$$SF = .00700E-5$$

$$ESB(J) = 2.51124 (KSB(J)) (DT) (DR1+DR2)$$

$$DR(I) = R(I) - R0(I)$$

A T O M S	THETA	TZERO	KB	EB	KSB	ESB
C(2)-C(1)-H(5)	110.875	110.000	.090	.0022	.360	.0060
C(2)-C(1)-H(6)	111.733	110.000	.090	.0044	.360	.0237
C(2)-C(1)-H(7)	111.149	110.000	.090	.0029	.360	.0104
H(5)-C(1)-H(6)	107.095	109.000	.320	.0254		
H(5)-C(1)-H(7)	107.658	109.000	.320	.0126		
H(6)-C(1)-H(7)	108.141	109.000	.320	.0052		
C(1)-C(2)-C(3)	113.460	109.500	.120	.0311	.450	.1546
C(1)-C(2)-H(8)	108.458	109.410	.090	-.0024	.360	.0071
C(1)-C(2)-H(9)	109.536	109.410	.090	.0003	.360	.0001
C(3)-C(2)-H(8)	108.746	109.410	.090	-.0022	.360	.0035
C(3)-C(2)-H(9)	109.615	109.410	.090	.0007	.360	.0003
H(8)-C(2)-H(9)	106.802	109.400	.320	.0473		
C(2)-C(3)-C(4)	113.461	109.500	.120	.0311	.450	.1548
C(2)-C(3)-H(10)	108.751	109.410	.090	-.0022	.360	.0034
C(2)-C(3)-H(11)	109.610	109.410	.090	.0007	.360	.0003
C(4)-C(3)-H(10)	108.459	109.410	.090	-.0024	.360	.0071
C(4)-C(3)-H(11)	109.533	109.410	.090	.0003	.360	.0001
H(10)-C(3)-H(11)	106.801	109.400	.320	.0474		
C(3)-C(4)-H(12)	110.875	110.000	.090	.0022	.360	.0060
C(3)-C(4)-H(13)	111.734	110.000	.090	.0044	.360	.0237
C(3)-C(4)-H(14)	111.148	110.000	.090	.0029	.360	.0104
H(12)-C(4)-H(13)	107.093	109.000	.320	.0255		
H(12)-C(4)-H(14)	107.663	109.000	.320	.0125		
H(13)-C(4)-H(14)	108.137	109.000	.320	.0052		

DIHEDRAL ANGLES, TORSIONAL ENERGY (ET) (27 ANGLES)

$$ET = (V1/2) (1+\cos(W)) + (V2/2) (1-\cos(2W)) + (V3/2) (1+\cos(3W))$$

SIGN OF ANGLE A-B-C-D 0 WHEN LOOKING THROUGH B TOWARD C,

IF D IS COUNTERCLOCKWISE FROM A, NEGATIVE.

A T O M S	OMEGA	V1	V2	V3	ET
C(1) C(2) C(3) C(4)	65.249	.200	.270	.093	.366
C(1) C(2) C(3) H(10)	-173.963	.000	.000	.267	.007
C(1) C(2) C(3) H(11)	-57.540	.000	.000	.267	.001
C(2) C(3) C(4) H(12)	175.465	.000	.000	.267	.004
C(2) C(3) C(4) H(13)	-65.151	.000	.000	.267	.005
C(2) C(3) C(4) H(14)	55.748	.000	.000	.267	.003
C(3) C(2) C(1) H(5)	175.388	.000	.000	.267	.004
C(3) C(2) C(1) H(6)	-65.226	.000	.000	.267	.005
C(3) C(2) C(1) H(7)	55.677	.000	.000	.267	.003
C(4) C(3) C(2) H(8)	-173.970	.000	.000	.267	.007
C(4) C(3) C(2) H(9)	-57.547	.000	.000	.267	.001
H(5) C(1) C(2) H(8)	54.445	.000	.000	.237	.005
H(5) C(1) C(2) H(9)	-61.774	.000	.000	.237	.001
H(6) C(1) C(2) H(8)	173.831	.000	.000	.237	.006
H(6) C(1) C(2) H(9)	57.613	.000	.000	.237	.001
H(7) C(1) C(2) H(8)	-65.265	.000	.000	.237	.004

H (7) C (1) C (2) H (9)	178.516	.000	.000	.237	.000
H (8) C (2) C (3) H (10)	-53.183	.000	.000	.237	.007
H (8) C (2) C (3) H (11)	63.240	.000	.000	.237	.002
H (9) C (2) C (3) H (10)	63.241	.000	.000	.237	.002
H (9) C (2) C (3) H (11)	179.665	.000	.000	.237	.000
H (10) C (3) C (4) H (12)	54.513	.000	.000	.237	.005
H (10) C (3) C (4) H (13)	173.898	.000	.000	.237	.006
H (10) C (3) C (4) H (14)	-65.203	.000	.000	.237	.004
H (11) C (3) C (4) H (12)	-61.703	.000	.000	.237	.000
H (11) C (3) C (4) H (13)	57.681	.000	.000	.237	.001
H (11) C (3) C (4) H (14)	178.580	.000	.000	.237	.000

FINAL STERIC ENERGY IS 3.0348 KCAL.

COMPRESSION	.1667
BENDING	.5930
STRETCHBEND	.0741
VANDERWAALS	
1,4 ENERGY	2.1122
OTHER	-.3621
TORSIONAL	.4510

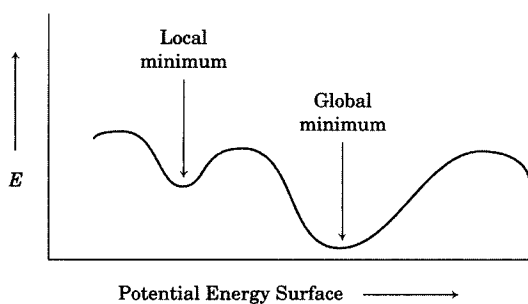
The steric energy of the minimized gauche conformation of butane is found by this calculation to be more than 0.6 kcal/mol lower than the initial conformation. Note that the C–C–C–C dihedral angle is no longer 60° but is now 65° and that a torsional strain of 0.366 kcal/mol is associated with the larger dihedral angle. Note also that the van der Waals strain decreases from 2.42 kcal/mol in the 60° conformer to 1.75 kcal/mol in the 65° conformer,¹²⁸ and most of the other strain parameters are also less in the 65° conformer. This example indicates two important points:

1. The minimum energy conformation is that conformation having the lowest *sum* of the components of steric strain, but some individual components of strain might be higher in a more stable conformation than they are in a less stable conformation.
2. A gauche conformer need not be exactly 60°.

If the initial conformation entered for butane is closer to 180° than to 60°, then the program finds an energy minimum in which the dihedral angle for the C–C–C–C bonds is 180°. That conformation has the following components of steric energy:

FINAL STERIC ENERGY IS 2.1714 KCAL.
COMPRESSION .1569
BENDING .2909
STRETCH-BEND .0524
VANDERWAALS
1,4 ENERGY 2.0697
OTHER -.4058
TORSIONAL .0073

¹²⁸ There is 2.11 kcal/mol of repulsive 1,4 van der Waals strain, but this is partially compensated for by 0.36 kcal/mol of attractive van der Waals interactions between other atoms.

**FIGURE 3.29**

Local(left)andglobal(right)minima on a simplified potential energy surface.

The difference in steric energy between the 65° gauche conformer and the anti conformer of butane is thus computed to be 0.86 kcal/mol, very close to the value used in our discussion of conformational analysis.

Why did the molecular mechanics program not optimize the initial 60° conformation to the anti conformation? The answer is that the gauche conformation is a **local minimum**, while the anti conformation represents a **global minimum** on the butane conformational potential energy surface. These terms are illustrated for a simplified two-dimensional potential energy surface in Figure 3.29. A minimization routine that starts with a geometry near a local minimum will generally optimize to that local minimum, even if there is a different geometry that is lower in energy. The problem is simple for butane because we can recognize likely minima and adjust the coordinates of the atoms in the input file so that the global minimum can be found. For large structures, determining the lowest energy conformation through computation can be difficult because the number of local minima increases dramatically with molecular size.¹²⁹ Therefore, it is essential to provide the molecular mechanics program with a wide variety of initial conformations so that all possible minima can be located.^{129,130}

The output from a molecular mechanics calculation on butane is quite lengthy, but that from a calculation on cyclohexane is even longer. Several results from the calculation on cyclohexane are shown in Table 3.6. The minimum energy geometry places atoms C1 and C4 2.959 Å apart, while the sum of their van der Waals radii is 3.800 Å.¹³¹ This gives rise to a calculated van der Waals repulsion of 0.31 kcal/mol between C1 and C4 (Figure 3.30). The same interaction energy is calculated for the repulsion between C2 and C5 as well as between C3 and C6, so carbon-carbon van der Waals repulsion accounts for 1.23 kcal/mol of the steric energy calculated for this conformation. Similarly, there is a repulsive van der Waals interaction between C1 and H11. They are calculated to be 2.810 Å apart, but the sum of their van der Waals radii is 3.340 Å. There is also 1,4-repulsion between hydrogen atoms on adjacent carbon atoms, such as H9 with H11 (0.204 kcal/mol) and H9 with H12 (0.171 kcal/mol). The interaction of the "1,3-diaxial hydrogens," such as H10 with H14, is only 0.009 kcal/mol, since they are about the same distance

¹²⁹ See, for example, Kolossváry, I.; Guida, W. C. *J. Am. Chem. Soc.* **1993**, *115*, 2107.

¹³⁰ A procedure for finding the global minimum in large molecules was reported by Saunders, M. *J. Am. Chem. Soc.* **1987**, *109*, 3150.

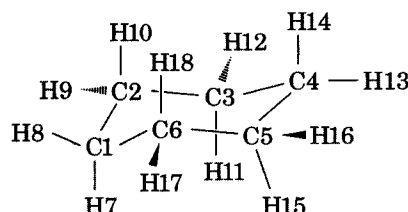
¹³¹ The van der Waals radii used in MM2 calculations differ somewhat from those tabulated in Chapter 1. In general they are 0.2–0.3 Å larger.

TABLE 3.6 Selected van der Waals Interactions from an MM2 Calculation

Atom Pair	r (Å)	Σr_{vdW} (Å)	Energy (kcal/mol)
C1–C4	2.959	3.800	0.312
C1–H11	2.810	3.340	0.102
C1–H12	3.499	3.340	–0.053
C1–H13	3.971	3.340	–0.035
C1–H14	3.376	3.340	–0.054
C1–H15	2.769	3.340	0.102
C1–H16	3.499	3.340	–0.053

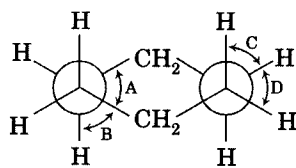
FIGURE 3.30

Atom numbering for discussion of van der Waals interactions in cyclohexane.



apart as the sum of their van der Waals radii (2.629 Å). Some of the van der Waals interactions are stabilizing dispersion effects, however, such as the interaction of C1 with H12.

The minimum energy conformation of cyclohexane calculated with a molecular mechanics program is shown in Figures 3.31 and 3.32, and the summary of the different contributions to the steric energy are listed in Table 3.7. Note that the C1–C2–C3–C4 dihedral angle is 56.33°, producing a torsional energy, E_T , of 0.343 kcal/mol. This value is quite close to the experimental value of 56.1°.¹³²



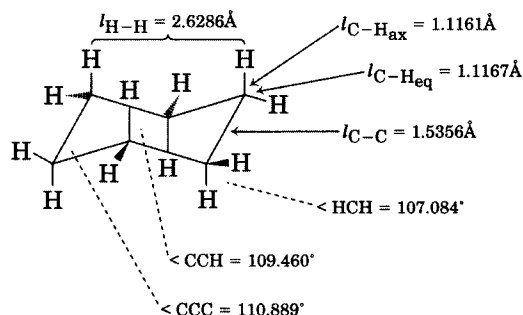
$$\begin{array}{ll} A = 56.33^\circ & B = 64.51^\circ \\ C = 57.26^\circ & D = 60.10^\circ \end{array}$$

FIGURE 3.31

Dihedral angles in chair cyclohexane from a molecular mechanics calculation.

In the discussions of Baeyer strain (page 123), we concluded that the chair conformation of cyclohexane has no angle strain, and the heat of combustion per methylene unit was found to be the same as that of an acyclic alkane. Examination of the chair conformation reveals that there are actually six butane gauche interactions, two evident from each conformation seen by a 120° rotation. Moreover, we have noted that there are three repulsive carbon–carbon transannular van der Waals interactions (e.g., the C1–C4 repulsion). Why, therefore, does cyclohexane not have 6 (0.8 kcal/mol) + 3 (0.31 kcal/mol) = 5.7 kcal/mol of strain energy? Wiberg noted that the heat of combustion comparison may be misleading.³⁸ Combustion of the alkanes is done on samples that are not at 0 K but are at room temperature, meaning that the population of alkane gauche conformations is not negligible. Therefore, cyclohexane is not being compared with a reference structure having all the CH₂ groups anti but, instead, is referenced to alkanes having a mixture of conformers. Wiberg calculated, however, that correcting for this mix of

¹³² Curtis, J.; Grant, D. M.; Pugmire, R. J. *J. Am. Chem. Soc.* **1989**, *111*, 7711.

**FIGURE 3.32**

Calculated minimum energy conformation of cyclohexane.

TABLE 3.7 Calculated Contributions to Steric Energy of Cyclohexane in the Chair Conformation

Parameter	E (kcal/mol)
Compression	0.3376
Bending	0.3652
Stretch-bend	0.0826
van der Waals	
1,4-Interaction	4.6733
Other	-1.0633
Torsional	2.1556
Total	6.5510

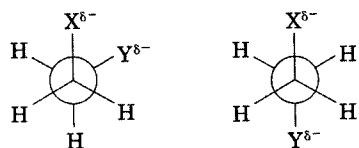
alkane conformations still suggested no more than 0.28 kcal/mol per cyclohexane gauche interaction.^{133,134}

This question serves as a reminder that the calculation of the components of internal energy in a molecular mechanics represents a model that is based on a set of nonobservables. Two molecular mechanics calculations that use different force fields might produce a similar value for the total strain of a structure, but they might partition that total into different internal contributions. For example, the MM1 and the MUB-2 procedures differed significantly in their handling of van der Waals forces. The MM1 procedure used a van der Waals potential for hydrogen that was large and hard but used a potential for carbon that was small. The potentials in the MUB-2 force field were smaller and softer for hydrogen, but they were larger for carbon. In the MM2 force field, the butane gauche interaction was modeled with a different torsional potential function, thus making the van der Waals characteristics of the atoms less important.¹⁰³ As Allinger has noted,

If different force-fields give the same results, as far as they can be checked against experimental values, but different results in terms of internal details which are not experimentally accessible, it is clear that one cannot assign physical significance to the different sets of internal details.¹⁰¹

¹³³ A possible explanation based on the electronic properties of the molecular orbitals used for sigma bonding was also offered by Dewar, M. J. S. *J. Am. Chem. Soc.* **1984**, 106, 669.

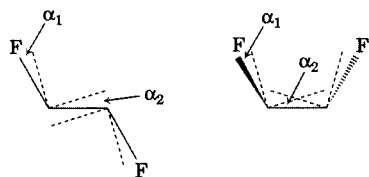
¹³⁴ Schleyer, P. v. R.; Williams, J. E.; Blanchard, K. R. *J. Am. Chem. Soc.* **1970**, 92, 2377 concluded that the gauche interactions in the cyclohexane skeleton are not comparable to those of gauche butane because the nonbonded hydrogen-hydrogen interactions are minimized in cyclohexane.

**FIGURE 3.33**

Electrostatic interactions in gauche (left) and anti (right) conformers of XCH_2CH_2Y .

This conclusion may be reinforced by considering conformations of compounds with the general structure $X-CH_2-CH_2-Y$. We have seen that when X and Y are both alkyl groups, the anti conformation is favored over the gauche conformation because of van der Waals strain. When X and Y are electronegative groups, we might expect that the gauche conformation would be even more destabilized through a combination of van der Waals forces and the electrostatic repulsion of the two partially negative substituents (Figure 3.33).

It may be surprising, therefore, that in the gas phase the gauche conformer of 1,2-difluoroethane is more stable than the anti conformer by about 1 kcal/mol. (For the other 1,2-dihaloethanes, the anti conformer is lower in energy, with the anti preference increasing along the series chlorine, bromine, and iodine.¹³⁵) Similar observations are made if X and Y are other electronegative atoms, such as oxygen, and the general trend is that the proportion of gauche conformer increases as X and Y become more electronegative.¹³⁶ This phenomenon is known as the **gauche effect**, which is "a tendency to adopt that structure which has the maximum number of gauche interactions between the adjacent electron pairs and/or polar bonds."¹³⁷

**FIGURE 3.34**

Effect of curved bond path on C–C bonding in anti (left) and gauche (right) conformers of 1,2-difluoroethane. (Reproduced from reference 138.)

An interesting explanation for the gauche effect was offered by Wiberg.¹³⁸ If the bond paths of methyl fluoride are curved as was discussed in Chapter 1, then those in 1,2-difluoroethane might be curved also. In Figure 3.34, the angle α_2 designates the difference between the carbon–carbon internuclear bond line and the preferred curved bond path from one carbon atom to another. Wiberg suggested that the curved bond path would lead to poor C–C orbital overlap in the anti conformer, but that bonding would not be affected as much in the case of the gauche conformer. Poorer orbital overlap would be expected to produce a longer carbon–carbon bond distance, and ab initio calculations did indicate that the C–C (internuclear) bond distance is 0.010 Å greater in the anti conformer than in the gauche conformer.¹³⁹ Because bond curvature is expected to increase as the electronegativity of the substituent increases, this explanation provides a simple model to explain a wide array of conformational phenomena.

Some theoretical work has supported Wiberg's proposal for bent carbon–carbon bonds in 1,2-difluoroethane. However, one study found mixing of a C–H bonding orbital with a C–F antibonding orbital (see Chapter 4) to be more significant than bond curvature in determining the minimum energy conformation of 1,2-difluoroethane.^{140–142} It remains noteworthy, however, that straight bonds are usually assumed in contemporary treatments of conformational analysis and molecular mechanics. If curved bonds are found to offer conceptual or computational advantages over straight bonds, then the straight bonds in contemporary model kits may be as deficient as was the hinged bond model that led Baeyer to propose angle strain in cyclohexane.

¹³⁵ Huang, J.; Hedberg, K. *J. Am. Chem. Soc.* **1990**, *112*, 2070.

¹³⁶ Phillips, L.; Wray, V. *J. Chem. Soc. Chem. Commun.* **1973**, 90.

¹³⁷ Wolfe, S. *Acc. Chem. Res.* **1972**, *5*, 102.

¹³⁸ Wiberg, K. B.; Murcko, M. A.; Laidig, K. E.; MacDougall, P. J. *J. Phys. Chem.* **1990**, *94*, 6956; Wiberg, K. B. *Acc. Chem. Res.* **1996**, *29*, 229.

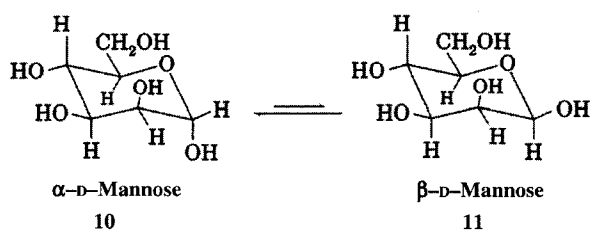
¹³⁹ Durig, J. R.; Liu, J.; Little, T. S.; Kalasinsky, V. F. *J. Phys. Chem.* **1992**, *96*, 8224.

¹⁴⁰ Goodman, L.; Gu, H.; Pophristic, V. *J. Phys. Chem. A* **2005**, *109*, 1223.

¹⁴¹ See also Freitas, M. P.; Rittner, R. *J. Phys. Chem. A* **2007**, *111*, 7233.

¹⁴² See the discussion of hyperconjugation in Chapter 4.

We saw in Chapter 2 that glucose can cyclize to form either the α or β hemiacetal. All of the substituents on the tetrahydropyran ring of glucose are equatorial except for the hemiacetal hydroxyl group, which may be either axial (for the α anomer) or equatorial (for the β anomer). If the conformational preferences of the tetrahydropyran ring are similar to those of cyclohexane, then an A value for OH of 0.87 in a protic solvent would predict that the axial anomer should comprise no more than 10% of the mixture. Experimentally, it has been determined that the α anomer is present to the extent of 34% of the equilibrium population of conformers. In the case of D-mannose, the α anomer (10) is the major isomer, and the β anomer (11) comprises only 32% of the equilibrium mixture.¹⁴³ This preference for axial conformer in carbohydrates has been termed the **anomeric effect**. This term is also used for any system R–Y–C–X, where X is an electronegative atom and Y is an atom with at least one lone pair.



This anomeric effect is considered a **stereoelectronic effect**—an effect that results from the “stereochemistry of particular electron pairs, bonded or nonbonded.”^{144,145} The origins of the anomeric effect have been discussed extensively.^{143,146,147} An early rationale was that local dipole moments interact more unfavorably in conformations when the R–Y–C–X conformation is gauche than when it is anti (Figure 3.35).¹⁴⁵ A more commonly cited explanation is an interaction of a nonbonded pair of electrons on oxygen with an antibonding orbital of the C–X bond in a process called hyperconjugation (Figure 3.36),¹⁴² but other origins have been suggested as well.^{148–150}

The ability to calculate conformational energies with molecular mechanics provides a useful means to correlate calculated structures with

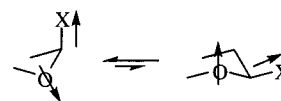


FIGURE 3.35

Dipole-dipole interactions suggested as an explanation for the anomeric effect.

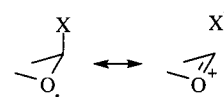


FIGURE 3.36

Hyperconjugation explanation for the anomeric effect.

¹⁴³ Kirby, A. J. *The Anomeric Effect and Related Stereoelectronic Effects at Oxygen*; Springer-Verlag: Berlin, 1983; p. 7.

¹⁴⁴ Deslongchamps, P. *Stereoelectronic Effects in Organic Chemistry*; Pergamon Press: Oxford, England, 1983.

¹⁴⁵ Thatcher, G. R. J., Ed. *The Anomeric Effect and Associated Stereoelectronic Effects*; American Chemical Society: Washington, DC, 1993.

¹⁴⁶ Juaristi, E.; Cuevas, G. *Tetrahedron* **1992**, *48*, 5019.

¹⁴⁷ Salzner, U.; Schleyer, P. v. R. *J. Am. Chem. Soc.* **1993**, *115*, 10231 and references therein.

¹⁴⁸ For more details, see chapter 2 of reference 143. See also reference 113, p. 220; Allinger, N. L.; Rahman, M.; Lii, J.-H. *J. Am. Chem. Soc.* **1990**, *112*, 8293; Cramer, C. J. *J. Org. Chem.* **1992**, *57*, 7034.

¹⁴⁹ For an explanation of the anomeric effect in terms of “hardness,” see Pearson, R. G. *J. Am. Chem. Soc.* **1988**, *110*, 7684; Hati, S.; Datta, D. *J. Org. Chem.* **1992**, *57*, 6056.

¹⁵⁰ See also Perrin, C. L.; Armstrong, K. B.; Fabian, M. A. *J. Am. Chem. Soc.* **1994**, *116*, 715; Roohi, H.; Ebrahimi, A.; Habibi, S. M.; Jarahi, E. *J. Mol. Struct.* **2006**, *772*, 65; Vila, A.; Mosquera, R. A. *J. Comput. Chem.* **2007**, *28*, 1516; Weinhold, F.; Landis, C. R. *Valency and Bonding: A Natural Bond Orbital Donor–Acceptor Perspective*; Cambridge University Press: Cambridge, UK, 2005; p. 240.

TABLE 3.8 Energies and Populations of 1-Bromo-2-methylbutane Conformers

Conformation	Relative E (kcal/mol)	Population (%)
G^-g^-	1.162	4.2
Ag^+	0.511	12.4
Aa	0.399	15.0
G^-a	0.311	17.4
G^+a	0.187	21.5
G^+g^+	0.00	29.5

experimental results. The relative population of a conformation is given by the Boltzmann distribution (equation 3.9), where E_i is the energy of the i th conformation and n is the number of conformations:⁸¹

$$P_i = \frac{e^{-E_i/RT}}{\sum_{i=1}^n e^{-E_i/RT}} \quad (3.9)$$

For example, six conformations of 1-bromo-2-methylbutane may be identified as shown in Table 3.8. Here the uppercase identifier refers to the C1–C2 bond, and the lowercase identifier designates the conformation of the C2–C3 bond.¹⁵¹ It may be seen that two conformations (G^+g^+ and G^+a) account for half of the equilibrium distribution, but the other four conformations are also present in significant amounts.

One very useful tool for studying conformations in solution is a relationship between dihedral angles and three-bond NMR coupling constants (3J) of vicinal protons. The relationship was derived theoretically by Karplus, and one form of the resulting equation is shown in equation 3.10, where ϕ is the H–C–C–H' dihedral angle:

$$^3J_{HH'} = A + B\cos\phi + C\cos 2\phi \quad (3.10)$$

For structural units having C–C bond lengths near 1.54 Å and bond angles near 109.5°, Karplus proposed values of 4.22, –0.5, and 4.5 for A , B , and C , respectively.¹⁵² As shown in Figure 3.37, values of ϕ near 90° lead to negligible coupling constants, while dihedral angles near 180° produce J values near 9 Hz. Karplus emphasized that equation 3.10 is only an approximation and that variations in bond lengths, bond angles, and electronegativities of substituents also need to be taken into account. Later authors have proposed empirical equations that account for such structural variations, and they enable more accurate correlations of NMR coupling constants with molecular geometry.¹⁵³

¹⁵¹ Wang, F.; Polavarapu, P. L.; Lebon, F.; Longhi, G.; Abbate, S.; Catellani, M. J. *Phys. Chem. A* **2002**, *106*, 12365. In this paper anti conformations are designated trans, so Aa in Table 3.8 is reported as Tt in the reference.

¹⁵² Karplus, M. J. *Chem. Phys.* **1959**, *30*, 11; *J. Am. Chem. Soc.* **1963**, *85*, 2870.

¹⁵³ Compare Haasnoot, C. A. G.; de Leeuw, F. A. A. M.; Altona, C. *Tetrahedron* **1980**, *36*, 2783.

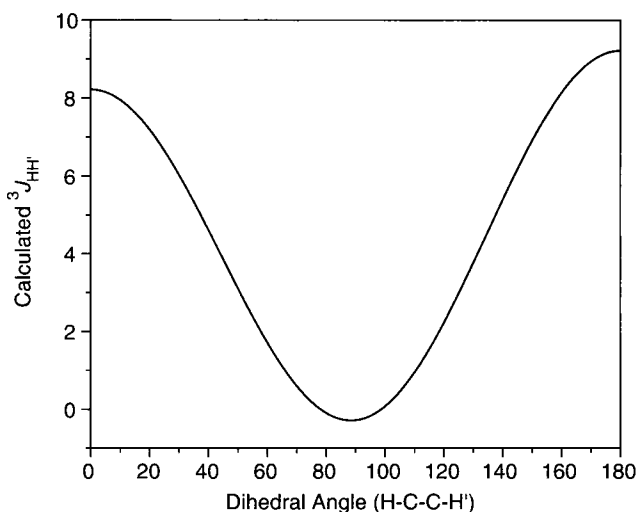


FIGURE 3.37

${}^3J_{HH}$ values calculated with equation 3.10.

Using the Karplus equation to calculate the J values expected for conformational minima and the distribution (mole fraction) of the conformations from their calculated relative energies allows the J value for a compound to be predicted from the relationship

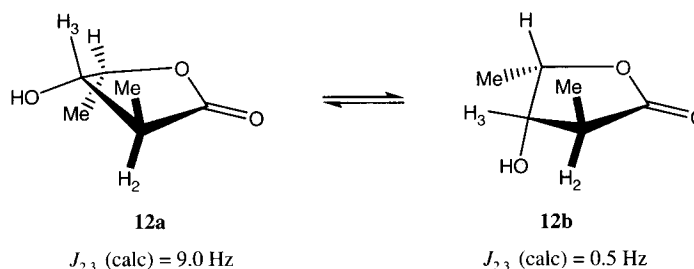
$$J = \sum_{i=1}^m n_i J_i \quad (3.11)$$

where n_i equals the mole fraction of the i th conformation and m is the number of conformers. As an example, two conformations of the γ -butyrolactone derivative **12** are shown in Figure 3.38. In conformation **12a** the hydrogen atoms on C2 and C3 are nearly anti, and the calculated $J_{2,3}$ value is 9.0 Hz. In **12b**, the $H_2-C_2-C_3-H_3$ dihedral angle is much smaller, and the calculated J value is 0.5 Hz. A molecular mechanics study indicated that **12a** and **12b** are very close in energy, so their equilibrium populations should be approximately 50 : 50. According to equation (3.11), the J value observed in solution should thus be 5.0, which matches the experimental value.¹⁵⁴

The principles of molecular mechanics may be used in a **molecular simulation** calculation, which is a type of computational statistical mechanics.¹⁵⁵ The goal of molecular simulation is to analyze a theoretical model of molecular behavior in order to determine the macroscopic properties of a substance. In one approach, known as **molecular dynamics** (MD), Newton's laws of motion for individual particles and a set of potential energy terms describing the forces on the structures are applied to all of the atoms in the calculation. Integration of the resulting differential equations over a short time period leads to new locations and new velocities for the atoms.

¹⁵⁴ Jaime, C.; Ortuño, R. M.; Font, J. *J. Org. Chem.* **1986**, *51*, 3946.

¹⁵⁵ Sadus, R. J. *Molecular Simulation of Fluids: Theory, Algorithms and Object-Oriented*; Elsevier: Amsterdam, 2002.

**FIGURE 3.38**

Calculated J values for conformers of **12**.

This stepwise process is repeated continually, allowing the system to evolve over time.

Molecular dynamics simulations may also be used to study the properties of individual molecules, such as probing the internal dynamics of cyclohexane and the intermolecular interactions of biomolecules^{156,157} and can provide insights into the bulk properties of substances. For example, Hammonds and co-workers reported a simulation of the properties of liquid *n*-octane at 20°. ¹⁵⁸ There are five C–C–C–C segments in *n*-octane, and each may exhibit either anti or one of two possible gauche conformations. As a result, there are 31 different possible conformational patterns possible. The results indicated that the all-anti (“zigzag”) conformation was exhibited by 11% of the molecules, while about 35% had a single gauche conformation somewhere along the chain. About 37% of the molecules had two gauche conformations along the chain, 15% had three, 2% had four gauche conformations, and less than 1% had five. These results were useful in modeling the distribution of end-to-end dimensions of the molecules, which could then be related to macroscopic properties such as diffusion.

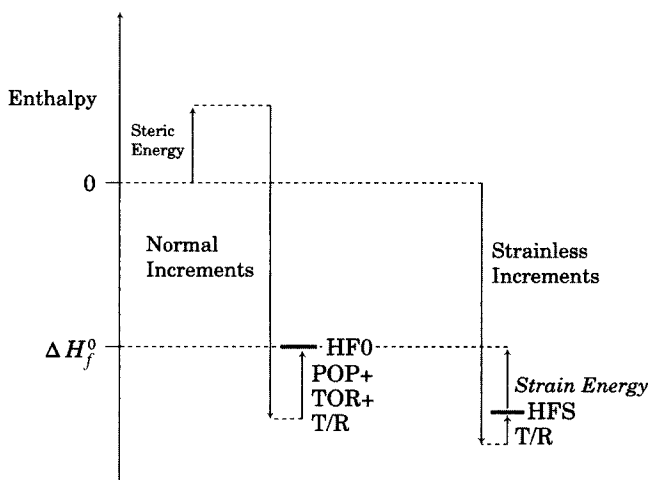
An alternative molecular simulation method is known as **Monte Carlo** statistical mechanics (MC).¹⁵⁵ In this approach, a trial configuration of the system is generated by *randomly* altering the positions of individual atoms or of entire molecules. The resulting changes in energy or other properties of the new arrangement are then used to determine an “acceptance criterion.” The acceptance criterion is compared with a random number, after which the new arrangement is either retained or rejected. Repeated application of the procedure yields a weighted-average model of the molecular structures and the thermodynamic properties of the system. This process is made more efficient through a technique known as Metropolis sampling, which generates trial arrangements that are more likely to make a significant contribution to the properties of the ensemble of molecules. In one study applying both molecular dynamics and Monte Carlo statistical mechanics to liquid hexane, the results of the two methods were found to be comparable, but the Monte Carlo method required less computer time.¹⁵⁹

¹⁵⁶ Kawai, T.; Tomioka, N.; Ichinose, T.; Takeda, M.; Itai, A. *Chem. Pharm. Bull.* **1994**, *42*, 1315; Beyer, A.; Schuster, P. *Monat. für Chemie* **1990**, *121*, 339.

¹⁵⁷ Compare Aleksandrov, A.; Simonson, T. J. *Am. Chem. Soc.* **2008**, *130*, 1114.

¹⁵⁸ Hammonds, K. D.; McDonald, I. R.; Ryckaert, J.-P. *Chem. Phys. Lett.* **1993**, *213*, 27.

¹⁵⁹ Jorgensen, W. L.; Tirado-Rives, J. J. *Phys. Chem.* **1996**, *100*, 14508.

**FIGURE 3.39**

Qualitative representation of enthalpy relationships used in calculating strain energies.

3.4 MOLECULAR STRAIN AND LIMITS TO MOLECULAR STABILITY

If a structure is well modeled by the parameters in the force field, molecular mechanics provides a means to calculate its ΔH_f° that is said to rival experiment for accuracy. Molecular mechanics can also be used to calculate a value for the strain energy of a structure. The strain energy of a molecule is not the same as the steric energy obtained from a molecular mechanics calculation, however, and the term *strain* is less precise than one might expect. "Qualitatively, organic chemists usually recognize a strained molecule when they see one,"¹²⁰ but strain is a parameter that can only be determined by reference to a model structure that is defined to be strain free.

Even the minimum energy conformation of a structure has some strain because it is impossible for every potential energy function to be at its energy minimum in the same geometry.¹¹³ For example, van der Waals interactions between nonbonded atoms might be optimized at a distance that is greater than the optimum bond distance for atoms to which those groups are bonded. Steric energies do give relative strain energies for conformers because the strainless reference compound is the same in both cases. However, the steric energy of butane cannot be compared directly with the steric energy of cyclobutane to determine the strain in cyclobutane. Therefore, strain calculations use "strainless" group contributions to determine a strainless heat of formation for the compound under consideration, and the difference between the two heats of formation can be said to be the strain energy of the structure. The relationships among strain energies, steric energies, and heats of formation are shown in Figure 3.39.¹²⁷

The relationships of the components used to calculate strain energy from steric energy may be made clearer by considering an example. A final portion of the output of the molecular mechanics calculation for the anti conformation of butane is shown here.

```
FINAL STERIC ENERGY IS 2.1714 KCAL.
HEAT OF FORMATION AND STRAIN ENERGY CALCULATIONS (UNITS ARE
KCAL.)
```

BOND ENTHALPY (BE) AND STRAINLESS BOND ENTHALPY (SBE) CONSTANTS AND SUMS

# BOND OR STRUCTURE	--- NORMAL ---	--- STRAINLESS ---
3 C-C SP3-SP3	.004 -.01	.493 1.48
10 C-H ALIPHATIC	-3.205 -32.05	-3.125 -31.25
2 C (SP3)-METHYL	-1.510 -3.02	-1.575 -3.15
	BE = -35.08	SBE = -32.92

PARTITION FUNCTION CONTRIBUTION (PFC)

CONFORMATIONAL POPULATION INCREMENT (POP)	.00
TORSIONAL CONTRIBUTION (TOR)	.00
TRANSLATION/ROTATION TERM (T/R)	2.40

PFC =	2.40

HEAT OF FORMATION (HF0) = E + BE + PFC	-30.51
STRAINLESS HEAT OF FORMATION (HFS) = SBE + T/R	-30.52
INHERENT STRAIN (SI) = E + BE - SBE	.01
STRAIN ENERGY (S) = POP + TOR + SI	.01

As indicated, the heat of formation (HF0) is taken as the sum of three terms. The first is the steric energy (E). The second is the bond enthalpy (BE), which is calculated from normal bond increments.¹⁶⁰ The third is a partition function increment (PFC), which is itself the sum of three terms: a conformational population increment (POP), a torsional contribution term (TOR), and a translation/rotation term (T/R).¹⁶¹ Since the molecular mechanics calculation has considered only one conformation, the POP and TOR terms are defined to be zero for this calculation (but see below). The T/R term is a molecular translational and rotational term that is always taken to be 2.4 kcal/mol at room temperature, since even an *anti*-butane molecule that is not rotating about the C2-C3 bond will still be undergoing translation and rotation of the entire molecule as a unit. Therefore, HF0 is the total of the bond increment contributions (BE = -35.08) plus the steric energy (E = 2.17) plus the partition function increment (PFC = 2.4). The sum, -30.51 kcal/mol, is slightly lower than the literature value of -30.15 kcal/mol.¹⁶²

¹⁶⁰ Neither the group increments nor the steric energies from one type of molecular mechanics calculation can be compared to the corresponding terms from calculations involving other force fields. The reason is that one force field might assign a particular interaction to a component of steric energy, but another force field might include some of that same energy in the bond or group increments used for calculation of ΔH_f^\ddagger . For example, Schleyer (reference 106) noted that three different force fields calculated values of 49.61, 31.48, and 40.40 kcal/mol as the steric energy of *tert*-butylmethane. However, the group contributions to ΔH_f^\ddagger for these same force fields were -102.69, -88.85, and -96.20 kcal/mol, respectively. Therefore, the calculated heats of formation were -53.08, -57.37 and -55.80 kcal/mol. The point is that the calculated heats of formation varied by only about 4 kcal/mol, even though the steric energies varied by more than 18 kcal/mol.

¹⁶¹ For details on the calculation of heats of formation from molecular mechanics, molecular orbital theory, or bond/group increments, see the discussion in Allinger, N. L.; Schmitz, L. R.; Motoc, I.; Bender, C.; Labanowski, J. K. *J. Am. Chem. Soc.* **1992**, *114*, 2880. The strain energy of a conformation can be calculated from values of heats of formation from these sources also. The relationships in Figure 3.39 among heat of formation, T/R, strainless increments, and strain energy hold no matter what the source of the heat of formation value.

¹⁶² Stull, D. R.; Westrum, E. F., Jr.; Sinke, G. C. *The Thermodynamics of Organic Compounds*; John Wiley & Sons: New York, 1969; p. 245.

We can also calculate a strainless heat of formation of *anti*-butane, which is the heat of formation of an anti structure made up of hypothetical *strainless* bonding interactions. As shown, we add the strainless bond increments to obtain the value of -32.92 kcal/mol for the strainless bond enthalpy (SBE). This value must also be corrected for the T/R term, but the POP and TOR terms are again taken to be zero. Thus, the strainless ΔH_f° (HFS) is the sum of -32.92 and $+2.40$, which is -30.52 kcal/mol. That differs from the heat of formation calculated with normal bond increments (-30.51 kcal/mol) by 0.01 kcal/mol, which is the inherent strain energy of *anti*-butane.¹⁶³

There is an important difference between the heat of formation (HFO) determined above and an experimental heat of formation, however. The calculated value is based on only one conformation, while the experimental value is determined from a sample of the *substance*, usually at or above room temperature, in which there is a distribution of conformations. For example, the POP term for butane should include the contribution to the ΔH_f° that arises because at 25° some butane molecules are in the gauche conformation. The excess enthalpy of butane that results from the presence of the higher energy conformers can be calculated from the knowledge of the energies of both the gauche and anti conformers and the Boltzmann distribution, and it is found to be 0.3 kcal/mol.¹¹³ We must also use a nonzero value for TOR to account for the change in enthalpy with temperature resulting from the presence of nonstaggered conformations, and that is calculated to be 0.36 kcal/mol.¹¹³ The T/R term remains 2.4 kcal/mol, since it does not vary with conformation. Therefore, the value of PFC becomes $0.3 + 0.36 + 2.4 = 3.06$ kcal/mol. Adding that value to the sum of the bond increments for butane (-35.08 kcal/mol) and the steric energy calculated for the anti conformer (2.17 kcal/mol) gives a ΔH_f° of butane of -29.85 kcal/mol, which is close to the literature value (-30.15 kcal/mol).

The strain energy at 25° of the *substance* butane should therefore be taken to be the difference between the strainless heat of formation and the heat of formation value that includes estimates of POP and TOR, and that difference is 0.67 kcal/mol. Notice that this value is not shown on the molecular mechanics output. Again, it must be emphasized that the strain energy shown on the molecular mechanics output above reflects only the inherent strain of the particular *conformer* calculated, not the strain in the *substance* represented by the computer model. A value of zero for POP and TOR on the output is an indication that appropriate values must be entered if the calculated value of ΔH_f° is expected to reproduce an experimental value and if a more accurate value for the strain energy is desired.

For molecules with many bonds about which rotation can occur and many conformations that might be populated at room temperature, the POP and TOR corrections can be significant. For relatively rigid molecules, however, these terms are less important, and the strain energies calculated from molecular mechanics can more closely approximate those that would be determined with consideration of POP and TOR. For example, consider the results of a molecular mechanics calculation for puckered cyclobutane, the final portion of which is reproduced here.

¹⁶³ Burkert and Allinger (reference 113) distinguished between inherent strain (shown as SI), which does not include POP and TOR, and total strain (shown as S), which does include those terms. By this distinction, one can either consider only the structural components of strain or both the structural and conformational components.

FINAL STERIC ENERGY IS 29.2202 KCAL.

COMPRESSION	.8020
BENDING	16.2111
STRETCH-BEND	-.9344
VANDERWAALS	
1,4 ENERGY	2.3242
OTHER	-.2521
TORSIONAL	11.0693

HEAT OF FORMATION AND STRAIN ENERGY CALCULATIONS (UNITS ARE KCAL.)

BOND ENTHALPY (BE) AND STRAINLESS BOND ENTHALPY (SBE) CONSTANTS AND SUMS

#	BOND OR STRUCTURE	-- NORMAL --	-- STRAINLESS --
4	C-C SP3-SP3	-.004	.493
8	C-H ALIPHATIC	-3.205	-3.125
		BE = -25.66	SBE = -23.03

PARTITION FUNCTION CONTRIBUTION (PFC)

CONFORMATIONAL POPULATION INCREMENT (POP)	.00
TORSIONAL CONTRIBUTION (TOR)	.00
TRANSLATION/ROTATION TERM (T/R)	2.40

PFC = 2.40

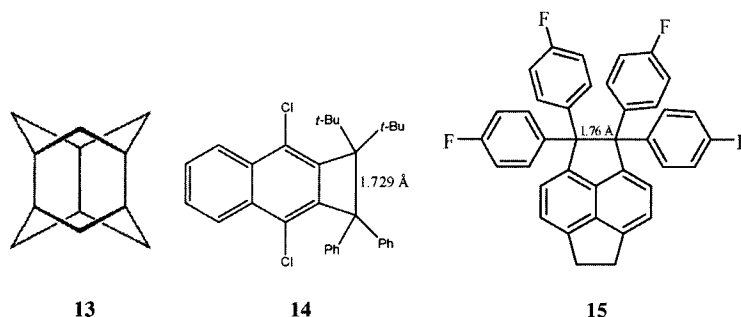
HEAT OF FORMATION (HF0) = E + BE + PFC	5.96
STRAINLESS HEAT OF FORMATION (HFS) = SBE + T/R	-20.63
INHERENT STRAIN (SI) = E + BE - SBE	26.59
STRAIN ENERGY (S) = POP + TOR + SI	26.59

The steric energy for cyclobutane is calculated to be 29.22 kcal/mol. Because the molecule is cyclic, there should not be free rotation about any bonds. Nevertheless, the conformational dynamics associated with inversion of puckered geometries (Figure 3.17) means that some internal energy must be included in the calculation of the heat of formation, and the total correction for POP and TOR amounts to 0.36 kcal/mol.¹¹³ Thus, the strain energy of cyclobutane should be greater than the amount shown by 0.36 kcal/mol, or a total of 26.95 kcal/mol.

Cyclobutane shows a significant amount of strain, but not as much as many compounds. One of the continuing challenges in organic chemistry is the design, synthesis, and characterization of novel molecular structures.¹⁶⁴ Molecular mechanics calculations (as well as quantum mechanics calculations, Chapter 4) are particularly helpful in these studies because they allow calculation of the heats of formation of highly strained molecules and the assignment of the components of the strain energy of the structures. This information can be a very useful guide to chemists trying to synthesize ever more strained organic compounds. Some of these structures are of interest primarily for their aesthetic appeal and intellectual challenge. Others allow chemists to put theories about molecular structure and bonding to extreme tests.

¹⁶⁴ For an introduction to the chemistry of strained organic molecules, see (a) reference 120; (b) Greenberg, A.; Liebman, J. F. *Strained Organic Molecules*; Academic Press: New York, 1978.

Some molecules are designed to test the limits on torsional strain. For example, the compound iceane (**13**) incorporates three cyclohexane boat conformations.¹⁶⁵ The limits on the lengths of carbon–carbon bonds can be estimated by experimental data on molecules with very long or very short bond distances. There are reports of structures having carbon–carbon bond lengths around 1.8 Å or more in highly strained molecules.^{166,167} Structure **14** has a C(*sp*³) – C(*sp*³) bond length that was found by X-ray diffraction to be 1.729 Å,^{168,169} and the “hexaphenylethane” single bond in **15** was determined to be 1.761 Å.¹⁷⁰ There was also one report of a system having a 2.9 Å carbon–carbon bond.¹⁷¹ On the other hand, the carbon–carbon *nonbonded* distance in derivatives of bicyclo[1.1.1]pentane is quite short. Adcock and co-workers have identified one derivative in which two carbon atoms that are not bonded to each other are only 1.80 Å apart.¹⁷² Thus, it appears that two carbon atoms that are formally bonded to each other in one molecule may be about the same distance apart as are two carbon atoms in another molecule that are not formally bonded to each other.¹⁷³



Steric strain in alkanes may also be due to van der Waals repulsion resulting from concentrated alkyl branching. Consider the structures in Figure 3.40, all of which have three *t*-butyl groups and one other alkyl group bonded to a central carbon. De Silva and Goodman studied these structures with molecular mechanics calculations and determined that **16**, **17**, and **18** should be stable at room temperature.¹⁷⁴ The possible existence of **19** was

¹⁶⁵ Cupas, C. A.; Hodakowski, L. *J. Am. Chem. Soc.* **1974**, *96*, 4668. See also Fărcașiu, D.; Wiskott, E.; Ōsawa, E.; Thielecke, W.; Engler, E. M.; Slutsky, J.; Schleyer, P. v. R. *J. Am. Chem. Soc.* **1974**, *96*, 4669.

¹⁶⁶ Bianchi, R.; Mugnoli, A.; Simonetta, M. *J. Chem. Soc. Chem. Commun.* **1972**, 1073; Bianchi, R.; Morosi, G.; Mugnoli, A.; Simonetta, M. *Acta Crystallogr. Sec. B* **1973**, *29*, 1196; Zhou, X.; Liu, R.; Allinger, N. L. *J. Am. Chem. Soc.* **1993**, *115*, 7525.

¹⁶⁷ An extensive review of organic molecules having atypical geometric parameters was provided by Komarov, I. V. *Russ. Chem. Rev.* **2001**, *70*, 991.

¹⁶⁸ Toda, F.; Tanaka, K.; Watanabe, M.; Tamura, K.; Miyahara, I.; Nakai, T.; Hirotsu, K. *J. Org. Chem.* **1999**, *64*, 3102.

¹⁶⁹ For a theoretical study of strained compounds, see Galasso, V.; Carmichael, I. *J. Phys. Chem. A* **2000**, *104*, 6271.

¹⁷⁰ Suzuki, T.; Takeda, T.; Kawai, H.; Fujiwara, K. *Pure Appl. Chem.* **2008**, *80*, 547.

¹⁷¹ Novoa, J. J.; Lafuente, P.; Del Sesto, R. E.; Miller, J. S. *Angew. Chem. Int. Ed. Engl.* **2001**, *40*, 2540.

¹⁷² Adcock, J. L.; Gakh, A. A.; Pollitte, J. L.; Woods, C. *J. Am. Chem. Soc.* **1992**, *114*, 3980.

¹⁷³ For a discussion of long bonds in strained molecules, see Ōsawa, E.; Kanematsu, K. in Liebman, J. F.; Greenberg, A., Eds. *Molecular Structure and Energetics*, Vol. 3; VCH Publishers: Deerfield Beach, FL, 1986; p. 329 ff.

¹⁷⁴ De Silva, K. M. N.; Goodman, J. M. *J. Chem. Inf. Model.* **2005**, *45*, 81.

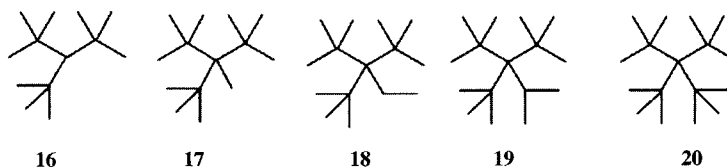


FIGURE 3.40
Highly branched alkanes.

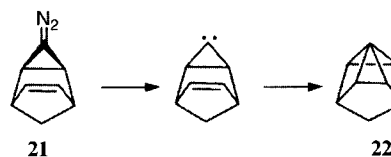


FIGURE 3.41
Proposed reaction sequence for generation of a structure containing a pyramidal carbon.

deemed questionable, and structure **20** was predicted to be unstable because of van der Waals strain. The authors suggested that **19** may be the “smallest saturated alkane that cannot be made.” Because of this strain, Paton and Goodman concluded that calculations of the number of hydrocarbon isomers having a given molecular formula overstate the number of stable structures.¹⁷⁵

Chemists have also sought to synthesize compounds with unusual bond angles. One goal has been to prepare compounds with **pyramidal carbon atoms**, meaning atoms in which the four valences are all directed toward one side of a plane passing through the carbon atom.¹⁷⁶ The reaction of *endo*-3-diazotriclo[3.2.1.0^{2,4}]oct-6-ene (**21**, Figure 3.41) produces products consistent with the intermediacy of the pentacyclooctane **22**, in which the carbon atom at the top of the structure (as drawn here) is constrained to be pyramidal.¹⁷⁷

Other interesting examples of compounds with this structural feature are the **propellanes**,¹⁷⁸ such as [1.1.1]propellane (**23**).¹⁷⁹ A theoretical analysis indicated that the C1–C3 bond has a bond order of about 0.7 and that the orbitals that comprise the bond have much *p* character.^{180,181} The compound has surprising stability, with a half-life for thermal rearrangement of 5 minutes at 114°. This example illustrates that we should not necessarily equate high strain with high chemical reactivity, because there may be a high activation barrier for chemical reaction, even for a very strained molecule.



¹⁷⁵ Paton, R. S.; Goodman, J. M. *J. Chem. Inf. Model.* **2007**, *47*, 2124.

¹⁷⁶ For reviews, see Wiberg, K. B. (a) *Acc. Chem. Res.* **1984**, *17*, 379; (b) *Chem. Rev.* **1989**, *89*, 975.

¹⁷⁷ Miesusset, J.-L.; Brinker, U. H. *J. Org. Chem.* **2006**, *71*, 6975.

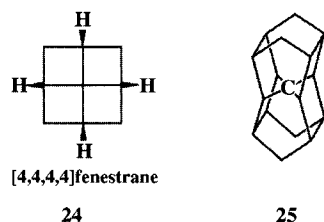
¹⁷⁸ The term propellane denotes a structure “having three nonzero bridges and one zero bridge between a pair of bridgehead carbons” (reference 176b).

¹⁷⁹ Wiberg, K. B.; Walker, F. H. *J. Am. Chem. Soc.* **1982**, *104*, 5239.

¹⁸⁰ Ebrahimi, A.; Deyhimi, F.; Roohi, H. *J. Mol. Struct.* **2003**, *626*, 223 and references therein.

¹⁸¹ Messerschmidt, M.; Scheins, S.; Grubert, L.; Pätzelt, M.; Szeimies, G.; Paulmann, C.; Luger, P. *Angew. Chem. Int. Ed.* **2006**, *44*, 3925.

One might expect that if a structure with a pyramidal carbon atom is capable of existence, then one with a flattened carbon atom should be more stable and therefore easier to synthesize. That has turned out not to be the case.¹⁸²⁻¹⁸⁴ For example, a great deal of interest was expressed in fenestranes, named for the Latin word for "window."^{185,186} Structure **24** would be [4.4.4.4]fenestrane, since each "pane" is composed of four carbon atoms. The figure suggests that the central carbon atom should be planar, but more detailed consideration suggests that nonplanar geometries are more stable.¹²⁰ Another approach to planar carbon is the proposed class of compounds named alkaplans, such as hexaplans (**25**), in which the central carbon atom is held with the right symmetry for the carbon atom to be planar.¹⁸⁷⁻¹⁸⁹



Many compounds are interesting because they represent novel geometric shapes that have not previously been identified in naturally occurring products. Tetrahedrane (**26**), in the shape of one of the Platonic solids, has not yet been synthesized,¹⁹⁰ but theoretical calculations suggest that it might

¹⁸² Interest in planar tetraligant carbon was stimulated by a paper by Hoffmann and co-workers, who used extended Hückel theory to consider how to stabilize a planar geometry so that it might serve as a transition state for isomerization of a chiral center. Hoffmann, R.; Alder, R. W.; Wilcox, C. F., Jr. *J. Am. Chem. Soc.* **1970**, *92*, 4992.

¹⁸³ Higher level calculations later indicated that planar methane could be characterized as a complex between a singlet methylene (see Chapter 5) and a side-on hydrogen molecule. Pepper, M. J. M.; Shavitt, I.; Schleyer, P. v. R.; Glukhovtsev, M. N.; Janoschek, R.; Quack, M. *J. Comput. Chem.* **1995**, *16*, 207.

¹⁸⁴ See also Perez-Peralta, N.; Sanchez, M.; Martin-Polo, J.; Islas, R.; Vela, A.; Merino, G. *J. Org. Chem.* **2008**, *73*, 7037.

¹⁸⁵ Georgian, V.; Saltzman, M. *Tetrahedron Lett.* **1972**, 4315. See also the discussion in Nickon, A.; Silversmith, E. F. *The Name Game. Modern Coined Terms and Their Origins*; Pergamon Press: New York, 1987; pp. 55-56.

¹⁸⁶ For a review, see Venepalli, B. R.; Agosta, W. C. *Chem. Rev.* **1987**, *87*, 399.

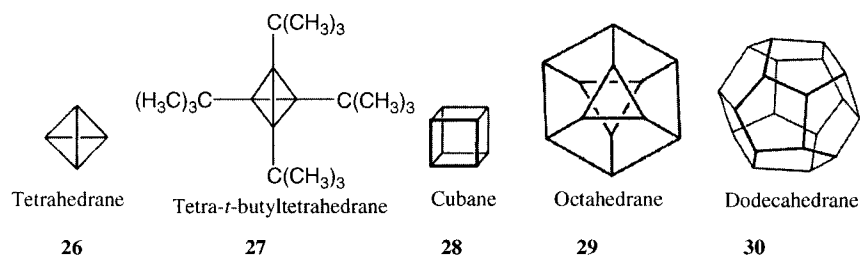
¹⁸⁷ McGrath, M. P.; Radom, L. *J. Am. Chem. Soc.* **1993**, *115*, 3320.

¹⁸⁸ Theoretical studies suggested that a C_5^{2-} structure could have a planar tetracoordinate carbon atom. Merino, G.; Méndez-Rojas, M. A.; Beltrán, H. I.; Corminboeuf, C.; Heine, T.; Vela, A. *J. Am. Chem. Soc.* **2004**, *126*, 16160.

¹⁸⁹ Keese, R. *Chem. Rev.* **2006**, *106*, 4787 summarized research directed toward the synthesis of planar tetraligant carbon compounds and the fenestranes.

¹⁹⁰ Scott, L. T.; Jones, M., Jr. *Chem. Rev.* **1972**, *72*, 181.

be sufficiently stable to be isolated.¹⁹¹ However, tetra-*t*-butyltetrahedrane (27) has been reported.¹⁹² Other compounds with geometries of Platonic solids are cubane (28),^{193,194} octahedrane (29),¹⁹⁵ and dodecahedrane (30).¹⁹⁶



Other structures with interesting geometries, such as those shown in Figure 3.42, are novel compounds that have provided challenges to synthetic chemists. Some, but not all, of these compounds have been synthesized.¹⁹⁷

The compounds in Figure 3.42 formally have only single carbon–carbon bonds. Even more strain can be present in structures that incorporate non-planar double or nonlinear triple bonds. The former case may arise if a double bond occurs at a bridgehead carbon atom, as was originally noted by Bredt. Therefore, the idea that such compounds are incapable of existence has become known as “Bredt’s Rule.”^{198,199} A formal statement of the rule was given by Fawcett:

In polycyclic systems having atomic bridges, the existence of a compound having a carbon–carbon or carbon–nitrogen double bond at a bridgehead position is not possible, except when the rings are large, because of the strain which would be introduced in its formation by the distortion of bond angles and/or distances. As a corollary, reactions which should lead to such compounds will be hindered or will give products having other structures.²⁰⁰

Violations of the rule are possible, especially if one of the rings has eight atoms or more, and structures such as 31 (Figure 3.43) are known as “anti-Bredt” compounds.²⁰¹ Anti-Bredt compounds with smaller rings may also

¹⁹¹ Nemirowski, A.; Reisenauer, H. P.; Schreiner, P. R. *Chem.–Eur. J.* **2006**, *12*, 7411.

¹⁹² Maier, G. *Angew. Chem. Int. Ed. Engl.* **1988**, *27*, 309.

¹⁹³ Eaton, P. E.; Cole, T. W., Jr. *J. Am. Chem. Soc.* **1964**, *86*, 3157.

¹⁹⁴ Griffin, G. W.; Marchand, A. P. *Chem. Rev.* **1989**, *89*, 997 reviewed the synthesis and chemistry of cubanes.

¹⁹⁵ de Meijere, A.; Lee, C.-H.; Kuznetsov, M. A.; Gusev, D. V.; Kozhushkov, S. I.; Fokin, A. A.; Schreiner, P. R. *Chem.–Eur. J.* **2005**, *11*, 6175.

¹⁹⁶ Ternansky, R. J.; Balogh, D. W.; Paquette, L. A. *J. Am. Chem. Soc.* **1982**, *104*, 4503.

¹⁹⁷ For a discussion of structures with multiple carbon rings, see Osawa, E.; Yonemitsu, O., Eds. *Carbocyclic Cage Compounds: Chemistry and Applications*; VCH Publishers: New York, 1992.

¹⁹⁸ A bridgehead carbon atom is part of two different rings.

¹⁹⁹ Bredt, J.; Thouet, H.; Schmitz, J. *Liebigs Ann. Chem.* **1924**, *437*, 1.

²⁰⁰ Fawcett, F. S. *Chem. Rev.* **1950**, *47*, 219.

²⁰¹ Prelog, V. *J. Chem. Soc.* **1950**, 420.

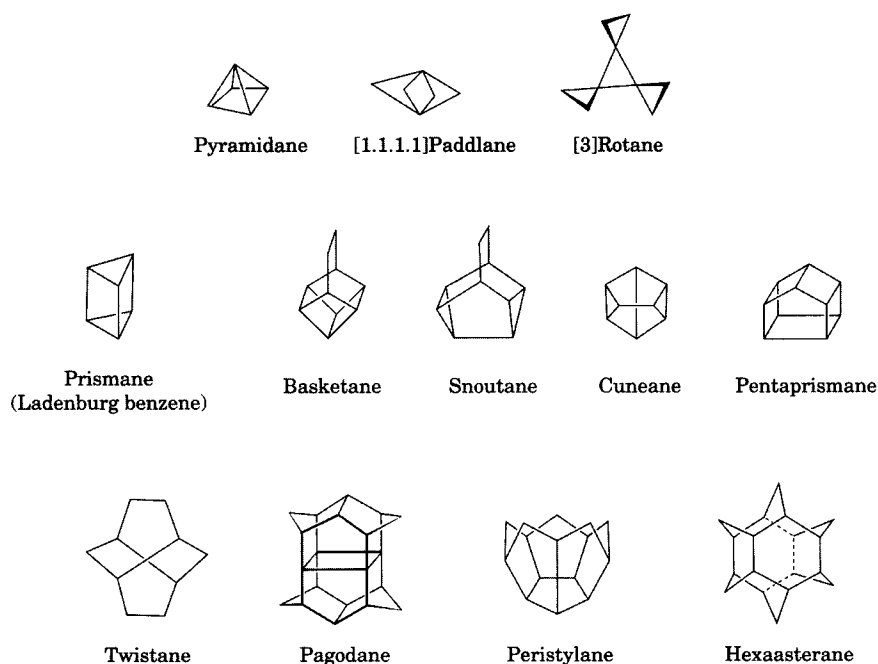


FIGURE 3.42
Challenging molecular structures.

exist as transient species. For example, bicyclo[2.2.0]hex-1(4)-ene (**32**) was produced but was found to polymerize at -23° with a half-life of less than 10 seconds.²⁰² Warner reviewed the wide variety of structures with strained bridgehead double bonds that have been studied.²⁰³

The geometry of a carbon-carbon double bond can also be distorted in monocyclic compounds. Cycloalkenes with a *trans* double bond show significant deviations from normal bond angles when the rings are small.²⁰⁴ Nevertheless, *trans*-cyclooctene (**33**) has been isolated,²⁰⁵ and *trans*-cycloheptene and *trans*-cyclohexene have been implicated as reaction intermediates.^{206–209} Even *cis* double bonds may be highly strained in very small rings. Billups and Haley obtained evidence for the existence of spirocyclopentadiene (**34**) as a transient species whose existence was confirmed by trapping with cyclopentadiene.²¹⁰

²⁰² Casanova, J.; Bragin, J.; Cottrell, F. D. *J. Am. Chem. Soc.* **1978**, *100*, 2264.

²⁰³ Warner, P. M. *Chem. Rev.* **1989**, *89*, 1067.

²⁰⁴ For a review, see Johnson, R. P. in *Molecular Structure and Energetics*, Vol. 3; Liebman, J. F.; Greenberg, A., Eds.; VCH Publishers: Deerfield Beach, FL, 1986; pp. 85–140.

²⁰⁵ Cope, A. C.; Pike, R. A.; Spencer, C. F. *J. Am. Chem. Soc.* **1953**, *75*, 3212; Turner, R. B.; Meador, W. R. *J. Am. Chem. Soc.* **1957**, *79*, 4133.

²⁰⁶ Corey, E. J.; Carey, F. A.; Winter, R. A. E. *J. Am. Chem. Soc.* **1965**, *87*, 934.

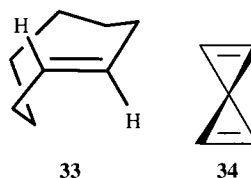
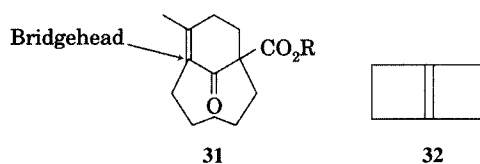
²⁰⁷ *trans*-Cycloheptene was prepared photochemically at -78°C by Inoue, Y.; Ueoka, T.; Kuroda, T.; Hakushi, T. *J. Chem. Soc. Perkin Trans. 2* **1983**, 983. The decay of *trans*-cycloheptene to the *cis* isomer was found to occur by a bimolecular process, suggesting that isolated *trans* isomers would be stable at higher temperatures: Squillacote, M. E.; DeFellipis, J.; Shu, Q. *J. Am. Chem. Soc.* **2005**, *127*, 15983.

²⁰⁸ Kropp, P. J. *Mol. Photochem.* **1978–79**, *9*, 39.

²⁰⁹ For a theoretical study of *trans*-cyclohexene, see Verbeek, J.; van Lenthe, J. H.; Timmermans, P. J. A. A.; Mackor, A.; Budzelaar, P. H. M. *J. Org. Chem.* **1987**, *52*, 2955.

²¹⁰ Billups, W. E.; Haley, M. M. *J. Am. Chem. Soc.* **1991**, *113*, 5084.

FIGURE 3.43
Anti-Bredt compounds.



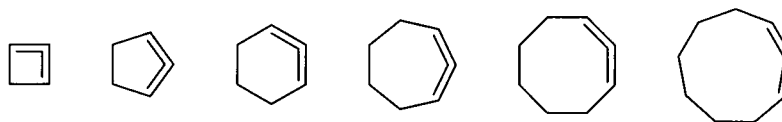
Cycloalkynes must also be strained if the ring does not allow the acetylenic carbon atoms to have 180° bond angles. A cycloalkyne with eight or more carbon atoms in the ring (e.g., cyclooctyne, **35**) is generally large enough to be stable,^{211,212} and smaller ring cycloalkynes have been proposed as reactive intermediates.^{213–215} For example, both cyclohexyne and cycloheptyne can be generated through elimination reactions of iodonium salts.²¹⁶



Isomeric with cycloalkynes are 1,2-cycloalkadienes (also known as cyclocumulenes). The structures in Figure 3.44 have been reported either as stable compounds or as reactive intermediates.²¹⁷

Acyclic alkenes may have strained π bonds due to steric hindrance. The isomers **36a** and **36b** are distorted because of steric strain associated with the

FIGURE 3.44
Cyclocumulenes.



²¹¹ (a) Brandsma, L.; Verkruijse, H. D. *Synthesis of Acetylenes, Allenes and Cumulenes: a Laboratory Manual*; Elsevier: Amsterdam, 1981. (b) For a discussion of triple bonds in small rings, see Sander, W. *Angew. Chem. Int. Ed. Engl.* **1994**, 33, 1455.

²¹² Blomquist, A. T.; Liu, L. H. *J. Am. Chem. Soc.* **1953**, 75, 2153.

²¹³ Erickson, K. L.; Wolinsky, J. *J. Am. Chem. Soc.* **1965**, 87, 1142.

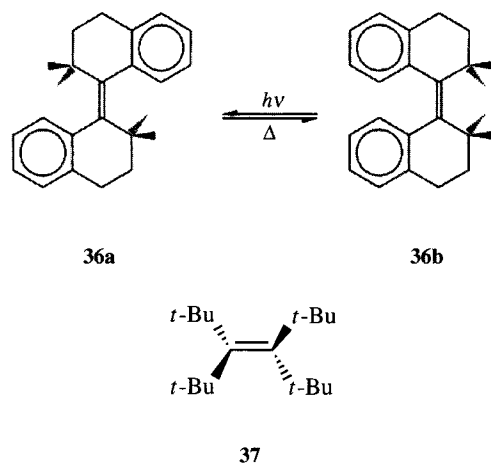
²¹⁴ Tseng, J.; McKee, M. L.; Shevlin, P. B. *J. Am. Chem. Soc.* **1987**, 109, 5474.

²¹⁵ Krebs, A.; Kimling, H. *Angew. Chem.* **1971**, 83, 540; Sander, W. *Angew. Chem. Int. Ed. Engl.* **1994**, 33, 1455.

²¹⁶ Okuyama, T.; Fujita, M. *Acc. Chem. Res.* **2005**, 38, 679.

²¹⁷ Daoust, K. J.; Hernandez, S. M.; Konrad, K. M.; Mackie, I. D.; Winstanley, J., Jr.; Johnson, R. P. *J. Org. Chem.* **2006**, 71, 5708.

bulky alkyl substituents about the carbon-carbon double bond. Compound **36a** is stable, and an X-ray analysis indicated that the double bond is twisted from planarity by 36.7° . Compound **36b** is even more strained and is unstable, isomerizing with an activation energy of only about 21 kcal/mol. Molecular mechanics calculations suggest that the substituents on **36b** are twisted by 73° .²¹⁸ Tetra-*t*-butylethylene (**37**) should also be highly twisted about the carbon-carbon double bond. The compound has not been synthesized, but a theoretical calculation suggested that it might be stable.²¹⁹



A particularly interesting case of a twisting distortion of the double bond is illustrated by a structure having the trivial name orthogonene (**38**, Figure 3.45).²²⁰ As the first part of the name suggests, the two substituents on one end of the double bond are oriented nearly perpendicular to the two substituents on the other end. Therefore the *p* orbitals of the alkene should be nearly perpendicular. Calculations indicated that the C_2 structure, which has an 83° dihedral angle across the double bond, is unstable with respect to rearrangement, but the D_2 isomer with an 88° dihedral angle (**39**) may be stable at room temperature.²²¹

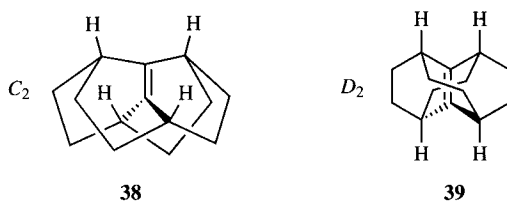


FIGURE 3.45

Orthogonene (**38**) and a possibly stable D_2 isomer (**39**).

²¹⁸ Gano, J. E.; Park, B. S.; Pinkerton, A. A.; Lenoir, D. J. *Org. Chem.* **1990**, *55*, 2688.

²¹⁹ Lenoir, D.; Wattenbach, C.; Liebman, J. F. *Struct. Chem.* **2006**, *17*, 419.

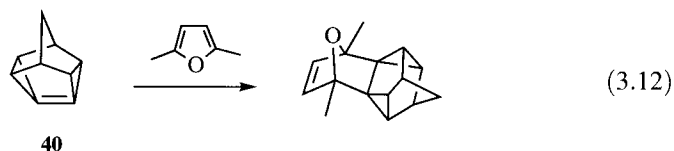
²²⁰ Jeffrey, D. A.; Maier, W. F. *Tetrahedron* **1984**, *40*, 2799.

²²¹ Lewars, E. G. J. *Phys. Chem. A* **2005**, *109*, 9827.

**FIGURE 3.46**

Definition of pyramidalization angle, ϕ .

A different kind of alkene distortion is pyramidalization, in which one or both of the substituents attached to a double-bonded carbon do not lie in the same plane as the other double-bonded carbon and its two substituents (as illustrated for distorted ethene in Figure 3.46).²²² The pyramidalization angle, ϕ , is defined as the angle through which the H–C–H plane deviates from the geometry expected for a planar alkene. As noted earlier, the energy barrier to distortion of bond angles around tetraligant carbon is relatively small. The same is true of bond angles to olefinic carbons. Rasul and co-workers calculated that an 18° deformation of both ends of a carbon–carbon double bond costs only 4.4 kcal/mol, and a 54° deformation costs only 38.3 kcal/mol.^{223,224} As an example, Forman and co-workers calculated the pyramidalization angle of pentacyclo[4.3.0.0^{2,4}.0^{3,8}.0^{5,7}]non-4-ene (**40**) to be about 65°.²²⁵ Such olefins can be used to generate other, strained structures, as is illustrated by the Diels–Alder reaction of **40** with 2,5-dimethylfuran (equation 3.12). Another intriguing example is the highly strained cubene (1,2-dehydrocubane, **41**), where the pyramidalization angle appears to be 90°.²²⁶ Some investigators have considered the possibility of “molecular loops and belts” based on pyramidalized double-bonded carbons. Among such structures are the beltene (e.g., **42**), which have double bonds only at each of the ring junctures, and cyclacenes (e.g., **43**), where each ring is formally a benzene ring (Figure 3.47).²²⁷ Structures such as **43** have not been reported, but Gleiter and co-workers synthesized [6.8]₃cyclacene (**44**), consisting of three six-membered benzene-like rings interspersed with three eight-membered cyclooctatetraene-like rings.²²⁸



Alkenes with unusual arrangements of double bonds are of interest in molecular orbital calculations (to be discussed in Chapter 4). Among

²²² For a review of pyramidalized alkenes, see Borden, W. T. *Chem. Rev.* **1989**, 89, 1095.

²²³ Rasul, G.; Olah, G. A.; Prakash, G. K. S. *J. Phys. Chem. A* **2006**, 110, 7197.

²²⁴ The theoretical foundations of these calculations will be discussed in Chapter 4.

²²⁵ Forman, M. A.; Moran, C.; Herres, J. P.; Stairs, J.; Chopko, E.; Pozzessere, A.; Kerrigan, M.; Kelly, C.; Lowchyj, L.; Salandria, K.; Gallo, A.; Loutzenhiser, E. *J. Org. Chem.* **2007**, 72, 2996.

²²⁶ Eaton, P. E.; Maggini, M. *J. Am. Chem. Soc.* **1988**, 110, 7230. Also see Hrovat, D. A.; Borden, W. T. *J. Am. Chem. Soc.* **1988**, 110, 4710.

²²⁷ Tahara, K.; Tobe, Y. *Chem. Rev.* **2006**, 106, 5274; Yao, T.; Yu, H.; Vermeij, R. J.; Bodwell, G. J. *Pure Appl. Chem.* **2008**, 80, 533.

²²⁸ Esser, B.; Rominger, F.; Gleiter, R. *J. Am. Chem. Soc.* **2008**, 130, 6716.

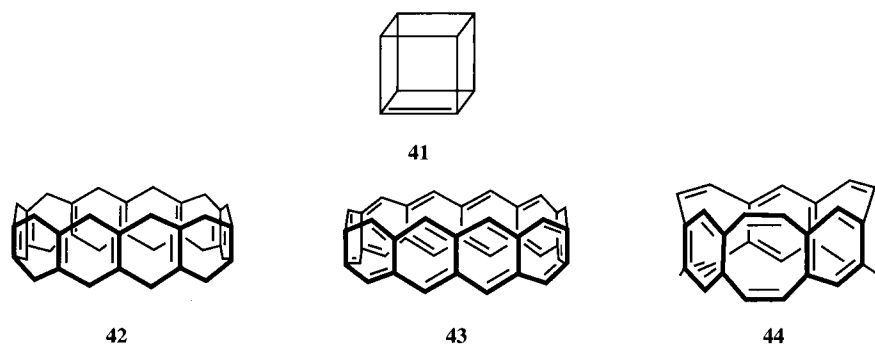
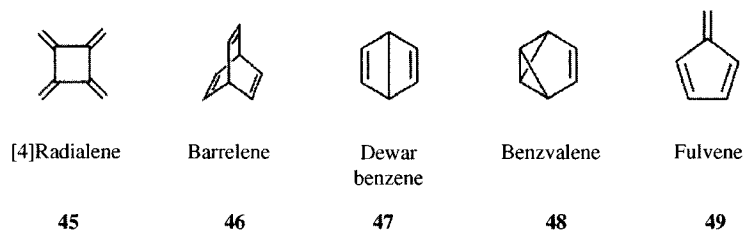


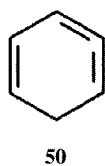
FIGURE 3.47

A beltene (42), a cyclacene (43), and [6.8]₃cyclacene (44).

structures that have been studied are [4]radialene (45),²²⁹ barrelene (46),²³⁰ and Dewar benzene (47).²³¹ Dewar benzene and benzvalene (48)²³² are **valence isomers** of benzene because they have the formula (CH)₆. Another isomer is fulvene (49), which is formed photochemically from benzene.²³³ Note that 49 is not a valence isomer of benzene because one carbon has two hydrogen substituents, while another carbon has no hydrogen substituent. Each valence isomer of benzene has only one hydrogen atom bonded to each carbon atom.



Compounds that are isomers of aromatic compounds are termed **isoaromatics**, and 1,2,4-cyclohexatriene is an **isobenzene** (50).²³⁴



²²⁹ Griffin, G. W.; Peterson, L. I. *J. Am. Chem. Soc.* **1963**, *85*, 2268. See also Hopf, H.; Maas, G. *Angew. Chem. Int. Ed. Engl.* **1992**, *31*, 931.

²³⁰ Zimmerman, H. E.; Paufler, R. M. *J. Am. Chem. Soc.* **1960**, *82*, 1514.

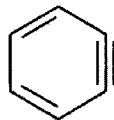
²³¹ van Tamelen, E. E.; Pappas, S. P. *J. Am. Chem. Soc.* **1963**, *85*, 3297.

²³² Wilzbach, K. E.; Ritscher, J. S.; Kaplan, L. *J. Am. Chem. Soc.* **1967**, *89*, 1031.

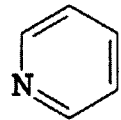
²³³ The heats of formation of the valence isomers of benzene were reported by Schulman, J. M.; Disch, R. L. *J. Am. Chem. Soc.* **1985**, *107*, 5059. The values for Dewar benzene, benzvalene, prismane, and 3,3'-bicyclopentenyl were 94.0, 90.2, 136.4, and 137.6 kcal/mol, respectively.

²³⁴ Christl, M.; Braun, M.; Müller, G. *Angew. Chem. Int. Ed. Engl.* **1992**, *31*, 473.

Arynes are structures having an additional bond in an aromatic ring. The classic aryne is benzyne (**51**),²³⁵ which is thought to be an intermediate in some substitution reactions (Chapter 8). Pyridyne (**52**) has also been detected.²³⁶

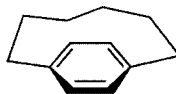


51

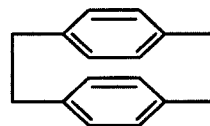


52

Cyclophanes are aromatic rings joined at two positions to form a cyclic structure.²³⁷ The smallest known is [6]paracyclophane (**53**), which is stable at room temperature. The aromatic ring carbon atoms attached to the alkyl chain are bent about 20° out of the plane defined by the other four aromatic carbon atoms.²³⁸ In [2.2]paracyclophane (**54**), one aromatic ring is held above another.²³⁹



53



54

Just as analytical chemists seem able to detect ever smaller quantities, so organic chemists seem able to synthesize increasingly strained species. Michl and Gladysz noted that

The concept of strain has fascinated organic chemists for about a century, and the interest shows no sign of abatement; if anything it is growing. Over this period of time, our attitudes have changed dramatically. Today, we accept the remarkable stability of [1.1.1]propellane and tetra-*tert*-butyltetrahedrane casually. Two decades ago, a student who would draw such "impossible" structures during an examination would have surely failed. We wonder what other marvels lie in store.²⁴⁰

²³⁵ The structure shown is that of 1,2-didehydrobenzene, more commonly known as *o*-benzyne. The 1,3-didehydro- and 1,4-didehydrobenzenes are known as *m*-benzyne and *p*-benzyne, respectively. The heats of formation of *o*-, *m*-, and *p*-benzyne have been determined to be 106 ± 3, 116 ± 3, and 128 ± 3 kcal/mol, respectively: Wenthold, P. G.; Paulino, J. A.; Squires, R. R. *J. Am. Chem. Soc.* **1991**, *113*, 7414.

²³⁶ Nam, H.-H.; Leroi, G. E. *J. Am. Chem. Soc.* **1988**, *110*, 4096.

²³⁷ For further reading, see Keehn, P. M.; Rosenfeld, S. M., Eds. *Cyclophanes*, Vols. I and II; Academic Press: New York, 1983. For a discussion of "super"phanes, see Gleiter, R.; Kratz, D. *Acc. Chem. Res.* **1993**, *26*, 311.

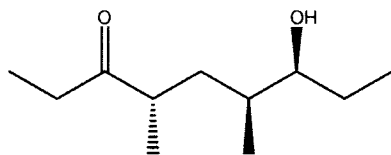
²³⁸ Tobe, Y.; Takemura, A.; Jimbo, M.; Takahashi, T.; Kobiuro, K.; Kakiuchi, K. *J. Am. Chem. Soc.* **1992**, *114*, 3479.

²³⁹ See Boekelheide, V. *Acc. Chem. Res.* **1980**, *13*, 65.

²⁴⁰ Michl, J.; Gladysz, J. A. *Chem. Rev.* **1989**, *89*, 973.

Problems

- 3.1. How many staggered conformations (other than those that involve rotation of a methyl group) are possible for 55.



55

- 3.2. Use the principles of conformational analysis to predict the difference in heats of combustion of *cis*- and *trans*-1,3-dimethylcyclohexane. How does your calculated value compare with the data in Table 3.3?
- 3.3. Rationalize the observation that only the more stable of the two isomers of 1,2-dimethylcyclohexane is chiral, but only the less stable isomer of 1,3-dimethylcyclohexane is chiral.
- 3.4. We usually expect larger substituents on cyclohexane rings to have *A* values that are greater than those of smaller substituents. The increase in equatorial preference is not linear with increasing size of alkyl substituents, however. Rationalize the data in Table 3.9.

TABLE 3.9 Equatorial Preference of Cyclohexane Substituents

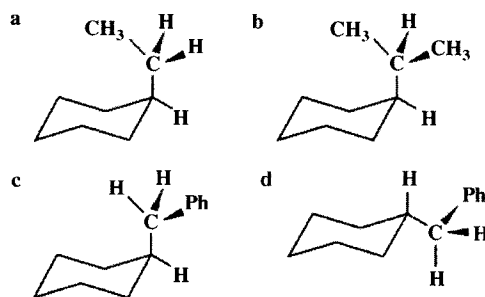
Substituent	<i>A</i> (kcal/mol)
Methyl	1.70
Ethyl	1.75
Isopropyl	2.15
<i>t</i> -Butyl	>5.4

- 3.5. At 202 K, the conformational equilibrium of *cis*-1-benzyl-4-methylcyclohexane favors the chair conformation having the benzyl group axial by 0.08 kcal/mol. However, at room temperature or higher, the equilibrium favors the chair conformation with the benzyl group equatorial by 0.04 kcal/mol. Explain this result.
- 3.6. Suggest explanations for the following observations concerning equatorial preferences (Table 3.2):
- The *A* values of the OH and NH₂ groups are different in protic and aprotic solvents.
 - The *A* value of the carboxylate (CO₂⁻) group is greater than that of the CO₂H group.
 - The *A* values of the halogens do not increase in the order F < Cl < Br < I.
- 3.7. The interconversion of the rotamers of the 2',6'-dialkyl-2-halo-*N*-methylacetanilides **8** and **9** (page 118) is slower in polar and hydrogen-bonding solvents than in nonpolar solvents. Rationalize this result.
- 3.8. The gas phase molecular structure of 2-fluoroethanol has been studied by electron diffraction and microwave spectroscopy at temperatures of 20°C, 156°C, and 240°C. At the two lower temperatures only the *gauche* conformation was seen; at 240°C the *anti* conformer was found to comprise 9.8% of the sample, while the *gauche* conformer comprised 90.2% of the sample.

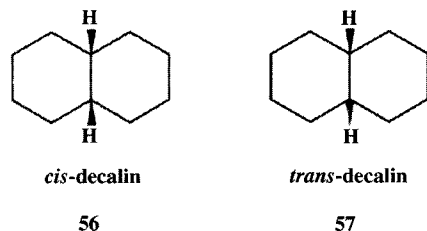
- a. Why is the anti conformer not the predominant conformer of 2-fluoroethanol?
- b. Calculate the difference in free energy between the gauche and anti conformers at 240°C.
- c. The calculated vibrational and rotational contributions to the entropies of each conformer were found to be very nearly equal. However, there are two gauche conformers (in each of which the OH group does not rotate because of hydrogen bonding), while there is one anti conformer (in which there are three potential energy minima for rotation of the OH group about the carbon–oxygen bond). Therefore, the ΔS° for conversion of the anti to the gauche conformer was determined to be $R \times (\ln 3 - \ln 2) = 0.81 \text{ cal K}^{-1} \text{ mol}^{-1}$. What is the ΔH° for conversion of the gauche conformer to the anti conformer?
- 3.9. Using the data in Table 1.7 (page 13), calculate ΔH_f° for the following compounds with molecular formula C_7H_{16} : *n*-heptane, 2-methylhexane, 3-methylhexane, 2,2-dimethylpentane, 2,3-dimethylpentane, and 3,3-dimethylpentane. Remember to include unavoidable butane gauche interactions in the calculations. Arrange the isomers in order of decreasing calculated ΔH_f° . Can you rationalize any apparent trends in this order? How do your values compare with literature values?
- 3.10. Locate a recent paper about the compounds listed below. (Some of them have been synthesized; some are still unknown.) Briefly summarize what the publications say about each of the compounds or its attempted synthesis. What types of strain would you expect to see in each of the compounds that have not yet been synthesized?

fenestrane
 twistane
 cubane
 prismane
 basketane
 tetrahedrane
 tricyclo[2.1.0.0^{1,3}]pentane

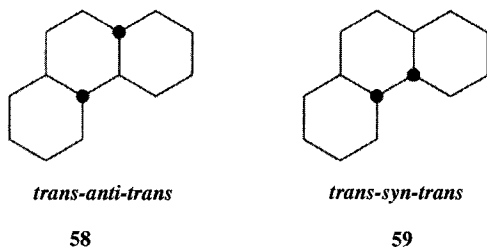
- 3.11. Tetrahedrane has not been synthesized, but the compound tetra-*t*-butyltetrahedrane has been prepared. Suggest reasons why the substituted compound has been made but the parent compound has not.
- 3.12. The heats of hydrogenation of 2,4,4-trimethyl-1-pentene and of 2,4,4-trimethyl-2-pentene are -25.5 kcal/mol and -26.8 kcal/mol , respectively. Which isomer is more stable? Is the result consistent with the common generalization that the more stable alkene isomer is the one with the greater number of alkyl substituents on the carbon–carbon double bond? If not, explain why the generalization does not offer the correct prediction in the case of these two compounds.
- 3.13. Classify each of the following conformations according to the nomenclature shown in Figure 3.3.



- 3.14. Which is more stable, the *sc* conformer of 3-(2-isopropylphenyl)-2,2,4,4-tetramethylpentan-3-ol or the *ap* conformer?
- 3.15. Predict whether *cis*- (56) or *trans*-decalin (57) should be more stable, and estimate the energy difference between them.



- 3.16. Use conformational analysis to explain why *trans-anti-trans*-perhydrophenanthrene (58) is about 5.7 kcal/mol more stable than the *trans-syn-trans* isomer (59).



- 3.17. The *A* value for the acetoxy ($-\text{O}_2\text{CCH}_3$) group at -88°C was determined to be 0.71 kcal/mol. Calculate the fraction of equatorial and axial conformers of that substituent present in cyclohexyl acetate at that temperature.
- 3.18. At -80°C the ratio of equatorial to axial cyclohexyl isocyanate was determined by NMR to be 3.74 : 1.0. Determine the *A* value for the NCO group.
- 3.19. At 40 K, the equatorial preference for alkyl substituents on cyclohexane is methyl > ethyl > isopropyl. However, the opposite trend is observed at room temperature. Explain this result.
- 3.20. ΔG for conversion of the *cis*-1-methyl-4-vinylcyclohexane conformation having the vinyl group axial to the conformation with the vinyl group equatorial is -0.06 kcal/mol. What is the *A* value for the vinyl group?
- 3.21. The ΔH° value for axial to equatorial conformational change of methylthiocyclohexane is -1.05 ± 0.09 kcal/mol. The corresponding ΔS° value is 0.48 ± 0.31 eu. What is the *A* value of the methylthio (CH_3S) group at 298 K? Is the equatorial conformer favored to a greater or lesser extent at 178 K?
- 3.22. Identify the local maxima, local minima, global maximum, and global minimum in Figure 3.13.
- 3.23. Predict the major kinds of strain present in any three of the structures in Figure 3.42.
- 3.24. In dilute CCl_4 solution, 1,2-disubstituted ethylene glycols (RCHOH-CHOHR) usually show two different O-H stretch peaks in the infrared spectrum. One peak near 3635 cm^{-1} is associated with the free OH stretch, while a peak in the region of 3585 cm^{-1} is associated with hydrogen-bonded OH stretch. The intensity of the hydrogen-bonded OH stretch varies with the stereochemistry

TABLE 3.10 Results of Molecular Mechanics Calculations on Two Conformations of Cyclobutane

Steric Energy Component	Cyclobutane Conformation A	Cyclobutane Conformation B
Stretch	0.68 kcal/mol	0.80 kcal/mol
Bend	13.47	16.24
Stretch–bend	–0.78	–0.94
Torsional	14.82	11.03
van der Waals	1.95	2.08

of the diol and the nature of the R groups. Hydrogen-bonded OH stretch is seen for the racemic diols when R = methyl, isopropyl, or *t*-butyl. For the corresponding meso diols, however, the IR absorption is strong for R = methyl, weak for R = isopropyl, and undetectable for R = *t*-butyl. Explain this result.

- 3.25. Table 3.10 shows the results of two different molecular mechanics calculations on cyclobutane.²⁴¹ In one calculation the C1–C2–C3–C4 dihedral angle was fixed at 0°, but all other parameters were optimized to obtain the lowest steric energy for the planar conformation. In the second calculation, that dihedral angle was also allowed to vary in the geometry optimization, and the final geometry of the cyclobutane ring was puckered. The results of one calculation are shown below the heading Conformation A, and the results of the other calculation are shown under the heading Conformation B. Which conformer is puckered cyclobutane and which is planar cyclobutane? Rationalize the relative magnitudes of stretch, bend, torsional, and van der Waals energies for the two conformations. (It may be helpful to use molecular models.)
- 3.26. A molecular mechanics calculation was used to identify two conformers of bicyclo[3.2.1]octane.²⁴¹ The components of steric energy for each are listed in Table 3.11.
- Which conformer, A or B, is lower in steric energy?
 - Using a set of molecular models and the energy parameters given in Table 3.11, suggest the most likely geometry for each of the two conformers.
 - Can you relate the difference in total steric energy between the two conformers to the energy difference predicted using conformational analysis for a model monocyclic compound?

TABLE 3.11 Steric Energy Parameters for Two Conformers of Bicyclo[3.2.1]octane

Steric Energy Component	Conformation A	Conformation B
Stretch	0.76 kcal/mol	0.86 kcal/mol
Bend	3.62	4.38
Stretch–bend	–0.05	–0.02
Torsional	9.70	12.55
van der Waals	5.24	6.97

- 3.27. Consider two twist boat conformations of methylcyclohexane—one in which the methyl group is in the “flagpole” position and one in which the methyl group is in the “bowsprit” position (page 124). A molecular mechanics calculation

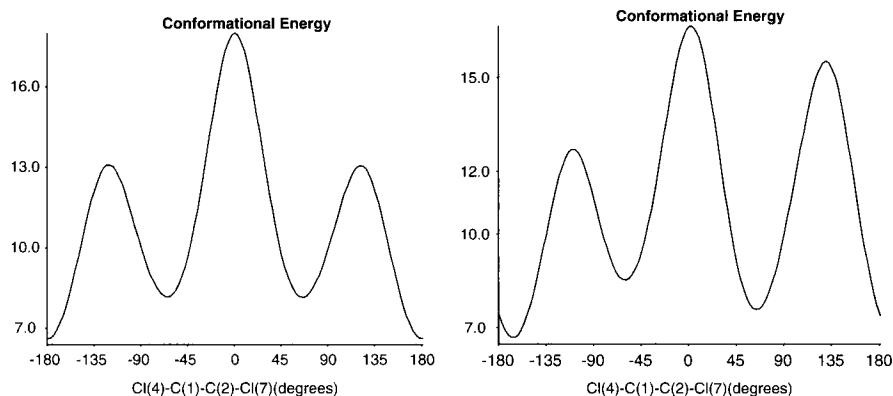
²⁴¹ The calculations were carried out with PCMODEL (Serena Software).

TABLE 3.12 Components of Steric Energy Calculated for Pentane Conformers

Steric Energy Component	Conformer A	Conformer B	Conformer C	Conformer D
Stretch	0.23	0.24	0.27	0.25
Bend	0.38	0.69	1.38	1.11
Stretch-bend	0.08	0.09	0.12	0.12
Torsion	0.01	0.47	1.83	0.79
Non-1,4-vdW	-0.62	-0.58	-0.68	-0.66
1,4-vdW	2.76	2.82	3.13	2.84

(Chem3D) indicates that conformation A has 6.6 kcal/mol of torsional strain, while conformation B has 5.5 kcal/mol of torsional strain. Which conformation is which?

- 3.28. Table 3.12 shows the results (in kcal/mol) of a Chem3D molecular mechanics calculations for four conformations of *n*-pentane. Identify each conformation as *aa*, g^+a , g^+g^- , or g^-g^- .
- 3.29. Consider a compound with a lowest energy conformation and two other accessible conformations—one of which is 0.43 kcal/mol higher in energy and another 1.79 kcal/mol higher in energy. What would be the relative population of these three conformations at 25°C?
- 3.30. A bicyclic structure is predicted by molecular mechanics calculations to have two low energy conformations—one involving a chair conformation in one portion of the structure and the other having a boat conformation instead. For one pair of vicinal hydrogens, $^3J_{\text{HH}}$ coupling constants predicted by a modified Karplus equation are 2.15 Hz for the chair conformer and 11.17 Hz for the boat conformer. The experimental *J* value is 3.90 Hz. What is the percentage of molecules that are in the chair conformation under the conditions of the NMR measurement?
- 3.31. One of the figures below shows potential energy as a function of rotation about the C2–C3 bond of *meso*-2,3-dichlorobutane, while the other figure shows a corresponding plot for one enantiomer of (2*R*,3*R*)-2,3-dichlorobutane. Which figure represents which isomer?



Applications of Molecular Orbital Theory and Valence Bond Theory

4.1 INTRODUCTION TO MOLECULAR ORBITAL THEORY

The discussions of stereochemistry and molecular mechanics in Chapters 2 and 3 were based implicitly on localized electron pair bonds. Now we will consider bonding models in which electrons are not restricted to the space between two atoms but are delocalized over a molecular structure. The approach we will consider in greatest detail is Hückel molecular orbital (HMO) theory, a simple method that nevertheless yields useful insights into structures and properties of organic compounds.^{1,2} Later we will consider some more advanced computational models.

Hückel Molecular Orbital Theory

The fundamental assumption of HMO theory is that we may calculate molecular orbitals through a process known as LCAO: the linear combination of atomic orbitals.³⁻⁵ That is, we use some combination of the wave functions of the atomic orbitals to produce a set of molecular orbitals. In the Hückel method, we combine a set of atomic p orbitals to produce a set of π molecular orbitals. For a set of n parallel p orbitals, the Hückel molecular orbitals have the form shown in equation 4.1. In this equation ψ_i is the wave function

¹ Hückel, E. *Grundzüge der Theorie ungesättigter und aromatischer Verbindungen*; Verlag Chemie: Berlin, 1938 and references therein.

² Sources for further reading include references cited below as well as (a) Flurry, R. L., Jr. *Molecular Orbital Theories of Bonding in Organic Molecules*; Marcel Dekker: New York, 1968; (b) Salem, L. *Electrons in Chemical Reactions: First Principles*; John Wiley & Sons: New York, 1982; (c) Coulson, C. A.; Streitwieser, A., Jr. *Dictionary of π -Electron Calculations*; W. H. Freeman and Co.: San Francisco, 1965; see especially reference 8; (d) Wiberg, K. B. *Physical Organic Chemistry*; John Wiley & Sons: New York, 1964; (e) Zimmerman, H. E. *Quantum Mechanics for Organic Chemists*; Academic Press: New York, 1975.

³ Coulson, C. A. *Q. Rev. Chem. Soc.* **1947**, *1*, 144.

⁴ Coulson, C. A. *J. Chem. Soc.* **1955**, 2069.

⁵ Pople, J. A. *Acc. Chem. Res.* **1970**, *3*, 217.

for the i th MO, ϕ_k is the wave function for a p orbital on the k th carbon atom, and c_n is a constant.

$$\psi_i = c_1\phi_1 + c_2\phi_2 + c_3\phi_3 + \cdots + c_k\phi_k = \sum_{\mu=1}^k c_{\mu}\phi_{\mu} \quad (4.1)$$

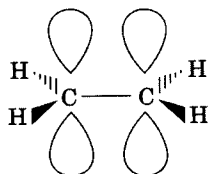


FIGURE 4.1
Relationship of p orbitals assumed in an HMO calculation for ethene.

In order to illustrate the nature and some of the limitations of the HMO procedure, we will begin with a very simple π molecular system, that of ethene. As shown in Figure 4.1, the HMO model uses the σ, π formulation for carbon-carbon double bonds.⁶ We assume that two carbon atoms are close enough to each other that a carbon-carbon σ bond can be formed through overlap of an sp^2 hybrid orbital on each. The other two sp^2 orbitals on each carbon atom are used to form C-H bonds. Each carbon atom has a remaining p orbital that is perpendicular to the plane defined by the sp^2 orbitals. It is the interaction of the two p orbitals that will produce the π molecular orbitals. Note that in HMO theory we assume that the σ and π systems may be treated separately and that the σ bonds and the π bonds do not interact.⁷ Rewriting equation 4.1 for the specific case of two p orbitals produces equation 4.2.

$$\psi_{\pi} = c_1\phi_1 + c_2\phi_2 \quad (4.2)$$

Now we use ψ_{π} in the Schrödinger equation, $\mathcal{H}\psi = E\psi$, and calculate the energies of the HMOs produced. Details of the procedure were given by Roberts, so only an outline is provided here.⁸ Multiplying both sides of $\mathcal{H}\psi = E\psi$ by ψ (or ψ^* as is appropriate), dividing by ψ^2 , and then integrating over all space in both the numerator and denominator gives equation 4.3.

$$E = \frac{\int \psi^* \mathcal{H} \psi d\tau}{\int \psi^2 d\tau} \quad (4.3)$$

We can use equation 4.3 to solve for ψ with a technique known as the **variational principle**.⁹ In essence, we assume that any wave function that we propose will underestimate the stability of a molecule. That was what we saw in the case of the MO and VB calculations of molecular hydrogen in Chapter 1, but must it always be so? A number of texts offer proofs of the variational principle,^{2d,9,10} but an intuitive approach will be sufficient here. A stable molecule has an arrangement of electrons and nuclei that represents an energy minimum. The best we can hope to do is describe that arrangement. If we propose a wave function that does not describe the most stable

⁶ The popularity of HMO theory has helped the σ, π formulation become the standard pictorial representation of double bonds. The applicability of the bent bond model to benzene was discussed by Schultz, P. A.; Messmer, R. P. *J. Am. Chem. Soc.* **1993**, *115*, 10943.

⁷ This is "an assumption that is often no more than a convenient fiction . . .": Coulson, C. A.; Stewart, E. T. in Patai, S., Ed. *The Chemistry of the Alkenes*, Vol. I.; Wiley-Interscience: London, 1964; p. 106.

⁸ Roberts, J. D. *Molecular Orbital Calculations*; W. A. Benjamin: New York, 1961.

⁹ Nesbet, R. K. *Variational Principles and Methods in Theoretical Physics and Chemistry*; Cambridge University Press: Cambridge, UK, 2003.

¹⁰ Eyring, H.; Walter, J.; Kimball, G. E. *Quantum Chemistry*; John Wiley & Sons: New York, 1944; p. 99.

arrangement of electrons, our calculation will err by predicting a higher energy.^{11,12} A mathematical statement of the variational principle is shown in equation 4.4.

$$E_{\text{calc}}(\psi_{\text{proposed}}) \geq E_{\text{calc}}(\psi_{\text{correct}}) \quad (4.4)$$

In HMO theory we assume that we know the \mathcal{H} for the system and that we know all but the coefficients c_1 and c_2 of ψ . If we minimize the energy of the wave function with respect to c_1 and c_2 by taking the partial derivatives of E with respect to c_1 and then with respect to c_2 , we will obtain the best estimate of the energy of the system that is possible with our theoretical model.

Expanding equation 4.3 by substituting $c_1\phi_1 + c_2\phi_2$ for ψ_π produces equation 4.5.

$$E = \frac{\int (c_1\phi_1 + c_2\phi_2) \mathcal{H}(c_1\phi_1 + c_2\phi_2) d\tau}{\int (c_1\phi_1 + c_2\phi_2)^2 d\tau} \quad (4.5)$$

Multiplying all of the terms in equation 4.5 produces equation 4.6.

$$E = \frac{\int (c_1\phi_1 \mathcal{H}c_1\phi_1 + c_1\phi_1 \mathcal{H}c_2\phi_2 + c_2\phi_2 \mathcal{H}c_1\phi_1 + c_2\phi_2 \mathcal{H}c_2\phi_2) d\tau}{\int (c_1^2\phi_1^2 + 2c_1c_2\phi_1\phi_2 + c_2^2\phi_2^2) d\tau} \quad (4.6)$$

Equation 4.6 can be simplified by making the following substitutions. First we note that the Hamiltonians are Hermitian (equation 4.7).¹³ Then we use the abbreviations and make the definitions shown in equations 4.8 through 4.11.

$$\int \phi_1 \mathcal{H} \phi_2 d\tau = \int \phi_2 \mathcal{H} \phi_1 d\tau \quad \text{Hermitian properties of Hamiltonian} \quad (4.7)$$

$$\int \phi_1 \mathcal{H} \phi_1 d\tau = H_{11} \quad \text{Coulomb integral (giving the energy of an electron in an isolated } p \text{ orbital)} \quad (4.8)$$

$$\int \phi_1 \mathcal{H} \phi_2 d\tau = H_{12} \quad \text{resonance integral} \quad (4.9)$$

$$\int \phi_1 \phi_1 d\tau = S_{11} \quad \text{normalization integral for identical atoms}^{14} \quad (4.10)$$

$$\int \phi_1 \phi_2 d\tau = S_{12} \quad \text{overlap integral for adjacent atoms} \quad (4.11)$$

¹¹ Applying the variational principle to obtain the best energy for a structure is often assumed to produce the best geometry and other observable properties as well, but that is not necessarily the case: Reed, L. H.; Murphy, A. R. *J. Chem. Educ.* **1986**, *63*, 757 and references therein.

¹² This argument covers only electron distribution or slight bond length or angle changes within the same structure, not isomerization to produce a different molecular structure.

¹³ Pilar, F. L. *Elementary Quantum Chemistry*; McGraw-Hill: New York, 1968; p. 71.

¹⁴ The value of this integral is unity if the wave functions are normalized.

Now we use the variational principle and set $\partial E/\partial c_1$ equal to 0 in order to determine the lowest energy that can be obtained by variation of the coefficient c_1 .

$$\frac{\partial E}{\partial c_1} = \frac{(c_1^2 S_{11} + 2c_1 c_2 S_{12} + c_2^2 S_{22})(2c_1 H_{11} + 2c_2 H_{12})}{(c_1^2 S_{11} + 2c_1 c_2 S_{12} + c_2^2 S_{22})} - \frac{(c_1^2 H_{11} + 2c_1 c_2 H_{12} + c_2^2 H_{22})(2c_1 S_{11} + 2c_2 S_{12})}{(c_1^2 S_{11} + 2c_1 c_2 S_{12} + c_2^2 S_{22})^2} = 0 \quad (4.12)$$

Rearranging terms gives equation 4.13.

$$(2c_1 H_{11} + 2c_2 H_{12}) = \frac{c_1^2 H_{11} + 2c_1 c_2 H_{12} + c_2^2 H_{22}}{(c_1^2 S_{11} + 2c_1 c_2 S_{12} + c_2^2 S_{22})} (2c_1 S_{11} + 2c_2 S_{12}) \quad (4.13)$$

Substituting E (from equation 4.5) for the fraction in equation 4.13 and then dividing both sides of the resulting equation by 2 gives equation 4.14.

$$c_1 H_{11} + c_2 H_{12} = E(c_1 S_{11} + c_2 S_{12}) \quad (4.14)$$

Rearranging the terms leads to equation 4.15.

$$c_1(H_{11} - ES_{11}) + c_2(H_{12} - ES_{12}) = 0 \quad (4.15)$$

Similarly, setting $\partial E/\partial c_2$ equal to 0 produces equation 4.16.

$$c_1(H_{21} - ES_{21}) + c_2(H_{22} - ES_{22}) = 0 \quad (4.16)$$

In these equations it is the coefficients c_1 and c_2 that we do not know—we presume that we know H_{11} , H_{12} , S_{11} , and S_{12} . Thus, we have two equations (equations 4.15 and 4.16) in two unknowns (c_1 and c_2). In order for there to be a solution for the two unknowns other than the trivial one ($c_1 = c_2 = 0$), it must be true that the secular determinant of the coefficients of the unknowns equals 0. The coefficients of the unknowns c_1 and c_2 are the terms in parentheses in equation 4.15 and equation 4.16. Thus, we have equation 4.17.

$$\begin{vmatrix} H_{11} - ES_{11} & H_{12} - ES_{12} \\ H_{21} - ES_{21} & H_{22} - ES_{22} \end{vmatrix} = 0 \quad (4.17)$$

For the more general HMO calculation (equation 4.1), the corresponding determinant is given by equation 4.18. Here k is the number of p orbitals combined, and the ellipses are place holders for one or more additional elements of the matrix.

$$\begin{vmatrix} H_{11} - ES_{11} & \cdots & H_{1k} - ES_{1k} \\ \cdots & \cdots & \cdots \\ H_{k1} - ES_{k1} & \cdots & H_{kk} - ES_{kk} \end{vmatrix} = 0 \quad (4.18)$$

Before solving the determinant in equation 4.17, we will make some simplifying assumptions and approximations. The overlap integral, S , is a measure of the degree to which two orbitals occupy the same volume of space. It is not too difficult to see the rationale for assuming that $S_{ii} \equiv 1$, since it is a property of normalized atomic orbitals that

$$\int \phi_i \phi_i d\tau = 1 \quad (4.19)$$

Now we must define the value of $\int \phi_i \phi_j d\tau$ if $i \neq j$. The overlap of two atomic orbitals on different atoms varies according to the distance between the two atomic nuclei and with the orientation of the two orbitals in space (except for spherically symmetric s orbitals). A calculation by Mulliken determined that the value of S_{ij} for two adjacent parallel p orbitals in ethene (1.34 Å apart) is 0.27, while that expected for two adjacent p orbitals in benzene (1.39 Å apart) is about 0.21.¹⁵ In general, we will not know the distance between p orbitals before starting a calculation. More important, trying to assign a value of S_{12} would make the computation more complex. Therefore, we make the obviously incorrect but very convenient assumption that $S_{ij} \equiv 0$ unless $i = j$.

H_{11} represents the energy of an electron in an isolated p orbital and is given the symbol α . Our reference system is an empty p orbital and an electron at infinite separation. If we define the energy of that reference system as 0, then the energy of the system is reduced as the electron and carbon atom approach each other. Therefore, α is a negative number.

A more difficult problem is that of H_{ij} , where $i \neq j$. There are two situations to consider. If atoms i and j are σ -bonded to each other, H_{ij} represents the extra stability of an electron brought from infinity and placed in the field of *both* nuclei. An intuitive model is that this H_{ij} is the "strength of the π -electron bond between these atoms"¹⁶ and is therefore expected to be a negative number. Since we do not have a numerical value for it now, we will use the symbol β for the value of H_{ij} when i and j are σ -bonded to each other.

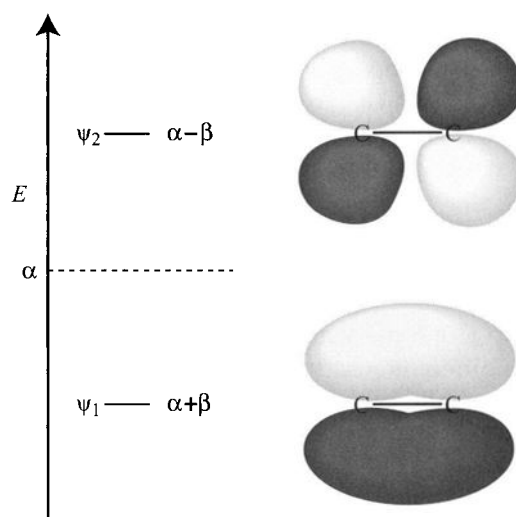
Determining the value of H_{ij} when atoms i and j are not σ -bonded to each other is more difficult. In general, atoms that are not σ -bonded are further apart than those that are bonded, and we would expect H_{ij} to be in the range from 0 to β , depending on the distance separating the two atoms and on the spatial relationship of the p orbitals involved. Here we run into the same problem we faced in evaluating the S_{ij} . Not only is it difficult to determine what value we should use, but also it will complicate the analysis if we use anything other than 0. Hence, we define $H_{ij} \equiv 0$ for all cases in which i and j are different atoms but are not σ -bonded to each other.⁸ Gutman noted that "it would be completely outdated to search for some physical justification of the above approximations," which were introduced before computers became available.¹⁷ Nevertheless, these approximations facilitate application of the HMO method.

¹⁵ Mulliken, R. S. *J. Am. Chem. Soc.* **1950**, *72*, 4493.

¹⁶ Brown, R. D. *Q. Rev. Chem. Soc.* **1952**, *6*, 63.

¹⁷ Gutman, I. *Top. Curr. Chem.* **1992**, *162*, 29.

FIGURE 4.2
Energy levels of HMOs of ethene.



Having made these assumptions, we can now rewrite the determinant in equation 4.17 as equation 4.20.

$$\begin{vmatrix} \alpha - E & \beta \\ \beta & \alpha - E \end{vmatrix} = 0 \quad (4.20)$$

Dividing through by β and representing $(\alpha - E)/\beta$ as X produces the determinant in equation 4.21.

$$\begin{vmatrix} X & 1 \\ 1 & X \end{vmatrix} = 0 \quad (4.21)$$

Solving the determinant by cross multiplication gives equation 4.22.¹⁸

$$X^2 - 1 = 0 \quad (4.22)$$

The solutions to this equation are $X=1$ and $X=-1$. Recalling that $X=(\alpha - E)/\beta$, we find that the energies of the two molecular orbitals are $E=\alpha + \beta$ and $E=\alpha - \beta$.¹⁹ We designate these two orbitals ψ_1 (having $E=\alpha + \beta$) and ψ_2 (having $E=\alpha - \beta$). Since α and β are both negative numbers, ψ_1 is a bonding orbital. That is, the energy of the π system is lower when an electron is in ψ_1 than would be the case ($E=\alpha$) if the two p orbitals did not interact. ψ_2 is an antibonding orbital because the energy of the π system is *greater* when an electron is in ψ_2 than would be the case if the two p orbitals did not interact. A schematic representation of the orbital energy levels is shown on the left in Figure 4.2.

In order to calculate the coefficients c_1 and c_2 for ψ_1 , we substitute $(\alpha + \beta)$ for E into both equations 4.15 and 4.16. Doing so generates two new

¹⁸ For this and other ways of solving determinants, see (a) reference 2e, chapters 1–3; (b) reference 2d, pp. 442–458.

¹⁹ As in the case of molecular hydrogen, combining two atomic orbitals produces two molecular orbitals—one bonding and one antibonding. To generalize, combining n atomic orbitals produces n molecular orbitals.

equations 4.23 and 4.24, and this time the unknowns really are c_1 and c_2 . Solving the equations produces the result in equation 4.25.

$$\begin{aligned} c_1(H_{11}-ES_{11}) + c_2(H_{12}-ES_{12}) &= c_1(\alpha - (\alpha + \beta)) + c_2\beta \\ &= -c_1\beta + c_2\beta = 0 \end{aligned} \quad (4.23)$$

$$c_1(H_{12}-ES_{12}) + c_2(H_{22}-ES_{22}) = c_1\beta + c_2(\alpha - (\alpha + \beta)) = c_1\beta - c_2\beta = 0 \quad (4.24)$$

$$c_1 = c_2 \equiv c \quad (4.25)$$

We know that molecular orbital wave functions must be normalized, just as atomic orbital wave functions must be. Therefore,

$$\int \psi^* \psi d\tau = 1 \quad (4.26)$$

which means that the probability of finding one electron in the molecular orbital should be calculated to be exactly 1.0. Substituting $(c\phi_1 + c\phi_2)$ for Ψ produces equation 4.27,

$$\int (c_1\phi_1 + c_2\phi_2)(c_1\phi_1 + c_2\phi_2) d\tau = 1 \quad (4.27)$$

which we can multiply through to produce equation 4.28.

$$c_1^2 \int \phi_1\phi_1 d\tau + c_2^2 \int \phi_2\phi_2 d\tau + 2c_1c_2 \int \phi_1\phi_2 d\tau = 1 \quad (4.28)$$

Ignoring the coefficients for the moment, we evaluate the integrals individually. The first integral is just the overlap integral S_{11} , which we have already defined to be 1.0. The second integral is S_{22} and is also 1.0. The third integral is the overlap of S_{12} , which we have defined to be 0. Therefore, equation 4.28 becomes

$$c_1^2 + c_2^2 = 1 \quad (4.29)$$

From equation 4.25 we know that $c_1 = c_2 = c$. Therefore, we are left with the result that

$$2c^2 = 1 \quad (4.30)$$

so

$$c = \frac{1}{\sqrt{2}} \quad (4.31)$$

An equally acceptable result is $c = -1/\sqrt{2}$. In that case all coefficients in the following discussion would be the negative of the ones shown, but bonding or antibonding interactions would be unchanged. Therefore, the physical picture of the orbital interactions, Figure 4.2, also would not be changed. Thus, ψ_1 is given by equation 4.32.

$$\psi_1 = \frac{1}{\sqrt{2}}\phi_1 + \frac{1}{\sqrt{2}}\phi_2 \quad (4.32)$$

Similarly, solving for the coefficients for the wave function having $E = \alpha - \beta$ produces

$$\psi_2 = \frac{1}{\sqrt{2}}\phi_1 - \frac{1}{\sqrt{2}}\phi_2 \quad (4.33)$$

The subscripts on the ψ terms follow the convention that the lowest energy orbital is numbered ψ_1 , with higher energy orbitals having higher numbered subscripts. The MOs ψ_1 and ψ_2 are the familiar π and π^* orbitals, so ψ_1 may be called π , and ψ_2 may be called π^* .

The physical meaning of ψ_1 is that the p orbitals on carbon atoms 1 and 2 combine to produce a molecular orbital with electron density over both carbon atoms. The shading of this wave function in Figure 4.2 indicates that it has a positive mathematical sign above the plane of the molecule and a negative mathematical sign of the wave function below the plane of the molecule. The bonding combination is thus formed by taking the combination of two p orbitals with the positive sign of the wave function in the same region of space (as indicated by the fact that both c_1 and c_2 are positive numbers in equation 4.32). Hence, ψ_1 is a *bonding orbital*.

In equation 4.33, on the other hand, c_1 has a positive sign and c_2 has a negative sign. This means that the mathematical sign is positive for the top lobe of the p orbital ϕ_1 but is negative for the top lobe of the p orbital ϕ_2 . The physical meaning of such an interaction is that one orbital cancels the other in the region of space between the two carbon atoms. This interference produces zero electron density in a plane perpendicular to the molecular plane and midway between the two carbon atoms. In other words, for ψ_2 there is a node between C1 and C2. Since the electrons in ψ_2 are not likely to be found between the two carbon nuclei, they cannot provide a force of attraction to overcome the nucleus-nucleus repulsion. Therefore, ψ_2 is an *antibonding orbital*, because electrons in this orbital produce molecular instability.

Now let us determine the HMOs of an allyl system by considering the combination of three parallel p orbitals (Figure 4.3). It does not matter whether we are interested in the allyl cation or the radical or the anion. In HMO theory the molecular orbitals are calculated on the basis of the number of p orbitals in the π system, not the number of electrons. We presume that we can determine the HMOs for the assembled nuclei and then add the electrons later.

Combining three p orbitals should produce three molecular orbitals, and the general format of each HMO should be

$$\psi = c_1\phi_1 + c_2\phi_2 + c_3\phi_3 \quad (4.34)$$

Fortunately, we do not have to go back to equation 4.1, make substitutions, take partial derivatives, and so on. Instead, we proceed directly to the secular determinant (equation 4.18). Thus, the determinant for allyl is shown in equation 4.35.

$$\begin{vmatrix} X & 1 & 0 \\ 1 & X & 1 \\ 0 & 1 & X \end{vmatrix} = 0 \quad (4.35)$$

It may be helpful to point out some features of this determinant that will be seen in other cases. The i th element of the determinant (the term in the i th

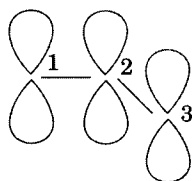
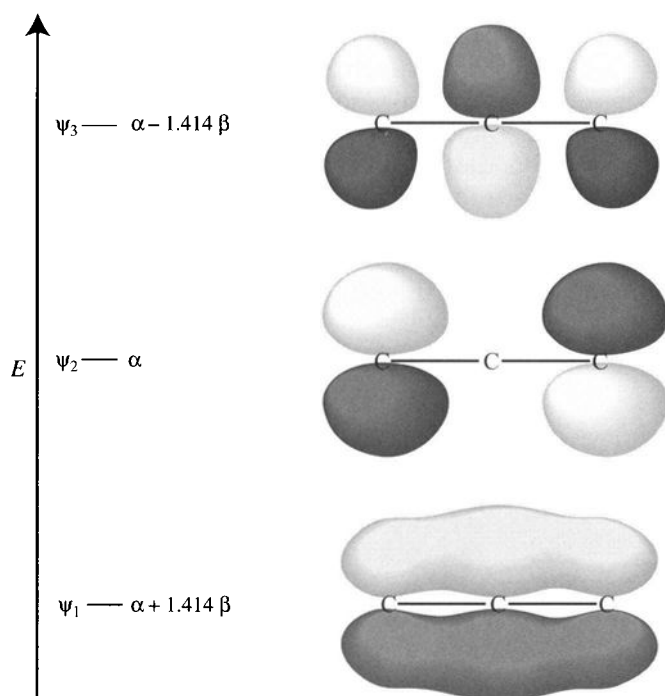


FIGURE 4.3
Basis set atomic orbitals for the allyl system.

**FIGURE 4.4**

Energy levels for allyl molecular orbitals.

column and i th row, i.e., on the diagonal from top left to bottom right) is X if the i th carbon atom has a p orbital participating in the π bonding. The ij th element of the determinant is 1 if C_i and C_j are σ -bonded to each other and 0 if they are not. That is a direct result of the assumptions about the overlap integrals and resonance integrals that we made on page 179.

We can now solve the determinant, which produces the equation

$$X^3 - 2X = 0 \quad (4.36)$$

Rearranging the terms on the left side of the equation produces

$$X(X - \sqrt{2})(X + \sqrt{2}) = 0 \quad (4.37)$$

So the three solutions are

$$X = 0, \pm \sqrt{2} \quad (4.38)$$

Again, $X = (\alpha - E)/\beta$. Therefore, the three molecular orbitals include an orbital (ψ_1) with energy of $\alpha + 1.414 \beta$ and an orbital (ψ_3) with energy $\alpha - 1.414 \beta$, as shown in Figure 4.4. ψ_1 is a bonding orbital, and ψ_3 is an antibonding orbital. The solution $X = 0$ produces a molecular orbital (ψ_2) with $E = \alpha$. The energy change associated with bringing an electron from a great distance and placing it into ψ_2 is the same as the energy change for bringing an electron from a great distance and placing it into an isolated p orbital. Adding an electron to that orbital thus does not increase the bonding energy of the π system, nor does it decrease it. Hence, ψ_2 is a *nonbonding* molecular orbital (NBMO).

We can determine the coefficients for each of the three molecular orbitals as before. The results are given in equations 4.39 – 4.41 and are shown

schematically in Figure 4.4. We see that these orbitals have electron density over the entire π system and thus are true molecular orbitals. Notice that there are no nodes in ψ_1 , one node in ψ_2 , and two nodes in ψ_3 . Now it is easy to see why ψ_2 is nonbonding. There is a node through C2, so electron density in ψ_2 cannot contribute to bonding between C1 and C2 nor between C2 and C3, but neither can an electron in that orbital contribute to any antibonding relationships. On the other hand, ψ_1 allows an electron to roam over all three carbon atoms in a bonding relationship. ψ_3 also allows electron movement over the entire molecule, but all interactions are antibonding.

$$\psi_3 = \frac{1}{2}\phi_1 - \frac{\sqrt{2}}{2}\phi_2 + \frac{1}{2}\phi_3 \quad (4.39)$$

$$\psi_2 = \frac{\sqrt{2}}{2}\phi_1 - \frac{\sqrt{2}}{2}\phi_3 \quad (4.40)$$

$$\psi_3 = \frac{1}{2}\phi_1 + \frac{\sqrt{2}}{2}\phi_2 + \frac{1}{2}\phi_3 \quad (4.41)$$

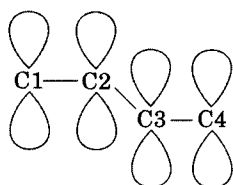


FIGURE 4.5
The butadiene system.

We will use the HMOs of the allyl system later, but let us first generate the HMOs of some larger systems. 1,3-Butadiene has four sp^2 -hybridized carbon atoms, which we may number as shown in Figure 4.5. Now the secular determinant can be written "by inspection" as shown in equation 4.42.

$$\begin{vmatrix} X & 1 & 0 & 0 \\ 1 & X & 1 & 0 \\ 0 & 1 & X & 1 \\ 0 & 0 & 1 & X \end{vmatrix} = 0 \quad (4.42)$$

The solution to the determinant is

$$X^4 - 3X^2 + 1 = 0 \quad (4.43)$$

from which we can obtain the solutions for X and the molecular orbital energy levels shown in Figure 4.6. From these energy levels, we may determine the coefficients of the MOs, thus producing the MOs shown in equations 4.44–4.47.

$$\psi_4 = 0.372\phi_1 - 0.602\phi_2 + 0.602\phi_3 - 0.372\phi_4 \quad (4.44)$$

$$\psi_3 = 0.602\phi_1 - 0.372\phi_2 - 0.372\phi_3 + 0.602\phi_4 \quad (4.45)$$

$$\psi_2 = 0.602\phi_1 + 0.372\phi_2 - 0.372\phi_3 - 0.602\phi_4 \quad (4.46)$$

$$\psi_1 = 0.372\phi_1 + 0.602\phi_2 + 0.602\phi_3 + 0.372\phi_4 \quad (4.47)$$

Note that the magnitude of the coefficients for ϕ_1 and ϕ_4 are the same in all the orbitals, as are the magnitudes of the coefficients for ϕ_2 and ϕ_3 in all four cases. This result must occur because of molecular symmetry: it should not matter whether we call the carbon atom on the left C1 or whether we start numbering from the right. As long as the two end carbon atoms have the same magnitude for the coefficient of a particular orbital, the bonding energies and other parameters we will calculate will be found to be the same, no matter which end of the molecule we start from when writing the determinant.

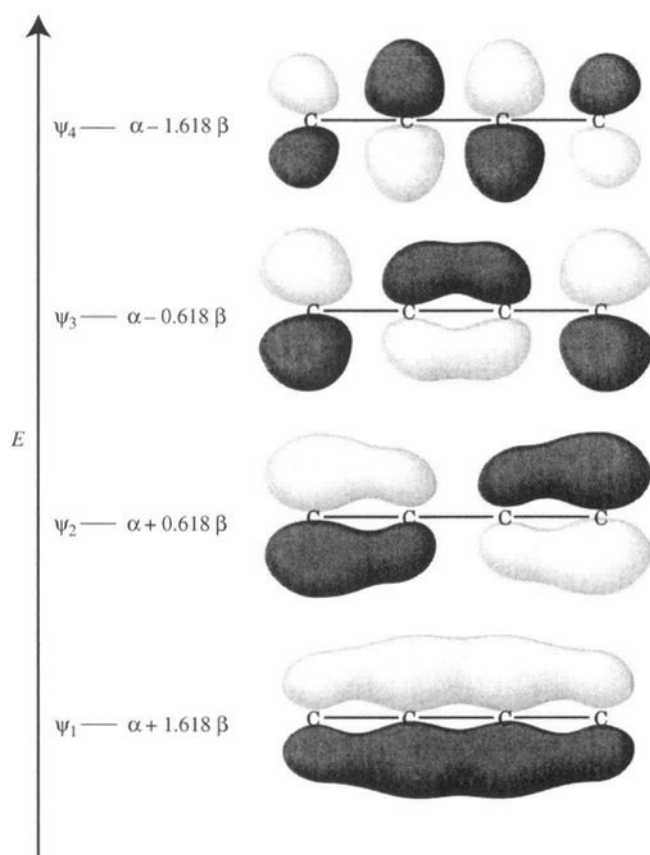
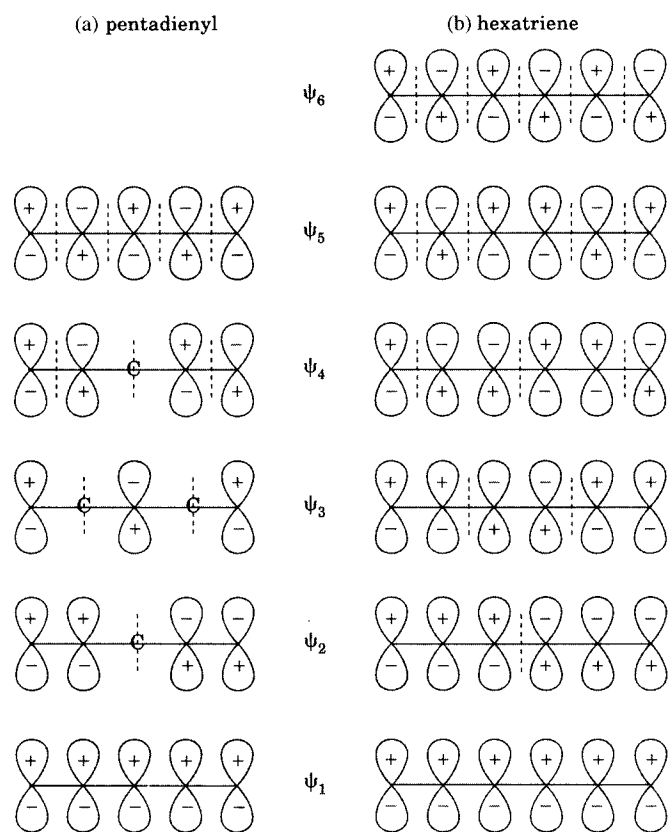


FIGURE 4.6
Orbitals and energy levels of
1,3-butadiene.

Figure 4.6 illustrates several other principles of Hückel molecular orbitals. The pattern of nodes is the same as in the case of the allyl system: 0 nodes in ψ_1 , one node in ψ_2 , and two nodes in ψ_3 . Continuing the pattern, there are three nodes in ψ_4 . This leads to the generalization that, for *linear* π systems, we will always see $n - 1$ nodes in ψ_n . Notice also that the bonding and antibonding orbitals are symmetrically placed above and below the nonbonding ($E = \alpha$) level. That is a general result for linear π systems with an even number of carbon atoms. For a linear π system with an odd number of p orbitals (such as in Figure 4.4), one orbital will have $E = \alpha$, and the rest of the orbitals will be displaced symmetrically above and below this orbital on an energy diagram.

It is the regularity of these features of molecular orbitals that makes them so useful to us in predicting molecular properties. Without actually doing the calculations, we can predict that the general pattern of the MOs for the pentadienyl system will be as shown in Figure 4.7(a), with two bonding MOs, one nonbonding MO, and two antibonding MOs. Similarly, we can predict that the MOs of hexatriene, Figure 4.7(b), will have three bonding and three antibonding MOs. In each case ψ_n has $n - 1$ nodes. It is important to note that Figure 4.7 shows not the actual molecular orbitals for the structure but only p orbital shapes that suggest the overlap pattern for each MO. Specifically, all of the p orbitals are drawn the same size no matter what the actual coefficients are for a particular MO. We infer the bonding and antibonding relationships from the mathematical signs on adjacent p orbital lobes or nonbonding

**FIGURE 4.7**

Qualitative representation of the molecular orbitals for linear π systems: (a) pentadienyl and (b) hexatriene. (Adapted from reference 8.)

interactions where there is a node (no p orbital shown on a carbon atom) between two p orbital shapes.

The HMO method produces different patterns of energy levels for cyclic π systems. For example, writing the 6×6 determinant for benzene gives equation 4.48. Note the 1 in the upper *right* corner and the lower *left* corner of the determinant, which results from the fact that C1 and C6 are σ -bonded.

$$\begin{vmatrix} X & 1 & 0 & 0 & 0 & 1 \\ 1 & X & 1 & 0 & 0 & 0 \\ 0 & 1 & X & 1 & 0 & 0 \\ 0 & 0 & 1 & X & 1 & 0 \\ 0 & 0 & 0 & 1 & X & 1 \\ 1 & 0 & 0 & 0 & 1 & X \end{vmatrix} = 0 \quad (4.48)$$

Solving the determinant for X and finding the energy levels for the six molecular orbitals gives the energy level diagram in Figure 4.8. Now we find a bonding orbital at $\alpha + 2\beta$, two bonding orbitals at $\alpha + \beta$,²⁰ two bonding orbitals at $\alpha - \beta$, and an antibonding orbital at $\alpha - 2\beta$. The shapes of the MOs are shown in Figure 4.9.

²⁰ Molecular orbitals having the same energy are said to be *degenerate*.

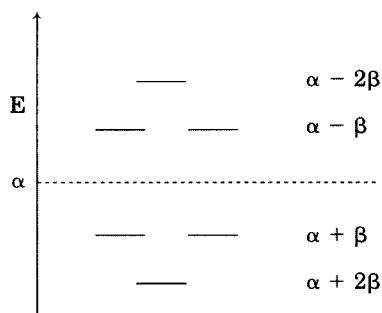


FIGURE 4.8
Benzene HMO energy levels.

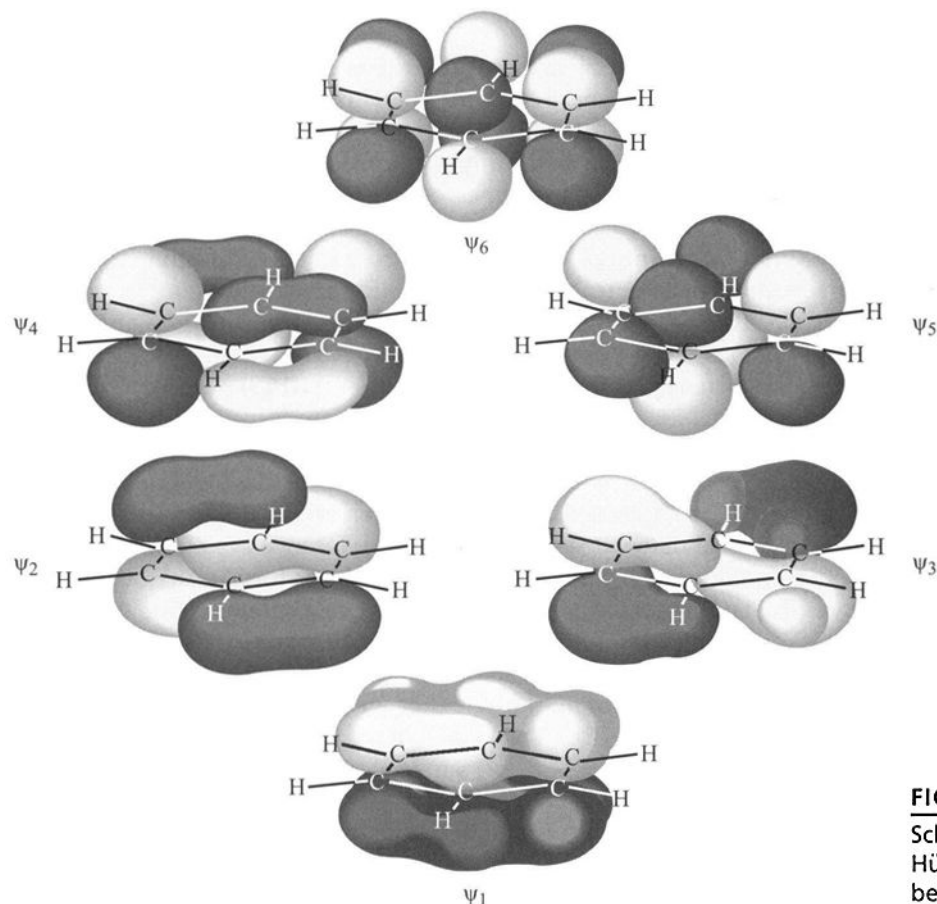


FIGURE 4.9
Schematic representation of Hückel molecular orbitals of benzene.

Correlation of Physical Properties with Results of HMO Calculations

So far we have considered only the energies of individual molecular orbitals. In order to determine the energy of a particular structure, we must take into account the number of electrons in each of those MOs. If electrons are placed into the molecular orbitals according to the aufbau principle, the first two electrons go into the lowest energy orbital, the next two electrons go into in the next lowest energy orbital, and so forth. In the case of ethene, there are two

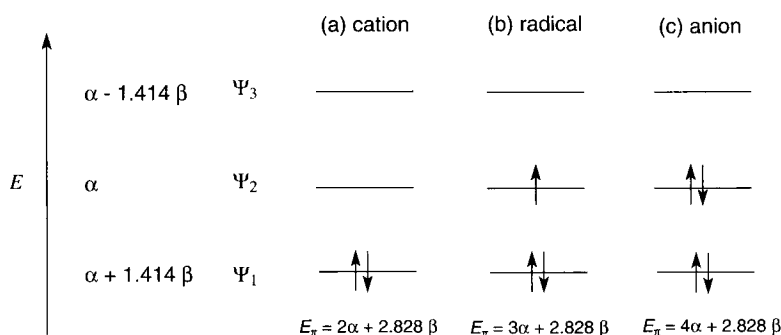


FIGURE 4.10
Electron population of HMOs in the allyl system: (a) cation, (b) radical, and (c) anion.

electrons in the π system (unless the structure has a charge). Both electrons can go into the orbital with energy $E = \alpha + \beta$. Therefore, the energy of the π system (E_π) is $2(\alpha + \beta) = 2\alpha + 2\beta$.

The number of electrons in the allyl system depends on the charge on the structure. The allyl cation has the same number of π electrons as a double bond and an empty p orbital. Thus, there are two electrons in the π HMOs of the allyl cation, so both can go into ψ_1 , as shown in Figure 4.10(a). The allyl radical has the same number of π electrons as a double bond and a methyl radical, so there are three electrons in the π system, as shown in Figure 4.10(b). The allyl anion has four electrons, so they are placed into the π HMOs as shown in Figure 4.10(c). Thus, the π energy of the allyl cation is $2(\alpha + 1.414\beta) = 2\alpha + 2.828\beta$. For the allyl radical it is $2\alpha + 2.828\beta$ (from the two electrons in ψ_1) plus α (from the one electron in ψ_2), so $E_\pi = 3\alpha + 2.828\beta$. Similarly, E_π for the allyl anion is $4\alpha + 2.828\beta$.

The actual E_π of a particular system is often not as informative as is the comparison of the delocalized system with a reference system having localized orbitals. Figure 4.11 shows the reference system for allyl: a double bond separated by an imaginary barrier from a p orbital that may have 0 (cation), 1 (radical), or 2 (anion) electrons.²¹ The molecular orbital description of that system, then, is simply a sum of the HMOs of the double bond and of the p orbital. Again, it does not matter whether we are talking about the cation, radical, or anion in Figure 4.11. The HMOs of the reference system are simply those of ethene ($E = \alpha + \beta$, $E = \alpha - \beta$) superimposed on the one HMO for an isolated p orbital ($E = \alpha$).

Putting electrons into the orbitals of the reference system according to the aufbau principle, we calculate that the E_π values of the reference *localized* cation, radical, and anion are $2\alpha + 2\beta$, $3\alpha + 2\beta$, and $4\alpha + 2\beta$, respectively (Figure 4.12). The difference in E_π between the delocalized system and the reference localized system is the **delocalization energy** (DE_π) of the structure. For the allyl cation, DE_π is $(2\alpha + 2.828\beta) - (2\alpha + 2\beta) = 0.828\beta$. Similarly, DE_π for the radical is $(3\alpha + 2.828\beta) - (3\alpha + 2\beta) = 0.828\beta$, and for the anion the delocalization energy is $(4\alpha + 2.828\beta) - (4\alpha + 2\beta) = 0.828\beta$. Therefore, each

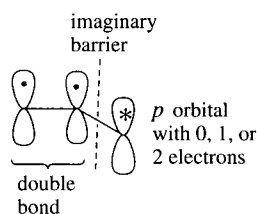
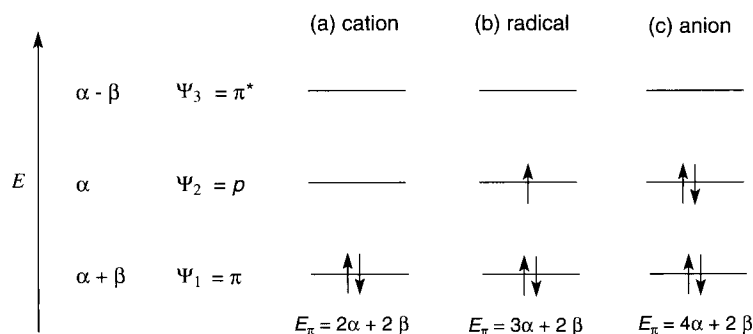
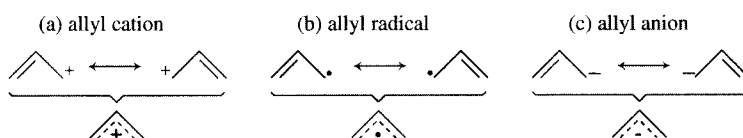


FIGURE 4.11
Reference system for allylic delocalization. (Adapted from reference 2e.)

²¹ A chemical structure in which one p orbital is perpendicular (and therefore orthogonal) to the p orbitals in the double bond, or one in which there is an insulating tetravalent carbon atom between the p orbital and the double bond, would have the same HMOs as does the reference system here.

**FIGURE 4.12**

Molecular orbitals for the allyl reference system shown in Figure 4.11.

**FIGURE 4.13**

Resonance structures (top) and resonance hybrid (bottom) for (a) allyl cation, (b) allyl radical, and (c) allyl anion.

of the three delocalized allylic species is predicted to be more stable than the reference localized systems with the same charge by 0.828β .²²

An alternative description of allyl species is provided by the concept of resonance, in which the best description of a structure is considered to be the resonance hybrid of two or more classical valence bond structures.^{23,24} For example, in Figure 4.13 the resonance hybrids of the allyl cation, radical, and anion are each shown as the average of a pair of contributing resonance structures. In each case the resonance hybrid is lower in energy than either one of the contributing resonance structures by an amount known as the resonance energy. Resonance energy is derived from valence bond theory, and delocalization energy is derived from molecular orbital theory. We recognize that they have the same conceptual basis, however, which is the extra stability of systems in which electrons are not localized between pairs of atoms.

Let us consider another correlation of HMO results with physical properties. As noted in Chapter 3, conjugated dienes such as 1,3-butadiene exhibit two main conformational minima for rotation about the C2–C3 bond, the *s-cis* conformation and the *s-trans* conformation. Figure 4.14 shows that rotation about the C2–C3 bond involves a transition state in which the *p* orbitals in the C1–C2 π system are perpendicular to the *p* orbitals in the C3–C4 π system. In that conformation the two π systems are orthogonal and therefore non-interacting. Thus, the HMOs in the transition structure are effectively those of two independent ethene systems, so the E_π of the transition structure is

²² Although the one electron in ψ_2 does not contribute to bonding in the radical, the two electrons in ψ_1 produce bonding that causes the radical to be planar. Electron diffraction measurements on the radical indicated a planar structure with C–C bond length of $1.428 \text{ \AA} \pm 0.013 \text{ \AA}$ and a C–C–C bond angle of $124.6 \pm 3.4^\circ$. Vajda, E.; Tremmel, J.; Rozsondai, B.; Hargittai, I.; Maltsev, A. K.; Kagramanov, N. D.; Nefedov, O. M. *J. Am. Chem. Soc.* **1986**, *108*, 4352. For a theoretical study of allyl species, see Gobbi, A.; Frenking, G. *J. Am. Chem. Soc.* **1994**, *116*, 9275 and references therein; Mo, Y. *J. Org. Chem.* **2004**, *69*, 5563; Linares, M.; Braida, B.; Humbel, S. *J. Phys. Chem. A* **2006**, *110*, 2505.

²³ Wheland, G. W. *Resonance in Organic Chemistry*; John Wiley & Sons: New York, 1955.

²⁴ Coulson, C. A. *Endeavour* **1947**, *6*, 42.

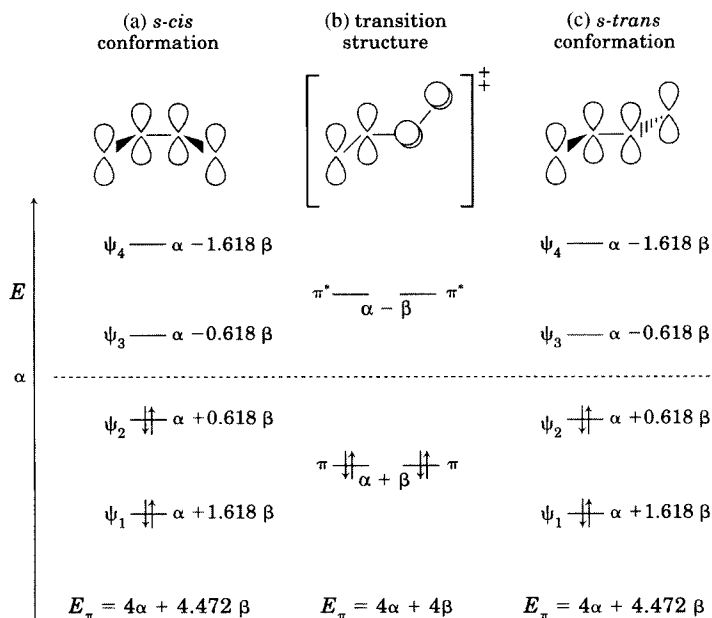


FIGURE 4.14
HMOs for 1,3-butadiene conformational change.

$2(2\alpha + 2\beta) = 4\alpha + 4\beta$. The E_π of planar 1,3-butadiene is $4\alpha + 4.472\beta$, so the *s-cis* to *s-trans* conversion should have an electronic energy barrier of 0.472β .

We have calculated that the rotation barrier for 1,3-butadiene is 0.472β , but what is β ? The value that appears most frequently in the literature is based on thermochemical data for benzene, which is considered to be the prototypical aromatic compound. With the six π electrons in the three bonding MOs shown in Figure 4.8, the value of E_π is $6\alpha + 8\beta$. A system of three noninteracting double bonds would have an energy of $3(2\alpha + 2\beta) = 6\alpha + 6\beta$. Therefore, the delocalization energy of benzene is 2β . If we equate this value to the commonly cited value for the resonance energy of benzene, 36 kcal/mol,²⁵ then β is 18 kcal/mol. Using this value means that the electronic barrier to rotation about C2–C3 in 1,3-butadiene should be about 8 kcal/mol. This is about twice the 3.7 kcal/mol conjugative stabilization of 1,3-butadiene estimated by Kistiakowsky on the basis of heat of hydrogenation data²⁶ and is also larger than the 5.7 kcal/mol calculated by Feller et al.²⁷ However, it is very close to the 8.2 kcal/mol value reported by Jarowski et al.²⁸ The HMO prediction may seem reasonably accurate, but that should not be regarded as a validation of the HMO method. Rather, this is likely to be the result of fortuitous cancellation of errors in the HMO calculation. An obvious fault in the HMO calculation is the set of approximations (e.g., $S_{ij} = 0$ unless $i = j$) inherent in the method. In addition, the schematic representation of the conformational change in Figure 4.14 ignores changes in bond angles and

²⁵ The value of 36 kcal/mol is not universally accepted; see the discussion on page 204.

²⁶ Kistiakowsky, G. B.; Ruhoff, J. R.; Smith, H. A.; Vaughan, W. E. *J. Am. Chem. Soc.* **1936**, *58*, 137, 146. See also the discussion in reference 28.

²⁷ Feller, D.; Craig, N. C.; Matlin, A. R. *J. Phys. Chem. A* **2008**, *112*, 2131.

²⁸ Jarowski, P. D.; Wodrich, M. D.; Wannere, C. S.; Schleyer, P. v. R.; Houk, K. N. *J. Am. Chem. Soc.* **2004**, *126*, 15036. This analysis took into account the effect of hyperconjugation on the ΔH values determined by Kistiakowsky. See also Cappel, D.; Tüllmann, S.; Krapp, A.; Frenking, G. *Angew. Chem. Int. Ed.* **2005**, *44*, 3617.

bond lengths that may occur during the rotation, and these bonding changes will also affect the transition state energy.

Another possible source of error in the rotational barrier predicted from the HMO calculation serves as a reminder of the inherent limitations of HMO theory. Specifically, the calculation here assumed a set of four p orbitals, each of which was capable of interacting equally with one or two p orbitals beside it. In fact, the C1–C2 bond length of 1,3-butadiene (1.3305 Å) is shorter than the C2–C3 bond length (1.454 Å).²⁹ Thus, the interaction of the p orbital on C2 with that on C3 is less than that with the p orbital on C1, so H_{23} is not equal to H_{12} . Still, Craig and co-workers determined that the C1–C2 bond is 0.016 Å longer and the C2–C3 bond is 0.007 Å shorter than the bond lengths that would be expected for a completely localized system (having noninteracting double bonds).²⁹ Thus, the π electrons do appear to be delocalized over the molecule to some extent.

Other Parameters Generated Through HMO Theory

Even though HMO theory cannot be relied upon for quantitatively correct predictions for some physical properties, it nevertheless provides a convenient framework for the development of a number of useful concepts in molecular bonding and reactivity. Among these are π electron density, charge density, bond order, and free valence. We calculate the **electron density** (ρ_i) at each atom by summing the electron density at that atom for each occupied molecular orbital. We have defined ψ_i in equation 4.1:

$$\psi_i = c_1\phi_1 + c_2\phi_2 + c_3\phi_3 + \cdots + c_k\phi_k = \sum_{\mu=1}^k c_{\mu}\phi_{\mu} \quad (4.1)$$

Again, the wave functions must be normalized. Solving equation 4.26 and taking the cross terms equal to 0³⁰ gives

$$c_1^2 \left[\int \phi_1\phi_1 d\tau \right] + c_2^2 \left[\int \phi_2\phi_2 d\tau \right] + \cdots + c_k^2 \left[\int \phi_k\phi_k d\tau \right] = 1 \quad (4.49)$$

Since the integrals in square brackets are unity (see equation 4.10), the sum of the squares of the coefficients for each MO must equal 1. That is,

$$c_1^2 + c_2^2 + \cdots + c_k^2 = 1 \quad (4.50)$$

Therefore, the square of the coefficient for ϕ_i in each wave function indicates the fraction of electron density to be found at the i th carbon atom when there is *one* electron in that ψ . If there are *two* electrons in a particular MO, then the electron density from that MO at the i th carbon atom is $2c_i^2$. To calculate the total electron density at a particular carbon atom, we must sum the electron density at that position in each of the MOs. The general expression for electron density at the i th position is then

$$\rho_i = \sum_{\text{occupied } \psi} n c_i^2 \quad (4.51)$$

²⁹ Craig, N. C.; Groner, P.; McKean, D. C. *J. Phys. Chem. A* **2006**, *110*, 7461.

³⁰ A *cross term* is the integral $\int \phi_j\phi_k d\tau$ for $j \neq k$.

TABLE 4.1 HMO Charge Densities for Allyl Cation, Radical, and Anion

Carbon Atom	Cation	Radical	Anion
1	$+\frac{1}{2}$	0	$-\frac{1}{2}$
2	0	0	0
3	$+\frac{1}{2}$	0	$-\frac{1}{2}$

where n is the number of electrons in each ψ . That is, ρ_i is equal to the sum of the squares of the coefficients at the i th carbon atom in each occupied orbital multiplied by the number of electrons in that orbital.

As an example of electron density calculations, consider again the allyl system (Figure 4.4). For the cation, there is electron density only in ψ_1 . The coefficient for ϕ_1 in ψ_1 is $\frac{1}{2}$, and there are two electrons in that MO. Thus, the electron density for C1 in the allyl cation is $\rho_1 = 2(\frac{1}{2})^2 = \frac{1}{2}$. The density is the same at C3, as we would expect from the symmetry of the molecule. The density at C2 is $2(1/\sqrt{2})^2 = 1$. For the allyl radical, there are two electrons in ψ_1 and one electron in ψ_2 , so the electron density on C1 is $2(\frac{1}{2})^2 + (1/\sqrt{2})^2 = 1$. The electron densities on C2 and C3 are also calculated to be 1. For the anion the electron densities on the three carbon atoms are $1\frac{1}{2}$, 1, and $1\frac{1}{2}$, respectively.

Electron densities allow us to calculate charge densities. The **charge density** on the i th atom (denoted q_i) is defined as³¹

$$q_i = 1 - \rho_i \quad (4.52)$$

An example will rationalize this relationship. In ethene, there are two electrons in the π bond, and by symmetry they must be distributed equally between the two carbon atoms. Since the molecule is electrically neutral, each carbon atom must also be electrically neutral,³² so $q_i = 0$. Since $\rho_i = 1$ and $q_i = 0$, equation 4.52 holds.

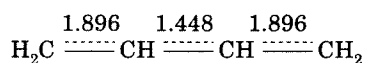
Equation 4.52 can be used to calculate the charge density for each position of the allyl cation, radical, and anion, and the results are shown in Table 4.1. These values are comforting, because they agree with our chemical experience with allylic systems. The resonance description of the allyl cation and radical (Figure 4.13) suggests that exactly half of the charge or unpaired electron density is associated with each of the terminal carbon atoms, and the HMO result is the same.

Bond order is the calculated amount of bonding between two atoms.³³ Since there is usually a σ bond between the same pair of atoms, we are most often interested in the π **bond order**, sometimes called mobile bond order. As in earlier examples (e.g., allyl, 1,3-butadiene), a pair of atoms may have the same sign for their atomic orbital coefficients (therefore a bonding relationship) for one molecular orbital but a different sign for their coefficients (thus

³¹ Wheland, G. W.; Pauling, L. J. *Am. Chem. Soc.* **1935**, *57*, 2086.

³² This statement is rigorously true only for HMO theory, which does not consider the possibility of charge on the carbon atoms arising due to opposite charge on the hydrogen atoms, because the hydrogen atoms are considered not to be involved in the π system.

³³ The concept of bond order was introduced by Coulson, C. A. *Proc. R. Soc. (London)* **1939**, *A169*, 413. Carbon-carbon bond lengths correlate with bond orders; see Jug, K. J. *Am. Chem. Soc.* **1977**, *99*, 7800. For further discussion of bond order and related parameters, see Sannigrahi, A. B.; Kar, T. J. *Chem. Educ.* **1988**, *64*, 674.

**FIGURE 4.15**

Total bond order for 1,3-butadiene C-C bonds.

an antibonding relationship) for a different molecular orbital. Bond order calculations simply sum the contributions to bonding between each pair of atoms over all the occupied molecular orbitals.

$$P_{ij} = \sum_{\text{occupied } \psi} n c_i c_j \quad (4.53)$$

Here P_{ij} is the π bond order between atoms i and j , n is the number of electrons in a particular MO, and c_i and c_j are the coefficients for the i th and j th carbon atoms, respectively, for that MO. If we consider 1,3-butadiene (Figure 4.6) we may calculate

$$P_{12} = \underset{\dots \dots \text{(from } \psi_1) \dots \dots}{2(0.372)(0.602)} + \underset{\dots \dots \text{(from } \psi_2) \dots \dots}{2(0.602)(0.372)} = 0.896 \quad (4.54)$$

$$P_{23} = \underset{\dots \dots \text{(from } \psi_1) \dots \dots}{2(0.602)(0.602)} + \underset{\dots \dots \text{(from } \psi_2) \dots \dots}{2(-0.372)(0.372)} = 0.448 \quad (4.55)$$

These values indicate that there is about 90% of a π bond between carbon atoms 1 and 2 and about 45% of a π bond between carbon atoms 2 and 3. By symmetry we also know $P_{34} = P_{12}$. These P values are for just the π bond order. If we add the σ bond between each of the carbon atoms, then the **total bond order** is the number indicated above the dotted lines in Figure 4.15.

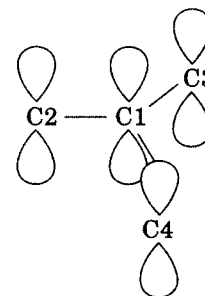
Calculating bond order allows us to determine one more property of π systems that will be useful in correlating the results of HMO theory with chemical experience. We would like to have a measure of the reactivity of each carbon atom in a π system. We define the parameter **free valence**, \mathcal{F}_i , as the difference between the maximum possible bond order of an atom and the actual total bond order.³⁴ What is the maximum possible bonding power of an atom? It would be difficult to imagine an sp^2 -hybridized carbon atom being more strongly bonded than C1 in the trimethylenemethyl system (Figure 4.16).

Calculation of the HMOs of that system shows that P_{12} , P_{13} , and P_{14} each have the value $\sqrt{3}/3$, so the total π bond order to C1 is $3(\sqrt{3}/3) = 1.732$. Since C1 also has three σ bonds, its total bond order is 4.732. Therefore, we define

$$\mathcal{F}_i = 4.732 - \sum_{\psi_{\text{occupied } j}} P_{ij} \quad (4.56)$$

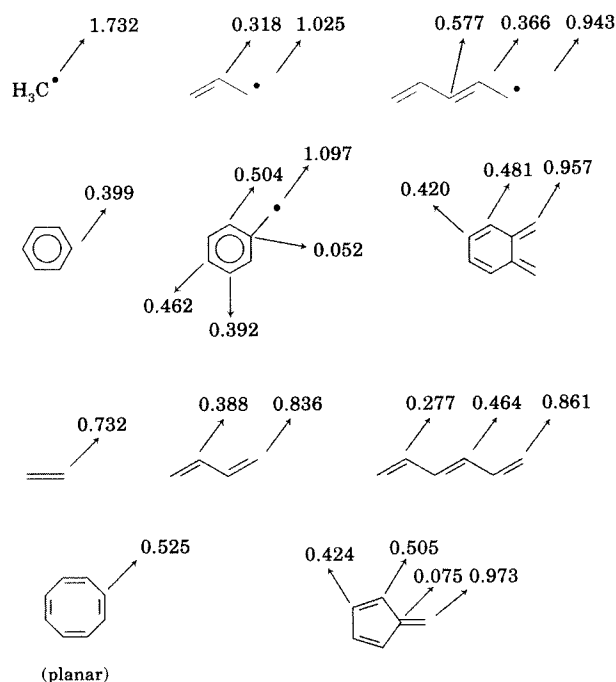
where P_{ij} includes σ bond order (usually 3) as well as π bond order. A free valence index of 1 or more is usually associated with high chemical reactivity.

As an example, let us calculate \mathcal{F}_1 , the free valence index for C1 of butadiene. P_{12} for butadiene is 0.896 (equation 4.54). The σ bond order is 3 (due to two σ bonds to hydrogen atoms and one σ bond to a carbon atom),

**FIGURE 4.16**

The trimethylenemethyl system.

³⁴ Coulson, C. A. *Trans. Faraday Soc.* **1946**, *42*, 265; Coulson, C. A. *Faraday Soc. Discuss.* **1947**, *2*, 9; Coulson, C. A. *J. Chim. phys.* **1948**, *45*, 243; Burkitt, F. H.; Coulson, C. A.; Longuet-Higgins, H. C. *Trans. Faraday Soc.* **1951**, *47*, 553.

**FIGURE 4.17**

\mathcal{F}_i values for unique positions in selected structures.

so the total bond order is 3.896. Subtracting 3.896 from 4.732 gives an \mathcal{F}_1 of 0.836. We represent \mathcal{F}_i as a number written at the end of an arrow drawn from a particular carbon atom. Figure 4.17 shows \mathcal{F}_i values for butadiene and for several other interesting structures.

Properties of Odd Alternant Hydrocarbons

For very large molecules, it is not trivial to produce the molecular orbital wave functions needed to calculate electron and charge densities, bond orders, and free valence indices without using a computer. Moreover, often our goal is to obtain the *results* of HMO calculations in order to solve chemical problems, not just to solve mathematical equations. It is more than legend to say that “back of the envelope” calculations or “napkin” calculations done during lunch may be the most stimulating to some chemists. Thus, many organic chemists are well served by methods that produce useful results from MO theory without requiring the actual calculations. Fortunately, there are shortcuts that greatly facilitate the use of HMO theory in this way.

We begin by defining two types of structures. A molecule is said to be **alternant** if every other π center can be “starred” with no stars adjacent to each other.^{35–38} It is **nonalternant** if two starred or two nonstarred positions must be adjacent. All linear structures are alternant, whether they have an even or odd number of π centers. All even-membered rings are alternant, but all odd-membered rings are nonalternant. Some bicyclic systems are alter-

³⁵ A π center is an atom that contributes a p orbital to the set of orbitals used in an HMO calculation.

³⁶ Coulson, C. A.; Longuet-Higgins, H. C. *Proc. R. Soc. (London)* **1947**, A192, 16.

³⁷ Longuet-Higgins, H. C. *J. Chem. Phys.* **1950**, 18, 265.

³⁸ Usually the symbol is an asterisk, but the terminology is “starred” nonetheless.

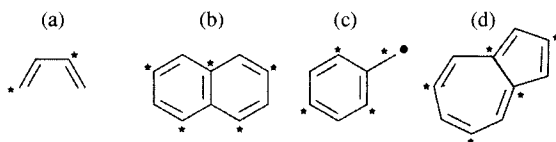


FIGURE 4.18
Alternant and nonalternant π systems.

nant, but some are not. Within the category of alternant structures, we further distinguish between **even alternant** systems, which have the same number of starred and nonstarred π centers, and **odd alternant** systems which do not. (We always label π centers so as to produce the greater number of starred positions, so odd alternant structures have more starred than nonstarred π centers.) In Figure 4.18, 1,3-butadiene (a) and naphthalene (b) are even alternant, the benzyl radical (c) is odd alternant, and azulene (d) is nonalternant.

Alternant π systems are of interest because the carbon atoms can be divided into two sets—the starred positions and the nonstarred positions—so that no carbon atoms in the same set have overlapping p orbitals.³⁷ This property means that some of the fundamental assumptions of HMO theory turn out to be valid for alternant systems but may not be valid for nonalternant systems. For example, in HMO theory we assume that all carbon atoms are electrically neutral. If that is true, then all values of H_{ii} are the same (α) and all values of H_{ij} for bonded atoms i and j are the same (β). If there are charges on any of the atoms, however, then the values of H_{ii} and H_{ij} will vary, and our assumptions are contradicted by the results of the calculation. A specific case is the nonalternant compound azulene, Figure 4.18(d). Even though azulene is neutral, none of the q_i values calculated with HMO theory are 0. Thus, there can be a fundamental inconsistency between the assumptions of an HMO calculation on a nonalternant structure and the calculated results. For alternant structures, however, the q_i values calculated from HMO theory are always found to be 0.

Alternant systems have other important properties as well:³⁹

1. Every even alternant conjugated π system has the bonding and antibonding MOs arranged symmetrically above and below the energy $E = \alpha$.
2. Every odd alternant conjugated π system has a nonbonding molecular orbital, **NBMO**, with $E = \alpha$. The remaining MOs are arranged symmetrically above and below the NBMO.

With this knowledge we could have predicted the *qualitative* ordering of the energy levels of the allyl and 1,3-butadiene systems (Figures 4.4 and 4.6) without having to do the HMO calculation.

Another important property of odd alternant systems will allow us to calculate the wave function of the NBMO without having to calculate the entire set of HMOs.

3. If we star an odd alternant system so as to have more starred than nonstarred positions, the NBMO will have nonzero coefficients only at the starred positions.

³⁹ For mathematical proofs of the properties of alternant systems, see Dewar, M. J. S. *The Molecular Orbital Theory of Organic Chemistry*; McGraw-Hill: New York, 1969; p. 199 ff.

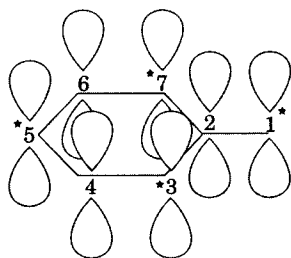


FIGURE 4.19
Determination of the NBMO of benzyl.

This was, in fact, the result obtained for the allyl system (page 184). The NBMO (ψ_2) has nonzero coefficients only on C1 and C3, which would be the starred positions if the allyl system were designated as an odd alternant system. ψ_1 and ψ_3 are arranged symmetrically above and below the NBMO.

The benzyl system (Figure 4.19) is an odd alternant system, so we can immediately determine that the NBMO of benzyl will have nonzero coefficients only at carbon atoms 1, 3, 5, and 7. Furthermore, we can determine the actual coefficients of the NBMO by using another result of HMO theory:

4. The sum of the coefficients of the atomic orbitals of the starred atoms directly linked to a given nonstarred atom is zero.^{2e}

Now we can write the following equations:

$$c_3 + c_5 = 0 \quad (4.57)$$

$$c_5 + c_7 = 0 \quad (4.58)$$

$$c_1 + c_3 + c_7 = 0 \quad (4.59)$$

If we let $c_5 = c$, then we have

$$c_3 = -c \quad (4.60)$$

$$c_7 = -c \quad (4.61)$$

$$c_1 = 2c \quad (4.62)$$

Since the wave function for the NBMO must be normalized, we know that

$$c_1^2 + c_3^2 + c_5^2 + c_7^2 = 1 \quad (4.63)$$

Substituting the values in equations 4.60–4.62 for each c_i in equation 4.63 gives

$$4c^2 + c^2 + c^2 + c^2 = 7c^2 = 1 \quad (4.64)$$

so

$$c = \pm \frac{1}{\sqrt{7}} \quad (4.65)$$

Thus,

$$\psi_{\text{NBMO}} = \frac{2}{\sqrt{7}}\phi_1 - \frac{1}{\sqrt{7}}\phi_3 + \frac{1}{\sqrt{7}}\phi_5 - \frac{1}{\sqrt{7}}\phi_7 \quad (4.66)$$

At first glance it may not seem important to calculate NBMOs for odd alternant systems. Most stable molecules have an even number of π centers, and the method presented here allows us to determine only one of several molecular orbitals. Nevertheless, the method is very valuable because odd alternant systems may be important intermediates in chemical reactions, and the properties of the NBMO are vital to their reactions. For example, the benzyl radical is an intermediate in the α -halogenation of toluene, and benzyl carbocations are intermediates in S_N1 reactions of benzyl halides. Therefore, calculating properties of these systems can give useful information about chemical reactions.

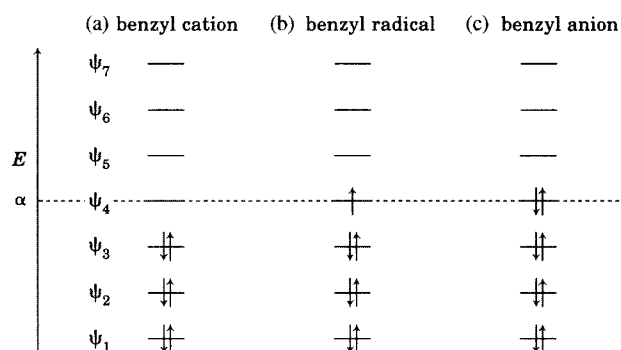


FIGURE 4.20
Population of HMOs in benzyl systems.

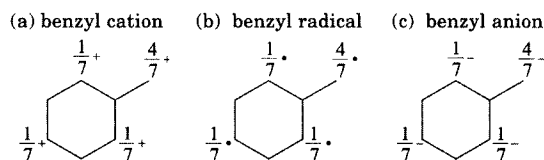


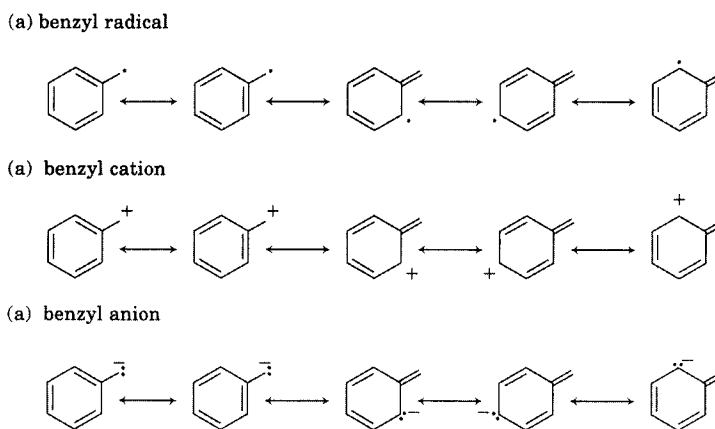
FIGURE 4.21
Charged and unpaired electron densities from HMO theory.

Note that equation 4.66 gives the coefficient of each ϕ in the NBMO. It is the *square* of the coefficient of each ϕ that tells us the electron density on each atom due to *one* electron in that orbital. That is, in the benzyl radical the unpaired electron density on C1 is $\frac{1}{7}$, while the unpaired electron density is $\frac{4}{7}$ on C3, on C5, and on C7. The electron densities in the NBMO determine the locations of charge density in an anion or cation produced by adding an electron to or removing an electron from the radical.³⁹ As shown in Figure 4.20, conversion of the benzyl radical to the benzyl cation removes electron density only from ψ_4 . Each carbon atom in the radical was electrically neutral, so removing $\frac{1}{7}$ th of the electron density from carbon atom 3 produces a positive charge of $+\frac{1}{7}$ at that position. Similarly, reduction of the radical to the anion adds electron density only to ψ_4 . Again, adding $\frac{1}{7}$ th of the charge of an electron to carbon atom 3 gives a net charge of $-\frac{1}{7}$ there. The unpaired electron densities and charge densities predicted for the benzyl radical, cation, and anion are shown in Figure 4.21.

It is interesting at this point to compare the HMO results with the predictions of resonance theory. The resonance structures for the benzyl systems are shown in Figure 4.22. We might expect the two resonance structures in which a benzene ring is maintained to be more stable than the other three and thus to make a greater contribution to the resonance hybrid. Thus, the charge on C1 should probably be greater than that at C3, C5, and C7, but we do not have a means for predicting how much. For now, therefore, we treat all of the resonance structures equally and estimate that C1 in the benzyl cation has a charge of $+\frac{2}{5}$.

Clearly, the predictions of HMO theory (Figure 4.21) and resonance theory (Figure 4.22) are qualitatively similar but quantitatively different. Which is incorrect? The electron paramagnetic resonance spectrum of the benzyl radical was interpreted to mean that about 50% of the unpaired electron density is on the benzylic carbon atom, while 15.8% is on each of the two *ortho* carbon atoms and 18.6% is on the *para* carbon atom.⁴⁰ These

⁴⁰ Fleming, I. *Frontier Orbitals and Organic Chemical Reactions*; Wiley-Interscience: London, 1976; p. 60.

**FIGURE 4.22**

Resonance theory description of benzyl systems.

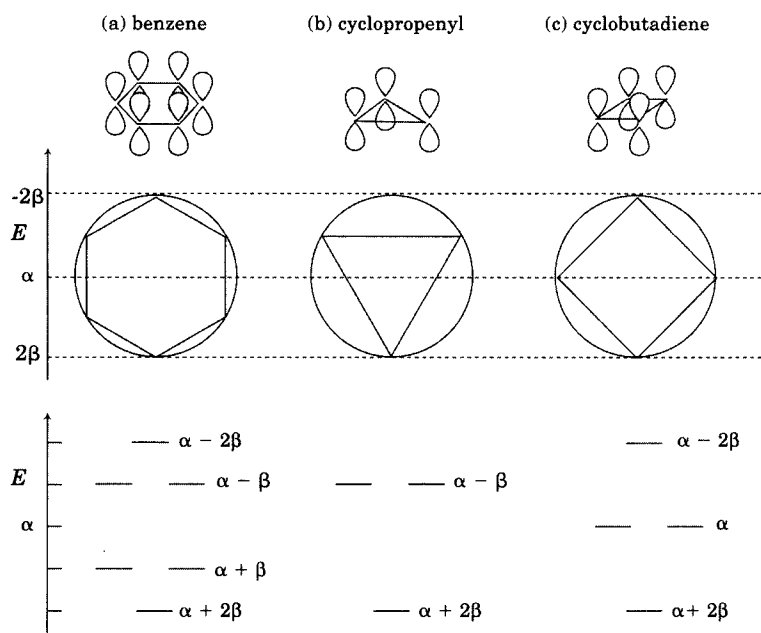
results are intermediate between the predictions of resonance theory and simple Hückel MO theory. By this measure, these two procedures are nearly equally "correct" (or equally incorrect, if one prefers). It is easy to account for differences between experiment and either theory. Because of the many assumptions and simplifications in the HMO analysis, it is not surprising that predictions of electron distribution by the HMO method are not quantitatively correct. Moreover, we did not quantify the resonance method by giving greater weight to some resonance structures than to others, so that prediction cannot be expected to be quantitatively correct either. Both theoretical approaches can be extended to yield more accurate predictions, but the greater complexity that results may reduce the utility that comes from working with simple conceptual models. Therefore, we will continue to use both simple resonance theory and Hückel molecular orbital theory, but with the understanding that they are only starting points for the calculation of molecular structure and properties.

The Circle Mnemonic

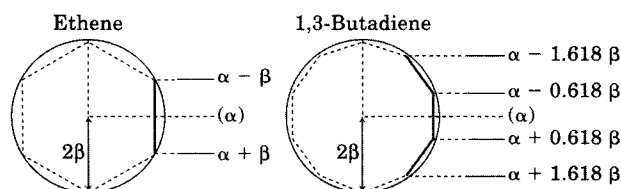
There is another shortcut to the results of HMO theory that organic chemists find particularly useful. As was noted by Frost and Musulin, the energy levels of a monocyclic π system can be determined, either mathematically or graphically, directly from the number of carbon atoms in the ring.⁴¹ The graphical procedure involves inscribing the polygon corresponding to the shape of the planar, monocyclic π system in a circle (with center at $E = \alpha$ and radius 2β) with **one vertex of the polygon** at the bottom of the circle. The height of each vertex (as measured on a scale drawn to one side of the circle) then gives the energy level of a molecular orbital for the π system. This procedure is illustrated in Figure 4.23 for benzene, cyclopropenyl, and cyclobutadiene. It may be seen that it predicts the energy of benzene to be the values we saw earlier (Figure 4.8). For cyclopropenyl and for cyclobutadiene the energy levels are the same as those that would be calculated by the HMO method.

The circle mnemonic has also been adapted for use with linear systems. A linear polyene with m p orbitals (where m is an integer ≥ 1) is transformed

⁴¹ Frost, A. A.; Musulin, B. J. *Chem. Phys.* **1953**, *21*, 572.

**FIGURE 4.23**

Application of the circle method to benzene, cyclopropenyl, and cyclobutadiene.

**FIGURE 4.24**

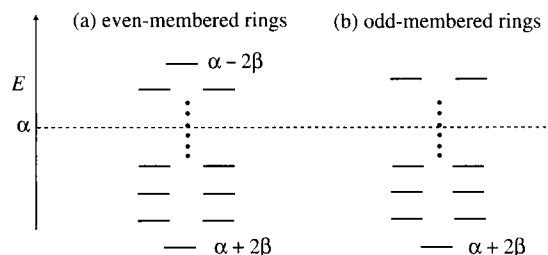
Application of the circle method to linear polyenes. (Adapted from reference 2e.)

into a monocyclic polyene with $2m + 2$ sides, and this polyene is inscribed in a circle of radius 2β , just as we did with the monocyclic systems above. In this case, however, the energy levels correspond only to the heights of vertices that correspond to carbon atoms in the *original* linear structure. Figure 4.24 illustrates this technique for ethene and for 1,3-butadiene. It may be seen that the energy levels so determined are the same as those we calculated earlier.

We should note two points about the circle method. First, we are not really *calculating* molecular orbital energy levels; we are simply using a graphical method to reproduce the results of HMO calculations. Second, the circle method works best for small linear or monocyclic polyenes—the very molecules for which we may most easily calculate the HMO energy levels by solving the secular determinant. With larger rings or longer polyenes, the levels pack together more tightly, making the graphical approach tedious. Thus, the circle method should be considered a mnemonic device to remind us of the pattern of the energy levels, not to derive them.

4.2 AROMATICITY

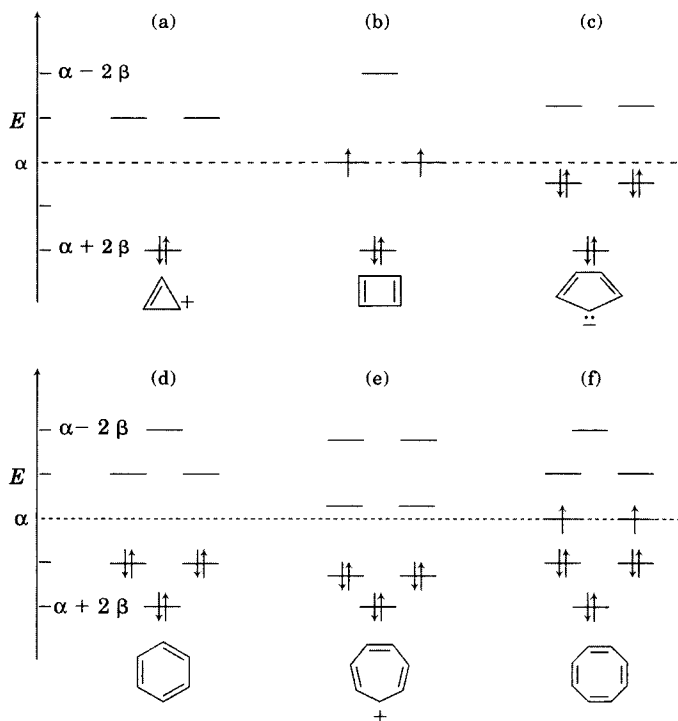
The circle mnemonic leads directly to a familiar result of HMO theory. As illustrated in Figure 4.25, the molecular orbitals of monocyclic conjugated π

**FIGURE 4.25**

Energy levels of monocyclic systems.

systems have energy levels that follow a recurring pattern. There is always one energy level at $E = \alpha + 2\beta$, and then there are pairs of degenerate energy levels at successively higher energy levels. The highest energy level may be a single orbital at $E = \alpha - 2\beta$ (if the ring has an even number of π centers) or there may be a pair of energy levels slightly lower in energy (if the ring has an odd number of π centers).

Figure 4.26 shows the HMOs for cyclopropenyl carbocation, square planar cyclobutadiene, cyclopentadienyl anion, benzene, cycloheptatrienyl carbocation, and planar (D_{8h}) cyclooctatetraene.^{42,43} If we place electrons into the molecular orbitals of each species according to the aufbau principle, we notice an important relationship between the stability of the systems and the

**FIGURE 4.26**

Energy levels of HMOs of cyclic systems. Note: All structures are assumed to be planar, and all carbon-carbon bond lengths in a given structure are the same.

⁴² Note the emphasis on *planar* cyclooctatetraene. As discussed on page 215, cyclooctatetraene has a tub shape.

⁴³ For a tabular summary, see Yates, K. *Hückel Molecular Orbital Theory*; Academic Press: New York, 1978; p. 143.

number of π electrons (not the number of carbon atoms). Systems with 2 or 6 electrons in the π system (examples in Figure 4.26 (a, c, d, e)) have the highest energy populated orbitals fully occupied. Therefore, these systems exhibit what is known as a **closed shell** configuration, meaning that there is not a partially filled HMO energy level. Consequently, there are not any unpaired electrons. Systems with 4 or 8 π electrons (e.g., Figure 4.26 (b, f)) are found by HMO theory to have two unpaired electrons, each in a different molecular orbital. Such systems are said to exhibit an **open shell** configuration.⁴⁴ Because there are both unpaired electrons and high energy orbital vacancies in these orbitals, structures with 4 or 8 electrons exhibit high chemical reactivity. Moreover, the delocalization energies of the cyclic π systems with 2 or 6 electrons are much lower than those of reference (localized or acyclic) systems with the same number of π electrons. For example, DE_π for benzene is 2β , while DE_π for 1,3,5-hexatriene is 0.99β . On the other hand, cyclic systems with 4 or 8 electrons do not have larger π delocalization energies than their acyclic analogs. For cyclobutadiene DE_π is 0β , while that for 1,3-butadiene is 0.47β .

The results observed in Figure 4.26 for cyclic systems with 2 or 6 π electrons can be shown to be true also for those with 10, 14, 18, . . . π electrons. Similarly, the trends observed for *planar cyclic systems* with 4 or 8 π electrons can be shown to be true for those with 12, 16, 20, . . . π electrons. Rewriting these series as arithmetical progressions leads to the Hückel $4n + 2$ rule, where n is an integer: planar cyclic systems with $(4n + 2)$ π electrons are said to be especially stable in comparison with acyclic analogs, while those with $4n$ π electrons are unstable in comparison with acyclic analogs. The name that we apply to monocyclic systems with $4n + 2$ electrons is **aromatic**, and we associate **aromaticity** with the properties of benzene.⁴⁵ Compounds with $4n$ electrons in a cyclic π system are unstable in comparison with acyclic analogs and are said to be **antiaromatic**.^{46,47} These terms have great significance in chemistry, since about two-thirds of known compounds are classified as having at least some aromatic character.⁴⁸

Benzene

In the early days of chemical science, molecular structures were unknown for substances such as benzaldehyde (from almonds) and methyl salicylate (from oil of wintergreen). These compounds have distinctive aromas, so they came to be called "aromatic." As chemistry developed, it was recognized that many of these aromatic compounds contain a benzene ring. In time the term *aromatic* came to mean a certain kind of structure and not a distinctive odor.

⁴⁴ By Hund's rule, two electrons in degenerate orbitals are more stable if they are in separate orbitals. The term *open shell* means that the orbitals at a particular energy level are only partially filled.

⁴⁵ For a historical overview of the concept of aromaticity, see Balaban, A. T. *Pure Appl. Chem.* **1980**, *52*, 1409.

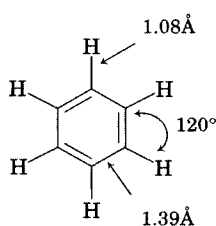
⁴⁶ Breslow, R. *Chem. Eng. News* **1965** (June 28), 43, 90.

⁴⁷ Our analysis will include only structures with an even number of electrons in the cyclic π system. For a discussion of the possibility of aromaticity in open shell, ion-radical cyclic π systems, see Rosokha, S. V.; Kochi, J. K. *J. Org. Chem.* **2006**, *71*, 9357.

⁴⁸ Balaban, A. T.; Oniciu, D. C.; Katritzky, A. R. *Chem. Rev.* **2004**, *104*, 2777.

**FIGURE 4.27**

Electron density data for benzene. (Reproduced from reference 53.)

**FIGURE 4.28**

Experimental bond lengths and angles in benzene.

Benzene itself is the simplest such neutral molecule. It was isolated by Faraday in 1825, and the accepted structure for benzene is usually attributed to a proposal by Kekulé in 1865.^{49,50} Most organic chemists are familiar with the (perhaps apocryphal) “snake tale” of Kekulé’s vision of cyclic benzene molecules.⁵¹ In the late 1800s there was great debate about the molecular structure of benzene, and a number of possible structures were proposed for it.⁵² The electron diffraction results shown in Figure 4.27 indicate a planar structure with hexagonal symmetry.⁵³ With other physical measurements, benzene was determined to have the structure shown in Figure 4.28.⁵⁴

The structure of benzene might not have been such an important question if it were not clear to early researchers that there is something special about benzene and its related compounds. In particular, benzene and its derivatives were seen to have four unusual traits:⁴⁹

1. Thermal stability, including ease of formation by pyrolytic methods
2. A pattern of substitution, not addition, with electrophilic reagents
3. An unusual resistance to oxidation

⁴⁹ For an account of the discovery of benzene and of the many names applied to it, see Badger, G. M. *Aromatic Character and Aromaticity*; Cambridge University Press: Cambridge, 1969; p. 1 ff. Visitors to London may visit the Faraday Museum in the Royal Institution, which has displayed what was reported to be the very sample of benzene isolated by Faraday in 1825. Also see Berson, J. A. *Chemical Discovery and the Logicians’ Program: A Problematic Pairing*, Wiley-Interscience: Weinheim, 2003.

⁵⁰ Wiswesser concluded that credit for the structure of benzene should be given to Johann Josef Loschmidt: Wiswesser, W. J. *Aldrichimica Acta* **1989**, 22, 17.

⁵¹ In most versions of the story, Kekulé was sitting before a fire in his room when he had a daydream of writhing snakes, one of which formed a circle by biting its tail. Some historians of chemistry have cast doubt on the validity of this part of chemical legend. For examples, see (a) Wotiz, J. H.; Rudofsky, S. *Chem. Br.* **1984**, 720; *J. Chem. Educ.* **1982**, 59, 23; (b) Wotiz, J. H., Ed. *The Kekulé Riddle*; Cache River Press: Vienna, IL, 1993; (c) Borman, S. A. *Chem. Eng. News*, **1993** (Aug 23), 20; (d) Heilbronner, E.; Dunitz, J. D. *Reflections on Symmetry*; Verlag Helvetica Chimica Acta: Basel, 1993; p. 47 ff. See also Seltzer, R. J. *Chem. Eng. News* **1985** (Nov 4), 22. For a physiological explanation of the snake legend, see Reese, K. M. *Chem. Eng. News* **1984** (Aug 13), 80.

⁵² Sementsov, A. *J. Chem. Educ.* **1966**, 43, 151; Kikuchi, S. *J. Chem. Educ.* **1997**, 74, 194; Balaban, A. T.; Schleyer, P. v. R.; Rzepa, H. S. *Chem. Rev.* **2005**, 105, 3436.

⁵³ Cox, E. G.; Cruickshank, D. W. J.; Smith, J. A. S. *Proc. R. Soc. A* **1958**, 247, 1. See also reference 49, p. 7 ff.

⁵⁴ Schomaker, V.; Pauling, L. *J. Am. Chem. Soc.* **1939**, 61, 1769.

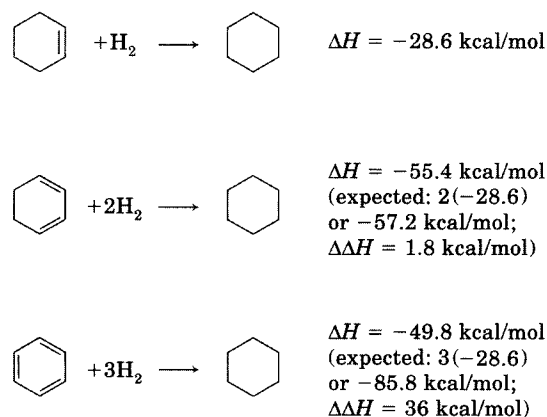


FIGURE 4.29
Heat of hydrogenation data.

4. Different physical properties from analogous aliphatic compounds: for example, aniline is less basic than cyclohexylamine, and phenol is more acidic than cyclohexanol.

Later, chemists associated other properties with benzene and structures judged to be similar to it.⁵⁵ Among these are

5. Geometric properties such that carbon–carbon bond lengths are intermediate between the lengths of single and double bonds⁵⁶
6. Indication of a significant resonance energy determined through comparison of ΔH values for a reaction with those of a reference system⁵⁷
7. Evidence from magnetic susceptibility measurements or NMR spectroscopy of a ring current in the π -electron system when the substance is placed in a magnetic field.⁵⁸

We have come to associate this set of molecular properties with benzene and similar structures, but defining exactly what aromaticity means remains difficult. Frenking and Krapp described aromaticity as one of the “unicorns in the world of chemical bonding models,” meaning that its characteristics are known to everyone, but aromaticity is nevertheless nonobservable.⁵⁹ Thus, we might ask the question: *Is benzene so stable because it is aromatic, or is it aromatic because it is so stable?*

First let us examine the question of stability and attempt to quantify it. The traditional method to determine the resonance energy of benzene is to analyze the heats of hydrogenation of cyclohexene, 1,3-cyclohexadiene, and benzene. Figure 4.29 shows the ΔH values for these reactions.²⁶ If each double bond in benzene were a single olefinic unit, then we might naively predict that its heat of hydrogenation should be $3(-28.6) = -85.8 \text{ kcal/mol}$. The experimental value is -49.8 kcal/mol , however, which is a difference of 36 kcal/mol .

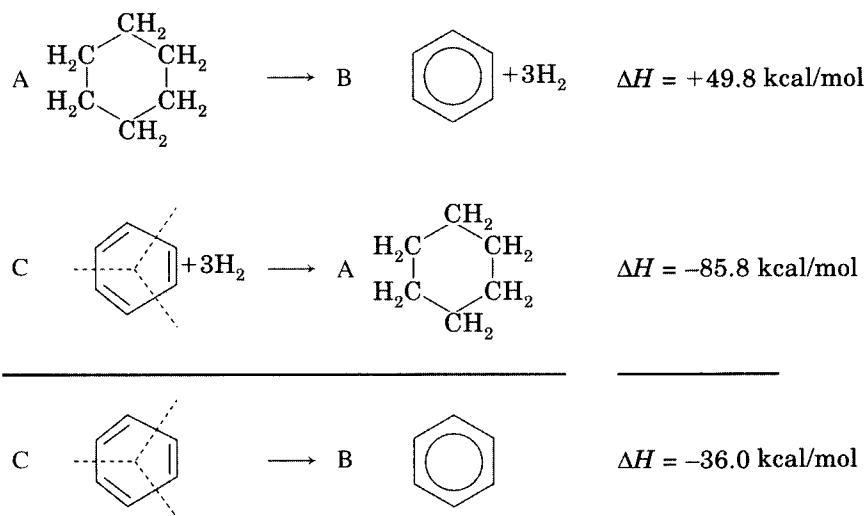
⁵⁵ For a discussion of the methods for evaluating aromatic stabilization energies, see Cyrański, M. K. *Chem. Rev.* **2005**, *105*, 3773.

⁵⁶ Krygowski, T. M.; Cyrański, M. K. *Chem. Rev.* **2001**, *101*, 1385.

⁵⁷ See, for example, Musci, Z.; Viskolcz, B.; Csizmadia, I. G. *J. Phys. Chem. A.* **2007**, *111*, 1123.

⁵⁸ Gomes, J. A. N. F.; Mallion, R. B. *Chem. Rev.*, **2001**, *101*, 1349.

⁵⁹ Frenking, G.; Krapp, A. J. *Comput. Chem.* **2007**, *28*, 15.

**FIGURE 4.30**

Enthalpy of conversion of 1,3,5-cyclohexatriene to benzene.

We may conclude from the data in Figure 4.29 that a conjugated diene is 1.8 kcal/mol more stable than two nonconjugated double bonds and that benzene is 36 kcal/mol more stable than three nonconjugated double bonds.⁶⁰ It might be just as reasonable to expect the ΔH value to be $3(-55.4/2)$ or 83.1 kcal/mol, since the double bonds in benzene really ought to be compared to linearly conjugated double bonds, not to isolated double bonds. By that reasoning, the resonance energy of benzene is only 33.3 kcal/mol.

The preceding analysis has omitted an important factor. Bond lengths and hybridizations change when a double bond is converted to a single bond, and there are energies associated with those changes. What we would like to calculate is the difference in energy between benzene and a 1,3,5-cyclohexatriene *with the same geometry as benzene* but with imaginary barriers that prevent electronic interaction of the π bonds. Therefore, let us consider the data in Figure 4.29 in a slightly different fashion. As shown in Figure 4.30, the ΔH value of -36 kcal/mol may be considered to be the sum of the enthalpies for two different processes: one is the removal of the imaginary barrier to resonance, and the other is the distortion of the molecule so that all carbon-carbon bonds are the same length.

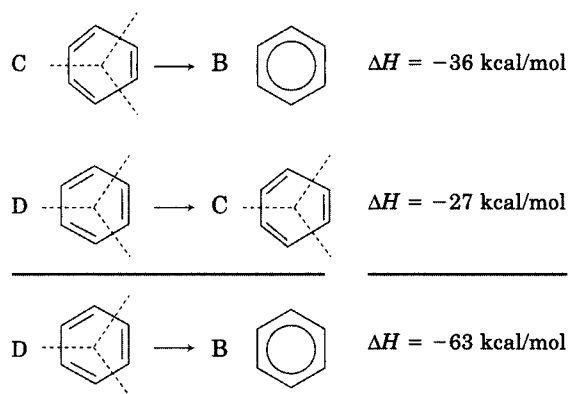
If we define resonance energy as the extra stabilization that a structure gains by delocalization of electrons *without movement of nuclei*, then we should separate the two factors that determine the net ΔH in Figure 4.30. Coulson determined that the distortion of a 1,3,5-cyclohexatriene molecule with short double bonds and long single bonds into a 1,3,5-cyclohexatriene structure in which all the carbon-carbon bonds are the same length requires a bond length distortion energy of $+27$ kcal/mol. Writing such a process in the reverse, as shown in Figure 4.31, leads us to calculate the resonance energy of benzene to be 63 kcal/mol.⁶¹⁻⁶³ A recent analysis by Mo and Schleyer determined the

⁶⁰ A value of 36 kcal/mol can also be calculated by comparing the observed heat of formation of benzene with that expected on the basis of group additivity values: Franklin, J. L. *J. Am. Chem. Soc.* **1950**, *72*, 4278.

⁶¹ Coulson, C. A.; Altmann, S. L. *Trans. Faraday Soc.* **1952**, *48*, 293.

⁶² For a detailed discussion, see Streitwieser, A., Jr. *Molecular Orbital Theory for Organic Chemists*; John Wiley & Sons: New York, 1961; p. 245.

⁶³ See also the analysis of George, P.; Bock, C. W.; Trachtman, M. *J. Chem. Educ.* **1984**, *61*, 225.

**FIGURE 4.31**

Determination of the resonance energy of 1,3,5-cyclohexatriene with all carbon-carbon bonds the same length.

resonance energy of benzene to be close to 57.5 kcal/mol.⁶⁴ Many other analyses are possible, and various authors reported values for the resonance energy of benzene ranging from 13 to 112 kcal/mol.^{62,65}

Not only is there evidence that the resonance energy of benzene is not the 36 kcal/mol that most organic chemists assume, but some theoreticians suggest that the special properties of benzene, while associated with the delocalized $4n + 2$ electrons, do not result from the propensity of these electrons to be delocalized. In particular, Shaik and Hiberty reported that “electronic delocalization in ... C_6H_6 turns out to be a byproduct of the σ -imposed geometric symmetry and not a driving force by itself.”^{66,67} This conclusion, which was supported by other investigators,⁶⁸ thus called into question a concept that has been called “the most important general concept for the understanding of organic chemistry.”⁶⁹

Let us return briefly to the idea that the heat of hydrogenation of benzene in Figure 4.29 should be -85.8 kcal/mol. One approach to determining the aromaticity of benzene has been to study structures with geometric features that make the bond length distortion upon hydrogenation less significant, such as compound **1**. The heat of hydrogenation of **1** is very close to predicted heat of hydrogenation of “1,3,5-cyclohexatriene” having equal C-C bond lengths (-85.8 kcal/mol) when the experimental value (-71.6 ± 1.5 kcal/mol) is adjusted for the ca. 11.4 kcal/mol of extra strain estimated for **2** because of the planarity of its cyclohexane ring.⁷⁰ Thus, these results were consistent with a model in which the central ring of **1** experiences strain-induced bond

⁶⁴ Mo, Y.; Schleyer, P. v. R. *Chem. Eur. J.* **2006**, *12*, 2009.

⁶⁵ Suresh, C. H.; Koga, N. *J. Org. Chem.* **2002**, *67*, 1965.

⁶⁶ Shaik, S. S.; Hiberty, P. C.; Lefour, J.-M.; Ohanessian, G. *J. Am. Chem. Soc.* **1987**, *109*, 363; Shaik, S. S.; Hiberty, P. C.; Ohanessian, G.; Lefour, J.-M. *J. Phys. Chem.* **1988**, *92*, 5086.

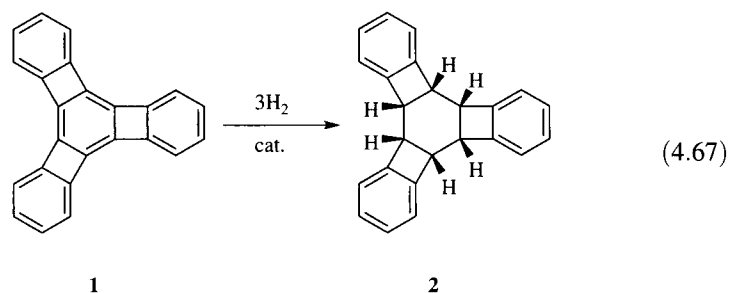
⁶⁷ Jug, K.; Hiberty, P. C.; Shaik, S. *Chem. Rev.* **2001**, *101*, 1477

⁶⁸ Stanger, A.; Vollhardt, K. P. C. *J. Org. Chem.* **1988**, *53*, 4889. See also Sironi, M.; Cooper, D. L.; Gerratt, J.; Raimondi, M. *J. Chem. Soc. Chem. Commun.* **1989**, 675; Jug, K.; Köster, A. M. *J. Am. Chem. Soc.* **1990**, *112*, 6772; Köster, A. M.; Calaminici, P.; Geudtner, G.; Gómez-Sandoval, Z. *J. Phys. Chem. A* **2005**, *109*, 1257; Pierrefixe, S. C. A. H.; Bickelhaupt, F. M. *Chem. Eur. J.* **2007**, *13*, 6321 and references therein.

⁶⁹ Katritzky, A. R.; Barczynski, P.; Musumarra, G.; Pisano, D.; Szafran, M. *J. Am. Chem. Soc.* **1989**, *111*, 7.

⁷⁰ Beckhaus, H.-D.; Faust, R.; Matzger, A. J.; Mohler, D. L.; Rogers, D. W.; Rüdhardt, C.; Sawhney, A. K.; Verevkin, S. P.; Vollhardt, K. P. C.; Wolff, S. *J. Am. Chem. Soc.* **2000**, *122*, 7819.

localization as a result of distortion of the σ -bond frame by the cyclobutane rings.



The idea that distortion of a benzene ring to produce alternating longer and shorter bonds could produce localization of the π -electron density is known as the Mills–Nixon effect and has been the subject of much debate in organic chemistry.⁷¹ An experimental result that is consistent with a particular model is supportive evidence for that model, but it can never be considered conclusive. For example, Mo and Schleyer found that bond alternation would not necessarily decrease the aromaticity of a 1,3,5-cyclohexatriene and that the heat of hydrogenation of 1 could be the result of other factors, such as the avoidance of antiaromaticity in the four-membered rings.⁶⁴

If the calculation of the stabilization of benzene by electron delocalization can be so complicated, the analysis of polycyclic aromatic compounds such as naphthalene, anthracene, and phenanthrene is even more complex (Figure 4.32). Their experimental resonance energies are found to be 61, 83.5, and 91.3 kcal/mol, respectively.²³ Naphthalene is like benzene in many ways, for example, by giving electrophilic aromatic substitution when treated with bromine. Phenanthrene, however, undergoes electrophilic addition with bromine,⁴⁹ which suggests that a greater resonance energy does not necessarily result in more “aromatic” behavior. On the other hand, aromatic character is also associated with thiophene (resonance energy 28 kcal/mol) and furan (resonance energy 16 kcal/mol).²³ How do we decide what magnitude of experimental resonance energy qualifies a structure to be called aromatic?

These questions take on even greater significance as the size of the π systems increase.⁷² Naphthalene and anthracene are the first members of a family of compounds known as acenes (also called polyacenes), which have

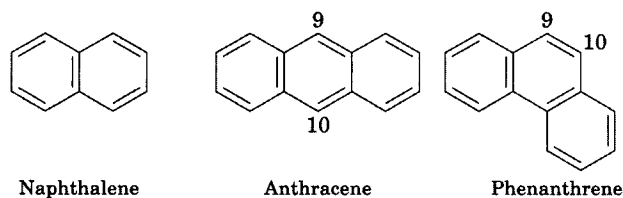


FIGURE 4.32
Polycyclic aromatic compounds.

⁷¹ Mills, W. H.; Nixon, I. G. *J. Chem. Soc.* **1930**, 2510. See also Baldrige, K. K.; Siegel, J. S. *J. Am. Chem. Soc.* **1992**, *114*, 9583; Siegel, J. S. *Angew. Chem. Int. Ed. Engl.* **1994**, *33*, 1721; Sakai, S. *J. Phys. Chem. A* **2002**, *106*, 11526; Alabugin, I. V.; Manoharan, M. *J. Comput. Chem.* **2007**, *28*, 373.

⁷² Schleyer, P. v. R.; Manoharan, M.; Jiao, H.; Stahl, F. *Org. Lett.*, **2001**, *3*, 3643.

the general structure shown in Figure 4.33.^{73,74} The next member of the series would be tetracene ($n=2$), then pentacene ($n=3$), hexacene ($n=4$), and heptacene ($n=5$). One major effect of increasing the dimensions of the acene π system is that the energy gap between the highest occupied MO and the lowest unoccupied MO decreases along the series. As a result, the wavelength of light absorbed by the acene changes with the size of the structure—from 312 nm for naphthalene to 475 nm to tetracene to 695 nm for hexacene.⁷⁵ This property makes the derivatives of tetracene and pentacene useful for a variety of microelectronic devices, such as organic light-emitting diodes.^{76–78} For example, Takahashi and co-workers demonstrated a light-emitting transistor based on a tetracene single crystal.⁷⁹ The larger acenes are not as suitable for these purposes because chemical reactivity increases through hexacene (and then remains constant because the molecular ground states become open shell, diradical in nature).⁸⁰ For example, hexacene is quite unstable in the presence of air or in solution at concentrations of 10^{-4} M, although it persists for 12 hours when generated photochemically in a polymethyl methacrylate matrix.⁸¹ Similarly, heptacene was generated photochemically in a polymer matrix, but it was not sufficiently stable to be observed in solution.⁸² Interestingly, some alkyl-substituted acenes are unstable with respect to their methylene-substituted tautomers. For example, 6,13-dipropylpentacene (**3**) is stable at 150°C in mesitylene solution, but it undergoes acid-catalyzed tautomerization by camphor-10-sulfonic acid (CSA) to 6-propylidene-13-propyl-6,13-dihydropentacene (**4**) in deuterated 1,1,2,2-tetrachloroethane (Figure 4.34).⁸³

If the system of fused benzene rings is extended in two dimensions, structures are formed that resemble a portion of a graphite layer (Figure 4.35).^{84,85} Even larger structures of this type are therefore called **graphenes**. Among such structures, those that are much longer than they are wide are called **graphene nanoribbons**.⁸⁶ If some sp^3 -hybridized carbon atoms are dispersed among the sp^2 -hybridized carbon atoms in a large graphene-like structure, then a three-dimensional lattice can be formed.

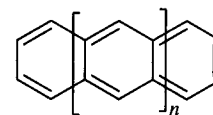


FIGURE 4.33

General formula for an acene ($n=0, 1, 2, \dots$).

⁷³ Kivelson, S.; Chapman, O. L. *Phys. Rev.* **1983**, *28*, 7236.

⁷⁴ For a discussion of the aromaticity of these compounds, see Aihara, J.; Kanno, H. *J. Phys. Chem. A* **2005**, *109*, 3717.

⁷⁵ Houk, K. N.; Lee, P. S.; Nendel, M. *J. Org. Chem.* **2001**, *66*, 5517.

⁷⁶ Anthony, J. E. *Chem. Rev.* **2006**, *106*, 5028.

⁷⁷ Anthony, J. E. *Angew. Chem. Int. Ed.* **2008**, *47*, 452.

⁷⁸ Such devices depend not only on the particular acene used but also on the orientations of the molecules. For an example, see Betti, M. G.; Kanjilal, A.; Mariani, C. *J. Phys. Chem. A* **2007**, *111*, 12454.

⁷⁹ Takahashi, T.; Takenobu, T.; Takeya, J.; Iwasa, Y. *Adv. Funct. Materials* **2007**, *17*, 1623.

⁸⁰ Bendikov, M.; Duong, H. M.; Starkey, K.; Houk, K. N.; Carter, E. A.; Wudl, F. *J. Am. Chem. Soc.* **2004**, *126*, 7416; Reddy, A. R.; Fridman-Marueli, G.; Bendikov, M. *J. Org. Chem.* **2007**, *72*, 51.

⁸¹ Mondal, R.; Adhikari, R. M.; Shah, B. K.; Neckers, D. C. *Org. Lett.* **2007**, *9*, 2505.

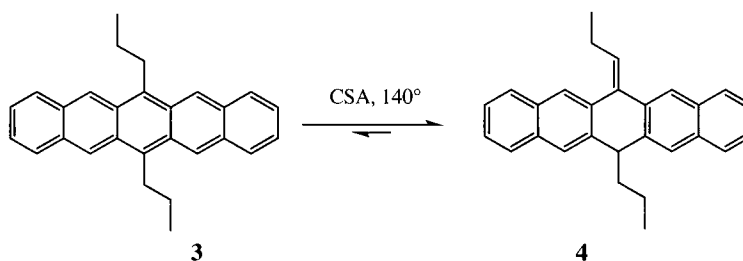
⁸² Mondal, R.; Shah, B. K.; Neckers, D. C. *J. Am. Chem. Soc.* **2006**, *128*, 9612.

⁸³ Takahashi, T.; Kashima, K.; Li, S.; Nakajima, K.; Kanno, K.-I. *J. Am. Chem. Soc.* **2007**, *129*, 15752.

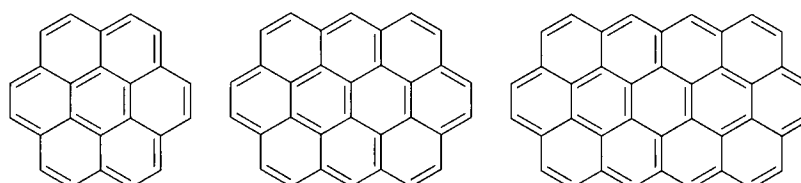
⁸⁴ See, for example, Aihara, J. *J. Chem. Soc. Perkin Trans. 2* **1996**, 2185. Also see Clar, E.; Robertson, J. M.; Schlägl, R.; Schmidt, W. *J. Am. Chem. Soc.* **1981**, *103*, 1320.

⁸⁵ For a discussion of the aromatic character of polycyclic conjugated systems, see Randić, M. *Chem. Rev.* **2003**, *103*, 3449.

⁸⁶ See, for example, Rudberg, E.; Salek, P.; Luo, Y. *Nano Lett.* **2007**, *7*, 2211.

**FIGURE 4.34**

Tautomerization of a 6,13-dialkylpentacene.

**FIGURE 4.35**

Coronene (left), ovalene (center), and circumanthracene (right).

Such structures show potential in nanoelectronics and for storage of H₂ in alternative energy systems.⁸⁷

If two edges of a graphene are connected, the structure becomes a single-walled nanotube (SWNT). This transformation decreases the planarity of the π system, so it decreases the overlap of the p orbitals and alters the π energy levels. As a result, formation of nanotubes is endothermic.⁸⁸ In addition, the electrical properties of the nanotube differ according to its dimensions, with some nanotubes behaving as metals and others as semiconductors.⁸⁹ Dekker and co-workers reported using a SWNT to create a nanoscale transistor that could be switched on or off with a single electron.⁹⁰ SWNTs may also have uses as electrode materials with extremely low background currents,⁹¹ as a means to follow reactions of a single molecule,⁹² as H₂ storage agents,⁹³ and as unique drug delivery systems and diagnostic agents.⁹⁴ Carbon nanotubes may be formed as one or more tubes inside another, and such multiwalled nanotube systems have their own unique properties. For example, Wei and co-workers used double-wall carbon nanotubes as both photogeneration sites and as charge carriers in a solar cell.⁹⁵ Incorporating a five-membered ring into a system of six-membered sp^2 -hybridized carbon atoms puckers the

⁸⁷ Li, D.; Kaner, R. B. *Science* **2008**, 320, 1170; Park, N.; Hong, S.; Kim, G.; Jhi, S.-H. *J. Am. Chem. Soc.* **2007**, 129, 8999.

⁸⁸ Gozzi, D.; Iervolino, M.; Latini, A. *J. Am. Chem. Soc.* **2007**, 129, 10269.

⁸⁹ For a review of the electronic and electrochemical properties of nanotubes, see Sgobba, V.; Guldi, D. M. *Chem. Soc. Rev.* **2009**, 38, 165.

⁹⁰ Postma, H. W. C.; Teepe, T.; Yao, Z.; Grifoni, M.; Dekker, C. *Science* **2001**, 293, 76. Also see Li, S.; Yu, Z.; Yen, S.-F.; Tang, W. C.; Burke, P. J. *Nano Lett.* **2004**, 4, 753.

⁹¹ Bertonecello, P.; Edgeworth, J. P.; Macpherson, J. V.; Unwin, P. R. *J. Am. Chem. Soc.* **2007**, 129, 10982.

⁹² Goldsmith, B. R.; Coroneus, J. G.; Kane, A. A.; Weiss, G. A.; Collins, P. G. *Nano Lett.* **2008**, 8, 189.

⁹³ Nikitin, A.; Li, X.; Zhang, Z.; Ogasawara, H.; Dai, H.; Nilsson, A. *Nano Lett.* **2008**, 8, 162.

⁹⁴ Prato, M.; Kostarelos, K.; Bianco, A. *Acc. Chem. Res.* **2008**, 41, 60.

⁹⁵ Wei, J.; Jia, Y.; Shu, Q.; Gu, Z.; Wang, K.; Zhuang, D.; Zhang, G.; Wang, Z.; Luo, J.; Cao, A.; Wu, D. *Nano Lett.* **2007**, 7, 2317.

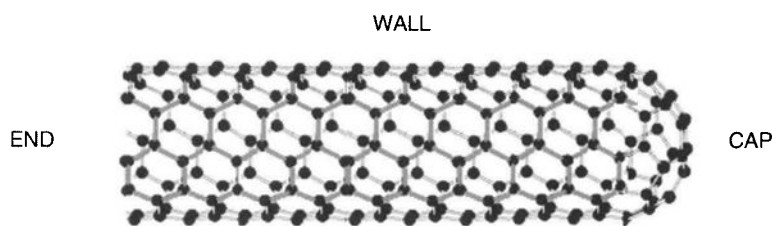
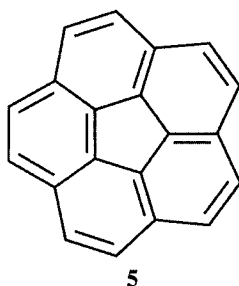


FIGURE 4.36
Carbon-capped single-walled
nanotube. (Adapted from
reference 98.)

π system and creates bowl-shaped structures.⁹⁶ The simplest example is corannulene (5). Fusion of a bowl-shaped structure to a nanotube results in a carbon-capped nanotube, which might be envisioned as the smallest possible test tube (Figure 4.36).⁹⁷



A graphene-like structure may be closed into a cage structure if 12 pentagons are mixed among the hexagonal pattern of the carbon π centers, as in C_{60} (6).⁹⁹ (The figure shows only the connectivity between atoms.) The π system in C_{60} is deformed about 11.6° from planarity at each carbon, thereby minimizing the overlap of the p orbitals and decreasing the aromaticity from what would be calculated for a planar π system of the same size.^{99,100} Therefore, C_{60} appears to have some aromatic character, but its aromaticity is much less than that of benzene, and it undergoes a variety of oxidation, reduction, cycloaddition, and other reactions.¹⁰¹ Still, C_{60} has been utilized as a single-molecule transistor,¹⁰² has also been incorporated into a variety of chemical and biomedical sensors and devices,¹⁰³ and has been proposed as a building block for molecular machines.¹⁰⁴ Fullerenes much larger than C_{60}

⁹⁶ Wu, Y.-T.; Siegel, J. S. *Chem. Rev.* **2006**, *106*, 4843.

⁹⁷ Hayashi, T.; Kim, Y. A.; Matoba, T.; Esaka, M.; Nishimura, K.; Tsukada, T.; Endo, M.; Dresselhaus, M. S. *Nano Lett.* **2003**, *3*, 887; Gasparac, R.; Kohli, P.; Mota, M. O.; Trofin, L.; Martin, C. R. *Nano Lett.* **2004**, *4*, 513.

⁹⁸ Haddon, R. C. *Acc. Chem. Res.* **2002**, *35*, 997.

⁹⁹ Lu, X.; Chen, Z. *Chem. Rev.* **2005**, *105*, 3643.

¹⁰⁰ For an introduction to curved polyarenes, see Scott, L. T.; Bronstein, H. E.; Preda, D. V.; Ansems, R. B. M.; Bratcher, M. S.; Hagen, S. *Pure Appl. Chem.* **1999**, *71*, 209.

¹⁰¹ For a review, see Hirsch, A.; Brettreich, M. *Fullerenes: Chemistry and Reactions*, Wiley-VCH: Weinheim, 2005.

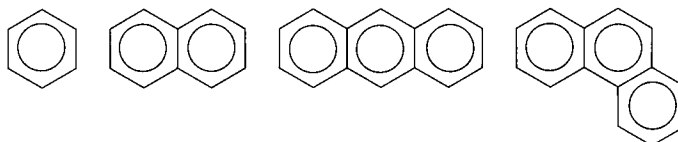
¹⁰² Yu, L. H.; Natelson, D. *Nano Lett.* **2004**, *4*, 79.

¹⁰³ See, for example, Qiao, R.; Roberts, A. P.; Mount, A. S.; Klaine, S. J.; Ke, P. C. *Nano Lett.* **2007**, *7*, 614; Goyal, R. N.; Gupta, V. K.; Bachheti, N. *Anal. Chim. Acta* **2007**, *597*, 82; Fletcher, J. S.; Lockyer, N. P.; Vaidyanathan, S.; Vickerman, J. C. *Anal. Chem.* **2007**, *79*, 2199; Sathish, M.; Miyazawa, K.; Sasaki, T. *Chem. Mat.* **2007**, *19*, 2398; Ikeda, A.; Doi, Y.; Nishiguchi, K.; Kitamura, K.; Hashizume, M.; Kikuchi, J.; Yogo, K.; Ogawa, T.; Takeya, T. *Org. Biomol. Chem.* **2007**, *5*, 1158.

¹⁰⁴ Mateo-Alonso, A.; Guldi, D. M.; Paolucci, F.; Prato, M. *Angew. Chem. Int. Ed.* **2007**, *46*, 8120.

FIGURE 4.37

One type of representation for aromatic character in benzene and larger systems.



have more aromatic character, because the deviation of the π system from planarity is lessened.¹⁰¹



6

We should note here some important aspects of the representation of polycyclic aromatic hydrocarbons. The depictions of naphthalene, anthracene, and phenanthrene in Figure 4.32 use only alternating single and double bonds and thus represent only one **Kekulé structure** for each compound. In the past chemists have tried to indicate the aromatic character of benzene by drawing a large circle inside a hexagon,¹⁰⁵ and by extension this representation has been used for polycyclic aromatic hydrocarbons as well (Figure 4.37). Such representations are now out of favor, in part because they may lead to misunderstandings of the structures. If such a circle indicates an aromatic sextet, then the depiction of naphthalene in Figure 4.37 might be interpreted to mean a system with twelve π electrons, even though the molecule has only ten.¹⁰⁶ Moreover, the circle representations suggest that all three of the rings in anthracene have equal aromatic character, but we have seen (page 206) that this is not the case.

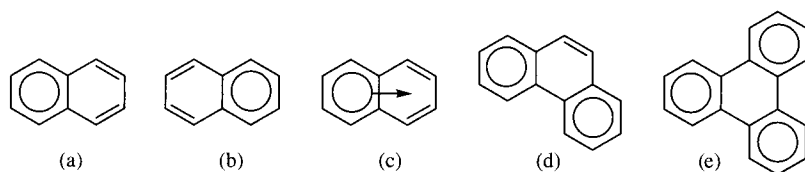
The circle notation is still used in a representation of aromatic systems proposed by Clar.^{107,108} In this system, as many aromatic circles as possible are drawn after the following conditions are met: (i) no circles may occupy adjacent hexagons, and (ii) the hexagons must either be “empty” or have only explicit single and double bonds. As an example, naphthalene could be represented as structure (a) in Figure 4.38. Of course, structure (b) is equally valid, so Clar proposed extending the notation to represent the “sextet migration” shown as Figure 4.38(c). The representation of phenanthrene in Figure 4.38(d) shows a structure with a double bond in one hexagon, and the representation of triphenylene in Figure 4.38(e) shows an “empty” hexagon. The last two examples illustrate cases in which the hexagons with circles represent regions with greater “local aromaticity,” while the other hexagons

¹⁰⁵ Armit, J. W.; Robinson, R. J. *Chem. Soc., Trans.* **1925**, 127, 1604.

¹⁰⁶ See, for example, Randić, M. *J. Chem. Inf. Comput. Sci.* **2004**, 44, 365.

¹⁰⁷ Clar, E. *The Aromatic Sextet*; John Wiley & Sons: London, 1972.

¹⁰⁸ Gutman, I.; Cyvin, S. J. *Introduction to the Theory of Benzenoid Hydrocarbons*; Springer-Verlag: Berlin, 1989.

**FIGURE 4.38**

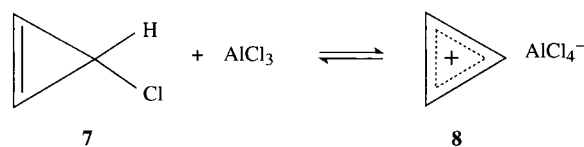
Clar representations of naphthalene (a–c), phenanthrene (d), and triphenylene (e).

represent regions with lesser “local aromaticity.”^{109,110} The Clar model is inherently qualitative, but it can be made quantitative when used in conjunction with graph theory.⁸⁵ Moreover, the Clar notation has proved useful in understanding the properties and reactivities of polycyclic aromatic compounds such as polyacenes¹¹¹ and carbon nanotubes.¹¹²

Aromaticity in Small Ring Systems

The discussion above has emphasized the properties of structures composed of six-membered rings with appreciable aromatic character. Let us return to the more general question of aromaticity by considering rings of other sizes. The cyclopropenyl carbocation (Figure 4.26) has only 2 π electrons. Both may be placed in the lowest energy MO, so the molecular energy is calculated to be $E_{\pi} = 2\alpha + 4\beta$. This is 2β lower in energy than the energy of a reference system composed of a double bond and a localized carbocation. Therefore, the delocalization energy of cyclopropenyl is calculated with HMO theory to be the same as that of benzene, so the cyclopropenyl carbocation is predicted to be much more stable than other carbocations. Consistent with this prediction, reaction of 3-chlorocyclopropene (7) with AlCl_3 led to the isolation of the cyclopropenyl cation (8, Figure 4.39).¹¹³ The structure of the triphenyl derivative of 8 was determined by X-ray crystallography. The carbon–carbon bonds in its three-membered ring were found to be 1.40 Å, which is very similar to the 1.39 Å bond lengths in benzene. Clark calculated the aromatic stabilization of 8 to be 49 kcal/mol.¹¹⁴

In contrast, both theoretical and experimental studies suggested that the cyclopropenyl radical distorts from a structure with D_{3h} symmetry to form

**FIGURE 4.39**

Synthesis of cyclopropenyl cation.

¹⁰⁹ Portella, G.; Poater, J.; Solà, M. *J. Phys. Org. Chem.* **2005**, *18*, 785.

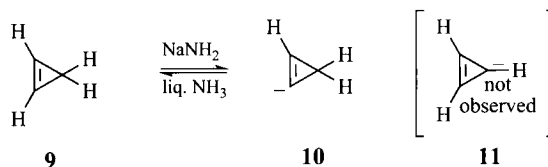
¹¹⁰ See also Randić, M.; Balaban, A. T. *J. Chem. Inf. Model.* **2006**, *46*, 57; Balaban, A. T.; Schmalz, T. G. *J. Chem. Inf. Model.* **2006**, *46*, 1563; Maksić, Z. B.; Barić, D.; Müller, T. *J. Phys. Chem. A* **2006**, *110*, 10135; Gutman, I.; Gojak, S.; Furtula, B.; Radenković, S.; Vodopivec, A. *Monatsh. Chem.* **2006**, *137*, 1127.

¹¹¹ Notario, R.; Abboud, J.-L. M. *J. Phys. Chem. A*, **1998**, *102*, 5290.

¹¹² Ormsby, J. L.; King, B. T. *J. Org. Chem.* **2004**, *69*, 4287; **2007**, *72*, 4035.

¹¹³ Breslow, R.; Groves, J. T. *J. Am. Chem. Soc.* **1970**, *92*, 984.

¹¹⁴ Clark, D. T. *J. Chem. Soc. D Chem. Commun.* **1969**, 637. For ab initio studies on the aromaticity of three-membered rings, see Byun, Y.-G.; Saebo, S.; Pittman, C. U., Jr. *J. Am. Chem. Soc.* **1991**, *113*, 3689.

**FIGURE 4.40**

Deprotonation of cyclopropane.

a nonaromatic structure with C_s symmetry.^{115,116} Similarly, the cyclopropenyl anion is unstable,¹¹⁷ and theoretical calculations indicated that the anion is destabilized by 40 kcal/mol if required to be planar but that pyramidalization of one carbon (thereby reducing the overlap of the three p orbitals) lowers the antiaromatic destabilization to 6 kcal/mol.^{116,118} Furthermore, the vinyl hydrogen atoms of cyclopropane (**9**, Figure 4.40) are more acidic than are the methylene hydrogen atoms.¹¹⁹ Breslow found that 1,2,3-triphenylcyclopropane does not undergo hydrogen exchange in ammonia, so the triphenylcyclopropenyl anion is apparently much harder to form than the anion of, for example, cyclopentadiene.¹²⁰ Cyclopropane itself does undergo proton loss in liquid ammonia, however, and the resulting carbanion is sufficiently concentrated in solution that an NMR spectrum can be obtained.¹²¹ The spectrum indicated the presence of the vinyl carbanion **10**, not the conjugated carbanion **11**. Thus, the carbanion **11** seems from these experiments to show *antiaromatic* character; at least, there is no evidence for any stabilization resulting from electron delocalization.

Cyclobutadiene is also predicted to be antiaromatic and, in fact, has been considered the "antiaromatic paradigm."¹²² The HMO model for the neutral structure has two electrons in an orbital of energy $\alpha + 2\beta$ and two other electrons, each of which must go into one of the two orbitals having energy α . The E_π of cyclobutadiene is thus $4\alpha + 4\beta$, which is the same E_π as two noninteracting double bonds, so the DE_π of cyclobutadiene is 0. Moreover, since there is one electron in each of the two orbitals having energy α , cyclobutadiene is an open shell structure with appreciable diradical character.¹²³

Cyclobutadiene has been the subject of much experimental effort. A number of reactions that were carried out in an effort to synthesize cyclobutadiene were found to produce other products instead.¹²⁴ The observation

¹¹⁵ Compare Davidson, E. R.; Borden, W. T. *J. Chem. Phys.* **1977**, *67*, 2191 and references therein; Closs, G. L.; Evanochko, W. T.; Norris, J. R. *J. Am. Chem. Soc.* **1982**, *104*, 350; Chipman, D. M.; Miller, K. E. *J. Am. Chem. Soc.* **1984**, *106*, 6236.

¹¹⁶ Glukhovtsev, M. N.; Laiter, S.; Pross, A. *J. Phys. Chem.* **1996**, *100*, 17801.

¹¹⁷ The 3-carbomethoxycyclopropen-3-yl anion has been studied in the gas phase: Sachs, R. K.; Kass, S. R. *J. Am. Chem. Soc.* **1994**, *116*, 783.

¹¹⁸ For a discussion and references, see Wiberg, K. B. *Chem. Rev.* **2001**, *101*, 1317.

¹¹⁹ Dorko, E. A.; Mitchell, R. W. *Tetrahedron Lett.* **1968**, 341.

¹²⁰ Breslow, R.; Dowd, P. *J. Am. Chem. Soc.* **1963**, *85*, 2729.

¹²¹ Schipperijn, A. J. *Recl. Trav. Chim. Pays-Bas* **1971**, *90*, 1110.

¹²² Bally, T. *Angew. Chem. Int. Ed.* **2006**, *45*, 6616.

¹²³ Characterization of cyclobutadiene by more advanced theoretical methods reveals many complexities not apparent in the HMO treatment, and Mo and Schleyer (reference 64) concluded that cyclobutadiene should be considered not an "antiaromatic paradigm" but a unique structure.

¹²⁴ Researchers have synthesized substituted cyclobutadienes in which substituents either retard reaction through steric effects or stabilize the ring through electronic effects. For a discussion see Hess, B. A., Jr.; Schaad, L. J. *J. Org. Chem.* **1976**, *41*, 3058.

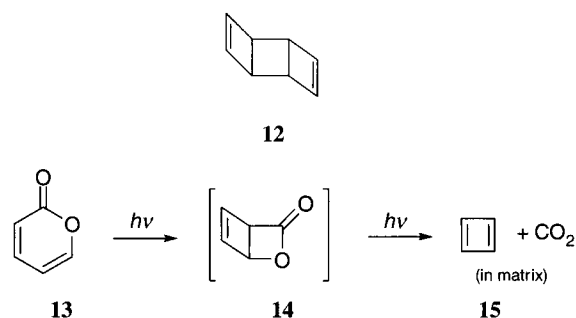


FIGURE 4.41
Matrix synthesis of cyclobutadiene.

that an apparent dimer (**12**) of cyclobutadiene was found in some reaction mixtures suggested that the elusive compound might have been formed as a transient species but was too reactive to characterize. Therefore, some investigators attempted to observe cyclobutadiene through matrix isolation spectroscopy.¹²⁵ In this method, a photochemically reactive compound is deposited in a frozen matrix of an unreactive medium (such as argon) on optical windows inside a spectrophotometer. The apparatus is designed to maintain a temperature low enough to keep the matrix solid, while allowing irradiation of the sample for photochemical reaction and then for spectroscopic analysis of the products.¹²⁶

Chapman and co-workers deposited pyranone (**13**) in the matrix and then photochemically generated bicyclopentanone (**14**), a compound expected to generate cyclobutadiene by photochemical elimination of CO₂ (Figure 4.41). Analysis of the infrared spectrum of the photoproduct suggested that cyclobutadiene (**15**) existed as a square planar molecule.¹²⁷ This result caused considerable discussion among theoreticians, since some calculations indicated that cyclobutadiene should exist as a rectangular molecule, with mostly single and mostly double bonds as shown in Figure 4.42.¹²⁸ The less symmetric rectangular structure (**16**) was thought to reduce, to some extent at least, the antiaromatic character of the π system.

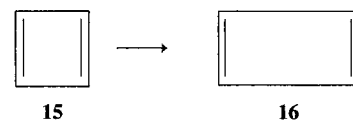


FIGURE 4.42
Distortion of cyclobutadiene to a rectangular structure.

Later, the experimental evidence for square cyclobutadiene was called into question. Krantz reported the photolysis of bicyclopentanone in which the carbon atom eliminated as CO₂ was labeled with ¹³C. One important infrared band that had been assigned to a vibration of square planar cyclobutadiene in earlier studies was altered by the isotopic change, suggesting that this band was due to CO₂ trapped with the cyclobutadiene in the rigid rare gas matrix.¹²⁹ Thus, the experimental data did not answer the question of the structure of cyclobutadiene. Later work on the theoretical determination of the infrared spectrum of cyclobutadiene¹³⁰ and further matrix isolation spectroscopy experiments,¹³¹ including the use of polarized IR spectroscopy

¹²⁵ Bally, T. in Moss, R. A.; Platz, M. S.; Jones, M., Jr., Eds. *Reactive Intermediate Chemistry*; Wiley-Interscience: Hoboken, NJ, 2004; pp. 797–845.

¹²⁶ Dunkin, I. R. in Horspool, W. M.; Lenci, F., Eds. *CRC Handbook of Organic Photochemistry and Photobiology*, 2nd ed.; CRC Press: Boca Raton, FL, 2003; p.14-1.

¹²⁷ Chapman, O. L.; McIntosh, C. L.; Pacansky, J. J. *Am. Chem. Soc.* **1973**, *95*, 614.

¹²⁸ Kollmar, H.; Staemmler, V. *J. Am. Chem. Soc.* **1977**, *99*, 3583.

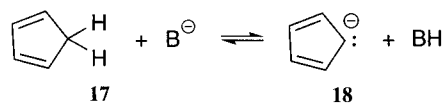
¹²⁹ Pong, R. G. S.; Huang, B.-S.; Laureni, J.; Krantz, A. J. *Am. Chem. Soc.* **1977**, *99*, 4153.

¹³⁰ Kollmar, H.; Staemmler, V. *J. Am. Chem. Soc.* **1978**, *100*, 4304.

¹³¹ Masamune, S.; Souto-Bachiller, F. A.; Machiguchi, T.; Bertie, J. E. *J. Am. Chem. Soc.* **1978**, *100*, 4889.

FIGURE 4.43

Reaction of cyclopentadiene as an acid.



and ¹³C NMR of labeled cyclobutadiene,¹³² appear to have settled the question in favor of a rectangular structure for cyclobutadiene.^{133–137}

The cyclopentadienyl anion has six electrons in the π system, giving the molecule an HMO π energy of $6\alpha + 6.47\beta$ and an HMO delocalization energy of 2.47β (Figure 4.26). This delocalization energy is not much different from the delocalization stabilization, 48 kcal/mol, calculated by more advanced methods.¹¹⁸ The pK_a of cyclopentadiene (17, Figure 4.43) is 16, which is nearly the same as that of water, suggesting that the cyclopentadienyl anion (18) is more stable than other carbanions.¹³⁸ In contrast, the cyclopentadienyl cation (19) is a very unstable species. 5-Iodo-1,3-cyclopentadiene did not react with silver perchlorate in propanoic acid at -15°C .¹³⁹ 5-Bromo-1,3-cyclopentadiene did react with SbF_5 in di-*n*-butyl phthalate at 78 K, and the spectral data suggested a structure with two unpaired electrons.¹⁴⁰ The antiaromatic destabilization of the cation was calculated to be 29 kcal/mol.^{118,141}

The cycloheptatrienyl carbocation (20) is also a six π electron system, and all six electrons can go into bonding orbitals. Its delocalization energy is calculated to be 2.99β (Figure 4.26), which is close to the value of 50 kcal/mol of delocalization stabilization calculated by other methods.¹¹⁸ Therefore, the cycloheptatrienyl cation is an especially stable carbocation,¹⁴² although it is still a cation and is certainly not as stable as benzene. On the other hand, the cycloheptatrienyl anion is a $4n$ π system and thus is predicted to be antiaromatic by HMO theory. More advanced calculations suggest that any energy consequences of electron delocalization in the anion must be very small.

¹³² Orendt, A. M.; Arnold, B. R.; Radziszewski, J. G.; Facelli, J. C.; Malsch, K. D.; Strub, H.; Grant, D. M.; Michl, J. *J. Am. Chem. Soc.* **1988**, *110*, 2648.

¹³³ Dewar, M. J. S.; Merz, K. M., Jr.; Stewart, J. J. P. *J. Am. Chem. Soc.* **1984**, *106*, 4040.

¹³⁴ Carpenter suggested that the rectangular forms of cyclobutadiene can interconvert by tunneling. Carpenter, B. K. *J. Am. Chem. Soc.* **1983**, *105*, 1700. See also Huang, M.-J.; Wolfsberg, M. *J. Am. Chem. Soc.* **1984**, *106*, 4039.

¹³⁵ See also Arnold, B. R.; Radziszewski, J. G.; Campion, A.; Perry, S. S.; Michl, J. *J. Am. Chem. Soc.* **1991**, *113*, 692; Lefebvre, R.; Moiseyev, N. *J. Am. Chem. Soc.* **1990**, *112*, 5052.

¹³⁶ The cyclobutadiene dication should have two electrons, both in ψ_1 , so it is predicted to have $DE = 2\beta$, the same as cyclopropenyl cation. There was a report that the dication had been observed: Olah, G. A.; Mateescu, G. D. *J. Am. Chem. Soc.* **1970**, *92*, 1430.

¹³⁷ The cyclobutadiene monocation should have a delocalization energy of 1β , and the EPR spectra (see Chapter 5) of substituted monocations was reported: Courtneidge, J. L.; Davies, A. G.; Luszyk, E.; Luszyk, J. *J. Chem. Soc. Perkin Trans. 2* **1984**, 155.

¹³⁸ Streitwieser, A., Jr.; Nebenzahl, L. L. *J. Am. Chem. Soc.* **1976**, *98*, 2188. See also Stewart, R. *The Proton: Applications to Organic Chemistry*; Academic Press: New York, 1985; pp. 72–74.

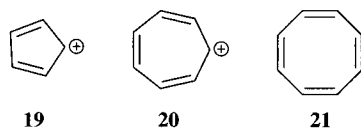
¹³⁹ Breslow, R.; Hoffman, J. M. *J. Am. Chem. Soc.* **1972**, *94*, 2110.

¹⁴⁰ The EPR spectrum indicated a species with two unpaired electrons having the same spin. Saunders, M.; Berger, R.; Jaffe, A.; McBride, J. M.; O'Neill, J.; Breslow, R.; Hoffman, J. M., Jr.; Perchonock, C.; Wasserman, E.; Hutton, R. S.; Kuck, V. J. *J. Am. Chem. Soc.* **1973**, *95*, 3017.

¹⁴¹ For a discussion, see Allen, A. D.; Tidwell, T. T. in Olah, G. A.; Prakash, G. K. S., Eds. *Carbocation Chemistry*, Wiley-Interscience: Hoboken, NJ, 2004; p. 103.

¹⁴² Doering, W. v. E.; Knox, L. H. *J. Am. Chem. Soc.* **1954**, *76*, 3203.

The anion was prepared in solution but was found to be highly reactive.^{118,143} It could also be formed in the gas phase but appeared to undergo rapid rearrangement to benzyl anion.¹⁴⁴



Planar cyclooctatetraene (COT, **21**) is predicted to have a π energy of $8\alpha + 9.657\beta$, giving it a delocalization energy of 1.66β . The HMO energy level diagram (Figure 4.26) predicts it to be an open shell molecule, however, and thus unstable. Nevertheless, COT is a commercially available compound and is regarded as a stable substance that is nonaromatic—that is, neither aromatic nor antiaromatic.^{145,146} The stability of COT is easily rationalized if we recall one of the fundamental assumptions of HMO theory—that the π system is planar with all of the p orbitals parallel to each other. Because a planar COT molecule would have ring bond angles of 135° , there would be considerable angle strain in addition to the electronic destabilization of planar COT. By adopting the tub-shaped conformation shown in Figure 4.44, COT can reduce both angle strain and electronic strain.¹⁴⁷ Therefore, the HMOs of COT are more like those of a system of four noninteracting double bonds, not those of an antiaromatic system.¹⁴⁸



FIGURE 4.44
Tub conformation of COT.

Adding two more electrons to planar COT would fill the vacancies in the partially filled HMOs, making the molecule an aromatic, closed shell structure. In fact, COT dianion is well known in organic chemistry.¹⁴⁹ Even though the C–C–C bond angles are required to be greater than 120° , the planar aromatic structure is more stable than a nonaromatic, nonplanar COT dianion. Similarly, removing two electrons from COT should generate a relatively stable dication, and Olah and co-workers have studied the properties of substituted COT dications.¹⁵⁰

Larger Annulenes

The term *annulene* refers to monocyclic compounds that can be represented with alternating single and double bonds.¹⁵¹ We indicate the size of the

¹⁴³ For a discussion and leading references, see Allen, A. D.; Tidwell, T. T. *Chem. Rev.*, **2001**, *101*, 1333.

¹⁴⁴ White, R. L.; Wilkins, C. L.; Heitkamp, J. J.; Staley, S. W. *J. Am. Chem. Soc.* **1983**, *105*, 4868.

¹⁴⁵ For a review, see Craig, L. E. *Chem. Rev.* **1951**, *49*, 103.

¹⁴⁶ The original synthesis of COT was a 13-step process: Willstätter, R.; Heidelberger, M. *Chem. Ber.* **1913**, *46*, 517.

¹⁴⁷ Karle, I. L. *J. Chem. Phys.* **1952**, *20*, 65. Dewar reported calculations showing that the chair-like conformation of cyclooctatetraene is unstable with respect to the tub conformation shown here: Dewar, M. J. S.; Merz, K. M., Jr. *J. Chem. Soc. Chem. Commun.* **1985**, 343.

¹⁴⁸ Theoretical calculations indicate that a D_{8h} (planar, antiaromatic) structure is a transition state in the double bond shifting reaction of cyclooctatetraene: Hrovat, D. A.; Borden, W. T. *J. Am. Chem. Soc.* **1992**, *114*, 5879.

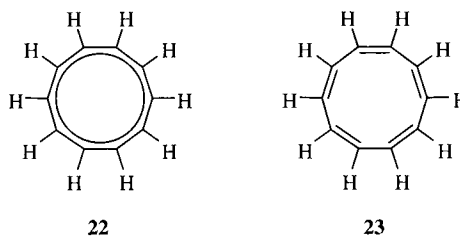
¹⁴⁹ Katz, T. J. *J. Am. Chem. Soc.* **1960**, *82*, 3784, 3785.

¹⁵⁰ Olah, G. A.; Staral, J. S.; Liang, G.; Paquette, L. A.; Melega, W. P.; Carmody, M. J. *J. Am. Chem. Soc.* **1977**, *99*, 3349.

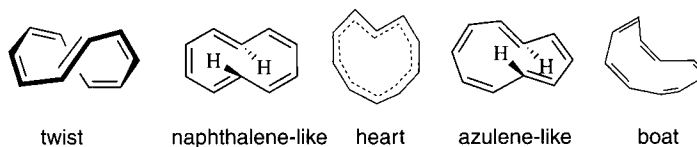
¹⁵¹ For reviews, see (a) Slayden, S. W.; Liebman, J. F. *Chem. Rev.* **2001**, *101*, 1541; (b) Kennedy, R. D.; Lloyd, D.; McNab, H. J. *Chem. Soc. Perkin Trans. 1* **2002**, 1601.

FIGURE 4.45

D_{10h} (left) and D_{5h} (right) structures for [10]annulene.

**FIGURE 4.46**

Nonplanar conformations considered for [10]annulene.



annulene by a number in brackets, $[n]$ annulene, where n is the number of π centers in the ring. By this definition cyclooctatetraene is [8]annulene. The next annulene is [10]annulene (cyclodecapentaene), which has $(4n + 2)$ π electrons and is predicted by HMO theory to be aromatic. As was the case for cyclooctatetraene, however, a planar $C_{10}H_{10}$ structure with all cis double bonds would have considerable angle strain. For example, the C–C–C bond angle in the D_{10h} structure 22 (Figure 4.45), in which all of the carbon–carbon bonds are the same length, is 144° . The D_{5h} structure 23, having alternating carbon–carbon bond lengths, would also have much angle strain. Attempts to synthesize [10]annulene have demonstrated that the compound is highly reactive and thus is hardly an example of aromatic stability.¹⁵²

Masamune and co-workers reported the synthesis and chromatographic separation at -80°C of two different [10]annulenes and recorded their NMR spectra at temperatures from -40°C to -160°C .¹⁵³ One isomer gave a single peak in both ^1H and ^{13}C NMR spectra, while the other showed one ^{13}C NMR peak at higher temperatures but five different peaks at -100°C . No subsequent experimental investigations of [10]annulene have been reported. Therefore, a variety of theoretical treatments have been used to study this system. Schaefer and co-workers considered the five nonplanar conformations shown in Figure 4.46. They found the $C_{10}H_{10}$ potential energy surface to be relatively flat, and different theoretical treatments led to different predictions of relative conformer stability.¹⁵⁴ The “twist” structure with four cis double bonds and one trans double bond was identified as the lowest energy minimum,¹⁵⁴ and its calculated NMR spectrum was consistent with its assignment as the Masamune isomer showing five signals at low temperature.¹⁵⁵ The identity of the other Masamune isomer is less certain,¹⁵⁵ but additional theoretical results are consistent with its assignment as the “heart” structure.¹⁵⁶

As the example of [10]annulene indicates, large annulenes having some trans double bonds can have lower angle strain than the corresponding all-cis

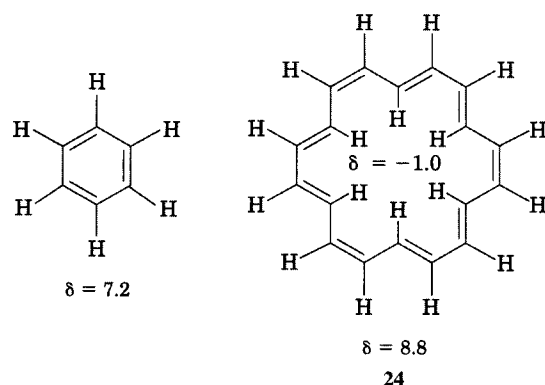
¹⁵² van Tamelen, E. E.; Burkoth, T. L. *J. Am. Chem. Soc.* **1967**, *89*, 151.

¹⁵³ Masamune, S.; Seidner, T. J. *J. Chem. Soc. Chem. Commun.* **1969**, 542; Masamune, S.; Hojo, K.; Hojo, K.; Bigam, G.; Rabenstein, D. L. *J. Am. Chem. Soc.* **1971**, *93*, 4966; Masamune, S.; Darby, N. *Acc. Chem. Res.* **1972**, *5*, 272.

¹⁵⁴ King, R. A.; Crawford, T. D.; Stanton, J. F.; Schaefer, H. F. III. *J. Am. Chem. Soc.* **1999**, *121*, 10788.

¹⁵⁵ Price, D. R.; Stanton, J. F. *Org. Lett.* **2002**, *4*, 2809.

¹⁵⁶ Castro, C.; Karney, W. L.; McShane, C. M.; Pemberton, R. P. *J. Org. Chem.* **2006**, *71*, 3001.

**FIGURE 4.47**

PMR data for benzene and [18]annulene (**24**).

structures. Furthermore, van der Waals strain from substituents on the resulting “internal” double bonds can be minimized if the ring size is large enough. For example, [18]annulene (**24**, Figure 4.47) is planar because it has six trans and three cis double bonds, an arrangement that puts six vinyl protons on the inside of the ring and twelve on the outside. Its ^1H NMR spectrum shows a singlet at $\delta -1.0$ for the six interior protons, while the twelve exterior protons are at $\delta 8.8$.¹⁵⁷ These shifts have been taken as evidence for a very strong ring current effect, which is one of the experimental criteria for aromaticity.^{158,159}

An alternative approach to characterizing the aromaticity of planar compounds is the calculation of a nucleus-independent chemical shift (NICS), which is a computed value of the magnetic shielding a virtual (ghost) nucleus would experience at specific locations near a π system.¹⁶⁰ A NICS(0) value refers to shielding in the center of the π system, while a NICS(1) value reports the shielding expected at a point 1 Å above the center of the molecular plane. Aromatic compounds have negative NICS(0) values, and antiaromatic structures have positive values. NICS values provide a quantitative measure of aromatic character and have been shown to correlate well with other measures of aromaticity.

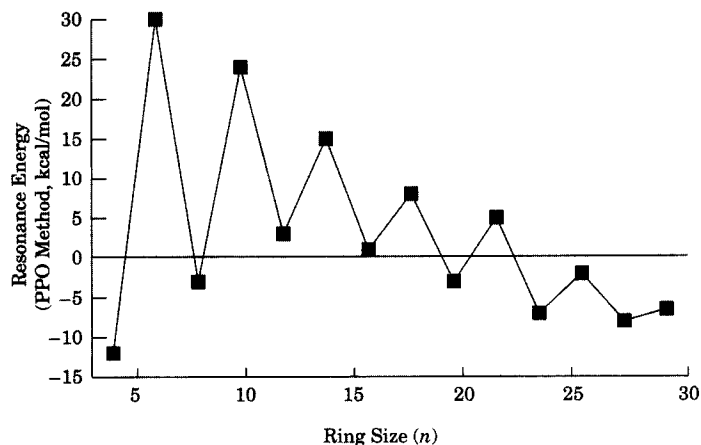
All of the [n]annulenes up to $n = 30$ have been synthesized except for $n = 26$ and $n = 28$.¹⁵¹ Both experimental data and theoretical calculations suggest that larger $4n + 2$ rings are less aromatic than are the smaller ones. As shown in Figure 4.25, the energy levels of monocyclic conjugated π systems are constrained to lie between $\alpha + 2\beta$ and $\alpha - 2\beta$. As the ring includes

¹⁵⁷ The ^1H NMR spectrum is temperature dependent. At 100°C all protons showed a single signal at $\delta 5.5$. At 20°C there are two bands, one at $\delta -1.0$ and one at $\delta 8.8$. At -60°C the spectrum consists of a quintet at $\delta -4.2$ and a quartet at $\delta 9.25$. Calder, I. C.; Garratt, P. J.; Sondheimer, F. *Chem. Commun.* **1967**, 41.

¹⁵⁸ [18]Annulene exhibits *diamagnetic anisotropy*, meaning that the effect of the ring current is not the same in every direction from a given point. The lines of force reinforce the applied field at the twelve exterior protons, but the induced field opposes the applied field in the vicinity of the six interior protons.

¹⁵⁹ Comparing annulene chemical shifts with those of benzene is not as precise as it might seem, however. Wannere, C. S.; Schleyer, P. v. R. *Org. Lett.* **2003**, *5*, 605 argued that the protons on benzene are not deshielded but are, instead, *shielded* by the π ring current. They attribute the chemical shift observed for benzene protons primarily to deshielding arising from the carbon-carbon σ bonds.

¹⁶⁰ Chen, Z.; Wannere, C. S.; Corminboeuf, C.; Puchta, R.; Schleyer, P. v. R. *Chem. Rev.* **2005**, *105*, 3842; Fallah-Bagher-Shaidaei, H.; Wannere, C. S.; Corminboeuf, C.; Puchta, R.; Schleyer, P. v. R. *Org. Lett.* **2006**, *8*, 863. See also Stanger, A. J. *Org. Chem.* **2006**, *71*, 883.

**FIGURE 4.48**

Change in calculated resonance energies for annulenes. (Figure based on data in reference 161.)

more π centers, there is an increasing number of HMO energy levels between those two limits, and the difference in delocalization energy between a $[4n]$ annulene and a $[4n + 2]$ annulene becomes smaller. Moreover, the HMO method has ignored overlap and the problem of electron-electron interactions. Figure 4.48 shows the resonance energy for a series of annulenes calculated by Dewar and Gleicher.¹⁶¹ If we take a large delocalization energy as a measure of aromaticity, then the distinction between what is aromatic and what is antiaromatic becomes progressively smaller with increasing ring size, and for a ring of around 26 π centers, even a member of the $4n + 2$ series is no longer calculated to be more stable than its acyclic analog. Now we are faced with a quantitative question: At what point in the series of annulenes does aromatic character end?¹⁶² It seems that the concept of aromaticity is useful for categorizing the properties and reactions of many compounds and for comparing some compounds with others, but a simple definition of aromaticity is elusive.

Dewar Resonance Energy and Absolute Hardness

There are two other approaches to defining aromaticity that we will consider. The first is based on a comparison of the heat of formation of an organic compound with the heat of formation calculated for a nondelocalized reference system. The difference between those two values would then be the resonance energy for this system.

$$\text{Resonance Energy}(\text{calc}) = \Delta H_f^\circ - \Delta H_{f, \text{ref}}^\circ \quad (4.68)$$

At first glance this approach would seem to be dependent on uncertain reference systems. However, it was given firm footing by the work of Dewar, and Baird elaborated Dewar's approach.^{39,163} Calculated values of resonance energy can thus be based only on knowledge of the molecular

¹⁶¹ Dewar, M. J. S.; Gleicher, G. J. *J. Am. Chem. Soc.* **1965**, *87*, 685.

¹⁶² For further reading, see (a) Chung, A. L. H.; Dewar, M. J. S. *J. Chem. Phys.* **1965**, *42*, 756; (b) Schaad, L. J.; Hess, B. A., Jr. *J. Chem. Educ.* **1974**, *51*, 640.

¹⁶³ Baird, N. C. *Can. J. Chem.* **1969**, *47*, 3535; *J. Chem. Educ.* **1971**, *48*, 509. See also Schaad, L. J.; Hess, B. A., Jr. *Chem. Rev.* **2001**, *101*, 1465.

TABLE 4.2 DRE Values for Selected Hydrocarbons

Compound	Experimental RE ^a	Calculated DRE ^b
Cyclobutadiene ^c	—	-17 kcal/mol
Benzene	+ 21 kcal/mol	+ 21
Cyclooctatetraene ^d	—	-10
Cyclodecapentaene	+ 10	+ 6
Naphthalene	+ 33	+ 33
Anthracene	+ 43	+ 42
Phenanthrene	+ 49	+ 49

^a Calculated from the experimental heat of formation given in reference 163 and equation 4.69.

^b Values taken from Tables 3 and 4 of reference 163.

^c Experimental heats of formation are not available.

^d Assumed to be planar.

structure and experimental data for a few reference compounds. The resonance energy so calculated is denoted the **Dewar resonance energy** (DRE). For a completely unsaturated compound with the formula $C_nH_mO_p\ddot{O}_q$, where p is the number of carbonyl-type oxygens and q is the number of ether-type oxygens, Baird showed that the DRE can be calculated as in equation 4.69:

$$\text{DRE} = 7.435n - 0.605m - 32.175p - 29.38q - \Delta H_f^\circ(C_nH_mO_p\ddot{O}_q) \quad (4.69)$$

where m is the number of C-H bonds present,

p is the number of C=O bonds present,

$(n - p)/2$ is the number of C=C bonds present,

$2q$ is the number of C-O bonds present, and

$\{n - q - m/2\}$ is the number of $C(sp^2)-C(sp^2)$ single bonds present.

This approach allows one to calculate indirectly the heat of formation of $C(sp^2)-C(sp^2)$ single bonds, which is difficult to determine directly. With this approach, the definition of aromaticity is that an *aromatic compound* has $\text{DRE} > 0$, an *antiaromatic compound* has a $\text{DRE} < 0$, and a compound that is neither aromatic nor antiaromatic has a DRE near 0. Results of DRE calculations by Baird are listed in Table 4.2.¹⁶³

The DRE values in Table 4.3 for a series of compounds containing benzene rings show that, for many compounds containing benzene rings conjugated with double bonds, the DRE values depend more on the number of benzene rings than on conjugation of double bonds with aromatic rings. Such DREs are useful in correlating chemical reactivity. As shown in Figure 4.49, the product

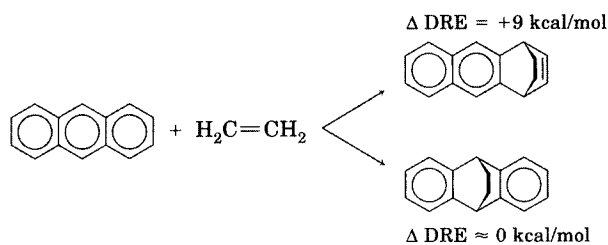
TABLE 4.3 DRE Values (kcal/mol) for Conjugated Benzenes

Compound	DRE	Benzene Rings	DRE/Benzene Ring
Benzene	21.2	1	21.2
Styrene	21.3	1	21.3
Biphenyl	43.6	2	21.8
Stilbene	42.1	2	21.0
benzophenone	43.8	2	21.9

Source: Reference 163.

FIGURE 4.49

DRE differences for addition reactions to anthracene. (Adapted from reference 163.)



of addition of ethene to anthracene is a structure with a naphthalene moiety, so its DRE is 33 kcal/mol (Table 4.2). Reaction by the bottom pathway yields a product with two benzene rings, so its DRE is $2 \times 21 = 42$ kcal/mol. Since the DRE of the reactant is 43 kcal/mol, the ΔDRE is +9 kcal/mol for the top pathway (based on calculated DRE values), but is approximately 0 for the lower pathway. Therefore, the lower pathway should be favored.

Another definition of aromaticity that does not depend explicitly on either experimental results or on comparison with reference compounds is derived from the concept of **absolute hardness**, η , which is defined as one-half of the energy difference between the highest occupied molecular orbital (HOMO) and the lowest unoccupied molecular orbital (LUMO) of a system (equation 4.70).^{164,165} According to Koopmans' theorem, E_{HOMO} is related to the ionization potential of the species, while E_{LUMO} is related to its electron affinity. A large gap between these two orbitals implies resistance to both oxidation and reduction, and low chemical reactivity is one of the defining characteristics of aromaticity.

$$\eta = \frac{E_{\text{LUMO}} - E_{\text{HOMO}}}{2} \quad (4.70)$$

Zhou, Parr, and Garst showed that absolute hardness correlates well with theoretical measures of aromaticity but that the value of η by itself does not allow the categorization of aromaticity.¹⁶⁶ Zhou and Parr later defined the **relative hardness** of a species as the difference between its hardness and the hardness of an acyclic reference compound.¹⁶⁷ Based on these correlations, the authors proposed that a compound is aromatic if its Hückel absolute hardness (determined from the Hückel HOMO–LUMO gap) is less than -0.2β , antiaromatic if the value of η is less than -0.15β , and nonaromatic if η is between those two values. The corresponding division based on relative hardness is 0. That is, a cyclic molecule that is harder than an acyclic analog is aromatic, while one that is not as hard as an acyclic analog is antiaromatic.

4.3 CONTEMPORARY COMPUTATIONAL METHODS

HMO theory can be a useful model for understanding the structure and reactivity of organic compounds, but its predictions should be seen as

¹⁶⁴ Pearson, R. G. *Acc. Chem. Res.* **1993**, *26*, 250 and references therein.

¹⁶⁵ For a discussion of the relationship between chemical hardness and macroscopic properties of substances, see Pearson, R. G. *J. Chem. Educ.* **1999**, *76*, 267.

¹⁶⁶ Zhou, Z.; Parr, R. G.; Garst, J. F. *Tetrahedron Lett.* **1988**, 4843.

¹⁶⁷ Zhou, Z.; Parr, R. G. *J. Am. Chem. Soc.* **1989**, *111*, 7371.

qualitative, not quantitative. Contemporary chemistry increasingly depends on computational methods that can provide accurate predictions of molecular structure and properties. As Cramer noted, chemical waste disposal is becoming increasingly expensive while computational technology is becoming increasingly affordable. "From an economic perspective, at least, theory is enormously attractive as a tool to reduce the costs of doing experiments."¹⁶⁸ Moreover, relatively sophisticated theoretical methods are becoming accessible to the bench top chemist through a variety of software packages. The following discussion will introduce some theoretical methods in order to provide context for the material in later chapters.¹⁶⁹

Extended Hückel Theory

The Hückel MO method assumes that the σ and π systems can be treated independently and then considers only the π system. The **extended Hückel theory** (EHT), developed by Hoffmann, considers all of the valence electrons in the system, but it does not deal with the core electrons (those in orbitals below the valence shell).¹⁷⁰ The EHT wave function is then written as a linear combination of functions describing each type of valence orbital on each atom in the structure. For hydrocarbons, the EHT wave functions include the 2s and all three 2p atomic orbitals of carbon as well as the 1s orbitals of hydrogen atoms. The overlap integrals (S_{ij}) are computed, whereas they were ignored in HMO theory. The H_{ii} elements of the secular determinant are assigned a value corresponding to the negative of the average ionization potential of an electron in the associated valence orbital. (This is the same as in HMO theory, where α represented the negative of the ionization potential of the methyl radical.) The off-diagonal overlap integrals (H_{ij}) are approximated with a parameter that depends on the values of H_{ii} , H_{jj} , and S_{ij} .¹⁶⁸

As an example of the EHT method, consider the lowest energy MO (ψ_1) of ethene, as shown in equation 4.71.¹⁷¹

$$\begin{aligned} \psi_1 = & -0.419 2s_{C1} + 0.042 2p_{xC1} + 0.0 2p_{yC1} + 0.0 2p_{zC1} \\ & -0.419 2s_{C2} - 0.042 2p_{xC2} + 0.0 2p_{yC2} + 0.0 2p_{zC2} \\ & -0.153 1s_{H3} - 0.153 1s_{H4} - 0.153 1s_{H5} - 0.153 1s_{H6} \end{aligned} \quad (4.71)$$

Analysis of the coefficients of each atomic orbital in this wave function indicates that there are bonding interactions between the 2s orbitals on the carbon atoms with each other and with the 1s orbitals on the hydrogen atoms to which they are bonded. As shown in Figure 4.50, this combination of atomic orbitals produces a molecular orbital that encompasses all of the atoms in the molecule.

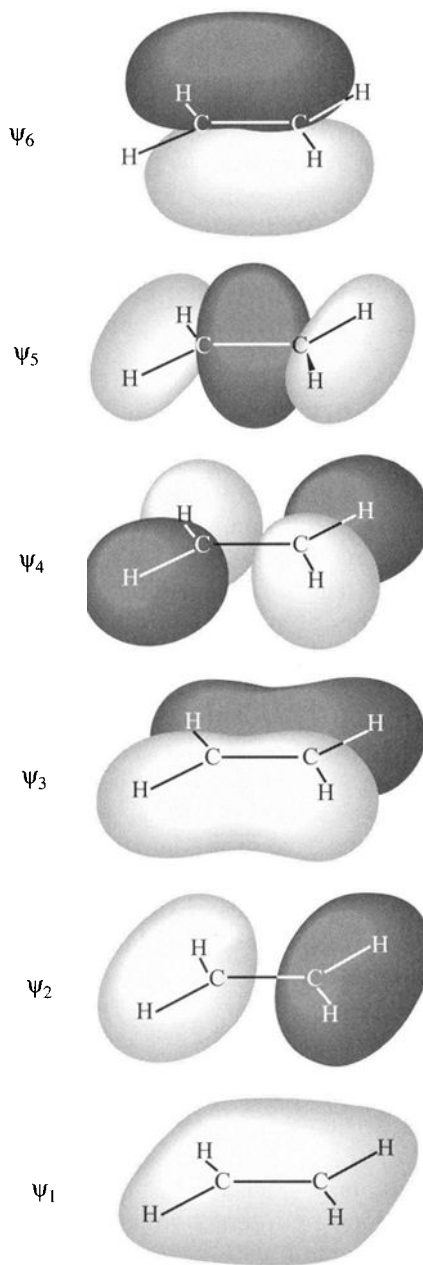
Figure 4.50 also shows the wave function for ψ_3 of ethene (equation 4.72) from the same EHT calculation. Now there are bonding interactions between the 2p_x orbitals on the carbon atoms with each other and with the 1s orbitals

¹⁶⁸ Cramer, C. J. *Essentials of Computational Chemistry: Theories and Models*, 2nd ed.; John Wiley & Sons: Chichester, 2004.

¹⁶⁹ For a glossary of terms that are used in theoretical organic chemistry, see Minkin, V. I. *Pure Appl. Chem.* **1999**, 71, 1919.

¹⁷⁰ Hoffmann, R. *J. Chem. Phys.* **1963**, 39, 1397.

¹⁷¹ Calculated with a CAChe™ WorkSystem.

**FIGURE 4.50**

Molecular orbitals of ethene calculated by extended Hückel theory.

on the hydrogen atoms to which each of the carbon atoms is bonded. Note that there is a nodal plane through the carbon atoms and perpendicular to the plane containing the carbons and hydrogens.

$$\begin{aligned}
 \psi_3 = & +0.0 \ 2s_{C1} + 0.0 \ 2p_{xC1} + 0.02 \ p_{yC1} - 0.255 \ 2p_{zC1} \\
 & + 0.0 \ 2s_{C2} + 0.0 \ 2p_{xC2} - 0.02 \ p_{yC2} - 0.355 \ 2p_{zC2} \\
 & + 0.267 \ 1s_{H3} - 0.267 \ 1s_{H4} + 0.267 \ 1s_{H5} - 0.267 \ 1s_{H6}
 \end{aligned} \quad (4.72)$$

The EHT HOMO of ethene is ψ_6 (equation 4.73). It is reassuring that this orbital includes contributions only from the $2p_y$ orbitals (which are perpendicular to the molecular plane in this calculation) and not from the other

orbitals. The shape of this MO (Figure 4.50) is very similar to the shape of the π bonding orbital of ethene determined earlier by a simple HMO calculation.

$$\begin{aligned} \psi_6 = & +0.0 2s_{C1} + 0.0 2p_{x_{C1}} - 0.612 2p_{y_{C1}} + 0.0 2p_{z_{C1}} \\ & + 0.0 2s_{C2} + 0.0 2p_{x_{C2}} - 0.612 2p_{y_{C2}} + 0.0 2p_{z_{C2}} \quad (4.73) \\ & + 0.0 1s_{H3} + 0.0 1s_{H4} + 0.0 1s_{H5} + 0.0 1s_{H6} \end{aligned}$$

Extended Hückel theory is a **semiempirical** method. That is, it has a theoretical foundation but uses some experimental data (the average ionization potentials) instead of solving some of the difficult mathematical functions exactly. Many other semiempirical methods have been developed, and several such methods continue to find wide application in organic chemistry. Among the procedures frequently used by organic chemists are AM1¹⁷² and PM3.¹⁷³ All of the semiempirical methods produce MOs based on combinations of valence shell orbitals only. The semiempirical methods differ from each other in the formalisms for handling some of the difficult overlap computations and also in the nature of the experimental data used to determine the optimum parameters in each method. Each method is parameterized to give good predictions for different sets of properties, such as heats of formation, geometry, spectroscopic transitions, and so on. As a result of this parameterization, each method also has its limitations. The appeal of semiempirical MO methodology is not that it is so accurate, except perhaps for problems very closely related to the structures used in its parameterization, but that it is computationally accessible. Therefore, it is important for the organic chemist to choose a method that is known to produce reliable results for the problem of interest.¹⁶⁸

An alternative to using semiempirical MO methods is to use *ab initio* (from the Latin for “from the beginning”) methods that consider all of the electrons in the system (not just the valence electrons) and that compute all of the complex integrals that arise during the calculation. *Ab initio* theory is built on Hartree–Fock (HF) theory.¹⁷⁴ That means that it is based on the Born–Oppenheimer approximation and that it assumes that each electron sees all of the other electrons in an average field.¹⁷⁵ Thus, it inherently neglects electron correlation, which is the tendency of electrons to minimize their mutual repulsion. *Ab initio* methods are much more demanding of computational resources than are semiempirical methods, but they are becoming more widely used due to advances in computing technology and the development of efficient mathematical procedures.^{176–178} In the Hartree–Fock method,

¹⁷² Dewar, M. J. S.; Zoebisch, E. G.; Healy, E. F.; Stewart, J. J. P. *J. Am. Chem. Soc.* **1985**, *107*, 3902.

¹⁷³ Stewart, J. J. P. *J. Comput. Chem.* **1989**, *10*, 209, 221. An extension known as PM6 was developed primarily for modeling biochemical structures: Stewart, J. J. P. *J. Mol. Model.* **2007**, *13*, 1173; **2008**, *14*, 499.

¹⁷⁴ For a review of the foundations of Hartree–Fock theory, see Echenique, P.; Alonso, J. L. *Mol. Phys.* **2007**, *105*, 3057.

¹⁷⁵ The Born–Oppenheimer approximation simplifies quantum mechanical calculations by considering the electronic wave function for a structure separately from that of the nuclei: Born, M.; Oppenheimer, J. R. *Ann. Phys.* **1927**, *84*, 457.

¹⁷⁶ Richards, W. G.; Cooper, D. L.; *Ab Initio Molecular Orbital Calculations for Chemists*, 2nd ed.; Clarendon Press: Oxford, England, 1983.

¹⁷⁷ For a commentary, see Davidson, E. R. in Lipkowitz, K. B.; Boyd, D. B., Eds. *Reviews in Computational Chemistry*; VCH Publishers: New York, 1990; p. 373.

¹⁷⁸ For an overview of *ab initio* molecular dynamics (Chapter 3) calculations, see Ifimie, R.; Minary, P.; Tuckerman, M. E. *Proc. Natl. Acad. Sci. U.S.A.* **2005**, *102*, 6654.

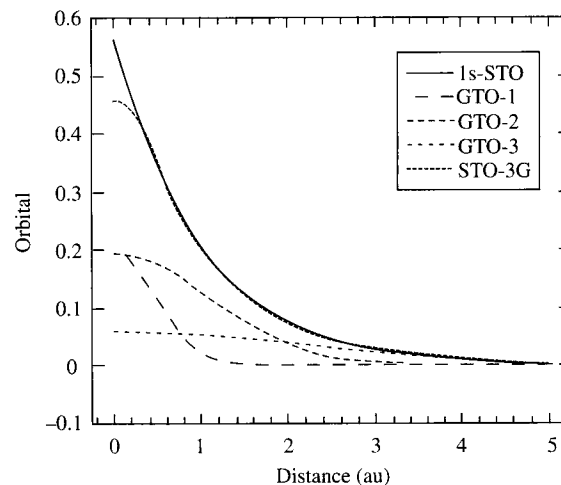


FIGURE 4.51

STO for a 1s basis function (solid line) and the STO-3G function (densely hashed line) formed from three GTOs. (Reproduced from reference 185.)

molecular orbitals are constructed as linear combinations of atomic orbitals, and the molecular orbitals are then optimized for energy by an SCF (self-consistent field) procedure.^{179,180} This means that the initial set of molecular orbitals is used to calculate a new set of molecular orbitals, and the process is repeated until the molecular orbitals no longer change. At that point the molecular orbitals have converged and the calculation is said to be self-consistent.¹⁰

Each HF molecular orbital is written as a linear combination of functions describing atomic orbitals. The entire set of such equations for the atomic orbitals in a molecule is called a basis set, and each equation is called a basis set function.¹⁸¹ Ideally, these basis set functions would have the properties of hydrogenic wave functions, particularly with regard to the radial dependence of electron density probability as a function of distance of the electron from the nucleus, r . A type of basis set function proposed by Slater uses a radial component incorporating $e^{-\alpha r}$, and such functions are called **Slater type orbitals (STOs)**. **Gaussian type orbitals (GTOs)** have $e^{-\alpha r^2}$ radial dependence and are easier to solve analytically, but they do not describe the radial dependence of electron density as well as do the STOs.

An effective trade-off between speed and accuracy in HF calculations is to use basis sets in which a linear combination of GTOs is used to approximate an STO. Figure 4.51 shows the radial dependence of a 1s-STO (solid line), three different GTOs (dashed lines), and the combination of those GTOs to produce a function that models the STO rather well except for distances very close to the nucleus. The linear combination of the three GTOs is thus indicated as STO-3G, meaning that it is constructed from three Gaussian "primitives" (GTOs). For some purposes, the STO-3G basis set provides an acceptable

¹⁷⁹ Roothaan, C. C. J. *Rev. Mod. Phys.* **1951**, 23, 69 and later papers.

¹⁸⁰ Davidson and Feller reviewed basis set selection for molecular calculations: Davidson, E. R.; Feller, D. *Chem. Rev.* **1986**, 86, 681; Feller, D.; Davidson, E. R. in Lipkowitz, K. B.; Boyd, D. B., Eds. *Reviews in Computational Chemistry*; VCH Publishers: New York, 1990; p. 1. For "an experimental chemist's guide to *ab initio* quantum chemistry," see Simons, J. *J. Phys. Chem.* **1991**, 95, 1017.

¹⁸¹ Quinn, C. M. *Computational Quantum Chemistry: An Interactive Guide to Basis Set Theory*; Academic Press: San Diego, 2002.

balance of computational accuracy and calculation time, but many calculations require much more complicated basis sets.

In theory there is no limit to the number of functions that could be included in a basis set. Indeed, theoreticians often refer to the "Hartree–Fock limit" as the energy that would be calculated for a system if an infinite number of basis functions were included in the calculation. That energy would still be greater than the energy of the molecular system, however, because the HF method cannot account for the additional stabilization to be gained through electron correlation. Nevertheless, HF calculations can provide very useful information if the electron correlation errors cancel when one compares one system to another. This is more likely to be the case for isodesmic reactions, in which types of bonds are the same in both the reactant and product.¹⁶⁸

There are several "post-Hartree-Fock" methods that were developed to account for electron correlation. One approach is called **configuration interaction (CI)**, which is a term for the mixing of electronic configurations (i.e., patterns of orbital populations), including configurations corresponding to states other than the ground electronic state. A method known as complete active space SCF (CASSCF) considers all of the configurations that can arise from placing the available electrons in the various molecular orbitals. In coupled cluster theory, different kinds of excited configurations are grouped together.¹⁸² For example, CCSD(T) means that single and double excitations are fully incorporated and triple excitations are treated indirectly. Another approach developed by Møller and Plesset is denoted MP_n , where the n indicates the level of the treatment (MP2, MP3, etc.). Commercially available software packages may provide the chemist with a number of options for handling electron correlation. There is an important trade-off between time and accuracy in ab initio calculations, and it is necessary to determine what computational resources can be allocated to a particular problem.

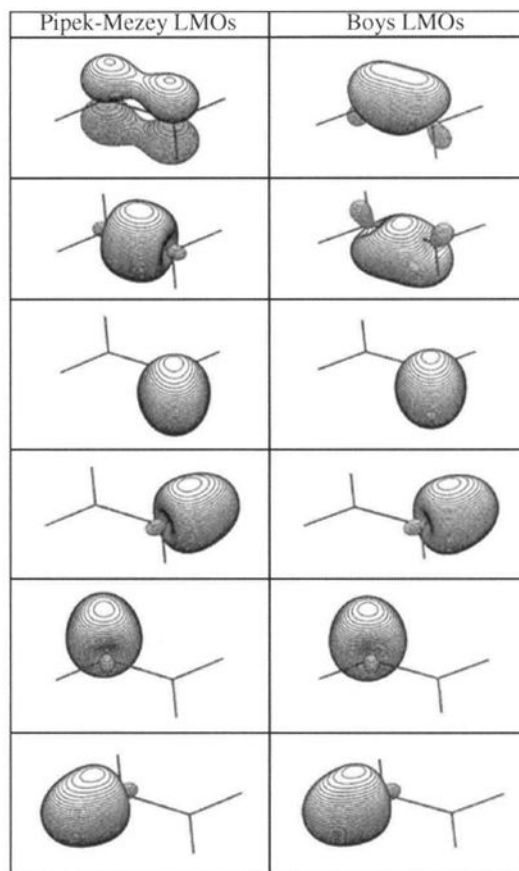
The molecular orbitals determined from Hartree–Fock theory are *canonical* (standard) MOs and therefore are delocalized over the structure. It is possible to transform the set of canonical MOs into an alternative set of **localized molecular orbitals (LMOs)** that are restricted to certain atoms. These LMOs have the advantage of indicating more directly which atoms are bonded to each other and also of being "chemically invariant" after a structural change at a distant location in the molecule.¹⁸³ There are several approaches for transforming canonical MOs into LMOs. These methods generally produce equivalent results for many types of structures, but they can give different results for systems with double bonds or nonbonded electron pairs. For example, Figure 4.52 shows the LMOs of ethene calculated by the Pipek–Mezey method¹⁸⁴ and by the Boys method.¹⁸³ The four LMOs associated with C–H bonding are very similar, but one method produces C–C bonding MOs that resemble σ and π orbitals, while the other produces LMOs that resemble the bent bonds discussed in Chapter 1.¹⁸⁵ It is important to note in this context that LMOs represent only a convenient repackaging of the

¹⁸² Crawford, T. D.; Schaefer, H. F. III. *Rev. Comp. Chem.* **2000**, *14*, 33.

¹⁸³ Boys, S. F. *Rev. Mod. Phys.* **1960**, *32*, 269.

¹⁸⁴ Pipek, J.; Mezey, P. G. *J. Chem. Phys.* **1989**, *90*, 4916.

¹⁸⁵ Jensen, F. *Introduction to Computational Chemistry*, 2nd ed.; John Wiley & Sons: Chichester, UK, 2007.

**FIGURE 4.52**

LMOs for ethene from two localization methods. (Reproduced from reference 185.)

information available from the full set of occupied canonical MOs and that LMOs do *not* indicate any change in the overall electron density or bonding of the molecule.

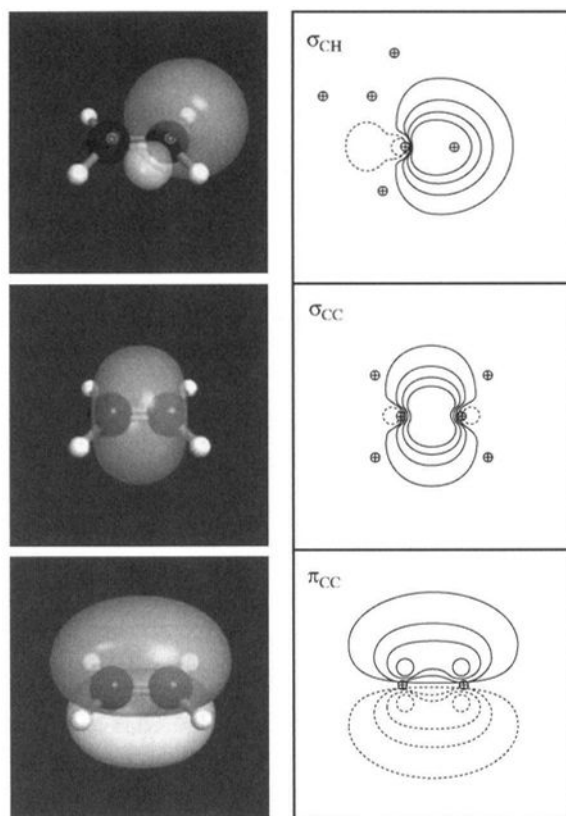
Similarly, the orbitals determined in both semiempirical and Hartree-Fock calculations may be transformed into **natural bond orbitals** (NBOs), which provide pictures of localized bonds and lone pairs that correspond closely with Lewis structure bonding models.^{186,187} For example, Figure 4.53 shows the NBOs for ethene σ_{CH} , σ_{CC} , and π_{CC} bonds.

Perturbational Molecular Orbital Theory

There is another extension of molecular orbital theory that organic chemists find quite useful. Perturbational molecular orbital (PMO) theory provides an estimate of the change in electronic energy levels and molecular orbitals that result from the interaction of one structure or molecular fragment having

¹⁸⁶ Foster, J. P.; Weinhold, F. *J. Am. Chem. Soc.* **1980**, *102*, 7211; Reed, A. E.; Curtiss, L. A.; Weinhold, F. *Chem. Rev.* **1988**, *88*, 899.

¹⁸⁷ Weinhold, F.; Landis, C. R. *Valency and Bonding: A Natural Bond Orbital Donor-Acceptor Perspective*; Cambridge University Press: Cambridge, UK, 2005.

**FIGURE 4.53**

Valence NBOs of ethene showing σ_{CH} (top), σ_{CC} (middle), and π_{CC} (bottom) bonds as electron density surface (left) and contour (right) views. (Reproduced from reference 187.)

known MOs with another structure or fragment having known MOs.¹⁸⁸ In a sense this process allows us to produce molecular orbitals by taking a linear combination of *molecular* orbitals, which is only a variation of the process of taking a linear combination of *atomic* orbitals (LCAOs). We are not so much seeking a complete MO description of the new structure, however, as we are trying to find the difference in energy between the new structure and the starting structures. This approach has an intuitive appeal because, as Lowe noted, “most chemists think perturbatively.” That is, they ask how the properties of a known substance will change if the structure is altered in some way.¹⁸⁹

Let us consider first a simple case involving the joining of two components, each of which has a single molecular orbital that will perturb (and be perturbed by) the molecular orbital of the other component. The MO of fragment *i* before the interaction is ψ_i^0 , and its energy is E_i^0 . The MO of fragment *j* before the interaction is ψ_j^0 , and its energy is E_j^0 . We also assume that the two energy levels are not degenerate and that $E_i^0 < E_j^0$. The Hamiltonian of the

¹⁸⁸ For a general introduction to PMO theory and its applications, see Dewar, M. J. S.; Dougherty, R. C. *The PMO Theory of Organic Chemistry*; Plenum Press: New York, 1975. See also Freeman, F. J. *Chem. Educ.* **1978**, 55, 26; Cooper, C. F. *J. Chem. Educ.* **1979**, 56, 568; Smith, W. B. *J. Chem. Educ.* **1971**, 48, 749; Whangbo, M.-H. in Csizmadia, I. G.; Daudel, R., Eds. *Computational Theoretical Organic Chemistry*; D. Reidel Publishing Company: Boston, 1981; pp. 233–252; Herndon, W. C. *J. Chem. Educ.* **1979**, 56, 448; Durkin, K. A.; Langler, R. F. *J. Phys. Chem.* **1987**, 91, 2422.

¹⁸⁹ Lowe, J. P.; Kafafi, S. A.; LaFemina, J. P. *J. Phys. Chem.* **1986**, 90, 6602.

initial system is \mathcal{H}° , and the new Hamiltonian of the perturbed system, \mathcal{H} , is $(\mathcal{H}^\circ + \mathcal{H}')$. The energy of the i th MO (E_i') after the perturbation will be

$$E_i' = E_i^\circ + \frac{|H'_{ij}|^2}{E_i^\circ - E_j^\circ} \quad (4.74)$$

Here H'_{ij} is given by equation 4.75.

$$H'_{ij} = \int \psi_i^\circ \mathcal{H} \psi_j^\circ d\tau \quad (4.75)$$

Since $E_i^\circ < E_j^\circ$, the second term on the right in equation 4.74 is a negative quantity. Therefore, $E_i' < E_i^\circ$, meaning that the perturbation has lowered the energy of the i th level. We also have

$$E_j' = E_j^\circ + \frac{|H'_{ij}|^2}{E_j^\circ - E_i^\circ} \quad (4.76)$$

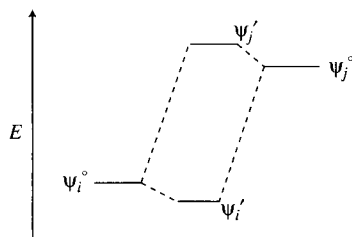


FIGURE 4.54

Effect of interaction on two nondegenerate orbitals.

Again, $E_i^\circ < E_j^\circ$, so the difference $E_j^\circ - E_i^\circ$ is a positive quantity. Therefore, $E_j' > E_j^\circ$, meaning that the perturbation has raised the energy of the j th level. Thus, the interaction raises the higher energy level and decreases the lower energy level, as shown in Figure 4.54.

Let us now consider the case of a perturbation involving the union of two systems having several nondegenerate orbitals.¹⁹⁰ The set of wave functions describing the system is ψ_n° , and their energy levels are E_n° . Now we introduce the perturbation, and again we represent the new Hamiltonian for the system, \mathcal{H} , as $(\mathcal{H}^\circ + \mathcal{H}')$. E_i , the energy of the i th MO after its interaction with the MOs of the other fragment, is given by equation 4.77.

$$E_i = E_i^\circ + \sum_{ij} \frac{|H'_{ij}|^2}{E_i^\circ - E_j^\circ} \quad (4.77)$$

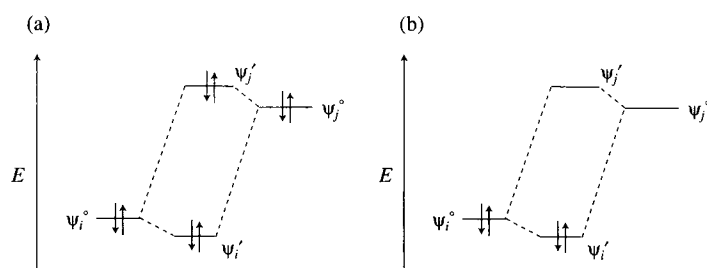
Here E_i° is the energy of the i th wave function before the perturbation and, as before,

$$H'_{ij} = \int \psi_i^\circ \mathcal{H} \psi_j^\circ d\tau \quad (4.75)$$

Equation 4.77 tells us that the changes in energy levels and wave functions can be predicted by determining the effect on E_i of the interaction of ψ_i with *each* of the wave functions of the perturbing system. In other words, the perturbations are "pairwise additive."

The calculation to this point has considered only the effect of a perturbation on the energies of molecular orbitals. The effect of a perturbation on the energy and electron distribution of a molecular structure will depend on the population of electrons in the energy levels that are perturbed. Figure 4.55

¹⁹⁰ Hoffmann, R. *Acc. Chem. Res.* **1971**, *4*, 1.

**FIGURE 4.55**

PMO interactions: (a) both ψ_i^o and ψ_j^o are doubly occupied; (b) only ψ_j^o is doubly occupied.

shows two situations of interest. In Figure 4.55(a), there are two electrons in ψ_i and two electrons in ψ_j . To the first approximation, the perturbation lowers the energy of ψ_i as much as it raises the energy of ψ_j . Since there are two electrons in ψ_i and two in ψ_j , the perturbation causes no net change in the energy of the system. In Figure 4.55(b) there are two electrons in ψ_i and no electrons in ψ_j . Therefore, there is a net lowering of the energy of the system, since this perturbation allows those two electrons to be in a more stable molecular orbital. Moreover, those electrons are now delocalized over the entire system.

The simple molecular orbital energy level diagrams in Figure 4.55 show only one orbital on each of the molecular fragments. In general, there will be many orbitals, some populated with electrons and some vacant. The highest occupied molecular orbital in a π system is called the **HOMO**, while the lowest unoccupied molecular orbital is called the **LUMO**.¹⁹¹ If there are noninteracting MOs lower in energy than ψ_i and ψ_j in Figure 4.55, then it is the interaction between the HOMO of fragment j and the LUMO of fragment i that determines the energy change of the union. The HOMO and LUMO of a molecular system are sometimes called the **frontier molecular orbitals (FMOs)**, since they are the orbitals from which it is easiest to remove an electron (HOMO) or add an electron (LUMO), and thus they are often involved in important chemical processes.^{40,192,193}

One process that can be described by FMO theory is the formation of a complex between two different molecules. The interaction occurs when the two structures come close enough together that their molecular orbitals can overlap. Complex formation then results in transfer of electron density from an orbital localized on fragment j to an orbital of the perturbed system that has electron density both on fragment i and fragment j (Figure 4.55(b)). Therefore, this type of interaction is called charge transfer complex or **electron donor-acceptor complex** formation.¹⁹⁴ An alternative representation of the process is depicted in equation 4.78. Charge transfer complexes may be characterized by the appearance of new UV-vis absorptions at frequencies that can be correlated by the Mulliken relationship: $h\nu = \text{IP} - \text{EA} - \omega$, where IP is the ionization potential of the electron donor, EA is the electron affinity of the

¹⁹¹ For radicals, a singly occupied molecular orbital is called a **SOMO**.

¹⁹² Another acronym for this approach is FO (frontier orbital) theory. The acronym FMO is also used for the fragment molecular orbital method. See, for example, Fedorov, D. G.; Kitaura, K. J. *Phys. Chem. A* **2007**, *111*, 6904.

¹⁹³ For a discussion of the scope and limitations of frontier orbital theory, see Anh, N. T.; Maurel, F. *New J. Chem.* **1997**, *21*, 861; Anh, N. T. *Frontier Orbitals: A Practical Manual*; John Wiley & Sons: Chichester, UK, 2007.

¹⁹⁴ Murrell, J. N. Q. *Rev. Chem. Soc.* **1961**, *15*, 191; Bender, C. J. *Chem. Soc. Rev.* **1986**, *15*, 475.

acceptor, and ω is the interaction energy between the two species in the charge transfer state.¹⁹⁵

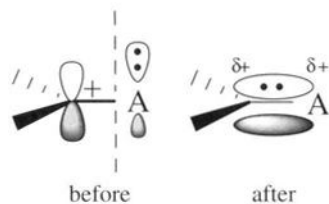


FIGURE 4.56

PMO analysis of the stabilization of a carbocation by an adjacent nonbonded pair.

An intramolecular example of the interaction in Figure 4.55(b) is the stabilization of a carbocation by an adjacent atom bearing a nonbonded pair of electrons. The structure on the left in Figure 4.56 represents the initial system, in which an artificial barrier represented by the dashed line prevents the interaction of the carbocation center with the adjacent nonbonded pair. In this case, ψ_i^0 is a nonbonding orbital on the atom with the electron pair, and ψ_j^0 is the empty p orbital of the carbocation. The interaction thus moves some electron density from an orbital that was localized on fragment i onto the carbocation carbon, fragment j , and lowers the energy of the structure. This is the same interaction that organic chemists would describe using resonance theory as shown in Figure 4.57.

A methyl group bonded to a carbocation center can also stabilize the carbocation, and the order of carbocation stabilities is $3^\circ > 2^\circ > 1^\circ > \text{methyl}$. One of the familiar rationalizations for this pattern is the idea that methyl groups are electron donating by a process called **hyperconjugation**.¹⁹⁶ The resonance description of this interaction, shown in Figure 4.58, is exactly parallel to that shown in Figure 4.57. The only difference is that the pair of electrons donated to the carbocation is not a lone pair but, instead, a pair of electrons drawn as a C-H bond. There is something unsettling about drawing a resonance structure that appears to show a proton no longer bonded to the rest of the structure. It is important to remember, however, that the resonance structure on the right in Figure 4.58 does not represent a real chemical species—and neither does the resonance structure on the left. Rather, Figure 4.58 is the valence bond representation of the delocalization of electrons in the C-H bond toward the carbocation center.

It is possible to describe the stabilization of a carbocation by an adjacent methyl group in a more familiar way with PMO theory by using a localized molecular orbital to represent the electron density associated with C-H σ bonding. The structure on the left in Figure 4.59 represents the nondelocalized carbocation, while the structure on the right shows the effect of the interaction described in Figure 4.55(b). Exactly as was the case in Figure 4.56, the

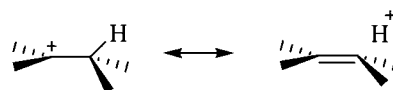
FIGURE 4.57

Resonance description of the stabilization of a carbocation by an adjacent nonbonded pair.



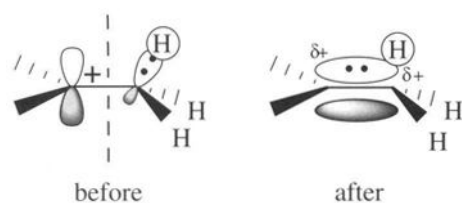
FIGURE 4.58

Hyperconjugation model for the stabilization of a carbocation by an adjacent C-H bond.



¹⁹⁵ Tsubomura, H.; Mulliken, R. S. *J. Am. Chem. Soc.* **1960**, *82*, 5966. See also Foster, R. *Organic Charge-Transfer Complexes*; Academic Press: New York, 1969.

¹⁹⁶ Mulliken, R. S.; Rieke, C. A.; Brown, W. G. *J. Am. Chem. Soc.* **1941**, *63*, 41.

**FIGURE 4.59**

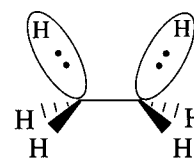
PMO analysis of the stabilization of a carbocation by an adjacent methyl group.

perturbation moves electron density onto the fragment that had the empty MO (the p orbital of the carbocation) and lowers the total energy of the structure.

Let us now apply the concepts of hyperconjugation and PMO theory to the torsional energy of ethane. As noted in Chapter 3, the eclipsed conformation is about 2.9 kcal/mol higher in energy than the staggered conformation. For much of the recent history of organic chemistry, the barrier was attributed to a steric interaction of the C-H bonds on one end of the molecule with those on the other end. The term *steric interaction* actually describes two closely related but different effects. One of these is a Coulombic interaction resulting from the repulsion of negatively charged electrons located near each other in space. The other is a quantum mechanical effect that arises when two doubly occupied orbitals are pushed together. In order to avoid a violation of the Pauli exclusion principle, the orbitals are forced to adopt high energy configurations to ensure their orthogonality.¹⁹⁷ It is the Pauli repulsion component of steric strain that was thought to be primarily responsible for the torsional barrier in ethane.¹⁹⁸ This interaction is greatest when the two C-H bonds are in the same plane (Figure 4.60) but is minimized when the H-C-C-H dihedral is 60°. This explanation for the torsional energy of ethane was not universally accepted, however. In particular, Eliel and Wilen argued against a steric basis for the torsional barrier because in the eclipsed conformation the distance between hydrogen atoms on C1 and the hydrogen atoms on C2 is barely less than the sum of their van der Waals radii.¹⁹⁹

An alternative explanation for the rotational barrier in ethane is that it results not from steric *destabilization* of the eclipsed conformation but, instead, from *stabilization* of the staggered conformation arising from a hyperconjugation interaction involving C-H σ bonding electrons (Figure 4.61). As with Figure 4.58, Figure 4.61 is simply the resonance theory model for a process that allows electrons associated with carbon-hydrogen bonding to provide additional carbon-carbon bonding. This interaction is not as favorable in the eclipsed conformation of ethane, so the staggered conformation is lower in energy.²⁰⁰

It is informative to consider the PMO description of the process leading to stabilization of the staggered conformation. Now the filled C-H bonding orbital on one of the ethane carbon atoms donates electron density to an (empty) C-H antibonding orbital on the other carbon atom. Figure 4.62 shows the filled ($\sigma_{\text{C-H}}$) and empty ($\sigma_{\text{C-H}}^*$) orbitals *before* the perturbation for the staggered conformation (left) and eclipsed conformation (right). There is

**FIGURE 4.60**

Pauli repulsion due to a pair of eclipsed C-H bonds.

¹⁹⁷ Weinhold, F. *Nature* **2001**, 411, 539.

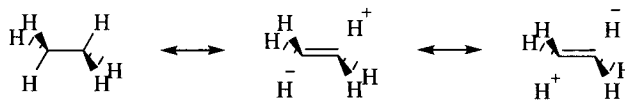
¹⁹⁸ Sovers, O. J.; Kern, C. W.; Pitzer, R. M.; Karplus, M. *J. Chem. Phys.* **1968**, 49, 2592.

¹⁹⁹ Eliel, E. L.; Wilen, S. H. *Stereochemistry of Organic Compounds*; John Wiley & Sons: New York, 1994.

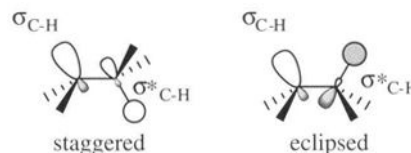
²⁰⁰ Alabugin, I. V.; Zeidan, T. A. *J. Am. Chem. Soc.* **2002**, 124, 3175.

FIGURE 4.61

Proposed hyperconjugation interaction in staggered ethane.

**FIGURE 4.62**

PMO description of the greater stabilization of the staggered conformation of ethane. (Adapted from reference 202.)



better overlap between the filled and unfilled orbitals in the staggered conformation than in the eclipsed conformation, so the interaction is more stabilizing in the staggered conformation.

The PMO interactions represented on the left in Figure 4.62 were supported by the results of a natural bond orbital analysis by Pophristic and Goodman, who calculated that the eclipsed conformation of ethane would be *lower* in energy than the staggered conformation if the hyperconjugation interaction did not occur.²⁰¹ Their conclusion that the lower energy of the staggered conformation must be due to the stabilizing effect of hyperconjugation was supported by some other studies.^{202–204} Results of other investigators, however, were taken as support for the steric basis for conformational energy differences.^{205,206} Interestingly, Mo and co-workers reported theoretical results indicating that *both* steric and hyperconjugation effects influence the torsional barrier in ethane. They concluded that about one-third of the energy barrier could be attributed to hyperconjugative stabilization of the staggered conformation, but most of the barrier was ascribed to steric repulsion in the eclipsed conformation.^{207–209}

Atoms in Molecules

Molecular orbital theory assumes a set of nuclei held together by a collection of electrons. This is a rather different view of matter from the intuitive view that molecules are made of atomic centers held together by electron pair bonds. There is a theoretical method that allows one to recover the concepts of atoms and bonds in chemical structures, and it does so in a rigorous, mathematical way. The approach was developed by Bader and co-workers and is known as atoms in molecules (AIM) or the quantum theory of atoms in

²⁰¹ Pophristic, V.; Goodman, L. *Nature* **2001**, *411*, 565.

²⁰² Schreiner, P. R. *Angew. Chem. Int. Ed. Engl.* **2002**, *41*, 3579

²⁰³ Weinhold, F. *Angew. Chem. Int. Ed. Engl.* **2003**, *42*, 4188. See also reference 187.

²⁰⁴ Juaristi, E.; Cuevas, G. *Acc. Chem. Res.* **2007**, *40*, 961.

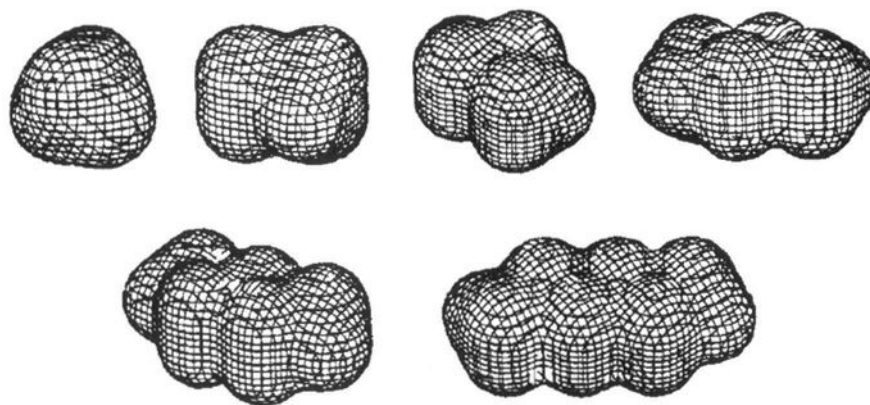
²⁰⁵ Bickelhaupt, F. M.; Baerends, E. J. *Angew. Chem. Int. Ed. Engl.* **2003**, *42*, 4183.

²⁰⁶ Bohn, R. K. *J. Phys. Chem. A* **2004**, *108*, 6814.

²⁰⁷ Mo, Y.; Wu, W.; Song, L.; Lin, M.; Zhang, Q.; Gao, J. *Angew. Chem. Int. Ed. Engl.* **2004**, *43*, 1986.

²⁰⁸ Mo, Y.; Gao, J. *Acc. Chem. Res.* **2007**, *40*, 113.

²⁰⁹ See also Liu, S.; Govind, N. *J. Phys. Chem. A* **2008**, *112*, 6690; Pendás, A. M.; Blanco, M. A.; Francisco, E. J. *Comput. Chem.* **2008**, *30*, 98.

**FIGURE 4.63**

The 0.001 au density envelopes of methane, ethane, propane, butane, pentane, and hexane. (Adapted from reference 216.)

molecules (QTAIM).^{210–214} Beginning with the three-dimensional electron density of a structure, $\rho(\mathbf{r})$, which can be obtained from either experimental measurement or theoretical calculations, the total molecular volume is defined as that volume of space included within a surface having a set electron density. For gas phase measurements this is typically chosen as $\rho(\mathbf{r}) = 0.001$ au because this surface incorporates over 99% of the electron density, and the volume within approximates the gas phase van der Waals volume of the structure.²¹⁵ For example, Figure 4.63 shows the isodensity surfaces determined for the linear alkanes from methane through hexane.²¹⁶ An organic chemist can instinctively map these shapes to the methyl and methylene units of the structures.

The surfaces shown in Figure 4.63 are called isodensity surfaces because the electron density is the same at all points on that surface. Within that surface, however, the electron density varies from one point in space to another. Figure 4.64 shows representations of the variation in the electron charge density in the ethene molecule as determined for three different slices through the molecular volume. Slice (a) is the plane of the molecule and passes through both carbon nuclei and all four hydrogen nuclei. Slice (b) is perpendicular to the first plane. It passes through the two carbon nuclei and bisects each of the H–C–H bond angles. Slice (c) is perpendicular to each of the other two planes and passes through the center of the carbon–carbon bond. The variation in electron density for each cross section of molecular volume is represented as a three-dimensional topographical map on the left and as a contour plot on the right. Contour lines around the nuclei indicate the increase in electron density from the outer surface of the molecule toward the nuclei. The three-dimensional representations provide a sense of scale for the contour plots and emphasize the much greater electron charge density near the carbon atoms than near the hydrogen atoms. (The flattened tops of the

²¹⁰ Bader, R. F. W.; Nguyen-Dang, T. T.; Tal, Y. *Rep. Prog. Phys.* **1981**, *44*, 893.

²¹¹ Bader, R. F. W. *Atoms in Molecules: A Quantum Theory*; Clarendon Press: Oxford, 1990.

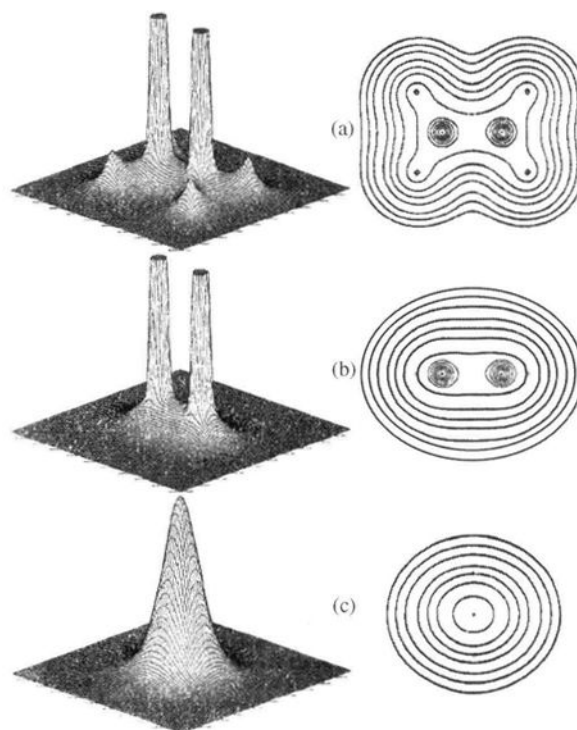
²¹² Bader, R. F. W.; Hernández-Trujillo, J.; Cortés-Guzman, F. J. *Comput. Chem.* **2007**, *28*, 4.

²¹³ Matta, C. F.; Boyd, R. J. *The Quantum Theory of Atoms in Molecules: From Solid State to DNA and Drug Design*; Wiley-VCH: Weinheim, 2007.

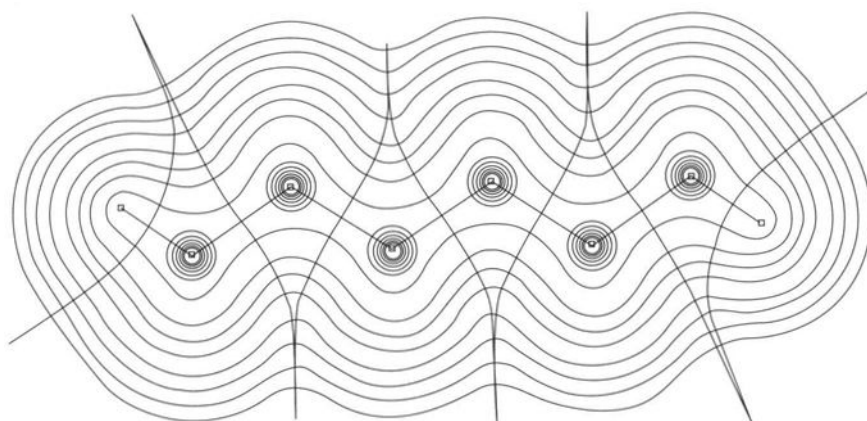
²¹⁴ Bader, R. F. W. *J. Phys. Chem. A* **2007**, *111*, 7966.

²¹⁵ 1.000 au equals 6.748 e/Å. A 0.002 electron density surface is a better match for van der Waals radii of molecules in the condensed phase.

²¹⁶ Bader, R. F. W.; Carroll, M. T.; Cheeseman, J. R.; Chang, C. J. *Am. Chem. Soc.* **1987**, *109*, 7968.

**FIGURE 4.64**

Representations of the electron charge density in three planes through ethene. (Reproduced from reference 210.)

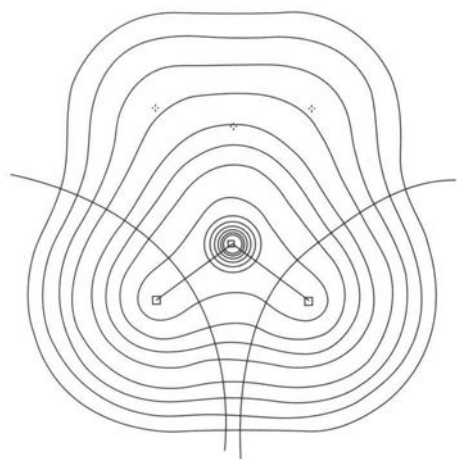
**FIGURE 4.65**

Contour map of the electron density in the "zigzag" conformation of hexane. (Adapted from reference 216.)

electron charge density for the carbon atoms in the three-dimensional drawings result from truncating the drawing to make it fit into the space available.)

Let us consider hexane again and view a contour plot for a cross section through the molecule in which the plane of the drawing includes all of the carbon nuclei and two of the hydrogen nuclei in the fully extended, "zigzag" conformation of the molecule (Figure 4.65). A cross section (passing through one methylene carbon) that is oriented perpendicular to this plane is shown in Figure 4.66.

In addition to the electron density contour lines in Figures 4.65 and 4.66, there are also essentially straight lines connecting the nuclei. Each of these lines indicates a **bond path**, which follows the path of maximum electron density from one nucleus to another. The concept of a bond path is thus quite

**FIGURE 4.66**

Contour map of the electron density of hexane in a plane perpendicular to that of Figure 4.65 (Adapted from reference 216.)

consistent with intuitive ideas about a chemical bond. In unstrained molecules the bond paths are straight lines, but in strained molecules, such as cyclopropane, the bond path curves away from the straight internuclear line.²¹⁷ The entire set of bond path lines for a structure comprises the molecular graph of the molecule.

Also shown in the figures are gradient lines that cross the bond path lines between the nuclei. The point of intersection of a gradient line with the bond path line indicates a **bond critical point (bcp)**. These gradient lines indicate the path of steepest ascent in the electron density and are thus perpendicular to each contour line and bond path in the infinitesimal region near the line intersections.²¹⁸ The effect of the gradient lines is to divide the electron density *in the plane shown* into areas that can reasonably be assigned to a nucleus encompassed by the gradient line and the outer isodensity surface contour line of the molecule. The total electron density at the bond critical point indicates the order of the bond between two nuclei, and bond orders correlate with bond lengths.²¹⁹ The distance from a nucleus to a bond critical point defines a bonded radius of the atom. If the bond is straight, the distance between the nuclei corresponds to the sum of the bonded radii of the two atoms.

If we now imagine the contour plots in Figures 4.65 and 4.66 as simultaneous cross sections through the three-dimensional isodensity surface of hexane in Figure 4.63, we recognize that the gradient lines in these figures are part of a surface composed of an infinite number of such gradient lines through the molecular volume. These internal surfaces along with the isodensity surface on the exterior of the molecule carve out segments of molecular volume containing exactly one nucleus. The volume of space inside each of these segments is termed an atomic volume, thus giving rise to the concept of atoms in molecules. Further detailed analysis of these atomic volumes can yield predictions of a wide variety of molecular properties.²²⁰

²¹⁷ Grimme, S. J. *Am. Chem. Soc.* **1996**, *118*, 1529.

²¹⁸ Runtz, G. R.; Bader, R. F. W.; Messer, R. R. *Can J. Chem.* **1977**, *55*, 3040.

²¹⁹ Bader, R. F. W.; Tang, T.-H.; Tal, Y.; Biegler-König, F. W. *J. Am. Chem. Soc.* **1982**, *104*, 946.

²²⁰ Mosquera, R. A.; González Moa, M. J.; Graña, A. M.; Mandado, M.; Vila, A. in Arnold, S. V., Ed. *Chemical Physics Research Trends*; Nova Science Publishers: New York, 2007.

This discussion has been deliberately qualitative in order to avoid complicating the fundamental concepts of QTAIM with the mathematical equations necessary to describe it completely. Further details of the theory and its applications are detailed in the references. The point to be made here is that there is a way to reconnect the results of molecular orbital theory with the familiar concepts of structure and bonding that have served organic chemists well. The QTAIM approach is not yet available in computational packages readily accessible to organic chemists, however.

Density Functional Theory

Most of the ideas of molecular orbital theory are familiar to organic chemists, even if the details of modern computational methods remain somewhat obscure. A very different and often less familiar approach to calculating structure and properties known as **density functional theory** (DFT) has become prominent in recent years.^{221–224} DFT calculates an observable property, electron density, instead of a nonobservable entity, a molecular orbital. It is important to note that a *functional* is not the same as a *function*. A function acts on a set of variables to produce a number, but a functional acts on another function to produce a number. For example, a wave function is a function, but the dependence of energy on a wave function is a functional. A function is denoted $f(x)$, while a functional is denoted $F[f]$.¹⁸⁵

The essential concepts of DFT are that the integral of electron density gives the number of electrons in a chemical system, that the local maxima in the density show the locations of the nuclei, and that the magnitudes of these maxima indicate the nuclear charges and thus the identity of the nuclei. Hohenberg and Kohn demonstrated that the ground state electronic energy of a structure is determined entirely by the electron density,^{225a} so each different density for a structure results in a different ground state energy. Moreover, the electron density determines the external potential, which in turn determines the Hamiltonian for the system, and it then determines the wave function, from which the energy can be computed.¹⁶⁸

Kohn and Sham proposed that the kinetic energy of the electrons could be calculated from a set of orbitals, χ , which are expressed with a basis set of functions for which the individual orbital coefficients are determined in a manner somewhat similar to that used to determine the coefficients of the orbitals in HF theory.^{225b} DFT thus becomes a self-consistent procedure in which one starts with a hypothetical system of noninteracting electrons that have the same electron density as the system of interest, determines the corresponding wave functions, and uses the variational principle to minimize the energy of the system and produce a new electron density. That density serves as a basis for a new iteration of the procedure, and the process is repeated until convergence is achieved.

The energy functional in DFT has several components, some of which can be determined in straightforward fashion. The “exchange-correlation”

²²¹ Bartolotti, L. J.; Flurchick, K. *Rev. Comp. Chem.* **1996**, *7*, 187.

²²² Kohn, W.; Becke, A. D.; Parr, R. G. *J. Phys. Chem.* **1996**, *100*, 12974.

²²³ Bickelhaupt, F. M.; Baerends, E. J. *Rev. Comp. Chem.* **2000**, *15*, 1.

²²⁴ Geerlings, P.; De Proft, F.; Langenaeker, W. *Chem. Rev.*, **2003**, *103*, 1793.

²²⁵ (a) Hohenberg, P.; Kohn, W. *Phys. Rev. B*, **1964**, *136*, 864; (b) Kohn, W.; Sham, L. J. *Phys. Rev.* **1965**, *4A*, 1133.

functional must be approximated, however, and it is the difference in the exchange-correlation functional that distinguishes one contemporary DFT implementation from another. A widely used functional is known as B3LYP, a hybrid based on the three-parameter functional of Becke²²⁶ and the functional of Lee, Yang, and Parr.²²⁷

DFT has become a primary tool in contemporary computational chemistry, but it is important to note that it has some limitations. In particular, it is unable to account for London dispersion forces. Also, investigators have demonstrated that DFT with the B3LYP functional does not handle medium-range electron correlation well and so cannot account for the fact that branched alkanes are more stable than their linear isomers.²²⁸ The cumulative errors become so large that results for systems with as few as eight carbon atoms may be useless.²²⁹ Other significant deficiencies are evident in predictions of molecular geometries, bond energies, and heats of formation.^{230,231} A number of investigators have proposed new functionals to address these problems.²³² For example, Truhlar and co-workers reported that the M05-2X functional, developed by fitting parameters to the data in a training set, gave good results for noncovalent interactions, alkyl bond dissociation energies, and predictions of energy differences among alkane isomers.^{233,234} Because the M05-2X functional is highly parameterized, it can give very good results for structures similar to those considered in its development, but it also can produce significant errors for other systems.²³⁰ As is the case with all theoretical methods, the organic chemist must carefully assess the performance of DFT methods for problems of interest.²³⁵

4.4 VALENCE BOND THEORY

Resonance Structures and Resonance Energies

We noted in Chapter 1 that valence bond theory and molecular orbital theory provide complementary beginning points for a theoretical description of H₂. This chapter has focused on applications of molecular orbital theory, particularly Hückel MO theory. Still, organic chemists have long used resonance theory, which is an approximate form of valence bond theory, to predict

²²⁶ Becke, A. D. *J. Chem. Phys.* **1993**, *98*, 5648.

²²⁷ Lee, C.; Yang, W.; Parr, R. G. *Phys. Rev. B* **1988**, *37*, 785.

²²⁸ (a) Grimme, S. *Angew. Chem. Int. Ed.* **2006**, *45*, 4460; (b) Wodrich, M. D.; Corminboeuf, C.; Schleyer, P. v. R. *Org. Letters* **2006**, *8*, 3631; (c) Schreiner, P. R.; Fokin, A. A.; Pascal, R. A., Jr.; de Meijere, A. *Org. Lett.* **2006**, *8*, 3635.

²²⁹ Schreiner, P. R. *Angew. Chem. Int. Ed.* **2007**, *46*, 4217.

²³⁰ Wodrich, M. D.; Corminboeuf, C.; Schreiner, P. R.; Fokin, A. A.; Schleyer, P. v. R. *Org. Lett.* **2007**, *9*, 1851.

²³¹ Cohen, A. J.; Mori-Sánchez, P.; Yang, W. *Science* **2008**, *321*, 792.

²³² See, for example, Benighaus, T.; DiStasio, Jr., R. A.; Lochan, R. C.; Chai, J.-D.; Head-Gordon, M. *J. Phys. Chem. A* **2008**, *112*, 2702; Csonka, G. I.; Ruzsinszky, A.; Perdew, J. P.; Grimme, S. *J. Chem. Theory Comput.* **2008**, *4*, 888; Schwabe, T.; Grimme, S. *Acc. Chem. Res.* **2008**, *41*, 569.

²³³ Zhao, Y.; Schultz, N. E.; Truhlar, D. G. *J. Chem. Theory Comput.* **2006**, *2*, 364.

²³⁴ Zhao, Y.; Truhlar, D. G. *Org. Lett.* **2006**, *8*, 5753.

²³⁵ Riley, K. E.; Op't Holt, B. T.; Merz, K. M., Jr. *J. Chem. Theory Comput.* **2007**, *3*, 407; Zhang, G.; Musgrave, C. B. *J. Phys. Chem. A* **2007**, *111*, 1554; Sousa, S. F.; Fernandes, P. A.; Ramos, M. J. *J. Phys. Chem. A* **2007**, *111*, 10439.

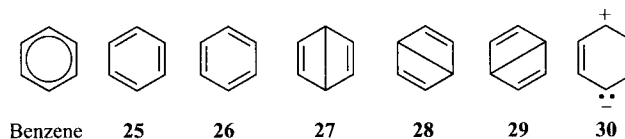
TABLE 4.4 Resonance Structures and Resonance Energies of Selected Aromatics

Compound	Number of Kekulé Structures	Resonance Energy (kcal/mol)
Benzene	2	36.0
Naphthalene	3	61.0
Anthracene	4	83.5
Phenanthrene	5	91.3

Source: Reference 23.

FIGURE 4.67

Some resonance structures for benzene.



properties of conjugated molecules. For example, chemical experience indicates a close relationship between the resonance energy of a neutral structure and the number of resonance structures of the system, as shown for several polycyclic aromatics in Table 4.4.²³⁶ Because of historical forces, VB theory has not been as widely used by organic chemists as have MO methods for quite some time.²³⁷ In recent years, however, valence bond theory has been attracting renewed interest.²³⁸

Let us first see how resonance theory can predict the properties of a planar, conjugated π system and then see how the valence bond approach can be used in higher level calculations. The calculation of resonance energies from valence bond descriptions of contributing resonance structures was discussed in a comprehensive treatise by Wheland.²³ Consider the calculation of the resonance energy of benzene. One begins by writing valence bond wave functions for each resonance structure that contributes to the resonance hybrid (Figure 4.67).²³⁹ Structures 25 and 26 are the familiar Kekulé structures. The VB method also considers non-Kekulé structures, such as those with elongated or formal bonds (27, 28, and 29) and ionic structures (e.g., 30). Because the latter structures seem high in energy, we suspect that they will make only a minor contribution to the overall properties of the resonance hybrid. Still, some contribution of high energy structures may be needed to accurately calculate the properties of the molecule.

The VB wave function for benzene is a linear combination of the VB wave functions for each of the contributing resonance structures and has the general form shown in equation 4.79:

$$\Phi_{\text{benzene}} = k_{25}\theta_{25} + k_{26}\theta_{26} + \cdots + \sum_G k_G\theta_G \quad (4.79)$$

²³⁶ Kekulé resonance structures are those structures with only single and double bonds and no extended or formal bonds or diradicals.

²³⁷ For a commentary, see Shaik, S. *New J. Chem.* **2007**, 31, 2015.

²³⁸ Compare Shurki, A. *Theor. Chem. Acc.* **2006**, 116, 253.

²³⁹ As with HMO theory, the valence bond description of these resonance structures is limited to wave functions involving the resonance electrons (i.e., those that correspond to the π electrons in the MO method). The σ bonds are not explicitly considered.

where θ_G is the VB wave function of the G th contributing resonance structure. As in HMO theory, we determine the coefficients (k) in the wave function as well as the resonance energy of benzene by use of the variational principle. Thus, we find the mix of contributing resonance structures that minimizes the calculated energy of benzene by setting the partial derivative of the energy with respect to each of the k values equal to zero and then finding the solution to the secular determinant that results.²³ Consideration of five contributing structures (25–29 in Figure 4.67) leads to a 5×5 determinant. There are assumptions, approximations, and substitutions that facilitate the calculation, just as there are in the HMO method. Solving the determinant leads to a set of energy levels, and determination of the coefficients for the lowest energy level leads to the VB function for benzene reported by Wheland (equation 4.80).

$$\Phi_{\text{benzene}} = 0.37(\theta_{25} + \theta_{26}) + 0.16(\theta_{27} + \theta_{28} + \theta_{29}) \quad (4.80)$$

The resonance energy determined in this calculation is the difference in energy between benzene and the most stable contributing resonance structure (25 or 26). The value obtained is $-1.11J$, where J is the *adjacent exchange integral*, a term that is reminiscent of β in the HMO method. In a number of such calculations, J is found to be approximately -30 kcal/mol, so the resonance energy of benzene is calculated to be about 33 kcal/mol.²⁴⁰ That value is quite close to the commonly accepted value of 36 kcal/mol and is almost identical to the 33.3 kcal/mol we identified as an alternative value for the benzene resonance energy (page 204). We have not carried out a detailed analysis, but it appears from this example that resonance theory can provide an accurate model for calculating the resonance energy of benzene.²⁴¹

The method just described is more difficult to apply to larger molecules. For naphthalene the HMO method leads to a 10×10 determinant because ten p orbitals are mixed to make the MO. For the resonance method, however, the size of the determinant is limited only by our willingness to include resonance structures. In general, there are many more resonance structures that should be considered than there are p orbitals, and a reasonable resonance treatment of naphthalene would require a 42×42 determinant.^{242,243} For anthracene and phenanthrene, the HMO determinant would be 14×14 , but the resonance method would require solution of a 429×429 determinant in each case. Consideration of symmetry can reduce the phenanthrene

²⁴⁰ See also Pauling, L.; Wheland, G. W. *J. Chem. Phys.* **1933**, *1*, 362. There is an interesting report that Albert Einstein attended one of Pauling's lectures on the applications of wave mechanics to chemical bonding and said afterward "It was too complicated for me." <http://osulibrary.oregonstate.edu/specialcollections/coll/pauling/bond/narrative/page29.html>.

²⁴¹ Cooper, D. L.; Cerratt, J.; Raimondi, M. *Nature* **1986**, *323*, 699 reported a spin-coupled valence bond method for calculation of molecular electronic structure and concluded that "our results suggest that the Kekulé description of benzene, as expressed in the classic VB form, is in fact much closer in reality than is a description in terms of delocalized molecular orbitals."

²⁴² This determinant size is a strict minimum. Even for benzene, determinants can be quite large. For example, Norbeck and Gallup used 175 resonance structures in an *ab initio* valence bond calculation for benzene and found that the ionic structures are major contributors to the calculated structure: Norbeck, J. M.; Gallup, G. A. *J. Am. Chem. Soc.* **1973**, *95*, 4460.

²⁴³ For a valence bond calculation of naphthalene, representations of the valence bond structures used in the calculation, and the relative contribution of these structures to the resonance hybrid, see Sherman, J. *J. Chem. Phys.* **1934**, *2*, 488.

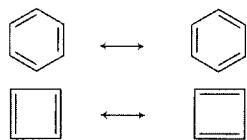


FIGURE 4.68

Kekulé resonance structures for benzene and cyclobutadiene.

problem to a 232×232 determinant and the anthracene problem to a 126×126 determinant.²³ Still, these determinants are much more difficult to solve than are the smaller determinants obtained from the HMO method. Therefore, HMO theory became the more widely accepted approach to calculating molecular structure in organic chemistry because the calculations are easier to carry out, not because it is inherently superior to the valence bond model.^{244,245}

There is one other aspect of the comparison of HMO and resonance methods that must be addressed. In general, the HMO method and resonance theory agree at least qualitatively (e.g., benzyl cation charge densities), and in some cases quantitatively as well (e.g., allyl cation charge densities). That is not always the case. As shown in Figure 4.68, both benzene and cyclobutadiene have two Kekulé resonance structures. Why, therefore, is cyclobutadiene an exceedingly unstable compound, but benzene is the standard of aromatic stability? The answer is that the intuitive form of resonance theory we often use in organic chemistry is an oversimplified version of valence bond theory, and stability cannot be predicted just by counting the number of resonance structures possible for a structure.²⁴⁶ A more complete form of valence bond theory correctly predicts the stabilities of aromatic systems and the instabilities of antiaromatic systems.^{247–248}

Hoffmann, Shaik, and Hiberty,²⁴⁹ with additional commentary by Roberts²⁵⁰ and by Streitwieser,²⁵¹ presented reasons why valence bond theory was initially appealing to organic chemists but was supplanted by molecular orbital theory. Roberts noted, in particular, the difficulty in carrying out valence bond calculations relative to that of using molecular orbital theory.²⁵⁰ An observation by Hiberty reinforces a point made in Chapter 1.

The two theories are not really different. They are rather two representations. . . of the same reality. Done well, done rigorously, VB and MO theory converge to the same exact description.²⁴⁹

Valence bond theory is the subject of continuing investigation in theoretical organic chemistry.^{245,252–255} Several workers described valence bond

²⁴⁴ Wheland, G. W. *J. Chem. Phys.* **1934**, *2*, 474 argued that the valence bond method as described by Heitler, London, Slater, and Pauling gives results closer to experimentally observed values than does the molecular orbital method attributed to Hund, Mulliken, and Hückel.

²⁴⁵ A summary of the development of VB theory and a discussion of the merits of VB and MO theories was given by Klein, D. J.; Trinajstić, N. *J. Chem. Educ.* **1990**, *67*, 633.

²⁴⁶ Fischer, H.; Murrell, J. N. *Theoret. Chim. Acta (Berlin)* **1963**, *1*, 463.

²⁴⁷ Epiotis, N. D. with Larson, J. R.; Eaton, H. L. *Unified Valence Bond Theory of Electronic Structure*; Springer-Verlag: Berlin, 1982.

²⁴⁸ Shaik, S.; Hiberty, P. C. *Helv. Chim. Acta* **2003**, *86*, 1063.

²⁴⁹ Hoffmann, R.; Shaik, S.; Hiberty, P. C. *Acc. Chem. Res.* **2003**, *36*, 750.

²⁵⁰ Roberts, J. D. *Acc. Chem. Res.* **2004**, *37*, 417.

²⁵¹ Streitwieser, A. *Acc. Chem. Res.* **2004**, *37*, 419.

²⁵² Mizoguchi, N. *J. Am. Chem. Soc.* **1985**, *107*, 4419; Shaik, S. S.; Hiberty, P. C. *J. Am. Chem. Soc.* **1985**, *107*, 3089.

²⁵³ Klein, D. J.; Trinajstić, N., Eds. *Valence Bond Theory and Chemical Structure*; Elsevier: Amsterdam, 1990.

²⁵⁴ Shaik, S.; Hiberty, P. C. *Rev. Comp. Chem.* **2004**, *20*, 1.

²⁵⁵ For leading references to the development of generalized valence bond (GVB) theory, see Goddard, W. A. III; Dunning, T. H., Jr.; Hunt, W. J.; Hay, P. J. *Acc. Chem. Res.* **1973**, *6*, 368; Voter, A. F.; Goddard, W. A. III *J. Am. Chem. Soc.* **1986**, *108*, 2830.

calculations for conjugated and aromatic π systems,²⁵⁶ and Hiberty used valence bond methods to calculate the effect of strained annulated rings on aromatic systems.²⁵⁷ Relationships between molecular orbital wave functions and valence bond wave functions have been developed,²⁵⁸ and Fox and Matsen reported a description of π -electron systems that employs features of both molecular orbital and valence bond theory.²⁵⁹ Molecular orbital theory remains more popular with organic chemists, but the proponents of VB theory suggest that the development of faster valence bond methods is helping in the “coming of age” of VB theory.

We will not explore the computational details of VB theory, but it is worth noting some results that can be obtained with it. Recall that one of the features of HMO theory is that it is possible to make useful predictions, such as the relative stabilities of cyclic π systems or the locations of unpaired electron density in a conjugated radical, without actually doing the HMO calculations. Similarly, it is not necessary to carry out a complete valence bond calculation to obtain useful quantitative predictions of resonance energies and some other properties of conjugated π systems. Herndon described a structure-resonance theory (SRT) method that enables one to calculate resonance energies *using only Kekulé structures*.²⁶⁰ The methods described in the references present

1. Some relatively easy ways to determine the number of Kekulé structures for a molecule (without having to draw all the imaginable structures and then determine which ones are redundant).
2. The definitions of some permutations of these structures.
3. Some formulas for calculation of resonance energies and other parameters.

Not only are the results of these procedures even easier to derive than are the results of simple HMO calculations, but they are very close to the results obtained with the more advanced MO methods described earlier.²⁶¹

The first step in the SRT method is the determination of the **structure count** (SC), which is the number of Kekulé structures for a given molecular structure.²⁶² In one procedure, a polycyclic molecule is constructed by drawing a single chain or ring containing all atoms of the molecule, followed by insertion of lines one at a time until the molecule is complete. With each line insertion the SC is obtained from equation 4.81.^{260a,263}

$$SC_a = SC_b + (SC_c \times SC_d) \quad (4.81)$$

²⁵⁶ Kuwajima, S. *J. Am. Chem. Soc.* **1984**, *106*, 6496; Klein, D. J. *Pure Appl. Chem.* **1983**, *55*, 299.

²⁵⁷ Hiberty, P. C.; Ohanessian, G.; Delbecq, F. *J. Am. Chem. Soc.* **1985**, *107*, 3095.

²⁵⁸ Živković, T. P. *Theor. Chim. Acta (Berlin)* **1983**, *62*, 335; Hiberty, P. C.; Leforestier, C. *J. Am. Chem. Soc.* **1978**, *100*, 2012; Chen, C. J. *Chinese Chem. Soc.* **1973**, *20*, 1; Imkampe, K. *J. Chem. Educ.* **1975**, *52*, 429; Sardella, D. J. *J. Chem. Educ.* **1977**, *54*, 217.

²⁵⁹ Fox, M. A.; Matsen, F. A. *J. Chem. Educ.* **1985**, *62*, 367, 477, 551.

²⁶⁰ (a) Herndon, W. C. *J. Chem. Educ.* **1974**, *51*, 10; (b) Herndon, W. C. *J. Am. Chem. Soc.* **1973**, *95*, 2404; (c) Herndon, W. C.; Ellzey, M. L., Jr. *J. Am. Chem. Soc.* **1974**, *96*, 6631.

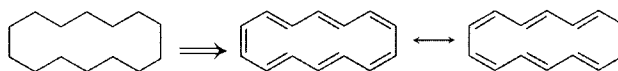
²⁶¹ The methods described also account for such antiaromatic structures.

²⁶² For a discussion of methods to determine the number of Kekulé structures for a molecule, see reference 108.

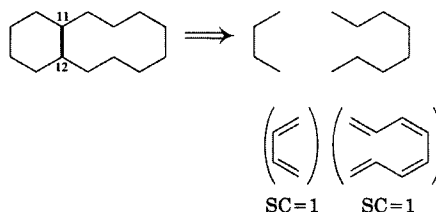
²⁶³ The method was developed by Wheland, G. W. *J. Chem. Phys.* **1935**, *3*, 356.

FIGURE 4.69

Kekulé structures for the open chain graph of anthracene.

**FIGURE 4.70**

Kekulé structures after inserting one σ bond



Here SC_a is the SC of the molecule or some fragment thereof, SC_b is the SC of the previous fragment, and SC_c and SC_d are the SCs of the fragments of the molecule without the line just inserted or its vertices.

This procedure may be illustrated by the example of anthracene. The graph of the molecule shown on the left of Figure 4.69 depicts the σ skeleton of cyclotetradecaheptaene, where each vertex represents a carbon atom with a p orbital. Two resonance structures can be written for this structure, so the SC for this fragment is 2.²⁶⁴

Next, we insert a line representing the σ bond from C11 to C12 in anthracene (shown in bold on the top left of Figure 4.70), then we delete that line *and its vertices* as indicated on the top right of Figure 4.70. The SC for each of the fragments so produced is 1, since each fragment would have only one Kekulé structure.²³⁶ From equation 4.81, the SC for the initial fragment on the top left of Figure 4.70 (*with the line in place*) is $2 + 1 \times 1 = 3$.

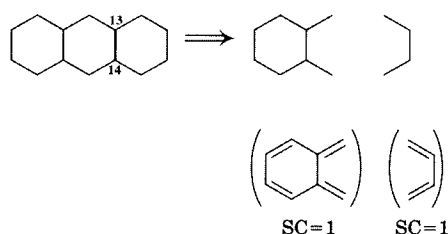
Now we insert the line corresponding to the C13–C14 σ bond of anthracene, then delete this line and its vertices to produce the two fragments shown on the top right in Figure 4.71. Both of these fragments have only one Kekulé structure, so the SC for the anthracene molecule is $3 + 1 \times 1 = 4$. That result agrees with the number of Kekulé resonance forms for anthracene determined by inspection (Table 4.4).

This method of determining the SC is somewhat tedious for large molecules, but there is another approach that is easier.^{260a,265} To determine the SC by this method, one deletes a vertex from the graph of the molecule and then writes the vertex coefficients (with no coefficient smaller than 1) that sum to zero around every vertex in the residual graph.²⁶⁶ Note that these

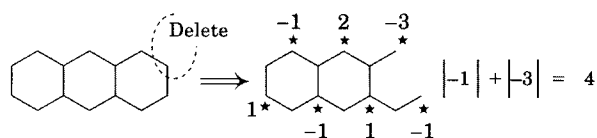
²⁶⁴ Because anthracene is planar, the cyclic polyene shown in Figure 4.69 is assumed to be planar for the purposes of this calculation.

²⁶⁵ Herndon, W. C. *Tetrahedron* **1973**, 29, 3.

²⁶⁶ The graph of the molecule is the outline of the molecule showing all σ bonds that comprise the skeleton of the π system. Much of the recent development in this area is inherently related to a branch of mathematics known as graph theory. See, for example, Hansen, P. J.; Jurs, P. C. *J. Chem. Educ.* **1988**, 65, 574, 661; Trinajstić, N.; Nikolić, S.; Knop, J. V.; Müller, W. R.; Szymanski, K. *Computational Chemical Graph Theory*; Ellis Horwood: London, 1991; Trinajstić, N. *Chemical Graph Theory*, 2nd ed.; CRC Press: Boca Raton, FL, 1992. For application of graph theory and the concept of conjugated circuits in determining aromaticity, see Randić, M.; Trinajstić, N. *J. Am. Chem. Soc.* **1987**, 109, 6923; Klein, D. J. *J. Chem. Educ.* **1992**, 69, 691. Graph theory can be used to extend the utility of valence bond calculations of aromatic systems: Alexander, S. A.; Schmalz, T. G. *J. Am. Chem. Soc.* **1987**, 109, 6933. Graph theoretical methods may also be used in MO theory: Dias, J. R. *J. Chem. Educ.* **1989**, 66, 1012; Mizoguchi, N. *J. Phys. Chem.* **1988**, 92, 2754 and references therein; Dias, J. R. *J. Chem. Educ.* **1992**, 69, 695. For applications of graph theory to structure–property relationships, see Mihalić, Z.; Trinajstić, N. *J. Chem. Educ.* **1992**, 69, 701.

**FIGURE 4.71**

Kekulé structures after inserting a second σ bond.

**FIGURE 4.72**

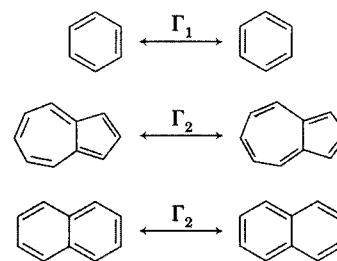
Determination of structure count by vertex deletion method.

coefficients are the *unnormalized* coefficients of the NBMO for the odd alternant structure left by removing a vertex from the graph. The SC is then determined by taking the sum of the absolute values of the coefficients adjacent to the deleted vertex.

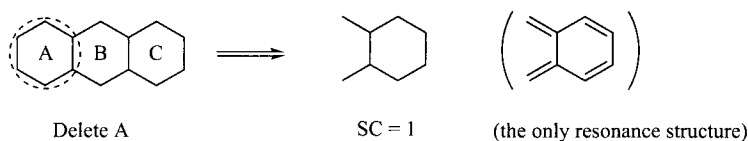
Again, it is instructive to consider the example of anthracene. Deleting a vertex from the graph of anthracene as shown on the left in Figure 4.72 generates the *odd alternant* structure on the right. We proceed as though we were determining the MO wave function for the NBMO of this fragment. Only the starred positions have nonzero coefficients, and the method requires that the smallest coefficient be unity. (If a trial run produces a coefficient smaller than 1 for a given carbon atom, we simply repeat the process starting at that position and assigning its coefficient to be 1.) The resulting coefficients are shown in Figure 4.72. Because the coefficients adjacent to the deleted vertex are -3 and -1 , the SC of anthracene is $|-3| + |-1| = 4$.

Next, we must define some types of electron permutations. A permutation of three pairs of electrons in a single ring is denoted by Γ_1 , and the permutation of five pairs of electrons in two rings is denoted by Γ_2 (Figure 4.73).

The number of Γ_1 permutations for each ring in the molecule is the SC for the *residual* molecule *with that particular ring excised from the structure*. The number of Γ_2 permutations is found by deleting *two adjacent rings* and summing the SCs for the residual system. Let us illustrate these concepts by continuing with the example of anthracene. If we identify the rings of anthracene as A, B, and C, then we first delete the A ring and determine that the SC for the residual fragment is 1 (Figure 4.74). By symmetry, deleting the C ring gives an SC of 1 as well. Deleting the B ring also gives an SC of 1 (Figure 4.75). Therefore, $n_1 = 3$.

**FIGURE 4.73**

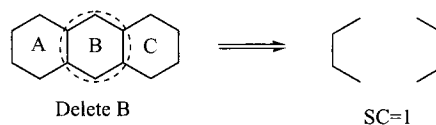
Γ_1 and Γ_2 permutations.

**FIGURE 4.74**

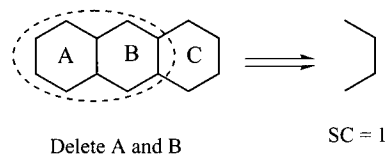
Determination of n_1 for anthracene: step 1, deleting ring A.

FIGURE 4.75

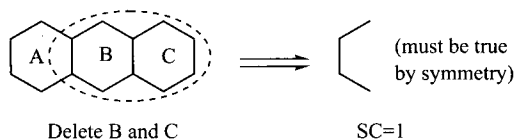
Determination of n_1 for anthracene: step 2, deleting ring B.

**FIGURE 4.76**

Determination of n_2 for anthracene: deletion of A and B rings.

**FIGURE 4.77**

Determination of n_2 for anthracene: deletion of B and C rings.



To compute the Γ_2 s, we delete the A and B rings together (Figure 4.76). The SC of the residual fragment is 1. Then we delete the B and C rings together (Figure 4.77). The SC of the residual system is also 1, as it must be by symmetry. Therefore, $n_2 = 2$.

The resonance energy associated with a particular structure is determined from the formula

$$RE = 2(n_1\Gamma_1 + n_2\Gamma_2)/K_{SC} \quad (4.82)$$

in which K_{SC} is the number of Kekulé structures for the molecule. The ratio Γ_2/Γ_1 is taken to be 0.40, which is an empirical value determined from the UV-vis absorption spectra of benzene and azulene,²⁶⁷ and Γ_1 is assigned a value of 0.838 eV (19.3 kcal/mol). For anthracene, therefore,

$$RE = 2(3\Gamma_1 + 2\Gamma_2)/4 \quad (4.83)$$

Substituting $0.4\Gamma_1$ for Γ_2 produces

$$RE = 0.5[3\Gamma_1 + 2(0.4\Gamma_1)] \quad (4.84)$$

so

$$RE = 1.9\Gamma_1 = 1.59 \text{ eV} \quad (4.85)$$

This result can be compared with the HMO DE_π , which is 5.38β . Taking β to be 18 kcal/mol means that DE_π is 4.2 eV. By contrast, SCF molecular orbital calculations give a delocalization energy of 1.60 eV.²⁶⁸ Clearly, the structure-resonance method result is closer to the result from more advanced molecular

²⁶⁷ Initially, a theoretical ratio of 0.37 was used (reference 260c).

²⁶⁸ 1 eV = 23.06 kcal/mol.

TABLE 4.5 Comparison of Measures of Delocalization and Resonance Energy

Compound	DE_{HMO} (eV) ^a	$DE_{\text{SCF-MO}}$ (eV)	RE_{SRT} (eV)
Benzene	1.56	0.87	0.84
Naphthalene	2.87	1.32	1.35
Phenanthrene	4.25	1.93	1.95
Pyrene	5.08	2.10	2.13
Styrene	1.89	0.86	0.84
Biphenyl	3.42	1.70	1.68
Stilbene	3.81	1.71	1.68
Ovalene	11.31	4.54	4.44

^a Published results in units of β are converted to eV: $1 \beta = 0.78 \text{ eV}$.

Source: Reference 260c.

orbital calculations than is the HMO result. Table 4.5 gives some results for other hydrocarbons, and it may be seen that the SRT method generally gives results that are very close to those obtained by SCF-MO calculation methods.²⁶⁹ Even though we will not use the SRT procedure again, this discussion serves as a useful introduction to some applications of graph theory in chemistry and as a reminder that MO theory is not the only route to useful chemical predictions.

Choosing a Computational Model

A wide variety of computational software is now available to the experimentalist who wishes to calculate the properties of a system of interest. The ready availability of these packages makes it is easy to lose sight of the many approximations and assumptions on which they are based. Different theoretical models can give quite different answers to the same question, and one can choose an approach that is not suited for a particular type of chemical problem. Thus, the results of any advanced calculation must always be examined to see whether it is reasonable in view of chemical intuition (which will most likely be expressed in terms of a simpler HMO or resonance model) and whether it reproduces experimental results for test structures. We must not forget that computer calculations, even those done with very large programs on very powerful computers, are only conceptual models. Theoretical calculations are subject to the same limitations as other models, and we should not put more faith into them than is warranted. This point was emphasized by Ross:

Computers do calculations. The equation solved may be that of a theory, such as Schrödinger's equation, or that of a model, such as a reaction-diffusion equation for a particular reaction mechanism. Solutions of such equations, whether obtained by analysis or numerical methods, are *predictions*, not

²⁶⁹ This method has been applied to other molecular properties, and a number of papers have examined its theoretical basis. See, for example, Herndon, W. C.; Párkányi, C. *J. Chem. Educ.* **1976**, *53*, 689; Herndon, W. C. *Tetrahedron* **1973**, *29*, 3; Gutman, I. *Chem. Phys. Lett.* **1984**, *103*, 475; Gutman, I.; Trinajstić, N.; Wilcox, C. F., Jr. *Tetrahedron* **1975**, *31*, 143; Cvetković, D.; Gutman, I.; Trinajstić, N. *J. Chem. Phys.* **1974**, *61*, 2700; Wilcox, C. F., Jr.; Gutman, I.; Trinajstić, N. *Tetrahedron* **1975**, *31*, 147; Gutman, I.; Herndon, W. C. *Chem. Phys. Lett.* **1984**, *105*, 281.

results of experiments. The validation of a prediction is confirmation by experiment. No one doubts the ability of computers to solve the equations of models; it is the models that require validation by experiments. . . .

All this may seem to be only a matter of proper usage of words; it is not. It is a matter of recognizing what science is about.²⁷⁰

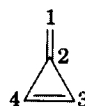
Problems

- 4.1. Demonstrate that using the relationship $E = \alpha - \beta$ in equations 4.15 and 4.16 produces the wave function for ψ_2 of ethene shown in equation 4.33.
- 4.2. Use the wave functions shown in equations 4.39 through 4.41 to calculate the π bond orders and the free valence indices for the allyl carbocation, radical, and carbanion.
- 4.3. We noted on page 195 that nonalternant compounds such as azulene may be found to have q_i values not equal to 0, even though that is a fundamental assumption of HMO theory. For what class of nonalternant structures *must* q_i values equal 0?
- 4.4. Using the indicated atom numbers, write the secular determinant for each of the following structures.

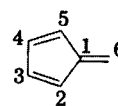
a



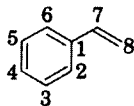
b



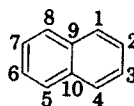
c



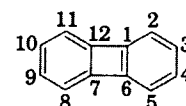
d



e



f



- 4.5. Use an HMO program to calculate the energy levels of the structures in Problem 4.4.²⁷¹ Draw an energy level diagram and calculate DE_π for each system.
- 4.6. Using the results of the HMO calculations in Problem 4.5, calculate \mathcal{F}_i , ρ_i , and q_i for each carbon atom and determine π bond order and total bond order for each bond. (Take advantage of molecular symmetry to minimize the number of calculations.)
- 4.7. Calculate the HMO energy levels of [3]-, [4]-, [5]-, and [6]radialene. What patterns in their energy levels do you notice? Can you predict the patterns of HMO energy levels for [7]- and [8]radialene without doing another calculation?
- 4.8. Use the symmetry properties of the Hückel molecular orbitals of linear, alternant hydrocarbons to sketch a representation like those in Figure 4.7 for each of the MOs of heptatrienyl, octatetraene, nonatetraenyl, and decapentaene. You will not be able to give a quantitative estimate of the coefficient of each atomic orbital, but your representation should indicate for each MO which coefficients are positive, which are negative, and which (at a node) are zero. For each structure

²⁷⁰ Ross, J. *Science* **1992**, 257, 860.

²⁷¹ For an online HMO calculator, see <http://www.chem.ucalgary.ca/SHMO/>.

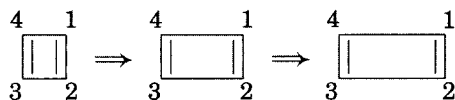
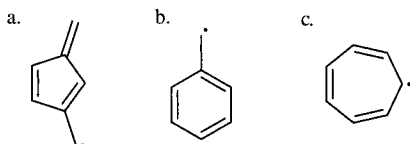


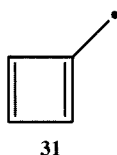
FIGURE 4.78
Distortion of cyclobutadiene.

rationalize the relative energy of each MO in terms of the bonding and antibonding interactions between atomic orbitals. (You should not need to carry out a calculation or consult the literature for this problem.)

- 4.9. Identify each of the radicals below as even alternant, odd alternant, or non-alternant. Use stars to illustrate your assignment.



- 4.10. Use the properties of odd alternant hydrocarbons to determine the unpaired electron density at the exocyclic carbon in the radical **31**. Is this result surprising to you? Show how resonance theory can easily rationalize the result.



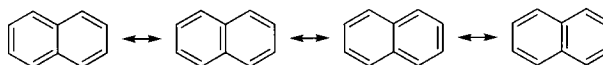
- 4.11. Methylene cyclopropene (structure b in Problem 4.4) is a nonalternant hydrocarbon. What did the results of the HMO calculation for methylene cyclopropene indicate about the charge density on each atom? Do those results agree with the statement on page 195 about the nature of alternant and nonalternant systems? How could you have predicted the polarity of methylene cyclopropene on the basis of resonance theory?
- 4.12. Cyclopropenone has a higher dipole moment than would be expected on the basis of a carbonyl group alone. Use the results of the HMO analysis of methylene cyclopropene in the previous problem to rationalize the dipole moment. How does resonance theory explain the polarity?
- 4.13. Calculate how distortion of square cyclobutadiene to a rectangular structure would affect the π energy of the molecule. To do this, solve the HMO determinant for a system such as the one in Figure 4.78, where H_{12} is β , but H_{23} varies from 1.0β to 0.7β to 0.5β to 0.3β to 0.0β . What is the effect of the distortion on the π energy of the system? What factors have we ignored in this analysis?
- 4.14. Predict the electronic and physical properties of the benzene dianion, $C_6H_6^{2-}$.
- 4.15. Use HMO theory to estimate the electronic energy barrier for rotation of an allyl radical about C2–C3 as shown in Figure 4.79. How does your result compare with an experimental activation energy? How does the calculated value compare with the electronic energy barriers calculated for the allyl cation and the allyl anion? How do the calculated values for the allyl systems compare with those of the corresponding benzyl systems?
- 4.16. Estimate the electronic energy barrier for rotation about the C1–C α bond of styrene.



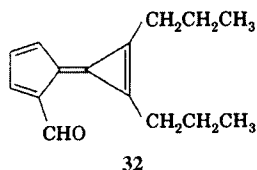
FIGURE 4.79
Rotation about C2–C3 in an allyl radical.

FIGURE 4.80

Incorrect representation of naphthalene resonance structures.



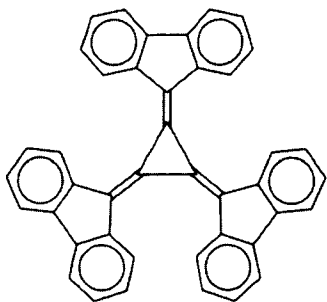
- 4.17. Ordinarily the barrier to rotation about a carbon–carbon double bond is quite high, but compound **32** was observed by NMR to have a rotational barrier of only about 20 kcal/mol. Explain this result.



- 4.18. Consider the \mathcal{F}_i values shown in Figure 4.17. The value of \mathcal{F}_i for the terminal carbon atom varies from 1.732 to 1.025 to 0.943 as the structure changes from methyl radical to allyl radical to pentadienyl radical. Conversely, the \mathcal{F}_i value for the terminal carbon atom increases along the series from ethene to 1,3-butadiene to 1,3,5-hexatriene.
- Predict the value of \mathcal{F}_i for the next member of each of these two series.
 - Why do the \mathcal{F}_i values increase in one case but decrease in the other?
 - Why should the \mathcal{F}_i value of a methylene carbon atom on 1,2-dimethylene-3,5-cyclohexadiene be nearly the same as for the terminal carbon atom of an allyl or pentadienyl radical?
 - The value of 0.525 for \mathcal{F}_i for a carbon atom in cyclooctatetraene is determined from a calculation that assumes the molecule is planar. What would you expect the \mathcal{F}_i value to be if the molecule is assumed to be tub shaped?
- 4.19. Apply the SRT method to phenanthrene and to styrene in order to verify the resonance energies listed in Table 4.5.
- 4.20. Consult the literature to find discussions of the aromaticity or antiaromaticity of the following structures: tropylium ion, cyclopentadienyl cation, COT dianion. Are the results consistent with familiar generalizations about aromatic character?
- 4.21. Figure 4.80 suggests that naphthalene has four resonance structures. Why is this not correct?
- 4.22. Phenanthrene has more Kekulé resonance structures than does naphthalene, so we expect it to be more aromatic, and the data in Table 4.4 indicate that it does have a larger resonance energy. However, naphthalene does not undergo electrophilic addition, and phenanthrene readily undergoes electrophilic addition across the 9,10 bond.
- Either by drawing all possible resonance structures or by applying the procedure described by Herndon, determine that the number of resonance structures indicated for phenanthrene in Table 4.4 is correct.
 - Use the nature of the resonance structures in each case to rationalize why phenanthrene adds electrophiles but naphthalene tends to undergo substitution instead. Can MO theory predict the same result? Are Clar structures informative in this analysis?
- 4.23. How many Kekulé structures are possible for (a) benzo[*a*]pyrene and for (b) benzanthracene?
- 4.24. Equation 4.69 is valid because the expression $7.435n - 0.605m - 32.175p - 29.38q$ represents the calculated heat of formation for a structure that does not exhibit

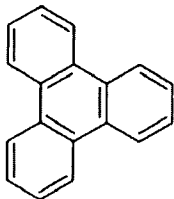
resonance. Verify that this is so by calculating ΔH_f° for glyoxal (O=CH-CH=O) and comparing your answer to the accepted value of -50.7 kcal/mol.¹⁶³

- 4.25. a. Calculate Δ DRE for addition of ethene across the 9,10 positions in anthracene and also for addition across the 1,2 positions. Which addition pathway should be favored?
- b. Also calculate Δ DRE for addition of ethene across the 9,10 positions and across the 1,2 positions in phenanthrene. Which reaction should be favored in this case?
- 4.26. Explain why tris(9-fluorenylidene)cyclopropane (**33**) undergoes two-electron reduction at a "remarkably positive" reduction potential.



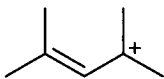
33

- 4.27. The Dewar resonance energy of triphenylene (**34**) is reported to be 65 kcal/mol. On the basis of the DRE value, is the central ring aromatic? Are Clar structures helpful in this analysis?

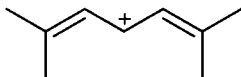


34

- 4.28. Rationalize the observation that the first absorption band of the naphthalene—tetracyanoethylene (TCNE) charge-transfer complex is at 550 nm, but the first absorption of the azulene—TCNE complex is at 686 nm.
- 4.29. Rationalize the observation that the cation **35** absorbs UV at 288 nm, while **36** absorbs at 363 nm.

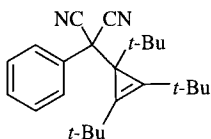


35



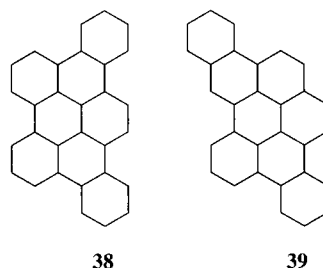
36

- 4.30. Compound **37** dissociates in acetonitrile with a ΔH_{dissoc} of about 4 kcal/mol. What are the products of the dissociation, and why is ΔH_{dissoc} so small?

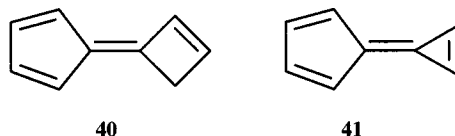


37

- 4.31. The figures below show the σ skeletons of two fully conjugated polycyclic aromatic structures. According to Clar's sextet theory, which of the two should be more reactive?



- 4.32. A semiempirical MO calculation on the two structures below indicated that one would be expected to have a dipole moment of 3 D, while the other would have a dipole moment of ca. 1.4 D. Which structure should have the larger dipole moment, and why?



- 4.33. One of the criteria for aromaticity (page 202) is a characteristic pattern of chemical reactivity. Which of these criteria cannot be applied to study the aromaticity of C_{60} and other fullerenes?
- 4.34. What is your response to the question posed on page 203: Is benzene aromatic because it is especially stable, or is it unusually stable because it is aromatic?
- 4.35. Consider the following statement made by E. Heilbronner after the opening paper of the Jerusalem symposium on aromaticity, pseudoaromaticity and antiaromaticity:

I think we should all realize that we are united here in a symposium on a non-existent subject. It must also be stated quite clearly at the beginning that aromaticity is not an observable property, i.e., it is not a quantity that can be measured and is not even a concept which, in my experience, has proved very useful. ...²⁷²

Do you agree with Heilbronner, or do you think that aromaticity is an existent subject? Discuss the role of aromaticity as a model of chemical structure and reactivity.

- 4.36. Respond to the statement that "one of the most fruitful concepts of organic chemistry is that of a substituent possessing a set of intrinsic individual properties."²⁷³ Is this view a product of historical, Lewis structure thinking, or is it also consistent with the model of chemical bonding that is implicit in molecular orbital theory and density functional theory?

²⁷² Bergmann, E. D.; Pullman, B., Eds. *Aromaticity, Pseudo-aromaticity, Anti-aromaticity*; Academic Press: New York, 1971.

²⁷³ Shubin, V. G. *Top. Curr. Chem.* **1984**, 116/117, 26

4.37. Kuhn discussed two related meanings of the term *paradigm*:

On the one hand, it stands for the entire constellation of beliefs, values, techniques, and so on shared by the members of a given community. On the other it denotes one sort of element in that constellation, the concrete puzzle solutions which, employed as models or examples, can replace explicit rules as a basis for the solution of the remaining puzzles of normal science.²⁷⁴

Using Kuhn's definition of paradigm, respond to the following statement:

It is apparent that virtual (but with orbital mixing) 1,3,5-cyclohexatriene (with bond-length alternation) would be nearly as aromatic as the real benzene. Instead of being the aromatic paradigm, benzene is the exception among all other benzenoid hydrocarbons, none of which have equal CC bond lengths.⁶⁴

²⁷⁴ Kuhn, T. S. *The Structure of Scientific Revolutions*, 2nd ed.; The University of Chicago Press: Chicago, 1970.

Reactive Intermediates

5.1 REACTION COORDINATE DIAGRAMS

Previous chapters have emphasized stable molecules—structures that persist for a long period of time under ambient conditions. In this chapter we consider some relatively less stable species that exhibit even greater structural diversity and that play central roles in the chemical transformations of organic compounds. The term **reactive intermediate** implies a species that is formed and then consumed during a reaction but which often cannot be isolated and characterized under ordinary conditions. Therefore, the methods we use to study reactive intermediates are frequently even more indirect than those we use to study stable structures. Furthermore, we often study reactive intermediates under conditions that are very different from the conditions in which these species are thought to be formed during chemical reactions.¹

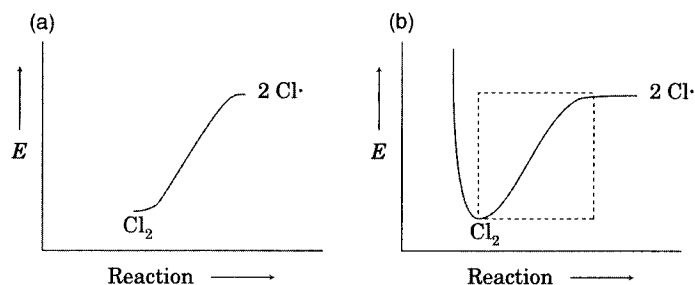
It is helpful to consider reactive intermediates in the context of a **reaction coordinate diagram**—a two-dimensional sketch that represents the potential energy of a system during some transformation. Usually the reactant is on the left of such figures and the product is on the right. The horizontal axis is often labeled *progress of reaction*. The simplest type of chemical reaction is a bond homolysis in a diatomic molecule, such as Cl₂. As shown in Figure 5.1(a), the reaction coordinate in this case corresponds to the distance between the two chlorine nuclei. The curve in Figure 5.1(a) is therefore only a portion, indicated with dotted lines, of a larger curve representing the ground electronic state of the chlorine molecule, Figure 5.1(b).

A bond homolysis in a polyatomic molecule would almost certainly involve changes in more than one bonding parameter (such as bond angles at the developing radical centers). To represent such a process, we should construct a potential energy surface in as many dimensions as there are bonding changes. The resulting surface, known as a **hypersurface**, would

¹ For examples of reactions that proceed differently under typical reaction conditions and under the conditions used to study the reactive intermediates, see Bethell, D.; Whitaker, D. in Jones, M., Jr.; Moss, R. A., Eds. *Reactive Intermediates*, Vol. 2; Wiley-Interscience: New York, 1981; p. 236 ff.

FIGURE 5.1

(a) Reaction coordinate diagram for dissociation of Cl_2 ; (b) electronic energy curve for $\text{Cl}-\text{Cl}$ σ bond.



indicate the energy of the species as a function of all relevant bond angle and length changes.² It is not possible to represent such a surface as a two-dimensional graph, however. A large table of numerical data indicating the energy of the structure as a function of each variable might be contemplated, but its complexity would offset its utility. Therefore, we do what we usually do when our models become too complex—we simplify them until they are more useful. The horizontal scale usually represents the change in the most significant bonding parameter associated with the reaction. If no single bonding parameter is physically meaningful for the changes we intend to represent, then we may draw a figure in which the horizontal scale is only a graphic convenience. In such cases the *x*-axis may be labeled *extent of reaction* or *reaction coordinate*.

One application of such a simplified reaction coordinate diagram is to provide a graphical distinction between a reaction in which an intermediate occurs and one in which there is not an intermediate. Figure 5.2 shows two possibilities for the ring inversion of a disubstituted bicyclo[2.1.0]pentane. If the solid line describes the reaction, the diradical is a local energy maximum on the potential energy surface, so it is a transition structure.³ If the reaction follows the dashed line, however, the diradical is a local minimum on the potential energy surface and is therefore an intermediate. To qualify as a chemical substance, the intermediate must have a lifetime long enough for at least one molecular vibration, or about 10^{-13} seconds.⁴ That means that the structure is stable with respect to small deformations, even though it is not sufficiently stable to be isolated for structural analysis. Both experimental and theoretical evidence suggest that the singlet diradical (in which the two unpaired electrons have opposite spins) is in fact a shallow minimum.⁵

Cruickshank and co-workers criticized the practice of using the terms *reaction coordinate* and *extent of reaction* interchangeably in such figures.⁶ They preferred *extent of reaction* to mean a macroscopic quantity—the composition

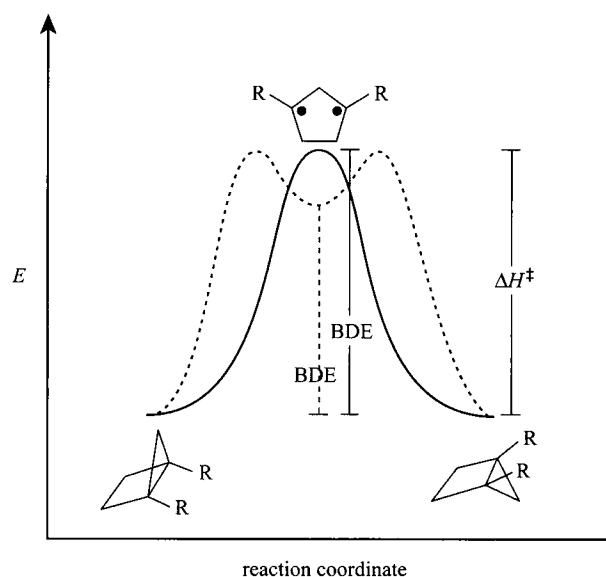
² For a discussion, see Mezey, P. G. *Potential Energy Hypersurfaces*; Elsevier: Amsterdam, 1987.

³ Coms, F. D.; Dougherty, D. A. *J. Am. Chem. Soc.* **1989**, *111*, 6894.

⁴ Wentrup, C. *Reactive Molecules*; John Wiley & Sons: New York, 1984; p. 2.

⁵ For theoretical calculations and leading references to previous work, see Sherrill, C. D.; Seidl, E. T.; Schaefer, H. F. III. *J. Phys. Chem.* **1992**, *96*, 3712. For 4-methylene-1,3-cyclopentenediyl, the energy well was determined to be 2.7 kcal/mol: Roth, W. R.; Bauer, F.; Breuckmann, R. *Chem. Ber.* **1991**, *124*, 2041.

⁶ Cruickshank, F. R.; Hyde, A. J.; Pugh, D. J. *Chem. Educ.* **1977**, *54*, 288.

**FIGURE 5.2**

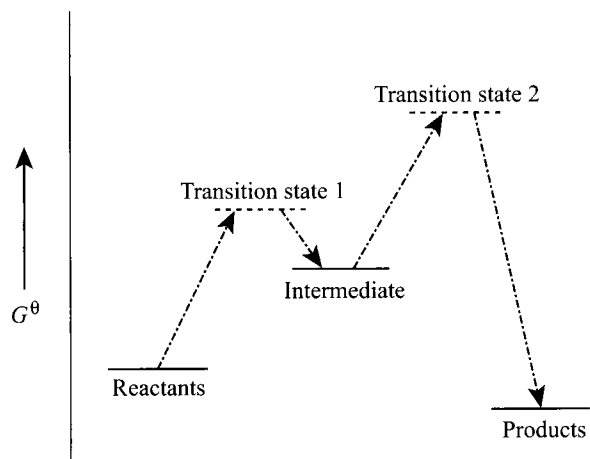
Reaction coordinate diagram for 1,3-cyclopentadienyl as an intermediate (dashed line) or transition structure (solid line) in the ring inversion of bicyclo[2.1.0]pentane. (Adapted from reference 3.)

of a reaction mixture as a function of time. They preferred *reaction coordinate* to be a molecular quantity—the progress toward product formation of an individual molecule (in a unimolecular process) or set of molecules (in a polymolecular process). With terms defined in this way, they noted that it is inappropriate to label the vertical axis of a reaction coordinate diagram as *free energy*, since a reaction coordinate does not actually define a thermodynamic state. These authors suggested that reaction–free energy diagrams be represented as a Gibbs diagram (Figure 5.3). There the vertical scale is G^θ , which refers to the free energy of a mole of the species shown, not to that of individual molecular units. The horizontal broken lines indicate that the transition states do not represent stable compounds. Such figures are often drawn to illustrate the results of theoretical calculations in which only the energies of reactants, transition states, and intermediates have been determined.

Both Figures 5.2 and 5.3 provide a starting point for the consideration of reactive intermediates and their roles in organic reactions. In the current discussion, we want to focus on the structural features that affect the stability of reactive intermediates and then relate this understanding to the chemical course and kinetics of a reaction. In most cases these reactive intermediates will be ions in which a carbon atom formally bears the positive or negative charge or radicals and carbenes in which the nonbonded electrons are formally localized on a carbon atom. Certainly there are other carbon-centered reactive intermediates (such as carbynes⁷ and atomic carbon⁸), and

⁷ Ruzsicska, B. P.; Jodhan, A.; Choi, H. K. J.; Strausz, O. P.; Bell, T. N. *J. Am. Chem. Soc.* **1983**, *105*, 2489; LaFrancois, C. J.; Shevlin, P. B. *J. Am. Chem. Soc.* **1994**, *116*, 9405; Seburg, R. A.; Hill, B. T.; Jesinger, R. A.; Squires, R. R. *J. Am. Chem. Soc.* **1999**, *121*, 6310.

⁸ Shevlin, P. B. in Moss, R. A.; Platz, M. S.; Jones, M., Jr., Eds. *Reactive Intermediate Chemistry*; John Wiley & Sons: Hoboken, NJ, 2004; chapter 10.

**FIGURE 5.3**

Gibbs diagram for a reaction with an intermediate.
(Reproduced from reference 6.)

there are important reactive intermediates centered on other atoms (including nitrenes,⁹ nitrenium ions,¹⁰ and silylenes^{11,12}). The processes used to generate these species are carried out relatively infrequently by most organic chemists, however. Focusing on reactive species more commonly proposed as intermediates in organic reactions will allow us to introduce many of the important techniques used to study reactive intermediates and thus will set the stage for discussions in following chapters.

5.2 RADICALS

A carbon-centered radical is a structure with a formal charge of 0 and one unpaired electron on a carbon atom.¹³ Examples include the methyl radical (1), the vinyl radical (2), the phenyl radical (3), and the triphenylmethyl radical (4). Radicals are often called *free radicals*, a term that arose from early nomenclature systems in which a *radical* was a substituent group that was preserved as a unit through a chemical transformation.¹⁴ Thus, the CH₃ group as a substituent was known as the methyl "radical," so a neutral •CH₃ group

⁹ Platz, M. S. in Moss, R. A.; Platz, M. S.; Jones, M., Jr., Eds. *Reactive Intermediate Chemistry*; John Wiley & Sons: Hoboken, NJ, 2004; chapter 11; Gritsan, N. P.; Platz, M. S. *Adv. Phys. Org. Chem.* **2001**, *36*, 255.

¹⁰ Falvey, D. E. in Moss, R. A.; Platz, M. S.; Jones, M., Jr., Eds. *Reactive Intermediate Chemistry*; John Wiley & Sons: Hoboken, NJ, 2004; chapter 13; Novak, M.; Rajagopal, S. *Adv. Phys. Org. Chem.* **2001**, *36*, 167.

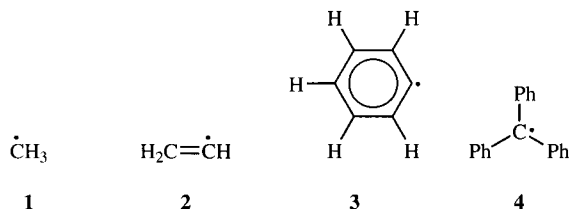
¹¹ Tokitoh, N.; Ando, W. in Moss, R. A.; Platz, M. S.; Jones, M., Jr., Eds. *Reactive Intermediate Chemistry*; John Wiley & Sons: Hoboken, NJ, 2004; chapter 14.

¹² For a discussion of the discovery of reactive intermediates, see Andraos, J. *Can. J. Chem.* **2005**, *83*, 1415.

¹³ The definition of radical given here is sufficient for our discussions, but there are more precise definitions. One is that a radical is "a species with one or more (spin-free) natural orbitals whose occupation numbers are near 1." Klein, D. J.; Alexander, S. A. in King, R. B.; Rouvray, D. H., Eds. *Graph Theory and Topology in Chemistry*; Elsevier: Amsterdam, 1987; p. 404.

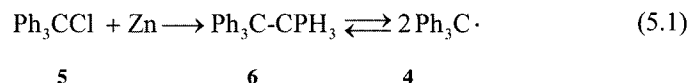
¹⁴ Walling, C. *Free Radicals in Solution*; John Wiley & Sons: New York, 1957; p. 2.

became a “free” radical. The terms *radical* and *free radical* are now used interchangeably.^{15,16}



Early Evidence for the Existence of Radicals

Before 1900 chemists considered carbon to be tetrasubstituted in virtually all organic compounds. Then, Gomberg's attempt to prepare hexaphenylethane from the reaction of triphenylmethyl chloride (5) with zinc dust (equation 5.1) gave colored solutions that reacted with reagents such as iodine (equation 5.2) to produce stable products. The results were interpreted in terms of an equilibrium between hexaphenylethane (6) and triphenylmethyl radicals.^{17–19}



Hexaphenylethane was accepted as the structure for the dimer of the triphenylmethyl radical for over sixty years. In 1968, however, Lankamp and co-workers reported that the ¹H NMR spectrum of the supposed “hexaphenylethane” indicated that it is most likely 7 (equation 5.3).^{20,21} That structural assignment was strengthened by a report that treating the dimer with *t*-BuOK produces 8.^{22,23}

¹⁵ Forrester, A. R.; Hay, J. M.; Thomson, R. H. *Organic Chemistry of Stable Free Radicals*; Academic Press: New York, 1968; p. 1.

¹⁶ For an overview of the chemistry of radicals, see (a) Kochi, J. K., Ed. *Free Radicals*, Vols. I and II; John Wiley & Sons: New York, 1973; (b) Leffler, J. E. *An Introduction to Free Radicals*; Wiley-Interscience: New York, 1993; (c) Fossey, J.; Lefort, D.; Sorba, J. *Free Radicals in Organic Chemistry*; John Wiley & Sons: Chichester, UK, 1995.

¹⁷ Gomberg, M. *Chem. Ber.* **1900**, 33, 3150; *J. Am. Chem. Soc.* **1900**, 22, 757.

¹⁸ Flürscheim, B. *J. Prakt. Chem.* **1905**, 71, 497; see the discussion in Skinner, K. J.; Hochster, H. S.; McBride, J. M. *J. Am. Chem. Soc.* **1974**, 96, 4301.

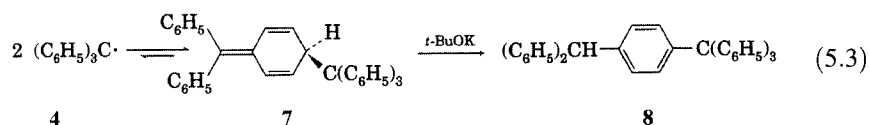
¹⁹ Tidwell, T. T. *Adv. Phys. Org. Chem.* **2001**, 36, 1; Ebersson, L. *Adv. Phys. Org. Chem.* **2001**, 36, 59.

²⁰ Lankamp, H.; Nauta, W. T.; MacLean, C. *Tetrahedron Lett.* **1968**, 249.

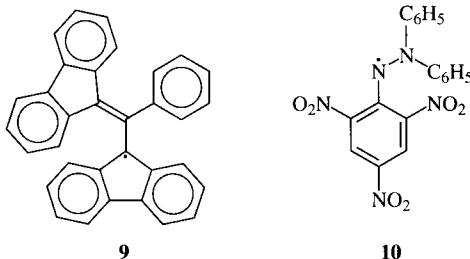
²¹ The bond dissociation energy of hexaphenylethane has been calculated to be 16.6 kcal/mol, suggesting that it might be possible to synthesize 6: Vreven, T.; Morokuma, K. *J. Phys. Chem. A* **2002**, 106, 6167.

²² Guthrie, R. D.; Weisman, G. R. *J. Chem. Soc. D* **1969**, 1316.

²³ McBride, J. M. *Tetrahedron* **1974**, 30, 2009 noted that 7 had been proposed as the structure for the dimer in 1904 and was supported by several lines of evidence in the following two years, and he discussed the process by which the incorrect structure became accepted.



Even though the proposal of **6** as the structure of the dimer was in error, the demonstration of the existence of radicals as transient species led to a great effort to study other radicals. Radicals reported in the literature range from some that are extremely unstable, short-lived species to others that can be isolated as pure substances.²⁴ For example, Koelsch reported that the radical α,γ -bisdiphenylene- β -phenylallyl (**9**) could be recovered in part after being subjected to molecular oxygen in boiling benzene for 6 hours.^{25,26} A well-known example of a nitrogen-centered radical is 2,2-diphenyl-1-picrylhydrazyl (DPPH), **10**, which is commercially available. DPPH has found increasing use in the measurement of the radical scavenging capabilities of a variety of synthetic compounds and dietary substances having antioxidant properties.^{27,28}



Detection and Characterization of Radicals

Experimental structure elucidation techniques can be used to characterize radicals if conditions can be found in which the radicals are produced in higher concentration and with longer lifetimes than is the case under typical reaction conditions. For example, the relative stability of the triphenylmethyl radical (**4**) allows it to be studied by magnetic susceptibility determination,

²⁴ Longer-lived radicals are termed *kinetically stable* or *persistent*. Extremely persistent radicals have been termed *inert*: Juliá, L.; Ballester, M.; Riera, J.; Castañer, J.; Ortin, J. L.; Onrubia, C. *J. Org. Chem.* **1988**, *53*, 1267.

²⁵ Koelsch, C. F. *J. Am. Chem. Soc.* **1957**, *79*, 4439.

²⁶ Persistent free radicals have found application as image-enhancing agents for studies of pH and of molecular oxygen concentrations in biological systems: Reddy, T. J.; Iwama, T.; Halpern, H. J.; Rawal, V. H. *J. Org. Chem.* **2002**, *67*, 4635; Bobko, A. A.; Dhimitruka, I.; Zweier, J. L.; Khramtsov, V. V. *J. Am. Chem. Soc.* **2007**, *129*, 7240.

²⁷ Cheng, Z.; Moore, J.; Yu, L. *J. Agric. Food Chem.* **2006**, *54*, 7429; Rackova, L.; Snirc, V.; Majekova, M.; Majek, P.; Stefek, M. *J. Med. Chem.* **2006**, *49*, 2543; Sendra, J. M.; Sentandreu, E.; Navarro, J. L. *J. Agric. Food Chem.* **2007**, *55*, 5512.

²⁸ For a discussion of substituent effects on the stability of radicals, see Creary, X. *Acc. Chem. Res.* **2006**, *39*, 761.

which involves weighing a sample both inside and outside a magnetic field.²⁹ The unpaired electron makes the radical paramagnetic, so the sample is drawn into the magnetic field. By this technique a 0.1 M solution of **7** was determined to be 0.2% dissociated.³⁰

A technique that has been of greater value to organic chemists is that of **electron paramagnetic resonance (EPR) spectroscopy**.^{31–33} The electron has a spin quantum number, m_s , which may have the value $+\frac{1}{2}$ or $-\frac{1}{2}$. If electrons are paired in an orbital, then one electron has $m_s = +\frac{1}{2}$ and the other has $m_s = -\frac{1}{2}$, and there is no net spin magnetic moment. If there is one unpaired electron, however, there will be a net magnetic moment of 9.284×10^{-19} erg-gauss. In the presence of an external magnetic field (H_0) the spin state having $m_s = -\frac{1}{2}$ is lower in energy, while that having $m_s = +\frac{1}{2}$ is higher in energy. The energy difference between the two spin states, ΔE , is

$$\Delta E = h\nu = g\beta_e H_0 \quad (5.4)$$

Here g is the spectroscopic splitting factor, which is the ratio of the magnetic moment (μ) to the angular momentum of the electron. The value of g is 2.002319 for a free electron, and it does not vary greatly for unpaired electrons in organic radicals.³⁴ The term β_e is the Bohr magneton, a constant with the value 9.2732×10^{-21} erg/gauss. Thus, at a field of 3400 gauss, the difference in energy between the electron spin states is

$$\begin{aligned} \Delta E &= 2.0023 \times (9.2732 \times 10^{-21} \text{ erg/gauss}) \times (3400 \text{ gauss}) \\ &= 0.63 \times 10^{-16} \text{ erg} \end{aligned} \quad (5.5)$$

which equals 0.91 cal/mol and which corresponds to a frequency of 9500 MHz.³⁵ Applying the Boltzmann distribution to this energy difference gives a relative population of 1,000,000 spins in the higher energy state to 1,001,500 spins in the lower energy state. Thus, at the same magnetic field strength, the difference between the two spin populations is greater than is the corresponding difference in spin populations in proton magnetic resonance. This is fortunate, because EPR measurements are usually made on materials in which only a fraction of the sample consists of free radicals.

In EPR spectroscopy, the sample is placed in a magnetic field and is irradiated with electromagnetic energy of an appropriate frequency. If the magnetic field is varied linearly, absorption of energy by the sample can be

²⁹ Selwood, P. W. in Weissberger, A., Ed. *Technique of Organic Chemistry*, Vol. I, Part IV; John Wiley & Sons: New York, 1960; p. 2873 ff.

³⁰ Roy, M. F.; Marvel, C. S. *J. Am. Chem. Soc.* **1937**, *59*, 2622.

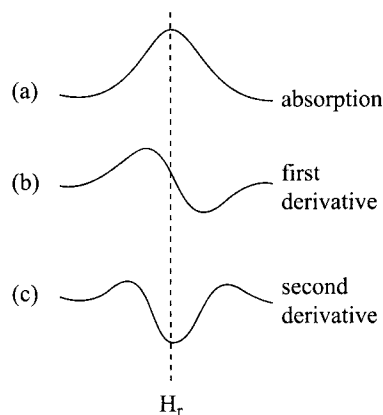
³¹ The technique is also known as *electron spin resonance (ESR) spectroscopy*. For a brief summary of the procedure, see Rieger, P. H. in Weissberger, A.; Rossiter, B. W., Eds. *Physical Methods of Organic Chemistry*, Vol. I, Part IIIA; Wiley-Interscience: New York, 1972; pp. 499–598.

³² Ayscough, P. B. *Electron Spin Resonance in Chemistry*; Methuen & Co.: London, 1967.

³³ Weil, J. A.; Bolton, J. R. *Electron Paramagnetic Resonance: Elementary Theory and Practical Applications*, 2nd ed.; John Wiley & Sons: Hoboken, NJ, 2007.

³⁴ Gordon, A. J.; Ford, R. A. *The Chemist's Companion*; John Wiley & Sons: New York, 1972; p. 336.

³⁵ Relationships between frequency and energy are discussed in Chapter 12.

**FIGURE 5.4**

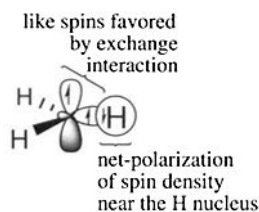
Representations of EPR spectra: (a) resonance signal, (b) first derivative, and (c) second derivative. (Reproduced from reference 37.)

recorded as a decrease in the radiofrequency energy received by a detector.³⁶ Thus, we could observe an absorption or *resonance* when the changing magnetic field strength makes the energy difference between the two spin states exactly equal to the energy of the electromagnetic radiation, as shown in Figure 5.4(a). Unlike NMR spectroscopy, however, the EPR signal is often recorded as the first derivative of absorption, Figure 5.4(b), or as the second derivative of the absorption, Figure 5.4(c).³⁷

The g value in equation 5.4 has been compared to the chemical shift (δ) in NMR spectroscopy. The very slight variation in g values from radical to radical means that g values seldom give chemically useful information for most organic compounds, however. What is of more value is the splitting of the EPR signal due to *hyperfine coupling* of the electron spin with the spins of nearby magnetic nuclei such as ^1H , ^2D , ^{13}C , and ^{17}O .³⁸ The mechanism of hyperfine coupling requires that the unpaired electron have spin density in an orbital having electron density at the nucleus. Because only s orbitals meet this requirement, hyperfine coupling depends on the s character of an orbital with unpaired electron density. The **hyperfine coupling constant** (termed the a value) of an electron in a $1s$ orbital of a hydrogen atom is 507 G, while the a value for an electron in a $2s$ orbital on ^{13}C is 1100 G. The unpaired electron in a methyl radical (Figure 5.5) is usually assumed to be localized in a p orbital on carbon. Since hyperfine coupling depends on the s character of an orbital, we might not expect to see hyperfine coupling of the unpaired electron in a methyl radical. Nevertheless, a $^{13}\text{C}_\alpha$ a value of 39 G is observed for the methyl radical, so it appears that about 4% s character is mixed into the orbital containing the unpaired electron.³⁹

**FIGURE 5.5**

Bonding model for planar methyl radical.

**FIGURE 5.6**

Mechanism of spin polarization for planar methyl radical.

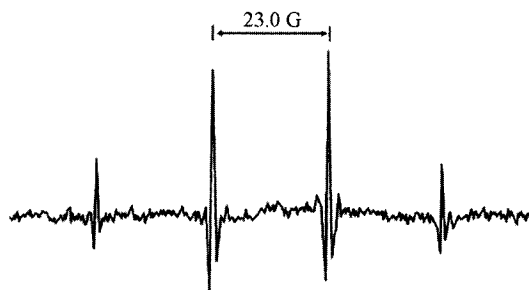
There are also hyperfine coupling interactions with the hydrogen nuclei of the methyl radical, which occurs through a process known as **spin polarization** (Figure 5.6). Due to the Pauli exchange principle, the energy of the electron pair responsible for bonding of the radical center (designated C_α) to a substituent is lower if the electron nearer C_α has the same spin as the

³⁶ This simplified description of the technique is for conceptual purposes only and does not represent modern Fourier transform spectroscopy.

³⁷ The figures are adapted from those presented by Bunce, N. J. *J. Chem. Educ.* **1987**, *64*, 907.

³⁸ In EPR spectroscopy the term *coupling* refers to interaction of one electron spin with another.

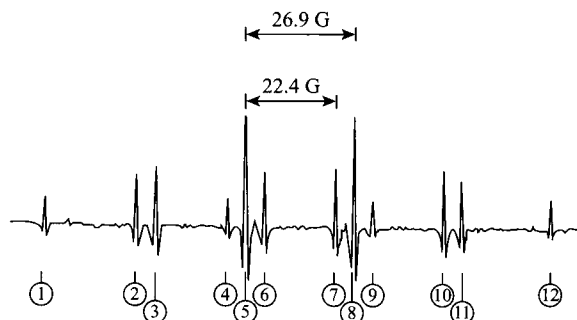
³⁹ Newcomb, M. in Moss, R. A.; Platz, M. S.; Jones, M., Jr., Eds. *Reactive Intermediate Chemistry*; John Wiley & Sons: Hoboken, NJ, 2004; p. 121.

**FIGURE 5.7**

EPR spectrum of methyl radical. (Reproduced from reference 44.)

unpaired electron. The electron closer to hydrogen is therefore more likely to have the *opposite* spin from that of the unpaired electron, giving rise to what is termed *negative spin polarization* near the hydrogen nucleus.^{40–43} The methyl radical has three hydrogen atoms bonded to C_α , so the EPR signal (shown as a second derivative spectrum in Figure 5.7) is split into a four-line pattern with relative intensities of 1:3:3:1.⁴⁴ Similarly, the unpaired electron in the benzene radical anion is split by six equivalent protons, so the signal is a septet with relative intensities 1:6:15:20:15:6:1.^{45–47} The magnitude of the splitting is indicated in gauss (G) or millitesla (mT). One tesla equals 10^4 gauss, so 1 mT = 10 G.

Figure 5.8 shows the EPR spectrum (also as a second derivative) of the ethyl radical.⁴⁴ Splitting of the signal by the two protons on the α carbon atom ($a_\alpha = 22.4$ G) gives rise to a three-line pattern, but each of those three lines is

**FIGURE 5.8**

EPR spectrum of ethyl radical. (Reproduced from reference 44.)

⁴⁰ Mile, B. *Curr. Org. Chem.* **2000**, 4, 55.

⁴¹ McConnell, H. M. *J. Chem. Phys.* **1956**, 24, 764; McConnell, H. M.; Heller, C.; Cole, T.; Fessenden, R. W. *J. Am. Chem. Soc.* **1960**, 82, 766.

⁴² See also Symons, M. C. R. *Chemical and Biochemical Aspects of Electron-Spin Resonance Spectroscopy*; John Wiley & Sons: New York, 1978.

⁴³ This type of coupling is called *isotropic* hyperfine coupling, since it does not depend on the orientation of the unpaired electron spin with the external magnetic field. There is also an *anisotropic* hyperfine coupling that depends on the orientation of the electron spin and the external magnetic field, but it is much weaker than the isotropic hyperfine coupling and is not observed for freely moving radicals in solution.

⁴⁴ Fessenden, R. W.; Schuler, R. H. *J. Chem. Phys.* **1963**, 39, 2147. Figure 5.7 is shown as the negative of the second derivative spectrum.

⁴⁵ Tuttle, T. R., Jr.; Weissman, S. I. *J. Am. Chem. Soc.* **1958**, 80, 5342.

⁴⁶ Carrington, A. *Q. Rev. Chem. Soc.* **1963**, 17, 67.

⁴⁷ The spectrum of the *t*-butyl radical shows a ten-line pattern with relative intensities 1:9:36:81:126:126:81:36:9:1 due to splitting by the nine equivalent protons (reference 32).

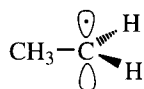


FIGURE 5.9
Localized model for ethyl radical (**11**).

further split into four lines by the β protons ($a_\beta = 26.9$ G). The combination of the two sets of splittings gives rise to a twelve-line pattern. Also of interest here are the magnitudes of the two a values. As noted above, the magnitude of the hyperfine coupling depends on the density of the unpaired electron in an orbital with s character about a magnetic nucleus. Therefore, it might seem surprising that the values of a_α and a_β for the ethyl radical are approximately equal, because such a result is not consistent with a simple model for the ethyl radical (**11**, Figure 5.9) in which the unpaired electron density is localized on C_α . Nevertheless, it is common for values of a_α and a_β to be similar.⁴⁸ Values of a_γ (e.g., the hyperfine coupling constant for splitting the signal of a 1-propyl radical by the terminal methyl group) are much smaller, typically less than 1 G.^{37,49}

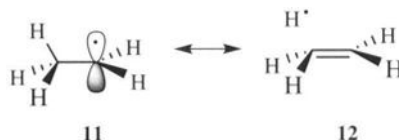


FIGURE 5.10
Hyperconjugation model for ethyl radical.

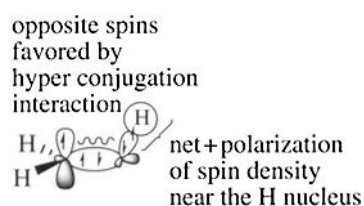


FIGURE 5.11
Representation of the hyperconjugation contribution to the a_β value of the ethyl radical.

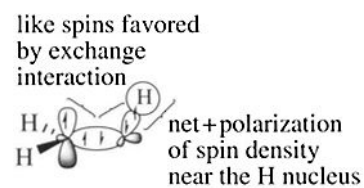


FIGURE 5.12
Illustration of the spin polarization contribution to the a_β value of the ethyl radical.

The valence bond explanation for the similarity of a_α and a_β values is based on the concept of hyperconjugation (Chapter 4).⁵⁰ As shown in Figure 5.10, we can write **12** as a resonance structure for **11**.⁵¹ Now the unpaired electron density is localized on one of the hydrogen atoms of the methyl group, but rotation about the C–C bond enables all three of the hydrogen atoms to participate equally in the hyperconjugation. The view that hyperconjugation can be rationalized meaningfully through the use of resonance structures such as **12** was a source of some controversy.⁵² Of course, Figure 5.10 does not mean that the ethyl radical is in *equilibrium* with structures without C $_\beta$ –H bonds, only that structures such as **12** contribute to the resonance hybrid of the ethyl radical. A more detailed description of the transfer of electron spin to the β hydrogen atoms of the ethyl radical by hyperconjugation is shown in Figure 5.11. In addition to hyperconjugation, a spin polarization effect (Figure 5.12) also causes electron spins near C $_\beta$ to be opposite that of the unpaired electron. As a result, the electron that is on average closer to the hydrogen nucleus in the C $_\beta$ –H bond will have the same spin as the unpaired electron, giving rise to positive spin polarization.

The preceding hyperconjugation model for hyperfine coupling is complemented by the perturbational molecular orbital analysis shown in Figure 5.13. Here the singly occupied molecular orbital (SOMO) is higher in energy than a π -like methyl group orbital that is parallel with the p orbital. The interaction of the SOMO and the HOMO produces two new orbitals, one

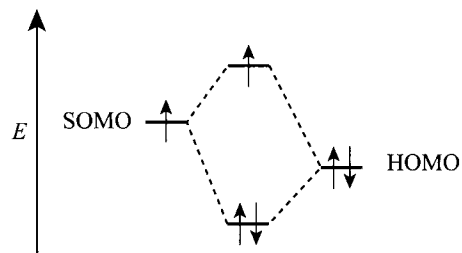
⁴⁸ Symons, M. C. R. *J. Chem. Soc.* **1959**, 277 and references therein.

⁴⁹ In special cases longer range coupling can be seen. 3-[n]Staffyl radicals (based on repeating units of [1.1.1]propellane) have been reported to show coupling with ϵ , ζ and even ι protons. McKinley, A. J.; Ibrahim, P. N.; Balaji, V.; Michl, J. *J. Am. Chem. Soc.* **1992**, *114*, 10631.

⁵⁰ Rossi, A. R.; Wood, D. E. *J. Am. Chem. Soc.* **1976**, *98*, 3452.

⁵¹ Wheland, G. W. *J. Chem. Phys.* **1934**, *2*, 474.

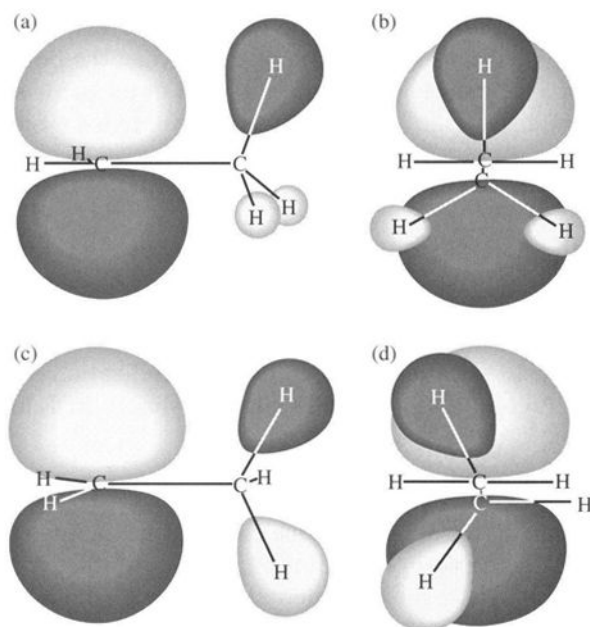
⁵² Dewar, M. J. S. *Hyperconjugation*; Ronald Press: New York, 1962; Shiner, V. J., Jr.; Campaigne, E. Eds. *Conference on Hyperconjugation*, proceedings of a conference held at Indiana University 2–4 June, 1958; Pergamon Press: New York, 1959.

**FIGURE 5.13**

PMO description of radical stabilization: interaction of SOMO with donor HOMO.

lower in energy than the HOMO and one higher in energy than the SOMO. Since two electrons go into the lower energy orbital but only one goes into the higher energy orbital, the effect is overall stabilizing. Moreover, the new, higher energy SOMO now has electron density on both the radical carbon and the adjacent methyl group.

Additional insight into the ethyl radical comes from an extended Hückel calculation. Figure 5.14 shows the orbital contours for the SOMO calculated for a conformation in which none of the C_{β} -H bonds eclipse either of the C_{α} -H bonds. We note first that this orbital does have π character, and the portion of the orbital near the CH_2 group resembles a p orbital. There is also density associated with the CH_3 end of the structure. Specifically, there is significant density on the hydrogen of the C_{β} -H bond that is parallel to the p orbital on the adjacent carbon atom, and there is some density on the other two hydrogen atoms also.⁵³ Figure 5.14 also shows that a similar picture results when one C_{β} -H bond eclipses a C_{α} -H bond. Although an analysis of all the

**FIGURE 5.14**

(a) Side and (b) end views of SOMO of ethyl radical in bisected conformation; (c) side and (d) end views of SOMO of ethyl radical in eclipsed conformation.

⁵³ Figure 5.14 does not mean that one of the CH_3 hydrogen atoms on the ethyl radical is different from the other two. Rotation about the C-C bond will introduce the same amount of unpaired electron density onto all of the hydrogen atoms.

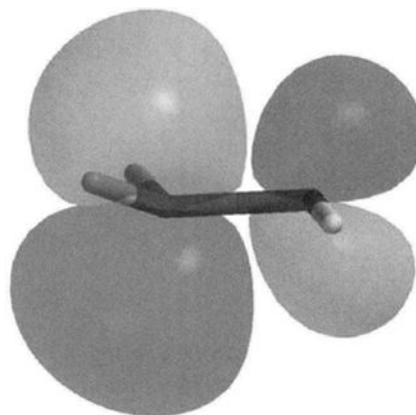


FIGURE 5.15
SOMO of hydroxymethyl radical, $\bullet\text{CH}_2\text{OH}$.

populated MOs would be necessary to draw firm conclusions, the orbital contour of the ethyl SOMO is consistent with the view both from hyperconjugation and from PMO theory that some electron density of the methyl group is delocalized into the half-empty p orbital, thus lowering the energy of the radical and giving rise to the large a_β value.⁵⁴

Other substituents capable of delocalizing the electron deficiency can also stabilize a radical center. For example, the tendency of ethers to form hydroperoxides upon exposure to oxygen results from the stabilization of a carbon radical by an adjacent oxygen atom. This interaction is illustrated in Figure 5.15 by the SOMO calculated for one conformation of the hydroxymethyl radical, which has density on both the oxygen and the carbon atoms.

The stabilizing effect of an α substituent on a radical center, relative to its effect on the parent hydrocarbon, is the **radical stabilization energy** (RSE). RSE values can be considered the difference between the bond dissociation energy (BDE) of a reference system and the BDE of the same system having that group as a substituent.⁵⁵ If methane is the reference system, then

$$\text{RSE of X in } \bullet\text{CH}_2\text{X} = (\text{BDE of CH}_4) - (\text{BDE of CH}_3\text{X}) \quad (5.6)$$

Alternatively, the RSE may be considered the ΔH of the isodesmic reaction



In both cases, a positive value of RSE indicates stabilization of the radical by the substituent. A compilation of RSE values is shown in Table 5.1.

Structure and Bonding of Radicals

The methyl radical (Figure 5.5) is shown having planar geometry at the radical center, and this geometry has been confirmed by both experimental and theoretical studies.⁵⁶ There is experimental evidence that other alkyl radicals either are planar structures or are pyramidal structures that can become

⁵⁴ For a summary of the shapes of all the orbitals of the $\text{CH}_3\text{CH}_2\bullet$ radical, see Jorgensen, W. L.; Salem, L. *The Organic Chemist's Book of Orbitals*; Academic Press: New York, 1973; p. 96.

⁵⁵ Menon, A. S.; Wood, G. P. F.; Moran, D.; Radom, L. *J. Phys. Chem. A* **2007**, *111*, 13638.

⁵⁶ Bickelhaupt, F. M.; Ziegler, T.; Schleyer, P. v. R. *Organometallics*, **1996**, *15*, 1477.

TABLE 5.1 Radical Stabilization Energies for Selected Substituents at 0 K

X in $\bullet\text{CH}_2\text{X}$	RSE (kcal/mol)
CH ₃	4.6 ± 0.3
OH	8.7 ± 0.2
OCH ₃	8.7
NH ₂	10.9 ± 2.0
SH	11.0 ± 2.0
F	3.6 ± 1.0
Cl	4.9 ± 0.6
Br	5.3 ± 0.6
CN	7.8 ± 1.0
CH=CH ₂	16.5 ± 0.7
C ₆ H ₅	14.7 ± 1.2

Source: Reference 55.

planar through inversion (like ammonia).⁵⁷ For example, chlorination of (+)-1-chloro-2-methylbutane (**13**) with Cl₂ produced racemic 1,2-dichloro-2-methylbutane (**14**). The results are most consistent with an intermediate radical that can react with Cl₂ equally well from either face of the radical center (Figure 5.16).⁵⁸

Spectroscopic data can be used to distinguish between planar and nonplanar, rapidly inverting radical centers. The hyperfine coupling constant (a_α) in the methyl radical is 23.0 G, which is a typical value for the splitting of an EPR signal by hydrogens attached to a radical center.⁵⁹ Theoretical analysis of the spectrum suggested that the methyl radical probably is flat, although a deviation from planarity of 10°–15° could not be ruled out.⁶⁰ There is also spectroscopic evidence that the methyl radical in the gas phase is essentially planar.⁶¹ Thus, the methyl radical is conveniently described by sp^2 hybridization, with the unpaired electron located primarily in the p orbital.

Substitution of a hydrogen atom on a methyl radical with fluorine or other electronegative atom makes the structure become less planar, and each

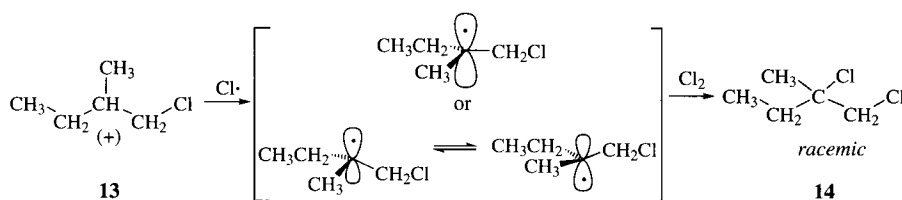


FIGURE 5.16
Racemization accompanying chlorination of (+)-1-chloro-2-methylbutane.

⁵⁷ Eliel, E. L. *Stereochemistry of Carbon Compounds*; McGraw-Hill: New York, 1962; pp. 380–384; Simamura, O. *Top. Stereochem.* **1969**, *4*, 1.

⁵⁸ Brown, H. C.; Kharasch, M. S.; Chao, T. H. *J. Am. Chem. Soc.* **1940**, *62*, 3435.

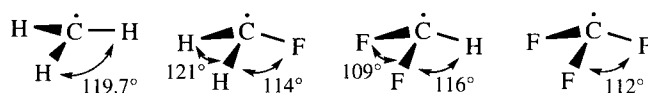
⁵⁹ More correctly, the *magnitude* of a_α is 23.0 G. In this experiment, only the magnitude of a_α is evident, but there is other evidence that the value is actually -23.0 G.

⁶⁰ Karplus, M. *J. Chem. Phys.* **1959**, *30*, 15.

⁶¹ Ellison, G. B.; Engelking, P. C.; Lineberger, W. C. *J. Am. Chem. Soc.* **1978**, *100*, 2556 and references therein.

FIGURE 5.17

Calculated geometries of fluoro-substituted methyl radicals.⁶⁴

**FIGURE 5.18**

Stabilization of ethyl radical through pyramidalization. (Adapted from reference 68.)



subsequent substitution makes the radical become more pyramidal.^{62,63} This conclusion is consistent with results of semiempirical calculations, and the geometries of fluoromethyl radicals calculated by this method are shown in Figure 5.17.^{64,65} A qualitative explanation of the geometry of fluoro-substituted radicals was provided by Pauling.⁶⁶ Pauling proposed that a carbon radical center would use sp^3 hybrid orbitals to bond substituents having the same electronegativity as carbon. Because of the electronegativity of fluorine, C–F bonds should be constructed with carbon orbitals having a greater degree of p character than would be the case for C–H bonds (see Chapter 1). Thus, there is less electron density near carbon in the orbitals used for C–F bonding than in orbitals used for C–H bonding. This has the effect of reducing the F–C–F bond angles to values less than 109.5° and increasing H–C–H bond angles to values greater than 109.5° .⁶⁷

Not only are fluoro-substituted radicals nonplanar, but alkyl-substituted radicals are found to be nonplanar as well. This result is consistent with Pauling's view that a carbon radical center would use sp^3 hybrid orbitals to bond substituents having the same electronegativity as carbon.⁶⁶ Paddon-Row and Houk ascribed the pyramidalization of the radical center to two other effects: (1) increased staggering of bonds to the radical center with respect to bonds on adjacent atoms, and (2) increased hyperconjugation of the p orbital with one of the adjacent σ bonds.⁶⁸ As shown in Figure 5.18, pyramidalization of the ethyl radical makes the C–H bonds on the CH_2 group more nearly staggered with respect to two of the C–H bonds on the CH_3 group. At the same time, the p orbital on the CH_2 group becomes more nearly parallel with the orbitals comprising a C–H bond of the methyl group, thus stabilizing the unfilled orbital system of the radical through hyperconjugation.

⁶² Fessenden, R. W.; Schuler, R. H. *J. Chem. Phys.* **1965**, *43*, 2704. See also Rogers, M. T.; Kispert, L. D. *J. Chem. Phys.* **1967**, *46*, 3193.

⁶³ Dolbier, W. R., Jr., in Chambers, R. D., Ed. *Organofluorine Chemistry: Fluorinated Alkenes and Reactive Intermediates*; Springer: New York, 1997, p. 97.

⁶⁴ Bernardi, F.; Cherry, W.; Shaik, S.; Epiotis, N. D. *J. Am. Chem. Soc.* **1978**, *100*, 1352 and references therein.

⁶⁵ Beveridge, D. L.; Dobosh, P. A.; Pople, J. A. *J. Chem. Phys.* **1968**, *48*, 4802.

⁶⁶ Pauling, L. *J. Chem. Phys.* **1969**, *51*, 2767.

⁶⁷ Of course, this explanation is based on the concept of straight (internuclear) C–F bonds and does not consider the possibility of curved bonds, which have since been advanced to explain the geometry of fluorocarbons.

⁶⁸ Paddon-Row, M. N.; Houk, K. N. (a) *J. Am. Chem. Soc.* **1981**, *103*, 5046; (b) *J. Phys. Chem.* **1985**, *89*, 3771.

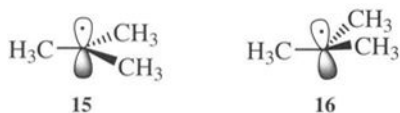
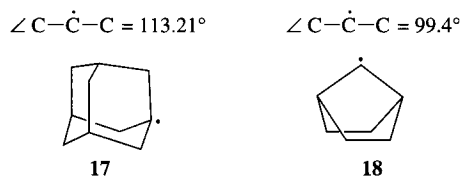


FIGURE 5.19

Planar (left) and nonplanar (right) geometries for *t*-butyl radical.

The *t*-butyl radical is an especially interesting case. We might expect the radical to be planar (15, Figure 5.19) because that geometry would minimize the steric repulsion of methyl groups. However, the experimental a_C value is 46.2 G, which was interpreted in terms of a C–C–C bond angle of 117.3° (16).⁶⁹ This result suggests that the electronic stabilization resulting from pyramidalization (Figure 5.18) outweighs the increase in energy due to steric effects.⁷⁰

The tendency of alkyl radicals to be nonplanar means that radicals can form at the bridgehead positions of bicyclic structures. Indeed, rates of radical reactions at bridgehead carbon atoms do not indicate significant strain due to pyramidalization, at least not in comparison with the strain due to bridgehead carbenium carbon atoms.⁷¹ Radicals such as 1-adamantyl (17) and 7-norbornyl (18) can be formed, although the stabilities of such species decrease with increasing deviation from the geometry observed for acyclic analogs.^{72,73} Thus, the general view that emerges from these studies is that only the methyl radical prefers to be planar, and even it has a low barrier to deformation.



Thermochemical Data for Radicals

We would like to determine the heats of formation and/or strain energies of radicals and correlate the data with their properties.⁷⁴ In principle, the heat of formation of a radical (R^\bullet) formed by homolytic dissociation of $R-X$ (equation 5.8) can be calculated according to equation 5.9, where all data refer to 298 K and ΔH_f° is the ΔH for the reaction in equation 5.8.⁷⁵



$$\Delta H_f^\circ(R^\bullet) = \Delta H_f^\circ - \Delta H_f^\circ(X^\bullet) + \Delta H_f^\circ(RX) \quad (5.9)$$

⁶⁹ Wood, D. E.; Williams, L. F.; Sprecher, R. F.; Lathan, W. A. *J. Am. Chem. Soc.* **1972**, *94*, 6241.

⁷⁰ This conclusion was questioned by Griller, D.; Ingold, K. U. *J. Am. Chem. Soc.* **1973**, *95*, 6459.

⁷¹ Compare Applequist, D. E.; Roberts, J. D. *Chem. Rev.* **1954**, *54*, 1065 and references therein. See also the discussion in Chapter 8.

⁷² Danen, W. C.; Tipton, T. J.; Saunders, D. G. *J. Am. Chem. Soc.* **1971**, *93*, 5186.

⁷³ For a review of bridgehead radicals, see Walton, J. C. *Chem. Soc. Rev.* **1992**, 105.

⁷⁴ Compare Simões, J. A. M.; Greenberg, A.; Liebman, J. F., *Energetics of Organic Free Radicals*; Chapman & Hall: London, 1996.

⁷⁵ Egger, K. W.; Cocks, A. T. *Helv. Chim. Acta* **1973**, *56*, 1516.

TABLE 5.2 Experimental and Predicted Thermochemical Data

Radical (R•)	BDE (R–H) ^a (kcal/mol)	ΔH_f° (lit) ^a (kcal/mol)	ΔH_f° (calc. with 1,3 repulsive) ^b (kcal/mol)	ΔH_f° (calc. with 1,3 attractive) ^c (kcal/mol)
Methyl	104.99 ± 0.03	35.05 ± 0.07	29.0	29.00
Ethyl	101.1 ± 0.04	29.0 ± 0.4	23.9	24.02
Isopropyl	98.6 ± 0.04	21.5 ± 0.4	21.5	21.29
sec-Butyl	98.2 ± 0.5	16.1 ± 0.5	16.1	16.31
t-Butyl	96.5 ± 0.4	12.3 ± 0.4	12.3	12.40

^a See reference 79.^b See reference 83.^c See reference 85.

ΔH_f° can be estimated from the activation energy for a bond homolysis if we assume that there is no activation energy for the recombination process. In some cases this assumption seems reasonable. For example, the activation energy for the dimerization of two ethyl radicals was determined to be ca. 0 ± 0.2 kcal/mol.⁷⁶ Some radical combination reactions do have activation energies, however. The combination of two 3-ethyl-3-pentyl radicals to give hexaethylethane was found to have an activation energy of about 20 kcal/mol, apparently as the result from steric hindrance in the dimer.^{4,77} In addition, if either of the radicals is delocalized, then part of the activation energy may result from loss of the delocalization energy.⁷⁸

Values for ΔH_f° of radicals and for the heats of dissociation reactions have been compiled and are available in the literature.^{75,79,80} Table 5.2 lists data for several small alkyl radicals as well as the C–H bond dissociation energies for the corresponding alkanes. The regular decrease in the C–H bond dissociation energies to form methyl, ethyl, isopropyl, or *t*-butyl radicals is the basis for the familiar generalization that the stability of radicals is methyl < 1° < 2° < 3°. As was the case for the ethyl radical, we can attribute increasing stability from increasing alkyl substitution at the radical center to either hyperconjugation (Figure 5.10) or delocalization (Figure 5.13).

While the bond dissociation energies and heats of formation of many carbon-centered radicals are well established, the role that hyperconjugation plays in determining these values has been a matter of dispute. Ingold and DiLabio calculated that 31% of the spin at the β hydrogens in the ethyl radical arises from the spin polarization mechanism, suggesting that the remaining 69% arises from hyperconjugation.⁸¹ They also calculated that the spin arising from hyperconjugation involving all of the β -CH₃ groups bonded to C _{α} varied from 0.11 for ethyl to 0.20 for isopropyl to 0.27 for *t*-butyl. These values correlated very well with the C–H bond dissociation energies for ethane, propane (for 2° C–H homolysis), and isobutane (3° C–H homolysis) and fit on the same line with the C3–H bond dissociation energy of propene (thus

⁷⁶ Hiatt, R.; Benson, S. W. *J. Am. Chem. Soc.* **1972**, *94*, 6886.⁷⁷ Beckhaus, H.-D.; Rüchardt, C. *Tetrahedron Lett.* **1973**, 1971.⁷⁸ For a discussion, see Dannenberg, J. J.; Tanaka, K. *J. Am. Chem. Soc.* **1985**, *107*, 671.⁷⁹ Blanksby, S. J.; Ellison, G. B. *Acc. Chem. Res.* **2003**, *36*, 255.⁸⁰ See also Seakins, P. W.; Pilling, M. J.; Niiranen, J. T.; Gutman, D.; Krasnoperov, L. N. *J. Phys. Chem.* **1992**, *96*, 9847.⁸¹ Ingold, K. U.; DiLabio, G. A. *Org. Lett.* **2006**, *8*, 5923.

forming an allyl radical) if one assumes that 40% of the unpaired electron density on C1 of allyl is delocalized by resonance. Thus, the investigators argued that hyperconjugation is an important factor in determining C–H bond dissociation energies.

The conclusions of Ingold and DiLabio were challenged by Gronert, who reported that plots of the C–X bond dissociation energies versus the C_{β} –H spin density attributed to hyperconjugation by Ingold and DiLabio are linear for the saturated alkanes but not for propene when X = OH, CH₃, SH, and I.⁸² Gronert concluded that the linear plot for C–H homolysis is a coincidental relationship and does not provide evidence of hyperconjugative stabilization of radicals. As noted in Chapter 1, Gronert also proposed that the stabilities of alkanes could be predicted by a model assuming that 1,3-geminal interactions are repulsive, not attractive.⁸³ Not only does the Gronert model account for the heats of formation of the alkanes, but it also uses the same parameters to predict the heats of formation of small alkyl radicals. For example, Table 5.2 illustrates the correlation between literature ΔH_f° values for a number of small alkyl radicals and values calculated by the Gronert approach. Therefore, Gronert argued that the differences in C–H bond strengths in alkanes arise from *differences* between the repulsive 1,3-interactions in the alkanes and the repulsive 1,3-interactions in the alkyl radicals, meaning that hyperconjugation is not responsible for the relative stability of alkyl radicals.⁸⁴ As was the case with the alkanes discussed in Chapter 1, however, Wodrich and Schleyer were able to predict the heats of formation of the alkyl radicals in Table 5.2 equally well by making the assumption that the 1,3-interactions are attractive.^{85,86}

Generation of Radicals

Radicals may be generated by thermal or photochemical processes that accomplish homolytic dissociation of a two-electron bond. Organic peroxides (equation 5.10) and azo compounds (equation 5.11) have weak bonds that undergo dissociation to radicals relatively easily.⁸⁷ Chemical or electrochemical oxidation or reduction of stable molecules can produce radicals as well.^{88,89} One approach for generating ethyl radicals is to add triethylborane to a reaction mixture from which not all the oxygen has been removed.^{39,90,91} Radicals may also be produced by photoinduced electron transfer (Chapter 12). Single electron transfer processes initially generate radical

⁸² Gronert, S. *Org. Lett.* **2007**, *9*, 2211.

⁸³ Gronert, S. *J. Org. Chem.* **2006**, *71*, 1209; 9560.

⁸⁴ Gronert, S. *J. Org. Chem.* **2006**, *71*, 7045.

⁸⁵ Wodrich, M. D.; Schleyer, P. v. R. *Org. Lett.* **2006**, *8*, 2135 and supporting information.

⁸⁶ Moreover, Stanger was able to correlate C–H dissociation energies of alkanes on the basis of the calculated hybridization of the orbital used for C–H bonding, which was in turn a function of molecular geometry. Stanger, A. *Eur. J. Org. Chem.* **2007**, 5717.

⁸⁷ Kita, Y.; Matsugi, M. in Renaud, P.; Sibi, M. P., Eds. *Radicals in Organic Synthesis, Vol. 1. Basic Principles*; Wiley-VCH: Weinheim, 2001; p. 1.

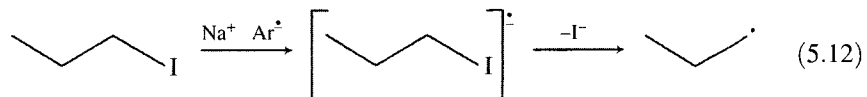
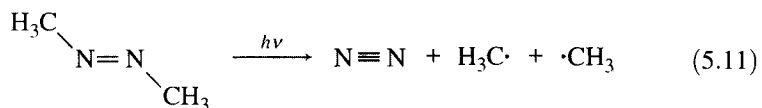
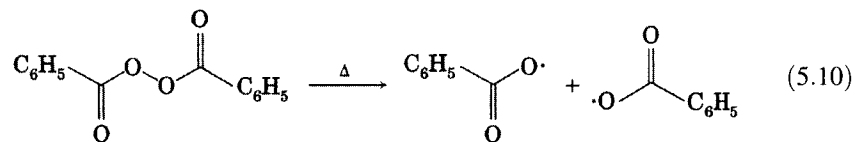
⁸⁸ Schäfer, H. J. in Renaud, P.; Sibi, M. P., Eds. *Radicals in Organic Synthesis, Vol. 1. Basic Principles*; Wiley-VCH: Weinheim, 2001; p. 250.

⁸⁹ Cossy, J. in Renaud, P.; Sibi, M. P., Eds. *Radicals in Organic Synthesis, Vol. 1. Basic Principles*; Wiley-VCH: Weinheim, 2001; p. 229.

⁹⁰ Nozaki, K.; Oshima, K.; Utimoto, K. *J. Am. Chem. Soc.* **1987**, *109*, 2547.

⁹¹ Yorimitsu, H.; Oshima, K. in Renaud, P.; Sibi, M. P., Eds. *Radicals in Organic Synthesis, Vol. 1. Basic Principles*; Wiley-VCH: Weinheim, 2001; p. 11.

cations (for oxidation) or radical anions (for reduction), which may then fragment to radicals and ions. For example, Sargent and co-workers determined that in 1,2-dimethoxyethane solution the radical anion of naphthalene (sodium naphthalenide, $\text{Na}^+ \text{Ar}^{\bullet-}$) transferred an electron to propyl iodide. Subsequent loss of iodide ion from the propyl iodide radical anion produced the propyl radical (equation 5.12).⁹²

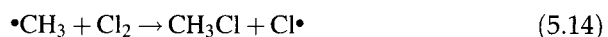
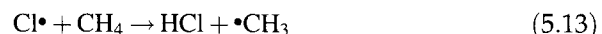


Reactions of Radicals

Radical reactions are frequently found to occur as chain reactions composed of three types of processes:

1. An **initiation** step, such as one of the generation reactions discussed in the previous section.
2. A series of **propagation** steps
3. One or more **termination** steps that stop the chain reaction.

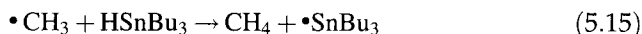
Each propagation step in a radical chain involves the reaction of a species with one unpaired electron to produce another species having one unpaired electron. Moreover, the reactant in one propagation step is a product in a subsequent propagation step. In the chlorination of methane, the first propagation step is the abstraction of a hydrogen atom by a chlorine atom (equation 5.13), and the second step is the abstraction of a chlorine atom from Cl_2 by the methyl radical (equation 5.14).



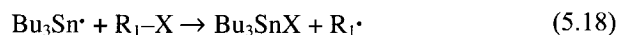
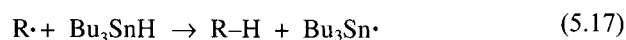
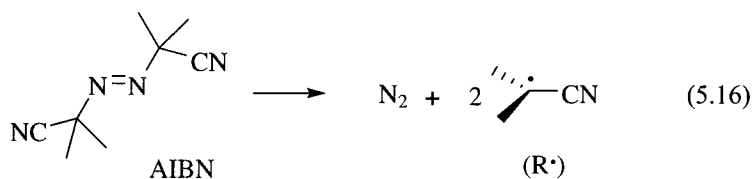
A carbon-centered radical can also abstract an atom from another molecule (or from another atom in the same molecule) to fill its outer shell if the free energy change for the abstraction is favorable. One example of this process is *radical trapping*, in which a radical abstracts a hydrogen atom from a

⁹² Sargent, G. D.; Cron, J. N.; Bank, S. J. *Am. Chem. Soc.* **1966**, *88*, 5363.

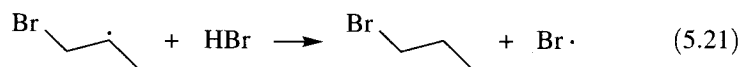
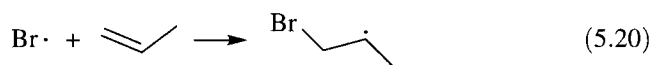
facile hydrogen atom donor such as tri-*n*-butyltin hydride (Bu_3SnH).^{93–95} The process is illustrated with methyl radical in equation 5.15. This reaction can serve as a means of detecting radical intermediates, because the appearance of the species R-H upon addition of Bu_3SnH to a reaction suggests the intermediacy of $\text{R}\cdot$ in the reaction.



Trialkyltin radicals can abstract chlorine, bromine, or iodine atoms from alkyl halides. Together with a radical initiator such as azobisisobutyronitrile (AIBN), trialkyltin hydrides and alkyl halides can give reduction or other radical-derived products.



Another common propagation step is addition of a radical to a double or triple bond, as in one of the propagation steps (equation 5.20) in the anti-Markovnikov addition of HBr to an alkene.



Radical addition to a multiple bond is the key step in radical polymerization.⁹⁶ For example, in the polymerization of styrene, the initiation step is homolysis of an initiator, which produces a radical that adds to a styrene molecule to begin the polymer chain. The propagation step illustrated in equation 5.22 is then repeated hundreds or thousands of times. Two carbon-carbon single bonds are about 20 kcal/mol more stable than one

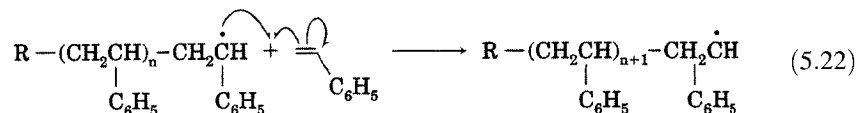
⁹³ Menapace, L. W.; Kuivila, H. G. *J. Am. Chem. Soc.* **1964**, *86*, 3047.

⁹⁴ Walling, C.; Cooley, J. H.; Ponnaras, A. A.; Racah, E. J. *J. Am. Chem. Soc.* **1966**, *88*, 5361.

⁹⁵ Kim, S.; Yoon, J.-Y. in Renaud, P.; Sibi, M. P., Eds. *Radicals in Organic Synthesis, Vol. 2. Applications*; Wiley-VCH: Weinheim, 2001; p. 1.

⁹⁶ Compare Georges, M. in Renaud, P.; Sibi, M. P., Eds. *Radicals in Organic Synthesis, Vol. 1. Basic Principles*; Wiley-VCH: Weinheim, 2001; p. 479.

carbon–carbon double bond, so the difference in the bond strengths provides the driving force for the reaction.⁹⁷ Increasingly, radical addition reactions are finding application in organic synthesis. Because charged species are not involved in the reaction, subtle effects due to orbital interactions and steric interactions can provide opportunities for stereoselective syntheses.⁹⁸ Radicals may have appreciable nucleophilic or electrophilic character, depending on substituents.^{99,100}



Another useful chain reaction involves the PTOC (pyridine-2-thione-*N*-oxycarbonyl) esters developed by Barton (Figure 5.20).¹⁰¹ Reaction of a carboxylic acid chloride (RCOCl) with the sodium salt of *N*-hydroxypyridine-2-thione produces an ester designated as R-PTOC. Addition of radical Y• (formed by an earlier initiation step) to the R-PTOC leads to the carboxy radical RCO₂•. The carboxy radical then decarboxylates to produce the radical R•, which can continue the chain reaction or can undergo other reactions.¹⁰²

Radicals are generally less susceptible to 1,2-hydrogen shifts and 1,2-alkyl shifts than are carbocations. For example, Brown and Russell found no evidence for the rearrangement of isobutyl radical to *t*-butyl radical in the chlorination of deuterium-labeled isobutane,¹⁰³ and the barrier for 1,2-shift in the ethyl radical was calculated to be ca. 55 kcal/mol.¹⁰⁴ Apparent 1,2-phenyl migration has been observed, however.^{16,105,106} Treatment of neophyl chloride (19) with phenylmagnesium bromide and cobaltous chloride produced *t*-butylbenzene (20, 27%), isobutylbenzene (21, 15%), 2-methyl-3-phenyl-1-propene (22, 9%), and β,β-dimethylstyrene (23, 4%).¹⁰⁷ The results suggest that rearrangement of neophyl radical (24, Figure 5.21) via the bridged 1,1-

⁹⁷ For an introduction, see Bevington, J. C. *Radical Polymerization*; Academic Press: London, 1961.

⁹⁸ Giese, B. *Radicals in Organic Synthesis: Formation of Carbon–Carbon Bonds*; Pergamon Press: Oxford, UK, 1986; Jasperse, C. P.; Curran, D. P.; Fevig, T. L. *Chem. Rev.* **1991**, *91*, 1237; Porter, N. A.; Giese, B.; Curran, D. P. *Acc. Chem. Res.* **1991**, *24*, 296.

⁹⁹ De Vleeschouwer, F.; Van Speybroeck, V.; Waroquier, M.; Geerlings, P.; De Proft, F. *Org. Lett.* **2007**, *9*, 2721. See also Schiesser, C. H.; Wille, U.; Matsubara, H.; Ryu, I. *Acc. Chem. Res.* **2007**, *40*, 303.

¹⁰⁰ For a survey of the synthetic applications of radicals in synthesis, see Renaud, P.; Sibi, M. P., Eds. *Radicals in Organic Synthesis, Vol. 2. Applications*; Wiley-VCH: Weinheim, 2001.

¹⁰¹ Barton, D. H. R.; Crich, D.; Motherwell, W. B. *Tetrahedron* **1985**, *41*, 3901.

¹⁰² PTOC esters are also useful in radical clock reactions: Newcomb, M.; Park, S. U. *J. Am. Chem. Soc.* **1986**, *108*, 4132; reference 111.

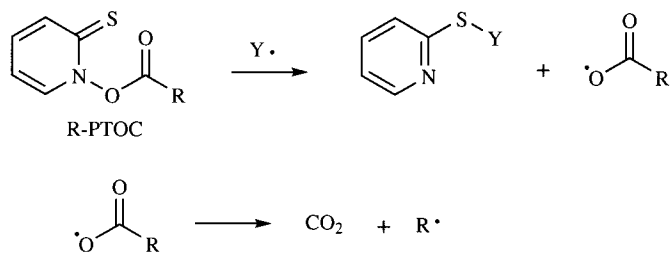
¹⁰³ Brown, H. C.; Russell, G. A. *J. Am. Chem. Soc.* **1952**, *74*, 3995.

¹⁰⁴ Hudson, C. E.; McAdoo, D. J. *Tetrahedron* **1990**, *46*, 331.

¹⁰⁵ Walling, C. in de Mayo, P., Ed. *Molecular Rearrangements*, Vol. 1; Wiley-Interscience: New York, 1963; pp. 407–455; Zipse, H. *Adv. Phys. Org. Chem.* **2003**, *38*, 111.

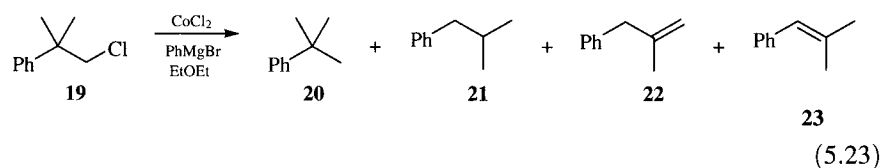
¹⁰⁶ 1,2-Hydrogen shifts in aryl radicals have been observed at high temperature. Calculated activation energies for the reaction are ca. 58 kcal/mol. Brooks, M. A.; Scott, L. T. *J. Am. Chem. Soc.* **1999**, *121*, 5444.

¹⁰⁷ Urry, W. H.; Kharasch, M. S. *J. Am. Chem. Soc.* **1944**, *66*, 1438.

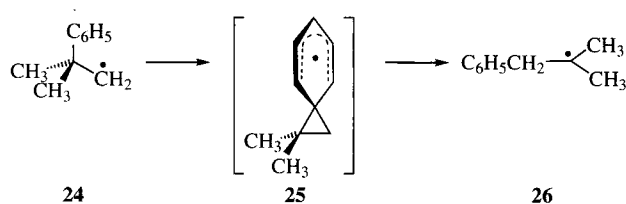
**FIGURE 5.20**

Generation of a radical through a PTOC ester.

dimethylspiro[2.5]octadienyl radical **25** leads to the formation of **26**, which is an intermediate in the formation of **21**, **22**, and **23**.^{108,109}



Radicals do exhibit facile intramolecular processes that may be classified as analogs of bimolecular addition or abstraction reactions. In some cases these reactions are considered to be diagnostic for the presence of radical intermediates in reactions under study. As illustrated for the 5-hexenyl radical (**27**) in equation 5.24, radicals easily cyclize to give a five-membered ring (**28**). Although the radical center is 1° in both reactant and product, the conversion of a carbon-carbon double bond to two carbon-carbon single bonds provides the driving force for the reaction. Formation of a 2° radical in a six-membered ring (**29**) would be favored thermodynamically, but the stereo-electronic requirement of the addition of the radical center to the alkene moiety favors the formation of the five-membered ring by a factor of 50 : 1.^{110,111} Such a process provides a diagnostic probe for radicals, since cations tend to cyclize to six-membered rings, while anions do not readily cyclize.¹¹²

**FIGURE 5.21**

Rearrangement of neophyl radical.

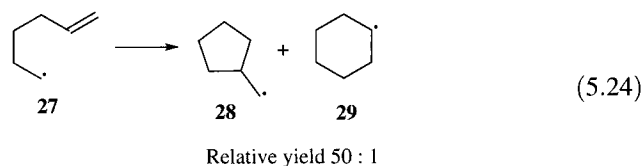
¹⁰⁸ Structure **24** cannot disproportionate because there is no hydrogen bonded to the β carbon atom. Moreover, steric hindrance may reduce the rate of its dimerization.

¹⁰⁹ For studies of the parent spiro[2.5]octadienyl radical, see Effio, A.; Griller, D.; Ingold, K. U.; Scaiano, J. C.; Sheng, S. J. *J. Am. Chem. Soc.* **1980**, *102*, 6063.

¹¹⁰ Beckwith, A. L. *J. Chem. Soc. Rev.* **1993**, *22*, 143.

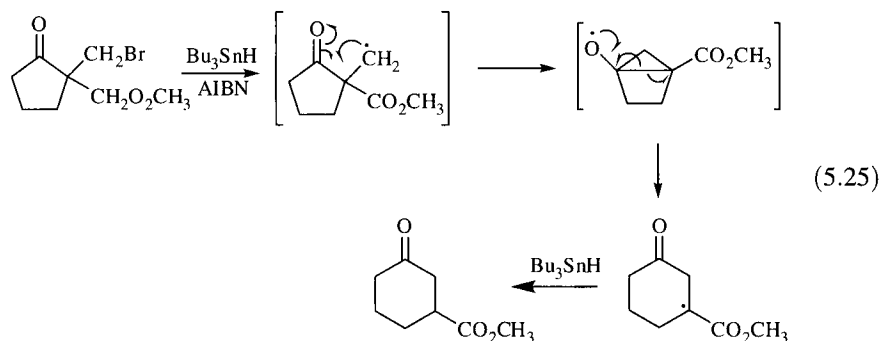
¹¹¹ Newcomb, M. *Tetrahedron* **1993**, *49*, 1151.

¹¹² Ingold, K. U. in Pryor, W. A., Ed. *Organic Free Radicals*; ACS Symposium Series 69, American Chemical Society: Washington, DC, 1978; p. 187 ff.



This pattern of reactivity is consistent with a set of empirical generalizations known as Baldwin's rules for ring-closing reactions.¹¹³ These rules are not restricted to intramolecular cyclizations involving radicals, but we will illustrate them in the context of radical reactions. The favored pathways for cyclizations are those in which the radical center approaches the olefinic carbon along a trajectory allowing better interaction orientation of the *p* orbital of a radical with the olefinic orbitals.^{40,114} If a radical forms a ring by adding to an intramolecular double bond, the process is described as *trig* (because the radical adds to a trigonal carbon). Addition to a triply bonded carbon is called *dig*, while reaction with a carbon bearing four substituents is called *tet*. If the closure leads to the smaller of the two possible rings, the process is called *exo*, while closure to form the larger of the two possible rings is termed *endo*. A number indicates the size of the ring formed by the closure. Thus, the 3-*exo-trig* closure in Figure 5.22 is termed 3 because a three-membered ring is formed, *exo* because the smaller of two possible rings is formed, and *trig* because the radical adds to a trigonal (olefinic) carbon atom. An alternative 4-*endo-trig* process would form the cyclobutyl radical, but it is not observed. Therefore, the energetically feasible processes are labeled "allowed," while noncompetitive cyclizations are labeled "forbidden."

Alkoxy radicals can undergo addition to a carbonyl group, followed by β -scission of the resulting alkoxy radical, and this pathway offers a useful route to ring expansion of appropriately substituted carbonyl compounds.^{115,116} For example, Dowd and Choi reported the formation of a cyclohexanone from a cyclopentanone by the reaction in equation 5.25.¹¹⁷



¹¹³ Baldwin, J. E. *Chem. Commun.* **1976**, 734, 738; Baldwin, J. E.; Cutting, J.; Dupont, W.; Kruse, L.; Silberman, L.; Thomas, R. C. *Chem. Commun.* **1976**, 736.

¹¹⁴ Spellmeyer, D. C.; Houk, K. N. *J. Org. Chem.* **1987**, 52, 959.

¹¹⁵ Baldwin, J. E.; Adlington, R. M.; Robertson, J. *Tetrahedron* **1989**, 45, 909.

¹¹⁶ Zhang, W. in Renaud, P.; Sibi, M. P., Eds. *Radicals in Organic Synthesis, Vol. 2. Applications*; Wiley-VCH: Weinheim, 2001; p. 234.

¹¹⁷ Dowd, P.; Choi, S.-C. *J. Am. Chem. Soc.* **1987**, 109, 3493.

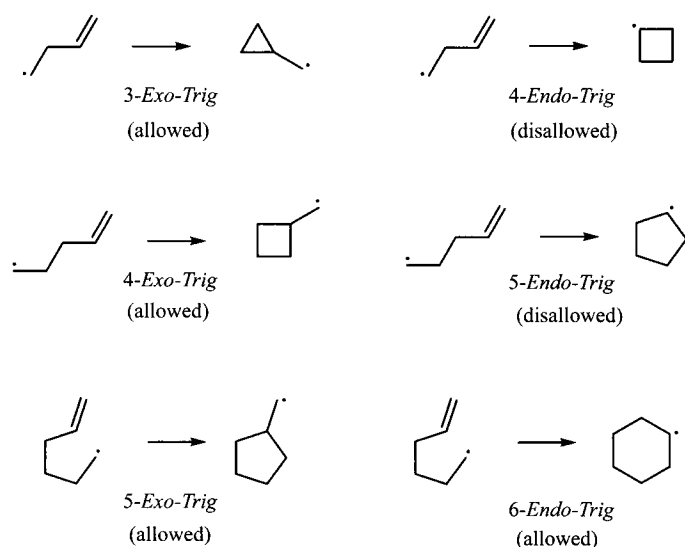


FIGURE 5.22
Baldwin designations for radical cyclizations.

The rate constants for several characteristic reactions of radicals have been shown to be relatively independent of solvent.¹¹⁸ If the radical partitions between one reaction with a known rate constant and another reaction with an unknown rate constant, the ratio of products can provide an estimate of the unknown rate constant.¹¹⁹ That is, the reactions can serve as a *radical clock* to determine the rate constant for the competing reaction.^{120–122}

As an example, consider the conversion of radical $\cdot R_1$ to $\cdot R_2$ and also the abstraction of a hydrogen atom from reagent $X-H$ by both $\cdot R_1$ and $\cdot R_2$, as shown in Figure 5.23. Plotting the product ratio, $[H-R_1]/[H-R_2]$ versus the concentration of the hydrogen atom donor, $[X-H]$, produces a linear correlation with slope equal to k_X/k_R (equation 5.26). If the rate constant for rearrangement, k_R , is known independently, then the rate constant for the competing reaction, k_X , is easily determined.

$$\frac{[R_1 - H]}{[R_2 - H]} = \frac{k_X}{k_R} [X - H] \quad (5.26)$$

For greatest accuracy, the rate constant of the radical clock reaction should be similar to the rate constant of the competing reaction. For this reason, investigators have developed a number of radical clocks with varying rate constants for reaction, as shown in Table 5.3. In addition to applications in the study of chemical reactions, radical clock reactions have been used extensively in studies of biological processes, such as the peroxidation of

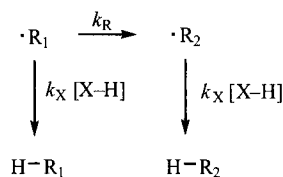


FIGURE 5.23
Reaction scheme for a radical clock reaction.

¹¹⁸ Fu, Y.; Li, R.-Q.; Liu, L.; Guo, Q.-X. *Res. Chem. Intermed.* **2004**, *30*, 279.

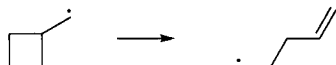
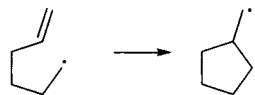



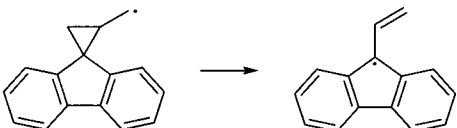
¹¹⁹ Newcomb, M. in Coxon, J. M., Ed. *Advances in Detailed Reaction Mechanisms*, Vol. 1; JAI Press: Greenwich, CT, 1991; pp. 1–33. Also see Hollis, R.; Hughes, L.; Bowry, V. W.; Ingold, K. U. *J. Org. Chem.* **1992**, *57*, 4284; Newcomb, M.; Johnson, C. C.; Manek, M. B.; Varick, T. R. *J. Am. Chem. Soc.* **1992**, *114*, 10915; Branchaud, B. P.; Glenn, A. G.; Stiasny, H. C. *J. Org. Chem.* **1991**, *56*, 6656; Nonhebel, D. C. *Chem. Soc. Rev.* **1993**, *22*, 347.

¹²⁰ Newcomb, M. *Tetrahedron* **1993**, *49*, 1151.

¹²¹ Newcomb, M. in Renaud, P.; Sibi, M. P., Eds. *Radicals in Organic Synthesis*, Vol. 1. *Basic Principles*; Wiley-VCH: Weinheim, 2001; p. 317.

¹²² Griller, D.; Ingold, K. U. *Acc. Chem. Res.* **1980**, *13*, 317.

TABLE 5.3 Room Temperature Rate Constants for Radical Clock Reactions

Reaction	k_R (s^{-1})	Reference
	1×10^3	127
	2×10^5	127
	4.5×10^7	128
	1.2×10^8	129
	4.8×10^{10}	130
	ca. 4×10^{12}	131

lipids¹²³ and the hydroxylation of C–H bonds by cytochrome P450.^{124,125,131} It is also possible to design probe molecules that can distinguish between radical and cationic pathways.^{126,131}

Radical chain reactions are terminated by processes that lead to species with an even number of electrons. The two most important termination steps are combination and disproportionation. Combination (equation 5.27) is the reverse of the thermal dissociation of a σ bond to produce two radicals. Radical combination is usually quite exothermic and thus has a small or negligible activation energy. As noted above, however, significant steric

¹²³ Roschek, B., Jr.; Tallman, K. A.; Rector, C. L.; Gillmore, J. G.; Pratt, D. A.; Punta, C.; Porter, N. A. *J. Org. Chem.* **2006**, *71*, 3527.

¹²⁴ Kumar, D.; de Visser, S. P.; Sharma, P. K.; Cohen, S.; Shaik, S. *J. Am. Chem. Soc.* **2004**, *126*, 1907.

¹²⁵ He, X.; Ortiz de Montellano, P. R. *J. Biol. Chem.* **2004**, *279*, 39479.

¹²⁶ He, X.; Ortiz de Montellano, P. R. *J. Org. Chem.* **2004**, *69*, 5684.

¹²⁷ Jin, J.; Newcomb, M. *J. Org. Chem.* **2007**, *72*, 5098.

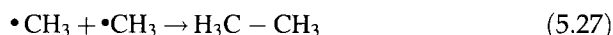
¹²⁸ Ha, C.; Horner, J. H.; Newcomb, M.; Varick, T. R.; Arnold, B. R.; Luszytk, J. *J. Org. Chem.* **1993**, *58*, 1194.

¹²⁹ Bowry, V. W.; Luszytk, J.; Ingold, K. U. *J. Am. Chem. Soc.* **1991**, *113*, 5687.

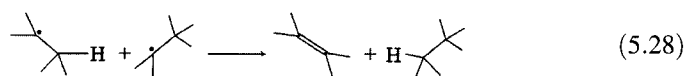
¹³⁰ Newcomb, M.; Glenn, A. G.; Williams, W. G. *J. Org. Chem.* **1989**, *54*, 2675.

¹³¹ Newcomb, M.; Toy, P. H. *Acc. Chem. Res.* **2000**, *33*, 449.

hindrance can lower the dissociation energy and introduce a barrier to recombination.



Disproportionation can be considered to be the abstraction of a hydrogen atom from one radical by another radical.¹³² One of the radical centers is converted to a carbon–hydrogen bond, while the other radical becomes an olefin (equation 5.28). Both combination and disproportionation represent bimolecular process of radicals. Combination is more exothermic than is disproportionation, but the ΔS for dimerization is much more negative than is ΔS for disproportionation. Therefore, the reaction of two radicals depends strongly on temperature, with higher temperature favoring disproportionation and lower temperature favoring combination.¹³³



There is one important exception to the statement that radical chain reaction termination steps produce products with an even number of electrons. A radical addition step may produce a radical product that is so much less reactive than its precursor that further chain reaction is precluded. This process, which is known as **spin trapping**, is primarily useful as a means of studying radicals that cannot be studied directly by EPR. Adding a nitroso compound or a nitron to a reaction mixture involving short-lived radicals can produce a **spin adduct**, a more persistent species that can be studied directly by EPR spectrometry (Figure 5.24).¹³⁴ The spectrum of the product is often diagnostic of its radical precursor.^{135,136} As shown in Figure 5.25, Caldwell and co-workers designed a spin trap capable of distinguishing between radicals and oxidative metal ions under biological conditions.¹³⁷

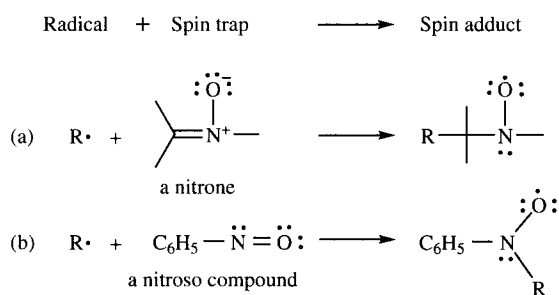


FIGURE 5.24

Reaction of a radical with a nitron (a) or a nitroso compound (b) in a spin trapping reaction.

¹³² Gibian, M. J.; Corley, R. C. *Chem. Rev.* **1973**, 73, 441.

¹³³ Bevington, J. C. *Trans. Faraday Soc.* **1952**, 48, 1045.

¹³⁴ Ebersson, L. *Adv. Phys. Org. Chem.* **1998**, 31, 91.

¹³⁵ For an introduction to spin trapping, see Janzen, E. G. *Acc. Chem. Res.* **1971**, 4, 31; Perkins, M. J. *Adv. Phys. Org. Chem.* **1980**, 17, 1.

¹³⁶ Janzen, E. G.; Evans, C. A.; Davis, E. R. in *Organic Free Radicals*, ACS Symposium Series 69; American Chemical Society: Washington, D. C., 1978; p. 433 ff.

¹³⁷ Caldwell, S. T.; Quin, C.; Edge, R.; Hartley, R. C. *Org. Lett.* **2007**, 9, 3499.

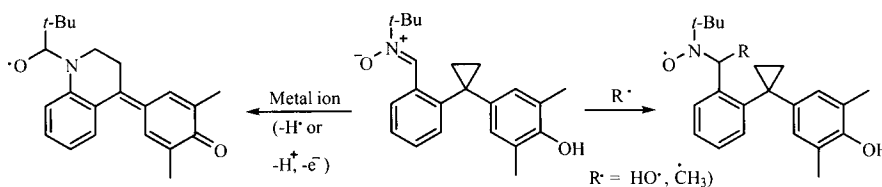


FIGURE 5.25
A discriminating spin trap.

5.3 CARBENES

Structure and Geometry of Carbenes

A **carbene** is a structure containing a neutral carbon atom that is bonded to only two other atoms, that has a formal charge of 0, and that has two nonbonded electrons localized on that carbon atom.¹³⁸ The simplest chemical example of such a structure is CH_2 , commonly called *methylene*. Figure 5.26 shows three different electronic states that could be proposed for methylene.¹³⁹ In **30a** the two electrons are both in the same orbital and therefore must be paired. In **30b** and **30c** they are in separate orbitals, so these two electrons may or may not have paired spins. Structures **30a** and **30b** are called *singlet* states, since the nonbonded electrons have their spins paired. In **30c** the spins of the nonbonded electrons are not paired, so this is a triplet state.¹⁴⁰ Based on Hund's rule, we expect the triplet to be lower in energy than the singlet, so **30b** is an excited state of **30c**. In theory all of the states in Figure 5.26 are possible, although they have different energies, patterns of reaction, and lifetimes.¹⁴¹

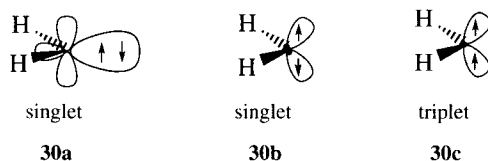


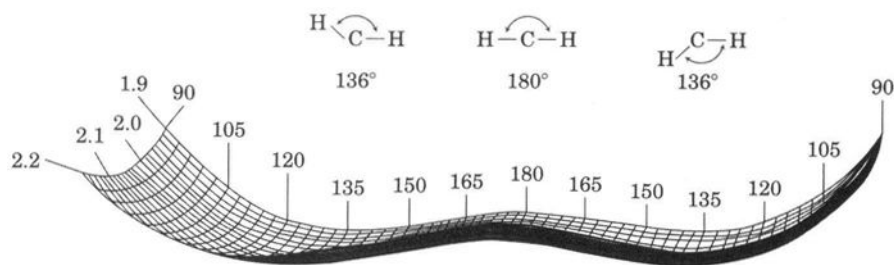
FIGURE 5.26
Singlet (**30a** and **30b**) and triplet (**30c**) states of methylene.

¹³⁸ For an introduction to the structures and reactions of carbenes, see (a) Liebman, J. F.; Simons, J. in Liebman, J. F.; Greenberg, A., Eds. *Molecular Structure and Energetics, Volume 1: Chemical Bonding Models*; VCH Publishers: Deerfield Beach, FL, 1986; p. 51; (b) Moss, R. A.; Jones, M., Jr., in Jones, M., Jr.; Moss, R. A., Eds. *Reactive Intermediates*, Vol. 2; John Wiley & Sons: New York, 1981; (c) Kirmse, W. *Carbene Chemistry*; Academic Press: New York, 1964; Gilchrist, T. L.; Rees, C. W. *Carbenes, Nitrenes and Arynes*; Appleton-Century-Crofts: New York, 1969; (d) Hine, J. *Divalent Carbon*; Ronald Press: New York, 1964; Bertrand, G. in Moss, R. A.; Platz, M. S.; Jones, M., Jr., Eds. *Reactive Intermediate Chemistry*; John Wiley & Sons: Hoboken, NJ, 2004; chapter 8; (e) Jones, M., Jr.; Moss, R. A. in Moss, R. A.; Platz, M. S.; Jones, M., Jr., Eds. *Reactive Intermediate Chemistry*; John Wiley & Sons: Hoboken, NJ, 2004; chapter 7.

¹³⁹ For further discussion, see Eisenthal, K. B.; Moss, R. A.; Turro, N. J. *Science* **1984**, 225, 1439; Gaspar, P. P.; Hammond, G. S. in reference 138d, pp. 235–274.

¹⁴⁰ The terms *singlet* and *triplet* arose from experiments in which singlet states gave emission at only one wavelength in certain spectroscopic experiments, while triplet states gave three lines (i.e., emission at three wavelengths). The distinction between singlet and triplet states will be especially important in the discussion of photochemistry (Chapter 12).

¹⁴¹ The **lifetime**, τ , of a transient species is the inverse of the sum of the rate constants for its disappearance (i.e., $\tau = 1/\Sigma k_i$).

**FIGURE 5.27**

Calculated potential energy surface for the lowest triplet state of methylene. (Adapted from reference 143.)

Structure **30a** has two electrons in one orbital and no electrons in another orbital. We would expect the carbon atom to be sp^2 hybridized, with the nonbonded electrons in an sp^2 orbital, leaving the p orbital empty. This arrangement allows the two electrons to be in a lower energy orbital having more s character. Structures **30b** and **30c** may be expected to have the same hybridization for the two singly occupied orbitals. If there is greater repulsion between pairs of electrons in the C–H bonds with each other than there is between the single electrons on carbon, then VSEPR theory would suggest that the H–C–H bond angle should be greater than 109.5° . The extreme angle of 180° , however, would be sp hybridization, and that would mean placing the two unpaired electrons into orbitals with no s character. Therefore, some hybridization intermediate between sp and sp^3 might be expected, but there is no obvious basis for predicting the hybridization for **30b** and **30c** exactly.

Theoretical and experimental studies support the expectation that the lowest energy electronic state of methylene is the triplet, **30c**. The singlet **30a** is a higher energy excited state, and the singlet **30b** is an even higher energy state. The exact difference in energy between **30c** and **30a** was the subject of some debate, however. Most theoretical calculations indicated a 10 kcal/mol energy separation, while an experimental value was reported to be about 20 kcal/mol. The issue was resolved when further experimental work gave a revised experimental value of 9 kcal/mol, which is very close to the calculated value.¹⁴²

The geometry of triplet methylene (**30c**) was also the subject of intensive theoretical and experimental work. Indeed, methylene was called a “paradigm for quantitative theoretical chemistry” because the success of computation in describing methylene, even in the face of initially contradictory experimental evidence, helped establish the credibility of computational chemistry.¹⁴³ Now the theoretical calculations and EPR data agree that triplet methylene is slightly bent, with an H–C–H angle of 136° (Figure 5.27).^{144–146} The species is thought to have only a small barrier to inversion in a process reminiscent of the inversion of nitrogen in amines.

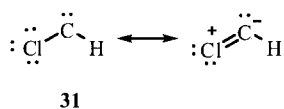
¹⁴² Leopold, D. G.; Murray, K. K.; Lineberger, W. C. *J. Chem. Phys.* **1984**, *81*, 1048. See also *Chem. Eng. News* **1984** (Nov 26), 30.

¹⁴³ Schaefer, H. F. III. *Science* **1986**, *231*, 1100. See also Wasserman, E. *Science* **1986**, *232*, 1319; Schaefer, H. F. III. *Science* **1986**, *232*, 1319; Wasserman, E.; Schaefer, H. F. III. *Science* **1986**, *233*, 829.

¹⁴⁴ Bender, C. F.; Schaefer, H. F. III. *J. Am. Chem. Soc.* **1970**, *92*, 4984.

¹⁴⁵ Wasserman, E.; Yager, W. A.; Kuck, V. J. *Chem. Phys. Lett.* **1970**, *7*, 409.

¹⁴⁶ Bunker, P. R.; Sears, T. J.; McKellar, A. R. W.; Evenson, K. M.; Lovas, F. J. *J. Chem. Phys.* **1983**, *79*, 1211; McKellar, A. R. W.; Yamada, C.; Hirota, E. *J. Chem. Phys.* **1983**, *79*, 1220; Bunker, P. R.; Jensen, P. *J. Chem. Phys.* **1983**, *79*, 1224.

**FIGURE 5.28**

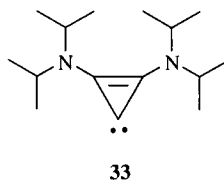
Stabilization of a singlet carbene by chlorine.

**FIGURE 5.29**

Stabilization of cyclopropenylidene (32) by adjacent p orbitals.

The structural principles discussed for methylene generally apply to other carbenes as well, but there are some additional considerations. Singlet carbenes are π -electron deficient because of the empty p orbital, but they are σ -electron rich because of the nonbonded pair of electrons in an sp^n orbital. Therefore, they are stabilized by groups that donate electrons to the empty p orbital of the carbene carbon by resonance and withdraw electrons through the σ framework by induction.¹⁴⁷ A halogen atom is such a substituent, and Moss and Mamantov found that a halogen bonded to the carbene center stabilizes the singlet state of the carbene relative to the triplet.^{148,149} Singlet chlorocarbene (31, Figure 5.28) is more stable than the triplet by about 6.8 kcal/mol, while singlet fluorocarbene is more stable than the triplet by ca. 14.5 kcal/mol.¹⁴⁷ The singlet of dichlorocarbene is calculated to be ca. 20 kcal/mol lower in energy than the triplet.^{150,151}

A particularly interesting singlet carbene is cyclopropenylidene, 32 (Figure 5.29), which may be the most abundant cyclic hydrocarbon in interstellar space.¹⁵² The structure is thought to be stabilized because the nonbonded pair of electrons is in an orbital with considerable s character, while the p orbital of the carbenic center is stabilized by electron donation from the adjacent olefinic system.¹⁵³ Cyclopropenylidene itself is not stable in the condensed phase, but the thermally stable bis(diisopropylamino) derivative 33 was reported to be stable.¹⁵²



Hyperconjugation can also stabilize singlet carbenes by donating C_β -C or C_β -H σ electron density to the empty p orbital of the carbene. This electron donation was calculated to lower the energy of singlet *t*-butylcarbene by about 18 kcal/mol.¹⁵⁴ Dialkylcarbenes may be stabilized by hyperconjugation involving two alkyl groups, but they may also be affected by steric interactions of the two alkyl groups. The resulting changes in bond angles at the carbene center affect the relative energies of the singlet and triplet states of the carbenes. The greater bond angle at the carbene carbon for di-*t*-butylcarbene,

¹⁴⁷ Scott, A. P.; Platz, M. S.; Radom, L. *J. Am. Chem. Soc.* **2001**, *123*, 6069.

¹⁴⁸ Moss, R. A.; Mamantov, A. *J. Am. Chem. Soc.* **1970**, *92*, 6951.

¹⁴⁹ Rate constants for rearrangements of alkylfluorocarbenes are about an order of magnitude lower than those of the alkylchlorocarbenes: Moss, R. A.; Ho, G.-J.; Liu, W. *J. Am. Chem. Soc.* **1992**, *114*, 959.

¹⁵⁰ Barden, C. J.; Schaefer, H. F. III. *J. Chem. Phys.* **2000**, *112*, 6515. See also Mukarakate, C.; Mishchenko, Y.; Brusse, D.; Tao, C.; Reid, S. A. *Phys. Chem. Chem. Phys.* **2006**, *8*, 4320.

¹⁵¹ Dichlorocarbene can be used to functionalize single-walled nanotubes: Hu, H.; Zhao, B.; Hamon, M. A.; Kamaras, K.; Itkis, M. E.; Haddon, R. C. *J. Am. Chem. Soc.* **2003**, *125*, 14893.

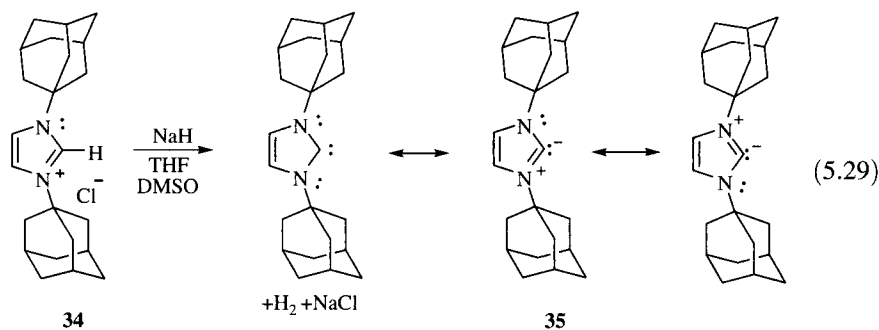
¹⁵² Lavallo, V.; Canac, Y.; Donnadiu, B.; Schoeller, W. W.; Bertrand, G. *Science* **2006**, *312*, 722.

¹⁵³ A QTAIM analysis suggested that the mechanism of stabilization may be more complicated: Johnson, L. E.; DuPré, D. B. *J. Phys. Chem. A* **2007**, *111*, 11066.

¹⁵⁴ Sulzbach, H. M.; Bolton, E.; Lenoir, D.; Schleyer, P. v. R.; Schaefer, H. F. III. *J. Am. Chem. Soc.* **1996**, *118*, 9908.

for example, means that the orbitals from the carbene carbon to the *t*-butyl groups must have greater *s* character. As a result, the orbital bearing the two nonbonded electrons in singlet di-*t*-butylcarbene have more *p* character. This destabilizes the singlet carbene, and the triplet becomes more stable by about 1 kcal/mol. Diphenylcarbene is also affected by the steric repulsion of the two phenyl groups, and it too has a triplet ground state. In a study of diphenylcarbene generated in diphenylethene crystals, the $C_{Ph}-C_{\alpha}-C_{Ph}$ bond angle was found to be 148° , and the phenyl rings were twisted 36° out of the plane defined by the carbene carbon atom and the two ring carbon atoms bonded to it.¹⁵⁵ Diarylcarbenes with substituents on the aryl groups may have even greater steric interactions, and the energy difference between the triplet ground state and the higher energy singlet state of a diarylcarbene tends to increase as steric effects make the carbene more nearly linear.¹⁵⁶

In some cases donation of nonbonded electrons by atoms β to the carbene carbon can stabilize singlet carbenes dramatically. Arduengo and co-workers reported that treating 1,3-di-1-adamantylimidazolium chloride (**34**) with the anion $CH_3SOCH_2^-$ in THF produced the singlet carbene 1,3-di-1-adamantylimidazol-2-ylidene (**35**, equation 5.29).¹⁵⁷ This carbene is stabilized thermodynamically by electron donation from the two amino groups, and it is stabilized kinetically by bulky adamantyl substituents that make it less likely to react intermolecularly. As a result, **35** is stable in the presence of air and moisture, and the crystals of **35** melt at $240\text{--}241^\circ\text{C}$.



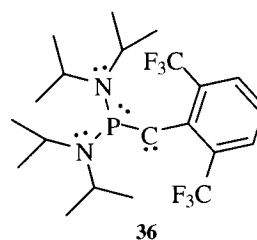
Compound **35** is known as a “push–push” carbene because two amino groups can donate electrons to the vacant *p* orbital of a singlet carbene. A “push–pull” carbene is a carbene stabilized both by resonance donation of electron density from an adjacent pair of nonbonded electrons to the empty *p* orbital of a singlet carbene and by stabilization of the nonbonded electron pair of the carbene through inductive or conjugative electron withdrawal by another substituent. For example, the singlet carbene **36**, where the phosphorus is the electron donor and the 2,6-bis(trifluoromethyl)phenyl group is the electron-withdrawing group, was found to be stable in solution at room temperature for weeks.¹⁵⁸

¹⁵⁵ Doetschman, D. C.; Hutchison, C. A., Jr. *J. Chem. Phys.* **1972**, *56*, 3964.

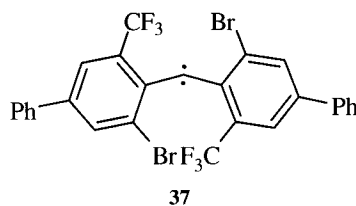
¹⁵⁶ Nazran, A. S.; Griller, D. *J. Am. Chem. Soc.* **1984**, *106*, 543.

¹⁵⁷ Arduengo, A. J. III; Harlow, R. L.; Kline, M. *J. Am. Chem. Soc.* **1991**, *113*, 361.

¹⁵⁸ The melting range of **36** was found to be $68^\circ\text{--}70^\circ\text{C}$. Buron, C.; Gornitzka, H.; Romanenko, V.; Bertrand, G. *Science* **2000**, *288*, 834.



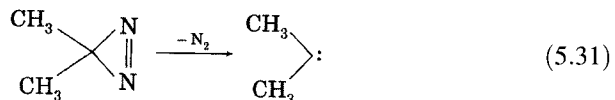
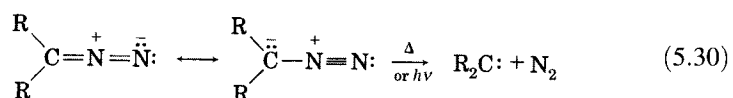
Hyperconjugation can stabilize triplet carbenes, but to a lesser extent than singlet carbenes, by donating $C_{\beta}-C$ σ or $C_{\beta}-H$ σ electron density to a half-filled orbital of the carbene center. It is more difficult to stabilize triplet carbenes than singlet carbenes with bulky alkyl substituents, because the radical character of triplet carbenes makes them much more reactive with C–H bonds.¹⁵⁹ Carbon–fluorine bonds are less reactive toward radicals, however, and the triplet carbene **37** was sufficiently stable to survive for nearly a day in solution at room temperature.¹⁶⁰



Generation of Carbenes

Carbenes may be synthesized by a variety of pathways that result in the elimination of two bonds from a tetravalent carbon atom. Among the more prominent of these reactions are the following:

1. Thermolysis or photolysis of diazoalkanes (equation 3.6) and dialkyl-diazirines (equation 3.7)

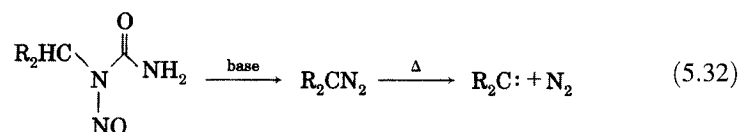


For example, *N*-nitrosoureas react with base to generate diazoalkanes, which can then eliminate nitrogen.¹⁶¹

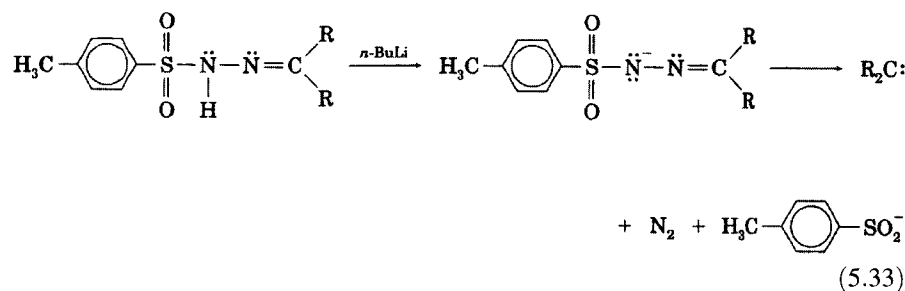
¹⁵⁹ For a discussion of factors that stabilize triplet carbenes, see Nemirowski, A.; Schreiner, P. R. *J. Org. Chem.* **2007**, *72*, 9533.

¹⁶⁰ Itoh, T.; Nakata, Y.; Hirai, K.; Tomioka, H. *J. Am. Chem. Soc.* **2006**, *128*, 957.

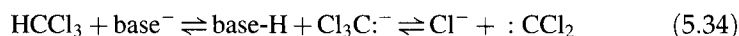
¹⁶¹ Jones, W. M.; Grasley, M. H.; Brey, W. S., Jr. *J. Am. Chem. Soc.* **1963**, *85*, 2754.



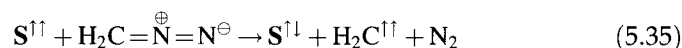
2. Reactions of tosylhydrazones with base.¹⁶²



3. α -Elimination reactions.¹⁶³



A carbene produced by elimination of N_2 or Cl^- is a singlet initially, but electronic relaxation to a lower energy triplet ground state can occur if reaction does not occur first. It is possible to produce a triplet carbene directly through a process known as **sensitization**, in which a triplet electronic excited state of a sensitizer (S) transfers energy to a carbene precursor and returns to its singlet ground electronic state (equation 5.35).¹⁶⁴ Conservation of electron spin requires that the carbene be produced in its triplet state.



4. Generation of carbenoids. The Simmons–Smith reaction produces a carbene equivalent that is stabilized by association with a metal and that reacts as a singlet carbene.¹⁶⁵



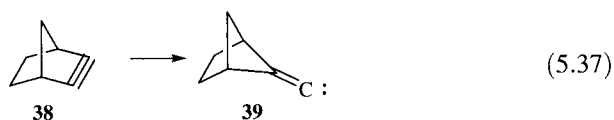
¹⁶² For a mechanism, see Figure 5.31.

¹⁶³ The base-promoted α -elimination of chloroform to dichlorocarbene was reported by Hine, J.; Dowell, A. M., Jr. *J. Am. Chem. Soc.* **1954**, *76*, 2688.

¹⁶⁴ A sensitizer is an electronically excited species that transfers energy to a ground state molecule, leading to the ground electronic state of the sensitizer and an electronically excited state of the energy acceptor. The symbol $\text{S}^{\uparrow\uparrow}$ means that the sensitizer is a triplet (i.e., the two electrons in singly occupied orbitals have the same spin). These terms will be discussed in Chapter 12.

¹⁶⁵ Simmons, H. E.; Smith, R. D. *J. Am. Chem. Soc.* **1958**, *80*, 5323.

5. Ring contraction of strained alkynes. For example, Gilbert and Yin reported evidence that ring contraction of norbornyne, **38**, produced the vinylidene **39**.¹⁶⁶



Reactions of Carbenes

The reactivity of a carbene is strongly influenced by its multiplicity—that is, whether it is a singlet or triplet. As noted above, some carbenes are produced as singlets, while others are formed as triplets or may convert to triplets before reaction.¹⁶⁷ Singlet and triplet carbenes exhibit similar reaction types, but there are some important differences between them.¹³⁸ Because it has both an empty *p* orbital (like a carbocation) and a nonbonded pair of electrons (like a carbanion), the singlet carbene exhibits both carbocation and carbanion character. However, the triplet carbene behaves more as a diradical. These characteristics influence the types and stereochemistries of carbene reactions.

One of the major reactions of carbenes is cycloaddition with double bonds:



A singlet carbene adds stereospecifically, meaning that reaction with a *cis*-alkene gives only *cis*-cyclopropane, and reaction with a *trans*-alkene gives *trans*-cyclopropane. The reaction of the triplet carbene is not stereospecific, however, and the product is a mixture of isomers. The difference in stereochemistry arises because the singlet carbene can add in one step (equation 5.39),

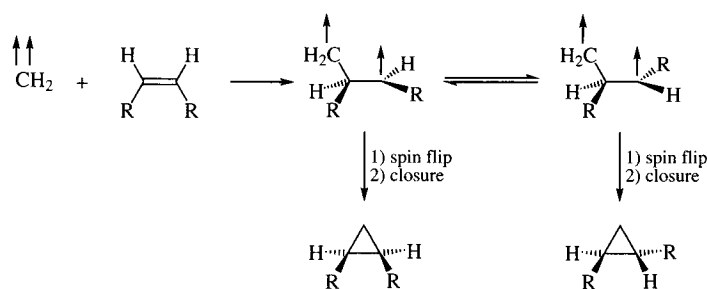


while the triplet cannot.¹⁶⁸ The triplet carbene adds first to one end of the double bond to produce a diradical, but it can only close to the cyclopropane after one electron flips its spin. As shown in Figure 5.30, this may allow rotation to occur around the C–C single bond before ring closure, so a mixture

¹⁶⁶ Gilbert, J. C.; Yin, J. *J. Org. Chem.* **2006**, *71*, 5658.

¹⁶⁷ The singlet–triplet energy gap also plays an important role in determining reactivity: Tomioka, H. in Moss, R. A.; Platz, M. S.; Jones, M., Jr., Eds. *Reactive Intermediate Chemistry*; John Wiley & Sons: Hoboken, NJ, 2004; chapter 9.

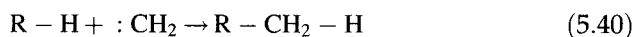
¹⁶⁸ If a triplet carbene were to add to an alkene in one step, there would be two unpaired electrons in one σ bond; that is, there would be an excited state of a σ bond, a very high energy species. For a summary of the reactions of triplet carbenes, see reference 167.

**FIGURE 5.30**

Nonstereospecific addition of triplet methylene to a *cis*-alkene.

of isomers results. Addition of singlet carbenes to conjugated dienes most often results in 1,2-addition, but 1,4-addition has been observed.^{169,170}

Another reaction of singlet carbenes is insertion into single bonds, as shown in equation 5.40.



Insertion into C–H bonds is more probable than insertion into C–C bonds. For example, photolysis of diazomethane in cyclopentane at -75°C produced only methylcyclopentane; cyclohexane was not observed.¹⁷¹ Singlet carbenes are thought to add to C–H bonds by a concerted process, while triplet carbenes can produce net addition through hydrogen abstraction and then recombination of the alkyl radicals. Addition to double bonds and C–H insertion reactions are competing processes. Irradiation of diazomethane in cyclohexene produced 1-methylcyclohexene (**40**, 10%), 3-methylcyclohexene (**41**, 25%), 4-methylcyclohexene (**42**, 25%), and norcarane (**43**, 40%). Thus, singlet methylene appeared to be indiscriminate with regard to allylic, 2° , or vinylic C–H bonds.¹⁷¹ Different carbenes exhibit different selectivities toward insertion and cycloaddition reactions, however, and halocarbenes tend to give more cycloaddition than insertion products. In particular, reaction of cyclohexene with dichlorocarbene resulted in a 60% isolated yield of the dichloro derivative of norcarane, 7,7-dichlorobicyclo[4.1.0]heptane (**44**).¹⁷² Insertion of dichlorocarbene into C–H bonds does occur to some extent, and the relative reactivity of different C–H bonds has been attributed to the ability of the carbon skeleton to accommodate partial positive charge buildup during donation of electron density to the carbene in the early stage of the addition.¹⁷³

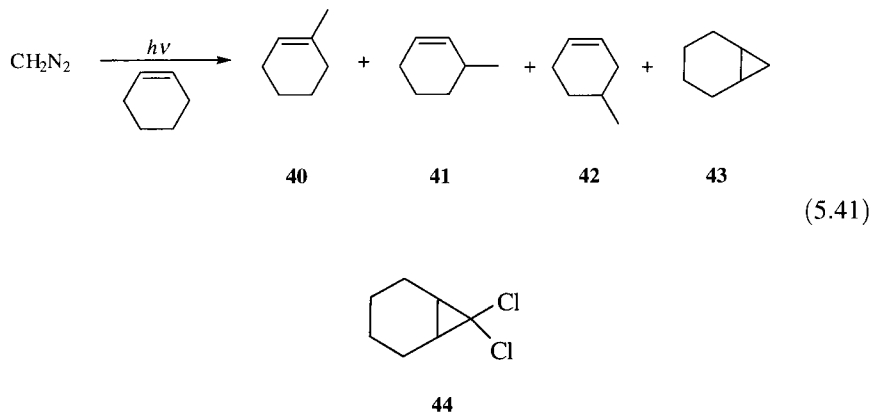
¹⁶⁹ For a theoretical study of the 1,2- and 1,4-addition pathways and for references to literature reports of 1,4-addition, see Evanseck, J. D.; Mareda, J.; Houk, K. N. *J. Am. Chem. Soc.* **1990**, *112*, 73.

¹⁷⁰ Turkenburg, L. A. M.; de Wolf, W. H.; Bickelhaupt, F. *Tetrahedron Lett.* **1982**, *23*, 769.

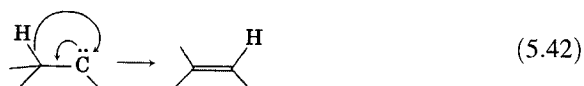
¹⁷¹ Doering, W. von E.; Buttery, R. G.; Laughlin, R. G.; Chaudhuri, N. *J. Am. Chem. Soc.* **1956**, *78*, 3224.

¹⁷² Doering, W. von E.; Hoffmann, A. K. *J. Am. Chem. Soc.* **1954**, *76*, 6162.

¹⁷³ The reaction pathway is different for acidic C–H bonds: Mieusset, J.-L.; Brinker, U. H. *J. Org. Chem.* **2007**, *72*, 10211.



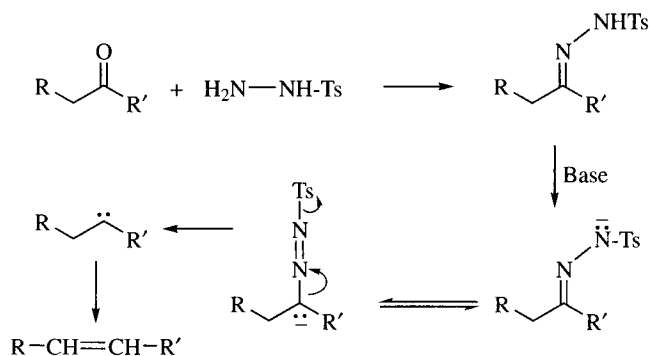
Singlet carbenes can rearrange to alkenes by a 1,2-hydrogen shift if hydrogen atoms are located on adjacent carbon atoms.^{174,175} Evanseck and Houk determined from *ab initio* calculations that the activation energy for the rearrangement of methylcarbene to ethene (equation 5.42) is only 0.6 kcal/mol.¹⁷⁶



This type rearrangement is the basis of the Bamford–Stevens reaction, in which the tosylhydrazone of an aliphatic ketone is converted to an alkene by the action of strong base, such as the sodium salt of ethylene glycol in ethylene glycol as solvent (Figure 5.31).¹⁷⁷

The extent to which any particular carbene exhibits the reactions discussed above depends on its structure and electronic state.¹⁷⁸ Alkyl and

FIGURE 5.31
Conversion of ketone to alkene through the Bamford–Stevens reaction.



¹⁷⁴ Schaefer, H. F. III. *Acc. Chem. Res.* **1979**, 12, 288.

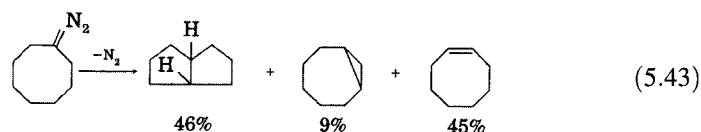
¹⁷⁵ Some carbenes with α -hydrogen atoms have been trapped and studied in matrices: Sander, W.; Bucher G.; Wierlacher, S. *Chem. Rev.* **1993**, 93, 1583.

¹⁷⁶ Evanseck, J. D.; Houk, K. N. *J. Phys. Chem.* **1990**, 94, 5518.

¹⁷⁷ Bamford, W. R.; Stevens, T. S. *J. Chem. Soc.* **1952**, 4735. For a mechanistic discussion and review, see Shapiro, R. H. *Org. React.* **1976**, 23, 405.

¹⁷⁸ For a review, see Nickon, A. *Acc. Chem. Res.* **1993**, 26, 84.

dialkyl carbenes undergo such rapid intramolecular reactions that intermolecular reactions are not competitive. For example, products from the decomposition of diazocyclooctane are shown in equation 5.43.¹⁷⁹



If intramolecular reactions cannot occur, the carbanion–carbocation character of a singlet carbene can lead to reactions that occur through ionic species. Singlet carbenes react with methanol by nucleophilic abstraction of a proton by the pair of electrons in the sp^n orbital of the carbene, resulting in a carbocation that subsequently reacts with the alcohol to produce an ether.^{138c} For example, the diphenylcarbene singlet (**45**, Figure 5.32), which cannot undergo rearrangement to form an alkene, abstracts a proton from methanol to form the diphenylmethyl carbocation (**46**). Methanol then adds as a nucleophile to **46** to produce the ether **47**.^{138c,180,181}

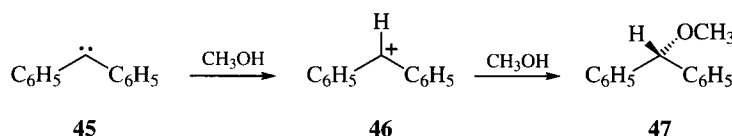


FIGURE 5.32

Reaction of diphenylcarbene with methanol to form benzhydryl methyl ether.

Singlet carbenes can also react with nucleophiles. For example, singlet chlorophenylcarbene reacts with pyridine to form the ylide **48** (Figure 5.33) with a rate constant of $3 \times 10^8 \text{ M}^{-1} \text{ s}^{-1}$.¹⁸² The formation and disappearance of such ylides may be detected spectroscopically, thus providing a method for determining the rate constants for other reactions of the carbenes. Platz and co-workers used this technique to determine that the first-order rate constant for the 1,2-hydrogen shift in benzylchlorocarbene to form the *cis* and *trans* isomers of β -chlorostyrene is $(4.9\text{--}6.7) \times 10^7 \text{ s}^{-1}$.¹⁸³ The second-order rate

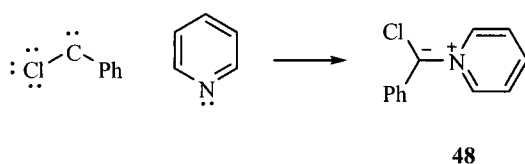


FIGURE 5.33

Formation of an ylide from pyridine and singlet chlorophenylcarbene.

¹⁷⁹ Friedman L.; Shechter, H. *J. Am. Chem. Soc.* **1961**, *83*, 3159.

¹⁸⁰ There is also the possibility that triplet diphenylcarbene can react with methanol, although this seems not to be the case for sterically more hindered diarylcarbenes such as dimesitylcarbene: Griller, D.; Nazran, A. S.; Scaiano, J. C. *J. Am. Chem. Soc.* **1984**, *106*, 198; reference 156; Jones, M. B.; Maloney, V. M.; Platz, M. S. *J. Am. Chem. Soc.* **1992**, *114*, 2163. See also Monguchi, K.; Itoh, T.; Hirai, K.; Tomioka, H. *J. Am. Chem. Soc.* **2004**, *126*, 11900.

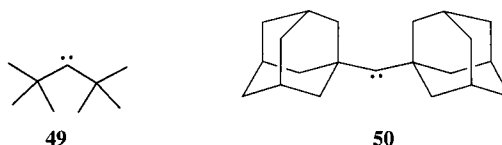
¹⁸¹ For an application of diaryl carbenes in the functionalization of diamond surfaces, see Wang, H.; Griffiths, J.-P.; Edgell, R. G.; Moloney, M. G.; Foord, J. S. *Langmuir* **2008**, *24*, 862.

¹⁸² Jackson, J. E.; Soundararajan, N.; Platz, M. S.; Liu, M. T. H. *J. Am. Chem. Soc.* **1988**, *110*, 5595.

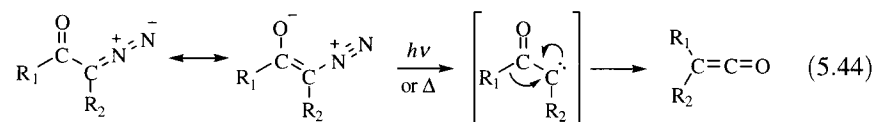
¹⁸³ Jackson, J. E.; Soundararajan, N.; White, W.; Liu, M. T. H.; Bonneau, R.; Platz, M. S. *J. Am. Chem. Soc.* **1989**, *111*, 6874.

constant for addition of benzylchlorocarbene to trans-3-hexene was found to be $6.8 \times 10^7 \text{ L mol}^{-1} \text{ s}^{-1}$.^{183,184}

Dialkylcarbenes that cannot undergo a hydrogen shift have longer lifetimes than do alkyl carbenes that can rearrange as shown in equation 5.42. Two have been studied spectroscopically: di-*t*-butylcarbene (**49**)¹⁸⁵ and diadamantylcarbene (**50**).¹⁸⁶ The studies indicated that both are ground state triplets, but the reactions of diadamantylcarbene in solution suggested involvement of both the singlet and triplet states. Spin-equilibrated **50** reacted with methanol ($k = 2 \times 10^7 \text{ L mol}^{-1} \text{ s}^{-1}$) to produce methyl diadamantylmethyl ether.¹⁸⁷ Reaction of the triplet state of **50** with oxygen (a triplet ground state molecule) gave a carbonyl oxide that could be reduced to diadamantyl ketone, confirming triplet reactivity.¹⁸⁸



α -Diazoketones can eliminate N_2 both photochemically and thermally.¹⁸⁹ The resulting ketocarbenes generally have triplet ground states. For example, the singlet of formylcarbene is about 2.4 kcal/mol higher in energy than the triplet.¹⁴⁷ Nevertheless, ketocarbenes readily undergo the Wolff rearrangement, in which alkyl and aryl groups migrate to the carbene center to produce a ketene (equation 5.44).^{190,191} Part of the energy barrier for the Wolff rearrangement (ca. 6 kcal/mol) is therefore due to the energy required to populate the singlet state before reaction can occur.¹⁴⁷ The ketenes produced by the Wolff rearrangement react readily with water to produce carboxylic acids (equation 5.45), with alcohols to produce esters, and with amines to produce amides. The synthesis of acids by this process makes diazoketones useful components in photoresists for the fabrication of microelectronic devices.¹⁹²



¹⁸⁴ The rate constant for the rearrangement of chloromethylcarbene to vinyl chloride was determined to be $3 \times 10^6 \text{ s}^{-1}$. (a) Bonneau, R.; Liu, M. T. H.; Rayez, M. T. *J. Am. Chem. Soc.* **1989**, *111*, 5973; (b) Liu, M. T. H.; Bonneau, R. *J. Am. Chem. Soc.* **1989**, *111*, 6873.

¹⁸⁵ Gano, J. E.; Wettach, R. H.; Platz, M. S.; Senthilnathan, V. P. *J. Am. Chem. Soc.* **1982**, *104*, 2326.

¹⁸⁶ Myers, D. R.; Senthilnathan, V. P.; Platz, M. S.; Jones, M., Jr. *J. Am. Chem. Soc.* **1986**, *108*, 4232.

¹⁸⁷ The term *spin-equilibrated* means that there is an equilibrium population of the singlet and triplet states.

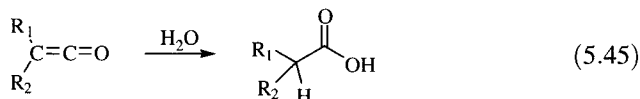
¹⁸⁸ Morgan, S.; Platz, M. S.; Jones, M., Jr.; Myers, D. R. *J. Org. Chem.* **1991**, *56*, 1351.

¹⁸⁹ For other applications of diazocarbonyl compounds in organic synthesis, see Ye, T.; McKervey, A. *Chem. Rev.* **1994**, *94*, 1091.

¹⁹⁰ Wolff, L. *Justus Liebigs Ann. Chem.* **1912**, 394, 23.

¹⁹¹ Kirmse, W. *Eur. J. Org. Chem.* **2002**, 2002, 2193.

¹⁹² Ito, H. *Adv. Polym. Sci.* **2005**, *172*, 37.



5.4 CARBOCATIONS

Carbonium Ions and Carbenium Ions

Carbocations are reactive intermediates having a formal charge of +1 on a carbon atom. Around 1900 it was observed that dissolving triarylmethyl halides in SO_2 produced electrically conducting solutions, which suggested that carbon atoms could be positively charged.^{193–195} In the gas phase, ions require more energy for formation than do the corresponding trivalent carbon radicals because energy is required both to break the bond to carbon and to separate the charged ions. The additional energy needed to form ions can be much smaller in solution because polar solvent molecules can solvate and stabilize the ions. This stabilization afforded by polar solvents means that any investigation of the cation is necessarily an investigation of both the ion and its environment.

During much of the history of organic chemistry, a structure with a positively charged carbon atom was called a *carbonium ion*, a term reminiscent of other positively charged species, such as ammonium, phosphonium, and sulfonium.¹⁹⁶ However, the latter terms all refer to a cation formed by adding a positively charged atom such as a proton to a neutral atom. To keep the nomenclature of organic chemistry consistent, Olah suggested that a species such as CH_3^+ should be considered the product of the addition of a proton to methylene (equation 5.46), so it should more properly be termed a *carbenium ion*, and that is the term now in general use for species in which a trivalent carbon atom bears a positive charge. Often, however, the more general term *carbocation* is used as a generic term for all cations of carbon compounds.¹⁹⁷



To continue the analogy of adding the suffix *-ium* to the term for a neutral species, Olah proposed that the term *carbonium ion* refer to a species that could be formed by adding a positive charge to a neutral, tetravalent carbon atom, as in equation 5.47. The carbon atom in the CH_5^+ ion appears to be bonded to more than four atoms at once, and such a structure is known as a

¹⁹³ Bethell, D.; Gold, V. *Carbonium Ions: An Introduction*; Academic Press: New York, 1967.

¹⁹⁴ Whitmore, F. C. *J. Am. Chem. Soc.* **1932**, *54*, 3274; Traynham, J. G. *J. Chem. Educ.* **1989**, *66*, 451.

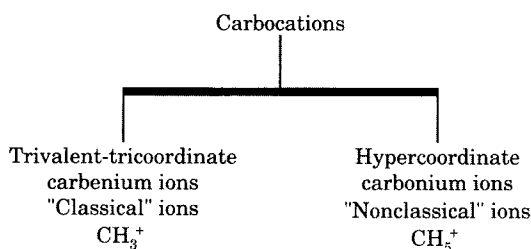
¹⁹⁵ Olah, G. A. *J. Org. Chem.* **2001**, *66*, 5943.

¹⁹⁶ The "waxing and waning" of the term *carbonium ion* was described by Traynham, J. G. *J. Chem. Educ.* **1986**, *63*, 930.

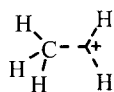
¹⁹⁷ Olah, G. A. *J. Am. Chem. Soc.* **1972**, *94*, 808.

FIGURE 5.34

Designations of carbocations.
(Adapted from reference 198.)



hypercoordinate carbon compound.^{198–200,226} The relationship between the two types of carbocations is summarized in Figure 5.34.¹⁹⁸

**FIGURE 5.35**

Structure proposed for methonium ion.

Structure and Geometry of Carbocations

The structure of CH_5^+ , also known as the methonium ion (Figure 5.35), has been the subject of extensive theoretical investigation. As originally proposed by Olah, the structure is a hypercoordinate species with a three-center, two-electron (3c–2e) bond.²²⁶

A variety of theoretical studies as well as an IR spectrum of the methonium ion led investigators to conclude that the potential energy surface for the structure is relatively flat, with one global energy minimum representing about 80% of the ions and two other structures relatively close in energy accounting for the rest of the structures.²⁰¹ Consequently, the hydrogen atoms interchange readily. As a simple model for bonding, the structure might be considered to have a CH_3^+ “tripod” unit with an H_2 molecule held to the carbon by a 3c–2e bond. However, other investigators concluded that the structure is better described as a $\text{H}_3\text{C}^\bullet$ pedestal with an H_2^+ ion attached by a 3c–2e bond.²⁰² An atoms-in-molecules analysis did not reveal a bond critical point between the two hydrogen atoms thought to be attached to carbon with the 3c–2e bond. This led to the conclusion that all five hydrogen atoms in the methonium ion are directly bonded to carbon,²⁰³ even though the AIM analysis did indicate the presence of 3c–2e bonds of other nonclassical

¹⁹⁸ Olah, G. A.; Prakash, G. K. S.; Williams, R. E.; Field, L. D.; Wade, K. *Hypercarbon Chemistry*; John Wiley & Sons: New York, 1987.

¹⁹⁹ CH_6^{2+} , a carbocation, is predicted to be an energy minimum also. For a discussion, see (a) Lammertsma, K.; Olah, G. A.; Barzaghi, M.; Simonetta, M. *J. Am. Chem. Soc.* **1982**, *104*, 6851; (b) Lammertsma, K. *J. Am. Chem. Soc.* **1984**, *106*, 4619 and references therein.

²⁰⁰ Olah noted that carbon can be *hypercoordinate* but not *hypervalent* because it is a first-row element and thus is not able to extend the valence shell. For a discussion of the terms *hypercoordinate* and *hypervalent*, see (a) Schleyer, P. v. R. *Chem. Eng. News* **1984** (May 28), 4; (b) Martin, J. C. *Chem. Eng. News* **1984** (May 28), 4.

²⁰¹ Asvany, O.; Kumar P, P.; Redlich, B.; Hegemann, I.; Schlemmer, S.; Marx, D. *Science*, **2005**, *309*, 1219; Huang, X.; McCoy, A. B.; Bowman, J. M.; Johnson, L. M.; Savage, C.; Dong, F.; Nesbitt, D. J. *Science*, **2006**, *311*, 60.

²⁰² Fleming, F. P.; Barbosa, A. G. H.; Esteves, P. M. *J. Phys. Chem. A* **2006**, *110*, 11903.

²⁰³ Okulik, N. B.; Peruchena, N. M.; Jubert, A. H. *J. Phys. Chem. A* **2006**, *110*, 9974.

carbocations.²⁰⁴ Therefore, further work will be necessary to clarify the structure and bonding of the methonium ion.

The methyl carbenium ion, a planar structure with 120° H–C–H bond angles (thus sp^2 hybridization) as shown in Figure 5.36, seems much less exotic to organic chemists. Because 2s orbitals are lower in energy than 2p orbitals, a carbocation is lower in energy if the empty orbital has as much p character as possible. Moreover, sp^2 hybridization allows the three substituents bonded to the carbon atom to be as far apart from each other as possible. This bonding model is consistent with the observed geometry for the *t*-butyl carbocation, which has been determined through both NMR²⁰⁵ and X-ray crystallographic²⁰⁶ studies to be planar, with 120° bond angles about the central carbon atom.²⁰⁷ Other evidence supporting a planar structure for carbenium ions comes from the racemization of chiral alkyl halides under solvolysis conditions. Moreover, the correlation of decreased solvolysis rate constants with increasing angle strain at a cationic carbon atom is also consistent with the view that carbenium ions prefer a planar geometry.^{208,209}

One fundamental aspect of carbocation chemistry is the large dependence of the energy of the cation on the substituents attached to the positively charged carbon atom. This dependence is most evident in the gas phase. Table 5.4 shows thermodynamic data for selected carbocations.^{210,211} The **hydride ion affinity**, $HIA(R^+)$, is defined as the negative of the ΔH for the attachment of a hydride ion to the cation in the gas phase. That is, the greater the $HIA(R^+)$, the more endothermic is the removal of a hydride ion from an alkane. We expect the trends to be the same for heterolytic dissociation of alkyl halides or other species that produce carbocations.

The data in Table 5.4 indicate that the ΔH for heterolytic dissociation of alkanes in the gas phase varies with the alkyl group as follows: methyl > ethyl > isopropyl > *t*-butyl,²¹³ which is consistent with the generalization that the ease of formation of carbocations is 3° > 2° > 1° > methyl. What is the source of this increase in stability? We can explain some, but not all, of the results by saying that an sp^3 hybrid orbital on carbon has a Pauling electronegativity of 2.5, while an sp^2 hybrid orbital on carbon is about 0.25 units more

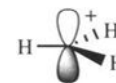


FIGURE 5.36

Simple representation of a methyl carbenium ion.

²⁰⁴ Okulik, N. B.; Peruchena, N. M.; Esteves, P. M.; Mota, C. J. A.; Jubert, A. J. *Phys. Chem. A* **1999**, *103*, 8491.

²⁰⁵ Yannoni, C. S.; Kendrick, R. D.; Myhre, P. C.; Bebout, D. C.; Petersen, B. L. *J. Am. Chem. Soc.* **1989**, *111*, 6440.

²⁰⁶ Hollenstein, S.; Laube, T. *J. Am. Chem. Soc.* **1993**, *115*, 7240.

²⁰⁷ Kato, T.; Reed, C. A. *Angew. Chem. Int. Ed.* **2004**, *43*, 2908.

²⁰⁸ Cf. Gleicher, G. J.; Schleyer, P. v. R. *J. Am. Chem. Soc.* **1967**, *89*, 582 and references therein. The authors concluded that the increase in angle strain with solvolysis to a carbenium ion is the most important effect, but by no means the only effect, in correlating molecular structure with reaction rate.

²⁰⁹ Bartlett, P. D.; Knox, L. H. *J. Am. Chem. Soc.* **1939**, *61*, 3184. For a review, see Applequist, D. E.; Roberts, J. D. *Chem. Rev.* **1954**, *54*, 1065.

²¹⁰ Aue, D. H.; Bowers, M. T. in Bowers, M. T., Ed. *Gas Phase Ion Chemistry*, Vol. 2; Academic Press: New York, 1979; p. 1.

²¹¹ Lossing, F. P.; Holmes, J. L. *J. Am. Chem. Soc.* **1984**, *106*, 6917 and references therein.

²¹³ Data of Stevenson, D. P., cited by Streitwieser, A., Jr. *Chem. Rev.* **1956**, *56*, 571. The ΔH values for allyl and benzyl chlorides were reported to be 158 and 152 kcal/mol, respectively.

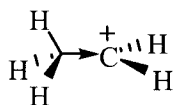
TABLE 5.4 Thermodynamic Data for Selected Alkyl Cations^a

Alkyl	$\Delta H_f^\circ(\text{R}^+)$ (kcal/mol)	HIA(R ⁺) (kcal/mol)
Methyl	261	313.4 ^b
Ethyl	216	270.7 ^b
<i>n</i> -Propyl	208	268
<i>n</i> -Butyl	201	266
<i>n</i> -Pentyl	194	264
Isopropyl	192	249.7 ^b
<i>sec</i> -Butyl	183	248
<i>sec</i> -Pentyl	174	244
Cyclopropyl	234	256
Cyclopentyl	193	246
Cyclohexyl	179	243
<i>t</i> -Butyl	166	236.9 ^b
<i>t</i> -Pentyl	159	230
<i>t</i> -Hexyl	152	228
Allyl	226	256
Propargyl	281	271
Benzyl	215	238
Vinyl	266 ^c	288.0 ^b
Phenyl	279	294

^a Except as noted, data are from reference 211.

^b See reference 212.

^c See reference 210.

**FIGURE 5.37**

Inductive model for stabilization of a carbocation by a methyl group.

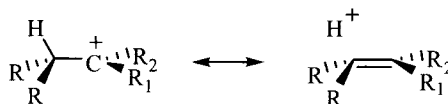
electronegative.²¹⁴ Thus, polarization (induction) of the electrons in a $\text{H}_3\text{C}-\text{C}^+$ σ bond toward the center of positive charge, as shown in Figure 5.37, may help stabilize the ion.

We may also explain the electron-donating ability of a methyl or other alkyl group in terms of hyperconjugation, a lowering of the energy of a system by delocalization of electrons through π bonds involving sp^3 -hybridized carbon atoms adjacent to the carbocation center, just as we did earlier for radicals.²¹⁵ In one formulation of the interaction, an alkyl group can conjugate with an adjacent positively charged carbon through the resonance structure shown on the right in Figure 5.38.

The resonance model is complementary to a perturbational MO analysis (Chapter 4).²¹⁶ Figure 5.39 shows the PMO description for the interaction of an empty p orbital with a $\pi(\text{CH}_3)$ localized methyl group orbital. The net effect is

FIGURE 5.38

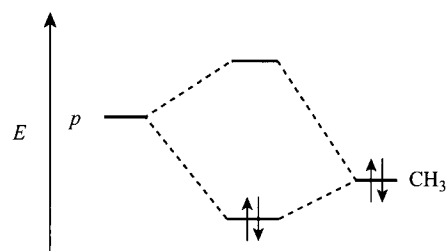
Stabilization of a carbocation through hyperconjugation.



²¹⁴ See the discussion in Huheey, J. E. *Inorganic Chemistry*, 3rd ed.; Harper & Row Publishers: New York, 1983; p. 153.

²¹⁵ Hyperconjugation has also been described as a through-space delocalization of electrons. For a comparison of induction and hyperconjugation, see White, J. C.; Cave, R. J.; Davidson, E. R. *J. Am. Chem. Soc.* **1988**, *110*, 6308 and references therein.

²¹⁶ Hoffmann, R.; Radom, L.; Pople, J. A.; Schleyer, P. v. R.; Hehre, W. J.; Salem, L. *J. Am. Chem. Soc.* **1972**, *94*, 6221 discussed the PMO description for methyl-substituted cations and anions.

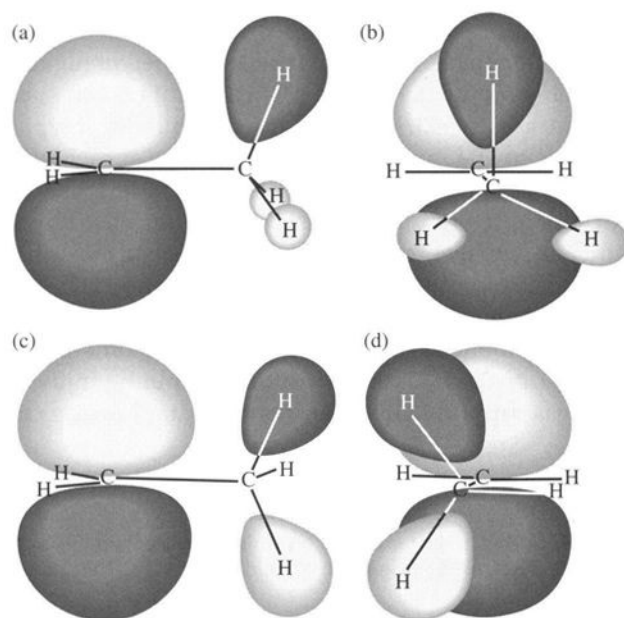
**FIGURE 5.39**

PMO description of stabilization of carbocation by methyl group.

to distribute the electron density from the methyl portion of the molecule into a new orbital that has density on both the methyl group and the adjacent carbocation center, thus delocalizing the positive charge and stabilizing the carbocation.

The PMO model is reinforced by the results of an extended Hückel calculation. Figure 5.40 shows four perspectives of the LUMO determined in extended Hückel calculations for the ethyl cation. Clearly, this empty orbital has some electron density on the β hydrogen atoms, indicating that there has been donation of electron density associated with C–H bonding toward the carbocation center.

Both the hyperconjugation model and the molecular orbital model for the stabilization of carbenium ions by alkyl groups suggest that there should be more bonding between the carbocation carbon (C_α) and an attached carbon atom (C_β) than between C_β and a substituent attached to it. These predictions were confirmed by the X-ray crystal structures for the *t*-butyl carbocation (**51**, Figure 5.41) and the 3,5,7-trimethyl-1-adamantyl cation (**52**). In both **51** and **52**, the length of the C_α – C_β bonds is 1.442(5) Å, whereas the typical length of a $C(sp^2)$ – $C(sp^3)$ bond is 1.503 Å.²¹⁷ The C_β – C_γ bond length in **52** (Figure 5.41) is

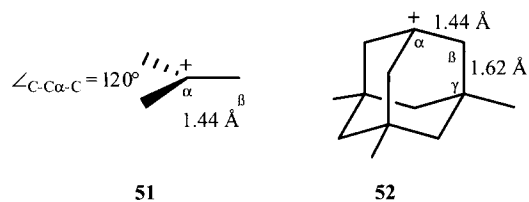
**FIGURE 5.40**

(a) Side and (b) end views of LUMO of ethyl cation in bisected conformation; (c) side and (d) end views of LUMO of ethyl cation in eclipsed conformation

²¹⁷ Laube, T. *Acc. Chem. Res.* **1995**, *28*, 399.

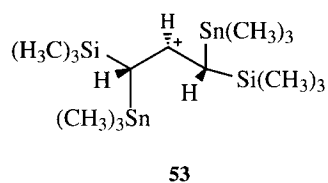
FIGURE 5.41

Geometries of *t*-butyl carbocation (**51**) and 3,5,7-trimethyl-1-adamantyl cation (**52**).



1.62 Å as a result of the weakening of this bond by donation of electron density to the carbocation center.²¹⁸

Hyperconjugation has been found to be important not only for carbocations having C_{β} -H and C_{β} -C bonds but also for structures having other elements bonded to C_{β} . The stabilization resulting from hyperconjugation increases along the series C_{β} -C \ll C_{β} -Si < C_{β} -Ge < C_{β} -Sn < C_{β} -Pb.²¹⁹ For example, the 2° carbocation **53** was found to be stable under N_2 for days at room temperature and to melt at 109°C. Although there are both C_{β} -Si and C_{β} -Sn bonds in the ion, the crystal structure revealed that it is the two C_{β} -Sn bonds that are aligned for maximum hyperconjugative interaction with the carbocation center.²²⁰



The simple models for hyperconjugation in the ethyl carbocation shown above were based on the implicit assumption that the ethyl cation could be described as a classical carbenium ion—specifically, a methyl-substituted methyl cation. The available data indicate that hyperconjugation involving the three alkyl substituents bonded to a 3° carbocation can stabilize the ion and help it retain a classical, carbenium ion structure. Hyperconjugation alone seems unable to stabilize 2° or 1° carbocations sufficiently for them to exist as carbenium ions, however. Many of the carbocations whose classical structures are familiar to organic chemists are calculated to have nonclassical structures, either as global energy minima or as local minima that are close in energy to the global minimum. For example, ab initio calculations indicate that a bridged C_{2v} structure (**54**) for the ethyl cation is more stable than the classical structure by about 3 kcal/mol. The classical geometry for ethyl cation was found to be a transition state for proton scrambling in the $C_2H_5^+$ ion.²²¹ This conclusion was supported by experimental data showing randomization

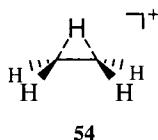
²¹⁸ The gas phase IR spectrum of the *t*-butyl cation is also consistent with the hyperconjugation model. Douberly, G. E.; Ricks, A. M.; Ticknor, B. W.; Schleyer, P. v. R.; Duncan, M. A. *J. Am. Chem. Soc.* **2007**, *129*, 13782.

²¹⁹ Fernández, I.; Frenking, G. *J. Phys. Chem. A* **2007**, *111*, 8028.

²²⁰ Schormann, M.; Garratt, S.; Hughes, D. L.; Green, J. C.; Bochmann, M. *J. Am. Chem. Soc.* **2002**, *124*, 11266.

²²¹ Raghavachari, K.; Whiteside, R. A.; Pople, J. A.; Schleyer, P. v. R. *J. Am. Chem. Soc.* **1981**, *103*, 5649.

of the protons in the ethyl cation both in the gas phase and in solution.^{222–224} In addition, the single-photon IR photodissociation spectrum of the $C_2H_5^+$ ion weakly complexed with a single Ar atom was consistent with the cation having the structure **54** in the gas phase.²²⁵



The bridging is symmetric in **54**, but Figure 5.42 indicates that many types of carbocation structures might be possible.²²⁶ We should note that bridging and hyperconjugation are closely related phenomena involving electron donation to the center of positive charge. In hyperconjugation, that donation results in shorter $C_\alpha-C_\beta$ bonds and longer $C_\beta-C_\gamma$ (or $C_\beta-H$) bonds, as well as decreased $C_\alpha-C_\beta-C_\gamma$ (or $C_\alpha-C_\beta-H$) bond angles. In bridging, $C_\alpha-C_\beta-C_\gamma$ (or $C_\alpha-C_\beta-H$) bond angles decrease so much that C_γ (or H) interacts directly with C_α . The extent to which a particular carbocation exhibits the bridging interactions illustrated in Figure 5.42 is a function of the nature of the bridging group, the nature of the substituents attached to the two carbon atoms involved in potential bridging, and the environment of the ion. Carbocations stabilized by resonance interactions or by multiple alkyl groups bonded to the carbocation center are more likely to exhibit classical carbenium ion behavior, while less stabilized carbocations show a greater tendency toward nonclassical structures.²²⁷

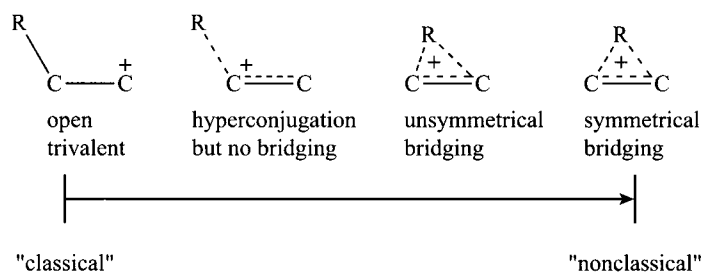


FIGURE 5.42

Representative members of a continuum of carbocation structures. (Adapted from reference 226.)

²²² Ausloos, P.; Rebbert, R. E.; Sieck, L. W.; Tiernan, T. O. *J. Am. Chem. Soc.* **1972**, *94*, 8939.

²²³ Vorachek, J. H.; Meisels, G. G.; Geanangel, R. A.; Emmel, R. H. *J. Am. Chem. Soc.* **1973**, *95*, 4078 and references therein.

²²⁴ Other carbocations are also calculated to have nonclassical structures: Hehre, W. J.; Radom, L.; Schleyer, P. v. R.; Pople, J. A.; *Ab Initio Molecular Orbital Theory*; John Wiley & Sons: New York, 1986; p. 379 ff; see also Klopper, W.; Kutzelnigg, W. *J. Phys. Chem.* **1990**, *94*, 5625.

²²⁵ Andrei, H.-S.; Solcà, N.; Dopfer, O. *Angew. Chem. Int. Ed.* **2008**, *47*, 395.

²²⁶ Olah, G. A. *J. Org. Chem.* **2005**, *70*, 2413.

²²⁷ Bridging may provide additional stabilization even to 3° structures, as evidenced by the structure of the *t*-pentyl carbocation. Schleyer, P. v. R.; Carneiro, J. W. de M.; Koch, W.; Forsyth, D. A. *J. Am. Chem. Soc.* **1991**, *113*, 3990.

This view of variable carbocation structure is the product of extensive experimentation and theoretical analysis.^{193,228–230} ^1H and ^{13}C NMR have been among the primary instrumental methods used to study the structures of carbocations.^{230–233} Other important tools include IR spectroscopy of long-lived carbocations in cryogenic matrices²³⁴ and X-ray crystal structure determination of carbocation salts.²³⁵ Studies of isotopically labeled compounds have also provided important insights.²³⁶ A pioneer in the use of NMR to study carbocations was Olah, who found that under appropriate conditions organic precursors dissolved in Brønsted superacids at low temperature gave solutions with spectra that were consistent with the presence of relatively long-lived carbocations.^{237–239} Useful Brønsted superacids include HSO_3F , $\text{CF}_3\text{SO}_3\text{H}$, and HClO_4 , while the nonnucleophilic solvents include SO_2 , SO_2ClF , and SO_2F_2 .²²⁶ A mixture composed of equimolar parts HSO_3F and SbF_5 is known as “Magic Acid” and is about 10^{16} times as acidic as 100% H_2SO_4 .²²⁶ These media are capable of ionizing alkyl halides and other compounds and are even able to protonate hydrocarbons such as methane (equation 5.48). ^{13}C NMR is a particularly useful tool for studying carbocations in superacid media because the chemical shifts for **carbenium** ions are observed at very low field. For example, the chemical shift for the 3° carbon atom in isobutane is 25.2 ppm, whereas the chemical shift for the corresponding carbon atom in $(\text{CH}_3)_3\text{C}^+$ in $\text{SO}_2\text{ClF-SbF}_5$ solution is 330.0 ppm.²⁴⁰ The large shift appears to result from decreased shielding due to

²²⁸ Olah, G. A.; Schleyer, P. v. R., Eds. *Carbonium Ions*, Vols. I–V; Wiley-Interscience: New York, 1968–1976.

²²⁹ Schleyer, P. v. R.; Maerker, C.; Buzek, P.; Sieber, S. Prakash, G. K. S. in Prakash, G. K. S.; Schleyer, P. v. R., Eds. *Stable Carbocation Chemistry*; John Wiley & Sons: New York, 1997, chapter 2.

²³⁰ Olah, G. A. *Carbocations and Electrophilic Reactions*; John Wiley & Sons: New York, 1974.

²³¹ Saunders, M.; Jiménez-Vázquez, H. A. *Chem. Rev.* **1991**, *91*, 375.

²³² Saunders, M.; Jiménez-Vázquez, H. A.; Kronja, O. in Prakash, G. K. S.; Schleyer, P. v. R., Eds., *Stable Carbocation Chemistry*; John Wiley & Sons: New York, 1997, chapter 9.

²³³ Myhre, P. C.; Yannoni, C. S. in Prakash, G. K. S.; Schleyer, P. v. R., Eds. *Stable Carbocation Chemistry*; John Wiley & Sons: New York, 1997, chapter 12.

²³⁴ Sunko, D. E. in Prakash, G. K. S.; Schleyer, P. v. R., Eds. *Stable Carbocation Chemistry*; John Wiley & Sons: New York, 1997, chapter 11.

²³⁵ Laube, T. in Prakash, G. K. S.; Schleyer, P. v. R., Eds. *Stable Carbocation Chemistry*; John Wiley & Sons: New York, 1997, chapter 14.

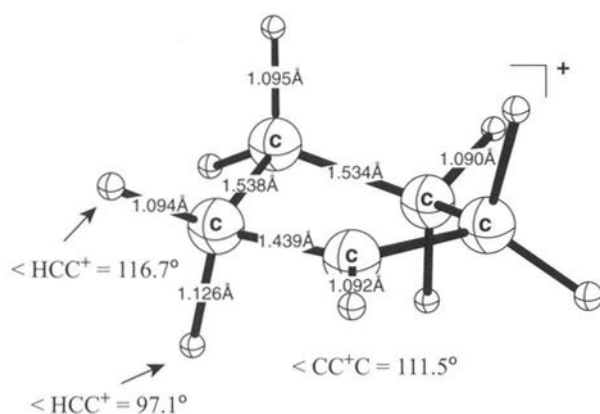
²³⁶ Forsyth, D. A. in Prakash, G. K. S.; Schleyer, P. v. R., Eds. *Stable Carbocation Chemistry*, John Wiley & Sons: New York, 1997, chapter 10.

²³⁷ Olah, G. A.; Tolgyesi, W. S.; Kuhn, S. J.; Moffatt, M. E.; Bastien, I. J.; Baker, E. B. *J. Am. Chem. Soc.* **1963**, *85*, 1328.

²³⁸ Olah, G. A.; Prakash, G. K. S.; Sommer, J. *Superacids*; John Wiley & Sons: New York, 1985.

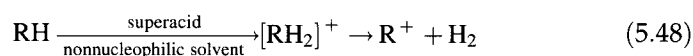
²³⁹ Brønsted superacids are acids stronger than 100% H_2SO_4 , while Lewis superacids are stronger than AlCl_3 (reference 226).

²⁴⁰ Absolute chemical shifts do not necessarily correlate with charge densities. The shielding constant for a carbon nucleus in ^{13}C NMR is thought to be the sum of several terms. For example, see Nelson, G. L.; Williams, E. A. *Prog. Phys. Org. Chem* **1976**, *12*, 229. However, we would expect such a correlation within a family of closely related compounds. A relationship between ^{13}C shifts and π -electron densities for aromatic compounds was developed by Spiess, H.; Schneider, W. G. *Tetrahedron Lett.* **1961**, 468. The correlation was extended by Olah, G. A.; Mateescu, G. D. *J. Am. Chem. Soc.* **1970**, *92*, 1430.

**FIGURE 5.43**

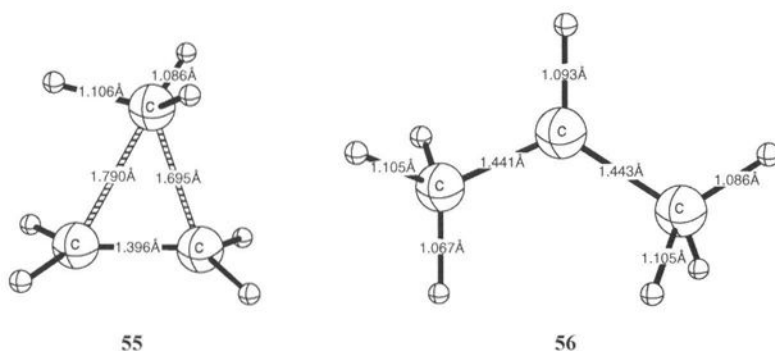
Calculated structure of the cyclopentyl carbocation. (Reproduced from reference 229.)

the decreased electron density at the carbenium center.



Among 2° carbocations, only the isopropyl, *sec*-butyl, and cyclopentyl carbocations have been observed in solution.²⁴¹ These three structures nevertheless illustrate the kinds of delocalization effects that may be expected in other 2° carbocations. The cyclic structure of the cyclopentyl cation prevents significant C–C–C bridging. The calculated geometry (Figure 5.43) shows a twisted C_2 structure with the C_β –H bonds aligned parallel with the empty p orbital for maximum hyperconjugative overlap.^{229,242}

The isopropyl cation is not prevented from bridging by a cyclic skeleton. Calculations reveal that an unsymmetrical corner-protonated cyclopropane (55) is about 7 kcal/mol higher in energy than a more classical structure having C_2 symmetry (56, Figure 5.44).²²⁹ As with the cyclopentyl cation, the C_β –H bonds in the open structure are aligned for maximum hyperconjugative interaction with the p orbital on C_α .

**FIGURE 5.44**

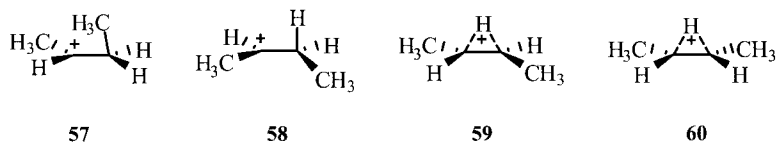
Asymmetric corner-protonated cyclopropane (55) and calculated geometry of classical isopropyl cation (56). (Structures reproduced from reference 229.)

²⁴¹ Vrček, V.; Kronja, O.; Saunders, M. J. *Chem. Theory Comput.* **2007**, *3*, 1223.

²⁴² There is evidence for partial bridging in a cyclopentyl cation derivative having methyl groups on the β carbons. Kronja, O.; Köhli, T.-P.; Mayr, H.; Saunders, M. J. *Am. Chem. Soc.* **2000**, *122*, 8067.

FIGURE 5.45

Energy minima for the 2-butyl carbocation.



The 2-butyl cation is a more challenging species. Unlike the isopropyl cation, it has a C_γ carbon, and unlike the cyclopentyl cation, there is not a ring structure to preclude orientation of the $C_\beta-C_\gamma$ bond so as to facilitate bridging. An intensive search at several levels of theory led to the identification of structures 57, 58, 59, and 60 (Figure 5.45) as energy minima on a rather flat potential energy surface.²⁴¹ Structure 57 exhibits partial bridging, while the less-bridged structure 58 is stabilized by hyperconjugation with the C_3-H bond (as illustrated) and the C_1-H bond (not illustrated). Structures 59 and 60 differ slightly in energy, depending on the relationship of the two methyl groups.

Structures that might be drawn in the simplest possible form as 1° carbocations are even more likely to be stabilized by bridging, but it is not possible to observe such species in solution. The lifetime of a 3° carbocation in dilute aqueous solution is estimated to be ca. 10^{-10} s, while that of a 2° carbocation is estimated to be ca. 5×10^{-12} s.^{243,244} The lifetime of a 1° carbocation, if it exists in water, should be even shorter. Ab initio studies of the 1-propyl cation with the FBH_3^- counterion indicated a nonclassical structure at large cation-anion distances. A geometry like that of a 1-propyl cation was found to be lower in energy at short ion pair distances, however.²⁴⁵ Thus, it appears that ion pairing effects may influence carbocation structure and provide relative stabilization of a more nearly classical structure. Nucleophilic solvent appears not to have a similar effect on the structure.^{246,247}

Primary alkyl halides do react in superacids, but ordinarily the products are 2° or 3° carbocations arising from rearrangements.²¹⁷ Nevertheless, there is evidence for the ethyl cation in mixtures of CH_3CH_2F and SbF_5 at low temperature in SO_2 solution as well as in a $H_3PW_{12}O_{40}$ pseudoliquid phase.^{248,249} There are also indications for formation of the ethyl cation in a reaction of ethene with methane and a $HF-TaF_5$ catalyst²⁵⁰ and in the solvolysis of ethyl tosylate in concentrated H_2SO_4 .^{248,251} In addition, a 1° carbocation-brosylate ion pair was proposed as an intermediate in the E1

²⁴³ Chiang, Y.; Kresge, A. J. *J. Am. Chem. Soc.* **1985**, *107*, 6363.

²⁴⁴ The lifetime of the isopropyl cation in aqueous acetonitrile was found to be 5×10^{-11} s. Pezacki, J. P.; Shukla, D.; Luszyk, J.; Warkentin, J. J. *Am. Chem. Soc.* **1999**, *121*, 6589.

²⁴⁵ Fărcașiu, D.; Hâncu, D. *J. Am. Chem. Soc.* **1999**, *121*, 7173.

²⁴⁶ Kirmse, W.; Zellmer, V.; Goer, B. *J. Am. Chem. Soc.* **1986**, *108*, 4912.

²⁴⁷ Casanova, J.; Kent IV, D. R.; Goddard, W. A. III. Roberts, J. D. *Proc. Nat. Acad. Sci. U.S.A.* **2003**, *100*, 15.

²⁴⁸ Olah, G. A.; DeMember, J. R.; Schlosberg, R. H.; Halpern, Y. *J. Am. Chem. Soc.* **1972**, *94*, 156.

²⁴⁹ Lee, K. Y.; Kanda, Y.; Mizuno, N.; Okuhara, T.; Misono, M.; Nakata, S.; Asaoka, S. *Chem. Lett.* **1988**, 1175.

²⁵⁰ Siskin, M. *J. Am. Chem. Soc.* **1976**, *98*, 5413.

²⁵¹ Myhre, P. C.; Brown, K. S. *J. Am. Chem. Soc.* **1969**, *91*, 5641.

reaction of the fluorene derivative **61**.²⁵² The investigators suggested that the π orbitals of the fluorenyl system stabilize the ion by overlap with the developing p orbital of the cation. In any case, a 1° carbocation is unlikely to be a solvent-equilibrated reactive intermediate in a typical S_N1 or E1 reaction.

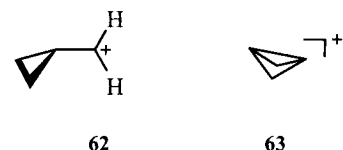
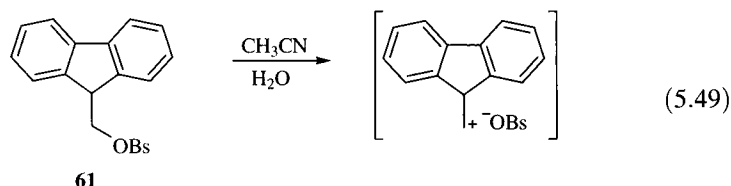


FIGURE 5.46
Two structures for the cyclopropylmethyl cation.

One very interesting structure that might at first glance appear to be a 1° carbocation is the cyclopropylmethyl cation. Calculations indicated, however, that this species is best described by a pair of rapidly equilibrating nonclassical structures (**62** and **63**, Figure 5.46) that are approximately equal in energy.²⁵³ Attempts to prepare the 1° cyclobutylmethyl cation were unsuccessful, however, with cyclopentyl cations being formed instead.²⁵⁴

The hydrogen-bridged C_2H_5 cation **54** (page 295) may be considered the smallest possible member of a type of nonclassical carbocation, **64**, in which hydrogen participates in a $3c-2e$ bond terminating at carbon on each end. The larger structures of this type are termed μ -hydridobridged cations.^{255,256} Although such μ -hydrido bridging may appear unusual, Sorensen has noted its conceptual similarity to the delocalization of charge in an allyl cation system (Figure 5.47).²⁵⁵

An example that illustrates the stability to be gained by μ -hydrido bridging is shown in equation 5.50. Protonolysis of *in*-bicyclo[4.4.4]-1-tetradecene (**65**) with trifluoromethanesulfonic acid in methylene chloride solution led to the μ -hydridobridged ion **66**. The room temperature 1H NMR spectrum showed a one-proton singlet at $\delta -3.5$, and the ^{13}C NMR

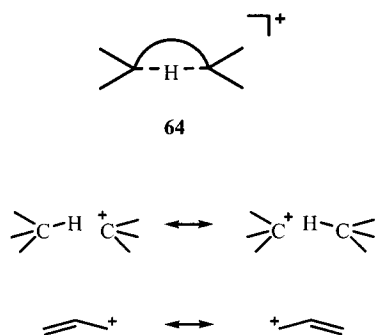


FIGURE 5.47
Resonance representations of μ -hydridobridged cation (top) and allyl cation (bottom).

²⁵² Meng, Q.; Thibblin, A. *J. Am. Chem. Soc.* **1997**, *119*, 4834.

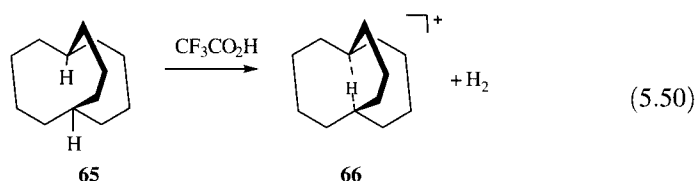
²⁵³ Vančik, H.; Gabelica, V.; Sunko, D. E.; Buzek, P.; Schleyer, P. v. R. *J. Phys. Org. Chem.* **1993**, *6*, 427.

²⁵⁴ Reddy, V. P.; Rasul, G.; Prakash, G. K. S.; Olah, G. A. *J. Org. Chem.* **2007**, *72*, 3076.

²⁵⁵ Sorensen, T. S. in Prakash, G. K. S.; Schleyer, P. v. R., Eds. *Stable Carbocation Chemistry*; John Wiley & Sons: New York, 1997, chapter 2.

²⁵⁶ McMurry, J. E.; Lectka, T. *Acc. Chem. Res.* **1992**, *25*, 47; *J. Am. Chem. Soc.* **1993**, *115*, 10167

spectrum showed only three peaks, consistent with the structure shown. The spectrum suggests that the inside hydrogen atom has partial negative charge, while both carbon atoms to which it is bonded have partial positive charge.^{257,258}



The Norbornyl Cation

Perhaps the "classic" example of a nonclassical carbocation is the 2-norbornyl cation, which was at the center of what has been called "the most heated chemical controversy in our time."²²⁹ In Chapter 8 we will review the experimental evidence, largely based on solvolysis reactions, that led to the proposal of the nonclassical carbonium ion structure shown in Figure 5.48. However, this description was not accepted by all researchers, and an alternative model for the 2-norbornyl cation was a pair of rapidly equilibrating classical (carbenium) ions, as shown in Figure 5.49. Many papers relating to the development of contrasting ideas in this area were published in a reprint and commentary volume by Bartlett.^{259,260}

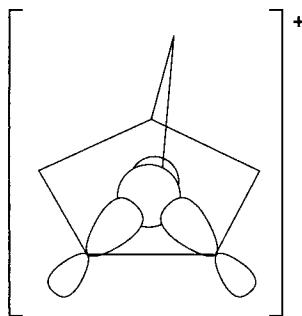


FIGURE 5.48
Nonclassical carbonium ion model for 2-norbornyl cation.

As with other carbocations, NMR spectroscopy was utilized to study the structure of the 2-norbornyl cation. The lowest temperatures used to record a spectrum for this system are 5 K (nonspinning) and 6 K (spinning) by Yannoni, Myhre, and co-workers.²⁶¹ Between 150 K and 5 K, the peak observed for C1 and C2 was at 125 ppm and did not change with temperature, suggesting that the 2-norbornyl cation was indeed a nonclassical carbonium ion (Figure 5.48). The authors concluded that if it were a pair of rapidly equilibrating classical ions (Figure 5.49), the activation energy for the equilibrium could be no more than 0.2 kcal/mol.²⁶² ESCA analysis^{263,264} and

²⁵⁷ McMurry, J. E.; Hodge, C. N. *J. Am. Chem. Soc.* **1984**, *106*, 6450.

²⁵⁸ Theoretical analyses of such structures indicated that the C–H–C 3c–2e bonds in tricyclic systems are highly sensitive to molecular geometry. Ponec, R.; Yuzhakov, G.; Tantillo, D. J. *J. Org. Chem.* **2004**, *69*, 2992.

²⁵⁹ Bartlett, P. D. *Nonclassical Ions: Reprints and Commentary*; W. A. Benjamin: New York, 1965.

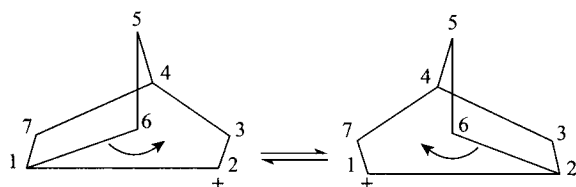
²⁶⁰ Sargent, G. D. *Q. Rev. Chem. Soc.* **1966**, *20*, 301 suggested that the "classical" period in carbocation history lasted less than ten years, from the time of Whitmore's publication (reference 194) until the first report of a bridged ion by Nevell, T. P.; de Salas, E.; Wilson, C. L. *J. Chem. Soc.* **1939**, 118; see also Saltzman, M. D.; Wilson, C. L. *J. Chem. Educ.* **1980**, *57*, 289.

²⁶¹ (a) Yannoni, C. S.; Macho, V.; Myhre, P. C. *J. Am. Chem. Soc.* **1982**, *104*, 7380; (b) Myhre, P. C.; Webb, G. G.; Yannoni, C. S. *J. Am. Chem. Soc.* **1990**, *112*, 8991. (c) Similar experiments on the C₄H₇⁺ ion were consistent with *ab initio* calculations suggesting that both a partially delocalized bisected cyclopropylcarbinyl cation and a nonclassical symmetrical bicyclobutonium ion (puckered cyclobutyl cation) are local energy minima on a very flat potential energy surface: Myhre, P. C.; Webb, G. C.; Yannoni, C. S. *J. Am. Chem. Soc.* **1990**, *112*, 8992 and references therein.

²⁶² This conclusion was based on the premise that tunneling of the carbon atoms was not important in the equilibration mechanism. For a discussion, see (a) Myhre, P. C.; McLaren, K. L.; Yannoni, C. S. *J. Am. Chem. Soc.* **1985**, *107*, 5294; (b) reference 261b.

²⁶³ Olah, G. A.; Mateescu, G. D.; Riemenschneider, J. L. *J. Am. Chem. Soc.* **1972**, *94*, 2529.

²⁶⁴ Johnson, S. A.; Clark, D. T. *J. Am. Chem. Soc.* **1988**, *110*, 4112.

**FIGURE 5.49**

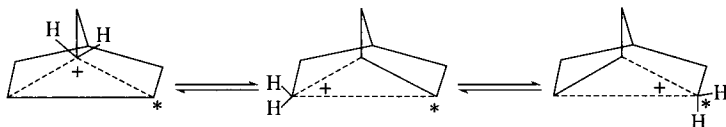
Rapidly equilibrating classical carbocation (carbenium ion) model for 2-norbornyl cation.

studies of carbocation stability in the gas phase²⁶⁵ also were interpreted as favoring the nonclassical structure.

At -70°C the ^{13}C NMR spectrum of the 2-norbornyl cation showed three peaks. One peak at $+101.8$ ppm ($J = 53.3$ Hz) was assigned to carbon atoms 1, 2, and 6; another peak at $+162.5$ ppm ($J = 140$ Hz) was assigned to carbon atoms 3, 5 and 7; a third peak at $+156.1$ ppm ($J = 153$ Hz) was assigned to carbon atom 4.²⁸¹ We expect carbon atoms 1 and 2 to be equivalent, whether we think the carbocation is classical or nonclassical, but their equivalence with carbon atom 6 is a surprise. Apparently there is a rapid hydride shift that interconverts these positions (Figure 5.50). Below 150 K the hydride shift could be frozen out, and a spectrum ascribed to a single ion was observed.

Further support for the nonclassical structure of the 2-norbornyl cation came from an application of ^{13}C NMR spectroscopy that is based on the difference between the total chemical shift of a carbocation and that of the corresponding alkane. Differences in total chemical shift of 350 ppm or more are associated with classical carbocations, while differences of less than 200 ppm are thought to indicate nonclassical, bridged carbonium ions. For example, the sum of the total ^{13}C NMR chemical shift of propane is 47 ppm, while the sum for the 2-propyl cation is 423 ppm. The difference, 376 ppm, indicates that the 2-propyl cation is a classical ion. For the 2-norbornyl system the total of the ^{13}C shifts is 408 ppm, while the total for norbornane is 233 ppm. The difference, 175 ppm, was taken as evidence for a nonclassical structure.²⁶⁶

The conclusion that the 2-norbornyl cation is a nonclassical carbocation was strengthened by the experimental determination of its infrared spectrum when the cation was generated in a cryogenic SbF_5 matrix. The experimental IR spectra agreed with those calculated for a nonclassical structure.²⁶⁷

**FIGURE 5.50**

1,2,6-Hydride shift in the 2-norbornyl cation.

²⁶⁵ Kaplan, F.; Cross, P.; Prinstein, R. J. *Am. Chem. Soc.* **1970**, *92*, 1445.

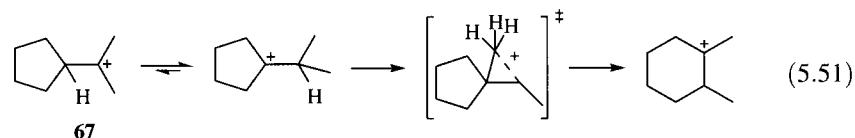
²⁶⁶ Schleyer, P. v. R.; Lenoir, D.; Mison, P.; Liang, G.; Prakash, G. K. S.; Olah, G. A. *J. Am. Chem. Soc.* **1980**, *102*, 683.

²⁶⁷ Koch, W.; Liu, B.; DeFrees, D. J.; Sunko, D. E.; Vancik, H. *Angew. Chem. Int. Ed. Engl.* **1990**, *29*, 183.

Additional experimental and theoretical evidence also support the conclusion that the 2-norbornyl cation is a nonclassical ion.^{268–270} However, there is theoretical evidence that the geometry of the cation can be shifted toward that expected for a classical carbocation when it is complexed with ammonia and benzene. These results may have implications for understanding the chemistry of carbocations involved in biocatalytic reactions.²⁷¹

Rearrangements of Carbocations

Every student of introductory organic chemistry learns that the relative stability of alkyl carbocations is $3^\circ > 2^\circ > 1^\circ > \text{methyl}$ and that a less stable carbocation will rearrange to a more stable carbocation whenever possible. Knowledge of this pattern is key to understanding important organic reactions, such as the formation of *sec*-butylbenzene from the reaction of benzene with 1-chlorobutane in the presence of AlCl_3 .²⁷² Contemporary studies, especially theoretical investigations, continue to explore these rearrangements. For example, Kronja and co-workers modeled the expansion of the five-membered ring to a six-membered ring that occurs during the biogenesis of steroids by studying the 2-cyclopentyl-2-propyl cation **67**.²⁷³ Both theoretical calculations and experimental results suggested that the reaction takes place by the pathway shown in equation 5.51.



Often carbocation rearrangements are evident from skeletal changes produced by a chemical reaction. In other cases, rearrangements may be unrecognized because the products are indistinguishable from the reactants without isotopic labeling. Spectroscopic studies reveal that many carbocations are surprisingly dynamic. For example, the ^1H NMR spectrum of the cyclopentyl carbocation (**68**, Figure 5.51) at -70°C is a singlet—indicating the equivalence of all the protons—not the multiplet expected for a system with three sets of magnetically nonequivalent protons.²³⁰ Similarly, the ^{13}C NMR spectrum indicates one carbon signal coupled with *nine* equivalent protons.

²⁶⁸ Olah, G. A.; Prakash, G. K. S.; Saunders, M. *Acc. Chem. Res.* **1983**, *16*, 440. Also see Walling, C. *Acc. Chem. Res.* **1983**, *16*, 448.

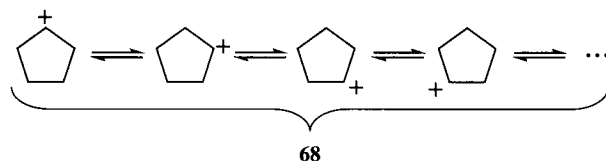
²⁶⁹ Lenoir, D.; Apeloig, Y.; Arad, D.; Schleyer, P. v. R. *J. Org. Chem.* **1988**, *53*, 661 and references therein; Schleyer, P. v. R.; Sieber, S. *Angew. Chem. Int. Ed. Engl.* **1993**, *32*, 1606.

²⁷⁰ A natural bond orbital analysis of 2-norbornyl and other nonclassical carbocations found evidence for a three-atom, two-center orbital and distribution of charge over all three atoms in the structures. Alkorta, I.; Abboud, J. L. M.; Quintanilla, E.; Dávalos, J. Z. *J. Phys. Org. Chem.* **2003**, *16*, 546.

²⁷¹ Hong, Y. J.; Tantillo, D. J. *J. Org. Chem.* **2007**, *72*, 8877.

²⁷² For a discussion, see Shubin, V. G.; Borodkin, G. I. in Prakash, G. K. S.; Schleyer, P. v. R., Eds. *Stable Carbocation Chemistry*; John Wiley & Sons: New York, 1997, chapter 7.

²⁷³ Vrček, V.; Siehl, H.-U.; Kronja, O. *J. Phys. Org. Chem.* **2000**, *13*, 616; see also Vrček, V.; Saunders, M.; Kronja, O. *J. Org. Chem.* **2003**, *68*, 1859.

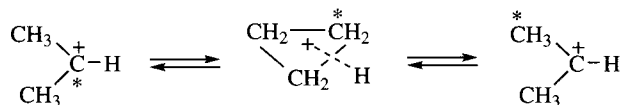
**FIGURE 5.51**

Equilibration of protons due to rapid rearrangement in cyclopentyl carbocation (68).

Apparently a rearrangement takes place rapidly on the NMR time scale, making all nine protons in the molecule equivalent.²⁷⁴

A study of the line broadening of the ^{13}C NMR spectrum of **68** by Saunders revealed an isomerization rate constant of $3.1 \times 10^7 \text{ s}^{-1}$ at -139°C , with a ΔG^\ddagger of 3.1 kcal/mol.^{275,276} The ESCA analysis of **68**, however, suggested the presence in the ion of four uncharged carbon atoms and one positively charged carbon atom.²⁷⁷ The NMR and ESCA results are different because NMR is a "slow camera" that sees only an average of the environments a nucleus experiences during its ca. 10^{-7} second "shutter speed."²⁷⁸ On the other hand, ESCA is a "fast camera" with a "shutter speed" of 10^{-16} second, so it is able to detect the discrete cyclopentyl ions.²⁷⁹

We might assume the isopropyl cation to be immune to the rearrangement exhibited by the cyclopentyl cation, since a 1,2-hydride shift would convert a 2° carbocation to a 1° carbocation in an endothermic process. Nevertheless, scrambling of hydrogen atoms in the isopropyl cation was inferred by Saunders from ^1H NMR spectra, and the E_a for the process was determined to be 16.4 kcal/mol.²⁸⁰ More surprising than the proton rearrangement is the rearrangement of the carbon skeleton. Olah observed that a sample of isopropyl cation labeled with ^{13}C at C2 underwent carbon skeletal rearrangement with a half-life of 1 hour at -78°C , and after several hours the label was evenly distributed along the carbon chain.²⁸¹ The mechanism shown in Figure 5.52 accounts for both proton and carbon scrambling.

**FIGURE 5.52**

Possible mechanism for rearrangement of isopropyl cation. (Adapted from reference 281.)

²⁷⁴ Schleyer, P. v. R.; Carneiro, J. W. de M.; Koch, W.; Raghavachari, K. *J. Am. Chem. Soc.* **1989**, *111*, 5475.

²⁷⁵ Saunders, M.; Kates, M. R. *J. Am. Chem. Soc.* **1978**, *100*, 7082.

²⁷⁶ Compare Saunders, M.; Kronja, O. in Olah, G. A.; Prakash, G. K. S., Eds. *Carbocation Chemistry*; Wiley-Interscience: Hoboken, NJ, 2004, p. 213.

²⁷⁷ For a discussion of ESCA, see Chapter 1.

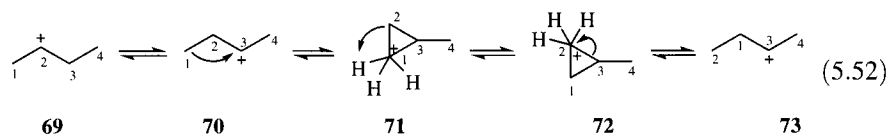
²⁷⁸ This is a very rough estimate based on rate constants of processes that lead to coalescence of peaks in variable temperature NMR.¹⁹⁸ The general rule is that the mean lifetime of a species to be detected by any spectroscopic technique must be greater than the inverse of $2\pi\Delta\nu$, where $\Delta\nu$ is the difference in frequencies of the two species in the spectroscopic technique being used. For a discussion, see (a) Oki, M. *Top. Stereochem.* **1983**, *14*, 1; (b) Bushweller, C. H. in Sarma, R. H., Ed. *Stereodynamics of Molecular Systems*; Pergamon Press: New York, 1979; pp. 39–51.

²⁷⁹ Olah, G. A.; Mateescu, G. D.; Riemenschneider, J. L. *J. Am. Chem. Soc.* **1972**, *94*, 2529.

²⁸⁰ Saunders, M.; Hagen, E. L. *J. Am. Chem. Soc.* **1968**, *90*, 6881.

²⁸¹ Olah, G. A.; White, A. M. *J. Am. Chem. Soc.* **1969**, *91*, 5801.

The situation for the *sec*-butyl cation is even more interesting. We might expect it to behave as does the cyclopentyl cation—that is, to undergo degenerate rearrangement among the two 2° carbocations at a rapid rate. The ^{13}C NMR spectrum of the 2-butyl cation in $\text{SbF}_5\text{-SO}_2\text{ClF}$ shows only two signals, one for the outside carbon atoms (C1 and C4) and another for the inside carbons (C2 and C3). The ^1H NMR spectrum also shows only two sharp peaks, one attributed to the six methyl protons and the other assigned to the five protons on C2 and C3. The simplicity of the spectrum suggests that **69** and **70** rapidly interconvert by a 1,2-hydride shift. When a sample of the 2-butyl cation was heated above -100°C , the ^1H NMR spectrum did show broadening. The results suggested that a process with an activation energy of about 7.5 kcal/mol interchanges the inside and outside methyl protons.²⁸² Isotopic labeling experiments were consistent with a process involving protonated cyclopropane intermediates **71** and **72**. Equation 5.52 shows the process that interchanges C1 and C2 to give **73**, and a similar process beginning with **69** can interchange C3 and C4. The ^{13}C NMR peaks did not show broadening down to -140°C , indicating that the energy barrier for the interconversion of **69** and **70** must be less than 2.4 kcal/mol.²⁸³

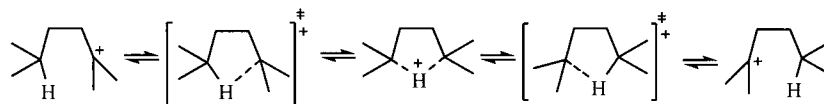


In addition to 1,2-hydride shifts, 1,3-, 1,4-, and higher hydride shifts can be observed. For example, the NMR spectrum of the 2,5-dimethyl-2-hexyl cation suggested rearrangement involving a 1,4-hydride shift by a process having an activation energy of 12–13 kcal/mol.²⁸⁴ Theoretical calculations suggested that the process occurs as shown in Figure 5.53, where the μ -hydridobridged carbocation was found to be an intermediate 5.6–10.5 kcal/mol (depending on the level of theory) higher in energy than the open chain carbocation.²⁸⁵ The μ -hydridobridged ions can be observed spectroscopically in monocyclic, bicyclic, and tricyclic systems.²⁸⁶

The discussion here has demonstrated that structures having a positive charge on the carbon skeleton exhibit structural variations that confound our attempts to represent them completely with simple valence bond structures. Even more intriguing structures having more than one positive charge on the

FIGURE 5.53

1,4-Hydride shift and μ -hydridobridged nonclassical ion intermediate.



²⁸² Walker, G. E.; Kronja, O.; Saunders, M. J. *Org. Chem.* **2004**, *69*, 3598.

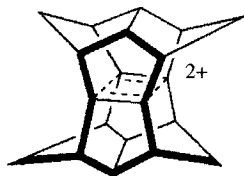
²⁸³ Saunders, M.; Kates, M. R. J. *Am. Chem. Soc.* **1978**, *100*, 7082.

²⁸⁴ Saunders, M.; Stofko, J. J., Jr. *J. Am. Chem. Soc.* **1973**, *95*, 252.

²⁸⁵ Vrček, I. V.; Vrček, V.; Siehl, H.-U. *J. Phys. Chem. A* **2002**, *106*, 1604.

²⁸⁶ Sun, F.; Sorensen, T. S. J. *Am. Chem. Soc.* **1993**, *115*, 77 and references therein.

carbon skeleton are known, such as the “remarkably stable” pagodane dication, **74**.²⁸⁷



74

Radical Cations

Each of the carbocations discussed to this point has been a species in which all of the electrons were spin-paired. Another type of positively charged reactive intermediate is the radical cation—a species that has both an unpaired electron and a positive charge.^{288,289} Radical cations play important roles in many radiochemical and photochemical reactions, and they may also be important in biological processes,²⁹⁰ including photosynthesis^{289b} and the biosynthesis of natural products.²⁹¹

Organic radical cations can be generated from neutral organic compounds through.^{289a}

1. Chemical oxidation by a wide variety of oxidizing agents, including Brønsted acids, Lewis acids, metal ions and oxides, nitrosonium ions, other organic radical cations, semiconductor materials, and some zeolites²⁹²
2. Electrochemical oxidation
3. Radiolysis with ionizing radiation (X-rays and γ -rays)

²⁸⁷ Prakash G. K. S. in Prakash, G. K. S.; Schleyer, P. v. R., Eds. *Stable Carbocation Chemistry*; John Wiley & Sons: New York, 1997, chapter 4.

²⁸⁸ Such species are also termed *cation radicals*, but the name *radical cation* is consistent with IUPAC terminology. (Commission on Physical Organic Chemistry, IUPAC, *Pure Appl. Chem.* **1994**, 66, 1077.) In the recommended nomenclature, the radical cation of molecule A is denoted $A^{\bullet+}$; that is, the symbols for cation and radical are written in the same order as indicated by the term *radical cation*.

²⁸⁹ For a discussion of radical ions in organic chemistry, see (a) Roth, H. D. *Top. Curr. Chem.* **1992**, 163, 131; (b) Kaiser, E. T.; Kevan, L., Eds. *Radical Ions*; Wiley-Interscience: New York, 1968; (c) Lund, A.; Shiotani, M., Eds. *Radical Ionic Systems: Properties in Condensed Phases (Topics in Molecular Organization and Engineering, Vol. 6)*; Kluwer Academic Publishers: Dordrecht, 1991; (d) Bauld, N. L. in Mariano, P.S., Ed. *Advances in Electron Transfer Chemistry*, Vol. 2; JAS Press: Greenwich, CT, 1992; pp. 1–66; (e) Chanon, M.; Rajzmann, M.; Chanon, F. *Tetrahedron* **1990**, 46 6193; (f) Hammerich, O.; Parker, V. D. *Adv. Phys. Org. Chem.* **1984**, 20, 55; (g) Shida, T.; Haselbach, E.; Bally, T. *Acc. Chem. Res.* **1984**, 17, 180; (h) Nelsen, S. F. *Acc. Chem. Res.* **1987**, 20, 269; (i) Roth, H. D. *Acc. Chem. Res.* **1987**, 20, 343; (j) Bauld, N. L.; Bellville, D. J. *Acc. Chem. Res.* **1987**, 20, 371; (k) Roth, H. D. in Moss, R. A.; Platz, M. S.; Jones, M., Jr., Eds. *Reactive Intermediate Chemistry*; John Wiley & Sons: Hoboken, NJ, 2004; chapter 6; Wiest, O.; Oxgaard, J.; Saettel, N. J. *Adv. Phys. Org. Chem.* **2003**, 38, 87.

²⁹⁰ For a study related of the cytochrome P-450 oxidative dealkylation of amines, see Dinnocenzo, J. P.; Karki, S. B.; Jones, J. P. *J. Am. Chem. Soc.* **1993**, 115, 7111.

²⁹¹ Hoffmann, U.; Gao, Y.; Pandey, B.; Klinge, S.; Warzecha, K.-D.; Krüger, C.; Roth, H. D.; Demuth, M. *J. Am. Chem. Soc.* **1993**, 115, 10358.

²⁹² Thermally activated Na-ZSM-5 zeolite was found to have a redox potential of 1.65 ± 0.1 V versus SCE in a study of the conversion of α,ω -diphenylpolyenes to their radical cations. Ramamurthy, V.; Caspar, J. V.; Corbin, D. R. *J. Am. Chem. Soc.* **1991**, 113, 594.

4. Photoinduced electron transfer (PET) resulting from bimolecular reaction of a photoexcited molecule with a ground state molecule²⁹³
5. Electron impact ionization (commonly used for the production of radical cations in mass spectrometry).

Among the major analytical tools for detecting and studying radical cations are mass spectrometry, EPR, and NMR.

Organic radical cations can be classified according to the type of orbital from which an electron is removed from a neutral parent compound. Compounds with nonbonded electrons, such as amines, ethers, and ketones, can be oxidized to produce *n*-radical cations. For example, the one-electron oxidation of methanol (equation 5.53) is conveniently viewed as the removal of an electron from the methanol HOMO, which we expect to be a nonbonding orbital associated with oxygen.²⁹⁴

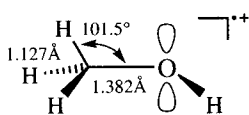
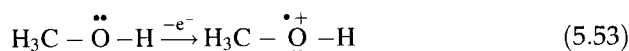
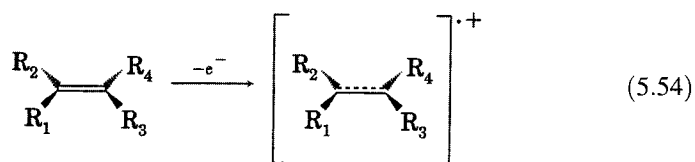


FIGURE 5.54
Calculated geometry of methanol radical cation. (Adapted from reference 295.)



The formulation of the radical cation of methanol shown in equation 5.53 might suggest a species in which both the positive charge and the unpaired electron density are localized on oxygen. As indicated by Figure 5.40, however, the LUMO of an ethyl cation is delocalized onto other atoms as well. Consistent with that model, the calculated geometry of the methanol radical cation (Figure 5.54) indicates that one C-H bond is aligned with the *p* orbital on oxygen, this C-H distance is lengthened, and the O-C distance is shortened in comparison with neutral methanol.^{295,296} The implication of this geometry is that hyperconjugative delocalization results in shifting of electron density from C-H bonding to C-O bonding.

One-electron oxidation of alkenes, alkynes, and arenes produces π -radical cations by removal of an electron from a π molecular orbital (equation 5.54).



²⁹³ Generation of radical cations by photoinduced electron transfer reactions of neutral molecules generates radical anion/radical cation pairs, which can undergo back electron transfer to regenerate neutral molecules. Polar solvents such as CH₃CN can make diffusive separation of the radical ions more probable, but the use of polar solvents increases the opportunity for reaction of solvent with the radical ions. The use of cationic acceptors for PET from photoexcited organic compounds forms a neutral radical/radical cation pair. With no Coulombic barrier to separation, yields of separated radical cations are increased. For a discussion, see Todd, W. P.; Dinnocenzo, J. P.; Farid, S.; Goodman, J. L.; Gould, I. R. *J. Am. Chem. Soc.* **1991**, *113*, 3601.

²⁹⁴ Budzikiewicz, H.; Djerassi, C.; Williams, D. H. *Mass Spectrometry of Organic Compounds*; Holden-Day: San Francisco, 1967; p. 94.

²⁹⁵ Ma, N. L.; Smith, B. J.; Pople, J. A.; Radom, L. *J. Am. Chem. Soc.* **1991**, *113*, 7903.

²⁹⁶ The calculated geometry depends to some extent on the level of theory employed. For other theoretical studies, see Gauld, J. W.; Glukhovtsev, M. N.; Radom, L. *Chem. Phys. Lett.* **1996**, *262*, 187; Belopushkin, S. I.; Belevskii, V. N.; Chuvylkin, N. D. *High Energy Chem.* **1998**, *32*, 92.

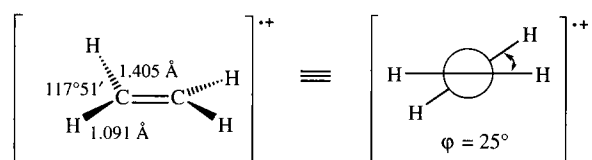
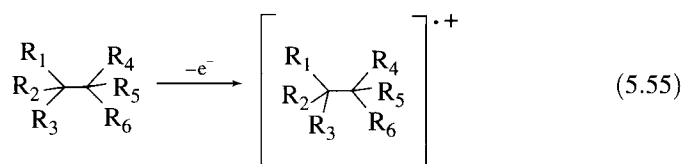


FIGURE 5.55
Geometry of radical cation of ethene.

From an analysis of the photoelectron spectrum of ethene, the ethene radical cation was found to have a torsion angle of 25° . The C–C bond length is 1.405 \AA , and the C–H bond length is 1.091 \AA . The H–C–H bond angle is $117^\circ 51'$.²⁹⁷ The geometry of the ethene radical cation (Figure 5.55) has been explained on the basis of a compromise between some remaining π bonding in the SOMO (optimized at a torsional angle of 0°) and hyperconjugative interaction of the p orbital on each carbon with the C–H bonding orbitals on the adjacent methylene group (optimized at a torsional angle of 90°).²⁹⁸

For larger alkenes, hyperconjugation with an alkyl group α to an olefinic carbon atom eliminates the need for rotation, so the radical cations of almost all alkenes other than ethene are planar.²⁹⁹ Eriksson and co-workers found that the radical cation formed by radiolysis of 1-pentene in a fluorochlorocarbon matrix at 77 K exhibits an EPR spectrum suggesting some delocalization of the SOMO over C3. In the case of the isomeric 2-pentenes, the results suggested that the SOMO is localized on the carbon atoms of the former double bond, C2 and C3. The difference in bonding was attributed to a lower ionization energy for the longer alkyl group attached to the double bond in 1-pentene in comparison with the higher ionization energy of the shorter alkyl group attached to the double bond in the 2-pentenes.³⁰⁰



One-electron oxidation of alkanes leads to σ -radical cations (equation 5.55).³⁰¹ Such ionization removes an electron from an orbital associated with σ bonding among carbon atoms. The radical cation of butane, for example, shows elongation of the C2–C3 bond to a distance of about 2.0 \AA and a much lower difference in energies of the anti and gauche conformers than is the case with the parent hydrocarbon.³⁰¹ Ionization of methane

²⁹⁷ Köppel, H.; Domcke, W.; Cederbaum, L. S.; von Niessen, W. *J. Chem. Phys.* **1978**, *69*, 4252.

²⁹⁸ Mulliken, R. S.; Roothan, C. C. *J. Chem. Rev.* **1947**, *41*, 219.

²⁹⁹ (a) Bellville, D. J.; Bauld, N. L. *J. Am. Chem. Soc.* **1982**, *104*, 294; (b) Clark, T.; Nelsen, S. F. *J. Am. Chem. Soc.* **1988**, *110*, 868.

³⁰⁰ Eriksson, L. A.; Sjöqvist, L.; Lunell, S.; Shiotani, M.; Usui, M.; Lund, A. *J. Am. Chem. Soc.* **1993**, *115*, 3244.

³⁰¹ For a theoretical study of the radical cations of alkanes and references to experimental data for these species, see Eriksson, L. A.; Lunell, S.; Boyd, R. J. *J. Am. Chem. Soc.* **1993**, *115*, 6896.

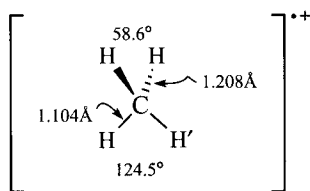
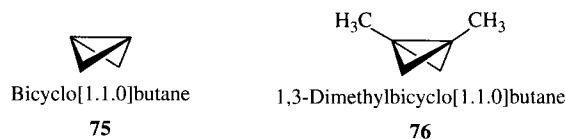


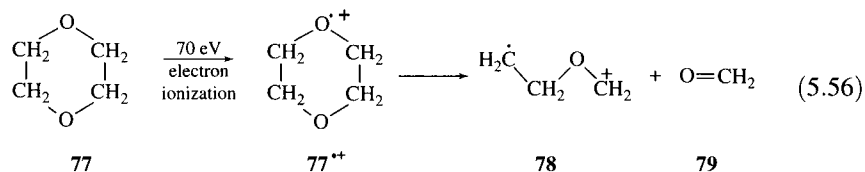
FIGURE 5.56
Geometry of methane radical cation. (Adapted from reference 301.)

produces a distorted structure (Figure 5.56) having two longer C–H bond distances, with an H–C–H angle of about 60° for these atoms, and two shorter C–H' bond distances associated with an H'–C–H' angle near 125° .³⁰²

Alkyl groups may also delocalize the unpaired electron and charge density in radical cations formed from strained alkanes. For example, radical cations of bicyclo[1.1.0]butane (**75**) and 1,3-dimethylbicyclo[1.1.0]butane (**76**) were detected in chlorofluorocarbon matrix following γ -irradiation of the parent hydrocarbon. The data suggested that much of the unpaired electron density in **75** \bullet^+ is associated with the two bridgehead carbon atoms, but that in **76** \bullet^+ about 15% of the unpaired electron density is associated with the methyl substituents at these positions.³⁰³



In each of the radical cation structures discussed so far, the unpaired electron and the positive charge have been closely associated. However, there are also radical cations in which the radical center and the cation center are separate from each other. For example, electron ionization of 1,4-dioxane (**77**) in a mass spectrometer produces the radical cation **77** \bullet^+ , which forms the radical cation **78** by elimination of formaldehyde (**79**).³⁰⁴ Species such as **78** were termed *distonic* by Radom to emphasize the distance between the charge and radical sites. Distonic radical cations can be significantly lower in energy than radical cations in which the charge and unpaired electron density are coincident.³⁰⁵



³⁰² The distortion from the tetrahedral geometry of methane is a Jahn–Teller effect: Jahn, H. A.; Teller, E. *Phys. Rev.* **1936**, *49*, 874; *Proc. R. Soc. London Ser. A* **1937**, *161*, 220. Experimental evidence for a C_{2v} structure for the methane radical cation (studied in a neon matrix at 4 K) was reported by Knight, L. B., Jr.; Steadman, J.; Feller, D.; Davidson, E. R. *J. Am. Chem. Soc.* **1984**, *106*, 3700. The EPR spectrum of CH_4^+ at 4 K suggests four magnetically equivalent protons, but the EPR spectrum of $CH_2D_2^+$ indicates the C_{2v} geometry shown. The apparent equivalence of the four protons in CH_4^+ is attributed to dynamic Jahn–Teller distortion making all protons equivalent on the NMR time scale. For a discussion and theoretical study, see Paddon-Row, M. N.; Fox, D. J.; Pople, J. A.; Houk, K. N.; Pratt, D. W. *J. Am. Chem. Soc.* **1985**, *107*, 7696.

³⁰³ Arnold, A.; Burger, U.; Gerson, F.; Kloster-Jensen, E.; Schmidlin, S. P. *J. Am. Chem. Soc.* **1993**, *115*, 4271.

³⁰⁴ A radical cation can be considered to be a cationized diradical in the sense that it is the hypothetical product of one-electron oxidation of a diradical. Conversely, neutralization of **78** produces the 1,4-biradical $\bullet CH_2CH_2OCH_2\bullet$, which offers a convenient method for studying its reactions in the gas phase: Polce, M. J.; Wesdemiotis, C. *J. Am. Chem. Soc.*, **1993**, *115*, 10849.

³⁰⁵ Yates, B. F.; Bouma, W. J.; Radom, L. *J. Am. Chem. Soc.*, **1984**, *106*, 5805.

Radical cations exhibit a wide variety of reactions,²⁸⁹ including unimolecular reactions such as rearrangement,³⁰⁶ fragmentation,³⁰⁷ and intramolecular bond formation, as well as bimolecular reactions with ionic, radical, or ground state species.³⁰⁸ Notable processes include reaction with nucleophiles to produce radicals, reaction with radicals to produce cations, reaction with electron donors to produce biradicals, and reactions with ground state molecules to give addition products.³⁰⁹ Often the products of reactions of radical cations with neutral species are different from those observed by reaction of the corresponding carbocation with the same reactant.³¹⁰

Radical cations of weak acids may react either by heterolytic cleavage (loss of a proton to produce a radical) or homolytic cleavage (loss of a hydrogen atom to form a carbocation).³¹¹ In a polar solvent, heterolytic cleavage is usually favored because of the favorable solvation energy of the proton, and radical cations ordinarily are much more acidic than the corresponding neutral compounds. For example, the pK_{HA} value of toluene in DMSO is 43, while the $pK_{\text{HA}^{+\cdot}}$ value for the radical cation of toluene is -20 . Therefore, the radical cation is 10^{63} more acidic than the neutral compound.³¹²

In the gas phase, heterolytic cleavage is favored because the positive charge can be stabilized by charge delocalization in the larger ion. Zhang and Bordwell determined that N–H and O–H bond dissociation energies (BDEHA \cdot^+) of radical cations are only slightly lower than those of their parent nitrogen or oxygen acid compounds. However, BDEHA \cdot^+ values are typically 30–50 kcal/mol lower than the BDE of the corresponding neutral compound.^{312b}

Reaction of a radical cation with a nucleophile can occur either by electron transfer to give a diradical or by attachment to give a radical. For example, the reaction of azide ion (N_3^-) with the radical cation of 4-methoxystyrene and its β -methyl and β,β -dimethyl derivatives was found to occur by electron transfer in acetonitrile (CH_3CN) solution but by nucleophilic attachment in 2,2,2-trifluoroethanol (TFE) solution. The change in mechanism was attributed to a change in the oxidation potential of azide ion with solvent (the value being 0.5 V more positive in TFE than in CH_3CN), suggesting that redox properties of nucleophiles and radical cations under reaction conditions can determine the reaction pathways of radical ions.³¹³

³⁰⁶ The radical cation of benzvalene was found to isomerize to the radical cation of benzene at a temperature of 135 K: Arnold, A.; Gerson, F.; Burger, U. *J. Am. Chem. Soc.* **1991**, *113*, 4359.

³⁰⁷ For a discussion of bond cleavage reactions of radical cations, see (a) Popielarz, R.; Arnold, D. *J. Am. Chem. Soc.* **1990**, *112*, 3068; (b) Camaioni, D. M. *J. Am. Chem. Soc.* **1990**, *112*, 9475; (c) Baciocchi, E.; Bietti, M.; Lanzalunga, O. *J. Phys. Org. Chem.* **2006**, *19*, 467.

³⁰⁸ Tedder, J. M. in Viehe, H. G.; Janousek, Z.; Merényi, R., Eds. *Substituent Effects in Radical Chemistry*; D. Reidel Publishing: Dordrecht, 1986; pp. 223–244.

³⁰⁹ For a theoretical study of the reaction of σ -radical cations with nucleophiles, see Shaik, S.; Reddy, A. C.; Ioffe, A.; Dinnocenzo, J. P.; Danovich, D.; Cho, J. K. *J. Am. Chem. Soc.* **1995**, *117*, 3205.

³¹⁰ Gassman, P. G.; Singleton, D. A. *J. Am. Chem. Soc.* **1984**, *106*, 7993.

³¹¹ Alkane radical cations in liquid hydrocarbon solution undergo ion–molecule reactions, such as proton transfer or hydrogen atom transfer, on a submillisecond time scale. Werst, D. W.; Bakker, M. G.; Trifunac, A. D. *J. Am. Chem. Soc.* **1990**, *112*, 40.

³¹² (a) Bordwell, F. G.; Cheng, J.-P. *J. Am. Chem. Soc.* **1989**, *111*, 1792.; (b) Zhang, X.-M.; Bordwell, F. G. *J. Am. Chem. Soc.* **1994**, *116*, 4251.

³¹³ Workentin, M. S.; Schepp, N. P.; Johnston, L. J.; Wayner, D. D. M. *J. Am. Chem. Soc.* **1994**, *116*, 1141.

Radical anions, which have both an unpaired electron and a negative charge, comprise another class of reactive intermediates. Radical anions can be made by one-electron reduction with metals such as potassium or by ionizing radiation.^{314,315} Many radical anions are difficult to study because their large, negative electron affinities (on the order of -2.3 eV) make them very unstable, and they are prone to fragmentation to an anion and a radical. Such processes are especially probable if a portion of the molecule can be detached as a relatively stable anion, such as a halide ion.³¹⁶ However, the ESR spectrum of the *trans*-3-hexene radical anion in *trans*-3-hexene/*n*-hexane-*d*₁₄ mixed crystals has been studied at 4.2 K. The results suggested pyramidalization of the olefinic carbon atoms, with half of the unpaired electron density delocalized onto the carbon atoms α to the olefinic carbon atoms.³¹⁷ In the gas phase, characteristic reactions of radical anions include electron transfer, proton transfer, hydrogen atom transfer, and substitution reactions.³¹⁸

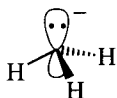


FIGURE 5.57
 sp^3 -Hybridized model for methyl anion.

5.5 CARBANIONS

Structure and Geometry of Carbanions

Carbanions are anions that contain an even number of electrons and that have an unshared pair of electrons on a triligant carbon atom.^{288,319–321} For the simplest carbanion, H_3C^- , we expect four pairs of electrons to be arranged around the carbon atom, with the nonbonded pair of electrons in an orbital that is approximately an sp^3 hybrid (Figure 5.57).^{322,323} This should produce a trigonal pyramid structure having a geometry similar to that of ammonia, and there is experimental evidence indicating that the methyl anion in the gas phase is pyramidal.³²⁴ NMR studies of alkyl Grignard reagents in solution also show evidence of a tetrahedral carbanion that can undergo inversion of

³¹⁴ Bauld, N. L. *Radicals, Ion Radicals, and Triplets: The Spin-Bearing Intermediates of Organic Chemistry*, Wiley-VCH: New York, 1997.

³¹⁵ For an example, see Stevenson, G. R.; Burton, R. D.; Reiter, R. C. *J. Am. Chem. Soc.* **1992**, *114*, 4514.

³¹⁶ For a discussion and leading references, see Maslak, P.; Narvaez, J. N.; Kula, J.; Malinski, D. S. *J. Org. Chem.* **1990**, *55*, 4550.

³¹⁷ Muto, H.; Nunome, K.; Matsuura, K. *J. Am. Chem. Soc.* **1991**, *113*, 1840.

³¹⁸ Born, M.; Ingemann, S.; Nibbering, N. M. M. *Mass Spectrom. Rev.* **1997**, *16*, 181.

³¹⁹ The term *carbanion* was proposed by Wallis, E. S.; Adams, F. H. *J. Am. Chem. Soc.* **1933**, *55*, 3838.

³²⁰ Pale, P.; Vogel, P. in Katritzky, A. R.; Taylor, R. J. K., Eds. *Comprehensive Organic Functional Group Transformations II*; Elsevier: Oxford, 2005; p. 889.

³²¹ Buncl, E.; Dust, J. M. *Carbanion Chemistry: Structures and Mechanisms*, Oxford University Press: New York, 2003.

³²² The application of molecular orbital theory to carbanions was discussed by Nobes, R. H.; Poppinger, D.; Li, W.-K.; Radom, L. in Buncl, E.; Durst, T., Eds. *Comprehensive Carbanion Chemistry. Part C. Ground and Excited State Reactivity*; Elsevier: Amsterdam, 1987; pp. 1–92.

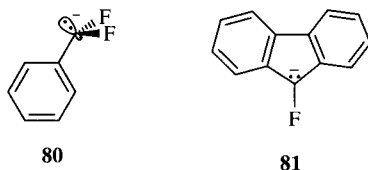
³²³ Often carbanions are shown without explicit depiction of the nonbonded pair of electrons. Thus, the methyl anion is also indicated by H_3C^- .

³²⁴ Ellison, G. B.; Engelking, P. C.; Lineberger, W. C. *J. Am. Chem. Soc.* **1978**, *100*, 2556.

the lone pair in a manner similar to ammonia.^{325,326} We would expect bridgehead carbanions to form without difficulty, and that is found to be the case.³²⁷

By similar arguments, vinyl carbanions are expected to exhibit sp^2 hybridization, and acetylenic carbanions should show sp hybridization. Based on the idea that the greater the s character in an orbital, the more easily it can accommodate a negative charge, we expect carbanions in which the negative charge is associated with a pair of nonbonded electrons in an sp hybrid orbital to be more easily formed than those in which the electrons are in sp^2 hybrid or sp^3 hybrid orbitals.³²⁸ Similarly, electron withdrawal by induction should stabilize a carbanion.

Although triligant carbanions are expected to be approximately pyramidal, carbanions with adjacent π systems may become planar due to the effects of resonance. Streitwieser proposed a way to distinguish between the two types of carbanions by noting the effect of an α -fluoro substituent. The fluorine has the effect of stabilizing a pyramidal carbanion, such as the α,α -difluorobenzyl anion **80**, but it destabilizes a planar carbanion such as 9-fluorofluorenyl anion, **81**.^{329,330}



In many cases, organic reactions involve organometallic compounds with carbanionic character, not free carbanions. In organometallic compounds, the carbon atom associated with the metal has much less than a full negative charge, and the interaction of the carbon atom with the metal atom has some covalent character. ^{13}C and ^7Li NMR studies of *n*-butyllithium and *t*-butyllithium in hydrocarbon solvent suggest a polar covalent C–Li bond with only a small negative charge on the carbon atom, and some calculations suggest that carbon–alkali metal bonds may be comparable in covalency to carbon–halogen bonds.^{331–333}

³²⁵ Whitesides, G. M.; Witanowski, M.; Roberts, J. D. *J. Am. Chem. Soc.* **1965**, *87*, 2854.

³²⁶ In general, we expect inversion to be facilitated when conditions allow a relatively free carbanion and to be inhibited when conditions cause the counterion to be held close to the carbanion.

³²⁷ Compare Applequist, D. E.; Roberts, J. D. *Chem. Rev.* **1954**, *54*, 1065.

³²⁸ Experimental results are consistent with this view. For details, see Cram, D. J. *Fundamentals of Carbanion Chemistry*; Academic Press: New York, 1965; p. 49 ff.

³²⁹ Streitwieser, A., Jr.; Mares, F. J. *Am. Chem. Soc.* **1968**, *90*, 2444.

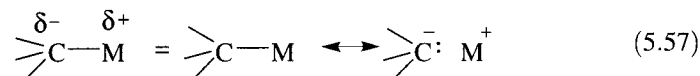
³³⁰ The effect was attributed to a decrease in carbanion stabilization arising from the greater electronegativity of the sp^2 hybrid orbital used for C–F bonding by Hine, J.; Mahone, L. G.; Liotta, C. L. *J. Am. Chem. Soc.* **1967**, *89*, 5911 and to an electron-donating resonance effect by Streitwieser and Mares (reference 329).

³³¹ McKeever, L. D.; Waack, R. J. *Chem. Soc. D Chem. Commun.* **1969**, 750.

³³² The investigation of carbanions by nuclear magnetic resonance was reviewed by O'Brien, D. H. in Bunce, E.; Durst, T., Eds., *Comprehensive Carbanion Chemistry. Part A. Structure and Reactivity*; Elsevier: Amsterdam, 1980; pp. 271–322.

³³³ Bickelhaupt, F. M.; Solà, M.; Guerra, C. F. *J. Chem. Theory Comput.* **2006**, *2*, 965.

In the valence bond model, organometallic compounds with carbanion character may be considered as resonance hybrids of two contributing structures, one purely covalent and one purely ionic (equation 5.57).



The degree of ionic character depends on the nature of the metal, the medium, and the substituents on the carbanionic carbon atom. The percent ionic character (i.e., the percent contribution of the ionic resonance structure to the hybrid) increases with increasing difference in electronegativity of the carbon and metal atoms. Pauling suggested an empirical relationship for estimating the fraction of ionic character in the carbon–metal bond (equation 5.58)

$$\text{Fraction ionic character} = 1 - e^{-0.25(\chi_A - \chi_B)^2} \quad (5.58)$$

where $\chi_A - \chi_B$ is the electronegativity difference between the two atoms involved.³³⁴ An alternative relationship (equation 5.59) was suggested by Hannay and Smyth (equation 5.59).³³⁵

$$\text{Fraction ionic character} = 0.16(\chi_A - \chi_B) + 0.035(\chi_A - \chi_B)^2 \quad (5.59)$$

The two equations predict comparable fractional ionic character for most atom pairs, although the latter equation correlates better with the experimental result that the H–F bond is 43% ionic and may also serve better for atoms with larger differences in electronegativity.³³⁶

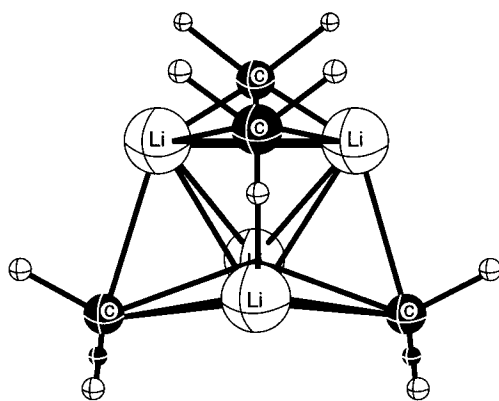
One conceptual difficulty with the covalent representation of an organometallic compound such as methyllithium is that the metal atom does not appear to have a filled outer shell. However, a formula such as CH_3Li should not be regarded as a true molecular formula because many organometallic compounds often are oligomeric, not monomeric, species. For example, methyllithium is reported to be a tetrahedral tetramer both in the solid state and the gas phase, although oligomers of different size can exist in solution. Figure 5.58 shows the calculated structure for the tetramer.³³⁷ The four lithium atoms are arranged at the vertices of a tetrahedron, while each carbon of the methyl groups is coordinated to one face of the tetrahedron. *n*-Butyllithium is reported to be hexameric in hydrocarbon solution and to exist as an equilibrium mixture of tetramers and dimers in THF

³³⁴ Pauling, L. *The Nature of the Chemical Bond*, 3rd ed.; Cornell University Press: Ithaca, NY, 1960; p. 98.

³³⁵ Hannay, N. B.; Smyth, C. P. *J. Am. Chem. Soc.* **1946**, *68*, 171.

³³⁶ For a tabulation of the partial ionic character of carbon–metal bonds, see Haiduc, I.; Zuckerman, J. J. *Basic Organometallic Chemistry*; Walter de Gruyter: Berlin, 1985; p. 9 ff.

³³⁷ Kwon, O.; Sevin, F.; McKee, M. L. *J. Phys. Chem. A* **2001**, *105*, 913; Kaufmann, E.; Raghavachari, K.; Reed, A. E.; Schleyer, P. v. R. *Organometallics* **1988**, *7*, 1597. See also Bickelhaupt, F. M.; Hommes, N. J. R. v. E.; Guerra, C. F.; Baerends, E. J. *Organometallics* **1996**, *15*, 2923.

**FIGURE 5.58**

Calculated structure of the methyl-lithium tetramer. (Reproduced from reference 337.)

solution.^{338,339} *n*-Propyllithium is a mixture of hexamers, octamers, and nonamers in cyclopentane solution, and there is rapid carbon–lithium bond exchange within the aggregates.³⁴⁰ Temperature can affect the degree of aggregation and the extent of solvation of organometallic compounds.³⁴¹

Carbanionic species in solution are strongly influenced by the counterion and by any added species such as bases that can coordinate a metallic counterion. For example, Kronzer and Sandel reported NMR studies of 1- and 2-naphthylmethyl lithium, -sodium, and -potassium in tetrahydrofuran (THF) and in hexamethylphosphoramide (HMPA) solution.³⁴² In THF the spectra showed a strong dependence on the metal, suggesting that there was close association of the carbanionic carbon with the metal. The spectra of the lithium and sodium species were identical in HMPA solution, however, suggesting that the carbanions were significantly separated from the cation, either as free ions or as ion pairs separated by solvent molecules.

Studies by Jackman and co-workers provided additional insight into the structure of the triphenylmethanide ion (82) in ethereal solvents.³⁴³ They determined that dissociation of contact ion pairs into solvent-separated ion pairs is exothermic due to the additional stabilization that results from better solvation of the two ions. The entropy term for the separation is negative, however, because solvent becomes more ordered around the separate ions. Therefore, the free energy change for ion separation is more negative at lower temperature. A greater delocalization of the negative charge favors ion separation. A smaller cation size also favors separation, although this appears to be the net result of destabilization arising from ion pair separation

³³⁸ For leading references, see Nichols, M. A.; Williard, P. G. *J. Am. Chem. Soc.* **1993**, *115*, 1568.

³³⁹ In addition to NMR, carbanions may also be investigated by UV–vis spectrophotometry (Buncel, E.; Menon, B. in Buncel, E.; Durst, T., Eds. *Comprehensive Carbanion Chemistry. Part A. Structure and Reactivity*; Elsevier: Amsterdam, 1980; pp. 97–124) and by infrared and Raman spectroscopy (Corset, J. in Buncel, E.; Durst, T., Eds. *Comprehensive Carbanion Chemistry. Part A. Structure and Reactivity*; Elsevier: Amsterdam, 1980; pp. 125–195).

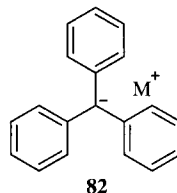
³⁴⁰ Fraenkel, G.; Henrichs, M.; Hewitt, J. M.; Su, B. M.; Geckle, M. J. *J. Am. Chem. Soc.* **1980**, *102*, 3345.

³⁴¹ Pratt, L. M.; Truhlar, D. G.; Cramer, C. J.; Kass, S. R.; Thompson, J. D.; Xidos, J. D. *J. Org. Chem.* **2007**, *72*, 2962.

³⁴² Kronzer, F. J.; Sandel, V. R. *J. Am. Chem. Soc.* **1972**, *94*, 5750.

³⁴³ Grutzner, J. B.; Lawlor, J. M.; Jackman, L. M. *J. Am. Chem. Soc.* **1972**, *94*, 2306.

combined with greater stabilization of the individual ions by polar solvent. For this reason a more polar solvent with greater ability to coordinate with the ions also favors separation. The effects of solvent on organometallic species can be quite dramatic. For example, a theoretical study revealed that the stereochemistry of an intramolecular carbolithiation could be reversed by coordination of a single molecule of THF to the lithium.³⁴⁴

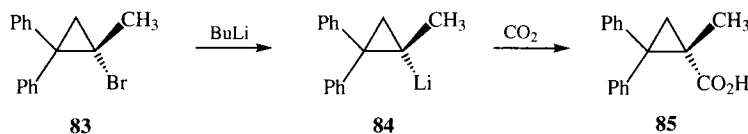


One way to study the structures of carbanions is to determine whether chiral carbanions undergo racemization. The retention of configuration at a chiral carbanionic center depends on solvent and temperature.^{345,346} Solvents such as ether decrease the covalent character of the carbon–metal interaction, thus facilitating epimerization at the chiral center.³⁴⁷ Racemization at a chiral center can be slowed if the rate of carbanion inversion can be decreased. Although cyclopropyl radicals racemize, cyclopropyl carbanions retain their configuration.^{348,349} For example, lithiation of the optically active bromocyclopropane derivative **83** produced a carbanion (**84**) that reacted with CO₂ to produce the cyclopropanecarboxylic acid **85**. The overall reaction took place with 100% retention of configuration, indicating that the three-membered ring inhibits the inversion of **84** (Figure 5.59).^{347,350}

In contrast, substituents that accept electron density by resonance can stabilize carbanionic centers, thus lessening the interaction with metal ions and facilitating racemization. The 1-lithio derivative of (–)-(R)-1-cyano-2,2-diphenylcyclopropane can be alkylated with methyl iodide to yield racemic-1-methyl-1-cyano-2,2-diphenylcyclopropane, indicating racemization at the carbanionic center.³⁵¹ This result could be ascribed either to a planar carbanion with appreciable C=C=N[–] character or to a rapidly inverting tetrahedral carbanion. The X-ray crystal structure of 1-cyano-2,2-dimethylcyclopropyllithium

FIGURE 5.59

Retention of configuration by a chiral cyclopropyl carbanion. (Adapted from reference 347.)



³⁴⁴ Liu, H.; Deng, K.; Cohen, T.; Jordan, K. D. *Org. Lett.* **2007**, *9*, 1911.

³⁴⁵ Letsinger, R. L. *J. Am. Chem. Soc.* **1950**, *72*, 4842.

³⁴⁶ Curtin, D. Y.; Koehl, W. J., Jr. *J. Am. Chem. Soc.* **1962**, *84*, 1967.

³⁴⁷ Walborsky, H. M.; Impastato, F. J.; Young, A. E. *J. Am. Chem. Soc.* **1964**, *86*, 3283.

³⁴⁸ Applequist, D. E.; Peterson, A. H. *J. Am. Chem. Soc.* **1960**, *82*, 2372.

³⁴⁹ This statement is a generalization. Whether one observes racemization with either radicals or carbanions depends on the reaction conditions and the rates of inversion and of bimolecular reaction.

³⁵⁰ Applequist, D. E.; Peterson, A. H. *J. Am. Chem. Soc.* **1961**, *83*, 862.

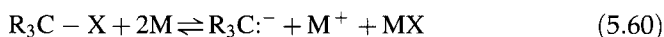
³⁵¹ Walborsky, H. M.; Hornyak, F. M. *J. Am. Chem. Soc.* **1955**, *77*, 6026.

indicated a tetrahedral carbanion carbon atom, supporting the latter explanation.^{352,353}

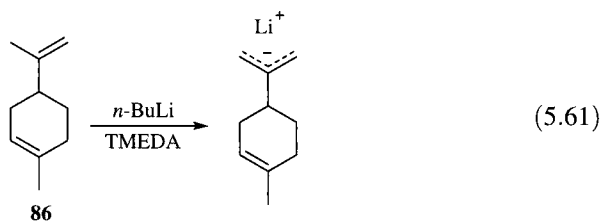
As in other areas of organic chemistry, computational investigations have provided important insights into the nature of carbanions, and the results complement the experimental studies. For example, *ab initio* calculations suggest that the inversion barrier of a methyl anion is ca. 2.2 kcal/mol and that the inversion barrier of the ethyl anion is 3.3 kcal/mol. These values contrast with the <0.2 kcal/mol inversion barrier of the resonance-stabilized cyanomethyl anion on the one hand and the ca. 15 kcal/mol barrier for inversion of the cyclopropyl anion via a highly strained transition structure on the other hand. By comparison, the inversion barrier of ammonia is about 5.5 kcal/mol.³²¹

Generation of Carbanions

A common procedure for the synthesis of organometallic compounds is the reduction of a carbon–halogen bond with a metal (M), as illustrated in equation 5.60.^{328,354} (This simple equation ignores the role of solvent molecules and aggregated species.)



Reagents such as *n*-butyllithium, methyllithium, and phenyllithium manufactured by this process are commercially available.³⁵⁵ Carbanions can also be formed by an acid–base reaction involving heterolytic dissociation of a carbon–hydrogen bond by a strong base. An example is the deprotonation of limonene (**86**) by *n*-butyllithium complexed with tetramethylethylenediamine (TMEDA), as shown in equation 5.61. Note that there is more than one kind of allylic proton in **86**, but the deprotonation preferentially produces the least-substituted carbanion.³⁵⁶



³⁵² Boche, G.; Harms, K.; Marsch, M. *J. Am. Chem. Soc.* **1988**, *110*, 6925.

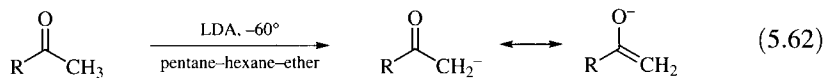
³⁵³ See also the theoretical calculations reported by Kaneti, J.; Schleyer, P. v. R.; Clark, T.; Kos, A. J.; Spitznagel, G. W.; Andrade, J. G.; Moffat, J. B. *J. Am. Chem. Soc.* **1986**, *108*, 1481.

³⁵⁴ Bates, R. B.; Ogle, C. A. *Carbanion Chemistry*; Springer-Verlag: Berlin, 1983; Stowell, J. C. *Carbanions in Organic Synthesis*; John Wiley & Sons: New York, 1979; Ayres, D. C. *Carbanions in Synthesis*; Oldbourne Book Co.: London, 1966.

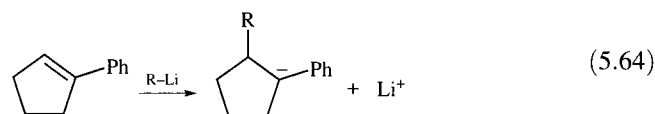
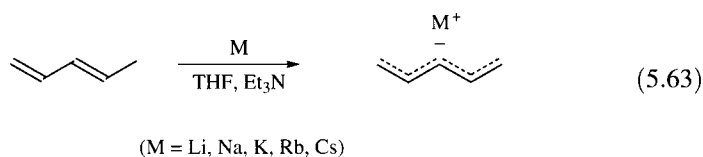
³⁵⁵ Durst, T. in Bunce, E.; Durst, T., Eds. *Comprehensive Carbanion Chemistry. Part B. Selectivity in Carbon–Carbon Bond Forming Reaction*; Elsevier: Amsterdam, 1984; pp. 239–291.

³⁵⁶ Crawford, R. J.; Erman, W. F.; Broadus, C. D. *J. Am. Chem. Soc.* **1972**, *94*, 4298.

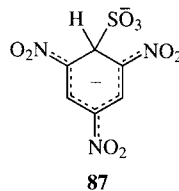
Because carbon–hydrogen bonds exhibit very low acidity (see Chapter 7), very strong bases are required for such reactions. However, C–H bonds adjacent to substituents such as carbonyl or cyano groups are more acidic. Nitrogen bases have been used effectively in these reactions to minimize the nucleophilic addition that can compete with proton removal when an organometallic compound such as *n*-butyllithium is used as the base. For example, methyl ketones react with lithium diisopropylamide (LDA) to form the enolate ion (equation 5.64),^{357–359}



In some cases metals will react directly with alkenes (equation 5.63).³⁶⁰ In addition, alkenes can undergo carbometalation, as illustrated in equation 5.64.^{361,362}



Addition of nucleophiles to aromatic compounds having many nitro or cyano groups leads to the formation of resonance-stabilized carbanions known as Jackson–Meisenheimer complexes. For example, addition of sulfite ion to 1,3,5-trinitrobenzene leads to **87**.³⁵⁴



³⁵⁷ House, H. O.; Phillips, W. V.; Sayer, T. S. B.; Yau, C.-C. *J. Org. Chem.* **1978**, *43*, 700.

³⁵⁸ An NMR spectrum of the lithium enolate of *t*-butyl acetate indicated that the carbon–carbon double bonded species was dominant. Rathke, M. W.; Sullivan, D. F. *J. Am. Chem. Soc.* **1973**, *95*, 3050.

³⁵⁹ Even more sterically hindered amides have been used: Olofson, R. A.; Dougherty, C. M. *J. Am. Chem. Soc.* **1973**, *95*, 582.

³⁶⁰ Yasuda, H.; Ohnuma, Y.; Yamauchi, M.; Tani, H.; Nakamura, A. *Bull. Chem. Soc. Jpn.* **1979**, *52*, 2036.

³⁶¹ Fraenkel, G.; Estes, D.; Geckle, M. J. *J. Organometal. Chem.* **1980**, *185*, 147.

³⁶² Yamataka, H.; Yamada, K.; Tomioka, K. in Rappoport, Z.; Marek, I., Eds. *The Chemistry of Organolithium Compounds*; Part 2, John Wiley & Sons: Chichester, UK, 2004; p. 901.

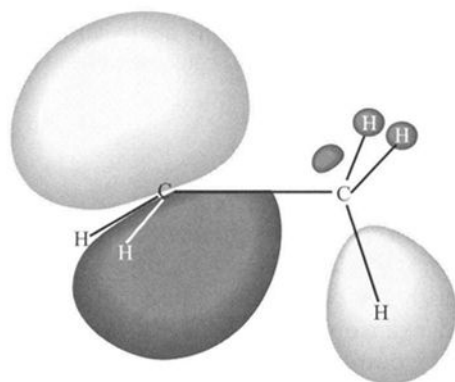


FIGURE 5.60
HOMO of ethyl anion.

Stability of Carbanions

We frequently measure anion stability in terms of the acidity of the corresponding protonated species. Thus, the acidity of carbon acids, in which the acidic proton is removed from a carbon atom, provides one measure of carbanion stability. There has been a significant change in the interpretation of carbanion stability over time. In 1979 a leading researcher summarized what was at that time the prevailing model of carbanion stabilities by saying that alkyl substitution at the carbanionic site results in an intensification of carbanionic character because of the electron-donating character of the alkyl groups. As we will see in more detail in Chapter 7, this view is no longer supported by theoretical or experimental evidence. Figure 5.60 shows the HOMO of ethyl anion as calculated with extended Hückel theory. It shows evidence of mixing a carbanion orbital having much p character with the orbitals of the methyl substituent, resulting in delocalization of negative charge away from the anionic center.³⁶³ This result is inconsistent with an explanation for decreasing acidity with increasing alkyl substitution that is based on electron-donating alkyl groups.

Major new insights into the electronic effects of substituents have resulted from measurements conducted in the gas phase, where the effects of solvent are eliminated.³⁶⁴ DePuy and co-workers determined the order of acidity to be ethane < propane (2° hydrogen atoms) < methane < isobutane (3° hydrogen atom) in the gas phase.³⁶⁵ This rather surprising result that methane is more acidic than ethane has some support in theoretical calculations.³⁶⁶ Therefore, the effect of alkyl substitution on a carbanion *in solution* may be better described as a solvation effect. As le Noble put it:

³⁶³ Theoretical calculations are in accord with stabilization of both cationic and anionic centers by methyl groups, with the affected C-H bond lengthened by the interaction. See the discussion by Forsyth, D. A.; Yang, J.-R. *J. Am. Chem. Soc.* **1986**, *108*, 2157 and references therein.

³⁶⁴ Three main types of experimental techniques have been used: high pressure mass spectrometry (HPMS), flowing afterglow (FA or FA-SIFT) studies, and pulsed ion cyclotron resonance (ICR) spectrometry. See Chapter 7 for further discussion and leading references.

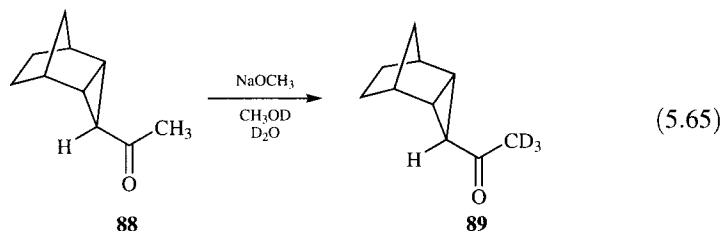
³⁶⁵ DePuy, C. H.; Bierbaum, V. M.; Damrauer, R. *J. Am. Chem. Soc.* **1984**, *106*, 4051; DePuy, C. H.; Gronert, S.; Barlow, S. E.; Bierbaum, V. M.; Damrauer, R. *J. Am. Chem. Soc.* **1989**, *111*, 1968.

³⁶⁶ Kollmar, H. *J. Am. Chem. Soc.* **1978**, *100*, 2660.

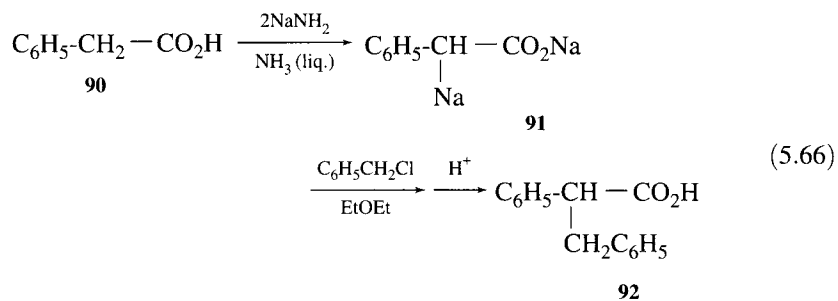
It becomes clear that much of the "truth" about carbanions to be found in current textbooks, however logical and convenient from a pedagogical point of view, is incorrect.³⁶⁷

Reactions of Carbanions

Because of the localization of electron density and negative charge, carbanions are both bases and nucleophiles. As a base, a carbanion can abstract a proton from any substance with a pK_a smaller than that of the protonated carbanion, and the use of isotopically labeled proton donors affords a useful synthesis of labeled compounds. For example, abstraction of a proton from the methyl group of *exo*-3-acetyl-*endo*-tricyclo[3.2.1.0^{2,4}]octane (**88**) gave an enolate ion that could abstract a deuterium ion from the solvent to produce a monodeuterated compound. Repeated exchange of the methyl protons led to a nearly quantitative yield of trideuterio product **89** (equation 5.65).³⁶⁸



As a nucleophile, a carbanion can react readily with a carbon atom bearing a good leaving group, which is a useful method for forming new carbon-carbon bonds. The aldol reaction and the Claisen condensation are familiar examples of carbanions (as enolates) undergoing nucleophilic addition to carbon-oxygen double bonds. Carbanions may also act as nucleophiles in S_N2 reactions. The reaction of phenylacetic acid (**90**) with sodium in liquid ammonia leads to a carbanion (**91**) that reacts with benzyl chloride to produce 2,3-diphenylpropionic acid (**92**, equation 5.66).³⁶⁹



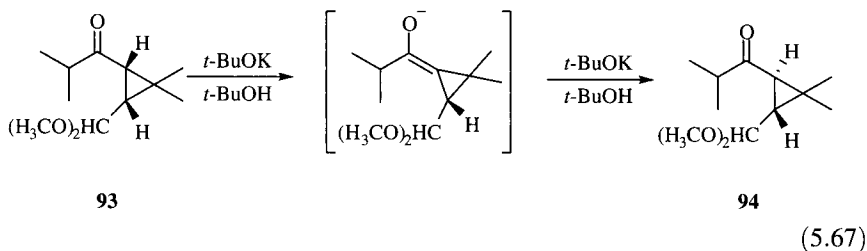
Carbanions are much less prone to unimolecular rearrangements than are carbocations or radicals, particularly with regard to 1,2-alkyl shifts

³⁶⁷ Ie Noble, W. J. in Jones, M., Jr.; Moss, R. A., Eds. *Reactive Intermediates*, Vol. 1; John Wiley & Sons: New York, 1978; pp. 27-67.

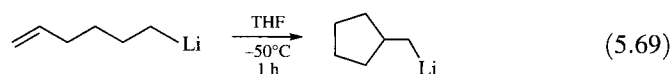
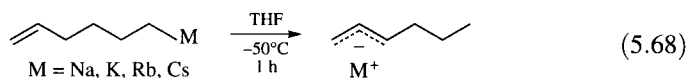
³⁶⁸ Creary, X. *J. Org. Chem.* **1976**, *41*, 3740.

³⁶⁹ Hauser, C. R.; Dunnivant, W. R. *Org. Synth. Collect. Vol. V* **1973**, 526.

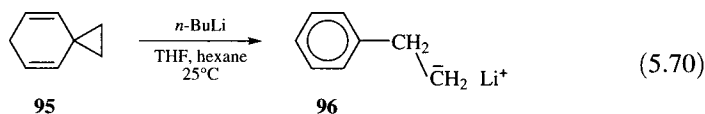
or 1,2-hydrogen shifts. However, some rearrangements of 1,2-migrations of aryl, vinyl, or acetylenic groups have been reported.³⁷⁰ In addition, the phenylcyclopropyl anion was found to open to the 2-phenylallyl anion in the gas phase with an E_a of 26 kcal/mol.³⁷¹ Carbanions stabilized by electron-withdrawing groups, such as carbonyls, are capable of other reactions. One example is epimerization of **93** to the more stable isomer **94** (equation 5.67), which was used in the synthesis of (\pm)-*trans*-chrysanthemic acid.³⁷² Here the configurational stability of the carbanion is lost because the intermediate is an enolate, so reprotonation of the intermediate can produce the more stable *trans* isomer of the cyclopropane.



The 5-hexenyl carbanions, where M is sodium, potassium, rubidium, and cesium, undergo rearrangement from a primary carbanion to the isomeric allylic carbanions in THF at -50°C (equation 5.68). However, 5-hexenyllithium rearranges to a cyclic structure (equation 5.69).³⁷³



Another example is the rearrangement of the carbanion formed by deprotonation of the spirodiene **95** by *n*-BuLi in THF. The product is the 2-phenylethyllithium species **96** (equation 5.70).³⁷⁴



Carbanions can take part in elimination reactions, as will be discussed in Chapter 10. The elimination of carbanions derived from THF is shown

³⁷⁰ Borosky, G. L. *J. Org. Chem.* **1998**, 63, 3337 and references therein.

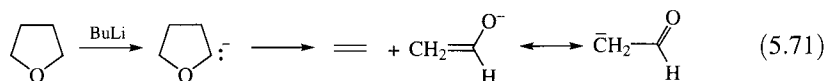
³⁷¹ Chou, P. K.; Dahlke, G.D.; Kass, S. R. *J. Am. Chem. Soc.* **1993**, 115, 315.

³⁷² Welch, S. C.; Valdes, T. A. *J. Org. Chem.* **1977**, 42, 2108.

³⁷³ Punzalan, E. R.; Bailey, W. F. *Abstracts of the 207th National Meeting of the American Chemical Society*; San Diego, CA, March 13–17, 1994; Abstract ORGN 384.

³⁷⁴ Staley, S. W.; Cramer, G. M.; Kingsley, W. G. *J. Am. Chem. Soc.* **1973**, 95, 5052.

in equation 5.71.³⁷⁵



Carbanions are also susceptible to oxidation.³⁷⁶ For example, ketone enolates can undergo oxidative coupling in the presence of CuCl_2 .³⁷⁷



Oxidation of carbanions by molecular oxygen is another important reaction. Equation 5.73 shows the oxidation of the anion of triphenylmethane by molecular oxygen in a solution composed of 80% DMF and 20% *t*-butyl alcohol. Addition of water to the reaction mixture allowed isolation of triphenylmethyl hydroperoxide in high yields (e.g., 87%).³⁷⁸



5.6 CHOOSING MODELS OF REACTIVE INTERMEDIATES

In this chapter we have developed models of reactive intermediates that are more complex than the models that organic chemists usually use. Just as our representation of cyclohexane in a chair conformation ignores rapid conformational changes, a picture of an isopropyl or a *sec*-butyl carbocation as a static carbenium ion is not consistent with the rapid internal bonding changes that can occur, even at low temperature. Moreover, there is experimental evidence that the 2-norbornyl cation is a nonclassical, hypercoordinate carbocation and that other ions exhibit varying degrees of bridging or nonclassical behavior. The simple picture of a carbanion ignores the critical role of metal ions and solvent molecules, and the model of a monomeric species ignores what may be very important effects of oligomerization.

In later chapters we will consider in more detail the energies and structures of reactants, transition states, intermediates, and products. It will be important to remember that the environment and lifetime of a reactive intermediate in a spectroscopic study, such as a carbocation in a frozen matrix or superacid solution at low temperature, are quite different from those of the

³⁷⁵ Bates, R. B.; Kroposki, L. M.; Potter, D. E. *J. Org. Chem.* **1972**, *37*, 560.

³⁷⁶ The electrochemistry of carbanions was discussed by Fox, M. A. in Buncl, E.; Durst, T., Eds. *Comprehensive Carbanion Chemistry. Part C. Ground and Excited State Reactivity*; Elsevier: Amsterdam, 1987; pp. 93–174.

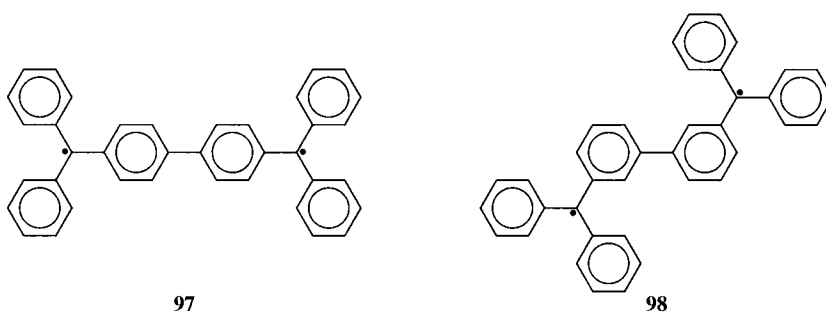
³⁷⁷ Ito, Y.; Konoike, T.; Harada, T.; Saegusa, T. *J. Am. Chem. Soc.* **1977**, *99*, 1487.

³⁷⁸ Russell, G. A.; Bemis, A. G. *J. Am. Chem. Soc.* **1966**, *88*, 5491.

species presumed to be involved in chemical reactions under much milder conditions or at room temperature. In all cases, it will be important to recognize that the structures and energy diagrams that we draw are at best simplified models of complex species in which certain components of a larger picture are emphasized and others are ignored.

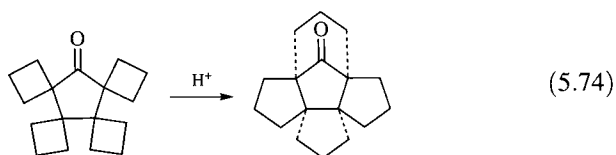
Problems

- 5.1. Diradicals **97** and **98** show rather different properties. Structure **97** shows predominantly singlet character at low temperature, although triplet character becomes evident at higher temperature. On the other hand, **98** displays predominantly triplet character under all conditions. Rationalize these results.

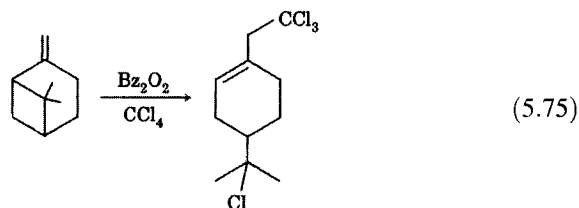


- 5.2. The EPR spectrum of the benzyl radical in solution shows a values for the α , ortho, meta, and para protons of 16.4 G, 5.17 G, 1.77 G, and 6.19 G, respectively. Interpret these results in terms of the relative unpaired electron density at each of these four positions. How do the results compare with the predictions of HMO theory or simple resonance theory from Chapter 4?
- 5.3. In the ^{13}C NMR spectrum of the isopropyl cation, the coupling constant between C2 and the hydrogen bonded to it is 169 Hz. Based on the relationship between ^{13}C NMR coupling constants and hybridization (see Chapter 1), what is the apparent hybridization of C2 in this ion?
- 5.4. When formic acid is dissolved in superacid media, the ^1H NMR spectrum indicates the presence of two isomeric species in a ratio of 2:1. Suggest a structure for these two species.
- 5.5. Although the ESCA spectrum of the *t*-butyl carbocation shows C 1s levels for both the carbenium carbon atom and the three methyl carbon atoms, the ESCA spectrum of the trityl cation (Ph_3C^+) suggests that all of the carbon 1s electrons have the same binding energy. Explain this result.
- 5.6. Rationalize the observation that the ^1H NMR spectrum of the 2,6-dimethyl-2-heptyl cation at -100°C shows only one peak for the four methyl groups at the ends of the chain.
- 5.7. When the *t*-butyl carbocation labeled with ^{13}C at the 3° position was heated in the superacid $\text{HSO}_3\text{F}:\text{SbF}_5:\text{SO}_2\text{ClF}$ at 70°C for 20 hours, complete scrambling of the label was observed. The activation energy for the process appeared to be 30 kcal/mol or more. Based on rearrangement processes of carbocations, suggest a mechanism by which the scrambling could occur. Is the E_a consistent with this mechanism?

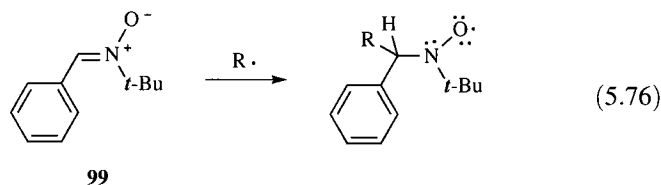
- 5.8. The 1-lithio derivative of (–)-(R)-2-cyano-1,1-diphenylcyclopropane was alkylated with methyl iodide to yield *racemic*-1-cyano-1-methyl-2,2-diphenylcyclopropane.³⁷⁹ However, the 1-lithio derivative of the isomeric (+)-(S)-2,2-diphenylcyclopropyl isocyanide reacted with methyl iodide to yield (+)-(S)-1-methyl-2,2-diphenylcyclopropyl isocyanide. Explain the racemization in the former compound and the retention of configuration in the latter.
- 5.9. In a study of 2,2-diphenylpropyllithium, a product isolated after addition of CO₂ and water was *o*-(1-phenyl-1-methylethyl)benzoic acid. Propose a mechanism to account for its formation.
- 5.10. The BDE for a C1–H bond in (*E*)-2-butene is 371 kJ/mol, while that for a C3–H bond in 1-butene is 360 kJ/mol. What is ΔH° for isomerization of (*E*)-2-butene to 1-butene?
- 5.11. Propose a mechanism for the acid-catalyzed rearrangement in equation 5.74. Be sure to account for the observed stereochemistry of the product.



- 5.12. Propose a mechanism for the reaction in equation 5.75. (Bz₂O₂ is dibenzoyl peroxide.)



- 5.13. In contrast to the reactivity of most simple carbenes, dimethoxycarbene does not readily undergo addition to alkenes unless the alkene is substituted with electron-withdrawing substituents. Propose an explanation for this behavior.
- 5.14. Propose a detailed mechanism for the reaction of a radical with α -phenyl-*N*-*t*-butylnitrone (**99**), and explain how such a reaction could be useful in studying the structures and properties of free radicals.



- 5.15. When cyclobutanone is subjected to the conditions for the Bamford–Stevens reaction, the major products are cyclobutene and methylenecyclopropane. Propose a mechanism to account for their formation.

³⁷⁹ Walborsky, H. M.; Hornyak, F. M. *J. Am. Chem. Soc.* **1955**, *77*, 6026.

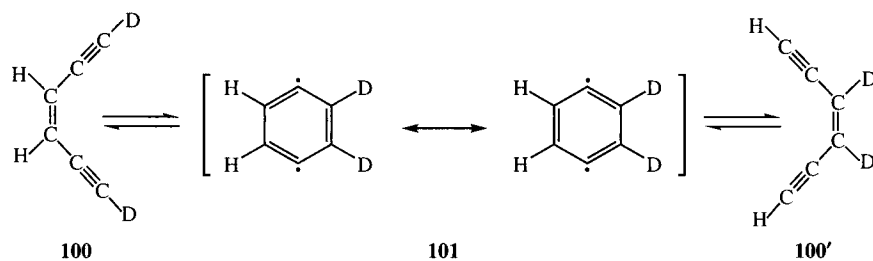
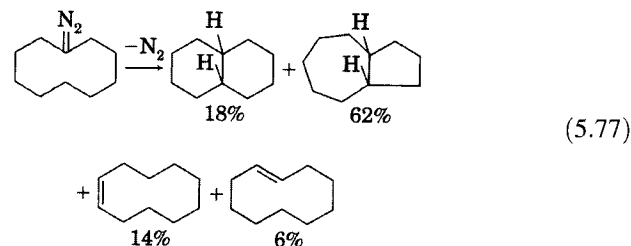


FIGURE 5.61
Proposed mechanism for rearrangement of **100**.

- 5.16. Propose a mechanism to account for the formation of products formed by decomposition of diazocyclodecane in the following reaction:



- 5.17. Deuterium-labeled *cis*-1,5-hexadiyn-3-ene (**100**, Figure 5.61) was found to undergo thermal rearrangement to **100'**, suggesting that the reaction involves cyclization to an intermediate or transition state having C_2 or higher symmetry. Based on this result and other data, the investigators proposed that 1,4-dehydrobenzene (benzene-1,4-diyl), **101**, is an intermediate in the reaction.

- Propose other possible C_6H_4 structures that have C_2 or higher symmetry and that might also be considered as possible intermediates in this reaction. In particular, consider candidate structures having (i) both carbocation and carbanion centers, (ii) two carbene centers, (iii) a highly strained bicyclic triene structure, and (iv) two allenic units.
- When the reaction was carried out in hydrocarbon solvent, benzene was formed as a by-product of the reaction. When the reaction was carried out in methanol, benzene and some benzyl alcohol were observed, but anisole was not detected. Reaction in toluene produced diphenylmethane, and reaction in CCl_4 produced 1,4-dichlorobenzene. (In each case, deuterium-labeled product was observed from the deuterium-labeled reactant.) How do these results reinforce the conclusion that the reactive intermediate is **101** and not one of the alternative structures?

- 5.18. What are the Baldwin designations for the radical closures shown below?

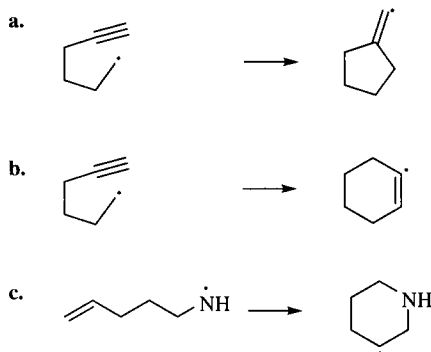
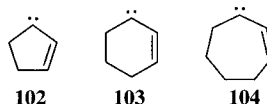


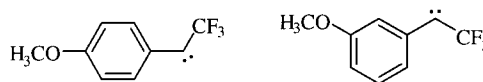
TABLE 5.5 Hyperfine Coupling Constants for Cycloalkyl Radicals

Radical	a_α (G)
Cyclopropyl	6.5
Cyclobutyl	21.2
Cyclopentyl	21.5
Cyclohexyl	21.3
Cycloheptyl	21.8

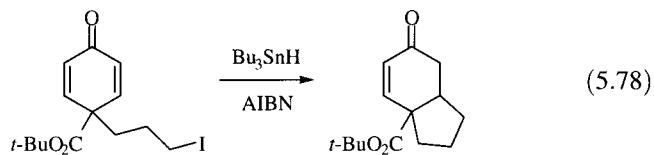
- 5.19. Isotropic α -proton hyperfine coupling constants (a_α) for cycloalkyl radicals are shown in Table 5.5. Why is the a_α value for cyclopropyl different from the a_α values of the other four radicals?
- 5.20. Predict the effects of ring size on the energy difference between singlet and triplet states of carbenes **102**, **103**, and **104**.



- 5.21. One of the carbenes below has a singlet ground state, and the other has a triplet ground state. Which is which?



- 5.22. Propose a mechanism for the reaction shown in equation 5.78.

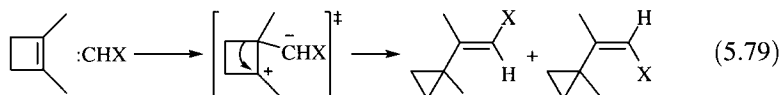


- 5.23. One of the arguments for the stabilization of radicals by hyperconjugation is that the C–H homolytic bond dissociation energies for alkanes vary as shown in Table 5.6. However, the C–F homolytic dissociation energies do not follow the same trend. Are these results consistent with the hyperconjugation model for radical stability?

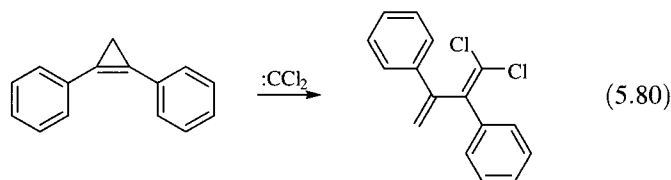
TABLE 5.6 Homolytic Dissociation Energies of Alkyl Halides and Fluorides (kcal/mol)

Alkyl	R–H	R–F
Methyl	102.4	108.2
Ethyl	99.0	111.3
Isopropyl	96.7	114.0
<i>t</i> -Butyl	95.3	116.1

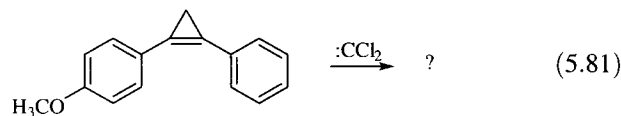
- 5.24. Show the structures of eleven reactants that could produce the methylcyclopentyl carbocation when added to a superacidic, nonnucleophilic medium.
- 5.25. When a solution of tris(1-adamantyl)methyl cation is held at -70°C , it decomposes to 1-adamantyl carbocation. What other reactive intermediate might be formed as a by-product of this process?
- 5.26. Why does the 2-adamantyl carbocation not rearrange to the ca. 18 kcal/mol more stable 1-adamantyl carbocation?
- 5.27. Explain the ^{13}C chemical shifts for the 1-adamantyl cation shown in Figure 5.62. Specifically, why should C_{γ} be deshielded more than C_{β} ?
- 5.28. A closer examination of the data in Table 5.4 indicates that not only does carbocation stability vary according to the familiar pattern $3^{\circ} > 2^{\circ} > 1^{\circ}$, but the stability for each type of carbocation varies according to the number of atoms in the ion. What is the mathematical relationship between the molecular mass of an ion and its thermodynamic stability in the gas phase, and how can you rationalize this pattern?
- 5.29. Theoretical calculations indicate that the barriers for 1,2-hydride shifts in carbocations are ordered as follows: cyclopropyl > cyclobutyl > cyclopentyl > *sec*-butyl. Propose an explanation for this trend.
- 5.30. Consider the mechanism shown in equation 5.79 for the reaction of 1,2-disubstituted cyclobutenes with halocarbenes: CHX ($\text{X} = \text{Cl}$ or I) to produce vinyl cyclopropanes.



- a. Propose an analogous mechanism for the reaction of dihalocarbenes with 1,2-diaryl cyclopropanes to produce butadienes (equation 5.80).



- b. Predict the major product expected when one aryl group in the reactant is phenyl and the other aryl group is *p*-methoxyphenyl.



- 5.31. Propose a mechanism for the base-promoted racemization of camphenilone (105).

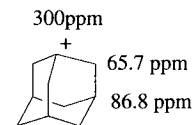
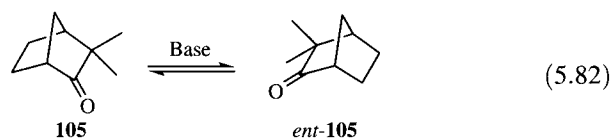
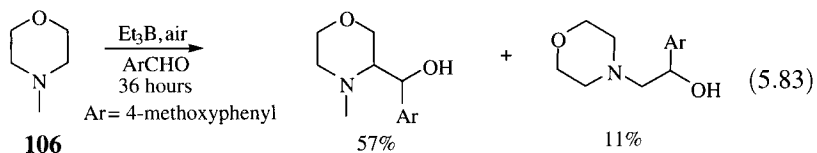


FIGURE 5.62
 ^{13}C chemical shifts reported for the 1-adamantyl cation.

- 5.32. Propose a mechanism to account for the formation of the two products in the reaction of 4-methylmorpholine (**106**) shown in equation 5.83. Explain the product distribution and also why substitution α to the oxygen atom is not also observed.



- 5.33. Summarize the results reported since the publication of this text of investigations of the methonium ion.
- 5.34. Summarize developments since the publication of this text in the debate about the role of hyperconjugation in stabilizing radicals.
- 5.35. McBride has written about the hexaphenylethane story that "this glaring, if relatively harmless, error dramatizes the importance of reviewing the basis in fact on which the classic generalizations of chemistry, however reasonable, are founded."²³ Do you agree with this view? Could there be other errors that are not so harmless but that persist only because no one has repeated crucial early experiments with more modern techniques?

Methods of Studying Organic Reactions

6.1 MOLECULAR CHANGE AND REACTION MECHANISMS

A reaction mechanism is a step-by-step description of a chemical transformation at the molecular level that gives information about the location of all nuclei and electrons, including those of solvent and other species present, as well as the total energy of the system. Gould called a mechanism a motion picture of the chemical transformation—one that we can stop and analyze frame by frame.¹ Such a motion picture should be viewed as a simulation, however. We cannot see the molecular events; we can only depict what we infer them to be.

The methods that we use to study mechanisms are never conclusive but are only indicative. That is, a mechanism can be disproved, but it can never be proved.² A mechanism may become *established*, which means that it is the only proposed mechanism that is able to predict the results of experiments designed to test possible mechanisms. Scientists are always open to the possibility that new data will conflict with current thinking, so they treat mechanisms as more or less thoroughly tested models and not as timeless realities.

6.2 METHODS TO DETERMINE REACTION MECHANISMS

Identification of Reaction Products

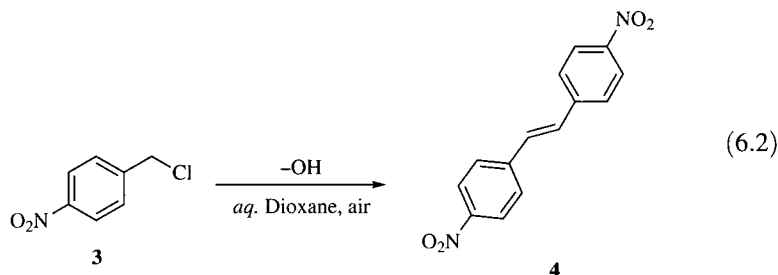
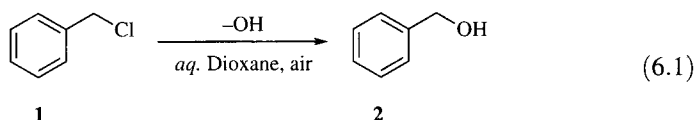
The most fundamental step in any investigation of a chemical reaction is the determination of the products of the reaction.³ This might appear to be

¹ Gould, E. S. *Mechanism and Structure in Organic Chemistry*; Holt, Rinehart and Winston: New York, 1959.

² The idea that scientific evidence can never prove a hypothesis but can only refute it is closely associated with the work of Karl Popper. See, for example, Popper, K. R. *Objective Knowledge*; Clarendon Press: Oxford, 1972.

³ This statement assumes that the reactants are well characterized. Obviously, a mechanistic study is also futile if the identity and purity of the reactants are not known.

a trivial statement, but it is not. Consider the study of the reaction of benzyl chloride (1) with hydroxide to give benzyl alcohol (2). One way to study the mechanism of the reaction is to determine what effect substituents on the benzene ring have on the rate constant for the reaction. Therefore, one might first determine the kinetics of the reaction of benzyl chloride with hydroxide ion and then determine the kinetics of the reactions of hydroxide with a series of substituted benzyl chlorides, including *p*-nitrobenzyl chloride (3). The product of the reaction of 3 is 4,4'-dinitrostilbene (4), however, not *p*-nitrobenzyl alcohol.⁴ Obviously, kinetic studies or other mechanistic investigation of all of the reactions cannot be interpreted in terms of one uniform mechanistic pattern if different reactants give different products.¹



Determination of Intermediates

The reactants and products fix only the end points of a reaction mechanism. To be complete, it is then necessary to fill in details of all that is between them. One important concept in mechanistic studies is the determination of the number of steps in the reaction. A reaction that involves only one step (reactants to transition structure to products) is called an **elementary reaction**. If there is more than one elementary step, then at least one intermediate must be involved in the reaction. As noted in Chapter 5, we may consider two hypothetical reaction coordinate diagrams (Figure 6.1) for a reaction in which

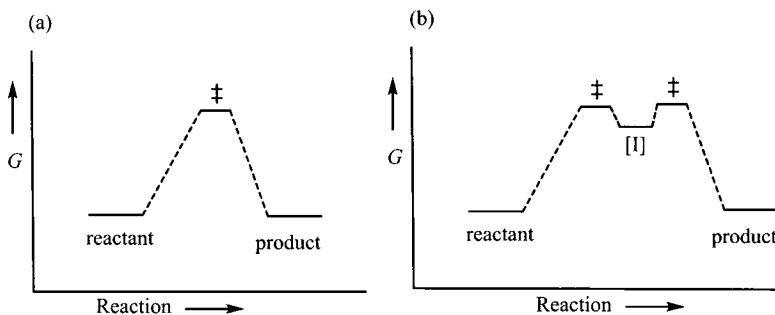


FIGURE 6.1

(a) Elementary reaction and
(b) reaction with an inter-
mediate (I).

⁴ For leading references, see Tewfik, R.; Fouad, F. M.; Farrell, P. G. *J. Chem. Soc. Perkin Trans. 2* 1974, 31.

at least one bond is broken and at least one bond is formed. Figure 6.1(a) represents a one-step reaction that is a **concerted process**, in which bonds are formed and broken simultaneously, while the presence of an intermediate as in Figure 6.1(b) requires the mechanism to be **stepwise**.⁵ In order for a reaction to have an intermediate, there must be a minimum on the Gibbs diagram that is at least as deep as the free energy available to the system at the reaction temperature.^{6,7} The deeper the dip in the free energy surface, the more stable is the intermediate and the more likely we will be able to detect it or perhaps even to isolate it.

The existence of intermediates can be demonstrated by several techniques. If a substance isolated from a reaction mixture is subjected to the reaction conditions and is found to proceed to the same products as the reactants, there is strong evidence that the isolated compound is indeed an intermediate (and not just a by-product) in the reaction. For example, Winstein and Lucas studied the conversion of 2,3-diacetoxybutane (**5**) to 2,3-dibromobutane (**6**) by fuming aqueous HBr (equation 6.3) and proposed 3-acetoxy-2-butanol (**7**), 2-acetoxy-3-bromobutane (**8**), and 3-bromo-2-butanol (**9**) as intermediates in the reaction (Figure 6.2). Each of these compounds could be isolated from the reaction mixture before the reaction had gone to completion, and subjecting each proposed intermediate to the reaction conditions produced 2,3-dibromobutane. The possibility that 2,3-butanediol (**10**) might also be an intermediate, even though it was not isolated from reaction mixtures, was eliminated by showing that it did not produce 2,3-dibromobutane under the reaction conditions.⁸

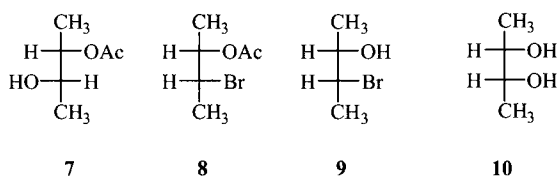
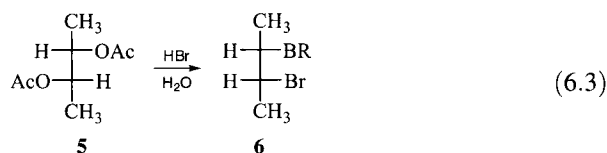


FIGURE 6.2

Likely intermediates (**7**, **8**, and **9**) and an unlikely intermediate (**10**) in the reaction shown in equation 6.3.

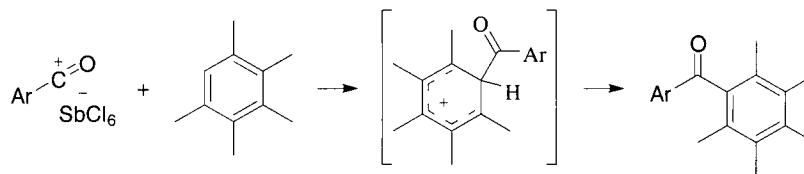
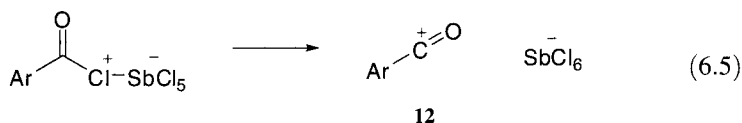
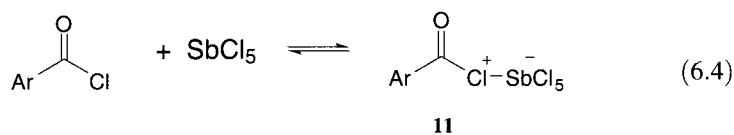
⁵ If several bonds are broken and several bonds are formed, bond breaking and bond formation might be synchronous for some processes but not for others. Lowe, J. P. *J. Chem. Educ.* **1974**, *51*, 785. See also the discussion by Bernasconi, C. F. *Acc. Chem. Res.* **1992**, *25*, 9.

⁶ As noted in Chapter 5, the intermediate must be able to survive for at least one molecular vibration before the reaction proceeds (i.e., the energy well must be at least as deep as the 0th vibrational level), otherwise it is simply a transition structure and not an actual intermediate.

⁷ We usually assume that the intermediate is a minimum on an *enthalpy* surface, but that need not be the case. Tetramethylene has been reported to be an intermediate without an enthalpy minimum because it occurs in an "entropy dominated free energy minimum." Doubleday, C., Jr.; Camp, R. N.; King, H. F.; McIver, J. W.; Mullally, D.; Page, M. *J. Am. Chem. Soc.* **1984**, *106*, 447; Doubleday, C., Jr. *J. Am. Chem. Soc.* **1993**, *115*, 11968.

⁸ Winstein, S.; Lucas, H. J. *J. Am. Chem. Soc.* **1939**, *61*, 1581. The stereochemistry of these interconversions will be considered in Chapter 8.

More recently, Kochi and co-workers isolated reactive intermediates in the Friedel–Crafts acylation of aromatics by acid chlorides.⁹ It had long been thought that the mechanism of the reaction involves complexation of an acid chloride by a Lewis acid catalyst, conversion of the Lewis acid–base complex to an acylium ion, reaction of the acylium with the aromatic to produce a Wheland intermediate, and loss of a proton to rearomatize the ring. By carrying out the reactions at low temperature in CH_2Cl_2 solution, the investigators were able to crystallize and obtain an X-ray structure of the Lewis acid–base complex (**11**, equation 6.4) and the acylium ion (**12**, equation 6.5). They were unable to crystallize the Wheland intermediate, **13**, but they did obtain evidence for such a species in solution by using UV–vis spectroscopy (equation 6.6). While these results strongly support the traditional mechanism for the electrophilic aromatic substitution reaction, the authors were careful to note that the species which can be crystallized from solution are not necessarily the principal intermediates in the reaction.



Wheland intermediate detected by UV–vis spectroscopy but not crystallized

(6.6)

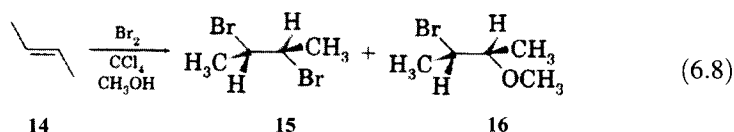
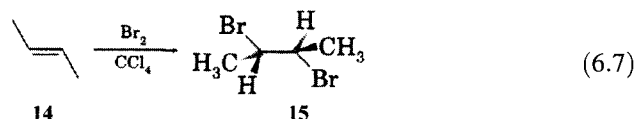
Finding that a substance proposed as an intermediate does produce the expected products when it is subjected to the conditions of a reaction under investigation suggests, but does not confirm, that the substance actually is an intermediate. It may be possible that the product can be formed by two different pathways, one proceeding through the intermediate in question and the other one a totally different pathway that does not involve that intermediate. In such a case, the role of a substance as an intermediate can be supported further if it can be shown that the proposed intermediate produces product at the rate expected under the reaction conditions.¹⁰

⁹ Davlieva, M. G.; Lindeman, S. V.; Neretin, I. S.; Kochi, J. K. *J. Org. Chem.* **2005**, *70*, 4013.

¹⁰ Conversely, a substance can be eliminated as an intermediate if it can be shown that the concentration of the substance in the reaction mixture must be less than would be required to produce the product at the observed rate. One way to do this utilizes the technique of isotopic dilution. For a discussion, see Swain, C. G.; Powell, A. L.; Sheppard, W. A.; Morgan, C. R. *J. Am. Chem. Soc.* **1979**, *101*, 3576. A general discussion of the use of isotopes to study organic reaction mechanisms was given by Collins, C. J. *Adv. Phys. Org. Chem.* **1964**, *2*, 1.

If an intermediate is not sufficiently stable to be isolated, it might nevertheless be formed in sufficient concentration to be detected spectroscopically. Techniques used for this purpose include UV–vis spectroscopy in stopped-flow kinetics experiments for relatively stable intermediates or IR spectroscopy in matrix isolation spectroscopy for more reactive species.^{11,12} For photochemical reactions, we can detect transient spectra of intermediates in the millisecond to microsecond (“conventional” flash spectroscopy) or nanosecond to picosecond or femtosecond (laser flash spectroscopy) time scale.^{13–15} In all cases we must be certain that the spectra observed are indeed indicative of the presence of the proposed intermediate and only the proposed intermediate. Theoretical calculations have been useful in determining the spectroscopic properties of a proposed intermediate, whether it is likely to be sufficiently stable for detection, and the type of experiment most likely to detect it.¹⁶ In addition, kinetic studies may suggest optimum conditions for spectroscopic detection of an intermediate.¹⁷

An intermediate that cannot be observed spectroscopically might be trapped by added reagents. In Chapter 5 we discussed the use of spin trap reagents to capture transient radicals for analysis by EPR spectrometry. Another example can be seen in the studies that led to the bromonium ion mechanism for the addition of bromine to *trans*-2-butene (**14**) to produce *meso*-2,3-dibromobutane (**15**, equation 6.7). Adding a nucleophile such as methanol to the reaction mixture led to a product incorporating the nucleophile (**16**) as shown in equation 6.8, which suggested that a cation may be an intermediate in the reaction.¹⁸ Additional evidence is necessary to determine the structure of the intermediate (*i.e.*, bromonium ion or bromine-substituted carbocation), but that is a matter of detail once the existence of an intermediate of some kind is established.



¹¹ Compare Gebicki, J.; Krantz, A. *J. Chem. Soc. Perkin Trans. 2* **1984**, 1623; Kesselmayer, M. A.; Sheridan, R. S. *J. Am. Chem. Soc.* **1986**, *108*, 99.

¹² For a review of techniques to measure extremely fast reactions, see Zuman, P.; Patel, R. C. *Techniques in Organic Reaction Kinetics*; John Wiley & Sons: New York, 1984; pp. 247–327; Krüger, H. *Chem. Soc. Rev.* **1982**, *11*, 227. Bell summarized the use of a variety of experimental methods for studying fast reactions with time scales ranging from 10^{-3} to 10^{-10} s: Bell, R. P. *The Proton in Chemistry*, 2nd ed.; Cornell University Press: Ithaca, NY, 1973; p. 111 ff.

¹³ Simon, J. D.; Peters, K. S. *Acc. Chem. Res.* **1984**, *17*, 277.

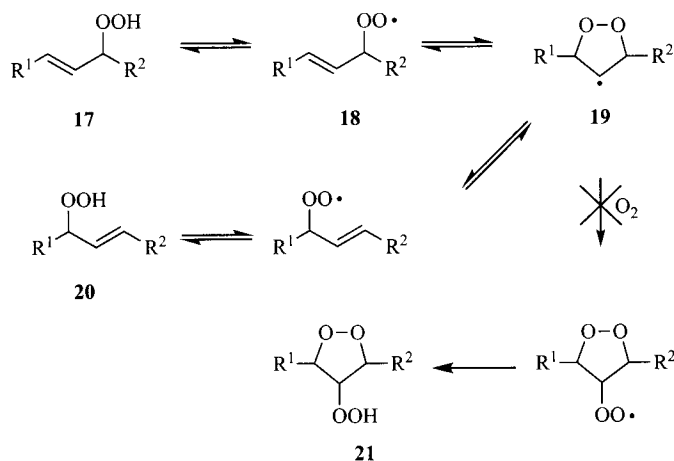
¹⁴ Noller, B.; Maksimenka, R.; Fischer, I.; Armone, M.; Engels, B.; Alcaraz, C.; Poisson, L.; Mestdagh, J.-M. *J. Phys. Chem. A* **2007**, *111*, 1771.

¹⁵ A nanosecond (ns) is 10^{-9} s. A picosecond (ps) is 10^{-12} s. A femtosecond (fs) is 10^{-15} s.

¹⁶ For an example, see Hu, C.-H.; Schaefer, H. F. III. *J. Phys. Chem.* **1993**, *97*, 10681.

¹⁷ Bernasconi, C. F.; Fassberg, J.; Killion, R. B., Jr.; Rappoport, Z. *J. Am. Chem. Soc.* **1990**, *112*, 3169.

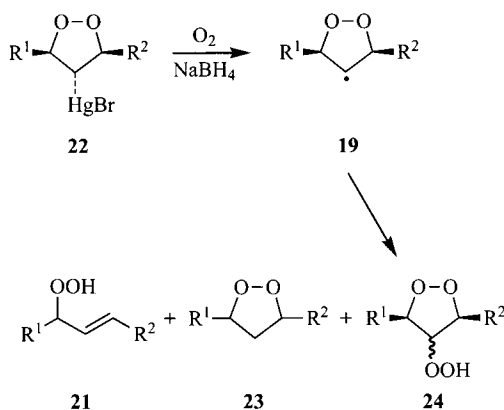
¹⁸ For an analysis of products formed by trapping the intermediate with nucleophiles, see Nagorski, R. W.; Brown, R. S. *J. Am. Chem. Soc.* **1992**, *114*, 7773.

**FIGURE 6.3**

Failure to observe **19** in the rearrangement of an allylic hydroperoxide. (R^1 is $-(\text{CH}_2)_4\text{CH}_3$; R^2 is $-\text{CH}=\text{CH}(\text{CH}_2)_7\text{CO}_2\text{CH}_3$. Reproduced from reference 20.)

Trapping reactions can also be used to demonstrate that a compound is *not* likely to be an intermediate in a reaction. This approach requires showing that a proposed intermediate cannot be trapped in a reaction but that it would be trapped if it actually were present. Porter and Zuraw used this approach in studying the rearrangement of allylic hydroperoxides such as **17** (Figure 6.3). The mechanism that had been proposed involved intramolecular reaction of a peroxy radical (**18**) with the double bond to produce intermediate **19** en route to the product, **20**. In earlier studies of the allylic hydroperoxide rearrangement, the proposed intermediate **19** had not been trapped with oxygen as compound **21**, even when the reaction was conducted under 500 lb/in.² of oxygen.¹⁹ Porter and Zuraw synthesized **19** by an unambiguous pathway beginning with **22** (Figure 6.4) and established that it could be trapped with oxygen at atmospheric pressure to yield **21**, **23**, and **24**. These results indicated that **19** could not be a "competent intermediate" in the allylic hydroperoxide reaction and that another mechanism must be followed.^{20a}

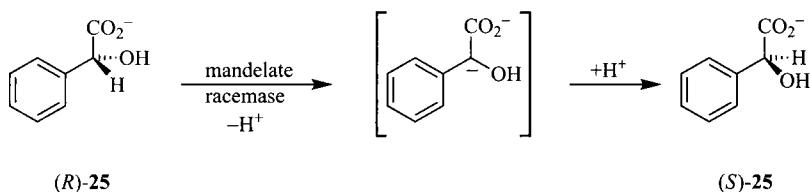
Sometimes the nature of an intermediate can be inferred from experiments in which changing reaction conditions provides a new reaction pathway for the intermediate. For example, a carbanion had been proposed as

**FIGURE 6.4**

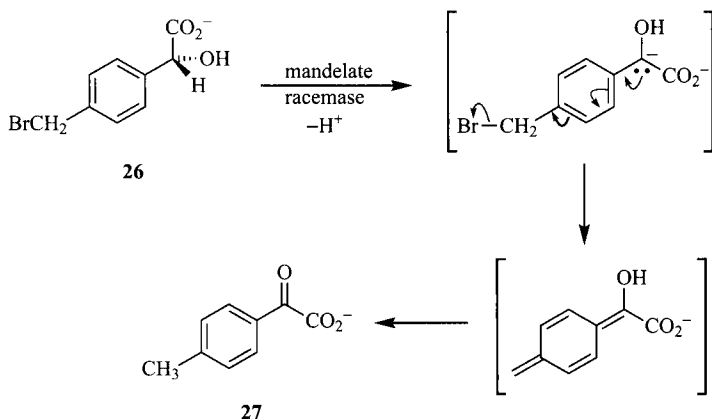
Demonstration that **19** can be trapped by oxygen. (Reproduced from reference 20.)

¹⁹ Brill, W. F. *J. Chem. Soc. Perkin Trans. 2* **1984**, 621.

²⁰ (a) Porter, N.; Zuraw, P. *J. Chem. Soc. Chem. Commun.* **1985**, 1472; (b) Lin, D. T.; Powers, V. M.; Reynolds, L. J.; Whitman, C. P.; Kozarich, J. W.; Kenyon, G. L. *J. Am. Chem. Soc.* **1988**, *110*, 323.

**FIGURE 6.5**

Racemization of mandelate via a carbanion intermediate.

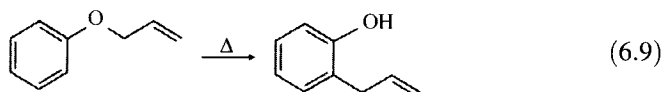
**FIGURE 6.6**

Elimination of bromide from a carbanion intermediate.

an intermediate in the interconversion of the enantiomers of the mandelate ion (**25**) by the enzyme mandelate racemase, as shown in Figure 6.5. The most likely reaction for the carbanion intermediate derived from mandelate ion itself is reprotonation. Lin and co-workers found that treatment of *p*-(bromomethyl)mandelate (**26**) with mandelate racemase led to *p*-methylbenzoylformate (**27**), as shown in Figure 6.6. That result suggested that a carbanion eliminated bromide ion to form **27**, supporting the intermediacy of a carbanion intermediate in the racemization of **25** also.^{20b}

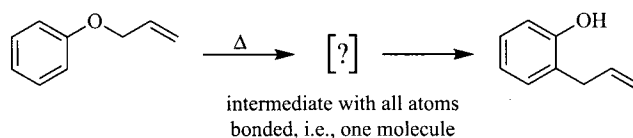
Crossover Experiments

A method of studying reaction mechanisms that is particularly relevant for many molecular rearrangements is the technique of **crossover experiments**. Consider the Claisen reaction (equation 6.9) in which an allyl group appears to migrate from one place in a molecule to another. We may propose two different *types* of mechanisms for the reaction. In the first, Figure 6.7(a), the rearrangement takes place so that there is bonding between the migrating group and the rest of the molecule at all times. In the second, Figure 6.7(b), the migrating group separates from the rest of the molecule to form two fragments, which then recombine. The notations # and * in that figure indicate that the fragments may both be radicals or that one may be an anion and the other a cation.

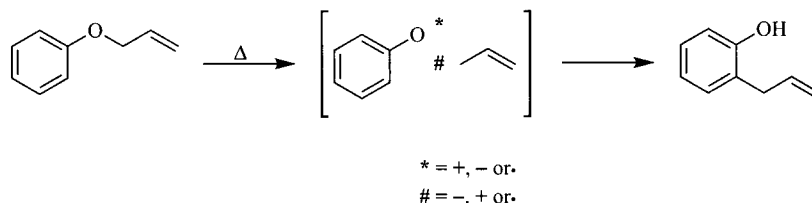


To apply the crossover technique to the Claisen rearrangement, we carry out the reaction with a mixture of two reactants, one of which bears a label on both of the possible fragments, while the other is not labeled on either fragment (Figure 6.8). For example, we first demonstrate that phenyl allyl

(a) A reaction pathway without dissociation



(b) A reaction pathway involving dissociation to ions or radicals

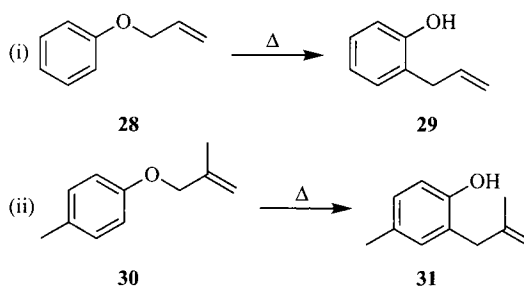
**FIGURE 6.7**

Nondissociative (a) and dissociative (b) processes for the Claisen rearrangement.

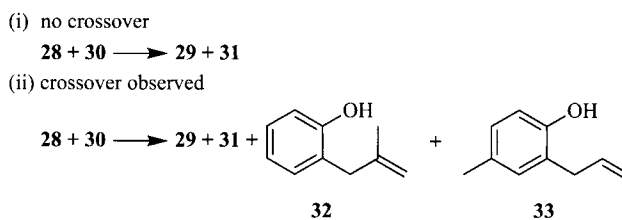
ether (**28**) yields only *o*-allylphenol (**29**) and that the labeled analog **30** produces only **31**. If we observe the new products **32** and **33**, then we conclude that there was recombination of fragments produced during the reaction.²¹ If, however, we find that a mixture of **28** and **30** produces only the products expected from each of the reactants alone (**29** and **31**), then the result of the crossover experiment is negative, suggesting that each reacting molecule does not separate into fragments during the reaction.

We must be careful in the interpretation of crossover experiments. If we find evidence of mixed products, we can conclude that the reaction mechanism involves fragmentation of the reactants and recombination of

(a) Reactions of labeled reactants carried out on individual samples of each



(b) Possible outcomes of crossover experiments

**FIGURE 6.8**

(a) Reactions of labeled reactants carried out on individual samples of each; (b) possible outcomes of crossover experiments.

²¹ Crossover studies of thermal Claisen rearrangement have not supported dissociative pathways for the reaction. For a discussion and references, see Tarbell, D. S. *Org. React.* **1944**, *2*, 1.

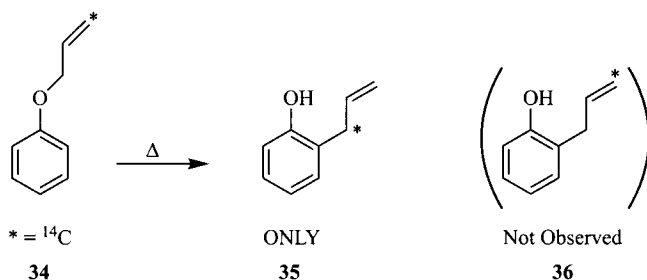


FIGURE 6.9
Isotopic label study of the Claisen rearrangement.

the fragments.²² If we do not see crossover products, however, we are more limited in our conclusions. It may be, for example, that dissociation occurs but recombination to give product is faster than diffusion of the fragments from the solvent cage. Thus, observation of the outcome predicted on the basis of a proposed mechanism can be taken as support for that mechanism, but failure to observe such an outcome does not necessarily rule out that mechanism.

Isotopic Labeling

Crossover experiments often use methyl or other alkyl groups as labels. There is always the possibility, however, that a label may alter the course of a reaction. Therefore, the minimum label that will allow us to distinguish the reaction pathway is best, and an isotopic replacement is the smallest perturbation to the molecular structure we can envision.²³ In the case of the Claisen reaction, labeling the allyl functionality of **34** with an isotope of carbon as shown in Figure 6.9 led to **35**, but **36** was not detected.²⁴ This result was further evidence that the mechanism does not involve molecular fragmentation, since a dissociative process would be expected to give both products.^{25,26}

In contrast to the thermal Claisen rearrangement, studies of isotopic labeling in the *photochemical* Claisen rearrangement support a dissociative mechanism. Figure 6.10 shows the results obtained from irradiation of 3-¹⁴C-allyl 2,6-dimethylphenyl ether (**37**) to produce 2,6-dimethylphenol (**38**) and 4-allyl-2,6-dimethylphenol (**39**). In **39**, the ¹⁴C label was distributed nearly equally between the α and γ positions, suggesting that it was formed by the recombination of 2,6-dimethylphenoxy and allyl intermediates and that rotation of the allyl fragment allows the label to become effectively scrambled between the two end carbon atoms of the allyl group by the time

²² We cannot conclude from this information alone that *all* product is formed by a dissociative pathway, only that the crossover products are formed through dissociation.

²³ Isotopic substitution can have structural consequences, however: Pasquini, M.; Schiccheri, N.; Piani, G.; Pietraperzia, G.; Becucci, M.; Biczysko, M.; Pavone, M.; Barone, V. *J. Phys. Chem. A* **2007**, *111*, 12363.

²⁴ Ryan, J. P.; O'Connor, P. R. *J. Am. Chem. Soc.* **1952**, *74*, 5866; Schmid, H.; Schmid, K. *Helv. Chim. Acta* **1952**, *35*, 1879; **1953**, *36*, 489.

²⁵ The mechanism of the thermal Claisen rearrangement is discussed in Chapter 11. Photo-dissociative reactions are discussed in Chapter 12.

²⁶ With isotopic labels, it is essential to verify that the label does not exchange with isotopes of the same atom in the solvent or other species present in the reaction mixture. For example, see Hengge, A. C. *J. Am. Chem. Soc.* **1992**, *114*, 2747.

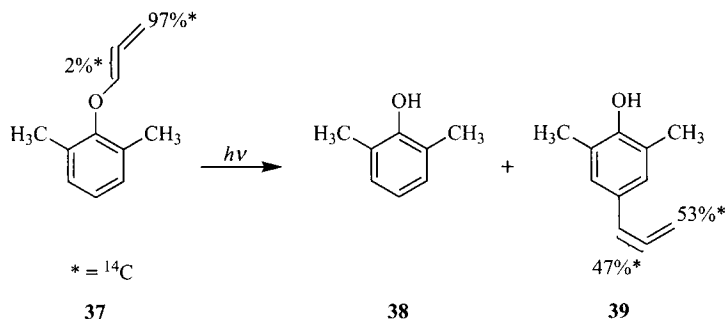
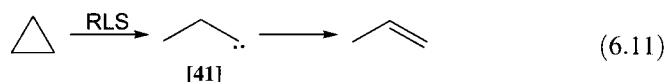
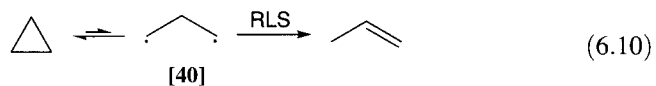


FIGURE 6.10
Scrambling of isotopic label in photochemical Claisen reaction.

of recombination. With other information, these results suggest that the photochemical reaction does involve the intermediacy of free radicals.²⁷

In the previous example, fragmentation to allyl and phenoxy groups appeared to be the most likely dissociative mechanism for the Claisen rearrangement. In other cases, there may be more than one feasible pathway for product formation. Often the nature of intermediates in these reactions can be inferred from the labeling experiments.²⁸ For example, two mechanisms were considered for the thermolysis of cyclopropane to propene. One was a reversible homolytic cleavage of a carbon–carbon bond to produce a trimethylene diradical (**40**), which could then undergo a [1,2]-hydrogen shift (equation 6.10) in the rate-limiting step (RLS). The second involved formation of singlet 1-propylidene (**41**) in the rate-limiting step for the reaction, followed by rearrangement to propene (equation 6.11).

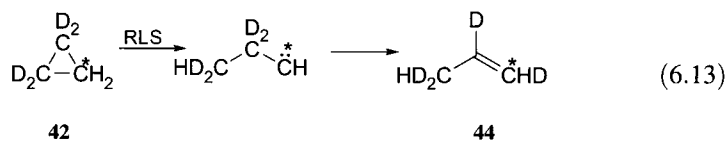
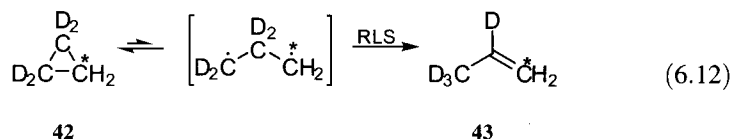


To distinguish between these two mechanisms, Baldwin and co-workers carried out the pyrolysis of 1- ^{13}C -2,2,3,3- d_4 -cyclopropane (**42**). As shown in equation 6.12, cleavage of a $^{13}\text{CH}_2\text{---CD}_2$ bond in **42** by the diradical pathway would lead to propene in which the ^{13}C label at C1 of the product bears two hydrogen (^1H) atoms (**43**). If the carbene mechanism (equation 6.13) operates, the ^{13}C label at C1 of the product (**44**) would be bonded to one H and one D. The ^{13}C NMR spectrum of the product mixture showed the presence of both **43** and **44**. The results were interpreted to mean that the pyrolysis of **42** occurred by both mechanisms, although relatively more of the product was formed by the diradical pathway.²⁹

²⁷ Schmid, K.; Schmid, H. *Helv. Chim. Acta* **1953**, *36*, 687.

²⁸ Baldwin, J. E. *J. Label. Compd. Radiopharm.* **2007**, *50*, 947.

²⁹ Baldwin, J. E.; Day, L. S.; Singer, S. R. *J. Am. Chem. Soc.* **2005**, *127*, 9370.



Stereochemical Studies

Stereochemical studies often yield useful information about mechanisms, as illustrated by the classical investigations of the S_N1 and S_N2 reactions. Consider the S_N2 reaction shown in Figure 6.11, in which a chiral substrate (45) reacts to give a chiral product (46) with inversion of configuration at the chiral center. The simplest mechanism that can explain both observations is the Walden inversion. In the S_N1 reaction (Figure 6.12), the substitution occurs so that an optically pure reactant (47) gives a racemic product (48). The chiral reactant must lose its asymmetry due to the formation of an achiral intermediate at some point along the reaction coordinate. A mechanism involving the formation of a planar carbocation fits comfortably with the experimental observations.³⁰

Solvent Effects

Determining the effect of solvent on the rate or course of a reaction can often provide insight into the reaction mechanism. One solvent property that may be important in extremely fast reactions is viscosity. If a reaction is encounter-controlled (also termed diffusion-controlled), the rate constant for the reaction is limited by the ability of the reacting species to reach each other. For example, in aqueous solution, the second-order rate constant for the encounter of two species is ca. $10^{10} \text{ L mol}^{-1} \text{ s}^{-1}$.³¹ In such cases, changing from a lower viscosity

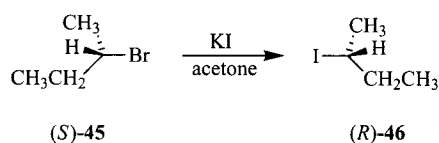
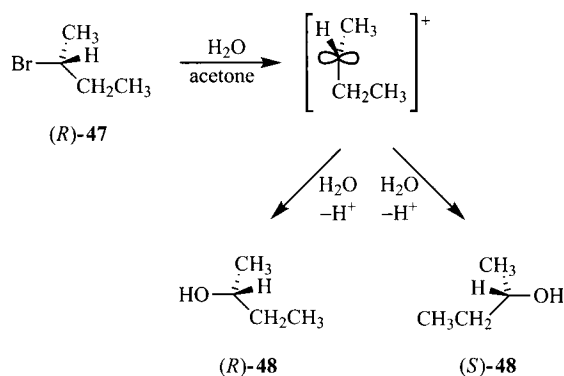


FIGURE 6.11
Stereochemical labels in mechanistic studies: S_N2 reaction.

³⁰ Another use of stereochemistry is a technique known as the endocyclic restriction test. In this procedure a cyclic molecule is constructed so that two substituents might react with each other in a mechanism analogous to a bimolecular reaction. However, because the transition structure for the reaction must be cyclic, only one of two possible mechanisms is sterically feasible. Determining whether the intramolecular reaction can occur for transition structures with various ring sizes provides some insight into the probable geometry of the reactants in the bimolecular reaction. For an example, see Li, J.; Beak, P. J. *Am. Chem. Soc.* **1992**, *114*, 9206. See also Beak, P. *Acc. Chem. Res.* **1992**, *25*, 215; *Pure Appl. Chem.* **1993**, *65*, 611.

³¹ IUPAC Compendium of Chemical Terminology, electronic version, <http://goldbook.iupac.org/>.

**FIGURE 6.12**

Stereochemical labels in mechanistic studies: S_N1 reaction.

solvent to a higher viscosity solvent with similar polarity (*e.g.*, from hexane to tetradecane) can decrease the rate of the reaction.

If we find that the rate constant of a reaction increases with increasing solvent polarity, as is the case with S_N1 reactions, then we may conclude that the transition structure is more polar than the reactants. Conversely, if we find that increasing solvent polarity decreases the rate constant of the reaction, we might deduce that there is less polarity in the transition structure than in the reactants. Solvent polarity is more difficult to quantify than we might expect because there is not a single way to measure it. Polarity is sometimes characterized by molecular dipole moment (μ), but that is a property of an individual molecule. Polarity is also characterized by the *dielectric constant* (ϵ), also known as the *relative static permittivity* of a substance, a property that can be measured by observing the effect of a substance on the electric field between two parallel, oppositely charged plates. Neither measure of polarity models the role of solvent molecules in a chemical reaction particularly well. A property of an individual molecule does not necessarily model the properties of a bulk solvent, and the orientation of solvent molecules around a charged or polar solute may be very different from the alignment of solvent molecules between charged metal plates.^{32,33} Furthermore, the properties of polar solvents can be altered by the addition of ionic species, and the resulting salt effects can increase the rates of organic reactions that occur faster in more polar solvents.³⁴

Many attempts have been made to develop empirical measures of solvent polarity that reflect the interaction of polar molecules with solutes and that correlate well with chemical reactivity, and Katritzky and co-workers discussed 184 such parameters.³⁵ For example, Kamlet, Taft, and co-workers proposed a general dipolarity/polarizability index, π^* , to measure the ability of a solvent to stabilize an ionic or polar species by means of its dielectric

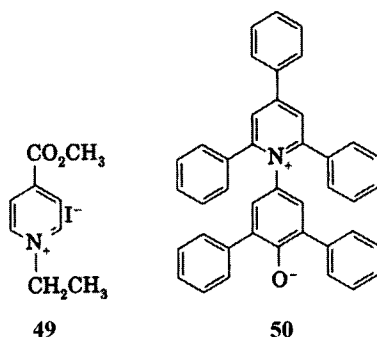
³² For definitions and compilations of solvent parameters, see Riddick, J. A.; Bunger, W. B.; Sakano, T. K. *Organic Solvents: Physical Properties and Methods of Purification*, 4th ed. (*Techniques of Chemistry*, Vol. II); Wiley-Interscience: New York, 1986.

³³ See also Kosower, E. M. *An Introduction to Physical Organic Chemistry*; John Wiley & Sons: New York, 1968; pp. 259–382.

³⁴ Addition of ions identical to those that are produced by the reaction (such as halide ions produced in elimination or substitution reactions) can decrease the rate of a reaction through a common ion effect, but some salts can increase reaction rates (see Chapter 8). For a general discussion, see Loupy, A.; Tchoubar, B. *Salt Effects in Organic and Organometallic Chemistry*; VCH: Weinheim, 1992.

³⁵ Katritzky, A. R.; Fara, D. C.; Yang, H.; Tamm, K.; Tamm, T.; Karelson, M. *Chem. Rev.* **2004**, *104*, 175.

effect.³⁶ Some scales are based on **solvatochromism**, which is a change in the shape, intensity, or position of the UV–vis absorption band of a diagnostic solute. Among the more widely cited scales are the Kosower Z scale, based on the charge transfer absorption spectra of 1-ethyl-4-carbomethoxy pyridinium iodide (**49**)^{33,37} and the $E_T(30)$ scale, based on the spectrum of a pyridinium *N*-phenol betaine (**50**).³⁸ Buncl and co-workers developed the π^*_{azo} scale based on the spectral properties of azo merocyanine dyes.³⁹



Solvent effects are not limited to polarity. Solvent molecules may act as electron pair donors or acceptors, as evidenced by the formation of charge transfer complexes or by the participation of solvent molecules as nucleophiles or electrophiles (Lewis bases or acids) in reactions. Solvent molecules may also behave as acids or bases in the Brønsted–Lowry sense,³⁸ and they may play important roles in reactions by serving as hydrogen bond donors or acceptors. Kamlet, Taft, and co-workers also developed the parameter α as a measure of the ability of solvent to act as a proton donor in a solvent–solute hydrogen bond and the parameter β to describe the ability of solvent to act as a proton acceptor in a solvent–solute hydrogen bond.^{36,40,41} A compilation of ϵ , μ , Z , $E_T(30)$, π^* , β , and α values for selected solvents is given in Table 6.1.⁴²

Computational Studies

Using theoretical methods such as those introduced in Chapter 4, chemists now routinely carry out virtual (*in silico*) experiments to evaluate possible reaction pathways. Often the calculation assumes that the reactants are in the gas phase, but increasingly computational methods are able to incorporate solvent molecules as well. As we noted in Chapter 4, each computational method has its particular set of inherent biases. Therefore, such studies

³⁶ Kamlet, M. J.; Abboud, J.-L. M.; Abraham, M. H.; Taft, R. W. *J. Org. Chem.* **1983**, *48*, 2877.

³⁷ Kosower, E. M. *J. Am. Chem. Soc.* **1958**, *80*, 3253.

³⁸ Reichardt, C. *Solvents and Solvent Effects in Organic Chemistry*, 2nd ed.; VCH: Weinheim, 1988.

³⁹ Buncl, E.; Rajagopal, S. *Acc. Chem. Res.* **1990**, *23*, 226 and references therein.

⁴⁰ For a review of these solvation parameters and their relationships with other parameters, see Marcus, Y. *Chem. Soc. Rev.* **1993**, *22*, 409.

⁴¹ Subsequently Abraham and co-workers extended this approach to develop a set of five analogous descriptors for solutes: *E* (excess molar refraction), *S* (dipolarity/polarizability), *A* (overall hydrogen bond acidity), *B* (overall hydrogen bond basicity), and *V* (a volume parameter related to dispersion interactions). For leading references, see Mintz, C.; Clark, M.; Acree, W. E., Jr.; Abraham, M. H. *J. Chem. Inf. Model.* **2007**, *47*, 115.

⁴² For a compilation of solvent parameters, see Abboud, J.-L. M.; Notario, R. *Pure Appl. Chem.* **1999**, *71*, 645.

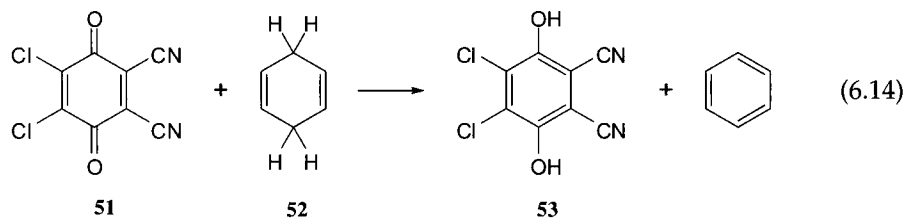
TABLE 6.1 Selected Solvent Parameters

Solvent	ϵ^a	$\mu(D)^a$	Z^b	$E_T(30)^c$	π^*	β	α^d
Formamide	111.0	3.37	83.3	56.6	0.97	0.48 ^e	0.71
Water	78.4	1.8	94.6	63.1	1.09	0.47 ^e	1.17
Formic acid	58.5	1.82		54.3	0.65 ^e	0.38 ^e	1.23 ^g
Dimethyl sulfoxide	46.5	4.06	71.1	45.1	1.00	0.76	0.00
<i>N,N</i> -Dimethylformamide	36.7	3.24	68.5	43.8	1.00 ^e	0.76 ^e	0.00
Nitromethane	35.9	3.56		46.3	0.85	0.06 ^e	0.22
Acetonitrile	35.9	3.53	71.3	45.6	0.75	0.40 ^e	0.19
Methanol	32.7	2.87	83.6	55.4	0.60	0.66 ^e	0.93
Hexamethylphosphoramide	29.3	4.31	62.8 ^f	40.9	0.87 ^e	1.05 ^e	0.00
Ethanol	24.5	1.66	79.6	51.9	0.54	0.75 ^e	0.83
1-Propanol	20.4	3.09	78.3	50.7	0.52	0.90 ^e	0.84 ^e
1-Butanol	17.5	1.75	77.7	50.2	0.47	0.84 ^e	0.84 ^e
Acetone	20.6	2.69	65.7	42.2	0.71	0.43 ^e	0.08
2-Propanol	19.9	1.66	76.3	48.4	0.48	0.84 ^e	0.76
Pyridine	12.9	2.37	64.0	40.5	0.87	0.64	0.00
<i>t</i> -Butyl alcohol	12.5	1.66	71.3	43.3	0.41	0.93 ^e	0.42 ^e
Methylene chloride	8.9	1.14	64.2	40.7	0.82	0.10 ^e	0.13 ^e
Tetrahydrofuran	7.58	1.75		37.4	0.58	0.55	0.00
1,2-Dimethoxyethane	7.20	1.71	62.1 ^f	38.2	0.53	0.41	0.00
Acetic acid	6.17	1.68	79.2	51.7	0.64	0.45 ^e	1.12
Ethyl acetate	6.02	1.82		38.1	0.55	0.45	0.00
Chloroform	4.80	1.15	63.2 ^g	39.1	0.58	0.10 ^e	0.20 ^e
Diethyl ether	4.2	1.15		34.5	0.27	0.47	0.00
Benzene	2.27	0	54.0 ^f	34.3	0.59	0.10	0.00
Carbon tetrachloride	2.23	0		32.4	0.28	0.10 ^e	0.00
<i>n</i> -Hexane	1.89	0.085		31.0	-0.04 ^e	0.00	0.00

^a Data from the compilation in reference 32.^b Data from reference 37.^c Data from the compilation in reference 38, pp. 365–371.^d Values for π^* , β , and α from reference 36.^e Data from the compilation in reference 40.^f Data from the compilation in reference 33, p. 301.^g(0.13 M EtOH).

should be considered as another useful tool to understanding reaction mechanisms but not as a window into reality.

A study of a transfer hydrogenation reaction provides a useful example of the mechanistic information available from a computational study and some of the caveats to be considered.⁴³ A transfer hydrogenation reaction involves the net transfer of two hydrogen atoms from one reactant to another, as illustrated for the reaction of 2,3-dichloro-5,6-dicyano-1,4-benzoquinone (DDQ, **51**) and 1,4-cyclohexadiene (**52**) to produce 2,3-dichloro-5,6-dicyano-1,4-benzenediol (**53**) and benzene (equation 6.14).

⁴³ Chan, B.; Radom, L. *J. Phys. Chem. A* 2007, 111, 6456.

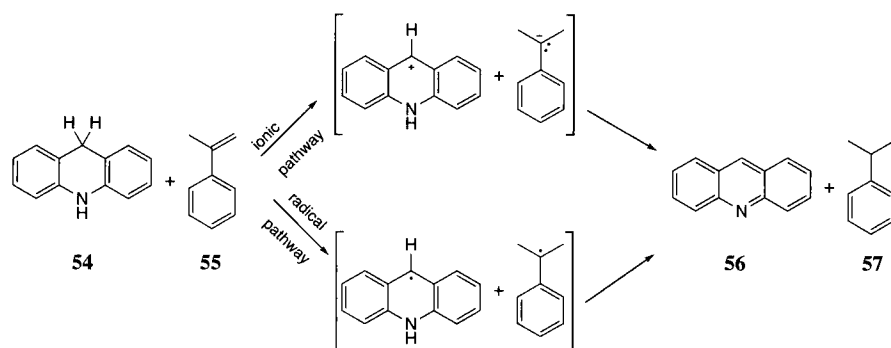


FIGURE 6.13
Ionic (top) and radical (bottom) pathways for the transfer hydrogenation of 55.

Figure 6.13 illustrates two pathways that had been proposed for the transfer hydrogenation reaction of acridan (**54**) and α -methylstyrene (**55**) to give acridine (**56**) and cumene (**57**). The top pathway proceeds by transfer of a hydride ion from **54** to **55** to give an ion pair intermediate, which subsequently transfers a proton to the anion to complete the reaction. The bottom pathway is a radical mechanism that involves a sequence of two hydrogen atom transfers. Previous reports suggested that the reaction of acridan with α -methylstyrene and the reaction of DDQ with 1,4-cyclohexadiene most likely involved the radical pathway but that some other transfer hydrogenation reactions followed the ionic pathway.

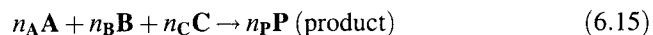
Chan and Radom carried out density functional theory computations for several transfer hydrogenations, both in the gas phase and in solution, using a variety of methods to calculate the energy of solvation of the reacting species.⁴³ They found that the calculated energy barrier for gas phase reactions was lower for the radical pathway than for the ionic pathway in all of the systems they studied. The results of calculations for solution reactions were more complex. Some reactions followed the radical pathway in all solvents, but other reactions followed the ionic pathway in polar solvents. In some cases, the results suggested that ionic and radical mechanisms might occur concurrently. As a result, trapping of a radical intermediate in such cases would not necessarily demonstrate that *only* the radical pathway was followed. The authors concluded that variations in reactant structure and solvent polarity can have dramatic effects on calculated reaction pathways, so investigators must be careful not to overgeneralize the results of a computational study.

6.3 APPLICATIONS OF KINETICS IN STUDYING REACTION MECHANISMS

A kinetic study is often the first tool chemists consider when planning a mechanistic investigation, but it is important to remember that kinetic studies do not “prove” any reaction mechanism. Rather, kinetics can only rule out proposed mechanisms that do not predict the experimental kinetic results, thus leaving as possibilities those mechanisms that are consistent with the kinetic data. We may say that a mechanism is *supported* by the

kinetic data, but we may not say that the mechanism is *confirmed* by the kinetic data.⁴⁴

The rate of a chemical reaction can be expressed as the time dependence of the appearance of a product or, alternatively, as the time dependence of the disappearance of a reactant.⁴⁵ Consider a reaction in which n_A molecules of **A** combine with n_B molecules of **B** and n_C molecules of **C** to produce n_P molecules of **P**.



We may find that the rate of the reaction depends on the concentration of some or all of the reactants, as shown equation 6.16.

$$\text{Rate} = \frac{1}{n_P} \frac{d[\mathbf{P}]}{dt} = -\frac{1}{n_A} \frac{d[\mathbf{A}]}{dt} = -\frac{1}{n_B} \frac{d[\mathbf{B}]}{dt} = -\frac{1}{n_C} \frac{d[\mathbf{C}]}{dt} = k_r[\mathbf{A}]^a[\mathbf{B}]^b[\mathbf{C}]^c \quad (6.16)$$

Here k_r is the rate constant for the reaction, and a , b , and c do not necessarily equal n_A , n_B , and n_C , respectively. In this expression, the **overall order** of the reaction is $a + b + c$, and the **order with respect to A** is a , the order with respect to **B** is b , and the order with respect to **C** is c . The order of a reaction with respect to a certain reagent is frequently a whole number, but fractional order is possible, and the order can be 0.

For an **elementary reaction** (involving a single step), the overall order of the reaction is the same as the **molecularity** (the number of reacting molecules in the rate-limiting step). Reactions composed of two or more elementary reactions are called **complex reactions**.^{46,47} A complex reaction may yield a complicated rate expression that includes concentration terms in the denominator or sums of terms that are similar to the right-hand side of equation 6.17. In such cases the overall order of the reaction is not defined.^{48,49} For example, we will see in Chapter 9 that the kinetic expression for the addition of bromine to an alkene in CCl_4 solution may take the form

$$-\frac{d[\text{Br}_2]}{dt} = [\text{alkene}](k_2[\text{Br}_2] + k_3[\text{Br}_2]^2 + k_{\text{Br}_3^-}[\text{Br}_3^-]) \quad (6.17)$$

The presence in equation 6.17 of a term that is second order with respect to bromine does not require that there be a step in which an alkene collides simultaneously with two bromine molecules. The more likely possibility, which is consistent with other experimental evidence, is that an alkene and one bromine molecule first react to produce an intermediate that subsequently reacts with another bromine molecule.

⁴⁴ Espenson, J. H. *Chemical Kinetics and Reaction Mechanisms*, 2nd ed.; McGraw-Hill: New York, 1995.

⁴⁵ The rate is sometimes called the *velocity* of the reaction, although that term occurs more frequently in biochemistry than in organic chemistry.

⁴⁶ For a discussion, see Connors, K. A. *Chemical Kinetics*; VCH Publishers: New York, 1990; pp. 3–4.

⁴⁷ The kinetics of complex reactions have been discussed by Noyes, R. M. in Lewis, E. S., Ed. *Investigation of Rates and Mechanisms of Reactions*, 3rd ed., Part I; Wiley-Interscience: New York, 1974; pp. 489–538.

⁴⁸ Laidler, K. J. *Chemical Kinetics*, 2nd ed.; McGraw-Hill: New York, 1965; p. 4.

⁴⁹ Reeve, J. C. *J. Chem. Educ.* **1991**, *68*, 728.

Let us consider in more detail a simpler reaction in which reactant **A** goes irreversibly to product **P** in a one-step reaction with rate constant k_1 . That is, $\text{A} \xrightarrow{k_1} \text{P}$. The rate expression is

$$\frac{d[\text{P}]}{dt} = -\frac{d[\text{A}]}{dt} = k_1[\text{A}] \quad (6.18)$$

The reaction is first order with respect to **A** and is overall first order. That order is consistent with a mechanism in which the rate-limiting step is unimolecular, meaning that one molecule of **A** reacts to give **P**. We can exclude a mechanism in which two molecules of **A** collide to give a molecule of **P** and one of **A**, since that process would give a different rate expression:

$$\frac{d[\text{P}]}{dt} = -\frac{d[\text{A}]}{dt} = k_2[\text{A}]^2 \quad (6.19)$$

Note that the term $d[\text{P}]/dt$ has units of concentration/time. The right-hand side of a rate equation must also have units of concentration/time, so the units of k_1 in equation 6.18 must be 1/time, while those of k_2 in equation 6.19 must be 1/(time \times concentration).

A **differential rate equation** such as equation 6.19 is generally not as useful to us as is the **integrated rate equation**, which allows us to compare experimental concentration data with that predicted by the rate expression. For a first-order reaction, the integrated rate expression is

$$\ln[\text{A}] = \ln[\text{A}]_0 - k_1 t \quad (6.20)$$

where t is time and $[\text{A}]_0$ is the value of $[\text{A}]$ at $t = 0$. In this case plotting the natural logarithm of the concentration of **A** versus time should produce a linear correlation with slope $-k_1$. For a second-order elementary reaction with stoichiometry $\text{A} + \text{A} \xrightarrow{k} \text{P}$, the integrated expression is

$$\frac{1}{[\text{A}]} - \frac{1}{[\text{A}]_0} = kt \quad (6.21)$$

Now plotting the reciprocal of the concentration of **A** versus time should produce a linear correlation, with slope $= k$.^{50,51}

⁵⁰ In general, for a reaction that is n th order (for $n > 1$) in **A**, the integrated rate expression is

$$\frac{1}{(n-1)} \left(\frac{1}{[\text{A}]^{n-1}} - \frac{1}{[\text{A}]_0^{n-1}} \right) = kt$$

For a detailed discussion of the kinetics of many kinds of reactions, see Capellos, C.; Bielski, B. H. J. *Kinetic Systems: Mathematical Description of Chemical Kinetics in Solution*; Wiley-Interscience: New York, 1972.

⁵¹ We may develop similar expressions for second- and third-order reactions in which two or three molecules of **A** collide in the rate-limiting step. See, for example, Gordon, A. J.; Ford, R. A. *The Chemist's Companion*; John Wiley & Sons: New York, 1972; p. 135 for a listing of the differential and integrated forms of zero-, first-, and second-order rate equations.

The rate expression for an elementary reaction with stoichiometry $\mathbf{A} + \mathbf{B} \rightarrow \mathbf{P}$ would be

$$\frac{d[\mathbf{P}]}{dt} = k[\mathbf{A}][\mathbf{B}] \quad (6.22)$$

Now the integrated expression becomes

$$\ln \frac{[\mathbf{A}]}{[\mathbf{B}]} + \ln \frac{[\mathbf{B}]_0}{[\mathbf{A}]_0} = ([\mathbf{A}]_0 - [\mathbf{B}]_0)kt \quad (6.23)$$

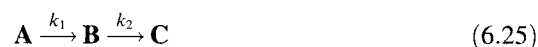
so plotting the natural logarithm of the term $[\mathbf{A}]/[\mathbf{B}]$ versus time should yield a linear correlation with slope $k([\mathbf{A}]_0 - [\mathbf{B}]_0)$.⁵²

If the concentration of \mathbf{B} is held essentially constant in a bimolecular reaction having the stoichiometry $\mathbf{A} + \mathbf{B} \rightarrow \mathbf{P}$, the rate expression will take the form⁵³

$$\frac{d[\mathbf{P}]}{dt} = k_{\text{observed}}[\mathbf{A}] \quad (6.24)$$

This type of reaction, which is said to be **pseudo-first order**, can occur if \mathbf{B} is an acid or base in a buffered solution, or if \mathbf{B} is a catalyst that is not consumed in the reaction, or if the ratio of $[\mathbf{B}]$ to $[\mathbf{A}]$ is very large. The last situation is typical in solvolysis reactions, in which the concentration of the solvent is large and essentially invariant.⁴⁶

Now let us consider a reaction in which reactant \mathbf{A} produces intermediate \mathbf{B} , which in turn goes on to product \mathbf{C} .



In this discussion the use of forward arrows (as opposed to equilibrium arrows) in the stoichiometric expressions is meant to imply that the two elementary steps are both **irreversible reactions**. This means that all molecules of \mathbf{B} go on to \mathbf{C} and do not revert to \mathbf{A} . Similarly, no \mathbf{C} molecules revert to \mathbf{B} . In theory, every reaction is reversible, and the energy and geometry of the transition structure should be the same in both directions.⁵⁴ If a particular step in a reaction is highly exothermic, however, the reverse reaction will be highly endothermic and thus may not be observed under our reaction conditions. By the term *irreversible*, therefore, we mean that the rate of the reverse reaction of each step is so slow as to be negligible under the reaction conditions.

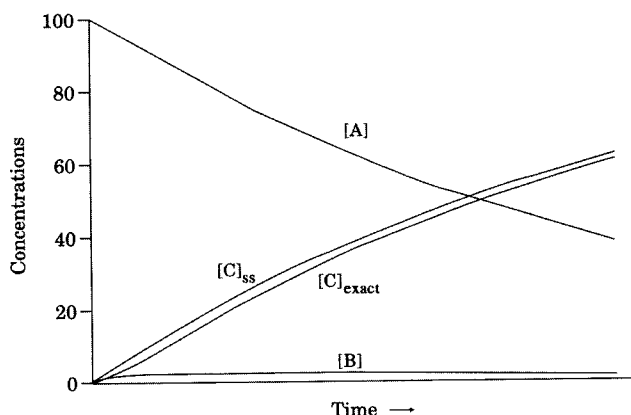
We can write an expression for the rate of product formation in equation 6.25 as follows:

$$\text{Rate} = \frac{d[\mathbf{C}]}{dt} = k_2[\mathbf{B}] \quad (6.26)$$

⁵² Bunnett, J. F. in Lewis, E. S., Ed. *Investigation of Rates and Mechanisms of Reactions*, 3rd ed., Part I; Wiley-Interscience: New York, 1974; pp. 140–141.

⁵³ The symbol k_{observed} is usually abbreviated k_{obs} . The symbols k_{ψ} and k_{app} (for k_{apparent}) have also been used for the rate constant in a pseudo-order reaction. See the discussion in reference 46, p. 23 ff.

⁵⁴ A formal statement of this theory is the **principle of microscopic reversibility**. For leading references, see (a) Morrissey, B. W. *J. Chem. Educ.* **1975**, *52*, 296; (b) Mahan, B. H. *J. Chem. Educ.* **1975**, *52*, 299.

**FIGURE 6.14**

Variation of [A], [B], and [C] with time for $k_1/k_2 = 0.033$.

The concentration of **B** is 0 at the start of the reaction and then varies with time. The rate expression for **[B]** is

$$\frac{d[\mathbf{B}]}{dt} = k_1[\mathbf{A}] - k_2[\mathbf{B}] \quad (6.27)$$

Integrating the rate expression for this system gives equations for the time dependence of the concentrations **[A]**, **[B]**, and **[C]**.⁵⁵ The relative concentrations of these species as a function of time are calculated for relative rate constants $k_1/k_2 = 0.033$ (Figure 6.14), $k_1/k_2 = 0.33$ (Figure 6.15), and $k_1/k_2 = 3.0$ (Figure 6.16).

In Figure 6.14, **[B]** does not change significantly once the reaction is underway. This observation is the basis for the **steady-state approximation** (also known as the quasi-steady-state approximation), a method that is commonly used to estimate the kinetics of systems involving intermediates.^{56–59} We assume that

$$\frac{d[\mathbf{B}]}{dt} = k_1[\mathbf{A}] - k_2[\mathbf{B}] \approx 0 \quad (6.28)$$

and so

$$k_2[\mathbf{B}] \approx k_1[\mathbf{A}] \quad (6.29)$$

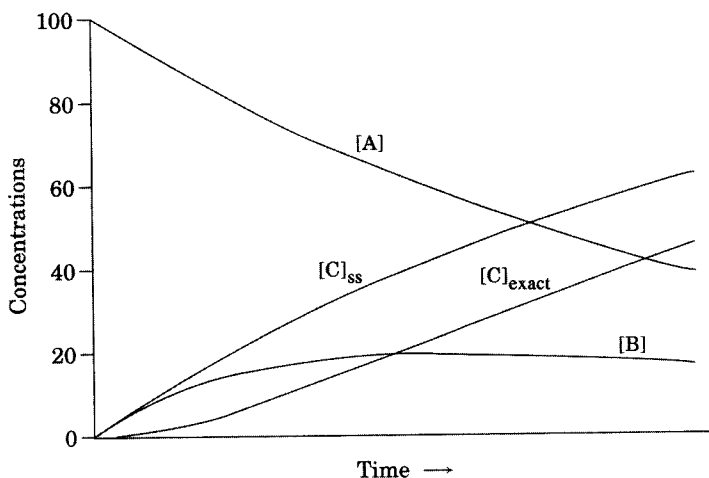
⁵⁵ Compare Frost, A. A.; Pearson, R. G. *Kinetics and Mechanism*, 2nd ed.; John Wiley & Sons: New York, 1961; p. 14 ff, p 166.

⁵⁶ (a) The steady-state approximation is commonly attributed to Bodenstein (Bodenstein, M.; Dux, W. Z. *Phys. Chem.* **1913**, *85*, 297; Bodenstein, M. Z. *Phys. Chem.* **1913**, *85*, 329). (b) However, Laidler, K. J. *Acc. Chem. Res.* **1995**, *28*, 187 noted that the method was used earlier by Chapman, D. L.; Underhill, L. K. *J. Chem. Soc.* **1913**, *103*, 496.

⁵⁷ See also the discussion by Bunnett, J. F. in Bernasconi, C. F., Ed. *Investigation of Rates and Mechanisms of Reactions*, 4th ed., Volume VI, Part I; John Wiley & Sons: New York, 1986; p. 251.

⁵⁸ Gilbert, H. F. *J. Chem. Educ.* **1977**, *54*, 492, presented a useful rule of thumb for writing steady-state equations in the general case. See also the discussion of the steady-state approximation and free energy profiles by Raines, R. T.; Hansen, D. E. *J. Chem. Educ.* **1988**, *65*, 757.

⁵⁹ For a discussion of the validity of the steady-state approximation, see Viostat, V.; Ben-Aim, R. I. *J. Chem. Educ.* **1993**, *70*, 732.

**FIGURE 6.15**

Variation of [A], [B], and [C] with time for $k_1/k_2 = 0.33$.

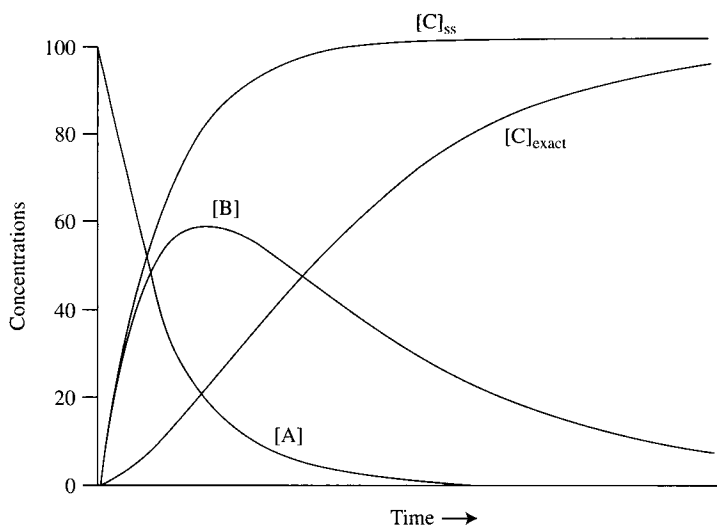
therefore

$$\text{Rate} = \frac{d[\text{C}]}{dt} = k_2[\text{B}] \approx k_1[\text{A}] \quad (6.30)$$

In other words, the overall reaction rate appears to be equal to the rate of the slowest step in the reaction sequence. If we make this assumption, the integrated expression for $[\text{C}]_{\text{ss}}$ (the concentration of C calculated on the basis of the steady-state approximation) becomes

$$[\text{C}]_{\text{ss}} = [\text{A}]_0 - [\text{A}] \quad (6.31)$$

Figures 6.14–6.16 illustrate the value of $[\text{C}]_{\text{ss}}$ as well as $[\text{C}]_{\text{exact}}$, the value of [C] calculated with the rate constants shown but without using the steady-state approximation. The figures suggest that the validity of the steady-state approximation depends on the relative magnitudes of the rate constants, k_1 and k_2 , and on the time scale of the measurement of [C]. Essentially, $[\text{C}]_{\text{ss}} = [\text{C}]_{\text{exact}} + [\text{B}]$. The larger the value of [B], the greater will be the error in

**FIGURE 6.16**

Variation of [A], [B], and [C] with time for $k_1/k_2 = 3.0$.

the value of $[C]_{ss}$. As the ratio k_1/k_2 becomes larger, both $[B]$ and the difference between $[C]_{ss}$ and $[C]_{exact}$ become larger as well.^{60,61}

Now let us consider a more complicated reaction involving at least one bimolecular step.⁶²



The rate of the reaction is:

$$\text{Rate} = \frac{d[D]}{dt} = k_2[C] \quad (6.33)$$

The exact integrated rate expression for this system is not known, but it is possible to approximate a solution using numerical integration methods such as the Runge–Kutta method.^{61,63} We may also apply the steady-state approximation to C :

$$\frac{d[C]}{dt} = k_1[A][B] - k_2[C] - k_{-1}[C] = 0 \quad (6.34)$$

so

$$[C] = \frac{k_1[A][B]}{(k_2 + k_{-1})} \quad (6.35)$$

Substituting the right-hand side of equation 6.35 for $[C]$ in equation 6.33 leads to

$$\frac{d[D]}{dt} = \frac{k_1 k_2}{(k_2 + k_{-1})} [A][B] \quad (6.36)$$

This complex equation may be simplified under certain conditions. If $k_2 \ll k_{-1}$, then the term $k_2 + k_{-1} \approx k_{-1}$, and equation 6.36 becomes

$$\frac{d[D]}{dt} = \frac{k_1 k_2}{k_{-1}} [A][B] = k_2 \frac{k_1}{k_{-1}} [A][B] \quad (6.37)$$

⁶⁰ The set of two consecutive irreversible reactions just considered is a subset of the more general case in which both reactions are reversible: $A \xrightleftharpoons[k_{-1}]{k_1} B \xrightleftharpoons[k_{-2}]{k_2} C$. The equations for this problem have been solved exactly for two limiting cases: (i) $[A]_0 = 1.00$ and both $[B]_0$ and $[C]_0 = 0$, and (ii) A is present as a saturated solution so that the concentration does not change with time. For details, see Lowry, T. M.; John, W. T. *J. Chem. Soc.* **1910**, 97, 2634 and references therein.

⁶¹ The kinetic expressions for more complicated reactions can become much more complex. Fortunately, there are exact solutions to some of these problems. Carpenter described the use of matrix methods to solve the problem of a “unimolecular array” in which a set of isomeric compounds and reaction intermediates are directly interconvertible. Carpenter, B. K. *Determination of Organic Reaction Mechanisms*; Wiley-Interscience: New York, 1984; p. 52 ff.

⁶² For a review of methods to model the kinetics of bimolecular reactions, see Fernández-Ramos, A.; Miller, J. A.; Klippenstein, S. J.; Truhlar, D. G. *Chem. Rev.* **2006**, 106, 4518.

⁶³ The exact solution for the time dependence of concentration for A , B , C , and D for the set of consecutive irreversible reactions $A + B \rightarrow C \rightarrow D$ has been reported: Anderson, R. L.; Nohr, R. S.; Spreer, L. O. *J. Chem. Educ.* **1975**, 52, 437.

where k_1/k_{-1} represents the equilibrium constant of the preequilibrium for formation of the species involved in the rate-limiting step. As was the case for the irreversible reaction, the concentrations calculated from the steady-state approximation will not be exact, although the magnitude of the error depends on the rate constants. If, however, $k_2 \gg k_{-1}$, then equation 6.36 simplifies to

$$\frac{d[\mathbf{D}]}{dt} = k_1[\mathbf{A}][\mathbf{B}] \quad (6.38)$$

If neither simplification is appropriate, then the reaction described by equation 6.32 may be studied by carrying out the reaction with a large initial concentration of **A** or **B** so that the first elementary reaction is carried out under pseudo-first-order conditions.

6.4 ARRHENIUS THEORY AND TRANSITION-STATE THEORY

One of the most important methods of investigating a reaction mechanism is the determination of the rate of the reaction as a function of temperature. The treatment of temperature effects that may be most familiar to organic chemists is the Arrhenius equation, which relates the rate constant of a reaction to the temperature and to the **activation energy**, E_a (also written as E_{act}).^{64,65} As shown in Figure 6.17, the activation energy is defined as the difference between the energy of the reactant(s) and the energy of the transition structure, which is the arrangement of electrons and nuclei at the high point on the reaction coordinate diagram for a one-step reaction.⁶⁶⁻⁶⁸

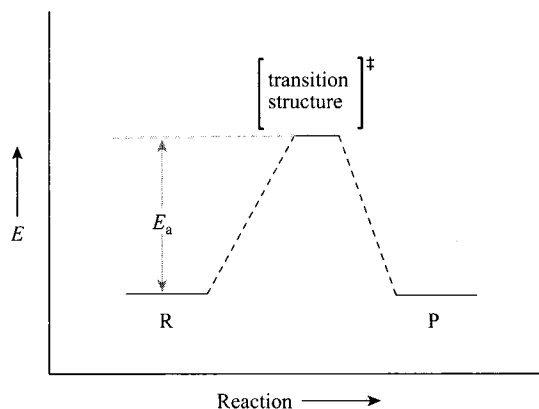


FIGURE 6.17

Reaction coordinate diagram illustrating E_a for a one-step reaction.

⁶⁴ See "The Development of the Arrhenius Equation," by Laidler, K. J. *J. Chem. Educ.* **1984**, *61*, 494; also see the comments regarding van't Hoff's pioneering work noted by Laidler in reference 56b.

⁶⁵ Arrhenius, S. Z. *Phys. Chem.* **1889**, *4*, 226. See the translation and commentary by Back, M. H.; Laidler, K. J. *Selected Readings in Chemical Kinetics*; Pergamon: Oxford, 1967.

⁶⁶ Laidler, K. J. *J. Chem. Educ.* **1988**, *65*, 540.

⁶⁷ For a discussion of the nature and depiction of transition states, see the anonymous note in *J. Chem. Educ.* **1987**, *64*, 208.

⁶⁸ For a discussion of the distinction between *transition state* and *transition structure*, see Williams, I. H. *Chem. Soc. Rev.* **1993**, *22*, 277.

TABLE 6.2 Experimental Data for the Thermolysis of 58

T ($^{\circ}\text{C}$)	$k \times 10^3$ (s^{-1})	$1/T$ (K)	$\ln k$
324.8	1.27	0.001672	-6.669
335.4	3.14	0.001643	-5.764
345.9	4.75	0.001615	-5.350
355.6	7.1	0.001590	-4.948
367.2	15.0	0.001562	-4.200
376.6	29.2	0.001539	-3.534
383.8	44.8	0.001522	-3.106
394.8	84.1	0.001497	-2.476

Source: Reference 71.

The usual expression of the Arrhenius equation is

$$k = Ae^{-E_a/RT} \quad (6.39)$$

in which k is the rate constant for the reaction, A is the preexponential factor, T is the temperature in Kelvin units, and R is the gas constant ($1.987 \text{ cal K}^{-1} \text{ mol}^{-1}$).⁶⁹ Taking the natural logarithm of both sides gives

$$\ln k = -\frac{E_a}{RT} + \ln A \quad (6.40)$$

Therefore, plotting $\ln k$ versus $1/T$ would be expected to give a straight line with slope $-E_a/R$ and intercept $\ln A$.⁷⁰

Consider the thermolysis of compound 58 to 59 (equation 6.41).⁷¹ Experimental temperatures and first-order rate constants determined at those temperatures are shown in the first two columns of Table 6.2. Note that the second column is labeled " $k \times 10^3$ (s^{-1})."

This means that the experimental rate constants have units of s^{-1} and that the numerical values were multiplied by 10^3 for the convenience of listing in the table. Therefore, the observed rate constant at 324.8°C is $1.27 \times 10^{-3} \text{ s}^{-1}$. The third column lists the inverse of the reaction temperature in K. As an example, the inverse of $(273.15 + 324.8)$ is 0.001672. The fourth column is the natural logarithm of the rate constant. For example, $\ln 0.00127$ is -6.669 . Plotting the parameters in the second two columns produces Figure 6.18. The slope of the best-fit line through the data points is -23295 , which equals $-E_a/R$. Multiplying the slope by the value of $-R$ therefore gives an E_a of $46,286 \text{ cal/mol} = 46.3 \text{ kcal/mol}$. The value of $\ln A$ is 32.3. Traditionally, chemists report values of

⁶⁹ A reaction may be slow at high temperature as well as at low temperature because of a small preexponential factor; that is, the reaction is improbable under all temperature conditions. The meaning of A in several theoretical treatments was discussed by Gouwenlock, B. G. *Q. Rev. Chem. Soc.* **1960**, *14*, 133.

⁷⁰ A long extrapolation of a plot of experimental data may produce an inaccurate value for $\ln A$. Therefore, an alternative approach is to calculate $\ln A$ from the calculated E_a value and data for the reaction rate constant at some temperature in the middle of the range of experimental temperature-rate data. Kalantar, A. H. *J. Phys. Chem.* **1986**, *90*, 6301 discussed the precision of E_a and A measurements. For a discussion of nonlinear Arrhenius plots, see Hulett, J. R. *Q. Rev. Chem. Soc.* **1964**, *18*, 227.

⁷¹ Wiberg, K. B.; Carangi, J. J.; Matturro, M. G. *J. Am. Chem. Soc.* **1990**, *112*, 5854.

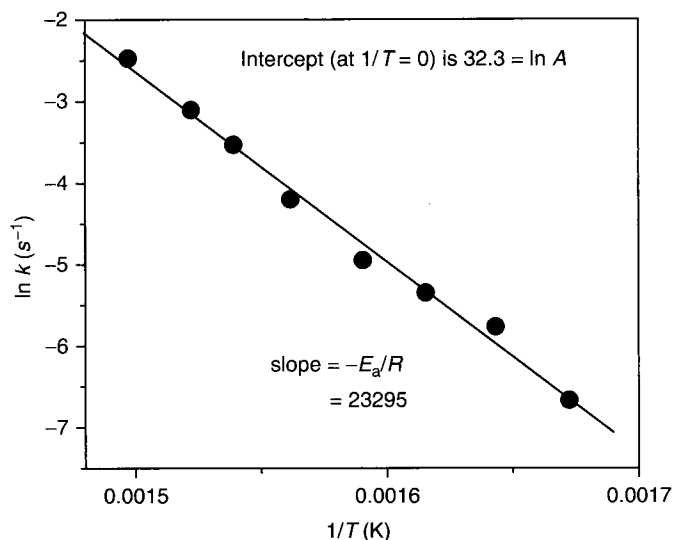
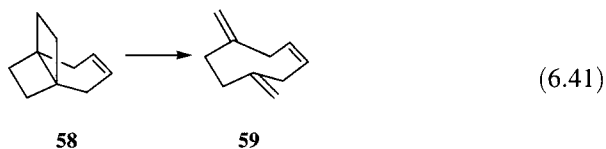


FIGURE 6.18
Arrhenius plot of data in Table 6.2.

log A , however, which in this case is $(32.3/2.303) = 14.0$.



In Figure 6.18 the slope of the best-fit line is negative, so E_a is positive. This is usually the case. If there is a preequilibrium between monomeric and complexed reactants prior to the rate-limiting step, however, the slope of the Arrhenius plot may be positive, and that would make the calculated E_a be negative. Such reactions are said to display a **negative kinetic temperature effect** or a **negative activation energy**. This does *not* mean that there is an elementary reaction step having a negative activation energy. Rather, such an observation suggests a multistep process involving an intermediate with two different reaction pathways.⁷²

An alternative to Arrhenius theory is **transition state theory**, which was put forward by Eyring and others in the 1930s.^{73,74} In this approach the **transition state**, also termed the **activated complex**, is considered a chemical species and is treated from the point of view of thermodynamics. Thus, we can define the activation free energy (ΔG^\ddagger), activation enthalpy (ΔH^\ddagger), and activation entropy (ΔS^\ddagger) for the transformation from reactants to the activated complex, as shown in Figure 6.19.^{75,76} The units of free energy and enthalpy

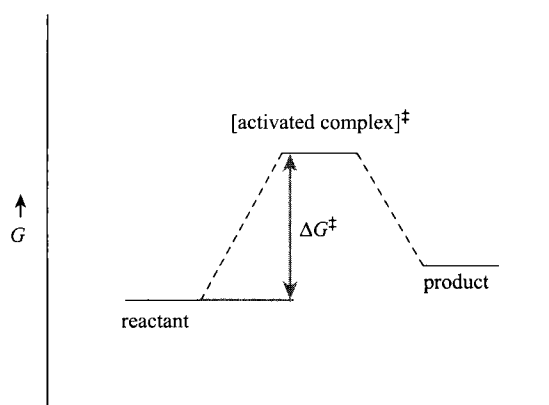
⁷² For example, see Turro, N. J.; Lehr, G. F.; Butcher, J. A., Jr.; Moss, R. A.; Guo, W. *J. Am. Chem. Soc.* **1982**, *104*, 1754; Albrecht-Gary, A.-M.; Dietrich-Buchecker, C.; Saad, Z.; Sauvage, J.-P. *J. Chem. Soc. Chem. Commun.* **1992**, 280; Zhu, X.-Q.; Zhang, J.-Y.; Cheng, J.-P. *J. Org. Chem.* **2006**, *71*, 7007.

⁷³ See "The Development of Transition-State Theory" by Laidler, K. J.; King, M. C. *J. Phys. Chem.* **1983**, *87*, 2657.

⁷⁴ For a review of developments in this area, see Truhlar, D. G.; Hase, W. L.; Hynes, J. T. *J. Phys. Chem.* **1983**, *87*, 2664; Albery, W. J. *Adv. Phys. Org. Chem.* **1993**, *28*, 139.

⁷⁵ The terms ΔG^\ddagger , ΔH^\ddagger , and ΔS^\ddagger are also written $\Delta^\ddagger G$, $\Delta^\ddagger H$, and $\Delta^\ddagger S$ and are defined as the Gibbs energy of activation, enthalpy of activation, and entropy of activation, respectively. *IUPAC Compendium of Chemical Terminology, Electronic Version*, <http://www.iupac.org/goldbook>.

⁷⁶ Another mechanistic tool is the activation volume, ΔV^\ddagger , which is determined by plotting $\ln k_{\text{observed}}$ versus pressure. For a review, see Van Eldik, R.; Asano, T.; le Noble, W. *J. Chem. Rev.* **1989**, *89*, 549; Whalley, E. *Adv. Phys. Org. Chem.* **1964**, *2*, 93.

**FIGURE 6.19**

Gibbs diagram illustrating ΔG^\ddagger for an elementary reaction.

are given in energy per mole (e.g., kcal/mol). The units of entropy are usually given as cal degree⁻¹ mol⁻¹, which is often abbreviated as eu (for "entropy units").

According to transition state theory, the rate constant k_r is defined as

$$k_r = \frac{\kappa \mathbf{k} T}{h} e^{-\Delta G^\ddagger / RT} \quad (6.42)$$

where h is Planck's constant (6.626×10^{-27} erg-s), T is the absolute temperature, κ is the transmission coefficient—a factor included because not all activated complexes go on to reaction products⁷⁷—and \mathbf{k} is the Boltzmann constant (1.380×10^{-16} erg/deg). Substituting $\Delta H^\ddagger - T \Delta S^\ddagger$ for ΔG^\ddagger gives

$$k_r = \frac{\kappa \mathbf{k} T}{h} e^{\Delta S^\ddagger / R} e^{-\Delta H^\ddagger / RT} \quad (6.43)$$

Dividing by T and then taking the natural logarithm of both terms in equation 6.43 gives

$$\ln \frac{k_r}{T} = \ln \frac{\kappa \mathbf{k}}{h} + \frac{\Delta S^\ddagger}{R} - \frac{\Delta H^\ddagger}{RT} \quad (6.44)$$

Taking \log_{10} instead of \ln gives

$$\log \frac{k_r}{T} = \log \frac{\kappa \mathbf{k}}{h} + \left[\frac{\Delta S^\ddagger}{2.303 R} - \frac{\Delta H^\ddagger}{2.303 RT} \right] \quad (6.45)$$

Replacing R with 1.987 cal deg⁻¹ mol⁻¹ produces the equivalent equation

$$\log \frac{k_r}{T} = \log \frac{\kappa \mathbf{k}}{h} + \frac{\Delta S^\ddagger}{4.575} - \frac{\Delta H^\ddagger}{4.575 T} \quad (6.46)$$

A plot of $\log(k_r/T)$ versus $1/T$, which is known as an Eyring plot, should be linear. Now ΔH^\ddagger can be calculated from the slope by the relationship

$$\Delta H^\ddagger = -4.575 \times \text{slope} \quad (6.47)$$

⁷⁷ The transmission coefficient is assumed to be a constant for all the variants of one reaction type.

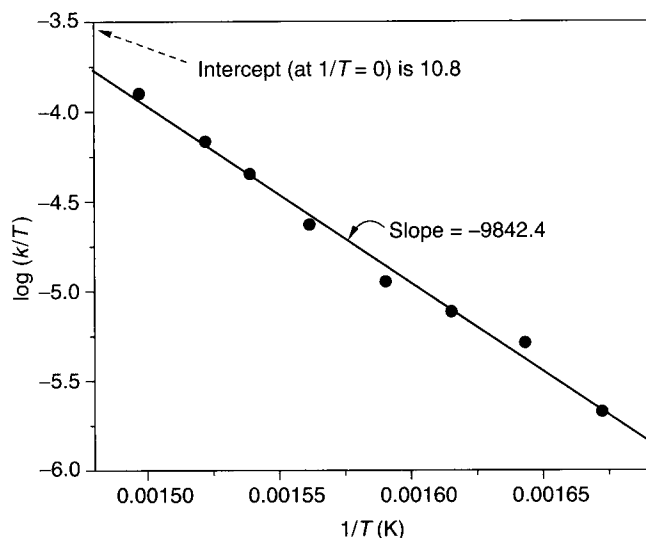


FIGURE 6.20

Eyring plot of the data in Table 6.2.

Note that the units of ΔH^\ddagger calculated from equation 6.47 are cal/mol, not kcal/mol. As an example, plotting the experimental data in Table 6.2 as $\log(k/T)$ versus $1/T$ produces Figure 6.20. Multiplying the slope by -4.575 gives a ΔH^\ddagger value of 45,039 cal/mol, or 45.0 kcal/mol. In solution, ΔH^\ddagger determined at room temperature is usually about 0.6 kcal/mol less than the Arrhenius E_a value, since⁷⁸

$$E_a = \Delta H^\ddagger + RT \quad (6.48)$$

and $RT = 0.6$ kcal/mol. Here the measurements were made at about 360°C (around 660 K), so the difference between E_a and ΔH^\ddagger is about 1.3 kcal/mol.

The value of ΔS^\ddagger can be calculated by rewriting equation 6.46 as

$$\Delta S^\ddagger = 4.575 \log \frac{k_r}{T} + \frac{\Delta H^\ddagger}{T} - 4.575 \log \frac{\kappa \mathbf{k}}{h} \quad (6.49)$$

Substituting for \mathbf{k} and h (and assuming that κ is unity) gives equation 6.50:

$$\Delta S^\ddagger = 4.575 \log \frac{k_r}{T} + \frac{\Delta H^\ddagger}{T} - 47.22 \quad (6.50)$$

Equation 6.50 thus allows the calculation of ΔS^\ddagger from the values of k_r and T for one experiment. For example, using the values for 376.6°C in Table 6.2 gives a ΔS^\ddagger of 2.2 eu. Alternatively, we may note from equation 6.46 that the intercept of a plot of $\log(k/T)$ versus $1/T$ is

$$\text{Intercept} = \log \frac{\kappa \mathbf{k}}{h} + \frac{\Delta S^\ddagger}{4.575} = 10.319 + \frac{\Delta S^\ddagger}{4.575} \quad (6.51)$$

⁷⁸ Leffler, J. E.; Grunwald, E. *Rates and Equilibria of Organic Reactions*; John Wiley & Sons: New York, 1963; p. 71.

so

$$\Delta S^\ddagger = 4.575 (\text{Intercept} - 10.319) \quad (6.52)$$

In the case of the experimental data considered here, $4.575 (10.795 - 10.319) = 2.2$ eu. Note that this example is based on a plot of $\log(k/T)$ versus $1/T$. Plotting $\ln(k/T)$ versus $1/T$ would give identical results when the log to ln conversion factor of 2.303 is included. Also, there is a close relationship between ΔS^\ddagger and the Arrhenius A value, as shown in equation 6.53 for A values expressed in units of s^{-1} and temperatures around 300 K.⁷⁸

$$\Delta S^\ddagger = 4.575 \log A - 60.53 \quad (6.53)$$

The value of ΔS^\ddagger for a reaction provides an estimate of the change in the order of the system upon going from reactants to the activated complex.⁷⁹ Consider the reactions shown in Figures 6.21 through 6.23. The dissociation of di-*t*-butyl peroxide (**60**, Figure 6.21) has been found to have an activation entropy of +13.8 eu in chlorobenzene solution, suggesting that the activated complex is less ordered than the reactant.⁸⁰ This result is compatible with a mechanism involving rate-limiting breaking of the O–O bond.⁸¹

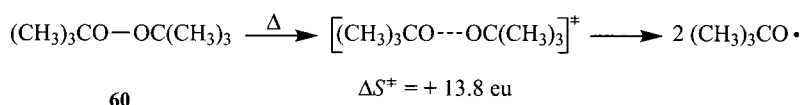


FIGURE 6.21

Cleavage of di-*t*-butyl peroxide.

On the other hand, the Cope rearrangement of *cis*-1,2-divinylcyclobutane (**61**) to *cis,cis*-1,5-cyclooctadiene (**62**, Figure 6.22) was found to have an activation entropy of –11.7 eu, meaning that the transition structure is more ordered than the reactant.⁸² This result suggests that the reaction does not proceed by a rate-limiting step involving breaking of the bond between the two carbon atoms with vinyl substituents. It is more consistent with a mechanism in which the two vinyl groups, which can rotate freely in the reactant, must become aligned in the transition structure.⁸³

The dimerization of cyclopentadiene (**63**) to produce **64** has a ΔS^\ddagger of –26 eu.⁵⁵ This large, negative activation entropy suggests a very highly

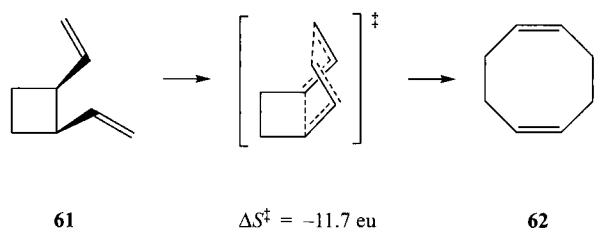


FIGURE 6.22

Rearrangement of *cis*-1,2-divinylcyclobutane to *cis,cis*-1,5-cyclooctadiene.

⁷⁹ For a discussion, see Schaleger, L. L.; Long, F. A. *Adv. Phys. Org. Chem.* **1963**, 1, 1.

⁸⁰ Bartlett, P. D.; Hiatt, R. R. *J. Am. Chem. Soc.* **1958**, 80, 1398.

⁸¹ Raley, J. H.; Rust, F. F.; Vaughan, W. E. *J. Am. Chem. Soc.* **1948**, 70, 1336.

⁸² Hammond, G. S.; DeBoer, C. D. *J. Am. Chem. Soc.* **1964**, 86, 899.

⁸³ In addition, the puckered cyclobutane ring may become more planar in the transition structure. The mechanism of this and similar reactions will be considered in Chapter 11.

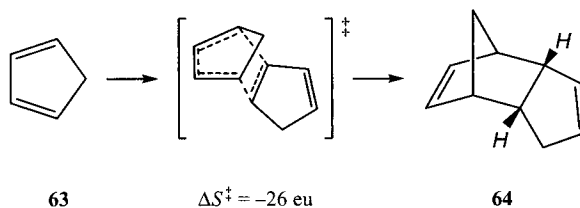


FIGURE 6.23
Dimerization of cyclopentadiene

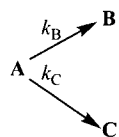


FIGURE 6.24
Competitive irreversible reactions of A to produce B and C.

ordered transition structure in which free rotations have been lost as two molecules come together in a very precise orientation. This result is consistent with the mechanism suggested in Figure 6.23. It is important to note that values of ΔH^\ddagger and ΔS^\ddagger for reactions in solution also include contributions from solvent molecules, not just the species that appear as reactants and products in the chemical equation.

While ΔH^\ddagger and ΔS^\ddagger provide important clues to reaction mechanisms, it is ΔG^\ddagger that determines the rate constant of a reaction. Knowledge of activation free energies is particularly useful in understanding parallel organic reactions, since relatively small differences in activation free energies can produce significant differences in product distributions. Consider the reaction of compound A to give either B or C in competitive, irreversible reactions (Figure 6.24) with rate constants k_B and k_C given by equations 6.54 and 6.55, respectively.

$$k_B = \frac{\kappa kT}{h} e^{-\Delta G_B^\ddagger/RT} \quad (6.54)$$

$$k_C = \frac{\kappa kT}{h} e^{-\Delta G_C^\ddagger/RT} \quad (6.55)$$

If these two reactions are irreversible, then the ratio of products ($[C]/[B]$) at any time will be a function of the ratio of rate constants, k_C/k_B , as shown in equation 6.56.

$$\ln \frac{k_C}{k_B} = \ln \frac{[C]}{[B]} = \frac{\delta \Delta G^\ddagger}{RT} \quad (6.56)$$

Equation 6.56 means that the natural log of the product ratio should tell us the difference in activation free energies (i.e., $\delta \Delta G^\ddagger$) for the two pathways, as shown in Figure 6.25.⁸⁴ Product ratios expected for different values of $\delta \Delta G^\ddagger/RT$ are listed in Table 6.3. As Saunders noted, at 25°C a change in the product ratio from 1:2 to 2:1 corresponds to a $\delta \Delta G^\ddagger$ of only about 0.8 kcal/mol, so small changes in relative activation energies can have pronounced changes in product distributions.⁸⁵

When using product distributions to estimate differences in activation free energies, we must be certain that the competing reactions really are irreversible. That is, we must ensure that the product distribution actually represents the relative magnitude of the rate constants for product formation.

⁸⁴ The term $\delta \Delta G^\ddagger$ is often written $\Delta \Delta G^\ddagger$, but the use of lowercase δ suggests that the ΔG^\ddagger values are significantly larger than the difference between them.

⁸⁵ Saunders, W. H., Jr. in Patai, S., Ed. *The Chemistry of Alkenes*; Wiley-Interscience: London, 1964; p. 184.

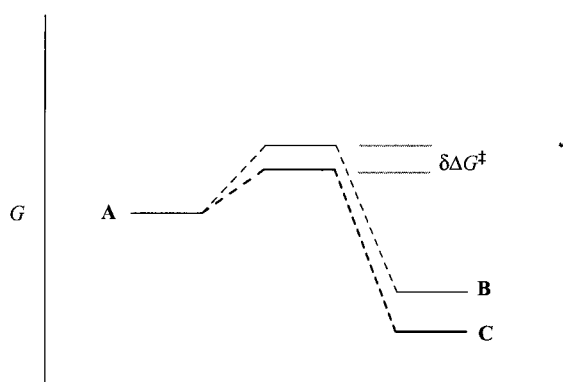
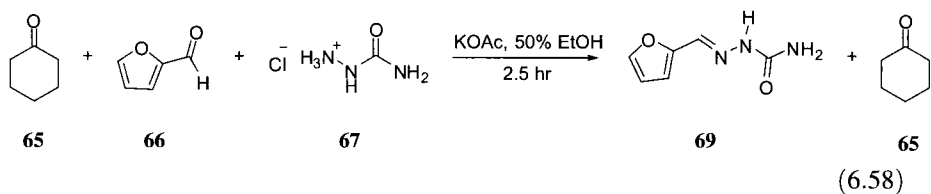
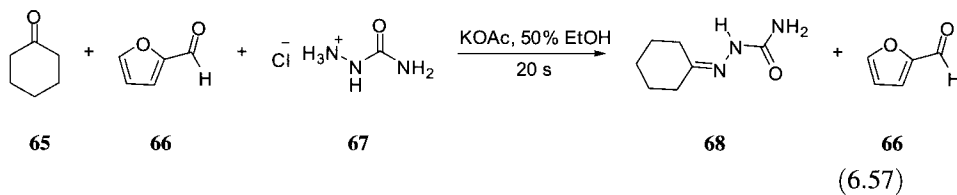
**FIGURE 6.25**

Illustration of the difference in free energies of activation for two competitive pathways.

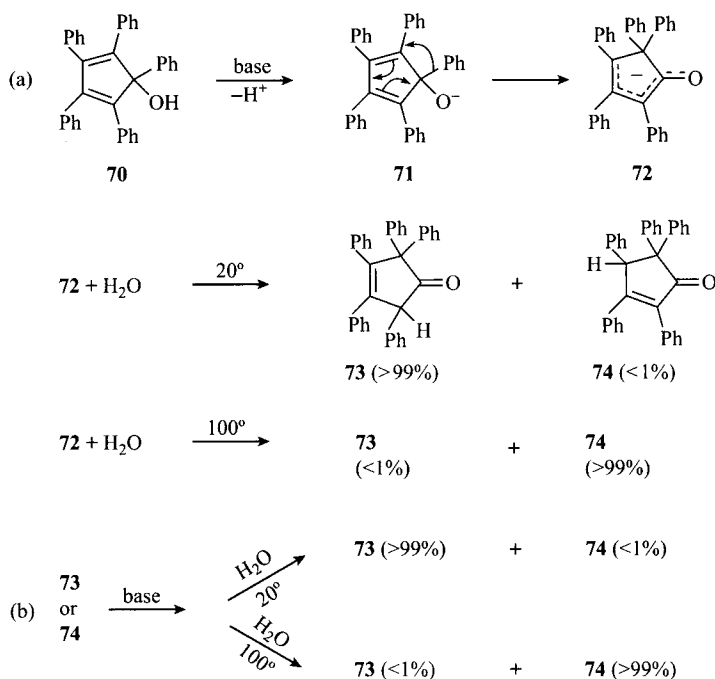
TABLE 6.3 Product Ratios and Differences in Activation Free Energy for Competitive, Irreversible Reactions

[C]/[B]	$\delta \Delta G^\ddagger$ at 25°C (kcal/mol)
1	0
2	0.41
5	0.96
10	1.36
100	2.73
1,000	4.09
10,000	5.45

For example, Conant and Bartlett studied the formation of semicarbazones from a solution composed initially of equal concentrations of cyclohexanone (**65**), furfural (**66**), and semicarbazide hydrochloride (**67**) in a solution of KOAc in 50% aqueous ethanol. The product isolated after a reaction period of 20 seconds was cyclohexanone semicarbazone (**68**, equation 6.57). However, when the reaction was allowed to proceed for 2.5 hours, the product was furfural semicarbazone (**69**, equation 6.58).⁸⁶



⁸⁶ Conant, J. B.; Bartlett, P. D. *J. Am. Chem. Soc.* **1932**, *54*, 2881.

**FIGURE 6.26**

Temperature ($^\circ\text{C}$) effects on the reaction of **72** with water.

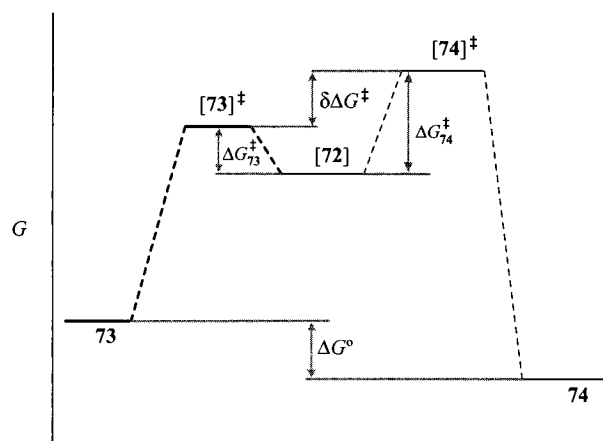
Similarly, reaction of chlorobenzene with isopropyl chloride under Friedel–Crafts conditions produced primarily the ortho and para alkylation products after a short reaction period. Allowing the reaction mixture to stand for a week before workup, however, produced primarily the meta product.⁸⁷ In both of these cases, the product isolated after a short time is said to be the product of **kinetic control** of the product distribution, since the product isolated is the one that is formed faster. The product isolated after a longer time is said to be the product of **thermodynamic control** of product distribution, since it is the more stable product.⁸⁸

In the example above, different products were obtained after different reaction times. Often questions about kinetic and thermodynamic control of product distribution arise in connection with reactions in which different products are found for reactions carried for the same amount of time but at different temperatures. Consider the reaction of 1,2,3,4,5-pentaphenyl-2,4-cyclopentadien-1-ol (**70**) with base, which leads to an alkoxide ion (**71**) that rearranges to the resonance-stabilized anion (**72**). Protonation of **72** gives the pentaphenylcyclopentenones **73** and **74** in ratios that were found to depend on the reaction temperature, as shown in Figure 6.26(a).⁸⁹ When the reaction was carried out at 20°C , quenching with water produced almost exclusively **73**. When the reaction was carried out at 100°C , quenching with water gave almost exclusively **74**. In a subsequent experiment, Figure 6.26(b), it was found that subjecting either **73** or **74** to the original reaction conditions at 20°C produced the same ratio of the two products as was observed from the reaction of **70** at 20°C . Similarly, subjecting either **73** or **74** to the original

⁸⁷ Kolb, K. E.; Standard, J. M.; Field, K. W. *J. Chem. Educ.* **1988**, *65*, 367.

⁸⁸ The terms *kinetic control* and *thermodynamic control* appear to have been introduced by Ingold. For a historical discussion, see Berson, J. A. *Angew. Chem. Int. Ed.* **2006**, *45*, 4724.

⁸⁹ Youssef, A. K.; Ogliaruso, M. A. *J. Chem. Educ.* **1975**, *52*, 473.

**FIGURE 6.27**

Reaction coordinate diagram for formation of kinetic and thermodynamic products.

reaction conditions at 100°C produced the same ratio of the two products as was observed from the reaction of 70 at 100°C.

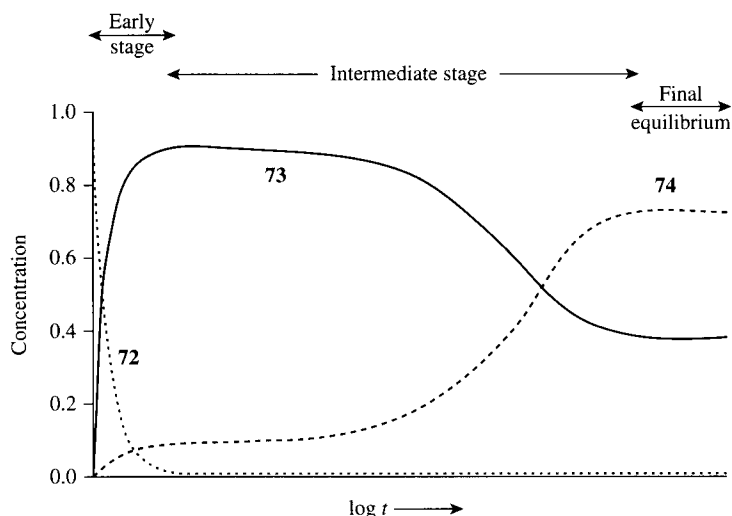
These results can be rationalized by the reaction coordinate diagram shown in Figure 6.27. Because ΔG^\ddagger for conversion of 72 to 73 is smaller than the value of ΔG^\ddagger for conversion of 72 to 74, formation of 73 is faster. Therefore, more of 73 is formed during the early stages of the reaction, so the distribution of products is said to reflect kinetic control. As the reaction proceeds, the much slower processes that convert 73 first to 72 and then to 74 become more significant. Eventually, equilibrium is established between 73 and 74, and the product distribution at the end of the reaction is said to reflect thermodynamic control.

The terms *thermodynamic control* and *kinetic control* were criticized by Brown and co-workers because both "thermodynamics and kinetics control all products," and the terms *kinetic* and *thermodynamic control* sometimes are thought to imply that temperature controls the reaction.⁹⁰ Snadden emphasized that the distinction between thermodynamic and kinetic control of product distributions is really one of *time* and not of *temperature*.⁹¹ The time dependence of reactant and product concentrations for a reaction such as that in Figure 6.26 would be qualitatively similar to that shown in Figure 6.28. (Note that the *x*-axis is logarithmic.) Because the equilibrium between the two products will be established more rapidly at a higher temperature, the effect of increasing the temperature of the reaction is to compress the curves along the *x*-axis, so that the thermodynamic product predominates in a shorter period. Keeping the temperature low would expand the curves along the *x*-axis, ensuring that the kinetic product would be formed in greater amount over the same time period. In other words, quenching of 72 at 20°C would also give a 99 : 1 ratio of 74 to 73 if we were to wait long enough before working up the reaction mixture.⁹²

⁹⁰ Brown, M. E.; Buchanan, K. J.; Goosen, A. *J. Chem. Educ.* **1985**, *62*, 575. Alternative terms are *rate control* and *equilibrium control*, which more precisely describe the factors that determine product distribution. For an example of this usage, see Solomons, T. W. G. *Organic Chemistry*, 4th ed.; John Wiley & Sons: New York, 1988; p. 470.

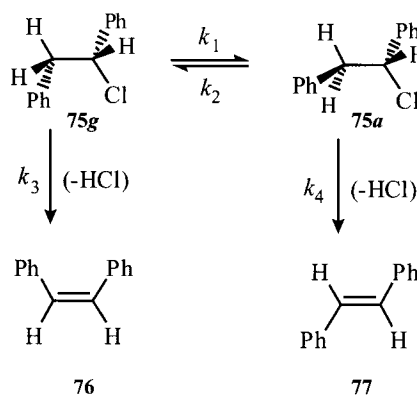
⁹¹ Snadden, R. B. *J. Chem. Educ.* **1985**, *62*, 653.

⁹² This discussion ignores a small temperature effect on the equilibrium between the two products.

**FIGURE 6.28**

Time dependence of the concentrations of **72**, **73**, and **74**. (Adapted from reference 91.)

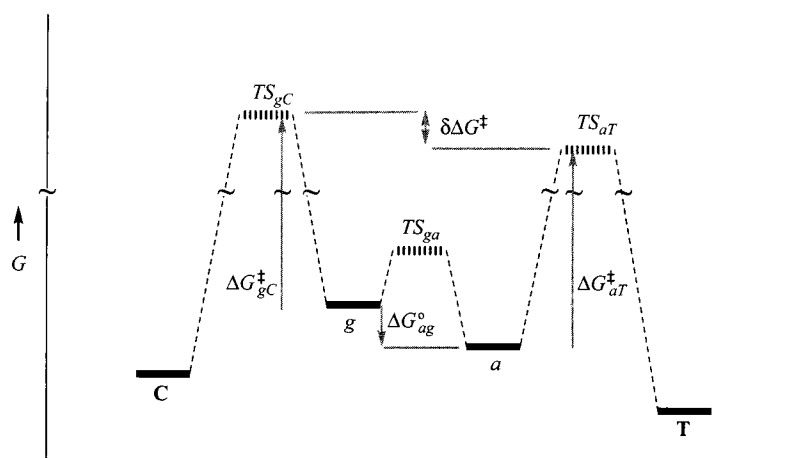
Another caution about the interpretation of chemical kinetics is called the **Curtin–Hammett principle**.^{93,94} The chemical reaction that led to the statement of the principle is the E2 elimination of 1-chloro-1,2-diphenylethane (**75**) to give *cis*-stilbene (**76**) and *trans*-stilbene (**77**, Figure 6.29). We may designate two conformations of the reactant as **75g** (with gauche phenyl groups) and **75a** (with anti phenyl groups). If we assume that the reaction requires an *anti-periplanar* relationship of the chlorine atom and a hydrogen atom, then the two conformations of the reactant should give two stereochemically different products. Here k_3 and k_4 are pseudo-first-order rate constants representing $k'_3[\text{base}]$ and $k'_4[\text{base}]$, respectively, under conditions of essentially constant base concentration.

**FIGURE 6.29**

Reaction scheme to illustrate the Curtin–Hammett principle.

⁹³ Curtin, D. Y. *Record Chem. Prog.* **1954**, *15*, 111. In the second edition of *Physical Organic Chemistry*, Hammett (reference 95) refers to the "Curtin Principle." Then, in a footnote, he says that "because Curtin is very generous in attributing credit, this is sometimes referred to as the Curtin–Hammett principle."

⁹⁴ For a memorial lecture summarizing the contributions of L. P. Hammett, see Shorter, J. *Prog. Phys. Org. Chem.* **1990**, *17*, 1.

**FIGURE 6.30**

Graphical representation of the Curtin–Hammett principle. Conformer **75a** is represented by *a*, and **75g** is represented by *g*. **T** and **C** represent *trans*- and *cis*-stilbene, respectively.

We know that the rate of formation of *trans*-stilbene (**T**) is

$$\frac{d[\mathbf{T}]}{dt} = k_4[a] \quad (6.59)$$

and the rate of formation of the *cis* isomer (**C**) is

$$\frac{d[\mathbf{C}]}{dt} = k_3[g] \quad (6.60)$$

The anti conformer **75a** should be more stable than the gauche conformer **75g**. If we observe that the yield of **77** is greater than that of **76**, then it is tempting to conclude that the product ratios provide a measure of the equilibrium between **75a** and **75g** in the reactant. In other words, we might assume that

$$[\mathbf{75a}]/[\mathbf{75g}] = [\mathbf{77}]/[\mathbf{76}] \quad (6.61)$$

This conclusion would be correct *only* if k_3 and k_4 are both much greater than k_1 and k_2 , however. In general, we would expect the rate of rotation about a carbon–carbon single bond to be much faster than the rate of a bimolecular elimination reaction, so equation 6.61 is almost certainly invalid.

Let us examine the kinetics of the reaction scheme in Figure 6.29 more closely by considering the Gibbs energy diagram in Figure 6.30. If the conformers of **75** are in equilibrium, then

$$K_{ag} = \frac{k_1}{k_2} = \frac{[a]}{[g]} \quad (6.62)$$

so

$$[a] = K_{ag}[g] \quad (6.63)$$

Now we can write

$$\frac{\frac{d[\mathbf{T}]}{dt}}{\frac{d[\mathbf{C}]}{dt}} = \frac{e^{-\Delta G_{aT}^\ddagger/RT} e^{-\Delta G_{ag}^\circ/RT}}{e^{-\Delta G_{gC}^\ddagger/RT}} = e^{-\delta\Delta G^\ddagger/RT} \quad (6.64)$$

and

$$\frac{[\mathbf{T}]}{[\mathbf{C}]} = e^{-\delta\Delta G^\ddagger/RT} \quad (6.65)$$

The Curtin–Hammett principle therefore states that the relative yield of the products from two competing, irreversible reactions is determined only by the difference in activation free energies ($\delta\Delta G^\ddagger$) for the pathways, provided that the interconversion of reactants is faster than product formation.^{95,96} This requirement is met if k_1 and k_2 are both at least 10 times greater than the larger of k_3 and k_4 and if the equilibrium between reacting species is no more than 10:1 in favor of one of the reactants.⁹⁶

Equation 6.65 concerns product distributions, not the overall rate of the reaction. A closely related expression is the Winstein–Holness equation (equation 6.66), which gives the total rate constant (k_{WH}) for the elimination reaction in terms of the individual rate constants for product formation (k_3 and k_4) and the mole fraction of each reactant present at equilibrium, n_g and n_a .⁹⁷

$$k_{\text{WH}} = n_g k_3 + n_a k_4 \quad (6.66)$$

An equivalent equation (6.67) was provided independently by Eliel and co-workers.⁹⁸

$$k_{\text{WH}} = \frac{k_3 K_{ag} + k_4}{K_{ag} + 1} \quad (6.67)$$

Detailed analyses of Curtin–Hammett kinetics were given by Zefirov⁹⁹ and by Seeman and co-workers.¹⁰⁰

6.5 REACTION BARRIERS AND POTENTIAL ENERGY SURFACES

In discussions to this point we have made frequent use of a Gibbs diagram (e.g., Figure 6.30), which shows the free energies of reactants, transition states, reactive intermediates, and products of a reaction. In such drawings the x -axis is only a convenience to separate the different entities. Dashed lines convey sequential relationships, but only in a qualitative way.

⁹⁵ Hammett, L. P. *Physical Organic Chemistry*, 2nd ed.; McGraw-Hill: New York, 1970; p. 120.

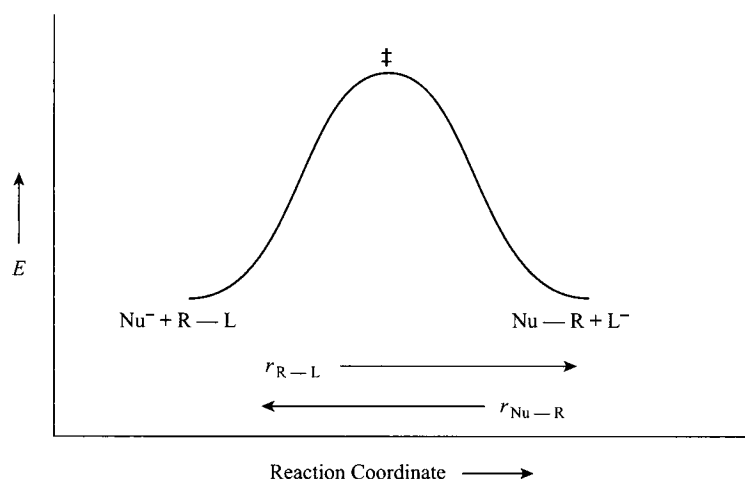
⁹⁶ See also the discussion by Eliel, E. L. *Stereochemistry of Carbon Compounds*; McGraw Hill: New York, 1962; pp. 151–152, 237–239; Eliel, E. L.; Wilen, S. H. *Stereochemistry of Organic Compounds*; Wiley-Interscience: New York, 1994; pp. 647–655.

⁹⁷ Winstein, S.; Holness, N. J. *J. Am. Chem. Soc.* **1955**, *77*, 5562. See also Eliel, E. L. *J. Chem. Educ.* **1960**, *37*, 126 and references therein.

⁹⁸ Eliel, E. L.; Ro, R. S. *Chem. Ind. London* **1956**, 251; Eliel, E. L.; Lukach, C. A. *J. Am. Chem. Soc.* **1957**, *79*, 5986.

⁹⁹ Zefirov, N. S. *Tetrahedron* **1977**, 2719; *Russ. J. Org. Chem.* **1997**, *33*, 138.

¹⁰⁰ Seeman, J. I.; Farone, W. A. *J. Org. Chem.* **1978**, *43*, 1854; Seeman, J. I. *Chem. Rev.* **1983**, *83*, 83; Perrin, C. L.; Seeman, J. I. *J. Org. Chem.* **1984**, *49*, 2887; Seeman, J. I. *J. Chem. Educ.* **1986**, *63*, 42.

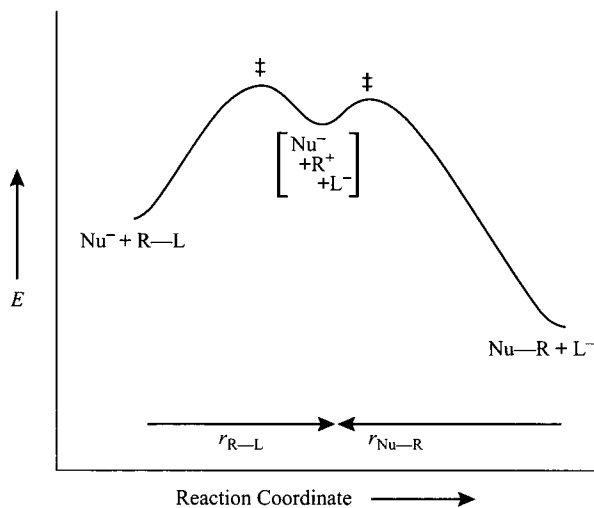
**FIGURE 6.31**

Reaction coordinate diagram for an S_N2 reaction. The reaction coordinate represents two parallel (but opposite in direction) bond distance measurements.

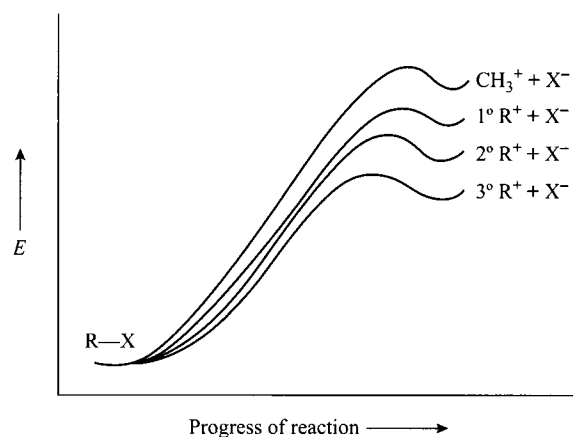
Organic chemists also represent the energetics of a reaction pathway with an alternative diagram, often called a reaction coordinate diagram, in which the x -axis does have meaning. This axis is often labeled “progress of reaction,” suggesting that it indicates the extent to which a reaction has progressed along some coordinate that characterizes the bonding changes necessary for reaction. Moreover, a continuous line connects the energy minima and maxima, implying knowledge (or at least some inference) about how the potential energy of the system changes during the course of the reaction. Although this coordinate is often only vaguely defined, it is useful to think about what it means.

Consider a substitution reaction involving $R-L$ and Nu^- . If the reaction follows the S_N2 mechanism, the reaction coordinate represents *both* the extent to which the C_R-L bond is broken and the extent to which the C_R-Nu bond is formed (Figure 6.31). In the case of an S_N1 reaction, however, the reaction coordinate measures first the extent to which the C_R-L bond is broken and then the extent to which the C_R-Nu bond is formed (Figure 6.32).

One purpose of drawings such as Figure 6.32 is to provide a graphical model for a correlation of structure and reactivity. For example, reactivity in

**FIGURE 6.32**

Reaction coordinate diagram for an S_N1 reaction. The reaction coordinate is composed of two consecutive bond distances.

**FIGURE 6.33**

Schematic representation of structure-energy relationships in S_N1 reactions.

an S_N1 reaction increases in the order $\text{CH}_3\text{-L} < C_{\text{primary}}\text{-L} < C_{\text{secondary}}\text{-L} < C_{\text{tertiary}}\text{-L}$. Therefore, the relative activation energies for these reactions must decrease in the order $\text{CH}_3\text{-L} > C_{\text{primary}}\text{-L} > C_{\text{secondary}}\text{-L} > C_{\text{tertiary}}\text{-L}$. We know that carbocation stability varies with alkyl structure in the order $\text{CH}_3^+ < C_{\text{primary}}^+ < C_{\text{secondary}}^+ < C_{\text{tertiary}}^+$. It is convenient to represent these energy relationships and reactivity trends in Figure 6.33, which indicates that the rate-limiting step in the S_N1 reaction should be faster for a 3° alkyl halide than for a 1° halide. Such drawings are familiar to every organic chemist, but it is worthwhile to ask what justifies their use.

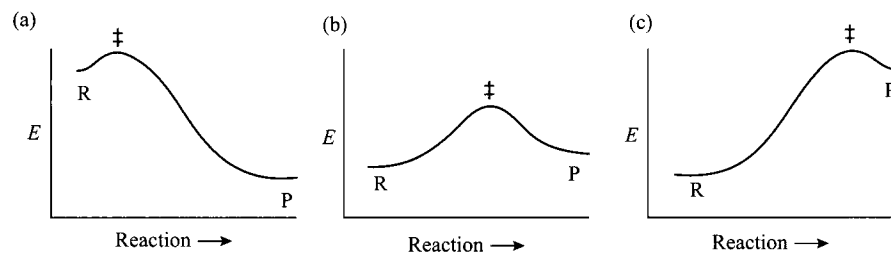
The shapes of the diagrams in Figures 6.31–6.33 follow from an intuitive argument most commonly known as the **Hammond postulate**. As it was stated by Hammond,

If two states, as for example, a transition state and an unstable intermediate, occur consecutively during a reaction process and have nearly the same energy content, their interconversion will involve only a small reorganization of the molecular structures.¹⁰¹

Hammond added that “in highly exothermic steps it will be expected that the transition states will resemble reactants closely and in endothermic steps the products will provide the best models for the transition states.” The postulate is a logical consequence of the idea that the energy of a chemical entity is a function of its structure. Therefore, two species that occur consecutively during a reaction and that have very similar energies might be expected to have very similar structures as well. In this context, the phrase “similar structures” means similar coordinates on the horizontal axis of the reaction coordinate diagram.

The Hammond postulate is illustrated by the diagrams in Figure 6.34. In an exothermic reaction, the energy of the transition state is necessarily closer to that of the reactant than to that of the product, so we draw it closer in structure also. That is, we draw the energy maximum to the left on the reaction coordinate diagram. The reverse is true for an endothermic reaction. Thus, we often say that an exothermic reaction has an “early” transition state and an endothermic reaction has a “late” transition state. In a thermoneutral reaction, the energy of the transition state is as different from that of the reactant as

¹⁰¹ Hammond, G. S. *J. Am. Chem. Soc.* 1955, 77, 334.

**FIGURE 6.34**

Typical reaction coordinate diagrams for (a) exothermic, (b) nearly thermoneutral, and (c) endothermic reactions.

it is from that of the product. According to the Hammond postulate, the structure of the transition state is as different from the reactant as from the product, so we show the transition state at the midpoint along the reaction coordinate. Leffler had earlier proposed a quantitative relationship between transition state energies and the energies of reactants and products, as shown in equation 6.68. Here α is said to indicate the resemblance of the transition state to the product and has a value ranging from 0 to 1.¹⁰² The ideas of Hammond and Leffler are sometimes cited together as the *Hammond–Leffler postulate*.¹⁰³

$$\Delta G^\ddagger = \alpha \Delta G^\circ + c \quad (6.68)$$

A closely related statement of the correlation of energy barriers with heats of reaction is known as the Bell–Evans–Polanyi (BEP) principle (equation 6.69).¹⁰⁴ Note that the BEP principle is concerned with the activation energies, while the Hammond and Leffler postulates are concerned with the structures of transition states. Of course, bonding and energy are inherently related, so the Hammond–Leffler postulate and the Bell–Evans–Polanyi principle are complementary.

$$E_a = \beta \Delta H_r^\circ + A \quad (6.69)$$

One way to rationalize these ideas is to describe the reactant and the product in an elementary reaction as structures with energies that vary parabolically with progress along the reaction coordinate. If this parabolic relationship is valid for large deformations along the coordinate, then the energy barrier for the reaction is determined by the overlap of the two parabolas. Figure 6.35 shows such a case for an exothermic reaction. Here the dashed line represents the energy of the system as it proceeds from reactant to product. Similar representations for a thermoneutral reaction (Figure 6.36) and an exothermic reaction (Figure 6.37) show how changing ΔH° affects both the activation energy for the reaction and the extent of similarity of the transition state to the reactant and product. In each case, the

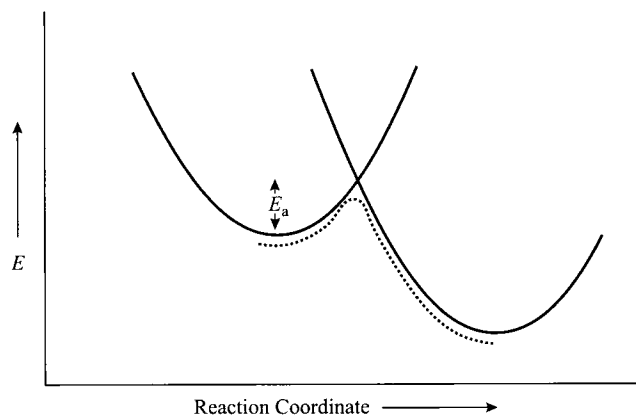
¹⁰² Leffler, J. E. *Science* **1953**, *117*, 340.

¹⁰³ Because a number of other authors contributed to our understanding of these and related concepts, Jencks (reference 112) proposed the acronym *Bema Hapothle* to incorporate references to the work of Bell, Evans, Marcus, Hammond, Polanyi, Thornton, and Leffler.

¹⁰⁴ Dewar, M. J. S.; Dougherty, R. C. *The PMO Theory of Organic Chemistry*; Plenum: New York, 1975, 212; Bell, R. P. *Proc. R. Soc. London Ser. A* **1936**, *154*, 414; Evans, M. G.; Polanyi, M. *Trans. Faraday Soc.* **1938**, *34*, 11 and earlier papers.

FIGURE 6.35

Representation of a reaction coordinate diagram as the sum of two parabolic potential energy surfaces for an exothermic reaction.



dashed line representing energy change along the reaction coordinate is qualitatively similar to the corresponding diagram in Figure 6.34.

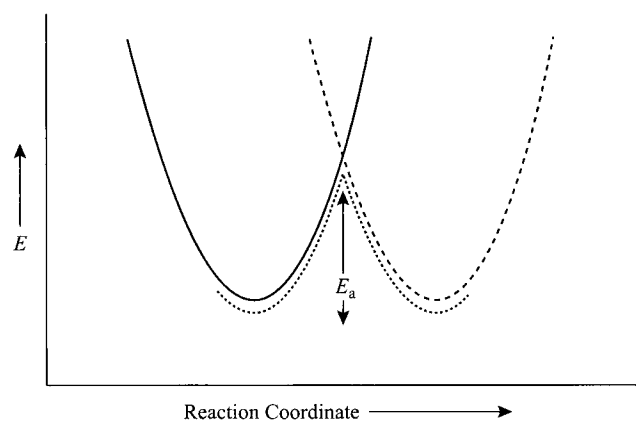
Drawings similar to Figures 6.35–6.37 were used by Marcus to develop a theory for the energetics of electron-transfer reactions.¹⁰⁵ The Marcus equation (one form of which is shown in equation 6.70) relates ΔG^\ddagger to the overall free energy change for the reaction (ΔG°) and an *intrinsic barrier* ($\Delta G^\ddagger_{\text{int}}$), which is the value of ΔG^\ddagger for an isoergonic reaction.¹⁰⁶

$$\Delta G^\ddagger = \Delta G^\ddagger_{\text{int}} + \frac{\Delta G^\circ}{2} + \frac{(\Delta G^\circ)^2}{16 \Delta G^\ddagger_{\text{int}}} \quad (6.70)$$

Moreover, Marcus demonstrated that it is possible for ΔG^\ddagger values for some electron-transfer reactions to *increase* as ΔG° values become more negative (Figure 6.38), giving rise to what is known as the *inverted region* in a plot of $\ln k$ versus $-\Delta G^\circ$.¹⁰⁵ Marcus theory has been extended to proton-, hydrogen- and group-transfer reactions as well.¹⁰⁷ For these processes, however, it is

FIGURE 6.36

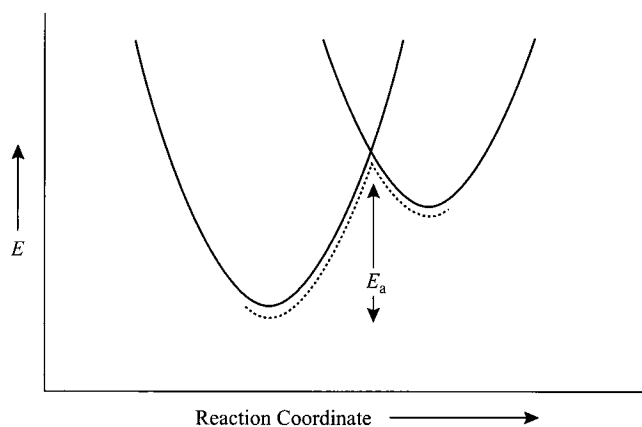
Representation of a reaction coordinate diagram as the sum of two parabolic potential energy surfaces for a thermoneutral reaction.



¹⁰⁵ Marcus, R. A. *J. Phys. Chem.* **1968**, *72*, 891; *Rev. Mod. Phys.* **1993**, *65*, 599.

¹⁰⁶ An *isoergonic* reaction has a zero value of ΔG° .

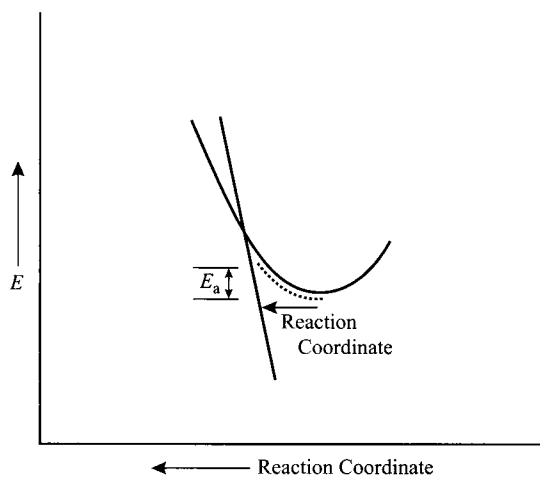
¹⁰⁷ Gonzales, J. M.; Allen, W. D.; Schaefer, H. F. III. *J. Phys. Chem. A* **2005**, *109*, 10613 and references therein.

**FIGURE 6.37**

Representation of a reaction coordinate diagram as the sum of two parabolic potential energy surfaces for an endothermic reaction.

ordinarily the case that activation energies approach zero as the reactions become more exothermic, so the inverted region is not observed.¹⁰⁸

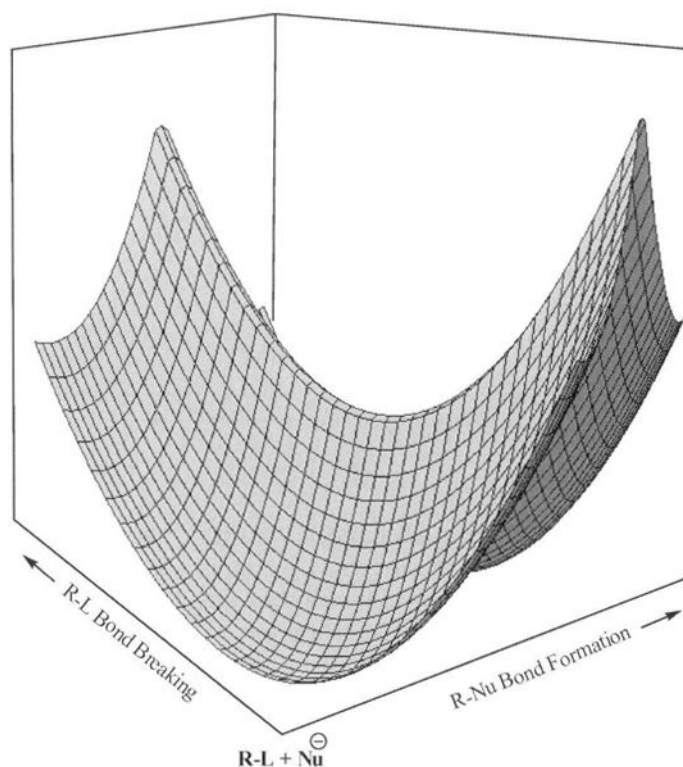
A common feature of all of the reaction diagrams presented in this discussion is the assumption that the properties of the transition state result from a linear blending of the properties of the reactant and product. However, Pross and Shaik argued that in some situations the character of the transition state need not be intermediate between the character of the reactants and products.¹⁰⁹ Moreover, Figures 6.31–6.37 all depict energy as a function of a single reaction coordinate, so these diagrams are valid only to the extent that the many structural changes associated with a chemical reaction can be represented by a single metric. This need not be the case if some bonding changes are not synchronous with other bonding changes. So-called anti-Hammond effects have been reported in which a transition state is thought to become *less* like a consecutive energy minimum as the energy of that

**FIGURE 6.38**

Origin of the energy barrier for a very exothermic reaction in the "inverted region" according to Marcus theory. (Only a portion of the parabola is shown for the very low energy product of the reaction.)

¹⁰⁸ Blowers, P.; Masel, R. I. *J. Phys. Chem. A* **1999**, *103*, 7047 proposed a modification of the Marcus equation that more accurately predicts activation barriers for group-transfer reactions.

¹⁰⁹ Pross, A.; Shaik, S. S. *J. Am. Chem. Soc.* **1982**, *104*, 1129.

**FIGURE 6.39**

A three-dimensional representation of the potential energy surface for a substitution reaction (oblique view).

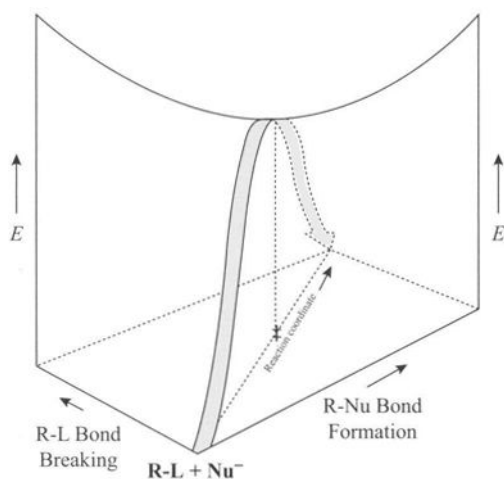
minimum increases.¹¹⁰ Therefore, simple reaction coordinate diagrams have their limitations.

It seems reasonable that a more complete depiction of the energy changes associated with a chemical reaction would result from using more than one measure of the bonding changes. We can generate a three-dimensional potential energy surface by choosing two dimensions of the reacting system as our x - and y -coordinates, with the z -coordinate representing energy. In the case of a substitution reaction, the x -coordinate could represent the C_R-L distance as the bond to the leaving group is broken, while the y -axis can represent the C_R-Nu distance as the new bond is formed. In the case of an "identity" S_N2 reaction, such as the reaction of Br^- and CH_3Br , the resulting three-dimensional potential energy surface might appear as shown in Figure 6.39.

Redrawing Figure 6.39 in schematic form produces Figure 6.40. Now we see more clearly that the transition state for the substitution reaction is an energy maximum on the diagonal path from reactants to products but is an energy minimum along a path diagonal to the reaction path. Thus, the transition structure corresponds to a *saddle point* on the three-dimensional potential energy surface. Viewing Figure 6.39 from the side gives Figure 6.41, which is shown schematically in Figure 6.42. An alternative representation of the same potential energy surface is the contour diagram shown in Figure 6.43.

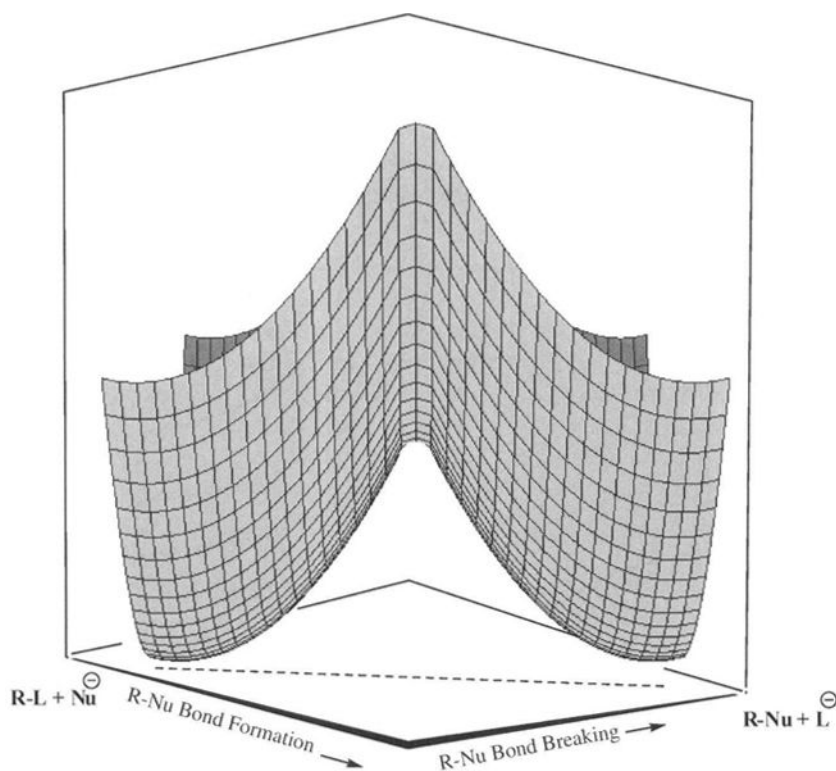
In Figures 6.40 and 6.43, the \ddagger symbol locates the transition state on the potential energy surface or on the contour plot representing the potential

¹¹⁰ See, for example, Lopez, X.; Dejaegere, A.; Karplus, M. *J. Am. Chem. Soc.* **2001**, *123*, 11755.

**FIGURE 6.40**

A simplified representation of the potential energy surface in Figure 6.39 (oblique view).

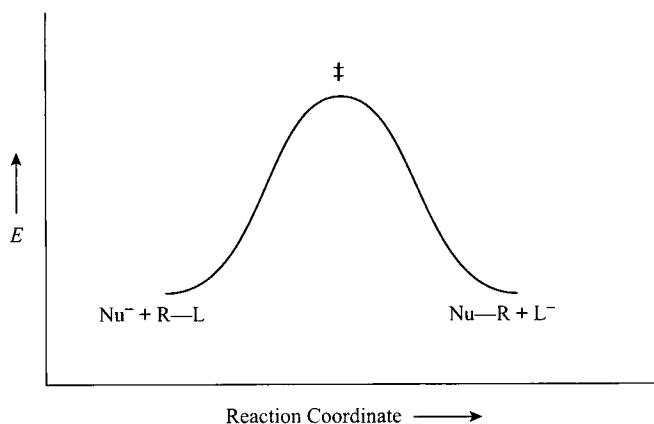
energy surface, while the dashed line from one corner to another indicates the reaction path from reactant to product. With the understanding that the dashed line represents the minimum energy path from reactants to products and the transition state is a saddle point, we may simplify Figure 6.43 by omitting the contour lines. The resulting drawing is called a More O'Ferrall–Jencks diagram.^{111,112} Such figures allow us to graphically depict

**FIGURE 6.41**

A three-dimensional representation of the potential energy surface for a substitution reaction (side view). The dashed line represents the reaction coordinate in Figure 6.40.

¹¹¹ More O'Ferrall, R. A. *J. Chem. Soc. B* **1970**, 274.

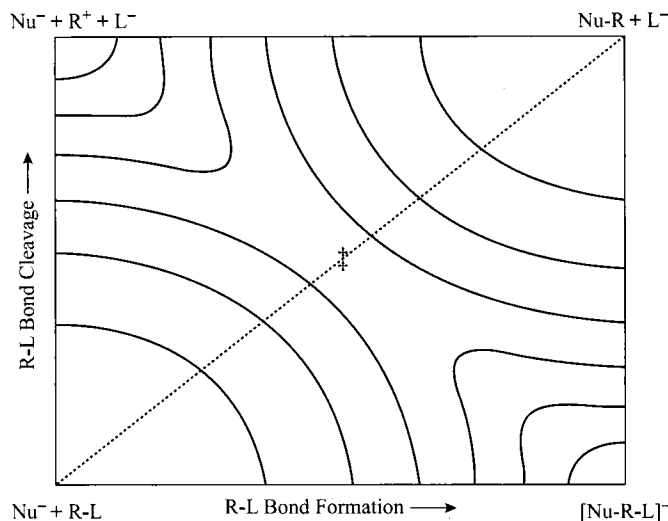
¹¹² Jencks, W. P. *Chem. Rev.* **1985**, 85, 511.

**FIGURE 6.42**

A reaction coordinate diagram derived from Figure 6.41.

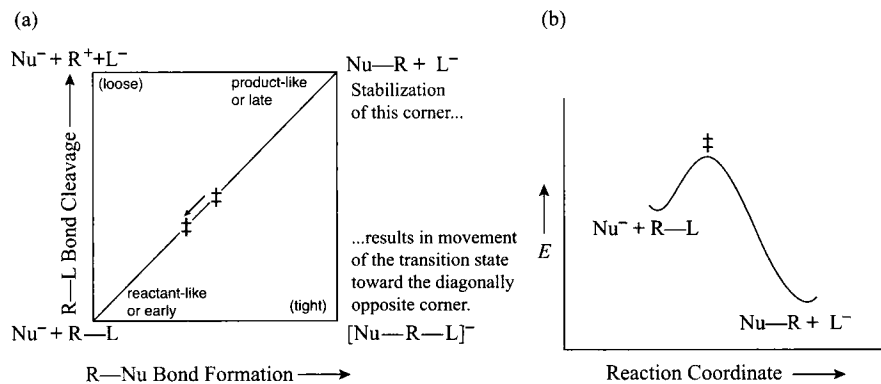
the consequences of changing the reactants or conditions of a reaction. For example, Figure 6.44(a) shows that lowering the product energy (the upper right corner of the figure) has the effect of moving the transition state along the diagonal toward the reactant. Figure 6.44(b) shows a side view of the resulting potential energy surface, confirming our expectations based on the Hammond postulate.

Now consider the effect of lowering the energy of the upper left corner in Figure 6.43 by making the carbocation R^+ more stable (Figure 6.45).¹¹³ The potential energy surface is lowered in a direction that is perpendicular to the diagonal line, so the transition state moves in that direction. Making the L^- a better leaving group lowers the energies of *both* the top left corner and the top right corner of Figure 6.43. The net effect is the vector sum of the two independent effects, one parallel to the reaction coordinate and one perpendicular to it (Figure 6.46). Depending on the extent to which R^+ and L^- are stabilized, there may be an infinite number of paths connecting reactants to products on a More O'Ferrall-Jencks diagram.

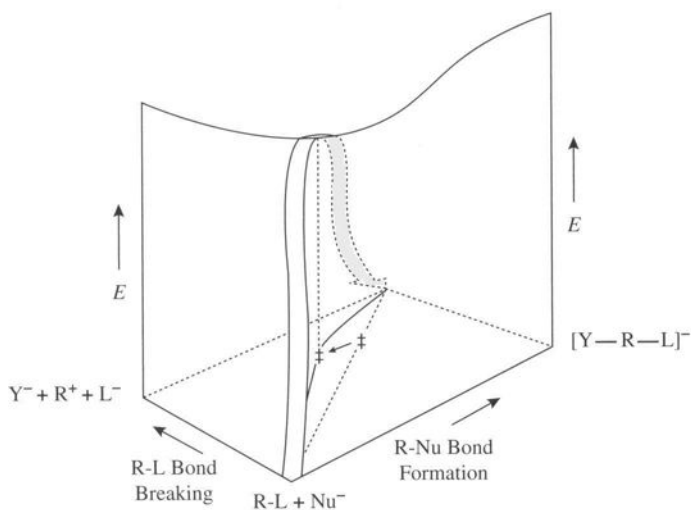
**FIGURE 6.43**

A contour diagram derived from Figure 6.39.

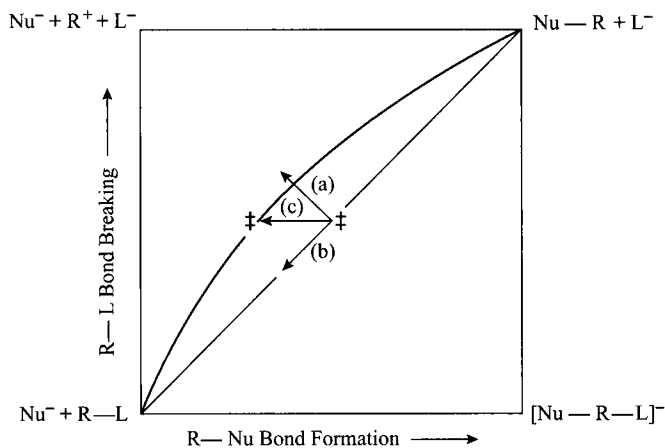
¹¹³ The following discussion is drawn in part from a paper by Harris, J. M.; Shafer, S. G.; Moffatt, J. R.; Becker, A. R. *J. Am. Chem. Soc.* **1979**, *101*, 3295.

**FIGURE 6.44**

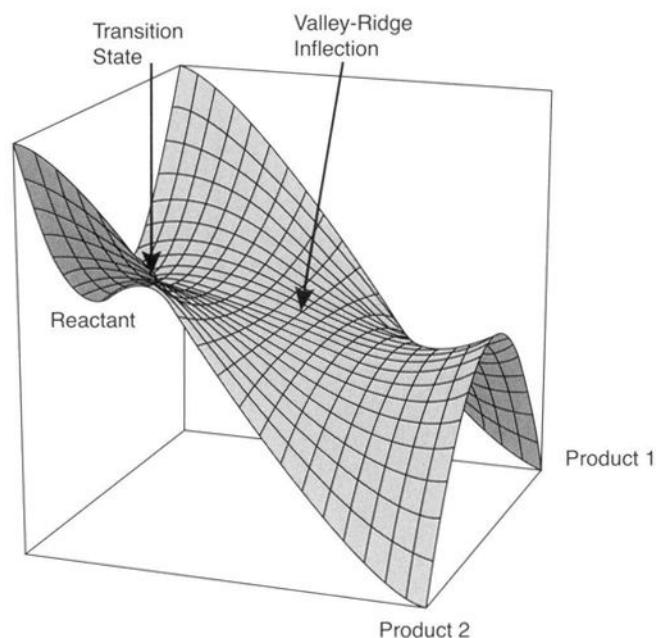
(a) A More O'Ferrall-Jencks diagram and (b) a reaction coordinate diagram for a substitution reaction in which the products are more stable than the reactants.

**FIGURE 6.45**

Effect on the transition state of lowering the energy of a corner of the three-dimensional potential energy surface.

**FIGURE 6.46**

Effect on the transition state of lowering the energy of both the top left and the top right corner of the three-dimensional potential energy surface. Vector (a) indicates the result of lowering the energy of the upper left corner. Vector (b) indicates the result of lowering the upper right corner. Vector (c) is the net result of vectors (a) and (b).

**FIGURE 6.47**

A potential energy surface with a valley–ridge inflection.

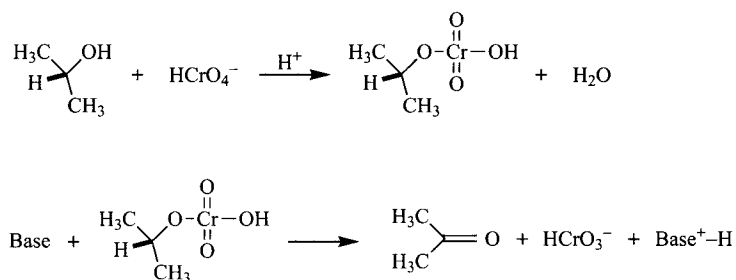
In the examples above, each reaction produced a single product. If two products can be formed from the same reactants, we usually assume that the pathway to each product can be described by unique pathways over a potential energy surface and that each pathway has its own transition state. In some cases, however, it appears that different reaction pathways can share the same transition state. This situation arises when there is a bifurcation in the potential energy surface connecting reactants to the products. As shown in Figure 6.47, such a potential energy surface is characterized by a valley–ridge inflection (VRI) point, where the valley along the pathway from the reactant to the transition state becomes a ridge separating the energy basin for one product from that for the other. In such cases, product distributions depend on the shape of the potential energy surface *after* the transition state.¹¹⁴

In later chapters we will find the types of energy–reaction progress diagrams described in this section to be useful in correlating the rates of reactions with the structures and energies of the reactants and products. It will be important to remember that these drawings are simplified models of more complex structure–energy relationships. They should not be considered complete descriptions of the systems under consideration. Nevertheless, these drawings will provide a useful framework for developing and applying some important methods for studying the mechanisms of organic reactions.

6.6 KINETIC ISOTOPE EFFECTS

So far we have considered reactions that are either one-step reactions or are multistep reactions in which the rate-limiting step is known. In many cases we may be able to propose a reasonable mechanism for a multistep reaction,

¹¹⁴ For a discussion of bifurcated potential energy surfaces for organic reactions, see Ess, D. H.; Wheeler, S. E.; Iafe, R. G.; Xu, L.; Çelebi-Ölçüm, N.; Houk, K. N. *Agnew. Chem. Int. Ed.* **2008**, *47*, 7592.

**FIGURE 6.48**

Two steps in the oxidation of isopropyl alcohol by chromic acid.

but we may not know which step is rate-limiting. Consider the oxidation of isopropyl alcohol by aqueous chromic acid (Figure 6.48). Two steps appear to be involved:^{115,116}

1. Formation of a chromate ester from isopropyl alcohol and chromic acid.
2. Decomposition of the chromate ester with concurrent oxidation of the alcohol and reduction of the chromium.

A central question about this reaction concerns the H–C bond shown in bold in Figure 6.48. Does the rate-limiting step occur before this bond is broken (perhaps during formation of the chromate ester), is it the breaking of this bond, or does it occur after this bond is broken (e.g., through the decomposition of a carbanionic intermediate in which the oxygen–chromium bond is still intact)?

There is a kinetic method that can, in principle, tell us about bonding changes in the rate-limiting step of a reaction and that was used to answer the questions just posed. The technique is the study of **kinetic isotope effects**, in which the rate constant of a reaction varies when one isotope of an atom is replaced by a different (usually heavier) isotope. If there is a kinetic effect upon replacement of an atom to which a bond is broken, then we observe a **primary (1°) kinetic isotope effect (PKIE)**. If the kinetic effect results from placing an isotope elsewhere in the reactant, then we observe a **secondary (2°) kinetic isotope effect**.¹¹⁷

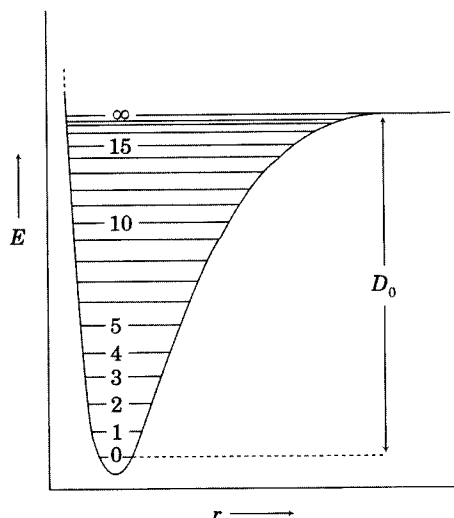
Primary Kinetic Isotope Effects

We will approach the theory of kinetic isotope effects with a somewhat intuitive conceptual model, leaving the detailed mathematical treatment to

¹¹⁵ Holloway, F.; Cohen, M.; Westheimer, F. H. *J. Am. Chem. Soc.* **1951**, *73*, 65; Roček, J.; Westheimer, F. H.; Eschenmoser, A.; Moldoványi, L.; Schreiber, J. *Helv. Chim. Acta* **1962**, *45*, 2554.

¹¹⁶ The overall mechanism is quite complex, and additional processes are involved in the reaction. For further discussion, see (a) Westheimer, F. H. *Chem. Rev.* **1949**, *45*, 419; (b) Watanabe, W.; Westheimer, F. H. *J. Chem. Phys.* **1949**, *17*, 61; (c) Wiberg, K. B.; Schäfer, H. *J. Am. Chem. Soc.* **1969**, *91*, 927, 933.

¹¹⁷ For further reading, see (a) Melander, L.; Saunders, W. H., Jr. *Reaction Rates of Isotopic Molecules*; John Wiley & Sons: New York, 1980; (b) Saunders, W. H., Jr. in Bernasconi, C. F., Ed. *Investigation of Rates and Mechanisms of Reactions*, 4th ed., Vol. VI, Part I; John Wiley & Sons: New York, 1986, p. 565; (c) Buncl, E.; Lee, C. C., Eds. *Isotopes in Organic Chemistry*, Vol. 7; Elsevier: Amsterdam, 1987.

**FIGURE 6.49**

Vibrational energy levels and bond dissociation energy. (Adapted from reference 119.)

the references.¹¹⁸ Consider first a unimolecular thermal dissociation of a C–H bond. The electronic energy of the molecule varies as a function of the internuclear distance and can be described by the curve in Figure 6.49. Superimposed on the electronic energy curve is a set of vibrational energy levels ($v = 0, 1, 2, \dots$) with widths that represent the vibrational amplitudes of the bond in the different vibrational energy levels. The vibrational energy levels become compressed near the dissociation limit because of the anharmonicity of the bond vibration.¹¹⁹ The energy of each vibrational level is given (to a first approximation) by the formula¹²⁰

$$E = hv\left(v + \frac{1}{2}\right) \quad (6.71)$$

where

$$v = \frac{\sqrt{\frac{k}{\mu}}}{2\pi} \quad (6.72)$$

Here k is the force constant for the molecular vibration and μ is the reduced mass, which is defined as

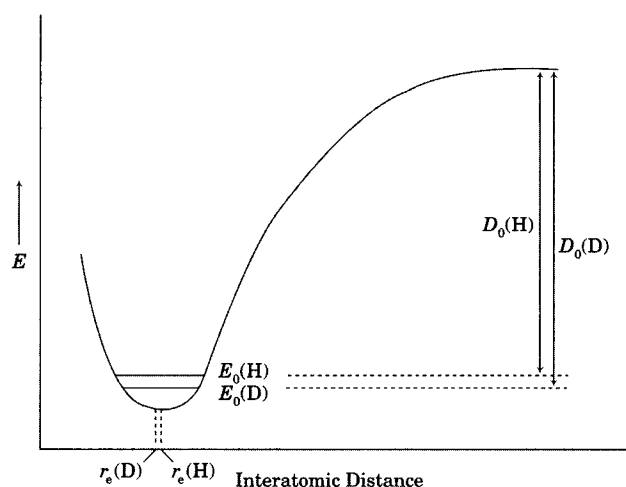
$$\mu = \frac{m_1 m_2}{(m_1 + m_2)} \quad (6.73)$$

for masses m_1 and m_2 . At room temperature 99% of molecules are in their 0th vibrational level,^{118b} so the vibrational energy of the molecule is greater than

¹¹⁸ See, for example, (a) Kresge, A. J. *J. Am. Chem. Soc.* **1980**, *102*, 7797; (b) Wiberg, K. B. *Chem. Rev.* **1955**, *55*, 713; (c) Westheimer, F. H. *Chem. Rev.* **1961**, *61*, 265; (d) Collins, C. J.; Bowman, N. S., Eds. *Isotope Effects in Chemical Reactions*; Van Nostrand Reinhold: New York, 1970; (e) Bell, R. P. *Chem. Soc. Rev.* **1974**, *3*, 513; (f) Kohen, A.; Limbach, H.-H., Eds. *Isotope Effects in Chemistry and Biology*; Taylor & Francis: Boca Raton, FL, 2006.

¹¹⁹ For a discussion, see King, G. W. *Spectroscopy and Molecular Structure*; Holt, Rinehart and Winston: New York, 1964; p. 160 ff.

¹²⁰ This equation implicitly models the bond vibration after a harmonic oscillator. Bonds are anharmonic oscillators, especially at higher vibrational levels, but at very low vibrational levels the approximation is not too bad.

**FIGURE 6.50**

Difference in bond dissociation energies for C–H and C–D bonds. (Adapted from reference 118b.)

the hypothetical energy at the electronic energy minimum by an amount equal to $\frac{1}{2}h\nu$. This energy is called the **zero point energy** or **ZPE**. The energy associated with the bond breaking (the **dissociation energy**, denoted E_D or D_0) is the difference in energy between the 0th vibrational energy level and the energy of the dissociated bond.¹²¹

There is a difference between the dissociation energy for a C–H bond in a CH_4 molecule and that of a C–D bond in a CH_3D molecule. If the CH_4 and CH_3D molecules are in their ground electronic states, they should have a common potential energy surface, and their energies should differ only in the vibrational and rotational energy levels associated with the C–H and C–D bonds.^{122,123} Due to the greater mass of deuterium, E_0 (the energy of the molecule in the 0th vibrational level) is lower for a C–D bond than for a C–H bond (Figure 6.50).

We can calculate the difference in E_0 values for C–H and C–D bonds from the reduced masses and an estimate of the stretching force constant. Alternatively, we can determine the energy difference empirically through infrared spectroscopy. As noted on page 372, the zero point energy for a bond stretching vibration is $\frac{1}{2}h\nu$. The zero point energy for a C–H bond is then determined from the frequency of the radiation corresponding to the stretching of a C–H bond in infrared spectroscopy, which is about 3000 cm^{-1} .

$$E_0(\text{H}) = \frac{1}{2} h\nu = \frac{1}{2}(3000\text{ cm}^{-1}) = 1500\text{ cm}^{-1} \quad (6.74)$$

The corresponding infrared stretching frequency of a C–D bond is seen around 2200 cm^{-1} , so the zero point energy is¹²⁴

$$E_0(\text{D}) = \frac{1}{2} h\nu = \frac{1}{2}(2200\text{ cm}^{-1}) = 1100\text{ cm}^{-1} \quad (6.75)$$

¹²¹ Figure 6.49 is adapted from the electronic curve and vibrational levels calculated for the HF molecule in reference 119.

¹²² In this discussion we are describing the system in terms of valence bond theory or in terms of “bonds” composed of localized molecular orbitals. An analysis using delocalized molecular orbitals would be equivalent, although less intuitive.

¹²³ Huskey, W. P. *J. Phys. Chem.* **1992**, *96*, 1263.

¹²⁴ For a discussion, see Pinchas, S.; Laulicht, I. *Infrared Spectra of Labelled Compounds*; Academic Press: London, 1971; p. 65 ff.

Then

$$\Delta E_0 = 1500 \text{ cm}^{-1} - 1100 \text{ cm}^{-1} = 400 \text{ cm}^{-1} \approx 1.15 \text{ kcal/mol} \quad (6.76)$$

This dissociation energy difference means that the activation energy for the thermal dissociation reaction should be 1.15 kcal/mol greater for the C–D dissociation than for the C–H dissociation.^{118c} The rate constants for the thermal C–H dissociation (k_H) and for the thermal C–D dissociation (k_D) are given by the following equations:

$$k_H = A_H e^{-E_a(\text{H})/RT} \quad (6.77)$$

$$k_D = A_D e^{-E_a(\text{D})/RT} \quad (6.78)$$

The terms $E_a(\text{H})$ and $E_a(\text{D})$ are each composed of two parts: an electronic part, E_e , which is presumed to be the same for the two cases, and a vibrational part, E_{vib} , which is different in the way described above. If the preexponential factors A_H and A_D are identical,¹²⁵ then the ratio k_H/k_D can be calculated to be

$$\frac{k_H}{k_D} = \exp \left[\frac{1.15 \times 10^3 \text{ cal mol}^{-1}}{(300 \text{ K})(1.98 \text{ cal mol}^{-1} \text{ K}^{-1})} \right] \quad (6.79)$$

so

$$\frac{k_H}{k_D} = e^{1.94} \approx 7 \quad (6.80)$$

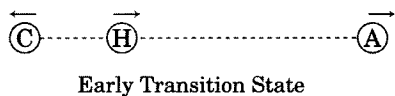
Thus, we predict that in a purely unimolecular, thermal reaction, the rate constant for a C–H bond dissociation should be approximately seven times greater than that for a C–D bond dissociation.^{118c} Slightly smaller values are predicted for homolytic dissociation of N–H and O–H bonds.^{118e} Primary kinetic isotope effects may be most pronounced for reactions that involve dissociation of bonds to hydrogen, since the mass of the leaving group doubles on going from hydrogen to deuterium and triples on going from hydrogen to tritium.¹²⁶ Nevertheless, kinetic investigations using isotopes

¹²⁵ This assumption is adequate for our purposes, but it is not always rigorously correct. See, for example, reference 117a, p. 146, for a discussion of A_H/A_D values in studies of bimolecular elimination reactions.

¹²⁶ The relationship between deuterium and tritium primary kinetic isotope effects is given by the Swain–Schaad equation:

$$\frac{k_H}{k_D} = \left(\frac{k_D}{k_T} \right)^x = \left(\frac{k_H}{k_T} \right)^{x/(x+1)}$$

where $x = 2.344$. Swain, C. G.; Stivers, E. C.; Reuwer, J. F., Jr.; Schaad, L. J. *J. Am. Chem. Soc.* **1958**, *80*, 5885. Also see Streitwieser, A., Jr.; Kaufman, M. J.; Bors, D. A.; Murdoch, J. R.; MacArthur, C. A.; Murphy, J. T.; Shen, C. C. *J. Am. Chem. Soc.* **1985**, *107*, 6983; Hirschi, J.; Singleton, D. A. *J. Am. Chem. Soc.* **2005**, *127*, 3294.

**FIGURE 6.51**

C · H · · · A vibration in an early transition state.

of other atoms can also provide useful information about reaction mechanisms.^{127,128}

Most organic processes of interest are not unimolecular thermolysis reactions.¹²⁹ Usually we investigate reactions in which one bond is broken and another is formed in the same elementary step. Based on the Hammond postulate (Figure 6.34), we can envision three scenarios for a reaction in which an atom A abstracts a hydrogen atom from a carbon atom.¹³⁰ In an exothermic reaction, the transition state occurs early (to the left on a reaction coordinate diagram). In an endothermic reaction, the transition state occurs late (to the right). In a thermoneutral reaction, the transition state occurs near the center of a reaction coordinate diagram.

If the transition state occurs early, the C–H or C–D bond will be broken only slightly in the transition structure. The stretching vibration in the transition state (shown in Figure 6.51) will be affected by the mass of the hydrogen (or deuterium) atom in much the same way as in the reactant. Therefore, the difference in transition state energy for the C–H or C–D species will be nearly the same in the transition structure as in the reactant. As shown on the hypothetical potential energy diagram for the abstraction shown in Figure 6.52, there will be only a small difference in activation energies for the C–H or C–D reactions. Therefore, k_H/k_D will be close to one for such a process.

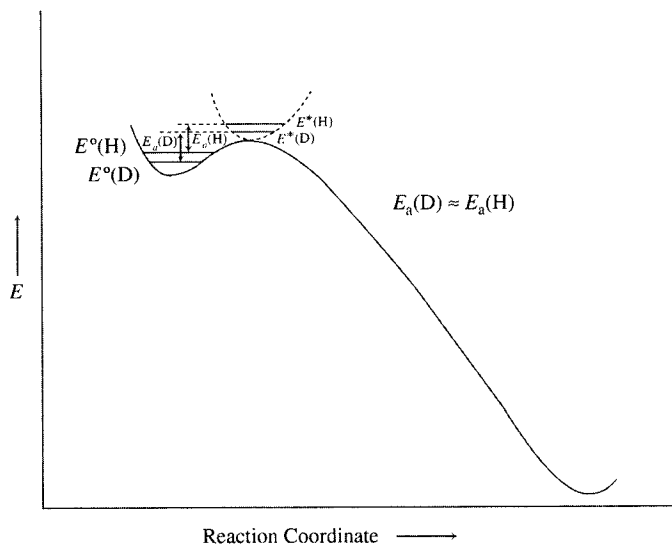
In a very endothermic reaction, the transition structure closely resembles the product (Figure 6.53). Although the original C–H or C–D bond will be almost fully broken, the bond between H or D and the abstracting atom (A) will be nearly fully developed. There will be almost the same difference in zero point energies for the developing A–H or A–D bond in the transition structure as there was in the C–H or C–D bond in the reactant (Figure 6.54). As a result, the activation energy for abstracting a deuterium will be very similar to that for abstracting a hydrogen atom, so again there will be only a very small primary kinetic isotope effect.

¹²⁷ Buncel, E.; Saunders, W. H., Jr., Eds. *Isotopes in Organic Chemistry*. Vol. 8. *Heavy Atom Isotope Effects*; Elsevier: Amsterdam, 1992. For an example of the application of both ¹³C and ¹⁸O isotope effects in the study of the same reaction, see Jacober, S. P.; Hanzlik, R. P. *J. Am. Chem. Soc.* **1986**, *108*, 1594; for the application of ¹⁴C, ³⁷Cl, and ²H isotope effects to a solvolysis reaction, see Burton, G. W.; Sims, L. B.; Wilson, J. C.; Fry, A. *J. Am. Chem. Soc.* **1977**, *99*, 3371; for the application of ¹¹C/¹⁴C kinetic isotope effects to study an enzymatic reaction, see Axelsson, B. S.; Bjurling, P.; Matsson, O.; Långström, B. *J. Am. Chem. Soc.* **1992**, *114*, 1502.

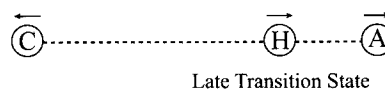
¹²⁸ In addition, isotope effects can have surprising effects in spectroscopy. For example, replacement of hydrogen by deuterium can alter ¹³C chemical shifts up to six bonds away from the site of the substitution. Berger, S.; Künzer, H. *Tetrahedron* **1983**, *39*, 1327; Servis, K. L.; Domenick, R. L. *J. Am. Chem. Soc.* **1986**, *108*, 2211.

¹²⁹ Some reactions of interest are unimolecular dissociations. For example, the shock tube dissociation of toluene to benzyl radical and hydrogen atom was studied by Hippler, H.; Troe, J. *J. Phys. Chem.* **1990**, *94*, 3803.

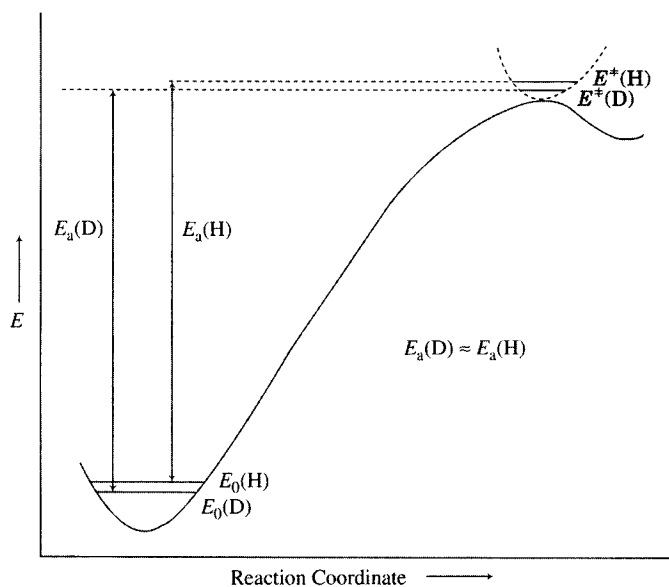
¹³⁰ Examples of such reactions include (a) the transfer of a hydrogen atom from diphenylmethane to a benzyl radical, reported by Bockrath, B. C.; Bittner, E. W.; Marecic, T. C. *J. Org. Chem.* **1986**, *51*, 15 and (b) the cytochrome P-450-catalyzed oxidation of octane reported by Jones, J. P.; Trager, W. F. *J. Am. Chem. Soc.* **1987**, *109*, 2171.

**FIGURE 6.52**

Origin of low k_H/k_D values for a very exothermic reaction. (Adapted from reference 118b.)

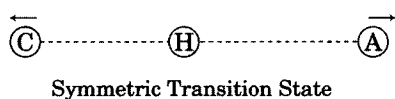
**FIGURE 6.53**

C ··· H · A vibration in a late transition state.

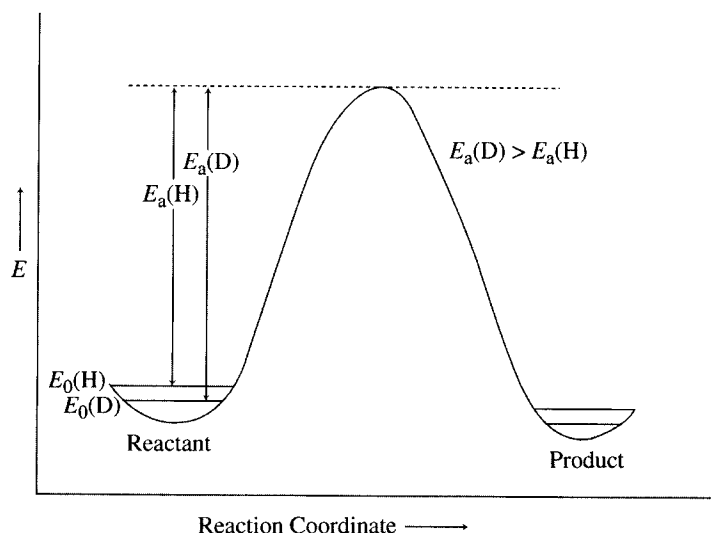
**FIGURE 6.54**

Origin of low k_H/k_D values for a very endothermic reaction. (Adapted from reference 118b.)

In a thermoneutral reaction, the transition state is symmetrically located along the reaction coordinate. Now the hydrogen atom does not move in the vibrational mode illustrated in Figure 6.55, so the frequency of the vibration does not depend on its mass. Therefore, $E^\ddagger(D) = E^\ddagger(H)$; that is, the transition

**FIGURE 6.55**

C · · H · · A vibrational mode in a symmetric transition state.

**FIGURE 6.56**

Origin of large $k_{\text{H}}/k_{\text{D}}$ value for a nearly thermoneutral reaction. (Adapted from reference 118b, p. 732.)

state energy is the same whether it is a hydrogen or deuterium atom that is being abstracted. As shown in Figure 6.56, the activation energies for the abstraction of H and D will differ by an amount equal to the difference in the C–H and C–D bond zero point energies, so there should be a significant kinetic isotope effect.^{131,132} This situation appears to describe the oxidation of $\text{CH}_3\text{CDOHCH}_3$ shown in Figure 6.48. Westheimer and Nicolaides found the value of $k_{\text{H}}/k_{\text{D}}$ for the reaction to be approximately 6, thereby supporting a mechanism in which the H–C bond is broken in the rate-limiting step of the reaction.¹³³

We might expect that the maximum hydrogen primary kinetic isotope effect for a reaction in which a C–H bond is broken would be $k_{\text{H}}/k_{\text{D}} = 7$, with smaller values for reactions that are either endothermic or exothermic. Indeed, the usual range for primary kinetic isotope effects is about 5–8. However, a ratio of $k_{\text{H}}/k_{\text{D}}$ of 25 was seen in one case,⁹⁵ and a value of 13,000 was reported in one unusual situation.¹³⁴ Obviously, our analysis of the possible magnitude of $k_{\text{H}}/k_{\text{D}}$ has been oversimplified. Two factors were specifically ignored above:

1. We considered C–H or C–D stretching vibrations but not C–H or C–D bending vibrations. If one adds these vibrations to the theoretical

¹³¹ The theoretical basis for kinetic isotope effects presented here is quite simplified. (See, for example, reference 118c, pp. 268–269.) For more theoretical discussions, see the sources cited in references 117 and 118. See also reference 46, pp. 296–297; Gilliom, R. *Introduction to Physical Organic Chemistry*; Addison-Wesley Publishing: Reading, MA, 1970.

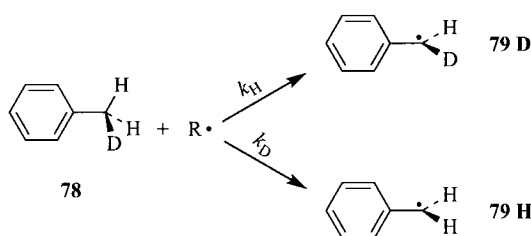
¹³² The effect of transition state location on kinetic isotope effects has been analyzed by Garrett, B. C.; Truhlar, D. G. *J. Am. Chem. Soc.* **1980**, *102*, 2559.

¹³³ Westheimer, F. H.; Nicolaides, N. *J. Am. Chem. Soc.* **1949**, *71*, 25.

¹³⁴ Brunton, G.; Griller, D.; Barclay, L. R. C.; Ingold, K. U. *J. Am. Chem. Soc.* **1976**, *98*, 6803.

FIGURE 6.57

The intramolecular primary hydrogen isotope effect.



determination of k_H/k_D values, the maximum value is larger. Bell estimated the maximum k_H/k_D value at 298 K to be 10.^{118e,135}

2. This analysis has ignored the possibility of tunneling, by which a hydrogen atom can move through an energy barrier with less than the energy needed to pass over it, but a more massive deuterium or tritium cannot easily do so.^{134,136–138}

The discussion to this point has considered only *intermolecular* effects, that is, the comparison of reaction rates for C–H or C–D bonds in different molecules. Let us now consider *intramolecular* kinetic isotope effects resulting from competition for reaction between C–H and C–D bonds in the same molecule.¹³⁹ Consider the free radical abstraction of a H or D atom from α -*d*-toluene (78) to give a benzyl radical (79, Figure 6.57).¹⁴⁰ The rate constants k_H and k_D represent the processes for abstracting hydrogen and deuterium, respectively.

The potential energy well of the reactant in Figure 6.58 shows only one vibrational energy level for 78, since any one molecule can have only one minimum vibrational energy level. However, abstraction of a hydrogen atom will leave behind a C–D bond, so the transition state will be lower in energy than that for abstraction of the deuterium atom, which would leave behind a C–H bond instead.¹⁴¹ As before, the removal of deuterium will require more energy, and thus it will be kinetically disfavored relative to the removal of hydrogen in this case as well.

The preceding analysis is consistent with experimental data for free radical halogenation of toluene. If the abstracting radical is a chlorine atom,

¹³⁵ The corresponding maximum k_H/k_T value at 298 K was calculated to be 27. For a discussion, see reference 118e.

¹³⁶ For a review see Bell, R. P. *The Tunnel Effect in Chemistry*; Chapman & Hall: New York, 1980.

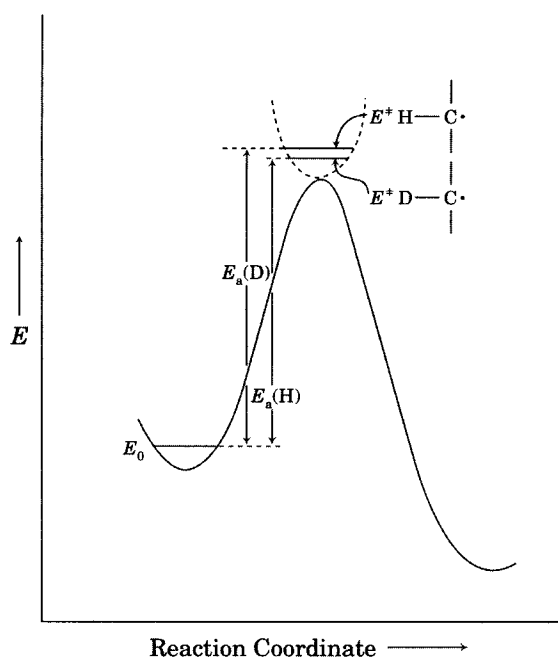
¹³⁷ Lewis, E. S.; Robinson, J. K. *J. Am. Chem. Soc.* **1968**, *90*, 4337.

¹³⁸ It has been calculated that 80% of the hydrogen atom transfer reaction $O + HD \rightarrow OH + D$ occurs by tunneling. Garrett, B. C.; Truhlar, D. G.; Bowman, J. M.; Wagner, A. F.; Robie, D.; Arepalli, S.; Presser, N.; Gordon, R. J. *J. Am. Chem. Soc.* **1986**, *108*, 3515.

¹³⁹ The magnitude of the secondary isotope effect is assumed to be small in comparison with the primary isotope effect for this reaction (reference 144). A method for the separation of primary and secondary isotope effects was reported by Hanzlik, R. P.; Hogberg, K.; Moon, J. B.; Judson, C. M. *J. Am. Chem. Soc.* **1985**, *107*, 7164, and a detailed analysis of primary and secondary isotope effects in this system was given by Hanzlik, R. P.; Schaefer, A. R.; Moon, J. B.; Judson, C. M. *J. Am. Chem. Soc.* **1987**, *109*, 4926.

¹⁴⁰ For a discussion of the abstraction of hydrogen atoms by radicals, see Tedder, J. M. *Q. Rev. Chem. Soc.* **1960**, *14*, 336. For a discussion of the photochlorination of alkanes in solution, see Ingold, K. U.; Luszyk, J.; Raner, K. D. *Acc. Chem. Res.* **1990**, *23*, 219.

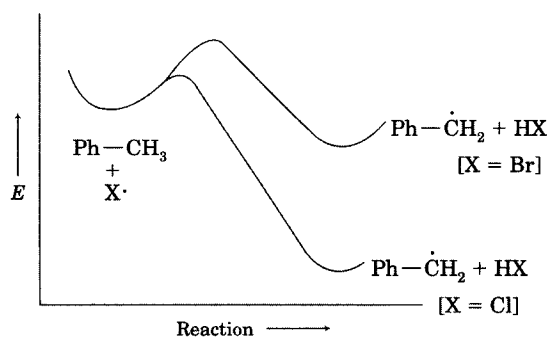
¹⁴¹ It is the vibrational zero point energy of the C–H or C–D bond remaining in the molecule, not the vibrational zero point energy of the bond that is being broken, that produces the difference in transition state energy.

**FIGURE 6.58**

Reaction coordinate diagram for intramolecular primary hydrogen kinetic isotope effect. (Adapted from reference 118b.)

k_H/k_D is 1.3 for reaction in CCl_4 solution at 77°C . If the abstracting atom is bromine, however, the ratio is 4.6.¹⁴² We interpret the results to mean that the transition state lies further to the right for the bromine abstraction, so more radical character is developed at the transition state and there is a greater difference between the energies of the benzyl radical with deuterium and the radical without deuterium substitution (Figure 6.59).

Kinetic isotope effects generally decrease with increasing reaction temperature, since the small difference between C–H and C–D dissociation pathways becomes less significant as more energy is available to the system.¹⁴³ For example, Table 6.4 shows data for the free radical bromination of

**FIGURE 6.59**

Reaction coordinate diagram for abstraction of H by $\text{Br}\cdot$ and by $\text{Cl}\cdot$. (Adapted from reference 118b.)

¹⁴² Wiberg, K. B.; Slauch, L. H. *J. Am. Chem. Soc.* **1958**, *80*, 3033 and references therein.

¹⁴³ This statement is correct for PKIE measurements in which a single reaction step determines the observed reaction rate. In more complex cases, however, the observed PKIE can *increase* with increasing temperature. For example, see Koch, H. F.; Koch, A. S. *J. Am. Chem. Soc.* **1984**, *106*, 4536.

TABLE 6.4 Values of k_H/k_D for Gas Phase Bromination of α -Deuteriotoluene

T ($^{\circ}\text{C}$)	k_H/k_D
121	6.69
130	6.53
142	6.17
150	5.93
160	5.69

Source: Reference 144.

α -deuteriotoluene in the gas phase to give benzyl bromide and α -deuteriobenzyl bromide.¹⁴⁴

Secondary Kinetic Isotope Effects

All of the isotope effects discussed so far have been primary kinetic isotope effects. A secondary kinetic isotope effect can arise when a bond to the isotope is not broken during the rate-limiting step of a reaction. Generally, secondary kinetic isotope effects are much smaller in magnitude than are primary kinetic isotope effects.¹⁴⁵ Secondary kinetic isotope effects can nevertheless serve as useful probes of transition state structure because the magnitude of the effect generally increases as the transition structure changes from reactant-like to product-like.^{40,146}

We divide secondary kinetic isotope effects into subgroups depending on the location of the isotope with respect to the reaction site. If the isotope is bonded to the atom undergoing reaction, the effect is said to be an α secondary isotope effect. We further divide α effects into the following three categories:¹⁴⁵

1. Normal ($k_H/k_D > 1$) α secondary kinetic isotope effects are seen for hybridization changes of the type $sp^3 \rightarrow sp^2$ or $sp^2 \rightarrow sp$. Consider the ionization of an alkyl halide, Figure 6.60(a).¹⁴⁷ The carbon orbital used for C–H bonding changes from sp^3 to sp^2 upon formation of the carbocation. Such reactions are slower when a hydrogen bonded to C_α is replaced with deuterium due to the effect of hybridization change on the energies of C–H and C–D bending vibrations, and a k_H/k_D of 1.15 per D is typical for normal α secondary hydrogen kinetic isotope effects.¹⁴⁸ For example, the acid-catalyzed dehydration of *p,p'*-dimethoxybenzhydrol (**80**) in Figure 6.61(a) has a $k_H/k_D = 1.18$.¹⁴⁹

¹⁴⁴ Timmons, R. B.; de Guzman, J.; Varnerin, R. E. *J. Am. Chem. Soc.* **1968**, *90*, 5996. Product ratios were determined from ratios of H_2 , HD, and D_2 produced from the HBr and DBr by-products of the reaction. Because $\text{C}_6\text{H}_5\text{CH}_2\text{D}$ contains two abstractable hydrogen atoms and one deuterium atom, the ratio of the rate constant for hydrogen abstraction to that for deuterium abstraction was divided by 2 to give the k_H/k_D value for the reaction.

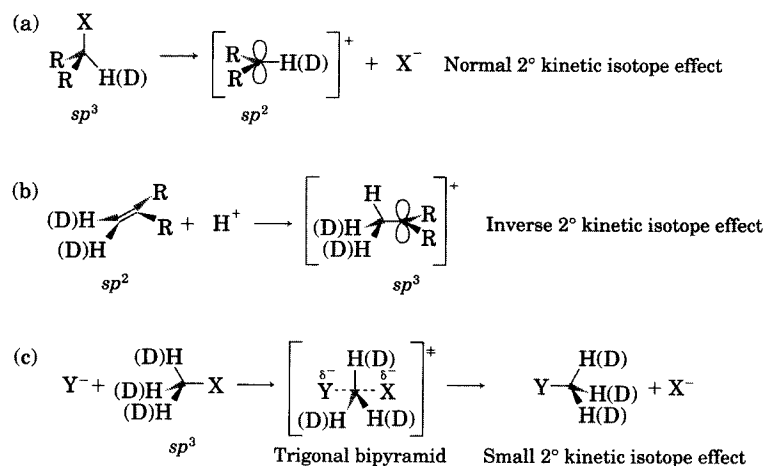
¹⁴⁵ Halevi, E. A. *Prog. Phys. Org. Chem.* **1963**, *1*, 109.

¹⁴⁶ Kovach, I. M.; Elrod, J. P.; Schowen, R. L. *J. Am. Chem. Soc.* **1980**, *102*, 7530.

¹⁴⁷ For a discussion of secondary deuterium isotope effects on reactions that involve carbocation formation, see Sunko, D. E.; Hehre, W. J. *Prog. Phys. Org. Chem.* **1983**, *14*, 205.

¹⁴⁸ Streitwieser, A., Jr.; Jagow, R. H.; Fahey, R. C.; Suzuki, S. J. *Am. Chem. Soc.* **1958**, *80*, 2326.

¹⁴⁹ Stewart, R.; Gatzke, A. L.; Mocek, M.; Yates, K. *Chem. Ind. (London)* **1959**, 331.

**FIGURE 6.60**Types of α secondary kinetic isotope effects.

2. **Inverse** ($k_H/k_D < 1$) α secondary kinetic isotope effects are seen for hybridization changes in the opposite direction ($sp \rightarrow sp^2$ or $sp^2 \rightarrow sp^3$). One process leading to an inverse secondary kinetic isotope effect would be the protonation of an alkene, as shown for structure **81** in Figure 6.61(b). For example, the thiocyanate-catalyzed *cis*-*trans* isomerization of maleic acid, Figure 6.61(b), has a k_H/k_D of 0.86 at 25°C.¹⁵⁰

3. Reactions that convert sp^3 -hybridized atoms to trigonal bipyramidal transition structures, as in S_N2 reactions, exhibit a third category of α effects. Even though we commonly describe such trigonal bipyramidal transition structures as sp^2 -hybridized, such k_H/k_D values are unity or very

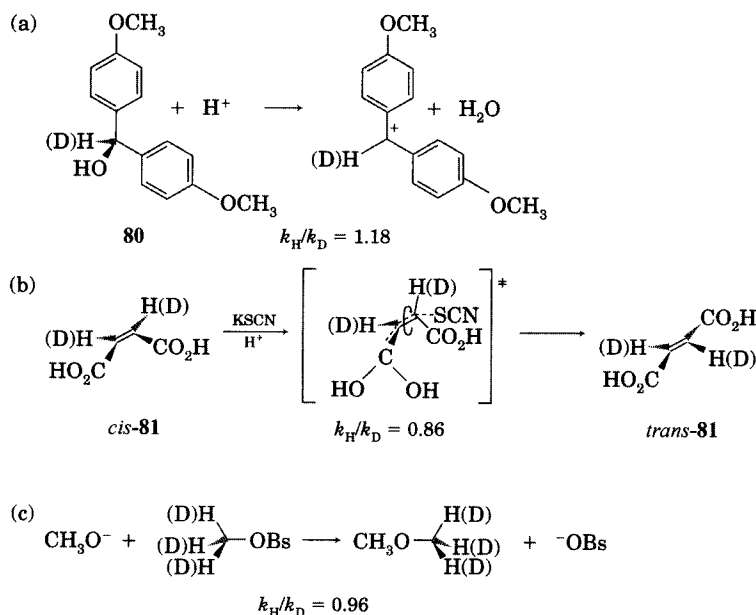
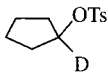
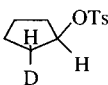
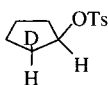
**FIGURE 6.61**Examples of α secondary kinetic isotope effects.¹⁵⁰ Seltzer, S. J. *Am. Chem. Soc.* **1961**, 83, 1861.

TABLE 6.5 Isotope Effects on Cyclopentyl Tosylate Solvolysis (Relative to Rate for Cyclopentyl Tosylate)

Compound	k_H/k_D
	1.15
	1.16
	1.22

Source: Reference 148.

slightly inverse for these kinds of reactions.^{145,151} For the reaction shown in Figure 6.61(c), $k_H/k_D = 0.96$.¹⁵²

If the isotope is bonded to an atom that is adjacent to the site of reaction, then a **β secondary isotope effect** may be observed. We might expect β secondary isotope effects to be smaller than α effects because the isotopic substituent is further from the reaction site, but this is not necessarily the case. S_N1 substitutions with β -D generally show $k_H/k_D > 1$, as indicated by the series of deuterated cyclopentyl tosylates in Table 6.5.¹⁴⁸ Numerous explanations have been advanced to explain results of this kind, but the most generally accepted view is that isotope effects on vibrations of β C–H or C–D bonds are most important. In short, donation of C–H or C–D bonding electron density to a center of positive charge decreases the strength of the C_β –H or C_β –D bonds. Thus, there is a smaller difference between the zero point energy of C–H and C–D in the transition structure than in the reactant, so the activation energy increases for the deuterated compound.¹⁵³ In addition to stretching vibrations, bending modes of the β -substituted atoms may also be important.^{148,154}

Isotope effects may be seen in equilibrium constants as well as in rate constants. The acidities of several carboxylic acids substituted with deuterium on the β carbon atom have equilibrium isotope effects, $K_{a(H)}/K_{a(D)}$ greater than 1.0 (Table 6.6).¹⁵⁵ The simplest explanation of the data is that CD_3 or CD_2 groups are electron-releasing with respect to CH_3 and CH_2 groups.¹⁵⁶

¹⁵¹ Westaway, K. C. in reference 117c, p. 275; McLennan, D. J. in reference 117c, p. 393.

¹⁵² Johnson, R. R.; Lewis, E. S. *Proc. Chem. Soc.* **1958**, 52.

¹⁵³ Boozer, C. E.; Lewis, E. S. *J. Am. Chem. Soc.* **1954**, 76, 794.

¹⁵⁴ For a theoretical study of the relationship between the structure of S_N2 transition states and secondary α -deuterium kinetic isotope effects, see Poirier, R. A.; Wang, Y.; Westaway, K. C. *J. Am. Chem. Soc.* **1994**, 116, 2526.

¹⁵⁵ Data from Streitwieser, A., Jr.; Van Sickle, D. E. *J. Am. Chem. Soc.* **1962**, 84, 254 and references therein. The values of $K_{a(H)}/K_{a(D)}$ in Table 6.6 reflect the contribution from all of the deuterium atoms in the structure indicated. The values shown are not on a per deuterium basis.

¹⁵⁶ See the discussion by Servis, K. L.; Domenick, R. L. *J. Am. Chem. Soc.* **1985**, 107, 7186; Halevi, E. A.; Nussim, M.; Ron, A. *J. Chem. Soc.* **1963**, 866.

TABLE 6.6 Isotope Effects on Acid Strengths

Deuterated Acid	$K_{a(H)}/K_{a(D)}$
C_6D_5OH	$1.12 \pm .02$
C_6D_5COOH	$1.024 \pm .006$
$C_6H_5CD_2COOH$	$1.12 \pm .02$
D_2COOH	$1.06 \pm .03$
CD_3COOH	$1.033 \pm .002$

Source: Reference 155.

This simple inductive explanation is not consistent with the results of theoretical calculations, however,¹⁵⁷ and 2° deuterium KIEs have been attributed to different hyperconjugation effects of C–H and C–D bonds.¹⁵⁸ It is possible to see effects still further removed, but γ kinetic isotope effects are usually very small.¹⁵⁹

Recall from Figure 6.50 that the lower ZPE of C–D compared to C–H and the anharmonicity of the electronic potential energy curve cause the C–D bond to be slightly shorter than the C–H bond. In fact, deuterium is taken to have a smaller van der Waals radius than hydrogen in molecular mechanics calculations.¹⁶⁰ This suggests the possibility of steric isotope effects.^{161–163} For the atropisomerization of the biphenyl **82**, k_H/k_D was found to be 0.84.¹⁶⁴ Cyclohexane-*d*₁ (**83**, Figure 6.62) was reported to prefer the conformation with the D equatorial over that with the D axial by 6.3 cal/mol (0.0063 kcal/mol)^{165,166}. Similarly, the equilibrium constant between the chair conformation of 1-trideuteriomethyl-1,3,3-trimethylcyclohexane (**84**) with the trideuterio group axial (**84a**) and the conformation with the trideuterio group equatorial (**84e**) was found to be 1.042 ± 0.001 . Theoretical calculations suggested that the greater stability of the axial trideuterio conformation arises from nonbonded interactions, making the conformational preference a true steric isotope effect.^{167,168}

¹⁵⁷ Perrin, C. L.; Dong, Y. *J. Am. Chem. Soc.* **2007**, *129*, 4490.

¹⁵⁸ Shiner, Jr., V. J. *J. Am. Chem. Soc.* **1956**, *78*, 2653; Lewis, E. S.; Johnson, R. R.; Coppinger, G. M. *J. Am. Chem. Soc.* **1959**, *81*, 3140; Leffek, K. T.; Llewellyn, J. A.; Robertson, R. E. *Can. J. Chem.* **1960**, *38*, 2171.

¹⁵⁹ Leffek, K. T.; Llewellyn, J. A.; Robertson, R. E. *J. Am. Chem. Soc.* **1960**, *82*, 6315.

¹⁶⁰ Allinger, N. L.; Flanagan, H. L. *J. Comput. Chem.* **1983**, *4*, 399.

¹⁶¹ Bartell, L. S. *J. Am. Chem. Soc.* **1961**, *83*, 3567.

¹⁶² For a more detailed description, see reference 118a, p. 189 ff; Carter, R. E.; Melander, L. *Adv. Phys. Org. Chem.* **1973**, *10*, 1; Bartell, L. S. *J. Am. Chem. Soc.* **1961**, *83*, 3567.

¹⁶³ See, however, Dunitz, J. D.; Ibberson, R. M. *Angew. Chem. Int. Ed.* **2008**, *47*, 4208.

¹⁶⁴ Melander, L.; Carter, R. E. *J. Am. Chem. Soc.* **1964**, *86*, 295.

¹⁶⁵ Anet, F. A. L.; Kopelevich, M. *J. Am. Chem. Soc.* **1986**, *108*, 1355, 2109; a value of 8.3 ± 1.5 cal/mol was reported later by Anet, F. A. L.; O'Leary, D. J. *Tetrahedron Lett.* **1989**, *30*, 1059.

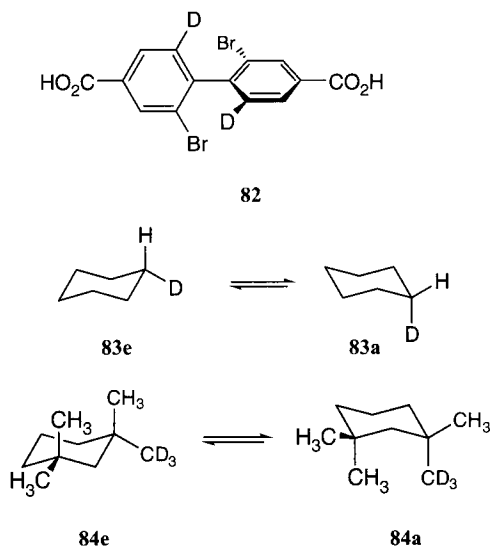
¹⁶⁶ Williams, I. H. *J. Chem. Soc. Chem. Commun.* **1986**, 627; Aydin, R.; Günther, H. *Angew. Chem. Int. Ed. Eng.* **1981**, *20*, 985.

¹⁶⁷ Saunders, M.; Wolfsberg, M.; Anet, F. A. L.; Kronja, O. *J. Am. Chem. Soc.* **2007**, *129*, 10276. For another example, see Hayama, T.; Baldridge, K. K.; Wu, Y.-T.; Linden, A.; Siegel, J. S. *J. Am. Chem. Soc.* **2008**, *130*, 1583.

¹⁶⁸ Steric isotope effects can also operate intermolecularly, for example, in supramolecular assemblies. Felder, T.; Schalley, C. A. *Angew. Chem. Int. Ed.* **2003**, *42*, 2258.

FIGURE 6.62

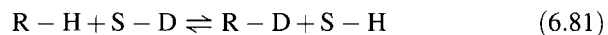
Conformations of deuterated cyclohexanes.



Solvent Isotope Effects

A **solvent isotope effect** is observed when the rate constant or the equilibrium constant for a process changes when a solvent is replaced with an isotopically substituted solvent.¹⁶⁹ Most often solvent isotope effect studies involve a hydroxylic solvent in which the OH group is replaced with an OD group. For example, the value of K_H/K_D for ionization of phenylacetic acid in H_2O versus ionization of phenylacetic acid-*O-d* in D_2O is 3.¹⁴⁵ Schowen has indicated three ways for solvent isotope effects to occur:^{169a}

1. The solvent may be a reactant. As with other reactions, there may be a 1° solvent isotope effect if proton is transferred in the rate-limiting step; otherwise there may be a 2° solvent isotope effect.
2. Solvent protons (or deuterons) may exchange with reactant protons, leading to labeled reactant. The **isotopic fractionation factor**, denoted ϕ , indicates the equilibrium distribution of the isotopic label between solute (R-H) and solvent (S-D). For the reaction



ϕ is defined as

$$\phi = \frac{[R - D][S - H]}{[R - H][S - D]} \quad (6.82)$$

3. Interactions of the transition structure with solvent molecules may be different in an isotopically labeled solvent.

¹⁶⁹ For an introduction, see (a) Schowen, R. L. *Prog. Phys. Org. Chem.* **1972**, 9, 275; (b) Kresge, A. J.; More O'Ferrall, R. A.; Powell, M. F. in Buncl, E.; Lee, C. C., Eds. *Isotopes in Organic Chemistry, Volume 7, Secondary and Solvent Isotope Effects*; Elsevier: Amsterdam, 1987; p. 177 ff.

Interpreting solvent kinetic isotope effects in terms of these interactions can provide information about the transition structure, its solvation, or both. With one technique, known as the **proton inventory** technique, the rate of a reaction is studied in a series of mixtures of H₂O and D₂O. The isotope effect, $k_n/k_{\text{H}_2\text{O}}$, is plotted versus the parameter n , the mole fraction of deuterium in the solvent. The slope and curvature of the resulting plot are then analyzed for information about the number and role of solvent molecules involved in the rate-limiting step.^{170,171}

6.7 SUBSTITUENT EFFECTS

In studying mechanisms, our goal is not just to write down the steps that occur in a reaction. We also want to use that information to make predictions about other reactions. Suppose we carry out a reaction such as



and then modify the reactant with a substituent, thus changing the group R₁ to R₂. Now the reaction is



We want to be able to predict the effect of this substituent on the rate constant or equilibrium constant of the new reaction.

Traditionally, the electronic effect of such a substituent has been described in terms of induction and resonance.^{172,173} Substituents that can donate or withdraw electrons by resonance are categorized as +R and -R, respectively.^{174,175} The substituent must have an orbital with p character (alone or as part of a π system) that can either donate one or more electrons to, or accept one or more electrons from, another part of the molecule. Some +R substituents include the halogens as well as OR and NR₂ groups (where R can be H). Methyl and other alkyl groups are also considered +R substituents, as we have noted in discussions of the PMO model for stabilization of carbocations and radicals by alkyl groups. Some -R groups include NO₂, CN, CO₂R, and C₆H₅.¹⁷²

Substituent groups may also be categorized according to their inductive effects as either electron-donating (+I) or electron-withdrawing (-I). The

¹⁷⁰ Batts, B. D.; Gold, V. *J. Chem. Soc. A* **1969**, 984.

¹⁷¹ For an example of the use of the proton inventory technique in the study of a reaction mechanism, see Bokser, A. D.; York, K. A.; Hogg, J. L. *J. Org. Chem.* **1986**, *51*, 92.

¹⁷² Additional effects can be classified as statistical considerations (e.g., the effect of an additional carboxylic acid group on the pK_a of a carboxylic acid), tautomeric, solvation, polarizability, and internal hydrogen bonding effects. Clark, J.; Perrin, D. D. *Q. Rev. Chem. Soc.* **1964**, *18*, 295.

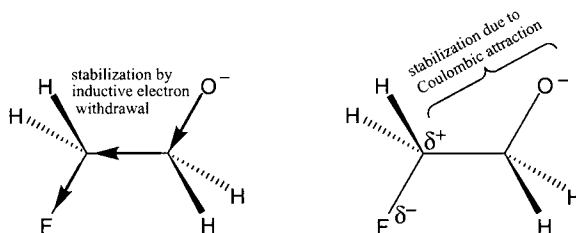
¹⁷³ Taft, R. W., Jr. in Newman, M. S., Ed. *Steric Effects in Organic Chemistry*; John Wiley & Sons: New York, 1956; p. 556 and references therein.

¹⁷⁴ See the listing in reference 1. Resonance effects are sometimes referred to as **mesomeric** effects. Substituents that interact through resonance interactions have been described as +M (electron-donating through resonance) or -M (electron-withdrawing through resonance) substituents. See, for example, Gold, V.; Loening, K. L.; McNaught, A. D.; Sehmi, P. *Compendium of Chemical Terminology. IUPAC Recommendations*; Blackwell Scientific Publications: Oxford, 1987; p. 250.

¹⁷⁵ For a more detailed analysis of possible interactions between substituents and a reaction site, see Katritzky, A. R.; Topsom, R. D. *J. Chem. Educ.* **1971**, *48*, 427.

FIGURE 6.63

(a) Inductive (through-bond) effect and (b) field (through-space) effect.



+I substituents are limited to alkyl groups such as methyl and to negatively charged substituents, such as O⁻ and NH⁻ groups. The -I substituents include all those groups that are deactivating in electrophilic aromatic substitution, as well as other groups that have electronegative atoms at the point of attachment.

The effect that we commonly call induction is often represented by arrows representing the polarization of σ bonds, as shown in Figure 6.63(a). For example, we could ascribe the greater acidity of 2-fluoroethanol than of ethanol to the electronegativity of the fluorine, which stabilizes the alkoxide ion by "pulling" electron density toward itself through the σ bond framework, thus reducing the extent of negative charge localization on the oxygen.¹⁷⁶ Induction may be more complex than is suggested by a simple model involving shifts of electrons in one σ bond after another through a molecule, however. We also have to consider the possibility of **field effects** (electrostatic effects) in which the substituent influences a remote site by an electrostatic potential operating through space, Figure 6.63(b). In most cases, increasing the number of bonds between a substituent and a probe site also increases the distance between them, so it is difficult to assign an effect to one or the other mode of transmission. Moreover, when model systems are chosen, the molecular skeletons must be fixed, otherwise conformational changes will allow a variety of orientations between the substituent and the reaction site.

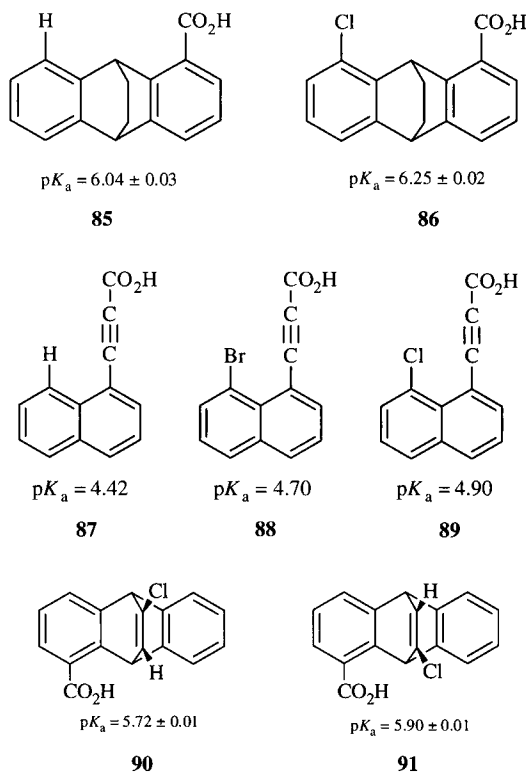
Several studies have been designed to determine the importance of through-space (field) and through-bond (inductive) effects. An electron-withdrawing substituent X that would be expected to increase the acidity of a model carboxylic acid by a through-bond effect could also *decrease* the acidity by a through-space effect if the negative end of the C-X dipole is closer to the carboxylate group than is the positive end of the dipole. In a study of the carboxylic acids **85** and **86**, the electron-withdrawing chlorine substituent in **86** was found to decrease the acidity of the parent compound (**85**).¹⁷⁷ Similarly, in a series of 3-(8-substituted-1-naphthyl)propionic acids (**87**, **88**, and **89**), acidity decreases as the substituent X is changed from H to Br to Cl.¹⁷⁸ The effect of angularity is seen even more clearly with compounds **90** and **91**. The acidity of **90** is greater, even though the electron-withdrawing chlorine is one bond closer to the carboxylic acid functionality in **91** than in **90**. The simplest explanation is that the negative end of the C-Cl dipole is aligned toward the carboxylate ion in **91** but away from it in **90**, suggesting that

¹⁷⁶ It might appear that the acid-strengthening effect of the fluorine is enthalpic, but there can also be an entropic effect due to differences in solvent reorganization upon deprotonation of ethanol and 2-fluoroethanol. This topic will be addressed in Chapter 7.

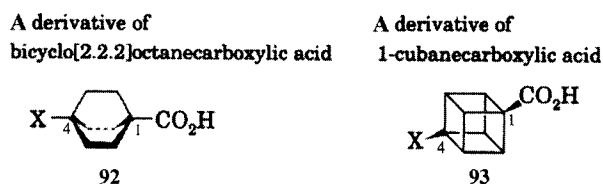
¹⁷⁷ Golden, R.; Stock, L. M. *J. Am. Chem. Soc.* **1966**, *88*, 5928.

¹⁷⁸ Bowden, K.; Hojatti, M. *J. Chem. Soc. Chem. Commun.* **1982**, 273; *J. Chem. Soc. Perkin Trans. 2* **1990**, 1197. See also Roberts, J. D.; Carboni, R. A. *J. Am. Chem. Soc.* **1955**, *77*, 5554.

through-space interactions are more important than through-bond interactions.¹⁷⁹ However, alternative explanations are possible. For example, it may be that substitution can affect acidities by altering solvation of the acid and carboxylate functions.



Another approach is to study compounds based on derivatives of bicyclo[2.2.2]octane and cubane.^{180,181} The carbon atoms labeled 1 and 4 are essentially the same distance apart in the two parent compounds ($\pm 0.01 \text{ \AA}$). There are three different three-bond paths connecting C1 and C4 in bicyclo[2.2.2]octane, but there are six analogous three-bond paths in cubane. A series of 4-substituted cubanecarboxylic acids (**92**)¹⁸² and 4-substituted bicyclo[2.2.2]octane-1-carboxylic acids (**93**)¹⁸³ showed similar effects of a substituent X on the pK_a of each parent compound.



¹⁷⁹ Grubbs, E. J.; Wang, C.; Deardurff, L. A. *J. Org. Chem.* **1984**, *49*, 4080.

¹⁸⁰ Davidson, R. B.; Williams, C. R. *J. Am. Chem. Soc.* **1978**, *100*, 2017 and references therein.

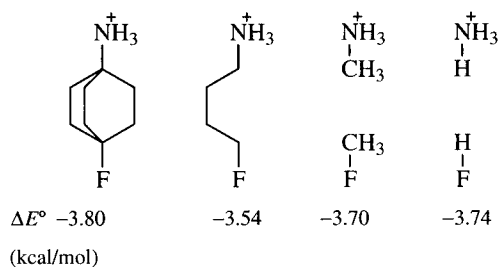
¹⁸¹ A study of 6-substituted derivatives of spiro[3.3]heptane-2-carboxylic acids also indicated that field and not inductive effects were dominant: Liotta, C. L.; Fisher, W. F.; Greene, G. H., Jr.; Joyner, B. L. *J. Am. Chem. Soc.* **1972**, *94*, 4891.

¹⁸² Cole, T. W., Jr.; Mayers, C. J.; Stock, L. M. *J. Am. Chem. Soc.* **1974**, *96*, 4555 and references therein.

¹⁸³ Wilcox, C. F.; Leung, C. *J. Am. Chem. Soc.* **1968**, *90*, 336.

FIGURE 6.64

Stabilization energies calculated for model compounds. (Reproduced from reference 185.)



These results might be interpreted to mean that field effects and not inductive effects are dominant. However, when conclusions about the magnitude of some nonobservable property are based on comparison of an experimentally determined value with the value expected for another system, it is essential to examine the assumptions made about the reference system. In this case, our expectation that inductive effects in compounds **92** and **93** should be different because of a different number of bond pathways may be invalid if we are intuitively viewing the molecules **92** and **93** as atoms held together by lines (perhaps thin metallic wires) that conduct electric charge. Davidson and Williams used semiempirical calculations to study the transmission of substituent electronic effects through the cubyl and bicyclo[2.2.2]-octyl systems in detail.¹⁸⁰ The calculations agreed with the experimental results in that both systems were seen to transmit substituent electronic effects equally—that is, equally poorly. The calculations revealed that the electronic effect of most substituents decreased to a negligible value through either molecular framework, so it was difficult to ascribe the effects of the substituents to any transmission of electronic properties through the σ framework.¹⁸⁴ This conclusion was reinforced by results of theoretical calculations in which the effect of a substituent on a molecular framework was found to be essentially the same, even when chemical bonds between the substituent and reacting sites were omitted (Figure 6.64).¹⁸⁵

The cumulative evidence from the studies cited here suggests that polarization effects generally are not transmitted through many carbon-carbon σ bonds and that often simple electrostatic effects can satisfactorily describe the experimental results.^{186,187} There are other analyses that seem more consistent with the dominance of an inductive effect for studies involving dissociation of positively charged ions or for investigations of the electrostatic theory in solvents of varying polarity.¹⁸⁸ However, any attempt to partition the effect of a substituent into separate inductive and field effects

¹⁸⁴ Similar results have been obtained in other investigations, such as those that determine the effect of substituents on NMR chemical shifts of atoms at various points on a molecular skeleton. Compare Adcock, W.; Butt, G.; Kok, G. B.; Marriott, S.; Topsom, R. D. *J. Org. Chem.* **1985**, *50*, 2551.

¹⁸⁵ Marriott, S.; Topsom, R. D. *J. Am. Chem. Soc.* **1985**, *107*, 2253 and references therein. See also Adcock, W.; Baran, Y.; Filippi, A.; Speranza, M.; Trout, N. A. *J. Org. Chem.* **2005**, *70*, 1029; Campanelli, A. R.; Domenicano, A.; Ramondo, F. *J. Phys. Chem. A* **2006**, *110*, 10122.

¹⁸⁶ (a) Stock, L. M. *J. Chem. Educ.* **1972**, *49*, 400; (b) Bowden, K.; Grubbs, E. J. *Prog. Phys. Org. Chem.* **1993**, *19*, 183.

¹⁸⁷ Bianchi, G.; Howarth, O. W.; Samuel, C. J.; Vlahov, G. *J. Chem. Soc. Chem. Commun.* **1994**, 629; analyzed NMR shifts of long-chain esters and acids in terms of inductive effects operating through up to fourteen carbon-carbon σ bonds.

¹⁸⁸ Exner, O.; Friedl, Z. *Prog. Phys. Org. Chem.* **1993**, *19*, 259.

may be futile. Shorter commented that “the electrostatic forces operating at a reaction centre are governed by the complete electron distribution of the molecule and it is this that is modified by the introduction of a substituent.” He also noted that it is misguided to think that one of the inductive and field models must be true and the other false. “This is an error. Both models are gross simplifications. . . .”¹⁸⁹ Exner and co-workers concluded that the field effects and induction are “two opposite approximations,” both of which are capable of being extended to produce more accurate results for most compounds.^{188,190} They also noted that this conclusion was put forth earlier by Hammett, who wrote that “both the inductive effect and the electric field effect should be recognized as methods of mathematical approximation. . . . The temptation to treat them as distinct physical phenomena should, however, be firmly resisted.”⁹⁵

Induction and field effects are, therefore, yet another example of complementary models that provide useful beginning points for the discussion of organic chemistry but that should not be viewed as pictures of reality.

6.8 LINEAR FREE ENERGY RELATIONSHIPS

It is useful to make a qualitative prediction of the effect of a substituent on one chemical reaction, but we would like to be able to extend this understanding to predict how the same substituent will affect some other reaction. Moreover, it would be helpful to have a procedure for using our knowledge of the effect that different substituents have on a particular reaction to help us understand the mechanism of that reaction. It is more difficult to treat both steric and electronic effects simultaneously, so we will first consider systems in which the effects of a substituent are primarily induction/field effects or resonance effects but not steric effects. The approach that we will take illustrates the use of a **linear free energy relationship** (LFER) to relate values of ΔG or ΔG^\ddagger from one reaction to another.^{78,191,192}

Consider a molecular system composed of three parts: a reactive site (R) is attached through a molecular framework (\square) to a substituent (S), as shown in Figure 6.65. The product of the reaction has the same structure except for a functional group change (P) resulting from the reaction. We assume that S and R (or P) are sufficiently far apart that they do not interact with each other sterically; that is, a change in the size of the substituent does not affect the reaction. The effect of the connecting framework is to transmit the electronic effect of the substituent to the site of the R \rightarrow P transformation.

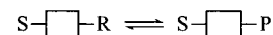


FIGURE 6.65

Schematic representation of a model system for studying equilibrium substituent effects.

¹⁸⁹ Shorter, J. in Zalewski, R. I.; Krygowski, T. M.; Shorter, J., Eds. *Similarity Models in Organic Chemistry, Biochemistry and Related Fields*; Elsevier: Amsterdam, 1991; p. 77.

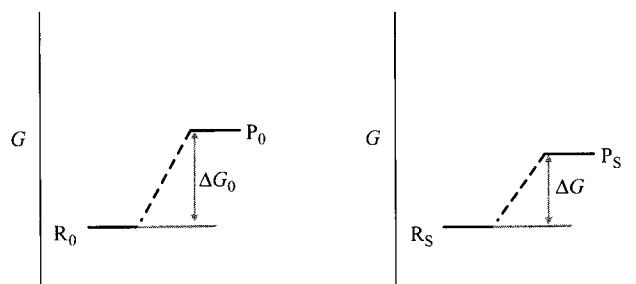
¹⁹⁰ Böhm, S.; Exner, O. *Collect. Czech. Chem. Commun.* **2004**, *69*, 984. See also Exner, O.; Böhm, S. *J. Phys. Org. Chem.* **2006**, *19*, 393.

¹⁹¹ Fuchs, R.; Lewis, E. S. in Lewis, E. S., Ed. *Investigation of Rates and Mechanisms of Reactions*, 3rd. ed., Part I; Wiley-Interscience: New York, 1974; pp. 777–824.

¹⁹² Buncl and Wilson discussed the relationship of linear free energy relationships to the larger problem of structure–activity relationships in organic chemistry: Buncl, E.; Wilson, H. *J. Chem. Educ.* **1987**, *64*, 475. Their conclusion—that the concept of structure–activity relationships is an oversimplification, but one that provides a model that is complementary to other approaches to studying organic chemistry—is entirely consistent with the major theme of this text.

FIGURE 6.66

Reaction coordinate diagrams for reference (left) and substituted (right) reaction.



Hammett proposed that for systems of this kind it should be possible to correlate the equilibrium constant with the substituent effect as shown in equation 6.85, which is known as the **Hammett equation**.^{95,193-195}

$$\log \frac{K}{K_0} = \sigma\rho \quad (6.85)$$

where K is the equilibrium constant for the reaction with a substituent S in place and K_0 is the equilibrium constant for a reference compound having a hydrogen atom as a substituent at that same position. The symbol σ in these equations is the **substituent constant**, which indicates the electronic effect of the substituent S at a particular position. The symbol ρ is the **reaction constant**, which measures the sensitivity of the reaction to the electronic effect of a substituent at a particular position in the molecular framework.

For the reaction of the "unsubstituted" compound (substituent = H) and the substituted analog (substituent = S), respectively, we can draw the Gibbs diagrams in Figure 6.66. Here ΔG_0 is the change in free energy for the conversion of reactant to product for the unsubstituted reactant, while ΔG is the free energy change for the reaction with a substituent S in place. In this example, the effect of the substituent is such that ΔG is less than ΔG_0 , but in some cases it might be larger.

Rewriting equation 6.85 as

$$\log \frac{K}{K_0} = \log K - \log K_0 = \sigma\rho \quad (6.86)$$

We calculate that

$$-\frac{\Delta G}{2.3RT} + \frac{\Delta G_0}{2.3RT} = \sigma\rho \quad (6.87)$$

So

$$\Delta G = \Delta G_0 - (2.3RT)\sigma\rho \quad (6.88)$$

Equation 6.88 makes it clear that equation 6.85 is a linear free energy relationship. That is, the free energy change for one reaction relative to the

¹⁹³ Hammett, L. P. *J. Am. Chem. Soc.* **1937**, 59, 96; reference 95, pp. 347 ff and references therein; see also Hammett, L. P. *Chem. Rev.* **1935**, 17, 125.

¹⁹⁴ Jaffé, H. H. *Chem. Rev.* **1953**, 53, 191.

¹⁹⁵ Johnson, C. D. *The Hammett Equation*; Cambridge University Press: Cambridge, England, 1973.

other is directly proportional to the product of two parameters, one that depends on the nature of the reaction (ρ) and one that depends on the nature of the substituent (σ) in the substituted reactant. We may consider the effect of a substituent on the rate constant for a reaction as well as for an equilibrium constant. Therefore, we can replace the equilibrium constant K by the reaction rate constant k in the discussion above and can substitute the transition state theory definition of k to arrive at the corresponding kinetic relationship:

$$\Delta G^\ddagger = \Delta G_0^\ddagger - (2.3RT)\sigma\rho \quad (6.89)$$

At this point, equation 6.85 is one equation with four unknowns. Therefore, it is necessary to establish a reference system with defined values of σ and ρ before using the relationship for other reactions. Hammett adopted the ionization of benzoic acid derivatives in water as the reference reaction and arbitrarily set the value of ρ for that equilibrium to 1.0. Therefore, K_0 is the ionization constant for benzoic acid itself. Hydrogen is the substituent in the "unsubstituted" compound, so the substituent constant σ for hydrogen was set equal to 0. Then the σ values for another substituent could be determined from the value of K for the substituted benzoic acid bearing that substituent from the relationship

$$\sigma = \log\left(\frac{K}{K_0}\right) \text{ for } \rho \equiv 1 \quad (6.90)$$

Some σ values obtained in this manner are listed in Table 6.7.¹⁹⁶

We can rationalize the results easily, and we might have predicted them qualitatively even if not quantitatively. The Cl, CN, and NO₂ substituents are electron-withdrawing by induction and/or resonance, so they would be expected to increase the stability of the benzoate ion, thus increasing the acidity of the corresponding acid. The methyl and amino groups are electron-donating and thus destabilize the benzoate ion, decreasing the acidity of the corresponding acid.

Using the σ values for each substituent determined in this way, we may now analyze the effect of substituents on other reactions. Our approach is to measure the K (or k) for each substituted compound and then plot the value of $\log K/K_0$ (or $\log k/k_0$) versus σ . If we can draw a straight line through the data

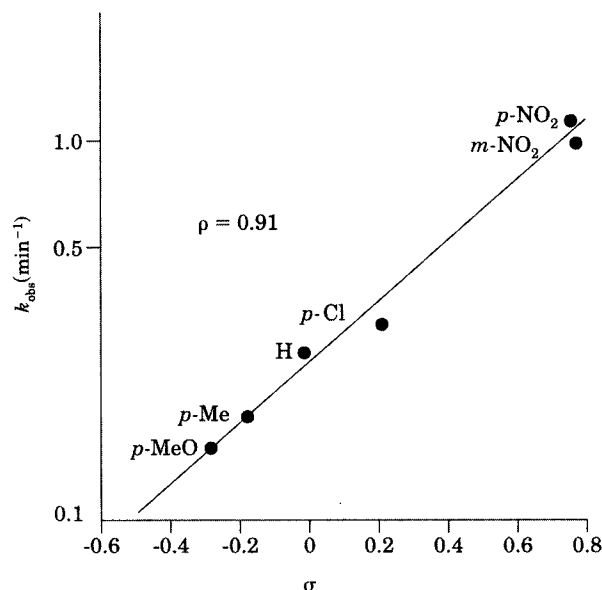
TABLE 6.7 Some σ Values

Benzoic Acid Substituents	$\sigma \equiv \log (K/K_0)$
<i>p</i> -NH ₂	-0.66
<i>p</i> -CH ₃	-0.17
H	0 ^a
<i>p</i> -Cl	0.23
<i>p</i> -CN	0.66
<i>p</i> -NO ₂	0.78

^a By definition.

Source: Reference 196.

¹⁹⁶ McDaniel, D. H.; Brown, H. C. *J. Org. Chem.* **1958**, *23*, 420.

**FIGURE 6.67**

Linear Hammett correlation observed in the formation of benzaldehyde semicarbazone at pH 1.75. (Reproduced from reference 204. Note that the vertical axis is a log scale.)

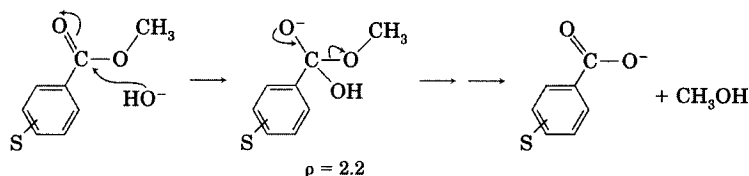
points, we say that a **linear Hammett correlation** is obtained, and the slope of the line is ρ . An example is the correlation of $\log k_{\text{obs}}$ with σ in the reaction of benzaldehyde with semicarbazide in 25% ethanol at pH 1.75 (Figure 6.67), where $\rho = +0.91$.¹⁹⁷ The linear correlation tells us that the reaction or equilibrium is affected in a consistent way by the electron-donating or electron-withdrawing ability of substituents. A positive ρ , as in Figure 6.67, means that the equilibrium or reaction rate constant increases with electron-withdrawing substituents. Conversely, a negative ρ indicates that the equilibrium or reaction rate constant is favored by electron-donating substituents.

Frequently, we seek further meaning from ρ values. For example, we may reason that a positive ρ indicates the development of negative charge in the transition structure (for a kinetic measurement) or in the product (for an equilibrium measurement) of a reaction. Conversely, we often conclude that there is an accumulation of positive charge in the transition structure or product for reactions with a negative value of ρ . It is more difficult to interpret the magnitude of ρ . Technically, we may say only that the greater the magnitude of ρ , the more sensitive is the reaction (or the equilibrium) to the electron-donating or electron-withdrawing power of substituents. We sometimes *infer*, however, that the magnitude of ρ can tell us about the extent to which charge develops in the product or transition structure during the reaction. For example, anionic polymerization involving benzylic anions produced a ρ value of +5.0, but the corresponding radical polymerization of the same compounds produced a ρ of +0.5.¹⁹⁸

Relating the magnitude of ρ to the extent of charge development must be done with caution. The ionization of benzoic acids, for which ρ was defined

¹⁹⁷ In this plot, the y -axis is $\log k$, not $\log(k/k_0)$. Problem 6.20 (at end of chapter) asks the reader to demonstrate that this approach is equivalent to plotting $\log(k/k_0)$ versus σ . The unit of the rate constant, min^{-1} , suggests a first-order rate constant. The study was conducted with a large excess of semicarbazide, so the kinetics are pseudo-first-order.²⁰⁴

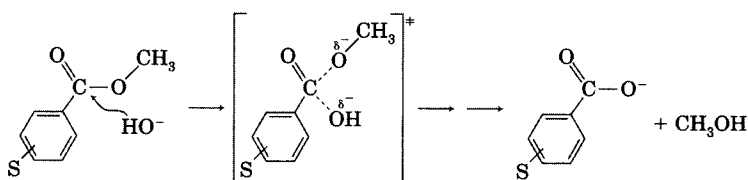
¹⁹⁸ Shima, M.; Bhattacharyya, D. N.; Smid, J.; Szwarc, M. *J. Am. Chem. Soc.* **1963**, *85*, 1306.

**FIGURE 6.68**

Accepted mechanism for the hydrolysis of an ester.

to be 1 in water, has a ρ of 1.7 in 40% aqueous ethanol.¹⁹⁹ We presume that the charge on the carboxylate ion is nearly the same in both solvent systems, but the difference in the polarity of the solvents causes the sensitivity of the equilibrium to substituent effects to be different. In other words, the effect of a substituent is less significant when solvent stabilizes the carboxylate ion more effectively. Values of ρ can also vary among members of a series of acids in the same solvent. Ionization of substituted phenylacetic acids in water gives a ρ of 0.49, while ionization of β -phenylpropionic acids in water gives a ρ of 0.212.¹⁹⁴ Thus, the magnitude of ρ decreases with increasing distance between the substituent and the reaction site. Again, the extent of charge developing at the reaction site is not changing, just the sensitivity of the reaction to the effect of remote substituents.

If we compare closely related structures under identical reaction conditions, then we may use Hammett correlations to investigate charge development in transition structures with more confidence.²⁰⁰ Consider the alkaline hydrolysis of methyl benzoate, which has a ρ value of +2.2 (Figure 6.68).^{201,202a} If the reaction were a direct S_N2 -type displacement, as shown in Figure 6.69, we would not expect much charge to develop on the benzoyl system. In fact, small values of ρ (either positive or negative) are observed in typical S_N2 reactions. The reaction of benzyl chloride with hydroxide ion by an S_N2 pathway (Figure 6.70) has a ρ of -0.3 .^{202b} On the other hand, the reaction of benzyl chloride with iodide in acetone (Figure 6.71) has a ρ of $+0.8$.^{202c} This contrast indicates that small positive or negative ρ values can appear in S_N2 reactions, depending on the degree to which bond forming or bond breaking is greater in the transition structure. Still, the

**FIGURE 6.69**

Hypothetical mechanism for ester hydrolysis.

¹⁹⁹ Reference 194, based on data reported by Bright, W. L.; Briscoe, H. T. *J. Phys. Chem.* **1933**, 37, 787.

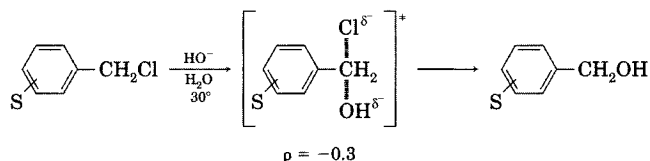
²⁰⁰ "Almost every kind of organic reaction has been treated via the Hammett equation, or its extended form." Hansch, C.; Leo, A.; Taft, R. W. *Chem. Rev.* **1991**, 91, 165.

²⁰¹ The following examples are taken from the compilation by Jaffé (reference 194).

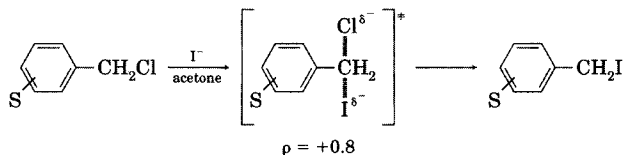
²⁰² Reference 194, based on data reported by (a) Tommila, E.; Hinshelwood, C. N. *J. Chem. Soc.* **1938**, 1801; (b) Olivier, S. C. J.; Weber, A. P. *Rec. Trav. Chim. Pays-Bas* **1934**, 53, 869; (c) Bennett, G. M.; Jones, B. J. *Chem. Soc.* **1935**, 1815; (d) Boyd, D. R.; Marle, E. R. *J. Chem. Soc.* **1914**, 105, 2117; (e) Goldsworthy, L. J. *J. Chem. Soc.* **1926**, 1254; (f) Williams, E. G.; Hinshelwood, C. N. *J. Chem. Soc.* **1934**, 1079.

FIGURE 6.70

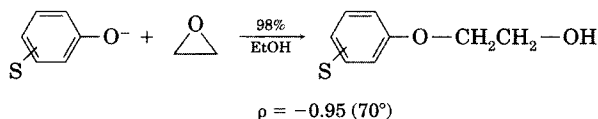
S_N2 reaction of benzyl chlorides with hydroxide ion.

**FIGURE 6.71**

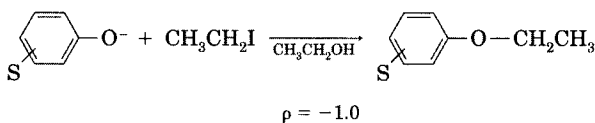
S_N2 reaction of benzyl chlorides with iodide ion.

**FIGURE 6.72**

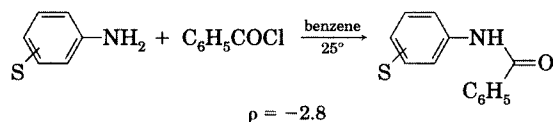
Reaction of phenoxides with ethylene oxide.

**FIGURE 6.73**

Reaction of phenoxides with ethyl iodide.

**FIGURE 6.74**

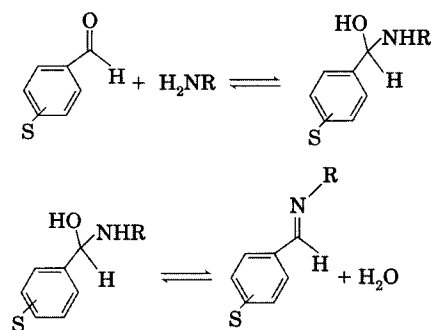
Reaction of anilines with benzoyl chloride.



magnitude of ρ is much smaller for this kind of reaction than for the hydrolysis of methyl benzoate. The ρ of +2.2 for ester hydrolysis can therefore be taken as evidence for the mechanism in Figure 6.68.

Somewhat larger ρ values may be observed in S_N2 reactions if the substituent is attached to the nucleophile or the leaving group. For the reaction of phenoxide with ethylene oxide (Figure 6.72), $\rho = -0.95$.^{202d} For phenoxide reacting with ethyl iodide (Figure 6.73), ρ was found to be -1 .^{202e} Reaction of aniline with benzoyl chloride in benzene solution gave a Hammett correlation with $\rho = -2.8$ (Figure 6.74).^{202f}

In some cases curved or bent Hammett correlation plots are found. These situations can arise when a reaction mechanism involves more than one step, either of which can be rate-limiting under certain conditions, or when different mechanisms may occur, depending on substituents. In such cases, changing a substituent can change the step that is rate-limiting or can change

**FIGURE 6.75**

Two steps in the mechanism of formation of benzaldehyde semicarbazone.

the mechanism itself, thus changing the apparent ρ for the reaction.²⁰³ Figure 6.75 shows the two steps involved in the formation of a semicarbazone from the reaction of benzaldehyde and semicarbazide.²⁰⁴ Both the rate and equilibrium of the first step are favored by electron-withdrawing substituents on the aldehyde, while the rate of the second step is favored by electron-donating substituents on the aldehyde. The effects of a substituent oppose each other at neutral pH, and there is little variation of rate with σ . At pH 1.75, the first step is rate-limiting, so a positive value of ρ is observed (Figure 6.67). However, at pH 3.9, the first step is rate-limiting for electron-withdrawing substituents but not for electron-donating substituents. Therefore, the Hammett correlation has two linear segments but, overall, is sharply bent concave downward (Figure 6.76).^{197,205} Such bending is usually associated with a change in the rate-limiting step of a reaction, while a correlation that is bent upward is expected for a system exhibiting change in mechanism with substitution.²⁰³

Similarly, two steps (addition of the amine, elimination of water) occur in the uncatalyzed formation of the *n*-butyl imine of a series of benzaldehydes (Figure 6.77). Again, the two steps of the reaction are favored by different substituent effects. In this case the maximum rate constant is observed for benzaldehyde itself, so the Hammett plot shows a maximum.²⁰⁶

As noted above, the σ value for a substituent depends on its position on the aromatic ring relative to the site of the reaction. Consider the para and meta σ values for the substituents shown in Table 6.8.¹⁹⁶ For the first two, the magnitude of σ_m is greater than that of σ_p . For the second two, the magnitude of σ_p is greater than that of σ_m . For the final entry, σ_p is negative but σ_m is positive.

We expect the trimethylammonio substituent to be electron-withdrawing. As shown in Figure 6.78, both the inductive effect (represented by arrows

²⁰³ Ammal, S. C.; Mishima, M.; Yamataka, H. *J. Org. Chem.* **2003**, *68*, 7772.

²⁰⁴ Anderson, B. M.; Jencks, W. P. *J. Am. Chem. Soc.* **1960**, *82*, 1773.

²⁰⁵ For a discussion of nonlinear Hammett correlations, see Schreck, J. O. *J. Chem. Educ.* **1971**, *48*, 103. See also Henri-Rousseau, O.; Texier, F. *J. Chem. Educ.* **1978**, *55*, 437; Jencks, W. P. *Chem. Soc. Rev.* **1981**, *10*, 345.

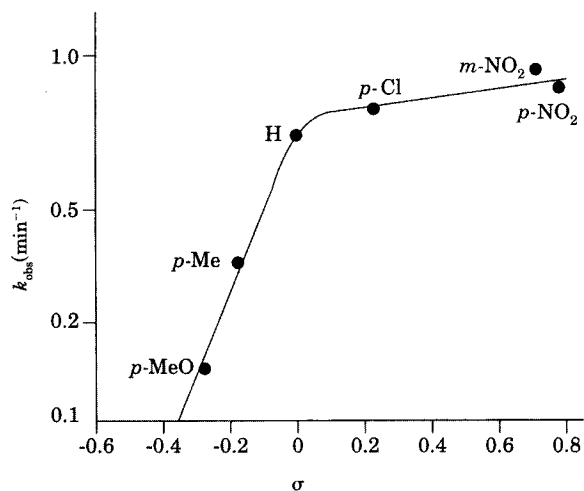
²⁰⁶ The reaction was carried out in methanol solution. The rate expression for the reaction was

$$\text{Rate} = (k_0 + k_{\text{HOAc}}[\text{HOAc}])[\text{RCHO}][\text{BuNH}_2]$$

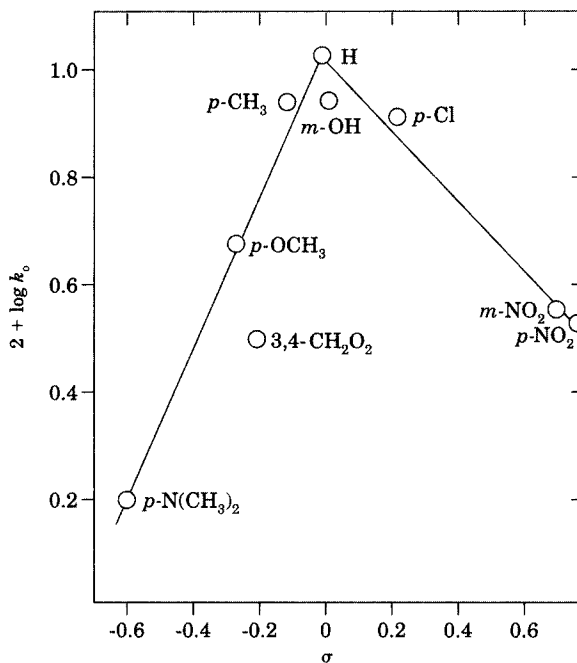
Here $\log k_0$ (for the reaction in the absence of acid catalysis) is plotted versus σ . The constant factor of 2 added to $\log k_0$ makes the units of the *y*-axis easier to read but does not affect the slope of the line. Santerre, G. M.; Hansroto, C. J., Jr.; Crowell, T. I. *J. Am. Chem. Soc.* **1958**, *80*, 1254.

FIGURE 6.76

Nonlinear Hammett correlation observed for formation of benzaldehyde semicarbazone at pH 3.9. (Reproduced from reference 204. Note that the vertical axis is a log scale.)

**FIGURE 6.77**

Hammett correlation for uncatalyzed reaction of benzaldehydes with *n*-butylamine. (Reproduced from reference 206.)

**TABLE 6.8 Comparison of para and meta σ Values**

Substituent	σ_p	σ_m
F	0.06	0.34
NMe ₃ ⁺	0.82	0.88
NH ₂	-0.66	-0.16
COCH ₃	0.50	0.38
OCH ₃	-0.27	0.12

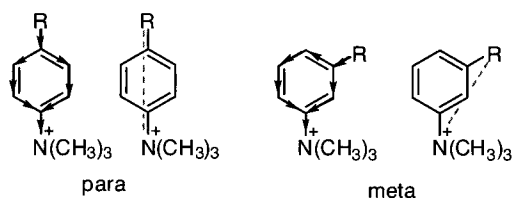
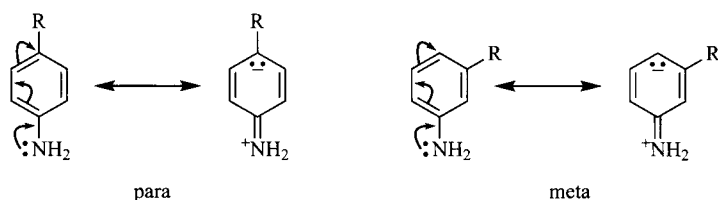
**FIGURE 6.78**

Illustration of inductive (arrows) and field (dashed line) effects for para (left) and meta (right) trimethylammonio substituent. R = site of reaction.

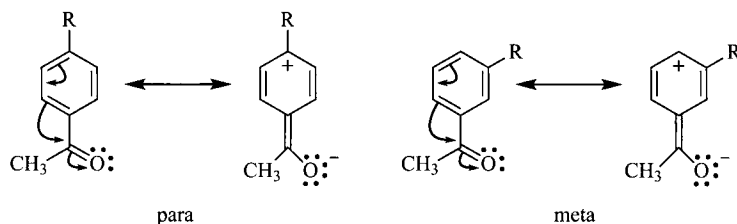
**FIGURE 6.79**

Resonance effect of para (left) and meta (right) NH_2 substituent.

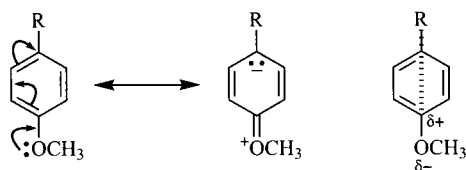
superimposed on the σ bonds) and the field effect (represented by a dashed line) are expected to decrease with increasing distance between the positively charged nitrogen atom and the site of the reaction (R). The decreasing ability of the electronic effect of the substituent to be transmitted to the reaction site can account for the lower magnitude of σ_p compared to that of σ_m .

The next two substituents in Table 6.8 are expected to have resonance interactions with the benzene ring in addition to their inductive effects. The NH_2 group is able to donate electron density by resonance (Figure 6.79), while the COCH_3 group is able to accept electron density by resonance (Figure 6.80). Since resonance effects are more pronounced in para positions than meta positions, resonance makes the magnitude of σ greater when the substituents are para to the carbon atom that is attached to the reaction site than when the substituents are in the meta position.

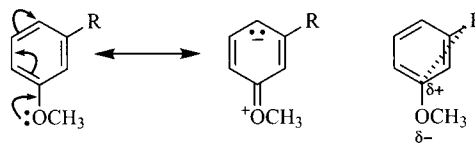
In the previous examples it was possible to discuss the effect of a substituent only in terms of the induction/field effect or primarily in terms of the resonance effect. Both effects are important for many substituents, and the location of the substituent on the ring influences how the effects influence the reaction site. The positive σ_m value for the methoxy group indicates that it functions primarily as an electron-withdrawing substituent by induction when it is meta to the reaction site, but the negative σ_p value means that it functions primarily as an electron-donating group when it para (Figure 6.81). In the para position, inductive withdrawal of electron density still operates, but it is weakened by the greater distance to the reaction site. Resonance donation of electron density now overcomes the inductive effect, and the substituent is overall electron-donating as judged by the ionization of benzoic acids. The much larger difference in σ_m and σ_p values for fluoro than for

**FIGURE 6.80**

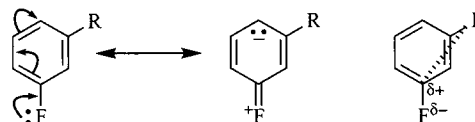
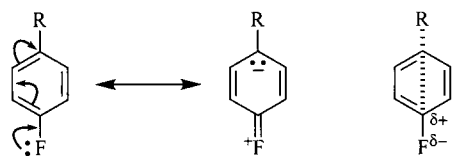
Resonance effect of para (left) and meta (right) COCH_3 substituent.

**FIGURE 6.81**

Resonance (left) and field (right) interactions for a methoxy substituent in the para (top) and meta (bottom) positions.

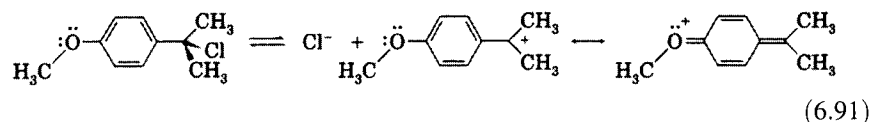
**FIGURE 6.82**

Resonance (left) and field (right) interactions for a fluoro substituent in the para (top) and meta (bottom) positions.



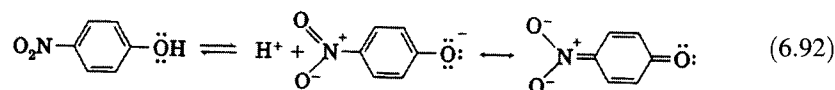
trimethylammonio suggests that an electron-donating resonance effect may be operating with *p*-F also, but that the electron-withdrawing field/induction effect is stronger (Figure 6.82).

It is important to remember that the initial definition of σ values was based on substituent effects for the ionization of benzoic acids. For these reactions we can imagine the stability of the resulting benzoate ion to be influenced by charge density accumulating on the benzene carbon atom that is attached to the carboxylate, no matter whether that charge density results from field or resonance effects. For other reactions, however, the relative effects of induction and resonance might be quite different. Solvolysis of a series of cumyl chlorides by a mechanism involving carbocation formation (equation 6.91) proceeds much faster when a para substituent is capable of direct resonance interaction with the carbocation center. The ionization of benzoic acids therefore provides a poor model for such systems. Brown and Okamoto suggested the designation of a new substituent constant, σ^+ , for this kind of reaction.²⁰⁷



²⁰⁷ Okamoto, Y.; Brown, H. C. *J. Org. Chem.* **1957**, *22*, 487; Brown, H. C.; Okamoto, Y. *J. Am. Chem. Soc.* **1958**, *80*, 4979.

Similarly, the ionization of a substituted phenol should be enhanced if there is a para substituent that can stabilize the resulting negatively charged oxygen through extended conjugation. Thus, we can also define σ^- values for substituents such as *p*-nitro, as shown in equation 6.92.²⁰⁸



Unless we already know something about the mechanism of a reaction, we may not know ahead of time whether $\log(k/k_0)$ values are more likely to correlate with σ , with σ^+ , or with σ^- . Consider a reaction in which electron-donating substituents are observed to increase the reaction rate constant. One way to choose between σ and σ^+ is to plot the $\log(k/k_0)$ versus both σ and σ^+ and determine which correlation is more linear. Another approach is to try to separate the influence of induction and resonance on the reaction. Yukawa and Tsuno proposed the relationship

$$\log\left(\frac{k}{k_0}\right) = \rho[\sigma + r(\sigma^+ - \sigma)] \quad (6.93)$$

where the r parameter measures the influence of resonance relative to the ionization of benzoic acids.²⁰⁹ Experimentally, ρ is determined first by plotting $(\log k/k_0)$ versus σ for those substituents that do not act as strong electron donors by resonance. Then one plots $[(\log k/k_0)/\rho - \sigma]$ versus $(\sigma^+ - \sigma)$ for those substituents for which $\sigma^+ \neq \sigma$. The slope of the correlation is r . In some cases, Hammett plots that are not linear versus σ exhibit a linear Yukawa–Tsuno correlation, so it is not always the case that a nonlinear traditional Hammett plot indicates a two-step or two-mechanism process.²¹⁰

As we have seen, σ values may involve some resonance contribution, so the use of σ and σ^+ terms does not totally distinguish between field and resonance effects. Swain and Lupton proposed using discrete field (F) and resonance (R) substituent constants (equation 6.94).²¹¹ Instead of a single reaction constant ρ , two terms measured the influence of field effects (f) and resonance (r) on the reaction.²¹²

$$\log\left(\frac{k}{k_0}\right) = fF + rR \quad (6.94)$$

²⁰⁸ Reference 95, p. 360; Cohen, L. A.; Jones, W. M. *J. Am. Chem. Soc.* **1963**, *85*, 3397.

²⁰⁹ Yukawa, Y.; Tsuno, Y. *Bull. Chem. Soc. Jpn.* **1959**, *32*, 965, 971.

²¹⁰ Um, I.-H.; Han, H.-J.; Ahn, J.-A.; Kang, S.; Bunzel, E. *J. Org. Chem.* **2002**, *67*, 8475; Um, I.-H.; Lee, J.-Y.; Kim, H.-T.; Bae, S.-K. *J. Org. Chem.* **2004**, *69*, 2436.

²¹¹ Swain, C. G.; Lupton, E. C., Jr. *J. Am. Chem. Soc.* **1968**, *90*, 4328.

²¹² A comprehensive treatment of the dual parameter approach was given by Ehrenson, S.; Brownlee, R. T. C.; Taft, R. W. *Prog. Phys. Org. Chem.* **1973**, *10*, 1. See also the treatment of substituent effects in nonaromatic unsaturated systems by Charton, M. *Prog. Phys. Org. Chem.* **1973**, *10*, 81.

Several attempts have been made to define σ values for reactions in which only field effects could be important. These have involved the ionization of phenylacetic acids to generate a series of σ^0 values,²¹³ of acetic acids to generate σ_1 values,²¹⁴ or other reactions in which resonance was considered unimportant to generate σ^n values.²¹⁵

Taft and Topsom developed a detailed analysis of the role that substituent effects play in properties such as acidity and basicity.²¹⁶ The four primary kinds of substituent effects were considered to be electronegativity (induction), field, resonance, and polarizability effects. As in the Hammett equation, the σ values are substituent properties, while the ρ values represent the sensitivity of the reaction to each of these properties. The general form of such an equation is given in equation 6.95,²¹⁶ where the symbols F , χ , α , and R represent field, electronegativity, polarizability, and resonance effects, respectively.

$$\delta \Delta E^0 = \sigma_F \rho_F + \sigma_\chi \rho_\chi + \sigma_\alpha \rho_\alpha + \sigma_R \rho_R \quad (6.95)$$

In this study inductive effects were deemed to be important primarily as a source of electric dipoles that can cause field effects, so the effect of a substituent usually could be described in terms of only the other three effects. Just as with the Hammett equation, direct conjugation between substituents and reaction sites can cause resonance effects that are different from the effects when direct conjugation is not possible. Therefore, the σ_R term may be replaced by $\sigma_{\bar{R}}$ for substituents with available electron pairs for donation by resonance, or the term $\sigma_{\bar{R}}^+$ may be used for substituents that may accept electrons by resonance. Some values of the various σ parameters for common substituents are given in Table 6.9.²¹⁷

Taft proposed a substituent constant, σ^* , to measure the polar effect of alkyl substituents in aliphatic systems.¹⁷³ This method is based on the assumption that resonance is unimportant in aliphatic systems and that steric effects are the same for ester hydrolysis whether in acid or base, so only the polar effect of the substituent is different under the two reaction conditions.²¹⁸ The value of σ^* for a substituent, R, was based on the rate constants for acid-catalyzed and base-promoted hydrolysis of the ester $\text{RCO}_2\text{R}'$ relative to those for $\text{CH}_3\text{CO}_2\text{R}'$. A factor of 2.48 was used to relate σ^* values to the Hammett σ values. Thus,

$$\sigma^* = \frac{\log \left(\frac{k}{k_0} \right)_B - \log \left(\frac{k}{k_0} \right)_A}{2.48} \quad (6.96)$$

²¹³ Taft, R. W., Jr. *J. Phys. Chem.* **1960**, *64*, 1805.

²¹⁴ Charton, M. *J. Org. Chem.* **1964**, *29*, 1222.

²¹⁵ van Bekkum, H.; Verkade, P. E.; Wepster, B. M. *Rec. Trav. Chim. Pays-Bas* **1959**, *78*, 815.

²¹⁶ Taft, R. W.; Topsom, R. D. *Prog. Phys. Org. Chem.* **1987**, *16*, 1.

²¹⁷ For an extensive listing of substituent constants, see Hansch, C.; Leo, A.; Hoekman, D. *Exploring QSAR: Hydrophobic, Electronic, and Steric Constants*; American Chemical Society: Washington, DC, 1995.

²¹⁸ For a discussion, see Shorter, J. Q. *Rev. Chem. Soc.* **1970**, *24*, 433.

TABLE 6.9 Selected Substituent Constants^a

Substituent	σ_p	σ_m	σ_p^+	F	R	σ^*	E_s	σ_x	σ_α	σ_F	σ_R	σ_R^-
H	0.000	0.000	0.000	0.000	0.000	0.490		0.000	0.000	0.000	0.000	0.000
CH ₃	-0.170	-0.069	-0.256	-0.052	-0.141	0.000	0.00	0.00	-0.35	0.00	-0.08	
CH ₂ CH ₃	-0.151	-0.07	-0.218	-0.065	-0.114	-0.1000	-1.31					
C(CH ₃) ₃	-0.197	-0.10	-0.275	-0.104	-0.138	-0.3000	-2.78	-0.02	-0.75	-0.00	-0.07	
C ₆ H ₅	-0.01	0.06	-0.085	0.139	-0.088	0.600	-3.82					
CO ₂ H	0.45	0.37	0.472	0.552	0.140	2.94						
CO ₂ ⁻	0.0	-0.1	0.109	-0.221	0.124	0.92						
COCH ₃	0.502	0.376	0.567	0.534	0.202	1.65		-0.04	-0.55	0.26	0.17	0.00
CO ₂ CH ₂ CH ₃	0.45	0.37	0.472	0.552	0.140	2.26						
CO ₂ CH ₃						2.00		0.04	-0.49	0.24	0.16	0.00
CN	0.660	0.56	0.674	0.847	0.184	3.64	-0.51	0.30	-0.46	0.60	0.10	0.00
CF ₃	0.54	0.43	0.582	0.631	0.186	2.6	-2.40	0.02	-0.25	0.44	0.07	0.00
NH ₂	-0.66	-0.16	-1.111	0.037	-0.681	0.62	-0.61	0.33	-0.16	0.14	-0.52	-0.28
N(CH ₃) ₃ ⁺	0.82	0.88	0.636	1.460	0.000	4.16		0.46	-0.26	0.65	0.18	0.00
NO ₂	0.778	0.710	0.740	1.109	0.155	4.66	-2.52					
OH	-0.37	0.121	-0.853	0.487	-0.643	1.37	-0.55	0.54	-0.03	0.30	-0.38	-0.28
OCH ₃	-0.268	0.115	-0.648	0.413	-0.500	1.77	-0.55	0.55	-0.17	0.25	-0.42	-0.27
F	0.062	0.337	-0.247	0.708	-0.336	3.19	-0.55	0.70	0.13	0.44	-0.25	
Cl	0.227	0.373	0.035	0.690	-0.161	2.94	-0.97	0.16	-0.43	0.45	-0.17	
Br	0.232	0.391	0.025	0.727	-0.176	2.80	-1.16					
I	0.18	0.352	-0.034	0.672	-0.197	2.22	-1.62					
SCH ₃	0.00	0.15	-0.164	0.332	-0.186	1.56	-1.07	-0.15	-0.68	0.25	-0.27	
S(CH ₃) ₂ ⁺	0.90	1.00	0.660	1.687	-0.042	5.09						
Si(CH ₃) ₃	-0.070	-0.040	-0.040	-0.093	-0.047	-0.14	-2.91		-0.072	-0.02	0.02	0.00

^a Values of σ_p and σ_m are taken from reference 196. Values of σ_p^+ , F , and R are taken from reference 211. Values of σ^* and E_s are taken from reference 217. Values of σ_x , σ_α , σ_F , σ_R , and σ_R^- are taken from reference 216.

where k is the rate constant for hydrolysis with the substituent R, k_0 is the rate constant of hydrolysis of the ester with the reference substituent (CH₃), and A and B refer to acid and base conditions, respectively.^{219,220}

Taft was also able to deduce a steric substituent constant, E_s , from the relationship

$$E_s = \log \left(\frac{k}{k_0} \right)_A \quad (6.97)$$

on the assumption that polar effects do not affect acid-catalyzed hydrolysis, so only steric effects contribute to differences in rate constants. Combining the relationships for the electronic and steric effects of substituents produces the **Taft equation** (equation 6.98). The σ^* values measure polar effects in this series and the E_s values measure steric effects. The terms ρ^* and S are the

²¹⁹ In Table 6.9, the values of σ^* for H, CH₃, and CH₃CH₂ are +0.490, 0.000, and -0.100, respectively. However, Bordwell, F. G.; Bartmess, J. E.; Hautala, J. A. *J. Org. Chem.* **1978**, *43*, 3095 noted that while these values correlate well with rate constants of some reactions, they do not correlate well with many other reactions. Instead, better correlations may be obtained if the σ^* values for hydrogen and for alkyl groups in general are taken to be 0.000.

²²⁰ Ritchie, C. D.; Sager, W. F. *Prog. Phys. Org. Chem.* **1964**, *2*, 323 advocated the use of the σ_1 scale instead of the σ^* scale. This source provides an extensive listing of σ_1 values on pp. 334–337. Exner, O.; Böhm, S. *Eur. J. Org. Chem.* **2007**, 2870 recommended removing σ^* constants from the literature.

corresponding reaction constants. Table 6.9 shows such parameters for a number of common substituents.^{221,222}

$$\log\left(\frac{k}{k_0}\right) = \rho^* \sigma^* - SE_s \quad (6.98)$$

In discussions of substituents as electron-donating or electron-withdrawing groups, it is easy to think about intramolecular interactions primarily in terms of enthalpy effects. We must not forget that rate constants and equilibria depend on ΔG^\ddagger and ΔG , respectively, not just on ΔH^\ddagger and ΔH . Thus, we should expect the Hammett and related linear free energy relationships to hold only when one of two conditions applies. Either (i) the entropy change is constant for all of the reactants in the data set, or (ii) there is a linear relationship between the values of ΔH^\ddagger and ΔS^\ddagger (or ΔH° and ΔS°) for all of the reactants in the data set. The latter condition is expressed by equation 6.99, where α and β are constants.^{223,224}

$$\Delta H_i^\ddagger = \alpha + \beta \Delta S_i^\ddagger \quad (6.99)$$

This relationship is often termed **enthalpy–entropy compensation**, and such correlations have been reported for a wide variety of reactions.²²⁵ For example, Figure 6.83 shows the correlation of ΔH^\ddagger with $-\Delta S^\ddagger$ for the oxidation of a series of *o*- and *p*-substituted anilines by percarbonate in glacial acetic acid.²²⁶ One possible explanation for such correlations is that variations in the enthalpy of the transition state might be reflected in the extent to which transition structures become more or less ordered than the reactants.²²⁵

If equation 6.99 applies, then the difference between the activation enthalpies ($\delta\Delta H^\ddagger$) for any pair of closely related reactants will be related to the difference between their activation entropies ($\delta\Delta S^\ddagger$) as shown in equation 6.100. Thus, we may express the difference between the activation free energies with equation 6.101.^{227–229}

$$\delta\Delta H^\ddagger = \beta\delta\Delta S^\ddagger \quad (6.100)$$

$$\delta\Delta G^\ddagger = (1 - T/\beta)\delta\Delta S^\ddagger \quad (6.101)$$

Equation 6.101 indicates that the quantity $\delta\Delta G^\ddagger$ will be zero when the temperature is numerically equal to the constant β . The value of ΔG^\ddagger will thus be identical for all members of the data set at that temperature, so the rate constants for all of the reactions will be the same. In addition, the apparent value of ρ will be zero at that temperature. The constant β , which has units of

²²¹ Adapted from reference 211.

²²² For an extensive listing of substituent constants, see reference 200.

²²³ Exner, O. *Prog. Phys. Org. Chem.* **1973**, *10*, 411.

²²⁴ Linert, W.; Jameson, R. F. *Chem. Soc. Rev.* **1989**, *18*, 477; also see Linert, W. *Chem. Soc. Rev.* **1994**, *23*, 429.

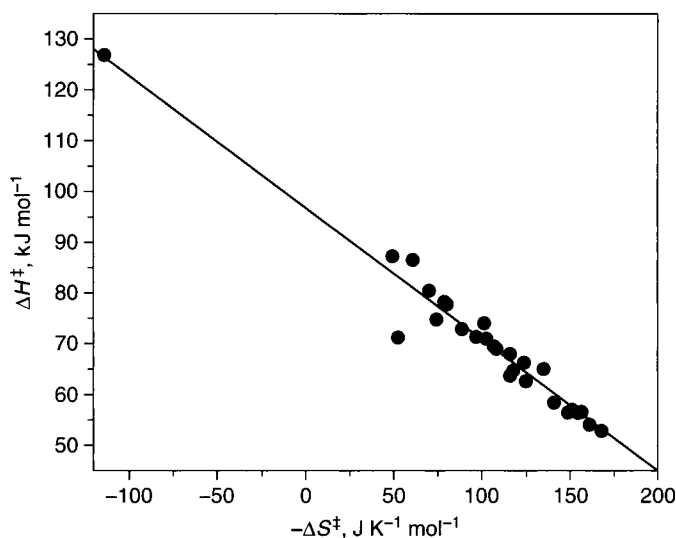
²²⁵ Liu, L.; Guo, Q.-X. *Chem. Rev.* **2001**, *101*, 673; Starikov, E. B.; Nordén, B. *J. Phys. Chem. B* **2007**, *111*, 14431.

²²⁶ Karunakaran, C.; Kamalam, R. *J. Org. Chem.* **2002**, *67*, 1118.

²²⁷ Leffler, J. E. *J. Org. Chem.* **1955**, *20*, 1202.

²²⁸ See also reference 78, pp. 324–342; reference 52, p. 412; reference 220, pp. 352–378.

²²⁹ The terms $\delta\Delta H^\ddagger$ and $\delta\Delta S^\ddagger$ are often written $\Delta\Delta H^\ddagger$ and $\Delta\Delta S^\ddagger$, respectively.

**FIGURE 6.83**

Enthalpy–entropy compensation observed in an oxidation reaction. (Based on data in reference 226.)

temperature, is therefore known as the **isokinetic temperature**. Systems of closely related reactants that exhibit such behavior are said to exhibit an **isokinetic relationship**.^{223,224,230} It is important to note in this context, however, that enthalpy–entropy compensation and the isokinetic relationship are related conceptually but are not equivalent. The compensation effect is established through a plot such as Figure 6.83, but an isokinetic relationship can be demonstrated only by the intersection at a common point of lines on a plot of $\log k$ versus $1/T$.^{225,231}

A number of publications have reported correlations between ΔH^\ddagger and ΔS^\ddagger values for a set of reactants, but there has been much discussion in the literature about whether such observations represent fundamental physical relationships or are merely statistical artifacts. Liu and Guo noted that in some cases a correlation between the enthalpy and entropy values for a series of related reactions may appear through experimental error because investigators considered only reactants having convenient rate constants or because an inappropriate kinetic model was used.²²⁵ For example, if a plot of the logs of experimental rate constants versus $1/T$ has a slope that is erroneously steep, then both ΔH^\ddagger and ΔS^\ddagger will be overestimated. Bunce and Forber used a technique of variable temperature kinetics to obtain the activation enthalpies and entropies of a single reactant in several different experiments. Even though the results produced an excellent correlation of ΔH^\ddagger with ΔS^\ddagger , the authors concluded that the relationship resulted only from a statistical correlation of the data because the different ΔH^\ddagger and ΔS^\ddagger values represented the same reaction under the same reaction conditions.²³² Nevertheless, Linert argued that the isokinetic relationship has a reasonable theoretical foundation based on the mechanisms of energy transfer from a heat bath to the reacting species.^{224,233}

²³⁰ A similar relationship involving ΔG° , ΔH° , and ΔS° is known as an **isoequilibrium relationship**.

²³¹ Petersen, R. C. *J. Org. Chem.* **1964**, *29*, 3133.

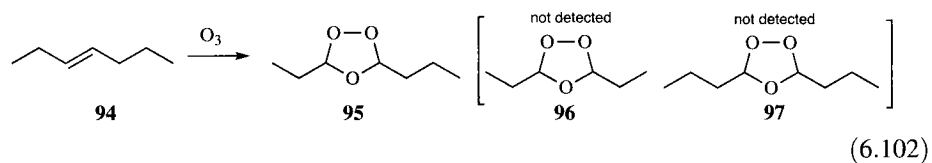
²³² Bunce, N. J.; Forber, C. L. *J. Chem. Res.*, **2000**, 36.

²³³ See also Pinheiro, L. M. V.; Calado, A. R. T.; Reis, J. C. R. *Org. Biomol. Chem.* **2004**, *2*, 1330.

In later chapters we will see other uses of the Hammett correlation as a tool to understand reaction mechanisms and the effect of substituents on them. We will also consider free energy relationships in the study of acid- and base-catalyzed reactions (such as the Brønsted equation) and substitution reactions (such as the Winstein–Grunwald equation).²³⁴ Indeed, a linear free energy correlation can be developed from the study of almost any reaction. What should be emphasized at this point is that trying to apply that equation (and the resulting substituent constants) to study a new reaction means that we are implicitly modeling the new reaction on the previous one. A linear free energy relationship must therefore be seen as just another of the conceptual models of organic chemistry.

Problems

- 6.1. The Criegee mechanism for the ozonolysis of alkenes is shown in Figure 6.84.²³⁵ As shown in equation 6.102, ozonolysis of 3-heptene (**94**) was found to give only the ozonide **95** and not **96** or **97**. Does this finding rule out a mechanism for ozonolysis that requires dissociation of one molecule into two fragments that recombine? What other experiments can you suggest to determine whether the Criegee mechanism might be occurring?



- 6.2. Two mechanisms have been considered for the isomerization of 1-chloropropane to 2-chloropropane with AlCl_3 . The first involves elimination of HCl to form propene, followed by addition of HCl to propene according to

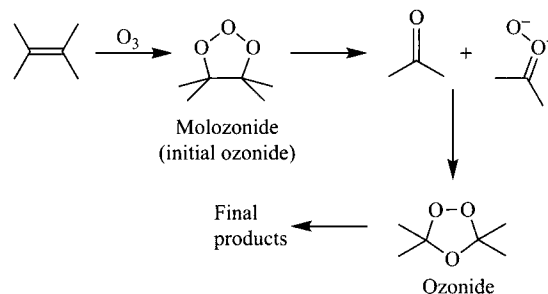


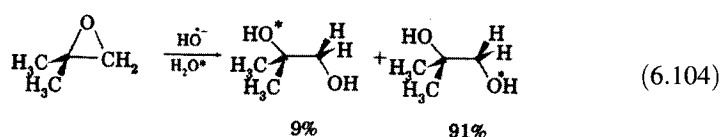
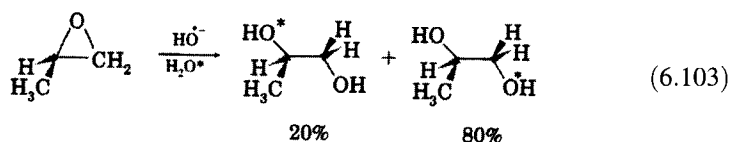
FIGURE 6.84
The Criegee mechanism.

²³⁴ Similar concepts are important in medicinal chemistry, in which the properties of a proposed drug are predicted on the basis of the effects of a series of known drugs. A leading researcher in this area is Corwin Hansch, for whom the Hansch correlation is named. For a discussion of quantitative structure–activity relationships, see Hansch, C.; Leo, A. *Exploring QSAR: Fundamentals and Applications in Chemistry and Biology*; American Chemical Society: Washington, DC, 1995.

²³⁵ Criegee, R. in Edwards, J. O. Ed. *Peroxide Reaction Mechanisms*; Wiley-Interscience: New York, 1962 and references therein.

Markovnikov's rule. The second involves heterolysis of 1-chloropropane to form Cl^- and the 2-propyl cation (either directly if hydride shift accompanies chloride departure or sequentially via a short-lived 1° carbocation), followed by ion combination. Propose an isotopic labeling experiment that would allow one to distinguish between these two mechanisms.

- 6.3. The reactions of propylene oxide and isobutylene oxide with ^{18}O -labeled hydroxide in ^{18}O -labeled water lead to the corresponding glycols in which the ^{18}O is distributed between the two oxygen atoms of each product as shown in equations 6.103 and 6.104. ($\text{O}^* = ^{18}\text{O}$.)



What do these results suggest about the regiochemistry of the hydrolysis of epoxides under basic conditions?

- 6.4. Derive the steady-state equation for $\text{A} + \text{B} \xrightleftharpoons[k_{-1}]{k_1} \text{C} \xrightarrow{k_2} \text{D}$ shown in equation 6.37 on page 347.
- 6.5. Verify the statement that a reactive intermediate having an energy minimum equal at least to RT has a lifetime of at least one vibration.
- 6.6. Demonstrate that ΔG^\ddagger for a first-order reaction of a species having a half-life of 24 hours at 24°C is about 24 kcal/mol.
- 6.7. Harcourt reported that the observed rate constant of a reaction doubled with every 10° increase in temperature, and this trend is sometimes offered as a "rule of thumb" in kinetics.²³⁶ Use the Arrhenius equation to evaluate the validity of the "rule" for a unimolecular reaction occurring over temperature ranges from 0°C to 100°C . Does the accuracy of the generalization depend on the activation energy for the reaction?
- 6.8. Propose a qualitative explanation for the observation that compound A reacts 9000 times faster than compound B at 0°C , but the two compounds have the same rate constant at a temperature of 103°C .
- 6.9. Rationalize the fact that ΔS^\ddagger for the dimerization of cyclopentadiene to dicyclopentadiene in the gas phase is -26 eu (Figure 6.23), whereas for the pyrolysis of dicyclopentadiene to cyclopentadiene the ΔS^\ddagger is 0 eu.
- 6.10. At 25°C the equilibrium constant, K , for an association reaction of methane with a host to form the complex " $\text{CH}_4@Host$ " is 81 M^{-1} (equation 6.105).

$$K = \frac{[\text{CH}_4@Host]}{[\text{CH}_4][Host]} = 81 \text{ M}^{-1} \quad (6.105)$$

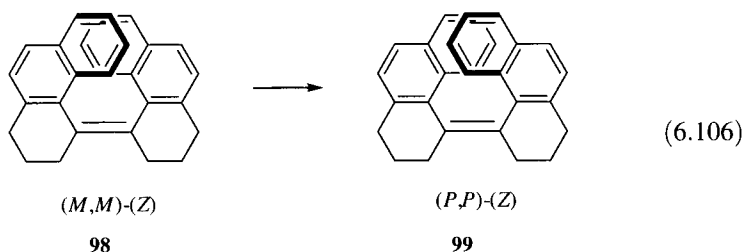
What is ΔG° for the complexation?

²³⁶ Harcourt, A. V. *J. Chem. Soc.* 1867, 20, 460.

TABLE 6.10 Kinetic Data for Isomerization of 98 to 99

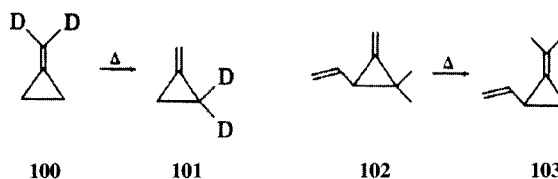
T ($^{\circ}\text{C}$)	k (s^{-1})
0.0	2.243×10^{-6}
9.8	6.747×10^{-6}
15.1	1.367×10^{-5}
19.9	2.214×10^{-5}
24.9	4.751×10^{-5}
101.1	8.45×10^{-2}
111.2	1.645×10^{-1}
121.7	3.310×10^{-1}
130.2	6.365×10^{-1}
140.2	1.209
150.2	2.121

- 6.11. A ketone can react with base to form either of two enolate ions. If the rate constant for formation of enolate E1 is twelve times greater than that for formation of enolate E2 at a certain temperature, what is the difference in the ΔG^{\ddagger} values for formation of the two enolates?
- 6.12. Consider the isomerization of 98 to 99 shown in equation 6.106.



The first-order rate constants observed for the isomerization at different temperatures are shown in Table 6.10. Calculate E_a for the isomerization from an Arrhenius plot and ΔH^{\ddagger} from an Eyring plot.

- 6.13. The thermal rearrangement of dideuteriomethylenecyclopropane (**100**) to methylenecyclopropane-2,2- d_2 (**101**) was found to have ΔH^{\ddagger} of 40.5 kcal/mol and ΔS^{\ddagger} of 1.5 eu. However, the rearrangement of **102** to **103** had a ΔH^{\ddagger} of 23.8 kcal/mol and ΔS^{\ddagger} of -6.0 eu. Explain these results, especially the appearance of a negative activation entropy for a reaction that apparently involves bond breaking.



- 6.14. Data for the thermal decarboxylation of the β -keto acid 2,2-dimethylbenzoylacetic acid (**104**) to 1-phenyl-2-methylpropanone (**105**, Figure 6.85) in 0.1 M HCl are shown in Table 6.11. (Note that the rate constants are multiplied by 10^5 . At 25.0°C the rate constant is $3.7 \times 10^{-5} \text{ s}^{-1}$.) Calculate ΔH^{\ddagger} and ΔS^{\ddagger} for the reaction and propose a possible mechanism for the decomposition.

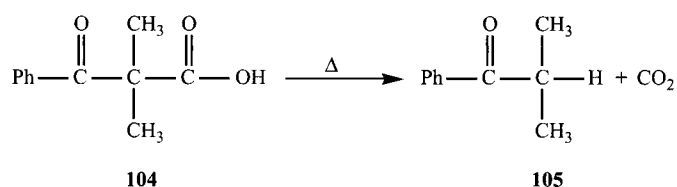


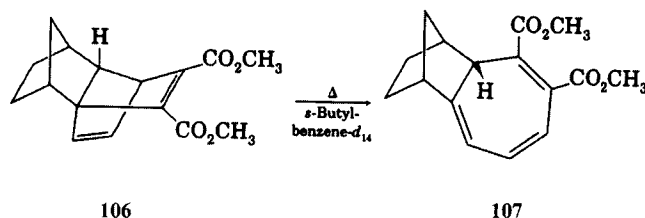
FIGURE 6.85

Decarboxylation of 2,2-dimethylbenzoylacetic acid.

TABLE 6.11 Kinetic Data for the Thermal Decarboxylation of 104

T ($^{\circ}\text{C}$)	$k \times 10^5$ (s^{-1})
25.0	3.7
48.5	69
63.0	300
79.0	1400

- 6.15. Compound **106** reacts thermally to form **107** in *sec*-butylbenzene. A kinetic study produced the following data: $\log A = 13.12$, $E_a = 30.6$ kcal/mol; $\Delta H^\ddagger = 29.8$ kcal/mol, $\Delta S^\ddagger = -11.3$ eu. Based on these values, would you favor a mechanism in which **106** dissociates into two molecules that recombine in a different way to form the product, or would you favor a mechanism in which the reactant rearranges without dissociation?



- 6.16. Indicate the kind of equilibrium isotope effect (e.g., primary or secondary, α or β , etc.) one would expect and predict the magnitude of the isotope effect on the equilibrium constant for the dissociation of cyclopentanone methyl hemiketal (**108**) to the ketone **109** and methanol (Figure 6.86).
- 6.17. Indicate the kind of equilibrium isotope effect one would expect and predict the magnitude of the isotope effect on the reaction of acetaldehyde- d_1 (**110**) with water to give the hydrate **111** (Figure 6.87).
- 6.18. Ozonolysis of propene-1- d , and propene-2- d gave the k_H/k_D values shown in Figure 6.88. What do these results suggest about the symmetry of the transition structure for the addition of ozone to propene?
- 6.19. Suggest an explanation for the fact that the ρ value for the ionization of benzoic acids in ethanol is 1.96, whereas in water it is 1.0.

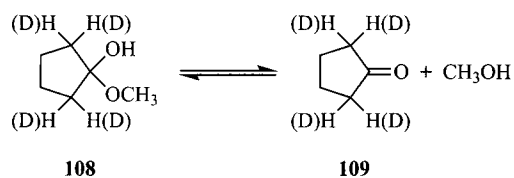
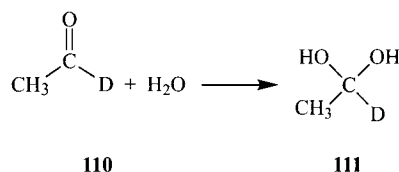
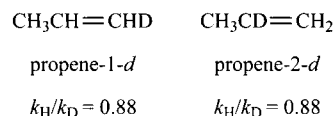


FIGURE 6.86

Dissociation of cyclopentanone methyl hemiketal.

**FIGURE 6.87**Hydration of acetaldehyde- d_1 .**FIGURE 6.88**

Kinetic isotope effects in addition of ozone to propene.

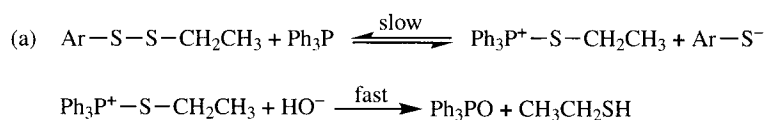
6.20. Some investigators try to observe a Hammett correlation without measuring the k_0 value for the unsubstituted compound (i.e., the substituent is hydrogen). Show that a plot of $\log k$ versus σ should give a linear Hammett correlation with the same slope one would obtain by plotting $\log(k/k_0)$ versus σ .

6.21. In a study of the reaction between ethyl (substituted)aryl disulfides with triphenylphosphine and water, the investigators proposed the mechanism shown in Figure 6.89(a), with step 1 being rate-limiting. They found that the rate constant for the first reaction varied according to the substituent (on the Ar of Ar-S-S-Et) as indicated in Table 6.12.

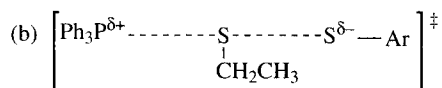
Show that these data give a linear Hammett correlation and calculate the value of ρ . Do you think this value of ρ supports the authors conclusion that the transition structure for step 1 is like the arrangement indicated in Figure 6.89(b)?

6.22. Consider the data in Table 6.13 for the reaction of a series of substituted phenoxides with *N*-chloroacetanilide (equation 6.107) and for the acidities of the phenols in water. (Values of σ^- are from the problem reference.)

- Determine whether the acidities correlate better with σ or with σ^- and rationalize the results.
- Determine whether the rate constants correlate better with σ or with σ^- . From the value of ρ you obtain, suggest a likely transition structure for the reaction of phenoxide with *N*-chloroacetanilide.

**FIGURE 6.89**

(a) Two steps in a proposed mechanism and (b) proposed transition structure for the first step.

**TABLE 6.12 Kinetic Data for the Reaction of Ethyl (Substituted)aryl Disulfides with Triphenylphosphine in Water**

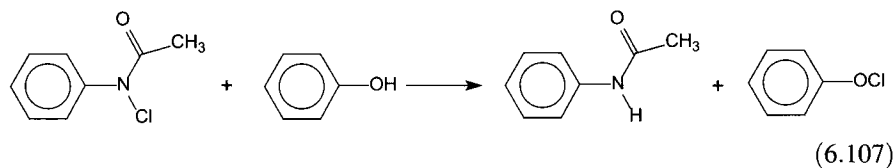
Substituent	$10^{-4}k_1$ ($\text{M}^{-1} \text{min}^{-1}$) ^a	Substituent	$10^{-4}k_1$ ($\text{M}^{-1} \text{min}^{-1}$) ^a
4-NO ₂	6.54	3-OCH ₃	0.355
3-NO ₂	6.19	4-OCH ₃	0.097
3-Cl	1.08	4-NH ₂	0.0219
4-Cl	0.684		

^a $k_1 = k_{\text{obs}}/[\text{Ph}_3\text{P}]$.

TABLE 6.13 Acidities and Rate Constants for Reaction of Substituted Phenoxides with *N*-Chloroacetanilide

Substituent	σ^-	pK_a^a	Rate Constant ($M^{-1} \text{min}^{-1}$)
<i>p</i> -CH ₃	0.16	10.28	1.1×10^3
H	0.00	9.95	5.3×10^2
<i>m</i> -Cl	0.37	9.42	3.6×10^2
<i>m</i> -NO ₂	0.74	8.52	8.5
<i>p</i> -NO ₂	1.25	7.13	4.1×10^{-1}

^a Under the reaction conditions.



- 6.23. Rate data for the ozonolysis of a series of substituted styrenes in CCl₄ at 25°C are summarized in Table 6.14. Do the data show a linear Hammett correlation with either σ , σ^+ , or σ^- ? (Ordinary σ values may be used for meta substituents in all three correlations.) If so, what is the value of ρ at 25°C? What do these results suggest about the reaction mechanism? Specifically, does the addition of ozone appear to be electrophilic or nucleophilic in nature?
- 6.24. In the Beckmann rearrangement (equation 6.108), oximes of ketones are converted to amides by acid catalysts.



In principle, two mechanisms can be considered for the rearrangement (Figure 6.90). Mechanism (a) involves a migration of an alkyl group that is concerted with dissociation of water. Mechanism (b) involves dissociation of the alkyl group instead of migration, leading to a nitrile and carbocation that can then undergo a Ritter reaction.²³⁷

TABLE 6.14 Rate Constants for the Reaction of Ozone with XC₆H₄CH=CH₂ in CCl₄ Solution at 25°C

X	k_2 ($M^{-1} \text{s}^{-1}$)
<i>p</i> -CH ₃	5.29
H	3.64
<i>p</i> -Cl	2.25
<i>m</i> -Cl	1.70
<i>m</i> -NO ₂	0.84

²³⁷ Ritter, J. J.; Minieri, P. P. *J. Am. Chem. Soc.* **1948**, *70*, 4045; Ritter, J. J.; Kalish, J. *J. Am. Chem. Soc.* **1948**, *70*, 4048.

FIGURE 6.90

(a) Nondissociative and (b) dissociative mechanisms for the Beckmann rearrangement.

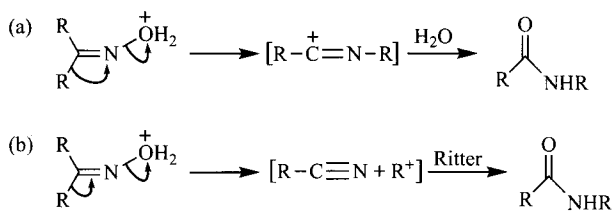
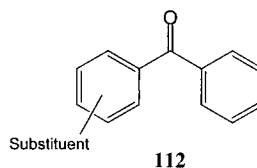


TABLE 6.15 Kinetic Data for Addition of Methylithium to Benzophenone Derivatives

Substituent	k_{rel}
3-CF ₃	2.82
3-Cl	2.47
4-Cl	1.72
4-F	1.19
H	1
3-CH ₃	0.84
4-OCH ₃	0.48

Most experimental studies have supported the nondissociative mechanism (a) for this reaction,²³⁸ but one study reported the following results: the polyphosphoric acid (PPA)-catalyzed Beckmann rearrangement of pinacolone oxime produced *N-t*-butylacetamide, while the PPA-catalyzed rearrangement of 2-methyl-2-phenylpropiophenone oxime produced *N*-benzoyl- α,α -dimethylbenzylamine and benzamide. Carrying out the rearrangement on a mixture of pinacolone oxime and 2-methyl-2-phenylpropiophenone oxime produced the products expected from each reactant, plus *N-t*-butylbenzamide and *N*-acetyl- α,α -dimethylbenzylamine.

- What does the observation of the last two products suggest about the mechanism of the Beckmann reactions in this study?
 - Can you propose a stereochemical study to further distinguish between the two possible pathways for the reaction?
 - For what types of oximes would a dissociative pathway be most likely?
- 6.25. Table 6.15 shows relative rate constants reported for the addition of methylithium to benzophenone derivatives having the general structure **112** in diethyl ether solution at 0°C. Determine the Hammett ρ for this reaction. Is the value of ρ consistent with your expectation for nucleophilic addition of methylithium to the carbonyl group?



²³⁸ For a review and leading references, see Donaruma, L. G.; Heldt, W. Z.; *Org. React.* **1960**, *11*, 1.

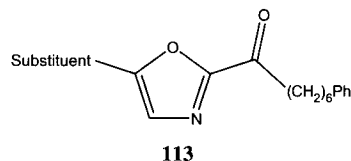
TABLE 6.16 Kinetic Data for Isomerization of 4-Substituted Aryl Compounds

T ($^{\circ}\text{C}$)	$k \times 10^5$ (s^{-1}) for the Indicated Substituent		
	4-OCH ₃	None (4-H)	4-NO ₂
170	3.46	2.01	1.47
190	16.9	9.94	7.26
210	78.6	45.2	33.4
230	396	228	166

TABLE 6.17 K_i Values for Derivatives of 113

Substituent	K_i (nM)
CH ₃	80
H	48
SCH ₃	25
Cl	5
CN	0.4

- 6.26. Consider the data in Table 6.16 for the first-order rate constants for the isomerization of a series of 4-substituted aryl compounds. How could you determine whether the relative reactivities are influenced primarily by ΔH^{\ddagger} or ΔS^{\ddagger} values without constructing an Arrhenius, Eyring, or Hammett plot?
- 6.27. 5-Substituted derivatives of 7-phenyl-1-(oxazol-2-yl)heptane-1-one (**113**) have been shown to inhibit the enzyme fatty acid amide hydrolase with inhibition constants K_i as shown Table 6.17. Predict the K_i value of the 5-trifluoromethyl derivative.



- 6.28. Second-order rate constants for the reaction of an amine with substituted benzyl bromides in methanol solution at several temperatures are shown in Table 6.18. Calculate ΔH^{\ddagger} and ΔS^{\ddagger} for the reaction of each of the benzyl bromides. Do the data exhibit an isokinetic relationship? If so, what is the isokinetic temperature?

TABLE 6.18 Rate Constants for a Substitution Reaction

Substituent	$k_2 \times 10^4$ ($\text{M}^{-1}\text{s}^{-1}$)			
	$T = 298\text{ K}$	$T = 303\text{ K}$	$T = 308\text{ K}$	$T = 313\text{ K}$
H	13.3	22.8	45.3	84.7
<i>p</i> -CH ₃	10.6	17.8	41.3	78.0
<i>p</i> -Br	18.8	27.6	49.3	91.8
<i>p</i> -NO ₂	41.6	52.7	66.8	98.6

Acid and Base Catalysis of Organic Reactions

7.1 ACIDITY AND BASICITY OF ORGANIC COMPOUNDS

Acid–Base Measurements in Solution

Acidity and basicity are fundamental properties of organic compounds, and acid–base reactions are essential steps in many organic transformations. Although there are several definitions of acidity and basicity, the Brønsted theory and the Lewis theory are used most often in organic chemistry.^{1,2} In Lewis theory, an **acid** is an electron pair acceptor and a **base** is an electron pair donor, as in the reaction of a trialkylamine as Lewis base with boron trifluoride as Lewis acid (equation 7.1).



In Brønsted theory, an acid is a proton donor and a base is a proton acceptor, as in the reaction of an amine with HCl in equation 7.2.^{3–5} There is a conceptual error in the latter definition, however. As Hawkes noted, “it makes no more sense to speak of HCl ‘donating’ a proton than of ‘donating’ your purse to a mugger.” It is more appropriate to speak of a Brønsted acid as

¹ For a discussion of acid–base theories, see Finston, H. L.; Rychtman, A. C. *A New View of Current Acid–Base Theories*; Wiley-Interscience: New York, 1982.

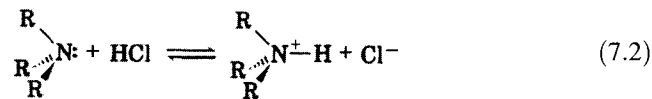
² A history of acid–base theories was given by Jensen, W. B. *The Lewis Acid–Base Concepts: An Overview*; Wiley-Interscience: New York, 1980.

³ The earlier Arrhenius theory held that an acid was a proton donor and a base was a hydroxide donor (reference 1). For a discussion of the merits of teaching this definition, see reference 6.

⁴ Brønsted, J. N. *Recl. Trav. Chim. Pays-Bas* **1923**, *42*, 718.

⁵ A proton donor is often defined as a Brønsted–Lowry acid. For a discussion of the degree to which Lowry should share credit with Brønsted, see the discussion in Bell, R. P. *The Proton in Chemistry*, 2nd ed.; Cornell University Press: Ithaca, NY, 1973.

being a substance "from which a proton can be removed" and of a Brønsted base as a substance "that can remove a proton from an acid."⁶



More precisely, a Brønsted acid is a substance from which a hydron can be removed and a Brønsted base is a substance that can remove a hydron from an acid.⁷ Hydron is a general term for H^+ , irrespective of isotope, and it includes the proton ($^1\text{H}^+$), deuteron ($^2\text{H}^+$), and triton ($^3\text{H}^+$).⁸ This distinction is useful in discussions of isotope effects, but it is seldom made otherwise. The term *proton* has long been used to represent H^+ in general as well as to represent the specific isotope $^1\text{H}^+$. Because of this familiar usage, a mechanistic discussion that uses the terms *protonation* and *deprotonation* may be clearer than an analysis that uses the terms *hydronation* and *dehydronation*. The discussion here will therefore retain the term *proton* as a general term for H^+ . Use of the term *proton* to mean the specific isotope $^1\text{H}^+$ can be understood in context.

The equilibrium constant for the Brønsted acid–base reaction of the acid A–H (equation 7.3) is the acidity constant, K_a , which is calculated as indicated in equation 7.4. It is convenient to indicate the acidity of a substance with its $\text{p}K_a$ value, which is defined in equation 7.5.^{9,10}



$$K_a = \frac{[\text{A}^-][\text{H}^+]}{[\text{A} - \text{H}]} \quad (7.4)$$

$$\text{p}K_a = -\log K_a = \text{pH} + \log \frac{[\text{A} - \text{H}]}{[\text{A}^-]} \quad (7.5)$$

Traditionally, the concentrations of A–H and A^- have been measured by UV–vis spectrophotometry or by potentiometry, although NMR and IR methods have also been utilized.¹¹ There are a number of tabulations of $\text{p}K_a$ values in aqueous solution, and correlations of $\text{p}K_a$ values with molecular structure have been presented.^{12–15}

⁶ Hawkes, S. J. *J. Chem. Educ.* **1992**, *69*, 542.

⁷ Commission on Physical Organic Chemistry, IUPAC, *Pure Appl. Chem.* **1994**, *66*, 1077.

⁸ For a discussion of the recommended terminology for hydrogen atoms and ions, see Commission on Physical Organic Chemistry, IUPAC, *Pure Appl. Chem.* **1988**, *60*, 1115.

⁹ The symbol $\text{p}X$ means the negative of the logarithm (base 10) of the quantity X . Thus, pH is $-\log a_{\text{H}^+}$, which we often approximate as $-\log [\text{H}^+]$. Here and in equation 7.6, a_{H^+} is the activity of H^+ and γ_{H^+} is the activity coefficient of H^+ . For a discussion, see Albert, A.; Serjeant, E. P. *The Determination of Ionization Constants: A Laboratory Manual*, 3rd ed.; Chapman and Hall: London, 1984; p. 203.

¹⁰ Bates, R. G. *Determination of pH: Theory and Practice*; John Wiley & Sons: New York, 1964.

¹¹ Cookson, R. F. *Chem. Rev.* **1974**, *74*, 5 and references therein.

¹² Serjeant, E. P.; Dempsey, B. *Ionisation Constants of Organic Acids in Aqueous Solution*; Pergamon Press: Oxford, England, 1979.

¹³ Kortüm, G.; Vogel, W.; Andrussow, K. *Dissociation Constants of Organic Acids in Aqueous Solution*; Butterworths: London, 1961.

¹⁴ Perrin, D. D.; Dempsey, B.; Serjeant, E. P. *pK_a Prediction for Organic Acids and Bases*; Chapman and Hall: London, 1981.

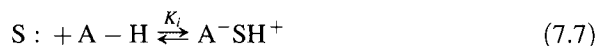
¹⁵ Barlin, G. B.; Perrin, D. D. *Q. Rev. Chem. Soc.* **1966**, *20*, 75.

The expression of pK_a values in terms of concentrations (equation 7.5) is not rigorously correct. Instead, the acidity of a solution at equilibrium should be defined by the **activity** (a) of each species or by the product of the concentration of each species and its **activity coefficient** (γ). Thus, the **thermodynamic acidity constant**, K_a^T , is defined as

$$K_a^T = \frac{a_{H^+} a_{A^-}}{a_{H-A}} = \frac{\gamma_{H^+} [H^+] \gamma_{A^-} [A^-]}{\gamma_{H-A} [A-H]} = K_a \frac{\gamma_{H^+} \gamma_{A^-}}{\gamma_{H-A}} \quad (7.6)$$

Since the activity coefficients are concentration dependent and approach unity as the solution becomes more dilute, K_a^T is approximately the same as K_a in very dilute solution.¹⁶

Equation 7.3 does not explicitly consider the role of the reaction medium. We have represented the product of the ionization as H^+ , but in solution the product involves solvent molecules as participants in the reaction. In water the products are solvated protons, $H(H_2O)_n^+$, and ion pairing effects may be important as well, so a more complete description of the reaction may be given by equations 7.7 and 7.8. The acid and base initially form an ion pair involving solvent (S) with equilibrium constant K_i , and then the ions dissociate (with an equilibrium constant K_d). Changes in the dielectric constant of the medium are thought to influence K_d more than K_i .^{11,17} Ordinarily, however, we use the simpler description of equation 7.3, in which the role of the solvent is considered only implicitly. Table 7.1 lists pK_a values for selected carboxylic acids, alcohols, phenols, and other compounds.



Even if literature acidity data are not readily available for a particular compound, empirical correlations may allow an estimation of its pK_a value. For example, a very good prediction of the pK_a value for a multiply substituted benzoic acid can be obtained from the relationship¹⁸

$$pK_a = 4.20 - \Sigma\sigma \quad (7.9)$$

in which $\Sigma\sigma$ is the sum of the Hammett σ values for the individual substituents on the benzene ring. Interestingly, almost any ortho substituent increases the acidity of benzoic acid (see Table 7.1), so almost all σ values for

¹⁶ The K_a from equation 7.4 might be called the "concentration-dependent acidity constant," since it varies with concentration (reference 9).

¹⁷ In this formulation K_a is defined as

$$K_a = \frac{K_i K_d}{1 + K_d}$$

See King, E. J. *Acid-Base Equilibria*; Pergamon Press: Oxford, England, 1965; reference 11.

¹⁸ Stewart, R. *The Proton: Applications to Organic Chemistry*; Academic Press: New York, 1985.

TABLE 7.1 pK_a Data for Selected Organic Compounds in Aqueous Solution

Compound	pK_a
<i>Carboxylic Acids</i>	
Formic acid	3.75 ^a
Performic acid	7.1 ^b
Acetic acid	4.76 ^c
Fluoroacetic acid	2.59 ^a
Chloroacetic acid	2.87 ^a
Bromoacetic acid	2.90 ^a
Iodoacetic acid	3.18 ^a
Cyanoacetic acid	2.47 ^a
Methoxyacetic acid	3.57 ^a
Nitroacetic acid	1.48 ^d
Mercaptoacetic acid	3.56 ^d
Hydroxyacetic acid	3.38 ^a
Phenylacetic acid	4.31 ^b
Phenoxyacetic acid	3.16 ^b
Difluoroacetic acid	1.34 ^d
Dichloroacetic acid	1.35 ^d
Dibromoacetic acid	1.48 ^b
Trifluoroacetic acid	0.52 ^b
Trichloroacetic acid	0.51 ^b
Tribromoacetic acid	0.72 ^b
Propanoic acid	4.87 ^a
Acrylic acid ($H_2C=CH-CO_2H$)	4.25 ^b
Propiolic acid ($HC\equiv C-CO_2H$)	1.89 ^d
Pyruvic acid (CH_3COCO_2H)	2.39 ^b
2,2,3,3,3-Pentafluoropropanoic acid	-0.41 ^b
Butanoic acid	4.82 ^c
<i>cis</i> -2-Butenoic acid	4.42 ^b
<i>trans</i> -2-Butenoic acid	4.70 ^b
2-Butynoic acid ($CH_3-C\equiv C-CO_2H$)	2.59 ^b
Cyclopentanecarboxylic acid	4.99 ^c
Cyclohexanecarboxylic acid	4.90 ^a
Benzoic acid	4.20 ^a
2-Methylbenzoic acid	3.91 ^d
3-Methylbenzoic acid	4.27 ^d
4-Methylbenzoic acid	4.37 ^d
2- <i>t</i> -Butylbenzoic acid	3.54 ^d
2-Bromobenzoic acid	2.85 ^d
3-Bromobenzoic acid	3.81 ^a
4-Bromobenzoic acid	4.00 ^a
2-Chlorobenzoic acid	2.91 ^d
3-Chlorobenzoic acid	3.83 ^a
4-Chlorobenzoic acid	3.99 ^a
2-Fluorobenzoic acid	3.27 ^d
3-Fluorobenzoic acid	3.86 ^d
4-Fluorobenzoic acid	4.14 ^d
2-Iodobenzoic acid	2.86 ^d
3-Iodobenzoic acid	3.85 ^d

TABLE 7.1 (Continued)

Compound	pK _a
4-Iodobenzoic acid	4.00 ^d
2-Hydroxybenzoic (salicylic) acid	2.97 ^a
3-Hydroxybenzoic acid	4.07 ^d
4-Hydroxybenzoic acid	4.58 ^a
2-Cyanobenzoic acid	3.14 ^d
3-Cyanobenzoic acid	3.60 ^d
4-Cyanobenzoic acid	3.55 ^a
2-Nitrobenzoic acid	2.21 ^d
3-Nitrobenzoic acid	3.49 ^d
4-Nitrobenzoic acid	3.44 ^a
Acetylsalicylic acid	3.38 ^b
Pentafluorobenzoic acid	1.75 ^b
1-Naphthoic acid	3.60 ^b
2-Naphthoic acid	4.14 ^b
<i>Alcohols, Thiols, Phenols, and Water</i>	
Water	15.74 ^d
Methanol	15.5 ^d
Ethanol	15.9 ^d
2-Chloroethanol	14.3 ^d
2-Methoxyethanol	14.8 ^d
2,2,2-Trifluoroethanol	12.4 ^d
1-Propanol	16.1 ^d
Allyl alcohol	15.5 ^d
2-Propanol	17.1 ^d
Propargyl alcohol (H-C≡C-CH ₂ OH)	13.6 ^d
1-Butanol	16.1 ^d
2-Butanol	17.6 ^d
<i>t</i> -Butyl alcohol	19.2 ^d
Benzyl alcohol	15.4 ^d
Phenol	10.0 ^f
1-Naphthol	9.39 ^f
2-Naphthol	9.59 ^f
Methanethiol	10.33 ^d
Ethanethiol	10.61 ^d
Thiophenol	6.52 ^f
<i>Other Acids</i>	
<i>p</i> -Toluenesulfonic acid	-1.34 ^b
Nitric acid	-1.44 ^e
HBr	-8. ^e
HCl	-6.1 ^e
HF	3.18 ^e
HCN	9.22 ^e

^a Data from the compilation in reference 71.^b Data from reference 12.^c Data from the compilation in reference 72.^d Data from reference 18.^e Data from reference 9.^f Data from the compilation in reference 15.

ortho substituents are positive.^{12,18} For example, the Hammett σ value for a methyl group at the ortho position in benzoic acid is +0.29, in contrast to the value of -0.14 for a methyl group in the para position and a value of -0.06 for a methyl group in the meta position. It has been suggested that ortho substituents reduce the extent of resonance of the carboxyl group with the benzene ring through a steric effect because ortho substituents perturb the solvation of the protonated carboxyl group more than they perturb the solvation of the carboxylate ion.¹⁹

The acidities of the aliphatic carboxylic acids (RCO₂H) in Table 7.1 correlate well with the Taft σ^* values of the substituents,²⁰ with the correlation being by equation 7.10.¹⁴

$$pK_a = 4.66 - 1.62\sigma^* \quad (7.10)$$

The corresponding equation for derivatives of acetic acid, RCH₂CO₂H, is¹⁴

$$pK_a = 5.16 - 0.73\sigma^* \quad (7.11)$$

For alcohols, RCH₂OH, the relationship is^{14,21}

$$pK_a = 15.9 - 1.42\sigma^* \quad (7.12)$$

As may be seen from equations 7.10 and 7.11, there is a large difference between the acidities of alcohols and carboxylic acids. Organic chemists have traditionally ascribed the greater acidity of acetic acid compared to isopropyl alcohol to resonance stabilization of the negative charge in the acetate ion, which makes it more stable than an isopropoxide ion. Siggel, Streitwieser, and Thomas concluded from *ab initio* calculations, however, that resonance contributes only about 2–5 kcal/mol to the stabilization of the carboxylate ion. Instead, about 80% of the difference in acidity between acetic acid and isopropyl alcohol was ascribed to the inductive effect of the carbonyl group on the adjacent OH function in acetic acid (Figure 7.1).^{22–24} This conclusion was supported by Taft and co-workers, who concluded that the 10^{22.5} greater acidity of acetic acid over ethanol in the gas phase arises primarily (by a factor of 10¹⁴) from a field or induction interaction, not from resonance. On the other hand, they also concluded that the greater acidity of phenol over cyclohexanol arises primarily through resonance. Burk and Schleyer observed that the Siggel–Thomas analysis of acidity from two different directions—dissociation of a neutral acid and protonation of its anion—led to different conclusions about the role of acid destabilization and anion stabilization in determining the acidity of carboxylic acids. This con-

¹⁹ Decouzon, M.; Ertl, P.; Exner, O.; Gal, J.-F.; Maria, P.-C. *J. Am. Chem. Soc.* **1993**, *115*, 12071.

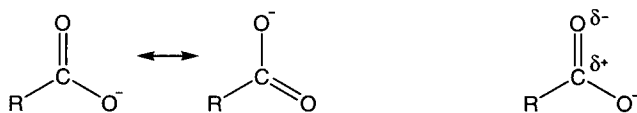
²⁰ Taft, R. W., Jr., in Newman, M. S., Ed. *Steric Effects in Organic Chemistry*; John Wiley & Sons: New York, 1956; p. 556 and references therein.

²¹ For an extensive list of Taft relationships for predicting the acidities of organic acids and protonated bases, see reference 12, pp. 126–135.

²² Siggel, M. R.; Thomas, T. D. *J. Am. Chem. Soc.* **1986**, *108*, 4360.

²³ Siggel, M. R. F.; Streitwieser, A., Jr.; Thomas, T. D. *J. Am. Chem. Soc.* **1988**, *110*, 8022. See also Bökman, F. *J. Am. Chem. Soc.* **1999**, *121*, 11217.

²⁴ McClard, R. W. *J. Chem. Educ.* **1987**, *64*, 416 noted that there should be a relatively flat potential energy surface between the transition state and the anion (ethoxide or acetate) in these acid–base reactions. For a discussion of the rate constants of proton transfer reactions, see reference 5.

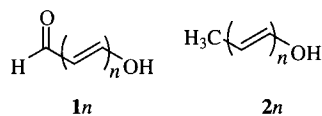
**FIGURE 7.1**

Resonance (left) and induction (right) stabilization of a carboxylate ion.

clusion suggested that the Siggel–Thomas analysis could not be used to determine the relative importance of induction and resonance in determining carboxylic acid acidity.²⁵

Hiberty and Byrman pointed out that the different conclusions reached by different investigators can result from the different assumptions that are implicit in each study.²⁶ They used *ab initio* valence bond theory to determine the difference in delocalization energies of the ionized and unionized forms of formic acid, vinyl alcohol, and ethanol. The results suggested that delocalization is primarily responsible for the greater acidity of vinyl alcohol than ethanol. They found that about half of the greater acidity of formic acid than ethanol is due to delocalization, with the remainder of the acidity increase being attributed to the inductive effect of the carbonyl group. Subsequent *ab initio* MO calculations by Wiberg and co-workers agreed qualitatively with the results of Hiberty and Byrman but ascribed even greater importance to Coulombic effects of the carbonyl group.²⁷

Holt and Karty used density functional theory (DFT) calculations to study the gas phase acidities of formic acid and a series of analogs with one or more carbon–carbon double bonds between the OH group and the carbonyl group.²⁸ By plotting the difference in calculated acidities for $1n$ and for a methanol derivative having the same number of vinyl groups ($2n$) and then extrapolating the resulting curve until $n = 0$, they concluded that the inductive effect of the carbonyl group is responsible for about 65% of the greater acidity of formic acid than methanol. The remaining 35% of acidity enhancement was attributed to resonance.



Exner and Čársky suggested that conclusions about the relative importance of resonance/delocalization versus Coulombic/inductive effects on the acidity of carboxylic acids in the gas phase should not be generalized implicitly to discussions of acidities in solution. They reported calculations indicating that both the inductive effect and the resonance effect of the carbonyl group are attenuated in aqueous solution but that the inductive effect is reduced to a greater extent.^{29,30} As Exner and Čársky noted, however,

²⁵ Burk, P.; Schleyer, P. v. R. *J. Mol. Struct.* **2000**, 505, 161.

²⁶ Hiberty, P. C.; Byrman, C. P. *J. Am. Chem. Soc.* **1995**, 117, 9875.

²⁷ Wiberg, K. B.; Ochterski, J.; Streitwieser, A. *J. Am. Chem. Soc.* **1996**, 118, 8291.

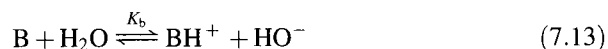
²⁸ Holt, J.; Karty, J. M. *J. Am. Chem. Soc.* **2003**, 125, 2797.

²⁹ Exner, O.; Čársky, P. *J. Am. Chem. Soc.* **2001**, 123, 9564.

³⁰ Calculations reported by Silva, C. O.; Nascimento, M. A. C. *Adv. Chem. Phys.* **2002**, 123, 423 also led to the conclusion that resonance effects are more important than inductive effects in the gas phase.

“the result will always depend on the definition and on the model applied; every model either operates with artificial structures or transfers some properties from one molecule to another.”²⁹ Thus, the familiar resonance explanation of carboxylic acid acidity is a useful conceptual model, but it—like all of our other models—offers only one perspective on the origin of acidities.

Basicities in water can be represented by K_b values for the equilibrium



but they usually are represented by K_{BH^+} values. K_{BH^+} is the equilibrium constant for deprotonation of the protonated base, BH^+ , in which H^+ is again the protonated solvent.³¹

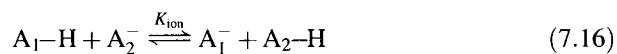


This approach allows equilibrium constants for acids and bases to be written on the same scale, so a smaller pK value corresponds to a stronger acid (or a weaker base), and a larger pK value corresponds to a weaker acid (or a stronger base).¹³ In aqueous solution, values of pK_b and pK_{BH^+} are related by equation 7.15.

$$pK_b + pK_{BH^+} = 14 \quad (7.15)$$

Values of pK_{BH^+} for the conjugate acids of selected nitrogen and oxygen bases in aqueous solution are shown in Table 7.2.^{32–34}

The range of pK_a values that can be measured in water is limited by the fact that water is both an acid ($pK_a = 15.75$) and a base ($pK_{BH^+} = -1.75$). Acid–base reactions can be carried out in other media, but the pK_a of a substance in a nonaqueous solvent may be very different from its pK_a in water. It is usually necessary to determine the pK_a of a substance (A_1-H) in a nonaqueous solvent indirectly by relating its pK_a to that of some other substance (A_2-H) having a known pK_a . The acid–base reaction used for the measurement is indicated in equation 7.16, and the pK_a is given by equation 7.17.³⁵



$$pK_{A_1H} = pK_{A_2H} - \log K_{ion} \quad (7.17)$$

In equation 7.16, the symbol for the equilibrium constant (K_{ion}) indicates that free anions are involved in the reaction. If the nonaqueous solvent is not

³¹ More rigorously, the acidity constants of protonated bases are calculated from activities instead of concentrations.

³² Arnett, E. M.; Wu, C. Y. *J. Am. Chem. Soc.* **1960**, *82*, 4999.

³³ Levy, G. C.; Cargioli, J. D.; Racela, W. J. *Am. Chem. Soc.* **1970**, *92*, 6238.

³⁴ Literature pK_{BH^+} values for several types of organic bases differ considerably. For example, Albert and Serjeant⁹ cite values for protonated alcohols ranging from -2.2 to -4.8 .

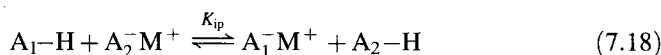
³⁵ For a review, see Streitwieser, A., Jr.; Juaristi, E.; Nebenzahl, L. L. in Buncl, E.; Durst, T., Eds. *Comprehensive Carbanion Chemistry, Part A: Structure and Reactivity*; Elsevier Scientific Publishing: Amsterdam, 1980; p. 323 and references therein. Some of the symbols used in this reference have been changed to avoid duplication of symbols used in other parts of the present discussion.

TABLE 7.2 Values of pK_{BH^+} for the Conjugate Acids of Selected Organic Compounds in Aqueous Solution

Protonated Base, BH^+	pK_{BH^+}
Methylamine· H^+	10.66 ^a
Dimethylamine· H^+	10.73 ^a
Trimethylamine· H^+	9.80 ^a
Pyridine· H^+	5.23 ^a
Aniline· H^+	4.87 ^a
<i>m</i> -Nitroaniline· H^+	2.46 ^a
<i>p</i> -Nitroaniline· H^+	1.02 ^a
Tetrahydrofuran· H^+	-2.08 ^b
Diethyl ether· H^+	-3.59 ^b
Anisole· H^+	-6.54 ^b
Acetophenone· H^+	-6.3 ^c
Acetone· H^+	-7.5 ^c
Cyclobutanone· H^+	-9.5 ^c
1-Fluoroacetone· H^+	-10.8 ^c
1,3-Difluoroacetone· H^+	-12.9 ^c
1,1,1-Trifluoroacetone· H^+	-14.9 ^c
1,1,3,3-Tetrafluoroacetone· H^+	≈-17 ^c

^a Reference 9.^b Reference 32. Uncertainties are ±0.18 for tetrahydrofuran, ±0.10 for diethyl ether, and ±0.02 for anisole.^c Reference 33. Values were determined by NMR from H_0 values (see page 430) at half-protonation in $H_2SO_4-H_2O$ mixtures.

sufficiently polar, the anions may be closely associated with cations, so the equilibria being measured (K_{ip}) may involve ion pairs (equations 7.18 and 7.19).



$$pK_{A_1H} = pK_{A_2H} - \log K_{ip} \quad (7.19)$$

Streitwieser and co-workers reported extensive measurements of pK_a values (designated as pK_{CsCHA} values) of weak acids in cyclohexylamine (CHA) solution using the cesium salt of cyclohexylamine as the base. They also established a pK_a scale involving Li^+ and Cs^+ counterions in tetrahydrofuran (THF) solution. These pK_a values are useful because THF is often used for synthetic reactions involving carbanions. The results suggested that lithium salts behave as solvent-separated ion pairs, while the cesium salts appeared to be contact ion pairs.^{36,37} The $pK_{Cs/THF}$ values of *p*-methylbiphenyl, fluorene, and 9-biphenylfluorene were found to be 38.73, 22.90, and 17.72, respectively.^{38,39}

³⁶ Kaufman, M. J.; Gronert, S.; Streitwieser, A., Jr. *J. Am. Chem. Soc.* **1988**, *110*, 2829.³⁷ The pK_a values were sometimes found to be concentration dependent because of aggregation of the ion pairs, primarily in the case of localized carbanions. Kaufman, M. J.; Streitwieser, A., Jr. *J. Am. Chem. Soc.* **1987**, *109*, 6092; Gronert, S.; Streitwieser, A., Jr. *J. Am. Chem. Soc.* **1988**, *110*, 2836.³⁸ Streitwieser, A.; Ciula, J. C.; Krom, J. A.; Thiele, G. J. *Org. Chem.* **1991**, *56*, 1074.³⁹ For those compounds that do not establish acid-base equilibria rapidly, studies of rates of isotopic exchange can be used to determine relative kinetic acidities of carbon acids. For a discussion of the correlation of kinetic acidities with equilibrium acidities, see Streitwieser, A., Jr.; Kaufman, M. J.; Bors, D. A.; Murdoch, J. R.; MacArthur, C. A.; Murphy, J. T.; Shen, C. C. *J. Am. Chem. Soc.* **1985**, *107*, 6983 and references therein.

TABLE 7.3 Equilibrium Acidities in DMSO and H₂O

Acid	pK _a (H ₂ O)	pK _a (DMSO)	Acid	pK _a (H ₂ O)	pK _a (DMSO)
F ₃ CSO ₃ H	-14 ^a	0.3	(CH ₃ CO) ₂ CH ₂	8.9	13.3
HBr	-9 ^a	0.9	HCN	9.1	12.9
HCl	-8 ^a	1.8	CH ₃ NO ₂	10.0	17.2
CH ₃ SO ₃ H	-0.6 ^a	1.6	C ₆ H ₅ OH	10.0	18.0
2,4,6-(NO ₂) ₃ C ₆ H ₂ OH	0.0	≈0	CH ₂ (CN) ₂	11.0	11.0
HF	3.2	15 ± 2	CH ₃ CONH ₂	15.1	25.1
C ₆ H ₅ CO ₂ H	4.25	11.1	CH ₃ OH	15.5	29.0
CH ₃ CO ₂ H	4.75	12.3	H ₂ O	15.75	32

^a These values are estimated by the *H*₀ method (see page 430).

Source: Reference 41.

Equilibrium acidity values in dimethyl sulfoxide (DMSO) solution are of wide interest because they have been shown to correlate with chemical reactivity and also to allow estimates of bond dissociation energies, relative radical stabilities, and the acidities of radical cations.^{39,40} As illustrated in Table 7.3, the pK_a values measured in DMSO differ from aqueous pK_a values in several important respects.⁴¹ First, values of pK_a as large as 32 can be determined without complications due to the leveling effect of the solvent (which has a pK_a of 35). In contrast, adding the same molar quantity of any one of the first four substances listed in Table 7.3 to water would produce the same concentration of H⁺ because they would all be fully dissociated.⁴² Second, pK_a values for a substance can vary dramatically with solvent because of differing solvation energies, particularly of the ions. For example, the two pK_a values for water shown in Table 7.3 differ by 16, and there are also large differences in the pK_a values for other acids that form oxyanions capable of strong hydrogen bonding with water. The delocalized anions formed by stronger acids do not hydrogen bond so strongly to water, however, so differences in the pK_a values of these compounds are smaller. For example, the pK_a value of 2,4,6-trinitrophenol (picric acid) is essentially the same in water as in DMSO.

Acid–Base Reactions in the Gas Phase

Gas Phase Acidity and Basicity Measurements

As discussed in the previous section, solvent effects have an important influence on pK_a values determined in solution. Indeed, there are pairs of acids for which the relative order of acidity can be reversed by a change of solvent.⁴³ The order of acidity of a pair of compounds may also be a function

⁴⁰ See also the discussion of structural and solvent effects on pK_a values measured in DMSO and in the gas phase by Taft, R. W.; Bordwell, F. G. *Acc. Chem. Res.* **1988**, *21*, 463.

⁴¹ Bordwell, F. G. *Acc. Chem. Res.* **1988**, *21*, 456.

⁴² The aqueous pK_a values shown are estimated from measurements using the acidity function, *H*₀, but there are uncertainties with these measurements.

⁴³ Allen, C. R.; Wright, P. G. *J. Chem. Educ.* **1964**, *41*, 251.

of temperature and of the effect of ion size on the enthalpy and entropy changes associated with ionization in solution.⁴⁴ In order to study the effects of structure on acidity and basicity in the absence of solvent, a variety of experimental techniques have been developed to study acid–base reactions in the gas phase. Three of the major experimental techniques are high pressure mass spectrometry (HPMS), flowing afterglow (FA) or flowing afterglow selected ion flow tube (FA-SIFT) studies,⁴⁵ and pulsed ion cyclotron resonance (ICR) spectrometry.^{46,47}

In principle, one might try to study the ionic dissociation of an acid (equation 7.3) directly in the gas phase, but ΔH for dissociation of a neutral species to a proton and an anion is usually quite large without solvent stabilization of the ions. For example, the ΔH for the gas phase dissociation of methane to methyl anion and a proton ($\Delta H_{\text{acid}}^{\circ}$) was calculated to be +417 kcal/mol.⁴⁸ This is much greater than the homolytic C–H bond dissociation energy of methane (+104 kcal/mol), so thermolysis of methane in the gas phase leads to radicals instead of ions. The pK_{a} value of an acid can be determined indirectly, however, by measuring the equilibrium for proton transfer from the acid to a base with a known pK_{a} . With a series of measurements, a scale of gas phase acidity values can be established by referencing one compound to another.

It is particularly difficult to determine the gas phase acidities of alkanes, because most alkyl anions cannot be produced as discrete species in the gas phase.⁴⁷ Indeed, some alkyl anions are expected to have either a negative or low positive ionization potential, meaning that the ionization of the corresponding hydrocarbon would produce a proton, a radical, and an electron, not a proton and a carbanion.⁴⁹ Again, indirect methods must be used. DePuy and co-workers measured the ratio of methane to alkane formed from the reactions of hydroxide ion with alkyltrimethylsilanes. A linear free energy relationship between the logarithm of the product ratios and the acidity of the corresponding alkanes, referenced to the known acidities of methane and benzene, allowed calculation of the gas phase acidity values of the alkanes. In these studies the alkyl anions are not produced as discrete carbanions but are thought to be formed as part of an ion–dipole complex in which the carbanion is stabilized through solvation by a trialkylsilanol molecule.^{47,50}

⁴⁴ Edward, J. T. *J. Chem. Educ.* **1982**, *59*, 354.

⁴⁵ Van Doren, J. M.; Barlow, S. E.; DePuy, C. H.; Bierbaum, V. M. *Int. J. Mass Spectrom. Ion Proc.* **1987**, *81*, 85.

⁴⁶ For a discussion of each of these techniques, see Pellerite, M. J.; Brauman, J. I. in Buncl, E.; Durst, T., Eds. *Comprehensive Carbanion Chemistry, Part A: Structure and Reactivity*; Elsevier Scientific Publishing: Amsterdam, 1980; p. 55 ff.

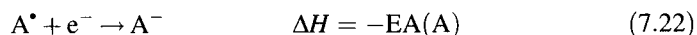
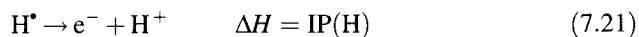
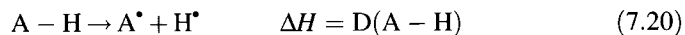
⁴⁷ Also see Aue, D.; Bowers, M. T. in Bowers, M. T., Ed. *Gas Phase Ion Chemistry*, Vol. 2; Academic Press: New York, 1979; pp. 1–51.

⁴⁸ DePuy, C. H.; Gronert, S.; Barlow, S. E.; Bierbaum, V. M.; Damrauer, R. J. *Am. Chem. Soc.* **1989**, *111*, 1968.

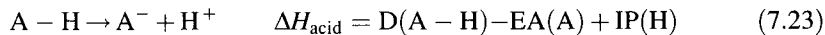
⁴⁹ Electron transfer from an anionic base to a neutral acid can also compete with proton transfer from the acid to the base in the gas phase. Han, C.-C.; Brauman, J. I. *J. Am. Chem. Soc.* **1988**, *110*, 4048.

⁵⁰ DePuy, C. H.; Bierbaum, V. M.; Damrauer, R. J. *Am. Chem. Soc.* **1984**, *106*, 4051.

ΔH_{acid} values can also be calculated from thermochemical cycles involving measurements of bond dissociation energies, ionization potentials, and electron affinities. Consider the reactions in equations 7.20 through 7.22:



Here $D(\text{A}-\text{H})$ is the gas phase homolytic dissociation energy of $\text{A}-\text{H}$, $\text{IP}(\text{H})$ is the ionization potential of the hydrogen atom, and $\text{EA}(\text{A})$ is the electron affinity of the radical A^{\bullet} . Summing the reactions in equations 7.20 through 7.22, and taking advantage of the fact that $\text{IP}(\text{H})$ is a constant, gives equation 7.23.^{51,52}



The standard state for reporting enthalpies and free energies of acid-base reactions in the gas phase is 298 K. The spectroscopic parameters must be corrected because homolytic dissociation energies are usually reported at 298 K, but electron affinity and ionization potential values derived from spectroscopic data refer to enthalpies at 0 K.^{53,54}

ΔH_{acid} values can be used to determine ΔG_{acid} values at 298 K if ΔS_{acid} values are known or can be estimated. Because ΔS° is nearly 0 for many proton transfer reactions in the gas phase, the difference in the ΔH_{acid} values for two compounds is essentially the same as the difference in the ΔG_{acid} values for the two compounds.⁵⁵ Table 7.4 lists gas phase acidity data for several carboxylic acids, alcohols, phenols, and C-H acids.

⁵¹ Ervin, K. M.; Gronert, S.; Barlow, S. E.; Gilles, M. K.; Harrison, A. G.; Bierbaum, V. M.; DePuy, C. H.; Lineberger, W. C.; Ellison, G. B. *J. Am. Chem. Soc.* **1990**, *112*, 5750.

⁵² Alternatively, if the acidity of the compound is known, the same relationship may be used to determine its bond dissociation energy. See, for example, Bordwell, F. G.; Cheng, J.-P.; Harrelson, J. A., Jr. *J. Am. Chem. Soc.* **1988**, *110*, 1229.

⁵³ For a discussion, see Bartmess, J. E.; McIver, R. T., Jr. in Bowers, M. T., Ed. *Gas Phase Ion Chemistry*, Vol. 2; Academic Press: New York, 1979; pp. 87-121.

⁵⁴ Also see Gal, J.-F.; Maria, P.-C. *Prog. Phys. Org. Chem.* **1990**, *17*, 159.

⁵⁵ For a discussion, see Majumdar, T. K.; Clairet, F.; Tabet, J.-C.; Cooks, R. G. *J. Am. Chem. Soc.* **1992**, *114*, 2897.

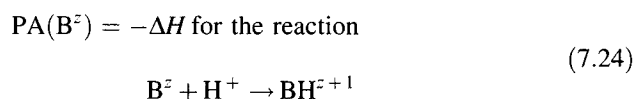
TABLE 7.4 Gas Phase Acidity Data for Selected Organic Compounds

Compound	ΔH_{acid} (kcal/mol)	ΔG_{acid} (kcal/mol)
<i>Carboxylic Acids</i>		
Formic acid	346.2 ± 1.2	339.2 ± 1.5
Acetic acid	348.1 ± 2.2	341.1 ± 2.0
Propanoic acid	347.4 ± 2.2	340.4 ± 2.0
Butanoic acid	346.8 ± 2.0	339.5 ± 2.0
Pentanoic acid	346.2 ± 2.1	339.2 ± 2.0
2-Methylpropanoic acid	346.0 ± 2.1	339.0 ± 2.0
2,2-Dimethylpropanoic acid	344.6 ± 2.1	337.6 ± 2.0
Benzoic acid	340.1 ± 2.2	332.9 ± 2.0
2-Methylbenzoic acid	339.3 ± 2.2	332.1 ± 2.0
3-Methylbenzoic acid	340.6 ± 2.1	333.6 ± 2.0
4-Methylbenzoic acid	341.0 ± 2.1	334.0 ± 2.0
Fluoroacetic acid	339.1 ± 2.2	331.6 ± 2.0
Chloroacetic acid	336.5 ± 2.2	329.0 ± 2.0
Bromoacetic acid	334.8 ± 2.3	328.2 ± 2.0
Iodoacetic acid	334.7 ± 2.2	327.7 ± 2.0
Difluoroacetic acid	331.0 ± 2.2	323.8 ± 2.0
Trifluoroacetic acid	323.8 ± 2.9	317.4 ± 2.0
<i>Water, Alcohols, and Phenol</i>		
Water	390.3	383.7 ± 0.3
Methanol	381.4 ± 1.0	375.0 ± 1.1
Ethanol	378.3 ± 1.0	371.7 ± 1.1
1-Propanol	375.7 ± 1.3	369.0 ± 1.4
2-Propanol	375.0 ± 1.0	368.5 ± 1.1
1-Butanol	375.2 ± 2.0	368.8 ± 2.1
2-Butanol	374.0 ± 2.0	367.6 ± 2.1
2-Methylpropanol	374.5 ± 2.0	367.8 ± 2.1
<i>t</i> -Butyl alcohol	374.8 ± 1.0	368.1 ± 2.0
2-Fluoroethanol	371.2 ± 2.9	364.5 ± 2.9
Phenol	349.7 ± 2.2	342.3 ± 2.0
<i>C-H Acids</i>		
Ethane	420.2 ± 2.0	411.8 ± 2.0
Propane (2° H)	419.4 ± 2.0	411.3 ± 2.1
Methane	416.7 ± 0.7	408.6 ± 2.0
Propane (1° H)	414.9 ± 2.0	407.3 ± 2.0
Butane (2° H)	414.9 ± 2.0	407.0 ± 2.0
Cyclobutane	417.3 ± 2.0	408.4 ± 2.1
Cyclopentane	416.1 ± 2.0	407.5 ± 2.1
Isobutane (3° H)	413.0 ± 2.0	405.6 ± 2.1
Isobutane (1° H)	413.0 ± 2.0	404.4 ± 2.1
Cyclopropane	411.1 ± 4.8	403.9 ± 7.2
Ethene	409.4 ± 0.6	401.0 ± 0.5
Benzene	401.7 ± 0.5	392.9 ± .04
Ethyne	380.0 ± 4.8	370.4 ± 4.8
Cycloheptatriene	375.2 ± 2.1	369.2 ± 2.0
Acetonitrile	372.8 ± 2.1	365.2 ± 2.0
Acetone	368.8 ± 2.0	361.9 ± 2.0
Cyclopentadiene	354.0 ± 2.2	347.8 ± 2.0

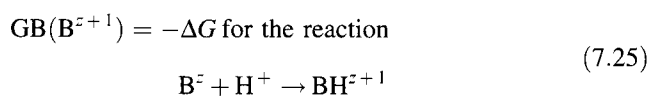
Source: Reference 56.

⁵⁶ Bartmess, J. E. in Linstrom, P. J.; Mallard, W. G., Eds. *NIST Chemistry WebBook, NIST Standard Reference Database No. 69*; National Institute of Standards and Technology: Gaithersburg, MD, 2005; <http://webbook.nist.gov>.

One can also measure the basicity of a substance in the gas phase.^{57,58} The **proton affinity** (PA) of species B with charge z is defined as the negative of the ΔH for the protonation of B^z (equation 7.24).



A larger proton affinity corresponds to greater difficulty in removing a proton from BH^{z+1} (i.e., to greater basicity of B^z) and a lower proton affinity corresponds to greater acidity of BH^{z+1} . A discussion of the measurement of PA values and an extensive compilation of experimental data were given by Szulejko and McMahon.⁵⁹ It is also possible to determine the **gas phase basicity** (GB), which is defined as



GB and PA are interconverted with the relationship⁶⁰

$$\text{PA} = \text{GB} - T \Delta S \quad (7.26)$$

Selected values of gas phase basicity are shown in Table 7.5.⁶¹

Comparison of Gas Phase and Solution Acidities

Measurement of gas phase acidity and basicity values allows a reexamination of the relationship of structure to acidity and basicity. The order of acidity of alcohols in the gas phase (Table 7.4) is *t*-butyl > isopropyl > ethyl > methyl, with methyl alcohol being more acidic than water. This is *opposite* the order of acidity of these compounds in aqueous solution (Table 7.1).⁶⁴ The decrease of acidity in solution with increasing alkyl substitution was traditionally

⁵⁷ For a discussion, see reference 1, p. 54 ff.

⁵⁸ Caldwell, G.; Renneboog, R.; Kebarle, P. *Can. J. Chem.* **1989**, *67*, 611.

⁵⁹ Szulejko, J. E.; McMahon, T. B. *J. Am. Chem. Soc.* **1993**, *115*, 7839.

⁶⁰ For a discussion, see Bouchoux, G.; Djazi, F.; Houriet, R.; Rolli, E. *J. Org. Chem.* **1988**, *53*, 3498.

⁶¹ Except as noted, ΔG values are measured at 300 K.

⁶² Hunter, E. P. L.; Lias, S. G. *J. Phys. Chem. Ref. Data* **1998**, *27*, 413.

⁶³ The relatively high basicity of cubane and dodecahedrane were ascribed primarily to bond strain and to polarizability effects, respectively. Santos, I.; Balogh, D. W.; Doecke, C. W.; Marshall, A. G.; Paquette, L. A. *J. Am. Chem. Soc.* **1986**, *108*, 8183.

⁶⁴ For a discussion of the gas phase acidities of these and other alcohols, see Brauman, J. I.; Blair, L. K. *J. Am. Chem. Soc.* **1968**, *90*, 6561.

TABLE 7.5 Selected Values of Proton Affinity (PA) and Gas Phase Basicity (GB) at 298 K

Base	PA (kcal/mol)	GB (kcal/mol)	Base	PA (kcal/mol)	GB (kcal/mol)
<i>Hydrocarbons</i>					
Methane	129.9	124.4	Isobutylamine	221.0	212.9
Ethane	142.5	136.2	<i>sec</i> -Butylamine	222.2	214.1
Ethene	162.6	155.7	<i>t</i> -Butylamine	223.3	215.1
Ethyne	153.3	147.4	Diethylamine	227.6	219.7
Propane	149.5	145.3	Pyrrole	209.2	201.7
Propene	179.6	172.6	Pyridine	222.3	214.7
Propyne	178.8	172.8	Aniline	210.9	203.3
Cyclopropane	179.3	172.6	<i>Compounds Containing Oxygen or Sulfur</i>		
Cyclopropene	195.6	188.3	CO ₂	129.2	123.3
Isobutane	162.0	160.4	Methanol	180.3	173.2
Isobutylene	191.7	185.4	Methanethiol	180.3	177.3
<i>trans</i> -2-Butene	178.5	172.1	Formaldehyde	170.4	163.3
Cyclobutene	187.5	180.1	Formic acid	177.3	169.7
1,3-Butadiene	187.2	181.1	Formamide	196.5	189.1
1,2-Butadiene	186.2	179.2	Nitromethane	180.4	172.5
2-Butyne	185.4	178.1	Ethanol	185.6	178.3
Cyclohexane	164.2	159.4	Dimethyl ether	189.3	182.7
1-Hexyne	191.2	185.2	Acetaldehyde	183.7	176.0
2-Hexyne	192.7	186.7	Trifluoroacetaldehyde	163.8	156.2
Cubane ^a	205.5	199.2	Acetic acid	187.3	179.9
Dodecahedrane ²³⁷¹	201.7	195.4	Trifluoroacetic acid	170.1	162.7
C ₆₀	—	197.8	Methyl formate	187.0	179.6
Benzene	179.3	173.4	Propanol	188.0	180.7
Hexafluorobenzene	154.9	149.2	2-Propanol	189.5	182.3
Toluene	187.4	180.8	Methyl acetate	196.4	189.0
Biphenyl	194.5	187.1	Acetone	194.1	186.9
Biphenylene	202.7	195.8	1-Butanol	188.6	181.4
<i>p</i> -Xylene	189.9	183.3	Isobutyl alcohol	189.7	182.2
<i>o</i> -Xylene	190.2	183.6	<i>t</i> -Butyl alcohol	191.8	184.6
Naphthalene	191.9	186.3	Diethyl ether	198.0	191.4
Azulene	221.1	214.1	THF	196.5	189.9
Anthracene	197.3	202.3	Furan	192.0	184.2
Phenanthrene	197.3	190.0	Thiophene	194.8	187.5
Tetracene	216.4	209.5	Cyclopentanone	196.9	189.8
Pryene	207.7	200.8	Cyclohexanone	201.0	193.9
Perylene	212.4	205.4	Phenol	195.3	187.9
Chrysene	201.0	193.6	Benzoic acid	197.0	188.8
Picene	203.5	196.1	Acetophenone	205.8	198.2
<i>Compounds Containing Nitrogen</i>			Cycloheptanone	202.1	195.0
Acetonitrile	186.2	178.8	Cyclooctanone	203.0	195.9
Ammonia	204.0	195.7	Cyclononanone	203.8	196.7
Methylamine	214.9	206.6	<i>Others</i>		
Dimethylamine	222.2	214.3	He	42.5	35.5
Ethylamine	218.0	209.8	Ne	47.5	41.7
Trimethylamine	226.8	219.4	Ar	88.2	82.8
Propylamine	219.4	211.3	Kr	101.5	96.2
Isopropylamine	220.8	212.5	Xe	119.4	114.3
Ethylmethylamine	225.2	217.3	H ₂ O	165.2	157.7
<i>n</i> -Butylamine	220.2	211.9			

(continued)

TABLE 7.5 (Continued)

Base	PA (kcal/mol)	GB (kcal/mol)	Base	PA (kcal/mol)	GB (kcal/mol)
H ₂ S	168.5	161.0	B ₂ H ₆	147.0	140.1
HF	115.7	109.2	N ₂	118.0	111.0
HCl	133.1	126.7	O ₂	100.6	94.7
HBr	139.6	133.3	O ₃	149.5	142.4
HI	150.0	143.7			

^a See reference 63.

Source: Reference 62.

attributed to the electron-donating property of alkyl groups, which was said to decrease the stability of alkoxide ions. The increase of acidity of an alcohol with alkyl substitution in the gas phase suggests that alkyl groups are able to polarize electrons *away* from a center of negative charge to stabilize an anion, just as they are able to polarize electrons *toward* a center of electron deficiency to increase the stability of a cation.⁶⁵ Theoretical calculations provide support for this view. Silla and co-workers determined from ab initio calculations that the charge associated with the carbon and oxygen atoms of the C–O[−] moiety of a series of alkoxides in the gas phase decreased along the series CH₃O[−], CH₃CH₂O[−], (CH₃)₂HCO[−], and (CH₃)₃CO[−].⁶⁶ The effect of this stabilization is to reduce the ΔG value calculated for gas phase deprotonation of methanol by 3.01, 4.98, and 6.21 kcal/mol for ethanol, 2-propanol, and *t*-butyl alcohol, respectively.⁶⁷

If a substituent has the same electronic effect in solution as in the gas phase, then the apparent acid-weakening effect of alkyl substituents in solution must arise because of a solvent effect that masks the charge-dispersing properties of the substituent.^{43,68} In solution methoxide anion is stabilized by 9.5 kcal/mol more than is the *t*-butoxide anion. Therefore, solvation of the anion overcomes the electronic effect, and methanol is the most acidic member of the series.^{69,70} Solvent effects also influence the relative acidity of carboxylic acids. In the gas phase the order of acidity is acetic acid < propionic acid < butanoic acid, but the opposite order is found in aqueous solution. Interestingly, formic acid might be predicted by this explanation to

⁶⁵ For a more detailed discussion of this point, see the discussion by Boand, G.; Houriet, R.; Gäumann, T. *J. Am. Chem. Soc.* **1983**, *105*, 2203.

⁶⁶ The sum of the fractional charges for the carbon and oxygen atoms in each case was calculated to be CH₃O[−], −0.957; CH₃CH₂O[−], −0.801; (CH₃)₂HCO[−], −0.664; (CH₃)₃CO[−], −0.548. The remaining negative charge was calculated to be dispersed among the atoms of the alkyl groups.

⁶⁷ Tuñón, I.; Silla, E.; Pascual-Ahuir, J.-L. *J. Am. Chem. Soc.* **1993**, *115*, 2226.

⁶⁸ Sebastian summarized some other experimental evidence that supports this view of the electronic effect of alkyl groups. Sebastian, J. F. *J. Chem. Educ.* **1971**, *48*, 97.

⁶⁹ There is a similar trend in the order of gas phase acidities of acetylenes, which were found to increase as CH₃C≡CH < CH₃CH₂C≡CH < HC≡CH. Dipole moments of hybrid orbitals may play a controlling role in this series. Brauman, J. I.; Blair, L. K. *J. Am. Chem. Soc.* **1971**, *93*, 4315.

⁷⁰ Siggel, M. R. F.; Thomas, T. D. *J. Am. Chem. Soc.* **1992**, *114*, 5795.

be less acidic in the gas phase than any of the three acids mentioned above, but formic acid is more acidic in the gas phase than is butanoic acid. Siggel and co-workers reported *ab initio* calculations that suggest an explanation for this apparent anomaly. In acetic acid the methyl group is bonded to a strongly electron-withdrawing carboxylic acid group and is highly polarized. There is less polarization of the methyl group in the acetate ion, however. As a result, replacing the $-H$ on formic acid with $-CH_3$ stabilizes the carboxylic acid function more than the carboxylate function, so there is a decrease in the acidity.⁷⁰

We might attribute the acid-weakening effect of alkyl substituents in solution to an increase in the enthalpy of the solvated anion because the substituents keep polar solvent molecules further away from the center of negative charge. Entropy changes associated with increased alkyl substitution on the anion cannot be ignored, however, because the magnitude of $T \Delta S$ can be greater than that of ΔH for ionization of many carboxylic acids in aqueous solution. For example, ΔH values for ionization of formic acid and acetic acid in water at 25°C are reported to be +0.01 and -0.02 kcal/mol, respectively, but the corresponding values of ΔS for the two ionizations are -17.1 and -21.9 eu.^{71,72} Furthermore, Bartmess and co-workers concluded from thermodynamic calculations that the *enthalpy* of ionization in solution is actually more favorable for acids with large, bulky R groups than for acids with small R groups, just as it is in the gas phase. They determined that the decrease in acidity that accompanies an increase in the size of the R group in RCH_2CO_2H actually arises from a less favorable *entropy* term. Specifically, the bulkier R group causes the solvent around the anion to become more ordered upon ionization, and this is the determining factor for acidities in solution.^{43,73}

It is also worthwhile to compare the values of ΔH for the ionization of halomethanes in the gas phase with their pK_a values in solution. In the gas phase, the relative acidities of methane and two halomethanes were found to be $CH_4 < CH_3F < CH_3Cl$ (Table 7.4). The greater acidity of methyl chloride than of methyl fluoride cannot be rationalized by any simple prediction based on electronegativity. Instead, the greater acidity of methyl chloride is attributed to the greater polarizability of chlorine than fluorine.^{74,75} The observation that the acidity of chloroform in water is 10^7 greater than that of fluoroform (Table 7.1) suggests that polarizability is important in solution as well.⁷⁶

⁷¹ Christensen, J. J.; Izatt, R. M.; Hansen, L. D. *J. Am. Chem. Soc.* **1967**, *89*, 213.

⁷² Christensen, J. J.; Oscarson, J. L.; Izatt, R. M. *J. Am. Chem. Soc.* **1968**, *90*, 5949.

⁷³ Wilson, B.; Georgiadis, R.; Bartmess, J. E. *J. Am. Chem. Soc.* **1991**, *113*, 1762.

⁷⁴ Schleyer, P. v. R.; Clark, T.; Kos, A. J.; Spitznagel, G. W.; Rohde, C.; Arad, D.; Houk, K. N.; Rondan, N. G. *J. Am. Chem. Soc.* **1984**, *106*, 6467.

⁷⁵ For theoretical calculations of the effects of multiple halogen substituents on methane, see Rodriguez, C. F.; Sirois, S.; Hopkinson, A. C. *J. Org. Chem.* **1992**, *57*, 4869.

⁷⁶ See also the discussion of kinetics of formation of carbanions from trihalomethanes in Hine, J. *Physical Organic Chemistry*, 2nd ed.; McGraw-Hill: New York, 1962; pp. 486-487.

Acidity Functions

As noted on page 422, dissolving the same molar quantity of two acids that are both fully dissociated in water will produce solutions with the same concentration of H_3O^+ . Because of this leveling effect, it is not possible to tell which of the acids is stronger (see equation 7.5).^{77,78} This observation led Hammett to consider ways to study acidities of species in more strongly acidic media, such as mixtures of water and sulfuric acid, because he considered an acid that is half-dissociated in 50% H_2SO_4 to be a stronger acid than one that is half-dissociated in 10% H_2SO_4 . To this end, Hammett suggested the use of an **acidity function**, H_0 , to categorize acidities in such environments.⁷⁹ In other words, the acidity function can be used to extend the pH scale beyond the range available in aqueous solutions.

As indicated by equation 7.14, we can represent the protonation equilibrium for a base by the relationship



Again, H^+ represents the protonated solvent. Letting the symbol I stand for the ratio of the concentrations of protonated to nonprotonated base, ($[\text{BH}^+]/[\text{B}]$), we may write

$$\text{p}K_{\text{BH}^+} = \log I + \text{pH} - \log \left(\frac{\gamma_{\text{B}}\gamma_{\text{H}^+}}{\gamma_{\text{BH}^+}} \right) \quad (7.27)$$

in which the γ terms represent the activity coefficients of the indicated species. If the activity coefficients are unity, then equation 7.27 reduces to

$$\text{p}K_{\text{BH}^+} = \log I + \text{pH} \quad (7.28)$$

If $[\text{BH}^+]$ is equal to $[\text{B}]$, then $\log I$ is 0, and $\text{p}K_{\text{BH}^+}$ is equal to pH. In most acidic solutions, however, the activity coefficients cannot be ignored. Therefore, the acidity function H_0 is defined as

$$H_0 = \text{pH} - \log \left(\frac{\gamma_{\text{B}}\gamma_{\text{H}^+}}{\gamma_{\text{BH}^+}} \right) \quad (7.29)$$

so

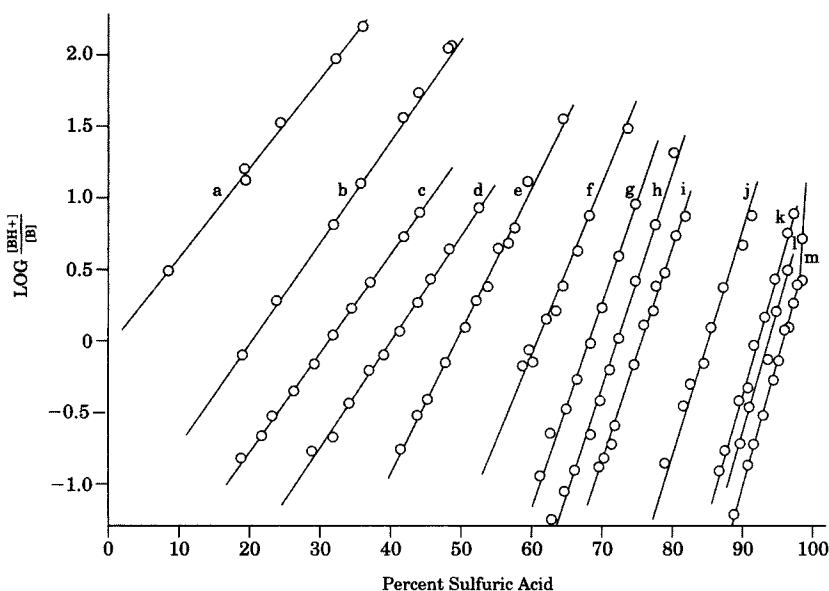
$$\text{p}K_{\text{BH}^+} = \log I + H_0 \quad (7.30)$$

Equation 7.30 provides a way to determine H_0 values for highly acidic solutions. We begin with a base having a known $\text{p}K_{\text{BH}^+}$ in aqueous solution. Then the ratio I is determined spectroscopically in a series of solutions having slightly different acidities. The protonated and nonprotonated bases show different absorption spectra, so UV-vis spectroscopy indicates the concentration of each species as a function of solution composition. The H_0 values

⁷⁷ Hammett, L. P. *Physical Organic Chemistry: Reaction Rates, Equilibria and Mechanisms*, 2nd ed.; McGraw-Hill: New York, 1970; pp. 272–273.

⁷⁸ See also Hammett, L. P. *J. Chem. Educ.* **1966**, *43*, 464.

⁷⁹ Hammett, L. P.; Deyrup, A. J. *J. Am. Chem. Soc.* **1932**, *54*, 2721.

**FIGURE 7.2**

Correlation of $\log ([\text{BH}^+]/[\text{B}])$ with percent H_2SO_4 for a series of nitroanilines. (Reproduced from reference 80. The figure also includes data from reference 79. The compounds are (a) 2-nitroaniline, (b) 4-chloro-2-nitroaniline, (c) 2,5-dichloro-4-nitroaniline, (d) 2-chloro-6-nitroaniline, (e) 2,6-dichloro-4-nitroaniline, (f) 2,4-dinitroaniline, (g) 2,6-dinitroaniline, (h) 4-chloro-2,6-dinitroaniline, (i) 2-bromo-4,6-dinitroaniline, (j) 3-methyl-2,4,6-trinitroaniline, (k) 3-bromo-2,4,6-trinitroaniline, (l) 3-chloro-2,4,6-trinitroaniline, and (m) 2,4,6-trinitroaniline.)

determined for these acid solutions are then used to determine the $\text{p}K_{\text{BH}^+}$ value for a second, weaker base. In turn, the second base is used to determine the H_0 value for each of a series of solutions with acid concentrations even greater than those used with the first base. These solutions are used to determine the $\text{p}K_{\text{BH}^+}$ value for a third, still weaker base, which is then used to extend the H_0 scale even further, and so on. By using a series of bases, H_0 values can be determined for a wide range of acid concentrations.

Hammett used the protonation of a series of nitroanilines in mixtures of water and sulfuric acid to establish the H_0 scale. Figure 7.2 shows the correlation of $\log I$ with percent H_2SO_4 for each of a series of nitroanilines.^{80,81} Figure 7.3 shows how H_0 varies over a concentration range from 0% H_2SO_4 (100% H_2O) to 100% H_2SO_4 .

Figure 7.3 also shows several other acidity functions, each of which has been developed with a different series of indicators. H''' is based on *N,N*-dialkylanilines and *N*-alkyldiphenylamines with nitro substituents on the aromatic rings, and H_A is based on a series of amides.⁸²⁻⁸⁴ Some of these functions change more rapidly with changing acid concentration than does H_0 , while others change less rapidly. All of the acidity functions change much more rapidly than does $-\log c_A$, where c_A is the molarity of the acid.

Some other acidity functions are defined for processes more complicated than simply protonating a particular type of atom. Consider the result of

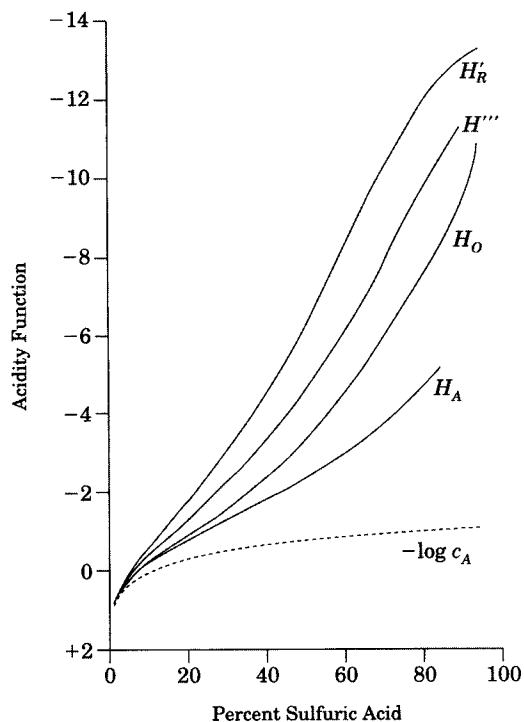
⁸⁰ Jorgenson, M. J.; Hartter, D. R. *J. Am. Chem. Soc.* **1963**, *85*, 878.

⁸¹ Note the increasing slope with increasing $[\text{H}_2\text{SO}_4]$.

⁸² Arnett, E. M.; Mach, G. W. *J. Am. Chem. Soc.* **1964**, *86*, 2671.

⁸³ The triple prime notation refers to the fact that the protonation takes place on the nitrogen atom of a 3° aromatic amine. The ordinary H_0 values are sometimes called H' or H_0' because they are based on measurements for the protonation of a 1° nitrogen in an aniline. Compare Arnett, E. M.; Mach, G. W. *J. Am. Chem. Soc.* **1966**, *88*, 1177.

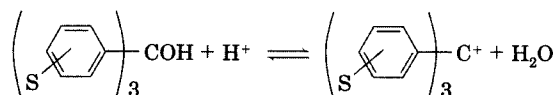
⁸⁴ Yates, K.; Stevens, J. B.; Katritzky, A. R. *Can. J. Chem.* **1964**, *42*, 1957.

**FIGURE 7.3**

Acidity functions of mixtures of water and sulfuric acid. (Reproduced from reference 77.)

FIGURE 7.4

Indicator reaction for acidity function H_R .



protonating the hydroxyl group of a triarylmethanol bearing a substituent (S) on each aromatic ring, as shown in Figure 7.4. The overall result is the formation of a carbocation and a water molecule. For this reaction, Deno and co-workers defined an acidity function H_R as shown in equation 7.31, in which a_W is the activity of water.⁸⁵ Reagan developed the H_C scale based on the protonation of carbon bases such as azulene, and acidity functions have also been developed for series of indoles (H_I), benzophenones (H_B), azulenes (H_m), and azo compounds (H_{Az}).^{86,87} Although sulfuric acid–water mixtures are often used for the definition of acidity functions, acidity functions have been measured for other water–acid mixtures, including perchloric, hydrochloric, phosphoric, nitric, and toluenesulfonic acids.

$$H_R = -\log a_{\text{H}^+} \left(\frac{a_{\text{ROH}}^\circ}{a_{\text{R}^+}^\circ} \right) + \log a_W \quad (7.31)$$

⁸⁵ Deno, N. C.; Jaruzelski, J. J.; Schriesheim, A. *J. Am. Chem. Soc.* **1955**, *77*, 3044. In Figure 7.3, the function H'_R is defined (reference 77) as $H'_R = -\log[a_{\text{H}^+} (a_{\text{ROH}}^\circ/a_{\text{R}^+}^\circ)]$.

⁸⁶ Reagan, M. T. *J. Am. Chem. Soc.* **1969**, *91*, 5506.

⁸⁷ Cox, R. A.; Yates, K. *J. Am. Chem. Soc.* **1978**, *100*, 3861.

It is possible to measure and compare the acidities of compounds that are not acidic enough to be ionized in water by using a more basic medium. Stewart and O'Donnell established the H_- scale for solutions of tetraalkylammonium hydroxide in sulfolane, DMSO–water, pyridine–water, and water.⁸⁸ In essence, the H_- scale extends upward the range for which pK_a values can be measured (which is effectively from 0 to 14 in aqueous solution) by another 12 pK units of basicity.^{39,89} A number of workers have modified the Hammett approach to acidity functions. In particular, Cox and Yates proposed the **excess acidity function**, X , which represents the difference between the acidity observed for a system and the acidity that would be observed if the system were ideal. In this approach, the activity coefficient ratio in equation 7.27 is taken to be the product of a coefficient m^* times the activity coefficient ratio, X , for a hypothetical standard base, B^* . Here m^* is a constant characteristic of each base, while X is a constant characteristic of the medium.^{18,86,90}

$$\log \left(\frac{\gamma_B \gamma_{H^+}}{\gamma_{BH^+}} \right) = m^* \log \left(\frac{\gamma_{B^*} \gamma_{H^+}}{\gamma_{B^*H^+}} \right) = m^* X \quad (7.32)$$

The different curves in Figure 7.3 indicate that the same water– H_2SO_4 solution can have very different acidity function values, depending on the system used to measure it. Hammett suggested that all of the functions are suitable as acidity functions, but noted that

It is now abundantly evident that a unique operational definition of the acidity of a system is a will-o'-the-wisp. Qualitatively one conveys some significant information by saying for instance that 80% aqueous sulfuric acid is more acid than 5% sulfuric acid. (This represents a semantic change, for 50 years ago one would have said that the 80% acid is less acid because it is less ionized.) But by one standard, that of reaction with bases of the H_R type, the 80% acid is 11.8 logarithmic units more acid than the 5% acid, and by another standard, that of reaction with bases of the H_A type, it is only 4.3 units more acid.⁷⁷

7.2 ACID AND BASE CATALYSIS OF CHEMICAL REACTIONS

Many organic reactions involve proton transfer, and acid-catalyzed or base-catalyzed reactions may be the “largest single class of organic mechanisms.”⁸³ We will not attempt to survey all possible acid-catalyzed and base-catalyzed reactions. Instead, we will first develop some ideas about how proton transfers are involved in organic reactions and then use these

⁸⁸ Stewart, R.; O'Donnell, J. P. *J. Am. Chem. Soc.* **1962**, *84*, 493.

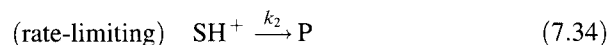
⁸⁹ For a review of the determination of acidity functions and their application to the study of kinetics and mechanisms, see Paul, M. A.; Long, F. A. *Chem. Rev.* **1957**, *57*, 1; Long, F. A.; Paul, M. A. *Chem. Rev.* **1957**, *57*, 935.

⁹⁰ Cox, R. A.; Yates, K. *Can. J. Chem.* **1980**, *59*; 2116; Cox, R. A. *Adv. Phys. Org. Chem.* **2000**, *35*, 1.

ideas to study selected reactions of carbonyl compounds and carboxylic acid derivatives. More complete discussions of these and related reactions are given in the references.^{5,18,91-93}

Specific Acid Catalysis

Consider the acid-catalyzed reaction in water of compound S to form product P, as shown in equations 7.33 and 7.34.⁹⁴ In these equations k_1 and k_{-1} are fast relative to k_2 , and H^+ represents protonated solvent.



Since the second step is the rate-limiting step, the rate of the reaction is

$$\text{Rate} = \frac{d[P]}{dt} = k_2[SH^+] \quad (7.35)$$

If we express the equilibrium in equation 7.33 as

$$K = \frac{[SH^+]}{[S][H^+]} \quad (7.36)$$

then

$$\frac{d[P]}{dt} = k_2K[S][H^+] = k_{SH^+}[S][H^+] \quad (7.37)$$

The concentrations of any acids that might ionize to produce H^+ do not appear in equation 7.37 because the proton has been fully transferred to the substrate before the rate-limiting step of the reaction.⁹⁵ The reaction rate depends only on the concentrations of S and H^+ , so the reaction is said to be subject to **specific acid catalysis**. The term *specific acid catalysis* therefore means that the reaction rate depends only on the concentration of protons in the solvent. In water the term often used is **specific oxonium ion catalysis**, which refers to the activity of H_3O^+ or, more generally, $H(H_2O)_n^+$. In other solvents, a more precise term is **specific lyonium ion**

⁹¹ Bunnett, J. F. in Bernasconi, C. F., Ed. *Investigation of Rates and Mechanisms of Reactions. Part I. General Considerations and Reactions of Conventional Rates*, 4th ed.; Wiley-Interscience: New York, 1986; p. 253.

⁹² Jencks, W. P. *Catalysis in Chemistry and Enzymology*; McGraw-Hill: New York, 1969.

⁹³ Frost, A. A.; Pearson, R. G. *Kinetics and Mechanism*; John Wiley & Sons: New York, 1953; p. 231 ff.

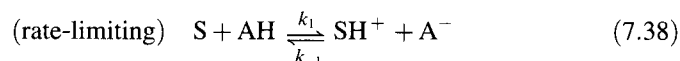
⁹⁴ Although it is not indicated explicitly in equation 7.34 or in equation 7.39, the proton is released in the rate-limiting step or in a subsequent step.

⁹⁵ For a discussion of many variations of the dependence of reaction rates on $[H^+]$, see Gupta, K. S.; Gupta, Y. K. *J. Chem. Educ.* **1984**, *61*, 972.

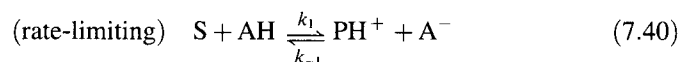
catalysis, referring to the protonated form of solvent in each medium (e.g., CH_3OH_2^+ in methanol).^{96,97}

General Acid Catalysis

If partial or complete proton transfer occurs *during* the rate-limiting step of a reaction, then the reaction is subject to **general acid catalysis**. Two processes can give rise to general acid catalysis. In the first, a proton is transferred from an acid, AH, to a substrate, S, in the rate-limiting step of the reaction. This transfer may occur as the rate-limiting step in a two-step reaction (equations 7.38 and 7.39) or the proton may be transferred during a one-step reaction leading directly to protonated product, PH^+ (equation 7.40).⁹⁸



or



followed by deprotonation of PH^+ . In either case the rate law is

$$\frac{d[\text{P}]}{dt} = k_1[\text{S}][\text{AH}] \quad (7.41)$$

The reaction is said to be subject to *general* acid catalysis because acids in general, not just H^+ , catalyze the reaction. If more than one acid is available to transfer protons, then the rate is a summation of the individual rates from the acid catalysis of all of the acids present (equation 7.42).⁹⁹

$$\frac{d[\text{P}]}{dt} = \sum_i k_i[\text{S}][\text{A}_i\text{H}] \quad (7.42)$$

The second process leading to general acid catalysis involves fast initial proton transfer from AH to S (equation 7.43), followed by rate-limiting

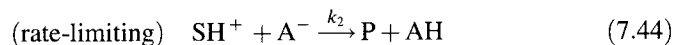
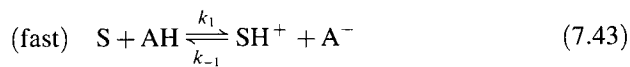
⁹⁶ Bunnett (reference 91, p. 317) noted that "it is doubtful whether any major chemical phenomena have been blessed with names more confusing than specific oxonium ion catalysis and general acid catalysis."

⁹⁷ A similar treatment for base-catalyzed reactions can be used to develop corresponding equations for **specific base catalysis**. Again, the terms *specific hydroxide ion catalysis* in water or *specific lyate ion catalysis* in another solvent (e.g., CH_3O^- in methanol) may be used for greater precision. (See reference 91.)

⁹⁸ In the latter case, the proton transfer may be concerted with some other bonding change in the substrate. For example, see Capon, B.; Nimmo, K. *J. Chem. Soc. Perkin Trans. 2* **1975**, 1113.

⁹⁹ A similar treatment for base-catalyzed reactions can be used to develop corresponding equations for **general base catalysis**. For a detailed discussion of general acid–base catalysis of aqueous reactions, see Jencks, W. P. *Chem. Rev.* **1972**, *72*, 705. See also Ault, A. *J. Chem. Educ.* **2007**, *84*, 38; Kwan, E. E. *J. Chem. Educ.* **2007**, *84*, 39.

proton transfer from the protonated substrate to the *conjugate base* of an acid (equation 7.44). Since the substrate is protonated before the rate-limiting step, this process can also be called **specific acid–general base catalysis**.



The rate of the reaction is

$$\frac{d[\text{P}]}{dt} = k_2[\text{SH}^+][\text{A}^-] \quad (7.45)$$

Incorporating the relationships in equations 7.46 and 7.47,

$$[\text{A}^-] = K_a \frac{[\text{AH}]}{[\text{H}^+]} \quad (7.46)$$

$$K'_{\text{eq}} = \frac{[\text{SH}^+]}{[\text{S}][\text{H}]} \quad (7.47)$$

we can rewrite equation 7.45 as

$$\frac{d[\text{P}]}{dt} = k_2[\text{SH}^+][\text{A}^-] = k_2 K'_{\text{eq}}[\text{S}][\text{H}^+][\text{A}^-] = k_2 K_a K'_{\text{eq}}[\text{S}][\text{AH}] \quad (7.48)$$

The product $k_2 K_a K'_{\text{eq}}$ can be written as k_{HA} , the observed experimental rate constant for catalysis by AH, so that equation 7.48 becomes

$$\frac{d[\text{P}]}{dt} = k_{\text{AH}}[\text{S}][\text{AH}] \quad (7.49)$$

If more than one acid is present, then the reaction rate is the sum of the rates of each of the individual general acid-catalyzed rates, and equation 7.42 again holds.

We should not expect that a given reaction will exhibit only general acid (or base) catalysis or specific acid (or base) catalysis. In principle, reactions may be subject to more than one kind of catalysis. For example, the catalytic rate expression for the reaction of iodine with acetone in buffer solutions was determined to be

$$k = k_{\text{H}_2\text{O}}[\text{H}_2\text{O}] + k_{\text{H}}[\text{H}^+] + k_{\text{OH}}[\text{HO}^-] + k_{\text{A}}[\text{A}^-] + k_{\text{AH}}[\text{AH}] \quad (7.50)$$

where $k_{\text{H}_2\text{O}}$ is the rate constant for the uncatalyzed or water-catalyzed reaction, and $[\text{AH}]$ and $[\text{A}^-]$ are the concentrations of the protonated and deprotonated form of the acid catalyst.¹⁰⁰ Therefore, this reaction was found

¹⁰⁰ Dawson, H. M.; Hall, G. V.; Key, A. J. *Chem. Soc.* **1928**, 2844 and references therein. See also the discussion in reference 5, p. 173 ff.

to be subject to both general and specific acid catalysis and to both general and specific base catalysis. Usually in such reactions, however, one may choose pH ranges and catalyst concentrations in which either acid or base catalysis is dominant.¹⁰¹ It is useful to make the substitutions indicated in equations 7.51 and 7.52.

$$K_W = [\text{H}^+][\text{HO}^-] \quad (7.51)$$

$$K_A = \frac{[\text{H}^+][\text{A}^-]}{[\text{AH}]} \quad (7.52)$$

$$r = \frac{[\text{AH}]}{[\text{A}^-]} \quad (7.53)$$

If the **buffer ratio**, r , is kept constant for a series of solutions that differ in $[\text{AH}]$, then

$$k = k'(r) + \left(k_{\text{AH}} + \frac{k_{\text{A}}}{r} \right) [\text{AH}] \quad (7.54)$$

A plot of k versus $[\text{AH}]$ should generate a linear plot with slope $(k_{\text{AH}} + k_{\text{A}}/r)$, and analysis of several studies, each with a different value of r , can yield the values of k_{AH} and k_{A} separately. If it can be demonstrated that only general acid catalysis is significant, then keeping a 1:1 buffer ratio ($r=1$) allows k_{AH} to be determined directly from a plot of k versus $[\text{AH}]$.^{92,102}

Brønsted Catalysis Law

For general acid catalysis, the relationship between the acidity of each acid present and the rate constant of the reaction is given by the **Brønsted catalysis law**.¹⁰³

$$k_{\text{AH}} = G_{\text{a}}(K_{\text{a}})^{\alpha} \quad (7.55)$$

Taking the logarithm of both sides of equation 7.55 produces equation 7.56.

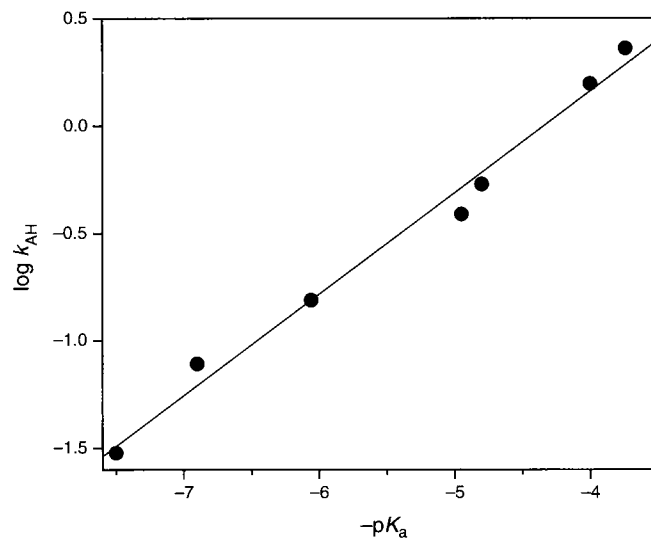
$$\log k_{\text{AH}} = \alpha \log K_{\text{a}} + \text{constant} \quad (7.56)$$

Thus, there should be a linear relationship between the logs of the rate constants and the logs of the K_{a} values for a general acid-catalyzed reaction involving a series of closely related compounds. Similarly, for general

¹⁰¹ The procedure for extracting values of k_{HA} was described by Stewart (reference 18).

¹⁰² Acid catalysis of the reaction of water-insoluble hydrocarbons with highly polar acid catalysts depends not only on H_0 but also on the extent of stirring. For a discussion, see Busca, G. *Chem. Rev.* **2007**, *107*, 5366.

¹⁰³ Brønsted, J. N. *Chem. Rev.* **1928**, *5*, 231. The representation of the first vowel in the last name here is the same as that in this publication.

**FIGURE 7.5**

A Brønsted catalysis plot for hydrolysis of diethylphenyl orthoformate in 50 : 50 dioxane : water. (Based on data reported in reference 104.)

base-catalyzed reactions with a series of bases

$$\log k_b = \beta \log K_b + \text{constant} \quad (7.57)$$

A linear plot of $\log k_{AH}$ versus $\log K_a$ (equivalently, $-pK_a$) for a series of acids confirms the Brønsted relationship, and the slope of the line is α . For example, Figure 7.5 shows a Brønsted plot for the hydrolysis of diethylphenyl orthoformate in 50 : 50 dioxane : water at 25°C. There is a linear correlation, and α is 0.47.¹⁰⁴ The value of α is said to represent the "sensitivity of the rate constant to the structural changes in the family of reactions."^{105,106} Some investigators relate α to the extent of proton transfer at the transition state of the general acid-catalyzed reaction, but this interpretation is not totally accepted.¹⁰⁷⁻¹¹¹

¹⁰⁴ Anderson, E.; Fife, T. H. *J. Org. Chem.* **1972**, *37*, 1993.

¹⁰⁵ Bender, M. L. *Chem. Rev.* **1960**, *60*, 53.

¹⁰⁶ For a discussion of the interpretation of α , see Lewis, E. S. *J. Phys. Org. Chem.* **1990**, *3*, 1.

¹⁰⁷ See, for example, Leffler, J. E. *Science* **1953**, *117*, 340; Richard, J. P.; Williams, K. B. *J. Am. Chem. Soc.* **2007**, *129*, 6952.

¹⁰⁸ Espenson, J. H. *Chemical Kinetics and Reaction Mechanisms*, 2nd ed.; McGraw-Hill: New York, 1995; p. 234.

¹⁰⁹ For leading references, see Streitwieser, A., Jr.; Kaufman, M. J.; Bors, D. A.; Murdoch, J. R.; MacArthur, C. A.; Murphy, J. T.; Shen, C. C. *J. Am. Chem. Soc.* **1985**, *107*, 6983. Also see Wiseman, F.; Kestner, N. R. *J. Phys. Chem.* **1984**, *88*, 4354.

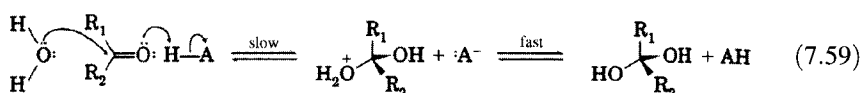
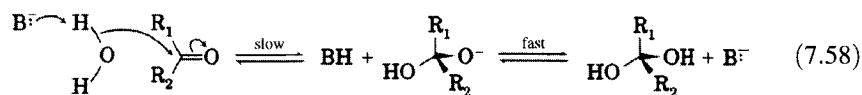
¹¹⁰ Bordwell reported α values outside the range of 0-1. Bordwell, F. G.; Boyle, W. J., Jr.; Yee, K. C. *J. Am. Chem. Soc.* **1970**, *92*, 5926; Bordwell, F. G.; Boyle, W. J., Jr. *J. Am. Chem. Soc.* **1972**, *94*, 3907.

¹¹¹ While the equations above suggest that Brønsted plots should be linear, curved plots can arise in some circumstances, as discussed by Kresge, A. J. *Chem. Soc. Rev.* **1973**, *2*, 475. Curved Brønsted plots may also result when a change in the rate-limiting step of a two-step mechanism accompanies the change in base or acid catalyst. For a discussion, see reference 199.

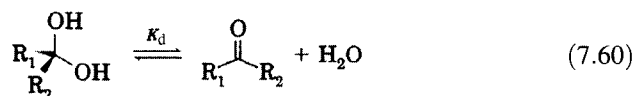
7.3 ACID AND BASE CATALYSIS OF REACTIONS OF CARBONYL COMPOUNDS AND CARBOXYLIC ACID DERIVATIVES

Addition to the Carbonyl Group

A characteristic reaction of the carbonyl group is addition of polar reagents across the carbon–oxygen double bond.^{112,113} Because of the polarity of the carbonyl group, polar additions take place so that the component of the adding reagent that is more acidic/electrophilic adds to the oxygen atom, while the component that is more basic/nucleophilic adds to the carbon atom. Familiar reactions of this type include cyanohydrin formation, bisulfite addition, hemiacetal or hemiketal formation, and addition of amines—the latter usually being followed by elimination of water to give products with carbon–nitrogen double bonds. One of the simplest reactions of aldehydes and some ketones is hydration, the addition of water across the carbon–oxygen double bond. Hydration reactions typically exhibit both general base and general acid catalysis, as illustrated in equation 7.58 and equation 7.59, respectively.¹¹⁴



Only rarely are the hydrates sufficiently stable to be isolated,¹¹⁵ but the hydration reaction allows an examination of the factors that influence addition to the carbonyl group. It is common to represent the equilibrium between an aldehyde or ketone and the corresponding hydrate in terms of a dissociation constant, K_d , as shown in equation 7.60.



¹¹² Ingold, C. K. *Structure and Mechanism in Organic Chemistry*, 2nd ed.; Cornell University Press: Ithaca, NY, 1969; p. 994 ff.

¹¹³ (a) For a review of additions in which an equilibrium is established between reactants and products, see Ogata, Y.; Kawasaki, A. in Zabicky, J., Ed. *The Chemistry of the Carbonyl Group*, Vol. 2; Wiley-Interscience: London, 1970. (b) For a theoretical and experimental study of the equilibria of formation of hydrates, hemiacetals, and acetals, see Wiberg, K. B.; Morgan, K. M.; Maltz, H. *J. Am. Chem. Soc.* **1994**, *116*, 11067.

¹¹⁴ Sørensen, P. E.; Jencks, W. P. *J. Am. Chem. Soc.* **1987**, *109*, 4675.

¹¹⁵ The isolation of the dihydrate from hexafluoroacetylacetone was reported by Schultz, B. G.; Larsen, E. M. *J. Am. Chem. Soc.* **1949**, *71*, 3250. The hydrate of *trans*-2,3-di-*tert*-butylcyclopropanone was reported to melt at 105–107°C by Pazos, J. F.; Pacifici, J. G.; Pierson, G. O.; Sclove, D. B.; Greene, F. D. *J. Org. Chem.* **1974**, *39*, 1990.

TABLE 7.6 Equilibrium Constants for Dissociation of Hydrates of Carbonyl Compounds^a

Compound	K_d^b	Compound	K_d^b
Cyclopropanone ^c	Very small	Pyruvic acid ^e	0.42
Chloral (α,α,α -trichloroacetaldehyde)	3.6×10^{-5}	Biacetyl ^e	0.50
Formaldehyde ^d	4.5×10^{-4}	Acetaldehyde ^f	0.83
α -Chloroacetaldehyde	2.7×10^{-2}	Propanol	1.4
α -Chlorobutyraldehyde	6.3×10^{-2}	Butanal	2.1
α,α' -Dichloroacetone	0.10	2-Methylpropanal	2.3
α,α -Dibromobutanal	0.11	Pivaldehyde ^e	4.1
α -Chloroheptanal	0.16	α -Chloroacetone ^g	9.1
2-Chloro-2-methylpropanal	0.19	Sodium pyruvate ^e	18.5
Methyl pyruvate ^e	0.32	Benzaldehyde ^h	120
α,α -Dichloroacetone ^e	0.35	Acetone ⁱ	720
α -Bromoheptanal	0.35	Acetophenone ^h	1.5×10^5
		Benzophenone ^h	8.5×10^6

^a Except as noted, data are from reference 116.

^b See reference 119.

^c See reference 124.

^d See reference 117.

^e See reference 122b.

^f See reference 114.

^g See reference 122.

^h See reference 120.

ⁱ See reference 118.

Values of K_d for several hydrates of interest are shown in Table 7.6.¹¹⁶⁻¹¹⁹ The data suggest that the carbonyl side of the equation is favored when R_1 and R_2 are electron-donating and is disfavored when R_1 and R_2 are electron-withdrawing. In an aromatic aldehyde or ketone, conjugation of the aryl group with the carbonyl group stabilizes the carbonyl side of the equilibrium, with the magnitude of the stabilization estimated at 2.7 kcal/mol.^{120,121} Steric factors are also important. The carbonyl side of the equation is favored when R_1 and R_2 are large alkyl groups because a 120° C–C(=O)–C bond angle provides more room for bulky substituents than does the 109° bond angle of the hydrate.¹²² In small cycloalkanones, however, steric strain can destabilize the carbonyl side of the equilibrium. For example, in cyclopropanone there is

¹¹⁶ Bell, R. P. *Adv. Phys. Org. Chem.* **1966**, 4, 1.

¹¹⁷ Sutton, H. C.; Downes, T. M. *J. Chem. Soc. Chem. Commun.* **1972**, 1.

¹¹⁸ Hine, J.; Redding, R. W. *J. Org. Chem.* **1970**, 35, 2769.

¹¹⁹ The K_d values shown in Table 7.6 are defined (reference 122) as $K_d = [R_1R_2C=O]/[R_1R_2C(OH)_2]$ and are therefore dimensionless because the concentration of water (55 M, with activity assumed to be unity) is included in the equilibrium constant. Literature values for equilibrium constants in which the concentration of water is not incorporated into the K_d term have been divided by 55.5 to make the values in Table 7.6 comparable.

¹²⁰ Guthrie, J. P. *Acc. Chem. Res.* **1983**, 16, 122.

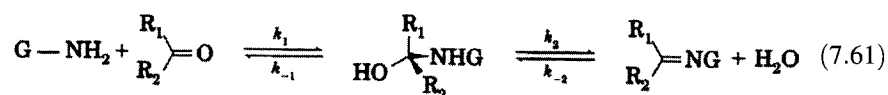
¹²¹ Greenzaid, P. J. *Org. Chem.* **1973**, 38, 3164.

¹²² (a) Bell (reference 116) calculated that the K_d values (equation 7.60) show a good correlation with Taft's polar and steric constants for alkyl groups: $\log K_d = 2.70 - 2.6 \Sigma\sigma^* - 1.3 \Sigma E_s$. (b) A somewhat better correlation was obtained by Greenzaid, P.; Luz, Z.; Samuel, D. *J. Am. Chem. Soc.* **1967**, 89, 749, who eliminated the need for the E_s term by treating aldehydes separately from ketones in the equation $-\log K_d = 1.70 \Sigma\sigma^* + 2.03 \Delta - 2.81$, in which Δ is the number of aldehyde hydrogen atoms (i.e., hydrogen atoms bonded to the carbonyl group) in the compound.

30° of angle strain at the carbonyl carbon atom because of the difference between the 60° internuclear C–C(=O)–C bond angle and the preferred angle of 120°. ¹²³ In cyclopropanone hydrate there is only 24.75° of angle strain, because of the smaller difference between the 60° C–C(OH)₂–C internuclear bond angle and the preferred angle of 109.5°. Formation of the hydrate relieves angle strain, so cyclopropanone is fully hydrated in the presence of water (Figure 7.6). ¹²⁴

The addition of an alcohol to an aldehyde produces a hemiacetal, and addition of an alcohol to a ketone produces a hemiketal. *K_d* values for dissociation of the hemiketals produced by reaction of methanol or ethanol with a number of ketones are shown in Table 7.7. The reduced stability of the hemiketals derived from ethanol, in comparison with those derived from methanol, is attributed to the greater steric requirements of the larger ethyl group. It is interesting to note that the methyl hemiketal of cyclobutanone is more stable (smaller *K_d*) than that of cyclohexanone, while the trend is the reverse for the hemiketals formed from ethanol. The results can be explained in terms of two conflicting trends. For both ketones, hemiketal formation relieves angle strain in the ketone, but the release of strain is greater for cyclobutanone. Therefore, the hemiketal formed from methanol is more stable for cyclobutanone than for cyclohexanone. Because of the larger size of the ethyl group, there is considerable steric strain in hemiketals formed from ethanol. That strain is greater in a hemiketal formed from cyclobutanone than in a hemiketal formed from cyclohexanone, so the ethyl hemiketal of cyclohexanone is more stable than is the ethyl hemiketal of cyclobutanone. ¹²⁵

The addition of a primary amine (H₂NG) to an aldehyde or ketone is the first step of a two-step reaction leading, after dehydration of an intermediate carbinolamine, to a structure with a carbon–nitrogen double bond (equation 7.61). Depending on the reagents and experimental conditions, either the addition step to form the carbinolamine or the dehydration step can be rate limiting. ¹²⁶ The pH dependence of the overall rate constant for the reaction of hydroxylamine with acetone is shown in Figure 7.7. ¹²⁷ From pH 7 to about pH 5, the rate-limiting step is the acid-catalyzed dehydration of the carbinolamine, so the rate constant increases with decreasing pH. Below pH 5, however, the rate-limiting step is the addition of unprotonated hydroxylamine to the carbonyl group. Since the concentration of free amine decreases with decreasing pH, the rate of the reaction decreases at lower pH. ¹²⁸ Therefore, a bell-shaped pH–rate constant curve is obtained.



¹²³ As was discussed in Chapter 3, angle strain is defined as *half* of the difference between the preferred bond angle and the observed bond angle.

¹²⁴ Lipp, P.; Buchkremer, J.; Seeles, H. *Liebigs Ann. Chem.* **1932**, 499, 1.

¹²⁵ Wheeler, O. H. *J. Am. Chem. Soc.* **1957**, 79, 4191.

¹²⁶ The two steps have different sensitivities to substituent effects, so the ρ values for Hammett correlations for the additions can vary according to conditions. See the discussion in Chapter 6.

¹²⁷ Jencks, W. P. *J. Am. Chem. Soc.* **1959**, 81, 475.

¹²⁸ In addition, there is a specific acid-catalyzed pathway for the addition of hydroxylamine to the protonated carbonyl group. Therefore, the rate does not fall off as fast at low pH as might be expected solely on the basis of the concentration of free hydroxylamine.

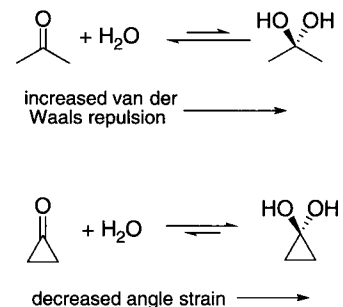


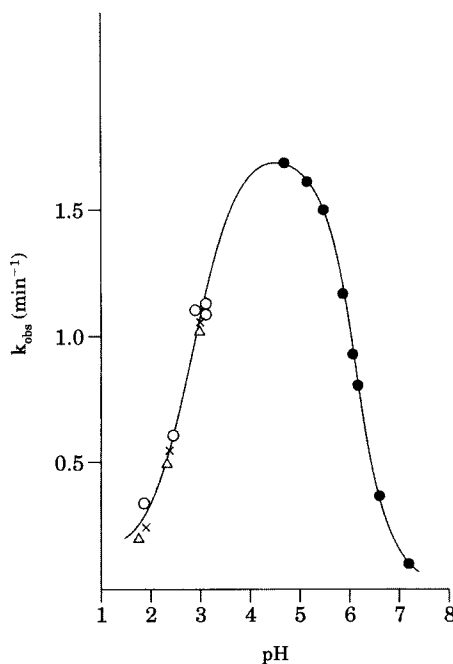
FIGURE 7.6

Changes in steric interactions upon hydration of acetone (top) and cyclopropane (bottom).

TABLE 7.7 Equilibrium Constants for Dissociation of Hemiketals Formed from Methanol or Ethanol

Ketone	K_d (Methanol)	K_d (Ethanol)
4-Heptanone	89.0	—
Cyclobutanone	1.11	327
Cyclopentanone	15.1	810
Cyclohexanone	2.16	237
Cycloheptanone	53.5	—
Cyclooctanone	268	—

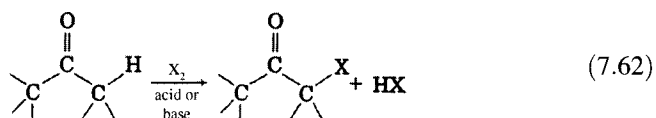
Source: Reference 125.

**FIGURE 7.7**

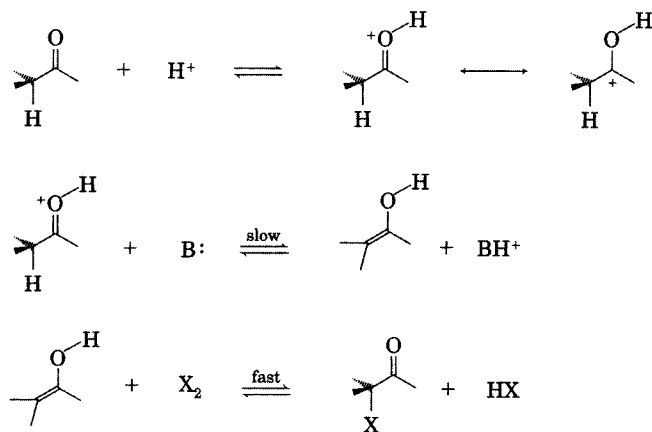
Dependence on pH of the rate constant for reaction of hydroxylamine with acetone. (Adapted from reference 127.)

Enolization of Carbonyl Compounds

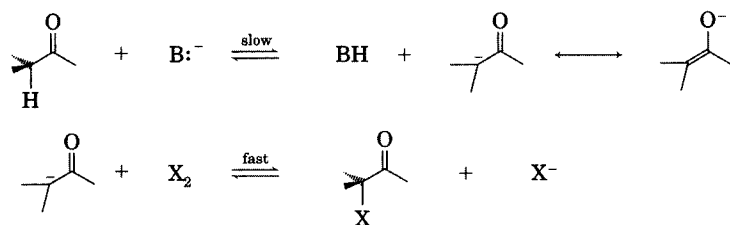
Ketones with α hydrogen atoms undergo substitution by halogen as shown in equation 7.62.



Lapworth found that the substitution reaction is catalyzed by both acids and bases. Since the HX produced as a by-product of the reaction can serve as a catalyst, the acid-catalyzed reaction is said to be **autocatalytic** because the rate of the reaction increases with time. The rate law for the reaction was found to be first order in ketone but zero order in halogen, meaning that halogen is not

**FIGURE 7.8**Lapworth mechanism for acid-catalyzed α -halogenation of a ketone.

involved in the rate-limiting step of the reaction.^{129–131} The simplest mechanisms consistent with the data involve rate-limiting, acid- or base-catalyzed conversion of the carbonyl compound to an intermediate, which then reacts with the halogen in a fast step. Because species with carbon–carbon double bonds are highly reactive toward halogen, Lapworth proposed mechanisms proceeding through an enol intermediate in the acid-catalyzed reaction (Figure 7.8) and an enolate intermediate in the base-catalyzed process (Figure 7.9).¹³²

**FIGURE 7.9**Lapworth mechanism for base-catalyzed α -halogenation of a ketone.

The mechanisms in Figures 7.8 and 7.9 are supported further by two observations: (i) chiral ketones undergo both acid- and base-catalyzed racemization, and (ii) exchange of hydrogen isotopes on the α carbon atoms is also observed. The rate constants for acid-catalyzed iodination and racemization are identical for phenyl *sec*-butyl ketone.¹³³ The same is true for acid-catalyzed bromination and racemization of (+)-2-(2-carboxybenzyl)indanone¹³⁴ as

¹²⁹ Lapworth, A. J. *Chem. Soc.* **1904**, 30.

¹³⁰ Watson, H. B. *Chem. Rev.* **1930**, 7, 173.

¹³¹ Obviously, the rate of the reaction is not totally independent of halogen concentration, because no reaction can occur in the total absence of halogen. Dependence on $[X_2]$ has been observed at low halogen concentration. At $[X_2]$ greater than 10^{-8} to $10^{-5} M^{-1}$, however, the reaction is apparently zeroth order in halogen. Dubois, J.-E.; El-Alaoui, M.; Toullec, J. J. *Am. Chem. Soc.* **1981**, 103, 5393.

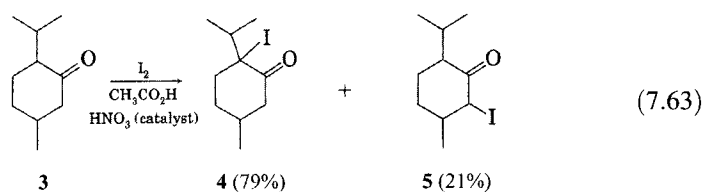
¹³² For a review of enolization, see Forsén, S.; Nilsson, M. in Zabicky, J., Ed. *The Chemistry of the Carbonyl Group*, Vol. 2; Wiley-Interscience: London, 1970; pp. 157–240.

¹³³ Bartlett, P. D.; Stauffer, C. H. *J. Am. Chem. Soc.* **1935**, 57, 2580. The rates of racemization and halogenation of a series of dialkyl ketones were found not to be identical in this study.

¹³⁴ Ingold, C. K.; Wilson, C. L. *J. Chem. Soc.* **1934**, 773.

well as for base-catalyzed racemization and bromination of the same reactant.¹³⁵ Hydrogen exchange rates were shown to be identical to those for racemization and halogenation with acid catalysis as well as for those reactions with base catalysis.^{136,137} The simplest explanation for the experimental results is that halogenation, racemization, and hydrogen exchange occur with identical rate constants because in each case the rate-limiting step is the deprotonation of the ketone to form an enolate (under base catalysis) or deprotonation of the protonated carbonyl to form an enol (under acid catalysis).¹¹²

If there is at least one hydrogen atom on each of the α carbon atoms of an unsymmetrically substituted ketone, then more than one substitution product might be observed. In such cases the regiochemistry of the halogenation depends on the other substituents on the two α carbon atoms and on whether the reaction is catalyzed by acid or base. Usually acid-catalyzed halogenation occurs on the α carbon bearing the greater number of alkyl substituents. For example, acid-catalyzed iodination of (-)-menthone (3) produced 79% of the product with halogen on the more substituted α carbon atom (4) and 21% of the product formed by substitution on the less substituted α carbon atom (5).¹³⁸ The results suggest that acid-catalyzed enolization of a ketone leads to preferential formation of the enol with the greater number of alkyl substituents on the carbon-carbon double bond.¹³⁹



In contrast, base-promoted halogenation tends to occur on the *less* substituted α carbon atom. For example, base-promoted iodination of methyl alkyl ketones leads initially to the iodomethyl alkyl ketone. Further reaction leads to the α, α -diiodo-, then to the α, α, α -triiodoketone, and then to iodoform and a carboxylate ion by the haloform reaction (Figure 7.10).

Two factors could contribute to the observed regiochemistry of base-promoted halogenation of ketones. One is a kinetic preference for formation of the less substituted enolate. Evidence for this effect can be seen in the rate constants for base-catalyzed iodination of phenyl alkyl ketones with the structure $\text{C}_6\text{H}_5\text{COCHR}_1\text{R}_2$, which are found to decrease with increasing alkyl substitution (Table 7.8).¹⁴⁰

A second possible explanation for the regiochemistry of base-promoted halogenation of ketones is a greater thermodynamic stability of the less substituted enolate, and there is evidence suggesting that this may be the case for some enolates. House and Kramar investigated the equilibria

¹³⁵ Hsü, S. K.; Wilson, C. L. *J. Chem. Soc.* **1936**, 623.

¹³⁶ Reitz, O. Z. *Phys. Chem.* **1937**, A179, 119.

¹³⁷ Hsü, S. K.; Ingold, C. K.; Wilson, C. L. *J. Chem. Soc.* **1938**, 78.

¹³⁸ Bartlett, P. D.; Vincent, J. R. *J. Am. Chem. Soc.* **1933**, 55, 4992.

¹³⁹ For a summary and leading references, see Cardwell, H. M. E.; Kilner, A. E. H. *J. Chem. Soc.* **1951**, 2430.

¹⁴⁰ Cardwell, H. M. E. *J. Chem. Soc.* **1951**, 2442.

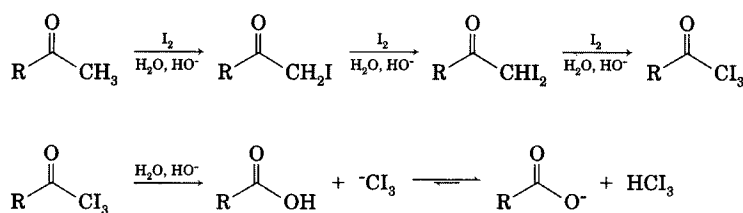
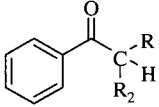


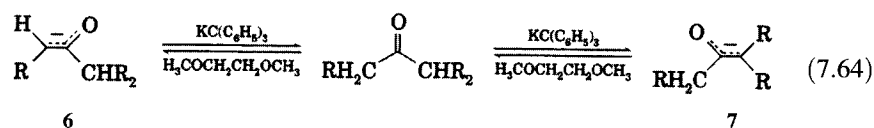
FIGURE 7.10
Iodoform reaction.

TABLE 7.8 Substituent Effects on Base-Promoted Iodination of Phenyl Alkyl Ketones

Reactant	R ₁	R ₂	Relative Rate Constant ^a
	H	H	238
	H	CH ₃	37
	H	CH ₂ CH ₃	29
	CH ₃	CH ₃	7

^a See reference 140.

between enolates **6** and **7** formed by reaction of unsymmetrical ketones with triphenylmethylpotassium in 1,2-dimethoxyethane solution (equation 7.64).^{141,142}

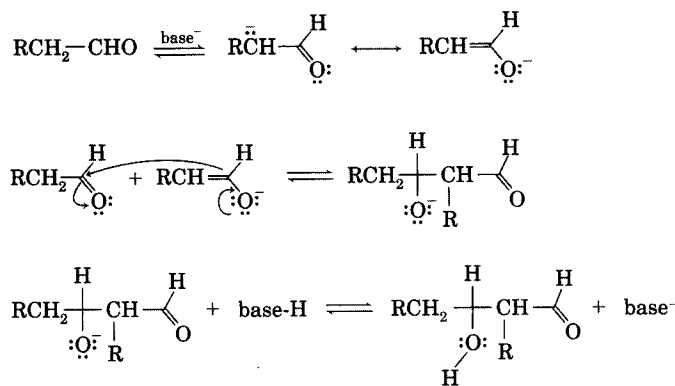


After equilibration, the enolates were allowed to react with D₂O, acetic anhydride, or methyl iodide. The results suggested that the less substituted enolate (**6**) was present in greater concentration at equilibrium when the starting ketone was monoalkyl substituted on one α carbon and dialkyl substituted on the other (e.g., R₂CHCOCH₂R). For methyl ketones (CH₃COCH₂R), however, the equilibrium favored the less substituted enolate if R was a branched alkyl group, but approximately equal concentrations of the two possible enolates were observed if R was a linear alkyl group.¹⁴³

¹⁴¹ House, H. O.; Kramar, V. J. *Org. Chem.* **1963**, *28*, 3362.

¹⁴² Synthetic applications of acid- and base-catalyzed α -halogenation of ketones have been discussed by House: House, H. O. *Modern Synthetic Reactions*, 2nd ed.; W. A. Benjamin: Menlo Park, CA, 1972; pp. 459–478.

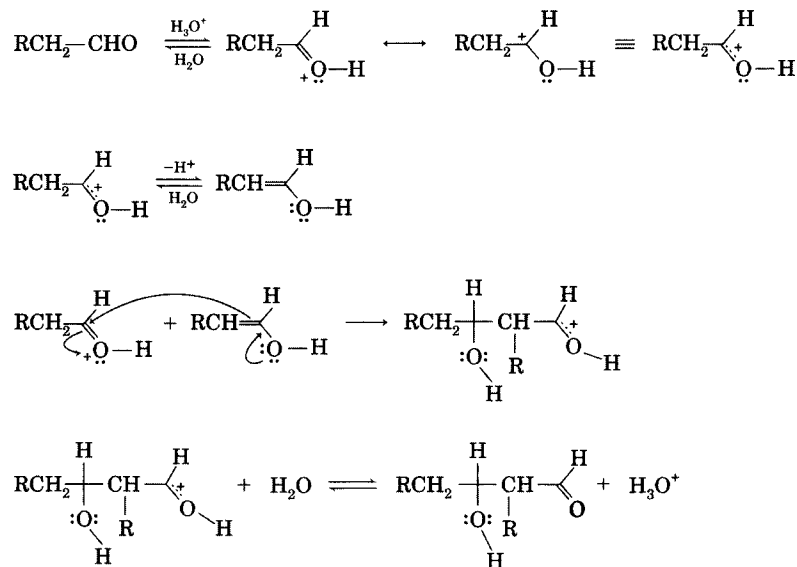
¹⁴³ The counterion was found to be a significant factor in the equilibrium, with the more highly substituted enolate increasingly favored as the cation varied from sodium or potassium to lithium. Beutelman, H. P.; Xie, L.; Saunders, W. H., Jr. *J. Org. Chem.* **1989**, *54*, 1703 determined that the primary hydrogen kinetic isotope effect for proton removal from alkyl ketones by strong bases such as lithium diisopropylamide in THF or DME was $k_{\text{H}}/k_{\text{D}} = 2.3$ to 5.9 at 0°C. The results suggested a very early transition state. The reactions appeared to depend on more than one base reacting with each ketone, however. See also Xie, L.; Saunders, W. H., Jr. *J. Am. Chem. Soc.* **1991**, *113*, 3123.

**FIGURE 7.11**

Base-catalyzed aldol reaction.

Acid catalysis of enol formation and base catalysis of enolate formation are also key steps in the aldol reaction.¹⁴⁴ The base-catalyzed reaction is shown in Figure 7.11, and the acid-catalyzed reaction is illustrated in Figure 7.12. The analogous reaction involving ketones is usually not synthetically useful because addition of an enolate ion to a ketone is less favorable than is addition to an aldehyde.¹⁴⁵

In recent years it has become possible to generate enols by processes other than enolization of carbonyl compounds.^{146,147} Kresge and co-workers found that the ketonization of photochemically generated acetophenone enol is

**FIGURE 7.12**

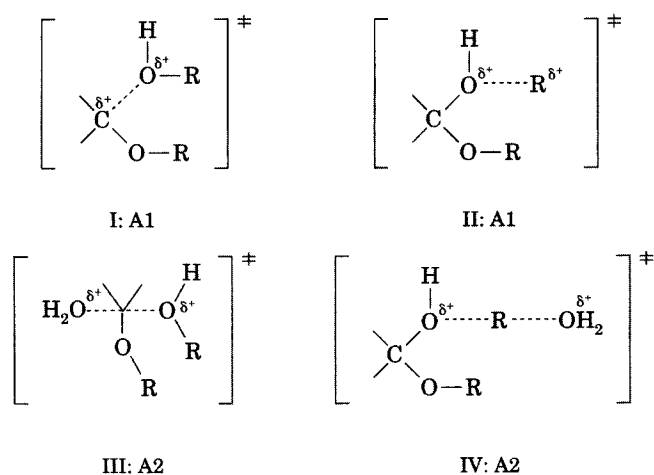
Acid-catalyzed aldol reaction.

¹⁴⁴ For leading references and synthetic applications, see chapter 10 of reference 142.

¹⁴⁵ Subsequent elimination of water from the aldol product leads to α,β -unsaturated carbonyl compounds, for example, in the Claisen-Schmidt reaction (reference 142).

¹⁴⁶ Capon, B.; Guo, B.-Z.; Kwok, F. C.; Siddhanta, A. K.; Zucco, C. *Acc. Chem. Res.* **1988**, *21*, 135.

¹⁴⁷ Keefe, J. R.; Kresge, A. J.; Schepp, N. P. *J. Am. Chem. Soc.* **1988**, *110*, 1993.

**FIGURE 7.13**

Possible transition structures for acid-catalyzed hydrolysis of an acetal. (Adapted from reference 151.)

subject to general acid catalysis and to general base catalysis.^{148,149} The results suggested that the uncatalyzed ketonization (i.e., the reaction without added acid or base catalysts) takes place in water through a process in which water acts as a base to deprotonate the enol, with subsequent reprotonation of the enolate ion.

Hydrolysis of Acetals

Hydrolysis of acetals is central to the chemistry of carbohydrates, and understanding the operation of enzymes is aided by understanding the mechanisms that can occur in solution.¹⁵⁰ Since acetals are stable in basic solutions, hydrolysis reactions are carried out with acid catalysis. Cordes discussed four possible transition structures for the acid-catalyzed hydrolysis of acetals (Figure 7.13).¹⁵¹ Structures I and II would be formed in unimolecular decompositions of protonated acetals, so reactions proceeding through these transition structures are termed **A1** (acid-catalyzed, unimolecular) mechanisms. A possible reaction coordinate diagram for a mechanism proceeding through transition structure I is shown in Figure 7.14.¹⁵² Structures III and IV would occur in bimolecular reactions of water with a protonated acetal, so reactions proceeding through these transition structures are termed **A2** (acid-catalyzed bimolecular) mechanisms.

The proposed mechanisms for acetal hydrolysis can be tested with the tools used to study other organic reactions. An A1 mechanism proceeding through transition structure II would lead to a carbocation centered on the departing R group, so racemization of a chiral center would be expected. On

¹⁴⁸ Chiang, Y.; Kresge, A. J.; Santaballa, J. A.; Wirz, J. *J. Am. Chem. Soc.* **1988**, *110*, 5506.

¹⁴⁹ One method of generating enols involves photohydration of phenylacetylene, while another method utilizes the Norrish Type II cleavage of γ -hydroxybutyrophenone. Photochemical reactions will be discussed in Chapter 12.

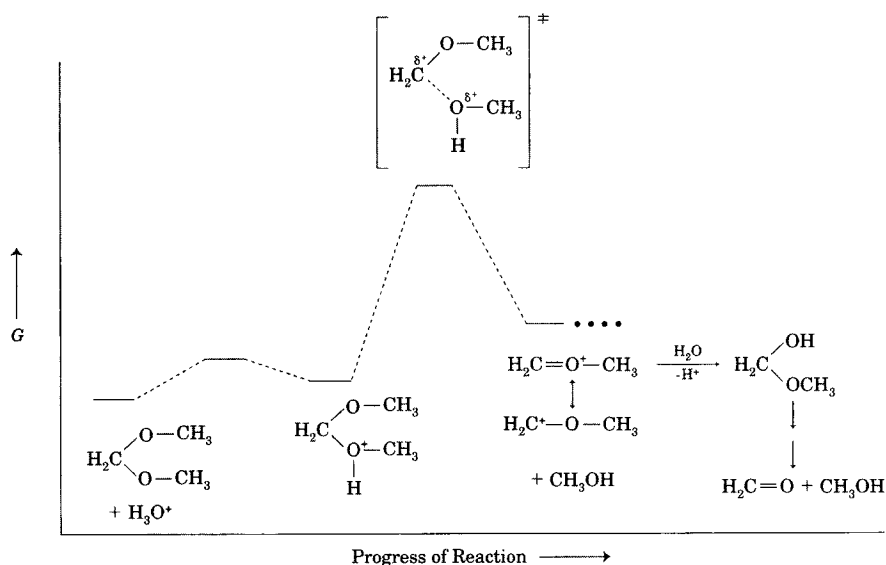
¹⁵⁰ Phillips, D. C. *Sci. Am.* **1966**, *215*, 78; Vernon, C. A. *Proc. R. Soc. London Ser. B* **1969**, *167*, 389. See also Capon, B. *Chem. Rev.* **1969**, *69*, 407.

¹⁵¹ Cordes, E. H. *Prog. Phys. Org. Chem.* **1967**, *4*, 1.

¹⁵² Anderson, E.; Capon, B. *J. Chem. Soc. (B)* **1969**, 1033.

FIGURE 7.14

Gibbs diagram for A1 hydrolysis of formaldehyde dimethyl acetal. (Adapted from reference 152.)



the other hand, an A2 mechanism proceeding through transition structure IV would lead to inversion of configuration of a chiral R group. Cordes summarized evidence obtained by a number of workers indicating that—even in the most favorable circumstances—neither inversion nor racemization of a chiral center is observed.¹⁵¹ Therefore, the acid-catalyzed hydrolysis of acetals appears not to occur through mechanisms involving either transition structure II or transition structure IV.¹⁶²

In transition structure I of Figure 7.13, there should be appreciable positive charge on the hemiacetal carbon atom, so there should be a negative slope to a Hammett correlation for rates of hydrolysis of acetals formed from aryl aldehydes. Transition structure III, on the other hand, does not show an appreciable positive charge on the acetal carbon atom, so a large Hammett ρ value would not be expected.¹⁵³ Fife and Jao found that hydrolysis of *m*-substituted benzaldehyde diethyl acetals gave a good Hammett correlation with σ , with a ρ value of -3.35 , which is more consistent with a mechanism involving transition structure I.¹⁵⁴ Observations of near-zero or positive values of ΔS^\ddagger also favor the mechanism shown in Figure 7.14 because a negligible or slightly positive ΔS^\ddagger would be expected for an A1 mechanism. An A2 mechanism, which requires two species to combine, should have a negative value of ΔS^\ddagger .¹⁵¹ Additional evidence from studies of activation volume and solvent kinetic isotope effects also supports the A1 pathway for acetal hydrolysis.^{155,162}

In contrast to acetals, hemiacetals can revert to aldehydes and alcohols through both acid and base catalysis.¹⁵⁶ Some catalysts incorporate both acid and base functions and can serve as bifunctional catalysts. This type of

¹⁵³ A small positive or negative charge might be present, depending on the relative rates of bond making and bond breaking in the transition structure.

¹⁵⁴ Fife, T. H.; Jao, L. K. *J. Org. Chem.* **1965**, *30*, 1492.

¹⁵⁵ For a discussion of the generality of the A1 mechanism, see Wann, S. R.; Kreevoy, M. M. *J. Org. Chem.* **1981**, *46*, 419.

¹⁵⁶ See, for example, Swain, C. G.; Brown, J. F., Jr. *J. Am. Chem. Soc.* **1952**, *74*, 2534.

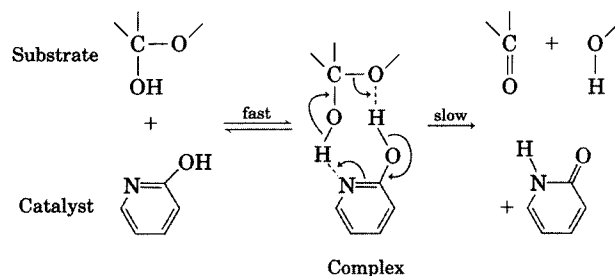
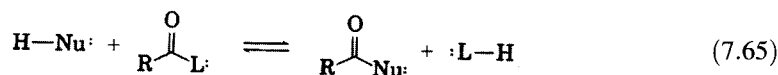


FIGURE 7.15
Catalysis of the hydrolysis of an acetal by 2-hydroxypyridine. (Adapted from reference 157.)

catalysis was demonstrated by Swain for the 2-hydroxypyridine-catalyzed mutarotation of tetramethylglucose in benzene solution, as shown schematically in Figure 7.15.^{157,158}

Acid-Catalyzed Hydrolysis of Esters

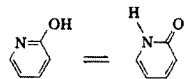
The characteristic reaction of carboxylic acid derivatives is substitution, not addition, because the $-\text{OH}$, $-\text{OR}$, $-\text{NH}_2$, $-\text{X}$, $-\text{OCOR}$, and $-\text{SR}$ groups are better leaving groups than are the hydride ions or carbanions that would be produced by the analogous substitution reaction of aldehydes or ketones.¹⁵⁹ A general reaction is shown in equation 7.65, where $\text{H}-\text{Nu}$ is the protonated form of the nucleophile and L is the leaving group. These reactions can be catalyzed by both acid and base.¹⁶⁰ Note that the hydrolysis of a carboxylic acid derivative with hydroxide ion consumes the hydroxide and generates a carboxylate ion. To the extent that carboxylate is a less effective base than hydroxide, catalyst is consumed during the reaction. To be precise, therefore, the process should be called base-promoted rather than base-catalyzed.



The mechanisms of acid-catalyzed hydrolysis of esters can also be categorized as A1 or A2. Two different pathways of each type can be defined, depending on whether the rate-limiting step involves cleavage of the

¹⁵⁷ Swain, C. G.; Brown, J. F., Jr. *J. Am. Chem. Soc.* **1952**, *74*, 2538.

¹⁵⁸ 2-Hydroxypyridine is the tautomer of 2-pyridone:



The equilibrium favors the hydroxy form in the gas phase and the keto form in polar solvents. In nonpolar solvents both tautomers are present in comparable concentrations. For leading references and a theoretical study, see Wong, M. W.; Wiberg, K. B.; Frisch, M. J. *J. Am. Chem. Soc.* **1992**, *114*, 1645.

¹⁵⁹ An exception to this generalization is the elimination of trihalomethyl anion in the haloform reaction (Figure 7.10).

¹⁶⁰ For reviews, see (a) Euranto, E. K. in Patai, S., Ed. *The Chemistry of Carboxylic Acids and Esters*; Wiley-Interscience: London, 1969; pp. 505–588; (b) Koskikallio, J. in Patai, S., Ed. *The Chemistry of Carboxylic Acids and Esters*; Wiley-Interscience: London, 1969; pp. 103–135; (c) Kirby, A. J. in Bamford, C. H.; Tipper, C. F. H., Eds. *Comprehensive Chemical Kinetics. Volume 10. Ester Formation and Hydrolysis and Related Reactions*; Elsevier Publishing: Amsterdam, 1972; pp. 57–207; (d) Talbot, R. J. E. in Bamford, C. H.; Tipper, C. F. H., Eds. *Comprehensive Chemical Kinetics. Volume 10. Ester Formation and Hydrolysis and Related Reactions*; Elsevier Publishing: Amsterdam, 1972; pp. 209–293.

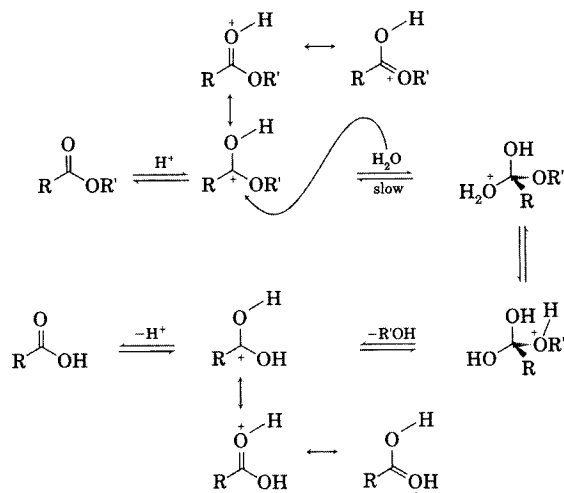


FIGURE 7.16
A_{Ac}2 mechanism for ester hydrolysis.

acyl–oxygen bond (A_{Ac}1 or A_{Ac}2) or the alkyl–oxygen bond (A_{Al}1 and A_{Al}2).¹⁶¹ Only three of these mechanisms are common, however.^{112,162} In the A_{Ac}2 mechanism (acid-catalyzed, **bimolecular**, with acyl-oxygen cleavage) shown in Figure 7.16, the rate-limiting step involves addition of water to the protonated ester.

The A_{Ac}1 (acid-catalyzed, **unimolecular**, acyl-oxygen cleavage) mechanism is shown in Figure 7.17. The reaction is unimolecular because the rate-limiting step involves dissociation of ROH from the protonated ester.¹¹² This

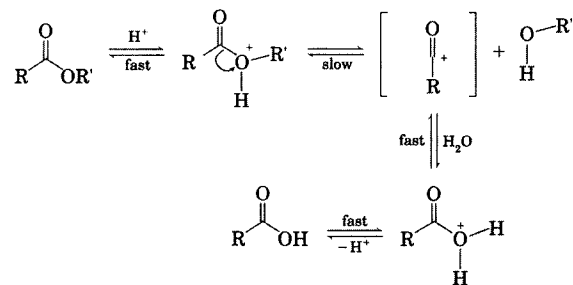


FIGURE 7.17
A_{Ac}1 mechanism for ester hydrolysis.

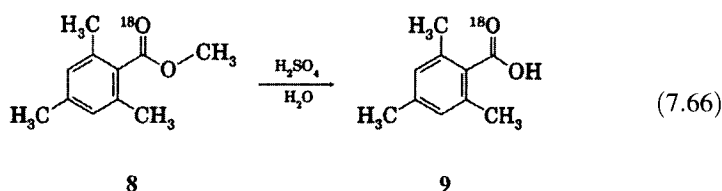
¹⁶¹ According to the 1989 IUPAC Recommendations for the Representation of Reaction Mechanisms (Commission on Physical Organic Chemistry, IUPAC *Pure Appl. Chem.* **1989**, 56, 23; also see Guthrie, R. D.; Jencks, W. P. *Acc. Chem. Res.* **1989**, 22, 343), bond-making (association) processes are denoted A, while bond-breaking (dissociation) processes are labeled D. An electrophilic or electrofugic process at a core atom is indicated with a subscript E, and a nucleophilic or nucleofugic process at a core atom is shown with a subscript N. Subscript H indicates hydron as electrophile or electrofuge at a core atom, and subscript h indicates a hydron as electrophile or electrofuge at a peripheral atom. Stepwise processes are indicated using a plus sign (+). Using this formalism, the A_{Ac}1 mechanism is denoted as A_h + D_N + A_N + D_h. The A_{Ac}2 mechanism is denoted A_h + A_N + A_hD_h + D_N + D_h. The A_{Al}1 reaction is called A_h + D_N + A_N + D_h.

¹⁶² Other mechanistic designations are possible. For a discussion of the B-A_{Ac}3 mechanism, for example, see Kanerva, L. T.; Euranto, E. K. *J. Chem. Soc. Perkin Trans. 2* **1986**, 721.

reaction pathway is most likely with esters of aromatic acids in which

1. the acylium ion is relatively stable, and
2. steric hindrance both destabilizes the ester by reducing resonance interaction of the carbonyl group with the aromatic ring and inhibits nucleophilic addition of water to the carbonyl carbon atom.

For example, acid-catalyzed hydrolysis of methyl mesitoate (**8**) labeled with ^{18}O in the carbonyl oxygen (equation 7.66) led to mesitoic acid (**9**) with no loss of ^{18}O label, even in solutions as low as 3.09 M in H_2SO_4 . Had the reaction occurred by the $\text{A}_{\text{Ac}2}$ pathway, proton exchange and loss of water from the tetrahedral intermediate would likely have resulted in loss of ^{18}O label from starting material and, therefore, from the product.¹⁶³



The $\text{A}_{\text{Al}1}$ (acid-catalyzed, **unimolecular**, alkyl-oxygen cleavage) mechanism involves formation of a carbocation in a process that is analogous to the ionization step in an $\text{S}_{\text{N}}1$ or $\text{E}1$ reaction (Figure 7.18).¹⁶⁴

Unlike acetals, for which one mechanism seems to describe most of the hydrolysis reactions that have been studied, the mechanism of acid-catalyzed hydrolysis of an ester depends on the structure of the ester and on the reaction conditions.¹⁶⁵ For example, Yates concluded that hydrolysis of primary esters occurs by the $\text{A}_{\text{Ac}2}$ mechanism below 90% H_2SO_4 but changes to the $\text{A}_{\text{Ac}1}$ mechanism in solutions with higher concentrations of sulfuric acid (and

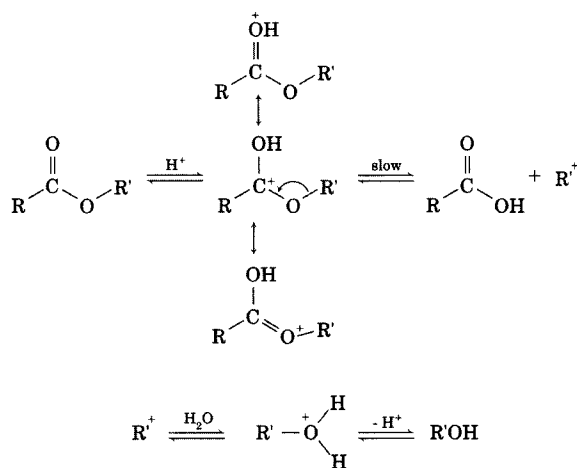


FIGURE 7.18

$\text{A}_{\text{Al}1}$ mechanism for ester hydrolysis.

¹⁶³ Bender, M. L.; Ladenheim, H.; Chen, M. C. *J. Am. Chem. Soc.* **1961**, *83*, 123.

¹⁶⁴ Figure 7.18 shows a mechanism proceeding through protonation of the carbonyl oxygen, which is generally agreed to be the predominant site of protonation of an ester. (Compare reference 160c.) Protonation of the alkyl oxygen also occurs to some extent, and an alternative mechanism involving this pathway can be written (reference 112).

¹⁶⁵ Yates, K. *Acc. Chem. Res.* **1971**, *4*, 136.

TABLE 7.9 Ester Hydrolysis Mechanisms in Concentrated Sulfuric Acid Solutions

Acetate	Changeover (%)	Mechanism
Methyl	75–90	A _{Ac} 2 → A _{Ac} 1
sec-Butyl	70–75	A _{Ac} 2 → A _{A1} 1
Phenyl	>60	A _{Ac} 2 → A _{Ac} 1
t-Butyl	—	A _{A1} 1
p-Methoxybenzyl	Dilute	(A _{Ac} 2) → A _{A1} 1

^a Source: Reference 166

therefore lower concentrations of water). Consistent with this conclusion, the acid-catalyzed hydrolysis of ethyl acetate in 40.2% H₂SO₄ exhibits a ΔH^\ddagger of 16.9 kcal/mol and a ΔS^\ddagger of -15.3 eu. For hydrolysis of the same compound in 98.4% H₂SO₄, ΔH^\ddagger is 23.7 kcal/mol and ΔS^\ddagger is +2.3 eu. The mechanism of hydrolysis of esters from secondary alcohols, as well as from benzyl and allyl alcohols, appears to change from A_{Ac}2 to A_{A1}1 at an acidity that varies with the stability of the carbocation being generated. For example, the mechanism of benzyl acetate hydrolysis changes from A_{Ac}2 to A_{A1}1 at a much lower concentration of H₂SO₄ than does the mechanism for hydrolysis of p-nitrobenzyl acetate. Table 7.9 shows a compilation of the mechanistic assignments for the acid-catalyzed hydrolysis of a series of alkyl and aryl acetates in H₂SO₄ solutions.

Marlier and co-workers reported detailed kinetic isotope effect studies of the hydrolysis of methyl formate in 0.5 M HCl at 20°C (Figure 7.19) that are consistent with an A_{Ac}2 pathway. The small kinetic isotope effect (KIE) observed for oxygen in the leaving group suggests that breakdown of the tetrahedral intermediate is not the rate-limiting step. The formyl hydrogen and carbonyl carbon KIEs suggest that formation of the tetrahedral intermediate is rate limiting. It appears that the reaction under acidic conditions has a “later” transition state, meaning that appreciable *sp*³ character is developed at the carbonyl carbon atom.¹⁶⁷

Alkaline Hydrolysis of Esters

Now consider the hydrolysis of esters under alkaline conditions (equation 7.67).^{168,169}

¹⁶⁶ To facilitate the interpretation of acid-catalyzed hydrolysis reactions, Yates defined an *r* value:

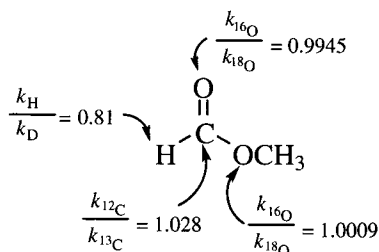
$$\log k_\psi + H_X = r \log a_{H_2O} + \text{constant}$$

where *k*_ψ is the pseudo-first-order rate constant and *H*_X is an acidity function appropriate for the type of compound being studied. Here the value of *r* is “the number of water molecules required to convert a protonated substrate molecule to the transition state, or the approximate ‘order’ of the reaction in water.” Values of *r* around 2 are associated with the A_{Ac}2 mechanism, since two water molecules are drawn in the step that converts a protonated ester to the transition state. Negative values of *r* result from transition states that are less highly solvated than are the protonated esters, suggesting that acylium ions or carbocations are involved in the reaction. Yates, K.; McClelland, R. A. *J. Am. Chem. Soc.* **1967**, *89*, 2686.

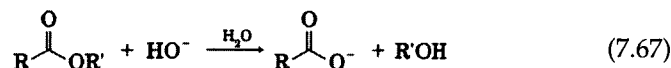
¹⁶⁷ Marlier, J. F.; Frey, T. G.; Mallory, J. A.; Cleland, W. W. *J. Org. Chem.* **2005**, *70*, 1737.

¹⁶⁸ Johnson, S. L. *Adv. Phys. Org. Chem.* **1967**, *5*, 237.

¹⁶⁹ For an overview of reactions of carboxylic acid derivatives, see Bender, M. L. *Chem. Rev.* **1960**, *60*, 53 and references therein.

**FIGURE 7.19**

Kinetic isotope effects for the acid-catalyzed hydrolysis of methyl formate.



The proposed reaction mechanisms can be distinguished by two factors: (i) whether ester cleavage occurs between the oxygen atom and the acyl carbon atom or between the oxygen atom and the alkyl carbon atom, and (ii) whether the reaction involves only a single step or involves an intermediate.¹⁷⁰

The **B_{Al}2** (base-promoted, **bimolecular**, with attack on the **alkyl** group) mechanism is essentially an S_N2 reaction, involving nucleophilic attack on the alkyl group by hydroxide (Figure 7.20). Since this mechanism predicts cleavage of the alkyl-carbon-oxygen bond, rather than the acyl-carbon-oxygen bond, isotopic labeling experiments can be used to determine whether this pathway operates. Hydrolysis of ethyl propionate labeled as shown in equation 7.68 led to product in which all of the label was found in the ethanol, therefore ruling out a B_{Al}2 mechanism for this reactant.¹⁷¹ The B_{Al}2 mechanism also predicts inversion at a chiral carbon atom bonded to the oxygen, but esters made from optically active alcohols do not show inversion.¹⁷² Therefore, it seems that *most* base-promoted hydrolysis reactions do not occur by the B_{Al}2 mechanism.¹⁷³



There is evidence for the B_{Al}2 pathway in certain cases, however. Olson and Miller found that hydrolysis of β-butyrolactone (**10**) to 4-hydroxybuta-

¹⁷⁰ The terminology used for mechanisms in this section is based on the Ingold system (reference 112). The IUPAC nomenclature (reference 161) for alkaline hydrolyses of esters is as follows: The B_{Ac}1 mechanism is D_N + A_N + A_{xh}D_h. The B_{Ac}2 reaction is termed A_N + D_N + A_{xh}D_h. For further discussion, see Guthrie, J. P. *J. Am. Chem. Soc.* **1991**, *113*, 3941.

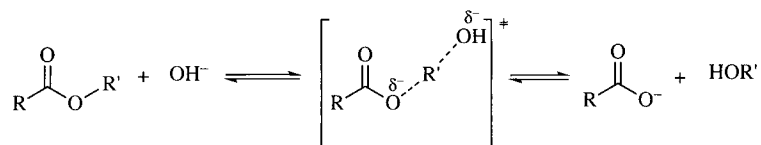
¹⁷¹ Kursanov, D. N.; Kudryavtsev, R. V. *Zh. Obshchei. Khim.* **1956**, *26*, 1040. See also reference 169 and *Chem. Abstr.* **1956**, *50*, 16666i.

¹⁷² Holmberg, B. *Chem. Ber.* **1912**, *45*, 2997.

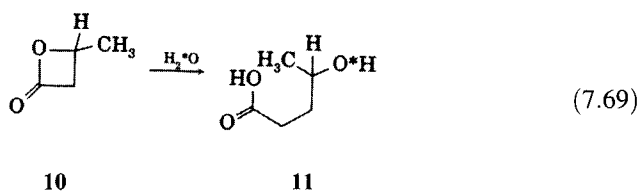
¹⁷³ This pattern of reaction was identified with methoxide ion as the nucleophile in the formation of dimethyl ether from the reaction of methoxide with methyl benzoate in methanol solution at 100°C. Bunnett, J. F.; Robison, M. M.; Pennington, F. C. *J. Am. Chem. Soc.* **1950**, *72*, 2378.

FIGURE 7.20

$B_{Al}2$ mechanism for ester hydrolysis.



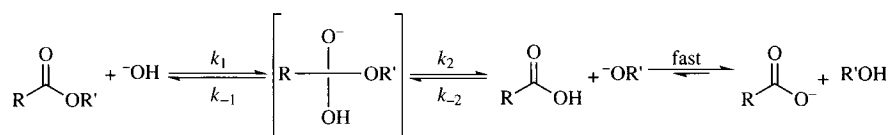
noic acid (11) is catalyzed by acid in very acidic solution ($pH < 1$) and by base at pH 9 and above. Between these pH regions the rate constant for hydrolysis is essentially constant. Hydrolysis of the lactone formed from (+)- β -bromobutyric acid at neutral pH led to a product that was optically active and that had the *opposite* rotation from that produced by the hydrolysis of the same lactone with either acid or base catalysis. The results suggested a mechanism involving back-side attack of water on the alkyl C–O bond in the neutral pH reaction, analogous to the mechanism shown in Figure 7.20.¹⁷⁴ This conclusion was supported by the results of hydrolysis of the lactone in $H_2^{18}O$ (equation 7.69), in which the labeled oxygen was found to be in the hydroxyl function.¹⁷⁵



The $B_{Ac}2$ (base promoted, **bimolecular**, with attack on the **acyl** group) mechanism is shown in Figure 7.21. In principle, either addition of hydroxide to the ester (with rate constant k_1) or decomposition of the tetrahedral intermediate (with rate constant k_2) may be the rate-limiting step in the reaction, so the kinetics of the reaction depend on the nucleophile and the leaving group.¹⁷⁶ For the hydrolysis of esters, the available data suggest that the attack of hydroxide ion is rate limiting.¹⁷⁷

FIGURE 7.21

$B_{Ac}2$ mechanism for ester hydrolysis.

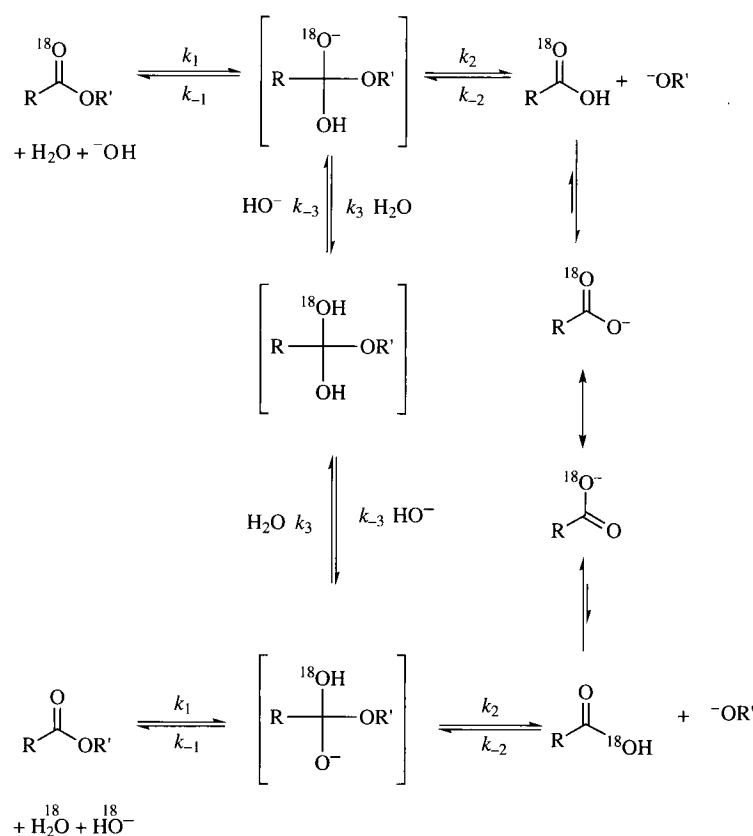


¹⁷⁴ Olson, A. R.; Miller, R. J. *J. Am. Chem. Soc.* **1938**, *60*, 2687.

¹⁷⁵ Olson, A. R.; Hyde, J. L. *J. Am. Chem. Soc.* **1941**, *63*, 2459. See also Olson, A. R.; Youle, P. V. *J. Am. Chem. Soc.* **1951**, *73*, 2468.

¹⁷⁶ The proposed expulsion of an alkoxide ion from the tetrahedral intermediate is consistent with theoretical calculations. Some studies have suggested that proton transfer to the oxygen may occur prior to breaking of the C–O bond. Maraver, J. J.; Marcos, E. S.; Bertrán, J. *J. Chem. Soc. Perkin Trans. 2* **1986**, 1323.

¹⁷⁷ For a detailed discussion of the kinetics of the base-promoted hydrolysis of esters, see Johnson, S. L. *Adv. Phys. Org. Chem.* **1967**, *5*, 237.

**FIGURE 7.22**

Isotopic exchange evidence for the tetrahedral intermediate in ester hydrolysis. (Adapted from reference 178b.)

Evidence for the $\text{B}_{\text{AC}2}$ mechanism has come from isotopic labeling studies.^{178,179} Hydrolysis of ethyl, isopropyl, or *t*-butyl benzoate labeled with ^{18}O in the carbonyl group (Figure 7.22) was found to yield a small amount of starting material that had lost the ^{18}O label. This result is most easily explained by a mechanism involving a tetrahedral intermediate, specifically the central structure in brackets shown in Figure 7.22 that can undergo a proton exchange and then loss of labeled water. It must be emphasized that failure to observe isotope exchange would not rule out a mechanism involving a tetrahedral intermediate, because that situation could result if the proton exchange required to produce the bracketed intermediate is too slow to compete with collapse of the anions with which it is in equilibrium. That is, isotopic exchange would not be observed unless $k_3 \gg k_2, k_{-1}$. Indeed, failure to observe isotopic exchange for reaction of phenyl benzoate and some other benzoates has been attributed to larger k_2 and k_{-1} values than k_3 values.^{180–183}

¹⁷⁸ (a) Bender, M. L. *J. Am. Chem. Soc.* **1951**, *73*, 1626; see also reference 169. (b) Bender, M. L.; Thomas, R. J. *J. Am. Chem. Soc.* **1961**, *83*, 4189.

¹⁷⁹ See also Kellogg, B. A.; Tse, J. E.; Brown, R. S. *J. Am. Chem. Soc.* **1995**, *117*, 1731.

¹⁸⁰ Bunton, C. A.; Spatcher, D. N. *J. Chem. Soc.* **1956**, 1079.

¹⁸¹ Bender, M. L.; Matsui, H.; Thomas, R. J.; Tobey, S. W. *J. Am. Chem. Soc.* **1961**, *83*, 4193.

¹⁸² Bruice, T. C.; Benkovic, S. J. *Bioorganic Mechanisms*, Vol. I; W. A. Benjamin: New York, 1966; p. 24.

¹⁸³ In some cases, a direct, $\text{S}_{\text{N}}2$ -type mechanism may occur. For example, Xie, D.; Zhou, Y.; Xu, D.; Guo, H. *Org. Lett.* **2005**, *7*, 2093 reported DFT calculations indicating that the reaction of *p*-nitrophenyl acetate can take place by a concerted pathway in aqueous solution.

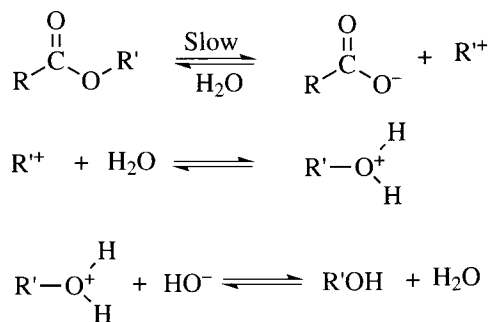


FIGURE 7.23

B_{A1} mechanism for ester hydrolysis.

The B_{A1} mechanism is illustrated in Figure 7.23. The rate-limiting step in the reaction is a unimolecular dissociation of the ester to a carboxylate ion and a carbocation. Such a mechanism is more likely if the ester is derived from a strong acid (so that the carboxylate ion is more stable), if R' is a tertiary or benzylic alkyl group (so that the carbocation is more stable), and if the concentration of base is low enough that the B_{Ac2} mechanism does not compete. For molecules in which the B_{A1} reaction is rapid, it can be observed through formation of racemized alcohol product even in the presence of hydroxide ions. For molecules in which the B_{A1} reaction is slow, however, reaction in the presence of aqueous base leads primarily to B_{Ac2} reaction, and the hydrolysis of an ester formed from an optically active alcohol leads to product in which there is retention of configuration in the alcohol product. For example, Ingold summarized studies of the hydrolysis of a series of alkyl hydrogen phthalates indicating that the B_{A1} process dominates in 10M NaOH solution when the alkyl group is *p*-methoxybenzhydryl and in dilute aqueous NaOH solution when the alkyl group is *p*-phenoxybenzhydryl. Only in neutral aqueous solution was racemization of the product alcohol observed when the alkyl group was 1-phenylethyl.¹¹²

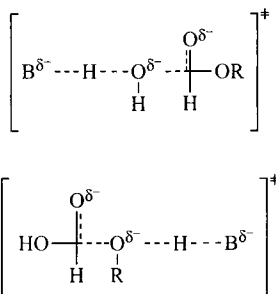


FIGURE 7.24

Possible transition states for general base-catalyzed hydrolysis of an ester: deprotonation of water (left) or protonation of the departing alkoxide ion (right).

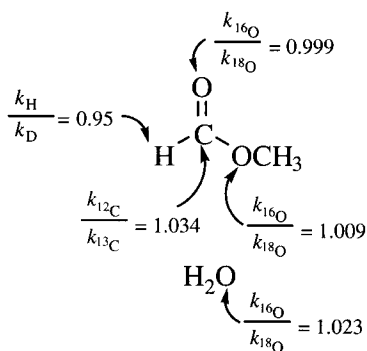
The mechanisms for alkaline hydrolysis of esters discussed to this point have indicated that the attacking nucleophile is a hydroxide ion, meaning that there is specific base catalysis. There are two processes that could lead to general base-catalyzed reactions, however: (i) general base catalysis of the addition of water or (ii) proton donation to the departing alkoxide ion in the second (rate-limiting) step of a specific base, general acid-catalyzed reaction (Figure 7.24).¹⁸⁴⁻¹⁸⁶ Marlier reported a detailed study of carbonyl oxygen, carbonyl carbon, formyl hydrogen, and nucleophile oxygen kinetic isotope effects in the hydrolysis of methyl formate (Figure 7.25).^{167,187} The small KIE observed for oxygen in the leaving group suggests that breakdown of the tetrahedral intermediate is not the rate-limiting step, while the formyl hydrogen and carbonyl carbon KIEs suggest that formation of the tetrahedral intermediate is rate limiting. These results indicated that the reaction under

¹⁸⁴ Jencks, W. P.; Carriuolo, J. J. *Am. Chem. Soc.* **1961**, *83*, 1743.

¹⁸⁵ See also Dawson, H. M.; Lowson, W. J. *Chem. Soc.* **1929**, 393; Gold, V.; Oakenfull, D. G.; Riley, T. *J. Chem. Soc. B* **1968**, 515.

¹⁸⁶ Sawyer, C. B.; Kirsch, J. F. *J. Am. Chem. Soc.* **1973**, *95*, 7375. Other reaction pathways can be kinetically equivalent to general base catalysis; for a discussion, see reference 188.

¹⁸⁷ Marlier, J. F. *J. Am. Chem. Soc.* **1993**, *115*, 5953.

**FIGURE 7.25**

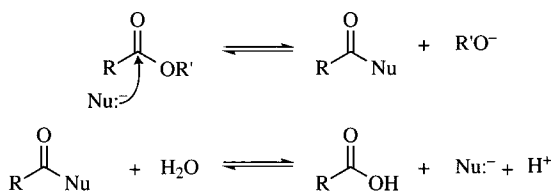
Kinetic isotope effects observed for the base-catalyzed hydrolysis of methyl formate.

basic conditions involves an “early” transition state in which the carbonyl carbon retains significant sp^2 character. The oxygen nucleophile isotope effect was attributed to the addition of a water oxygen to the carbonyl group, with general base assistance from hydroxide. Thus, the data suggest that the hydrolysis of methyl formate in aqueous hydroxide solution occurs through a stepwise mechanism in which the rate-limiting step is the formation of the tetrahedral intermediate by addition of a *water molecule*, not hydroxide, with assistance by a general base (Figure 7.25).¹⁸⁸

An alternative mechanism for base catalysis of ester hydrolysis is nucleophilic catalysis, as illustrated in Figure 7.26. In the first step of the reaction, a nucleophile replaces the alkoxy group. In the second step, that nucleophile is replaced by an OH group.¹⁸⁹ The catalytic effect arises if (at the pH of the experiment) Nu is both a more effective nucleophile than hydroxide ion and is also a better leaving group than the alkoxide ion.

Experimental evidence for such nucleophilic catalysis is summarized in Figure 7.27. Hydrolysis of 2,4-dinitrophenyl benzoate catalyzed by acetate ion labeled with ^{18}O on both oxygen atoms led to product in which both benzoic acid and acetic acid were labeled with ^{18}O , but about 75% of the label derived from one ^{18}O in the reactant was found in the benzoate ion.¹⁹⁰ The data were interpreted as evidence for the intermediacy of the mixed anhydride $\text{CH}_3\text{CO}_2\text{COC}_6\text{H}_5$.

The reaction in Figure 7.27 involves intermolecular nucleophilic catalysis, but *intramolecular* nucleophilic catalysis has also been observed. Fersht and Kirby found incorporation of ^{18}O in the product when acetyl-3,5-dinitrosalicylate ion was hydrolyzed in a solvent containing isotopically enriched

**FIGURE 7.26**

Nucleophilic catalysis in ester hydrolysis.

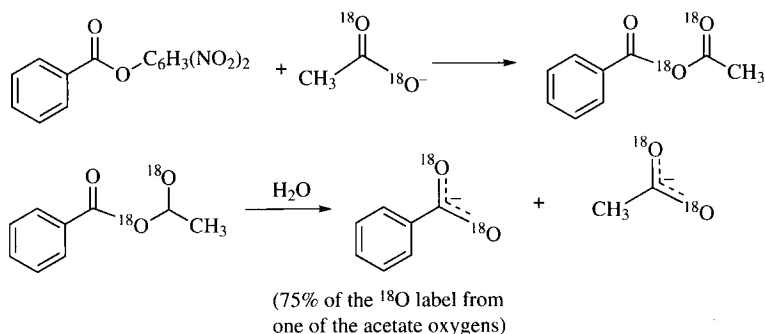
¹⁸⁸ Stefanidis, D.; Jencks, W. P. *J. Am. Chem. Soc.* **1993**, *115*, 6045 came to the same conclusion in studies of the hydrolysis of a series of alkyl formates on the basis of the increase in the Brønsted β value for base catalysis with the decrease in the pK_a of the leaving group and on the basis of solvent isotope effects

¹⁸⁹ For examples, see Bender, M. L.; Turnquest, B. W. *J. Am. Chem. Soc.* **1957**, *79*, 1652; Bender, M. L.; Glasson, W. A. *J. Am. Chem. Soc.* **1959**, *81*, 1590.

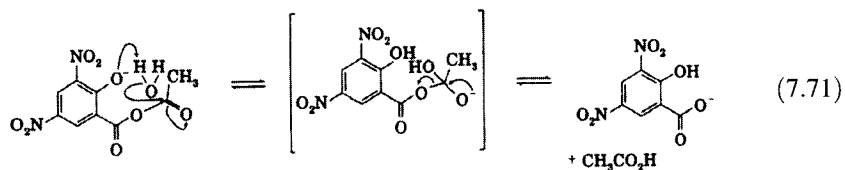
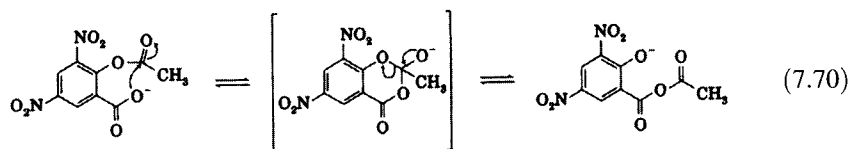
¹⁹⁰ Bender, M. L.; Neveu, M. C. *J. Am. Chem. Soc.* **1958**, *80*, 5388.

FIGURE 7.27

Nucleophilic catalysis by acetate ion in hydrolysis of a benzoic acid ester.



water. This result suggested the mechanism shown in equations 7.70 and 7.71. The reaction in equation 7.70 is the step involving intramolecular nucleophilic catalysis; it is followed by a reaction involving intramolecular base catalysis (equation 7.71).¹⁹¹ Intramolecular nucleophilic catalysis was also proposed for the hydrolysis of phthalic acid, methyl hydrogen phthalate, and nonenolizable β -keto esters.¹⁹²⁻¹⁹⁴



The discussion here has emphasized the hydrolysis of alkyl esters. *Aryl* esters may react differently because the greater acidity of phenols than of alcohols makes the phenolate ions much better leaving groups. Guthrie concluded that aryl esters with leaving groups formed from strongly acidic phenols ($\text{p}K_{\text{a}} < 1$) react by way of acylium ions, while esters with leaving groups of $\text{p}K_{\text{a}} > 11$ react by an associative mechanism that may involve a tetrahedral addition intermediate. Esters with $\text{p}K_{\text{a}}$ of the leaving group between 1 and 11, however, were determined to react by way of a concerted mechanism.^{185,195}

Hydrolysis and other acyl substitution reactions can be catalyzed by molecules that are bifunctional, and these reactions serve as models for enzymatic processes. In addition, metal ions can catalyze some of these

¹⁹¹ Fersht, A. R.; Kirby, A. J. *J. Am. Chem. Soc.* **1968**, *90*, 5818.

¹⁹² Bender, M. L.; Chow, Y.-L.; Chloupek, F. *J. Am. Chem. Soc.* **1958**, *80*, 5380.

¹⁹³ Bender, M. L.; Chloupek, F.; Neveu, M. C. *J. Am. Chem. Soc.* **1958**, *80*, 5384.

¹⁹⁴ Washburn, W. N.; Cook, E. R. *J. Am. Chem. Soc.* **1986**, *108*, 5962.

¹⁹⁵ Similar conclusions had been reached by Ba-Saif, S.; Luthra, A. K.; Williams, A. *J. Am. Chem. Soc.* **1989**, *111*, 2647.

reactions.¹⁸⁴ For example, the hydroxide-catalyzed hydrolysis of esters of picolinic acid is dramatically enhanced by low concentrations of Ni^{2+} and Cu^{2+} ions. The catalysis appears to occur through formation of a metal chelate, such as **12**, that reduces the barrier for the rate-limiting addition of the nucleophile to the carbonyl group.^{196,197} In addition, the hydrolysis of a 1° amide by a catalytic antibody was reported.¹⁹⁸



Hydrolysis is only one of many acyl substitution reactions of esters. If the attacking nucleophile is not hydroxide ion but is an amine, alkoxide ion, phenoxide ion, halide ion, or other nucleophile, then the mechanism may differ. For example, Jencks and co-workers made a detailed study of the reaction of substituted phenoxide ions as nucleophiles in substitutions with nitro-substituted phenyl formates and acetates.¹⁹⁹ In such reactions the fate of a tetrahedral intermediate, such as that shown in Figure 7.21, depends on both the nucleophile and the leaving group. If the nucleophile is the weaker base, then departure of the leaving group is rate limiting. If the nucleophile is the stronger base, then attack of the nucleophile is rate limiting. However, Jencks and co-workers were unable to detect evidence for a change in the rate-limiting step in the reaction of substituted phenoxide nucleophiles with a series of formate and acetate esters. This led to the conclusion that the tetrahedral species is so unstable that it is a transition structure rather than an intermediate. Similarly, DeTar concluded from a detailed analysis of the kinetics of acyl substitution reactions that aminolysis of aryl esters might not involve a "kinetically significant" tetrahedral intermediate and that a direct displacement should also be considered.²⁰⁰ Synchronous displacement was also proposed for reactions of acyl halides with nucleophiles such as 2-naphthoxide, the reaction of phenoxide ion with 2-aryloxazolin-5-one, reactions of phenol with chloroacetyl chloride in acetonitrile, alcoholysis of benzoyl chloride, and solvolyses of benzoyl chloride in some water-organic solvent mixtures.²⁰¹⁻²⁰⁵

¹⁹⁶ Fife, T. H.; Przystas, T. J. *J. Am. Chem. Soc.* **1985**, *107*, 1041 and references therein.

¹⁹⁷ Pronounced catalytic activity has been observed with some binuclear metal complexes. Göbel, M. W. *Angew. Chem. Int. Ed. Engl.* **1994**, *33*, 1141.

¹⁹⁸ Martin, M. T.; Angeles, T. S.; Sugasawara, R.; Aman, N. I.; Napper, A. D.; Darsley, M. J.; Sanchez, R. I.; Booth, P.; Titmas, R. C. *J. Am. Chem. Soc.* **1994**, *116*, 6508.

¹⁹⁹ Stefanidis, D.; Cho, S.; Dhe-Paganon, S.; Jencks, W. P. *J. Am. Chem. Soc.* **1993**, *115*, 1650.

²⁰⁰ DeTar, D. F. *J. Am. Chem. Soc.* **1982**, *104*, 7205.

²⁰¹ Haberfield, P.; Trattner, R. B. *Chem. Commun.* **1971**, 1481.

²⁰² Curran, T. C.; Farrar, C. R.; Niaz, O.; Williams, A. *J. Am. Chem. Soc.* **1980**, *102*, 6828.

²⁰³ Briody, J. M.; Satchell, D. P. N. *J. Chem. Soc.* **1965**, 168.

²⁰⁴ Peterson, P. E.; Vidrine, D. W.; Waller, F. J.; Henrichs, P. M.; Magaha, S.; Stevens, B. *J. Am. Chem. Soc.* **1977**, *99*, 7968.

²⁰⁵ Bentley, T. W.; Carter, G. E.; Harris, H. C. *J. Chem. Soc. Perkin Trans. 2* **1985**, 983.

There is also evidence for the role of acylium ions in some acyl substitutions, such as the reactions of acyl halides with nucleophilic reagents in acetonitrile, nitromethane, and ethanol and the hydrolysis of some acyl fluorides.^{203,206,207} Acylium ions are more likely candidates for reaction intermediates under acidic conditions. Bender reported that the hydrolysis of a series of substituted methyl 2,6-dimethylbenzoates in 9.7 M sulfuric acid proceeds through an acylium ion intermediate.²⁰⁸ Hydrolysis of a series of substituted 2,6-dimethylbenzoyl chlorides in 99% CH₃CN–H₂O was determined to involve an acylium intermediate under acidic or neutral conditions, and ρ values (measured by σ^+) were found to be -3.85 and -3.73 , respectively. The value of ρ under basic conditions was $+1.20$, suggesting that the base-promoted reaction does involve a tetrahedral addition intermediate.²⁰⁹

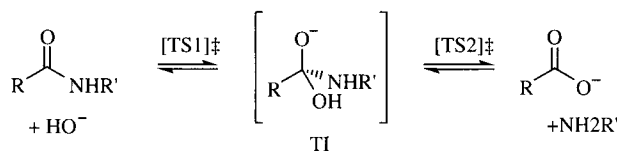
Hydrolysis of Amides

Because of its close relationship to the chemistry of peptides, the hydrolysis of amides has been the subject of extensive experimental and theoretical investigation. Observations of ¹⁸O exchange accompanying the basic hydrolysis of amides such as 1°, 2°, or 3° toluamides suggested that a tetrahedral intermediate (TI) is formed along the reaction path (Figure 7.28).²¹⁰

Experimental studies led to the conclusion that the rate-limiting step in the hydrolysis is departure of the amine from the tetrahedral intermediate, because greater oxygen exchange was observed with poorer leaving groups.^{211,212} Oxygen exchange was also observed in the acid-catalyzed hydrolysis of amides.²¹³ For the hydrolysis of many amides, the exchange data, as well as solvent kinetic isotope effect data, are consistent with the mechanism shown in Figure 7.28. As the basicity of the leaving amine decreases (so that the pK_a of the ammonium ion is less than 6), the nitrogen is less likely to be protonated in the tetrahedral intermediate. The nitrogen is therefore more likely to depart as an amide ion, and ¹⁸O exchange becomes proportionally less likely. Thus, amides formed from low-basicity amines

FIGURE 7.28

Proposed mechanism for the basic hydrolysis of an amide.



²⁰⁶ Kevill, D. N.; Daum, P. H.; Sapre, R. J. *Chem. Soc. Perkin Trans. 2* **1975**, 963.

²⁰⁷ Song, B. D.; Jencks, W. P. *J. Am. Chem. Soc.* **1987**, *109*, 3160; **1989**, *111*, 8470.

²⁰⁸ Bender, M. L.; Chen, M. C. *J. Am. Chem. Soc.* **1963**, *85*, 37.

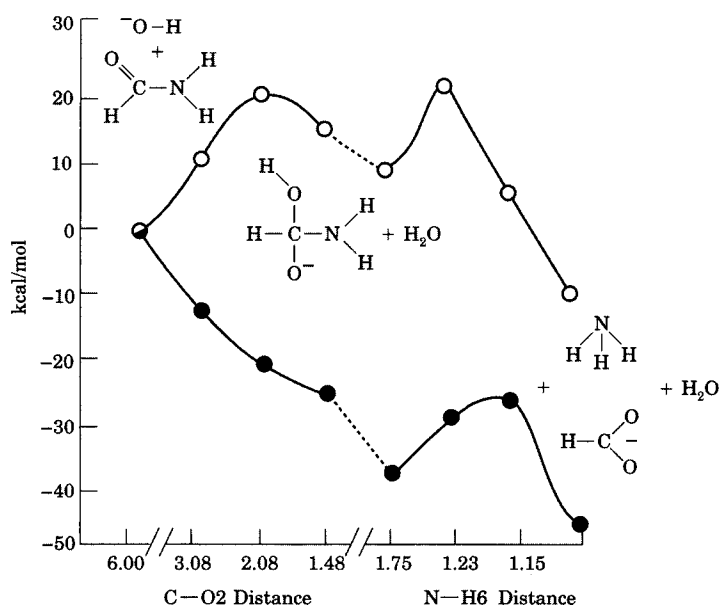
²⁰⁹ Bender, M. L.; Chen, M. C. *J. Am. Chem. Soc.* **1963**, *85*, 30.

²¹⁰ Ślebocka-Tilk, H.; Brown, R. S. *J. Org. Chem.* **1988**, *53*, 1153.

²¹¹ Ślebocka-Tilk, H.; Bennet, A. J.; Keillor, J. W.; Brown, R. S.; Guthrie, J. P.; Jodhan, A. J. *Am. Chem. Soc.* **1990**, *112*, 8507.

²¹² Ślebocka-Tilk, H.; Bennet, A. J.; Hogg, H. J.; Brown, R. S. *J. Am. Chem. Soc.* **1991**, *113*, 1288.

²¹³ Ślebocka-Tilk, H.; Brown, R. S.; Olekszyk, J. J. *Am. Chem. Soc.* **1987**, *109*, 4620. The compounds studied in this investigation were acetanilide and *N*-cyclohexylacetamide.

**FIGURE 7.29**

Calculated energy profiles for the hydrolysis of formamide in the gas phase (●) and in aqueous solution (○). (Adapted from reference 215.)

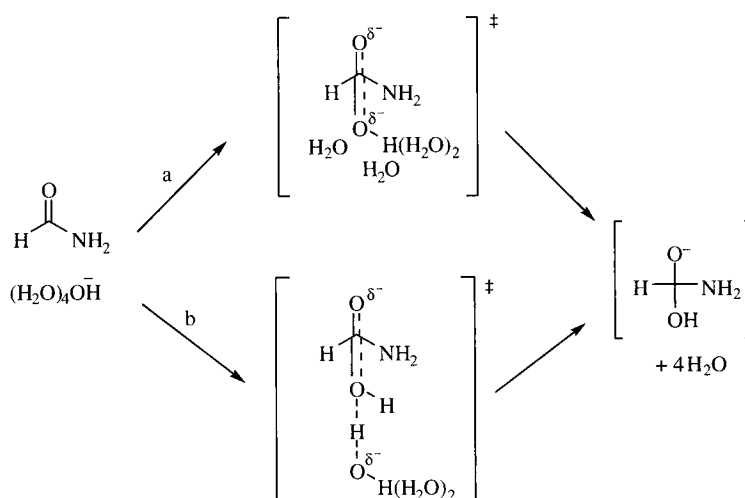
may undergo hydrolysis by expelling the deprotonated form of the amine from II.²¹⁴

Although the solvent is not depicted in Figure 7.28, protic solvents play an important role in amide hydrolysis both as polar solvents and as proton-donating and -accepting agents. Kollman and co-workers reported calculations for the hydrolysis of formamide in aqueous solution and in the gas phase.²¹⁵ Figure 7.29 shows the energies calculated for the gas phase reaction (filled circles) and for the solution reaction (open circles) at several points between reactants and products. The gas phase calculations include one molecule of water to lower the barrier for transfer of a proton from oxygen to nitrogen during the expulsion of ammonia. The calculations indicate that there is no activation barrier for formation of the tetrahedral addition intermediate in the gas phase, but there is a 12 kcal/mol barrier for the expulsion of ammonia. Calculations for reaction in aqueous solution indicated a 22 kcal/mol barrier for addition of the hydroxide to the carbon-oxygen double bond and a slightly smaller barrier for the departure of ammonia.²¹⁶ Later calculations provided even more detailed pictures of the role of conformational

²¹⁴ Brown, R. S.; Bennet, A. J.; Ślebocka-Tilk, H.; Jodhan, A. J. *Am. Chem. Soc.* **1992**, *114*, 3092; Brown, R. S.; Bennet, A. J.; Ślebocka-Tilk, H. *Acc. Chem. Res.* **1992**, *25*, 481.

²¹⁵ Weiner, S. J.; Singh, U. C.; Kollman, P. A. *J. Am. Chem. Soc.* **1985**, *107*, 2219.

²¹⁶ Krug, J. P.; Popelier, P. L. A.; Bader, R. F. W. *J. Phys. Chem.* **1992**, *96*, 7604 subsequently carried out ab initio calculations for the hydrolysis of formamide in the gas phase under four sets of conditions: (i) no acid or base catalysis, but with one molecule of water; (ii) reaction with hydroxide; (iii) reaction with H_3O^+ involving protonation of the carbonyl oxygen; and (iv) similar acid catalysis involving protonation of the amide nitrogen. The detailed model of the structure, charge, and energy changes that accompany the hydrolysis reaction provided by these calculations may be relevant to the mechanism of amide hydrolysis in the hydrophobic region of an enzyme.

**FIGURE 7.30**

Alternative pathways for the formation of the tetrahedral intermediate in the basic hydrolysis of formamide.

changes, nitrogen pyramidalization, substituents, and solvent in the hydrolysis reaction.^{217–220}

As noted above, there is not an activation barrier for the formation of a tetrahedral intermediate (TI) from hydroxide ion and formamide in the gas phase. The barrier in solution has been attributed to the increase in free energy that must accompany the partial desolvation of hydroxide ion that is required for formation of TI by attack of hydroxide on the carbonyl group. Two slightly different mechanisms for this process have been proposed, as shown in Figure 7.30. In path a, two water molecules are lost from the solvated hydroxide ion, (H₂O)₄HO⁻, before hydroxide adds to the carbonyl. In path b, one of the waters of hydration provides the nucleophilic oxygen, and the hydroxide ion then provides general-base catalysis for the reaction.

Blumberger and co-workers used ab initio metadynamics calculations to map a two-dimensional potential energy surface for the addition of hydroxide to formamide.²²¹ The analysis identified both of the possible mechanisms shown in Figure 7.30, but for path b it was determined that proton transfer from a solvated water molecule to hydroxide occurs before addition of that water oxygen to the carbonyl carbon, supporting the view that it is a hydroxide ion and not a water molecule (catalyzed by general base) that adds to the carbonyl. In addition, the analysis reaffirmed the view that the activation energy for the reaction is primarily associated with the loss of two hydrogen bonds from the hydroxide ion as the transition state is formed.²²²

Amide hydrolysis in aqueous solution is also catalyzed by acid. Marlier and co-workers reported a detailed kinetic isotope effect study of the acid-catalyzed hydrolysis of formamide (Figure 7.31).²²³ The large deuterium

²¹⁷ Lopez, X.; Mujika, J. I.; Blackburn, G. M.; Karplus, M. *J. Phys. Chem. A* **2003**, *107*, 2304.

²¹⁸ For a theoretical study, see Bakowies, D.; Kollman, P. A. *J. Am. Chem. Soc.* **1999**, *121*, 5712.

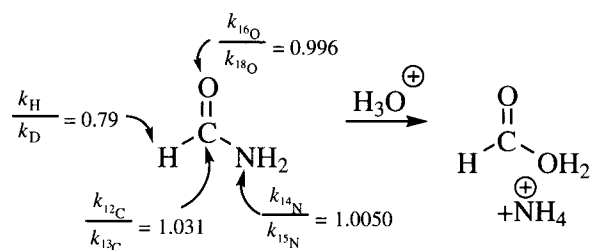
²¹⁹ Estiu, G.; Merz, K. M., Jr. *J. Phys. Chem. B* **2007**, *111*, 6507.

²²⁰ Xiong, Y.; Zhan, C.-G. *J. Phys. Chem. A* **2006**, *110*, 12644.

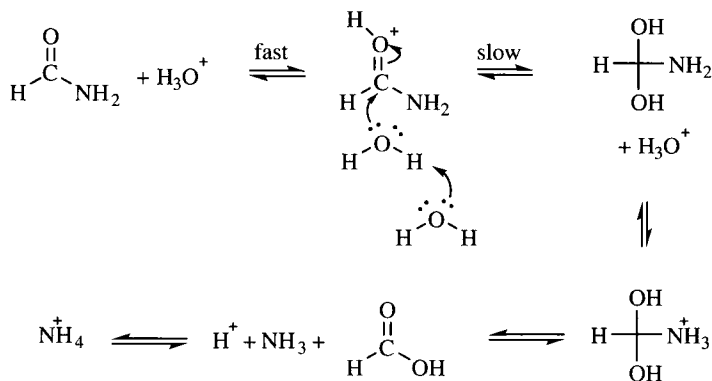
²²¹ Blumberger, J.; Ensing, B.; Klein, M. L. *Angew. Chem. Int. Ed.* **2006**, *45*, 2893.

²²² See also Šlebocka-Tilk, H.; Neverov, A. A.; Brown, R. S. *J. Am. Chem. Soc.* **2003**, *125*, 1851.

²²³ Marlier, J. F.; Campbell, E.; Lai, C.; Weber, M.; Reinhardt, L. A.; Cleland, W. W. *J. Org. Chem.* **2006**, *71*, 3829.

**FIGURE 7.31**

Kinetic isotope effects observed in the acidic hydrolysis of formamide.

**FIGURE 7.32**

Mechanism proposed for the hydrolysis of formamide in acidic solution.

kinetic isotope effect observed for the formyl hydrogen suggested that the carbonyl carbon is highly tetrahedral in the transition state, and the carbon KIE was consistent with this conclusion. The small nitrogen KIE suggested that breaking of the C–N bond is not rate limiting, while the carbonyl oxygen KIE was attributed to addition of water to the carbonyl group in the rate-determining step. Along with other evidence, these results supported the mechanism in Figure 7.32 for the acid-catalyzed hydrolysis.²¹⁴

In addition to acid and base catalysis of amide hydrolysis, there is evidence that neutral water can also react with amides. A detailed investigation of the hydrolysis of formamide in aqueous solution was reported by Slebocka-Tilk et al.²²⁴ The value of the observed rate constant (k_{obs}) was found to depend on temperature because of the variation of the autodissociation equilibrium constant of water, K_w , with temperature. Log k_{obs} for the reaction at 56°C was a minimum at pH 6.1 and then increased in either more acidic or more basic environments. By measuring the rate constants for the acid- and base-catalyzed reactions, the investigators determined the rate constant for reaction of formamide with neutral water. Thus, the overall observed rate constant for the reaction at 56°C was

$$k_{\text{obs}}^{56^\circ\text{C}} = 3.03 \times 10^{-3}[\text{H}_3\text{O}^+] + 3.2 \times 10^{-2}[\text{HO}^-] + 3.6 \times 10^{-9} \quad (7.72)$$

²²⁴ Slebocka-Tilk, H.; Sauriol, F.; Monette, M.; Brown, R. S. *Can. J. Chem.* **2002**, *80*, 1343.

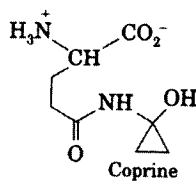
The activation parameters observed for the acid-catalyzed reaction were $\Delta H^\ddagger = 17.0 \pm 0.4$ kcal/mol and $\Delta S^\ddagger = -18.8 \pm 1.3$ cal mol⁻¹ K⁻¹. The corresponding values for the base-catalyzed reaction were $\Delta H^\ddagger = 17.9 \pm 0.2$ kcal/mol and $\Delta S^\ddagger = -11.1 \pm 0.5$ cal mol⁻¹ K⁻¹. The value of k_w at 25°C was then calculated to be 1.1×10^{-10} s⁻¹, meaning that the half-life for the hydrolysis of formamide by water at 25°C is approximately 200 years.

Problems

- Use equation 7.9 to predict the pK_a of vanillic acid (4-hydroxy-3-methoxybenzoic acid).
- Convert the ΔG_{acid} values in kcal/mol for acetic and propionic acids in Table 7.4 to pK_a values at 25°C by using the relationship $\Delta G = -RT \ln K$. Explain the difference in magnitude of the pK_a values in the gas phase and in solution, and rationalize the different order of acidities of the compounds in the two media.
- Use the data for ab initio calculations of the stabilities of alkoxide ions on page 428 to compare the effect, in kcal/mol, of replacing first one, then two, then three hydrogen atoms on methoxide with methyl groups. Rationalize the trend you observe.
- Explain the order of the K_d values for hemiketals of cyclobutanone, cyclopentanone, and cyclohexanone listed in Table 7.7.
- Demonstrate that equation 7.57 can be written in terms of the pK_a value of the protonated base, BH^+ as shown in equation 7.73, where c is a constant.

$$\log k_b = \beta pK_{BH^+} + c \quad (7.73)$$

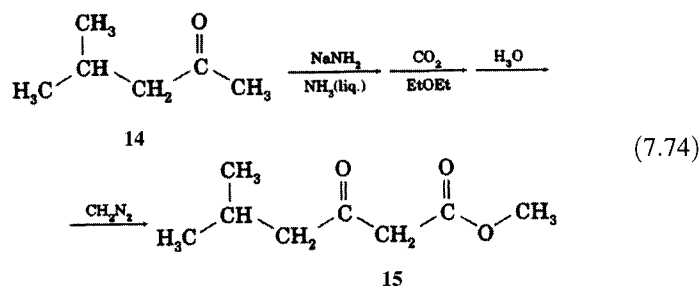
- Toxicity has been associated with the coincident ingestion of the mushroom *Coprinus atramentarius* along with ethanol. A compound found to the extent of 0.1% by weight of the dried mushroom has been identified as coprine (13). Although coprine itself is inactive in vitro, a derivative of coprine identified as cyclopropanone hydrate was found to be an inhibitor of acetaldehyde dehydrogenase, an enzyme that is involved in the physiological oxidation of ethanol.
 - Propose a mechanism for the nonenzymatic formation of cyclopropanone hydrate from coprine.
 - Explain why cyclopropanone hydrate would exist in physiological solution almost entirely as the hydrate and not as the ketone.



13

- Predict the position of acid-catalyzed bromination of each of the following ketones: (a) 2-butanone, (b) 2-pentanone, (c) 3-methyl-2-butanone, (d) 2-methylcyclohexanone, and (e) methyl cyclohexyl ketone.

- 7.8. Treatment of methyl isobutyl ketone (14) with sodium amide and then CO_2 produces, after workup, a carboxylic acid that is converted by diazomethane to methyl isovalerylacetate (15). Propose a mechanism for the reaction, and explain the regiochemical preference that leads to the observed product.

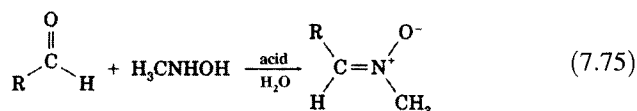


- 7.9. Pyridine bases have been found to catalyze the aldol reaction of D-glyceraldehyde. Rate constants for reactions carried out with a series of catalysts in water at pH 7.0 and 30°C are shown in Table 7.10. (The observed reaction rates were divided by the molar concentration of unprotonated base at the reaction pH in order to obtain the rate constants shown.) Determine whether the reaction is subject to general or specific base catalysis. Do the data suggest any role of steric hindrance in the catalysis of the reaction by pyridine bases?
- 7.10. Treatment of 5,5-dimethyl-1,3-cyclohexanedione with NaOCl and KOH in aqueous solution at 35°C , followed by acidification of the reaction mixture, leads to the formation of 3,3-dimethylpentanedioic acid. Propose a detailed mechanism to account for the formation of this product.
- 7.11. Should a tetrahedral intermediate formed by the addition of a nucleophile to the $\text{C}=\text{O}$ group of an ester be more stable for phenyl acetate or phenyl formate? Explain your answer.
- 7.12. Construct a More O'Ferrall-Jencks diagram for the general base-catalyzed hydration of acetaldehyde. Let the horizontal scale represent proton transfer from water to the general base (to form hydroxide ion), and let the vertical scale represent addition of the oxygen atom of water to the carbonyl carbon atom. The upper right corner of the diagram will represent the products, protonated base and the oxyanion of the hydrate. What structural features of the base and the carbonyl compound would affect the location of the transition structure and the reaction coordinate on this projection of the potential energy surface?

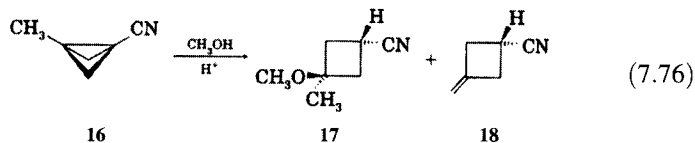
TABLE 7.10 Rates of Aldolization of D-Glyceraldehyde Catalyzed by Pyridine Bases

Catalyst	$\text{p}K_{\text{BH}^+}$	k_2 ($\text{M}^{-1} \text{s}^{-1}$)
Pyridine	5.17	1.74×10^{-5}
2-Methylpyridine	5.97	1.90×10^{-5}
3-Methylpyridine	5.68	2.91×10^{-5}
4-Methylpyridine	6.02	3.65×10^{-5}
2,4-Dimethylpyridine	6.63	3.24×10^{-5}
2,5-Dimethylpyridine	6.40	2.74×10^{-5}
3,4-Dimethylpyridine	6.46	7.32×10^{-5}
2,6-Dimethylpyridine	6.72	0.60×10^{-5}

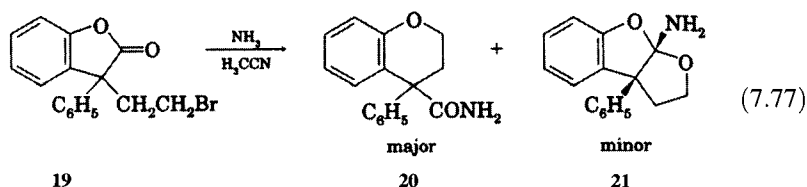
- 7.13. Propose an explanation for the fact that the apparent molecular weight of freshly prepared 1,3-dihydroxyacetone is 180 g/mol.
- 7.14. The extinction coefficients (ϵ) at ca. 286 nm determined from the UV-vis spectra of 4-methoxybutanal and 4-hydroxybutanal dissolved in 75 : 25 (v : v) dioxane-water were found to be 17.4 and 1.99, respectively. For 5-methoxy- and 5-hydroxypentanal, the corresponding values were 19.2 and 1.17. The ϵ values were much closer for 6-methoxy- and 6-hydroxyhexanal, however: 19.4 and 16.6. Explain the origin of the difference in the ϵ values for each compound, and explain why the difference varies among members of the series.
- 7.15. Hydrolysis of acetals in H_2^{18}O produces alcohols with virtually no ^{18}O label. Predict the stereochemistry of the product from the hydrolysis of the acetal formed from acetaldehyde and (-)- α -phenylethyl alcohol.
- 7.16. Rationalize the observation that sterically hindered esters are more likely to react via acylium ions than are unhindered esters.
- 7.17. Reaction of an aldehyde with *N*-methylhydroxylamine in the presence of an acid catalyst in aqueous solution leads to the formation of a structure known as a nitron, as shown in equation 7.75. Experimental evidence indicates that the reaction occurs in two steps, with the second step showing general acid catalysis. Propose a mechanism for the reaction.



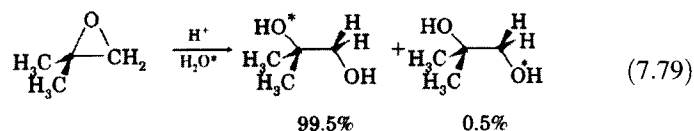
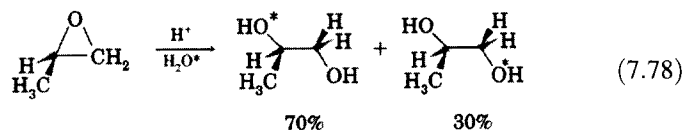
- 7.18. When the hydrolysis of optically active β -butyrolactone is carried out in neutral solution, the product is optically active and has the opposite rotation from the product obtained by hydrolysis of the same lactone under conditions of base catalysis by carbonate ion. When acetate ion is used as a base catalyst, however, the optical activity of the product is identical to that observed at neutral pH. Explain these results.
- 7.19. In methanol solution, 3-methylbicyclobutanecarbonitrile (**16**) undergoes acid-catalyzed addition of solvent to form as major products the cyclobutanes **17** and **18** (equation 7.76). The reaction was investigated by carrying out the addition in a series of buffered methanol solutions at 50°C and constant ionic strength. The second-order rate constants observed for the acid-catalyzed addition of methanol (and the $\text{p}K_{\text{a}}$ values of the buffers under the experimental conditions) were found to be as follows: 2.24×10^{-1} (2.75), 1.06×10^{-3} (4.98), 3.52×10^{-5} (6.41), 8.13×10^{-7} (8.35), and $7.8 \times 10^{-8} \text{ M}^{-1} \text{ s}^{-1}$ (9.42). Show that the reaction is subject to general acid catalysis, and determine the value of α for the reaction.



- 7.20. Treatment of 3-(2-bromoethyl)-3-phenyl-2-benzofuranone (**19**) with ammonia in acetonitrile led to the isolation of a product mixture consisting primarily of **20**, but about 10% of **21** was also formed (equation 7.77). Propose a mechanism to account for the formation of these products.

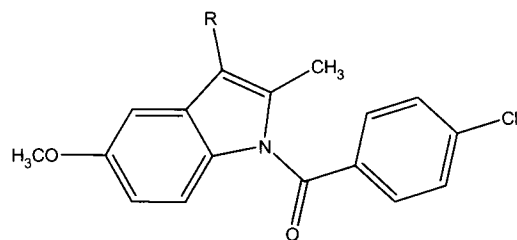


- 7.21. The reaction of ketones with acetic anhydride in the presence of BF_3 provides a convenient synthesis of β -diketones. For example, reaction of acetone with AcOAc produces acetylacetone. Two different β -diketones may be formed from unsymmetrical ketones. With a series of methyl ketones having the general structure $\text{CH}_3\text{COCH}_2\text{R}$, the yield of the two possible products $\text{CH}_3\text{COC}(\text{COCH}_3)\text{HR}/\text{CH}_3\text{COCH}_2\text{COCH}_2\text{R}$ varied with R as follows: R = methyl (100%/0%); R = ethyl (90%/10%); R = isopropyl (45%/55%). Propose a mechanism for the general reaction, and account for the distribution of products in each of these cases.
- 7.22. In contrast to the case with base-promoted hydrolysis of epoxides in ^{18}O -labeled water (Problem 6.3 in Chapter 6), the corresponding hydrolysis of unsymmetrical alkene oxides under acid-catalyzed conditions leads to product mixtures in which the majority of the labeled oxygen is on the carbon atom with the greater number of alkyl groups. For example, products from hydrolysis of propylene oxide and isobutylene oxide are shown in equations 7.78 and 7.79 ($\text{O}^* = ^{18}\text{O}$).



Isobutylene oxide reacts 100 times faster than does propylene oxide under the same conditions. In both cases the log of the rate constant is linear with $-H_0$. Propose an explanation for these results.

- 7.23. Propose an explanation for the fact that the enol of 2-oxocyclobutanecarboxylate ion is 10^4 times more acidic than the enol of the 2-oxocyclopentanecarboxylate ion.
- 7.24. Consult the literature to find ΔH_{acid} and ΔG_{acid} values for the methyl group of propene, 1-butene, and methylcyclopropane. Rationalize the results.
- 7.25. Propose both an A1 mechanism and an A2 mechanism for the hydrolysis of the amide group in compound 22.



R = substituent group terminating in CO_2H .

- 7.26. The gas phase basicities of a series of ring-substituted styrene derivatives are shown in Table 7.11. Predict the gas phase basicity of styrene itself.

TABLE 7.11

Ring Substituent	GB (kcal/mol)
<i>p</i> -OCH ₃	207.4
<i>p</i> -CH ₃	199.8
<i>m</i> -Br	190.7
<i>m</i> -CF ₃	187.6

- 7.27. Pseudo-first-order rate constants for the HCl-catalyzed hydrolysis of dimethoxymethane are shown in Table 7.12. Do the data correlate better with $[H^+]$ or with H_0 ? What do the results suggest about the mechanism of the reaction?

TABLE 7.12

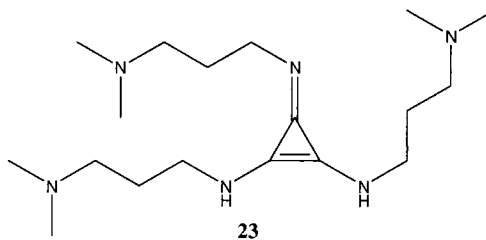
[HCl] (M)	k_h (min ⁻¹)	$-H_0$
0.371	7.66×10^{-3}	-0.43
0.495	1.08×10^{-3}	-0.31
1.303	4.96×10^{-3}	0.24
2.606	2.02×10^{-2}	0.74
3.909	1.40×10^{-1}	1.30

- 7.28. Propose an explanation for the differences in gas phase acidities (ΔG°) reported for the cyclohexanediols listed in Table 7.13.

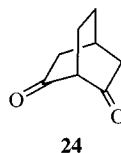
TABLE 7.13

Compound	ΔG° (kcal/mol)
<i>trans</i> -1,3-Cyclohexanediol	363.2
<i>cis</i> -1,3-Cyclohexanediol	352.3
<i>trans</i> -1,4-Cyclohexanediol	363.7
<i>cis</i> -1,4-Cyclohexanediol	356.1

- 7.29. Compound **23** has been termed a "superbase." What accounts for its unusually high basicity?



- 7.30. β -Diketones are usually much more acidic than other diketones. Structure **24** is much less acidic than acyclic analogs, however. Rationalize this acidity difference.



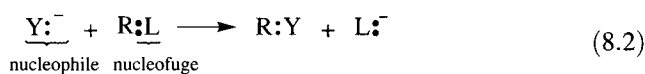
Substitution Reactions

8.1 INTRODUCTION

In a substitution reaction, an atom or group of atoms (Y) replaces another atom or group of atoms (L) in some molecular entity (RL). In shorthand notation,

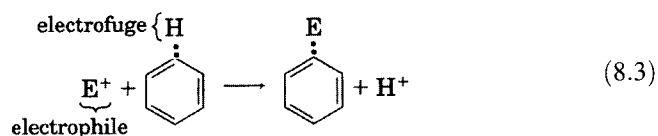


Replacement of one functional group by another may occur either with or without accompanying change in the molecular framework, so R' need not be identical to R. The general substitution reaction shown in equation 8.1 does not indicate the source of the electrons that are used to make the R'-Y bond. In nucleophilic substitution, those electrons originate with Y, which is a **nucleophile** (from the Greek, *philein*, "to love").¹ In electrophilic substitution, an **electrophile** forms a Y-R bond by using both of the electrons in the R-L bond. Leaving groups also are categorized according to the fate of the electrons that bond the leaving group to the molecule. If these electrons depart with the leaving group (as is typically the case in a nucleophilic substitution), then the leaving group is a **nucleofuge** (equation 8.2). If these electrons do *not* depart with the leaving group (as is typically the case in an electrophilic substitution), then that group is an **electrofuge** (equation 8.3).² In both equations, the pair of electrons that originally comprises the R-L bond is shown as a bold pair of dots.

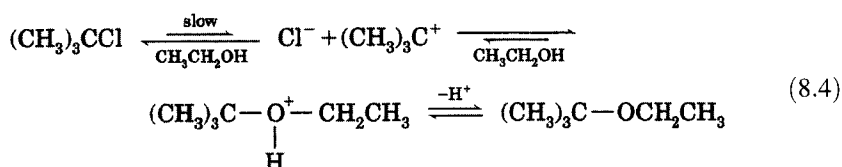


¹ Commission on Physical Organic Chemistry, IUPAC. *Pure Appl. Chem.* **1994**, 66, 1077.

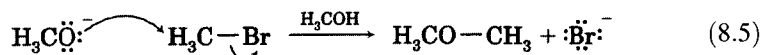
² These terms are derived from the Latin *fugere* ("to flee"). Compare Nickon, A.; Silversmith, E. F. *Organic Chemistry: The Name Game*; Pergamon Press, New York: 1987; p. 258-259.



It is convenient to categorize reactions with concise descriptive labels. For substitution reactions we often use the notation S_xM , in which the letter S indicates a substitution reaction. The subscript x indicates something of the mechanism, such as N for nucleophilic or E for electrophilic. M usually indicates the molecularity of the reaction, the nature of the reacting species, or additional information.³⁻⁵ The most familiar terms for substitution reactions are S_N1 (for substitution nucleophilic unimolecular⁶), as shown in equation 8.4,



and S_N2 (for substitution nucleophilic bimolecular), as illustrated in equation 8.5,



These terms were suggested by Ingold and are familiar to all organic chemists.

Typically, the kinetics of simple aliphatic substitutions are overall second order for S_N2 reactions and overall first order for S_N1 reactions. That is, an S_N2 reaction between Y^- and $R-L$ leads to the rate equation

$$\text{Rate} = -\frac{d[\text{R-L}]}{dt} = k_2[\text{R-L}][\text{Y}^-] \quad (8.6)$$

We expect the kinetic expression for an S_N1 reaction to be

$$\text{Rate} = -\frac{d[\text{R-L}]}{dt} = k_1[\text{R-L}] \quad (8.7)$$

³ Ingold, C. K.; Rothstein, E. *J. Chem. Soc.* **1928**, 1217.

⁴ Ingold, C. K. *Structure and Mechanism in Organic Chemistry*, 2nd ed.; Cornell University Press: Ithaca, NY, 1969; p. 427.

⁵ For a listing of the Ingold terminology for other kinds of substitution reactions not considered here, see Orchin, M.; Kaplan, F.; Macomber, R. S.; Wilson, R. M.; Zimmer, H. *The Vocabulary of Organic Chemistry*; Wiley-Interscience: New York, 1980.

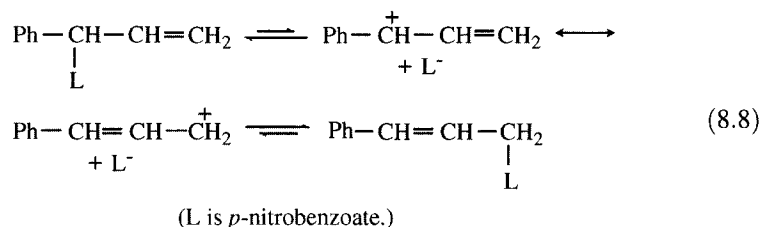
⁶ The term *unimolecular* does not mean that no other molecules are involved in the rate-limiting step, since the reaction is not observed in the absence of solvent. Therefore, the designation *polymolecular* was used by Steigman, J.; Hammett, L. P. *J. Am. Chem. Soc.* **1937**, 59, 2536, and the term *termolecular* (based on a specific model of solvent interaction) was suggested by Swain, G. C. *J. Am. Chem. Soc.* **1948**, 70, 1119.

It is important to note that the terms S_N1 and S_N2 do not merely identify the kinetic results observed in studies of nucleophilic substitution. Rather, these terms are intended to characterize the mechanisms of those reactions. It is sometimes thought that the 1 and 2 refer to kinetics, but Ingold wrote that "the numerical indication in the symbolic label, no less than in the verbal name, refers to the *molecularity* of the reaction, and not to its kinetic order."⁴ To put it another way, those terms designate *nonobservable* mechanistic and not *observable* kinetic properties.

Although the Ingold mechanistic labels for substitution reactions are very familiar, some chemists proposed terminology to denote the details of mechanisms more explicitly. A formalism suggested by the IUPAC Commission on Physical Organic Chemistry designates the steps of a substitution as A (attachment) and D (detachment).⁷ A suffix N indicates a nucleophilic attachment (A_N) or a nucleofugic detachment (D_N). Similarly, a suffix E denotes an electrophilic or electrofugal process. The placement of the terms A_N and D_N with other symbols can be used to convey the mechanism of the reaction. For example, they

1. May be combined without an intervening symbol to indicate that they occur at the same time.
2. May be combined with a "+" symbol to indicate that they occur with enough time between them that any intermediates have time to equilibrate with solvent and other ions in solution.
3. May be combined with a "*" to indicate that the two steps occur so quickly that equilibrium with outside species is not attained.

With this terminology we may not only describe a fully concerted, one-step S_N2 reaction ($A_N D_N$), and a stepwise S_N1 reaction involving intermediate ions that diffuse apart ($D_N + A_N$), but we may also concisely represent a stepwise reaction involving a transient ion pair ($D_N^* A_N$).^{8,9} The IUPAC nomenclature system can also be used to describe other substitution reactions. Among them are the S_N1' (substitution nucleophilic unimolecular with rearrangement) reaction, equation 1.8, which is denoted by IUPAC as an ($1/D_N + 3/A_N$) reaction. The numbers before the slash symbols indicate atoms involved in the dissociation and association steps. Thus, $1/D_N$ means that the nucleofuge dissociates from one atom (1), while the $3/A_N$ term means that the nucleophile associates at an allylic position (3).

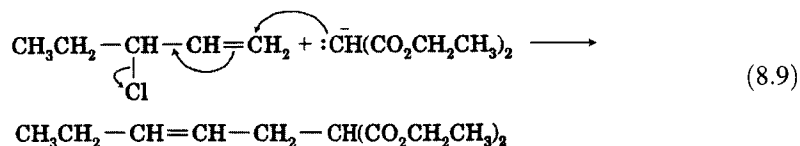


⁷ Commission on Physical Organic Chemistry, IUPAC. *Pure Appl. Chem.* **1989**, *61*, 23; see also Guthrie, R. D.; Jencks, W. P. *Acc. Chem. Res.* **1989**, *22*, 343.

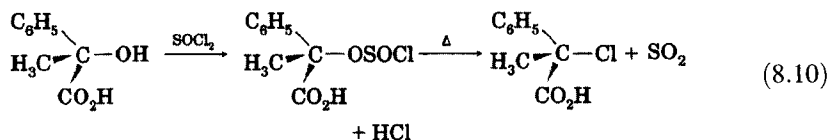
⁸ See the discussion of the roles of ion pairs in nucleophilic substitution reactions beginning on page 480.

⁹ Catchpole, A. G.; Hughes, E. D. *J. Chem. Soc.* **1948**, 1.

Similarly, the S_N2' (substitution nucleophilic bimolecular with rearrangement) reaction, equation 8.9,¹⁰ is described as a (3/1/ $A_N D_N$) process.



The S_{Ni} (substitution nucleophilic internal) reaction, equation 8.10,¹¹ is denoted a ($D_N + D + A_N$) reaction, where D without a subscript refers to a unimolecular dissociation. This system for labeling reaction mechanisms did not meet with wide acceptance, however, and most of the chemical literature still utilizes the Ingold system to describe substitution reactions.¹²



As the discussion above suggests, substitution reactions are much more complicated than the S_N1/S_N2 picture suggests. In the sections that follow, we will explore the explicit and implicit models we use to describe substitution reactions.

8.2 NUCLEOPHILIC ALIPHATIC SUBSTITUTION

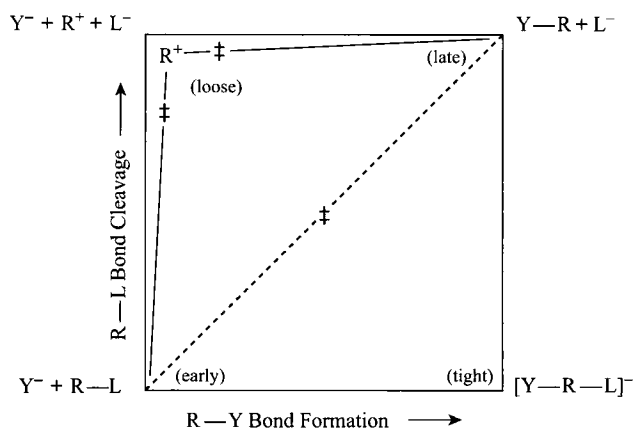
Introduction

Nucleophilic substitution is often one of the first examples of chemical reactivity in introductory organic chemistry because classification of substitution reactions either as S_N1 or as S_N2 serves to illustrate the application of chemical kinetics, stereochemical labeling, solvent effects, and structural effects in studying organic reactions. The S_N1 and S_N2 models are familiar to all organic chemists, but such models are two-edged swords. They enable us to assimilate a large volume of diverse material into one conceptual framework, but at the same time they can restrict our ability to envision new mechanistic possibilities. Consider the More O'Ferrall-Jencks diagram for a nucleophilic substitution (Figure 8.1). The dashed diagonal line with one transition state represents the concerted, synchronous S_N2 pathway, while the solid line with two transition states represents the S_N1 pathway. Now we see that these two reactions describe only two of an infinite number of possible reaction paths on the potential energy surface leading from reactants to

¹⁰ Kepner, R. E.; Winstein, S.; Young, W. G. *J. Am. Chem. Soc.* **1949**, *71*, 115; DeWolfe, R. H.; Young, W. G. *Chem. Rev.* **1956**, *56*, 753. For a review of the intramolecular S_N' reaction, see Paquette, L. A.; Stirling, C. J. M. *Tetrahedron* **1992**, *48*, 7383; for a review of the intermolecular S_N2' reaction, see Magid, R. M. *Tetrahedron* **1980**, *36*, 1901.

¹¹ McKenzie, A.; Clough, G. W. *J. Chem. Soc.* **1910**, 97, 2564.

¹² Olah, G. A. *Acc. Chem. Res.* **1990**, *23*, 31. See also Jencks, W. P. *Acc. Chem. Res.* **1990**, *23*, 32; Guthrie, R. D. *Acc. Chem. Res.* **1990**, *23*, 33.

**FIGURE 8.1**

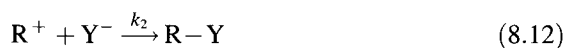
S_N1 (solid line) and S_N2 (dashed line) pathways for a substitution reaction.

products.¹³ The familiar S_N1 and S_N2 landmarks of nucleophilic aliphatic substitution reactions are therefore only convenient reference points for discussions of the mechanisms of nucleophilic aliphatic substitution reactions.

The S_N1 Reaction

Kinetics

In the usual mechanism for the S_N1 reaction (equations 8.11 and 8.12), the rate-limiting step is the dissociation of the substrate to form a carbocation and an anion.¹⁴ Therefore, we commonly write that the rate of the reaction is effectively the rate of the unimolecular first step, as shown in equation 8.13. Clearly, equation 8.13 cannot be exact, however, because there must be some Y^- in the solution or the substitution step (equation 8.12) cannot occur.



$$\text{Rate} = k_1[\text{R-L}] \quad (8.13)$$

A more exact kinetic expression results from applying the steady-state approximation to $[\text{R}^+]$, which produces equation 8.16.

$$\frac{d[\text{R}^+]}{dt} \equiv 0 = k_1[\text{R-L}] - k_{-1}[\text{R}^+][\text{L}^-] - k_2[\text{R}^+][\text{Y}^-] \quad (8.14)$$

¹³ For a review of the mechanisms of nucleophilic aliphatic substitution, see Katritzky, A. R.; Brycki, B. E. *Chem. Soc. Rev.* **1990**, 19, 83.

¹⁴ The carbocation intermediate has been observed spectroscopically in some systems: Mayr, H.; Minegishi, S. *Angew. Chem. Int. Ed.* **2002**, 41, 4493; Schaller, H. F.; Tishkov, A. A.; Feng, X.; Mayr, H. *J. Am. Chem. Soc.* **2008**, 130, 3012. For an example of "carbocation watching" in solvolysis, see Schaller, H. F.; Mayr, H. *Angew. Chem. Int. Ed.* **2008**, 47, 3958.

and

$$[\text{R}^+] = \frac{k_1[\text{R-L}]}{k_{-1}[\text{L}^-] + k_2[\text{Y}^-]} \quad (8.15)$$

so

$$\text{Rate} = \frac{k_1[\text{R-L}]k_2[\text{Y}^-]}{k_{-1}[\text{L}^-] + k_2[\text{Y}^-]} \quad (8.16)$$

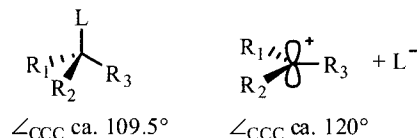
In early phases of the reaction, $[\text{L}^-]$ is close to zero, so the term $k_{-1}[\text{L}^-]$ is also about zero. Making the assumption that $k_{-1}[\text{L}^-] + k_2[\text{Y}^-] \approx k_2[\text{Y}^-]$ allows us to cancel the $k_2[\text{Y}^-]$ terms in the numerator and denominator of equation 8.16, which leads to the *approximate* expression of equation 8.13. As the reaction proceeds, $[\text{L}^-]$ increases and the apparent rate of the reaction may decrease if $k_{-1}[\text{L}^-]$ becomes significant relative to $k_2[\text{Y}^-]$. Adding L^- to the solution would also decrease the rate of formation of R-Y , a phenomenon known as the **common ion effect** or **mass law effect**.¹⁵ In **solvolysis reactions**, in which the solvent is the nucleophile, the concentration of the nucleophile is effectively constant and cannot be varied. The reaction is therefore more properly described as **pseudo-first order**, since only the concentration of the substrate can be varied.

Structural Effects in $\text{S}_{\text{N}}1$ Reactions

The central role of carbocations in the $\text{S}_{\text{N}}1$ reaction is supported by the finding that the reactivity of R-L compounds follows the order of carbocation stability. That is, solvolysis rate constants decrease as the stability of the carbocation decreases, from 3° to 2° to 1° to methyl, with 1° and methyl systems being essentially unreactive by the $\text{S}_{\text{N}}1$ pathway. This correlation seems reasonable in view of the Hammond postulate. Because ionization is highly endothermic, the transition structure should resemble the carbocation being formed. Indeed, calculations have suggested that the charge separation in the transition structure for *t*-butyl chloride solvolysis is about 80% of full ionization.¹⁶

Steric effects can play a role in $\text{S}_{\text{N}}1$ reactivity. In Figure 8.2, the reactant carbon atom bearing the leaving group has bond angles that ordinarily are close to 109.5° . The preferred geometry of the carbocation intermediate is trigonal planar with bond angles of 120° . Thus, three alkyl groups attached to

FIGURE 8.2
Steric relief accompanying ionization.



¹⁵ Addition of other ionic species could increase the rate by changing the effective polarity of the microenvironment through a salt effect, and some salts exhibit a special salt effect. See the discussion on page 483.

¹⁶ Abraham, M. H.; Abraham, R. J. *J. Chem. Soc. Perkin Trans. 2* **1974**, 47; Clarke, G. A.; Taft, R. W. J. *Am. Chem. Soc.* **1962**, 84, 2295.

TABLE 8.1 Rate Constants for the Hydrolysis of 3° Halides, $R(\text{CH}_3)_2\text{CCl}$, in 80% Aqueous Ethanol at 25°C

R	k_1 (h^{-1})	k_1 (rel)
Me	0.033	1.00
Et	0.055	1.67
Pr	0.052	1.58
Isopropyl	0.029	0.88
Bu	0.047	1.42
<i>t</i> -Bu	0.040	1.21
Neopentyl	0.74	22.4

Source: Reference 18.

the reaction site are sterically more crowded in the reactant than they are in the intermediate, and steric relief can accelerate the rate of the ionization step. Such a trend is observed in the rate constants for hydrolysis of the 3° alkyl halides shown in Table 8.1.^{17,18}

With some structures, the geometry imposed by a molecular skeleton leads to greater steric strain in the carbocation than in the reactant. This effect is particularly notable in 1-substituted bridgehead systems in which the molecular framework forces the carbocation to be nonplanar.¹⁹ In **1**, for example, the carbocation is decidedly nonplanar, with C–C–C bond angles at the carbocation center calculated to be 110°. The strain associated with formation of this carbocation means that 4-tricyclyl derivatives are very resistant to solvolysis.²⁰ The relative reactivities of several structures substituted at the bridgehead position (Figure 8.3) confirm that solvolytic reactivity decreases as the size of the bridges decreases.²¹



Substituents that can stabilize a carbocation by resonance can increase the rate constants for S_N1 reactions dramatically. For example, benzyl (**2**), benzhydryl (**3**), and trityl (**4**) cations (Figure 8.4) are stabilized by the aromatic rings, with a resulting dramatic increase in the reactivity of the corresponding chlorides in solvolysis reactions (Table 8.2).²¹

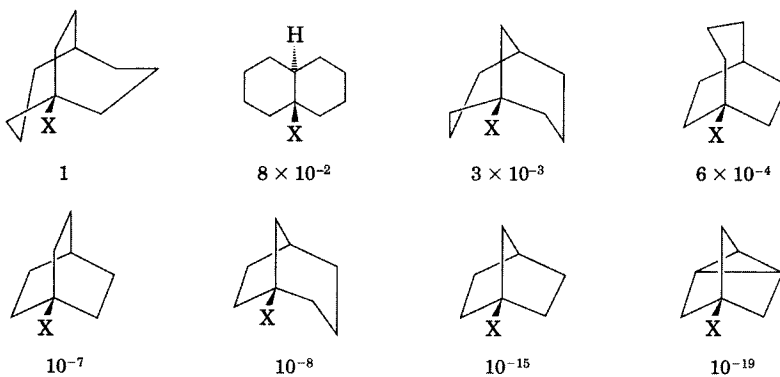
¹⁷ Brown, H. C.; Fletcher, R. S. *J. Am. Chem. Soc.* **1949**, *71*, 1845.

¹⁸ Brown, H. C.; Fletcher, R. S.; Johannesen, R. B. *J. Am. Chem. Soc.* **1951**, *73*, 212.

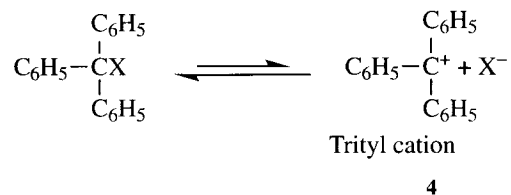
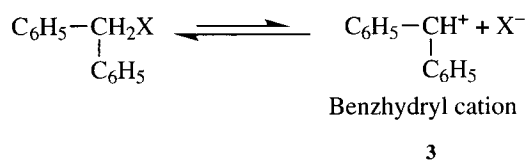
¹⁹ For a discussion of the reactivity of bridgehead systems in solvolysis reactions, see Bingham, R. C.; Schleyer, P. v. R. *J. Am. Chem. Soc.* **1971**, *93*, 3189.

²⁰ Sherrod, S. A.; Bergman, R. G.; Gleicher, G. J.; Morris, D. G. *J. Am. Chem. Soc.* **1972**, *94*, 4615.

²¹ Nixon, A. C.; Branch, G. E. *J. Am. Chem. Soc.* **1936**, *58*, 492.

**FIGURE 8.3**

Approximate relative reactivities in solvolysis reactions.¹⁹

**FIGURE 8.4**

Ionization of benzyl, benzhydryl, and trityl systems.

TABLE 8.2 Relative Reactivities of Aryl Halides in $\text{S}_{\text{N}}1$ Reactions^a

Alkyl Halide	Reactivity
$\text{C}_6\text{H}_5\text{CH}_2\text{-Cl}$	1
$(\text{C}_6\text{H}_5)_2\text{CH-Cl}$	1.75×10^3
$(\text{C}_6\text{H}_5)_3\text{C-Cl}$	2.5×10^7

^a Data for ethanolysis in 60% diethyl ether, 40% ethanol.

Source: Reference 21.

Solvent Polarity and Nucleophilicity

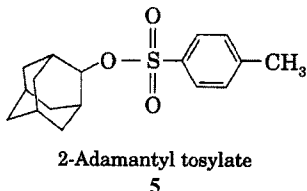
Because the S_N1 reaction involves dissociation of a neutral species to two oppositely charged ions, greater solvent polarity accelerates the rate of reaction.²² In general, however, solvolysis rate constants do not correlate well with solvent dipole moment (μ) or dielectric constant (ϵ).²³ Other solvent polarity parameters have been developed, including the Z and E_T scales discussed in Chapter 6, but solvent molecules do more than simply provide a benign polar medium for ion stabilization. Solvent molecules with electrophilic properties may enhance reactivity by assisting in the solvation of the departing nucleofuge. In addition, solvent molecules that can act as nucleophiles can compete with other species for product formation or can assist in the ionization process so that another nucleophile can react to produce a substitution product.

One of the earliest attempts to describe solvent behavior in solvolysis reactions quantitatively was the Grunwald–Winstein equation, which is a linear free energy relationship analogous to the Hammett equation.²⁴

$$\log \frac{k}{k_0} = mY \quad (8.17)$$

Here, k is the rate constant for reaction of a compound in a particular solvent and k_0 is the rate constant of the compound in the reference solvent system. Y is the ionizing power of a solvent, and m is the sensitivity of the substrate to solvent ionizing power. Defining m to be 1.00 for the reaction of *t*-butyl chloride in methanol, the value of Y for another solvent is then calculated from equation 8.18.

$$Y = \log \frac{k_{t\text{-BuCl, solvent}}}{k_{t\text{-BuCl, methanol}}} \quad (8.18)$$



A two-parameter scale of solvent ionizing power is the Y_{OTs} scale introduced by Schleyer and co-workers.²⁵ This system is based on the solvolysis of 2-adamantyl tosylate (5). The free energy relationship is

$$\log \frac{k}{k_0} = lN + mY \quad (8.19)$$

²² For a theoretical study of the effect of solvent polarity on the transition structures for S_N1 reactions, see Mathis, J. R.; Kim, H. J.; Hynes, J. T. *J. Am. Chem. Soc.* **1993**, *115*, 8248.

²³ Fainberg, A. H.; Winstein, S. *J. Am. Chem. Soc.* **1956**, *78*, 2770.

²⁴ Grunwald, E.; Winstein, S. *J. Am. Chem. Soc.* **1948**, *70*, 846; Winstein, S.; Grunwald, E.; Jones, H. W. *J. Am. Chem. Soc.* **1951**, *73*, 2700.

²⁵ Schadt, F. L.; Bentley, T. W.; Schleyer, P. v. R. *J. Am. Chem. Soc.* **1976**, *98*, 7667.

TABLE 8.3 Values of Y , Y_{OTs} , and N_{OTs} for Selected Solvents ^a

Solvent	Y	Y_{OTs}	N_{OTs}
80% Aqueous ethanol	0.0	0.00	0.00
Ethanol	-2.0	-1.96	0.06
50% Ethanol	1.7	1.29	-0.09
Methanol	-1.1	-0.92	-0.04
95% Acetone	-2.8	-2.95	
50% Acetone	1.4	1.26	-0.39
Acetonitrile		-3.21	
50% Acetonitrile		1.2	
30% Acetonitrile		1.9	
10% Acetonitrile		3.6	
Water	3.5	4.1	-0.44
2-Propanol	-2.7	-2.83	0.12
2-Methyl-2-propanol	-3.3	-3.74	
Acetic acid	-1.6	-0.9	-2.28
Trifluoroacetic acid		4.57	-5.56
60% (w/w) Sulfuric acid in water		5.29	-2.02
<i>N,N</i> -Dimethylformamide		-4.14	
<i>N,N</i> -Dimethylacetamide		-4.99	

^a Values of Y are from reference 23. Values of Y_{OTs} and N_{OTs} are from reference 28.

where k is the rate constant for reaction in a given solvent, k_0 is the rate constant for reaction in the reference solvent (80% aqueous ethanol), Y is the solvent ionizing power, and m is the sensitivity of the substrate to solvent ionizing power. Some substrates show evidence of nucleophilic solvent participation in solvolysis, so N is the solvent nucleophilicity and l is the sensitivity of the substrate to solvent nucleophilicity.^{26,27} N_{OTs} values are determined from studies of the solvolysis of methyl tosylate according to equation 8.20:

$$N_{OTs} = \log \left(\frac{k}{k_0} \right)_{CH_3OTs} - 0.3Y_{OTs} \quad (8.20)$$

Values of Y_{OTs} and N_{OTs} for selected solvents are shown in Table 8.3. Many other Y scales have been developed for particular reaction systems.²⁸ As noted in Chapter 6, however, writing a linear free energy relationship implies the modeling of one reaction on another. The ability of the linear free energy equation to correlate experimental data thus depends to some extent on the degree to which the model reaction is appropriately chosen.

²⁶ For a discussion, see references 25 and 28.

²⁷ Abraham and co-workers concluded that at least four solvent parameters are necessary to adequately correlate solvolysis of *t*-butyl chloride with solvent properties in the most general case. These four properties are solvent dipolarity, solvent hydrogen bond acidity, solvent hydrogen bond basicity, and the cohesive energy density of the solvent. They note, however, that a smaller number of parameters may be adequate for studies in which solvent properties vary in more restricted ways. Abraham, M. C.; Doherty, R. M.; Kamlet, M. J.; Harris, J. M.; Taft, R. W. J. *Chem. Soc. Perkin Trans. 2* **1987**, 913, 1097.

²⁸ For a discussion of Y_X scales of solvent ionizing power, see Bentley, T. W.; Llewellyn, G. *Prog. Phys. Org. Chem.* **1990**, 17, 121.

If the reaction mixture for an S_N1 reaction includes added nucleophiles, particularly anions, then not only the rate but also the product of the reaction can be affected. For example, adding 0.05 M sodium azide to a solution of 4,4'-dimethylbenzhydryl chloride in 85% aqueous acetone was seen to increase the observed rate constants for the solvolysis reaction by 50%, and the product was found to consist of 66% of 4,4'-dimethylbenzhydryl azide and 34% of the alcohol.^{29,30} This increase in reactivity is explained on the basis of a **normal salt effect**, meaning that the increased ionic strength of the reaction medium increases the effective "polarity" of the reaction medium. Various theoretical and empirical treatments suggest that the rate constant should increase with the log of the concentration of added salt,³¹ with the first power of concentration of added salt,³¹ or with the square root of the concentration of added salt,³² depending on the reactants and solvents.

The product distribution resulting from the addition of nucleophiles to a solvolysis reaction depends on the relative abilities of the added nucleophile and the solvent to compete for attachment to the carbocation intermediate. The relative reactivity of nucleophiles toward carbocations often does not vary dramatically with the structure of the carbocation alone, however. Rather, the distribution of products of nucleophilic attachment to a cation depends on the structures of both the nucleophile and the solvent in which the reaction occurs. Ritchie determined that many cation–nucleophile reactions could be described by the equation

$$\log(k/k_{\text{H}_2\text{O}}) = N_+ \quad (8.21)$$

where k is the rate constant for the reaction of a nucleophile with a given carbocation, $k_{\text{H}_2\text{O}}$ is the rate constant for reaction of water as a nucleophile under the same conditions, and N_+ is a nucleophilicity parameter for the nucleophile–solvent system.³³ Selected values of N_+ are shown in Table 8.4. The trends in N_+ values, in particular, the observation that higher N_+ values are observed for systems in which the nucleophiles are not strongly solvated, suggest that nucleophilic reactivity is a function of a *system* consisting of both a nucleophile and the solvent.³⁶ Failure to observe a dependence of relative nucleophilicity on the structure of the cation in equation 8.21 suggests that the transition structures strongly resemble the carbocations; that is, there is negligible bond formation, and there has been little disturbance of the cation or its solvation shell in the transition state.³⁴

²⁹ Bateman, L. C.; Church, M. G.; Hughes, E. D.; Ingold, C. K.; Taher, N. A. *J. Chem. Soc.* **1940**, 979.

³⁰ Huisgen, R. *Angew. Chem. Int. Ed. Engl.* **1970**, *9*, 751.

³¹ Fainberg, A. H.; Winstein, S. *J. Am. Chem. Soc.* **1956**, *78*, 2763.

³² Winstein, S.; Klinedinst, P. E. Jr.; Robinson, G. C. *J. Am. Chem. Soc.* **1961**, *83*, 885.

³³ Ritchie, C. D. *Acc. Chem. Res.* **1972**, *5*, 348 and references therein.

³⁴ As the carbocation becomes more stable, the transition structure would be expected to become somewhat more product-like (Chapter 6), and some selectivity of the cation for the more nucleophilic species might be expected. For a discussion, see (a) Sneen, R. A.; Carter, J. V.; Kay, P. S. *J. Am. Chem. Soc.* **1966**, *88*, 2594; (b) Raber, D. J.; Harris, J. M.; Hall, R. E.; Schleyer, P. v. R. *J. Am. Chem. Soc.* **1971**, *93*, 4821. Ritchie (reference 33) discussed the possible origins of such correlations. Shaik, S. S. *J. Org. Chem.* **1987**, *52*, 1563 found that nucleophilicities toward one cation in water correlated with the vertical ionization potential of the nucleophile. A discussion of the barrier for carbocation–nucleophile combinations was given by Richard, J. P. *Tetrahedron* **1995**, *51*, 1535.

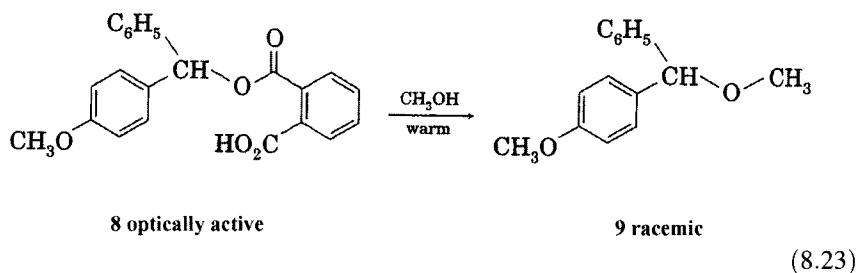
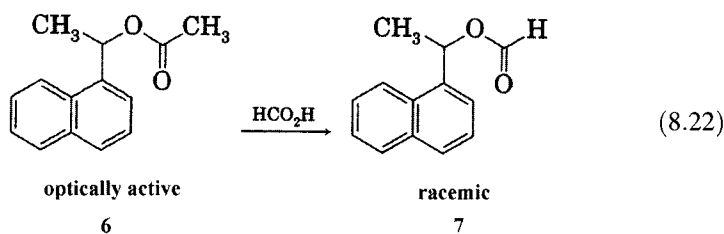
TABLE 8.4 N_+ Values for Nucleophile and Solvent Systems at 25°C

Nucleophile (solvent)	N_+	Nucleophile (solvent)	N_+
H ₂ O (H ₂ O)	0.0	CH ₃ O ⁻ (CH ₃ OH)	7.5
CH ₃ OH (CH ₃ OH)	0.5	N ₃ ⁻ (CH ₃ OH)	8.5
CN ⁻ (H ₂ O)	3.8	CN ⁻ (CH ₃ SOCH ₃)	8.6
C ₆ H ₅ SO ₂ ⁻ (CH ₃ OH)	3.8	CN ⁻ (HCON(CH ₃) ₂)	9.4
HO ⁻ (H ₂ O)	4.5	N ₃ ⁻ (CH ₃ SOCH ₃)	10.7
N ₃ ⁻ (H ₂ O)	5.4	C ₆ H ₅ S ⁻ (CH ₃ OH)	10.7
CN ⁻ (CH ₃ OH)	5.9	C ₆ H ₅ S ⁻ (CH ₃ SOCH ₃)	13.1

Source: Reference 33.

Solvated Ions and Ion Pairs

Discussion of reactivity in the S_N1 reaction often emphasizes the structure of the carbocation, but the roles of the solvent and the nucleofuge are also significant. The simplest model of the S_N1 reaction at a single stereogenic center predicts racemization of an optically active starting material because the nucleophile is able to add equally well to the top lobe of an empty *p* orbital. For example, **formolysis** (solvolysis in formic acid) of optically active 1-(α -naphthyl)ethyl acetate (**6**) gave the racemic formate (**7**).³⁵ Similarly, **methanolysis** of (-)-*p*-methoxybenzhydryl hydrogen phthalate (**8**) produced the totally racemic ether (**9**).³⁶



In a number of cases, solvolysis reactions of chiral substrates show some degree of inversion of configuration. For example, Steigman and Hammett

³⁵ Balfe, M. P.; Downer, E. A. W.; Evans, A. A.; Kenyon, J.; Poplett, R.; Searle, C. E.; Tárnoky, A. L. J. *Chem. Soc.* **1946**, 797.

³⁶ Balfe, M. P.; Doughty, M. A.; Kenyon, J.; Poplett, R. J. *Chem. Soc.* **1942**, 605.

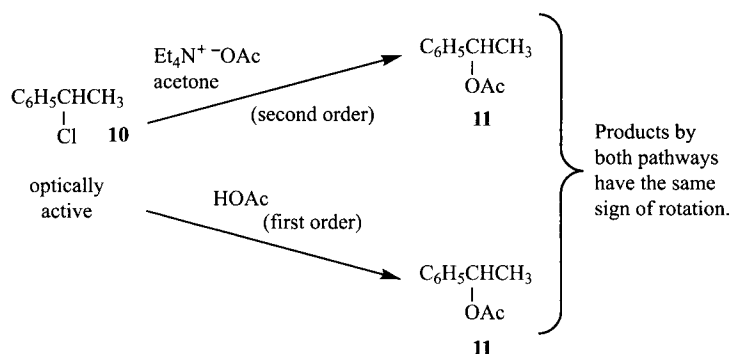


FIGURE 8.5
Acetolysis of α -phenylethyl chloride.

found that **acetolysis** (solvolysis in acetic acid) of α -phenylethyl chloride (10) gave the corresponding acetate (11) by a strictly first-order process (Figure 8.5). That is, the rate was not affected by added acetate ion.^{37,38} The product 11 could also be formed by a second-order reaction between 10 and tetraethylammonium acetate in acetone. The product formed by both pathways had the same *sign* of rotation of polarized light, although the product obtained through solvolysis had a much smaller rotation. One possible explanation for such behavior is that the reaction takes place by a mixture of $\text{S}_{\text{N}}1$ and $\text{S}_{\text{N}}2$ pathways. If the enantiomeric purity of the product(s) is not affected by changes in concentration of nucleophile (meaning that the kinetics are strictly first order), however, then competing $\text{S}_{\text{N}}1$ and $\text{S}_{\text{N}}2$ pathways cannot be occurring. Therefore, any observed retention of configuration must be associated with a first-order process.

Numerous other cases of partial net inversion in first-order solvolysis reactions led to a variety of proposals for participation of solvent in these reactions. Doering and Zeiss found that methanolysis of the phthalate ester 12 gave 54% inversion and 46% racemization in the product (13, Figure 8.6).³⁹ They suggested that the intermediate in solvolyses should not be considered a

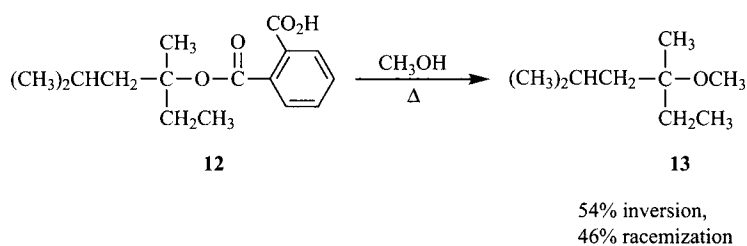


FIGURE 8.6
Methanolysis of an optically active phthalate.

³⁷ Determination of first-order kinetics is complicated by the need to keep the ionic strength of the medium constant during the reaction.

³⁸ Steigman, J.; Hammett, L. P. *J. Am. Chem. Soc.* **1937**, *59*, 2536. This paper marks an early use of the word *solvolysis*.

³⁹ Doering, W. v. E.; Zeiss, H. H. *J. Am. Chem. Soc.* **1953**, *75*, 4733.

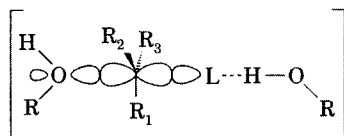


FIGURE 8.7

Doering-Zeiss intermediate.

free carbocation but, instead, a carbocation strongly coordinated by available electron pair donors (Figure 8.7).^{40,41} This intermediate (shown as I in Figure 8.8) could then undergo complete bond formation with solvent to form inverted product or could undergo exchange of the departing nucleofuge by another solvent molecule to produce intermediate II. Products resulting from II would be racemic, half showing retention of configuration and half showing inversion (Figure 8.8). The net result would be a slight excess of inversion.

Early evidence for ion pairing was reported by Winstein from the reaction of α,α -dimethylallyl chloride (**14**) in acetic acid with added acetate. Although the major product of the reaction was the expected acetate, there was rapid isomerization of **14** to the isomeric γ,γ -dimethylallyl chloride (**15**, equation 8.24). Formation of **15** can be explained by a mechanism in which the nucleofuge, Cl^- , competes as a nucleophile with solvent and rebonds to the allyl cation at the less hindered position. The rate of formation of **15** was found not to be a function of the concentration of added chloride ion, however. This finding is significant because the rate of the solvolysis should be decreased by addition of chloride ion if the mechanism involves dissociation of **14** to free ions (see equation 8.16). It appears, therefore, that the chloride ion in **15** must originate in the same molecule and not from the bulk medium. This process was characterized as **internal return** of a chloride ion held as part of intimate ion pair (**16**) within a solvent shell.⁴² Similar conclusions were obtained from

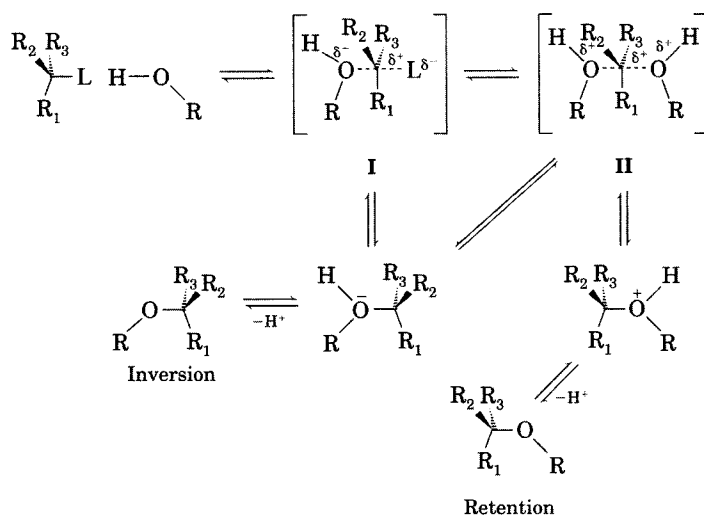


FIGURE 8.8

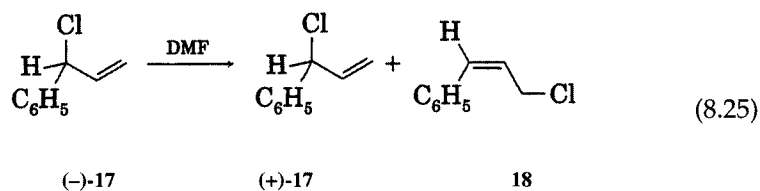
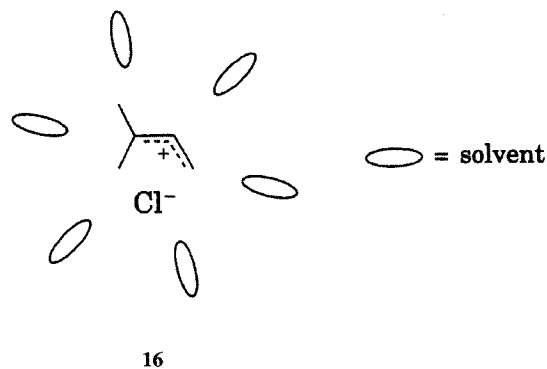
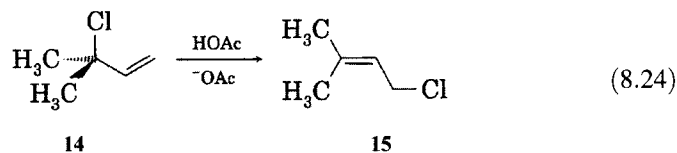
Doering-Zeiss mechanism.

⁴⁰ The term *encumbered* has been used to describe carbocations having strong interactions with Lewis base solvents. For a discussion, see Keating, J. T.; Skell, P. S. in Olah, G. A.; Schleyer, P. v. R., Eds. *Carbonium Ions. Volume II. Methods of Formation and Major Types*; Wiley-Interscience: New York, 1970; pp. 573-653 and references therein.

⁴¹ Streitwieser, A., Jr.; Schaeffer, W. D. *J. Am. Chem. Soc.* **1957**, *79*, 2888 found that solvolysis of 1-butyl-1-*d* *p*-nitrobenzenesulfonate in 75% dioxane-25% acetic acid occurred with 46% net inversion. Furthermore, no products indicating rearrangement of a 1° to a 2° carbocation were found.

⁴² Young, W. G.; Winstein, S.; Goering, H. L. *J. Am. Chem. Soc.* **1951**, *73*, 1958.

the study of other systems. For example, Weinstock found that optically active 3-chloro-3-phenylpropene (17, equation 8.25) underwent racemization 50% faster than it isomerized to cinnamyl chloride (18), which suggested a tight ion pair as an intermediate in the reaction.⁴³



Some systems show a distinctive kinetic behavior with added salt that is known as the **special salt effect**. Winstein and co-workers reported that adding lithium tosylate to reaction mixtures of alkyl tosylates in acetic acid produced only a small increase in rate, consistent with a small ionic strength effect. Adding lithium perchlorate, however, caused the observed initial rate constants to vary as shown in Figure 8.9.³⁴ The linear part of the curve, at higher salt concentrations, is a normal salt effect. The steeply rising initial portion of the curve for LiClO_4 is an indication of a special salt effect. Winstein explained the results in terms of two kinds of ion pairs—an intimate ion pair and a solvent-separated ion pair (Figure 8.10). For substrates that undergo internal return only from intimate ion pairs, only a normal salt effect is observed. For substrates in which the intimate ion pair separates further to external (solvent-separated) ion pairs, some added salts can trap the nucleofuge and interfere with its return to form the intimate ion pair, thus leading to faster solvolysis.^{44,45} The external ion pairs can also dissociate further to free

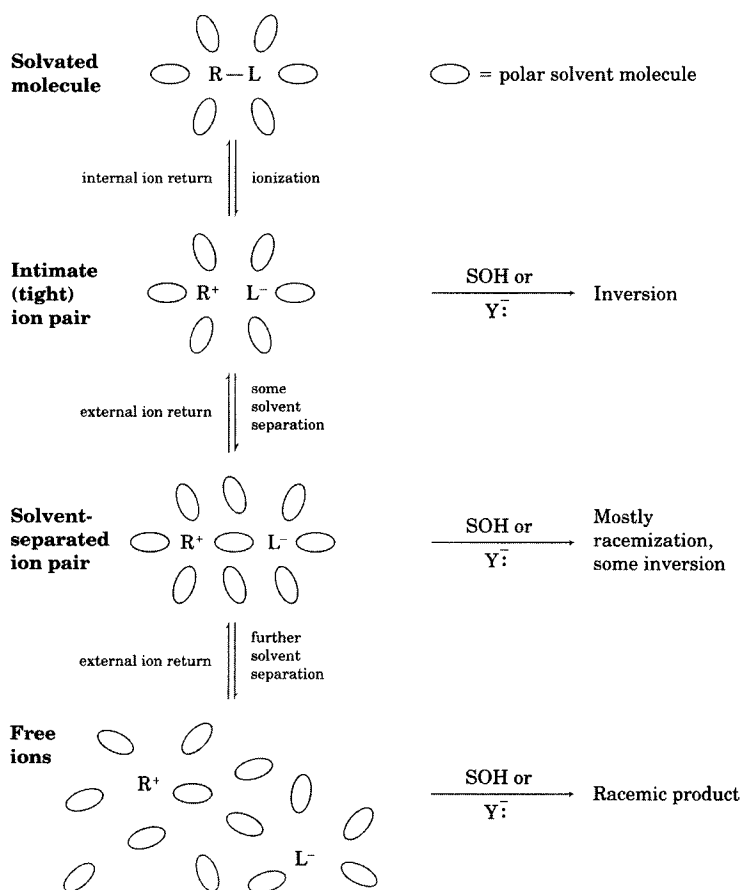
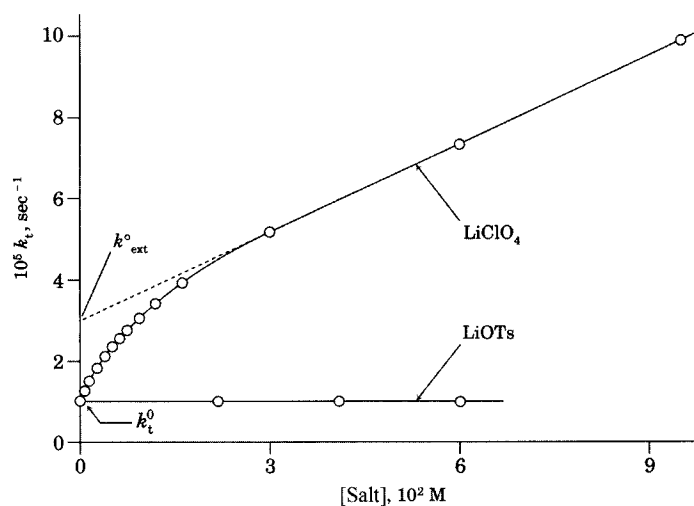
⁴³ Shandala, M. Y.; Waight, E. S.; Weinstock, M. J. *Chem. Soc. B* **1966**, 590.

⁴⁴ Winstein, S.; Clippinger, E.; Fainberg, A. H.; Robinson, G. C. *J. Am. Chem. Soc.* **1954**, *76*, 2597.

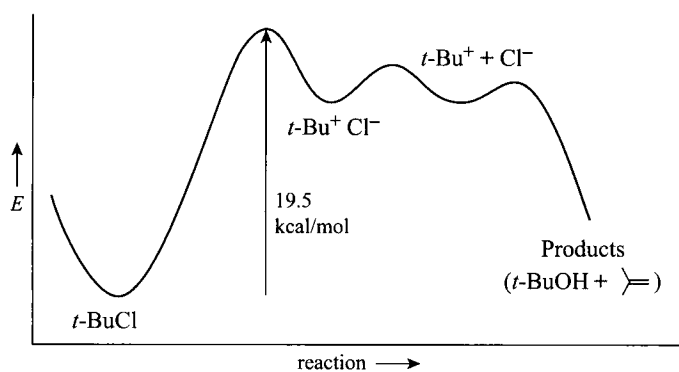
⁴⁵ Winstein, S.; Klinedinst, P. E., Jr.; Clippinger, E. *J. Am. Chem. Soc.* **1961**, *83*, 4986.

FIGURE 8.9

An example of the special salt effect in the solvolysis of an alkyl tosylate. (Adapted from reference 32.)

**FIGURE 8.10**

Species proposed as intermediates in solvolysis reactions.

**FIGURE 8.11**

Schematic diagram of a possible reaction profile for the solvolysis of *t*-butyl chloride in water. (Adapted from reference 47.)

ions. Depending on the relative stability of each species and the reactivity of each species with nucleophilic solvent, there may be varying amounts of racemization and inversion of chiral centers.⁴⁶

Theoretical calculations support the existence of discrete ion pair intermediates in solvolysis reactions. Figure 8.11 shows a reaction coordinate diagram, and Figure 8.12 shows calculated structures for the solvolysis of *t*-butyl chloride in water. The $(\text{CH}_3)_3\text{C}^+\text{Cl}^-$ contact ion pair and the solvent-separated ion pair are distinct species, with calculated energies indicating that each is a local minimum. The more widely separated ion pair in Figure 8.12(c) is similar in energy to the solvent-separated ion pair.⁴⁷

Anchimeric Assistance in S_N1 Reactions

The stereochemistry of a solvolysis reaction can be affected if the substrate has a substituent that can donate a pair of electrons to the developing carbocation center. For example, treatment of (\pm)-*threo*-3-bromo-2-butanol (**19**) with HBr gave only the racemic 2,3-dibromobutane (**20**). There was none of the *meso* compound that would have been expected if the reaction involved protonation, loss of water, and formation of a free carbocation intermediate. Similarly, reaction of (\pm)-*erythro*-3-bromo-2-butanol with HBr gave only *meso*-2,3-dibromobutane. The reaction of **19** seems best explained by nucleophilic participation of the bromine on the adjacent atom in concert with departure of the water. The result is a bridged intermediate (**21**) that is the same bromonium ion expected from the electrophilic addition of Br_2 to *cis*-2-butene (Figure 8.13).⁴⁸ Back-side attack by bromide ion on either carbon atom involved in the three-membered bromonium ring is equally likely, so a racemic mixture results.

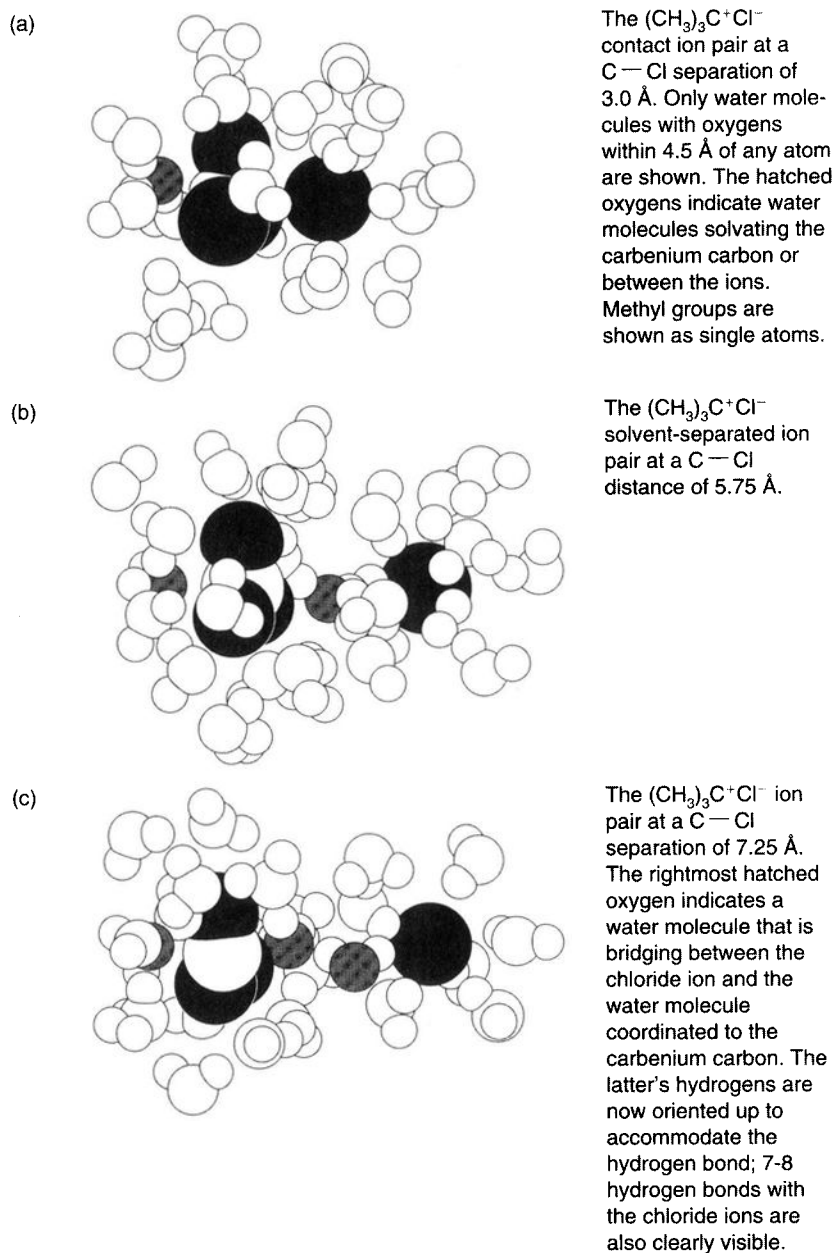
There is also kinetic evidence for intramolecular participation in some S_N1 reactions. Acetolysis of *trans*-2-acetoxycyclohexyl tosylate (**22**) gave only the *trans* diacetate (**23**), suggesting the intermediacy of **24** (Figure 8.14).⁴⁹

⁴⁶ For a review of studies of the role of ions and ion pairs in solvolysis reactions, see Raber, D. J.; Harris, J. M.; Schleyer, P. v. R. in Szwarc, M., Ed. *Ions and Ion Pairs in Organic Reactions*, Vol. 2; Wiley-Interscience: New York, 1974; pp. 247–374.

⁴⁷ Jorgensen, W. L.; Buckner, J. K.; Huston, S. E.; Rossky, P. J. *J. Am. Chem. Soc.* **1987**, *109*, 1891.

⁴⁸ Winstein, S.; Lucas, H. J. *J. Am. Chem. Soc.* **1939**, *61*, 1576.

⁴⁹ The literature describing this work uses the term *retention of configuration* to describe the products. Since racemic starting materials were used, the terminology refers to the formation of *trans* product from *trans* starting material. Retention of optical activity was not involved.

**FIGURE 8.12**

Calculated structures in the solvolysis of *t*-butyl chloride: (a) contact ion pair at 3.0 Å; (b) solvent-separated ion pair at 5.75 Å; and (c) ion pair at 7.25 Å. (Adapted from reference 47. The notes to the right of each part of the figure are from that reference.)

Furthermore, the rate constant for the reaction with the *trans*-2-acetoxy compound was found to be nearly 10^3 greater than that of the *cis* isomer and five times greater than that of cyclohexyl tosylate itself.⁵⁰ This evidence supported the view that the acetoxy group participates in the rate-limiting step of the reaction, not in a subsequent step after formation of the intermediate carbocation. The ionization of the tosylate is said therefore to be assisted

⁵⁰ Winstein, S.; Grunwald, E.; Buckels, R. E.; Hanson, C. J. *Am. Chem. Soc.* **1948**, *70*, 816 and references therein.

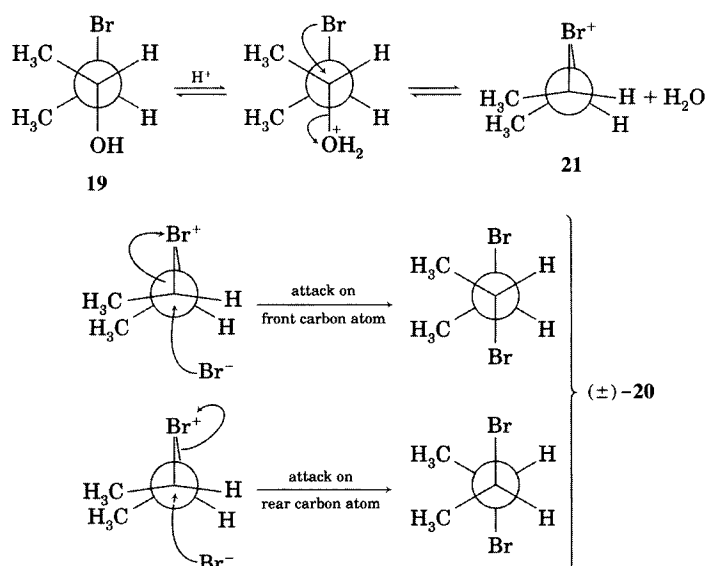


FIGURE 8.13

Anchimeric assistance via bromonium ion intermediate.

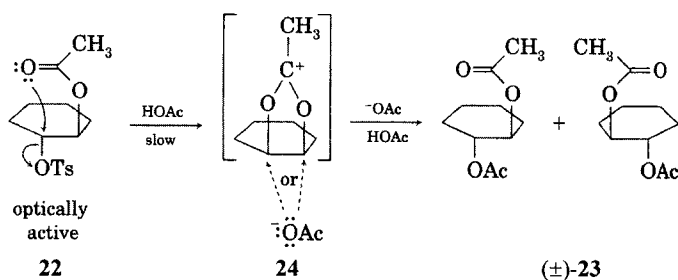


FIGURE 8.14

Anchimeric assistance in the reaction of *cis*-2-acetoxycyclohexyl tosylate.

by **neighboring group participation** by the acetoxy group. This process is often called **anchimeric assistance** and is generalized in Figure 8.15.⁵¹⁻⁵³ Note that the acetoxy group reacts by donating electron density to the back side of the C-OTs bond in a process similar to an S_N2 reaction. A *cis* acetoxy group would not be able to react by this pathway.

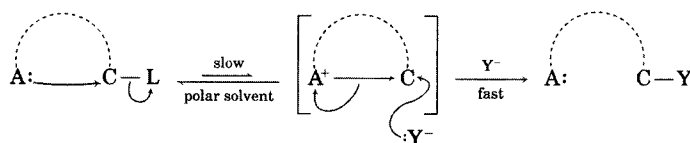


FIGURE 8.15

Schematic representation of anchimeric assistance.

⁵¹ The term is derived from the Greek *anhi* and *meros*, meaning "neighboring parts:" Winstein, S.; Lindgren, C. R.; Marshall, H.; Ingraham, L. L. *J. Am. Chem. Soc.* **1953**, *75*, 147.

⁵² For a discussion of terminology used in discussions of these assisted reactions, see Bartlett, P. D. *Nonclassical Ions*; W. A. Benjamin: New York, 1965; p. 65.

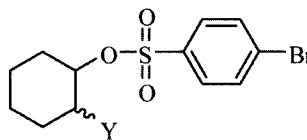
⁵³ The interacting groups must be spatially close but need not be adjacent along a carbon skeleton. For a report of a neighboring group interaction involving functional groups that interact through a 17-membered ring that arises from medium-induced coiling of a linear molecule, see Jiang, X.-K.; Fan, W.-Q.; Hui, Y.-Z. *J. Am. Chem. Soc.* **1984**, *106*, 7202.

TABLE 8.5 Rate Constants for Acetolysis of 2-Substituted Cyclohexyl *p*-Bromobenzenesulfonates

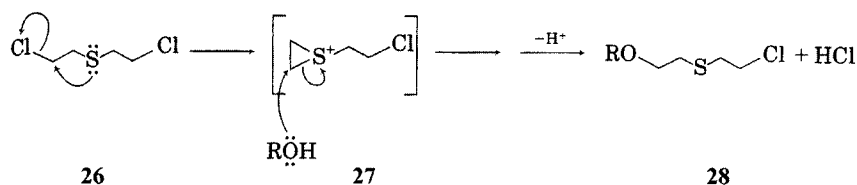
Substituent (Y)	$k_{\text{(rel)}}$	ΔH^\ddagger (kcal/mol)	ΔS^\ddagger (eu)
H	1.00	27.0	+1.5
<i>trans</i> -OAc	0.24	26.0	-4.2
<i>cis</i> -OAc	3.8×10^{-4}	30.9	-3.5
<i>trans</i> -Br	0.1	28.4	+0.8
<i>trans</i> -OCH ₃	0.06	27.3	-3.4
<i>trans</i> -Cl	4.6×10^{-4}	33.0	+2.7

Source: Reference 54.

Table 8.5 lists data for acetolysis of 2-substituted cyclohexyl brosylates having the general structure **25**.⁵⁴ The data confirm that a *trans* acetate reacts faster than does a *cis* acetate. The activation entropy data suggest a more ordered transition structure for the acetolysis of the *trans* isomer, consistent with the model of anchimeric assistance. A *trans* bromine is nearly as effective as a *trans* acetoxo, but a *trans* chloro group is far less effective—apparently due to the low stability of a chloronium ion in comparison with a bromonium ion.

**25**

A dramatic example of the role of neighboring group participation is provided by 2,2'-dichlorodiethyl sulfide (**26**). This compound reacts rapidly with nucleophiles to give substitution products, with kinetic rate expressions that are first order in **26** but independent of added nucleophile.⁵⁵ Thus, the kinetics are consistent with rate-limiting intramolecular cyclization to the intermediate **27**, which then reacts with nucleophiles to give substitution products (**28**) as shown in Figure 8.16. Alkoxy, hydroxyl, or amino groups are rapidly alkylated by **27**, and HCl is liberated as a by-product, making **26** a powerful vesicant and irritant. Compound **26** was used as a poison gas in World War I, and it is still known as mustard gas.

**FIGURE 8.16**

Anchimeric assistance in reaction of **26**.

⁵⁴ Winstein, S.; Grunwald, E.; Ingraham, L. L. *J. Am. Chem. Soc.* **1948**, *70*, 821.

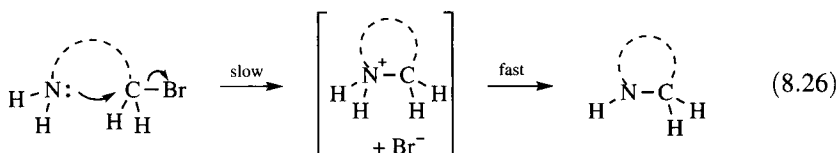
⁵⁵ Bartlett, P. D.; Swain, C. G. *J. Am. Chem. Soc.* **1949**, *71*, 1406.

TABLE 8.6 Rate Constants for Cyclization of ω -Aminoalkyl Bromides in Water at 25°C

Reactant	Rate Constant (min^{-1})
$\text{Br}-(\text{CH}_2)_2-\text{NH}_2$	3.6×10^{-2}
$\text{Br}-(\text{CH}_2)_3-\text{NH}_2$	5.0×10^{-4}
$\text{Br}-(\text{CH}_2)_4-\text{NH}_2$	ca. 30
$\text{Br}-(\text{CH}_2)_5-\text{NH}_2$	0.5
$\text{Br}-(\text{CH}_2)_6-\text{NH}_2$	1.0×10^{-3}

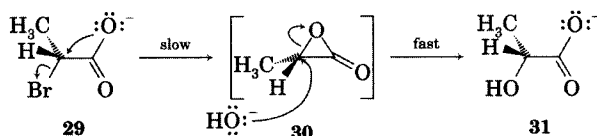
Source: Reference 56.

The intramolecular participation of the sulfur in reactions of **26** involves the formation of a three-membered ring in the intermediate. A study of the analogous reaction of nitrogen compounds to form cyclic amines (equation 8.26) led to the conclusion that three-membered ring formation occurs with a greater rate constant than does formation of a four-membered ring (Table 8.6). The rate constant for formation of five-membered rings is fastest of all of the compounds studied, however.⁵⁶



The ease of three-membered ring formation is an important factor in other solvolytic reactions. Reaction of α -bromocarboxylates (e.g., **29**, Figure 8.17) with nucleophiles proceeds with retention of configuration due to the double inversion resulting from two steps: (i) ionization assisted by participation of the carboxylate group to form an α -lactone (**30**), followed by (ii) fast attack of a nucleophile to generate a product with the same configuration as the reactant (**31**).⁵⁷

Anchimeric assistance does not require heteroatoms with nonbonded electrons; electrons associated with π bonds on carbon atoms may also accelerate first-order substitution reactions. Acetolysis of 2,2,2-triphenylethyl tosylate (**32**, Figure 8.18) gives products suggesting that rearrangement has accompanied the ionization. Moreover, the reaction takes place 7700 times faster (Table 8.7) than with 2,2-dimethyl-2-phenylpropyl tosylate (**33**), even though inductively withdrawing phenyl groups in **32** would be expected to

**FIGURE 8.17**

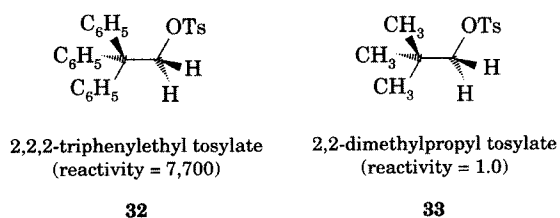
Retention of configuration in a solvolysis reaction via anchimeric assistance.

⁵⁶ Freundlich, H.; Kroepelin, H. Z. *Phys. Chem.* **1926**, 122, 39.

⁵⁷ Grunwald, E.; Winstein, S. J. *Am. Chem. Soc.* **1948**, 70, 841 and references therein.

FIGURE 8.18

Comparison of reactivity of 2,2,2-triphenylethyl tosylate and 2,2-dimethylpropyl tosylate.



retard a reaction that forms a carbocation.⁵⁸ Correcting for the expected inductive effect of the phenyl groups means that **32** reacts 10^7 times as fast as a compound with no participation by one of the phenyl groups.^{58,59} The data suggest that ionization is accompanied by concurrent migration of a phenyl group toward the developing carbocation to form an intermediate **phenonium ion**, which can be represented by the resonance-stabilized structure **34** (Figure 8.19).^{60–62}

Stereochemical evidence for the participation of β -aromatic rings was provided by Cram, who found that the acetolysis of *D-erythro*-3-phenyl-2-butyl tosylate (**35**) gave **36** with complete retention of configuration. On the other hand, acetolysis of the optically active threo isomer (**37**) gave racemic product (**38**).⁶³ The results can most easily be rationalized by mechanisms involving the bridged intermediates (**39** and **40**) shown in Figure 8.20.⁶⁴

TABLE 8.7 Acetolysis Rate Constants and Activation Parameters for Primary Tosylates

Substrate	k (s^{-1})	ΔH^\ddagger (kcal/mol)	ΔS^\ddagger (eu)
2,2-Dimethylpropyl tosylate	2.17×10^{-9}	31.5	-1.0
2-Methyl-2-phenylpropyl tosylate	9.92×10^{-7}	25.7	-6.4
2,2,2-Triphenylethyl tosylate	1.68×10^{-5}	25.2	-2.5

Source: Reference 58.

⁵⁸ Winstein, S.; Morse, B. K.; Grunwald, E.; Schreiber, K. C.; Corse, J. J. *Am. Chem. Soc.* **1952**, *74*, 1113.

⁵⁹ See also Charlton, J. C.; Dostrovsky, I.; Hughes, E. D. *Nature* **1951**, *167*, 986; Brown, F.; Hughes, E. D.; Ingold, C. K.; Smith, J. F. *Nature* **1951**, *168*, 65.

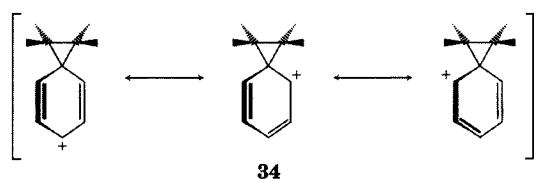
⁶⁰ For a theoretical study of the phenonium ion, see Sieber, S.; Schleyer, P. v. R.; Gauss, J. J. *Am. Chem. Soc.* **1993**, *115*, 6987.

⁶¹ To view the process differently, the carbocation character that develops as the leaving group starts to depart leads to attachment of the incipient carbocation to the aromatic ring in what is essentially the first step of an electrophilic aromatic substitution.

⁶² Olah and co-workers used NMR spectroscopy to study the relative stability of phenonium ions, benzylic ions, and phenethyl cations as a function of substituents on the benzene ring. For the unsubstituted benzene ring, the phenonium ion was more stable than the other two possible structures. With a *p*-methoxy substituent, however, the benzylic ion was most stable, while the phenethyl cation was most stable for a *p*-trifluoromethyl substituent. Olah, G. A.; Comisarow, M. B.; Kim, C. J. *J. Am. Chem. Soc.* **1969**, *91*, 1458. Also see Olah, G. A.; Head, N. J.; Rasul, G.; Prakash, G. K. S. *J. Am. Chem. Soc.* **1995**, *117*, 875.

⁶³ Note that the intermediate phenonium ion formed from the threo reactant is a meso structure. Optical activity has already been lost at this stage, so the product cannot be optically active.

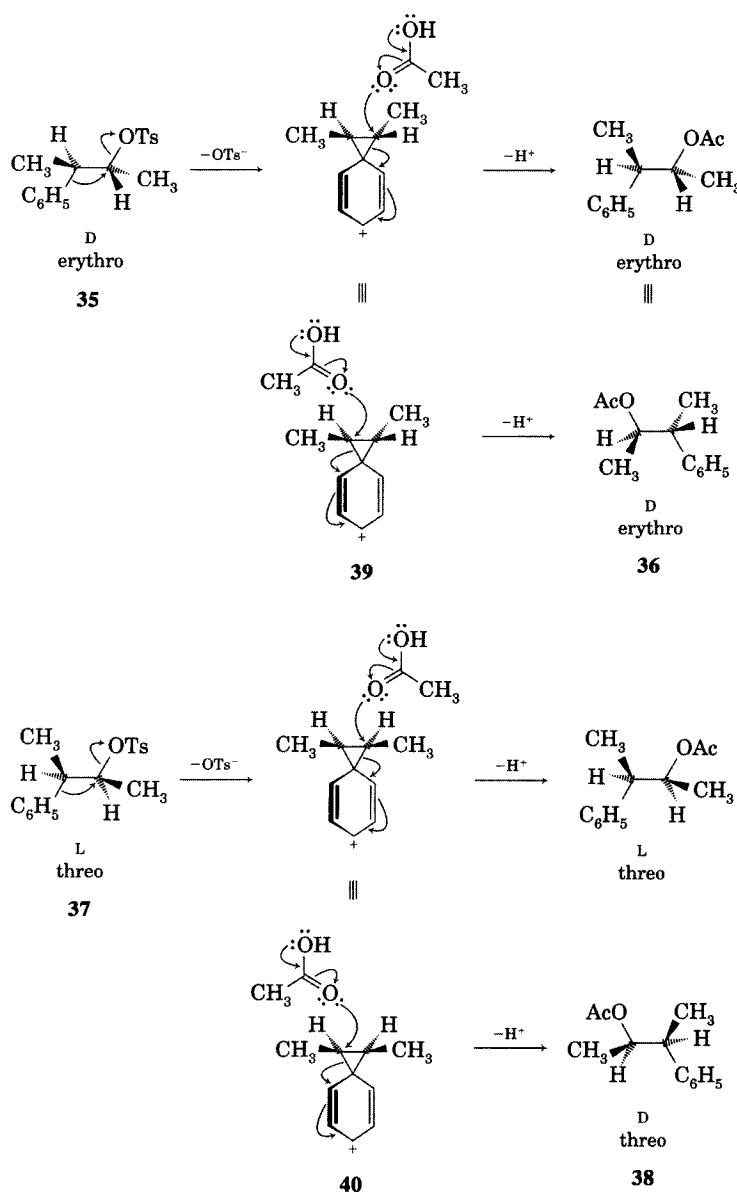
⁶⁴ Cram, D. J. *J. Am. Chem. Soc.* **1949**, *71*, 3863. For a more detailed discussion of this and related papers, see Gould, E. S. *Mechanism and Structure in Organic Chemistry*; Holt, Rinehart and Winston: New York, 1959; p. 575 ff.

**FIGURE 8.19**

Resonance structures for a phenonium ion generated by participation of a phenyl group in a solvolysis reaction.

Nonclassical Carbocations in S_N1 Reactions

An olefinic π system can also participate in a solvolysis reaction. Acetolysis of cholesteryl tosylate (**41**, Figure 8.21) gave the β -acetoxy product (**43**), plus some rearrangement product (**44**) with a rate constant around 100 times greater than the rate constant for acetolysis of cyclohexyl

**FIGURE 8.20**

Stereochemical evidence for phenonium ion intermediates.

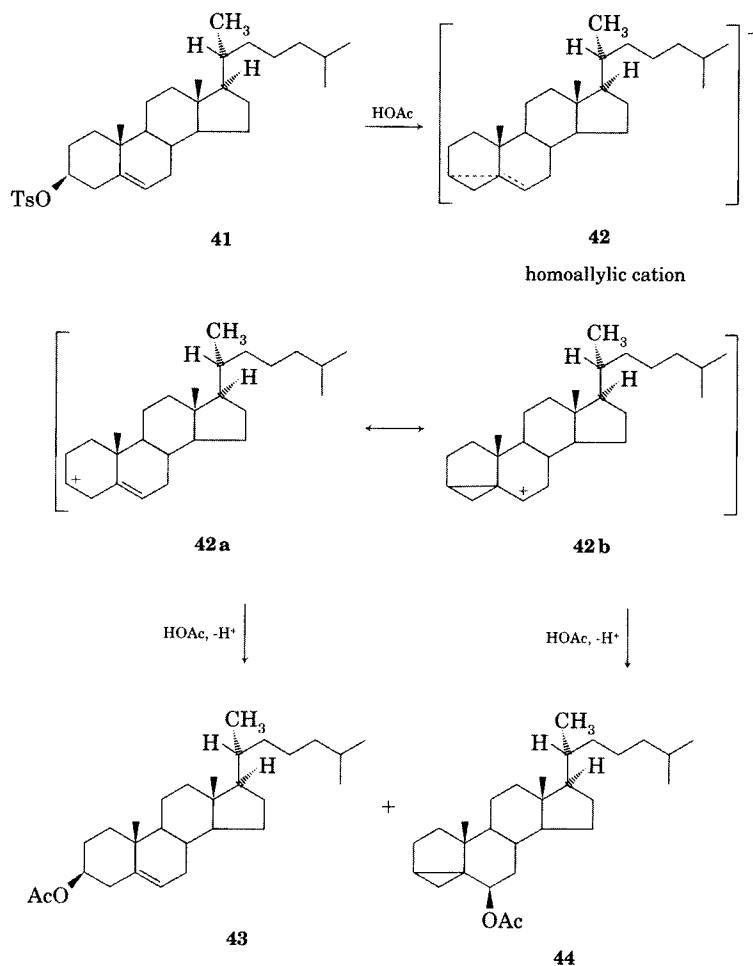


FIGURE 8.21

Acetolysis of cholesteryl tosylate.

tosylate.⁶⁵ The results were consistent with anchimeric assistance by the double bond concurrent with ionization to give a delocalized carbocation intermediate, shown both as the delocalized structure **42** and as a hybrid of the resonance structures **42a** and **42b**. Nucleophilic attack on **42** by acetic acid can yield the two products, **43** and **44**.

There is evidence that σ bonds can also participate in the formation of nonclassical carbocation intermediates in solvolysis reactions. In the Wagner–Meerwein rearrangement, camphene hydrochloride (**45**) rearranges to isobornyl chloride (**46**).^{66,67} It is possible to write a mechanism in which

⁶⁵ Winstein, S.; Adams, R. J. *Am. Chem. Soc.* **1948**, *70*, 838. Qualitatively similar results had been reported by Shoppee, C. W. *J. Chem. Soc.* **1946**, 1147 for the methanolysis of cholesteryl tosylate.

⁶⁶ The conversion of camphene hydrochloride to isobornyl chloride is the prototypical Wagner–Meerwein rearrangement, but the term *Wagner–Meerwein rearrangement* is a general term for 1,2-alkyl and 1,2-hydride shifts in carbocation rearrangements. Because of the contributions of Whitmore in elucidating these shifts, they are sometimes called Wagner–Meerwein–Whitmore rearrangements. Compare reference 5. For a review, see Pocker, Y. in de Mayo, P., Ed. *Molecular Rearrangements*, Part 1; Wiley-Interscience: New York, 1963, 1; Berson, J. A. *ibid.*, p. 111.

⁶⁷ Isotopic labeling experiments by Roberts and Lee not only confirmed the rearrangement shown Figure 8.22 but also revealed even more extensive rearrangements involving hydride shifts in this system. Roberts, J. D.; Lee, C. C. *J. Am. Chem. Soc.* **1951**, *73*, 5009; Roberts, J. D.; Lee, C. C.; Saunders, W. H., Jr. *J. Am. Chem. Soc.* **1954**, *76*, 4501. See also the discussion by Bartlett (reference 52), pp. 65–67 and references therein.

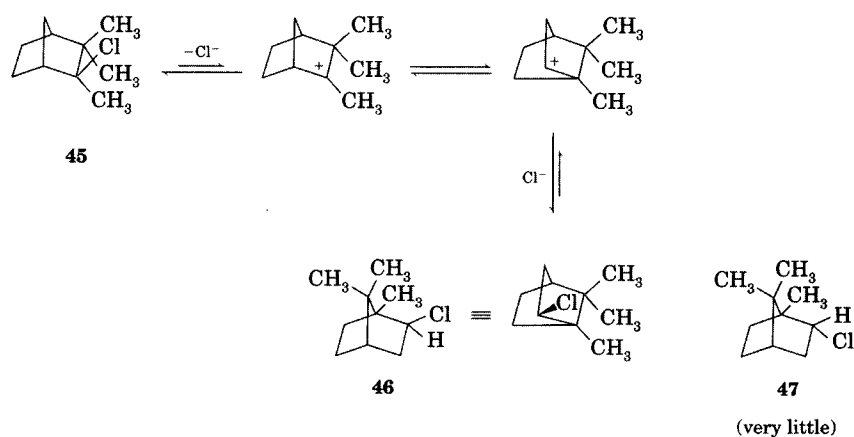


FIGURE 8.22
Wagner-Meerwein
rearrangement.

only classical (carbenium) ions are intermediates in the reaction, as shown in Figure 8.22. The major product of the rearrangement is the exo isomer of bornyl chloride (**46**), and very little of the endo isomer (**47**) of the product is seen. We might expect faster formation of **47** than **46** if the reaction involves a free carbocation, because the pathway leading to **47** would not require chloride ion to attack the carbocation near the methyl group on the bridge.

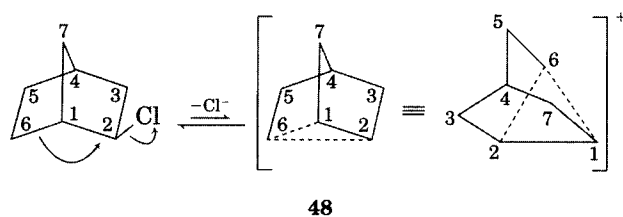


FIGURE 8.23
Formation of a nonclassical carbocation in solvolysis of a 2-norbornyl derivative.

Winstein proposed that the intermediate in the solvolysis of 2-norbornyl (bicyclo[2.2.1]heptyl) systems is the nonclassical carbocation **48** (Figure 8.23; see also the discussion in Chapter 5), which is formed by σ bond participation in the solvolysis reaction. As shown in Figure 8.24, nucleophilic attack on the back side of either partial carbon-carbon bond leads to the formation of exo product. Moreover, the presence of the plane of symmetry (passing through carbon atoms 4, 5, and 6) in **48** means that the product must be racemic. As a means of formalizing the information in this area, Winstein and others proposed the concepts of **homoconjugation** (conjugation involving orbitals on atoms not formally σ -bonded to each other) and of **homoaromaticity**

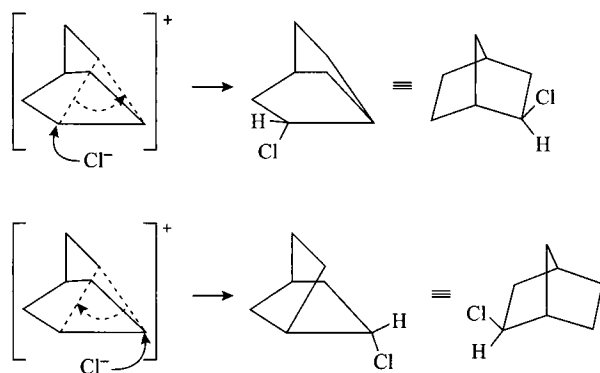


FIGURE 8.24
Formation of racemic product from solvolysis of a 2-norbornyl compound.

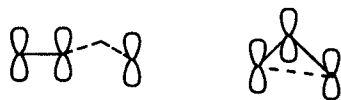


FIGURE 8.25

Basis set orbitals illustrating homoconjugation (left) and homoaromaticity (right).

(aromaticity achieved through homoconjugation). These interactions are illustrated in Figure 8.25, where the dashed lines indicate connectivity through tetraligant carbon atoms. For example, the intermediate (42) in the solvolysis of cholesteryl tosylate would be *homoallylic* since it is allylic with one overlap involving atoms not σ -bonded to each other. Similarly, the norbornyl cation (48) would be *bishomocyclopropenyl*, since it is like cyclopropenyl except for two missing σ bonds.⁶⁸

Although there were many proponents of nonclassical ions and anchimeric assistance in solvolysis reactions, there was also resistance to these ideas. In particular, Brown argued that all of the kinetic and stereochemical results cited in support of nonclassical ions could also be explained in terms of classical carbocations.^{69,70} In the case of the solvolysis of the 2-norbornyl derivatives, he pointed out that the apparent rate increase might be the result of steric acceleration of ionization (see Table 8.1), not anchimeric assistance. He suggested that the formation of exclusively *exo* product from solvolysis of *exo*-2-norbornyl compounds could result from a higher transition state energy for *endo* product formation than for *exo* product formation, and he ascribed the racemization accompanying such solvolyses to the intermediacy of **rapidly equilibrating classical carbocations** as shown in Figure 8.26.⁷¹ As noted in Chapter 5, several lines of evidence support the existence of nonclassical carbocations—at least under spectroscopic conditions—and the role of nonclassical ions in solvolysis reactions is now widely accepted. Nevertheless, the discussions of classical and nonclassical carbocations in solvolysis reactions prompted physical organic chemists to reexamine many fundamental concepts of structure and reactivity.⁵⁸

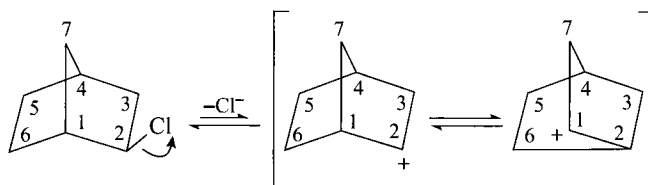
The S_N2 Reaction

Stereochemistry

Prior to 1895, it was thought that all substitution reactions occur with retention of configuration.⁷² In that year, however, Walden reported that inversion of configuration accompanied a substitution reaction.⁷³ As

FIGURE 8.26

Rapidly equilibrating classical carbocation model for the norbornyl cation.



⁶⁸ Homoconjugation and homoaromaticity were topics of great interest in physical organic chemistry, and Winstein summarized much of the work in this area: Winstein, S. Q. *Rev. Chem. Soc. (London)* **1969**, 23, 141.

⁶⁹ Brown, H. C. *Chem. Soc. (London) Spec. Publ.* **1962**, 16, 140. This paper is reproduced in reference 52 (p. 438 ff). See also the commentary by Bartlett, p. 461 ff in reference 52.

⁷⁰ See also Brown, H. C. with commentary by Schleyer, P. v. R. *The Nonclassical Ion Problem*; Plenum: New York, 1977.

⁷¹ For a discussion of the arguments against nonclassical ions by H. C. Brown and a commentary offering the opposing view, see reference 70.

⁷² Eliel, E. L. *Stereochemistry of Carbon Compounds*; McGraw-Hill: New York, 1962; p. 116.

⁷³ Walden, P. *Ber. Dtsch. Chem. Ges.* **1895**, 28, 1287; *Ber. Dtsch. Chem. Ges.* **1897**, 30, 3146.

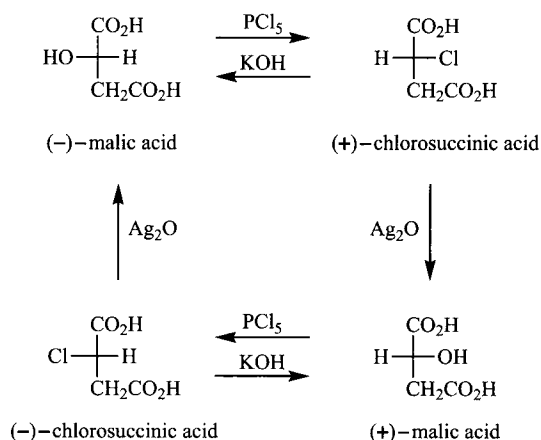


FIGURE 8.27
The Walden cycle.

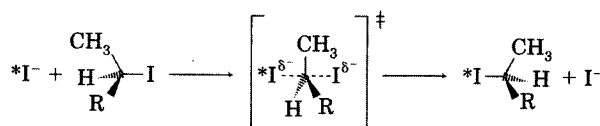


FIGURE 8.28
Stereochemistry of the back-side pathway in the S_N2 reaction.

shown in Figure 8.27, conversion of (–)-malic acid to (+)-malic acid by two substitution reactions indicates that one of the two steps must take place with inversion of configuration and the other must take place with retention. Later, racemization of optically active 2-iodooctane was found to occur at twice the rate of incorporation of radioactive iodine into the structure.⁷⁴ The simplest mechanism to explain this result is the reaction pathway shown in Figure 8.28, which is the familiar S_N2 back-side displacement mechanism. Molecular beam studies of the reaction of methyl iodide and chloride ion in the gas phase subsequently provided direct evidence for substitution by back-side attack.⁷⁵

An alternative pathway for a bimolecular substitution that would give retention of configuration is the front-side attack mechanism shown in Figure 8.29. One explanation for the failure to observe retention of configuration in many S_N2 reactions is that a front-side attack would give a transition structure with two partial negative charges close to each other. Such a geometry should be less stable than a transition structure with the charges

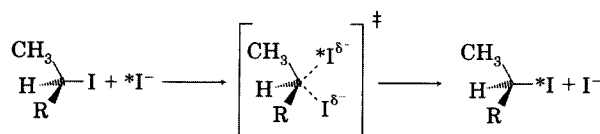
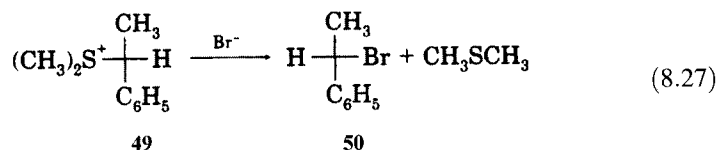


FIGURE 8.29
Stereochemistry of a hypothetical front-side attack pathway for the S_N2 reaction.

⁷⁴ Hughes, E. D.; Juliusburger, F.; Masterman, S.; Topley, B.; Weiss, J. J. *Chem. Soc.* **1935**, 1525. The rate constant for racemization was *twice* the rate constant for inversion. Because inversion both removes one stereoisomer and produces its enantiomer, the rate constant for radioactive iodine incorporation was presumed to equal the rate constant for inversion.

⁷⁵ Interestingly, the results also suggested a novel alternative mechanism in which chloride ion first collides with the side of the methyl group and spins the methyl iodide 360° around the iodine atom before colliding again and displacing the iodide ion. Mikosch, J.; Trippel, S.; Eichhorn, C.; Otto, R.; Lourderaj, U.; Zhang, J. X.; Hase, W. L.; Weidemüller, M.; Wester, R. *Science* **2008**, 319, 183. See also the commentary by Brauman, J. I. *Science* **2008**, 319, 168.

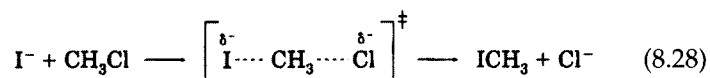
further apart, as is the case with back-side displacement. Such electrostatic interactions seem not to be dominant, however. S_N2 reactions with negatively charged nucleophiles and positively charged leaving groups also react by back-side displacement, even though the front-side attack would appear to be more stable due to positive-negative attraction. For example, the reaction of L-(-)-dimethyl- α -phenylethylsulfonium ion (49) with bromide ion gives D-(+)- α -phenylethyl bromide (50, equation 8.27).^{76,77} It appears therefore that back-side attack generates a transition structure with lower electronic energy than does front-side attack, and theoretical studies utilizing both semiempirical and ab initio calculations have confirmed this explanation.⁷⁸



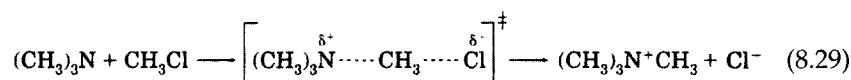
Solvent Effects

The effect of solvent on an S_N2 reaction depends on the difference between the solvation energies of the reactants and that of the transition structure. In terms of solvent polarity, the important question is the change both in total charge and in charge distribution between reactants and transition structures. Ingold identified four different patterns that might be observed in S_N2 reactions:⁴

- (i) Negative nucleophile and neutral substrate, such as the substitution of iodide for chloride in methyl chloride



- (ii) Neutral nucleophile and neutral substrate, such as the reaction of trimethylamine with methyl chloride

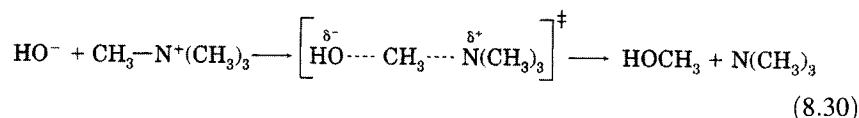


- (iii) Negative nucleophile and positive substrate, such as the reaction of hydroxide ion with tetramethylammonium ion

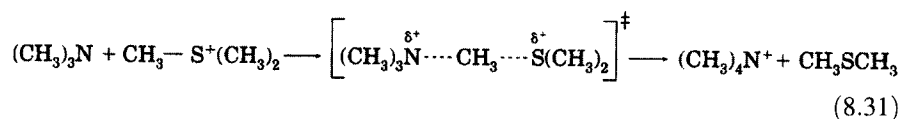
⁷⁶ Siegel, S.; Graeffe, A. F. *J. Am. Chem. Soc.* **1953**, *75*, 4521.

⁷⁷ Cowdrey, W. A.; Hughes, E. D.; Ingold, C. K.; Masterman, S.; Scott, A. D. *J. Chem. Soc.* **1937**, 1252.

⁷⁸ (a) Allinger, N. L.; Tai, J. C.; Wu, F. T. *J. Am. Chem. Soc.* **1970**, *92*, 579; (b) Ritchie, C. D.; Chappell, G. A. *J. Am. Chem. Soc.* **1970**, *92*, 1819; (c) Dedieu, A.; Veillard, A. *J. Am. Chem. Soc.* **1972**, *94*, 6730; *Quantum Theory Chem. React.* **1980**, *1*, 69. Also see Hu, W.-P.; Truhlar, D. G. *J. Am. Chem. Soc.* **1994**, *116*, 7797.



- (iv) Neutral nucleophile and positive substrate, such as the reaction of trimethylamine with trimethylsulfonium to produce tetramethylammonium ion and dimethyl sulfide,



Let us illustrate the effects of solvent polarity by considering the first two types of reactions. Because all of the charge in a type (i) reaction is initially localized on the nucleophile, there is strong solvation of the nucleophile by a polar solvent, but the solvation of the neutral substrate is weaker. In the transition structure, the negative charge is still present, but it is dispersed over the entire transition structure. The stabilization of the transition structure by solvent is diminished because the charge is less localized.⁷⁹ Consequently, the activation energy for the reaction is greater in a more polar solvent than in a less polar solvent, and the rate constant for the reaction decreases with increasing solvent polarity (Figure 8.30). The data in Table 8.8 are consistent with this view.

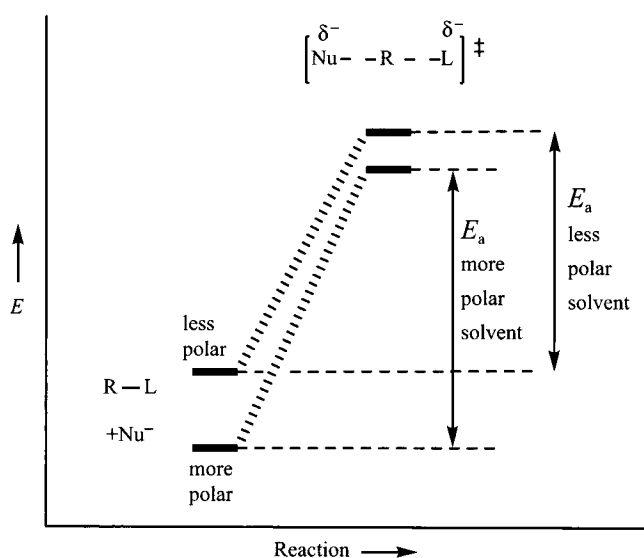


FIGURE 8.30
Effect of solvent polarity on a type (i) substitution reaction.

⁷⁹ For the reaction of chloride ion with methyl chloride in water, Jorgensen calculated that the heats of hydration of the transition structure and reactants differ by 22 kcal/mol. Chandrasekhar, J.; Smith, S. F.; Jorgensen, W. L. *J. Am. Chem. Soc.* **1985**, *107*, 154.

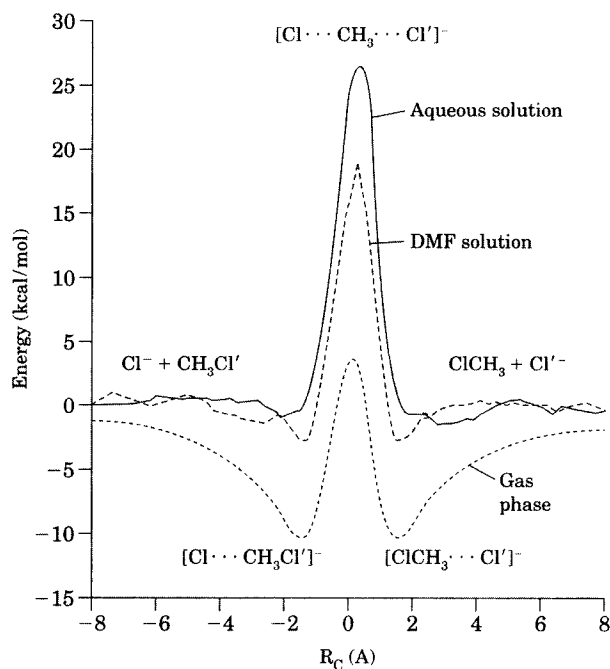
TABLE 8.8 Solvent Effect on Rate Constants for the S_N2 Reaction of CH₃I with Cl⁻

Solvent	<i>k</i> (rel.)
CH ₃ OH	0.9
H ₂ O	1.0
HCONH ₂	14.1
CH ₃ NO ₂	14,100
CH ₃ CN	35,800
DMF	708,000
Acetone	1,410,000

Source: Reference 80.

The data in Table 8.8 also indicate that faster rate constants are associated with **aprotic** (i.e., nonhydrogen bonding) solvents that do not strongly solvate anions. For example, the rate constant for reaction of methyl iodide with chloride ion increases by a factor of 1.5×10^6 as the solvent is changed from methanol to acetone.⁸⁰ Moreover, changing from a protic solvent to acetone reverses the order of nucleophilicity of halide ions⁸¹ ($I^- > Br^- > Cl^-$ in protic solvent), indicating that the energy required to remove hydrogen-bonded solvent molecules from the smaller ions is a significant factor in decreasing their nucleophilicity.

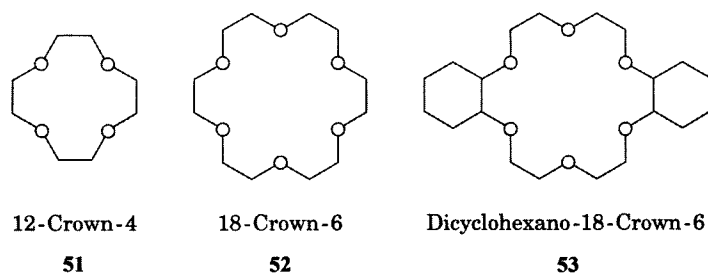
Theoretical calculations are also informative in interpreting solvent effects in type (i) S_N2 reactions. Figure 8.31 shows the results obtained with

**FIGURE 8.31**

Calculated energies for reaction of Cl⁻ with CH₃Cl. (Reproduced from reference 82.)

⁸⁰ Parker, A. J. *Chem. Rev.* **1969**, *69*, 1.

⁸¹ Winstein, S.; Savedoff, L. G.; Smith, S.; Stevens, I. D. R.; Gall, J. S. *Tetrahedron Lett.* **1960**, *9*, 24.

**FIGURE 8.32**

Structures of some crown ethers.

Monte Carlo statistical mechanics calculations by Chandrasekhar and Jorgensen for the reaction of chloride ion with methyl chloride in the gas phase, in dimethylformamide (DMF), and in water. It is interesting that in the gas phase there is an energy minimum both before and after the energy maximum, the first minimum corresponding to a $[\text{Cl} \cdots \text{CH}_3\text{Cl}]^-$ complex. A simple way to think of the complex is that the polar methyl chloride molecule can partially solvate the chloride ion, since no other solvent is available. The calculated reaction barrier is only slightly higher than the initial energy of the reactants. In DMF solution the complex is less evident, and the reaction barrier is 19.3 kcal/mol. In aqueous solution the complexes are not apparent, and the reaction barrier is 26.3 kcal/mol.⁸²

Equation 8.28 shows only the anionic nucleophile explicitly, since the counterion does not appear to take part in the reaction. Nevertheless, the counterion affects the solubility of a nucleophilic salt, which therefore can influence the polarity of the solvent needed for the reaction. An alternative to the use of a more polar solvent to dissolve a salt for nucleophilic substitution is to use crown ether additives. Crown ethers are cyclic polyethers that can coordinate with cations and therefore increase their solubility in organic solvents. The nomenclature provides the total number of atoms and the number of oxygen atoms in the ring. Compound 51 is 12-crown-4, and 52 is 18-crown-6 (Figure 8.32). Coordination of a crown ether with a cation helps to dissolve the salt in a less polar solvent and leaves the anion relatively unsolvated. The activation energy for substitution therefore does not include a large term for desolvation of the nucleophilic anion, and the reactions are fast.⁸³ For example, adding dicyclohexano-18-crown-6 (53) to a solution of 1-bromobutane in dioxane was found to increase its reactivity with potassium phenoxide by a factor of 1.5×10^4 .⁸⁴ Moreover, Liotta and Harris were able to use KF solubilized with 18-crown-6 (52) to carry out $\text{S}_{\text{N}}2$ reactions on 1-bromooctane in benzene.⁸⁵

⁸² Chandrasekhar, J.; Jorgensen, W. L. *J. Am. Chem. Soc.* **1985**, *107*, 2974. The study with DMF involved the calculation of the energy of the two reactants plus 180 molecules of DMF. For a discussion, see Shaik, S. S.; Schlegel, H. B.; Wolfe, S. *Theoretical Aspects of Physical Organic Chemistry: The $\text{S}_{\text{N}}2$ Mechanism*; John Wiley & Sons: New York, NJ, 1992.

⁸³ Similarly, $\text{S}_{\text{N}}2$ reactions can be carried out in other solvents if appropriate phase transfer agents (highly soluble organic cations) are used to carry the "naked" nucleophile into solution. For example, Carpino and Sau used tetra-*n*-butylammonium chloride to solubilize KF in acetonitrile for such a reaction. Carpino, L. A.; Sau, A. C. *J. Chem. Soc. Chem. Commun.* **1979**, 514.

⁸⁴ Thomassen, L. M.; Ellingsen, T.; Ugelstad, J. *Acta Chem. Scand.* **1971**, *25*, 3024. See also the discussion in de Jong, F.; Reinhoudt, D. N. *Stability and Reactivity of Crown-Ether Complexes*; Academic Press: New York, 1981; p. 35 ff.

⁸⁵ Liotta, C. L.; Harris, H. P. *J. Am. Chem. Soc.* **1974**, *96*, 2250.

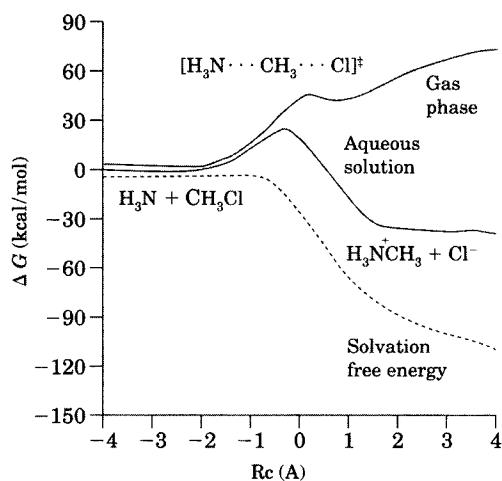


FIGURE 8.33

Free energy profiles calculated for reaction of ammonia with methyl chloride. (Adapted from reference 87.)

The effect of changing solvent polarity is exactly the opposite in type (ii) S_N2 reactions. Because the reactants are neutral but partial charges develop in the transition structure, type (ii) reactions are facilitated by polar solvent.⁸⁶ Figure 8.33 shows the calculated free energy for the reaction of ammonia with methyl chloride in the gas phase and in aqueous solution as a function of the reaction coordinate (Rc).^{87,88} The top line shows that the energy increases throughout the reaction in gas phase reactions because there is no solvent to stabilize the developing ions. The middle curve shows the free energy for reaction in aqueous solution. The bottom, dotted curve shows the calculated free energy of solvation for the reaction. A solvent less polar than water should produce somewhat less stabilization, resulting in a curve between those for reaction in water and in the gas phase.⁸⁹

Substrate Effects

The second-order rate constants for the substitution reactions of alkyl halides generally decrease as the alkyl halide varies from methyl to 1° to 2° to 3° . This trend is illustrated in Table 8.9, which summarizes kinetic data for alkyl bromides (R–Br) reacting with bromide ion.⁹⁰ This trend is usually ascribed to increasing steric hindrance to back-side attack of the nucleophile as hydrogens bonded to the C–Br carbon atom are replaced with larger alkyl groups. Theoretical calculations⁹¹ and gas phase studies⁹² have provided support for this explanation. It is notable that neopentyl bromide is less reactive than

⁸⁶ For examples, see Cox, H. E. *J. Chem. Soc.* **1921**, 119, 142; McCombie, H.; Scarborough, H. A.; Smith, F. F. P. *J. Chem. Soc.* **1927**, 802.

⁸⁷ Gao, J. *J. Am. Chem. Soc.* **1991**, 113, 7796. See also Gao, J.; Xia, X. *J. Am. Chem. Soc.* **1993**, 115, 9667.

⁸⁸ This reaction is a Menshutkin—also spelled Menshutkin—reaction, which is generally described as the S_N2 alkylation of a nitrogen nucleophile, usually by an alkyl halide. For a discussion, see Abboud, J.-L. M.; Notario, R.; Bertrán, J.; Solà, M. *Prog. Phys. Org. Chem.* **1993**, 19, 1.

⁸⁹ For a valence bond analysis of the Menshutkin reaction, see Su, P.; Ying, F.; Wu, W.; Hiberty, P. C.; Shaik, S. *ChemPhysChem* **2007**, 8, 2603.

⁹⁰ de la Mare, P. B. D. *J. Chem. Soc.* **1955**, 3180.

⁹¹ Vayner, G.; Houk, K. N.; Jorgensen, W. L.; Brauman, J. I. *J. Am. Chem. Soc.* **2004**, 126, 9054.

⁹² Gronert, S.; Fagin, A. E.; Okamoto, K.; Mogali, S.; Pratt, L. M. *J. Am. Chem. Soc.* **2004**, 126, 12977.

TABLE 8.9 Kinetic Data for $^*Br^- + R-Br \rightarrow ^*R-Br + Br^-$ in Acetone at 25°C

R	<i>k</i> (rel.)	<i>E_a</i> (kcal/mol)	log <i>A</i>
CH ₃	76	15.8	10.7
CH ₃ CH ₂	1.0	17.5	10.1
CH ₃ CH ₂ CH ₂	0.65	17.5	9.8
(CH ₃) ₂ CH	0.011	19.7	9.7
(CH ₃) ₂ CHCH ₂	0.033	18.9	9.6
(CH ₃) ₃ C	0.003	21.8	10.7
(CH ₃) ₃ CCH ₂	0.000015	22.0	8.6

Source: Reference 90.

t-butyl bromide, even though neopentyl bromide is formally a 1° alkyl halide. Space-filling models indicate that hydrogen atoms on β methyl groups can provide a steric barrier to reaction that is comparable to that of hydrogen atoms on α methyl groups.⁹⁵ Moreover, the effect of steric hindrance to back-side attack appears to be greater in solution than in the gas phase because solvation has the effect of making the nucleophile larger.⁹²

This explanation for the reduction in reactivity with increasing substitution of the reaction site might be interpreted to mean that the steric effect is primarily enthalpic, but that is an oversimplification. Table 8.10 summarizes some data for the reaction of chloride ion with a series of alkyl iodides in acetone.⁹³ The *E_a* values for the first five entries in the table differ by only 2 kcal/mol, although that for neopentyl is several kcal/mol higher. On the other hand, the log *A* values are quite different among this series of compounds. The log *A* values suggest that the activation entropy plays an important role in determining the rate constants of S_N2 reactions in which many nuclei must move simultaneously in order to go from the reactant to the transition state. This decrease in S_N2 reactivity has been called the **ponderal effect**, meaning that it depends on the mass of the substituents near the carbon atom undergoing substitution and not just on their space-filling properties.⁹⁴

TABLE 8.10 Kinetic Data for Reaction of R-I with Chloride in Acetone

R	<i>k</i> (rel.)	<i>E_a</i> (kcal/mol)	log <i>A</i>
CH ₃	11.1	16.0	9.4
CH ₃ CH ₂	1.0	17.0	9.1
CH ₃ CH ₂ CH ₂	0.58	17.0	8.8
(CH ₃) ₂ CH	0.032	18.0	8.3
(CH ₃) ₂ CHCH ₂	0.038	17.8	8.3
(CH ₃) ₃ CCH ₂	0.000014	22.0	7.9

Source: Reference 93.

⁹³ Hughes, E. D.; Ingold, C. K.; Mackie, J. D. H. *J. Chem. Soc.* **1955**, 3177.

⁹⁴ de la Mare, P. B. D.; Fowden, L.; Hughes, E. D.; Ingold, C. K.; Mackie, J. D. H. *J. Chem. Soc.* **1955**, 3200.

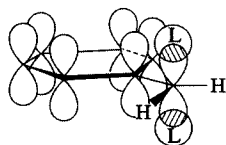
TABLE 8.11 Relative Reactivities of R–Cl with Iodide in Acetone at 50°C

R	<i>k</i> (rel.)	R	<i>k</i> (rel.)
Cyclohexyl	$<10^{-3}$	PhCH ₂	1.95×10^2
<i>n</i> -Butyl	1.0	EtOCOCH ₂	1.72×10^3
<i>n</i> -Heptyl	1.3 ^a	NCCH ₂	3.07×10^3
Allyl	79	CH ₃ COCH ₂	3.57×10^4
H ₂ NCOCH ₂	99	PhCOCH ₂	1.05×10^{5b}

^a See reference 93b.^b See reference 95c.

Source: Reference 95a.

Not all substituents decrease the rate constants of S_N2 reactions. Table 8.11 summarizes reactivity data for a series of alkyl chlorides with iodide ion in acetone.⁹⁵ *n*-Butyl chloride is much less reactive than allyl chloride, benzyl chloride, and other structures with a π system bonded to the carbon atom undergoing substitution. A simple model for the reaction of the benzyl system (Figure 8.34) suggests that the sp² hybridization proposed for the transition structure means that a *p* orbital developing at the reaction center can be conjugated with the attached π system, thus stabilizing the transition structure and lowering the activation energy for the reaction.^{96,97} It was also suggested that this type of resonance interaction can lower the energy of the transition structure by delocalizing the nucleophilic electrons into the aromatic ring. However, the reactivity of benzylic systems is enhanced by both electron-donating and electron-withdrawing substituents, and a number of explanations have been proposed to explain the results. A combined ab initio and density functional theory study led to the conclusion that the reactivity of benzyl fluoride derivatives in the gas phase is determined primarily by electrostatic interactions among the reactants and that delocalization of nucleophilic charge into the aromatic ring is not a significant factor.⁹⁸

**FIGURE 8.34**

Transition state interactions with π systems. (Adapted from reference 96.)

The fact that the reactivity of α-chloroacetone is 450 times greater than that of allyl chloride suggested an additional rate accelerating factor in α-halo carbonyl compounds and similar structures. An early rationale for the reactivity of these compounds is that the partial positive charge on the carbonyl carbon atom augments the partial charge on the C–L carbon atom, thereby increasing its attraction for a nucleophile.⁹⁹ Another explanation was that compounds of this type could undergo nucleophilic attack on the carbonyl group, leading to a tetrahedral intermediate that subsequently rearranges to the substitution product (equation 8.32).¹⁰⁰ Pearson and co-

⁹⁵ (a) Conant, J. B.; Kirner, W. R.; Hussey, R. E. *J. Am. Chem. Soc.* **1925**, *47*, 488; (b) Conant, J. B.; Hussey, R. E. *J. Am. Chem. Soc.* **1925**, *47*, 476; (c) Conant, J. B.; Kirner, W. R. *J. Am. Chem. Soc.* **1924**, *46*, 232; (d) Kirner, W. R. *J. Am. Chem. Soc.* **1926**, *48*, 2745.

⁹⁶ Streitwieser, A., Jr.; *Solvolytic Displacement Reactions*; McGraw-Hill: New York, 1962; pp. 13–20.

⁹⁷ King, J. F.; Tsang, G. T. Y.; Abdel-Malik, M. M.; Payne, N. C. *J. Am. Chem. Soc.* **1985**, *107*, 3224 and references therein.

⁹⁸ Galabov, B.; Nikolova, V.; Wilke, J. J.; Schaefer, H. F. III; Allen, W. D. *J. Am. Chem. Soc.* **2008**, *130*, 9887.

⁹⁹ Hughes, E. D. *Trans. Faraday Soc.* **1941**, *37*, 603.

¹⁰⁰ Baker, J. W. *Trans. Faraday Soc.* **1941**, *37*, 632. (See especially the discussion beginning on page 643.)

workers summarized data that is inconsistent with either of these mechanisms, however. They also ruled out a third possibility, that the tetrahedral intermediate formed by attachment of a nucleophile to a carbonyl group might form an epoxide, which could react with another nucleophile to form the substitution product (equation 8.33).^{101,102} Instead, Pearson suggested that the increased reactivity of α -halo carbonyl compounds might result from the additional electrostatic attraction of the carbonyl dipole for the approaching nucleophile, a mechanism commonly called *dual attraction* (Figure 8.35).^{103,104}

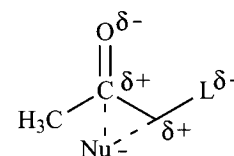
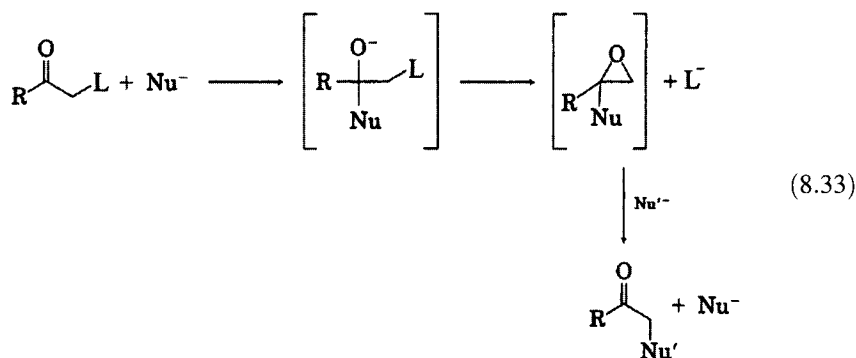
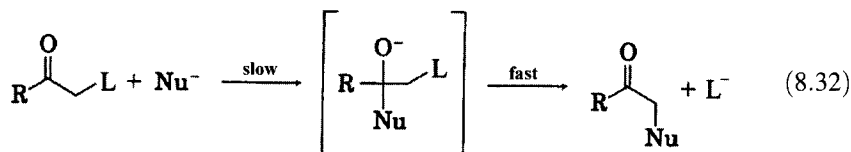


FIGURE 8.35

Dual attraction model for nucleophilic substitution.



Bach and co-workers presented a theoretical analysis suggesting that the enhanced reactivity of α -halo carbonyl compounds arises in part from overlap of the p orbital on C_α that develops in the transition structure with the π orbitals of the carbonyl group. Figure 8.36 shows a similar representation of the basis set orbitals for the transition structure for the $\text{S}_{\text{N}}2$ reaction of chloroacetaldehyde with a nucleophile. The additional reactivity of the α -halocarbonyl system over that of a benzyl system was attributed to the fact that the carbonyl group is more polarizable than the phenyl group. Therefore, the carbonyl group is better able to delocalize the negative charge in the transition structure.¹⁰⁵

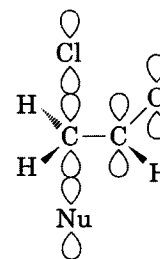


FIGURE 8.36

Basis set orbitals for the $\text{S}_{\text{N}}2$ reaction of chloroacetaldehyde with a nucleophile. (Adapted from reference 105.)

¹⁰¹ Pearson, R. G.; Langer, S. H.; Williams, F. V.; McGuire, W. J. *J. Am. Chem. Soc.* **1952**, *74*, 5130.

¹⁰² An epoxide was isolated and determined to be an intermediate in the hydrolysis of 2-chloro-2-phenylacetophenone by Ward, A. M. *J. Chem. Soc.* **1929**, 1541.

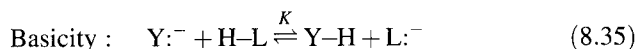
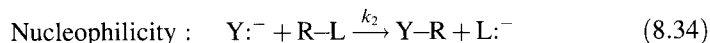
¹⁰³ Eliel, E. L. in Newman, M. S., Ed. *Steric Effects in Organic Chemistry*; John Wiley & Sons: New York, 1956; p. 105.

¹⁰⁴ For a summary and discussion of α - and β -substituent effects on $\text{S}_{\text{N}}2$ reactions, see Shaik, S. S. *J. Am. Chem. Soc.* **1983**, *105*, 4359.

¹⁰⁵ Bach, R. D.; Coddens, B. A.; Wolber, G. J. *J. Org. Chem.* **1986**, *51*, 1030.

Quantitative Measures of Nucleophilicity

Nucleophilicity and basicity are inherently related, because both involve donation of electrons. Although one definition is that a nucleophile is "an electron pair donor, i.e., a Lewis base,"¹⁰⁵ we often consider nucleophilicity to be a *kinetic concept* (equation 8.34), whereas basicity is usually considered to be an *equilibrium concept* (equation 8.35).¹⁰⁶

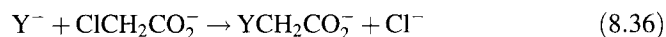


Comparison of the nucleophilicities of species in which the nucleophilic atoms bear the same charge and are in the same column of the periodic table generally shows that nucleophilicity increases with increasing atomic number. For example, H₂S is a better nucleophile than is H₂O. This result is consistent with a model in which the polarizability of the electron cloud increases with atomic size. Greater polarizability is said to enable a nucleophile to form a developing covalent bond without incurring strong repulsive electron-electron interactions with substituents near the site of the nucleophilic attack.¹⁰⁷ On the other hand, sodium hydride, a strong base but a small, nonpolarizable nucleophile, is unreactive in S_N2 reactions.¹⁰⁸ Furthermore, solvation forces are stronger for small nucleophilic ions than for large ones, especially in protic solvents. Consistent with these factors, the order of nucleophilicities of halide ions in protic solvents is I⁻ > Br⁻ > Cl⁻ > F⁻.⁸⁷

There have been many attempts to develop linear free energy relationships for nucleophilicity so that rate constants of substitution reactions could be predicted quantitatively and so that the effects on reactivity of changing reaction conditions could be ascribed to particular aspects of the intermediates involved. This has not been easy to accomplish, however, because at least seventeen different factors have been suggested as contributors to nucleophilic reactivity.^{109,110} The following discussion will highlight some of the more prominent methods that have been proposed. Further details are available in reviews.¹¹¹⁻¹¹³

Brønsted Correlations

One of the earliest correlations of nucleophilicity with basicity was provided by Smith for the reaction of carboxylate ions (Y⁻ = RCO₂⁻ or ArCO₂⁻) with chloroacetate ion.



¹⁰⁶ This "feeling" is ascribed to Swain, C. G.; Scott, C. B. *J. Am. Chem. Soc.* **1953**, *75*, 141, but it was challenged by Edwards, J. O. *J. Am. Chem. Soc.* **1954**, *76*, 1540.

¹⁰⁷ See footnote 9 in reference 101.

¹⁰⁸ Cristol, S. J.; Ragsdale, J. W.; Meek, J. S. *J. Am. Chem. Soc.* **1949**, *71*, 1863.

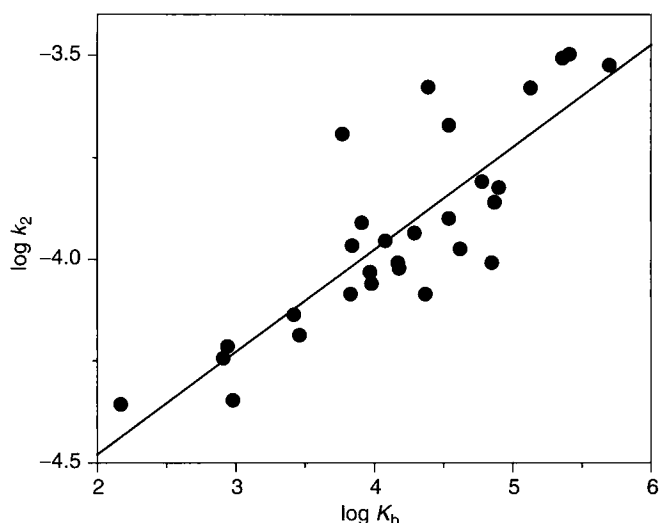
¹⁰⁹ Bunnett, J. F. *Annu. Rev. Phys. Chem.* **1963**, *14*, 271.

¹¹⁰ Pearson, R. G. *J. Org. Chem.* **1987**, *52*, 2131.

¹¹¹ Wells, P. R. *Chem. Rev.* **1963**, *63*, 171.

¹¹² Ibne-Rasa, K. M. *J. Chem. Educ.* **1967**, *44*, 89.

¹¹³ Harris, J. M.; McManus, S. P. in Harris, J. M.; McManus, S. P., Eds. *Nucleophilicity*; American Chemical Society: Washington, DC, 1987; pp. 1-20.

**FIGURE 8.37**

Correlation of nucleophilic reactivity with basicity in the hydrolysis of chloroacetate ion. (Figure based on data in reference 114.)

As shown in Figure 8.37, a reasonably linear correlation of $\log k_2$ versus $\log K_b$ was obtained for this series of nucleophiles.¹¹⁴ Basicity alone cannot explain nucleophilicity, however, as evidenced by reactions in which the nucleophilic atom is different. For example, phenoxide is more than 10^3 times more basic than thiophenoxide, but thiophenoxide is more than 10^4 times more nucleophilic than phenoxide.¹¹⁵ Uggerud concluded that strong bases have large intrinsic barriers for nucleophilic reaction but stabilize the products relative to reactants, so basicity and nucleophilicity are strongly correlated only for highly exothermic reactions.¹¹⁶

Hard–Soft Acid–Base Theory and Nucleophilicity

Pearson and Edwards noted that some substrates in S_N2 reactions seem more susceptible to the Brønsted basicity of a nucleophile, while other substrates seem more susceptible to its polarizability.¹¹⁷ Pearson proposed that bases be divided into two categories: soft (polarizable) and hard (nonpolarizable).¹¹⁸ On the basis of equilibrium data, Pearson concluded that H^+ , Li^+ , Na^+ , Mg^{2+} , and Ca^{2+} are hard acids, while Cu^+ , Ag^+ , Hg^{2+} , I^+ , Br^+ , I_2 , and Br_2 are soft. Pearson noted that hard acids show greater association with hard bases, while soft acids prefer soft bases.¹¹⁹ One explanation for this behavior is the ionic/covalent bond description, in which it is assumed that hard acids and hard bases are attracted primarily through ionic interactions, while soft acids and soft bases associate through covalent bonds. In addition, the two

¹¹⁴ Smith, G. F. *J. Chem. Soc.* **1943**, 521. For the data plotted, the correlation coefficient is only 0.7, but a general trend is evident.

¹¹⁵ Data are for reaction of the two ions with CH_3I in methanol solution. See Pearson, R. G.; Sobel, H.; Songstad, J. *J. Am. Chem. Soc.* **1968**, *90*, 319.

¹¹⁶ Uggerud, E. *Chem. Eur. J.* **2006**, *12*, 1127.

¹¹⁷ Edwards, J. O.; Pearson, R. G. *J. Am. Chem. Soc.* **1962**, *84*, 16.

¹¹⁸ Pearson, R. G. *J. Am. Chem. Soc.* **1963**, *85*, 3533.

¹¹⁹ For a discussion, see Pearson, R. G.; Songstad, J. *J. Am. Chem. Soc.* **1967**, *89*, 1827.

TABLE 8.12 Hardness of Bases

Base	η	Base	η
F ⁻	7.0	HO ⁻	5.6
Cl ⁻	4.7	H ₂ O	7.0
Br ⁻	4.2	HS ⁻	4.1
I ⁻	3.7	H ₂ S	5.3
H ⁻	6.8	H ₂ N ⁻	5.3
CH ₃ ⁻	4.0	H ₃ N	6.9

Source: Reference 121.

types of acids are expected to differ with regard to π -bonding possibilities. Solvation is generally said to "soften" both hard and soft acids.¹²⁰

Pearson applied the concept of hard and soft acids and bases to nucleophilicity in the S_N2 reaction by using the concept of absolute hardness, η .^{110,121}

$$\eta = \frac{I-A}{2} = \frac{1}{\sigma} \quad (8.37)$$

Here, A is the electron affinity and I is the gas phase ionization potential of the acid under consideration. "Absolute softness," σ , is the inverse of η . The term $I - A$ is a measure of the energy gap between the LUMO and the HOMO calculated for a π system in MO theory, so this term is equivalent to the polarizability term used previously to define hardness or softness. Selected values of η are shown in Table 8.12. This approach is somewhat more successful at predicting relative reactivities (such as the increasing ratio of the reactivity of CH₃I relative to CH₃F as the hardness of the base increases) and in explaining solvent effects on reactivity.¹¹⁰ One clear example of the utility of the theory is its ability to explain why nucleophiles such as *p*-toluenesulfonate react with the oxygen serving as the nucleophile with hard acids (to give an ester) but with the sulfur serving as the nucleophile with soft acids (to produce a sulfone).¹²² In general, however, the hard-soft acid-base theory has been more widely used to explain the reactions of coordination compounds than to describe reactivity in organic substitution reactions quantitatively.

Edwards Equations

Edwards attempted to improve the correlation of nucleophilicity with substrate reactivity by considering separately two different components of nucleophilic reactivity. Two equations were presented, and the distinction between them is not always clear in the literature. In deriving equation 8.38, Edwards noted that basicity is only one measure of a nucleophile's tendency to donate electrons, the other being its oxidation potential.¹²³ To the extent that the transition structure for an S_N2 reaction resembles a partially oxidized

¹²⁰ Hard and soft acid and base theory was not universally accepted by organic chemists. For example, Parker noted the reversal of nucleophilicity of halide ions in protic and nonprotic solvents, adding that "one cannot sensibly claim that saturated carbon is 'soft' in protic solvents and 'hard' in dipolar solvents, and yet this is required if the hard acids-soft bases theory is to be applied to this observation" (reference 80).

¹²¹ Parr, R. G.; Pearson, R. G. *J. Am. Chem. Soc.* **1983**, *105*, 7512.

¹²² Meek, J. S.; Fowler, J. S. *J. Org. Chem.* **1968**, *33*, 3422.

¹²³ Edwards, J. O. *J. Am. Chem. Soc.* **1954**, *76*, 1540.

species, the oxidation potential may be correlated with nucleophilic reactivity. Moreover, he suggested that different substrates might require different contributions from basicity and from oxidation of the nucleophile. Therefore, Edwards wrote that

$$\log(k/k_0) = \alpha E_n + \beta H \quad (8.38)$$

As before, k and k_0 are the rate constants for a nucleophile n and of a standard nucleophile (chosen as H_2O), respectively. H is a measure of the basicity of the nucleophile,

$$H = \text{p}K_a + 1.74 \quad (8.39)$$

where the $\text{p}K_a$ is that of the conjugate acid of the nucleophile. E_n is related to the oxidation potential of the nucleophile (Y^-) in the reaction



by the relationship

$$E_n = E_0 + 2.60 \quad (8.41)$$

The parameters α and β then relate the sensitivity of the substrate to each of these measures of nucleophilicity.¹²⁴

Application of equation 8.38 led to situations in which β was found to be negative for some substrates. The most satisfying explanation for this result was that the parameters E_n and H are not totally separable because factors that determine basicity can also influence the electrochemical properties of the nucleophile. To preserve the two-parameter nucleophilicity equation, Edwards proposed equation 8.42, in which substrate reactivity is correlated with the basicity (B) and polarizability (P) of the nucleophile.¹²⁵ This equation is often written as $\log(k/k_0) = \alpha P + \beta H$.¹¹⁷ Thus, it is sometimes difficult to know whether the Edwards parameters refer to the original α and β definitions or to the new A and B terms.

$$\log(k/k_0) = AP + BH \quad (8.42)$$

Swain–Scott Equation

Swain and Scott developed a linear free energy relationship for nucleophilicity (equation 8.43) in the same form as the Hammett equation.

$$\log(k_n/k_0) = sn \quad (8.43)$$

The term n is the nucleophilicity parameter for a given nucleophile, while s is the measure of the sensitivity of the substrate to the nucleophilicity of the attacking reagent. The rate constants k_n and k_0 are the rate constants for reaction of the nucleophile and of water, respectively, and the n value of water

¹²⁴ Equation 8.38 has been called an *oxibase scale*, since the E_n term is an oxidation term, while the H term is a basicity term: Davis, R. E. in Janssen, M. J., Ed. *Organosulfur Chemistry*; Wiley-Interscience: New York, 1967; pp. 311–328.

¹²⁵ The relationships $A = \alpha a$ and $B = \beta + \alpha b$ may be used to convert equation 8.38 to equation 8.42: Edwards, J. O. *J. Am. Chem. Soc.* **1956**, *78*, 1819.

TABLE 8.13 Selected Values of Swain Nucleophilicity Parameter, n

Nucleophile	n	Nucleophile	n
H ₂ O	0.00	NO ₃ ⁻	1.03
2,4,6-(NO ₂) ₃ C ₆ H ₂ O ⁻	1.9	Cl ⁻	2.70
HCO ₂ ⁻	2.75	C ₆ H ₅ O ⁻	3.5
Br ⁻	3.53	HCO ₃ ⁻	3.8
N ₃ ⁻	4.00	HO ⁻	4.20
I ⁻	5.04	HS ⁻	5.1
NC ⁻	5.1		

Source: Reference 111.

TABLE 8.14 Selected Values of Swain–Scott s Value

Substrate	s	Substrate	s
Methyl bromide	1.00	Benzenesulfonyl chloride	1.25
Ethyl iodide	1.15	Benzoyl chloride	1.43
Chloroacetate	1.0	β-Propionolactone	0.77
Bromoacetate	1.1	Ethylene-β-chloroethylsulfonium	0.95
Iodoacetate	1.33	Ethyl tosylate	0.66
Benzyl chloride	0.87	Trityl fluoride	0.61

Source: Reference 111.

was taken to be 1.0.¹²⁶ Both n and s values are determined empirically and are not related to other parameters. Table 8.13 shows the n values determined for the reaction of methyl bromide with various nucleophiles, and Table 8.14 collects some values of s .¹²⁷ Note that n values are logarithmic values. For example, iodide ion is 100,000 times more reactive than water.

The format of the Swain–Scott equation implies that the relative nucleophilicity of a nucleophile is invariant, that is, it is not a function of the substrate. As Ibne-Rasa noted, the success of the Swain–Scott equation is greatest for nucleophilic reactions involving attack on a tetrasubstituted carbon atom.¹¹² The deviations from linearity in the determination of s were severe in other cases. The conclusion may be that the Swain–Scott n values are most properly denoted as n_C values (for attack on a tetravalent carbon atom) and that different n values (n_H for attack on hydrogen, n_{Ar} for attack on an aromatic carbon atom, etc.) would need to be devised for individual systems.¹¹²

Mayr Equations

Mayr and co-workers developed an expression for the prediction of nucleophilic reactivity that considers both the nature of the nucleophile and the nature of the electrophile (equation 8.44). Here k is the rate constant for the

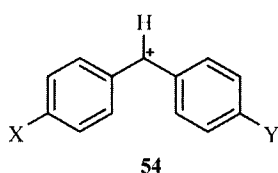
¹²⁶ Swain, C. G.; Scott, C. B. *J. Am. Chem. Soc.* **1953**, *75*, 141; Swain, C. G.; Dittmer, D. C. *J. Am. Chem. Soc.* **1953**, *75*, 4627; Swain, C. G.; Mosley, R. B. *J. Am. Chem. Soc.* **1955**, *77*, 3727; Swain, C. G.; Mosley, R. B.; Brown, D. E. *J. Am. Chem. Soc.* **1955**, *77*, 3731; Swain, C. G.; Dittmer, D. C.; Kaiser, L. E. *J. Am. Chem. Soc.* **1955**, *77*, 3737.

¹²⁷ Data from the compilation by Wells (reference 111) and references therein. A summary is also given by Gordon, A. J.; Ford, R. A. *The Chemist's Companion*; Wiley-Interscience: New York, 1972; p. 151.

reaction, s_N is a nucleophile-specific slope parameter, N is a nucleophilicity parameter, and E is a nucleophile-independent electrophilicity parameter.¹²⁸

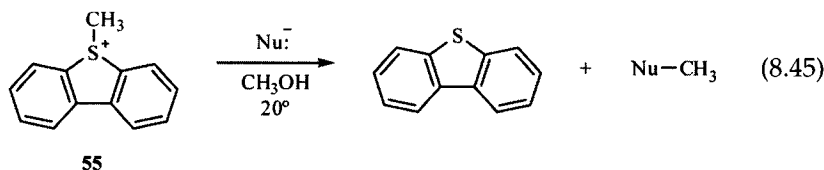
$$\log k = s_N(N + E) \quad (8.44)$$

The scale was developed using a series of benzhydrylium ions having the general structure **54**, where the E value was taken to be 0.00 for system with both X and $Y = \text{OCH}_3$. This system allowed the study of a wide range of reactivity, because the E value for **54** having X and $Y = \text{Cl}$ is 6.0, while that for **54** with X and $Y = \text{N}(\text{CH}_3)_2$ is -7.4 . The nucleophiles in the initial study were all π -nucleophiles, and the nucleophile-specific slope parameter was chosen to be 1.00 for the case of 2-methyl-1-pentene, which was found to have an N value of 0.96. Each nucleophile is identified with both an N and an s_N value, so the listing for 2-methyl-1-pentene is 0.96 (1.00).



This approach was subsequently extended to the determination of the electrophilicities of other cations, such as metal-coordinated cations, electron-deficient alkenes, and arenes. Moreover, the method has been used to study the nucleophilicities of alkynes, ethers, enamines, delocalized carbanions, alcohols, alkoxides, metal- π -complexes, hydride donors, and amines as well as aqueous and alcoholic solvent systems.¹²⁹⁻¹³¹

Mayr and co-workers further extended the method by studying reactions of nucleophiles with the *S*-methylthiophenium ion (**55**, equation 8.45).¹³¹ The investigators plotted values of $(\log k)/s_N$ versus N for a series of nucleophiles and solvents reacting with **55** and obtained a linear correlation with slope 0.6. A subset of the experimental data is shown in Table 8.15 and plotted in Figure 8.38. The results indicated that the reaction of **55** with nucleophiles is affected only 60% as much by the nucleophilicity of the nucleophile as is the reaction of **54**.



¹²⁸ Mayr, H.; Patz, M. *Angew. Chem. Int. Ed. Engl.* **1994**, 938.

¹²⁹ Mayr, H.; Bug, T.; Gotta, M. F.; Hering, N.; Irrgang, B.; Janker, B.; Kempf, B.; Loos, R.; Ofial, A. R.; Remennikov, G.; Schimmel, H. *J. Am. Chem. Soc.* **2001**, 123, 9500.

¹³⁰ Brotzel, F.; Chu, Y. C.; Mayr, H. *J. Org. Chem.* **2007**, 72, 3679.

¹³¹ Phan, T. B.; Breugst, M.; Mayr, H. *Angew. Chem. Int. Ed.* **2006**, 45, 3869 and references therein.

TABLE 8.15 Selected Values of Mayr Nucleophilicity Parameters and Kinetic Data for Reactions of 55

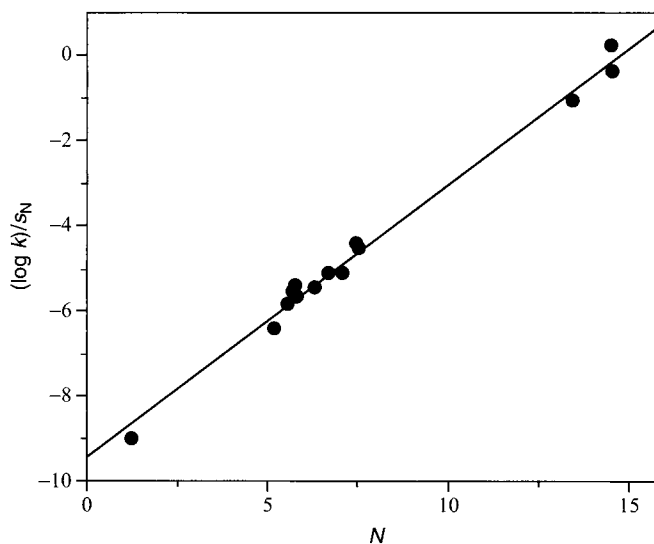
Nucleophile	N	s_N	k
Azide	14.54	0.822	5.08×10^{-1g}
Methoxide	14.51	0.68	1.5^g
Benzylamine	13.46	0.624	2.25×10^{-1g}
<i>n</i> -Propylamine	13.41	0.657	2.01×10^{-1g}
Methanol	7.54	0.92	7.23×10^{-5g}
Ethanol	7.44	0.9	1.14×10^{-4g}
1-Propanol	7.05	0.8	8.50×10^{-5g}
80E 20W ^a	6.68	0.85	4.84×10^{-5h}
60E 40W ^b	6.28	0.87	1.99×10^{-5h}
40E 60W ^c	5.81	0.9	8.91×10^{-6h}
80A 20W ^d	5.77	0.87	2.06×10^{-5h}
90A 10W ^e	5.7	0.85	2.14×10^{-5h}
20E 80W ^f	5.54	0.94	3.32×10^{-6h}
Water	5.2	0.89	2.03×10^{-6h}
2,2,2-Trifluoroethanol	1.23	0.92	5.66×10^{-9h}

^a 80% Ethanol–20% water (v/v).^b 60% Ethanol–40% water (v/v).^c 40% Ethanol–60% water (v/v).^d 80% Acetone–20% water (v/v).^e 90% Acetone–10% water (v/v).^f 20% Ethanol–80% water (v/v).^g Second-order rate constant ($M^{-1} s^{-1}$) in methanol at 20°C.^h First-order rate constant at 25°C.

These results suggested that it should be possible to elaborate equation 8.44 in the form of equation 8.46. Here s_E is an electrophile-specific slope parameter (0.6 for 55), and the other parameters have the same meaning as in equation 8.44.

$$\log k = s_E s_N (N + E) \quad (8.46)$$

One interesting aspect of equation 8.46 is that it can be shown to incorporate both the Ritchie equation (equation 8.21, page 479) and the Swain–Scott

**FIGURE 8.38**

Determination of s_E of 55 using kinetic data for nucleophiles in Table 8.15.

equation (equation 8.43, page 507).¹³¹ Making the assumption that s_N is about 0.6 for most *n*-nucleophiles (those that donate nonbonded electrons to an electrophile) reduces equation 8.46 to equation 8.47,

$$\log k = 0.6s_E E + 0.6s_E N \quad (8.47)$$

which can be rewritten as equation 8.48:

$$\log k = \log k_0 + 0.6s_E N \quad (8.48)$$

In turn, equation 8.48 can be rearranged to have the form of the Swain–Scott equation (equation 8.49):

$$\log k - \log k_0 = \log \frac{k}{k_0} = s'_E N \quad (8.49)$$

Making the additional assumption that s_E is about 1 for most carbocations reduces equation 8.46 to equation 8.50,

$$\log k = 0.6N + 0.6E \quad (8.50)$$

which can be rewritten (equation 8.51) in the form of the Ritchie equation. In the systems reported so far, either the electrophile or the nucleophile (or both) has a carbon at the reaction center. More work remains before this approach can be applied with confidence to other nucleophile–electrophile systems.^{131,132}

$$\log k - 0.6E = \log k - \log k_0 = \log \frac{k}{k_0} = 0.6N = N_+ \quad (8.51)$$

Finally, it is interesting that equation 8.46 has the form of a general relationship between the kinetics of nucleophilic substitution reactions and the empirical nucleophilicity and electrophilicity parameters of the reactants. Since most organic reactions may be considered to be combinations of nucleophiles with electrophiles, equation 8.46—if validated for the great diversity of reaction possibilities—might be considered the prototype of a general equation to describe organic reactivity.¹³³

The α Effect

Subsequent to the work of Edwards, it was shown that some anions are more nucleophilic than would be expected on the basis of *P* and *H* values.¹³⁴ These nucleophiles are characterized by the formula: Z–Y, where: Z represents a relatively electronegative atom with an unshared pair of electrons that is adjacent (α) to a nucleophilic atom, Y. For example, the basicity of hydroxide (HO[−]) is about 16,000 times greater than that of hydroperoxide (HOO[−]), but hydroperoxide is more than 200 times as nucleophilic as hydroxide in

¹³² Mayr, H.; Ofial, A. R. *J. Phys. Org. Chem.* **2008**, *21*, 584.

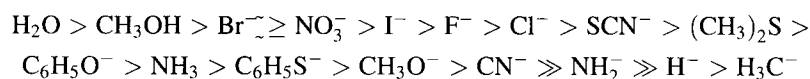
¹³³ Mayr, H.; Ofial, A. R. *Pure Appl. Chem.* **2005**, *77*, 1807.

¹³⁴ Jencks, W. P.; Carriuolo, J. J. *Am. Chem. Soc.* **1960**, *82*, 1778.

addition reactions to carbonyl groups.¹³⁵ This enhanced nucleophilicity of species such as HOO^- has been called the α effect, and a number of investigators have explored its origins.¹³⁶ One theoretical explanation was the proposal by Ibne-Rasa and Edwards that the presence of α -nonbonded electrons destabilizes the nucleophile in the ground state, thus lowering the activation energy.¹³⁷ DuPuy found that HOO^- is less reactive than HO^- for reaction with CH_3F in the gas phase, however, and calculations by Jorgensen indicated that HOO^- should be less reactive than HO^- for reaction with methyl chloride in the gas phase.^{138,139} The origins of the α effect are complex and are not completely understood. Some investigators suggested that the apparently greater reactivity of HOO^- than HO^- in solution could be due to solvation effects,¹⁴⁰⁻¹⁴² but others have concluded that effects on the energy of the transition state may be most important.¹⁴³

Leaving Group Effects in $\text{S}_{\text{N}}2$ Reactions

One of the common generalizations about substitution reactions is that the more stable the detached leaving group (usually an anion or neutral molecule), the greater will be its **nucleofugality** (kinetic leaving group ability). For example, an important principle in the reactions of alcohols is that C–O bonds are broken more easily in substitution reactions when the oxygen atom departs as a weaker base (such as water or tosylate ion) than when the oxygen departs as a strong base (such as hydroxide ion). Such observations give rise to the general statement that the activation energy for the $\text{S}_{\text{N}}2$ reaction decreases as the basicity of the leaving group decreases.¹⁴⁴ Pearson determined theoretically that the order of nucleofugality should therefore be¹²⁹



Just as nucleophiles can interact differently with protic and dipolar aprotic solvents, so can leaving groups, and solvation energies can affect the energies of transition states. The data in Table 8.16 show considerable variation in the experimental values for the relative rate constants for reaction of methyl derivatives with a series of nucleophiles, Y^- . For example, methyl tosylate reacts with azide ion nearly ten times faster than methyl iodide in

¹³⁵ Edwards, J. O.; Pearson, R. G. *J. Am. Chem. Soc.* **1962**, *84*, 16.

¹³⁶ One review concluded that “the sources of the α -effect are remarkable in their ambiguity.” Hoz, S.; Buncl, E. *Israel J. Chem.* **1985**, *26*, 313.

¹³⁷ Ibne-Rasa, K. M.; Edwards, J. O. *J. Am. Chem. Soc.* **1962**, *84*, 763.

¹³⁸ DePuy, C. H.; Della, E. W.; Filley, J.; Grabowski, J. J.; Bierbaum, V. M. *J. Am. Chem. Soc.* **1983**, *105*, 2481.

¹³⁹ Evanseck, J. D.; Blake, J. F.; Jorgensen, W. L. *J. Am. Chem. Soc.* **1987**, *109*, 2349.

¹⁴⁰ See also Gao, J.; Garner, D. S.; Jorgensen, W. L. *J. Am. Chem. Soc.* **1986**, *108*, 4784.

¹⁴¹ Hudson, R. F.; Hansell, D. P.; Wolfe, S.; Mitchell, D. J. *J. Chem. Soc. Chem. Commun.* **1985**, 1406.

¹⁴² Hudson, R. F. in reference 113, p. 195.

¹⁴³ Um, I.-H.; Hwang, S.-J.; Buncl, E. *J. Org. Chem.* **2006**, *71*, 915; Ren, Y.; Yamataka, H. *Org. Lett.* **2006**, *8*, 119; *J. Org. Chem.* **2007**, *72*, 5660.

¹⁴⁴ This correlation has been called an “illusion” based on inadequate and perhaps unobtainable data: Stirling, C. J. M. *Acc. Chem. Res.* **1979**, *12*, 198.

TABLE 8.16 Relative Rate Constants of S_N2 Reactions of CH₃L

Y ⁻	Solvent	log [k(CH ₃ L)/k(CH ₃ I)]				
		L = Cl	Br	I	OTs	Me ₂ S ⁺
N ₃ ⁻	CH ₃ OH	-2.0	-0.2	0.0	+0.8	-3.3
	DMF	-3.3	-0.9	0.0	-1.8	-4.8
Cl ⁻	CH ₃ OH	—	+0.3	0.0	+0.4	—
	DMF	—	-0.8	0.0	-1.7	—

Source: Reference 80.

methanol, but methyl iodide reacts with azide ion nearly 100 times faster than methyl tosylate in DMF.

Mayr and co-workers extended their investigations of nucleophilicity and basicity scales to the development of a scale of nucleofugality as well. They found that kinetic data could be correlated with a relationship in the form of equation 8.52.¹⁴⁵

$$\log k_{25^\circ} = s_f(N_f + E_f) \quad (8.52)$$

Here s_f and N_f are nucleofuge-specific parameters, and E_f is an electrofuge-specific parameter. It is important to note that these nucleofugality parameters are a function of both the leaving group and the solvent. Selected values of N_f and s_f are listed in Table 8.17.

Aliphatic Substitution and Single Electron Transfer

The discussion so far has considered only heterolytic processes for substitution reactions, but there is increasing evidence that substitutions may take place by a single electron shift synchronous with bond displacement or by a **single electron transfer** (SET) pathway in which electron transfer precedes bond displacement.¹⁴⁶ To understand the basis of this theory, it is useful to discuss a conceptual model for organic reactions that has been called the valence bond configuration mixing (VBCM) model.^{147,148} As described by

TABLE 8.17 Values of N_f (s_f) for Selected Leaving Groups and Solvents

L	Solvent System			
	90% Acetone-10% Water (v/v)	CH ₃ CH ₂ OH	CH ₃ OH	CF ₃ CH ₂ OH
OTs	5.42 (0.89)	6.05 (0.75)	—	9.82 (0.89)
Br	2.31 (1.00)	2.97 (0.92)	4.27 (0.98)	6.20 (0.92)
Cl	0.69 (0.99)	1.87 (1.00)	2.95 (0.98)	5.56 (0.82)
CF ₃ CO ₂	0.12 (0.94)	0.30 (1.10)	—	—

¹⁴⁵ Denegri, B.; Streiter, A.; Jurić, S.; Ofial, A. R.; Kronja, O.; Mayr, H. *Chem. Eur. J.* **2006**, *12*, 1648.

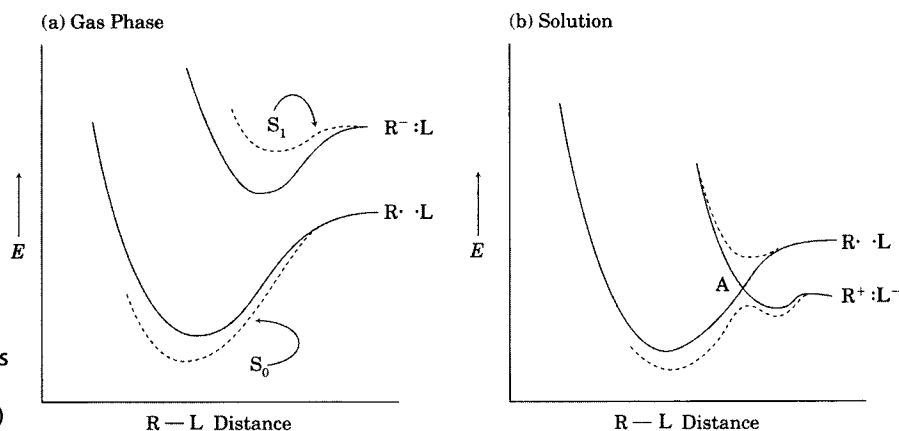
¹⁴⁶ For a review, see Shaik, S. S. *Acta Chem. Scand.* **1990**, *44*, 205.

¹⁴⁷ Shaik, S. S. *J. Am. Chem. Soc.* **1981**, *103*, 3692.

¹⁴⁸ Pross, A.; Shaik, S. S. *Acc. Chem. Res.* **1983**, *16*, 363 and references therein.

FIGURE 8.39

Energy diagrams for homolytic and heterolytic dissociation: (a) gas phase and (b) solution. (Reproduced from reference 148.)



Pross and Shaik, the method is based on an analysis of the energies of all possible valence bond configurations of the reactants and products as a function of the reaction coordinate.

Consider the homolysis of a polar covalent R–L bond in the gas phase and in solution (Figure 8.39). The ground electronic state (denoted S_0) of R–L is described by equation 8.53, in which the polar bond is considered to result from mixing of two configurations, one nonpolar and the other polar. It is also useful to describe the first electronically excited state (S_1) by equation 8.54, in which the polar character is dominant, although there is some mixing of nonpolar character as well.¹⁴⁹ Figure 8.39(a) shows the calculated energies of the pure nonpolar and polar configurations (solid lines) as a function of the R–L bond distance as well as the energies of S_0 and S_1 (dashed lines) when mixing is included.

$$(\text{R-L})_{S_0} \approx (\text{R} \cdot \cdot \text{L}) + \lambda(\text{R}^+ \cdot \text{L}^-) \quad (8.53)$$

$$(\text{R-L})_{S_1} \approx (\text{R}^+ \cdot \text{L}^-) - \lambda'(\text{R} \cdot \cdot \text{L}) \quad (8.54)$$

where

$$(\text{R-L}) = \left(1/\sqrt{2}\right)[(\text{R}\uparrow\downarrow\text{L}) \leftrightarrow (\text{R}\downarrow\uparrow\text{L})] \quad (8.55)$$

In solution the energy of ionic states is reduced by solvation, so the two solid curves cross as shown in Figure 8.39(b). The mixing of the two states prevents their crossing, so the energies of the two states in solution are described by the dashed curves.^{148,150} Figure 8.39(b) thus suggests that stretching of the R–L bond leads at first to a slight *decrease* in polarity until the energy maximum (at the avoided crossing) is reached, then to an *increase*

¹⁴⁹ Electronically excited states are discussed in Chapter 12.

¹⁵⁰ Such *avoided crossings* are discussed in Chapter 11.

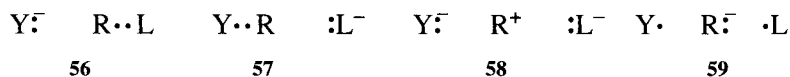
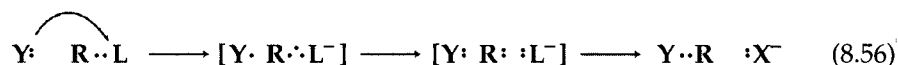


FIGURE 8.40

Valence bond representations of reactant (56), product (57), and possible intermediate configurations for a substitution reaction (58 and 59).

in polarity as ions are formed. This increase in polarity is effectively brought about by a *single* electron shift from R· to ·L in the developing R·L configuration to form the R⁺:L⁻ configuration.

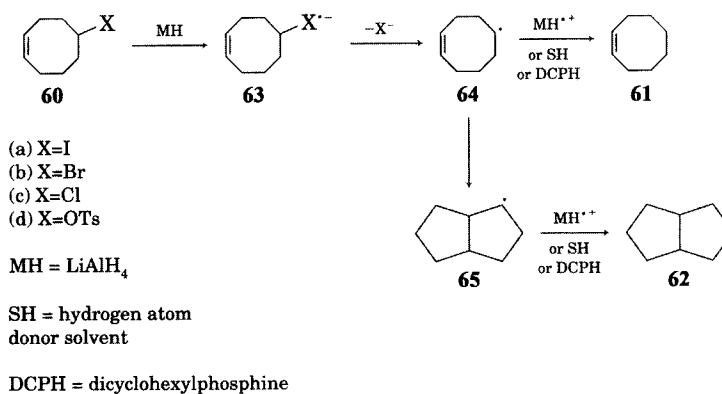
Now let us apply this model to a nucleophilic substitution reaction in which the R–L bond is broken and a new bond is formed from R to a nucleophile, Y (which is present initially as the nucleophilic anion, Y⁻). We can define valence bond representations 56, 57, 58, and 59 (Figure 8.40), where 56 is the reactant configuration, 57 is the product configuration, and 58 and 59 are species with positive and negative charge, respectively, on the carbon atom at the site of the substitution. Pross and Shaik used these descriptions to illustrate their suggestion that S_N2 reactions involve a single electron shift, as indicated in equation 8.56. There is an analogy to this mechanism in the electrochemical reduction of alkyl halides. Reduction of methyl halide apparently adds an electron to the σ_{R-L}^{*} orbital, and that leads to dissociation of the radical anion to a methyl radical and a halide ion, R· and L⁻.¹⁴⁴ In SET reactions, the R· may bond with Y· so rapidly that free radicals are not observed outside the solvent cage.



Even though long-lived radicals need not be formed in S_N2 reactions that proceed by the SET pathway, evidence for radical intermediates was found in some cases by using diagnostic tools such as cyclizable radical probes, radical traps, and chiral alkyl halides. These studies have suggested that the extent of single electron transfer is a function of the substrate, the leaving group, the solvent, and the reducing agent.¹⁵¹ Cyclizable radical probes were particularly useful in these studies. For example, the reduction of alkyl halides by LiAlH₄ had long been considered to be an S_N2 reaction because inversion of configuration was observed in the reduction of (+)-1-chloro-1-phenylethane with LiAlD₄.¹⁵² When 5-substituted cyclooctenes, 60a–60d, were reduced with LiAlH₄, the product mixture was a function of the substituent. In addition to cyclooctene (61), a significant amount of bicyclo[3.3.0]octane (62) was formed in reactions of the iodide and bromide, but not with the chloride and tosylate (Figure 8.41). The results suggested that when the carbon–halogen bond is easily reduced, single electron transfer leads to the radical anion 63, which loses an anion to form 4-cyclooctenyl radical (64). In

¹⁵¹ Ashby, E. C.; DePriest, R. N.; Goel, A. B.; Wenderoth, B.; Pham, T. N. *J. Org. Chem.* **1984**, *49*, 3545.

¹⁵² Eliel, E. L. *J. Am. Chem. Soc.* **1949**, *71*, 3970.

**FIGURE 8.41**

Evidence for SET in the metal hydride reduction of 5-halocyclooctenes. (Adapted from reference 153; not all processes are shown.)

turn, **64** cyclizes to **65**, which abstracts a hydrogen atom from solvent to form **62**.^{153,154}

Other studies also indicated SET behavior in substitution reactions. As shown in Figure 8.42, SET reduction of 6-iodo-5,5-dimethyl-1-hexene (**66**) can lead to a radical capable of cyclization to a five-membered ring. Both the initial and cyclized radicals can react with a radical (from the nucleophile) in the solvent cage to produce substitution products or can abstract a hydrogen atom from solvent to give reduction products. In the case of reduction of **66** with LiAlH₄ in solvents in which only protium is abstractable, products **67** and **68** are identical, as are products **69** and **70**. When the reduction was carried out with LiAlD₄ in a nondeuterated solvent, however, those pairs of products were isotopically different and could be distinguished. In a study of the reduction of **66** with LiAlD₄ in a nondeuterated solvent, it was found that 31% of the noncyclized product was the nondeuterated **68**. Formation of this product is most simply explained by a mechanism involving abstraction of protium from solvent by the radical formed through single electron transfer.¹⁵²

Leaving group effects can also distinguish between S_N2 and SET processes. For alkyl halides, the relative reactivity in S_N2 reactions is I ≈ OTs > Br > Cl, while relative reactivity in SET processes is I > Br > Cl > OTs.¹⁵⁵ For reduction of cyclizable 2° alkyl derivatives, it appears that the tosylates and chlorides undergo reduction only by an S_N2 pathway, that the bromides give mostly S_N2 reduction (but some SET reduction also occurs), and the iodides undergo significant SET reactions. With stronger one-electron donors, such as (CH₃)₃Sn⁻, even alkyl chlorides can undergo SET reaction.¹⁵⁶ Stereochemical

¹⁵³ Ashby, E. C.; Pham, T. N. *J. Org. Chem.* **1986**, *51*, 3598.

¹⁵⁴ Ashby, E. C.; Argyropoulos, J. N. *J. Org. Chem.* **1985**, *50*, 3274 also found that the enolate of propiophenone reacts with 1-iodo-2,2-dimethyl-5-hexene to give a number of products, including a significant yield of the cyclized products expected if single electron transfer and halide loss produce an alkyl radical intermediate. Cyclization was not observed with the corresponding bromide or chloride. The results suggest that the apparent S_N2 reaction of enolates with alkyl halides proceeds with some amount of single electron transfer, the degree depending on the leaving group. Bordwell, F. G.; Wilson, C. A. *J. Am. Chem. Soc.* **1987**, *109*, 5470 found evidence for SET in one system when the redox potentials of the nucleophile and substrate are favorable and when steric hindrance inhibits the two-electron S_N2 reaction.

¹⁵⁵ Ashby, E. C.; Park, B.; Patil, G. S.; Gadru, K.; Gurumurthy, R. *J. Org. Chem.* **1993**, *58*, 424.

¹⁵⁶ Ashby, E. C.; Pham, T. N.; Amrollah-Madjdabadi, A. *J. Org. Chem.* **1991**, *56*, 1596.

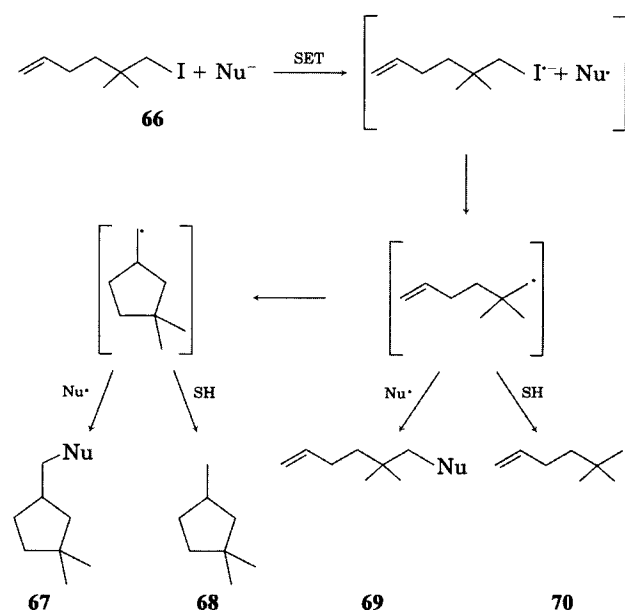


FIGURE 8.42
Product formation in SET reaction with a cyclizable probe.

studies reinforce these conclusions. A study of the reduction of optically active 2-octyl derivatives with LiAlH₄ indicated that reduction of the iodide occurs with racemization but that the tosylate, chloride, and bromide react with inversion of configuration.^{147,157} The more easily reduced alkyl geminal dichlorides do undergo SET reaction with LiAlH₄.¹⁵⁸

It must be emphasized that isomerization of a probe can be taken as positive evidence for a radical intermediate in a substitution reaction, but failure to observe cyclization with such a probe does not rule out a radical intermediate. For example, reaction of 6-bromo-1-hexene with NaSN(CH₃)₃ in THF was found not to produce cyclized product.¹⁵⁹ Cyclized product was observed when the same reaction was carried out in 1:1 THF-pentane, however.¹⁶⁰ These results suggested that cyclization of the radical probe occurs outside the solvent cage in which it is formed and that a lower viscosity solvent allows more radicals to diffuse from the radical cage so that cyclization can occur.

There may be varying degrees of single electron transfer and Y-R bond formation in substitution reactions.¹⁶¹ One may view the "pure" SET process represented by the solid line marked SET on Figure 8.43 as a limiting case in

¹⁵⁷ Ashby, E. C.; DePriest, R. N.; Pham, T. N. *Tetrahedron Lett.* **1983**, 24, 2825.

¹⁵⁸ Ashby, E. C.; Deshpande, A. K. *J. Org. Chem.* **1994**, 59, 3798.

¹⁵⁹ Park, S.-U.; Chung, S.-K.; Newcomb, M. J. *J. Org. Chem.* **1987**, 52, 3275.

¹⁶⁰ (a) Ashby, E. C.; Su, W.-Y.; Pham, T. *Organometallics* **1985**, 4, 1493; (b) Tolbert, L. M.; Sun, X.-J.; Ashby, E. C. *J. Am. Chem. Soc.* **1995**, 117, 2861.

¹⁶¹ In addition to references cited above, leading references include (a) Pross, A. *Acc. Chem. Res.* **1985**, 18, 212; (b) Shaik, S. S. *J. Am. Chem. Soc.* **1984**, 106, 1227; (c) McLennan, D. J.; Pross, A. *J. Chem. Soc. Perkin Trans. 2* **1984**, 981; (d) Shaik, S. S. *Prog. Phys. Org. Chem.* **1985**, 15, 197; *Acta Chem. Scand.* **1990**, 44, 205 and references therein; (e) Shaik, S. S. *Israel J. Chem.* **1985**, 26, 367; (f) Shaik, S.; Ioffe, A.; Reddy, A. C.; Pross, A. *J. Am. Chem. Soc.* **1994**, 116, 262; (g) Shaik, S. S.; Schlegel, H. B.; Wolfe, S. *Theoretical Aspects of Physical Organic Chemistry: The S_N2 Mechanism*; Wiley-Interscience: New York, 1992. See also Perrin, C. L. *J. Phys. Chem.* **1984**, 88, 3611.

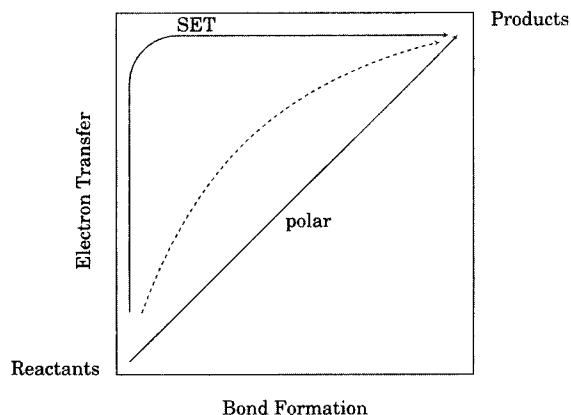


FIGURE 8.43
Relationship between polar and SET pathways. (Reproduced from reference 161a.)

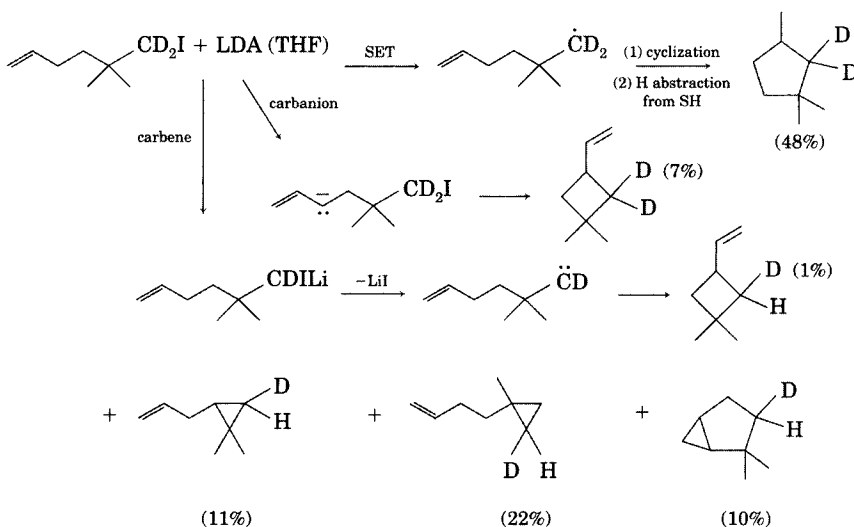


FIGURE 8.44
Competing radical, carbanion, and carbene pathways in the reaction of 6-iodo-5,5-dimethyl-1-hexene with LDA in THF. (Adapted from reference 155.)

which one electron is completely transferred from Y^- to $R-L$ before the $R-L$ bond dissociation occurs. An alternative limiting case is one in which the electron transfer occurs simultaneously with $Y-R$ bond formation (the diagonal line), meaning a “pure” or “classical” two-electron S_N2 process. The dashed line in Figure 8.43 suggests one of a continuum of possible transition states, ranging from pure SET to pure “polar.”

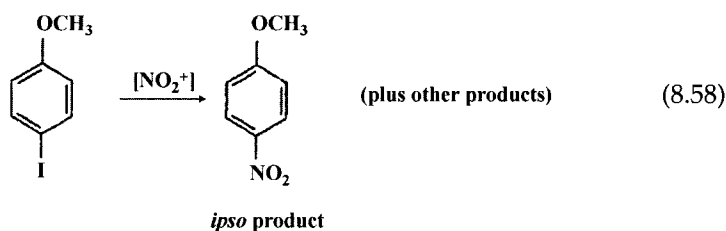
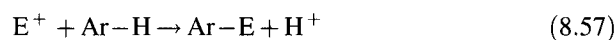
Although this discussion has emphasized the competition between SET and S_N2 processes, other pathways are also possible in the reaction of alkyl halides with reagents that are strong bases and electron donors. For example, in the case of reduction of 6-iodo-5,5-dimethyl-1-hexene with lithium diisopropylamide (LDA) in THF, products resulting from competing radical, carbanion, and carbene pathways were identified (Figure 8.44).¹⁵¹

8.3 ELECTROPHILIC AROMATIC SUBSTITUTION

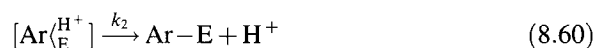
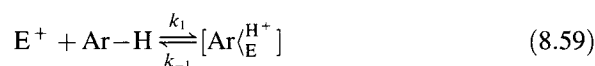
The S_EAr Reaction

Electrophilic aromatic substitution (S_EAr) involves reaction of an electrophile, E^+ , with an aromatic compound to produce a substituted aromatic

compound. As shown in equation 8.57, this substitution usually displaces a proton from the aromatic ring, but that is not always the case. In *ipso* substitution there is replacement of another substituent, as is illustrated in equation 8.58.



If equation 8.57 represents a one-step process, then a primary hydrogen kinetic isotope effect should be observed for the reaction. In most cases, however, $k_{\text{H}}/k_{\text{D}}$ is near unity for typical $\text{S}_{\text{E}}\text{Ar}$ reactions such as nitration or bromination.¹⁶²⁻¹⁶⁵ Therefore, we surmise that the loss of the C–H bond usually does not occur in the rate-limiting step. Since two essential processes in the reaction are formation of a bond between E^+ and a carbon atom in the aromatic ring and the loss of a proton from the same carbon atom, a minimum kinetic formulation consistent with the data is the following two-step process



with the first step being rate limiting (i.e., $k_2 \gg k_{-1}$) for most reactions. This would give rise to the reaction coordinate diagram shown in Figure 8.45.

The simple mechanism represented in equations 8.45 and 8.46 underestimates the complexity of the $\text{S}_{\text{E}}\text{Ar}$ reaction. First, generation of the electrophile may be a multistep process with equilibria that vary according to reagents and experimental conditions.¹⁶⁶ In the case of bromination, for

¹⁶² Lauer, W. M.; Noland, W. E. *J. Am. Chem. Soc.* **1953**, *75*, 3689.

¹⁶³ de la Mare, P. B. D.; Dunn, T. M.; Harvey, J. T. *J. Chem. Soc.* **1957**, 923.

¹⁶⁴ A primary kinetic isotope effect is seen for sulfonation: Melander, L.; Saunders, W. H., Jr. *Reaction Rates of Isotopic Molecules*; Wiley-Interscience: New York, 1980; p. 162 ff.

¹⁶⁵ A pronounced kinetic isotope effect can also be seen in diazonium ion coupling reactions (Zollinger, H. *Helv. Chim. Acta* **1955**, *38*, 1617) and mercuriation of benzene (Perrin, C.; Westheimer, F. H. *J. Am. Chem. Soc.* **1963**, *85*, 2773).

¹⁶⁶ (a) de la Mare, P. B. D.; Harvey, J. T. *J. Chem. Soc.* **1956**, 36; (b) Sato, Y.; Yato, M.; Ohwada, T.; Saito, S.; Shudo, K. *J. Am. Chem. Soc.* **1995**, *117*, 3037 reported that in some cases the electrophile in a Friedel–Crafts acylation reaction may be a dication.

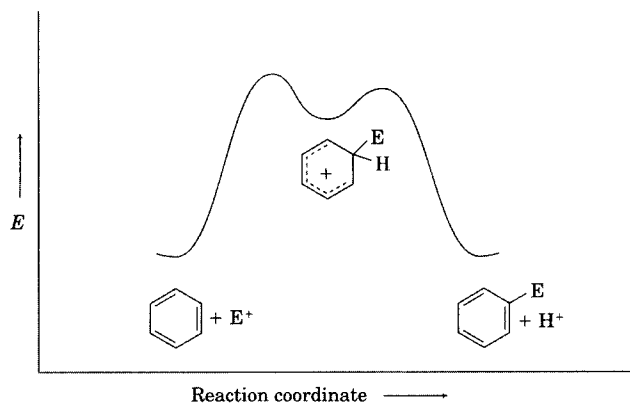


FIGURE 8.45

Reaction coordinate diagram for electrophilic aromatic substitution.

example, the active electrophile may be either Br^+ or HO_2Br^+ when the reagent is HOBr in aqueous dioxane with perchloric acid catalysis, but it may be molecular bromine under other conditions.^{166a} Second, π complexes may also be involved in the reaction. Let us consider as an example one of the most thoroughly studied $\text{S}_{\text{E}}\text{Ar}$ reactions, the nitration of benzene and its derivatives (Figure 8.46).¹⁶⁷⁻¹⁶⁹ Formation of the nitronium ion, NO_2^+ , occurs by protonation of nitric acid and subsequent elimination of water. The nitronium ion then forms an **encounter complex** with benzene, and the encounter complex then proceeds to a **σ complex** (because the electrophile is bonded to a carbon atom of the aromatic ring by a σ bond), which is often termed a *Wheland intermediate* after the contributions of Wheland.^{170,171}

In some cases the formation of the σ complex can be the rate-limiting step in the reaction, while in other cases formation of the encounter complex can be rate limiting. Figure 8.47(a) illustrates the former situation in the nitration of toluene. The latter case is illustrated for reaction of nitronium ion with 1,2,4-trimethylbenzene in Figure 8.47(b).^{172,176} Here the greater stability of the more highly alkyl-substituted σ complex lowers the activation energy for its formation.

In both reactions in Figure 8.47, we presume that proton removal to rearomatize the ring is not rate limiting, but this is not necessarily the case. Forlani and co-workers demonstrated that reaction of 1,3,5-tris(*N*-piperidyl)benzene with 4-substituted benzenediazonium tetrafluoroborates led to the

¹⁶⁷ Deno, N. C.; Stein, R. J. *Am. Chem. Soc.* **1956**, *78*, 578.

¹⁶⁸ For a review of work in this area, see reference 176.

¹⁶⁹ For a detailed discussion, see Olah, G. A.; Malhotra, R.; Narang, S. C. *Nitration: Methods and Mechanisms*; VCH Publishers: New York, 1989.

¹⁷⁰ Wheland, G. W. *J. Am. Chem. Soc.* **1942**, *64*, 900.

¹⁷¹ Wheland, G. W. *Resonance in Organic Chemistry*; John Wiley & Sons: New York, 1955; pp. 476-507.

¹⁷² The formation of a complex prior to reaction is well supported in the case of bromination. Molecular bromine forms charge transfer complexes with benzene even in the absence of Lewis acid catalysts. The complexes can be detected spectroscopically and can even be crystallized for structure determination. Complexes of Br^+ with the aromatic compound may also be formed. For a summary of experimental data in this area, see the discussion in reference 178.

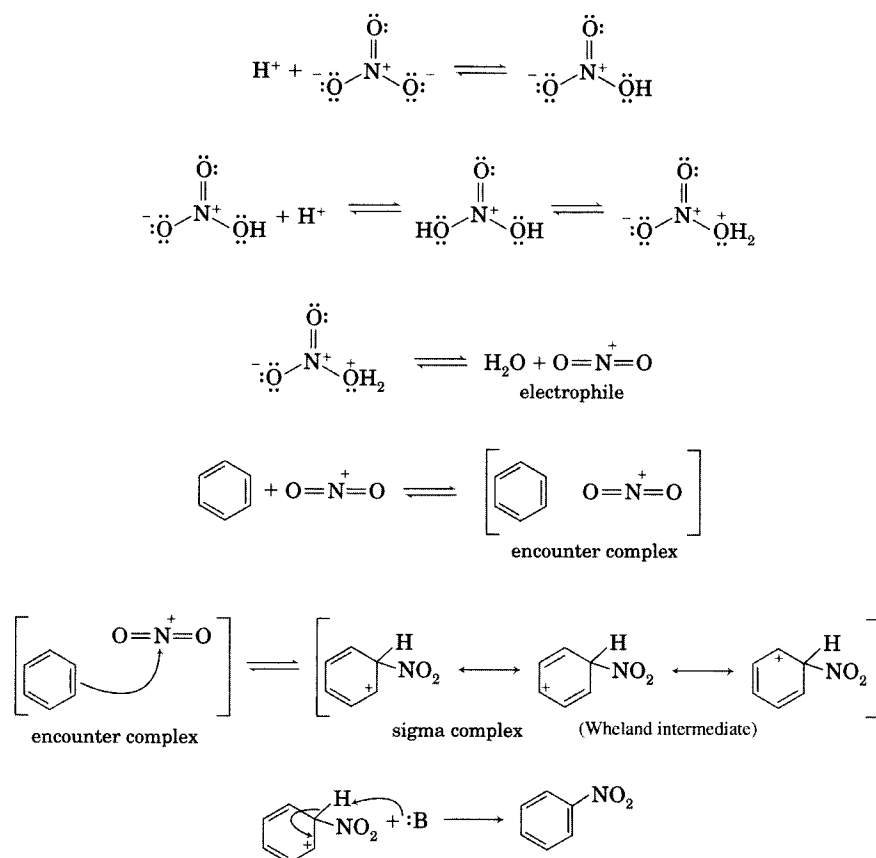
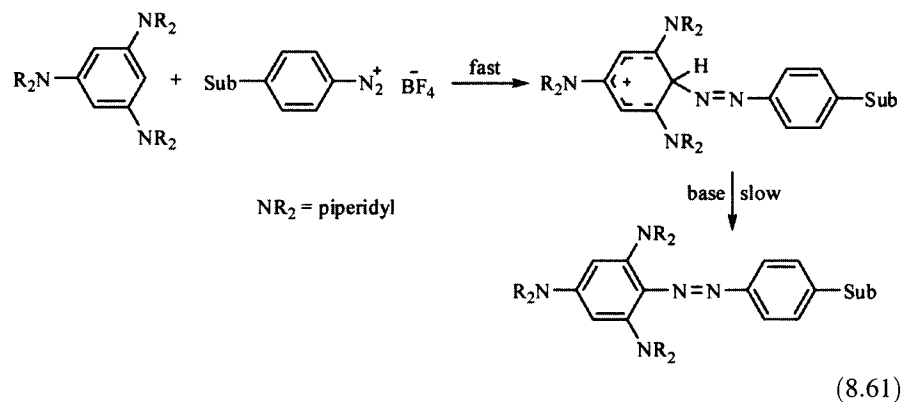


FIGURE 8.46
Detailed mechanism for nitration of benzene.

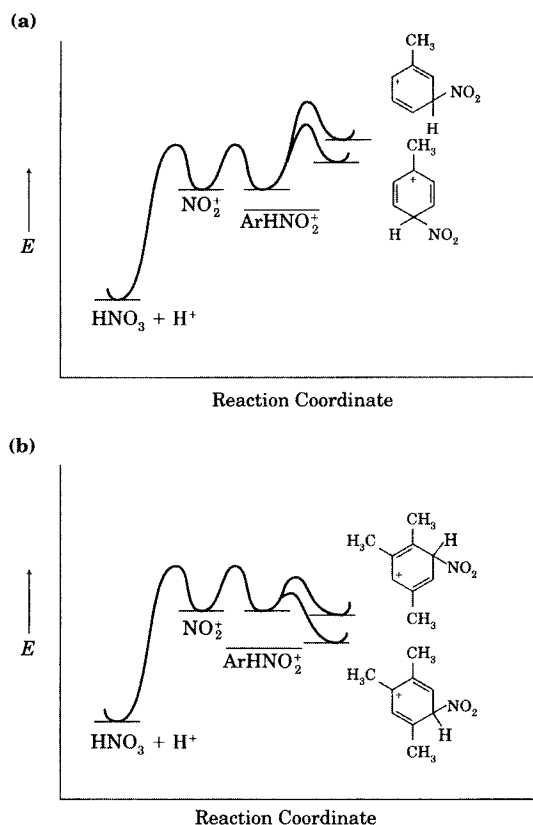
rapid formation of σ -adducts that underwent rate-limiting, base-catalyzed formation of the aromatic substitution products (equation 8.61).¹⁷³



Quantitative Measurement of $S_{\text{E}}\text{Ar}$ Rate Constants: Partial Rate Factors

Benzene has six equivalent sites for $S_{\text{E}}\text{Ar}$ reaction. A monosubstituted benzene has only five sites, and these sites are not equivalent because two

¹⁷³ Forlani, L.; Boga, C.; Del Vecchio, E.; Ngobo, A.-L. T. D.; Tozzi, S. J. *Phys. Org. Chem.* **2007**, *20*, 201.

**FIGURE 8.47**

Possible reaction coordinate diagrams for nitration of (a) toluene and (b) 1,2,4-trimethylbenzene. (Adapted from reference 176.)

are ortho to the substituent, two are meta, and one is para. Often it is desirable to compare the reactivity at *one* site in benzene with the reactivity at *one* site of each type in a substituted derivative of benzene. The reactivities so determined are called **partial rate factors** (denoted f^Z) and are defined as follows:^{4,174,175}

$$f_o^Z = \frac{\frac{k'}{2}}{\frac{k}{6}} \frac{\% \text{ ortho product}}{100} = 0.03 \frac{k'}{k} (\% \text{ ortho product}) \quad (8.62)$$

$$f_m^Z = \frac{\frac{k'}{2}}{\frac{k}{6}} \frac{\% \text{ meta product}}{100} = 0.03 \frac{k'}{k} (\% \text{ meta product}) \quad (8.63)$$

$$f_p^Z = \frac{\frac{k'}{1}}{\frac{k}{6}} \frac{\% \text{ para product}}{100} = 0.06 \frac{k'}{k} (\% \text{ para product}) \quad (8.64)$$

¹⁷⁴ Taylor, R. *Electrophilic Aromatic Substitution*; John Wiley & Sons: Chichester, England, 1990; p. 40 ff.

¹⁷⁵ The superscript Z refers to a substituent on the aromatic ring. In some sources the partial rate factor is represented with the symbol $f^{\phi Z}$, in which superscript ϕZ more explicitly indicates a monosubstituted derivative of benzene. (See, for example, reference 5.) Also used in the literature are symbols in which the positions of the letter f and the positional indicator are reversed. For example, f_o^Z may be shown as o_f , as in reference 176.

where k is the rate constant for reaction of benzene and k' is the rate constant for reaction of the derivative. The statistical factors are included in the equations because there are six equivalent sites for reaction on benzene, while a monosubstituted benzene has two equivalent ortho sites, two equivalent meta sites, but only one para site. Thus, f_o^Z is the relative reactivity at one of the two sites ortho to a substituent in a monosubstituted benzene in comparison with the reactivity of one of the six sites on benzene under the same conditions.

As an example, the bromination of toluene with HOBr in dioxane–water proceeds 36.2 times as fast as does bromination of benzene under the same conditions, and the product is composed of 70.3% *ortho*-, 2.3% *meta*-, and 27.4% *para*-bromotoluene.¹⁶³ Thus, the partial rate factors are

$$f_o^Z = (0.03)(36.2)(70.3) = 76.3 \quad (8.65)$$

$$f_m^Z = (0.03)(36.2)(2.3) = 2.5 \quad (8.66)$$

$$f_p^Z = (0.06)(36.2)(27.4) = 59.5 \quad (8.67)$$

Partial rate factors are indicated by small numbers shown near each reaction site (Figure 8.48).

Partial rate factors quantify the qualitative terms “activating, ortho, para directing,” “deactivating, meta directing,” and “deactivating, ortho, para directing” that are used to label substituents in S_EAr reactions. If $f^Z > 1$, then that site is activated, since it reacts faster than a site on benzene. Conversely, if $f^Z < 1$, then the site is deactivated. If $f_o^Z, f_p^Z > f_m^Z$, the substituent is an ortho, para director. If $f_m^Z > f_o^Z, f_p^Z$, the substituent is a meta director. Although the ortho and para positions are treated together in qualitative discussions of directing effects, the values of f_o^Z and f_p^Z can be significantly different. Table 8.18 shows the partial rate factors for nitration of four substituted benzenes.¹⁷⁶ Note that the relative reactivity of ortho and para positions is quite different in toluene and *t*-butylbenzene, apparently

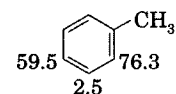


FIGURE 8.48

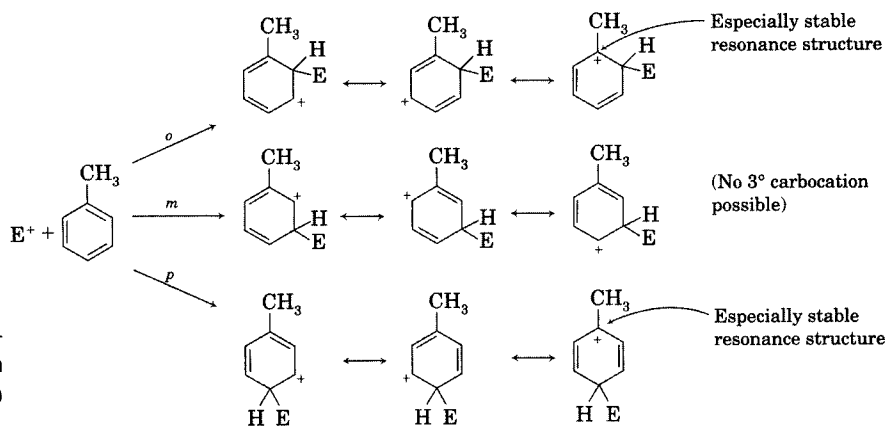
Partial rate factors for the S_EAr bromination of toluene. (Data from reference 166.)

TABLE 8.18 Partial Rate Factors for Nitration with Nitric Acid in Nitromethane at 25°C

Compound	k/k_b	Isomer Distribution			Partial Rate Factor		
		ortho	meta	para	f_o^Z	f_m^Z	f_p^Z
<i>t</i> -Butylbenzene	15	12.2	8.2	79.6	5.5	3.7	71.6
Toluene	21	61.7	1.9	36.4	38.9	1.3	45.8
Chlorobenzene	0.031	29.6	0.9	69.5	0.028	0.00084	0.130
Bromobenzene	0.028	36.5	1.2	62.4	0.030	0.00098	0.103

Source: Reference 176.

¹⁷⁶ Stock, L. M. *Prog. Phys. Org. Chem.* **1976**, 12, 21.

**FIGURE 8.49**

Resonance structures for the Wheland intermediates resulting from ortho, meta, and para attack of an electrophile on toluene.

because of steric hindrance to the approach of the electrophile in the latter compound.^{177,178}

Lewis Structures as Models of Reactivity in S_EAr Reactions

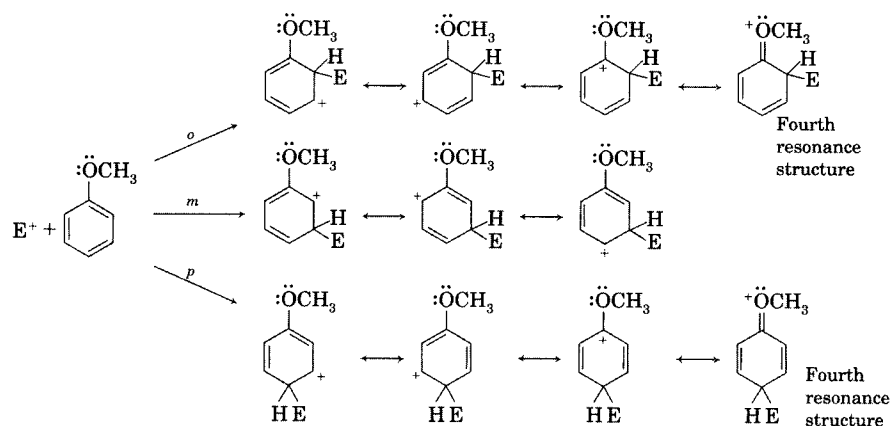
The partial rate factor concept suggests that there is a unique rate constant for reaction at each position of a benzene derivative. Therefore, competitive reactions at different sites within one molecule may be described in the same way as are competitive reactions at sites in different molecules. In a comparison of the ortho and para sites of toluene with the meta position, it is useful to compare the energies of the σ -intermediates for ortho and para reactions to that for meta substitution. Lewis structures for the σ -intermediates formed by reaction of an electrophile with toluene are shown in Figure 8.49. In the case of ortho and para substitution, one of the three resonance structures for the intermediate can be described as a 3° carbocation, while all the contributing resonance structures for the intermediate in meta substitution are 2° carbocations.¹⁶⁸ Based on the Hammond postulate, we expect a lower activation energy for formation of a more stable intermediate, so the rate constants for formation of the ortho and para substitution products should be greater than the rate constant for formation of the meta product.

For highly activated derivatives such as anisole, the intermediate for ortho and para reaction has a contribution from a fourth resonance structure, but a similar resonance structure is not possible for reaction at the meta position (Figure 8.50).

On the other hand, the intermediates formed upon electrophilic substitution at the ortho or para positions on benzene rings with strongly deactivating substituents (such as nitro or trialkylammonio groups) involve contributions from resonance structures representing unstable carbocations. Such unstable resonance structures do not contribute to the resonance hybrid for the intermediate in the meta reaction (Figure 8.51). Therefore, the activation

¹⁷⁷ Product distribution can also be altered by carrying out reactions in heterogeneous environments. For example, the percent yield of *p*-nitrotoluene increases from 34% in homogeneous solution to 55% when the reaction is carried out on a clay support. For a discussion, see Delaude, L.; Laszlo, P.; Smith, K. *Acc. Chem. Res.* **1993**, *26*, 607.

¹⁷⁸ Reaction conditions have strong effects on relative reactivities of benzene derivatives. Under some conditions toluene is 30 times as reactive as benzene, but under other conditions the two compounds have essentially the same reactivity. Berliner, E. *Prog. Phys. Org. Chem.* **1964**, *2*, 253.

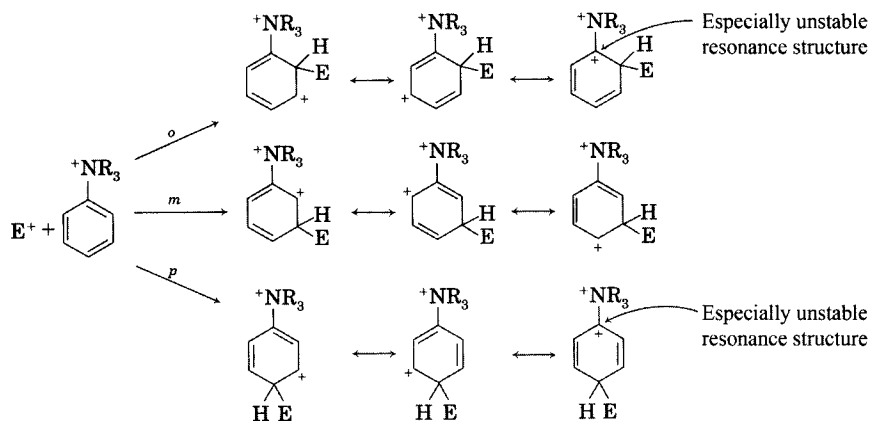
**FIGURE 8.50**

Resonance structures for the Wheland intermediates resulting from ortho, meta, and para attack of an electrophile on anisole.

energy for formation of the σ -intermediate should be lower for meta substitution than for ortho or para substitution, so more meta product should be observed.

Perhaps the most interesting case is that of halogen-substituted aromatics. Intuitively, we consider the halogens to be electron-withdrawing by induction, conveniently viewed as a through-bond interaction, while they are electron-donating through the π system. The π donation can be described by the fourth resonance structure in Figure 8.52. The halogens are thus deactivating but are still ortho, para-directing substituents.¹⁷⁹

Although the mechanism of the S_EAr reaction as described here is widely accepted, alternative explanations have been advanced for some familiar S_EAr reactions. In particular, since single electron transfer processes have been observed in S_N2 reactions, we might consider them a possibility in S_EAr reactions as well. Perrin suggested that such reactions could occur through the mechanism for nitration shown in equations 8.68 and 8.69.^{180,181} Here, the

**FIGURE 8.51**

Resonance structures for the Wheland intermediates resulting from ortho, meta, and para attack of an electrophile on phenyltrialkylammonium ion.

¹⁷⁹ The effect of multiple substituents is usually described in terms of the same resonance (Lewis structure) approaches that are described here for benzene and its monosubstituted derivatives. For a discussion, see Bures, M. G.; Roos-Kozel, B. L.; Jorgensen, W. L. *J. Org. Chem.* **1985**, *107*, 4490.

¹⁸⁰ Perrin, C. *J. Am. Chem. Soc.* **1977**, *99*, 5516. Although the conclusions of this paper were questioned (reference 181), there is experimental evidence for the electron transfer pathway in the nitration of naphthalene: Johnston, J. F.; Ridd, J. H.; Sandall, J. P. B. *J. Chem. Soc. Chem. Commun.* **1989**, 244.

¹⁸¹ Compare Ebersson, L.; Radner, F. *Acc. Chem. Res.* **1987**, *20*, 53.

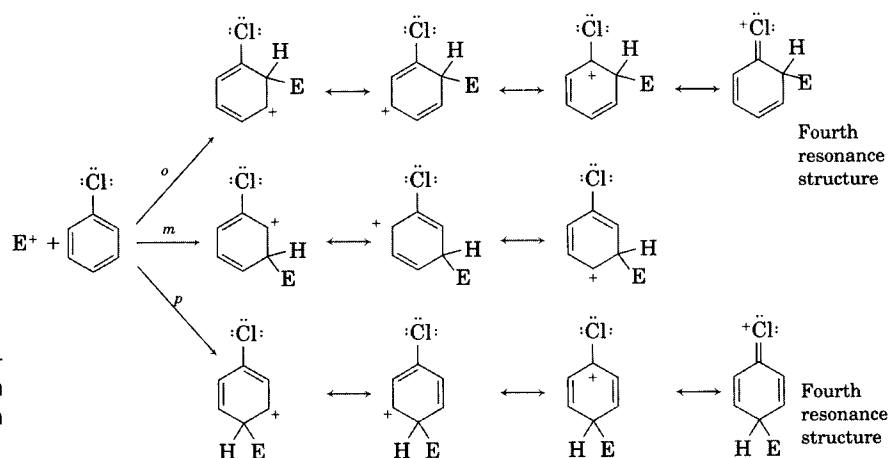
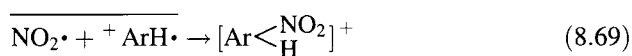
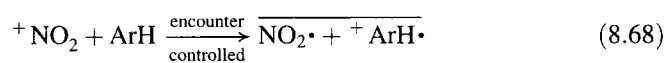


FIGURE 8.52

Resonance structures for the Wheland intermediates resulting from ortho, meta, and para attack of an electrophile on chlorobenzene.

nitronium ion and the aromatic compound form a radical ion pair in a solvent cage (represented by the bar in the equations below), and the radical ion pair then collapses to the σ complex.¹⁸²



Experimental and theoretical studies by Head-Gordon, Kochi, Esteves, Olah, Xiao, and their co-workers found evidence to support the role of single electron transfer processes in the nitration of benzene.^{183–185} Esteves and Olah concluded that there are three distinct intermediates in the substitution reaction. The first is a charge transfer complex between the nitronium ion and the aromatic compound. The second is a radical cation–molecule pair ($\text{C}_6\text{H}_6 \cdot^+ / \text{NO}_2$) formed by transfer of a single electron from the aromatic ring to the nitronium ion. The third intermediate is the σ complex.¹⁸⁴ Similarly, there is evidence that the bromination of benzene with Br_2 may also involve a single electron transfer step.^{186,187} Some investigators have concluded that the classical Wheland mechanism and the SET mechanism should be viewed as the extremes of a continuum of mechanistic possibilities.^{184,188}

¹⁸² Theoretical calculations reinforced this conclusion: Gleghorn, J. T.; Torossian, G. *J. Chem. Soc. Perkin Trans. 2* **1987**, 1303.

¹⁸³ Gwaltney, S. R.; Rosokha, S. V.; Head-Gordon, M.; Kochi, J. K. *J. Am. Chem. Soc.* **2003**, *125*, 3273.

¹⁸⁴ Esteves, P. M.; Carneiro, J. W. de M.; Cardoso, S. P.; Barbosa, A. G. H.; Laali, K. K.; Rasul, G.; Prakash, G. K. S.; Olah, G. A. *J. Am. Chem. Soc.* **2003**, *125*, 4836.

¹⁸⁵ Chen, L.; Xiao, H.; Xiao, J.; Gong, X. *J. Phys. Chem. A* **2003**, *107*, 11440.

¹⁸⁶ Smith, W. B. *J. Phys. Org. Chem.* **2003**, *16*, 34.

¹⁸⁷ Vasilyev, A. V.; Lindeman, S. V.; Kochi, J. K. *New J. Chem.* **2002**, *26*, 582.

¹⁸⁸ de Queiroz, J. F.; Carneiro, J. W. de M.; Sabino, A. A.; Sparrapan, R.; Eberlin, M. N.; Esteves, P. M. *J. Org. Chem.* **2006**, *71*, 6192.

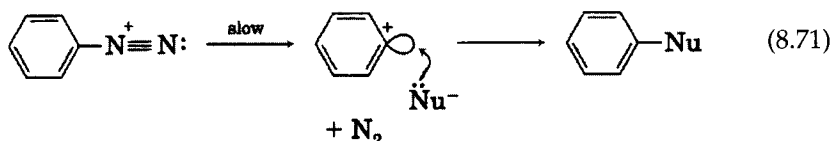
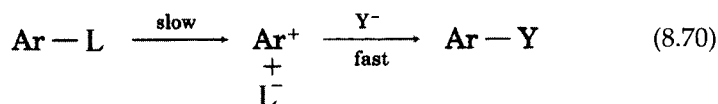
8.4 NUCLEOPHILIC AROMATIC AND VINYLIC SUBSTITUTION

Nucleophilic Aromatic Substitution

As is the case with nucleophilic aliphatic substitution, nucleophilic aromatic substitution (S_NAr) can occur by processes that exhibit either first- or second-order kinetics.^{189,190} In contrast to the aliphatic reactions, however, the first- and second-order aromatic reactions are quite different in character.

First-Order S_NAr Reactions

The first-order S_NAr reaction requires a mechanism in which the rate-limiting step is the unimolecular departure of a leaving group, resulting in the formation of an intermediate that can then react with a nucleophile. If the substitution is to occur on an aromatic ring, then the most feasible structure for the intermediate is a carbocation having an empty sp^2 hybrid orbital in the plane of a benzene ring, as is illustrated in equation 8.70. Since phenyl carbocations are much less stable than are alkyl carbocations, there must be a strong driving force for the departure of the leaving group.¹⁹¹ For this reason, first-order nucleophilic aromatic substitution reactions almost always involve decomposition of arenediazonium ions to phenyl carbocations and molecular nitrogen, as illustrated in equation 8.71.¹⁹²



Swain and co-workers reported a kinetic study of the uncatalyzed reaction of benzenediazonium ions in aqueous solution. They found very low selectivity among nucleophiles, nearly identical rate constants for reaction in H_2O and D_2O , and essentially invariant rate constants in solutions with very different concentrations of H_2SO_4 . The value of ΔS^\ddagger was $+10.5$ eu. Secondary kinetic isotope effects, $k_{\text{H}}/k_{\text{D}}$, were 1.22 for each ortho position, 1.08 for each meta position, and 1.02 for the para position on the aromatic ring. These results were consistent with the mechanism shown in equation 8.71, in which the rate-limiting step is loss of N_2 , resulting in the formation of a highly reactive carbocation that is stabilized to some extent by hyperconjugative delocalization of the positive charge onto the ortho and meta positions of

¹⁸⁹ Miller, J. *Aromatic Nucleophilic Substitution*; Elsevier Publishing: Amsterdam, 1968.

¹⁹⁰ Terrier, F. *Nucleophilic Aromatic Displacement: The Influence of the Nitro Group*; VCH Publishers: New York, 1991.

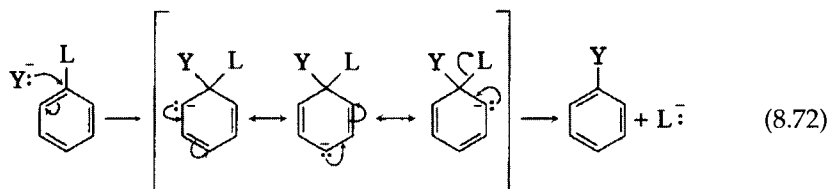
¹⁹¹ Orbitals with more s character are more electronegative, so it is more difficult to produce a vacant sp^2 hybrid orbital than a vacant sp^3 hybrid orbital.

¹⁹² For another example of a first-order S_NAr reaction, see Himeshima, Y.; Kobayashi, H.; Sonoda, T. *J. Am. Chem. Soc.* **1985**, *107*, 5286.

the ring.^{193,194} Note that this conclusion applies only to uncatalyzed arenediazonium reactions. Metal ion-catalyzed reactions, such as the Sandmeyer reaction, are thought to proceed by radical pathways.¹⁹⁵

Second-Order S_NAr Reactions

The second-order nucleophilic aromatic substitutions are more varied. Although there was some initial consideration of one-step, S_N2 -like bimolecular mechanisms for these reactions,¹⁹⁶ Bunnett and Zahler argued against such pathways on theoretical grounds.¹⁹⁷ They suggested that the reactions instead proceed through an attachment-detachment ($A_N + D_N$) mechanism analogous to the mechanism for electrophilic aromatic substitution (equation 8.72). It is important to note a major difference between nucleophilic and electrophilic aromatic substitutions, however. In the electrophilic reactions, there are usually several good electrofugal groups (the protons), so substituents can exert an influence both on the overall reactivity of the molecule and on the site of the reaction. In S_NAr reactions, however, there is seldom more than one good nucleofugal group. The detachment of a hydride ion is highly unlikely, so the nucleophilic aromatic substitution replaces a good leaving group such as a halide ion. Other substituents on the aromatic ring can influence the reactivity of the molecule but usually not the site of the reaction.¹⁹⁸⁻²⁰⁰



Several lines of evidence support the mechanism shown in equation 8.72.^{201,202} Cryoscopic measurements suggest the formation of an adduct

¹⁹³ Swain, C. G.; Sheats, J. E.; Harbison, K. G. *J. Am. Chem. Soc.* **1975**, *97*, 783; Swain, C. G.; Sheats, J. E.; Gorenstein, D. G.; Harbison, K. G. *J. Am. Chem. Soc.* **1975**, *97*, 791.

¹⁹⁴ Wu, Z.; Glaser, R. *J. Am. Chem. Soc.* **2004**, *126*, 10632 argued that the nucleophilic substitution of a benzenediazonium ion should be considered an S_N2Ar pathway because strictly first-order reactions cannot occur in solvolyses.

¹⁹⁵ Galli, C. *Chem. Rev.* **1988**, *88*, 765.

¹⁹⁶ Compare Chapman, N. B.; Parker, R. E.; Soanes, P. W. *J. Chem. Soc.* **1954**, 2109 and earlier papers cited therein.

¹⁹⁷ Bunnett, J. F.; Zahler, R. E. *Chem. Rev.* **1951**, *49*, 273.

¹⁹⁸ It is possible to determine the effects of substituents on the regiochemistry of the S_NAr reaction in the case of monosubstituted derivatives of pentafluorobenzene because there are now nucleofugal groups in the ortho, meta, and para positions. In molecules with the structure C_6F_5X , for example, the NH_2 group is found to be a deactivating, meta director in S_NAr reactions. For a discussion and leading references, see reference 189.

¹⁹⁹ Makosza, M.; Winiarski, J. *J. Org. Chem.* **1984**, *49*, 1494; Makosza, M.; Ludwiczak, S. *J. Org. Chem.* **1984**, *49*, 4562; Makosza, M.; Winiarski, J. *Acc. Chem. Res.* **1987**, *20*, 282.

²⁰⁰ A theoretical study suggested that charge transfer complexes may also be involved in the S_NAr reaction. Dotterer, S. K.; Harris, R. L. *J. Org. Chem.* **1988**, *53*, 777.

²⁰¹ Ross, S. D. *Prog. Phys. Org. Chem.* **1963**, *1*, 31.

²⁰² Bunnett, J. F. *Q. Rev. Chem. Soc.* **1958**, *12*, 1.

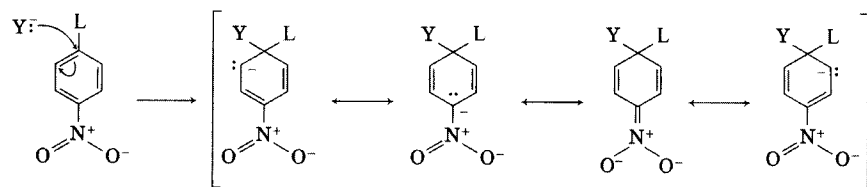
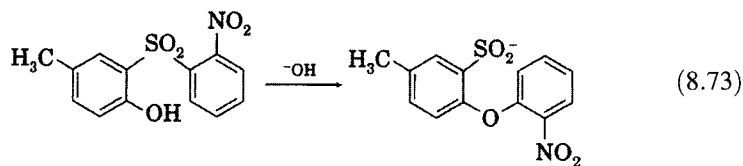


FIGURE 8.53
Resonance interaction of a *p*-nitro substituent in an S_NAr intermediate.

between the aromatic compound and a nucleophilic solvent,²⁰³ and adducts known as Jackson–Meisenheimer complexes (analogous to the σ complexes of electrophilic aromatic substitution) can be isolated in some cases.²⁰⁴ The S_NAr reaction is accelerated by groups such as nitro and cyano that can accept electrons by resonance in the ortho and para positions (Figure 8.53), and a Hammett correlation confirms the accelerating effect of electron-withdrawing substituents.²⁰⁵ In addition, there is generally no **element effect** on the reaction, meaning that the rate constants are not affected by the identity of the leaving group. For example, reactions of several 1-substituted-2,4-dinitrobenzenes with piperidine in methanol solution show rate constants and activation parameters that are very similar (Table 8.19), indicating that the C–L bond is broken only slightly (if at all) in the transition structures for reaction of these compounds.^{206–208} S_NAr reactions may be intramolecular as well as intermolecular, as is illustrated by the Smiles rearrangement (equation 8.73).²⁰⁹



There are some notable exceptions to the general rule that nucleophilic aromatic substitution does not lead to replacement of a hydrogen. In

²⁰³ Baliah, V.; Ramakrishnan, V. *Rec. Trav. Chim. Pays-Bas* **1959**, 78, 783.

²⁰⁴ For a discussion see Crampton, M. R. *Adv. Phys. Org. Chem.* **1969**, 7, 211; also see Mariella, R. P.; Callahan, J. J.; Jibril, A. O. *J. Org. Chem.* **1955**, 20, 1721.

²⁰⁵ Berliner, E.; Monack, L. C. *J. Am. Chem. Soc.* **1952**, 74, 1574; Bunnett, J. F.; Moe, H.; Knutson, D. *J. Am. Chem. Soc.* **1954**, 76, 3936.

²⁰⁶ Bunnett, J. F.; Garbisch, E. W. Jr.; Pruitt, K. M. *J. Am. Chem. Soc.* **1957**, 79, 385.

²⁰⁷ In protic solvents, solvation of the departing nucleofuge makes the attachment of the nucleophile rate limiting, so no leaving group effect is seen. The rate-limiting step in S_NAr reactions in aprotic solvents such as THF appears to be the detachment of the nucleofuge. Nudelman, N. S.; Mancini, P. M. E.; Martinez, R. D.; Vottero, L. R. *J. Chem. Soc. Perkin Trans. 2* **1987**, 951. In addition, an $^{18}F/^{19}F$ fluorine kinetic isotope effect of 1.0262 has been observed for the reaction of piperidine with 2,4-dinitrofluorobenzene in THF, suggesting that the C–F bond is broken in the rate-limiting step. Matsson, O.; Persson, J.; Axelsson, B. S.; Långström, B. *J. Am. Chem. Soc.* **1993**, 115, 5288.

²⁰⁸ A leaving group effect ($Br > Cl > F$) is observed for the 4-chlorobenzoylCoA dehalogenase-catalyzed substitution of OH for halogen in *p*-halogenbenzoate ion in aqueous solution. One explanation for this result is that the enzyme lowers the activation energy for the first step (attachment of the nucleophile to the aromatic ring), making the second step (detachment of halide ion) rate limiting. Crooks, G. P.; Copley, S. D. *J. Am. Chem. Soc.* **1993**, 115, 6422.

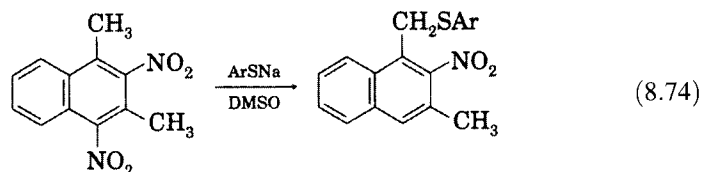
²⁰⁹ Levy, A. A.; Rains, H. C.; Smiles, S. *J. Chem. Soc.* **1931** 3264. For an extensive discussion, see Truce, W. E.; Kreider, E. M.; Brand, W. W. *Org. React.* **1970**, 18, 99.

TABLE 8.19 Kinetic Data for Reaction of Piperidine with 1-Substituted-2,4-Dinitrobenzenes in Methanol Solution at 0°C

Substituent	Rate Constant ($M^{-1} \text{ min}^{-1}$)	E_a (kcal/mol)	ΔS^\ddagger (eu)
Br	0.118	11.8	-29.5
Cl	0.117	11.6	-30.2
$C_6H_5SO_2$	0.0860	12.0	-29.3
$p\text{-NO}_2C_6H_4O$	0.0812	10.5	-35.3
I	0.0272	12.0	-31.7

Source: Reference 206.

one example of the **von Richter reaction** (Figure 8.54), cyanide and *p*-nitrochlorobenzene produce *m*-chlorobenzoic acid. Results of isotopic labeling experiments suggested the mechanism shown in Figure 8.54, and this proposed mechanism was supported by studies demonstrating that both the *o*-nitrosobenzamide and the subsequent indazolone produce benzoic acid when subjected to the reaction conditions.²¹⁰ This reaction can be called a **cine substitution** (from the Greek meaning "to move"), since the nucleophilic atom becomes bonded ortho to the leaving group.²¹¹ Substitution leading to replacement of a substituent more than one atom removed (usually meta or para to the original substituent on an aromatic ring) is called **tele substitution** (equation 8.74).²¹²



Another type of S_NAr reaction that can lead to net displacement of a hydrogen atom from the aromatic ring is known as "vicarious" nucleophilic aromatic substitution. In equation 8.75, the nucleophile bears a leaving group, L. Attachment of such a nucleophile to an aromatic ring (at a position determined by the electron-withdrawing groups on the ring) has been reported to produce an intermediate that can then undergo base-promoted elimination of HL (where H is on the aromatic ring and L is a substituent on the nucleophile). The result is a second intermediate, which can tautomer-

²¹⁰ (a) Rauhut, M. M.; Bunnett, J. F. *J. Org. Chem.* **1956**, *21*, 939; Bunnett, J. F.; Rauhut, M. M. *J. Org. Chem.* **1956**, *21*, 944 and references therein; (b) Samuel, D. *J. Chem. Soc.* **1960**, 1318; (c) Rosenblum, M. *J. Am. Chem. Soc.* **1960**, *82*, 3796; (d) Ibne-Rasa, K. M.; Koubek, E. *J. Org. Chem.* **1963**, *28*, 3240. For further discussion, see Jones, R. A. Y.; *Physical and Mechanistic Organic Chemistry*, 2nd ed.; Cambridge University Press: Cambridge, UK, 1984; pp. 2-5.

²¹¹ The original meaning of *cine* was loss of a substituent from one position and replacement with another group at any other site on the molecular framework. *Cine* has come to mean that the replacement occurs on the carbon atom adjacent to the site of the original substituent, while *tele* has come to mean substitution at some other site. For a discussion, see reference 2, pp. 249-250.

²¹² Novi, M.; Dell'Erba, C.; Sancassan, F. *J. Chem. Soc. Perkin Trans. 1* **1983**, 1145.

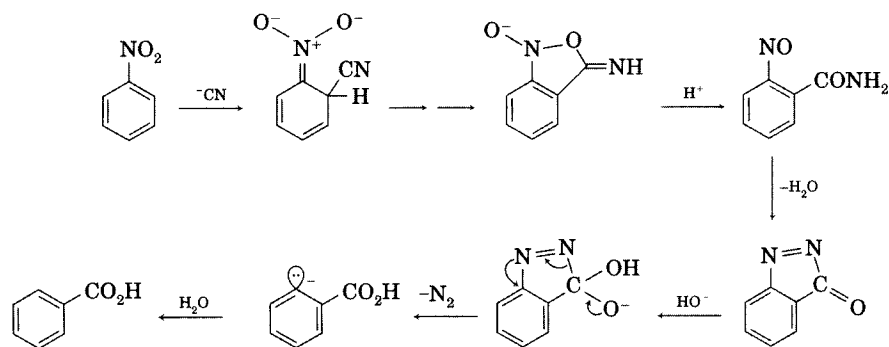
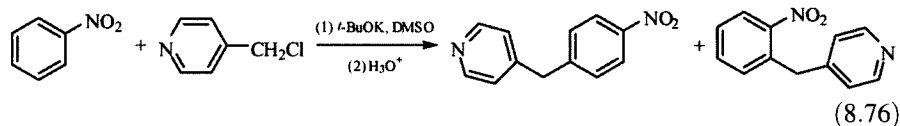
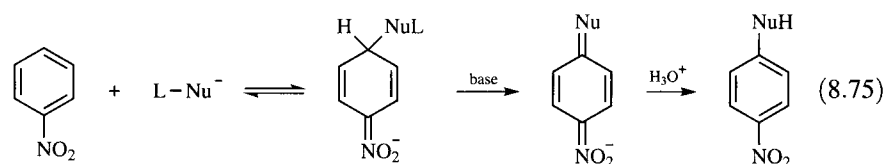


FIGURE 8.54
Mechanism proposed for the von Richter reaction. (Adapted from reference 210c.)

ize to give the final product.¹⁹⁹ An example of the synthetic utility of this procedure can be seen in the synthesis of pyridine derivatives in equation 8.76.²¹³



Single Electron Transfer in S_NAr Reactions

We have noted that both S_N2 and S_EAr reactions may occur through SET processes. There is good evidence that the S_NAr reaction may involve such a pathway also. Figure 8.55 shows species identified by Bacaloglu and co-workers in a fast kinetic spectroscopy study of the reaction of hydroxide ion with 1-chloro-2,4,6-trinitrobenzene (picryl chloride, **71**).²¹⁴ Depending on reaction conditions, these workers could see transients ascribed to the π complex (**72**), an intermediate produced by single electron transfer (**73**), and one or more σ complexes (**74**, **75**). In addition, evidence was obtained for the reversible formation of a phenyl carbanion (**76**) and a dianion (**77**) that probably do not lead directly to the substitution product (**78**). Further support for the role of SET processes in S_NAr reactions comes from the detection of radical intermediates by EPR spectrometry²¹⁵ and by correlations of reactivity with the oxidation potentials of the nucleophiles in some studies.²¹⁶

²¹³ Florio, S.; Lorusso, P.; Luisi, R.; Granito, C.; Ronzini, L.; Troisi, L. *Eur. J. Org. Chem.* **2004**, 2118.

²¹⁴ Bacaloglu, R.; Bunton, C. A.; Cerichelli, G. *J. Am. Chem. Soc.* **1987**, *109*, 621. See also Bacaloglu, R.; Blaskó, A.; Bunton, C. A.; Ortega, F.; Zucco, C. *J. Am. Chem. Soc.* **1992**, *114*, 7708.

²¹⁵ Grossi, L.; Strazzari, S. *J. Chem. Soc. Perkin Trans. 2*, **1999**, 2141.

²¹⁶ Terrier, F.; Mokhtari, M.; Goumont, R.; Hallé, J.-C.; Buncel, E. *Org. Biomol. Chem.* **2003**, *1*, 1757.

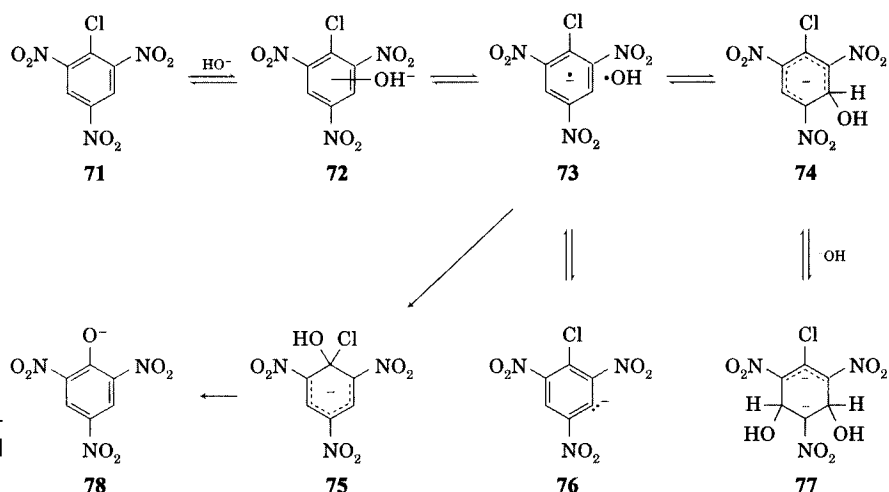
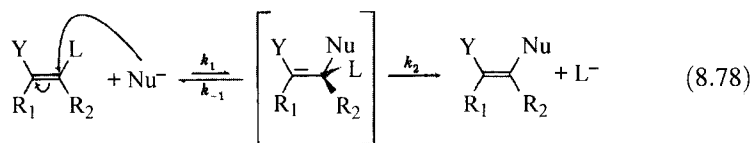
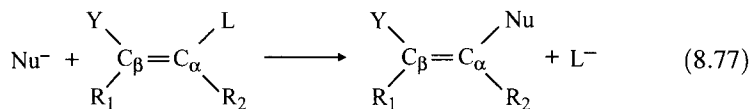


FIGURE 8.55
Evidence for single electron transfer in an S_NAr reaction. (Adapted from reference 214.)

Nucleophilic Vinyl Substitution

Analogous to nucleophilic aromatic substitution is nucleophilic vinylic substitution (equation 8.77), in which a nucleophile replaces a leaving group on an olefinic carbon atom. Reactions of the type shown in equation 8.78 may take place by a variety of mechanisms. Rappoport identified sixteen different processes for nucleophilic substitution of a leaving group attached to an olefinic carbon,²⁰⁵ including an S_N1 reaction involving a vinyl cation,²¹⁷ a one-step substitution similar to an S_N2 reaction, an elimination–addition process (analogous to the benzyne process discussed on page 537), and an attachment–detachment pathway analogous to the S_NAr reaction.^{218–220} The reaction in this area that has received most interest, and the process that most closely resembles the S_NAr mechanism, is the attachment–detachment pathway (equation 8.78).²²¹



²¹⁷ Stang, P. J.; Rappoport, Z.; Hanack, M.; Subramanian, L. R. *Vinyl Cations*; Academic Press: New York, 1979.

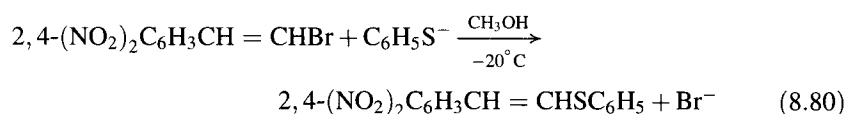
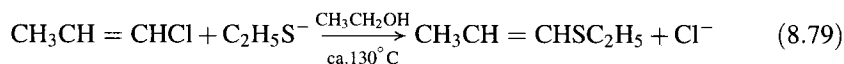
²¹⁸ Rappoport, Z. *Adv. Phys. Org. Chem.* **1969**, *7*, 1.

²¹⁹ Modena, G. *Acc. Chem. Res.* **1971**, *4*, 73.

²²⁰ Rappoport, Z. *Acc. Chem. Res.* **1981**, *14*, 7.

²²¹ An ab initio study suggested that a concerted S_N2 reaction is possible in the case of *unactivated* substrates in which the attachment–detachment pathway is not favored by electron-withdrawing substituents, and some experimental data are consistent with this prediction: Glukhovtsev, M. N.; Pross, A.; Radom, L. *J. Am. Chem. Soc.* **1994**, *116*, 5961.

The rate-limiting step in nucleophilic vinylic substitution is usually thought to be the attachment of the nucleophile to the unsaturated system. The presence of groups on the β carbon atom that can stabilize negative charge therefore lowers the energy of the intermediate in brackets and increases the rate constant for the reaction.²²² For example, Modena noted the enhancement of reactivity achieved by replacing a methyl group with a 2,4-dinitrophenyl group at the β position of a vinyl halide. The reaction in equation 8.79 requires temperatures around 130°C, while that in equation 8.80 occurs at -20°C.²⁰⁶



The attachment-detachment mechanism shown in equation 8.78 is supported by several lines of evidence. The reactions typically show overall second-order kinetics, first order in the vinyl halide and first order in the nucleophile.²²³ Particularly significant is the lack of an element effect. That is, for most vinyl halides, the rate constants for substitution are about the same for the chloride as for the bromide, which suggests that the halide is not eliminated in the rate-limiting step for the reaction. Moreover, the intermediate shown in brackets in equation 8.78 has been observed spectroscopically in a few cases.²²⁴ The lifetime of the intermediate depends on the relative magnitude of the rate constants for the attachment and detachment steps, which are complex functions of the activating group(s) on the β carbon atom as well as the other substituent on the α carbon atom, the strength of the nucleophile, and the nucleofugality of the leaving group. In some cases the mechanism may approach a one-step process involving a transition state and not a true intermediate.^{207,225}

One of the interesting aspects of nucleophilic vinylic substitution is the observation that the product often retains the configuration of the reactant, as illustrated by the reactions of (*Z*)- and (*E*)- β -bromoethyl crotonate in equations 8.81 and 8.82.²²⁶ Not all reactions are stereospecific, however, and the stereochemical outcome depends on the nature of the nucleophile,

²²² In discussions of nucleophilic vinylic substitution, the carbon atom bearing the leaving group is commonly denoted the α carbon atom, while the other olefinic carbon atom is the β position.²¹⁹

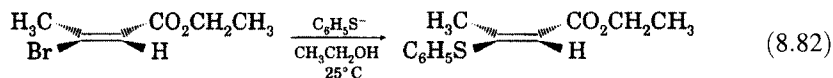
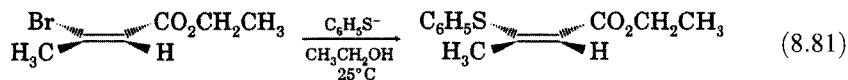
²²³ See, for example, Silversmith, E. F.; Smith, D. *J. Org. Chem.* **1958**, *23*, 427.

²²⁴ Bernasconi, C. F.; Killion, R. B., Jr.; Fassberg, J.; Rappoport, Z. *J. Am. Chem. Soc.* **1989**, *111*, 6862; Bernasconi, C. F.; Fassberg, J.; Killion, R. B., Jr.; Rappoport, Z. *J. Am. Chem. Soc.* **1990**, *112*, 3169; also see Bernasconi, C. F.; Fassberg, J.; Killion, R. B., Jr.; Schuck, D. F.; Rappoport, Z. *J. Am. Chem. Soc.* **1991**, *113*, 4937.

²²⁵ For a theoretical study of nucleophilic vinylic substitution, see Cohen, D.; Bar, R.; Shaik, S. S. *J. Am. Chem. Soc.* **1986**, *108*, 231.

²²⁶ Théron, F. *Bull. Soc. Chim. France* **1969**, 278. See also the discussion in Peishoff, C. E.; Jorgensen, W. L. *J. Org. Chem.* **1985**, *50*, 1056.

leaving group, and especially on the activating group(s) on the β carbon atom.²²⁷



The tendency for nucleophilic vinylic substitution to give retention of configuration can be explained on the basis of the scheme in Figure 8.56, with the following additional restrictions:^{205,206,228}

1. The nucleophile approaches the α carbon atom on a line perpendicular to the plane of the olefin.
2. The α carbon atom is nearly tetrahedral in the transition structure because bond making from the nucleophile to the carbon atom is more advanced than is $\text{C}_\alpha\text{-L}$ bond breaking.
3. The β carbon atom remains relatively planar (especially if there is resonance delocalization of the negative charge) or is pyramidal but inverts so rapidly that its time-averaged geometry is planar.
4. The leaving group departs on a line that is perpendicular to the plane of the developing double bond.

This last restriction means that some rotation about the olefinic carbon-carbon bond must occur in order for the leaving group to depart. A 60° rotation followed by detachment gives a substitution product in which the original stereochemistry is retained. A 120° rotation followed by detachment gives the diastereomer of that product. Several studies suggest that the 60° rotation is faster than the 120° rotation, so retention is most likely with short-lived carbanionic intermediates.²²⁰

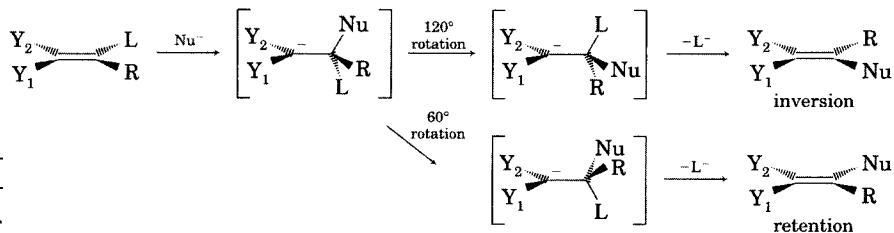


FIGURE 8.56

Inversion (top) and retention (bottom) of configuration in nucleophilic vinylic substitution reactions.

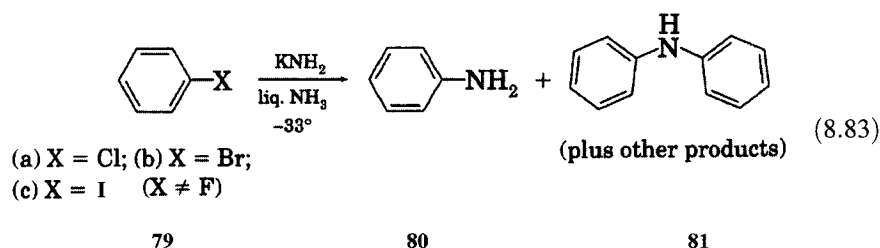
²²⁷ Rappoport, Z.; Gazit, A. *J. Org. Chem.* **1956**, *51*, 4112.

²²⁸ This figure is a considerably simplified version of more detailed schemes provided in the references.

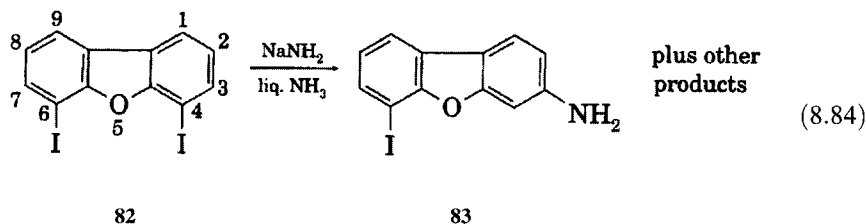
Nucleophilic Substitution Involving Benzyne Intermediates

Introduction

Because of the requirement for S_NAr reactions to have nitro or other electron-withdrawing groups ortho or para to the leaving group, unsubstituted benzenes generally react only slowly with nucleophiles. In an investigation of the effect of activating, ortho, para-directing substituents on such reactions, Bergstrom and co-workers found that chlorobenzene and other unactivated aromatic halides (**79**) do react to give aniline (**80**) plus diphenylamine (**81**) and other products when treated with amide ion in liquid ammonia at -33°C (equation 8.83). They do not react with sodium amide in diethyl ether at room temperature, however.^{229,230}



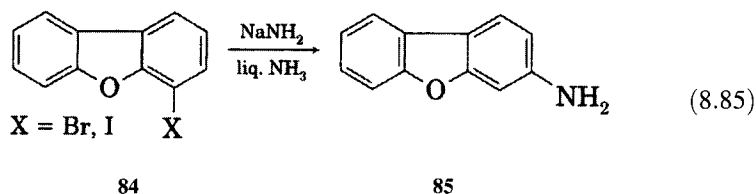
Later, Gilman and Avakian reported an unusual substitution reaction of 4,6-diiodobenzofuran (**82**) when they attempted to prepare the 4,6-diamino derivative by substitution of **82** with sodium amide in liquid NH_3 . Instead of the expected product (4-amino-6-iodobenzofuran), they observed formation of 3-amino-6-iodobenzofuran (**83**) plus other products. They also found that 4-iododibenzofuran (**84**) gave the 3-amino derivative (**85**), but that 2-iododibenzofuran gave the 2-amino derivative.²³¹ Extending the study to derivatives of benzene, Gilman and Avakian found that under the same conditions *m*-anisidine was obtained from reaction of *o*-iodoanisole, *o*-bromoanisole, or *o*-chloroanisole. They concluded that the apparent rearrangement of *o*-halo aromatic ethers to yield *m*-amino aromatic ethers was characteristic of molecules with a halogen ortho to an aromatic ether oxygen.



²²⁹ Bergstrom, F. W.; Wright, R. E.; Chandler, C.; Gilkey, W. A. *J. Org. Chem.* **1936**, *1*, 170.

²³⁰ The diphenylamine and triphenylamine were found to be formed as secondary products of the reaction of aniline and diphenylamine, respectively. Wright, R. E.; Bergstrom, F. W. *J. Org. Chem.* **1936**, *1*, 179.

²³¹ Gilman, H.; Avakian, S. *J. Am. Chem. Soc.* **1945**, *67*, 349.



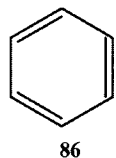
In subsequent investigations, Gilman and co-workers observed rearranged product from the reaction of *o*-bromodimethylaniline under similar conditions.²³² Further studies showed that *p*-bromoanisole reacted to give *m*-methoxyaniline.²³³ Reaction of *o*-chlorotrifluoromethylbenzene gave *m*-trifluoromethylaniline, as did reaction of *m*-chlorotrifluoromethylbenzene. The language in these papers suggests that the authors believed the "normal" reaction (taking place without apparent rearrangement) to be a typical S_NAr reaction, while the rearrangement product was believed to result from a different mechanism.

Experimental Evidence for Benzyne Intermediates

A very different mechanism for these reactions was put forward by Roberts and co-workers.²³⁴⁻²³⁶ Summarizing the various reactions reported in the literature, Roberts noted the following:

1. The amino group was always found either on the carbon atom from which the leaving group departed or, at most, one carbon atom away.
2. Neither the starting materials (aryl halides) nor the products (arylamines) appeared to isomerize under the reaction conditions.
3. The reactivities of the halogens were $\text{Br} > \text{I} > \text{Cl} > > \text{F}$.

Two mechanistic alternatives could explain these results. One possibility is that the aryl halide reacts with the incoming amino group by competitive "normal" (equation Figure 8.57) and "abnormal" (Figure 8.58) pathways. The second possibility is that both types of product result from an elimination-addition mechanism involving benzyne (**86**), an aromatic ring with a formal triple bond, as shown in Figure 8.59.



²³² Gilman, H.; Kyle, R. H.; Benkeser, R. A. *J. Am. Chem. Soc.* **1946**, *68*, 143.

²³³ Gilman, H.; Kyle, R. H. *J. Am. Chem. Soc.* **1948**, *70*, 3945.

²³⁴ Roberts, J. D.; Semenow, D. A.; Simmons, H. E., Jr.; Carlsmith, L. A. *J. Am. Chem. Soc.* **1956**, *78*, 601.

²³⁵ Particularly noteworthy is the use of quotation marks around the word 'prove' in the statement by Roberts (reference 234) that "the above facts strongly indicate but do not 'prove' that benzyne is the intermediate in the [reaction]. Therefore, other reaction mechanisms will be considered in order to determine whether a more satisfactory formulation can be found."

²³⁶ The benzyne mechanism can be denoted as an $S_N(EA)$ (substitution nucleophilic elimination addition) reaction (reference 7).

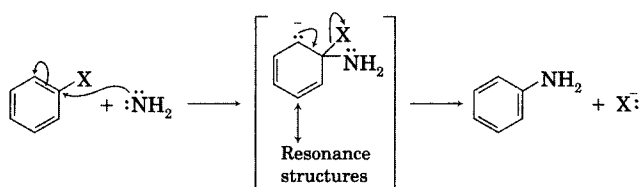


FIGURE 8.57
"Normal" mechanism for aniline formation.

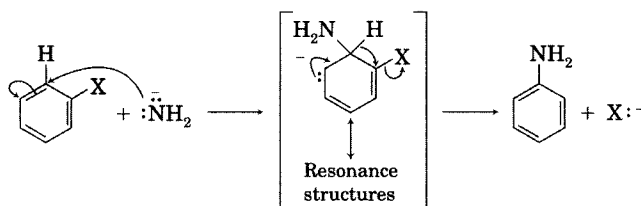


FIGURE 8.58
Hypothetical "abnormal" mechanism for aniline formation.

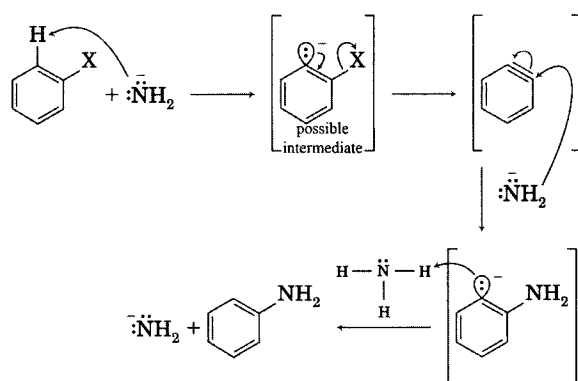
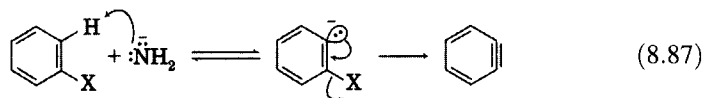
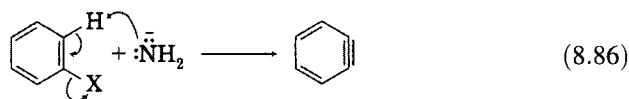


FIGURE 8.59
Benzyne mechanism for aniline formation.

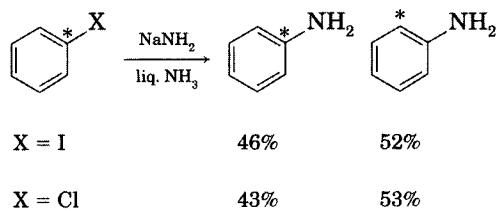
To determine the regiochemistry of halide replacement by amide ion, Roberts and co-workers studied the reaction of chlorobenzene-1-¹⁴C and iodobenzene-1-¹⁴C with KNH₂ in liquid NH₃, as shown in Figure 8.60. The observation of nearly equal yields of the two products is most consistent with the benzyne mechanism (Figure 8.59).²³⁷

The mechanism shown in Figure 8.59 requires that both a C–H and a C–L bond be broken in order to form the benzyne intermediate. Roberts and co-workers considered that these two groups might be lost in a concerted process (equation 8.86) or in consecutive steps (equation 8.87).



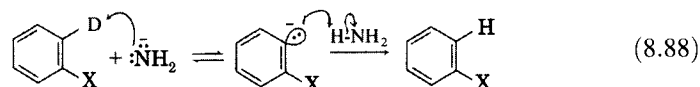
Use of halobenzenes labeled with deuterium on *one* of the positions ortho to the halogen gave further insight into the reaction. If the reaction occurs in

²³⁷ The relative yields are not exactly 50:50 due to a small carbon isotope effect favoring attachment of the nucleophile to ¹²C.

**FIGURE 8.60**

Distribution of isotopic label after substitution.

stepwise fashion, then the initial carbanion might be reprotonated (equation 8.88), leading to loss of deuterium label in the reactant. Table 8.20 summarizes the results found with a series of reactants.



The data indicate that the reaction is effectively concerted (equation 8.86) for bromobenzene, because deuterium loss in the reactant is negligible. Chlorobenzene appears to react by a stepwise process (equation 8.87), however. During a reaction period sufficient to convert 28% of reactant to product, 13% of the reactant underwent proton exchange (deuterium loss). The fluorobenzenes also underwent rapid proton exchange, but the reaction did not lead to anilines. The ease with which an ortho hydrogen is abstracted from a halobenzene ($F > Cl > Br > I$) varies directly with the electronegativity of the halogen. That is, the greater the electronegativity of X, the easier the *o*-hydrogen can be abstracted. The opposite trend is observed for the ease of departure of the leaving group: $I > Br > Cl > F$. For bromobenzene and iodobenzene, the rate-limiting step is proton removal; for fluorobenzene and chlorobenzene the rate-limiting step is halide ion departure. Thus, the overall reactivity of aryl halides varies as $Br > I > Cl > > F$.²²¹

Product Ratios in Benzyne Reactions

The near-equivalence of the rate constants for protonation and for departure of halide ion from the aryl carbanion derived from chlorobenzene suggests an explanation for the effects of substituents on the rate constants and product distributions observed in benzyne reactions. Table 8.21 summarizes the

TABLE 8.20 Deuterium Loss and Aniline Formation in the Reaction of *o*-Deuterioaryl Halides with KNH₂ in Liquid Ammonia

Aryl Halide	Deuterium Loss from Reactant	Aniline Formation (%)
Fluorobenzene-2,4,6- ² H ₃	100%	0
Fluorobenzene-3,5- ² H ₂	100%	0
Fluorobenzene-2- ² H	100%	0
Chlorobenzene-2- ² H	13%	28
Bromobenzene-2- ² H	—	72

Source: Reference 234.

TABLE 8.21 Product Distributions for Reaction of Substituted Halobenzenes with NH_2^- in Liquid Ammonia

R	X	Yield (%)	% Ortho	% Meta	% Para
<i>o</i> -CF ₃	Cl	28	—	100	—
<i>o</i> -CH ₃	Cl	66	45	55	—
<i>o</i> -CH ₃	Br	64	48.4	51.5	—
<i>o</i> -OCH ₃	Br	33	—	100	—
<i>p</i> -CF ₃	Cl	25	—	50	50
<i>p</i> -CH ₃	Cl	35	—	62	38
<i>p</i> -OCH ₃	Br	31	—	49	51
<i>m</i> -CF ₃	Cl	16	—	100	—
<i>m</i> -CH ₃	Cl	66	40	52	8
<i>m</i> -CH ₃	Br	61	22	56	22
<i>m</i> -OCH ₃	Br	59	—	100	—

Source: Reference 238.

distribution of substituted aniline products observed in the reaction of substituted bromo- and chlorobenzenes with amide ion in liquid ammonia.²³⁸ For the ortho-substituted compounds, benzyne formation can only occur so as to give the intermediate with the triple bond located between carbon atoms 2 and 3 (relative to the substituent), as shown in Figure 8.61. Attachment of a nucleophile to the triple bond of such a benzyne could yield only the ortho and meta products. For R = *o*-CF₃, only the meta product is formed. We infer that the transition state leading to phenyl carbanion **87** is lower in energy than that leading to **88** because of the greater stability of the developing carbanion having the negative charge closer to the electron-withdrawing CF₃ group. When R = *o*-CH₃, which we traditionally consider to be weakly electron-donating in electrophilic aromatic substitution, approximately equal amounts of ortho and meta products are formed. Similar arguments apply to the intermediates (**89** and **90**) when *para*-substituted halobenzenes react (Figure 8.62).

Two different benzyne intermediates can be formed by reaction of meta-substituted halobenzenes, but we expect a lower activation energy (and therefore faster reaction and thus more product) for the pathway involving benzyne formation via the more stable carbanion. Therefore, if R is electron-donating, the proton para to R will be removed faster by amide ion, as shown in Figure 8.63. If R is electron-withdrawing, then the carbanion with the

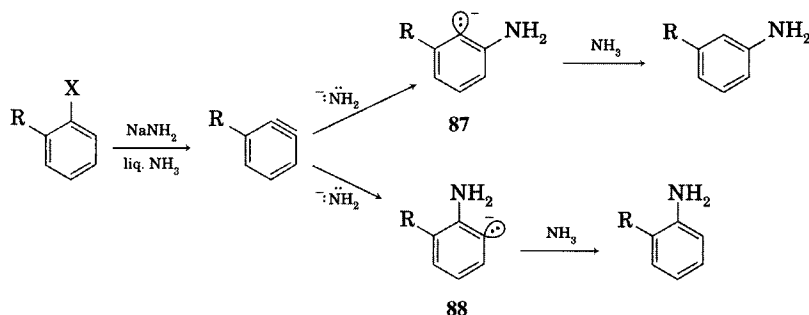
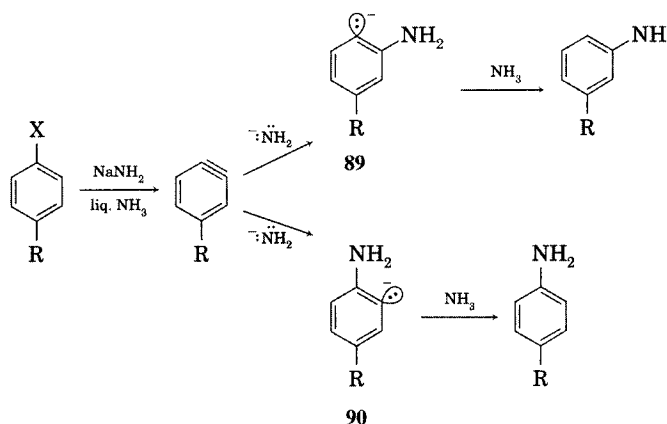


FIGURE 8.61
Effect of ortho substituents on patterns of benzyne substitution.

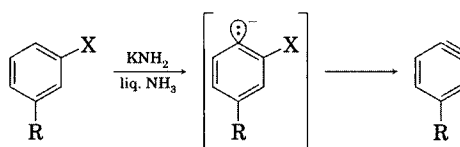
²³⁸ Roberts, J. D.; Vaughan, C. W.; Carlsmith, L. A.; Semenov, D. A. *J. Am. Chem. Soc.* **1956**, *78*, 611.

**FIGURE 8.62**

Effect of para substituents on patterns of benzyne substitution.

FIGURE 8.63

Effect of substituent on elimination step in benzyne mechanism: favored pathway if R is electron-donating.



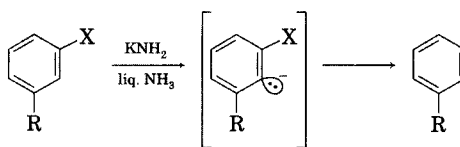
negative charge ortho to R will be formed preferentially, as shown in Figure 8.64. Similar considerations apply to the prediction of the site of reaction of the resulting benzyne with amide ion, as shown in Figures 8.65 and 8.66.

Benzyne Substituent Effects and Implicit Models

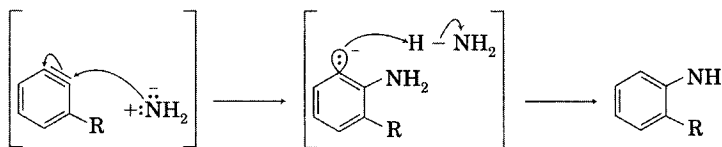
The preceding explanation would seem to explain most of the data in Table 8.21, but there is one apparent discrepancy. We might have expected the methoxy substituent to be electron-donating, but it gives the same product orientation as does trifluoromethyl. This intuitive expectation of the substituent effect of methoxy is based primarily on its influence on electrophilic aromatic substitution (S_EAr) and on nucleophilic aromatic substitution (S_NAr) reactions, both of which involve attachment of a species to an aromatic ring to form a σ complex. In contrast, the carbanionic intermediates presumed to be formed in the benzyne reaction have the nonbonded pair of electrons in

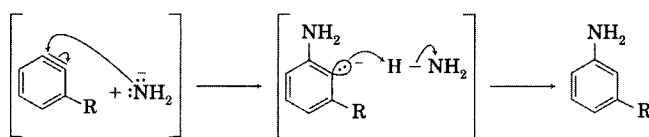
FIGURE 8.64

Effect of substituent on elimination step in benzyne mechanism: favored pathway if R is electron-withdrawing.

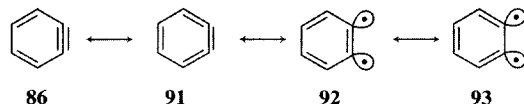
**FIGURE 8.65**

Effect of substituent on addition step in benzyne mechanism: favored pathway if R is electron-donating.



**FIGURE 8.66**

Effect of substituent on addition step in benzyne mechanism: favored pathway if R is electron-withdrawing.

**FIGURE 8.67**

Representations of benzyne.

an sp^2 hybrid orbital in the plane of the aromatic ring. This sp^2 hybrid orbital is orthogonal to the aromatic π system, so interaction of this orbital with the π system and with p orbitals on ring substituents is precluded. In other words, the geometry of the carbanion prevents resonance interactions between the carbanion and the substituent, so the effect of a substituent in benzyne reactions is limited to inductive (field) effects. Due to the electronegativity of oxygen, methoxy is electron-withdrawing by induction, so its effect is qualitatively the same as trifluoromethyl. This example shows the potential pitfalls in transferring models from one reaction to another without explicitly considering the underlying bases of those models.

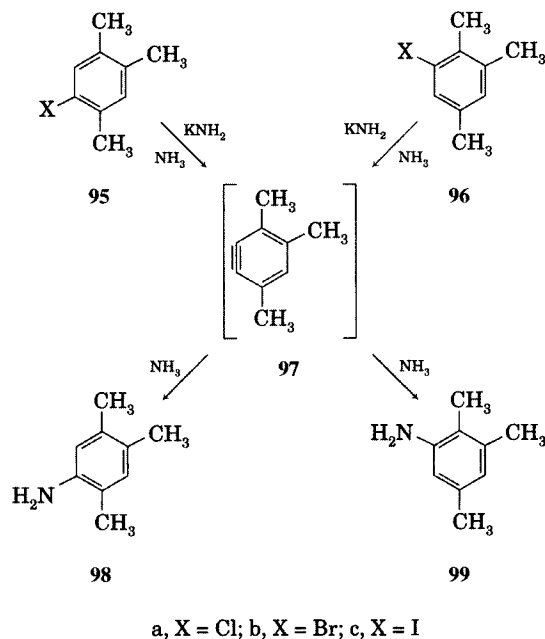
One other aspect of benzyne chemistry deserves mention. We have drawn the benzyne structure as **86** (Figure 8.67), which might be called the aryne representation. We cannot a priori state that a structure with what is formally one triple bond and two double bonds in a six-membered ring is more stable than a structure with four double bonds, which is the cumulene representation of benzyne (**91**). We should also consider the possibility of some biradical nature of benzyne, as suggested by the resonance structures **92** and **93**. There have been several attempts to determine experimentally and theoretically which drawing is the best graphical representation of benzyne, and Laing and Berry found that analysis of infrared absorption bands of matrix-isolated benzyne suggested the aryne structure (**86**).²³⁹ Nevertheless, our structural models should not be limited by our desire to draw simple graphical models in synthetic or mechanistic schemes, and there may be utility in remembering the possible contribution of the other resonance structures also.

Radical-Nucleophilic Substitution

Just as the benzyne mechanism was proposed in order to explain apparent anomalies in reactions considered initially to be S_NAr reactions, another mechanism for nucleophilic aromatic substitution was developed because of results of studies under conditions in which the benzyne mechanism was expected. Kim and Bunnett investigated the reaction of halogen-substituted isomers of pseudocumene (1,2,4-trimethylbenzene, **94**) with KNH_2 in liquid NH_3 .²⁴⁰ As shown in Figure 8.68, elimination of HX from both the 5-halopseudocumenes (**95a,b,c**) and the 6-halopseudocumenes (**96a,b,c**) should produce the same aryne intermediate, **97**. Therefore, the distribution of

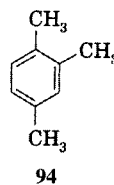
²³⁹ Laing, J. W.; Berry, R. S. *J. Am. Chem. Soc.* **1976**, *98*, 660.

²⁴⁰ Kim, J. K.; Bunnett, J. F. *J. Am. Chem. Soc.* **1970**, *92*, 7463.

**FIGURE 8.68**

Aryne mechanism for reaction of isomeric halopseudocumenes with KNH_2 in liquid NH_3 . (Adapted from reference 245.)

5- (**98**) and 6-pseudocumidine (**99**) formed via a benzyne reaction should be the same, no matter whether the reactant is **95a**, **95b**, **95c**, **96a**, **96b**, or **96c**.

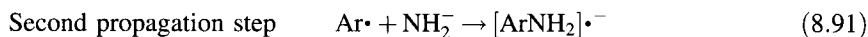
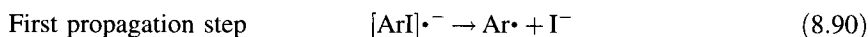
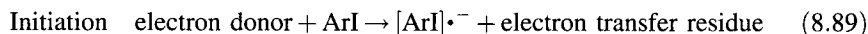


The ratio of products from reaction of **95a**, **95b**, **96a**, and **96b** were found to be identical within experimental error. (Ratios of **98** to **99** ranged from 1.45 to 1.55.) There was a large difference in the product distributions formed from the iodopseudocumenes, however. When the reactant was **95c**, the ratio of **99** to **98** was 0.63 : 1.0; when the reactant was **96c**, the ratio of **99** to **98** was 5.86 : 1.0. Furthermore, significant yields of **94** were observed from reactions with **95c** and **96c**.²⁴⁰

The observation that some **99** formed in the reaction of **95c** and some **98** resulted from the reaction of **96c** suggested that at least some product must arise through the aryne mechanism shown in Figure 8.68. The observation of relatively greater amounts of **98** than **99** from **95c** and of greater amounts of **99** than **98** from **96c** indicated that there must also be a competing mechanism leading to the unrearranged products. It was considered unlikely that this alternative mechanism could be an $\text{S}_{\text{N}}\text{Ar}$ pathway, because that process is more favorable for aryl bromides and chlorides than for iodides.²⁴⁰

Kim and Bunnett also found that the product ratios from reactions of **95c** and **96c** could be shifted toward the ratios observed with other halogens by adding a radical trap such as tetraphenylhydrazine to the solvent (liquid ammonia) or by carrying out the reaction in a solvent composed of 50% ammonia and 50% diethyl ether. The authors therefore proposed a radical chain mechanism, shown in equations 8.89 through 8.93, for formation of

unrearranged products. In the initiation step, an unspecified electron donor transfers an electron to either **95c** or **96c** (both denoted as Ar). In the first propagation step of the chain reaction, the radical anion of the aryl iodide detaches an iodide ion and forms an aryl radical. The aryl radical reacts with amide ion to form the radical anion of the product, **98** or **99**. The product radical anion then transfers an electron to the aryl iodide, and the chain continues. Termination steps, such as the reaction of the aryl radical with a hydrogen donor to produce the arene, **94**, interrupt the chain reaction.²⁴¹



This chain reaction is analogous to radical chain mechanisms for nucleophilic aliphatic nucleophilic substitution that had been suggested independently by Russell and by Kornblum and their co-workers.^{242,243} The descriptive title $S_{RN}1$ (substitution radical-nucleophilic unimolecular) was suggested for this reaction by analogy to the S_N1 mechanism for aliphatic substitution.²⁴⁴ The IUPAC notation⁷ for the $S_{RN}1$ reaction is (T + D_N + A_N), in which the symbol T refers to an electron transfer. When the reaction was carried out in the presence of solvated electrons formed by adding potassium metal to the ammonia solution, virtually no aryne (rearranged) products were observed. Instead, reaction of **95c** produced only **98** (40%) and **94** (40%) but no **99**, and reaction of **96c** produced **99** (54%) and **94** (30%) with only a trace of **98**.²⁴⁵

Subsequent research showed the $S_{RN}1$ mechanism to occur with many other aromatic compounds.²⁴⁴ The reaction was found to be initiated by solvated electrons, by electrochemical reduction, and by photoinitiated electron transfer.²⁴⁶ Not only I, but also Br, Cl, F, SC_6H_5 , $N(CH_3)_3^+$, and $OPO(OCH_2CH_3)_2$ have been found to serve as electrofuges. In addition to amide ion, phosphanions, thiolate ions, benzeneselenolate ion ($C_6H_5Se^-$), ketone and ester enolate ions, as well as the conjugate bases of some other carbon acids, have been identified as nucleophiles. The $S_{RN}1$ reaction was observed with naphthalene, phenanthrene, and other polynuclear aromatic systems, and the presence of alkyl, alkoxy, phenyl, carboxylate, and benzoyl groups on the aromatic ring does not interfere with the reaction.²⁴⁷

The $S_{RN}1$ mechanism is also important for many aliphatic structures that are unreactive in either S_N2 or S_N1 reactions. Such compounds include

²⁴¹ Under some conditions, termination by dimerization of aryl radicals may lead to appreciable yields of Ar-Ar. Ettayeb, R.; Savéant, J.-M.; Thiébaud, A. *J. Am. Chem. Soc.* **1992**, *114*, 10990.

²⁴² Kornblum, N.; Michel, R. E.; Kerber, R. C. *J. Am. Chem. Soc.* **1966**, *88*, 5662.

²⁴³ Russell, G. A.; Danen, W. C. *J. Am. Chem. Soc.* **1966**, *88*, 5663; **1968**, *90*, 347.

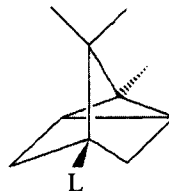
²⁴⁴ For a detailed discussion, see Rossi, R. A.; de Rossi, R. H. *Aromatic Substitution by the $S_{RN}1$ Mechanism*, ACS Monograph 178; American Chemical Society: Washington, DC, 1983.

²⁴⁵ Kim, J. K.; Bunnett, J. F. *J. Am. Chem. Soc.* **1970**, *92*, 7463; 7464.

²⁴⁶ For a review of photochemically stimulated $S_{RN}1$ reactions, see Bowman, W. R. in Fox, M. A.; Chanon, M., Eds. *Photoinduced Electron Transfer*, Part C; Elsevier: Amsterdam, 1988; pp. 487-552.

²⁴⁷ Bunnett, J. F. *Acc. Chem. Res.* **1978**, *11*, 413.

perfluoroalkyl iodides, 1-substituted bridgehead compounds, substituted cyclopropanes, and neopentyl halides.^{234,248,249} As noted on page 475, the 1-substituted bridgehead compounds are unreactive in S_N1 reactions because the resulting carbocations are nonplanar.²¹ For example, 4-tricyclyl triflate (**100**) was calculated to undergo solvolysis in 60% aqueous ethanol at 25°C with a half-life of 4.6×10^9 years.²² On the other hand, 4-iodotricyclene (**101**) readily undergoes the $S_{RN}1$ reaction with $(C_6H_5)_2P^-$ ions in liquid ammonia at $-33^\circ C$.²⁵⁰



100 (L = OTf) **101** (L = I)

The Impermanence of Mechanistic Labels for Substitution Reactions

Substitution processes are diverse in both scope and mechanism. Upon detailed investigation, even those reactions that seem most familiar to us offer degrees of complexity that confound our attempts to fit all of organic chemistry into a few distinct compartments. As one author put it, "in summary, nitration—the classic example of electrophilic aromatic substitution—is not always an electrophilic aromatic substitution."²⁵¹

We are reminded again of the need to consider all mechanisms in chemistry as temporary descriptions that may change as new theories and experimental results become available. There is truth in the statement of Coulson that "reaction mechanisms in general are elucidated in successive approximation."²⁵² In this regard it may be useful to remember the words of Lucretius:

No single thing abides, but all things flow.
 Fragment to fragment clings, and thus they grow
 Until we know and name them.
 Then by degrees they change and are no more
 The things we know.²⁵³

²⁴⁸ Rossi, R. A.; Pierini, A. B.; Palacios, S. M. *J. Chem. Educ.* **1989**, *66*, 720.

²⁴⁹ Kornblum and co-workers found evidence for a radical chain mechanism initiated by electron transfer from the nucleophile to the nitroaromatic ring in the reaction of *p*-nitroacetyl chloride with nucleophiles such as azide ion in hexamethylphosphoramide (HMPA) solution. Kornblum, N.; Wade, P. A. *J. Org. Chem.* **1987**, *52*, 5301. See also Kornblum, N.; Cheng, L.; Davies, T. M.; Earl, G. W.; Holy, N. L.; Kerber, R. C.; Kestner, M. M.; Manthey, J. W.; Musser, M. T.; Pinnick, H. W.; Snow, D. H.; Stuchal, F. W.; Swiger, R. T. *J. Org. Chem.* **1987**, *52*, 196.

²⁵⁰ The corresponding chloride is not reactive under the same conditions, apparently because of the less favorable reduction potential of the chloride. Santiago, A. N.; Morris, D. G.; Rossi, R. A. *J. Chem. Soc. Chem. Commun.* **1988**, 220.

²⁵¹ Perrin, C. L. *J. Am. Chem. Soc.* **1977**, *99*, 5516.

²⁵² Coulson, C. A. *Proc. Chem. Soc.* **1962**, 265.

²⁵³ The quotation is from *No Single Thing Abides*, translated by Mallock, W. H. in Van Doren, M., Ed. *An Anthology of World Poetry*; Reynal & Hitchcock, 1936. It was previously used in the introduction to Chapter 4 of Leffler, J. E.; Grunwald, E. *Rates and Equilibria of Organic Reactions*; John Wiley & Sons: New York, 1963; p. 57.

Problems

- 8.1. Predict the products and effect of increasing solvent polarity on the rate of each of the following reactions:
- $\text{I}^- + (\text{CH}_3)_4\text{N}^+ \rightarrow$
 - $\text{NH}_3 + (\text{CH}_3)_3\text{S}^+ \rightarrow$
- 8.2. Complete the diagram shown in Figure 8.69 for nucleophilic aromatic substitution by adding the structures corresponding to the lower left and upper right corners. Identify the reaction pathway indicated by each of the two dashed lines leading from reactant to product.

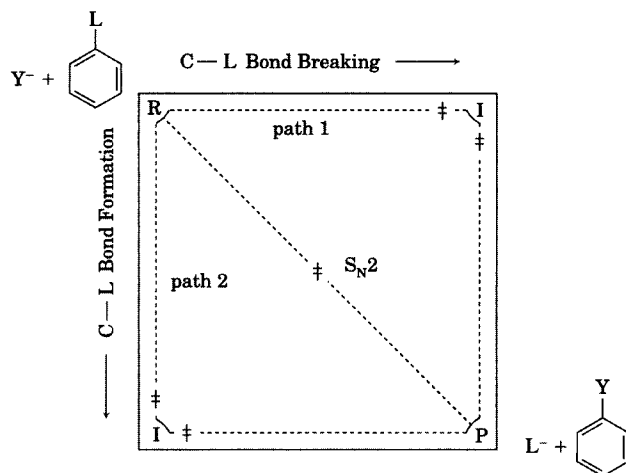
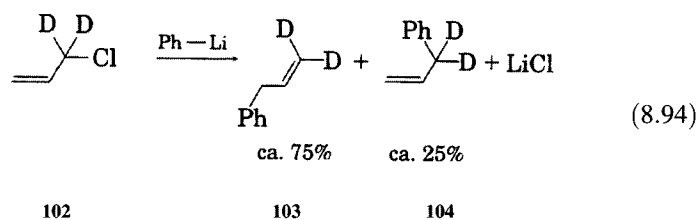


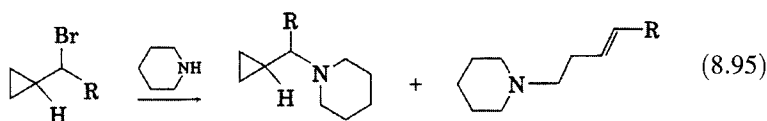
FIGURE 8.69

- 8.3. Reaction of allyl-1,1- d_2 chloride (**102**) with phenyllithium produces allylbenzene in which about 75% of the product is allylbenzene-3,3- d_2 (**103**) and about 25% is allylbenzene-1,1- d_2 (**104**).



What do these results suggest about the relative contributions of $\text{S}_{\text{N}}2$ and $\text{S}_{\text{N}}2'$ processes in this reaction?

- 8.4. Cyclopropylcarbinyl halides react with piperidine to give products as shown in equation 8.95. Both products are formed by second-order processes. The distribution of the two products varies with the nature of the R group: the larger the R group, the greater is the yield of rearranged product.
- Propose a mechanism for the formation of each product.
 - Explain why the size of the R group affects the product distribution.



- 8.5. (+)-D- α -Bromopropionate reacts in aqueous NaOH with second-order kinetics to give (-)-L- α -hydroxypropionate. In water it undergoes first-order reaction to give (+)-D- α -hydroxypropionate, however. Propose an explanation for these results.
- 8.6. Treatment of (-)-2-hydroxy-2-phenylpropanoic acid with SOCl_2 leads to the formation of (-)-2-chloro-2-phenylpropanoic acid. When the same reactant is treated with PCl_5 , however, the product that is isolated is (+)-2-chloro-2-phenylpropanoic acid. Explain the different stereochemical outcome of these two synthetic procedures.
- 8.7. The relative rate constants for solvolysis in buffered acidic solution of compounds with the structure $\text{H}_2\text{NCH}_2\text{CR}_2\text{CH}_2\text{CH}_2\text{Br}$ vary with the structure of the R group as follows: R = hydrogen, 1.0; R = methyl, 158; R = ethyl, 594; R = isopropyl, 9190. Explain this variation in reactivity.
- 8.8. a. Verify that the stereochemical assignments for each structure in Figure 8.20 are correct.
b. What stereoisomer of 3-phenyl-2-pentyl tosylate gives acetolysis products that are the mirror image of those obtained by acetolysis of L-threo-2-phenyl-3-pentyl tosylate?
- 8.9. Sketch the expected shape of plots of ΔG versus reaction coordinate (as in Figure 8.33) for the reaction of ammonia with methyl chloride in acetone solution and in hexane solution.
- 8.10. When treated with fuming HBr, (\pm)-2,3-diacetoxybutane is converted to meso-2,3-dibromobutane. There is evidence that (\pm)-erythro-3-bromo-2-butanol is an intermediate in the reaction. Propose a mechanism to account for the stereospecificity of the reaction.
- 8.11. For nitration of toluene, the partial rate factors under one set of experimental conditions are $f_o^Z = 41$, $f_m^Z = 2.1$, $f_p^Z = 51$. What is the relative reactivity of toluene compared to benzene under these conditions?
- 8.12. The crown ether 21-crown-7 (21C7) was found to influence the rate and selectivity of nitration of anisole with tetrabutylammonium nitrate and trifluoroacetic acid in methylene chloride solution. Table 8.22 shows the relative reactivity and product distribution for various concentrations of the crown ether.²⁵⁴
- a. Calculate the partial rate factor for the ortho and para positions for each [21C7].
- b. Rationalize the change (if any) seen in the partial rate factors as a function of [21C7].

TABLE 8.22 Effect of [21C7] on Nitration of Anisole

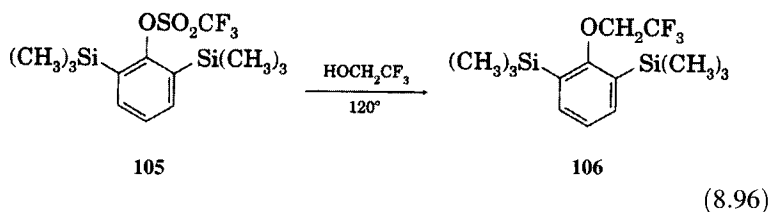
	[21C7]			
	0.0 M	0.0082 M	0.032 M	0.131 M
k/k_B	2220	4940	10800	27600
% Ortho	78.1	33.8	13.2	4.8
% Para	21.9	66.2	86.8	95.2

²⁵⁴ Masci, B. J. *Org. Chem.* 1985, 50, 4081.

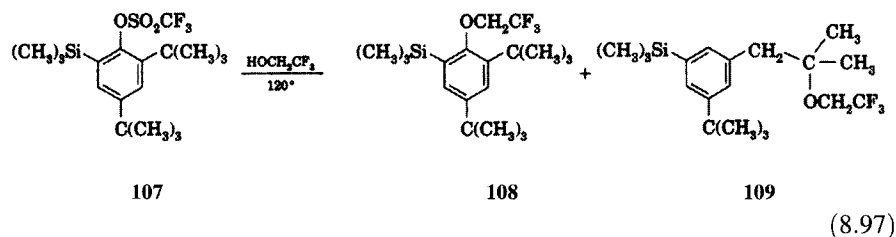
TABLE 8.23 Kinetic Data for Benzoylation of Benzene and Derivatives in Benzoyl Chloride Solution at 25°C

Compound	k ($M^{-1} \text{ min}^{-1}$)
Benzene	0.00297
Toluene	0.326
<i>t</i> -Butylbenzene	0.215

- 8.13. Rate constants reported for the AlCl_3 -catalyzed benzoylation of benzene and its derivatives in benzoyl chloride solution are shown in Table 8.23.
- Calculate the relative rate of reaction (with the rate of reaction of benzene set equal to 1.0) for each compound. Are the results consistent with your expectations based on the activating or deactivating nature of the substituent groups?
 - The relative isomer distribution of products from benzoylation of toluene is 9.3% ortho, 1.45% meta, and 89.3% para. Calculate the partial rate factor for reaction of toluene at each position.
 - Use the data in Table 8.23 to determine whether a Hammett correlation is observed in this reaction. Do the data fit better with σ or with σ^+ ? Interpret the meaning of the sign and magnitude of the value of ρ you obtain.
- 8.14. a. When heated in 2,2,2-trifluoroethanol (TFE) buffered with 2,6-lutidine at 120°C for 5 hours, 2,6-bis(trimethylsilyl)phenyl triflate (**105**) gave a quantitative yield of the trifluoromethyl ether **106**. The reaction was found to be first order in **105** and zero order in 2,6-lutidine. The ΔH^\ddagger and ΔS^\ddagger values for the reaction were found to be 26.5 kcal/mol and -5.5 eu, respectively. Propose a mechanism and give a mechanistic label for the reaction.



- b. Trifluoroethanolysis of the triflate **107** at 100°C produced the two ethers, **108** (66%) and **109** (27%). Propose a mechanism for the formation of **109** that involves both a 1,4-hydride shift and a 1,2-aryl shift.



- 8.15. In a study of the iodination of phenol, the second-order rate constant for the reaction of 2,4,6-trideuteriophenol with iodine in aqueous solution was found to

be $3.05 \times 10^{-4} \text{ M}^{-1} \text{ s}^{-1}$, while the corresponding rate constant for reaction of undeuterated phenol was found to be $1.21 \times 10^{-3} \text{ M}^{-1} \text{ s}^{-1}$.²⁵⁵

- Calculate the 1° hydrogen kinetic isotope effect for the reaction.
 - Propose a mechanism involving the formation of an intermediate that will account for both the observed second-order kinetics and the kinetic isotope effect.
 - A 1° hydrogen kinetic isotope effect was also observed in the sulfonation of benzene and in the cyclodehydration of 2-anilino-2-pentene-4-one. Based on the intermediates expected in each case, explain why 1° hydrogen kinetic isotope effects are observed in these reactions but not in most other $\text{S}_{\text{E}}\text{Ar}$ reactions?
- Propose a detailed mechanism for the Smiles rearrangement shown as equation 8.74, page 530.
 - Summarize the types of labeling experiments that could be used to study the proposed mechanism for the von Richter reaction (Figure 8.54).
 - Propose an explanation for the observation that potassium amide enhances the rate of formation of tetraphenylmethane in the reaction of chlorobenzene with potassium triphenylmethide in liquid ammonia.
 - Consider an alternative mechanism (Figure 8.70) for the formation of *m*-trifluoromethylaniline by reaction of *o*-chlorotrifluoromethylbenzene with KNH_2 in liquid ammonia in which a phenyl carbanion isomerizes prior to an $\text{S}_{\text{N}}\text{Ar}$ reaction. Suggest experiments to determine whether such a mechanism occurs in this case or in other reactions of aryl halides with KNH_2 in liquid ammonia.

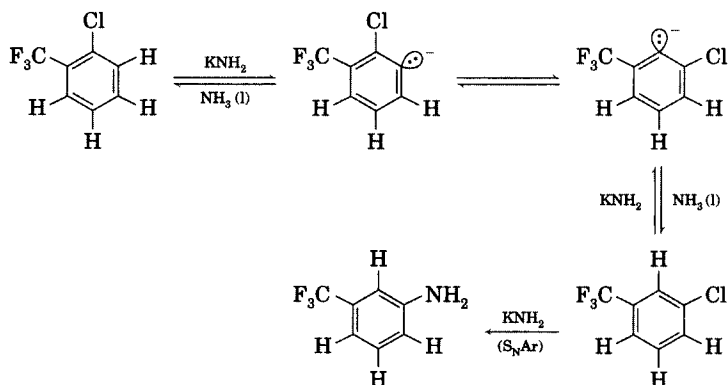
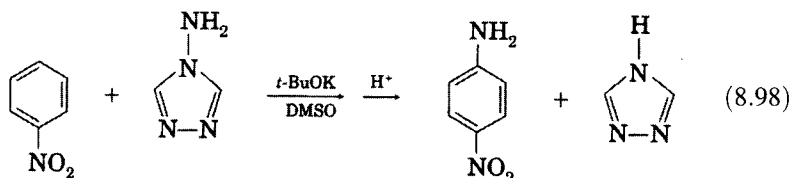


FIGURE 8.70

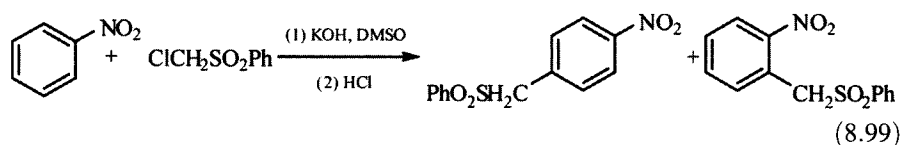
- Propose a detailed mechanism for the transformation of nitrobenzene to *p*-nitroaniline with 4-amino-1,2,4-triazole shown in equation 8.98.



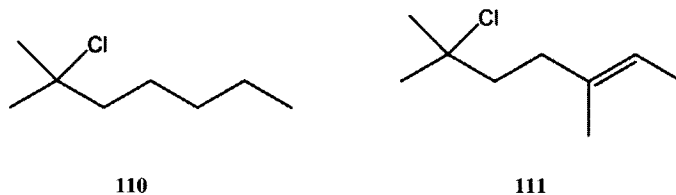
- Based on the data in Table 8.19, draw a reaction coordinate diagram for the reaction of piperidine with 1-bromo-2,4-dinitrobenzene.

²⁵⁵ Initial concentrations were $8 \times 10^{-3} \text{ M}$ phenol, $1.96 \times 10^{-3} \text{ M}$ iodine, 0.5 M acetic acid, 0.05 M sodium acetate, 0.23 M sodium perchlorate, and 0.02 M sodium iodide.

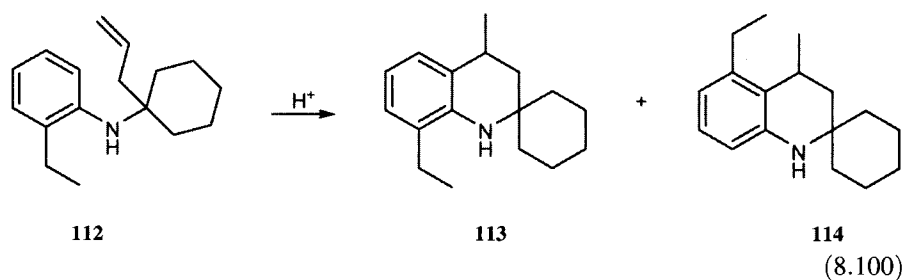
- 8.22. Rationalize the distribution of products from the reaction of *o*-bromotoluene with KNH₂ in liquid ammonia (Table 8.21).
- 8.23. One of the observations that led to the formulation of the benzyne mechanism was the failure of either bromomesitylene or bromodurene to react with sodium amide in liquid ammonia.
- Why are these compounds unreactive by the benzyne mechanism?
 - Why is the lack of reaction of these compounds alone insufficient to establish the benzyne mechanism for reactions of compounds such as bromobenzene with amide ion in liquid ammonia? That is, what factors might make bromomesitylene and bromodurene unreactive with amide ion in liquid ammonia whether or not the reaction of bromobenzene involves a benzyne mechanism?
- 8.24. Propose a detailed mechanism to account for the formation of the products in equation 8.99.



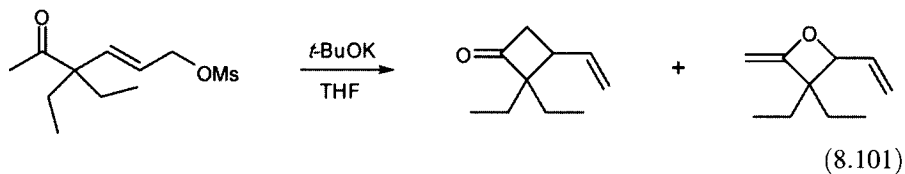
- 8.25. Measurements of the rate constants for solvolysis of **110** and **111** in 80% (v/v) aqueous ethanol indicated that ΔG^\ddagger is 91 kJ/mol for **110** and 82 kJ/mol for **111**. The ΔS^\ddagger value is $-31 \text{ J K}^{-1} \text{ mol}^{-1}$ for **110** and $-67 \text{ J K}^{-1} \text{ mol}^{-1}$ for **111**. Explain these results.



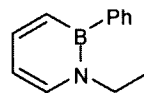
- 8.26. Propose a detailed mechanism for the reaction of **112** to form **113** and **114**.



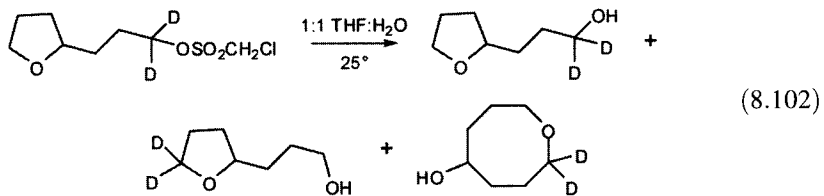
- 8.27. Propose S_Ni' mechanisms for the reactions in equation 8.101.



- 8.28. Predict the major substitution product of the reaction of 1-ethyl-2-phenyl-1,2-azaborine (**115**) with Br_2 in CH_2Cl_2 at 0°C .

**115**

- 8.29. Propose a mechanism to account for the formation of the products in equation 8.102.



- 8.30. The rate constant for solvolysis of compound **116** in 60% aqueous ethanol at 25°C is ca. $2.7 \times 10^{-20} \text{ s}^{-1}$. Why is the rate constant so low? What is the half-life of the compound under these conditions?

**116**

- 8.31. Propose the propagation steps that might be expected in an $\text{S}_{\text{RN}}2$ mechanism for the conversion of ArL and Y^- to ArY and L^- .

Addition Reactions

9.1 INTRODUCTION

An addition reaction occurs when two molecular entities combine to form a single product containing all of the atoms of the reactants. In this process two bonds are formed, one bond breaks in the adding reagent, and there is a net reduction of bond multiplicity in the other reactant.¹ The structure undergoing addition can be any species with a multiple bond, but our focus will be on alkenes, alkynes, and carbonyl compounds. While addition to other functional groups is certainly important, alkenes and alkynes exhibit a wide range of electrophilic addition reactions, and additions to the carbonyl group will illustrate some theoretical aspects of nucleophilic addition.

Addition mechanisms are broadly defined to be heterolytic, homolytic, or cyclic, which are processes that involve ionic or radical intermediates or are concerted, respectively.² Concerted reactions will be discussed in Chapter 11. The emphasis here will be heterolytic (ionic) additions, although we will also consider some aspects of radical reactions. Addition reactions may be categorized further as being electrophilic or nucleophilic. In an electrophilic addition, a compound with a multiple bond reacts with an electrophilic reagent to produce an intermediate that subsequently reacts with a nucleophile. In nucleophilic addition, the unsaturated substrate reacts with a nucleophile to produce an intermediate that subsequently reacts with an electrophile to produce the final product.³

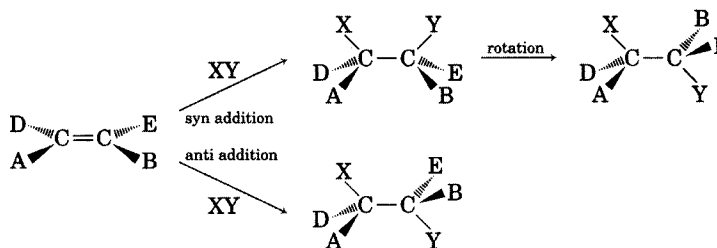
¹ Commission on Physical Organic Chemistry, IUPAC. *Pure Appl. Chem.* **1994**, 66, 1077.

² de la Mare, P. B. D.; Bolton, R. *Electrophilic Additions to Unsaturated Systems*, 2nd ed.; Elsevier Scientific Publishing: New York, 1982; p. 2.

³ We generally think of electrophilic and nucleophilic additions as being heterolytic processes, but there can be electrophilic and nucleophilic character to radical additions also. Alkyl or aryl substituents on a carbon-centered radical make the radical more nucleophilic than a methyl radical, while electron-withdrawing substituents make it more electrophilic. For a discussion, see Zipse, H.; He, J.; Houk, K. N.; Giese, B. J. *Am. Chem. Soc.* **1991**, 113, 4324. Perfluoroalkyl radicals are strongly electrophilic; see, for example, Avila, D. V.; Ingold, K. U.; Lusztyk, J.; Dolbier, W. R.; Pan, H.-Q. *J. Am. Chem. Soc.* **1993**, 115, 1577.

FIGURE 9.1

Diastereomeric products of syn and anti addition to an alkene.



One important stereochemical distinction to be made in additions to alkenes is that syn addition and anti addition to a carbon-carbon double bond may produce stereoisomeric products.⁴ The term *anti* means that one group adds from the top of the molecule (as defined by the plane of the substituents on the double bond), while the other adds from the bottom. In *syn* addition, both substituents add from the same face. As noted in Figure 9.1, the syn and anti pathways produce different configurations at one of the two tetrahedral centers created by the addition to a carbon-carbon double bond. In older terminology, these processes were referred to as *trans* or *cis* additions, but currently it is preferred to use the terms *syn* and *anti* for *mechanisms* and to reserve the terms *cis* and *trans* for *structures*.⁵

Many different mechanisms have been proposed for addition reactions, and they have long been described in terms of the Ingold formalism.⁶ In this system, addition reactions are labeled with symbols incorporating Ad for addition, E or N for electrophilic or nucleophilic, and a number indicating the molecularity of the reaction.⁷ For example, an Ad_E2 mechanism involves attachment of an electrophile to the substrate, followed by attachment of a nucleophile to the resulting intermediate. The corresponding IUPAC term for the same reaction would be (A_E + A_N).⁸ Because most of the literature of organic chemistry has been written using the Ingold terminology, we will note the IUPAC nomenclature but will usually discuss reactions in terms of the more familiar Ingold designations.

⁴ Whether stereoisomeric products are formed and, if so, whether the products are enantiomers or diastereomers depend on the substitution pattern of the olefin and on whether the adding reagent is symmetric (X-X) or not (X-Y).

⁵ Eliel, E. L.; editor's comment, p. 328, in Fahey, R. C. *Top. Stereochem.* **1968**, 3, 237.

⁶ Ingold, C. K. *Structure and Mechanism in Organic Chemistry*, 2nd ed.; Cornell University Press: Ithaca, NY, 1969. See also Fahey, R. C.; Lee, D.-J. *J. Am. Chem. Soc.* **1968**, 90, 2124.

⁷ Wilson, M. A. *J. Chem. Educ.* **1975**, 52, 495 summarized the Ingold terminology for many of the mechanistic possibilities.

⁸ Commission on Physical Organic Chemistry, IUPAC. *Pure Appl. Chem.* **1989**, 61, 23. For a discussion, see Guthrie, R. D.; Jencks, W. P. *Acc. Chem. Res.* **1989**, 22, 343.

9.2 ADDITION OF HALOGENS TO ALKENES

Electrophilic Addition of Bromine to Alkenes

Introduction

One of the classic reactions of organic chemistry is the addition of bromine to an alkene.⁹⁻¹¹ We will first summarize the evidence that led to the textbook mechanism (shown in Figure 9.2), and then we will survey experimental data that reveal the complexities underlying this simple mechanistic representation.

Two important features of the mechanism shown in Figure 9.2 are:

1. The intermediate is a **bromonium ion**, a three-membered ring containing a bromine atom bearing a formal charge of +1. The structure is also called a σ complex, because the valence bond representation implies a full or partial σ bond between the olefinic carbon atoms and the bromine atom.¹²
2. The attachment of the two bromine atoms to the carbon-carbon double bond is anti. This stereochemistry results because a bromide ion attacks the back side of one of the bromonium ion C-Br bonds in a process much like an S_N2 reaction.¹³⁻¹⁵

The bromonium ion in Figure 9.2 was proposed by Roberts and Kimball to explain the stereospecificity of the addition to alkenes.¹⁶ Independent evidence for the existence of bromonium ions was provided by Winstein and Lucas, who found that (\pm)-*erythro*-3-bromo-2-butanol was converted to *meso*-2,3-dibromobutane upon reaction with fuming HBr (equation 9.1), but the (\pm)-*threo* reactant formed the (\pm)-2,3-dibromobutane. These authors suggested that the bromine provides anchimeric assistance to the departure of the protonated OH group and forms a bromonium ion which, upon nucleophilic attack by bromide ion, gives a

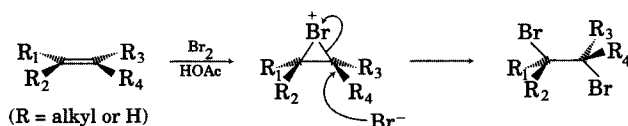


FIGURE 9.2

General mechanism for addition of bromine to an alkene.

⁹ de la Mare, P. B. D.; Bolton, R. *Electrophilic Addition to Unsaturated Systems*; Elsevier Publishing Company: Amsterdam, 1966; p. 32.

¹⁰ Schmid, G. H.; Garratt, D. G. in Patai, S., Ed. *The Chemistry of Double-bonded Functional Groups*, Supplement A, Part 2; John Wiley & Sons: London, 1977; pp. 725-912.

¹¹ Schmid, G. H. in Patai, S., Ed. *The Chemistry of Double-bonded Functional Groups*, Supplement A, Volume 2, Part 1; John Wiley & Sons: London, 1989; pp. 679-731.

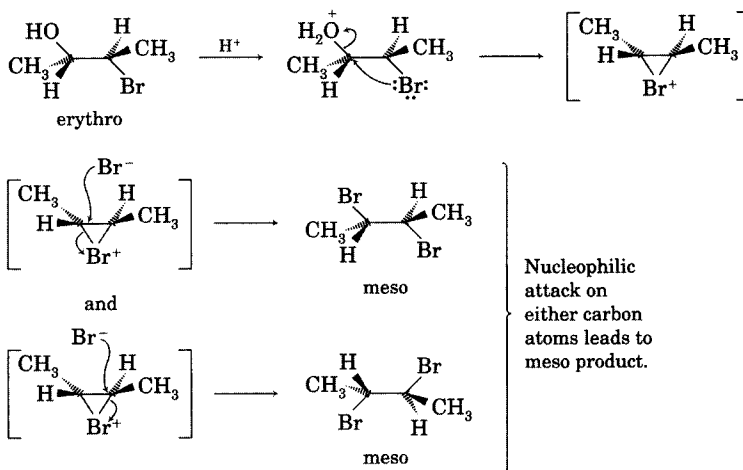
¹² The results of ab initio calculations (reference 75) suggested that it might be more correctly described as a strong π -complex.

¹³ Meer, N.; Polanyi, M. Z. *physik. Chem.* **1932**, B19, 164; Bergmann, I. E.; Polanyi, M.; Szabo, A. Z. *phys. Chem.* **1933**, B20, 161.

¹⁴ Olson, A. R. J. *Chem. Phys.* **1933**, 1, 418; Olson, A. R.; Voge, H. H. J. *Am. Chem. Soc.* **1934**, 56, 1690.

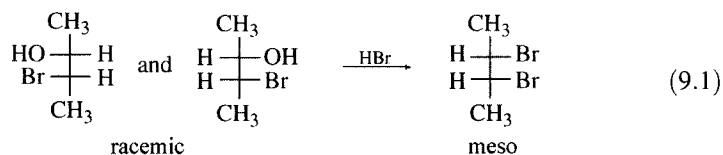
¹⁵ A frontier MO rationalization for *anti*-1,2 addition (as well as for *syn*-1,4 addition and *anti*-1,6 addition) was provided by Fukui, K. *Tetrahedron Lett.* **1965**, 2427.

¹⁶ Roberts, I.; Kimball, G. E. J. *Am. Chem. Soc.* **1937**, 59, 947.

**FIGURE 9.3**

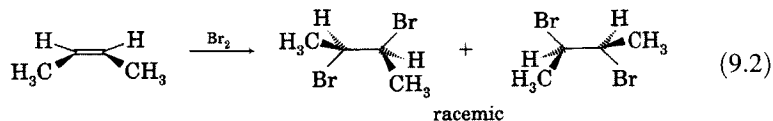
Proposed mechanism for the conversion of *erythro*-3-bromo-2-butanol into *meso*-2,3-dibromobutane.

dibromide with retention of configuration of the original bromohydrin (Figure 9.3).¹⁷



The mechanism of bromine addition shown in Figure 9.2 is further supported by several lines of evidence:

1. Addition of bromine to an alkene is highly stereospecific and gives products with stereochemistry consistent with an anti addition mechanism.¹⁸ For example, addition of bromine to cyclohexene produces *trans*-1,2-dibromocyclohexane.¹⁹ Addition of bromine to *cis*-2-butene produces (\pm)-2,3-dibromobutane (equation 9.2), while addition to the *trans* isomer gives the *meso* product (equation 9.3).²⁰⁻²²



¹⁷ Winstein, S.; Lucas, H. J. *J. Am. Chem. Soc.* **1939**, *61*, 1576, 2845.

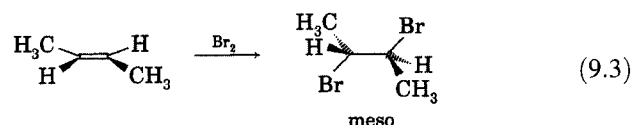
¹⁸ For a summary of reactions illustrating the stereochemistry, see Terry, E. M.; Eichelberger, L. *J. Am. Chem. Soc.* **1925**, *47*, 1067 and references therein. See also the discussion by Fahey (reference 5).

¹⁹ Winstein, S. *J. Am. Chem. Soc.* **1942**, *64*, 2792.

²⁰ Dillon, R. T.; Young, W. G.; Lucas, H. J. *J. Am. Chem. Soc.* **1930**, *52*, 1953.

²¹ Rolston, J. H.; Yates, K. *J. Am. Chem. Soc.* **1969**, *91*, 1469.

²² Addition of bromine to cholesterol produced the 5 α ,6 β isomer of cholesterol dibromide. Barton, D. H. R.; Miller, E. J. *J. Am. Chem. Soc.* **1950**, *72*, 1066.



2. The reaction is faster with electron-rich alkenes.²³ The rate constants for addition of bromine to a series of alkenes were found to increase in the order ethene < propene < 2-butene \approx isobutene < 2-methyl-2-butene.²⁴ In other words, each methyl group that replaces a hydrogen atom on ethene increases reactivity. The addition of bromine to substituted ethenes in methanol with added sodium bromide can be correlated to the equation

$$\log k_2 = -3.10 \Sigma \sigma^* + 7.02 \quad (9.4)$$

where $\Sigma \sigma^*$ is the sum of the Taft σ^* values for the four substituents.²⁵ Since the polar effects of the alkyl groups are additive, regardless of their position on the double bond, the results were interpreted as evidence for a symmetrical distribution of positive charge on the two olefinic carbon atoms in the transition structure for the addition.^{26,27} Moreover, the rate constant for the reaction is decreased if electron-withdrawing groups are near the double bond, as is shown by the series of halogen-substituted olefins in Table 9.1.²⁸

3. The cationic intermediate suspected in the reaction can be trapped by added nucleophiles (including nucleophilic solvent molecules) if its lifetime is long enough for diffusion to bring the two species together.

TABLE 9.1 Relative Reactivity of Alkenes in Bromine Addition

Alkene	Relative Reactivity
Ethene	1
Allyl bromide	0.3
Vinyl bromide	3.0×10^{-4}
<i>cis</i> -1,2-Dichloroethene	1.0×10^{-7}
Trichloroethene	3.0×10^{-10}
Tetrachloroethene	Too low to measure

Source: Reference 28.

²³ The term *electron rich* has been applied to alkenes with several alkyl substituents because these compounds typically react rapidly with electrophiles. Vardhan and Bach (reference 219) attributed the greater reactivity of more substituted alkenes to the higher energy (and thus greater electron-donating ability) of the olefinic HOMO.

²⁴ Davis, H. S. *J. Am. Chem. Soc.* **1928**, *50*, 2769.

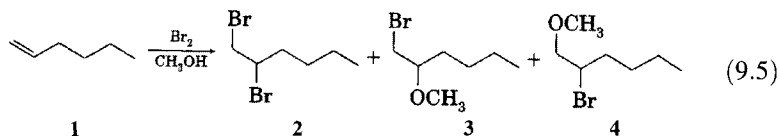
²⁵ Linear free energy relationships, including the use of σ^* and σ^+ constants, were discussed in Chapter 6.

²⁶ Ruasse, M.-F. *Acc. Chem. Res.* **1990**, *23*, 87 and references therein.

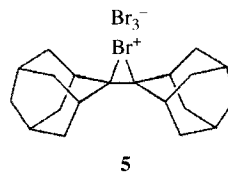
²⁷ The steric effects of alkyl substituents can retard bromine addition reactions, however, and this effect can be large enough to mask the electronic effect of alkyl substituents. Ruasse, M.-F.; Motallebi, S.; Gal, B.; Lomas, J. S. *J. Org. Chem.* **1990**, *55*, 2298.

²⁸ Swedlund, B. E.; Robertson, P. W. *J. Chem. Soc.* **1947**, 630.

For example, the addition of bromine to *trans*-2-butene in acetic acid gave 98% of the expected *meso*-2,3-dibromobutane, but 2% of 1-acetoxy-2-bromobutane was also observed.²¹ Addition of bromine to 1-hexene (1) in methanol was found to produce 31% of 1,2-dibromohexane (2), and 59% of a 4 : 1 ratio of 1-bromo-2-methoxyhexane (3) and 2-bromo-1-methoxyhexane (4), as shown in equation 9.5.²⁹ The formation of 4 implies that the cationic intermediate is not simply a secondary carbocation.



4. Olah obtained direct evidence for the existence of the tetramethylethylene bromonium ion (and also the chloronium ion and iodonium ion but not the fluoronium ion) by ¹H NMR spectra of halogenated precursors in antimony pentafluoride-sulfur dioxide solution at -60°C.³⁰⁻³²
5. A yellow solid identified as a bromonium ion was isolated by Wynberg and co-workers from the reaction of bromine with adamantylidene-adamantane.³³ Brown and co-workers obtained an X-ray crystal structure of the species 5 as a tribromide salt.³⁴⁻³⁶



All of the data cited so far are consistent with the mechanism suggested in Figure 9.2, but additional experimental results suggest a much more complex range of interactions among alkene, halogen, solvent, and added nucleophiles than is apparent from that figure.³⁷

²⁹ Puterbaugh, W. H.; Newman, M. S. *J. Am. Chem. Soc.* **1957**, *79*, 3469. See also Ecke, G. G.; Cook, N. C.; Whitmore, F. C. *J. Am. Chem. Soc.* **1950**, *72*, 1511 and references cited therein.

³⁰ Olah, G. A.; Bollinger, J. M. *J. Am. Chem. Soc.* **1967**, *89*, 4744.

³¹ Also see Olah, G. A. *Halonium Ions*; Wiley-Interscience: New York, 1975.

³² Evidence for the existence of the fluoronium ion in the gas phase was reported by Nguyen, V.; Cheng, X.; Morton, T. H. *J. Am. Chem. Soc.* **1992**, *114*, 7127.

³³ Strating, J.; Wieringa, J. H.; Wynberg, H. *J. Chem. Soc. Chem. Commun.* **1969**, 907.

³⁴ Slebocka-Tilk, H.; Ball, R. G.; Brown, R. S. *J. Am. Chem. Soc.* **1985**, *107*, 4504.

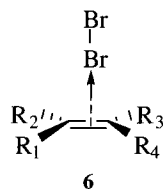
³⁵ Bennet, A. J.; Brown, R. S.; McClung, R. E. D.; Klobukowski, M.; Aarts, G. H. M.; Santarsiero, B. D.; Bellucci, G.; Bianchini, R. *J. Am. Chem. Soc.* **1991**, *113*, 8532.

³⁶ An X-ray structure of the corresponding triflate salt confirmed the symmetrical geometry of the three-membered ring containing bromine. Brown, R. S.; Nagorski, R. W.; Bennet, A. J.; McClung, R. E. D.; Aarts, G. H. M.; Klobukowski, M.; McDonald, R.; Santarsiero, B. D. *J. Am. Chem. Soc.* **1994**, *116*, 2448.

³⁷ The results of an NMR study using deuterated structures gave results more consistent with equilibrating β -bromocarocations than with a static bromonium ion: Ohta, B. K.; Hough, R. E.; Schubert, J. W. *Org. Lett.* **2007**, *9*, 2317.

Role of Charge Transfer Complexes in Bromine Addition Reactions

One of the earliest observations about bromine addition reactions is that mixing bromine and alkenes leads to a new, transient UV–vis absorption band, suggesting the formation of a bromine–olefin π complex (**6**).³⁸ The stabilities of these charge transfer complexes depend significantly on the ionization potentials of the alkenes, although the polarizabilities of the alkenes can be a significant factor also.³⁹



Quantifying the extent of weak complex formation is a difficult task.⁴⁰ Furthermore, observation of a complex between two reactants does not necessarily mean that the complex is a necessary step in the reaction. Formation of the complex might be only a nonproductive detour from the reaction path. Because there was a correlation between the CT complex stabilization energies (determined by spectroscopy) and the rate constants of bromine addition, Dubois and Garnier concluded that complex formation may be a fast step that precedes the formation of the bromonium ion.⁴¹ Moreover, spectroscopic studies reported by Bellucci and co-workers indicated that the decay of the absorption of the CT complex from bromine and cyclohexene (λ_{max} near 287 nm) corresponded to the rate constant for formation of the bromine addition product. The kinetic data pointed to an apparent negative activation energy, -7.8 kcal/mol, for the bromination, while the formation of the CT complex in 1,2-dichloroethane was exothermic, with $\Delta H = -4.6$ kcal/mol and $\Delta S = -17.0$ eu in the range of 15°C to 35°C . These results were consistent with a mechanism in which the CT complex is an essential step in the addition of bromine to cyclohexene. The results were not consistent with a mechanism in which complex formation is an unproductive pathway that serves only to reduce the concentrations of the reactants.⁴² The results of stopped-flow kinetics experiments, coupled with *ab initio* and density functional theory (DFT) calculations, provided further evidence that 1:1 and 1:2 π complexes are intermediates in the electrophilic addition of halogens to alkenes.⁴³

Not only does the experimental evidence support the role of a CT complex as an intermediate in bromine addition reactions, but it appears that many different CT complexes may occur in mixtures of alkenes and bromines.

³⁸ Because of the evidence for charge transfer complexation, Garnier and Dubois proposed that the mechanistic description should be $\text{Ad}_\text{E}\text{C}1$ (unimolecular electrophilic addition proceeding through a CT complex) for the process in which progression from the CT complex to the bromonium ion is the rate-limiting step and $\text{Ad}_\text{E}\text{C}2$ (bimolecular electrophilic addition involving reaction of a CT complex with a nucleophile) for processes in which the CT complex reacts with another species in the rate-limiting step. Garnier, F.; Dubois, J.-É. *Bull. Soc. Chim. France* **1968**, 3797.

³⁹ Chiappe, C.; Detert, H.; Lenoir, D.; Pomelli, C. S.; Ruasse, M. F. *J. Am. Chem. Soc.* **2003**, *125*, 2864. See also Chiappe, C.; Lenoir, D.; Pomelli, C. S.; Bianchini, R. *Phys. Chem. Chem. Phys.* **2004**, *6*, 3235.

⁴⁰ Person, W. B. *J. Am. Chem. Soc.* **1965**, *87*, 167.

⁴¹ Dubois, J. E.; Garnier, F. *Tetrahedron Lett.* **1966**, 3047; *Chem. Commun.* **1968**, 241.

⁴² Bellucci, G.; Bianchini, R.; Ambrosetti, R. *J. Am. Chem. Soc.* **1985**, *107*, 2464.

⁴³ Lenoir, D.; Chiappe, C. *Chem. Eur. J.* **2003**, *9*, 1037.

Bellucci and co-workers reported evidence for the interaction of adamantylideneadamantane and bromine to form complexes with different stoichiometries, having alkene: Br₂ ratios of 2:1, 1:1, 1:2, and 1:3.⁴⁴ Conductivity experiments suggested that the 1:2 and 1:3 complexes are tribromide and pentabromide salts, respectively, of the adamantylideneadamantane bromonium ion.

Kinetics of Bromine Addition Reactions

The kinetics of bromine addition to alkenes can be more complex than the simple model in Figure 9.2 would suggest.⁴⁵ Early studies revealed considerable kinetic variation with solvent, temperature, and the presence of additives such as water. The kinetic investigations can also be complicated because of the involvement of HBr₃ (from Br₂ and HBr) or of termolecular processes involving an alkene, Br₂, and Br⁻.⁴⁶ The Br⁻ can be produced if the bromonium ion is intercepted by solvent or solvent anion (e.g., acetate ion). The equilibrium constant for dissociation of Br₃⁻ to Br₂ and Br⁻ was determined to be 5 × 10⁻² M in water and 2 × 10⁻³ M in methanol.⁴⁷ Thus, a general kinetic expression for the addition of bromine to alkenes can be represented as^{21,48}

$$-\frac{d[\text{Br}_2]}{dt} = (k_2[\text{Br}_2] + k_3[\text{Br}_2]^2 + k_{\text{Br}_3^-}[\text{Br}_3^-])[\text{alkene}] \quad (9.6)$$

Some early studies suggested that only the k_2 process should occur in polar solvents at low [Br₂], that the k_3 process alone should be seen in nonpolar solvents, and that both the k_2 and k_3 processes can occur in polar solvents at higher [Br₂]. Fukuzumi and Kochi demonstrated that both second-order and third-order reactions could occur in CCl₄.⁴⁹ Schmid and Toyonaga determined that the rate constants for the second-order and third-order processes for addition of bromine to *cis*-2-butene in CCl₄ at 25°C are $k_2 = 8.9 \times 10^{-4} \text{ M}^{-1} \text{ s}^{-1}$ and $k_3 = 4.0 \text{ M}^{-2} \text{ s}^{-1}$, respectively.⁴⁸ Thus, for *cis*-2-butene there is a concentration range (Br₂ < 10⁻⁴ M) in which the second-order process dominates, a region (Br₂ > 10⁻² M) in which the third-order process dominates, and a range in between in which both processes are significant.⁴⁸ The Br₃⁻ process is thought to be unimportant in most cases unless bromide ion has been added as a reagent. Because of the kinetic complexity, mechanistic discussions based on kinetics studies must take account of the concentration of the brominating agent(s).

⁴⁴ Bellucci, G.; Bianchini, R.; Chiappe, C.; Marioni, F.; Ambrosetti, R.; Brown, R. S.; Slebocka-Tilk, H. *J. Am. Chem. Soc.* **1989**, *111*, 2640. The formation constants observed for these species in 1,2-dichloroethane were $K_{2:1} = 1.11 \times 10^3 \text{ M}^{-2}$, $K_{1:1} = 2.9 \times 10^2 \text{ M}^{-1}$, $K_{1:2} = 3.2 \times 10^5 \text{ M}^{-2}$, and $K_{1:3} = 7.2 \times 10^6 \text{ M}^{-3}$, respectively.

⁴⁵ For a discussion and compilation of kinetic parameters for electrophilic addition to unsaturated compounds, see Bolton, R. in Bamford, C. H.; Tipper, C. F. H., Eds. *Comprehensive Chemical Kinetics. Volume 9. Addition and Elimination Reactions of Aliphatic Compounds*; Elsevier: Amsterdam, 1973; pp. 1–86.

⁴⁶ Morton, I. D.; Robertson, P. W. *J. Chem. Soc.* **1945**, 129 and references therein.

⁴⁷ Bartlett, P. D.; Tarbell, D. S. *J. Am. Chem. Soc.* **1936**, *58*, 466.

⁴⁸ Schmid, G. H.; Toyonaga, B. *J. Org. Chem.* **1984**, *49*, 761 and references therein.

⁴⁹ Fukuzumi, S.; Kochi, J. K. *J. Am. Chem. Soc.* **1982**, *104*, 7599.

One possible mechanism for reactions of Br_3^- with alkenes involves the dissociation of Br_3^- to Br_2 and Br^- ion before reaction of Br_2 with the alkene.⁵⁰ Alternatively, Br_3^- might act as an electrophile and add directly to the alkene.^{47,51} Bellucci and co-workers used the stopped-flow technique to study the kinetics of addition of bromine to cyclohexene in 1,2-dichloroethane solution.⁵² With molecular bromine the kinetics were overall third order, first order in cyclohexene and second order in Br_2 .

$$-\frac{d[\text{Br}_2]}{dt} = k_3[\text{Br}_2]^2[\text{alkene}] \quad (9.7)$$

With tetrabutylammonium tribromide, the reaction was second order, first order in [cyclohexene] and first order in Br_3^- .

$$-\frac{d[\text{Br}_2]}{dt} = k_2[\text{Br}_3^-][\text{alkene}] \quad (9.8)$$

There was a solvent kinetic isotope effect on the tribromide reaction in $\text{CHCl}_3/\text{CDCl}_3$, with $k_{\text{H}}/k_{\text{D}} = 1.175$, but there was no solvent isotope effect for the addition of Br_2 . Reaction with Br_2 (the third-order reaction, equation 9.7) gave a ΔH^\ddagger value of -8.4 kcal/mol, while the reaction with tribromide (equation 9.8) gave a ΔH^\ddagger value of $+6.0$ kcal/mol.⁴² For reactions exhibiting third-order kinetics, the rate-limiting step appears to involve formation of a bromonium ion-tribromide ion pair from a complex of one alkene and two bromine molecules. With tetra-*n*-butylammonium tribromide as the source of bromine, the rate-limiting step is thought to be a backside nucleophilic attack at an olefin- Br_2 charge transfer complex (in equilibrium with Br_3^- and the olefin) by the ammonium bromide ion pair that has become detached from Br_2 at the moment of formation of the CT complex or that is present as added salt.⁵³

Kinetic isotope effects also indicate a difference in mechanism when the brominating agents are Br_2 and Br_3^- . Brown and co-workers measured rate constants for addition of molecular bromine to cyclohexene, to 3,3,6,6-tetra-deuteriocyclohexene, and to cyclohexene- d_{10} with Br_2 and with Br_3^- in acetic acid.⁵⁴ For bromination with Br_2 , the β secondary isotope effect (found by comparison of the reactivities of cyclohexene and 3,3,6,6-tetadeuteriocyclohexene) was 1.0 (Figure 9.4). Addition of bromine to cyclohexene and to cyclohexene- d_{10} , however, gave an inverse secondary kinetic isotope effect, $k_{\text{H}}/k_{\text{D}} = 0.53$. The results suggested that there is significant rehybridization of the alkene carbon atoms from sp^2 toward sp^3 in the transition structure for addition with Br_2 . For addition of bromine with Br_3^- , however, the value of $k_{\text{H}}/k_{\text{D}}$ calculated for cyclohexene/cyclohexene- d_{10} was 0.78, suggesting less

⁵⁰ Wolf, S. A.; Ganguly, S.; Berliner, E. *J. Org. Chem.* **1985**, *50*, 1053 and references therein.

⁵¹ DeYoung, S.; Berliner, E. *J. Org. Chem.* **1979**, *44*, 1088 and references therein.

⁵² Bellucci, G.; Bianchini, R.; Ambrosetti, R.; Ingrosso, G. *J. Org. Chem.* **1985**, *50*, 3313.

⁵³ Further support for the difference in mechanism for addition with Br_2 and Br_3^- comes from the observation that the two reagents give different stereochemical results upon addition of bromine to 3-substituted cyclohexenes. Bellucci, G.; Bianchini, R.; Vecchiani, S. *J. Org. Chem.* **1986**, *51*, 4224. Furthermore, the two reagents yield diastereomeric products upon reaction with chiral ketals. Giordano, C.; Coppi, L. *J. Org. Chem.* **1992**, *57*, 2765.

⁵⁴ Slebocka-Tilk, H.; Zheng, C. Y.; Brown, R. S. *J. Am. Chem. Soc.* **1993**, *115*, 1347 and references therein.

FIGURE 9.4

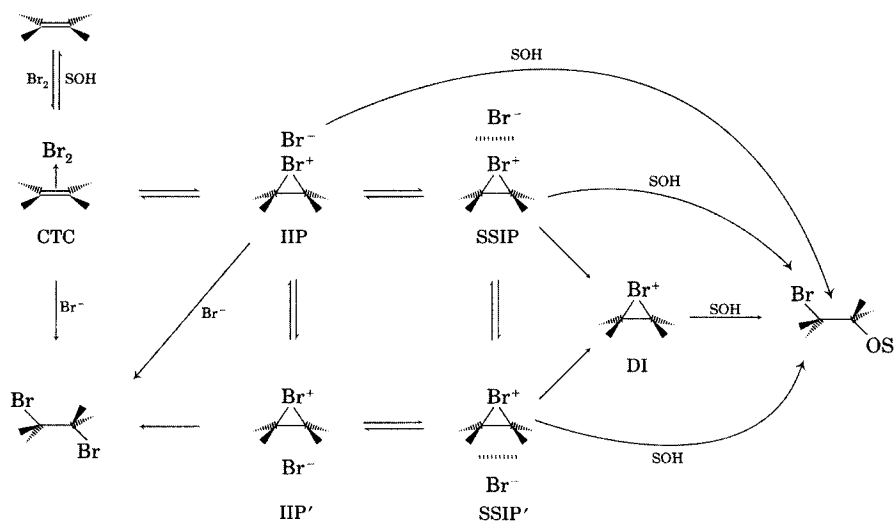
Kinetic isotope effects in the bromination of cyclohexene with Br_2 and Br_3^- .

	3,3,6,6-Tetradeuterio-cyclohexene	Cyclohexene- d_{10}
Brominating agent	$k_{\text{H}}/k_{\text{D}} = 1.0$	$k_{\text{H}}/k_{\text{D}} = 0.53$
Br_2	$k_{\text{H}}/k_{\text{D}} = 1.0$	$k_{\text{H}}/k_{\text{D}} = 0.53$
Br_3^-	-	$k_{\text{H}}/k_{\text{D}} = 0.78$

extensive rehybridization of the alkene carbon atoms in the transition structure.

Another product formed by the reaction of bromine with cyclohexene in acetic acid is *trans*-1-acetoxy-2-bromocyclohexane.⁵⁴ The yield of this product varies with the concentration of added LiBr (with ionic strength held constant). With $[\text{LiBr}] = 0$, Brown and co-workers found that the product mixture consisted of 27% 1,2-dibromo and 73% 1-acetoxy-2-bromo adducts. At $[\text{LiBr}]$ 0.1 M, 90% of the product was 1,2-dibromocyclohexane and only 10% was the 1-acetoxy-2-bromo derivative. Based on the conclusion that the low α -secondary deuterium KIE requires a nucleophilic (not electrophilic) role for Br^- , Brown and co-workers proposed the detailed mechanism shown in Figure 9.5. Here, CTC is a charge transfer complex; IIP and IIP' are intimate ion pairs; SSIP and SSIP' are solvent-separated ion pairs; DI is a dissociated ion; and SOH is a hydroxylic solvent. The key feature of the mechanism is the necessity for Br^- migration to occur in the rearrangement of IIP to IIP' so that backside attack can produce the dibromo product. The SSIP can rearrange to SSIP', but the latter must then reorganize to form IIP' (so that the Br^- is inside the solvent shell) before nucleophilic attack can occur. Added Br^- can react with the CTC or with IIP to produce the dibromo product.

The complex mechanism in Figure 9.5 can rationalize some observations about yields of the solvent incorporation products. In acetic acid, the bromoacetoxy product can arise from nucleophilic backside attack by solvent on IIP, IIP', and SSIP', and all of these processes can compete with pathways leading to the dibromo product. Once the SSIP or SSIP' has dissociated to free ions (DI), however, only nucleophilic attack by solvent is likely, so DI

**FIGURE 9.5**

Mechanism proposed for bromination of cyclohexene in acetic acid (SOH). (Adapted from reference 54.)

participation leads only to the bromoacetoxy product. It should be emphasized that the pathways shown in Figure 9.5 are suggested by the observed kinetics and product distributions, but they are not the only possibilities.⁵⁵ Any one of the reaction pathways might be replaced by another process that is its kinetic equivalent. For example, an alternative pathway for Br^- participation in the reaction would be one in which it acts as a base to facilitate removal of a proton from acetic acid in the transition structure for nucleophilic attack by the acetoxy oxygen.⁵⁴ Whatever may be the case, the mechanism in Figure 9.5 shows considerably more detail than the simplified form in Figure 9.2.

Solvent Effects in Bromine Additions

The mechanism in Figure 9.5 also provides a rationalization for some observations of solvent effects in bromine addition reactions. The major product of the reaction of bromine with cyclohexene in methanol is *trans*-2-bromo-1-methoxycyclohexane. *trans*-1,2-Dibromocyclohexane is observed if Br^- is added to the solution, but the yield of the dibromo adduct approaches 0% as $[\text{Br}^-]$ approaches 0 M.⁵⁶ This result stands in contrast to the 27% of 1,2-dibromo adduct obtained from the corresponding reaction in acetic acid. It appears that the greater polarity of methanol accelerates the dissociation of IIP to DI, and the greater nucleophilicity of methanol enhances the reaction of solvent with IIP, SSIP, DI, and SSIP'.⁵⁴

In addition to polarity and nucleophilicity toward the bromonium ion, other solvent properties may come into play. The rate-limiting step in electrophilic bromine addition is thought to be the conversion of a CT complex to a cation–bromide ion pair, which is consistent with the observation that the rate constant for bromine addition increases as solvent polarity increases.³⁸ Solvent may also electrophilically assist the removal of the bromide ion from the alkene– Br_2 CT complex by hydrogen bonding to a developing bromide ion (Figure 9.6).^{57,58} It has been estimated that this electrophilic solvent participation can lower the energy of bromonium ion formation by 60 kcal/mol.^{59,60} Additional support for the role of electrophilic

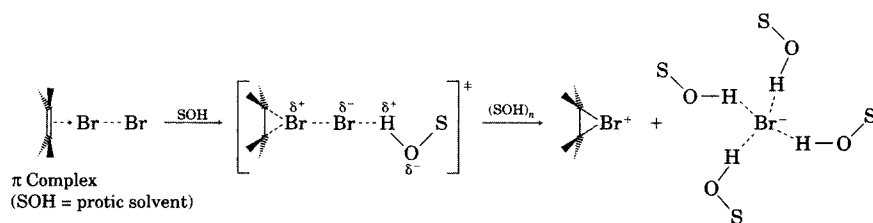


FIGURE 9.6

Possible role for electrophilic properties of solvent in addition of bromine to alkenes.

⁵⁵ Because the mechanistic scheme has many more rate constants than there are observables, consistency between a calculated rate expression and experimental results does not ensure that the mechanism is correct.

⁵⁶ Nagorski, R. W.; Brown, R. S. *J. Am. Chem. Soc.* **1992**, *114*, 7773.

⁵⁷ (a) Garnier, F.; Donnay, R. H.; Dubois, J.-E. *J. Chem. Soc. D Chem. Commun.* **1971**, 829; (b) Modro, A.; Schmid, G. H.; Yates, K. *J. Org. Chem.* **1979**, *44*, 4221.

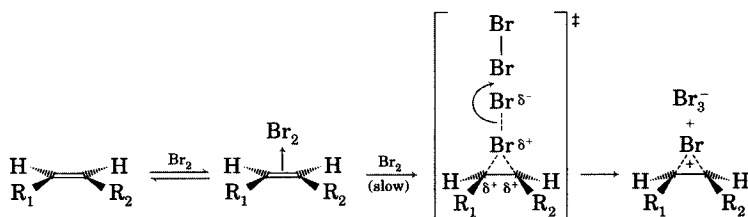
⁵⁸ Modro, A.; Schmid, G. H.; Yates, K. *J. Org. Chem.* **1977**, *42*, 3673.

⁵⁹ Ruasse, M.-F.; Zhang, B.-L. *J. Org. Chem.* **1984**, *49*, 3207.

⁶⁰ Ruasse, M.-F.; Motallebi, S.; Galland, B. *J. Am. Chem. Soc.* **1991**, *113*, 3440 and references therein.

FIGURE 9.7

Model for electrophilic assistance of departing Br^- by Br_2 in a non-protic solvent.



participation of protic solvent comes from solvent kinetic isotope effect studies. The value of $k_{\text{H}}/k_{\text{D}}$ for addition of bromine to 1-pentene in methanol/methanol- d was found to be 1.21, while for addition in acetic acid/acetic acid- d_4 it was 1.25.⁵⁷ In an aprotic solvent, a second Br_2 molecule may assist the collapse of the charge transfer complex by removing the departing Br^- as a Br_3^- ion (Figure 9.7).⁶⁰⁻⁶²

Based on solvent isotope effects and on the sensitivity of reaction rates to solvent, it has also been proposed that solvent molecules can provide nucleophilic assistance to the conversion of the CT complex to the bromonium ion, as shown in Figure 9.8.^{58,60} This process is analogous to that proposed for one possible mechanism (Figure 9.9) for the bromide-catalyzed addition to highly deactivated alkenes such as cinnamic acid.^{51,63}

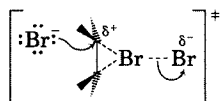


FIGURE 9.9

Proposed nucleophilic role of bromide ion in reaction of CT complex.

Reversibility of the Addition of Bromine

Most studies of bromine addition to alkenes have presumed that the intermediate proceeds to product and does not revert to alkene and bromine.⁶⁴ Brown and co-workers determined that bromonium ions generated from the solvolysis of the *trans*-2-bromo-1-brosylates of cyclohexene or cyclopentene could react with added Br^- to produce Br_2 .⁶⁵ Furthermore, *erythro*-2-bromo-1,2-diphenylethanol was found to react with anhydrous HBr (in 1,2-dichloroethane or chloroform) to produce both *trans*-stilbene and *meso*-1,2-dibromo-1,2-diphenylethane. The reaction of the *erythro* diastereomer can be explained by a mechanism involving anchimeric assistance in departure of water, which leads to a bromonium ion that reverts to the stilbene, as shown in Figure 9.10.^{66,67}

Under the same reaction conditions, *threo*-2-bromo-1,2-diphenylethanol was also found to produce *trans*-stilbene and *meso*-stilbene dibromide. It

⁶¹ Yates, K.; McDonald, R. S.; Shapiro, S. A. *J. Org. Chem.* **1973**, *38*, 2460.

⁶² For a more detailed discussion, see the mechanism proposed by Islam, S. M.; Poirier, R. A. *J. Phys. Chem. A* **2007**, *111*, 13218.

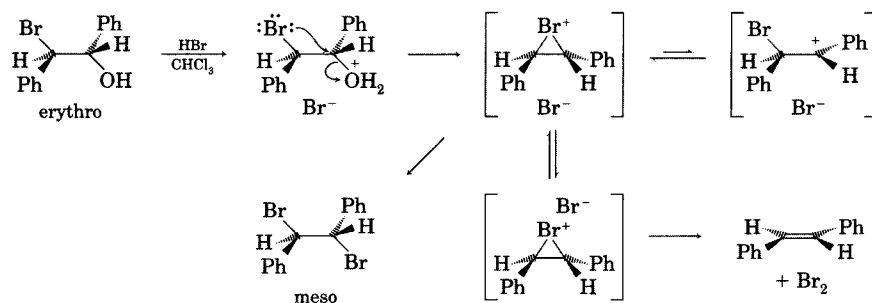
⁶³ The role of nucleophilic solvent participation is more clearly developed in the case of bromine addition to alkynes: Modena, G.; Rivetti, F.; Tonellato, U. *J. Org. Chem.* **1978**, *43*, 1521.

⁶⁴ Addition of bromine to cholesterol initially produced $5\alpha,6\beta$ -dibromocholestan- 3β -ol (reference 22). Upon standing in methanol solution at room temperature for 3 days, the initial product was converted to a 4 : 1 mixture of $5\beta,6\alpha$ -dibromocholestan- 3β -ol and the $5\alpha,6\beta$ isomer. The rate constant for the rearrangement was not affected by a 30-fold molar excess of cyclohexene, suggesting that the rearrangement did not occur by dissociation of the cholesterol dibromide to cholesterol and bromine.

⁶⁵ Brown, R. S.; Gedye, R.; Slebocka-Tilk, H.; Buschek, J. M.; Kopecky, K. R. *J. Am. Chem. Soc.* **1984**, *106*, 4515.

⁶⁶ Bellucci, G.; Chiappe, C.; Marioni, F. *J. Am. Chem. Soc.* **1987**, *109*, 515.

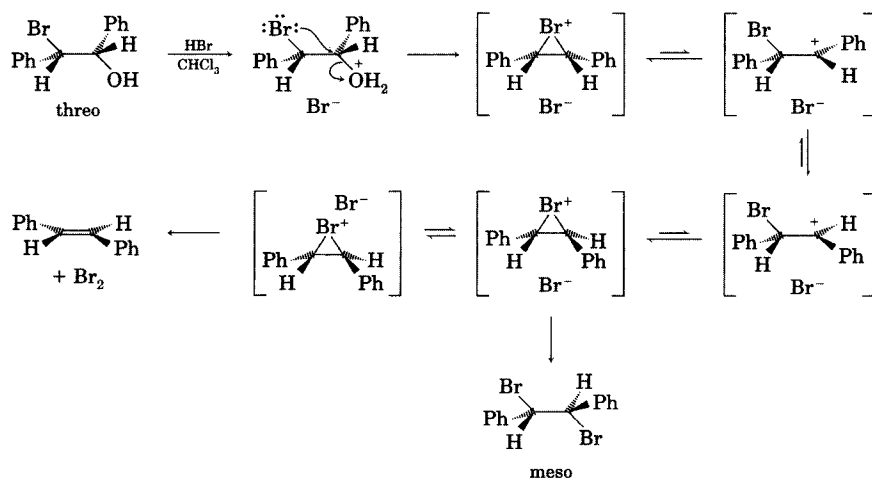
⁶⁷ Also see Brown, R. S.; Slebocka-Tilk, H.; Bennet, A. J.; Bellucci, G.; Bianchini, R.; Ambrosetti, R. *J. Am. Chem. Soc.* **1990**, *112*, 6310 and references therein.

**FIGURE 9.10**

Evidence for reversibility of bromonium ion formation from an erythro bromohydrin. (Adapted from reference 66.)

appears that the internal strain of the bromonium ion initially formed by loss of water can be relieved by isomerization, via a β -bromocarbenium ion, to the isomeric bromonium ion having the same stereochemistry as that in Figure 9.10. Thus, both diastereomers of starting material lead to the same stereoisomeric products, as shown in Figure 9.11.

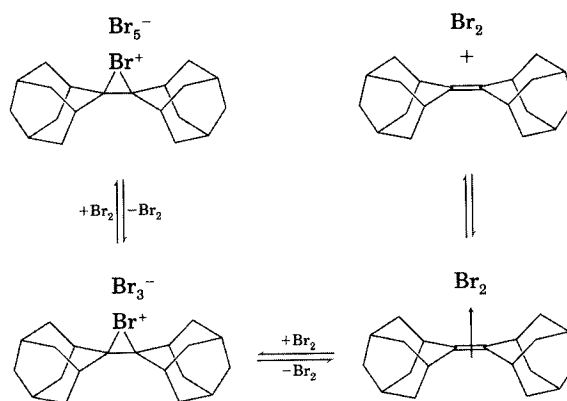
Reversibility of bromonium ion formation has been observed directly in the regeneration of adamantylideneadamantane from the bromonium ion salt (Figure 9.12).^{68,69} Further evidence for reversibility is the observation that the bromonium ion from adamantylideneadamantane can transfer Br^+ to cyclohexene in CH_2Cl_2 solution. Since a sterically hindered bromonium ion can transfer Br^+ , it seems reasonable that bromonium ions that are not sterically hindered should also be capable of transferring Br^+ . Therefore, reversibility of bromonium ion formation could be a general process.³⁵ Reversibility may

**FIGURE 9.11**

Evidence for reversibility of bromonium ion formation from a threo bromohydrin. (Adapted from reference 66.)

⁶⁸ Reversibility is also not anticipated for unsymmetrical alkenes such as *gem*-disubstituted alkenes. As is discussed in the following section, the cationic intermediates in such reactions are highly asymmetric, with much of the positive charge on the carbon atom and relatively little on the bromine. Since reversibility implies nucleophilic attack of bromide ion on the bromine in the intermediate, the smaller the charge on bromine, the less likely is that nucleophilic attack. For further discussion, see reference 60.

⁶⁹ Furthermore, from the solvolysis of the *trans*-2-bromo-1-trifluoromethanesulfonate of cyclohexane in the presence of Br^- in both acetic acid and methanol, it was determined that the solvolytic bromonium ions actually react with Br^- preferentially on the Br^+ , thus generating free Br_2 . Zheng, C. Y.; Slebocka-Tilk, H.; Nagorski, R. W.; Alvarado, L.; Brown, R. S. *J. Org. Chem.* **1993**, *58*, 2122.

**FIGURE 9.12**

Multiple equilibria in the formation of bromine from the adamantylideneadamantane bromonium ion. (Adapted from reference 44.)

be less likely with bromonium ions formed from sterically unhindered alkenes in nucleophilic protic solvents because capture by solvent is very rapid. As noted above, the protic solvent provides about 60 kcal/mol of electrophilic assistance in removal of bromide ion to form the bromonium ion (or β -bromocarocation), so this barrier would have to be overcome in the reverse reaction. Moreover, lack of steric hindrance would lower the barrier to attack of the bromide ion on the bromonium ion, so the lifetime of the bromonium ion should be decreased.

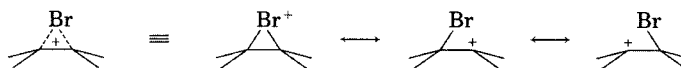
Intermediates in the Addition of Bromine to Alkyl-Substituted Alkenes

The Lewis structure of the bromonium ion in Figure 9.2 shows all of the positive charge on the bromine atom. Polarization of the C–Br bonds might be expected to result in some positive charge on the two carbon atoms as well. One way to indicate the charge distribution is to depict the bromonium ion as a resonance hybrid of three Lewis structures, as shown in Figure 9.13.⁷⁰ Still, we often find it convenient to represent the bromonium ion with just the Lewis structure having the positive charge on the bromine atom, just as we frequently represent benzene with only one of the Kekulé structures.

Even though there is experimental evidence for the existence of bromonium ions, it need not be the case that all bromine addition reactions involve identical intermediates. The totally symmetric structure represented in Figure 9.13 may be only one member (I in Figure 9.14) of a range of possible intermediates for electrophilic halogen addition reactions. At the other extreme would be the bromo-substituted carbocation **III**, a species capable of rotation about the former carbon–carbon double bond. Since carbocation stability is strongly affected by substituents on the positively charged carbon atom, we might expect structure **III** to be more likely with *gem*-dialkyl olefins. In between these two extremes could be intermediates that are formally described as carbocations but in which stabilization of the ion and restricted

FIGURE 9.13

Resonance structures contributing to the bromonium ion.



⁷⁰ Dewar proposed that the intermediate might be a π complex: Dewar, M. J. S. *J. Chem. Soc.* **1946**, 406.

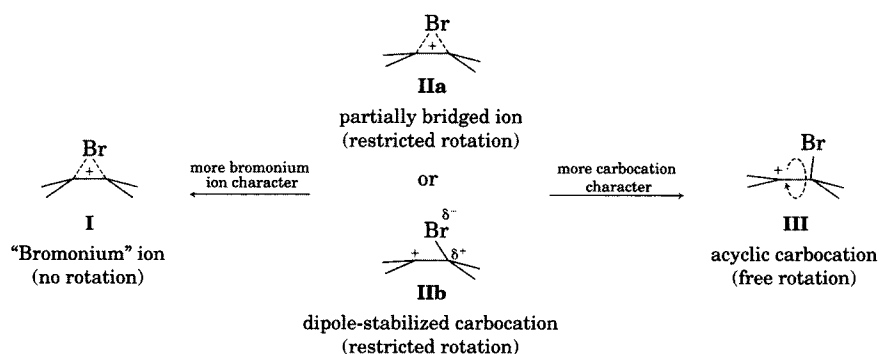
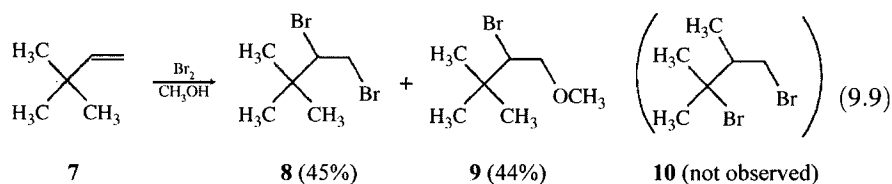


FIGURE 9.14

Spectrum of possible intermediates in the bromination of alkenes.

rotation about the C–C bond results from some interaction between the bromine atom and the more distant olefinic carbon atom.^{71,72} The stabilizing interaction could be described either as partial bonding (**IIa**) or as an ion–dipole interaction involving the positive charge and the partially negative end of the carbon–bromine bond dipole (**IIb**). Structures such as **IIa** and **IIb** are said to be *partially bridged*.

One way to test for the intermediacy of carbocations in reaction mechanisms is to look for rearrangements, for example, from a 2° carbocation to a 3° carbocation. In the addition of bromine to 3,3-dimethyl-1-butene (**7**) in methanol, however, the only products observed were 1,2-dibromo-3,3-dimethylbutane (**8**), 45%, and 2-bromo-1-methoxy-3,3-dimethylbutane (**9**), 44%.²⁹ There was no evidence for products such as **10**, which might have been expected if a free 2° carbocation were formed and then underwent a methyl shift to yield a 3° carbocation. Therefore, the intermediate in the addition of bromine to alkyl-substituted alkenes appears not to behave like a carbocation.



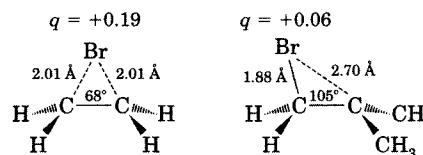
There is also kinetic evidence that the intermediate in the addition of bromine to aliphatic alkenes is not a carbocation. Nagorski and Brown studied the addition of bromine to alkenes in methanol containing varying concentrations of added bromide ion or azide ion. The ratios of the rate constants for formation of addition products incorporating azide ion or methanol ($k_{\text{N}_3^-}/k_{\text{CH}_3\text{OH}}$) were found to be 5.9 M^{-1} and 4.9 M^{-1} , respectively, for cyclopentene and cyclohexene. Since azide ion is a much stronger nucleophile than is methanol, the relatively small ratios suggested that the intermediate is a highly reactive (nonselective) species. Assuming that the reaction of the intermediate with N_3^- is diffusion limited (meaning a rate constant of about $10^{10} \text{ M}^{-1} \text{ s}^{-1}$), the lifetimes of the intermediates from these alkenes were calculated to be $5.9 \times 10^{-10} \text{ s}$ and $5.0 \times 10^{-10} \text{ s}$, respectively.⁵⁶

⁷¹ Yates, K.; McDonald, R. S. *J. Org. Chem.* **1973**, *38*, 2465.

⁷² The structures in Figure 9.14 are based on those presented in reference 71.

FIGURE 9.15

MNDO structures for intermediates in the bromination of ethene (left) and 2-methylpropene (right). (Data from reference 78.)



These lifetimes are two orders of magnitude greater than the lifetime expected for a secondary carbocation.^{73,74} The longer lifetimes and the observation of exclusive anti addition support the view that the intermediates are bromonium ions and not β -bromocarboxocations.⁵⁶

The bromonium ion derived from ethene has been studied by ab initio methods. The results of one study found the bromonium ion to be an energy minimum on the $C_2H_4Br^+$ hypersurface, with the open β -bromocarboxocation higher in energy.⁷⁵ Contrary to the depiction in Figure 9.2, the bromine atom in the bromonium ion was calculated by one theoretical method to be almost neutral, with the charge residing primarily on the carbon atoms.⁷⁶ A study of the bromonium ion derived from ethene by another theoretical approach led to the conclusion that there is appreciable positive charge on the bromine, but that the magnitude of the charge is sensitive to solvent, to substituents, and to the orientation of the bromide ion with respect to the bromonium ion.⁷⁷

An semiempirical MO study of methyl-substituted bromonium ions indicated that *symmetrical* bromonium ions are energy minima only when the two carbon atoms in the bromonium ion ring *each* have the same number of methyl groups. When one of the carbon atoms has a greater number of alkyl groups than does the other one, the structures corresponding to energy minima were found to be highly asymmetric, with a longer distance from the bromine atom to the more substituted carbon atom (Figure 9.15). The resulting picture is more nearly consistent with a structure in which there is only a small bonding interaction between the bromine and the more substituted carbon atom.⁷⁸ Klobukowski and Brown found that the geometry calculated for the bromonium ion derived from isobutene depends strongly on the level of the calculation. Higher order calculations predicted a more symmetric ion but with a rather flat potential energy surface for variation of the C-CH₂-Br angle. (A 10°–15° variation from an angle near 85° caused an energy change of only about 2 kcal/mol.) Although the resulting geometry differs somewhat from that shown in Figure 9.15, the higher order calculations did indicate greater positive charge on the carbon atom bearing the methyl substituents. Furthermore, Klobukowski and Brown suggested the flat potential energy surface for variation of the C-CH₂-Br angle may be perturbed by an incoming nucleophile.⁷⁹

⁷³ Chiang, Y.; Chwang, W. K.; Kresge, A. J.; Powell, M. F.; Szilagyi, S. J. *Org. Chem.* **1984**, *49*, 5218.

⁷⁴ Chiang, Y.; Kresge, A. J. *J. Am. Chem. Soc.* **1985**, *107*, 6363.

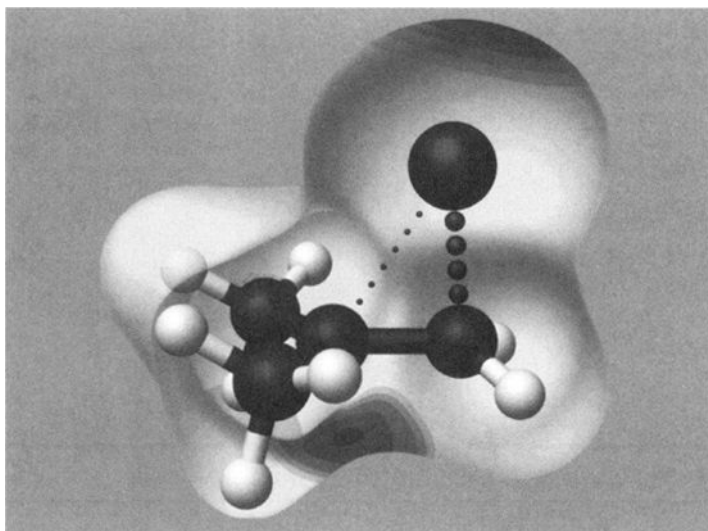
⁷⁵ Hamilton, T. P.; Schaefer, H. F. III. *J. Am. Chem. Soc.* **1990**, *112*, 8260.

⁷⁶ Cioslowski, J.; Hamilton, T.; Scuseria, G.; Hess, B. A.; Hu, J.; Schaad, L. J.; Dupuis, M. *J. Am. Chem. Soc.* **1990**, *112*, 4183.

⁷⁷ Cossi, M.; Persico, M.; Tomasi, J. *J. Am. Chem. Soc.* **1994**, *116*, 5373.

⁷⁸ Galland, B.; Evleth, E. M.; Ruasse, M.-F. *J. Chem. Soc. Chem. Commun.* **1990**, 898.

⁷⁹ Klobukowski, M.; Brown, R. S. *J. Org. Chem.* **1994**, *59*, 7156.

**FIGURE 9.16**

Electron density surface of the bromonium ion from isobutene, shaded by nucleophilic susceptibility.

Figure 9.16 shows a portion of the PM3 electron density surface of the bromonium ion derived from isobutene.⁸⁰ The C–CH₂–Br bond angle was fixed at 80° in accordance with the results reported in reference 77. The shading illustrates regions of similar nucleophilic susceptibility, which was calculated on the basis of the density of frontier MOs by the method of Fukui et al.⁸¹ The nucleophilic susceptibility on the carbon atom with the two hydrogen atoms is 0.04, while that for the carbon atom with two methyl substituents is 1.18. Therefore, an incoming nucleophile would be attracted more strongly to the more substituted carbon atom of the bromonium ion.⁸²

Further insight into the nature of bromonium ions came from studies of the competitive reactions of Br[−] and methanol with bromonium ions in methanol solution. The reaction can be categorized with regard to both the *chemoselectivity*—relative reactivity with bromide ion and with methanol—and *regioselectivity*—Markovnikov or anti-Markovnikov orientation of the bromomethoxy product. In this context, Markovnikov orientation is defined as the formation of product in which the bromine is bonded to the carbon atom having fewer alkyl or aryl substituents, which is the orientation expected upon attachment of Br⁺ to give the more stable carbocation. (See page 585.) The carbon atom with the greater number of alkyl substituents is designated as C_α in Figure 9.17. The results, some of which are shown in Table 9.2, are that the more unsymmetrical bromonium ions were found to produce greater amounts of methanol addition products relative to dibromide. Moreover, the more unsymmetrical alkenes also gave relatively greater amounts of Markovnikov bromomethoxy compounds. On the other hand, the

⁸⁰ The PM3 surface is drawn at a density of 0.01 e/Å³.

⁸¹ Fukui, K.; Yonezawa, T.; Nagata, C.; Shingu, H. *J. Chem. Phys.* **1954**, *22*, 1433.

⁸² By comparison, nucleophilic susceptibility was found to be 0.46 for each of the two carbon atoms in the bromonium ion formed from ethene. These results are consistent with the tendency for the bromonium ion from isobutene to react with nucleophiles at the more highly substituted position, but the calculated structures implicitly represent gas phase species. Structures in solution may be affected by solvent or counterions.

FIGURE 9.17

Chemo- and regioselectivity in bromination of alkenes. (Adapted from reference 83.)

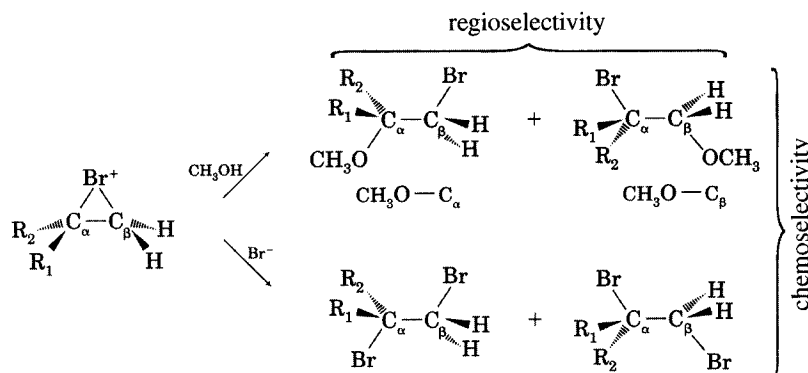


TABLE 9.2 Chemoselectivity and Regioselectivity in Addition of Bromine to Alkenes

Alkene	R ₁	R ₂	Bromomethoxyalkane		
			Yield	CH ₃ O-C _α	CH ₃ O-C _β
Ethene	H	H	38%	(not defined)	(not defined)
Propene	CH ₃	H	61%	50%	11%
2-Methylpropene	CH ₃	CH ₃	85%	85%	0%

Source: Reference 83.

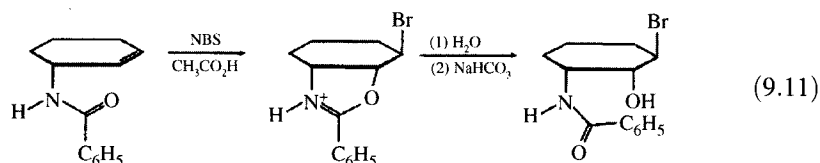
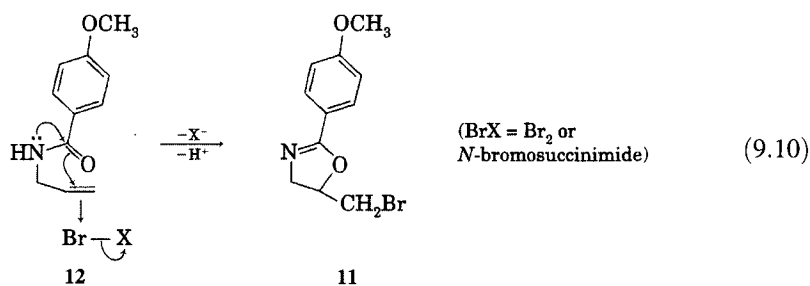
more symmetrical alkenes gave higher yields of dibromo products, and the bromomethoxy products that were produced were composed of relatively more of the anti-Markovnikov (CH₃O-C_β) products.

These results are consistent with a model in which the bromonium ion from a symmetrically substituted alkene behaves more like a bromonium ion and less like a carbocation. That is, with a symmetric ion there is relatively little solvent incorporation, and solvent is relatively indiscriminate in attacking the two carbon atoms of the bromonium ion. On the other hand, there is more solvent incorporation product formed from the more unsymmetrical ions, and the solvent is more likely to add to the more highly substituted carbon atom than to the less highly substituted carbon atom. This behavior suggests that solvent is attracted to the center of greater partial positive charge.⁸³

Product regiochemistry can also be affected by other functional groups in the alkene. In particular, the observation of anchimeric assistance in solvolysis reactions suggests that similar interactions could occur in electrophilic addition reactions, and neighboring group participation has been noted in the addition of bromine to *N*-allylbenzamides. For example, *N*-*p*-methoxybenzoylallylamine (**12**) reacted with NBS in acetic acid to give a 95% yield of the oxazoline **11** (equation 9.10).⁸⁴ This methodology was also shown to be useful for the synthesis of cyclohexane derivatives with specific 2-*cis*, 3-*trans* orientation with respect to the benzamide functionality, as shown in equation 9.11.

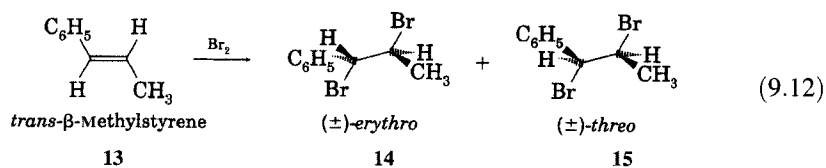
⁸³ Dubois, J.-E.; Chretien, J. R. *J. Am. Chem. Soc.* **1978**, *100*, 3506. Regioselectivity could be correlated with the difference in partial positive charge at the two carbon atoms as determined by NMR.

⁸⁴ Winstein, S.; Goodman, L.; Boschan, R. *J. Am. Chem. Soc.* **1950**, *72*, 2311.



Intermediates in the Addition of Bromine to Aryl-Substituted Alkenes

The discussion to this point has focused on the addition of bromine to double bonds bearing alkyl substituents. There are significant differences in the addition of bromine to alkenes with aryl substituents. For example, the addition of bromine to aryl-substituted alkenes is not stereospecific. Reaction of *cis*- β -methylstyrene (**13**) with bromine in CCl₄ led to the formation of 17% of *erythro*- (**14**) and 83% of *threo*-(1,2-dibromopropyl)benzene (**15**, equation 9.12). Reaction of *trans*- β -methylstyrene under the same conditions yielded 88% of the *erythro* and 12% of the *threo* product. When the benzene ring in the *trans* reactant was substituted with a 4-methoxy group (*trans*-anethole), the reaction became even less stereoselective, giving 63% *erythro* and 37% *threo* product.^{85,86}



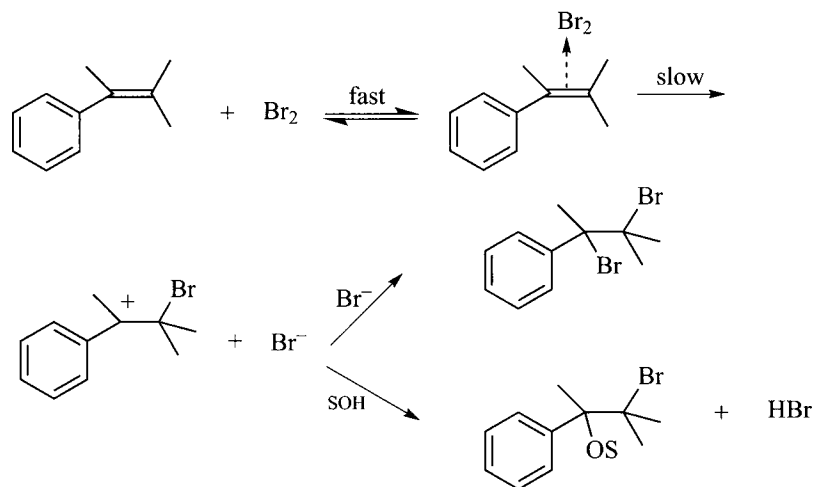
Yates, McDonald, and Shapiro studied the addition of bromine in acetic acid to ring-substituted styrenes under concentration conditions ($<10^{-3}$ M) in which second-order kinetics were observed.⁸⁷ Reactivity was decreased by electron-withdrawing substituents on the aromatic ring, and the rate constants correlated ($r = 0.997$) with σ^+ to give a ρ of -4.8 .²⁵ That ρ value is very nearly the same as the ρ value observed for the solvolysis of cumyl chloride in ethanol (-4.67) or 90% aqueous acetone (-4.54),⁸⁸ suggesting that the

⁸⁵ Fahey, R. C.; Schneider, H.-J. *J. Am. Chem. Soc.* **1968**, *90*, 4429.

⁸⁶ The reaction of bromine with the methylstyrenes is *not* said to be stereospecific because it is not observed that stereoisomeric reactants give different stereoisomeric products. Rather, the two reactions can only be said to be stereoselective, meaning that each of the two reactants gives more of one stereoisomer than of another.

⁸⁷ Yates, K.; McDonald, R. S.; Shapiro, S. A. *J. Org. Chem.* **1973**, *38*, 2460.

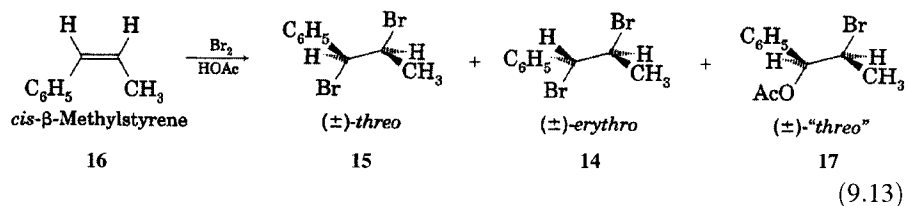
⁸⁸ Brown, H. C.; Okamoto, Y. *J. Am. Chem. Soc.* **1958**, *80*, 4979.

**FIGURE 9.18**

Mechanism proposed for second-order bromination of styrenes. (Adapted from reference 87.)

addition of bromine involves a species that closely resembles a benzylic carbocation (Figure 9.18).⁸⁹

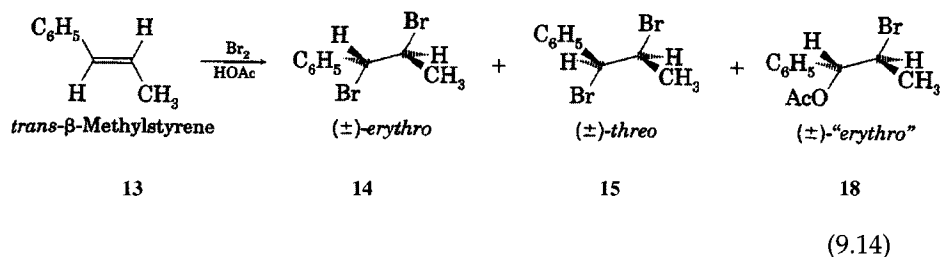
It is unlikely that a free carbocation (or a solvent-separated ion pair) is the intermediate in these addition reactions, however. Rolston and Yates studied the addition of bromine to derivatives of styrene in acetic acid and other solvents.^{21,90} In acetic acid, the products were found to be the 1,2-dibromo addition products plus variable amounts of the bromoacetoxylated products derived from solvent. For all of the styrene derivatives studied except β,β -dimethylstyrene, the solvent incorporation product in each case was exclusively the 1-acetoxy-2-bromo compound—the product expected from nucleophilic attack of solvent on a benzylic carbocation. The dibromo and bromoacetoxylated products were formed with different stereoselectivity. The reaction of *cis*- β -methylstyrene (**16**) produced (\pm)-*threo*-1,2-dibromo-1-phenylpropane (**15**, 58%), (\pm)-*erythro*-1,2-dibromo-1-phenylpropane (**14**, 22%), and (\pm)-*threo*-1-acetoxy-2-bromo-1-phenylpropane (**17**, 20%).



Reaction of *trans*- β -methylstyrene (**13**) produced 64% of **14**, 13% of **15**, and 23% of (\pm)-*erythro*-1-acetoxy-2-bromo-1-phenylpropane (**18**, 20%).

⁸⁹ The second- and third-order reactions showed interesting differences. For the second-order reaction, ΔH^\ddagger values were 9.0 kcal/mol and 4.7 kcal/mol for addition of bromine to *p*-nitrostyrene and to styrene, respectively, while the corresponding ΔS^\ddagger values were -39.5 eu and -37.6 eu for these two compounds. For the third-order reaction, however, the values of ΔH^\ddagger were 0.9 and 0.01 kcal/mol, and the ΔS^\ddagger values were -50.5 and -37.6 eu, respectively, for addition to *m*-nitrostyrene and to styrene. Thus, the second-order reaction was said to be "enthalpy controlled," while the third-order reaction was said to be "entropy controlled" (reference 87).

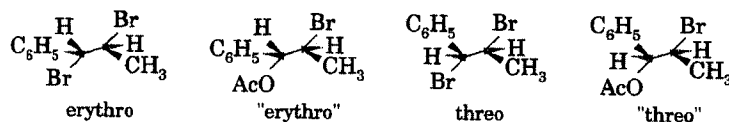
⁹⁰ Rolston, J. H.; Yates, K. *J. Am. Chem. Soc.* **1969**, *91*, 1477.



In both cases, therefore, the bromoacetoxy products were those expected from anti addition, while formation of the dibromo products was much less stereoselective.^{21,91,92} Furthermore, the fraction of dibromide formed by apparent syn addition to *cis*- β -methylstyrene varied with solvent polarity, from 27% in acetic acid to 55% in nitrobenzene.⁹⁰ The results were discussed in terms of initial formation of an intimate bromo-carbocation-bromide ion pair that can undergo attachment of acetic acid from the face of the ion away from the bromide ion, thus leading to anti formation of bromoacetoxy compounds. Reorientation of the bromide ion within the solvent shell for backside attachment to the bromonium ion provides time for rotation about the carbon-carbon single bond of the bromocarbocation, so the dibromo products are formed with less stereoselectivity.

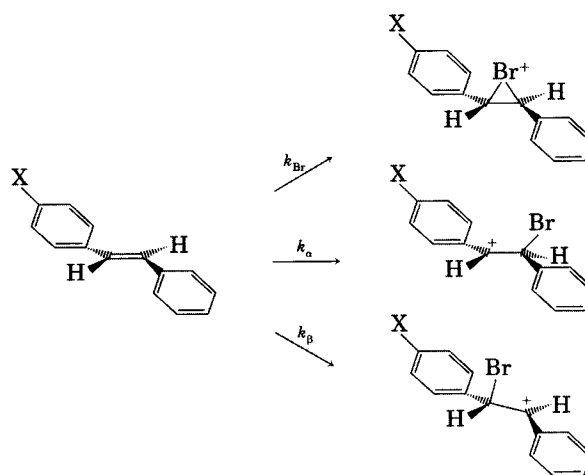
There is also kinetic evidence that the addition of bromine to styrene involves an intermediate that is neither a bromonium ion nor a carbocation but a structure in which there is some interaction between the bromine atom and the phenyl-substituted carbon atom. The lifetime of a 1-phenylethyl cation was determined to be 10^{-11} s,⁷⁴ but the lifetime estimated by Nagorski and Brown for the intermediate in the addition of bromine to styrene is 2.7×10^{-10} s. Thus, the longer lifetime of the intermediate in the addition

⁹¹ The terms *erythro* and *threo* are shown in quotation marks for those structures in which the labels would apply if the two groups that added to the olefinic carbon atoms were identical, even though they are not the same. In the structures below, the erythro structure would become a meso structure if the phenyl and methyl were made equivalent. In the "erythro" structure to its right, however, the bromine and acetoxy groups would also have to be made identical in order for the compound to become a meso structure.



The "erythro" and "threo" labels provide a convenient shorthand notation for unsymmetrical adducts. For further discussion, see footnote 18 of Ruasse, M. F.; Argile, A.; Dubois, J. E. *J. Am. Chem. Soc.* **1978**, *100*, 7645.

⁹² Similar results were obtained in a study of the reaction of *trans*- β -methylstyrene and its derivatives with bromine in methylene chloride. Only when the aromatic ring was substituted with trifluoromethyl groups at the 3 and 5 positions was the reaction 100% anti stereospecific. With one trifluoromethyl group at the three position, 91% of the product was the "erythro" product, while 9% was the "threo" product. With no substituent other than hydrogen on the aromatic ring, 81% of the product was erythro, while with a 4-methoxy substituent, only 63% was erythro (reference 91).

**FIGURE 9.19**

Competitive pathways proposed for the electrophilic addition of bromine to stilbene derivatives.

reaction supports the view of some kind of stabilization, such as a dipolar interaction or weak bridging.^{56,93} That would mean that the intermediate is somewhat closer to the center of the range in Figure 9.14.

It is also possible that there is not just one intermediate but several intermediates that are formed and react in parallel. In the case of addition of bromine to stilbene, Ruasse and co-workers argued for the competitive formation of three discrete intermediates: two different carbocations and a bromonium ion (Figure 9.19).²⁶ If formation of the intermediates is irreversible, then the rate constant for the reaction, k , is the sum of the rate constants for the three processes; that is,

$$k = k_{\alpha} + k_{\beta} + k_{\text{Br}} \quad (9.15)$$

If X is a strongly electron-donating group, then a carbocation adjacent to the substituted ring will be most stable. Therefore, k_{α} will dominate k , and a Hammett correlation with σ^{+} will be observed. If X is a strongly electron-withdrawing group, however, then the carbocation with positive charge further away from the substituted ring will be most stable. In this case, k_{β} will make the greatest contribution to k , and $\log k$ will correlate with σ .²⁵ If X is neither strongly electron donating nor withdrawing, then the intermediate may be a bromonium ion, and there should again be a correlation of $\log k$ with σ . The curved $\sigma\rho$ plot (Figure 9.20) shows a change of slope as X varies from electron donating to electron withdrawing, suggesting a mechanistic changeover consistent with the role of discrete intermediates.⁹⁴

Another report suggested that a single intermediate with a variable degree of bridging might be involved in the addition of bromine to stilbene derivatives. Bellucci and co-workers found evidence for reversibility in the

⁹³ The intermediacy of a species with appreciable charge on the benzylic carbon atom is also supported by the observation of a Hammett correlation with σ^{+} , which had a ρ value of -4.21 for the addition of bromine to styrene derivatives in acetic acid: Rolston, J. H.; Yates, K. *J. Am. Chem. Soc.* **1969**, *91*, 1483.

⁹⁴ For further discussion and results for styrene derivatives, see reference 26.

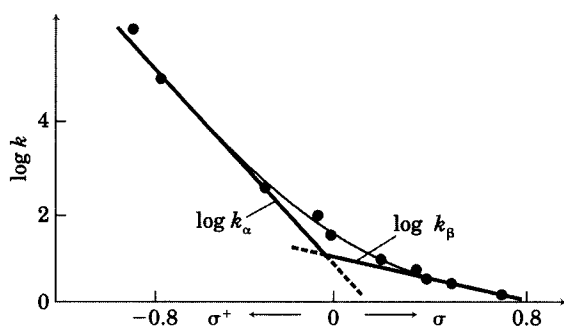


FIGURE 9.20
Curved Hammett plot for bromination of monosubstituted stilbenes. (Reproduced from reference 26.)

addition of bromine to stilbene derivatives in 1,2-dichloroethane solution (Figure 9.21).⁹⁵ The *cis* isomers of *p*-methylstilbene, stilbene, *p*-trifluoromethylstilbene, and *p,p'*-bis(trifluoromethyl)stilbene each showed some conversion to the corresponding *trans* isomer during the reaction. Isomerization of starting material was greatest with the *p,p'*-bis(trifluoromethyl) isomer and least with the *p*-methyl isomer. The ratio of meso to racemic product was essentially constant at about 70 : 30 for the *p*-methyl isomer regardless of whether the *cis* or *trans* isomer was used as starting material. This result suggested that the intermediate resembles an open bromocarocation. For the other three compounds, the product ratio for the *cis* reactant was different from that obtained when the *trans* isomer was the starting material. For the *trans* isomer of *p,p'*-bis(trifluoromethyl)stilbene, the formation of almost exclusively meso product suggested stereospecific anti addition. The investigators concluded that the cationic intermediates formed from these stilbenes have properties similar to those of β -bromocarocations but with some stabilization or bridging involving the bromine (as shown by the dashed line in the central structures in Figure 9.21) and that the degree of bridging

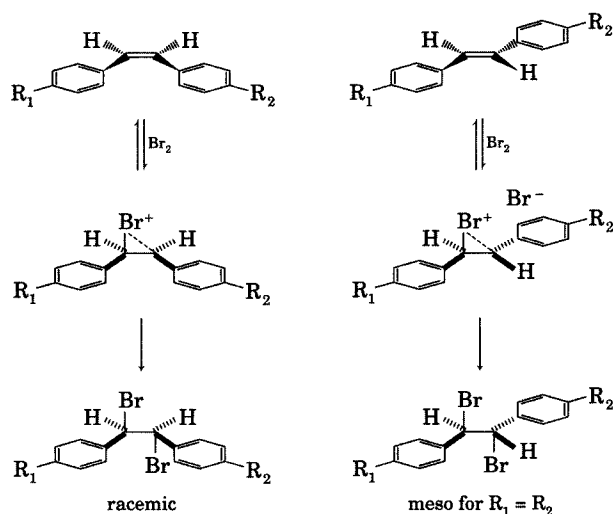


FIGURE 9.21
Proposed mechanism for bromine addition to stilbenes. (Note the process leading to *cis*-*trans* isomerization.)

⁹⁵ Bellucci, G.; Bianchini, R.; Chiappe, C.; Brown, R. S.; Slebocka-Tilk, H. *J. Am. Chem. Soc.* **1991**, *113*, 8012.

increases as the electron-withdrawing properties of the substituents increase.⁹⁶

Summary of Bromine Addition

Addition of bromine to an alkene is much more complicated than the simple representation in Figure 9.2 would suggest. The classical bromonium ion description of electrophilic addition of bromine to an alkene is useful only as a beginning point to describe the mechanistic options. The structure of the intermediate, the kinetics of the reaction, and both the stereochemistry and the regiochemistry of the products are all complex functions of the nature and concentration of the brominating agent, the solvent, any added nucleophiles, and the structure of the alkene.

Only symmetrical alkenes react by means of true bromonium ions (i.e., strongly bridged, symmetrical structures). If the alkene is unsymmetrically substituted with alkyl groups, the bromonium ion takes on the character of a β -bromocarocation with restricted rotation about the formerly olefinic carbon-carbon bond. If an aryl group is present on one or both of the olefinic carbon atoms, the evidence points to an intermediate that is even more nearly like a benzylic carbocation.

Preceding the cationic intermediate is at least one charge transfer complex, with the rate-limiting step usually being the conversion of the CT complex to a bromonium ion or bromocarocation intermediate. A protic solvent can assist this ionization process by acting as an electrophile to remove Br^- through hydrogen bonding. Nonpolar aprotic solvents cannot assist in that way, but a second Br_2 molecule may participate in the reaction by removing Br^- as a Br_3^- ion, and Br_5^- ions may be involved at high bromine concentration. Formation of the cationic intermediate is reversible, although the reverse reaction is usually not seen unless the solvent is aprotic or the alkene provides a steric barrier to the nucleophilic attack needed to complete the addition reaction.

The cationic intermediate is probably formed as a tight ion pair whose subsequent reaction depends on the nucleophilicity and polarity of the solvent. In a less polar solvent, the initially formed tight ion pair may rearrange to an ion pair in which the bromide ion is on the back side of the C-Br bonds, which facilitates the second step of the addition reaction. In a more polar solvent, the bromide ion is more likely to diffuse away from the cation, so nucleophilic attack by solvent becomes more likely. Regardless of whether the intermediate is a bromonium ion or a β -bromocarocation and whether the product is the dibromide or solvent incorporation product, the stereochemistry of the addition is anti with alkyl-substituted alkenes. If the alkene is unsymmetrically substituted with aryl groups, the tendency for the cationic intermediate to behave as a β -bromocarocation is even greater, and both syn and anti addition are observed.

⁹⁶ The authors further concluded that for *p*-methylstilbene the activation energy for formation of the β -bromocarocation intermediate is higher than the activation energy for formation of the dibromide. For the reaction of *trans-p,p'*-bis(trifluoromethyl)stilbene, however, the activation energy appeared to be greater for addition of the nucleophile to the cation. This conclusion is consistent with the hypothesis that reversibility is most likely when the intermediate is a bromonium ion (so that significant positive charge is localized on the bromine), and it is least likely when the intermediate is a β -bromocarocation (with little charge on the bromine). For a discussion, see reference 95.

Addition of Other Halogens to Alkenes

Chlorine

The study of the addition of chlorine to alkenes is even older than the study of bromine addition. The synthesis of 1,2-dichloroethane was first reported by a group of Dutch chemists in 1795, and Michael Faraday investigated the addition of chlorine to ethene in 1821.⁹⁷ In many ways the addition of chlorine to alkenes is similar to the addition of bromine to alkenes. For example, each additional alkyl group increases the relative reactivity of an olefin by a factor of 50 to 100 (Table 9.3). A Taft $\rho^*\sigma^*$ correlation is observed, and the ρ^* for chlorine addition is -2.9 , which is similar to the value of -3.1 for addition of bromine. This result suggests that charges on the alkenyl carbon atoms in the transition structures for addition of chlorine are similar to those in the addition of bromine.⁹⁸

The chloronium ion (the chlorine equivalent of the bromonium ion) was proposed by Lucas and Gould,⁹⁹ and Olah reported evidence for a stable chloronium ion by NMR.³⁰ Addition of chlorine to 2-butene was found to occur by an anti pathway, with *trans*-2-butene giving the meso

TABLE 9.3 Reactivities of Alkenes and Yields of Substitution Products in Reactions of Cl_2 with Neat Alkenes

Reactivity ^a	Substitution Products (% Yields)	
1.00		$\text{ClCH}_2\text{CH}=\text{CH}_2$ 3%
1.15		CH_2Cl 10%
50		Cl 20%
58		CH_2Cl 87%
160		CH_2Cl 58% CH_2Cl 29% CH_2Cl 8%
1,100		Cl 85%
43,000		Cl >99%

^a Substitution and addition.

Source: Adapted from reference 107.

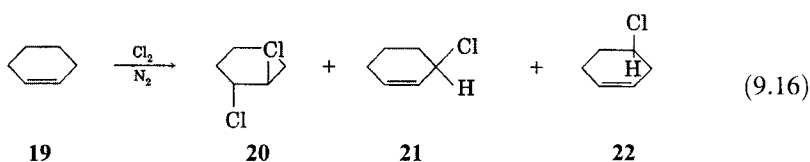
⁹⁷ Anantkrishnan, S. V.; Venkataraman, R. *Chem. Rev.* **1943**, 33, 27 and references therein.

⁹⁸ Bienvenüe-Goëtz, E.; Ratsimandresy, B.; Ruasse, M. F.; Dubois, J. E. *Tetrahedron Lett.* **1982**, 3273.

⁹⁹ Lucas, J. J.; Gould, C. W. *J. Am. Chem. Soc.* **1941**, 63, 2541.

adduct, while the cis isomer yields racemic product.⁹⁹ Thus, we might expect the stereochemistry of chlorine addition to be quite similar to that for bromine.

There are significant differences between the bromine addition and chlorine addition reactions, however. The addition reaction of ethene and chlorine is exothermic by 44 kcal/mol, which is 15 kcal/mol more exothermic than the addition of ethene and bromine.¹⁰⁰ Poutsma noted that addition of chlorine to alkenes in nonpolar solvents can occur by either radical or ionic pathways, but that oxygen inhibits the radical reaction.^{101,102} For example, addition of chlorine to neat (i.e., not diluted by solvent) cyclohexene (**19**) gave *trans*-1,2-dichlorocyclohexane (**20**), 3-chlorocyclohexene (**21**), and 4-chlorocyclohexene (**22**) in a 1.95 : 1.00 : 0.60 ratio when the reaction was carried out under a nitrogen atmosphere. In the presence of oxygen, the ratio was 3–4 : 1.00 : 0.¹⁰²



Poutsma found that the tendency to give substitution as well as addition with Cl₂ is general for the reaction of neat alkyl-substituted alkenes and that this tendency increases with increasing alkyl substitution. Table 9.3 shows the yields of substitution products obtained from a series of alkenes.¹⁰³ The formation of substitution products in chlorine addition reactions had been explained as resulting from a β-chlorocarocation.¹⁰⁴ Addition of chlorine to *cis*-1,2-di-*t*-butylethylene in carbon tetrachloride solvent with oxygen present gave racemic 3,4-dichloro-2,2,5,5-tetramethylhexane, however, meaning that a carbocation rearrangement did not occur. Similar reaction of the *trans* isomer gave the meso dichloride, although substitution product was also formed.¹⁰⁵ The results suggest that the isomerizational stability of the intermediate ion must be at least enough to overcome the greater steric strain of the *cis* alkene than that of the *trans*, which is about 9 kcal/mol. An intermediate carbocation would be expected to relax to a conformation with less steric strain, but a chloronium ion could provide isomerizational stabilization. Therefore, Fahey concluded that the reactions must proceed either through a bridged intermediate or through an open chlorocarocation with sufficient interaction between the chlorine atom and the carbocation carbon atom to provide significant stabilization. A mechanism that can account for the

¹⁰⁰ Conn, J. B.; Kistiakowsky, G. B.; Smith, E. A. *J. Am. Chem. Soc.* **1938**, *60*, 2764.

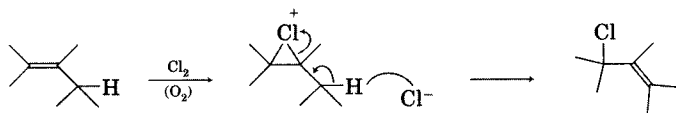
¹⁰¹ The addition of bromine to alkenes can also occur by a free radical pathway if the reaction is carried out in a nonpolar solvent such as CCl₄ and if the reaction mixture is irradiated with light. Allylic substitution can be a competing reaction if the alkene contains allylic hydrogens. For a discussion of the competing substitution and addition reactions, see McMillen, D. W.; Grutzner, J. B. *J. Org. Chem.* **1994**, *59*, 4516.

¹⁰² Poutsma, M. L. *J. Am. Chem. Soc.* **1965**, *87*, 2161.

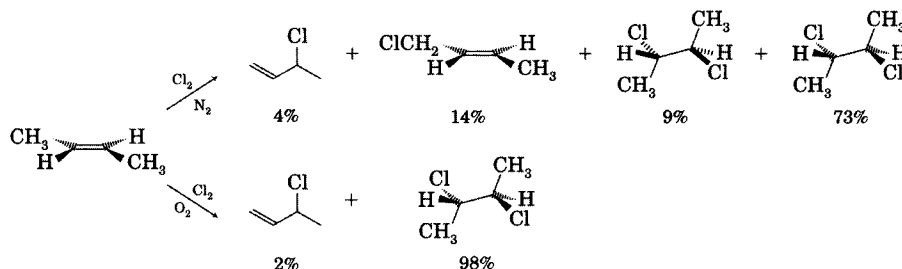
¹⁰³ The material balance not accounted for by the sum of the percent yields was addition product.

¹⁰⁴ Taft, R. W., Jr. *J. Am. Chem. Soc.* **1948**, *70*, 3364.

¹⁰⁵ Fahey, R. C. *J. Am. Chem. Soc.* **1966**, *88*, 4681.

**FIGURE 9.22**

Possible mechanism for substitution via a chloronium ion intermediate.

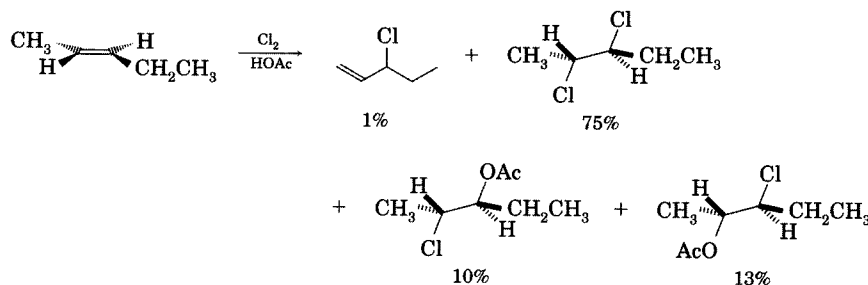
**FIGURE 9.23**

Products of reaction of *trans*-2-butene with Cl₂ in pentane.

formation of substitution product by way of a chloronium ion is shown in Figure 9.22.^{106,107}

Addition of chlorine to the isomers of 2-butene gave 97–98% anti addition product and 2–3% substitution product when the alkene was neat or was dissolved in a nonpolar solvent with oxygen present to suppress radicals. Under a nitrogen atmosphere, however, 18% of the product was substitution, and the 82% of the product that was derived from adding Cl₂ was not formed stereospecifically (Figure 9.23). Poutsma concluded that radical reactions are difficult to suppress in chlorine addition because they do not require an initiator and seem to begin spontaneously.¹⁰⁸

Electrophilic addition of Cl₂ to alkenes in a polar solvent seems not to be affected as severely by radical reactions as does addition in a nonpolar solvent. Figure 9.24 shows results for the addition of Cl₂ to *trans*-2-pentene

**FIGURE 9.24**

Addition of Cl₂ to *trans*-2-pentene in acetic acid. (All products are racemic.)

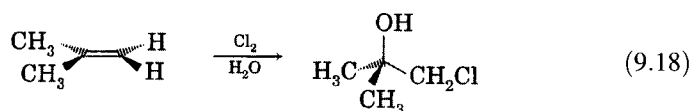
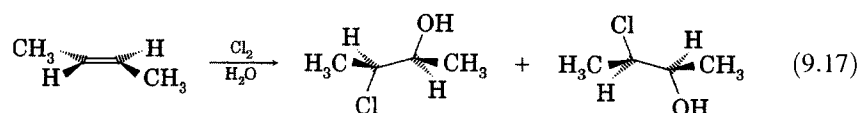
¹⁰⁶ Except for the complication of bridging by chlorine, the competition between addition and elimination in the second step to each product is reminiscent of the E1/S_N1 competition exhibited by other carbocations.

¹⁰⁷ Addition of chlorine to neat *t*-butylethylene gave not only the expected dichloride but also 10% of 4-chloro-2,3-dimethyl-1-butene, indicating that a rearrangement consistent with a methyl shift in a carbocation had occurred. Poutsma, M. L. *J. Am. Chem. Soc.* **1965**, *87*, 4285. Small amounts of substitution products accompanied the addition. Addition of chlorine to linear alkenes gave mostly addition, but addition of chlorine to branched alkenes gave mostly allylic substitution products. Addition is favored at lower temperatures, as is the case with the competition between S_N1 and E1 reactions.

¹⁰⁸ Poutsma, M. L. *J. Am. Chem. Soc.* **1965**, *87*, 2172.

in acetic acid.¹⁰⁹ Along with a small amount of substitution product, both the dichloride and two chloroacetoxy adducts were observed. Because the dichloride and the chloroacetoxy products were formed by anti addition, a mechanism involving a chloronium ion–chloride ion pair (similar to the mechanism for dibromide formation) was proposed for the reaction. Formation of both the 2-acetoxy-3-chloro and 3-acetoxy-2-chloro products was attributed to nucleophilic attack on the chloronium ion by the solvent. There appeared to be a slight preference for solvent attack on the carbon atom with the smaller alkyl group, perhaps for steric reasons.

Reaction of an unhindered alkene with chlorine in aqueous solution results in the addition of the elements of hypochlorous acid, HOCl, to produce a chlorohydrin (β -hydroxyalkyl chloride).¹¹⁰ The stereochemistry of chlorohydrin formation is anti. For example, reaction of *trans*-2-butene with chlorine and water produces (\pm)-*threo*-2-chloro-2-butanol (equation 9.17).¹¹¹ Chlorohydrin formation is generally highly regioselective, with the OH group becoming attached to the alkene carbon atom bearing the greater number of alkyl groups. For example, the chlorohydrin of methylcyclohexene is 2-chloro-1-methylcyclohexanol,¹¹² and isobutene reacts with chlorine in water to produce 1-chloro-2-methyl-2-propanol (equation 9.18).¹¹³ The results are explicable in terms of an unsymmetrical intermediate chloronium ion that has a greater partial positive charge on the carbon atom bearing the greater number of alkyl groups, as is the case for unsymmetrically substituted bromonium ions (Figure 9.15). Then nucleophilic attack by water is favored at the olefinic carbon atom bearing the greater partial positive charge.^{114,115}



¹⁰⁹ Poutsma, M. L.; Kartch, J. L. *J. Am. Chem. Soc.* **1967**, *89*, 6595.

¹¹⁰ Gomberg, M. J. *Am. Chem. Soc.* **1919**, *41*, 1414.

¹¹¹ Collis, M. J.; Merrall, G. T. *Chem. Ind. (London)* **1964**, 711. The stereochemistry of the chlorohydrin was determined indirectly by noting that reaction of the chlorohydrin with aqueous base produced *cis*-2,3-epoxybutane. Bartlett, P. D. *J. Am. Chem. Soc.* **1935**, *57*, 224, had earlier concluded that addition of HOCl to cyclohexene produces *trans*-2-chlorocyclohexanol.

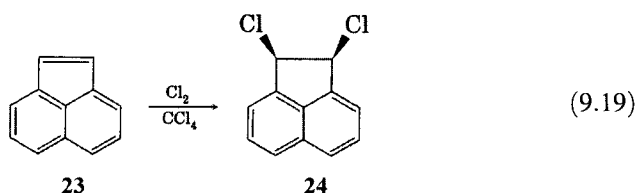
¹¹² Bartlett, P. D.; Rosenwald, R. H. *J. Am. Chem. Soc.* **1934**, *56*, 1990.

¹¹³ de la Mare, P. B. D.; Salama, A. J. *Chem. Soc.* **1956**, 3337.

¹¹⁴ The argument is closely analogous to that used to explain the regioselectivity of formation of bromoacetoxy compounds (Table 9.2) formed in the addition of bromine to alkenes in acetic acid.

¹¹⁵ Similarly, addition of bromine to alkenes in water produces bromohydrins. Although they are more difficult to synthesize, iodohydrins and fluorohydrins are also known. For a review of the synthesis and reactions of halohydrins, see Rosowsky, A. in Weissberger, A., Ed. *Heterocyclic Compounds with Three- and Four-Membered Rings*, Part One; Wiley-Interscience: New York, 1964; p. 1.

In contrast to the anti addition of chlorine to 2-butene, addition of chlorine to 1-phenylpropene (β -methylstyrene) is nonstereospecific in both polar and nonpolar solvents. While 2-butene reacts via a chloronium ion, 1-phenylpropene probably reacts through an open (benzylic) carbocation.¹¹⁶ *cis*-Stilbene was found to react with chlorine to give a 9 : 1 mixture of meso to racemic product, while *trans*-stilbene gave a 35 : 65 mixture of those two products.¹¹⁷ The addition to stilbene must have proceeded through intermediate(s) similar to chlorocarocations so that appreciable syn reaction could take place. Similarly, addition of chlorine to phenanthrene gave appreciable *cis*-9,10-dichloro-9,10-dihydrophenanthrene,¹¹⁸ and acenaphthylene (**23**) reacted with chlorine in CCl_4 to give the *cis*-1,2-dichloroacenaphthene (**24**) exclusively.¹¹⁹



An attractive mechanism to explain these results is shown in Figure 9.25.¹¹⁶ The addition of chlorine to the double bond of *cis*-stilbene produces a benzylic carbocation–chloride ion pair. Attachment of Cl^- to the carbocation before rearrangement gives net syn addition. Either rearrangement of the initial ion pair to an ion pair with the chloride ion on the other face

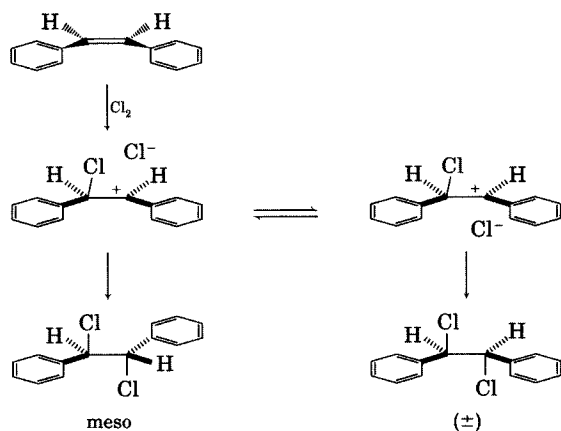


FIGURE 9.25

Ion pair intermediates proposed for the addition of chlorine to *cis*-stilbene.

¹¹⁶ Fahey, R. C.; Schubert, C. J. *Am. Chem. Soc.* **1965**, *87*, 5172.

¹¹⁷ Buckles, R. E.; Knaack, D. F. *J. Org. Chem.* **1960**, *25*, 20 reported that tetrabutylammonium iodotetrachloride gives stereospecific anti addition of chlorine to stilbene and other compounds. The stereospecificity of the reaction was attributed to an unspecified role for the iodotetrachloride or iododichloride ions present in the reaction mixture.

¹¹⁸ de la Mare, P. B. D.; Koenigsberger, R. J. *Chem. Soc.* **1964**, 5327.

¹¹⁹ Cristol, S. J.; Stermitz, F. R.; Ramey, P. S. *J. Am. Chem. Soc.* **1956**, *78*, 4939. Acenaphthene was found to react with iodobenzene dichloride in chloroform to give the *trans* isomer.

of the molecule (shown) or rotation about the C–C bond (not shown) could produce apparent anti addition. Since rotation about the single bond cannot occur in the case of chlorine addition to phenanthrene or acenaphthylene, reaction through rearrangement of the tight ion pair must be the main route to cis product formation for these compounds, and it could be the main route for the formation of racemic dichlorostilbenes also. Ab initio calculations indicated that the chloronium ion is a minimum on the $C_2H_4Cl^+$ potential energy surface. The 2-chloroethyl carbocation was calculated not to be a minimum, however. Instead, it was found to isomerize without an energy barrier to the 1-chloroethyl carbocation, which was a global minimum (4.3 kcal/mol more stable than the chloronium ion). The activation barrier for conversion of the chloronium ion to the 1-chloroethyl carbocation was about 28 kcal/mol.¹²⁰

Fluorine

The exothermicity of the addition of F_2 to an alkene makes it difficult to study the mechanism and also limits the synthetic utility of the addition. Merritt suggested that carrying out the addition of fluorine at low temperature would prevent some secondary reactions that result from the heat generated by addition of fluorine to alkenes, and reactions at $-78^\circ C$ were found to be synthetically useful.¹²¹

Because its small size makes fluorine inefficient as a bridging atom,³⁰ we might consider it likely that addition of fluorine would occur through a two-step mechanism involving a β -fluorocarocation. The stereochemistry of the fluorine addition reaction has generally been found to be that resulting from syn addition, however, which suggests that the reaction does not proceed through a long-lived carbocation that can undergo nucleophilic attachment from either the top or the bottom lobe of the empty p orbital. The results could be explained if the reaction proceeds through a short-lived carbocation–fluoride ion pair that quickly collapses to syn product. An alternative possibility is a concerted, four-center pathway, as shown in Figure 9.26.^{122,123}

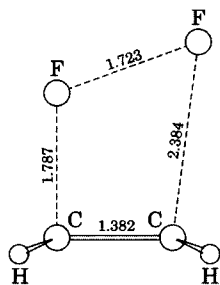


FIGURE 9.26
Transition structure calculated for the addition of F_2 to alkenes. (Distances in Å. Adapted from reference 123.)

The four-center concerted pathway was criticized, however, both on theoretical grounds and on the basis of experimental data supporting an alternative method of fluorine addition. Rozen and Brand¹²⁴ carried out the direct addition of fluorine to alkenes by bubbling a gas mixture composed

¹²⁰ Theoretical calculations also support the intermediacy of chloronium ions in addition reactions. Rodriguez, C. F.; Bohme, D. K.; Hopkinson, A. C. *J. Am. Chem. Soc.* **1993**, *115*, 3263. Also see Reynolds, C. H. *J. Am. Chem. Soc.* **1992**, *114*, 8676. There was also experimental evidence for the existence of chloronium ions from ion cyclotron resonance spectrometry experiments. Berman, D. W.; Anicich, V.; Beauchamp, J. L. *J. Am. Chem. Soc.* **1979**, *101*, 1239 reported that the stability of cyclic ions varies with the atom or group that is bonded to two carbon atoms in a three-membered ring. For the following species as the bridging group, relative stability is $OH < Cl < Br < SH$, $PH_2 < NH_2$.

¹²¹ Merritt, R. F.; Johnson, F. A. *J. Org. Chem.* **1966**, *31*, 1859. See also Merritt, R. F.; *J. Org. Chem.* **1966**, *31*, 3871; Merritt, R. F. *J. Am. Chem. Soc.* **1967**, *89*, 609.

¹²² The concerted mechanism is termed an Ad_E2M pathway.

¹²³ Yamabe, S.; Minato, T.; Inagaki, S. *J. Chem. Soc. Chem. Commun.* **1988**, 532. The same calculations identified three-centered transition structures for the addition of chlorine and bromine; such transition structures should lead to chloronium and bromonium ions, respectively.

¹²⁴ Rozen, S.; Brand, M. *J. Org. Chem.* **1986**, *51*, 3607.

of 1% fluorine in nitrogen into a solution of the alkene dissolved in a mixture of CFCl_3 , CHCl_3 , and ethanol, a solvent system chosen to diminish the probability of radical reactions competing with the ionic addition process. For alkenes substituted with alkyl groups (e.g., cycloheptene) or with electron-withdrawing groups (*cis*- or *trans*-ethyl cinnamate), the products isolated were exclusively from those of syn addition. When *cis*-stilbene was treated under the same conditions, the major product was the *meso*-1,2-difluoro-1,2-diphenylethane isomer, but an appreciable yield of the racemic product was also found. The results were interpreted to mean that in most cases the additions take place through electrophilic addition of fluorine to the alkene to produce a tight β -fluorocarocation--fluoride ion pair. The ion pair can collapse to give syn addition before rotation about a carbon-carbon single bond or reorientation of the fluoride ion in the ion pair can result in anti addition. When stilbene reacts, however, the β -fluorocarocation is a benzylic carbocation and is sufficiently stable for some reorientation to occur before attack of the fluoride ion to the cation. In no case is there evidence for a long-lived carbocation or even for a solvent-separated ion pair, since no ethyl ethers are observed in the product mixture.¹²⁵

Synthetic chemists have sought other reagents for addition of fluorine to alkenes because of the danger and difficulty of working with molecular fluorine. One such reagent is XeF_2 , which was found to react with ethene to give a 35% yield of 1,1-difluoroethane and a 45% yield of 1,2-difluoroethane. Propene reacted with XeF_2 to give 1,1-difluoropropane as the main product.¹²⁶ The investigators suggested that 1,2-difluoropropane is formed as a kinetic (rate-controlled) product, but that it rearranges to the thermodynamically more stable 1,1-difluoropropane (equilibrium-controlled product).¹²⁷

A significant complication in understanding the mechanism of addition of fluorine to alkenes with XeF_2 is uncertainty about the possible role of single electron transfer in the reaction. Figure 9.27 shows that the hydrogen fluoride-catalyzed reaction of XeF_2 with a styrene derivative could produce the same carbocation by either a one-step transfer of F^+ to the alkene or by a two-step route involving single electron transfer to form the radical cation of the alkene, which then abstracts a fluorine atom from FXe^* . Stavber and co-workers studied the HF-catalyzed reaction of a series of phenyl-substituted alkenes with XeF_2 in CH_2Cl_2 at room temperature. The logarithms of the relative rate constants for addition across the carbon-carbon double bond were found to correlate with the ionization potentials of the alkenes, with a lower IP being associated with a faster rate constant for addition.¹²⁸ The authors concluded that the rate-limiting step in the addition is disruption of

¹²⁵ The observation of increasing proportion of syn addition of X_2 with increasing electronegativity of X is also consistent with the suggestion by Phillips, L.; Wray, V. *J. Chem. Soc. Chem. Commun.* **1973**, 90 that there is a parallel between the vicinal relationship of the halogen atoms in syn addition to an alkene and the relationship of vicinal halogen atoms in molecules that exhibit a gauche effect. These authors suggest that the electronic factors responsible for the gauche effect may also be reflected in the potential energy surface for electrophilic addition of X_2 , even if the reaction proceeds through an unsymmetrical carbocation.

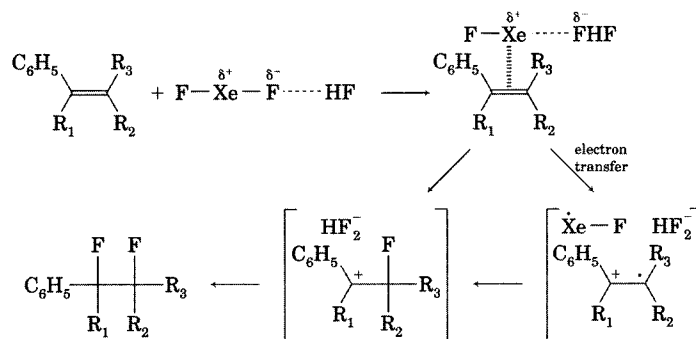
¹²⁶ Shieh, T.-C.; Yang, N. C.; Chernick, C. L. *J. Am. Chem. Soc.* **1964**, *86*, 5021.

¹²⁷ For a discussion of the origins of the greater stability of *gem*-difluorides than of *vic*-dihalides, see Hine, J. *J. Am. Chem. Soc.* **1963**, *85*, 3239.

¹²⁸ Stavber, S.; Sotler, T.; Zupan, M.; Popovič, A. *J. Org. Chem.* **1994**, *59*, 5891.

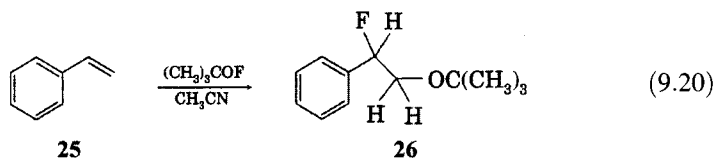
FIGURE 9.27

Competitive pathways for reaction of XeF_2 with alkenes. (Adapted from reference 128.)



the π bond, but that did not allow exclusion of either of the two pathways shown in Figure 9.27. It might be the case that not all addition reactions occur by the same mechanism. The operation of the ionic or electron transfer mechanism of addition in a particular case might be a function of the structure of the alkene, the concentration of the reagents, the solvent, and the temperature.¹²⁸

If a synthetic scheme requires that only one fluorine be attached to the carbon skeleton, then other reagents are available. Appelman and Rozen and their co-workers described the synthesis and reactions of *t*-butyl hypofluorite, $(\text{CH}_3)_3\text{COF}$.¹²⁹ Reaction of $(\text{CH}_3)_3\text{COF}$ with styrene (**25**) in CH_3CN solution produced 1-fluoro-1-phenyl-2-*t*-butoxyethane (**26**) as the major product (equation 9.20).¹³⁰ This regiochemistry suggests that the reaction involves reaction of the alkene with the *t*-butoxyl cation, $(\text{CH}_3)_3\text{CO}^+$, followed by subsequent attachment of F^- to the cationic intermediate.



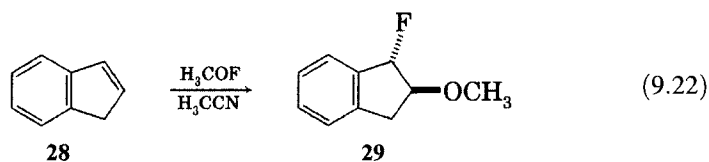
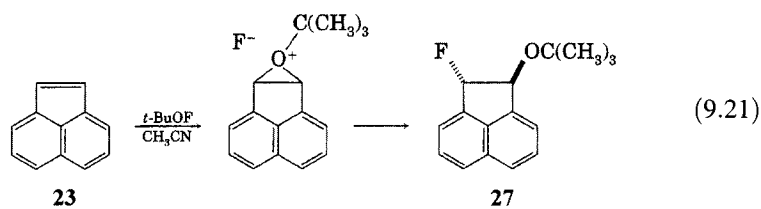
The cationic intermediate in this reaction appears to have some bridged ion character. Addition of $(\text{CH}_3)_3\text{COF}$ to acenaphthylene (**23**) gave *threo*-1-fluoro-2-*t*-butoxyacenaphthene (**27**) as the only adduct (equation 9.21).¹³¹ Similarly, methyl hypofluorite (H_3COF , prepared in situ from the reaction of F_2 with methanol) also adds to alkenes, as in the conversion of indene (**28**) into (\pm)-*trans*-1-fluoro-2-methoxyindane (**29**, equation 9.22).¹³²

¹²⁹ Appelman, E. H.; French, D.; Mishani, E.; Rozen, S. *J. Am. Chem. Soc.* **1993**, *115*, 1379.

¹³⁰ Small amounts of 1-fluoro-1-phenyl-3-cyanopropane were also observed, perhaps as a result of radical ion reactions involving solvent.

¹³¹ The addition of *t*-BuOF stands in contrast to the pattern of reaction of other alkyl hypofluorites, such as CF_3OF and $\text{CF}_3\text{CF}_2\text{OF}$, since they add in a syn process and with the opposite regiochemistry for fluorine addition: Lerman, O.; Rozen, S. *J. Org. Chem.* **1980**, *45*, 4122; Rozen, S.; Lerman, O.; Kol, M.; Hebel, D. *J. Org. Chem.* **1985**, *50*, 4753.

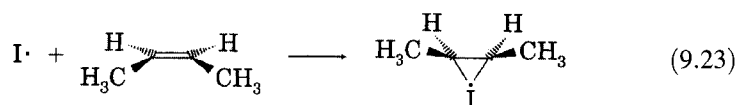
¹³² Rozen, S.; Mishani, E.; Kol, M.; Ben-David, I. *J. Org. Chem.* **1994**, *59*, 4281.



Iodine

Because iodine is the best of the halogens at bridging, we might expect the iodonium ion to be the intermediate in the addition of iodine to alkenes. Indeed, an iodonium ion was isolated from the reaction of iodine with adamantylideneadamantane.³⁶ The addition of iodine to alkenes is generally not synthetically useful, however, primarily because the formation of 1,2-diodo compounds from I_2 and alkenes is not as exothermic as are the additions of other halogens to alkenes. For example, the ΔH for addition of iodine to ethene is exothermic by only about 11 kcal/mol in the gas phase. Since ΔS is -31.5 eu, adduct stability decreases with increasing temperature.¹³³ In one study it was found that a mixture of styrene and iodine produced styrene diiodide; the product could be collected by filtration at 0°C , but it decomposed at room temperature to styrene and iodine.¹³⁴

The addition of iodine to alkenes takes place through radical as well as ionic pathways. Addition of I_2 to 1-butene occurred photochemically to give a product, presumed to be 1,2-diiodobutane, that was stable only below -15°C . Addition of iodine to *trans*-2-butene produced 2,3-diiodobutane, which melted with decomposition at -11°C .¹³⁵ Alkenes were also found to add iodine photochemically in refluxing propane at -42°C to produce crystalline diiodides that decomposed at room temperature.¹³⁶ The stereochemistry of the addition was found to be anti, with *cis*-2-butene producing racemic diiodide and *trans*-2-butene producing *meso*-2,3-diiodobutane. For these additions, the authors proposed a radical chain mechanism involving a bridged radical intermediate (with propagation steps 9.23 and 9.24) and suggested that the relative bridging power of β -halogenated radicals is $F \ll Cl < Br < I$.¹³⁷



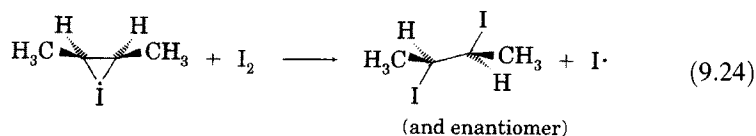
¹³³ Benson, S. W.; Amano, A. *J. Chem. Phys.* **1962**, *36*, 3464.

¹³⁴ Fraenkel, G.; Bartlett, P. D. *J. Am. Chem. Soc.* **1959**, *81*, 5582.

¹³⁵ Forbes, G. S.; Nelson, A. F. *J. Am. Chem. Soc.* **1937**, *59*, 693.

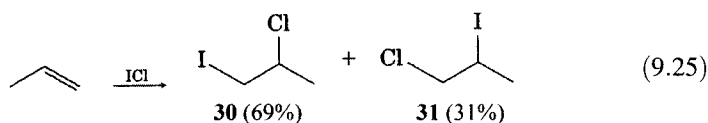
¹³⁶ Skell, P. S.; Pavlis, R. R. *J. Am. Chem. Soc.* **1964**, *86*, 2956.

¹³⁷ Investigators have also concluded that both radical chain and nonradical chain mechanisms are possible: (a) reference 134; (b) Trifan, D. S.; Bartlett, P. D. *J. Am. Chem. Soc.* **1959**, *81*, 5573.



Addition of Mixed Halogens

The mixed halogens ICl, IBr, and BrCl also add to alkenes. White and Robertson found third-order kinetics for the reaction and determined the relative reactivities to be $\text{BrCl} > \text{ICl} > \text{Br}_2 > \text{IBr} > \text{I}_2$.¹³⁸ The large reactivity of BrCl means that addition of BrCl can occur when alkenes react with mixtures of Br_2 and Cl_2 .¹³⁹ The regioselectivity of addition of mixed halogens was reported by Ingold and Smith. Addition of ICl to propene gave 69% of 2-chloro-1-iodopropane (**30**) and 31% of 1-chloro-2-iodopropane (**31**), and addition to styrene gave more than 95% of 1-chloro-2-iodo-1-phenylethane.¹⁴⁰



This regiochemistry can be rationalized by imagining that the X–Y molecule first adds X^+ to the alkene when Y is the more electronegative of the atoms X and Y.¹⁴¹ Furthermore, attachment of X^+ may result in a halonium ion if such an intermediate is formed in the addition of X_2 to the same alkene. For example, *cis*-stilbene reacted in a mixture of Br_2 and Cl_2 to produce 68% of *threo*-1-bromo-2-chloro-1,2-diphenylethane and only about 5% of the *erythro* diastereomer.¹³⁹

Addition of XY to alkenes can also be accomplished by indirect means. Buckels and Long¹⁴² used *N*-bromoacetamide and HCl to add BrCl to alkenes. The stereochemistry of the reaction suggested an anti addition, which was consistent with attachment of Br^+ from protonated *N*-bromoacetamide to give a bromonium ion (or β -bromocarocation), followed by attachment of Cl^- . Reaction of *N*-bromoacetamide and HF in a proton-accepting solvent such as THF (which increases the solubility of HF) gave anti addition of FBr to cyclohexene. Similarly, reaction of cyclohexene with *N*-iodoacetamide and HF produced *trans*-1-fluoro-2-iodocyclohexane.^{143,144}

¹³⁸ White, E. P.; Robertson, P. W. *J. Chem. Soc.* **1939**, 1509.

¹³⁹ Buckles, R. E.; Forrester, J. L.; Burham, R. L.; McGee, T. W. *J. Org. Chem.* **1960**, *25*, 24.

¹⁴⁰ Ingold, C. K.; Smith, H. G. *J. Chem. Soc.* **1931**, 2742

¹⁴¹ Ingold, C. K. *Chem. Rev.* **1934**, *15*, 225 (see especially pp. 270–271).

¹⁴² Buckels, R. E.; Long, J. W. *J. Am. Chem. Soc.* **1951**, *73*, 998.

¹⁴³ Bowers, A.; Cuéllar Ibáñez, L.; Denot, E.; Becerra, R. *J. Am. Chem. Soc.* **1960**, *82*, 4001.

¹⁴⁴ These reactions are useful for the synthesis of steroids, where fluorine substitution has been found to give useful pharmacological properties. Bowers, A.; Denot, E.; Becerra, R. *J. Am. Chem. Soc.* **1960**, *82*, 4007.

9.3 OTHER ADDITION REACTIONS

Addition of Hydrogen Halides to Alkenes

Regiochemistry of Addition: Markovnikov's Rule

The addition of HCl to propene to produce isopropyl chloride is the classic example of Markovnikov's rule.^{145,146} As translated by Kharasch and Reinmuth, Markovnikov wrote that the addition of halogen acids to unsymmetrical alkenes occurs so that the halogen becomes attached to the less hydrogenated carbon atom (Figure 9.28).¹⁴⁷ Contemporary textbooks often state that the addition of HX to an unsymmetrical alkene occurs so that the proton becomes bonded to the olefinic carbon atom that already had the greater number of hydrogen atoms. Although this statement may be easier to remember, it is not precisely the original rule. Both statements are easily seen as manifestations of ionic addition proceeding through the more stable of two possible carbocations.¹⁴⁸ In the case of vinyl chloride and other haloalkenes, the halogen of the HX adds to the carbon atom that already has a halogen substituent.¹⁴⁷

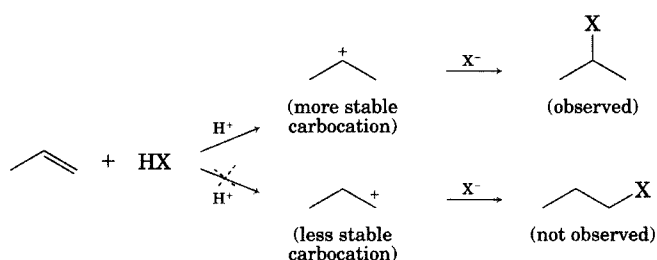


FIGURE 9.28

Rationale for Markovnikov regiochemistry in terms of carbocation stability.

Just as Figure 9.2 is an extremely simplified mechanism for bromine addition, so it appears that Figure 9.28 understates the complexity of the addition of HX to an alkene. Figure 9.28 suggests that the addition should be overall second order, first order in alkene and first order in hydrogen halide, but this is generally not the case. In nonpolar solvents the addition of HBr to an alkene is first order in alkene and either second order or third order in HBr. Mayo and Savoy found that it was quite difficult to eliminate all traces of the competing radical reaction (see page 589), but the kinetic expression most closely resembled

$$\text{Rate} = k[\text{alkene}][\text{HBr}]^3 \quad (9.26)$$

¹⁴⁵ The spelling currently popular is Markovnikov, although different spellings were used in the first publications in German and French: (a) Markownikoff, W. *Liebigs Ann. Chem.* **1870**, 153, 228 (particularly the discussion beginning on p. 256); (b) Markownikoff, V. *Compt. Rend.* **1875**, 81, 668.

¹⁴⁶ A brief autobiography of Markovnikov was given by Leicester, H. M. *J. Chem. Educ.* **1941**, 18, 53. Several authors have discussed the history of Markovnikov's rule and its various forms and spellings. Jones, G. J. *J. Chem. Educ.* **1961**, 38, 297 noted the contribution of Henry in writing a more general form of Markovnikov's rule in which the more negative group in a molecule XY adds to the carbon atom with the fewer number of hydrogen atoms (i.e., the carbon atom with the greater number of alkyl substituents). See also Tierney, J. J. *J. Chem. Educ.* **1988**, 65, 1053.

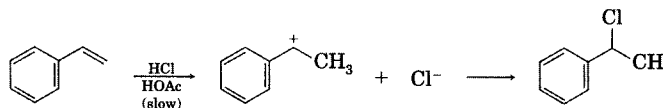
¹⁴⁷ Kharasch, M. S.; Reinmuth, O. *J. Chem. Educ.* **1931**, 8, 1703.

¹⁴⁸ A density functional theory analysis supported this model for Markovnikov orientation: Aizman, A.; Contreras, R.; Galván, M.; Cedillo, A.; Santos, J. C.; Chamorro, E. *J. Phys. Chem. A*, **2002**, 106, 7844.

When hydroxylated solvents were added, the rate of reaction increased, and the rate expression appeared to be of lower order.¹⁴⁹ The addition of HBr to cyclohexene in acetic acid was found to give both cyclohexyl bromide and cyclohexyl acetate. Through deuterium labeling of the cyclohexene, the predominant pattern of addition was found to be anti, with the proportion of syn HBr addition varying from 4% to 6% over the temperature range 15–60°C. The formation of cyclohexyl acetate was greater at the higher temperature.^{150–152} Instead of a bare H⁺, therefore, the electrophile may be one or more molecules of HBr, and there may also be one or more HBr molecules required to solvate the departing Br⁻ ion.¹⁵³

Addition of HCl shows similar complexity. The addition of HCl to isobutylene also indicated fourth-order kinetics overall, third order in HCl.¹⁵⁴ Studies by Fahey and co-workers suggested that anti addition of HCl to cyclohexene occurs by a termolecular process depending on [alkene], [HCl], and [Cl⁻]⁻—an Ad_E3 mechanism—along with syn addition through a carbocation–chloride ion pair—^{an Ad_E2 mechanism.}^{155–157} The mechanism of the addition also depends on the structure of the alkene. The addition of HCl to styrene in acetic acid was reported to occur by an Ad_E2 pathway (Figure 9.29),¹⁵⁸ but the addition of HCl to cyclohexene was reported to occur at least partly by an Ad_E3 mechanism (Figure 9.30).^{156,159}

FIGURE 9.29
Ad_E2 addition of HCl to styrene.



¹⁴⁹ Mayo, F. R.; Savoy, M. G. *J. Am. Chem. Soc.* **1947**, *69*, 1348.

¹⁵⁰ Fahey, R. C.; Smith, R. A. *J. Am. Chem. Soc.* **1964**, *86*, 5035.

¹⁵¹ Addition of HI to propene gave only 2-iodopropane, whether antioxidants or peroxides were added. Addition of HI to allyl bromide produced only 1-bromo-2-iodopropane, and addition of HI to allyl chloride gave only 1-chloro-2-iodopropane. The reason for the Markovnikov orientation may be that HI reacted with peroxides to give iodine, thus stopping initiation of radical chain reaction. Kharasch, M. S.; Norton, J. A.; Mayo, F. R. *J. Am. Chem. Soc.* **1940**, *62*, 81.

¹⁵² Addition of HF to alkenes has been shown to follow Markovnikov's rule (Sharts, C. M.; Sheppard, W. A. *Org. React.* **1974**, *21*, 125 and references therein). Direct addition of HF is seldom carried out because of the danger of working with that reagent and because of the development of newer synthetic reagents. Moreover, it is both safer and more convenient to use KF to synthesize a 2-fluoroalkane from the corresponding 2-chloroalkane than to add HF to a 1-alkene.

¹⁵³ Solvent molecules might also serve to facilitate the reaction. Isenberg, N.; Grdinic, M. *J. Chem. Educ.* **1969**, *46*, 601.

¹⁵⁴ Mayo, F. R.; Katz, J. J. *J. Am. Chem. Soc.* **1947**, *69*, 1339.

¹⁵⁵ Fahey, R. C.; McPherson, C. A. *J. Am. Chem. Soc.* **1971**, *93*, 2445.

¹⁵⁶ Fahey, R. C.; Monahan, M. W.; McPherson, C. A. *J. Am. Chem. Soc.* **1970**, *92*, 2810; Fahey, R. C.; Monahan, M. W. *J. Am. Chem. Soc.* **1970**, *92*, 2816.

¹⁵⁷ In one case it was also suggested that the addition of HCl could occur through a concerted, four-center pathway (Ad_E2M) in solution. Freeman, P. K.; Raymond, F. A.; Grostic, M. F. *J. Org. Chem.* **1967**, *32*, 24.

¹⁵⁸ Fahey, R. C.; McPherson, C. A. *J. Am. Chem. Soc.* **1969**, *91*, 3865; see also the discussion in reference 7.

¹⁵⁹ The intermediate has been proposed as a nonclassical carbocation in some cases. See, for example, Cristol, S. J.; Caple, R. *J. Org. Chem.* **1966**, *31*, 2741; Cristol, S. J.; Sullivan, J. M. *J. Am. Chem. Soc.* **1971**, *93*, 1967.

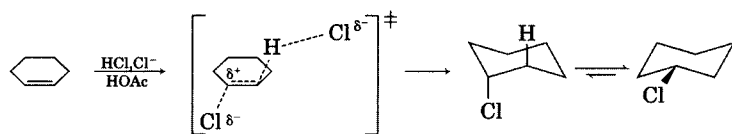
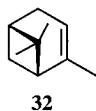


FIGURE 9.30
Ad_E3 addition of HCl to cyclohexene.

The addition of HCl to alkenes is slower than is the addition of HBr, and often addition of HCl is not observed unless the alkene is substituted with many alkyl groups, is substituted with at least one aryl group, or is strained. For example, (–)- α -pinene (**32**) reacts with HCl in CHCl₃ solution, but 1-octene does not.^{160,161} Solvent effects are also important in HCl addition. The rate constant for addition of HCl to α -pinene was found to vary with solvent as follows: CHCl₃ > xylene > nitrobenzene \gg methanol > dioxane > diethyl ether (no apparent reaction).¹⁶² Investigators concluded that the rate constant for the addition reaction decreases with an increasing tendency of HCl to coordinate with an electron pair donor of the solvent.¹⁶³ Kropp and co-workers reported that the addition of HCl to 1-octene can be carried out in CHCl₃ solution when the HCl is generated in the presence of silica gel or alumina. The surface-mediated reaction appears to involve a longer lived carbocation intermediate, since 3-chlorooctane is isolated along with 2-chlorooctane, and both (*E*)- and (*Z*)-2-octene can also be recovered from the reaction mixture.^{161,164}



Although a carbocation is not the only possible intermediate in the addition of hydrogen halides to alkenes,¹⁶⁵ the observation of characteristic carbocation rearrangement products strongly supports the role of a carbocation-like species in this reaction under these surface-mediated conditions. Addition of HCl to neat 3,3-dimethyl-1-butene (**7**) produced 60% of the rearranged product (2-chloro-2,3-dimethylbutane, **33**) and about 40% of the unrearranged 2-chloro-3,3-dimethylbutane (**34**).¹⁶⁶ Fahey and

¹⁶⁰ Kropp, P. J.; Daus, K. A.; Crawford, S. D.; Tubergen, M. W.; Kepler, K. D.; Craig, S. L.; Wilson, V. P. *J. Am. Chem. Soc.* **1990**, *112*, 7433.

¹⁶¹ The greater reactivity of HBr in addition reactions means that HBr does add to 1-octene in CHCl₃. Kropp, P. J.; Daus, K. A.; Tubergen, M. W.; Kepler, K. D.; Wilson, V. P.; Craig, S. L.; Baillargeon, M. M.; Breton, G. W. *J. Am. Chem. Soc.* **1993**, *115*, 3071.

¹⁶² Hennion, G. F.; Irwin, C. F. *J. Am. Chem. Soc.* **1941**, *63*, 860. Products from the reaction of pinene with HCl in methanol were not reported.

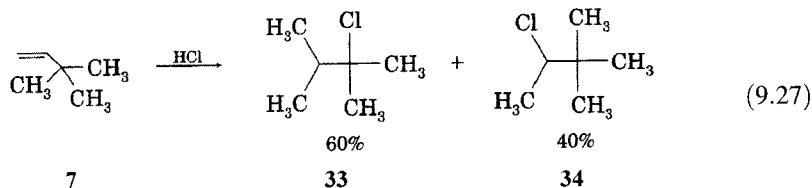
¹⁶³ O'Connor, S. F.; Baldinger, L. H.; Vogt, R. R.; Hennion, G. F. *J. Am. Chem. Soc.* **1939**, *61*, 1454.

¹⁶⁴ The surface-mediated reaction enables the addition of HBr to 1-octene to proceed at room temperature without the formation of 1-bromooctane by free radical chain reaction addition.

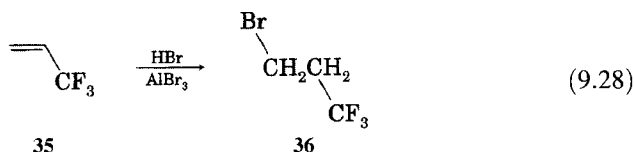
¹⁶⁵ Brown, H. C.; Liu, K.-T. *J. Am. Chem. Soc.* **1975**, *97*, 600.

¹⁶⁶ Less rearrangement was observed with addition of HI, with only 10% of the product being the 2-iodo-3,3-dimethylbutane. Ecke, G. G.; Cook, N. C.; Whitmore, F. C. *J. Am. Chem. Soc.* **1950**, *72*, 1511.

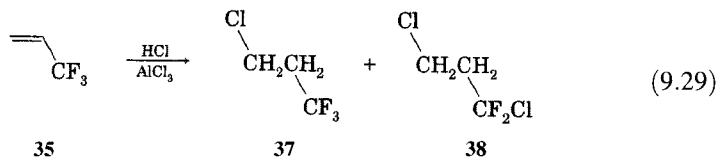
McPherson found that reaction of 7 with HCl in acetic acid also gave both 33 and 34.^{167,168}



The strongly electron-withdrawing trifluoromethyl group destabilizes an adjacent carbocation and reduces the rate constant for addition of hydrogen halides to an alkene. For example, adding HBr to 3,3,3-trifluoropropene (35) produced the anti-Markovnikov product, 3-bromo-1,1,1-trifluoropropane (36), but only when the reactants were heated in a sealed tube at 100°C with AlBr₃ catalyst (equation 9.28).¹⁶⁹



If this addition occurs through a carbocation intermediate, as in Figure 9.28, then the regiochemistry might be attributed to the greater stability of a 1° cation in which the trifluoromethyl group is further removed (CF₃CH₂CH₂⁺) than a 2° carbocation with an adjacent trifluoromethyl group (CF₃CH⁺CH₃). The mechanism must be more complex, however, because the reaction of 3,3,3-trifluoropropene with HCl and AlCl₃ produced nearly equal amounts of CF₃CH₂CH₂Cl (37) and CF₂ClCH₂CH₂Cl (38, equation 9.29).¹⁷⁰



The investigators proposed that AlCl₃-promoted removal of fluoride from the starting material would give 1,1-difluoroallyl cation, which could add Cl⁻ to

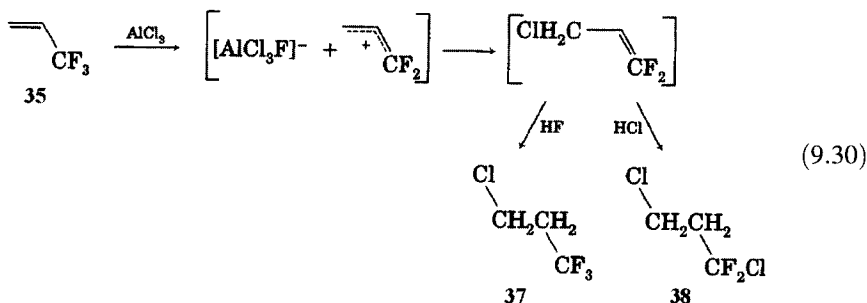
¹⁶⁷ Fahey, R. C.; McPherson, C. A. *J. Am. Chem. Soc.* **1969**, *91*, 3865

¹⁶⁸ This result confirmed the earlier work of Whitmore, F. C.; Johnston, F. J. *Am. Chem. Soc.* **1933**, *55*, 5020, who had found that the addition of HCl to 3-methyl-1-butene without solvent, in a sealed reaction tube for 7 weeks, gave both 2-chloro-3-methylbutane and 2-chloro-2-methylbutane. This result contradicted the suggestion of earlier investigators that the 3° alkyl halide was formed by rearrangement of the 2° alkyl halide formed from the addition reaction. Hammond, G. S.; Collins, C. H. *J. Am. Chem. Soc.* **1960**, *82*, 4323 found that addition of HCl to 1,2-dimethylcyclopentene produced 1-chloro-*trans*-1,2-dimethylcyclopentane as the major (perhaps only) addition product, but it isomerized to 1-chloro-*cis*-1,2-dimethylcyclopentane.

¹⁶⁹ Henne, A. L.; Kaye, S. *J. Am. Chem. Soc.* **1950**, *72*, 3369.

¹⁷⁰ Myhre, P. C.; Andrews, G. D. *J. Am. Chem. Soc.* **1970**, *92*, 7596.

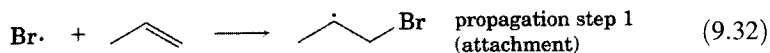
give 1,1-difluoro-3-chloropropene. That product could then add either HCl or HF to give the two products observed (equation 9.30).¹⁷¹



Anti-Markovnikov Addition of HBr to Alkenes

For some time the regiochemistry of the addition of HBr to alkenes was the subject of controversy because the results did not appear to be the same from laboratory to laboratory. Sometimes even the same researchers found different results under apparently similar conditions.¹⁴⁹ In 1933 Kharasch and Mayo distinguished between *normal* (now called Markovnikov) addition of HBr to allyl bromide in the presence of radical inhibitors and the *abnormal* or *unnatural* reaction observed in the presence of peroxides, air, and some other reagents.^{172,173} Addition of HBr to propene gave 2-bromopropane if antioxidants were present but 1-bromopropane if peroxides were added.¹⁷⁴ Similar results were obtained in the addition of HBr to pentene.^{175,176} In these reactions the dielectric constant of the solvent did not appear to influence the *orientation* of the addition, but it did affect the *rate constant* for the normal addition.

The mechanism proposed for the *peroxide effect* involves a radical chain reaction.¹⁷⁷ The initiation step (equation 9.31) produces a bromine atom, which then attaches to the less alkyl-substituted carbon atom of a carbon-carbon double bond (equation 9.32). The resulting alkyl radical then abstracts a hydrogen atom from HBr to produce the anti-Markovnikov product and regenerate a bromine atom in the second propagation step (equation 9.33). Termination steps, not shown, interrupt the chain reaction.



¹⁷¹ A similar mechanism might be expected in the reaction with HBr/AlBr₃, but 3-bromo-1,1,1-trifluoropropane was the only product of the reaction. Newton, T. A. *J. Chem. Educ.* **1987**, *64*, 531.

¹⁷² Credit has also been given to Hey and Waters for independent discovery of the radical nature of anti-Markovnikov addition of HBr to alkenes: Hey, D. H.; Waters, W. A. *Chem. Rev.* **1937**, *21*, 169.

¹⁷³ Kharasch, M. S.; Mayo, F. R. *J. Am. Chem. Soc.* **1933**, *55*, 2468.

¹⁷⁴ Kharasch, M. S.; McNab, M. C.; Mayo, F. R. *J. Am. Chem. Soc.* **1933**, *55*, 2531.

¹⁷⁵ Kharasch, M. S.; Hinckley, J. A., Jr.; Gladstone, M. M. *J. Am. Chem. Soc.* **1934**, *56*, 1642.

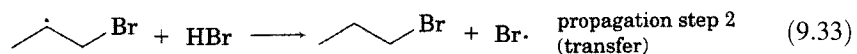
¹⁷⁶ Vaughan, W. E.; Rust, F. F.; Evans, T. W. *J. Org. Chem.* **1942**, *7*, 477.

¹⁷⁷ Kharasch, M. S.; Engelmann, H.; Mayo, F. R. *J. Org. Chem.* **1938**, *2*, 288.

TABLE 9.4 Enthalpies of the Propagation Steps in the Radical Addition of HX to Ethene

HX	Attachment (equation 9.32)	Transfer (equation 9.33)
HF	-46 kcal/mol	36 kcal/mol
HBr	-3 kcal/mol	-11 kcal/mol
HCl	-17 kcal/mol	4 kcal/mol
HI	12 kcal/mol	-27 kcal/mol

Source: Reference 153.



Among the hydrogen halides, only HBr is known to undergo radical addition readily, even though the addition of HX to a carbon-carbon double bond is exothermic for all the hydrogen halides.¹⁷⁸ Calculation of the ΔH values for the two propagation steps in the chain reaction suggests a reason for the singular reactivity of HBr: only for HBr are *both* propagation steps exothermic (Table 9.4).¹⁷⁹ The endothermic radical attachment step precludes radical chain addition of HI, and the highly endothermic transfer step prevents the addition of HF. For radical addition of HCl to an alkene, the slightly endothermic transfer step minimizes the importance of radical chain addition, although the photochemical addition of HCl to ethene in the gas phase was considered to be a radical chain addition process.¹⁸⁰ Furthermore, addition of anhydrous HCl to neat 3,3-dimethyl-1-butene in the presence of dibenzoyl peroxide produced up to 24% of 1-chloro-3,3-dimethylbutane, apparently as a result of radical chain addition. However, this anti-Markovnikov product was only seen at low concentrations of HCl.¹⁶⁶

The regiochemistry of anti-Markovnikov addition can be rationalized conveniently by the argument that the reaction proceeds through the intermediacy of the more stable free radical. Tedder noted an important limitation of this rationalization, however.¹⁸¹ Since the attachment of a bromine atom to an alkene (equation 9.32) is strongly exothermic, the transition state should be early. Therefore, differences in thermodynamic stabilities of the developing radicals need not result in significant differences in transition state energies. A more satisfying explanation for the tendency of the bromine atom to bond to the less alkyl-substituted carbon atom is that steric effects are minimized in the transition structure.¹⁸² Thus, in equation 9.32 the observed pathway does

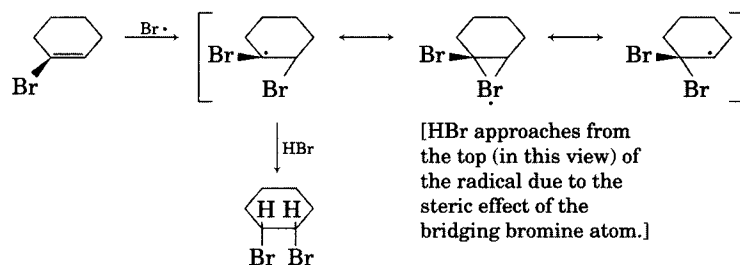
¹⁷⁸ The addition of HI to propene, 1-bromopropene, allyl chloride, or allyl bromide gave only the normal addition products, and antioxidants did not inhibit the reaction. Moreover, HI inhibited the radical addition of HBr to alkenes. One possible route for this inhibition would be the reaction of peroxides with HI to produce I_2 . Kharasch, M. S.; Norton, J. A.; Mayo, F. R. *J. Am. Chem. Soc.* **1940**, *62*, 81.

¹⁷⁹ For a discussion see reference 153. The values in Table 9.4 and those in that reference differ slightly due to the use here of more recent bond strength data. See also Pryor, W. A. *Chem. Eng. News* **1968** (Jan 15), 46, 70.

¹⁸⁰ Raley, J. H.; Rust, F. F.; Vaughan, W. E. *J. Am. Chem. Soc.* **1948**, *70*, 2767.

¹⁸¹ Tedder, J. M. *J. Chem. Educ.* **1984**, *61*, 237.

¹⁸² Tedder (reference 181) also discussed the importance of polar effects, for example, in the case of attachment of methyl or trifluoromethyl radicals to vinyl fluoride.

**FIGURE 9.31**

Mechanism proposed for formation of *cis*-1,2-dibromocyclohexane by free radical addition of HBr to 1-bromocyclohexene.

form the more stable radical, but primarily because it also proceeds through the less sterically hindered addition pathway.¹⁸³

As in other cases, the reactive intermediates in additions to alkenes are often more complex than the simple models suggest. This is apparently true also for the intermediate in the free radical addition of HBr to alkenes. Peroxide-promoted addition of HBr to 1-bromocyclohexene in pentane solution was reported to give *cis*-1,2-dibromocyclohexane (equation 9.34). Similarly, addition to 1-methylcyclohexene gave *cis*-1-bromo-2-methylcyclohexane. In both cases, the *trans* products would have been thermodynamically more stable. These results suggest that a planar carbon free radical is not the intermediate. Rather, the intermediate radical seems to be a bromine-bridged species analogous to a bromonium ion. As shown in Figure 9.31, a bridging bromine atom effectively blocks one face of the cyclohexane ring. This interaction causes the reaction of the radical with HBr to occur from the other face of the structure, thus accounting for the observed stereochemistry.¹⁸⁴



This discussion has focused on the addition of HBr, but radical addition pathways have been elucidated for other reagents as well, and some of these reactions lead to the formation of carbon-carbon bonds.¹⁸⁵ For example, ethanol adds to 1-hexene to give 2-octanol in low yield in the presence of di-*t*-butyl peroxide at 125°C and in the presence of light.¹⁸⁶ In the presence of diacetyl peroxide initiator, CCl_3COCl and $\text{CHCl}_2\text{COOCH}_3$ add to alkenes by

¹⁸³ Goering and Larsen reported that the radical chain addition of HBr (or DBr) to 2-bromo-2-butene is stereospecific anti addition at -80°C but is not stereospecific at room temperature. Goering, H. L.; Larsen, D. W. *J. Am. Chem. Soc.* **1959**, *81*, 5937.

¹⁸⁴ Goering, H. L.; Abell, P. I.; Aycock, B. F. *J. Am. Chem. Soc.* **1952**, *74*, 3588.

¹⁸⁵ Walling, C.; Huyser, E. S. *Org. React.* **1963**, *13*, 91.

¹⁸⁶ Urry, W. H.; Stacey, F. W.; Huyser, E. S.; Juveland, O. O. *J. Am. Chem. Soc.* **1954**, *76*, 450.

a free radical mechanism.¹⁸⁷ Other free radical chain reaction additions to alkenes include mercaptans,¹⁸⁸ CCl₄, CBr₄, CHCl₃, and CHBr₃;¹⁸⁹ CBr₂Cl₂ and CHBrCl₂;¹⁹⁰ CF₂I₂;¹⁹¹ and CBrCl₃.¹⁹² A radical chain mechanism was reported for the addition of perfluoroalkyl iodides to alkenes.¹⁹³

Hydration of Alkenes

Hydration of alkenes is the addition of the elements of water (H and OH) across the carbon-carbon double bond. There is substantial evidence that acid-catalyzed addition of water to an alkene involves a cationic intermediate. Rate constants for hydration increase with the electron-donating ability of the substituents on the double bond, and rate constants for hydration of unsymmetrical alkenes with the general formula R₁R₂C=CH₂ give a good correlation with σ^+ values,

$$\log k_2 = \rho^+ \Sigma \sigma^+ + C \quad (9.35)$$

where $\rho^+ = -12.3$ and $C = -10.1$.¹⁹⁴ Because of the lower acidity of water in comparison with hydrogen halides, addition of water is carried out with acid catalysis. For hydration of 2-methyl-2-butene in aqueous nitric acid solutions, the reaction was found to be overall second order, first order in alkene and first order in H⁺, with $E_a = 18.9$ kcal/mol.¹⁹⁵

Acid-catalyzed hydration reactions occur with Markovnikov orientation. For example, hydration of 2-methyl-2-butene gives 2-methyl-2-butanol, consistent with the intermediacy of the 3° 2-methyl-2-butyl carbocation. Moreover, hydration of 2-methyl-1-butene was also found to produce 2-methyl-2-butanol, and there was no indication of isomerization to 2-methyl-2-butene during hydration.¹⁹⁶ These results suggest, but do not confirm,⁹ that the cationic intermediate undergoes nucleophilic attack by water faster than it loses a proton to revert to starting material.¹⁹⁷

¹⁸⁷ Kharasch, M. S.; Urry, W. H.; Jensen, E. V. *J. Am. Chem. Soc.* **1945**, *67*, 1626.

¹⁸⁸ Jones, S. O.; Reid, E. E. *J. Am. Chem. Soc.* **1938**, *60*, 2452.

¹⁸⁹ With a generalized unsymmetrical alkene, RCH=CH₂, the products from these reagents are RCHClCH₂CCl₃, RCHBrCH₂CBr₃, RCH₂CH₂CCl₃, and RCHBrCH₂CCL₃, respectively. Kharasch, M. S.; Jensen, E. V.; Urry, W. H. *J. Am. Chem. Soc.* **1947**, *69*, 1100.

¹⁹⁰ With a generalized unsymmetrical alkene, RCH=CH₂, the products from these reagents are BrCHRCH₂CBrCl₂ and BrCHRCH₂CHCl₂, respectively. Kharasch, M. S.; Kuderna, B. M.; Urry, W. *J. Org. Chem.* **1948**, *13*, 895.

¹⁹¹ With a generalized unsymmetrical alkene, RCH=CH₂, the product from this reagent is RCHICH₂CF₂I. Elsheimer, S.; Dolbier, W. R., Jr.; Murla, M.; Seppelt, K.; Paprott, G. *J. Org. Chem.* **1984**, *49*, 205.

¹⁹² With a generalized unsymmetrical alkene, RCH=CH₂, the product from this reagent is RCHBrCH₂CCl₃. Kharasch, M. S.; Reinmuth, O.; Urry, W. H. *J. Am. Chem. Soc.* **1947**, *69*, 1105.

¹⁹³ Feiring, A. E. *J. Org. Chem.* **1985**, *50*, 3269 and references therein.

¹⁹⁴ Oyama, K.; Tidwell, T. T. *J. Am. Chem. Soc.* **1976**, *98*, 947.

¹⁹⁵ Lucas, H. J.; Liu, Y.-P. *J. Am. Chem. Soc.* **1934**, *56*, 2138.

¹⁹⁶ Levy, J. B.; Taft, R. W., Jr.; Hammett, L. P. *J. Am. Chem. Soc.* **1953**, *75*, 1253. In the older literature, 2-methyl-1-butene was sometimes named *asym*-methylethylethylene, where the prefix *asym* means asymmetric.

¹⁹⁷ Lucas cited unpublished data of Welge indicating that the hydration is reversible but that the equilibrium lies heavily in favor of the alcohol in aqueous solution, $K = 7.5 \times 10^3$ at 25°C. The dehydration step has an activation energy of 34.8 kcal/mol. Eberz, W. F.; Lucas, H. J. *J. Am. Chem. Soc.* **1934**, *56*, 1230.

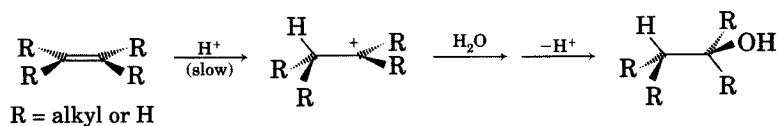


FIGURE 9.32

A_{SE2} mechanism for hydration of alkenes.

Early studies of acid-catalyzed hydration were interpreted in terms of a π complex as an intermediate,¹⁹⁸ and ab initio calculations do suggest that a hydrogen-bridged structure is more stable than an open cation structure for both the 2-butyl cation and the ethyl cation (Chapter 5).^{199,200} It is not necessarily the case that structures that are lowest in energy in the gas phase are also lowest in energy in solution, however, and there is no compelling evidence for bridged carbocations as significant intermediates in the hydration of alkenes.²⁰⁰ The available experimental data suggest that hydration and other electrophilic reactions involving proton attachment to alkenes proceed directly through formation of carbocations (by an A_{SE2} mechanism, Figure 9.32),²⁰¹ and that π complexes are not required intermediates.^{202,203} Currently, hydration of alkenes is taken as the model for electrophilic additions that do not involve cyclic bridged intermediates.²⁰⁴

General acid catalysis was observed in the hydration of both *trans*-cyclooctene and 2,3-dimethyl-2-butene, which helped to establish the A_{SE2} mechanism for hydration of alkenes.²⁰⁵ Furthermore, 1,1-dicyclopropylethene was found to react much faster than either *cis*- or *trans*-1,2-dicyclopropylethene, which indicates that substituent location (and not just the total electron-donating ability of the substituents) affects the rate constant for hydration reactions. It appears that the approaching proton is undergoing bond formation to one of the olefinic carbon atoms in the transition structure but not to the other, so the regiochemistry of the hydration reaction is determined by the approach that leads to the development of the more stable carbocation.²⁰⁶

Several lines of evidence led to the acceptance of the A_{SE2} mechanism for the acid-catalyzed hydration of styrenes also. In a study of the rate constants and equilibria, Schubert and Keeffe noted the following conclusions:²⁰⁷

¹⁹⁸ Purlee, E. L.; Taft, R. W., Jr. *J. Am. Chem. Soc.* **1956**, *78*, 5807.

¹⁹⁹ Carneiro, J. W. de M.; Schleyer, P. v. R.; Koch, W.; Raghavachari, K. *J. Am. Chem. Soc.* **1990**, *112*, 4064.

²⁰⁰ Kloppe, W.; Kutzelnigg, W. *J. Phys. Chem.* **1990**, *94*, 5625.

²⁰¹ The mechanism shown can also be described as an A_{DE2} reaction. A_{SE2} (or $A-S_{E2}$) has often been used in the literature to describe reactions, including the hydration of alkenes by the mechanism shown in Figure 9.32, in which a rate-limiting proton transfer from a general acid leads to product formation. Stewart, R. *The Proton: Applications to Organic Chemistry*; Academic Press: New York, 1985; pp. 259–261 indicated that the terminology is derived from the prototypical $A-S_{E2}$ reaction, the exchange of ring protons on aromatic compounds, with the S_E standing for electrophilic substitution.

²⁰² For a discussion and leading references, see Nowlan, V. J.; Tidwell, T. T. *Acc. Chem. Res.* **1977**, *10*, 252.

²⁰³ See also footnote 4 in reference 207.

²⁰⁴ Schmid, G. H.; Tidwell, T. T. *J. Org. Chem.* **1978**, *43*, 460.

²⁰⁵ Kresge, A. J.; Chiang, Y.; Fitzgerald, P. H.; McDonald, R. S.; Schmid, G. H. *J. Am. Chem. Soc.* **1971**, *93*, 4907.

²⁰⁶ Knittel, P.; Tidwell, T. T. *J. Am. Chem. Soc.* **1977**, *99*, 3408.

²⁰⁷ Schubert, W. M.; Keeffe, J. R. *J. Am. Chem. Soc.* **1972**, *94*, 559 and references therein.

1. Rate constants for hydration (k_{hyd}) correlate well with $-H_0'$ and $-H_R'$. The correlation of k_{hyd} with the acidity of the medium indicates that a proton is transferred in the rate-limiting step of the reaction.
2. Observation of general acid catalysis for the reaction suggests that a proton is transferred in the rate-limiting step.
3. Proton transfer apparently does not occur prior to the rate-limiting step. When β,β -dideuteriostyrene was subjected to hydration conditions, loss of deuterium label in the starting material was not observed in the initial stages of the reaction.²⁰⁸ If proton transfer occurred prior to the rate-limiting step, then the reverse of such a fast step should have led to deuterium loss.
4. Observation of a good Hammett correlation ($\rho^+ = -3.58$) for the hydration of *p*-substituted styrenes suggests that appreciable positive charge is developed on the incipient benzylic carbon atom in the transition structure. A ρ^+ value of -3.2 was found for acid-catalyzed hydration of 2-arylpropenes.²⁰⁹ Both values are somewhat smaller in magnitude than the value expected for a fully developed benzylic carbocation.²¹⁰
5. A primary solvent isotope effect suggests that a proton is undergoing bonding change in the transition structure. The value of $k_{\text{H}_3\text{O}^+}/k_{\text{D}_3\text{O}^+}$ was found to vary from 2 to 4, depending on reactant and conditions. A somewhat smaller solvent isotope effect of 1.45 was found for the hydration of isobutene in aqueous perchloric acid solutions,²¹¹ suggesting that the nature of substituents (alkyl or aryl) on the olefinic carbon atoms can affect the degree of proton transfer in the transition structure of hydration reactions. With other data, the results suggest that proton transfer is more nearly complete in the transition structure for hydration of alkyl-substituted alkenes than for hydration of aryl-substituted alkenes.^{207,211}

Before leaving this section, we should note that the simple carbocation structure in Figure 9.32 may camouflage a complex ion-solvent species with considerable variation possible from one alkene-solvent system to another.²¹² Chiang and Kresge determined that the 3° carbocation intermediate formed by protonation of 2,3-dimethyl-2-butene has a lifetime (τ) of about 10^{-10} s in aqueous solution and therefore is a conformationally equilibrated carbocation. The 2° cyclooctyl carbocation was found to have a lifetime that varied with the solvent; τ was found to be on the order of 10^{-8} s in highly acidic solutions (about 50% HClO₄) such as those used to study the reaction of *cis*-cyclooctene, but τ was around 5×10^{-12} s in dilute acid solutions used to study the reaction of *trans*-cyclooctene.⁷⁴ The investigators concluded that the hydration of *trans*-cyclooctene probably occurs through an early transition

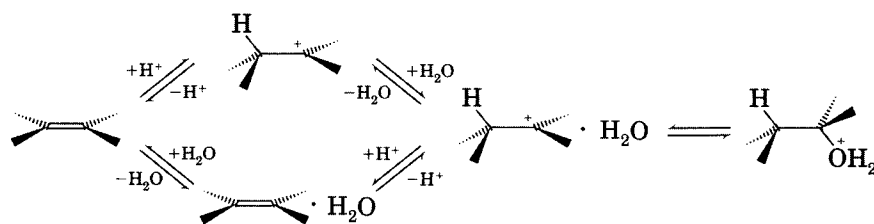
²⁰⁸ Because of the equilibrium between styrene and α -phenylethanol under the reaction conditions, some loss of deuterium label in the starting material can occur as the hydration reaction nears completion. When the concentration of alcohol is minimal in the early stages of the reaction, however, the return path is negligible, and loss of label is not detected.

²⁰⁹ Deno, N. C.; Kish, F. A.; Peterson, H. J. *J. Am. Chem. Soc.* **1965**, *87*, 2157.

²¹⁰ Brown, H. C.; Okamoto, Y. *J. Am. Chem. Soc.* **1957**, *79*, 1913.

²¹¹ Gold, V.; Kessick, M. A. *J. Chem. Soc.* **1965**, 6718.

²¹² Another complication not discussed here is that the cyclooctyl carbocation may have a bridged structure, not the simple 2° structure shown. See Chapter 5 and reference 74.

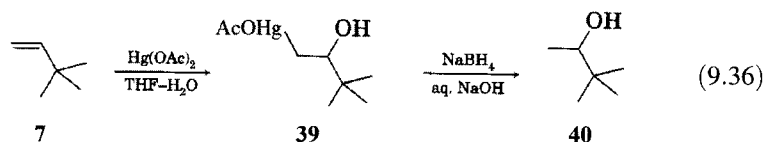
**FIGURE 9.33**

Hydration of an alkene through an equilibrated carbocation (upper pathway) or by a preassociation mechanism (lower pathway).

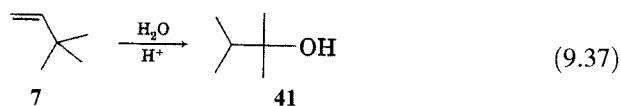
state in which there is still appreciable double bond character between the olefinic carbon atoms in the transition structure. For 2° carbocations formed from unstrained alkenes in dilute aqueous acid solutions, such a short lifetime would be less than the rotational correlation time of water. If the lifetime of the carbocation is shorter than the solvent reorientation time, then proton removal to reform the alkene will be faster than nucleophilic attack by water. In that situation the water reorientation becomes the rate-limiting step in the reaction. Reaction will only occur by the bottom pathway in Figure 9.33, in which a water molecule is already properly oriented for nucleophilic attack before protonation of the alkene. Therefore, the reaction of *trans*-cyclooctene may be said to occur by a **preassociation** mechanism.⁷⁴

Oxymercuration

Alkenes can also be converted to alcohols through a sequence of reactions known collectively as oxymercuration–demercuration.²¹³ In the oxymercuration reaction, an alkene combines with a salt of Hg^{2+} and a nucleophile (usually protic solvent) to give an organomercury compound. The demercuration reaction involves reduction of the organomercury compound with NaBH_4 or another reducing agent to produce the final product (equation 9.36). The synthetic utility of the oxymercuration–demercuration reaction lies primarily in the mild conditions that can hydrate an alkene with Markovnikov orientation (i.e., with attachment of the OH group to the alkene carbon atom bearing the greater number of alkyl groups). For example, treatment of 3,3-dimethyl-1-butene with a suspension of mercuric acetate in water–tetrahydrofuran for 10 minutes produced an organomercurial (**39**) that was reduced in situ by NaBH_4 in aqueous NaOH to produce 3,3-dimethyl-2-butanol (**40**) in 94% yield.²¹⁵



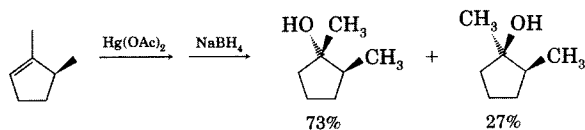
This reaction produced none of the rearrangement product (**41**) that would be expected from acid-catalyzed hydration of the reactant via an intermediate carbocation.



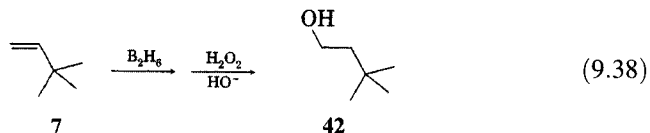
²¹³ Chatt, J. *Chem. Rev.* **1951**, *48*, 7.

FIGURE 9.34

Stereoselectivity in the oxymercuration–demercuration of 2,3-dimethylcyclopentene.



Furthermore, this method offers complementary regiochemistry to that observed (42) from carrying out the hydroboration–oxidation procedure (see page 600) on the same reactant.

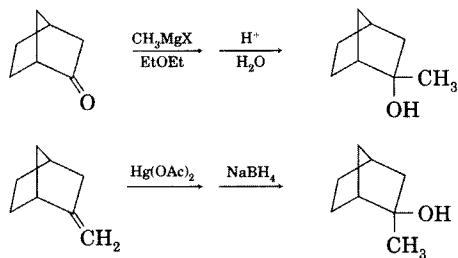


In addition to avoiding the carbocation rearrangements common with hydration reactions that involve carbocations, the oxymercuration–demercuration procedure offers another synthetic advantage. As shown in Figure 9.34, hydration of the alkene proceeds more easily from the less hindered side of the molecule, which is the same side from which attack of a Grignard reagent on the corresponding ketone would occur. Oxymercuration–demercuration therefore provides stereochemistry that is complementary to stereochemistry available through the synthesis of alcohols by reaction of carbonyls with Grignard reagents (Figure 9.35).²¹⁴

The oxymercuration reaction is thought to be a two-step process. In the first step, electrophilic attachment of the mercury ion to the alkene produces a positively charged intermediate (equation 9.39). In the second step of oxymercuration, a nucleophile (most likely a solvent molecule, SOH) reacts with the intermediate to produce the organomercury compound (equation 9.40). For reactions in water, both the organomercurial and the final product are alcohols.²¹⁵ The reaction produces an ether if the hydroxylic solvent is an alcohol, and the reaction is called solvomercuration or alkoxymercuration. Better yields are obtained if the anion of the mercuric salt is a weaker nucleophile than is the solvent. For this reason, mercuric

FIGURE 9.35

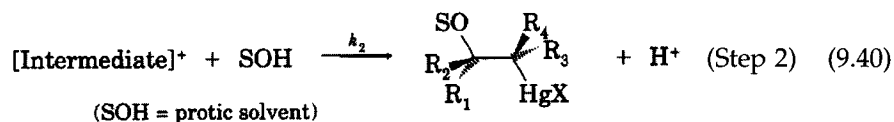
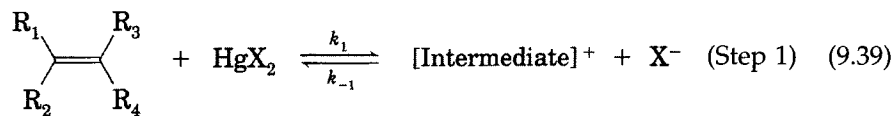
Different stereochemistry of Grignard and oxymercuration–demercuration alcohol syntheses.



²¹⁴ Brown, H. C.; Hammar, W. J. *J. Am. Chem. Soc.* **1967**, *89*, 1524.

²¹⁵ Brown, H. C.; Geoghegan, P., Jr. *J. Am. Chem. Soc.* **1967**, *89*, 1522.

trifluoroacetate is often used instead of mercuric acetate for reactions in tertiary alcohols.^{216,217}

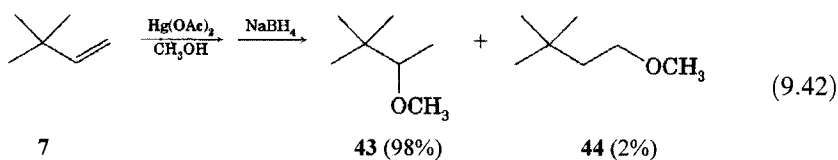


Typically, the oxymercuration reaction is second order overall, first order in alkene and first order in mercuric salt.²¹⁸ Vardhan and Bach concluded that the oxymercuration reaction involves fast equilibrium formation of an intermediate (with $K_1 = k_1/k_{-1}$), followed by rate-limiting attack of the nucleophile on this species (with rate constant k_2).²¹⁹ Thus, the rate law for the reaction would be

$$k_{\text{obs}} = \frac{k_1 k_2}{k_{-1}} [\text{alkene}][\text{Hg salt}] = K_1 k_2 [\text{alkene}][\text{Hg salt}] \quad (9.41)$$

Since *formation* of the intermediate is rate limiting in addition of bromine, but *reaction* of the intermediate is rate limiting in oxymercuration, there is a large difference in substituent effects between these two reactions.²¹⁹ Alkyl groups greatly enhance the rate constant for bromine addition,²⁴ but their effect on the rate constant for oxymercuration is more complex. For example, reactivity in oxymercuration increases from ethene to propene to isobutene, but the rate constant for reaction of either *cis*- or *trans*-2-butene is much less than that of isobutene, and alkenes with four alkyl substituents undergo oxymercuration quite slowly.²¹⁸ These relative reactivities were attributed to a much larger effect of the size of the alkyl substituents on reactivity in oxymercuration than is the case for bromine addition.²¹⁹

Steric effects may play a role in the regiochemistry of the reaction as well. While the oxymercuration–demercuration reaction is generally considered to give only Markovnikov hydration, as shown by predominant formation of **43**, this regioselectivity is not absolute. For example, methoxymercuration of 3,3-dimethyl-1-butene produced 2% of 3,3-dimethylbutyl methyl ether (**44**, equation 9.42).²¹⁶



We have not yet defined the structure of the intermediate in equations 9.39 and 9.40. By analogy with other electrophilic additions, it seems reasonable to

²¹⁶ Brown, H. C.; Rei, M.-H. *J. Am. Chem. Soc.* **1969**, *91*, 5646.

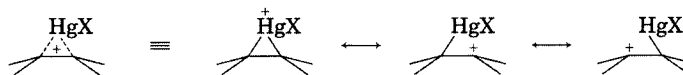
²¹⁷ Solvomercuration in acetonitrile can be used as a route to amines. Brown, H. C.; Kurek, J. T. *J. Am. Chem. Soc.* **1969**, *91*, 5647.

²¹⁸ Halpern, J.; Tinker, H. B. *J. Am. Chem. Soc.* **1967**, *89*, 6427.

²¹⁹ Vardhan, H. B.; Bach, R. D. *J. Org. Chem.* **1992**, *57*, 4948.

FIGURE 9.36

Resonance description of mercurinium ion. (Compare with Figure 9.13.)



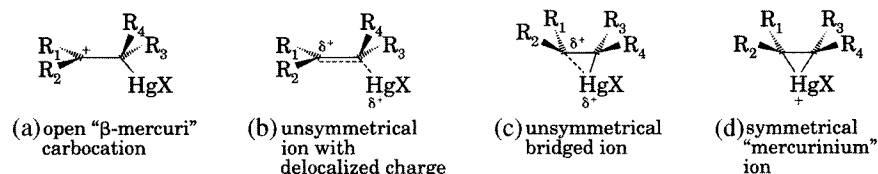
propose a cyclic ion analogous to the bromonium ion as an intermediate.²²⁰ Lucas, Hepner, and Winstein proposed a symmetrically bridged mercurinium ion, which might be described as a resonance hybrid of valence bond structures having positive charge on the mercury and on each of the olefinic carbon atoms (Figure 9.36).^{221,222} Experimental evidence for a symmetrical mercurinium ion formed from ethene was found by NMR and by ion cyclotron resonance (ICR) spectrometry.^{223–225} Semiempirical molecular orbital calculations also indicated an energy minimum for a symmetrically bridged ion composed of Hg^{2+} ion and ethene, but Bach and Henneike concluded that the bridged ion could be described as a π complex instead of a σ -bonded three-membered ring.²²⁶

In Figure 9.36 the mercurinium ion is depicted as a structure in which the mercury ion is symmetrically placed over the olefinic carbon atoms. Figure 9.37 shows four structures that span a spectrum of possible structures for the organomercury intermediate.²²⁷ Semiempirical calculations revealed only a shallow energy minimum on the potential energy surface associated with shifting the mercury along the C–C axis toward an unsymmetrical ion, so the unsymmetrical ion might be lower in energy for unsymmetrically substituted alkenes.²²⁶ As was the case with bromonium and chloronium ions, backside nucleophilic attack by solvent (leading to anti addition) is thus favored at the mercurinium carbon atom bearing the greater number of alkyl groups because that site bears the greater positive charge.

The theoretical results are consistent with experimental data. Oxymercuration of ethene appears to proceed through a symmetrical mercurinium ion with most of the positive charge on mercury, not on the olefinic carbon atoms.²²⁷ If one of the olefinic carbon atoms has an aryl substituent

FIGURE 9.37

Possible geometries for the intermediate in the oxymercuration reaction.



²²⁰ The positively charged intermediate in the oxymercuration reaction has also been called a *mercuronium* ion (e.g., see reference 219). Because the term mercurinium has been used so extensively in the literature of organic chemistry, that is the term that will be used in the present discussion.

²²¹ Lucas, H. J.; Hepner, F. R.; Winstein, S. *J. Am. Chem. Soc.* **1939**, *61*, 3102.

²²² Evidence for such an intermediate was deduced from steric effects by Pasto, D. J.; Gontarz, J. A. *J. Am. Chem. Soc.* **1970**, *92*, 7480.

²²³ Olah, G. A.; Clifford, P. R. *J. Am. Chem. Soc.* **1971**, *93*, 1261, 2320.

²²⁴ Bach, R. D.; Gauglhofer, J.; Kevan, L. *J. Am. Chem. Soc.* **1972**, *94*, 6860.

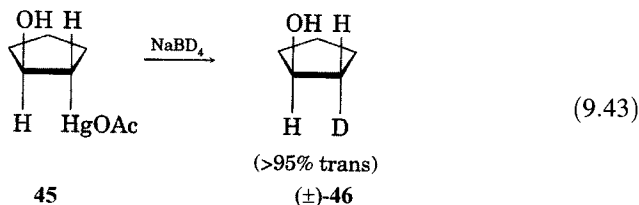
²²⁵ Bach, R. D.; Richter, R. F. *J. Org. Chem.* **1973**, *38*, 3442.

²²⁶ Bach, R. D.; Henneike, H. F. *J. Am. Chem. Soc.* **1970**, *92*, 5589.

²²⁷ Ambidge, I. C.; Dwight, S. K.; Rynard, C. M.; Tidwell, T. T. *Can. J. Chem.* **1977**, *55*, 3086.

(particularly a benzene ring substituted with an electron-donating substituent), then an unsymmetrical mercurinium ion or partially bridged mercury-substituted carbocation is proposed as the intermediate.²²⁸ With substituents such as cyclopropyl groups that are very effective at stabilizing carbocations, the intermediate appears to be an open carbocation.²²⁷

Although the oxymercuration reaction is stereospecific, the demercuration reaction often is not. Reduction of the *trans*-2-hydroxycyclopentylmercuric acetate (45) from oxymercuration of cyclopentene with NaBD₄ led to 2-deuteriocyclopentanol, which was determined to be at least 95% pure *trans* isomer (46).



In contrast, oxymercuration of either *cis*-2-butene or *trans*-2-butene, followed by reduction with NaBD₄, led to a 50 : 50 mixture of *erythro*- and *threo*-3-deuterio-2-butanols (Figure 9.38).²²⁹

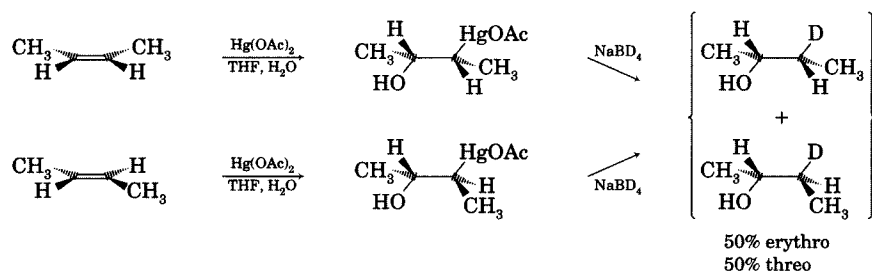


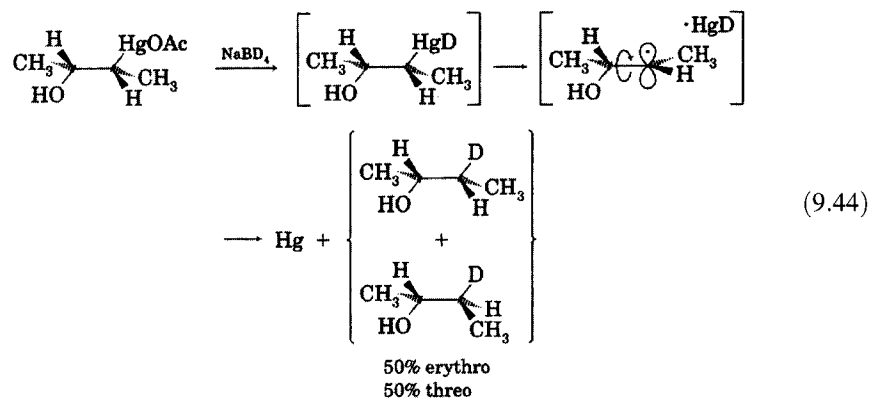
FIGURE 9.38

Loss of stereochemistry in the demercuration. All products are racemic. (Adapted from reference 229.)

These results can be rationalized with a radical mechanism in which an organomercury hydride, produced by borohydride reduction of R–Hg–X, dissociates to alkyl and •Hg–H radicals within a solvent cage. Abstraction of the hydrogen atom from •Hg–H by the alkyl radical would produce the carbon–hydrogen bond and elemental mercury.²²⁹ With a substrate derived from an acyclic alkene, rotation about the central carbon–carbon single bond can occur faster than hydrogen abstraction, leading to loss of stereochemistry of the reactant (equation 9.44). With a reactant derived from a cyclic alkene, it is more likely that the alkyl radical can abstract a hydrogen atom from •Hg–H before reorientation can occur within the solvent cage. As a result, the carbon–hydrogen bond is more likely to have the same stereochemistry as the carbon–mercury bond it replaces (equation 9.43). The stereochemistry of the demercuration reaction therefore depends strongly on the structure of the organomercury compound.²²⁹

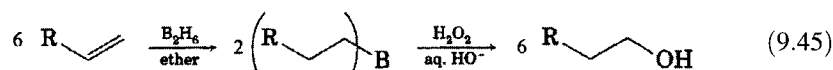
²²⁸ Lewis, A.; Azoro, J. J. *J. Org. Chem.* **1981**, *46*, 1764 and references therein. See also Lewis, A. J. *J. Org. Chem.* **1984**, *49*, 4682.

²²⁹ Pasto, D. J.; Gontarz, J. A. *J. Am. Chem. Soc.* **1969**, *91*, 719.



Hydroboration

The hydroboration–oxidation procedure is a valuable method to hydrate an alkene with anti-Markovnikov orientation and with syn addition of the H and OH groups.^{230,231} Addition of BH_3 (which may be added to the reaction mixture as diborane, B_2H_6) to an alkene occurs readily in diethyl ether, THF, or similar solvent. The hydroboration is strongly exothermic, with a ΔH of -33 kcal/mol per B–H bond that reacts.²³² If stoichiometry and the steric requirements of the alkyl substituents on the boron atom permit, the reaction proceeds until three alkyl groups are attached to each boron atom. The trialkylborane can then be oxidized with hydrogen peroxide in aqueous base to produce the alcohol.



The hydroboration reaction is generally highly, but not completely, regioselective. For example, reaction of 1-hexene with diborane, followed by oxidation, produces 1-hexanol (**48**) in high yield, with only a small amount of 2-hexanol (**49**, equation 9.46).^{233,234} Brown determined that the preference for the boron atom to add to the less-substituted carbon atom is about 94% for monosubstituted alkenes such as 1-pentene, 99% for *gem*-disubstituted alkenes such as 2-methyl-1-butene, and 98% for trisubstituted alkenes such as 2-methyl-2-butene.²³³

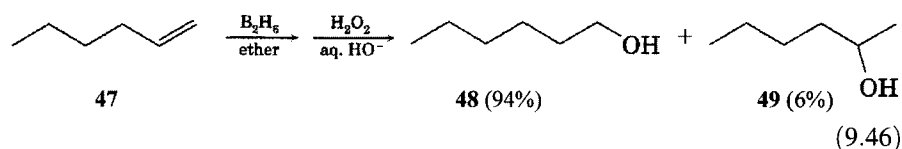
²³⁰ (a) Brown, H. C.; Subba Rao, B. C. *J. Am. Chem. Soc.* **1956**, *78*, 5694; **1959**, *81*, 6423; (b) Brown, H. C. *Hydroboration*; W. A. Benjamin: New York, 1962; (c) Brown, H. C. *Boranes in Organic Chemistry*; Cornell University Press: Ithaca, NY, 1972.

²³¹ Numerous other reactions include the synthesis of trialkylcarbinols from trialkylboranes (Brown, H. C. *Acc. Chem. Res.* **1969**, *2*, 65) and hydroboration–protonolysis leading to alkanes (Brown, H. C.; Murray, K. *J. Am. Chem. Soc.* **1959**, *81*, 4108). Isomerization and disproportionation of the alkylboranes was also seen (reference 230b).

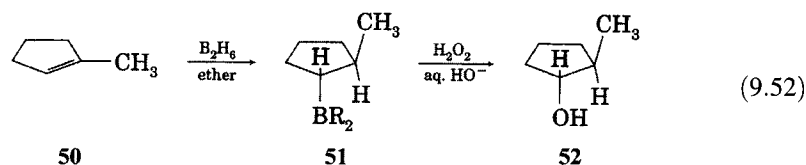
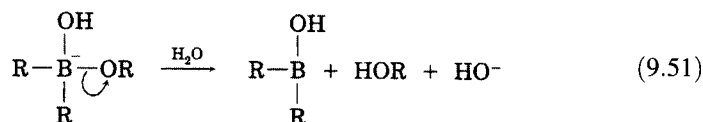
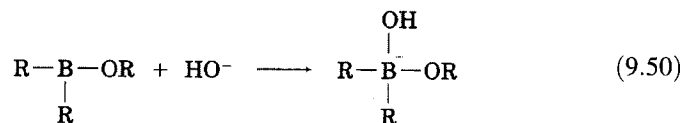
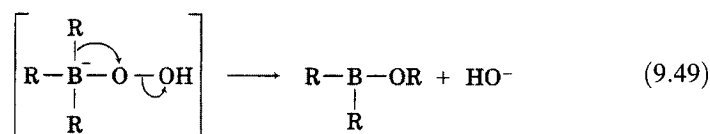
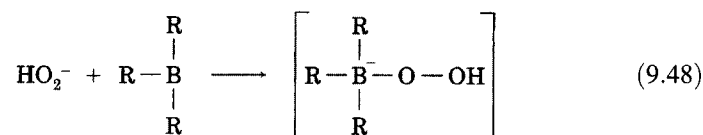
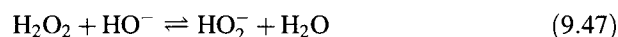
²³² Pasto, D. J.; Lepeska, B.; Cheng, T.-C. *J. Am. Chem. Soc.* **1972**, *94*, 6083.

²³³ Brown, H. C.; Zweifel, G. *J. Am. Chem. Soc.* **1960**, *82*, 4708.

²³⁴ Synthetic applications have been discussed: Zweifel, G.; Brown, H. C. *Org. React.* **1963**, *13*, 1.



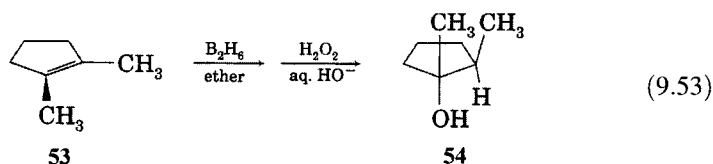
The addition of boron and hydrogen across the carbon-carbon double bond appears to occur by stereospecific syn addition. The replacement of the C-B bond by a C-OH bond in the oxidation step is also stereospecific. The mechanism proposed for the oxidation of one of the carbon-boron bonds is shown in equations 9.47 through 9.51, so the configuration of the carbon-boron bond is retained in the product.^{234,235} As an example, hydroboration-oxidation of 1-methylcyclopentene (**50**, equation 9.52) followed by oxidation of the organoborane (**51**) gave only the *trans*-2-methylcyclohexanol (**52**).



The reaction in equation 9.52 does not provide a convincing demonstration of the stereochemistry of hydroboration-oxidation, since **52** is thermodynamically more stable than the corresponding *cis* isomer. Therefore, Brown and Zweifel also carried out the procedure on 1,2-dimethylcyclopentene (**53**, equation 9.53). The product of that reaction was the less stable stereoisomer

²³⁵ House, H. O. *Modern Synthetic Reactions*, 2nd ed.; W. A. Benjamin: Menlo Park, CA, 1972; pp. 106-144.

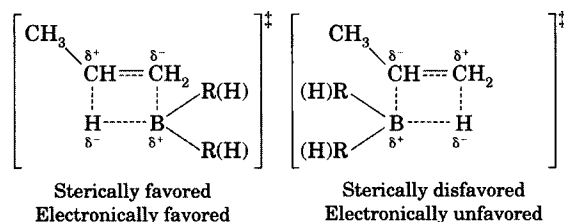
with the two methyl groups cis to each other (54), confirming the syn pathway for the addition.^{236,237}



The observation of consistent syn addition in the hydroboration step suggests that the mechanism for addition of BH_3 is different from all of the addition mechanisms discussed so far except one. As discussed on page 580, a one-step, four-center mechanism was considered in the syn addition of F_2 to an alkene, and a similar mechanism can explain the stereochemistry of BH_3 addition. Moreover, the regiochemistry of addition to unsymmetrical alkenes can be rationalized in terms of the steric and electronic effects present in such a transition structure.

FIGURE 9.39

Transition structure models for hydroboration of an alkene with one alkyl substituent.



The transition structures in Figure 9.39 show two possible orientations for concerted addition of borane to an unsymmetrical alkene. The B–H bond is presumed to be polarized so that the hydrogen atom has a slight negative charge and the boron atom has a slight positive charge. Association of boron with the alkene would be expected to drain electron density from the double bond, and partial charge development should be more pronounced on the carbon atom that will become bonded to hydrogen. As suggested in Figure 9.39, this interaction could result in a slight electronic effect favoring the attachment of boron to the carbon atom having fewer alkyl substituents because this approach places a partial positive charge on the more highly substituted carbon atom. This explanation merits closer examination, however. The partial charge development is likely to be small in the case of an early transition state.²³⁸ Moreover, there is also the possibility of steric hindrance between the other substituents on boron with the substituents on the alkene. Such a steric effect also correctly predicts the attachment of the boron atom to the less-substituted carbon atom of the alkene.

Analogous transition structures for addition of BH_3 to styrene and its derivatives are shown in Figure 9.40. Again, the steric factor should favor

²³⁶ The production of *exo*-norborneol from hydroboration–oxidation of norbornene further supported the syn pathway. Brown, H. C.; Zweifel, G. *J. Am. Chem. Soc.* **1959**, *81*, 247.

²³⁷ Syn addition of molecular hydrogen to alkenes can be accomplished by protonolysis of organoboranes with carboxylic acids. For a discussion of the mechanism of the reaction and examples of its use in synthesis, see reference 235.

²³⁸ Some investigators do not draw the partial charges in the transition state. For example, see reference 251.

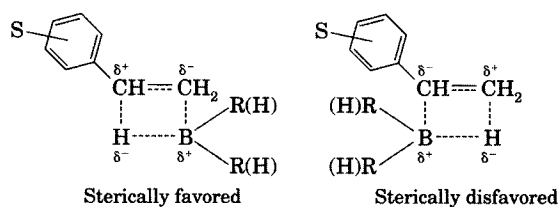
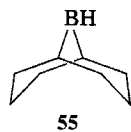


FIGURE 9.40

Transition structure models for hydroboration of an alkene with one aryl substituent.

attachment of boron to the carbon atom with fewer alkyl substituents. Now, however, the ability of the phenyl group to provide some delocalization of a partial negative charge on the α carbon atom means that there can be some electronic stabilization for the addition pathway leading to attachment of boron to the carbon atom bearing the phenyl group. This effect would be more important for compounds such as *p*-nitrostyrene than for styrene, and less important for styrenes with electron-donating groups.

To investigate the roles of charge and steric effects on the regiochemistry of hydroboration, Vishwakarma and Fry studied the relative rates of reaction of *p*-substituted styrenes with 9-borabicyclo[3.3.1]nonane (9-BBN, **55**) in THF at 25°C.²³⁹ In all cases the hydroboration–oxidation was highly regioselective, with the β -phenylethanol comprising more than 97% of the product. (The remaining product was the α -phenylethanol.) Apparently the steric requirements of the 9-BBN were able to overcome any electronic stabilization of the alternative addition pathway. The rate constants for the addition reactions gave a Hammett correlation with σ^+ ($r = 0.94$), with a ρ value of -0.49 . The results suggest that there is only a small amount of charge developed on the α carbon atom in the transition structure for the reaction.²⁴⁰ The investigators concluded that substituents on the styrene moiety exert electronic influences that change the *rate constant* for hydroboration, but that steric factors are the primary determinant of *regioselectivity*.



While the four-center transition structure for BH_3 addition is a widely used model, other reaction pathways have also been considered. In a synthesis of optically active (–)-1-butanol-1-*d*, Streitwieser and co-workers used the optically active borane formed from diborane and (+)- α -pinene (R_2BH) to carry out the hydroboration–oxidation of (*Z*)-1-butene-1-*d*.²⁴¹ To explain the observed stereochemistry of the reduction, they proposed that hydroboration involves a π complex between R_2BH and the alkene (Figure 9.41). Note the close resemblance of such a complex to the cyclic structures

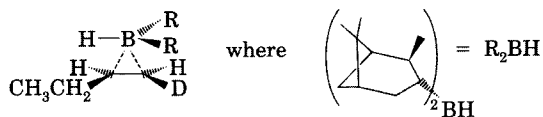
²³⁹ Vishwakarma, L. C.; Fry, A. J. *Org. Chem.* **1980**, *45*, 5306.

²⁴⁰ These results differed somewhat from the results of hydroboration of substituted styrenes reported by Brown, H. C.; Sharp, R. L. *J. Am. Chem. Soc.* **1966**, *88*, 5851, who found that the Markovnikov hydration product was formed in nearly 20% yield. With electron-donating substituents, the yield of anti-Markovnikov product was increased, while for electron-withdrawing substituents the yield of Markovnikov products was increased. See also the discussion in reference 233.

²⁴¹ Streitwieser, A., Jr.; Verbit, L.; Bittman, R. *J. Org. Chem.* **1967**, *32*, 1530.

FIGURE 9.41

Proposed π complex in the hydroboration of an alkene.



proposed for halogen addition or oxymercuration.²⁴² The structure shown in Figure 9.41 is proposed as an energy minimum and therefore might be an intermediate in the reaction, but the four-center structure shown on the left in Figure 9.39 is proposed as a transition structure. It is also conceivable that the π complex might be an intermediate on the path to the four-center transition structure.^{243,244}

The nature of the transition structure in hydroboration has been the subject of extensive theoretical investigation. Nelson found that the rate constants for hydroboration of alkenes by 9-BBN correlate with the HOMO energy of the alkenes (from an MNDO calculation) and that the regiochemical preference for C–B bond formation is predicted by the larger olefinic carbon atomic orbital in the alkene HOMO.²⁴⁵ Dewar and McKee used the MNDO method to study the hydroboration of alkenes and alkynes.²⁴⁶ In the cases of ethene, propene, and isobutene, there was a transition state leading to a loose π -type adduct along the reaction coordinate and another transition state leading away from the complex. In each case, however, the complex was marginally stable and required little or no activation to proceed to product. Lipscomb and co-workers also studied hydroboration with semiempirical MO theory and concluded that the mechanism involves a loosely bound complex that is formed prior to a transition state for the reaction.²⁴⁷

The results of ab initio calculations for the addition of borane to ethene depend on the level of the calculation.^{248,249} For the reaction of borane with propene in the gas phase, Houk and co-workers identified a π complex and two transition states, one for attachment of the boron atom to the carbon bearing two hydrogen atoms and one for attachment of the boron atom to the methyl-substituted carbon atom. As in the case of ethene, the π complex formed from propene was found to be lower in energy than the reactants. The transition state for attachment of the boron atom to the CH_2 position was found to be 3.7 kcal/mol lower in energy than the alternative transition state, and the difference in energy was attributed to a combination of electronic and steric factors.²⁴⁸

²⁴² For further discussion, see Pasto, D. J.; Klein, F. M. *J. Org. Chem.* **1968**, *33*, 1468; Jones, P. R. *J. Org. Chem.* **1972**, *37*, 1886.

²⁴³ Klein, J.; Dunkelblum, E.; Wolff, M. A. *J. Organometal. Chem.* **1967**, *7*, 377.

²⁴⁴ Sundberg, K. R.; Graham, G. D.; Lipscomb, W. N. *J. Am. Chem. Soc.* **1979**, *101*, 2863.

²⁴⁵ Nelson, D. J.; Cooper, P. J. *Tetrahedron Lett.* **1986**, *27*, 4693.

²⁴⁶ Dewar, M. J. S.; McKee, M. L. *Inorg. Chem.* **1978**, *17*, 1075.

²⁴⁷ See reference 244. The overall reaction was described as a two-step, donation–backdonation mechanism, with the boron having considerable negative charge in the transition structure but releasing this charge as the reaction proceeds. The calculation also indicated significant charge separation involving the two olefinic carbon atoms, with the carbon atom nearest boron acquiring considerable negative charge, while the other olefin carbon atom becomes more positive.

²⁴⁸ Wang, X.; Li, Y.; Wu, Y.-D.; Paddon-Row, M. N.; Rondan, N. G.; Houk, K. N. *J. Org. Chem.* **1990**, *55*, 2601.

²⁴⁹ Hommes, N. J. R. v. E.; Schleyer, P. v. R. *J. Org. Chem.* **1991**, *56*, 4074.

The calculations discussed so far are for reaction of monomeric BH_3 with alkenes in the gas phase. In solution the borane is most likely to be a dimer or, in ether solvents such as THF, a borane–solvent complex. It is difficult to study the kinetics of borane addition in solution because the reaction is complicated by three addition steps (one for each B–H bond), three redistribution equilibria (in which borane and the alkyl boranes exchange substituents), and five different monomer–dimer equilibria involving all the species with at least one B–H bond.²⁵² In the hydroboration of 2,3-dimethyl-2-butene with diborane in THF, the reacting species is most likely a borane–THF complex. The reaction was found to be second order overall, first order in alkene and first order in BH_3 –THF. The E_a was found to be 9.2 kcal/mol, while the activation entropy was -27 eu. These results stand in contrast to the value of 2 kcal/mol determined for ΔH^\ddagger for the reaction of BH_3 with ethene in the gas phase.²⁵⁰

Pasto and Kang studied the addition of monochloroborane (BClH_2) to olefins in THF solution.²⁵¹ The advantages of this reagent are (i) it is monomeric (as the THF complex); (ii) it reacts only to the monoalkylmonochloroborane stage; and (iii) the addition product is monomeric in THF and does not disproportionate. Therefore, the kinetics are somewhat easier to study than is the case for BH_3 –THF. The rate constants for addition to *p*-nitrostyrene, styrene, and *p*-methoxystyrene were found to be $3.24 \times 10^{-3} \text{ M}^{-1} \text{ min}^{-1}$, $7.31 \times 10^{-3} \text{ M}^{-1} \text{ min}^{-1}$, and $27.8 \times 10^{-3} \text{ M}^{-1} \text{ min}^{-1}$, respectively. The regioselectivity of product formation varied among these compounds, with 67%, 90%, and 93.3%, respectively, of the product formed through attachment of the boron atom to the β (CH_2) carbon atom. Separation of the overall rate constant data into rates for attachment to α and β carbon atoms gave a Hammett correlation for each, with ρ values of -0.65 and -1.43 , respectively. Reaction with BClD_2 gave isotope effects of 1.78 and 1.87, respectively, for the α and β reactions. Pasto concluded from these data that the addition is electrophilic in nature, but with a very early transition state such that there is little charge development on either carbon atom of the double bond in the transition structure. The results support the four-center model for the transition structure advanced by Brown.

Epoxidation

Epoxidation of an alkene produces a three-membered ring containing one oxygen atom. Reagents often used for this reaction are peroxides, either H_2O_2 or a peroxy acid (peracid) having the general formula RCO_3H , such as peroxyacetic acid (equation 9.54).^{252–254}

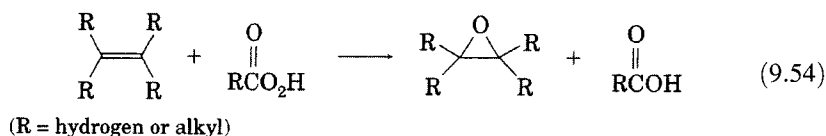
²⁵⁰ Fehlner, T. P. *J. Am. Chem. Soc.* **1971**, *93*, 6366.

²⁵¹ Pasto, D. J.; Kang, S.-Z. *J. Am. Chem. Soc.* **1968**, *90*, 3797.

²⁵² Epoxides may also be formed by oxidation of alkenes with other reagents. For a summary, see Hudlický, M. *Oxidations in Organic Chemistry*, ACS Monograph No. 186; American Chemical Society: Washington, DC, 1990. Dehydrohalogenation of halohydrins is another path to epoxides.

²⁵³ Swern, D. *Org. React.* **1953**, *7*, 378. Credit for the discovery of the peracid reaction is given to N. Prileschajew in 1908.

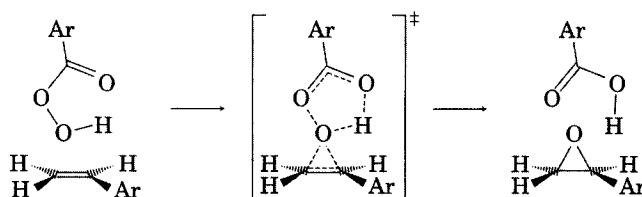
²⁵⁴ *m*-Chloroperbenzoic acid (*m*CPBA) is often the reagent of choice for epoxidation of alkenes because it is soluble in CH_2Cl_2 , but the *m*-chlorobenzoic acid by-product is not. Precipitation of the acid from solution reduces the possibility that the epoxide will undergo subsequent acid-catalyzed ring-opening reaction.



Epoxidation appears to involve electrophilic addition to the alkene, since the reaction is favored by electron-withdrawing groups on the peracid and electron-donating groups on the alkene.²⁵⁵ The epoxidation reaction is highly exothermic, with an experimental heat of reaction of -38 kcal/mol.²⁵⁶ The kinetic expression is overall second order, first order in the alkene and first order in the peracid.²⁵⁷ Steric effects do not appear to be important. The rate constant for the reaction increases with the number of alkyl substituents on the double bond, but the location of the alkyl groups is not important. For example, *cis*-2-butene, *trans*-2-butene, and isobutene have nearly the same reactivity.²⁵³ The rate constant for the reaction is sensitive to strain, with faster rates observed for alkenes that produce greater relief of strain upon epoxidation. For example, *trans*-cyclooctene is epoxidized about 100 times faster than *cis*-cyclooctene.²⁵⁸

An early suggestion for the mechanism of peracid epoxidation of alkenes was the "butterfly" mechanism proposed by Bartlett (Figure 9.42).^{259,260} The transition structure shown in that figure is symmetric, but there are variations of the Bartlett mechanism in which the three-membered ring of the developing epoxide is asymmetric, with the incoming oxygen atom over one of the carbon atoms.²⁶¹ Plesničar and co-workers studied the reaction with ab initio calculations and identified several possible transition structures, including the butterfly structure (Figure 9.42), a spiro structure with the oxygen centered over the middle of the two alkene carbon atoms, Figure 9.43(a), a spiro structure with the oxygen centered over one of the carbon atoms,

FIGURE 9.42
Bartlett mechanism for epoxidation.



²⁵⁵ Lynch, B. M; Pausacker, K. H. *J. Chem. Soc.* **1955**, 1525.

²⁵⁶ Plesničar, B.; Tasevski, M.; Ažman, A. *J. Am. Chem. Soc.* **1978**, *100*, 743.

²⁵⁷ In most cases peroxidation is found not to be acid catalyzed, although catalysis by trichloroacetic acid was reported by Berti, G.; Bottari, F. *J. Org. Chem.* **1960**, *25*, 1286.

²⁵⁸ Shea, K. J.; Kim, J.-S. *J. Am. Chem. Soc.* **1992**, *114*, 3044.

²⁵⁹ Bartlett, P. D. *Rec. Chem. Prog.* **1950**, *11*, 47. See also Mimoun, H. *Angew. Chem. Int. Ed. Engl.* **1982**, *21*, 734.

²⁶⁰ See the discussion in Rebek, J., Jr.; Marshall, L.; McManis, J.; Wolak, R. *J. Org. Chem.* **1986**, *51*, 1649.

²⁶¹ Ogata, Y.; Tabushi, I. *J. Am. Chem. Soc.* **1961**, *83*, 3440.

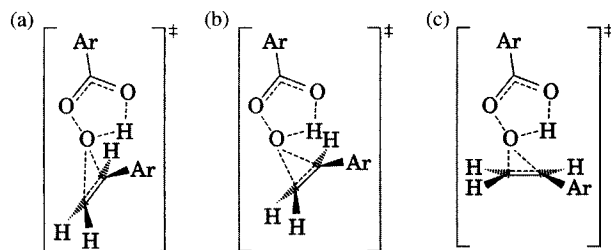


FIGURE 9.43

Alternative transition structures considered for peracid epoxidation of alkenes.

Figure 9.43(b), and a planar structure with the oxygen centered over one of the alkene carbon atoms, Figure 9.43(c).^{256,262}

Woods and Beak used the endocyclic restriction test to study the epoxidation of alkenes. In this test, two functional groups that normally react in an intermolecular process are tethered together on a series of molecular skeletons, each of which restricts the possible orientations of the two functional groups in a different way. By determining which skeletons allow the same reaction seen in the intermolecular reaction to occur and which do not, it is possible to estimate the orientation of the two reacting groups in the intermolecular reaction. Woods and Beak concluded that this mechanistic test strongly supported the Bartlett mechanism for the intermolecular epoxidation of alkenes. The endocyclic restriction test cannot distinguish between the several butterfly and spiro variants of the Bartlett mechanism that differ in the orientation of the alkenyl and peracid moieties, however.²⁶³

Hanzlik and Shearer found a ρ of -1.1 for epoxidation of substituted *trans*-stilbenes with perbenzoic acid, but a ρ of $+1.4$ for epoxidation of *trans*-stilbene with substituted peroxybenzoic acids. A $k_{\text{H}}/k_{\text{D}}$ value of 1.17 was observed for reaction with $\text{C}_6\text{H}_5\text{CO}_3\text{D}$, suggesting that the proton on the peracid was either only slightly (or, alternatively, nearly fully) transferred in the transition structure. A secondary deuterium kinetic isotope effect was observed for the alkenyl hydrogen atoms on the β carbon atom of styrene ($k_{\text{H}}/k_{\text{D}} = 0.82$) as well as on the α carbon atom ($k_{\text{H}}/k_{\text{D}} = 0.99$), indicating that rehybridization from sp^2 to sp^3 is further advanced for the β carbon atom than for the α carbon atom in the transition structure. These observations led to the proposal of the asymmetric transition structure shown in Figure 9.44.²⁶⁴ Substituent effects on the epoxidation of ring-substituted α -methylstilbenes with peroxybenzoic acid suggested that the nature of the transition structure varies according to the electron-donating ability of the alkene substituents

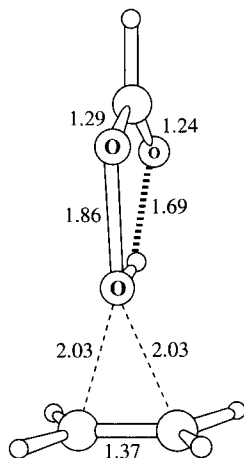
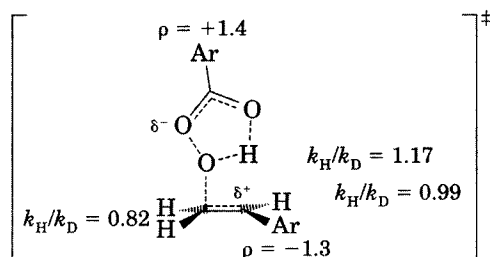
²⁶² An alternative mechanism involving a rather different geometry for the transition structure was proposed by Kwart, H.; Hoffman, D. M. *J. Org. Chem.* **1966**, *31*, 419; Kwart, H.; Starcher, P. S.; Tinsley, S. W. *Chem. Commun.* **1967**, 335.

²⁶³ Woods, K. W.; Beak, P. J. *Am. Chem. Soc.* **1991**, *113*, 6281. For leading references to the development and use of the endocyclic restriction test, see Tenud, L.; Farooq, S.; Seibl, J.; Eschenmoser, A. *Helv. Chim. Acta* **1970**, *53*, 2059; Hogg, D. R.; Vipond, P. W. *J. Chem. Soc. C* **1970**, 2142; Beak, P.; Basha, A.; Kokko, B.; Loo, D. *J. Am. Chem. Soc.* **1986**, *108*, 6016.

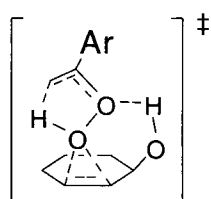
²⁶⁴ Hanzlik, R. P.; Shearer, G. O. *J. Am. Chem. Soc.* **1975**, *97*, 5231.

FIGURE 9.44

Kinetic isotope data and model for the transition structure in the epoxidation of styrene.²⁶⁴

**FIGURE 9.45**

Calculated transition structure for the epoxidation of ethene with peroxyformic acid. The numbers indicate distances in Å. (Adapted from reference 269.)

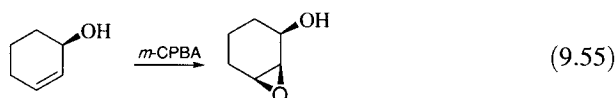
**FIGURE 9.46**

Proposed transition structure for epoxidation of allylic alcohols.

and the electron-withdrawing ability of substituents on the peroxybenzoic acid ring.²⁶¹ Thus, the transition structure may be symmetric for epoxidation of ethene or symmetrically substituted alkenes, but it may be highly asymmetric when one carbon atom is substituted with a group that can stabilize a carbocation (such as in Figure 9.44).²⁶⁵

Both experimental and theoretical studies of the peracid epoxidation of ethene and alkyl-substituted olefins have suggested that a spiro transition structure is favored over a planar one.^{266–268} For example, DFT calculations indicated that the transition structure for the reaction of peroxyformic acid and ethene has the geometry shown in Figure 9.45.²⁶⁹ In this case the two C–O distances are identical, indicating synchronous formation of the two C–O bonds. If the olefin is substituted with a methyl, methoxy, vinyl, or cyano group, however, the transition structure can become asynchronous, meaning that one C–O bond has been formed to a greater extent than the other in the transition structure.²⁶⁹

If an alkene has a hydroxyl (or other functional group capable of donating a proton in a hydrogen bonding interaction) in the allylic position, that group can affect the stereochemistry of the epoxide product. For example, reaction of cyclic allylic alcohols produces a 10 : 1 ratio of product with the epoxide cis to the alcohol function (equation 9.55) relative to the trans product. This diastereoselectivity has been attributed to hydrogen bonding in the transition structure for the epoxidation (Figure 9.46).^{270,271}



²⁶⁵ For arguments against this point of view, see the discussion in reference 264.

²⁶⁶ Singleton, D. A.; Merrigan, S. R.; Liu, J.; Houk, K. N. *J. Am. Chem. Soc.* **1997**, *119*, 3385.

²⁶⁷ Bach, R. D.; Glukhovtsev, M. N.; Gonzalez, C. *J. Am. Chem. Soc.* **1998**, *120*, 9902.

²⁶⁸ Koerner, T.; Slebocka-Tilk, H.; Brown, R. S. *J. Org. Chem.* **1999**, *64*, 196.

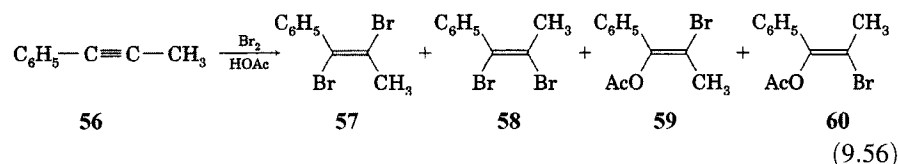
²⁶⁹ Houk, K. N.; Liu, J.; DeMello, N. C.; Condroski, K. R. *J. Am. Chem. Soc.* **1997**, *119*, 10147.

²⁷⁰ For a review, see Hoveyda, A. H.; Evans, D. A.; Fu, G. C. *Chem. Rev.* **1993**, *93*, 1307.

²⁷¹ Freccero, M.; Gandolfi, R.; Sarzi-Amadè, M.; Rastelli, A. *J. Org. Chem.* **2004**, *69*, 7479.

Electrophilic Addition to Alkynes and Cumulenes

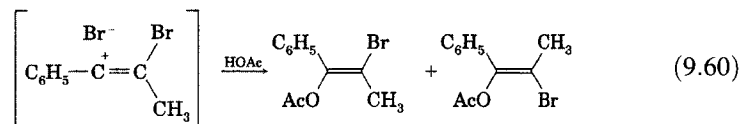
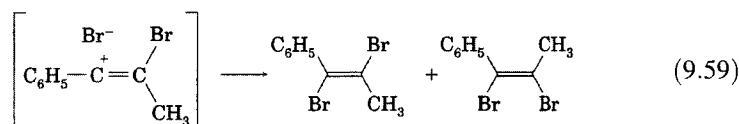
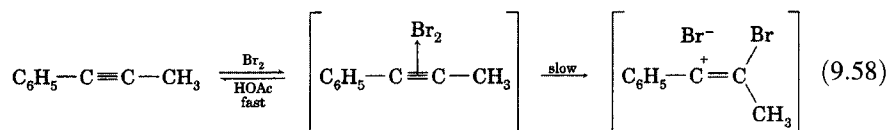
The electrophilic additions discussed above also occur with alkynes and cumulenes, but there can be significant differences in reactivity between alkenes and these other compounds.²⁷² The reaction of bromine and 1-phenylpropyne (56) in acetic acid led to the formation of four primary products, 57, 58, 59, and 60 (equation 9.56).^{273,274}



The rate expression for this reaction was found to be

$$\text{Rate} = (k_2[\text{Br}_2] + k_3[\text{Br}_2]^2 + k_{\text{Br}^-}[\text{Br}_2][\text{Br}^-])[\text{alkyne}] \quad (9.57)$$

In the absence of Br^- and at low concentrations of Br_2 , the kinetic expression is first order in alkyne and first order in bromine. A ρ value of -5.17 for bromine addition to substituted derivatives of 56 is consistent with the intermediacy of a vinyl cation–bromide ion pair that can combine to form both *cis* and *trans* dibromide adducts or can react with solvent to form *cis*- and *trans*-1-acetoxy-2-bromo-1-phenylpropene, as shown in equations 9.58 through 9.60.^{275,276}



²⁷² Schmid, G. H. in Patai, S., Ed. *The Chemistry of the Carbon–Carbon Triple Bond*; Wiley-Interscience: Chichester, England, 1978; pp. 275–341.

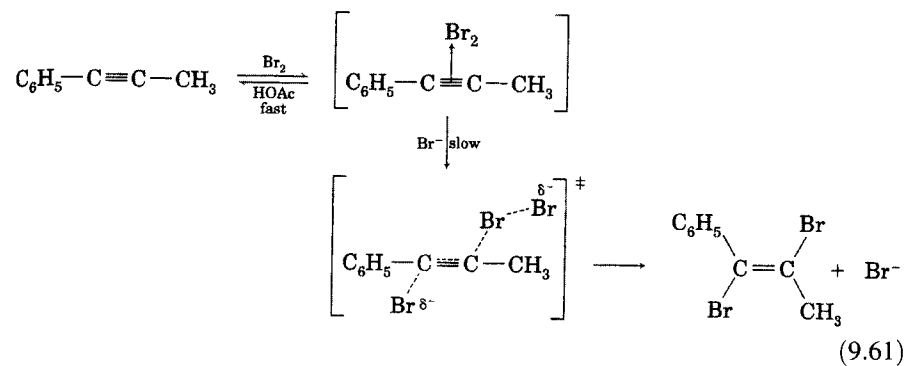
²⁷³ Pincock, J. A.; Yates, K. *J. Am. Chem. Soc.* **1968**, *90*, 5643. In addition to the products shown, 1,1-dibromoethyl phenyl ketone was formed as a result of subsequent reaction of products 59 and 60.

²⁷⁴ Pincock, J. A.; Yates, K. *Can. J. Chem.* **1970**, *48*, 3332.

²⁷⁵ For a discussion of vinyl cations and electrophilic additions to alkynes, see Stang, P. J.; Rappoport, Z.; Hanack, M.; Subramanian, L. R. *Vinyl Cations*; Academic Press: New York, 1979.

²⁷⁶ Apparently the 1-phenylpropene is the intermediate in the nonstereospecific addition of trifluoroacetic acid to 1-phenylpropene, which produces approximately equal yields of the *cis* and *trans* adducts. Peterson, P. E.; Dudley, J. E. *J. Am. Chem. Soc.* **1966**, *88*, 4990. In addition to the vinyl esters, hexaethylbenzene was also formed, with the proportion of this product increasing with increasing initial concentration of 1-phenylpropyne.

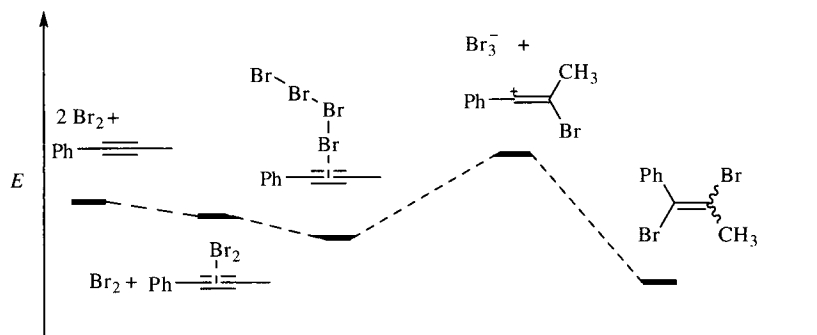
The k_{Br^-} term in equation 9.57 is significant only in the presence of added Br^- . The ratio of **57** to **58** was found to be 4.2 : 1 in the absence of added bromide ion, but the ratio increased with increasing bromide ion concentration. Essentially 100% anti addition was observed at the highest concentrations of bromide ion studied.²⁷⁷ These observations led the investigators to conclude that there could be an $\text{Ad}_{\text{E}}3$ mechanism (equation 9.61) in the presence of bromide ion.



Bianchini and co-workers found that the reaction of 1-phenylpropyne with Br_2 in 1,2-dichloroethane produced a 78 : 22 mixture of the *E* and *Z* diastereomers of 2,3-dibromo-1-phenylethene.²⁷⁸ In addition, the reaction was found to have a ΔH^\ddagger of -1.2 kcal/mol and a ΔS^\ddagger of -56 eu. These observations were consistent with both the essential role of a π complex in the reaction mechanism and a reaction pathway involving an open β -bromovinyl cation, as shown in Figure 9.47.²⁷⁹

In contrast to the results for 1-phenylpropyne, 3-hexyne (**61**) formed only the *E* bromine addition product (**62**) in acetic acid. The reaction appears to occur through the intermediacy of a bromonium ion (equation 9.62) in the

FIGURE 9.47
Energy diagram for the addition of bromine to 1-phenylpropyne.
(Adapted from reference 278.)

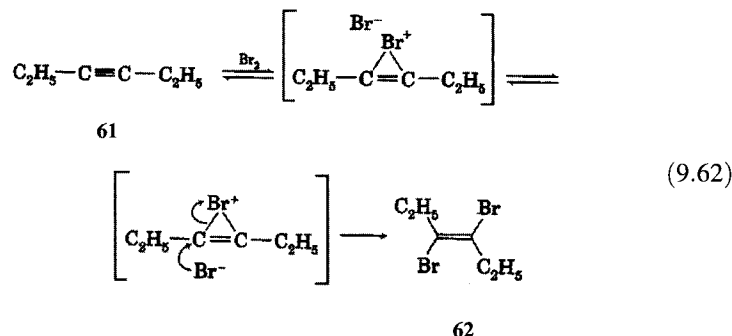


²⁷⁷ Similarly, the addition of bromine to phenylacetylene in acetic acid was found to give a mixture of (*E*)- to (*Z*)-1,2-dibromo-1-phenylethene that varied from 70 : 30 without added bromide to 97 : 3 with 0.1 M LiBr. König, J.; Wolf, V. *Tetrahedron Lett.* **1970**, 1629.

²⁷⁸ Bianchini, R.; Chiappe, C.; Lo Moro, G.; Lenoir, D.; Lemmen, P.; Goldberg, N. *Chem. Eur. J.* **1999**, *5*, 1570.

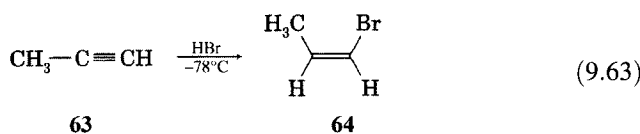
²⁷⁹ For an experimental study of the bromination of arylalkynes in ionic liquids, see Chiappe, C.; Conte, V.; Pieraccini, D. *Eur. J. Org. Chem.* **2002**, 2831. For theoretical investigations of halogen addition to alkynes, see Okazaki, T.; Laali, K. K. *J. Org. Chem.* **2005**, *70*, 9139; Zabalov, M. V.; Karlov, S. S.; Lemenovskii, D. A.; Zaitseva, G. S. *J. Org. Chem.* **2005**, *70*, 9175.

absence of bromide ion, or an $\text{Ad}_{\text{E}3}$ mechanism in the presence of bromide ion.^{274,278}



As the results presented above suggest, alkynes with alkyl substituents on the acetylenic carbons are more likely to react through cyclic halonium ions than are those with aryl groups that are capable of stabilizing vinyl cations. The tendency for the reaction to proceed through a cyclic ion instead of an open cation increases along the series Cl, Br, I as the bridging ability of the halogen increases.^{280,281} Mixed halogens also add to alkynes, and the kinetics of the reactions can be complex, especially when the alkyne reacts slowly and considerable assistance by other molecules of mixed halogen is necessary to evoke reaction.²⁸²

Hydrogen halides also add to alkynes. The addition of HBr to alkynes can be difficult to interpret because (as with alkenes) both ionic and free radical mechanisms may occur, and the free radical process can be difficult to suppress.²⁸³ Reaction of HBr with propyne (63) in the liquid phase at -78°C led to the formation of (*Z*)-1-bromopropene (64, equation 9.63), indicating stereoselective anti addition.²⁸⁴ When the reaction was carried out at room temperature, however, a mixture of *Z* (64) and *E* (65) isomers was obtained (equation 9.64).²⁸⁵ The results suggested that addition of a bromine atom to propyne produces the vinyl radical 66, which abstracts a hydrogen from HBr to produce 64 at -78°C but which can isomerize (with $E_a > 17$ kcal/mol) to the radical 67 at room temperature.



²⁸⁰ Bassi, P.; Tonellato, U. *J. Chem. Soc. Perkin Trans. 1* **1973**, 669.

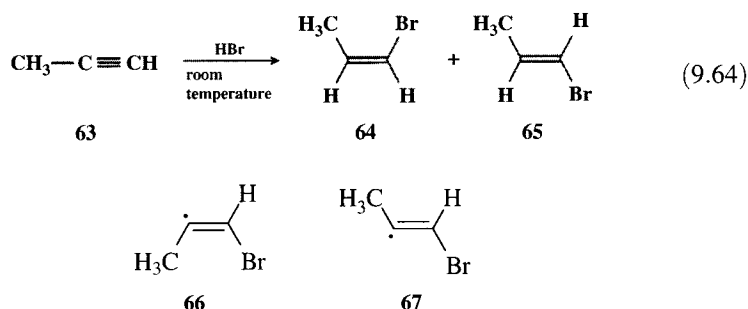
²⁸¹ Addition of I_2 appears to occur by anti addition also (reference 272). Addition of fluorine to alkynes occurs to give the tetrafluoroalkane, even when the fluorinating reagent is XeF_2 : Zupan, M.; Pollak, A. *J. Org. Chem.* **1974**, 39, 2646.

²⁸² For example, the addition of ICl to ethyl but-3-ynoate in propionic acid was reported to occur by a combination of $\text{Ad}_{\text{E}3}$ and $\text{Ad}_{\text{E}4}$ pathways. Tendil, J.; Verney, M.; Vessiere, R. *Tetrahedron* **1974**, 30, 579.

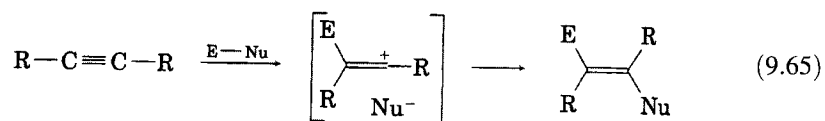
²⁸³ Fahey, R. C.; Lee, D.-J. *J. Am. Chem. Soc.* **1968**, 90, 2124 and references therein.

²⁸⁴ Skell, P. S.; Allen, R. G. *J. Am. Chem. Soc.* **1958**, 80, 5997.

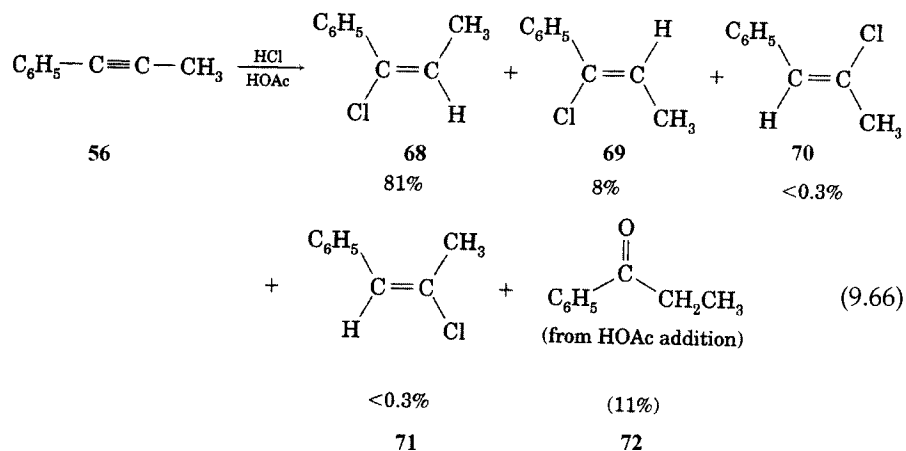
²⁸⁵ Skell, P. S.; Allen, R. G. *J. Am. Chem. Soc.* **1964**, 86, 1559.



The reaction of alkynes with HCl in acetic acid solution does take place by a heterolytic pathway. By analogy to the addition of electrophiles to alkenes, one might write a mechanism involving a vinyl cation, which could then combine with the nucleophile anion to produce the adduct (equation 9.65).²⁷⁵ Vinyl cations are much less stable than are 2° or 3° alkyl cations and allyl or benzyl cations, however.²⁸⁶



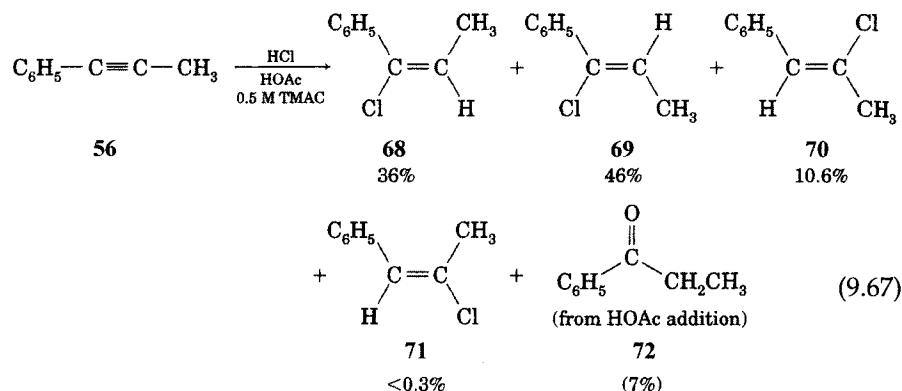
The reaction of 1-phenylpropyne (**56**) with 0.1M HCl in acetic acid solution produced five products, as shown in equation 9.66.²⁸⁷ The major product (**68**) was the result of syn addition of HCl, with attachment of the proton to C2 of the reactant. There was also a stereoisomer (**69**) with the same regiochemistry, indicating some anti addition of HCl. Both of these products are consistent with the intermediacy of a vinyl cation–chloride ion pair. Trace amounts of the regioisomers **70** and **71** apparently were formed by electrophilic addition with initial protonation of C1 of the alkyne. Propiophenone (**72**) was also formed in the reaction. Apparently solvent reacts with the vinyl cation intermediate to produce vinyl acetates, which then react with trace water to hydrolyze to unstable enols that tautomerize to the ketone.



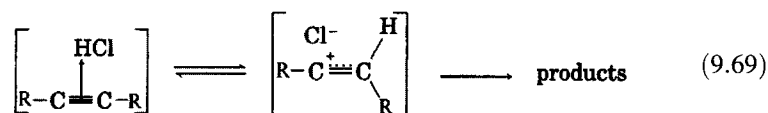
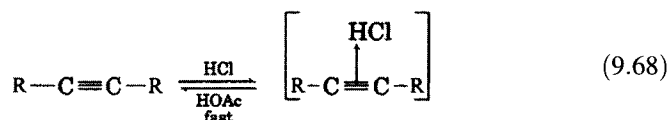
²⁸⁶ Some authors have estimated that vinyl cations are comparable in stability to methyl or, perhaps, primary carbocations. For a discussion, see Weiss, H. M. *J. Chem. Educ.* **1993**, *70*, 873. See also Tidwell, T. T. *J. Chem. Educ.* **1996**, *73*, 1081; Weiss, H. M. *J. Chem. Educ.* **1996**, *73*, 1082.

²⁸⁷ Fahey, R. C.; Payne, M. T.; Lee, D.-J. *J. Org. Chem.* **1974**, *39*, 1124.

When 0.5 M chloride ion (as tetramethylammonium chloride, TMAC) was added to the reaction mixture, the rate constant for the reaction shown in equation 9.66 increased by a factor of 5, and the product distribution had a much greater proportion of **69** and **70** (equation 9.66).

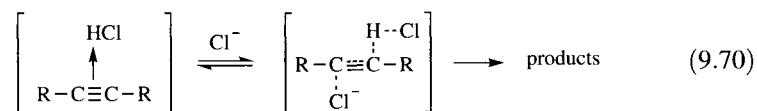


To account for the rates of reaction and product distributions observed in these and other studies, Fahey and co-workers suggested that two competitive processes are involved.²⁸⁷ As shown in equations 9.68 through 9.70, both processes begin with the formation of an alkyne–HCl complex or its kinetic equivalent, an association of the alkyne and HCl in a solvent cage.²⁸⁸ If the developing carbocation is sufficiently stable, the complex can proceed to a vinyl cation–chloride ion pair, leading to product formation by an Ad_E2 mechanism (equation 9.69). Alternatively, the complex can react with added chloride ion to form product by an Ad_E3 mechanism (equation 9.70). In the absence of added chloride ion, another molecule of HCl may serve the same purpose.²⁸⁹

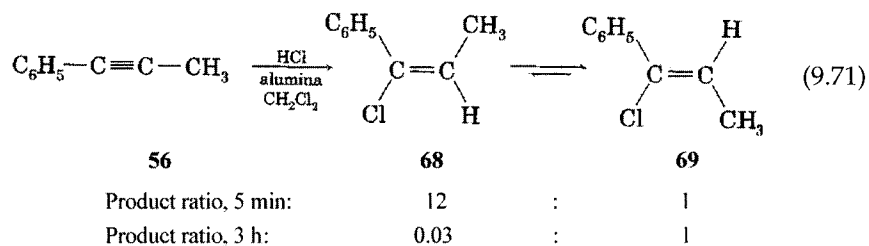


²⁸⁸ Evidence for the existence of alkyne–HCl complexes was reported by Mootz, D.; Deeg, A. J. *Am. Chem. Soc.* **1992**, *114*, 5887, who obtained an X-ray structure for a 1 : 1 complex of HCl and 2-butyne. The complex was found to be a T-shaped structure, with the H–Cl bond axis perpendicular to the axis of the carbon–carbon triple bond. The authors also obtained an X-ray structure for a 2 : 1 HCl : 2-butyne complex.

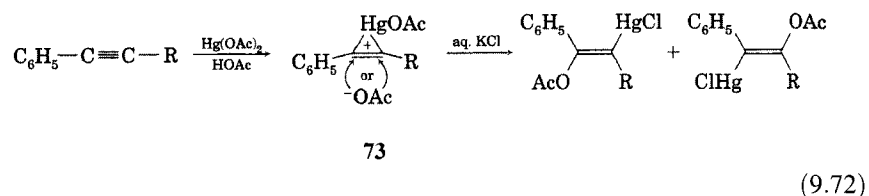
²⁸⁹ Fahey and Lee (reference 283) found the addition of HCl to 3-hexyne in acetic acid to be termolecular, first order in the alkyne and second order in HCl. The reaction showed primarily anti addition at 25°C, although there was more syn addition at higher temperatures. Similar considerations apply in the addition of other electrophiles to alkynes (reference 275).



The complexities associated with the addition of hydrogen halides to alkynes in homogeneous solution limit the synthetic utility of these reactions. Kropp and Crawford found that the surface-mediated addition of hydrogen halides to alkynes in heterogeneous mixtures proceeds more rapidly and gives less complex product mixtures than does reaction in homogeneous solution.²⁹⁰ For example, addition of HCl to 1-phenylpropyne on a suspension of alumina in CH₂Cl₂ gave a high yield of (*E*)-1-chloro-1-phenylpropene at short reaction times. At longer reaction times, product equilibration produced a high yield of the (*Z*)-diastereomer (equation 9.71). Furthermore, surface-mediated addition of HBr to alkynes was not accompanied by products of radical reaction.²⁹⁰



Dialkylacetylenes and phenylalkylacetylenes also add mercuric acetate in acetic acid solution. The products point to exclusively anti addition, but with a regiochemistry that depends on the nature of the alkyl group.^{291,292} The results suggest that the solvomercuration of alkynes appears to take place through mercurinium ions (e.g., **73**), as does solvomercuration of alkenes.²⁹³



Alkynes also undergo acid-catalyzed hydration to yield ketones. Alkynes substituted with alkoxy or phenoxy groups undergo hydration readily, and butyl acetate was obtained by heating butoxyacetylene in distilled water.²⁹⁴

²⁹⁰ Kropp, P. J.; Crawford, S. D. *J. Org. Chem.* **1994**, *59*, 3102.

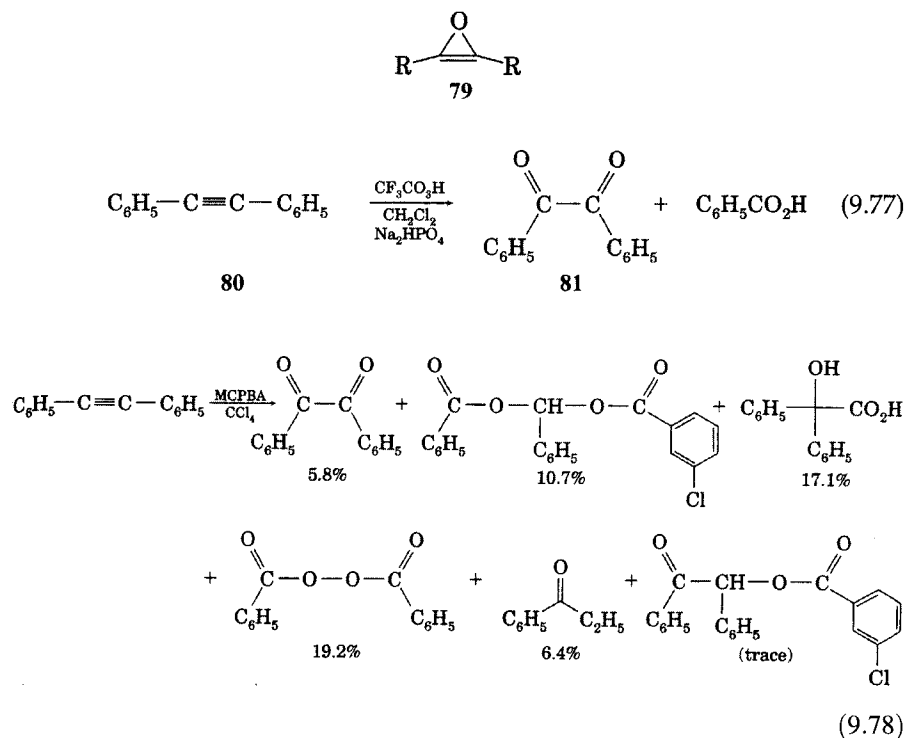
²⁹¹ See, for example, Uemura, S.; Miyoshi, H.; Okano, M. *J. Chem. Soc. Perkin Trans. 1* **1980**, 1098.

²⁹² The kinetics of the addition are first order in alkyne and first order in the mercurating agent. Bassetti, M.; Floris, B. *J. Org. Chem.* **1986**, *51*, 4140.

²⁹³ Diphenylacetylene gives exclusively syn addition. See the discussion in reference 291; also see Bach, R. D.; Woodard, R. A.; Anderson, T. J.; Glick, M. D. *J. Org. Chem.* **1982**, *47*, 3707.

²⁹⁴ Jacobs, T. L.; Searles, S., Jr. *J. Am. Chem. Soc.* **1944**, *66*, 686 and references therein.

the formation of an oxirene intermediate (79), which can then undergo further oxidation by peracid, addition of solvent, or rearrangement to a ketene.^{305,306} For example, reaction of diphenylacetylene (80) with pertrifluoroacetic acid in methylene chloride produced mostly benzil (81) and benzoic acid (equation 9.77).³⁰⁵ However, peroxidation with *m*-chloroperoxybenzoic acid (*m*-CPBA) in CCl₄ solution produced only a 5.8% yield of benzil, no benzoic acid, and a total of 53% yield of five other products (equation 9.78).³⁰⁶



Electrophilic additions also occur to cumulated dienes (allenes).³⁰⁷ Caserio and co-workers established that the mechanisms of both the oxymercuration reaction and the electrophilic addition of bromine to allenes are similar to the corresponding additions to olefins.³⁰⁸ The oxymercuration of (*R*)-(-)-2,3-pentadiene (82) in methanol produced 83% of (*S*)-*trans*-3-acetoxymercuri-4-methoxy-2-pentene (83), confirming the anti pathway for the addition. Also formed was 17% of *cis*-3-acetoxymercuri-4-methoxy-2-pentene (84), which was presumed to have the *R* configuration.³⁰⁹ As shown in Figure 9.48, the product ratios can be explained on the basis of preequilibrium formation of mercurinium ions resulting from attachment of mercury to either the top or the bottom of one of the double bonds. Subsequent rate-limiting attack of methanol on the mercurinium ions is easier for the pathway

³⁰⁵ McDonald, R. N.; Schwab, P. A. *J. Am. Chem. Soc.* **1964**, *86*, 4866.

³⁰⁶ Stille, J. K.; Whitehurst, D. D. *J. Am. Chem. Soc.* **1964**, *86*, 4871.

³⁰⁷ See, for example, Fischer, H. in Patai, S., Ed. *The Chemistry of Alkenes*; Wiley-Interscience: London, 1964; pp. 1025-1159.

³⁰⁸ Waters, W. L.; Linn, W. S.; Caserio, M. C. *J. Am. Chem. Soc.* **1968**, *90*, 6741.

³⁰⁹ Although the acetoxymercuri compound is shown in Figure 9.48, the investigators treated the initial oxymercuration product with aqueous sodium chloride and isolated the corresponding chloromercuri compounds.

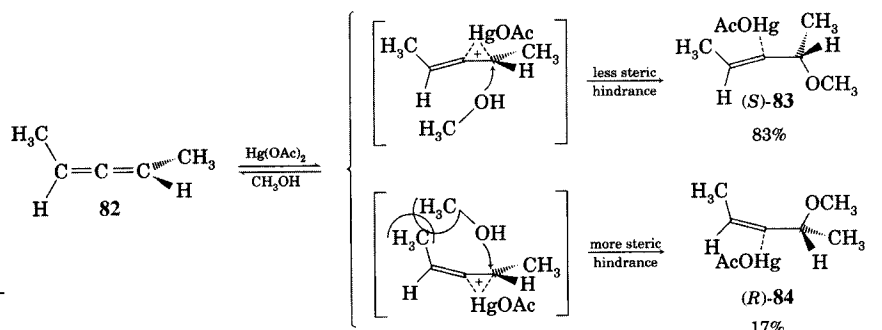


FIGURE 9.48

Addition of $\text{Hg}(\text{OAc})_2$ to (R)-(-)-2,3-pentadiene in methanol.

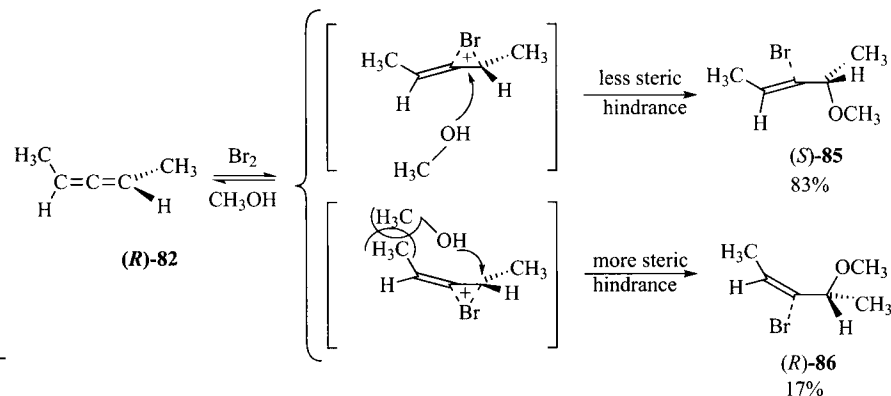


FIGURE 9.49

Addition of bromine to (R)-(-)-2,3-pentadiene in methanol.

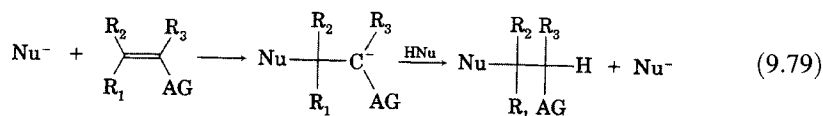
in which solvent can avoid the steric hindrance due to the remaining vinyl methyl group, so formation of (S)-83 predominates.

Addition of bromine to the same allene in methanol led to the formation of 83% of the (S)-*trans*-3-bromo-4-methoxy-2-pentene (85), confirming the anti pathway for the addition of bromine under these conditions. Also formed was 17% of *cis*-3-bromo-4-methoxy-2-pentene (86), which was again presumed to have the R configuration. As shown in Figure 9.49, the same ratio of diastereomers was observed in the oxymercuration reaction. This result is consistent with an anti addition mechanism for bromine addition that is closely analogous to the mechanism of oxymercuration.

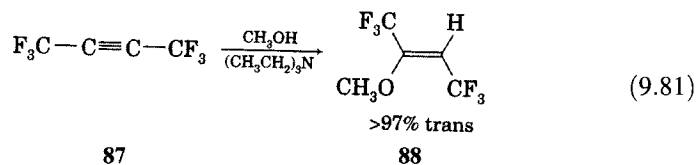
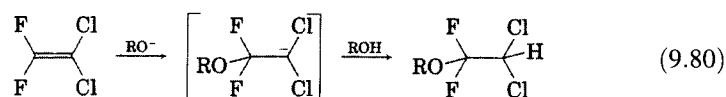
Nucleophilic Addition to Alkenes and Alkynes

Nucleophilic additions to alkenes and alkynes are also possible, but these reactions generally require that the substrate have substituents that can stabilize a carbanionic intermediate. Therefore, nucleophilic additions are most likely for compounds with carbon-heteroatom multiple bonds, such as carbonyl compounds, imines, and cyano compounds. We may distinguish two main types of substituents that activate alkenes and alkynes for nucleophilic attack. The first type consists of those activating groups (labeled AG in equation 9.79) that can stabilize an adjacent carbanion by induction.³¹⁰

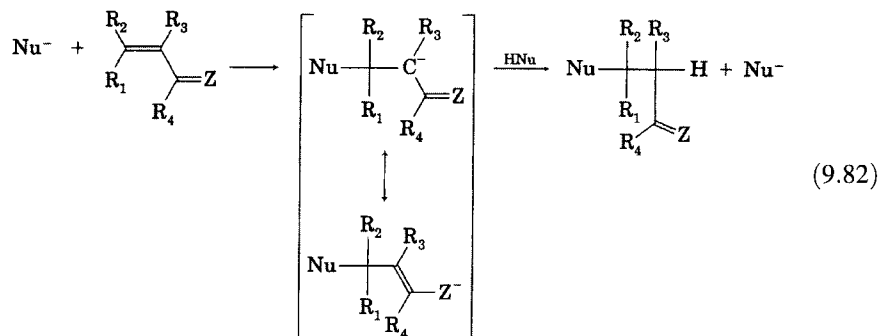
³¹⁰ In some cases, the addition is followed by elimination of one of the olefinic substituents, so the result of addition-elimination is nucleophilic vinylic substitution. Rappoport, *Z. Adv. Phys. Org. Chem.* **1969**, *7*, 1.



The synthesis of fluoroalkyl and chlorofluoroalkyl ethers occurs readily by base-catalyzed nucleophilic addition of alcohols to haloalkenes. An example is the synthesis of the alkyl 2,2-dichloro-1,1-difluoroethyl ethers, where R is methyl or 1° or 2° alkyl (equation 9.80).³¹¹ Nucleophilic addition can also occur with alkynes that are activated by the presence of groups such as trifluoromethyl. An example is the addition of methoxide to hexafluoro-2-butyne (**87**) to produce the methoxy ether with trans trifluoromethyl groups (**88**, equation 9.81).³¹² Note that the orientation of addition to the alkyne is anti, a pattern that is frequently—but not always—observed.^{313,314}



The second type of activating group stabilizes the carbanion primarily through resonance, as illustrated in equation 9.82.



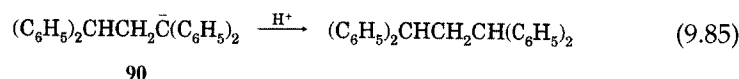
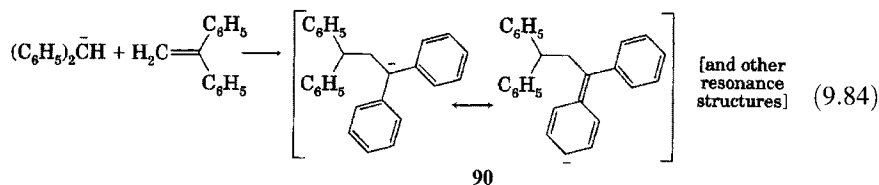
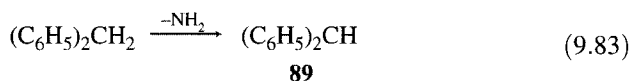
³¹¹ Tarrant, P.; Brown, H. C. *J. Am. Chem. Soc.* **1951**, *73*, 1781. For related examples, see Miller, W. T., Jr.; Fager, E. W.; Griswold, P. H. *J. Am. Chem. Soc.* **1948**, *70*, 431; Park, J. D.; Sharrah, M. L.; Breen, W. H.; Lacher, J. R. *J. Am. Chem. Soc.* **1951**, *73*, 1329.

³¹² Raunio, E. K.; Frey, T. G. *J. Org. Chem.* **1971**, *36*, 345.

³¹³ See, for example, (a) Truce, W. E.; Simms, J. A. *J. Am. Chem. Soc.* **1956**, *78*, 2756; (b) Miller, S. I. *J. Am. Chem. Soc.* **1956**, *78*, 6091.

³¹⁴ For discussions of nucleophilic addition to alkynes, see Miller, S. I.; Tanaka, R. in Thyagarajan, B. S., Ed. *Selective Organic Transformations*, Vol. I; Wiley-Interscience: New York, 1970; pp. 143–238; Dickstein, J. I.; Miller, S. I. in Patai, S., Ed. *The Chemistry of the Carbon-Carbon Triple Bond*, Part 2; Wiley-Interscience: Chichester, England, 1978; pp. 843–911.

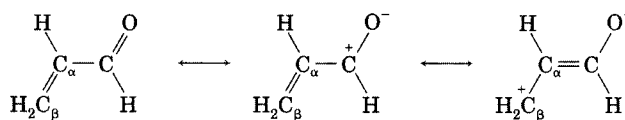
For example, reaction of the diphenylmethide ion **89** with 1,1-diphenylethene was reported to occur by nucleophilic addition to the carbon–carbon double bond (equations 9.83 through 9.85).³¹⁵ In this case, delocalization of the negative charge over the two phenyl groups stabilizes the intermediate carbanion (**90**).



Substituents that are particularly effective at stabilizing nucleophilic addition to alkenes and alkynes are those in which the group C=Z in equation 9.82 is a C=O (including aldehydes, ketones, esters, acid halides, and other carboxylic acid derivatives except amides), C=NR, S=O, and P=O group.³¹⁶ One significant complication with compounds of this type, particularly with carbonyl compounds, is that two different pathways for addition are possible. The resonance structures for propenal in Figure 9.50 suggest that there should be appreciable positive charge on both the carbonyl carbon atom and the β carbon atom. A nucleophile might therefore add directly to the carbonyl carbon atom in a 1,2-addition, or it could add to the β carbon atom of the α,β -unsaturated carbonyl compound in a 1,4- or conjugate addition reaction, also known as Michael addition (Figure 9.51).^{317,318}

The regiochemistry of nucleophilic addition to an alkene or alkyne stabilized by a carbonyl group is a function of both the substrate and the nucleophile. Hard nucleophiles such as Grignard reagents tend to add

FIGURE 9.50
Resonance structures for propenal.

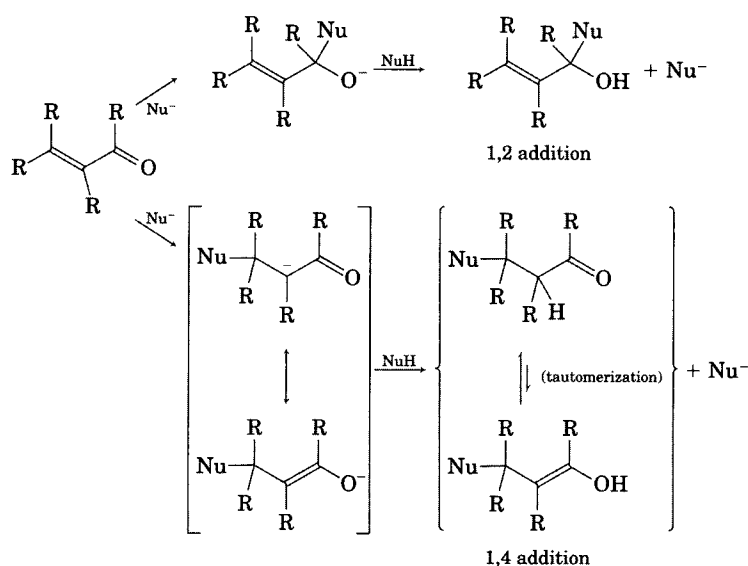


³¹⁵ Kofron, W. G.; Goetz, J. M. J. *Org. Chem.* **1973**, *38*, 2534.

³¹⁶ Perlmutter, P. *Conjugate Addition Reactions in Organic Synthesis*; Pergamon Press: Oxford, England, 1992.

³¹⁷ For a discussion of the terminology of conjugate addition reactions, see reference 316.

³¹⁸ For a review of Michael addition in synthesis, see Bergmann, E. D.; Ginsburg, D.; Pappo, R. *Org. React.* **1959**, *10*, 179. For a review of the stereochemistry of the base-promoted Michael addition, see Oare, D. A.; Heathcock, C. H. *Top. Stereochem.* **1989**, *19*, 227.

**FIGURE 9.51**

1,2- (top) and 1,4-addition (bottom) to an α,β -unsaturated carbonyl compound

preferentially at the carbonyl carbon atom, but soft nucleophiles such as organocopper compounds tend to give 1,4-addition.³¹⁹ For example, use of a catalytic amount of CuCl with a CH_3MgBr solution in diethyl ether changed the regiochemistry of the reaction from 1.5% to more than 80% conjugate addition.^{320,321} The greater LUMO coefficient on the β carbon atom than on the carbonyl carbon atom of an α,β -unsaturated carbonyl compound (Figure 9.52) makes the softer nucleophile more reactive with the β site.³²² Steric hindrance can also be a factor in determining the preference for 1,2- or 1,4-addition, and a large substituent on the carbonyl carbon atom greatly increases the yield of conjugate addition product.³²³ One of the best-known examples of a conjugate addition is the first step of the Robinson annulation, as shown by the conjugate addition of the enolate of cyclohexanone to methyl styryl ketone, followed by an aldol reaction (Figure 9.53).³²⁴

As a general rule, nucleophiles add to α,β -unsaturated carbonyl compounds only at the carbonyl carbon atom or the β carbon atom. However, the

	$\text{H}_2\text{C}=\text{CH}-\text{CH}=\text{O}$
	$\beta \quad \alpha \quad \text{carbonyl}$
LUMO coefficient	0.59 -0.48 -0.30

FIGURE 9.52

LUMO coefficients for acrolein.

³¹⁹ Organolithium reagents show an even greater preference for 1,2-addition. Wakefield, B. J. *The Chemistry of Organolithium Compounds*; Pergamon Press: Oxford, England, 1974.

³²⁰ Kharasch, M. S.; Tawney, P. O. *J. Am. Chem. Soc.* **1941**, *63*, 2308.

³²¹ Organocopper reagents are widely used to carry out addition to the β carbon atom of α,β -unsaturated carbonyl compounds. For a discussion, see Posner, G. H. *Org. React.* **1972**, *19*, 1. The nature of the organocopper compound is a significant factor in these reactions. See, for example, Lipshutz, B. H.; Wilhelm, R. S.; Kozlowski, J. A. *J. Org. Chem.* **1984**, *49*, 3938.

³²² Fleming, I. *Frontier Orbitals and Organic Chemical Reactions*; Wiley-Interscience: London, 1976; pp. 70, 163.

³²³ See, for example, (a) DeMeester, W. A.; Fuson, R. C. *J. Org. Chem.* **1965**, *30*, 4332; (b) Cooke, M. P., Jr. *J. Org. Chem.* **1986**, *51*, 1638.

³²⁴ Rapson, W. S.; Robinson, R. *J. Chem. Soc.* **1935**, 1285.

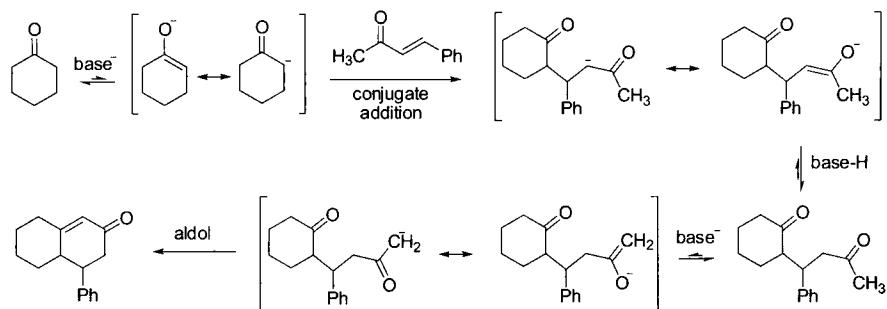
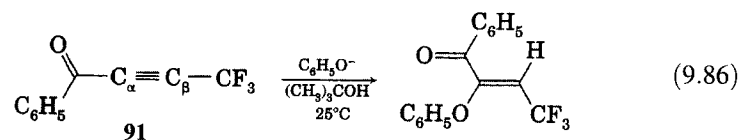


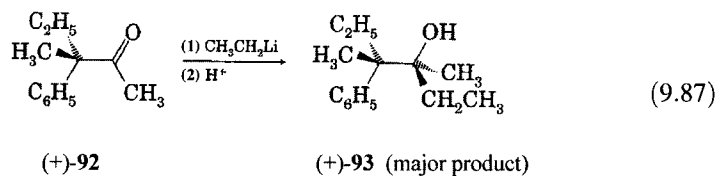
FIGURE 9.53
Conjugate addition in the Robinson annulation reaction.

addition of phenoxide to benzoyl(trifluoromethyl)acetylene (**91**) was found to occur at the α carbon atom (equation 9.86). In this case the anti-Michael orientation is consistent with the observation that both the partial positive charge and the coefficient of the LUMO of the reactant are greater at C_{α} than at C_{β} . Also, the intermediate carbanion resulting from nucleophilic attachment to C_{α} in this case is believed to be more stable than the carbanion intermediate generated by nucleophilic attachment to C_{β} .³²⁵



Nucleophilic Addition to Carbonyl Compounds

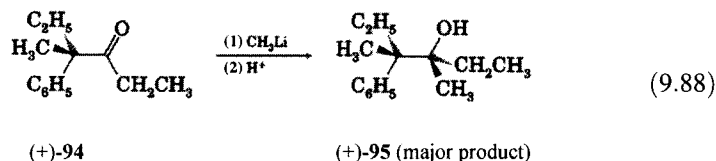
Regiochemistry is ordinarily not a concern in the addition of nucleophiles to structures having carbon–heteroatom multiple bonds that are not conjugated with carbon–carbon double or triple bonds, because only 1,2-addition is expected.³²⁶ If the addition creates a new chiral center, however, then stereoisomeric addition products can be formed. Considerable interest in this area was sparked by a report by Cram that nucleophilic addition to ketones having chiral α carbon atoms gave unequal yields of the possible diastereomeric adducts. For example, addition of ethyllithium to the methyl ketone (+)-**92** gave primarily the erythro product (+)-**93**.



³²⁵ Bumgardner, C. L.; Bunch, J. E.; Whangbo, M.-H. *J. Org. Chem.* **1986**, *51*, 4082.

³²⁶ The most important reactions of this type involve addition to the carbonyl group, but reactions involving imines, iminium ions, and nitriles are also synthetically important.

In contrast, addition of methyllithium to the ethyl ketone (+)-**94** produced the threo diastereomer (+)-**95** as the major product.³²⁷



To explain this diastereoselectivity, Cram proposed that the asymmetric induction at the carbonyl group is determined by steric effects in the encounter between the ketone and the nucleophilic reagent.^{328,329} As shown in Figure 9.54, the preferred conformation of a chiral ketone was considered to be one in which the large substituent (L) is anti-periplanar to the carbonyl group, especially if coordination of the oxygen with the metal atom (Z) of the nucleophilic reagent $\text{R}'\text{-Z}$ increases the effective size of the oxygen atom. The other two substituents on the α carbon atom were designated S (for small) and M (for medium). The sterically less hindered route of attack was thought to bring the incoming nucleophile to the back of the carbonyl on the side of the small substituent. This **rule of steric control of asymmetric induction** (often called Cram's rule) was found to correctly predict the major diastereomer in the synthesis of 3-cyclohexyl-2-butanol with methylmagnesium iodide, with methyllithium in ether or pentane, with lithium aluminum hydride, or with sodium borohydride.³³⁰

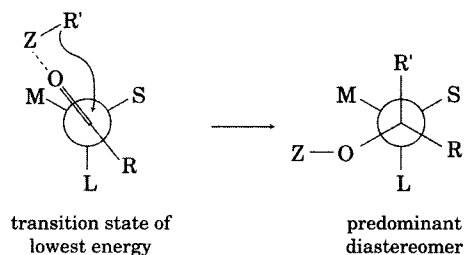


FIGURE 9.54

Steric model for asymmetric induction in chiral ketones. (Adapted from reference 329.)

For those ketones in which one of the substituents on the α carbon atom is also capable of coordinating with the metal (Z in $\text{R}'\text{-Z}$), a second model, termed the rigid model, was proposed.³²⁹ A five-membered ring was said to be formed by the carbonyl carbon atom, the α carbon atom, the electron-donating α substituent, the metal Z, and the carbonyl oxygen atom (Figure 9.55). Again, the nucleophile was considered more likely to attack from the side of the smaller substituent (S) than the larger one (L), leading to the diastereoselectivity. This rule correctly predicted the addition of methyllithium to the ketone **96** to produce the erythro diastereomer (**97**, equation 9.89),³²⁹ and Eliel and co-workers obtained evidence

³²⁷ Cram, D. J.; Knight, J. D. *J. Am. Chem. Soc.* **1952**, *74*, 5835.

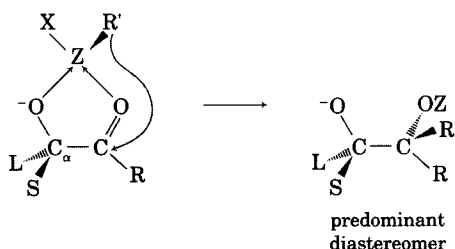
³²⁸ Cram, D. J.; Abd Elhafez, F. A. *J. Am. Chem. Soc.* **1952**, *74*, 5828.

³²⁹ Cram, D. J.; Kopecky, K. R. *J. Am. Chem. Soc.* **1959**, *81*, 2748.

³³⁰ It did not predict the correct product when 3-cyclohexyl-2-butanone was reduced by aluminum isopropoxide, however. Cram, D. J.; Greene, F. D. *J. Am. Chem. Soc.* **1953**, *75*, 6005.

FIGURE 9.55

Rigid model for diastereoselectivity in nucleophilic addition to carbonyl compounds. (Reproduced from reference 329.)



for the role of chelates in the addition of nucleophiles to α -alkoxy ketones.^{331–333}

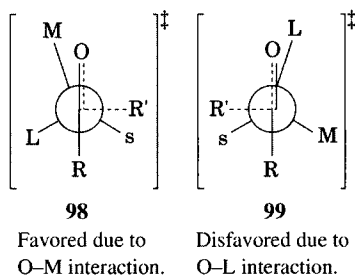
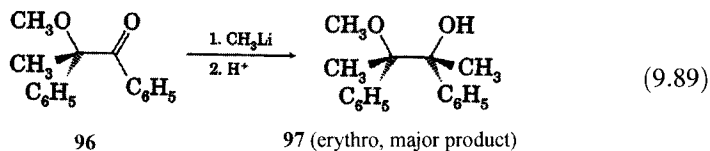


FIGURE 9.56

Transition structures proposed for asymmetric induction by Karabatsos. (Adapted from reference 334.)

The Cram model was questioned by Karabatsos, however, who noted that results for some compounds suggested that the apparent size of methyl was greater than that of isopropyl. Furthermore, he noted that the Curtin–Hammett principle requires knowledge of transition state energies, not just the energies of initial conformations. He proposed an alternative model in which there is a very early transition state for the addition and in which the incoming nucleophile (R') prefers to approach near the smallest group, as shown in the two transition structures in Figure 9.56. Then the sum of the steric interactions between the *other* substituents (particularly between the carbonyl oxygen and the substituent M or L on the eclipsed bond) was used to predict the diastereomeric preference of the addition reaction.³³⁴ Thus, a pathway that involves **98** would be favored over a pathway that involves **99**.

Cornforth proposed a different explanation for the diastereoselective addition of Grignard reagents to α -chloro aldehydes and ketones.³³⁵ The underlying premise of this model is that electrostatic effects such as dipole–dipole interactions favor a reactant conformation in which the C=O group and the C_α –Cl bonds are oriented anti-coplanar. The preferred path for approach of the nucleophile could then be predicted on the basis of the sizes of the other substituents on the α carbon (Figure 9.57).

Still another model was proposed by Felkin and co-workers, who suggested that the most important steric interaction is between the large group (L) and the incoming nucleophile (Nu).³³⁶ According to this model, the lowest

³³¹ Frye, S. V.; Eliel, E. L. *J. Am. Chem. Soc.* **1988**, *110*, 484.

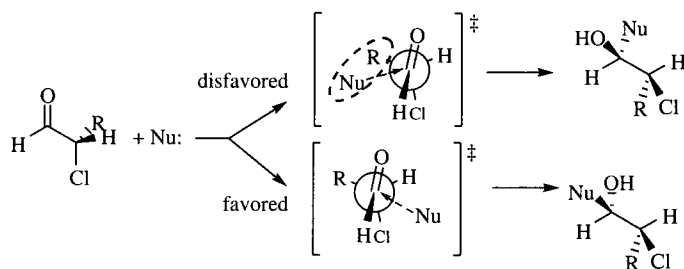
³³² Chen, X.; Hortelano, E. R.; Eliel, E. L.; Frye, S. V. *J. Am. Chem. Soc.* **1992**, *114*, 1778. A key piece of evidence suggesting that the chelates are true intermediates (and not structures that are in equilibrium with the reactants but are not along the reaction path) was the fact that the most reactive compounds also gave the greatest diastereoselectivity. The authors noted that this result also suggests an analogy between chelates and enzymatic processes.

³³³ Further evidence supporting the role of chelates was reported by Reetz, M. T. *Acc. Chem. Res.* **1993**, *26*, 462 and references therein.

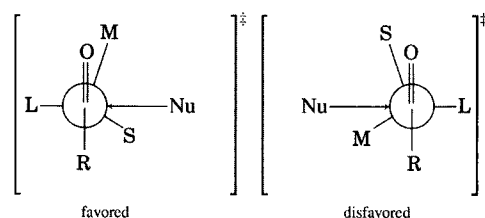
³³⁴ Karabatsos, G. J. *J. Am. Chem. Soc.* **1967**, *89*, 1367.

³³⁵ Cornforth, J. W.; Cornforth, R. H.; Mathew, K. K. *J. Chem. Soc.* **1959**, 112.

³³⁶ Chérest, M.; Felkin, H.; Prudent, N. *Tetrahedron Lett.* **1968**, 2199.

**FIGURE 9.57**

Cornforth model for nucleophilic addition to an α -chiral aldehyde. Note that Cl and O are anti-coplanar.

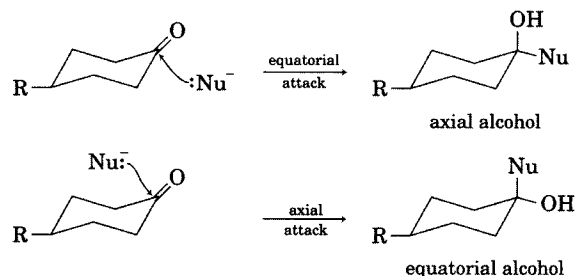
**FIGURE 9.58**

Representations of the pathways for addition of a nucleophile to a carbonyl group according to the Felkin model. Note that Nu and L are anti-coplanar. (Adapted from reference 343.)

energy transition structure is one in which L and Nu are anti-periplanar, so the nucleophile should approach between the medium and small substituents. The preferred path according to this model, therefore, is the one in which the *small* substituent is closer to the substituent R on the carbonyl carbon atom (Figure 9.58). The authors also suggested the possibility that there might be some torsional energy associated with interaction of the incipient σ bond with the σ bonds already present in the molecule.

The consideration of the development of torsional strain in the transition state for nucleophilic addition afforded an explanation for product distributions observed in the addition of nucleophiles to substituted cyclohexanones. Dauben and co-workers reported that reduction of 4-methylcyclohexanone with LiAlH_4 produced 81% of the trans alcohol and 19% of the cis isomer.³³⁷ With 4-*t*-butylcyclohexanone, a conformationally more rigid structure, a similar product distribution was obtained.³³⁸ Initially, the results were explained in terms of **product development control**, in which the more stable alcohol (with the equatorial OH group) is formed by axial attack of the nucleophile on the carbon–oxygen double bond (Figure 9.59).³³⁷

Most theoretical models now indicate that the transition state in nucleophilic addition to a carbonyl group is very early, meaning that the transition

**FIGURE 9.59**

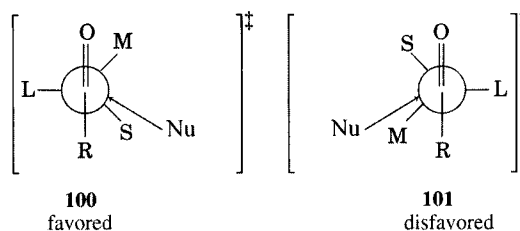
Equatorial (top) and axial (bottom) attack of a nucleophile on a cyclohexanone carbonyl group.

³³⁷ Dauben, W. G.; Fonken, G. J.; Noyce, D. S. *J. Am. Chem. Soc.* **1956**, *78*, 2579 and references therein.

³³⁸ Cieplak, A. S. *J. Am. Chem. Soc.* **1981**, *103*, 4540.

FIGURE 9.60

Models for the transition structures for nucleophilic addition to a carbonyl group according to the Anh and Eisenstein model. (Adapted from reference 343.)



structures more nearly resemble the reactants than the products. Therefore, product distributions need not reflect the thermodynamic stability of products. As an alternative explanation, Felkin proposed that the equatorial attack of a nucleophile (leading to axial alcohol) involves torsional strain between the incipient Nu–C bond and the equatorial C_α–H bond. On the other hand, axial attack of the nucleophile (leading to equatorial alcohol) should involve some repulsive van der Waals interaction with axial substituents. The product distribution in a particular case, then, was said to be determined by the competing factors favoring axial and equatorial addition of the nucleophile.³³⁹

Although the models considered above have emphasized steric interactions, Anh, Eisenstein, and their co-workers proposed that stereoelectronic factors are comparable in importance.³⁴⁰ Ab initio calculations suggested that the electron cloud around the carbonyl group is dissymmetric in chiral aldehydes and ketones and that this dissymmetry might be a factor in nucleophilic attack. Moreover, the calculations indicated that the approach of the nucleophile is not along a path perpendicular to the carbon–oxygen double bond but instead is closer to an O–C···Nu bond angle of 109.5°.³⁴¹ Anh and Eisenstein therefore proposed that the group anti-periplanar to the incoming nucleophile is not necessarily the largest group but is, instead, the group with the lowest energy σ* orbital.³⁴² Now the preferred pathway for attack of the nucleophile (100) is near the small group rather than the medium group (101, Figure 9.60). Also, some stabilization may arise from mixing of the developing σ orbital with a σ* orbital on the α carbon atom. The more electronegative the group anti-periplanar to the incoming nucleophile, the lower would be the energy of that σ* orbital, and the more stable the transition structure (Figure 9.61).³⁴³

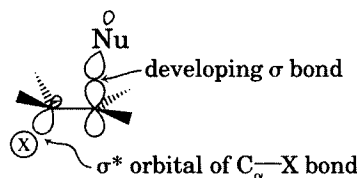


FIGURE 9.61

Interaction of a developing Nu–C σ bond with an adjacent C_β–X σ* orbital. Greater electronegativity of X is thought to produce greater stabilization of the transition structure. (Adapted from reference 344.)

³³⁹ Chérest, M.; Felkin, H. *Tetrahedron Lett.* **1968**, 2205.

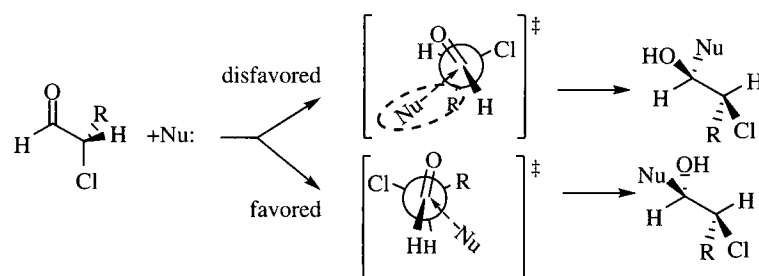
³⁴⁰ Anh, N. T.; Eisenstein, O.; Lefour, J.-M.; Trân Huu Dâu, M.-E. *J. Am. Chem. Soc.* **1973**, *95*, 6146.

³⁴¹ Bürgi, H. B.; Dunitz, J. D.; Shefter, E. *J. Am. Chem. Soc.* **1973**, *95*, 5065; Bürgi, H. B.; Lehn, J. M.; Wipff, G. *J. Am. Chem. Soc.* **1974**, *96*, 1956.

³⁴² Anh, N. T.; Eisenstein, O. *Nouv. J. Chem.* **1977**, *1*, 61.

³⁴³ Lodge, E. P.; Heathcock, C. H. *J. Am. Chem. Soc.* **1987**, *109*, 3353 tested the theoretical models by determining diastereoselectivity in the addition of a lithium enolate to a series of chiral aldehydes. The results were in general agreement with the Anh–Eisenstein adaptation of the Felkin model, but the authors concluded that steric effects were as important as electronic effects (energy of the σ* orbital) in determining the transition state for attack of the nucleophile on the carbonyl carbon atom.

³⁴⁴ Cieplak, A. S.; Tait, B. D.; Johnson, C. R. *J. Am. Chem. Soc.* **1989**, *111*, 8447.

**FIGURE 9.62**

Polar Felkin–Anh model for nucleophilic addition to a carbonyl group.

The concepts of Felkin, Anh, and Eisenstein are now recognized collectively with the term *polar Felkin–Anh model*, which is illustrated in Figure 9.62.^{345,346} The favored approach of the nucleophile allows maximum hyperconjugative stabilization of the developing Nu–C bond (the HOMO) with the anti-bonding orbital associated with the C_α–Cl group (the LUMO) and also avoids steric interaction of the nucleophile with the larger group attached to C_α. These models for nucleophilic addition to carbonyl groups prompted extensive experimental and theoretical study. Typically, steric effects are dominant, but electrostatic effects and hyperconjugative effects have been found to be significant in some cases.^{345,347–350}

Problems

- In the addition of bromine to 1,2-diarylethenes, why is the observation that addition of Br₂ to *trans*-stilbene produces almost exclusively meso product not sufficient to show that the mechanism of the addition is anti? That is, why is it necessary to study addition to the *cis* isomer also?
- Predict the product of the reaction of *trans*-cinnamic acid with a mixture of Br₂ and Cl₂ in CH₂Cl₂ solution.
- A reaction mixture composed of 5×10^{-2} M Br₂ and 2.5×10^{-2} M cyclohexene in acetonitrile (containing less than 0.5% water) produced a 90% yield of a product identified as *trans*-1-(*N*-acetylamino)-2-bromocyclohexane. Propose a mechanism for the formation of this compound.
- Refluxing phenylacetaldehyde in acetic anhydride with some potassium acetate leads to the formation of a product, **A**, which has molecular formula C₁₀H₁₀O₂. Treatment of **A** with bromine in CCl₄ leads to a solution containing compound **B**. Adding methanol and allowing the mixture to sit at room temperature leads to a solution from which can be isolated compound **C**, which has the molecular formula C₁₀H₁₃O₂Br. Identify compounds **A**, **B**, and **C**.

³⁴⁵ For a discussion, see Cee, V. J.; Cramer, C. J.; Evans, D. A. *J. Am. Chem. Soc.* **2006**, *128*, 2920.

³⁴⁶ The term Felkin–Anh model refers to a system in which the α chiral center has substituents that differ primarily in terms of size and not in electronic effects.³⁴⁵

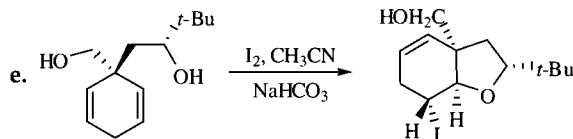
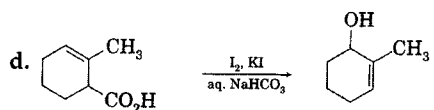
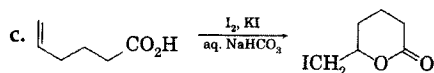
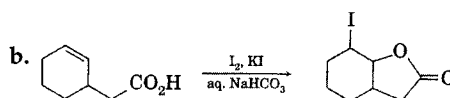
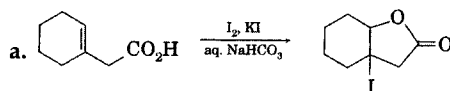
³⁴⁷ Mehta, G.; Chandrasekhar, J. *Chem. Rev.* **1999**, *99*, 1437.

³⁴⁸ Mengel, A.; Reiser, A. *Chem. Rev.* **1999**, *99*, 1191.

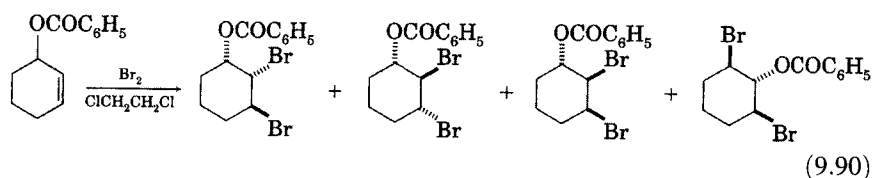
³⁴⁹ Adcock, W.; Trout, N. A. *J. Phys. Org. Chem.* **2008**, *21*, 68.

³⁵⁰ For a summary of theoretical investigations of nucleophilic additions to carbonyl groups, see Bachrach, S. M. *Computational Organic Chemistry*, John Wiley & Sons: Hoboken, NJ, 2007, p. 301 ff.

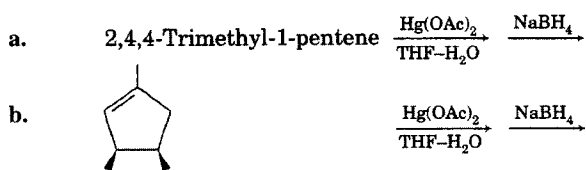
- 9.5. When the disodium salt of (*E*)-2,3-dimethyl-2-butenedioic acid is allowed to react with chlorine in water, a product described as a chloro β -lactone is isolated. When the (*Z*) diastereomer reacts under the same conditions, an isomeric product is found. What are the structures of the products, and how are they formed?
- 9.6. Addition of bromine to *cis*- β -methylstyrene was found to give primarily anti addition in solvents of low polarity (e.g., acetic acid, $\mu = 6$) but primarily syn addition in solvents of higher polarity (e.g., nitrobenzene, $\mu = 35$). In dioxane ($\mu = 2.2$), however, the bromine adduct is formed with only 20% anti addition. Explain this apparent contradiction.
- 9.7. Propose a detailed mechanism to account for each of the following transformations:



- 9.8. Reaction of 5-chloro-5-deuterio-1-hexene in trifluoroacetic acid leads to the formation of 5-chloro-5-deuterio-2-hexyl trifluoroacetate (60%) and 5-chloro-2-deuterio-2-hexyl trifluoroacetate (40%). Propose a mechanism for the formation of these products.
- 9.9. One of the products isolated from the photochemical reaction of iodine with styrene is 1,4-diiodo-2,3-diphenylbutane. Account for the formation of this compound.
- 9.10. Treatment of 2-ethoxy-1,3-butadiene with acid in 80% aqueous acetone yields methyl vinyl ketone. Propose a mechanism to account for the formation of this product.
- 9.11. The addition of bromine to 2-cyclohexenyl benzoate in 1,2-dichloroethane produces four dibromide derivatives (equation 9.90; all products are racemic). Propose a mechanism to account for the formation of each of these compounds.



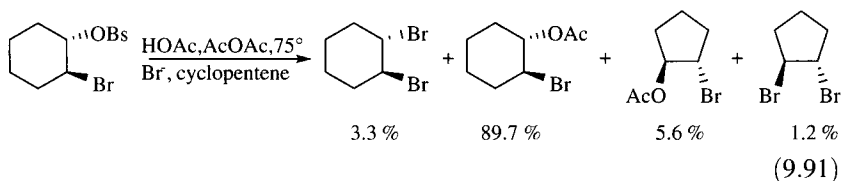
- 9.12. Rationalize the differences in percentage of product formed by syn addition (shown in parentheses) when 1-phenylpropene reacts with each of the following electrophiles: DBr (88%), F₂ (78%), Cl₂ (62%), and Br₂ (17%).
- 9.13. In a study of the addition of bromine to styrene derivatives in acetic acid solution, it was found that reaction of β,β-dimethylstyrene produces both 1-acetoxy-2-bromo and 2-acetoxy-1-bromo derivatives (in roughly a 3 : 1 ratio) as well as the 1,2-dibromo product. Only the 1,2-dibromo adduct and the 1-acetoxy-2-bromo compound were observed in the reaction of styrene, 3-chlorostyrene, 3-nitrostyrene, *cis*-β-methylstyrene, or *trans*-β-methylstyrene under the same conditions. Explain why β,β-dimethylstyrene gives different results from those of other styrene derivatives, and suggest other compounds that might give the same or a greater amount of the 2-acetoxy-1-bromo derivative.
- 9.14. Reaction of chlorine with methyl *trans*-cinnamate in acetic acid leads to the formation of both methyl *erythro*- and methyl *threo*-3-acetoxy-2-chloro-3-phenylpropionate and both methyl *erythro*- and methyl *threo*-2,3-dichloro-3-phenylpropionate in a ratio of 41 : 7 : 12 : 40. Explain the origin of each of these products, and rationalize their relative yields.
- 9.15. Give the structure and stereochemistry of the major product expected from reaction at -78°C of *trans*-3-hexen-1-ol acetate (dissolved in a mixture of CFCl₃, CHCl₃, and ethanol) with a mixture of 1% fluorine in nitrogen that is bubbled into the reaction mixture.
- 9.16. Propose a detailed mechanism for the specific acid-catalyzed formation of butyl acetate when butoxyacetylene is heated in water, and explain why this compound is more reactive toward hydration in water than is butylacetylene.
- 9.17. Oxymercuration of the following pentenols was found to occur with the rate constants indicated (units of M⁻¹s⁻¹) at 25°C: 1-penten-3-ol, 1.5 × 10²; 1-penten-4-ol, 6.1 × 10³; 1-penten-5-ol, >10⁶.
- Rationalize the rate constants for these three compounds.
 - Show the structure of the product(s) expected in each case.
- 9.18. Predict the stereochemistry (*erythro* or *threo*) of the products resulting from the reaction of (*E*)- and (*Z*)-1-hexene-1,2-*d*₂ with dicyclohexylborane.
- 9.19. Predict the products (specifying both regiochemistry and stereochemistry) of the following reactions:



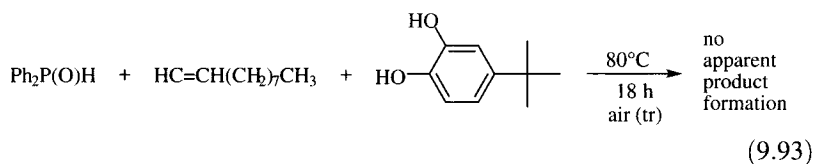
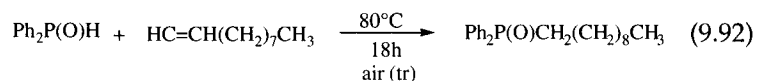
- 9.20. Solvomercuration of cyclohexene with mercuric nitrate in acetonitrile, followed by reduction with sodium borohydride, leads to a product with the molecular formula C₈H₁₅NO.
- What is the structure of the product?
 - Propose a mechanism to account for its formation.
 - Why would mercuric nitrate be used in this reaction instead of mercuric acetate?
- 9.21. Predict which double bond will be epoxidized faster in each of the following compounds:
- isoprene

- b. methyl 2,4-hexadienoate
c. 2-methyl-2,3-butadiene

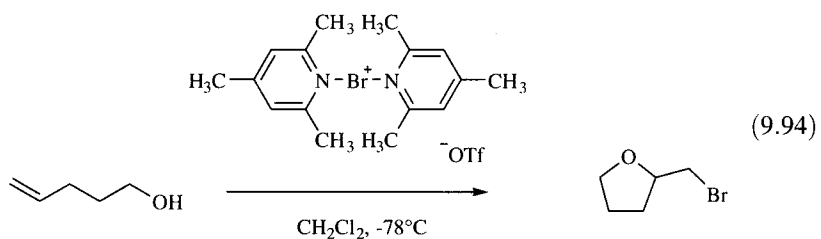
- 9.22. Propose an explanation for the observation that the addition of bromine to propene is 550 times faster than the corresponding addition to ethene when the reaction is carried out in 1,1,2,2-tetrachloroethane but is 80 times faster in acetic acid, 61 times faster in methanol, and 26 times faster in water.
- 9.23. It has been proposed that there is a close analogy between the S_N1 reaction and the electrophilic addition of bromine to an alkene. Compare and contrast the two reactions in terms of (a) gross mechanistic features (especially charge development), (b) substituent effects, and (c) solvent effects.
- 9.24. Propose a mechanism to explain the distribution of products in equation 9.91.



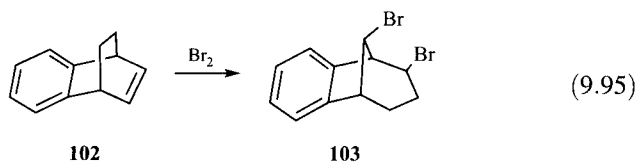
- 9.25. Propose a mechanism to account for the following observations:



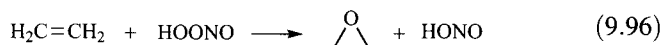
- 9.26. Propose a mechanism for the following reaction:



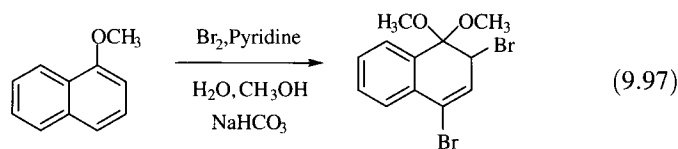
- 9.27. Propose a mechanism to explain the reaction of **102** with bromine to produce **103**.



- 9.28. Reaction of *trans*-cinnamic acid with Br₂ in solution gives *erythro*-2,3-dibromo-3-phenylpropionic acid. Addition of bromine to *trans*-cinnamic acid that has been coordinated with a dicobalt species in an organic "capsule" gives (±)-*threo*-2,3-dibromo-3-phenylpropionic acid, however. What do these results suggest about the differing mechanisms of the two addition reactions?
- 9.29. Propose a mechanism for the reaction of ethene with peroxyntrous acid (equation 9.96).



- 9.30. Propose a mechanism to account for the transformation shown in equation 9.97.



- 9.31. Respond to the following statement by discussing the similarities and differences between conceptual models used in mechanistic chemistry and those used in synthetic chemistry:

Halogenation in polar solvents now assumes a formal resemblance to general acid catalysis initiated by proton donors, which latter can be arranged in a series of decreasing efficacy which parallels their decreasing acid strength. Although we regard positive halogen ions as a fiction, it is not to be ignored that free hydrogen ions in solution are also a fiction, and it may develop that for purposes of classification, positive halogen ions may be just as useful a fiction as free protons.³⁵¹

- 9.32. Do you agree with Kerber's assertion that Markovnikov's rule should not be discussed in introductory organic chemistry textbooks because it "allows students to think for a while that they can avoid getting into the more complex considerations of relative carbocation stabilization. It therefore hinders their learning the general principles that underlie organic reactivity."³⁵² Include in your answer a discussion of the pedagogical value of some other "named" rules taught in introductory organic chemistry.

³⁵¹ Bartlett, P. D.; Tarbell, D. S. *J. Am. Chem. Soc.* **1936**, *58*, 466.

³⁵² Kerber, R. C. *Found. Chem.* **2002**, *4*, 61.

Elimination Reactions

10.1 INTRODUCTION

In an elimination reaction, a substrate loses two substituents, with a resulting increase in its number of units of unsaturation.¹ The familiar E1 and E2 reactions of alkyl halides provide some of the fundamental conceptual models for understanding and categorizing the reactions of organic compounds. As with substitution and addition reactions, however, simple mechanistic labels serve only as beginning points for the discussion of a wide range of elimination pathways.

The most familiar elimination reactions are 1,2-eliminations, which are commonly known as β -eliminations and which are termed 1/2-eliminations in the IUPAC system.¹ In such reactions, a leaving group departs from one (α) atom, while a proton or other group leaves from the adjacent (β) atom (Figure 10.1).² Many fundamental aspects of 1,2-elimination reactions were developed through the work of Hughes, Ingold, and their co-workers and were reported in 1948.^{3,4} The common mechanistic designations E1 (elimination unimolecular) and E2 (elimination bimolecular) were also suggested by Ingold.⁵

As with addition reactions, an important stereochemical distinction in elimination reactions is that of *syn* and *anti* pathways. These pathways were sometimes referred to in older terminology as “*trans*” or “*cis*” eliminations. As was noted in Chapter 9, current preference uses the terms *syn* and *anti* for mechanisms and reserves the terms *cis* and *trans* for structures. When applied to an elimination reaction, the term *anti* means that one group detaches from the top of the molecule (as defined by the developing bond) while the other group

¹ Commission on Physical Organic Chemistry, IUPAC. *Pure Appl. Chem.* **1994**, *66*, 1077.

² The equation is not balanced because the by-products depend on the reaction conditions.

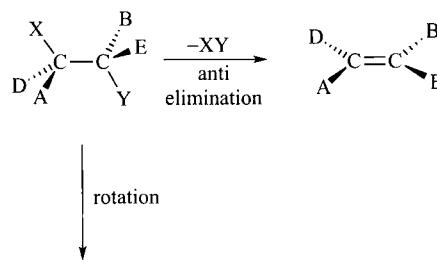
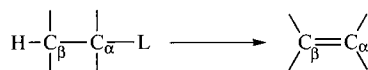
³ A series of papers culminated in a discussion of the mechanisms of elimination reactions by Dhar, M. L.; Hughes, E. D.; Ingold, C. K.; Mandour, A. M. M.; Maw, G. A.; Woolf, L. I. *J. Chem. Soc.* **1948**, 2093.

⁴ An earlier series of investigations was reported by Hughes, E. D.; MacNulty, B. J. *J. Chem. Soc.* **1937**, 1283 and earlier papers in that volume.

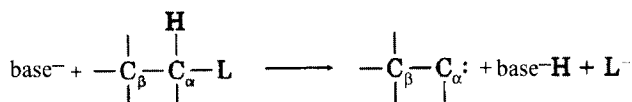
⁵ Hughes, E. D.; Ingold, C. K.; Scott, A. D. *J. Chem. Soc.* **1937**, 1271.

FIGURE 10.1

A 1,2-elimination reaction.

**FIGURE 10.2**

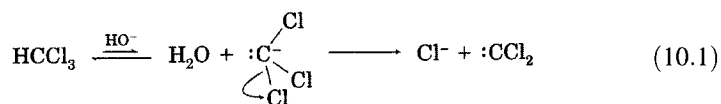
Diastereomeric products of syn and anti elimination.

**FIGURE 10.3**

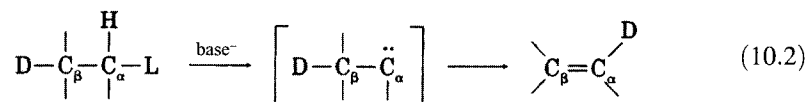
A 1,1-elimination.

detaches from the bottom. In syn elimination, both groups detach from the same face. As shown in Figure 10.2, the syn and anti pathways may be distinguished by the formation of diastereomeric products from appropriately substituted reactants.

There are also elimination reactions in which the two departing groups are not located on adjacent atoms. In a 1,1-elimination (α -elimination), the two leaving groups are bonded to the same atom, so a carbene is produced (Figure 10.3).⁶ A specific example is the base-promoted synthesis of dichlorocarbene from chloroform (equation 10.1).



A 1,1-elimination pathway has also been considered as a possible mechanism for the elimination of trialkylamines from tetraalkylammonium ions. Rearrangement of the carbene produces an alkene, so such a pathway can be distinguished from 1,2-elimination only through isotopic labeling (equation 10.2).



⁶ The base-promoted 1,1-cleavage of chloroform to dichlorocarbene was reported by Hine, J.; Dowell, A. M., Jr. *J. Am. Chem. Soc.* **1954**, *76*, 2688.

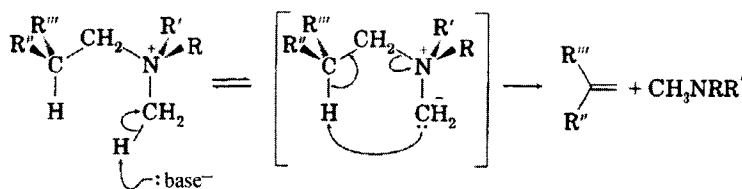
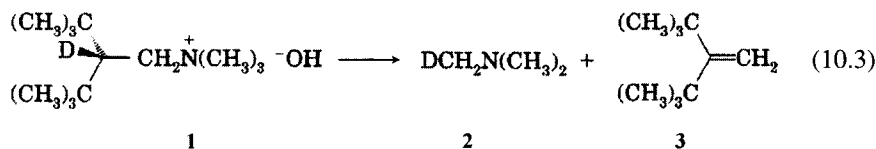
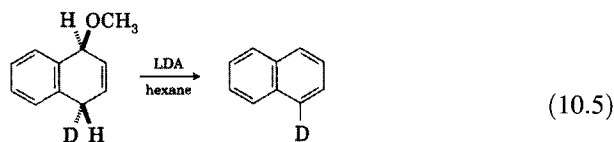
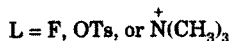
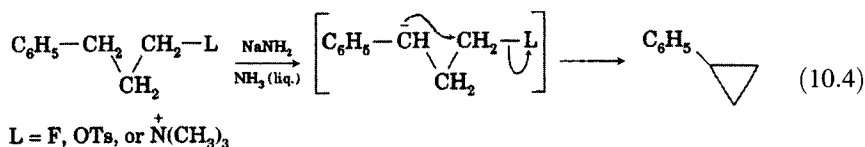


FIGURE 10.4
An α',β -elimination pathway.

An alternative pathway for the elimination of tetraalkylammonium ions is the ylide (α,β) pathway shown in Figure 10.4.⁷ Evidence for the ylide mechanism in the reaction of 1 was reported by Cope and Mehta, who found that the deuterium label appeared in one of the methyl groups of trimethylamine (2) and not in the alkene (3, equation 10.3).⁸



Reactions that are formally 1,3-eliminations (γ -eliminations) have also been observed, as in the example shown in equation 10.4.⁹ Reactions of this type could also be termed intramolecular S_N2 reactions. 1,4- or δ -Eliminations can occur when there is a double bond between the atoms bearing the leaving groups, as in the reaction shown in equation 10.5.^{10,11}



(LDA = lithium diisopropylamide)

⁷ The mechanism of the ylide reaction is very similar to the concerted mechanism proposed for pyrolytic eliminations. See the discussion beginning on page 681.

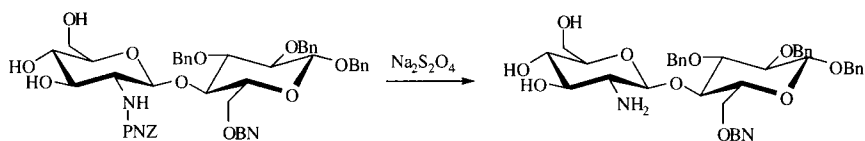
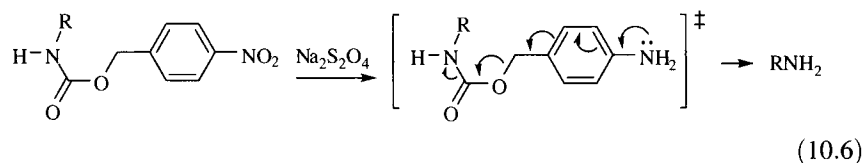
⁸ Cope, A. C.; Mehta, A. S. *J. Am. Chem. Soc.* **1963**, *85*, 1949.

⁹ Bumgardner, C. L. *Chem. Commun.* **1965**, 374. 1,2-Dehydrohalogenation (and subsequent reaction with sodium amide and additional starting material to produce diphenylhexenes) predominates when L is bromine or chlorine. The results also suggest that the rate constant for 1,2-elimination is more sensitive to leaving group ability than is the rate constant for 1,3-elimination.

¹⁰ Moss, R. J.; Rickborn, B. *J. Org. Chem.* **1986**, *51*, 1992.

¹¹ These elimination reactions can be synthetically useful. See, for example, Tobia, D.; Rickborn, B. *J. Org. Chem.* **1986**, *51*, 3849; Banwell, M. G.; Papamihail, C. *J. Chem. Soc. Chem. Commun.* **1981**, 1182.

An example of a 1,6-elimination is the removal of the *p*-nitrobenzyloxy-carbonyl protecting group in organic synthesis. As illustrated in equation 10.6, reduction of the nitro group with $\text{Na}_2\text{S}_2\text{O}_4$ produces an amino group that can instigate the elimination reaction, releasing RNH_2 under relatively mild conditions. An application of this reaction in carbohydrate synthesis is shown in equation 10.7.



PNZ = *p*-nitrobenzyloxycarbonyl; Bn = benzyl

(10.7)

The 1,6- and higher elimination reactions are also finding use in the design of prodrugs—substances that can be administered in a biologically inactive form but that can be converted *in vivo* into a pharmacologically active compound. Such a prodrug might incorporate a segment that acts as a “trigger” for enzymatic conversion into a derivative, which can then undergo an elimination reaction to release the active form of the drug (Figure 10.5).¹² An analogous prodrug delivery system incorporates a naphthalene moiety to enable a 1,8-elimination to release the drug after removal of a protecting group (PG, Figure 10.6).^{13,14}

All of the reactions above maintain the molecular skeleton that connects the groups being eliminated. There is also a class of elimination reactions, elucidated by Grob, that are known as *fragmentation reactions* because carbon skeletal bonds are broken during the reaction.¹⁵ In the generalized fragmentation shown in equation 10.8, the letters a, b, c, and d generally represent carbon, nitrogen, or oxygen atoms, and L is a leaving group. (For the purpose of generality, charges are deliberately omitted.) Fragmentation reactions may

¹² Compare Greenwald, R. B.; Pendri, A.; Conover, C. D.; Zhao, H.; Choe, Y. H.; Martinez, A.; Shum, K.; Guan, S. *J. Med. Chem.* **1999**, *42*, 3657.

¹³ de Groot, F. M. H.; Loos, W. J.; Koekkoek, R.; van Berkom, L. W. A.; Busscher, G. F.; Seelen, A. E.; Albrecht, C.; de Bruijn, P.; Scheeren, H. W. J. *Org. Chem.* **2001**, *66*, 8815.

¹⁴ For examples of 1,6-, 1,8-, and 1,10-eliminations, respectively, see van Boom, J. H.; Brandsma, L.; Arens, J. F. *Recl. Trav. Chim. Pays-Bas* **1966**, *85*, 952; Rudolf, K.; Koenig, T. *Tetrahedron Lett.* **1985**, *26*, 4835; Rappoport, Z.; Greenblatt, J.; Apeloig, Y. *J. Org. Chem.* **1979**, *44*, 3687.

¹⁵ (a) Grob, C. A. in *Theoretical Organic Chemistry*; Butterworths Scientific Publications: London, 1959; pp. 114–126; (b) Grob, C. A.; Schiess, P. W. *Angew. Chem. Int. Ed. Engl.* **1967**, *6*, 1; (c) Grob, C. A. *Angew. Chem. Int. Ed. Engl.* **1969**, *8*, 535.

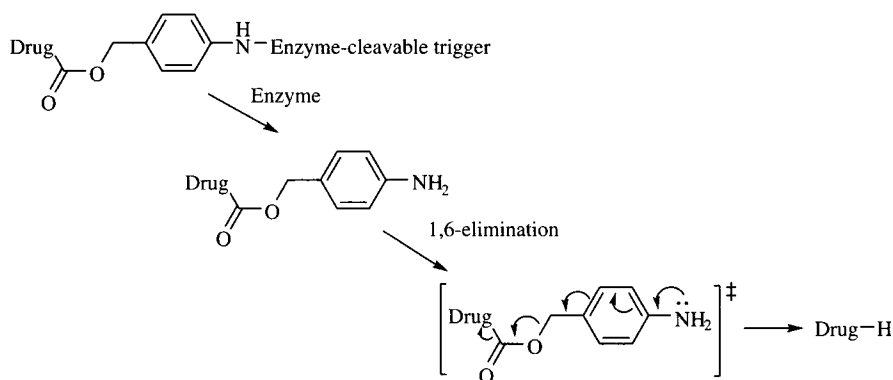


FIGURE 10.5
1,6-Elimination in a prodrug delivery system.

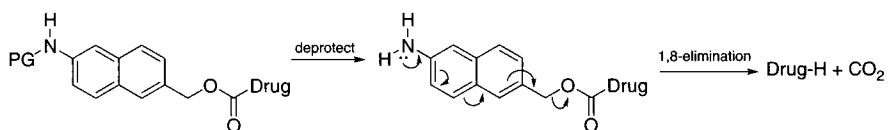
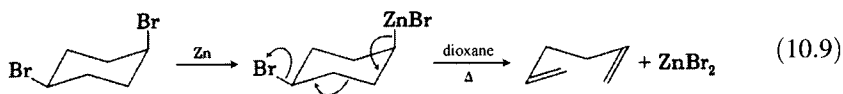
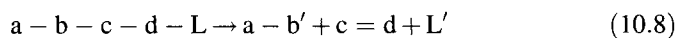
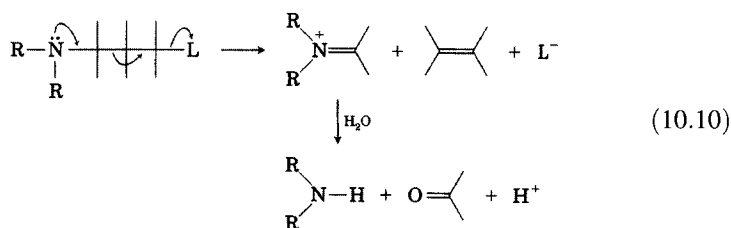


FIGURE 10.6
1,8-Elimination in a prodrug delivery system.

occur by one-step or by multistep mechanisms.^{15c,16} Such reactions are useful for both structure elucidation and synthesis.^{15b} One example of a fragmentation reaction is the reaction of *cis*-1,4-dibromocyclohexane with zinc in hot dioxane solution (equation 10.9).¹⁷



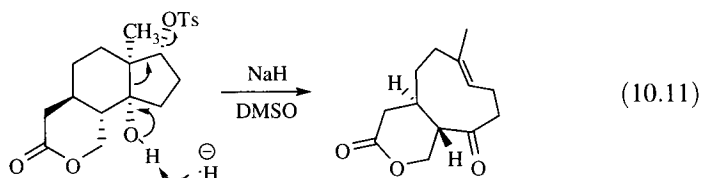
Another example is the fragmentation that accompanies solvolysis of γ -aminoalkyl compounds.



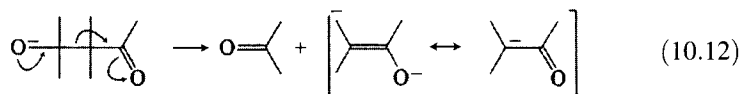
¹⁶ As noted in reference 20, fragmentation reactions can be described as F1, F2, and F1cb by analogy to E1, E2, and E1cb reactions.

¹⁷ The mechanism shown is intended to illustrate a possible pattern of electron movement leading to bond breaking. Grob, C. A.; Baumann, W. *Helv. Chim. Acta* **1955**, *38*, 594.

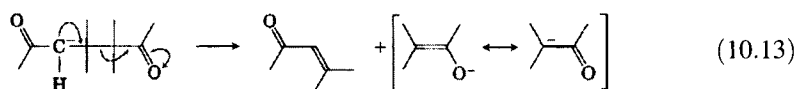
Grob fragmentation reactions have proved useful in organic synthesis, as, for example, in the synthesis of compounds with larger rings (equation 10.11).¹⁸



Fragmentation reactions also formally include the reverse aldol reaction,



and reverse Michael addition,



Extensive discussion of these and many other types of elimination reactions can be found in several reviews.^{19–22} We will focus here on 1,2-eliminations, especially dehydrohalogenation, dehydration, dehalogenation, deamination reactions, and pyrolytic eliminations.

10.2 DEHYDROHALOGENATION AND RELATED 1,2-ELIMINATION REACTIONS

Potential Energy Surfaces for 1,2-Elimination

There are three essential aspects of a 1,2-elimination reaction such as that shown in Figure 10.1:

1. the bond between C_β and a hydrogen atom is lost,
2. the bond between C_α and the leaving group (L) is lost, and
3. an additional bond forms between C_α and C_β .

We can distinguish three general classifications of elimination reactions on the basis of the timing of these processes, and transition structures for each are

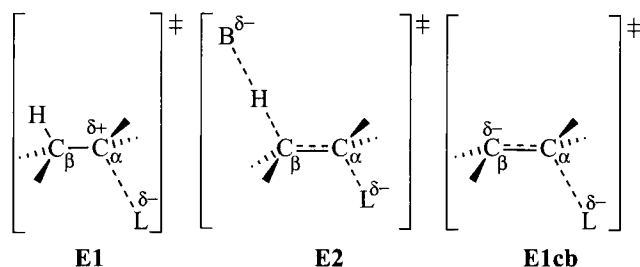
¹⁸ Renneberg, D.; Pfander, H.; Leumann, C. J. *J. Org. Chem.* **2000**, *65*, 9069.

¹⁹ Banthorpe, D. V. *Elimination Reactions*; Elsevier Publishing: Amsterdam, 1963.

²⁰ Saunders, W. H., Jr.; Cockerill, A. F. *Mechanisms of Elimination Reactions*; Wiley-Interscience: New York, 1973.

²¹ Bartsch, R. A.; Závada, J. *Chem. Rev.* **1980**, *80*, 453.

²² Cockerill, A. F.; Harrison, R. G. in Patai, S., Ed. *The Chemistry of Double-Bonded Functional Groups*, Part I; Wiley-Interscience: New York, 1977; pp. 155–189.

**FIGURE 10.7**

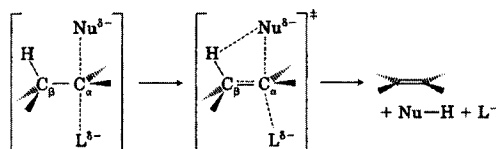
Transition structure models for 1,2-elimination reactions.

shown in Figure 10.7.²³ If the $C_\alpha-L$ bond dissociates first, the reaction is termed an E1 reaction. If both the $C_\alpha-L$ and the $C_\beta-H$ bonds are lost at the same time, the reaction is an E2 mechanism. If the C_β proton is abstracted first, then we call the reaction an E1cb (elimination unimolecular conjugate base) reaction, since proton removal leaves a carbanion that is the conjugate base of the original substrate.²⁴

In the nomenclature system recommended by the IUPAC Commission on Physical Organic Chemistry,²⁵ the E2 reaction is denoted $A_{xh}D_H D_N$. Here A_{xh} indicates that loss of a proton is not spontaneous but occurs through association of a base (nucleophile) with the proton. The E1 reaction can be termed $D_N + D_E$ but is more completely described as $D_N + A_{xh}D_H$. In this case the plus sign indicates that dissociation of the leaving group occurs first, followed by abstraction of a proton by base. The E1cb reaction is termed $A_{xh}D_H + D_N$, signifying that removal of the proton by base occurs first, then the leaving group departs.

The three categories of 1,2-eliminations can be represented as paths on a More O'Ferrall-Jencks diagram, a two-dimensional projection of a

²³ All of the 1,2-elimination mechanisms discussed here have assumed that, at some point, a base abstracts a proton β to the leaving group by directly attacking that proton. Some authors have distinguished between the E2H ("normal E2") pathway and an E2C pathway, in which the base interacts with the α -carbon atom attached to the leaving group prior to removal of the β -hydrogen atom:



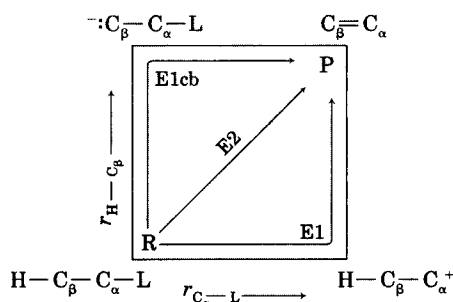
It was thought that this model could provide for a weaker $C_\beta-H$ bond that could more easily be removed by the weak base by allowing the base to act first as a nucleophile to loosen the $C_\alpha-L$ bond partially. The degree to which the E2C mechanism might compete with the E2H mechanism was thought to be a function of the substitution of the substrate and the polarity of the medium. Elimination mechanisms are not currently discussed in terms of the E2C pathway, however. For leading references to literature discussions of this issue, see Ford, W. T. *Acc. Chem. Res.* **1973**, *6*, 410; Biale, G.; Cook, D.; Lloyd, D. J.; Parker, A. J.; Stevens, I. D. R.; Takahashi, J.; Winstein, S. *J. Am. Chem. Soc.* **1971**, *93*, 4735; Parker, A. J. *Chem. Tech.* **1971**, 297; Kwart, H.; Wilk, K. A. *J. Org. Chem.* **1985**, *50*, 3038; McLennan, D. J. *Annu. Rep. Prog. Chem.* **1970**, *B*, 59; Bunnett, J. F.; Midgal, C. A. *J. Org. Chem.* **1989**, *54*, 3041.

²⁴ In Figure 10.7 the transition structure for the E1cb reaction indicates that the β -proton has already been abstracted by a base, so the rate-limiting step is detachment of the leaving group. As discussed on page 642, there are many variations of the E1cb mechanism.

²⁵ Commission on Physical Organic Chemistry, IUPAC. *Pure Appl. Chem.* **1989**, *61*, 23.

FIGURE 10.8

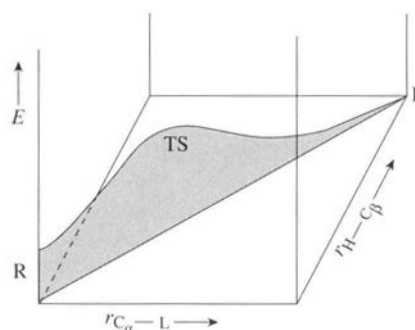
Structure–energy surface for 1,2-elimination reactions.



three-dimensional potential energy surface for a reaction (Chapter 6).^{26,27} In Figure 10.8 the vertical axis on the printed page represents the dissociation of the $\text{H}-\text{C}_{\beta}$ bond, while the horizontal axis represents the dissociation of the $\text{C}_{\alpha}-\text{L}$ bond. The energy of the species at any point on the surface would be represented in the third dimension, coming out of the page toward the viewer. Each of the reactions represented in Figure 10.7 would have its own three-dimensional potential energy surface, with a line in Figure 10.8 showing the projection onto the plane of a path that follows the lowest energy pathway from reactant to product on the surface above.

Figure 10.8 indicates graphically that the key differences among the E1, E2, and E1cb pathways are the timing of the two bond-breaking steps and the possible existence of an intermediate along the reaction coordinate. If the proton and leaving group have departed to the same extent at any point along the reaction coordinate, then the reaction follows the diagonal line from reactant to product, and there is a concerted E2 reaction. The E1 reaction, in which departure of the leaving group produces a cation that later undergoes proton removal, is represented by the line proceeding through the lower right corner. The E1cb pathway, in which proton removal forms a carbanion intermediate, proceeds through the upper left corner. Note that this figure represents only the bonding changes for the reacting substrate, not for any bases or solvent molecules that may be important to the reaction.

The idea that Figure 10.8 is a projection of a three-dimensional surface may be made clearer by Figure 10.9, in which the shaded portion of the

**FIGURE 10.9**

Cross section through potential energy surface for E2 reaction.

²⁶ Compare More O'Ferrall, R. A. *J. Chem. Soc. B* **1970**, 274; More O'Ferrall, R. A. in Patai, S., Ed. *The Chemistry of the Carbon-Halogen Bond*, Vol. 2; John Wiley & Sons: New York, 1973; Jencks, D. A.; Jencks, W. P. *J. Am. Chem. Soc.* **1977**, 99, 7948.

²⁷ Bunnett, J. F. *Angew. Chem. Int. Ed. Engl.* **1962**, 1, 225.

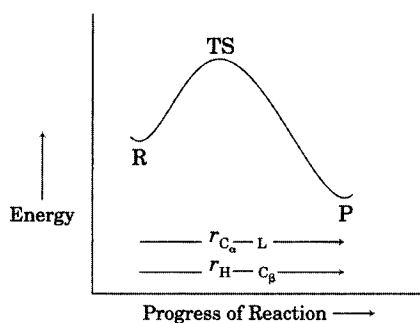


FIGURE 10.10
Reaction coordinate diagram for E2 reaction.

drawing represents a cross section from reactant to product through the potential energy surface. Any deviation perpendicular to the curve shown in Figure 10.9 requires an increase in energy of the system. Thus, the transition state is only an energy maximum for the diagonal pathway from $\text{H}-\text{C}_{\beta}-\text{C}_{\alpha}-\text{L}$ to $\text{C}_{\beta}=\text{C}_{\alpha}$. It is an energy minimum on another cross section, from $^-\text{C}_{\beta}-\text{C}_{\alpha}-\text{L}$ to $\text{H}-\text{C}_{\beta}-\text{C}_{\alpha}^+$. In other words, the transition state is a saddle point on the three-dimensional surface for this E2 reaction. This diagonal cross section can be redrawn in two dimensions as Figure 10.10, and that is the diagram commonly used to represent the lowest energy pathway from reactants to products in an E2 reaction.

An analogous cross section of the minimum energy path for an E1 reaction is shown in Figure 10.11. Now the reaction pathway appears to hug the boundaries of the drawing. Again, any perpendicular deviation from this pathway represents an increase in energy. As noted in Chapter 6, the reaction coordinate diagram for the E1 reaction (Figure 10.12) has a horizontal scale labeled progress of reaction that can conveniently be viewed as a combination of two different sets of nuclear coordinates. From the reactant (R) to the

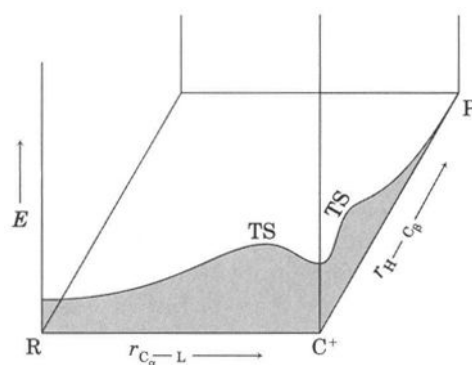


FIGURE 10.11
Potential energy surface for E1 reaction.

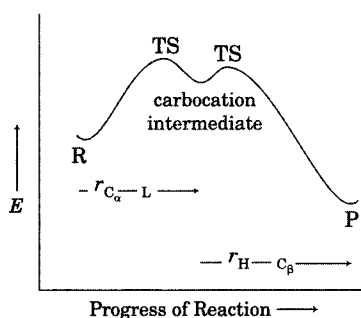
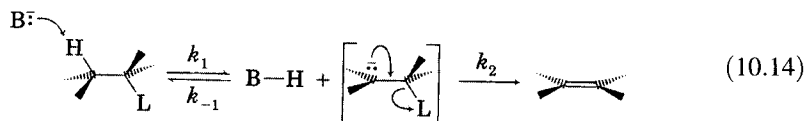


FIGURE 10.12
Reaction coordinate diagram for E1 reaction.

carbocation intermediate, the reaction coordinate is approximated by the distance between C_α and L, while from the intermediate to the product (P), the reaction coordinate is essentially the change in the distance between C_β and a proton.

Analogous drawings can be made for the E1cb reaction, but the situation is more complicated because there are many variations of this type of reaction. It is useful to differentiate among several categories of E1cb reactions with reference to the rate constants shown in equation 10.14.^{28,29}



Applying the steady-state approximation to the carbanion intermediate in equation 10.14 leads to the rate expression

$$\text{Rate} = \frac{k_2 k_1 [\text{RL}][\text{B}^-]}{k_{-1} [\text{BH}] + k_2} \quad (10.15)$$

The apparent rate law for a particular E1cb reaction depends on the relative magnitudes of k_1 , k_{-1} , and k_2 and on the concentrations of B^- and BH . If k_1 is much greater than both k_{-1} and k_2 , and if the initial concentration of B^- is larger than the initial concentration of RL , then essentially all of RL is converted to the carbanion intermediate. Changes in the concentration of B^- therefore have no appreciable effect on the rate of the reaction, and the reaction appears to follow first-order kinetics,

$$\text{Rate} \approx k_{\text{exp}} [\text{RL}] \quad (10.16)$$

Such a reaction is termed $\text{E1}_{(\text{anion})}$ or $\text{E1cb}_{(\text{anion})}$. For a deuterium-labeled reactant ($\text{D}-\text{C}_\beta-\text{C}_\alpha-\text{L}$), this type of reaction is characterized by rapid exchange of deuterium with protons from protic solvents and by a β -hydrogen 1° kinetic isotope effect ($k_{\text{H}}/k_{\text{D}}$) of 1.0. There is also an appreciable element effect, meaning that the rate constant for the reaction depends on the leaving group ability of L. An example of an $\text{E1}_{(\text{anion})}$ mechanism is the elimination of methanol from 2-phenyl-*trans*-2-methoxy-1-nitrocyclopentane (4) by the mechanism shown in Figure 10.13.³⁰

If $k_{-1}[\text{BH}]$ is much greater than k_2 but is less than $k_1[\text{RL}][\text{B}^-]$, the equilibrium for the first step in equation 10.14 does not lie completely in favor of the anion. Now equation 10.15 becomes

$$\text{Rate} = \frac{k_2 k_1 [\text{RL}][\text{B}^-]}{k_{-1} [\text{BH}]} \quad (10.17)$$

²⁸ Bordwell, F. G. *Acc. Chem. Res.* **1972**, *5*, 374 analyzed a range of mechanisms for elimination reactions.

²⁹ See also (a) Rappoport, *Z. Tetrahedron Lett.* **1968**, 3601; (b) reference 21.

³⁰ Bordwell, F. G.; Yee, K. C.; Knipe, A. C. *J. Am. Chem. Soc.* **1970**, *92*, 5945; see also Bordwell, F. G.; Vestling, M. M.; Yee, K. C. *J. Am. Chem. Soc.* **1970**, *92*, 5950.

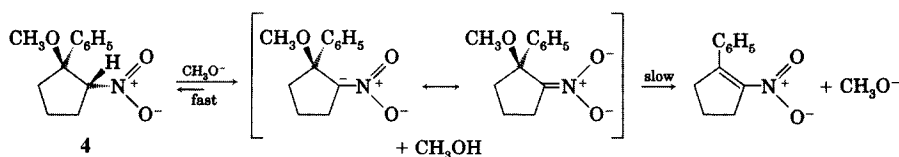


FIGURE 10.13
E1_(anion) mechanism for 1,2-elimination.

If BH is also the solvent for the reaction, then its concentration effectively does not vary during the reaction. Therefore, the rate expression becomes

$$\text{Rate} = k_{\text{obs}}[\text{RL}][\text{B}^-] \quad (10.18)$$

This type of elimination is known as an E1_{cbR} (elimination, unimolecular, conjugate base, reversible) reaction, and a generalized reaction coordinate diagram is shown in Figure 10.14. Such reactions exhibit C_β-H/D exchange and a 1° hydrogen kinetic isotope effect ($k_{\text{H}}/k_{\text{D}}$) of 1.0. An example of an E1_{cbR} is shown in Figure 10.15.³¹

Just as ion pair intermediates are important in substitution reactions, they may also play an important role in elimination reactions.³² Figure 10.16 shows an example of an E1_{cbip} (elimination, unimolecular, conjugate base, ion pair) mechanism.^{31b} Here again there is a fast preequilibrium formation of a carbanion. In this case, however, the carbanion and the cation are held together as an ion pair due to Coulombic forces that are not overcome by solvation.

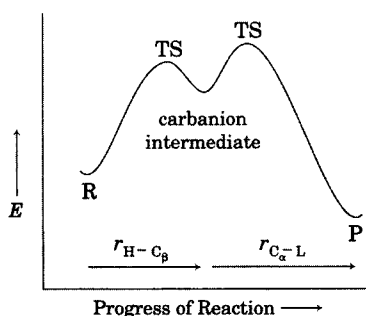
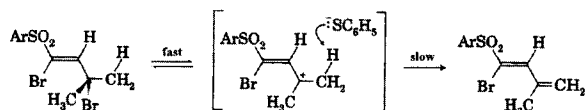


FIGURE 10.14
Reaction coordinate diagram for an E1_{cbR} reaction. (Note that the first transition state is lower in energy than the second.)

³¹ (a) Miller, S. I.; Lee, W. G. *J. Am. Chem. Soc.* **1959**, *81*, 6313; (b) Kwok, W. K.; Lee, W. G.; Miller, S. I. *J. Am. Chem. Soc.* **1969**, *91*, 468.

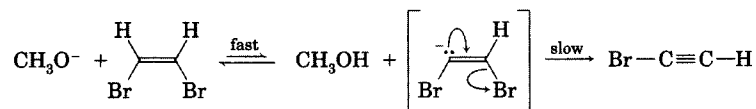
³² As another example, the E2_{ip} (elimination, bimolecular, ion pair) mechanism is characterized by dissociation of the C_α-L bond to form a tight carbocation-L⁻ ion pair that then undergoes rate-limiting proton abstraction by a base:



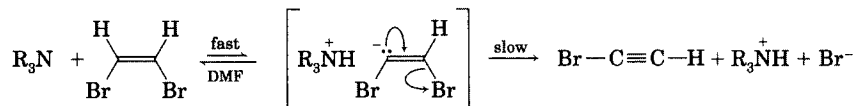
For a discussion, see reference 28. Also see Bordwell, F. G.; Mecca, T. G. *J. Am. Chem. Soc.* **1972**, *94*, 2119. It may also be possible that the ion pair forms during, and not before, attack of the base on the substrate. Saunders, W. H., Jr. *Acc. Chem. Res.* **1976**, *9*, 19 discussed the approaches used to distinguish concerted and nonconcerted elimination mechanisms.

FIGURE 10.15

E1cb_R mechanism. (Adapted from reference 31b.)

**FIGURE 10.16**

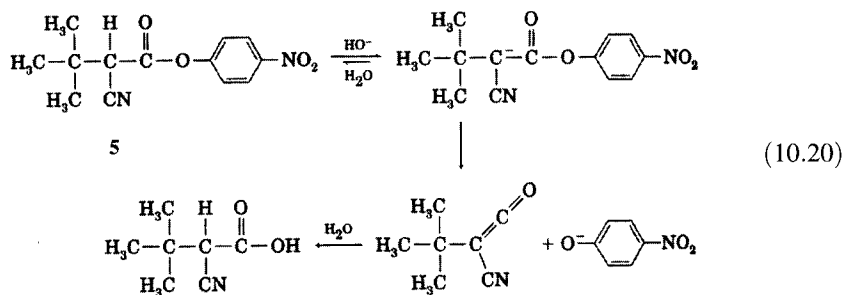
E1cb_{ip} mechanism. (Adapted from reference 31b.)



If k_2 is much greater than $k_{-1}[\text{BH}]$ and if $k_{-1}[\text{BH}]$ is much greater than k_1 (a situation that may arise if the intermediate carbanion is strongly hydrogen bonded in a protic solvent), then equation 10.15 becomes

$$\text{Rate} \approx k_1[\text{RL}][\text{B}^-] \quad (10.19)$$

That is, the reaction exhibits second-order kinetics even though the actual loss of the leaving group occurs by a unimolecular decomposition of the conjugate base of the reactant.³³ Such a mechanism is termed E1cb₁ (elimination, unimolecular, conjugate base, irreversible) and is characterized by negligible C_β-H isotope exchange with solvent and with a substantial 1° hydrogen kinetic isotope effect ($k_{\text{H}}/k_{\text{D}}$ in the range of 2 to 8). The hydrolysis of *p*-nitrophenyl 2-cyano-3,3-dimethylbutanoate (**5**) was found to occur by an E1cb₁ mechanism at pH values at which *p*-nitrophenyl 2-cyanoacetate reacted by an E1cb_R mechanism. In this case it appears that the deprotonation is effectively irreversible because the methyl groups in **5** provide a steric barrier to reprotonation of the intermediate anion.³⁴

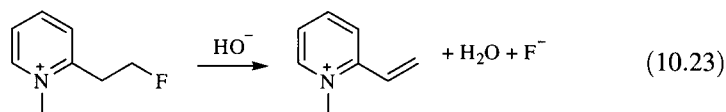
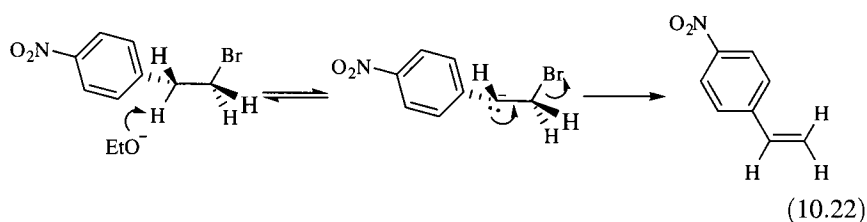
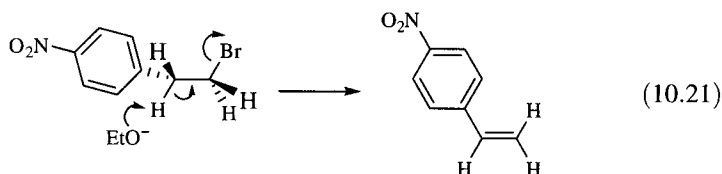


The IUPAC nomenclature system provides precise terminology for these elimination reactions.²⁵ The E1cb_R reaction is A_{xh}D_H + D_N[‡], where ‡ indicates that departure of the leaving group is the rate-limiting step. The E1cb₁ reaction is A_{xh}D_H + D_N. The E1cb_{ip} reaction is A_{xh}D_H[‡]*D_N if removal of proton is rate limiting. Here * indicates that the species does not persist long enough to equilibrate with the species in its environment. If the departure of the leaving group is rate limiting, then the E1cb_{ip} reaction is termed A_{xh}D_H*D_N[‡].

³³ Bordwell, F. G.; Weinstock, J.; Sullivan, T. F. *J. Am. Chem. Soc.* **1971**, *93*, 4728.

³⁴ Inoue, M.; Bruce, T. C. *J. Org. Chem.* **1986**, *51*, 959.

The distinction between various mechanistic possibilities for 1,2-elimination reactions is sometimes difficult, and more detailed investigations can reveal greater mechanistic complexity than we might assume. For example, there was a report that the elimination of HBr from 2-(4-nitrophenyl)ethyl bromide, the “classical E2 reaction” (equation 10.21), occurs instead by an E1cb mechanism (equation 10.22).³⁵



De Angelis and co-workers found from experimental and theoretical studies that the E1cb and E2 paths seemed to “merge smoothly” into each other in the hydroxide-promoted elimination of HF from 2-(2-fluoroethyl)-1-methylpyridinium ion in aqueous solution (equation 10.23).^{36,37} The potential energy surface in Figure 10.17 suggests that the energy barrier for fluoride loss decreases continually as the bond from carbon to the abstracted proton lengthens. As a result, the potential energy surface is nearly flat for C–H distances of ca. 1.8 Å, and the carbanion intermediate can lose fluoride “almost instantaneously.”³⁷

Competition Between Substitution and Elimination

It is an axiom of organic chemistry that substitution and elimination reactions are competitive processes.⁵ Elimination is generally favored at higher temperatures, while lower temperatures result in a higher percentage of substitution product in both E1 and E2 reactions. For example, in the solvolysis of *t*-butyl chloride in 80% aqueous ethanol, the percentage of isobutene

³⁵ Handoo, K. L.; Lu, Y.; Zhao, Y.; Parker, V. D. *Org. Biomol. Chem.* **2003**, *1*, 24.

³⁶ Alunni, S.; De Angelis, F.; Ottavi, L.; Papavasileiou, M.; Tarantelli, F. *J. Am. Chem. Soc.* **2005**, *127*, 15151.

³⁷ De Angelis, F.; Tarantelli, F.; Alunni, S. *J. Phys. Chem. B.* **2006**, *110*, 11014.

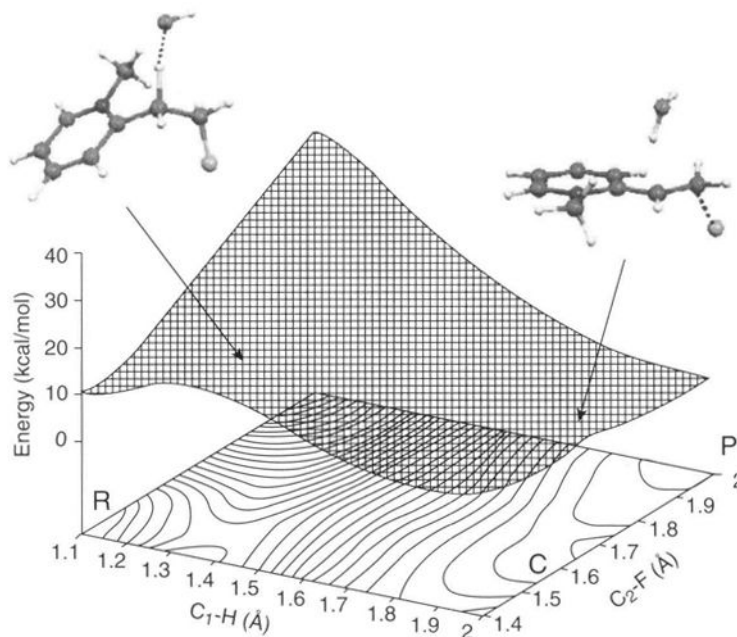


FIGURE 10.17

Calculated potential energy surface for the elimination reaction in equation 10.23. (Reproduced from reference 37.)

increased from 16.8% to 36.3% as the temperature was increased from 25°C to 65°C.^{38,39} The effect of temperature on the ratio of substitution to elimination in a 2° substrate was smaller: the percentage of elimination product from the reaction of 2-bromopropane with ethoxide in ethanol was 53% at 45°C and 57% at 75°C. These trends can be explained by the kinetic data for competition between S_N2 and E2 pathways for reactions of several substrates with sodium ethoxide (Table 10.1). Both E_a and log A are seen to be greater for elimination than for substitution.^{38,40}

Elimination becomes more competitive with substitution as the number of alkyl substituents on the substrate increases. Table 10.2 shows rate constants for S_N2 and E2 reactions of a series of alkyl bromides with sodium ethoxide in ethanol at 55°C.⁴¹ The rate constant for elimination increases along the series from ethyl bromide to propyl bromide to isobutyl bromide. The more substituted alkenes formed with propyl bromide and (to a greater extent) with isobutyl bromide are more stable than the alkene formed from ethyl bromide. Because the transition structures have some double bond

³⁸ Cooper, K. A.; Hughes, E. D.; Ingold, C. K.; Maw, G. A.; MacNulty, B. J. *J. Chem. Soc.* **1948**, 2049. Kinetic studies revealed an E_a of 23.2 kcal/mol and a log A of 11.9.

³⁹ In many early papers, the solvent composition is reported in quotation marks, as in "80% ethanol," meaning a solvent mixture composed by mixing 80 volumes of absolute ethanol and 20 volumes of water. Due to volume changes on mixing, the volume of ethanol added is not necessarily 80% of the final volume of the mixture.

⁴⁰ In addition, reactions of the neutral substrates are seen to have higher activation energies and smaller A values for E2 reaction than do the corresponding reactions of ionic substrates. The smaller A values (i.e., more negative values of ΔS^\ddagger) for neutral reactants may be related to the change in solvent order between the reactants and the transition structures for these species. We expect less change in solvent entropy on going from a charged reactant to a transition structure with dispersed charge than would be the case for the conversion of a neutral substrate to a transition structure with developing charges.

⁴¹ Dhar, M. L.; Hughes, E. D.; Ingold, C. K.; Masterman, S. *J. Chem. Soc.* **1948**, 2055.

TABLE 10.1 Activation Parameters for Substitution and Elimination Reactions

Substrate	Solvent	log A (S_N2)	E_a (S_N2) (kcal/mol)	log A (E2)	E_a (E2) (kcal/mol)
2-Bromopropane	60% Ethanol	9.4	20.8	10.4	22.1
2-Bromopropane	80% Ethanol	10.1	21.7	10.9	22.6
2-Iodopropane	60% Ethanol	10.1	20.7	11.1	22.2
2-Chloropropane	80% Ethanol	9.4	23.1	10.7	24.8
<i>t</i> -Butyl bromide	100% Ethanol	—	—	10.1	19.7
<i>t</i> -Butyldimethylsulfonium	100% Ethanol	—	—	14.9	24.9
(2-Phenylethyl)dimethylsulfonium	100% Ethanol	—	—	15.0	23.9

Source: Reference 38.

character, the Hammond postulate predicts lower transition state energies and faster rates of formation of the more substituted products. Steric effects can also be seen in elimination reactions. For example, the rate constants for the E2 reactions of the 1° alkyl bromides decrease slightly along the series from *n*-propyl to *n*-butyl to *n*-pentyl bromides. The trend closely parallels the decrease in the rate constants of S_N2 reactions along the same series, a trend that is attributed to the dominance of steric effects on the rates of S_N2 reactions.

Stereochemistry of 1,2-Elimination Reactions

It is useful to discuss the stereochemistry of bimolecular elimination reactions in terms of the H–C–C–L dihedral angle (Figure 10.18). In an anti-periplanar conformation, the dihedral angle H–C_β–C_α–L is near 180°, while it is near 0° in a syn-periplanar conformation. If the dihedral angle is exactly 180°, the conformation is anti-coplanar, while it is syn-coplanar if the dihedral is exactly 0°. ⁴² An anti-clinal conformation has a dihedral angle of approximately 120°, while a syn-clinal conformation has a dihedral of about 60°.

Representing the C_α–L and C_β–H bonds as shown in Figure 10.19 makes it apparent that both the anti-coplanar and syn-coplanar conformations allow the development of π bonding without the necessity for rotation about the carbon–carbon double bond as the elimination occurs. With the anti-clinal

TABLE 10.2 Structural Effects on Rate Constants of E2 and S_N2 Reactions with Sodium Ethoxide in Ethanol Solution at 55°C

Alkyl Bromide	10 ⁴ k for S_N2 (M ⁻¹ s ⁻¹)	10 ⁵ k for E2 (M ⁻¹ s ⁻¹)
CH ₃ CH ₂ Br	17.2	1.6
CH ₃ CH ₂ CH ₂ Br	5.5	5.3
CH ₃ CH ₂ CH ₂ CH ₂ Br	4.0	4.3
CH ₃ CH ₂ CH ₂ CH ₂ CH ₂ Br	3.6	3.5
(CH ₃) ₂ CHCH ₂ Br	0.6	8.5

Source: Reference 41.

⁴² See the discussion of coplanar and periplanar by Kane, S.; Hersh, W. H. J. *Chem. Educ.* 2000, 77, 1366.

FIGURE 10.18

Conformational designations.

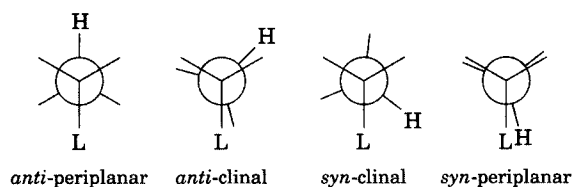
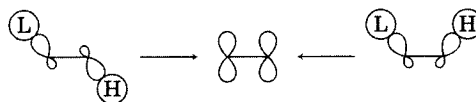


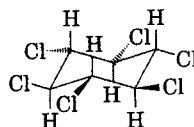
FIGURE 10.19

Orbital model for anti-coplanar (left) and syn-coplanar (right) elimination.



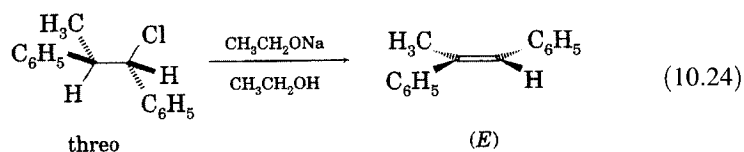
and syn-clinal conformations, however, rotation of 60° about the carbon-carbon bond would be needed in order to develop the parallel p orbitals of the developing double bond. Thus, we might expect the electronic energies to be lower for transition structures having syn-coplanar and anti-coplanar conformations than for other conformations.

Experimental data indicate that the anti pathway for E2 reactions is favored over the syn pathway. In one of the earliest studies of the stereochemistry of the E2 reaction, Cristol found the rate constant for the dehydrochlorination of the β isomer of benzene hexachloride (1,2,3,4,5,6-hexachlorocyclohexane, **6**), in which each chlorine is cis to the hydrogen atoms on either side of it, to be only 10^{-4} times those of the other benzene hexachloride isomers. Since each of the other isomers has at least one hydrogen atom trans to a chlorine atom on an adjacent carbon atom, the low reactivity of **6** suggested that the E2 reaction occurs preferentially when there is a trans relationship for the hydrogen atom and chlorine atom on cyclohexane.⁴³



6

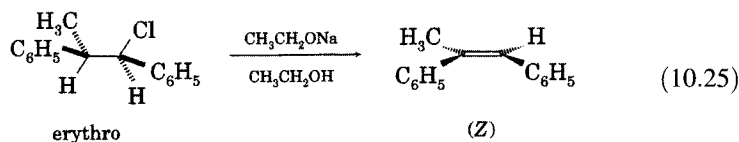
A similar preference for an anti-periplanar relationship in acyclic compounds was reported by Cram and co-workers. *threo*-1,2-Diphenyl-1-propyl chloride was found to undergo E2 elimination to give exclusively (*E*)-1,2-diphenylpropene (equation 10.24), while the erythro diastereomer produced only the (*Z*)-1,2-diphenylpropene (equation 10.25).^{44,45}



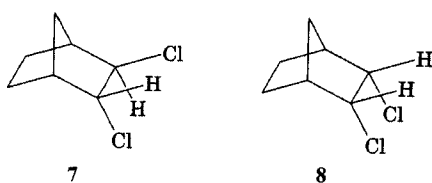
⁴³ Cristol, S. J. *J. Am. Chem. Soc.* **1947**, *69*, 338. See also Cristol, S. J.; Hause, N. L.; Meek, J. S. *J. Am. Chem. Soc.* **1951**, *73*, 674.

⁴⁴ Cram, D. J.; Greene, F. D.; DePuy, C. H. *J. Am. Chem. Soc.* **1956**, *78*, 790.

⁴⁵ Winstein, S.; Pressman, D.; Young, W. G. *J. Am. Chem. Soc.* **1939**, *61*, 1645 had reported earlier that *meso*-2,3-dibromobutane reacts with sodium iodide in propanol to give only *trans*-2-butene, while (\pm)-2,3-dibromobutane produces only the *cis* isomer.



Despite the electronic and steric factors favoring anti elimination, syn elimination can occur. One situation that gives rise to syn elimination is a molecular structure that precludes an anti-coplanar transition structure geometry.⁴⁶ For example, *trans*-2,3-dichloronorbornane (**7**) underwent dehydrohalogenation to form 2-chloronorbene 85 times faster than did the endo-cis isomer (**8**). This reactivity difference was attributed to the fact that a syn-coplanar relationship is feasible in the transition structure for reaction of **7**, but an anti-coplanar relationship is not feasible for the transition structure in the reaction of **8**.⁴⁷



Similarly, the rate constant for dehydrochlorination of **9**, which can react by syn-coplanar elimination, was found to be about eight times greater than the rate constant for **10**, which can only react from an anti-clinal conformation (Figure 10.20).⁴⁸

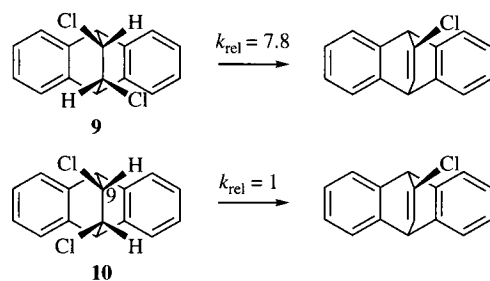


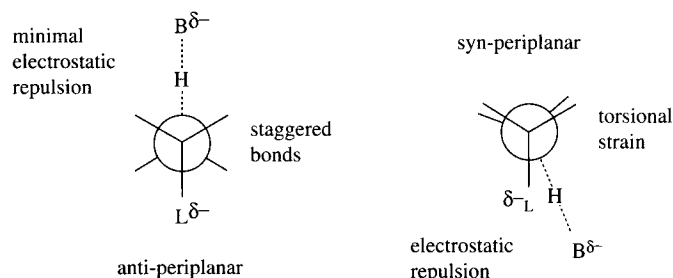
FIGURE 10.20
Relative rates of syn and anti elimination.

One explanation that was offered for the prevalence of anti E2 eliminations is based on steric differences between the syn and anti elimination pathways. The bonds from the C_β and C_α atoms to their substituents are eclipsed in the transition structure for syn 1,2-elimination (Figure 10.21). On the other hand, such torsional strain is not present in the transition structure for anti 1,2-elimination because those bonds are staggered. Torsional strain in a conformation leading to syn elimination might thus be expected to raise the barrier for syn elimination in a conformationally mobile substrate. The syn pathway also involves greater steric interactions between the base and the leaving group, but these steric interactions are avoided in the anti pathway.

⁴⁶ Cristol, S. J.; Arganbright, R. P. *J. Am. Chem. Soc.* **1957**, *79*, 3441 and references therein.

⁴⁷ Cristol, S. J.; Hoegger, E. F. *J. Am. Chem. Soc.* **1957**, *79*, 3438.

⁴⁸ Cristol, S. J.; Hause, N. L. *J. Am. Chem. Soc.* **1952**, *74*, 2193.

**FIGURE 10.21**

Anti-periplanar and syn-periplanar conformations for 1,2-elimination.

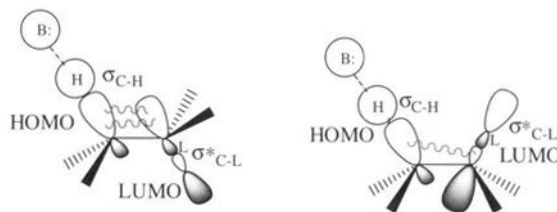
Moreover, there could be electrostatic repulsion between a base (bearing a negative charge or a nonbonded pair of electrons) and a leaving group that is becoming negatively charged (or developing a nonbonded pair of electrons) as shown in Figure 10.21.

There can also be an electronic preference favoring anti elimination over syn elimination.^{49,50} The anti orientation allows electron density in the C_{β} -H σ bonding orbital (the HOMO as the proton removal begins) to interact with the C-L σ^* orbital, which is essentially localized along the C_{α} -L axis (Figure 10.22). Population of the LUMO helps to expel the leaving group, with concomitant production of the carbon-carbon double bond. The corresponding interaction is less favorable in the case of syn elimination because of poorer overlap of orbitals on the C_{β} and C_{α} carbons.

Bach determined that syn elimination arises from a transition structure with considerable E1cb character. Inversion at the developing carbanion center can then lead to donation of electron density to the C-L σ^* orbital, promoting the departure of L and formation of the double bond.^{51,52} DePuy and co-workers found evidence for this view in the base-promoted elimination of *cis*- and *trans*-2-arylcyclopentane tosylates (Figure 10.23).⁵³ The observation of a Hammett ρ value of +2.8 for syn elimination, in contrast to a ρ of +1.5 for anti elimination, supported the view that syn elimination occurs by a mechanism with considerable E1cb character.

FIGURE 10.22

Interaction of the σ_{C-H} HOMO with the σ^*_{C-L} LUMO in concerted anti-coplanar (left) and syn-coplanar (right) elimination. (Adapted from reference 52.)



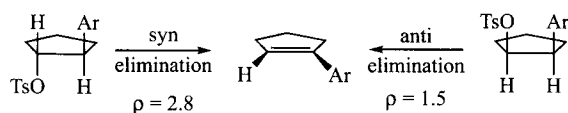
⁴⁹ See also Ingold, C. K. *Proc. Chem. Soc.* **1962**, 265.

⁵⁰ This intuitive view received theoretical support from a number of investigators. See, for example, Lowe, J. P. *J. Am. Chem. Soc.* **1972**, *94*, 3718.

⁵¹ (a) Bach, R. D.; Badger, R. C.; Lang, T. J. *J. Am. Chem. Soc.* **1979**, *101*, 2845. (b) This conclusion was supported by calculations of Minato, T.; Yamabe, S. *J. Am. Chem. Soc.* **1988**, *110*, 4586.

⁵² Dohner, B. R.; Saunders, W. H., Jr. *J. Am. Chem. Soc.* **1986**, *108*, 245 also concluded that syn elimination has more carbanion character than does anti elimination.

⁵³ DePuy, C. H.; Morris, G. F.; Smith, J. S.; Smat, R. J. *J. Am. Chem. Soc.* **1965**, *87*, 2421. Cyclopentyl derivatives were studied because coplanarity is achieved more easily in five-membered rings than in six-membered rings.

**FIGURE 10.23**

ρ Values for syn and anti elimination from 2-arylcyclopentyl tosylates.

Bickelhaupt reported a density functional theory study of the E2 reaction of fluoride ion with fluoroethane that offered additional insight into the preference for anti elimination.⁵⁴ The eclipsed conformation necessary for syn elimination was found to be only 2.3 kcal/mol higher in energy than the staggered conformation. Therefore, torsional strain could account for less than one-third of the 9 kcal/mol preference for anti elimination. Bickelhaupt also noted that, in accordance with the Curtin–Hammett principle, differences in transition state energies for the two pathways and not reactant conformational energies control relative rates of reaction. The calculations revealed that the transition state for syn elimination is reached relatively early, when the C_{β} –H bond has been stretched 39% but the C_{α} –F bond has been stretched only 11%. On the other hand, the transition state for anti elimination occurs only after the C_{α} –F bond has been stretched more than 50%. The energetic preference for anti elimination could thus be explained as the result of a more favorable electronic interaction of the HOMO of the base with the lower energy LUMO of the substrate *in its transition state geometry for anti elimination* than would be the case for interaction of the HOMO of the base with a higher energy LUMO of the substrate in the geometry for syn elimination.

Because the syn pathway for bimolecular elimination appears to have E1cb character, the preference for syn-coplanar (as opposed to syn-periplanar) orientation is not as strong as is the preference for anti-coplanar (as opposed to anti-periplanar) orientation. Gronert calculated the potential energy surface for syn elimination to be relatively flat with respect to the H_{β} – C_{β} – C_{α} –L dihedral angle. In some systems there was a slight preference for dihedral angles in the 20°–60° range instead of 0°. These geometries allowed a balance between lower torsional strain and greater electronic energy of the transition state.⁵⁵

Steric interactions can also favor syn elimination. Tao and Saunders found considerable syn elimination in reactions of compounds having the general formula $R_1R_2CHCHD(CH_3)_3N^+$ with hydroxide ion in 50 : 50 $(CH_3)_2SO : H_2O$ at 80°C.⁵⁶ When R_1 was phenyl, the percent of syn elimination was found to be 68.5% when R_2 was isopropyl but was 26.5% when R_2 was CH_3 . The results were rationalized in terms of a greater steric barrier between the leaving group and the substituents R_1 and R_2 in the transition structure for anti elimination compared to that for syn elimination (Figure 10.24). For these compounds both the syn and anti elimination pathways appear to have some carbanion character, although the carbanion character is still greater for syn elimination. For example, ρ values for substituted aryl derivatives were found to be 3.02 ± 0.22 for anti elimination and 3.69 ± 0.20 for syn elimination.⁵²

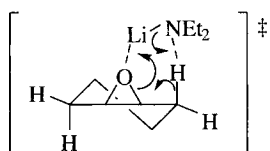
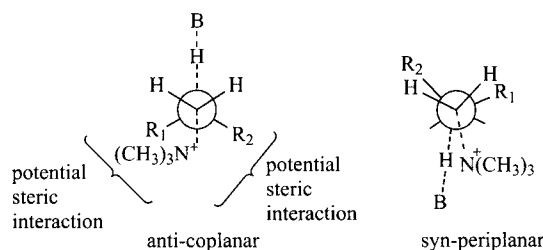
⁵⁴ Bickelhaupt, F. M. J. *Comput. Chem.* **1999**, *20*, 114.

⁵⁵ Gronert S. J. *Am. Chem. Soc.* **1992**, *114*, 2349; **1993**, *115*, 652; *J. Org. Chem.* **1994**, *59*, 7046.

⁵⁶ Tao, Y.-T.; Saunders, W. H., Jr. *J. Am. Chem. Soc.* **1983**, *105*, 3183.

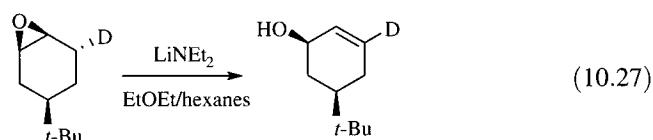
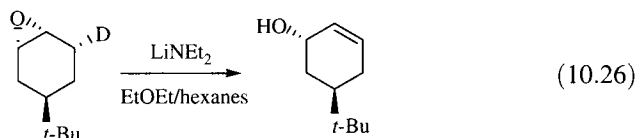
FIGURE 10.24

Greater steric interaction in anti (left) than in syn (right) transition structures.

**FIGURE 10.25**

Transition state for syn isomerization of cyclohexene oxide to allylic cyclohexenol. (Adapted from reference 58.)

Ion pairing effects also make syn elimination more likely. Cyclohexene oxides react with lithium diethylamide in a low polarity solvent to give allylic cyclohexenols. Deuterium labeling experiments summarized in equations 10.26 and 10.27 demonstrated that the C–O bond that breaks during the reaction is syn to the H (or D) removed by base.⁵⁷ A transition structure proposed for the syn elimination is shown in Figure 10.25.⁵⁸ Disruption of ion pairing reduces the tendency for syn elimination. For example, the percent of syn elimination from reaction of *meso*-1,2-dichloro-1,2-diphenylethane with *t*-BuOK in *t*-BuOH decreased from 13% to 0% when 18-crown-6 was added to the reaction mixture.⁵⁹ Similarly, syn elimination is not observed with a neutral nucleofuge because the positive charge on $-L^+$ in the reactant disrupts the Li–N ion pairing seen in Figure 10.25.⁶⁰



The reactions in equations 10.26 and 10.27 were carried out in homogeneous solution. Syn elimination is also seen under heterogeneous conditions, as in the dehydrohalogenation of β -halogen-activated *trans*-1,2-dichlorocycloalkanes with mixtures of NaNH_2 and *t*-BuONa in THF.⁶¹ The ratio of the rate constants for anti and syn elimination to form 1-chlorocycloheptene from *cis*- and *trans*-1,2-dichlorocycloheptane, respectively, was about 9. This relatively small ratio was attributed to enhancement of the rate of syn elimination as a result of a cyclic transition structure (Figure 10.26) in which both the halogen and the β -hydrogen atom interact with the surface of the complex base.

⁵⁷ Thummel, R. P.; Rickborn, B. *J. Am. Chem. Soc.* **1970**, *92*, 2064. See also the discussion by Morgan, K. M.; Gronert, S. *J. Org. Chem.* **2000**, *65*, 1461.

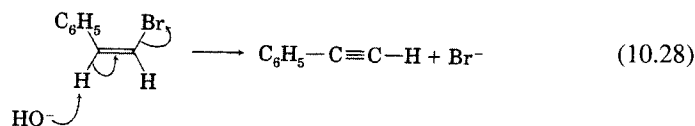
⁵⁸ For a discussion of asymmetric epoxide isomerizations promoted by chiral bases, see Magnus, A.; Bertilsson, S. K.; Andersson, P. G. *Chem. Soc. Rev.* **2002**, *31*, 223.

⁵⁹ Baciocchi, E.; Ruzziconi, R. *J. Org. Chem.* **1984**, *49*, 3395 and references therein.

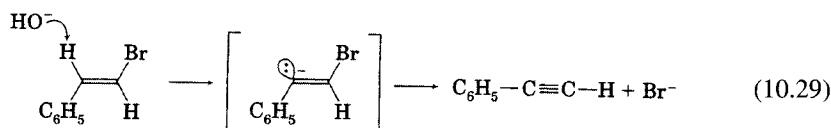
⁶⁰ Saunders, W. H., Jr. *J. Org. Chem.* **2000**, *65*, 681.

⁶¹ Croft, A. P.; Bartsch, R. A. *J. Org. Chem.* **1994**, *59*, 1930 and references therein.

The dehydrohalogenation of vinyl halides in the synthesis of alkynes shows steric preferences analogous to those of alkyl halides.⁶² The reaction of (*Z*)- β -bromostyrene with hydroxide ion in isopropyl alcohol at 43°C was 2.1×10^5 faster than the reaction of the (*E*) isomer. The results were interpreted in terms of differing mechanisms for the eliminations of the two compounds. As shown in equation 10.28, the (*Z*) isomer can undergo concerted elimination of hydrogen and bromine because they are in the proper orientation for anti-coplanar elimination.



The anti-coplanar relationship is not possible with the (*E*) isomer, however, so an E1cb mechanism involving formation of a vinyl carbanion and subsequent elimination of the bromide ion was proposed (equation 10.29).⁶³ The ratio of the rate constant for reaction of (*Z*)-*p*-nitro- β -bromostyrene to that of the (*E*) isomer was an order of magnitude smaller than the ratio of rate constants for (*Z*)- and (*E*)- β -bromostilbenes. This difference was attributed to the stabilization of the carbanion intermediate by the *p*-nitro group.⁶⁴ With a less acidic $\text{C}_\beta\text{-H}$ proton, the carbanion mechanism in equation 10.29 is slower, but the concerted mechanism in equation 10.28 is not as significantly affected. Therefore, the ratio of rate constants is much greater for elimination of HCl from isomeric chloroalkenes.



Still another reaction pathway may become operative with a very strong base, such as amide ion or an alkyllithium. When treated with phenyllithium in diethyl ether, for example, both (*Z*)- and (*E*)- β -bromostyrene are converted to phenylacetylene (equations 10.30–10.33). Because the ratio of rate constants for reaction of the (*E*) and (*Z*) isomers differed only by a factor of 2 in this case, the results seemed more consistent with a 1,1-elimination mechanism.⁶⁵

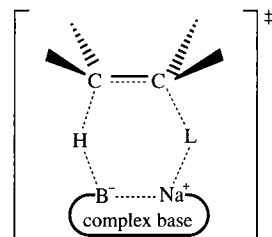
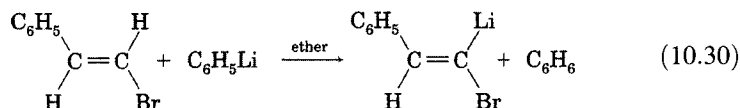


FIGURE 10.26

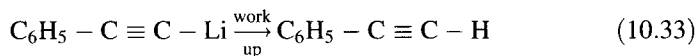
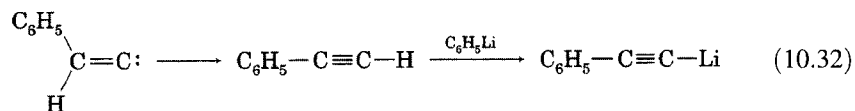
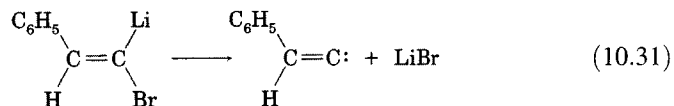
Cyclic transition structure suggested for syn dehydrohalogenation with heterogeneous base. (Adapted from reference 61.)

⁶² For a discussion of elimination reactions used for the synthesis of alkynes, see Jacobs, T. L. *Org. React.* **1949**, *5*, 1.

⁶³ The electronic reorganization associated with the formation of the alkyne is similar to the inversion of vinyl carbanion. Bach, R. D.; Evans, J. C. *J. Am. Chem. Soc.* **1986**, *108*, 1374.

⁶⁴ Cristol, S. J.; Norris, W. P. *J. Am. Chem. Soc.* **1954**, *76*, 3005.

⁶⁵ Cristol, S. J.; Helmreich, R. F. *J. Am. Chem. Soc.* **1955**, *77*, 5034.



Most concerted 1,4-eliminations have been found to occur with syn stereochemistry.^{66,67} The reaction shown in equation 10.5 (page 635) was found to be more than 99% syn, consistent with the mechanism shown in Figure 10.27.¹⁰ In some cases, it appears that 1,4-eliminations occur not by a concerted pathway but by a mechanism with considerable carbanion character.⁶⁸ In the gas phase, 1,4-elimination of methanol from 3-methoxycyclohexene was found to occur by a concerted syn pathway with a weak base (such as fluoride), but by a nonstereoselective carbanion pathway with a stronger base (such as amide or hydroxide).⁶⁹

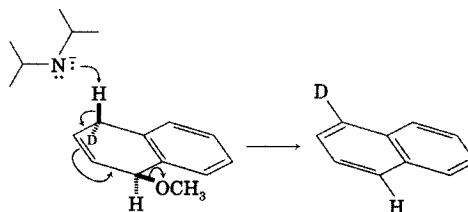


FIGURE 10.27

Possible mechanism for syn 1,4-elimination.

Regiochemistry of 1,2-Elimination Reactions

Many substrates have nonequivalent β -protons, so a 1,2-elimination may produce more than one alkene.⁷⁰ For example, ethoxide-promoted elimination of 2-iodo-3-methylbutane produced 82% of 2-methyl-2-butene and 18% of 3-methyl-1-butene (equation 10.34).⁷¹ The generalization that 1,2-elimination reactions of alkyl halides usually give the more substituted alkene is known as the **Saytzeff rule**. Saytzeff observed that the regiochemistry of elimination could be correlated with removal of a hydrogen atom from the

⁶⁶ See, for example, Hill, R. K.; Bock, M. G. *J. Am. Chem. Soc.* **1978**, *100*, 637; Cristol, S. J.; Barasch, W.; Tieman, C. H. *J. Am. Chem. Soc.* **1955**, *77*, 583.

⁶⁷ Failure to observe syn stereochemistry in an enzyme-catalyzed 1,4-elimination suggested that the enzyme-catalyzed reaction is a two-step process and not a concerted reaction: (a) Hill, R. K.; Newkome, G. R. *J. Am. Chem. Soc.* **1969**, *91*, 5893; (b) Onderka, D. K.; Floss, H. G. *J. Am. Chem. Soc.* **1969**, *91*, 5894.

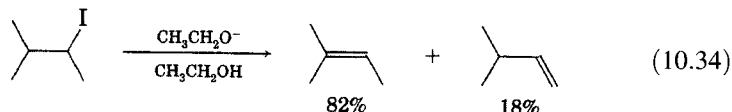
⁶⁸ Cristol, S. J. *Acc. Chem. Res.* **1971**, *4*, 393.

⁶⁹ Rabasco, J. J.; Kass, S. R. *J. Org. Chem.* **1993**, *58*, 2633.

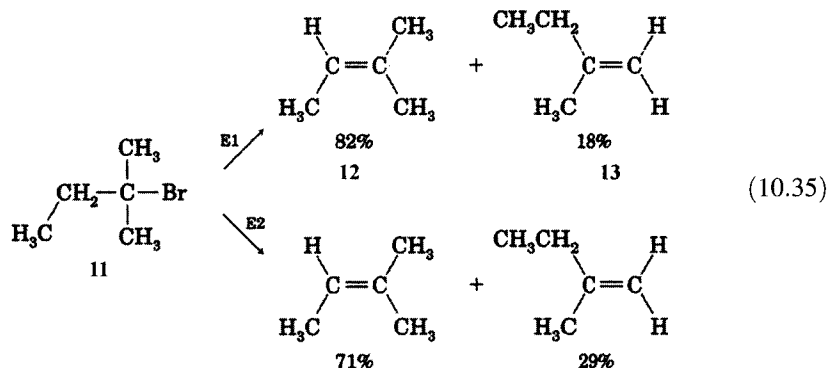
⁷⁰ That is, β -protons that are constitutionally heterotopic.

⁷¹ Hughes, E. D.; Ingold, C. K.; Mandour, A. M. *J. Chem. Soc.* **1948**, 2090.

β -carbon atom of an alkyl halide that has the smaller number of hydrogen atoms.⁷² Hughes and Ingold generalized this observation to mean that elimination from alkyl halides generally produces a higher yield of the alkene with the greater number of alkyl substituents on the carbon-carbon double bond.³



The Saytzeff rule applies to both E1 and E2 reactions. For example, the reaction of *t*-amyl bromide (11) with 0.05 M sodium ethoxide in ethanol at 25°C was found to occur by competing E1 and E2 pathways.⁷³ Both the E1 and E2 reactions produced higher yields of 2-methyl-2-butene (12) than of 2-methyl-1-butene (13). The percent yield of 12 was found to be 71% by the E2 pathway and 82% by the E1 pathway. The percent of 2-methyl-2-butene decreases with increasing concentration of ethoxide in the reaction mixture because a greater portion of the product is formed by the E2 reaction.⁷⁴



The tendency for alkyl halides to eliminate with Saytzeff orientation can be rationalized with the Hammond postulate. Figure 10.28 is a modification of Figure 10.10 to show two competing E2 reactions. Because the more substituted alkene is more stable than the less substituted isomer and because the transition structure for each pathway has some double bond character, the transition structure leading to the more substituted alkene should be lower in energy than the transition structure leading to the less substituted isomer.³ If the eliminations are effectively irreversible under the reaction conditions, then the product produced by the pathway with lower activation energy will be the major product (assuming that activation entropies for the two pathways are similar). An analogous argument applies to the distribution of products formed by proton removal from a carbocation intermediate in an E1 reaction (Figure 10.29).

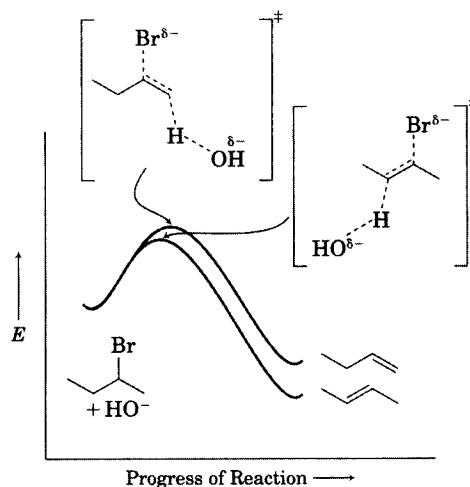
⁷² Saytzeff, A. *Liebigs Ann. Chem.* **1875**, 179, 296. See also the discussion in reference 3.

⁷³ The reaction produced a total of 56% elimination and 44% substitution.

⁷⁴ Dhar, M. L.; Hughes, E. D.; Ingold, C. K. *J. Chem. Soc.* **1948**, 2065.

FIGURE 10.28

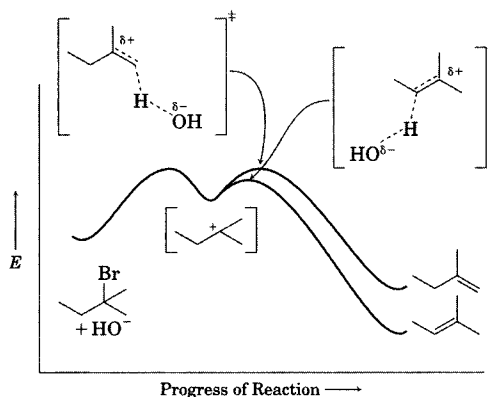
Reaction coordinate diagram for dehydrobromination of 2-bromobutane to 1-butene and 2-butene with Saytzeff orientation.



Not all eliminations follow the Saytzeff rule. The Hofmann elimination involves heating a tetraalkylammonium hydroxide to produce an alkene along with a trialkylamine and water as by-products, as illustrated by the reaction shown in equation 10.37.⁷⁵ Hofmann reported that elimination of a quaternary ammonium hydroxide with different alkyl groups on the nitrogen always produced ethene if an ethyl group was one of the substituents. Since the quaternary ammonium ion **14** has three β -protons on the ethyl group and two β -protons on the propyl group, reaction of hydroxide ion with the alkyl groups on a purely statistical basis would lead to 60% ethene and 40% propene. The data in Table 10.3 show that product distributions from Hofmann elimination reactions are usually very different from a statistical prediction based only on the number of β -hydrogen atoms of each alkyl group. The observation that the Hofmann elimination usually produces the less substituted alkene (ethene instead of propene in the example shown) in greater yield is known as the **Hofmann rule**.⁷⁶

FIGURE 10.29

Reaction coordinate diagram for E1 elimination of HBr from 2-bromo-2-methylbutane.



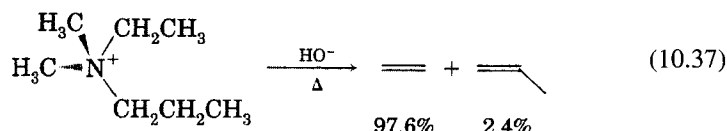
⁷⁵ Cope, A. C.; LeBel, N. A.; Lee, H.-H.; Moore, W. R. J. *Am. Chem. Soc.* **1957**, *79*, 4720.

⁷⁶ Hofmann, A. W. *Liebigs Ann. Chem.* **1851**, *78*, 253; **1851**, *79*, 11.

TABLE 10.3 Product Distributions in Hofmann Eliminations of $R_1R_2(CH_3)_2N^+ HO^-$

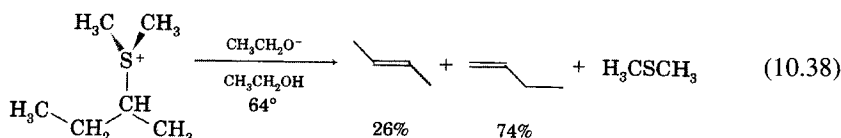
Alkyl Groups		Olefinic Products			
R ₁	R ₂	Experimental Results		Statistical Prediction	
Ethyl	Propyl	97.6% Ethene	2.4% Propene	60% Ethene	40% Propene
Ethyl	Isopropyl	41.2% Ethene	58.8% Propene	33.3% Ethene	67.7% Propene
Ethyl	Isobutyl	99.1% Ethene	0.9% Isobutene	75% Ethene	25% Isobutene
<i>n</i> -Butyl	Isobutyl	64% 1-Butene	36% Isobutene	67.7% 1-Butene	33.3% Isobutene

Source: Reference 75.



14

Hughes, Ingold, and co-workers generalized Hofmann's observation to mean that elimination of an alkene from a quaternary ammonium ion bearing only alkyl groups will produce as the major product that alkene with the fewer alkyl substituents on the carbon-carbon double bond.^{3,77} This generalization was not limited to the Hofmann elimination itself, but it was also applied to any bimolecular elimination in which the leaving group bears a positive charge when bonded to the substrate (and thus leaves as a neutral species). As an example, Ingold and co-workers noted that ethoxide-promoted elimination of dimethyl-*sec*-butylsulfonium ion (**15**) produced 26% of the 2-butenes (predominantly *trans*) and 74% of 1-butene (equation 10.38).⁷⁸ Other molecules that give similar selectivity include tetraalkylphosphonium salts, so Hofmann orientation is said to be a characteristic of the "–onium" (sulfonium, ammonium, etc.) compounds.

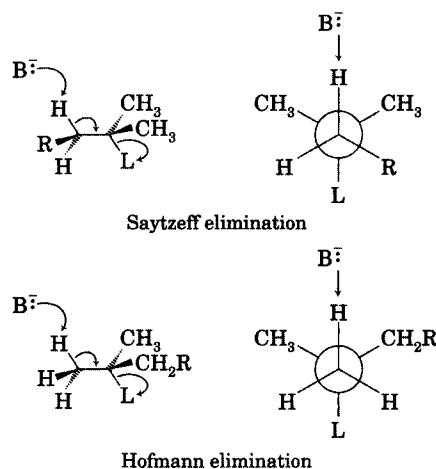


15

The anti-coplanar reaction pathways that lead to Saytzeff or Hofmann orientation are shown in Figure 10.30. Why should a reactant with one leaving group react preferentially by one pathway, while a species with a different leaving group reacts primarily by a different pathway? If the elimination reaction is not reversible under the experimental conditions, then a higher yield of Hofmann product than Saytzeff product suggests that the transition state leading to the Saytzeff product must be higher in energy than that

⁷⁷ Hanhart, W.; Ingold, C. K. *J. Chem. Soc.* **1927**, 997.

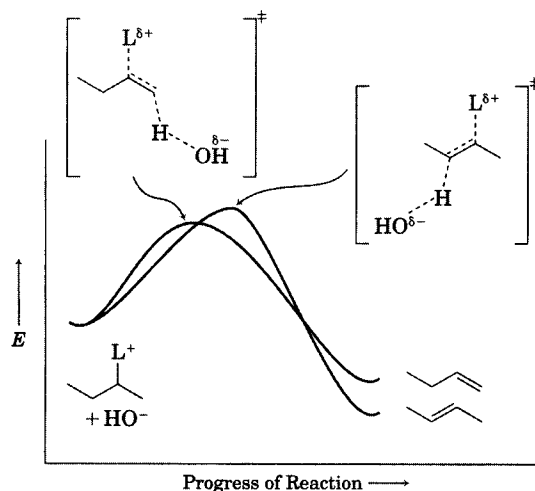
⁷⁸ Hughes, E. D.; Ingold, C. K.; Maw, G. A.; Woolf, L. I. *J. Chem. Soc.* **1948**, 2077. The product distributions in equation 10.38 reflect only the elimination products. More than 30% substitution product was also obtained.

**FIGURE 10.30**

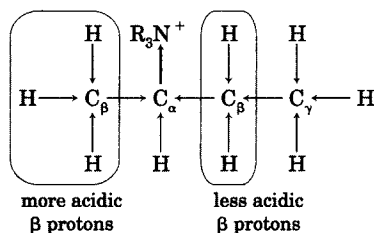
Two views of the generalized Saytzeff and Hofmann eliminations.

leading to Hofmann product. The more substituted alkene is more stable than the less substituted alkene, no matter the pathways by which these products are formed. Therefore, the transition state energies in a reaction producing Hofmann orientation cannot reflect product stabilities. That conclusion suggests a reaction coordinate diagram such as that shown in Figure 10.31, in which some interaction either raises the energy of the transition state leading to the more substituted alkene or lowers the energy of the transition state leading to the less substituted alkene.

Hughes and Ingold attributed Hofmann orientation to an inductive effect of the positively charged leaving group.³ As shown in Figure 10.32, they suggested that a cationic substituent would withdraw electron density from the α -carbon atom, which in turn would withdraw electron density from the other atoms in the structure. This electron withdrawal was thought to increase the acidity of a β -hydrogen atom, thus lowering the energy of a transition structure involving removal of the β -proton by base. A β -carbon atom with more alkyl substituents was said to have less acidic hydrogen atoms due to the electron-donating ability of the alkyl group(s) attached to it. The more acidic protons on the less substituted β -carbon atom would, therefore, be expected

**FIGURE 10.31**

Reaction coordinate diagram for elimination leading to predominant Hofmann orientation.

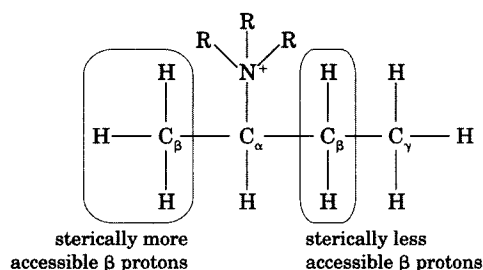
**FIGURE 10.32**

An inductive model for Hofmann elimination.

to react faster with a base, leading to Hofmann orientation.⁷⁹ Calculations suggested that the activation energy differences resulting from such electron withdrawal might be as much as 1 kcal/mol, which was considered adequate to explain the experimental results.⁸⁰

The induction explanation for Hofmann orientation suggests that breaking of the C_β -H bond precedes C_α -L dissociation in the transition structure, so the reaction might have some E1cb character.⁸¹ Indeed, the Hofmann elimination does seem to be more sensitive to the electronic effect of electron-withdrawing substituents than is the Saytzeff elimination. For example, a Hammett correlation for the bimolecular elimination of a series of 2-phenylethyl bromides gave a ρ of 2.1, while elimination of dimethyl sulfide from a series of 2-phenylethyldimethylsulfonium bromides gave a ρ value of 2.6.⁸²

Steric effects must also be considered as an explanation for Hofmann orientation in bimolecular elimination reactions of “-onium” compounds. The leaving group in “-onium” compounds is usually much larger than the leaving group in substrates that exhibit Saytzeff orientation.⁸³ As shown in Figure 10.33, approach of a base to a β -proton on a molecule with a bulky leaving group will be more difficult on a β -carbon atom with many substituents than on a β -carbon with few substituents. This interaction could cause the transition state energy for the Hofmann pathway to be lower than the transition state energy for the Saytzeff pathway.

**FIGURE 10.33**

Steric explanation for Hofmann elimination.

⁷⁹ This discussion is couched in terms of electron-donating alkyl groups and in terms of through-bond induction. As we have seen, these may not be the most generally applicable models for these phenomena.

⁸⁰ Banthorpe, D. V.; Hughes, E. D.; Ingold, C. K. *J. Chem. Soc.* **1960**, 4054.

⁸¹ See the discussion in Ford (cited in reference 23), p. 411 and in Wolfe, S. *Acc. Chem. Res.* **1972**, 5, 102.

⁸² DePuy, C. H.; Froemsdorf, D. H. *J. Am. Chem. Soc.* **1957**, 79, 3710; Saunders, W. H., Jr.; Williams, R. A. *J. Am. Chem. Soc.* **1957**, 79, 3712.

⁸³ This idea was suggested by Schramm, C. H. *Science* **1950**, 112, 367, but experimental evidence was not provided.

TABLE 10.4 Hofmann Product Formation in Dehydrohalogenation of $\text{RCH}_2\text{C}(\text{CH}_3)_2\text{Br}$ with Pyridine or Ethoxide Bases

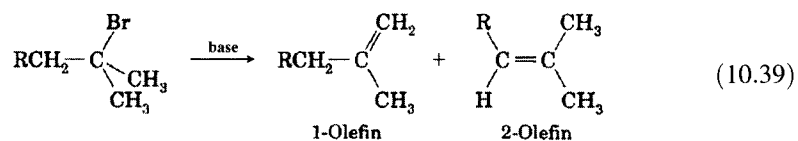
3° Bromide	R	% 1-Olefin with Pyridine ^a	% 1-Olefin with Ethoxide ^b
2-Bromo-2-methylbutane	Methyl	25	30
2-Bromo-2-methylpentane	Ethyl	32	50
2-Bromo-2,4-dimethylpentane	Isopropyl	44	54
2-Bromo-2,4,4-trimethylpentane	<i>t</i> -Butyl	70	86

Source: Reference 84.

^a Neat pyridine, 70°C.

^b 1 M KOCH_2CH_3 in ethanol 70°C.

In a series of papers in 1956, Brown and co-workers reported evidence that increasing the size of any one or all of the alkyl substituents on the β -carbon atom(s), the leaving group, and the attacking base can shift the proportion of products from Saytzeff orientation toward Hofmann orientation. For example, Brown investigated the elimination of HBr from a series of 3° bromides, $\text{RCH}_2\text{C}(\text{CH}_3)_2\text{Br}$, by pyridine and by potassium ethoxide (equation 10.39).⁸⁴ The results, shown in Table 10.4, indicate that increasing the number of alkyl substituents on the β -carbon atom increases the percentage of Hofmann orientation.



Brown and Wheeler studied the effect of the leaving group on product distribution in ethoxide-promoted E2 reactions of a series of 2-pentyl compounds in ethanol solution (Table 10.5).⁸⁵ The data are consistent with a model in which a larger leaving group produces a greater yield of the less substituted alkene, whether or not the leaving group has a positive charge on the atom bonded to the α -carbon atom.

To study the effect of base size, Brown and co-workers determined the product distribution for dehydrobromination of 2-bromo-2-methylbutane by a series of alkoxides.⁸⁶⁻⁸⁸ The percent of 1-alkene (2-methylbutene) formed with each base was found to be 30% with $\text{CH}_3\text{CH}_2\text{O}^-$, 72.5% with $(\text{CH}_3)_3\text{CO}^-$, and 88.5% with $(\text{CH}_3\text{CH}_2)_3\text{CO}^-$, indicating greater Hofmann orientation

⁸⁴ Brown, H. C.; Moritani, I.; Nakagawa, M. *J. Am. Chem. Soc.* **1956**, *78*, 2190.

⁸⁵ Brown, H. C.; Wheeler, O. H. *J. Am. Chem. Soc.* **1956**, *78*, 2199.

⁸⁶ Brown, H. C.; Moritani, I.; Okamoto, Y. *J. Am. Chem. Soc.* **1956**, *78*, 2193.

⁸⁷ The tendency for highly hindered bases to give more Hofmann orientation has been used synthetically, as in the isomerization of 1-methylcyclohexene to methylenecyclohexane by first adding HCl and then eliminating HCl with a sterically hindered base. Acharya, S. P.; Brown, H. C. *Chem. Commun.* **1968**, 305.

⁸⁸ Gould, E. S. *Mechanism and Structure in Organic Chemistry*; Holt, Rinehart and Winston: New York, 1959; p. 485 noted that this result could occur because of steric effects between the base and the substrate or because of intramolecular strain in the substrate in conformations required for E2 elimination to occur.

TABLE 10.5 Dependence of Elimination Products on Leaving Group in Elimination of HL from 2-Pentyl Compounds

2-Pentyl Derivative	L	% 1-Pentene	% <i>cis</i> -2-Pentene	% <i>trans</i> -2-Pentene
Bromide ^a	Br	31	18	51
Iodide ^a	I	30	16	54
Tosylate ^a	OTs	48	18	34
Dimethylsulfonium ^a	(CH ₃) ₂ S ⁺	87	5	8
Methyl sulfone ^b	SO ₂ CH ₃	89	2.5	9
Trimethylammonium ^b	(CH ₃) ₃ N ⁺	98	1	1

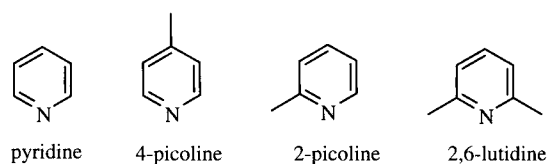
Source: Reference 85.

^a 1 M KOCH₂CH₃, 80°C.

^b 4 M KOCH₂CH₃, 130°C.

with larger bases. Brown and Nakagawa also investigated the effects of base strength and size on the products of dehydrobromination of 2-bromo-2-methylbutane by a series of pyridine bases (Figure 10.34).⁸⁹ Here the distribution of 1-alkene in the products was found to vary with base as follows: pyridine, 25%; 4-picoline, 25%; 2-picoline, 30%; and 2,6-lutidine, 44.5%. Since 4-picoline and pyridine differ in base strength but should have similar steric requirements in elimination, while 2- and 4-picoline have similar base strengths but different steric requirements, the results were consistent with the view that it is the steric requirement of the larger base in the transition structure for E2 elimination that leads to a greater proportion of Hofmann elimination.

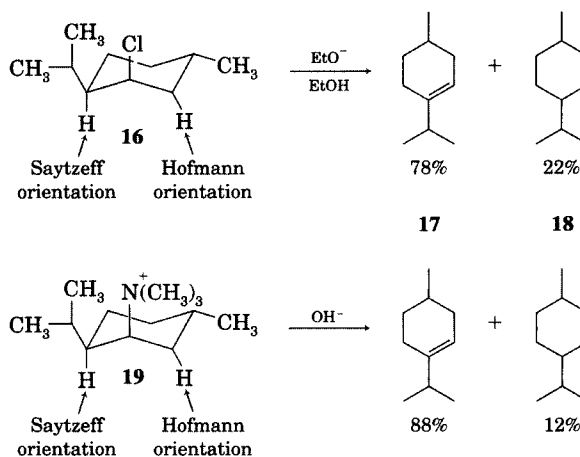
In some cases changing the strength of the base in a series of alkoxides can affect product distributions. Froemdsdorf and Robbins studied the elimination of *sec*-butyl tosylate in DMSO and found that 31% of 1-butene was formed when the base was phenoxide, but only 16% of the 1-butene was formed when *p*-nitrophenoxide was the base. The two anions have different basicities, but the steric environments near the oxygen anions should be similar. This result suggested that change in base strength does influence the regioselectivity of the E2 elimination, which is consistent with the induction model of Ingold.⁹⁰ The finding of a slightly larger yield of 1-alkene with ethoxide than with pyridine in Table 10.4 is also consistent with a tendency toward more Hofmann product with increasing base strength. This effect need not be related to the acidities of the different β -protons, however. Instead, it may reflect an earlier transition state and, as a result, a smaller dependence of the

**FIGURE 10.34**

Pyridine bases differing in basicity and alkyl substitution near nitrogen.

⁸⁹ Brown, H. C.; Nakagawa, M. J. *Am. Chem. Soc.* **1956**, *78*, 2197.

⁹⁰ Froemdsdorf, D. H.; Robbins, M. D. J. *Am. Chem. Soc.* **1967**, *89*, 1737.

**FIGURE 10.35**

Product distributions from second-order eliminations from neomenthyl chloride (**16**) and neomenthyltrimethylammonium hydroxide (**19**).

difference in ΔG^\ddagger values for the two elimination pathways on the thermodynamic stability of the two alkenes.

The results of one experiment strongly suggest that steric effects can overcome any inductive effect by an “-onium” group. As shown in Figure 10.35, neomenthyl chloride (**16**) underwent E2 reaction with ethoxide ion in ethanol at 100°C to give 78% of 3-menthene (**17**) and 22% of 2-menthene (**18**). With trimethylammonio as the leaving group instead of chlorine in **19**, the product of elimination with hydroxide as base in water at 156°C consisted of 88% of 3-menthene.⁹¹ In other words, this Hofmann elimination gave Saytzeff orientation. A possible explanation for this seemingly contradictory result may be that the molecule adopts a conformation in which steric effects are less important, so the transition states for the two elimination pathways more closely reflect stabilities of the products. Conversely, it might be argued that steric effects are actually more important in this reaction than in most Hofmann eliminations, because steric strain of the axial (CH₃)₃N⁺ group weakens the C–N bond and changes its leaving group ability.²⁰ Finally, it is interesting to consider the possibility that the theory of Hofmann orientation as presented by Hughes and Ingold was based in part on a typographical error. Hughes and Ingold cited the report by Hückel that neomenthyl chloride underwent base elimination to give 75% 3-menthene, while neomenthyltrimethylammonium ion gave 80% 2-menthene.⁹² However, Brown noted that Hückel’s experimental data indicated that the trimethylammonio compound actually gave 80% 3-menthene and that the report of 80% 2-menthene was an error in the discussion section of the paper.⁹³ A repetition of the experiment by McNiven and Read confirmed that 3-menthene is the major product.⁹⁴

The idea that leaving group ability, and not just leaving group size or charge, can determine the orientation of E2 reactions is supported by detailed studies of the dehydrohalogenation of alkyl halides. Saunders and co-workers found the major product from reaction of 2-fluoropentane with

⁹¹ Hughes, E. D.; Wilby, J. J. *Chem. Soc.* **1960**, 4094. The product distributions reflect second-order elimination. Some first-order elimination accompanied the reaction.

⁹² Hückel, W.; Tappe, W.; Legutke, G. *Liebigs Ann. Chem.* **1940**, 543, 191.

⁹³ Brown, H. C.; Moritani, I. *J. Am. Chem. Soc.* **1956**, 78, 2203.

⁹⁴ McNiven, N. L.; Read, J. J. *Chem. Soc.* **1952**, 153.

TABLE 10.6 Product Distributions from Reaction of 2-Halohexanes with NaOCH₃ in CH₃OH at 100°C

Leaving Group	% 1-Hexene	% <i>trans</i> -2-Hexene	% <i>cis</i> -2-Hexene	Saytseff/ Hofmann Ratio	<i>trans/cis</i> - 2-Hexene Ratio
F	69.9	21.0	9.1	0.43	2.3
Cl	33.3	49.5	17.1	2.0	2.9
Br	27.6	54.5	17.9	2.6	3.0
I	19.3	63.0	17.6	4.2	3.6

Source: Reference 96.

sodium ethoxide in ethanol to be 1-pentene, even though the fluorine atom is neither large nor positively charged.⁹⁵ Furthermore, Bartsch and Bunnett found a definite trend toward more Hofmann orientation with a *smaller* leaving group (Table 10.6) in the reactions of 2-halohexanes with methoxide ion in methanol, which is exactly opposite the trend predicted on the basis of size of the leaving group.^{96,97}

Bartsch and Bunnett calculated the rate constants for formation of each of the products at several temperatures and determined the values of ΔH^\ddagger and ΔS^\ddagger for the formation of each product from each halide. As shown in Table 10.7, the magnitudes of both ΔH^\ddagger and ΔS^\ddagger increase along the series I < Br < Cl < F. With all of the halogens, the ΔS^\ddagger value for formation of 1-hexene is less negative than the ΔS^\ddagger value for formation of 2-hexene. Bartsch and Bunnett suggested that this trend may reflect some difference in entropies of the products being formed, or it may be a measure of the entropies of the transition structures themselves.⁹⁶ In either case, the $T\Delta S^\ddagger$ term tends to favor 1-hexene formation.⁹⁸ The more negative values of ΔS^\ddagger for compounds with Cl and—to a greater degree—F than for compounds with Br or I were attributed to greater hydrogen bonding between the departing anion and

TABLE 10.7 Activation Parameters for Reactions of 2-Halohexanes with Methoxide Ion^a

Leaving Group	1-Hexene		<i>trans</i> -2-Hexene		<i>cis</i> -2-Hexene	
	ΔH^\ddagger	ΔS^\ddagger	ΔH^\ddagger	ΔS^\ddagger	ΔH^\ddagger	ΔS^\ddagger
F	30.2	-13.5	29.1	-16.6	29.0	-18.7
Cl	27.1	-9.0	25.1	-11.2	26.2	-10.6
Br	25.3	-6.2	23.7	-7.1	24.1	-8.5
I	24.7	-6.0	22.1	-7.8	23.1	-7.5

Source: Reference 96.

^a Values of ΔH^\ddagger in kcal/mol; values of ΔS^\ddagger in eu.

⁹⁵ Saunders, W. H., Jr.; Fahrenholtz, S. R.; Caress, E. A.; Lowe, J. P.; Schreiber, M. J. *Am. Chem. Soc.* **1965**, *87*, 3401.

⁹⁶ Bartsch, R. A.; Bunnett, J. F. *J. Am. Chem. Soc.* **1968**, *90*, 408.

⁹⁷ The tendency for the Saytzeff elimination to give *trans*-2-hexene followed the trend F < Cl < Br < I. Some substitution product, 2-hexyl methyl ether, was also formed in the reactions.

⁹⁸ Among other factors to be considered in predicting the products of bimolecular elimination reactions is the role of aggregation of the base, which can be particularly significant for *t*-BuOK in *t*-BuOH solution. A variety of different models have been proposed to account for the interaction of aggregated bases with substrates in E2 reactions. For a discussion, see reference 21.

solvent molecules in the transition structures for reactions of the alkyl chloride and fluoride. The authors concluded that the polar effects of the halogens could not be the basis for the tendency toward Hofmann orientation because the Taft σ^* values for XCH_2 groups vary only slightly along the series.

Bartsch and Bunnett explained these results in terms of a variable transition state theory.²⁷ According to this model, the E2 mechanism can be synchronous, or it can have more E1 character or more E1cb character. That is, the reaction path could follow the diagonal line from reactant to product in Figure 10.7 (page 640) or it could follow a path that curves toward one or the other of the corners corresponding to E1 or E1cb reaction. The effect of changing the reactant, solvent, or base in a particular elimination would then depend on whether the transition structure for the reaction is more like a carbanion (E1cb-like) or a carbocation (E1-like). Among the trends suggested by Bunnett are the following:²⁷

1. Introduction of an α -aryl substituent or (to a smaller extent) an α -alkyl substituent should stabilize a developing carbocation and make the transition structure more E1-like.
2. Introduction of a β -aryl substituent should enhance the tendency toward E1cb reaction by stabilizing a developing carbanion at the β -carbon atom.
3. Introduction of a β -alkyl substituent should make the reaction more E1-like (or less E1cb-like). That is, an E1cb-like reaction should become more synchronous because the alkyl substituent would be expected to destabilize a developing carbanion and stabilize the incipient carbon-carbon double bond. An E1-like reaction should become even more E1-like.
4. Change to a better leaving group should make the reaction more nearly E1-like; conversely, change to a poorer leaving group should make the reaction more nearly E1cb-like.
5. Change to a more electronegative leaving group should lead to a transition structure with less carbocation character on the α -carbon atom and greater carbanion character on the β -carbon atom.

The last two trends are particularly relevant to the elimination reactions of the 2-hexyl halides. As indicated by the data in Table 10.7, leaving group ability in methanol solution follows the trend $I > Br > Cl > F$. In comparison with the other 2-hexyl halides, therefore, the transition structure for 2-hexyl fluoride should have relatively more carbanion character. Therefore, the stabilities of the developing carbon-carbon double bonds are less important in determining values of ΔG^\ddagger for 2-hexyl fluoride than is the case for the other 2-hexyl halides.^{99,100}

Using the variable transition state model, the tendency for the “-onium” compounds to give Hofmann orientation can be explained simply as the result of the R_3N and R_2S moieties being relatively poor leaving groups. This model can also account for the failure to observe Hofmann orientation in the bimolecular elimination of trimethylamine from **19** (page 662). Steric

⁹⁹ The enhanced E1cb character does not mean that the reaction is fully E1cb, however. Saunders, W. H., Jr.; Schreiber, M. R. *Chem. Commun.* **1966**, 145 found that there was no hydrogen isotope exchange in the elimination of 2-pentyl fluoride with ethoxide in CH_3CH_2OD solution.

¹⁰⁰ This argument can also rationalize the observation of more *cis*-2-hexene as the atomic number of the halogen decreases.

repulsion (1,3-diaxial interactions) between $(\text{CH}_3)_3\text{N}^+$ and the other axial substituents, particularly the isopropyl group, would raise the energy of the reactive conformation of the starting material. This *steric compression* should therefore make the trimethylamine a better leaving group in this molecule, so the elimination should be more nearly E2-like. As a result, the stability of the developing double bond lowers the energy of the pathway leading to 3-menthene, and a greater yield of the Saytzeff product is observed.²⁷

Eubanks and co-workers reported a detailed experimental and theoretical study of the effects of isotopic substitution on the Hofmann elimination reaction that are consistent with the variable transition state model.¹⁰¹ Data for ethoxide-promoted elimination of (2-phenylethyl)trimethylammonium-1-¹⁴C and (2-phenylethyl)trimethylammonium-2-¹⁴C bromide led the authors to conclude that the mechanism occurs through an E2 mechanism with considerable E1cb character. The β -proton was said to be more than half transferred to base in the transition structure (Figure 10.36). Kinetic isotope effect data for derivatives with substituents on the benzene ring suggested that there is a progression of transition structures as the aryl substituent varies from electron-withdrawing to electron-donating. This effect was attributed to stabilization of the carbanion character of the transition structure by electron-withdrawing aryl substituents. As indicated by the points representing *p*-substituents in Figure 10.37, the investigators concluded that the transition structures become both more reactant-like and more E1cb-like as the substituents on the benzene ring become more electron-withdrawing.¹⁰¹

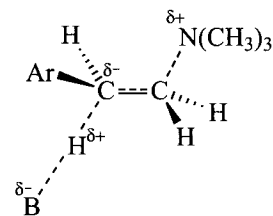


FIGURE 10.36

Transition structure proposed for Hofmann elimination of (2-phenylethyl)trimethylammonium ion. (Reproduced from reference 101.)

10.3 OTHER 1,2-ELIMINATION REACTIONS

Dehalogenation of Vicinal Dihalides

In each of the examples of 1,2-elimination reactions discussed above, one of the groups eliminated was a proton. Another type of 1,2-elimination reaction is the dehalogenation of vicinal dihalides.^{20,102} Iodide ion can be used as the dehalogenating agent in both protic and aprotic solvents (equation 10.40).

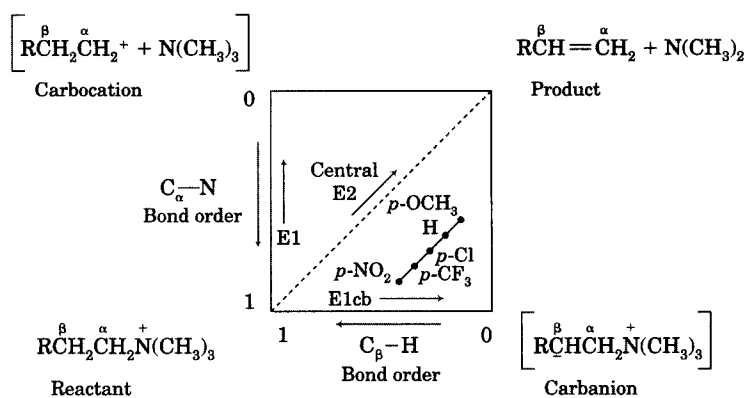


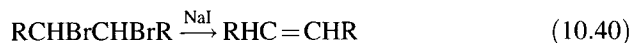
FIGURE 10.37

Transition state spectrum for elimination from substituted (2-phenylethyl)trimethylammonium ions. (Adapted from reference 101.)

¹⁰¹ Eubanks, J. R. I.; Sims, L. B.; Fry, A. J. *Am. Chem. Soc.* **1991**, *113*, 8821.

¹⁰² At least one report in the literature dates to 1871. See the discussion in Mathai, I. M.; Schug, K.; Miller, S. I. *J. Org. Chem.* **1970**, *35*, 1733 and references therein.

Chloride and bromide ions are effective in aprotic solvents such as DMF but not in protic solvents, and the reaction of 1,2-dihalides with iodide is faster in DMF than in protic solvents. The overall process may be viewed either as the attack of a nucleophilic halide ion on a halogen atom or as a net two-electron reduction of the organic dibromide. The reaction can also be accomplished with other two-electron reducing agents, such as zinc or other metals.¹⁰³ Reactions with one-electron reducing agents have also been reported, so radical pathways for the elimination may be possible.¹⁰⁴ While the substrate is most commonly a 1,2-dihalide, either or both of the halogens may instead be another leaving group, including hydroxyl and alkoxy groups.^{102,105}



The stoichiometry of the elimination in equation 10.40 is¹⁰⁶



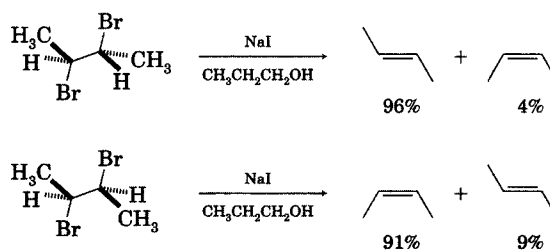
Kinetic and stereochemical studies provided early clues to the mechanism of the reaction. The dehalogenation of a vicinal dibromide with iodide shows second-order kinetics.¹⁰⁷

$$\text{Rate} = k_2[\text{BrCH}_2\text{CH}_2\text{Br}][\text{I}^-] \quad (10.42)$$

Substituent effects on the rates of elimination of aryl-substituted 1,2-diphenyl-1,2-dihaloethanes are small, suggesting that double bond formation is advanced in the transition structure and that most of the charge is localized on the departing halide ion.¹⁰³ The debromination of 2,3-dibromobutane with iodide ion is highly stereospecific, with the *meso* diastereomer giving almost exclusively *trans*-2-butene, and the racemic diastereomer producing mostly *cis*-2-butene (Figure 10.38).⁴⁵ The results were taken as evidence for a

FIGURE 10.38

Stereospecific anti elimination in the debromination of *meso*- (top) and *racemic*-2,3-dibromobutane (bottom).



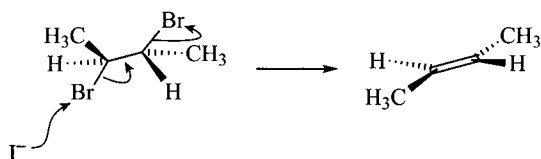
¹⁰³ Baciocchi, E.; Schioli, A. *J. Chem. Soc. B* **1969**, 554.

¹⁰⁴ Strunk, R. J.; DiGiacomo, P. M.; Aso, K.; Kuivila, H. G. *J. Am. Chem. Soc.* **1970**, *92*, 2849 reported that tri-*n*-butyltin hydride leads to predominantly anti elimination of Br₂ from both (±)- and *meso*-2,3-dibromobutanes by a free radical chain reaction.

¹⁰⁵ Kochi, J. K.; Singleton, D. M. *J. Am. Chem. Soc.* **1968**, *90*, 1582.

¹⁰⁶ Goering, H. L.; Espy, H. H. *J. Am. Chem. Soc.* **1955**, *77*, 5023.

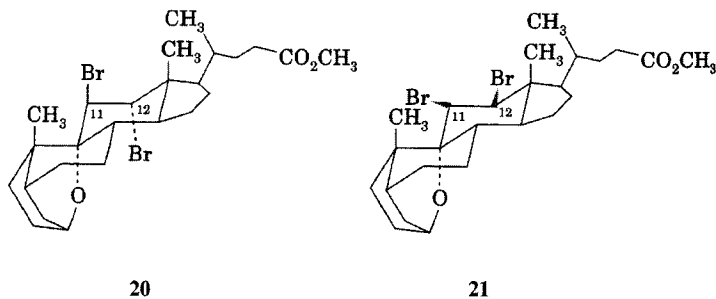
¹⁰⁷ Hine, J.; Brader, W. H., Jr. *J. Am. Chem. Soc.* **1955**, *77*, 361.

**FIGURE 10.39**

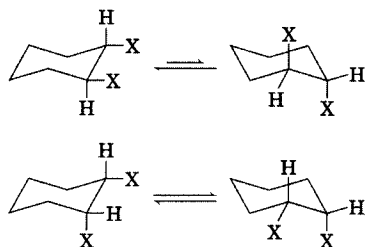
Concerted mechanism proposed for iodide-promoted dehalogenation reaction.

concerted, anti elimination analogous to the E2 dehydrohalogenation reaction, as suggested in Figure 10.39.¹⁰⁸

The relative reactivities of two diastereomeric vicinal dibromide derivatives of cholanic acid also provided evidence for an anti-coplanar orientation of the two carbon–bromine bonds in iodine-promoted dehalogenation. In the 11 α ,12 β -dibromo compound **20**, each of the two bromine atoms is held in an axial conformation by the rigid steroid skeleton. On the other hand, each of the two bromine atoms is held in an equatorial conformation in the 11 β ,12 α -dibromo isomer **21**. As a result, the conformation of the Br–C–C–Br grouping is anti in **20** but is gauche in **21**. When treated with sodium iodide in acetone, **20** underwent debromination readily, while **21** was unreactive under the same conditions.¹⁰⁹



The conformational relationship of the bromine atoms is clear in **20** and **21** because of the rigidity of the steroid structure. Individual cyclohexane rings usually have considerable conformational mobility, however, and *trans*-1,2-dihalocyclohexanes exist as a mixture of diaxial and diequatorial conformers (Figure 10.40). While the diequatorial conformer is expected to be the major conformer, the anti-coplanar elimination suggested in Figure 10.39 must occur from the minor diaxial conformer. In the case of *cis*-1,2-dihalocyclohexanes,

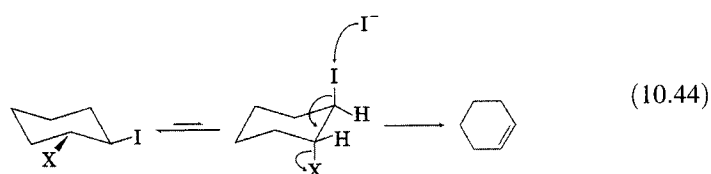
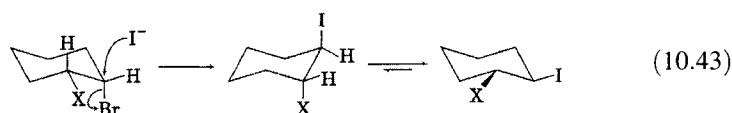
**FIGURE 10.40**

Conformational equilibria in *trans*- (top) and *cis*-1,2-dihalocyclohexane (bottom).

¹⁰⁸ Failure to observe complete stereospecificity may be the result of some S_N2 displacement of bromide or iodide prior to the elimination.

¹⁰⁹ Barton, D. H. R.; Rosenfelder, W. J. J. *Chem. Soc.* **1951**, 1048.

however, each of the two possible chair conformers has one axial and one equatorial halogen substituent. It would appear therefore that *cis*-1,2-dihalo-cyclohexanes should be unreactive. Nevertheless, iodide-promoted elimination does occur with *cis* isomers. For example, *cis*-1,2-dibromocyclohexane is debrominated by potassium iodide in methanol at 80°C, although the *trans* isomer was debrominated more than eleven times faster under the same conditions. Furthermore, *cis*-1-bromo-2-chlorocyclohexane reacted at nearly the same rate as the *trans* isomer. Goering and Espy explained the reactivity of the *cis* isomers by proposing that they react by a two-step mechanism. In the first step (equation 10.43), the *cis* isomer undergoes a rate-limiting S_N2 reaction that produces a *trans*-1-iodo-2-cyclohexyl system, which then rapidly undergoes the concerted elimination (equation 10.44).¹⁰⁶



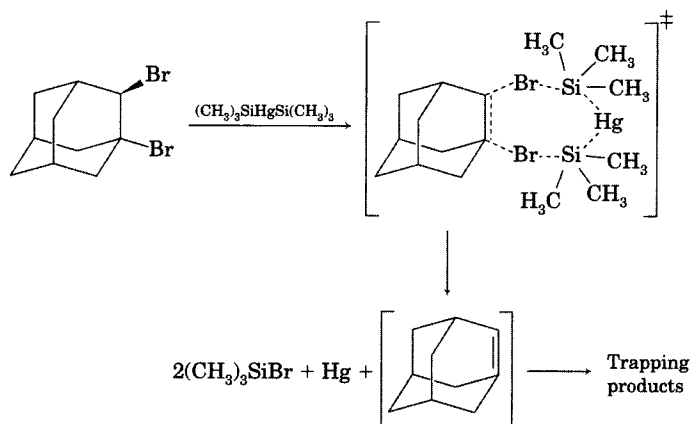
Similarly, both *cis*- and *trans*-2-bromo-1-cyclohexyl arenesulfonates were converted to cyclohexene upon treatment with sodium iodide in propanol, although the *trans* isomers were more reactive. For example, *trans*-2-bromo-1-cyclohexyl tosylate was 62 times as reactive as the *cis* isomer, and *trans*-2-bromo-1-cyclohexyl brosylate was 48 times as reactive as its *cis* isomer. Again, the data suggested that the rate-limiting step in the case of the *cis* isomers is an S_N2 substitution of iodide for bromide, followed by anti elimination of the *trans*-1-halo-2-iodocyclohexane.¹¹⁰

Although eliminations promoted by iodide ion have been studied most extensively, a wide variety of other dehalogenating reagents have been used as well. The stereospecificity of the reaction depends on the reducing agent. Miller and co-workers found that all reducing agents convert *meso*-1,2-dibromo-1,2-diphenylethane to *trans*-stilbene but that the reduction of *racemic*-1,2-dibromo-1,2-diphenylethane gives yields of *cis*-stilbene ranging from 96% (with sodium iodide in acetone) to 0% (with FeCl₂ in DMF). The authors suggested that the failure to observe complete stereospecificity could arise from one or more alternative pathways for the elimination reaction, including the intermediacy of halonium ions such as those proposed for the addition of halogen to alkenes.^{102,111,112}

¹¹⁰ Cristol, S. J.; Weber, J. Q.; Brindell, M. C. *J. Am. Chem. Soc.* **1956**, *78*, 598.

¹¹¹ Lee, C. S. T.; Mathai, I. M.; Miller, S. I. *J. Am. Chem. Soc.* **1970**, *92*, 4602.

¹¹² The intermediacy of bromonium ions in the debromination of vicinal dibromides is consistent with the formation of stilbene from stilbene dibromide in 1,2-dichloroethane solution. Bellucci, G.; Bianchini, R.; Chiappe, C.; Brown, R. S.; Slebocka-Tilk, H. *J. Am. Chem. Soc.* **1991**, *113*, 8012. See also Zheng, C. Y.; Slebocka-Tilk, H.; Nagorski, R. W.; Alvarado, L.; Brown, R. S. *J. Org. Chem.* **1993**, *58*, 2122.

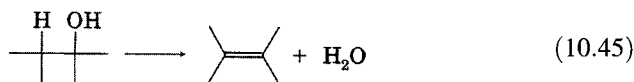
**FIGURE 10.41**

Syn elimination in the debromination of 1,2-dibromoadamantane with bis(trimethylsilyl)mercury. (Adapted from reference 114.)

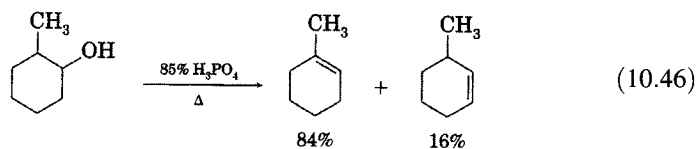
Stereospecific debromination by a nearly syn pathway has also been observed with bis(trimethylsilyl)mercury and bis(trimethylgermyl)mercury.¹¹³ A mechanistic scheme proposed for the debromination of 1,2-dibromoadamantane to form the highly reactive compound adamantene is illustrated in Figure 10.41.¹¹⁴

Dehydration of Alcohols

The dehydration of alcohols (equation 10.45) is one of the fundamental reactions of organic chemistry.¹¹⁵



The most common way to carry out the reaction is by heating the alcohol in the presence of a catalytic amount of a strong mineral acid such as sulfuric acid or phosphoric acid. The dehydration of 2-methylcyclohexanol is illustrated in equation 10.46.¹¹⁶

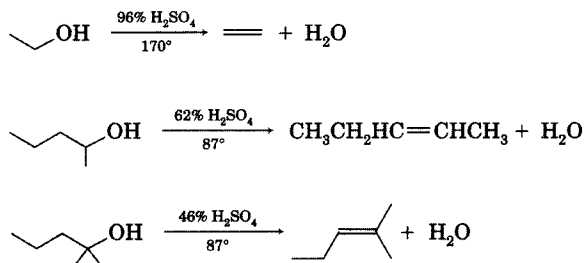


¹¹³ Bennett, S. W.; Eaborn, C.; Jackson, R. A.; Walsingham, R. W. J. *Organometal. Chem.* **1971**, 27, 195.

¹¹⁴ Cadogan, J. I. G.; Leardini, R. J. *Chem. Soc. Chem. Commun.* **1979**, 783.

¹¹⁵ For a more detailed discussion, see (a) reference 20, pp. 221–274; (b) reference 19, pp. 145–156; (c) Knözinger, H. in Patai, S., Ed. *The Chemistry of the Hydroxyl Group*, Part 2; Wiley-Interscience: London, 1971; pp. 641–718.

¹¹⁶ Taber, R. L.; Champion, W. C. *J. Chem. Educ.* **1967**, 44, 620.

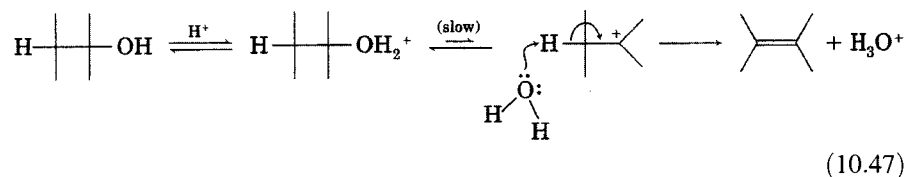
**FIGURE 10.42**

Conditions required for dehydration of 1°, 2°, and 3° alcohols with sulfuric acid. (Adapted from reference 117.)

The preferential formation of the more substituted alkene is the common pattern in such reactions, but this product distribution could be the result of an acid-catalyzed interconversion of the products. That is, there may be an equilibrium-controlled and not a rate-controlled product distribution in acid-catalyzed reactions.

Many experimental observations are consistent with an E1 mechanism for the acid-catalyzed dehydration of alcohols. The relative reactivities of 1°, 2°, and 3° alcohols parallel the stabilities of the corresponding carbocations. Consequently, higher temperatures or more concentrated acid solutions are required for dehydration of 1° than 2° than 3° alcohols, as illustrated in Figure 10.42.¹¹⁷ Furthermore, rearranged products are observed in reactions in which the intermediate carbocations can undergo alkyl or hydride shifts to form more stable carbocations.^{118,119}

The simplest mechanism for a specific acid-catalyzed E1 dehydration of an alcohol is shown in equation 10.47. The rate-limiting step is the formation of the carbocation intermediate, which is followed by abstraction of a β -proton by base. In aqueous solutions of sulfuric acid, water is the most likely base for the proton abstraction.¹²⁰



There is evidence that the dehydration reaction is much more complex than is suggested by equation 10.47, however, because for most alcohols exchange of OH with solvent is considerably faster than elimination. For example, Dostrovsky and Klein found that 1-butanol undergoes oxygen exchange with ¹⁸O-labeled water three times faster than it undergoes elimination at 125°C. Neopentyl alcohol, on the other hand, was found to undergo carbocation rearrangement and subsequent elimination of water 37 times faster than it

¹¹⁷ Fieser, L. F.; Fieser, M. *Advanced Organic Chemistry*; Reinhold Publishing: New York, 1961; p. 138 ff.

¹¹⁸ See, for example, Dostrovsky, I.; Klein, F. S. *J. Chem. Soc.* **1955**, 4401.

¹¹⁹ Collins, C. J. Q. *Rev. Chem. Soc.* **1960**, *14*, 357.

¹²⁰ The elimination can be subject to general base catalysis. Loudon and Noyce found general base catalysis in the dehydration of substituted 1-aryl-2-phenylethanols in aqueous dioxane solution with 1 : 1 dichloroacetic acid–sodium dichloroacetate buffers. Loudon, G. M.; Noyce, D. S. *J. Am. Chem. Soc.* **1969**, *91*, 1433.

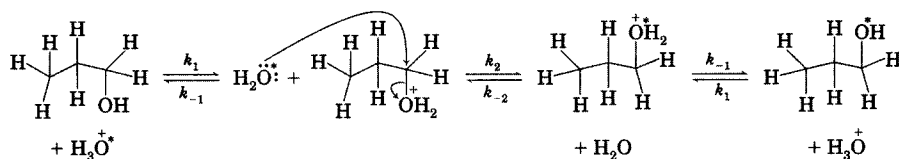
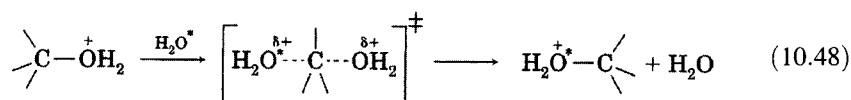


FIGURE 10.43

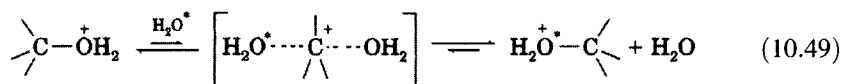
S_N2 mechanism for acid-catalyzed exchange of OH in 1-propanol.

exchanged oxygen with solvent.¹¹⁸ Because 1° carbocations are unstable and because neopentyl systems react slowly in concerted substitution reactions, the results suggested an S_N2 mechanism for oxygen exchange with 1° alcohols, as illustrated for 1-propanol in Figure 10.43.

There is evidence that the S_N2 mechanism for oxygen exchange also operates in 2° alcohols. For example, the rate of oxygen exchange of optically active 2-butanol in $H_2^{18}O$ was found to be exactly half the rate of racemization, as is expected for a Walden inversion (equation 10.48).¹²¹



An alternative mechanism for oxygen exchange could be dehydration of the alcohol to an alkene, followed by rehydration of the alkene with labeled water. However, that process would lead to racemization (not inversion) of the chiral center, and the rate of oxygen exchange would be more than half the rate of racemization. There is also another possibility that is consistent with the experimental data. A rate of oxygen exchange that is half the rate of inversion could also result from a mechanism involving a tightly solvated symmetric carbocation that collapses to reactant (protonated alcohol) or product (protonated alcohol with labeled oxygen) faster than one of the solvating water molecules can diffuse away from the carbocation center and be replaced by another water molecule from the solution.¹²²



With a 3° alcohol, the tendency for S_N2 reaction is greatly diminished, and the stability of an intermediate carbocation is much greater than is the case with 2° alcohols. Still, oxygen exchange with solvent is faster than elimination even with 3° alcohols. For example, in 0.09 N aqueous H_2SO_4 at 55°C, *t*-butyl alcohol underwent oxygen exchange about 30 times faster than it underwent elimination.¹²³ At 75°C, the ratio of the rate constants for exchange and elimination was about 21. That trend is consistent with the general observation that higher temperatures favor elimination over substitution.¹²⁴ Because

¹²¹ Bunton, C. A.; Konasiewicz, A.; Llewellyn, D. R. *J. Chem. Soc.* **1955**, 604; Bunton, C. A.; Llewellyn, D. R. *J. Chem. Soc.* **1957**, 3402.

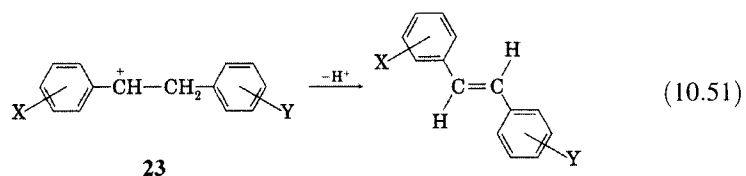
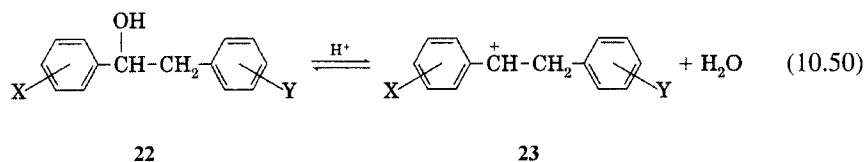
¹²² Dietze, P. E.; Jencks, W. P. *J. Am. Chem. Soc.* **1987**, 109, 2057.

¹²³ Dostrovsky, I.; Klein, F. S. *J. Chem. Soc.* **1955**, 791.

¹²⁴ Higher acid concentrations also favor elimination (references 121 and 123).

the S_N2 pathway is unlikely, it is probable that oxygen exchange with 3° alcohols occurs by an S_N1 mechanism.

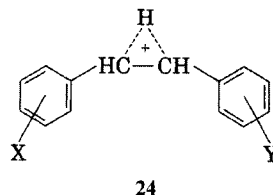
Exchange of oxygen with solvent is an important process even with benzylic alcohols.¹²⁵ Racemization of optically active 1,2-diphenylethanol in 50–60% aqueous sulfuric acid was found to be 58 times faster than the dehydration to *trans*-stilbene.¹²⁶ The results suggest that under these conditions there is reversible formation of a 1,2-diphenylethyl cation (equation 10.50), followed by rate-limiting detachment of a proton from the carbocation (equation 10.51).



Furthermore, a study of the dehydration of a series of substituted 1,2-diarylethanols (**22**, equation 10.50) showed very different effects of the substituents X and Y.¹²⁷ The Hammett correlation for the rate constant for dehydration was found to be

$$k_{X,Y} = -3.78\sigma_X^+ + 0.23\sigma_Y - 3.19 \quad (10.52)$$

The correlation with σ_X^+ suggests that the equilibrium population of the benzylic carbocation (**23**) is enhanced by a substituent X that can stabilize the carbocation through a resonance interaction. The correlation with σ_Y suggests that substituent Y has a much weaker effect. This result is not compatible with an alternative mechanism involving rate-limiting formation of a bridged cationic intermediate such as **24**, since in that case the X and Y substituents would be expected to have a similar effect on cation stability.¹²⁸

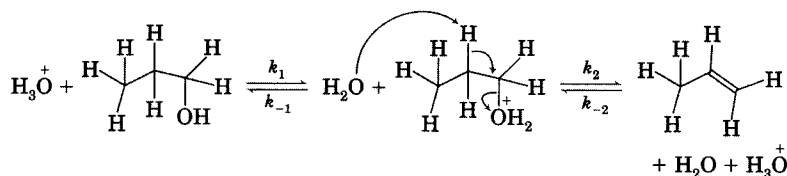


¹²⁵ Grunwald, E.; Heller, A.; Klein, F. S. *J. Chem. Soc.* **1957**, 2604.

¹²⁶ Noyce, D. S.; Hartter, D. R.; Pollack, R. M. *J. Am. Chem. Soc.* **1968**, *90*, 3791.

¹²⁷ Noyce, D. S.; Hartter, D. R.; Miles, F. B. *J. Am. Chem. Soc.* **1968**, *90*, 3794.

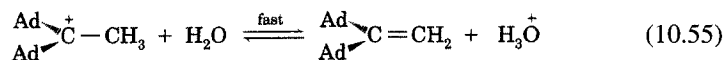
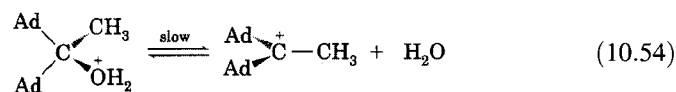
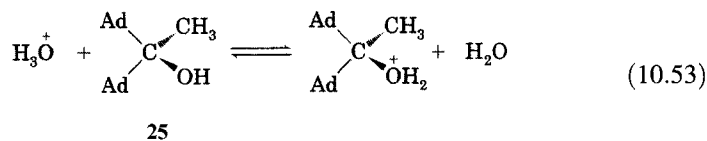
¹²⁸ For a discussion and leading references to proposals of a proton-alkene π complex as an intermediate in the dehydration of alcohols and the protonation of alkenes, see reference 120.

**FIGURE 10.44**

Concerted mechanism for dehydration of 1-propanol. (Adapted from reference 129.)

Because of the instability of 1° carbocations and the conclusion that 1° alcohols undergo acid-catalyzed oxygen exchange by an S_N2 process, there may be some question whether 1° carbocations are true intermediates in elimination reactions. An alternative mechanistic possibility for dehydration of 1° alcohols is an acid-catalyzed E2 mechanism. Narayan and Antal proposed such a mechanism for the specific acid-catalyzed dehydration of 1-propanol with sulfuric acid in supercritical water (Figure 10.44).¹²⁹

The concerted E2 process in Figure 10.44 seems not to apply to benzylic or 3° (alkyl) alcohols, which can react by an E1 pathway, but the situation for 2° alcohols in aqueous solution is less certain. Lomas studied the acid-catalyzed dehydration of 1,1'-diadamantylethanol (**25**) to 1,1-bis(1-adamantyl)ethene (**26**) in anhydrous acetic acid solution.¹³⁰ Dehydration of the trideuterio-methyl analog produced a deuterium kinetic isotope effect, with $k_{\text{H}}/k_{\text{D}}$ equal to 1.32. This result is not consistent with a mechanism in which the β-proton is lost in the rate-limiting step, but it is consistent with rate-limiting formation of the carbocation intermediate (with the $k_{\text{H}}/k_{\text{D}}$ ratio reflecting a secondary kinetic isotope effect), as shown in equation 10.54.



26

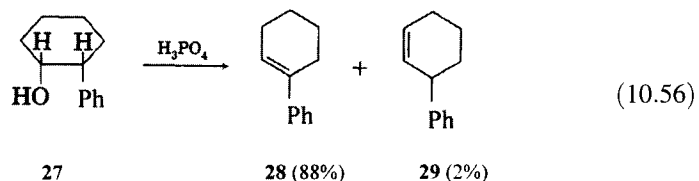
On the other hand, Dietze and Jencks concluded that the hydration of 1-butene and the oxygen exchange between solvent water and 2-butanol do not involve a common carbocation intermediate.¹²² A common intermediate would be expected to partition to the same products under identical conditions, but the investigators found that different ratios of *cis*- to *trans*-2-butene are formed when 1-butene and 2-butanol are subjected to the same reaction conditions. Furthermore, the two reactants gave different ratios of products derived from deprotonation and water addition. Dietze and Jencks concluded

¹²⁹ Narayan, R.; Antal, M. J., Jr. *J. Am. Chem. Soc.* **1990**, *112*, 1927.

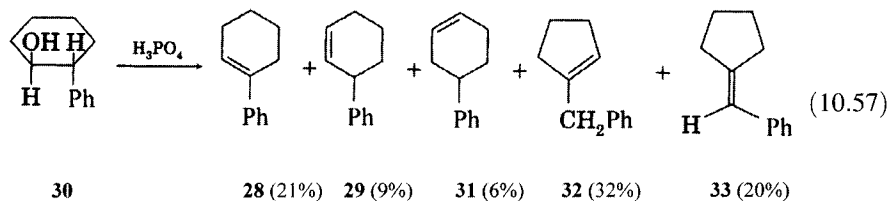
¹³⁰ Lomas, J. S. *J. Org. Chem.* **1981**, *46*, 412.

that isomerization of 1-butene and oxygen exchange of 2-butanol may occur through parallel concerted mechanisms in which there is significant carbocation character in the transition structures. A possible explanation for the failure to observe a common carbocation intermediate is that ordinary 2° carbocations do not have a significant lifetime in the presence of water.¹²²

Even though the dehydration reactions of many alcohols may occur by processes that do not produce solvent-equilibrated carbocations, it is clear that considerable carbocationic character does develop during the course of the reaction. This carbocationic character can lead to hydride, alkyl, and aryl shifts. For example, the dehydration of *cis*-2-phenylcyclohexanol (**27**) with phosphoric acid produced an 88% yield of 1-phenylcyclohexene (**28**) and a 2% yield of 3-phenylcyclohexene (**29**).¹³¹



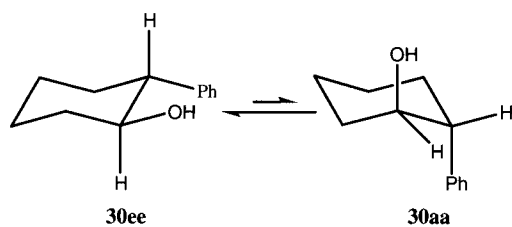
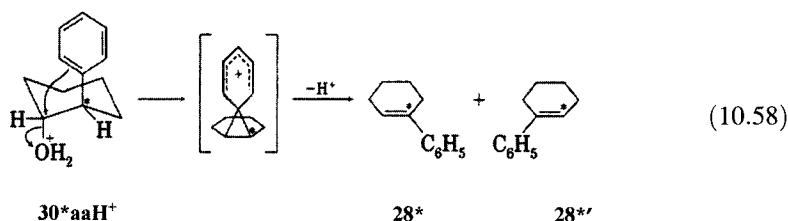
In contrast, the *trans* isomer (**30**) was found to give 21% of **28**, 9% of **29**, 6% of 4-phenylcyclohexene (**31**), 32% of 1-benzylcyclopentene (**32**), and about 20% of 1-benzalicyclopentane (**33**).



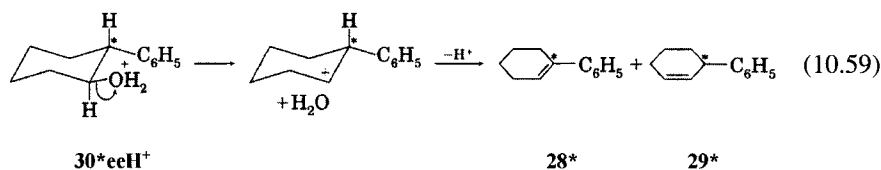
To explain these results, the investigators suggested that the two chair conformers of **30** could give rise to different reaction pathways. The diaxial conformer **30aa** (Figure 10.45) has a phenyl group that is properly oriented for anchimeric assistance to the departure of water from the protonated alcohol, with the resulting formation of a symmetrical phenonium ion. Loss of a proton from the phenonium ion produces **28**. Confirmation of the phenyl migration pathway in the dehydration reaction was found in the reaction of 2-phenylcyclohexanol-2-¹⁴C, which produced 1-phenylcyclohexene labeled with ¹⁴C at both C1 and C2 (equation 10.58). This mechanism cannot be the only pathway to **28**, because the symmetrical phenonium ion should give product with the ¹⁴C label distributed equally on C1 and C2. Instead, only about 25% of **28** was found to have the ¹⁴C label on C2. (In equation 10.58, the notation **30*aaH⁺** means that **30** is labeled with ¹⁴C, is protonated, and is in the diaxial conformation. The notations **28*** and **28*'s** indicate isotomers of labeled **28**.)¹³²

¹³¹ Schaeffer, H. J.; Collins, C. J. *J. Am. Chem. Soc.* **1956**, *78*, 124.

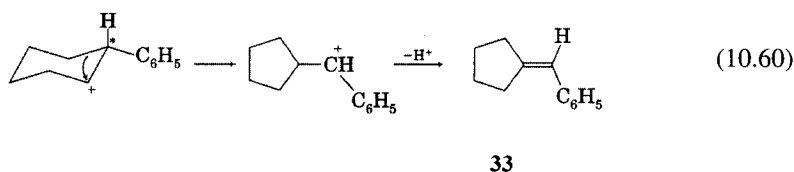
¹³² *Isotomers*, such as CH₂DCH₂OH and CH₃CHDOH, are isomers that differ only in the location of one or more atomic isotopes.

**FIGURE 10.45**Chair conformations of *trans*-2-phenylcyclohexanol.

To explain the formation of some of the **28** without phenyl rearrangement and to explain the high yields of the other products, the investigators proposed that loss of water from the protonated diequatorial conformer **30ee** (the major conformer) leads to a 2-phenylcarbocation, which can lose a proton to form either unrearranged **28** or **29**. Reprotonation of **29** and subsequent deprotonation of the 3-phenylcyclohexyl carbocation could lead to **31**.



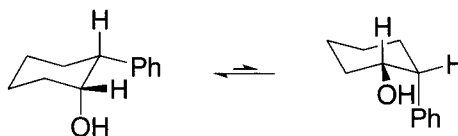
The ring contraction products were explained by an alkyl shift involving C6. The C1–C6 bond is anti to the departing water molecule, which facilitates the alkyl shift shown in equation 10.60. The alkyl shift forms a benzylic carbocation that can lose a proton to form **33**. Reprotonation of **33** and subsequent deprotonation of the benzyliccyclopentyl carbocation would lead to **32**.



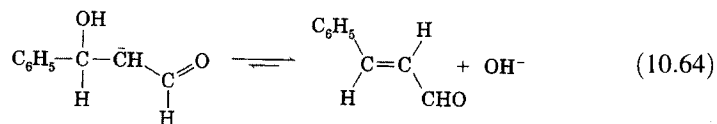
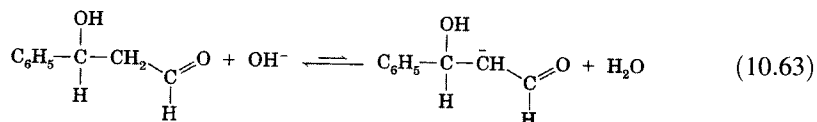
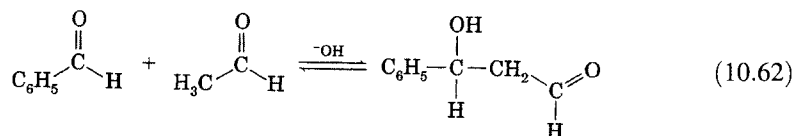
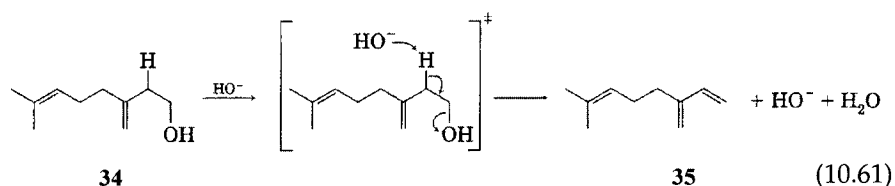
The products of dehydration of the *cis* isomer (equation 10.56) are quite different from those produced from the *trans* isomer because each of the two chair conformations of the *cis* isomer has one axial and one equatorial substituent (Figure 10.46). In neither conformation is the phenyl group anti to the departing water molecule, so phenyl migration does not accompany loss of water from the protonated alcohol.

FIGURE 10.46

Chair conformations of *cis*-2-phenylcyclohexanol.



Although the dehydration of most alcohols is acid catalyzed, base-catalyzed eliminations can be observed if the elimination of water leads to a conjugated product. For example, equation 10.61 shows a concerted mechanism for the dehydration of 7-methyl-3-methyleneoct-6-en-1-ol (**34**) to myrcene (**35**).^{115c,133} A carbanion (E1cb) mechanism has been proposed for the dehydration step in the base-catalyzed aldol reaction of benzaldehyde and acetone (equations 10.62–10.64).^{134,135}



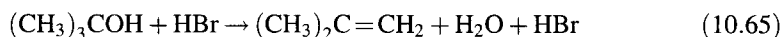
Heating alcohols in the gas phase to temperatures above 500°C can lead to dehydration, but dehydrogenation to carbonyl compounds also occurs.^{115c} Better yields of dehydration products are obtained if catalysts are added to the reaction mixture. Heating *t*-butyl alcohol in the gas phase at 315–422°C

¹³³ Ohloff, G. *Chem. Ber.* **1957**, *90*, 1554.

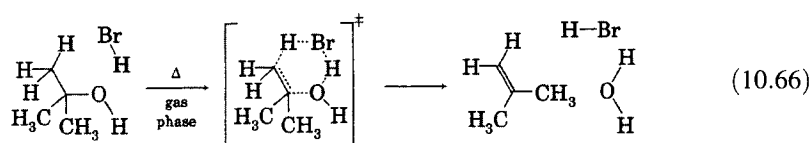
¹³⁴ Noyce, D. S.; Reed, W. L. *J. Am. Chem. Soc.* **1959**, *81*, 624.

¹³⁵ See also Crowell, T. I. in Patai, S., Ed. *The Chemistry of Alkenes*; Wiley-Interscience: London, 1964; pp. 241–270.

with a catalytic amount of HBr produced isobutene and water.¹³⁶ The stoichiometry of the reaction is



Similarly, heating 2-butanol in the gas phase with a catalytic amount of HBr at temperatures of 387–510°C was found to produce a mixture of water, 1-butene, *cis*-2-butene, and *trans*-2-butene. The reaction was overall second order, first order in alcohol and first order in HBr. The reaction was unaffected by additives expected to retard the rates of radical reactions, so a molecular reaction pathway seemed most likely.¹³⁷ Several bimolecular mechanisms were considered, but a mechanism involving the transition structure shown in equation 10.66 is particularly interesting because of the resemblance of this transition structure to those proposed for pyrolytic eliminations (page 681).^{136,138}



One of the most active areas of research in dehydration reactions is the use of heterogeneous catalysts (such as metal oxides, alumina, and zeolites) to catalyze the elimination of water from alcohols. Not only do the catalysts lower the temperatures required for dehydration, but they can also alter product distributions. For example, dehydration of 2-butanol produced 45% of 1-butene when the dehydration was catalyzed by alumina but 90% of 1-butene when zirconia was the catalyst.¹³⁹ A wide variety of mechanisms have been considered for these reactions.¹¹⁵ The effect of the catalyst is a function of the nature of the acidic and basic sites on the catalyst surface, the size of openings into which organic molecules may fit, molecular shape, and reaction temperature.¹⁴⁰ In the case of zeolites, carbocations and alkyl silyl ethers have been detected as reactive intermediates.¹⁴¹

Deamination of Amines

The reaction of 1° amines with nitrous acid produces diazonium ions (equation 10.67).^{142,143}

¹³⁶ Maccoll, A.; Stimson, V. R. *J. Chem. Soc.* **1960**, 2836.

¹³⁷ Failes, R. L.; Stimson, V. R. *J. Chem. Soc.* **1962**, 653.

¹³⁸ Another possibility for the transition structure is an ion pair composed of the protonated alcohol and bromide ion.

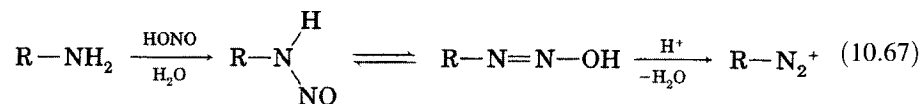
¹³⁹ Davis, B. H. *J. Org. Chem.* **1982**, *47*, 900.

¹⁴⁰ For example, see Yue, P. L.; Olaofe, O. *Chem. Eng. Res. Des.* **1984**, *62*, 167; Paukstis, E.; Jiratova, K.; Soltanov, R. I.; Yurchenko, E. N.; Beranek, L. *Collect. Czech. Chem. Commun.* **1985**, *50*, 643.

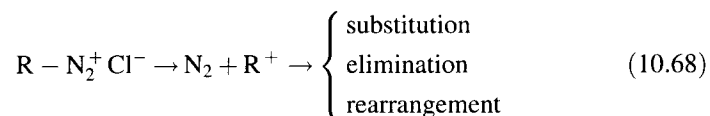
¹⁴¹ Stepanov, A. G.; Zamaraev, K. I.; Thomas, J. M. *Catal. Lett.* **1992**, *13*, 407.

¹⁴² Ridd, J. H. *Q. Rev. Chem. Soc.* **1961**, *15*, 418.

¹⁴³ White, E. H.; Woodcock, D. J. in Patai, S., Ed. *The Chemistry of the Amino Group*; Wiley-Interscience: London, 1968; pp. 407–497.



The aryldiazonium ions derived from 1° aromatic amines are useful intermediates in the synthesis of a wide variety of substituted aromatic compounds. The alkyldiazonium ions derived from 1° aliphatic amines are not regarded as being synthetically useful, however, because they generally lead to a mixture of products. For example, treatment of *n*-butylamine with sodium nitrite in aqueous HCl produced 1-butanol (25%), 2-butanol (13.2%), 1-chlorobutane (5.2%), 2-chlorobutane (2.8%), a mixture of butenes (36.5%), and unidentified higher boiling compounds (7.6%).¹⁴⁴ An explanation for the variety of products arising from 1° alkyldiazonium ions is shown in equation 10.68, in which loss of N₂ produces a carbocation that can then give a mixture of substitution, elimination, and rearrangement products.



There is evidence that carbocations do play a role in the reaction of some diazonium ions.¹⁴⁵ For example, the products of nucleophilic addition to *t*-butyl carbocations are essentially the same whether the carbocations are produced from aliphatic amines or from solvolysis of the corresponding alkyl halide.¹⁴⁶ The decomposition of the diazonium ion to form a carbocation should become less favorable as the stability of the carbocation decreases, and the formation of an ethyl cation from ethyldiazonium ion in the gas phase has been calculated to be endothermic by 13.9 kcal/mol.¹⁴⁷ The decomposition of a 1° alkyldiazonium ion to N₂ and a 1° carbocation in solution may be energetically more favorable, perhaps even exothermic, but it is questionable whether a free carbocation is formed from a 1° alkyldiazonium ion.¹⁴⁸ For example, the distribution of olefinic products from deamination of *sec*-butylamine was different from that obtained by solvolysis of the corresponding tosylate (Figure 10.47).¹⁴⁹ The results suggested that products from the deamination reaction must arise, at least in part, by some pathway not involving a 2° carbocation intermediate.¹⁵⁰

¹⁴⁴ Whitmore, F. C.; Langlois, D. P. *J. Am. Chem. Soc.* **1932**, *54*, 3441.

¹⁴⁵ For a review, see Friedman, L. in Olah, G. A.; Schleyer, P. v. R., Eds. *Carbonium Ions*, Vol. II; Wiley-Interscience: New York, 1970; pp. 655–713.

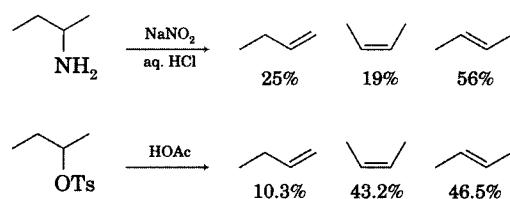
¹⁴⁶ Streitwieser, A., Jr. *J. Org. Chem.* **1957**, *22*, 861 and references therein.

¹⁴⁷ Ford, G. P.; Scribner, J. D. *J. Am. Chem. Soc.* **1983**, *105*, 349.

¹⁴⁸ The reaction is known to have an activation energy on the order of 3–5 kcal/mol (reference 149).

¹⁴⁹ Streitwieser, A., Jr.; Schaeffer, W. D. *J. Am. Chem. Soc.* **1957**, *79*, 2888.

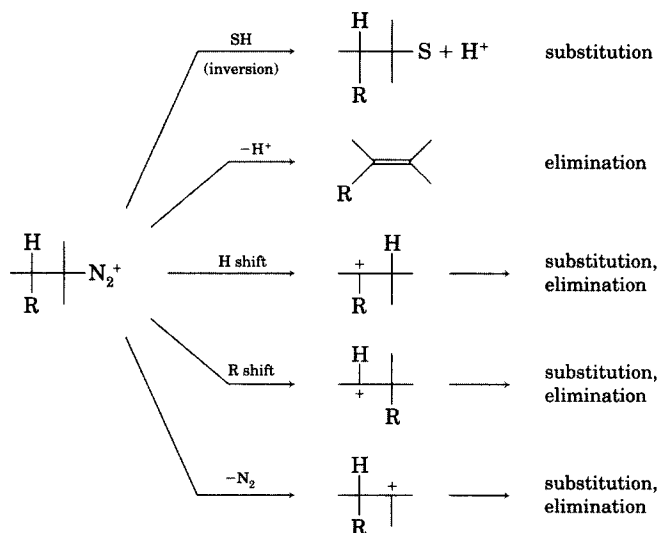
¹⁵⁰ It has been proposed in some cases that differences in product distributions from deamination reactions and those expected from solvolyses reactions expected to produce the same carbocations can be explained if the deamination produces a "hot" (distorted) carbocation. See, for example, Semenow, D.; Shih, C.-H.; Young, W. G. *J. Am. Chem. Soc.* **1958**, *80*, 5472. In other cases ion pairing effects have been suggested as important in determining the products in deamination reactions (reference 157).

**FIGURE 10.47**

Distribution of butenes from deamination and solvolysis reactions. (Data from reference 149.)

As an alternative to mechanistic schemes requiring carbocation intermediates, Streitwieser suggested that loss of N_2 from an alkyldiazonium ion may occur during, not before, bonding changes that lead to the reaction products.^{146,149} As shown in Figure 10.48, N_2 loss could be concerted with displacement by solvent, with loss of a proton to form an alkene, with a hydride shift to form a rearranged carbocation, or with an alkyl or aryl shift to form a different rearranged carbocation. The possibility that a free carbocation might be formed was also included in the reaction scheme.

One of the strongest arguments against the formation of 1° carbocations in the deamination of 1° amines comes from stereochemical studies. Reaction of nitrous acid with optically active 1- ^{2}H -1-butanamine (**36**) produced the diazonium ion **37**, which then formed 1-butanol (**38**) with essentially complete inversion of configuration (equation 10.69).^{151,152} This result suggested that the formation of **38** does not occur by capture of the 1° butyl cation by water but is, instead, the product of an S_N2 reaction on **37**.¹⁵³

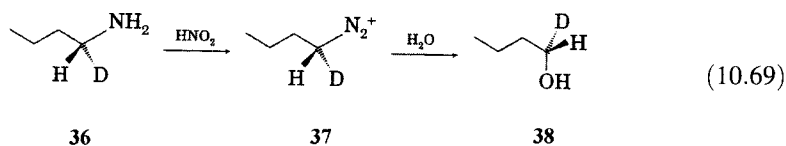
**FIGURE 10.48**

Reaction pathways in diazonium ion decomposition. (Adapted from reference 149.)

¹⁵¹ Brosch, D.; Kirmse, W. *J. Org. Chem.* **1991**, *56*, 907.

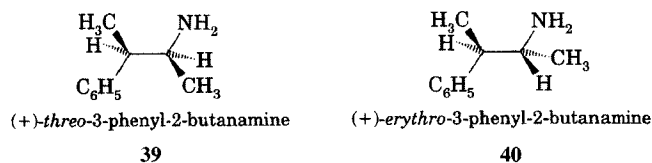
¹⁵² Deamination of **36** was accompanied by the formation of 2-butanol (30%) as well as 1-butanol (51%).

¹⁵³ Similar results were obtained in the study of an optically active secondary amine. Radical pathways have also been implicated in the deamination of 1-octanamine in micellar media. Brosch, D.; Kirmse, W. *J. Org. Chem.* **1993**, *58*, 1118.



Streitwieser rationalized the propensity for deamination reactions to give a wide variety of products with an argument based on the Hammond postulate. Because the transition states in the reactions shown in Figure 10.48 are likely to be early (reactant-like), there should be only small differences in their activation energies, and a wide variety of reactions should be competitive. In contrast, solvolysis and other reactions have much higher activation energies, so their transition states are later. As a result, there should be much larger differences in activation energies for the various pathways available to the reactant in solvolysis reactions, and that should give much larger preferences for one reaction pathway over another.¹⁴⁹

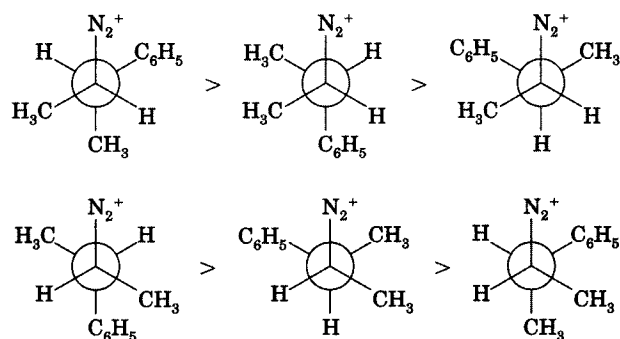
Streitwieser also noted that the small activation energies for diazonium ion decomposition are comparable to energy barriers for rotation about carbon-carbon single bonds. As a result, the product distributions from deamination reactions might be affected by the distribution of conformations of the diazonium ions.¹⁴⁹ Evidence for this view came from a study of the deamination of 3-phenyl-2-butanamine in acetic acid by Cram and McCarty.¹⁵⁴ The mixture of acetate products was reduced with LiAlH_4 to produce 1-methyl-1-phenylpropanol (the product of a phenyl migration to the site of the departing N_2 moiety) and 2-methyl-1-phenylpropanol (the product of a corresponding methyl migration), along with diastereomeric 3-phenyl-2-butanols. The product distribution was found to be a function of the stereochemistry of the starting amine. Product ratios from deamination of the threo diastereomer (**39**) were consistent with a 1.5 to 1 ratio of methyl to phenyl migration. Product ratios from deamination of the erythro diastereomer (**40**) suggested an 8 to 1 preference for phenyl migration over methyl migration. Solvolysis of the corresponding tosylates in acetic acid did not produce any product of methyl migration, however.



To explain these results, the investigators suggested that the rate constant for product formation from the carbocation intermediate is greater than the rate constant for rotation about the carbon-carbon single bond.¹⁵⁵ Therefore, the product distribution is determined by the relative stability of the conformers of each enantiomer. As shown in Figure 10.49, the relative stability of the conformers of the (+)-threo diastereomer (top) suggests that migration

¹⁵⁴ Cram, D. J.; McCarty, J. E. *J. Am. Chem. Soc.* **1957**, *79*, 2866.

¹⁵⁵ Central to this argument is the assumption that reaction of the incipient carbocations is significantly faster than is rotation about carbon-carbon single bonds. As noted in Chapter 6, the Curtin-Hammett principle applies to situations in which conformational interconversion is faster than the rates of reaction of conformers.

**FIGURE 10.49**

Relative stabilities of *threo*- (top) and *erythro*-3-phenyl-2-butanamine (bottom) conformers. (Adapted from reference 154.)

of a methyl group may occur more often than migration of a phenyl group because of the greater population of conformers in which a methyl group is anti-coplanar to the departing N_2 . Similarly, the greater population of conformers of the (+)-*erythro* diastereomer (bottom) in which a phenyl group is anti-coplanar to the departing N_2 is entirely consistent with the observation that phenyl migration is the dominant process in reactions of this diastereomer.^{156,157}

Pyrolytic Eliminations

Some intramolecular eliminations that occur thermally are known as **pyrolytic eliminations**,¹⁵⁸ and many of these reactions result in *syn* elimination.^{159,160} Often these reactions are carried out in the gas phase, where they are not affected by solvent, counterions, or other species that can affect reactions in solution.¹⁶¹ One of the most-studied pyrolytic eliminations is the Chugaev reaction (equation 10.70).^{162,163} Reaction of an alcohol having a β -hydrogen atom with sodium or potassium metal or with a strong base

¹⁵⁶ A similar conclusion was reached by Monera, O. D.; Chang, M.-K.; Means, G. E. *J. Org. Chem.* **1989**, *54*, 5424, who investigated the deamination of 1-octanamine in a series of solutions ranging from pH 2 to pH 10. The relative distribution of products—1-octanol, 2-octanol, 1-octene, and 2-octenes (80% *trans*, 20% *cis*)—did not vary significantly as a function of pH. The authors interpreted the results in terms of conformationally determined reactions of the alkyl diazonium ion.

¹⁵⁷ Although the discussion in reference 154 was presented in terms of methyl or phenyl migration to a carbocation, after the loss of N_2 , the arguments can also apply to concurrent migration and loss of N_2 . The deamination of optically active 2-octanamine was found to produce 2-octanol with 24% net inversion, suggesting that some S_N2 reaction with solvent occurs in this 2° system also: Moss, R. A.; Talkowski, C. J.; Reger, D. W.; Powell, C. E. *J. Am. Chem. Soc.* **1973**, *95*, 5215. The reaction was sensitive to medium effects, and the stereochemistry changed to 6% retention of configuration in micellar media. However, Collins, C. J. *Acc. Chem. Res.* **1971**, *4*, 315 argued that free carbocations are formed, at least with some 2° alkyl and benzylic amines.

¹⁵⁸ Reference 20, pp. 377–482; reference 19, pp. 167–195.

¹⁵⁹ For a review of pyrolytic *syn* eliminations, see DePuy, C. H.; King, R. W. *Chem. Rev.* **1960**, *60*, 431.

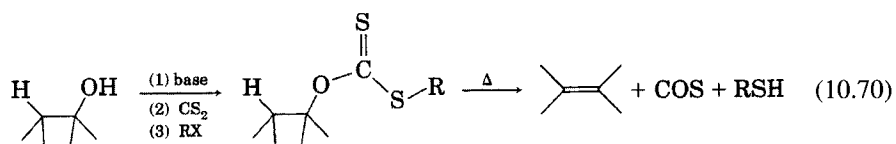
¹⁶⁰ In the IUPAC nomenclature system (reference 25), this mechanism is termed a cyclo- $D_E D_N A_n$ mechanism.

¹⁶¹ There may be complications due to surface effects of the reaction vessel. See the discussion on page 687.

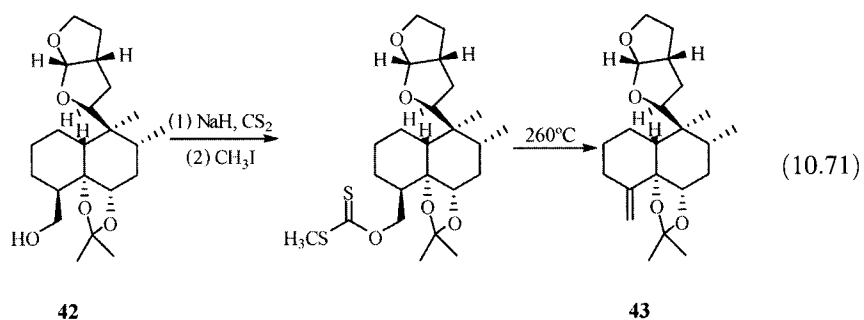
¹⁶² (a) O'Connor, G. L.; Nace, H. R. *J. Am. Chem. Soc.* **1952**, *74*, 5454; (b) O'Connor, G. L.; Nace, H. R. *J. Am. Chem. Soc.* **1953**, *75*, 2118; (c) Nace, H. R. *Org. React.* **1962**, *12*, 57.

¹⁶³ Chugaev, L. A. *Chem. Ber.* **1899**, *32*, 3332. An alternate spelling is "Tschugaeff" (reference 164), but "Chugaev" is used more commonly now.

such as sodium amide, followed by reaction of the alkoxide with CS_2 and then $\text{S}_{\text{N}}2$ reaction with an alkyl halide, usually methyl iodide, produces a xanthate ester (**41**, equation 10.70). The xanthate ester is purified as much as possible and is then heated, usually by distillation at atmospheric pressure, to induce decomposition to an alkene, along with carbon oxysulfide and a mercaptan.¹⁶² This alkene synthesis is particularly useful because it provides a means of dehydration of an alcohol without the possible complications of carbocation rearrangements.^{164–166} An example of the application of xanthate pyrolysis in organic synthesis is the conversion of **42** to **43**, a key intermediate in the synthesis of the natural product lupulin C (equation 10.71).¹⁶⁷ This selective method of alcohol dehydration avoids acidic conditions that would cause unwanted side reactions in other parts of the structure.



41



Cram demonstrated that the Chugaev reaction is a syn elimination by showing that the pyrolysis of the *S*-methyl xanthate of diastereomeric 3-phenyl-2-butanols is stereospecific, as shown in equations 10.72 and 10.73.^{168–170} As noted, the eliminations also produced 3-phenyl-1-butene (in 30–40% yield).

¹⁶⁴ See, for example, Stevens, P. G. *J. Am. Chem. Soc.* **1932**, *54*, 3732 and references therein.

¹⁶⁵ Schurman, I.; Boord, C. E. *J. Am. Chem. Soc.* **1933**, *55*, 4930.

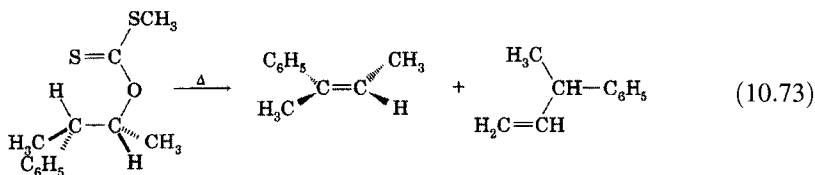
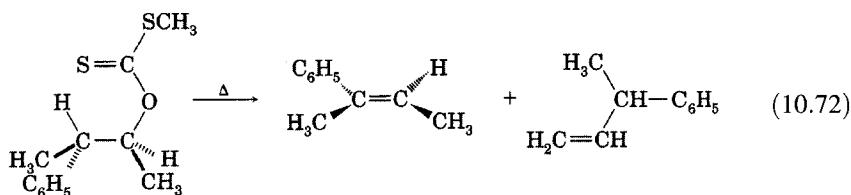
¹⁶⁶ If more than one $\text{C}_\beta\text{-H}$ bond is present, a mixture of alkenes can be produced. As discussed in reference 159, the product distribution depends on the number of $\text{C}_\beta\text{-H}$ bonds that can lead to each product, steric factors in conformations in which each $\text{C}_\beta\text{-H}$ bond is syn-coplanar to the $\text{C}_\alpha\text{-O}$ bond, and the relative thermodynamic stabilities of the products.

¹⁶⁷ Meulemans, T. M.; Stork, G. A.; Macaev, F. Z.; Jansen, B. J. M.; de Groot, A. *J. Org. Chem.* **1999**, *64*, 9178.

¹⁶⁸ Cram, D. J. *J. Am. Chem. Soc.* **1949**, *71*, 3883.

¹⁶⁹ Syn elimination provides a means of determining stereochemical relationships in natural product structure elucidation. Barton, D. H. R. *J. Chem. Soc.* **1949**, 2174.

¹⁷⁰ In some cases product distributions suggest the possibility that anti elimination might occur, but uncertainties about reactant purity can make it difficult to quantify the amount of non-syn elimination. For a discussion, see reference 159, p. 444 ff.



The pyrolysis of cholesteryl methyl xanthate was found to have an E_a of 32.9 kcal/mol and a ΔS^\ddagger of -4.7 eu.^{162a} The low activation energy suggested a concerted reaction (in which bond forming and bond breaking occur simultaneously), and the negative activation entropy suggested a cyclic transition structure. Two slightly different mechanisms are consistent with the kinetic and stereochemical results. The mechanism currently accepted is a two-step process. The first, rate-limiting step is a concerted unimolecular elimination (E_i) involving hydrogen abstraction by the thione sulfur atom in a cyclic transition structure, while the second step is decomposition of the RSCOSH to COS and RSH (Figure 10.50).¹⁷¹

An alternative cyclic mechanism (Figure 10.51) involves hydrogen abstraction by the thioether sulfur atom, which leads to the observed products in one step. Bader and Bourns reported a combination of carbon and sulfur isotope effects that are consistent with the mechanism in Figure 10.50 but are not consistent with the mechanism in Figure 10.51.^{172,173}

Generalizing the Chugaev reaction as shown in Figure 10.52 suggests that many other organic compounds should pyrolyze to alkenes.¹⁷⁴ Unimolecular syn elimination has been reported for alkyl esters,^{175,176} carbonates, carbamates,^{162b} amides, vinyl ethers, and carboxylic acid anhydrides.¹⁵⁹ The mechanistic resemblance of several of these eliminations to the Chugaev reaction was noted by O'Connor and Nace, who found activation entropies for the pyrolyses of cholesteryl carbamate, acetate, and methyl xanthate to be

¹⁷¹ The cyclic transition structure was proposed by Hurd and Blunck for pyrolysis of esters having a β -hydrogen atom (reference 175).

¹⁷² Bader, R. F. W.; Bourns, A. N. *Can. J. Chem.* **1961**, *39*, 348.

¹⁷³ In some cases, the presence of peroxide impurities may introduce an alternative radical mechanism for xanthate decomposition. Nace, H. R.; Manly, D. G.; Fusco, S. *J. Org. Chem.* **1958**, *23*, 687. Radical processes were also proposed for the formation of minor products in the pyrolysis of alkyl acetates. Shi, B.; Ji, Y.; Dabbagh, H. A.; Davis, B. H. *J. Org. Chem.* **1994**, *59*, 845.

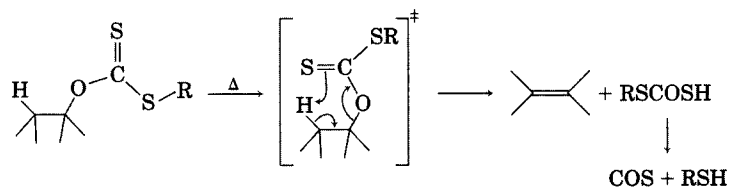
¹⁷⁴ If b is CH and a, c, d, and e are all CH_2 , then the reaction shown in Figure 10.52 is a retro-ene reaction, which is discussed in Chapter 11.

¹⁷⁵ Hurd, C. D.; Blunck, F. H. *J. Am. Chem. Soc.* **1938**, *60*, 2419.

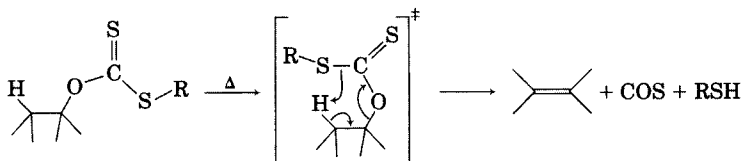
¹⁷⁶ In one case, pyrolysis of an ester led to anti elimination. The results were explained on the basis of a mechanism incorporating anchimeric assistance: Smismann, E. E.; Li, J. P.; Creese, M. W. *J. Org. Chem.* **1970**, *35*, 1352. Anchimeric assistance was also proposed for a gas phase elimination of hydrogen chloride: Hernandez, J. A.; Chuchani, G. *Int. J. Chem. Kinet.* **1978**, *10*, 923; Chuchani, G.; Martin, I. *J. Phys. Chem.* **1986**, *90*, 431.

FIGURE 10.50

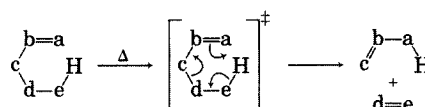
Concerted mechanism proposed for Chugaev reaction.

**FIGURE 10.51**

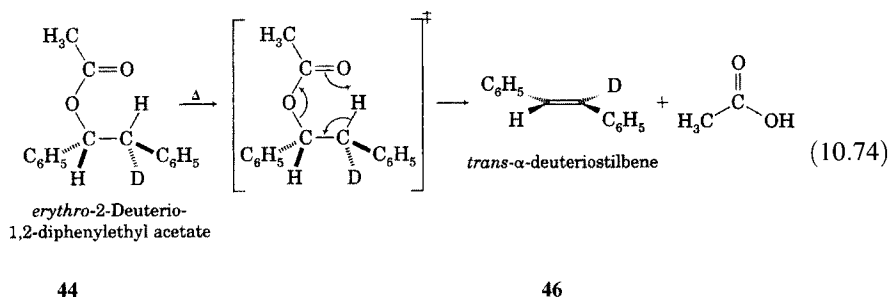
Alternative mechanism for Chugaev reaction.

**FIGURE 10.52**

A general mechanism for concerted pyrolytic eliminations.



very similar (Table 10.8).¹⁷⁷ Kinetic isotope effect studies indicate that the C_{β} -H bond is being broken in the transition structure in these reactions also.¹⁵⁹ Furthermore, Curtin and Kellom demonstrated that ester pyrolysis occurs primarily through syn elimination by studying the pyrolysis of *erythro*- and *threo*-2-deuterio-1,2-diphenylethyl acetate (**44** and **45**, respectively).¹⁷⁸ Although the product of both reactions is *trans*-stilbene, the product of reaction of **44** retains almost all of the deuterium label (**46**, equation 10.74), but the olefinic product of pyrolysis of **45** has lost most of the deuterium label (**47**, equation 10.75).^{179,180}



¹⁷⁷ The lower activation energy for the xanthate pyrolysis means that it occurs at lower temperatures than do the other pyrolyses. As a result, xanthate pyrolysis avoids the necessity of vapor phase pyrolysis that the other eliminations require, and the products are less likely to undergo further reaction at the lower temperature of xanthate pyrolysis. For a discussion, see reference 159.

¹⁷⁸ Curtin, D. Y.; Kellom, D. B. *J. Am. Chem. Soc.* **1953**, *75*, 6011.

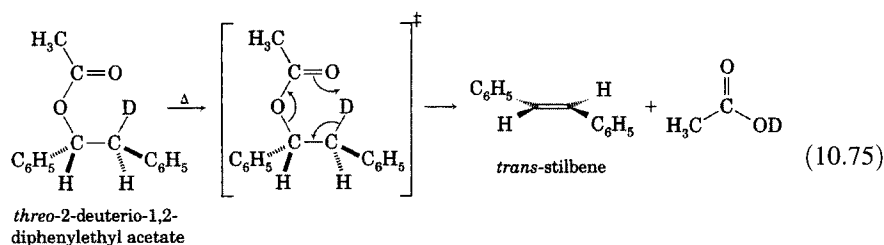
¹⁷⁹ Quantitative interpretation of the percent of deuterium retention is subject to uncertainty because the stilbenes are not completely stable at the temperature of the pyrolysis reaction. See the footnote to Table 1 in reference 178.

¹⁸⁰ For a theoretical study of the gas phase pyrolysis of esters, see Lee, I.; Cha, O. J.; Lee, B.-S. *J. Phys. Chem.* **1990**, *94*, 3926.

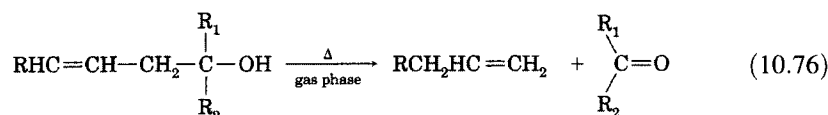
TABLE 10.8 Activation Parameters for Pyrolysis of Cholesteryl Derivatives

Compound	E_a (kcal/mol)	ΔS^\ddagger (eu)
Cholesteryl ethyl carbamate	41.0	-4.3
Cholesteryl acetate	44.1	-3.6
Cholesteryl methyl xanthate	32.9	-4.7

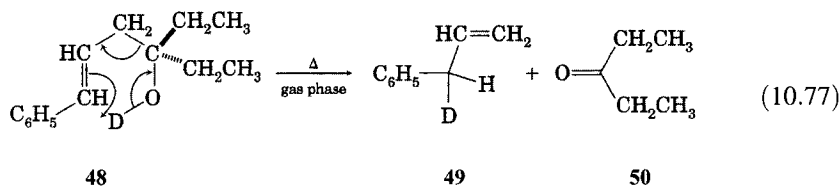
Source: Reference 162b.



Similarly, β -hydroxyalkenes undergo elimination at 500°C in the gas phase to form an alkene and an aldehyde or ketone (equation 10.76).



Arnold and Smolinsky determined that the pyrolysis of 3-deuterio-3-ethyl-6-phenyl-5-hexen-3-ol (48) produced 3-deuterio-3-phenylpropene (49) and 2-pentanone (50). This result confirmed a syn elimination and suggested a cyclic transition structure for the reaction (equation 10.77).¹⁸¹



This conclusion was supported by the observation that pyrolysis of 3-butenol has a ΔS^\ddagger of -8.8 eu, which is similar to the activation entropy values reported for pyrolysis of ethyl formate and for 3-butenic acid, and the activation energies for all three pyrolyses are also similar (about 40 kcal/mol).¹⁸²

Another well-known concerted syn elimination is the **Cope elimination**, which involves the thermal elimination of an alkene from an amine oxide (Figure 10.53).^{183,184} Unlike the reactions discussed above, all of which have

¹⁸¹ Arnold, R. T.; Smolinsky, G. J. *Org. Chem.* **1960**, *25*, 129.

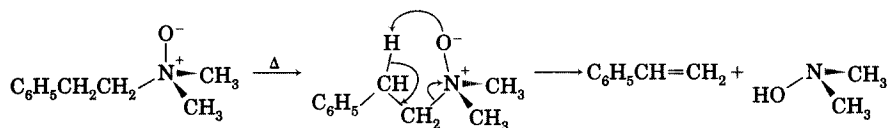
¹⁸² Smith, G. G.; Yates, B. L. *J. Chem. Soc.* **1965**, 7242.

¹⁸³ Cope, A. C.; Foster, T. T.; Towle, P. H. *J. Am. Chem. Soc.* **1949**, *71*, 3929.

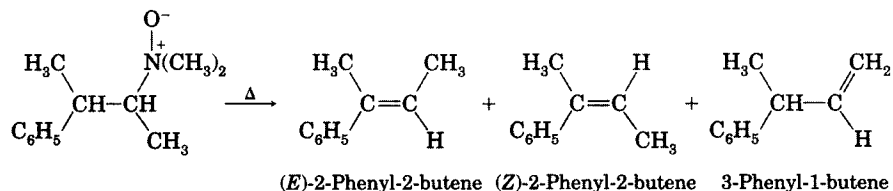
¹⁸⁴ Cope, A. C.; Trumbull, E. R. *Org. React.* **1960**, *11*, 317.

FIGURE 10.53

Concerted mechanism for the Cope elimination.

**FIGURE 10.54**

Products from pyrolysis of diastereomers of 2-amino-3-phenylbutane oxide.¹⁸⁵



Diastereomer (racemic)	Percent yield		
Erythro	4	89	7
Threo	93	0.2	7

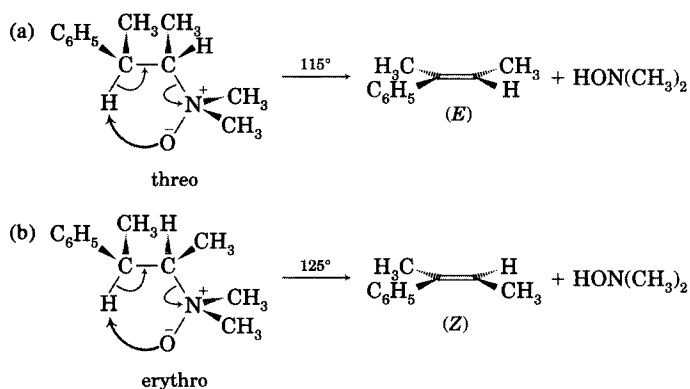
a six-membered ring in the transition structure, the Cope elimination has a five-membered ring in the transition structure.

Cram and McCarty demonstrated that the stereochemistry of the Cope elimination is syn by showing that diastereomeric 2-amino-3-phenylbutane oxides produce different product distributions (Figure 10.54).¹⁸⁵ Interestingly, the threo diastereomer undergoes pyrolysis at a lower temperature than does the erythro diastereomer. As shown in Figure 10.55(a), the Cope elimination of the threo diastereomer can occur through a transition structure in which a carbon-phenyl bond is eclipsed with a carbon-hydrogen bond. Elimination of the erythro diastereomer requires a more strained transition structure in which a carbon-phenyl bond eclipses a carbon-methyl bond, as shown in Figure 10.55(b).

The regiochemistry of the Cope elimination is different from that of the Hofmann elimination. As shown by the data in Table 10.9, there seems to be

FIGURE 10.55

Stereospecificity of Cope elimination. (Adapted from reference 185.)



¹⁸⁵ Cram, D. J.; McCarty, J. E. *J. Am. Chem. Soc.* 1954, 76, 5740.

TABLE 10.9 Product Distributions in Cope Eliminations from $R_1R_2CH_2N^+ - O^-$

Alkyl Groups		Olefinic Products			
R_1	R_2	Experimental Results		Statistical Prediction	
Ethyl	Propyl	62.5% Ethene	37.5% Propene	60% Ethene	40% Propene
Ethyl	Isopropyl	27.5% Ethene	72.5% Propene	33.3% Ethene	67.7% Propene
Ethyl	Isobutyl	67.6% Ethene	32.4% Isobutene	75% Ethene	25% Isobutene
<i>n</i> -Butyl	Isobutyl	64.8% 1-Butene	35.2% Isobutene	67.7% 1-Butene	33.3% Isobutene

Source: Reference 75.

only a slight tendency for a more substituted alkene to be formed in preference to a less substituted alkene. Instead, the product distributions are closely predicted on the basis of the number of β -hydrogen atoms that could be abstracted on each alkyl group.¹⁸⁴ If the β -carbon atom is substituted with a phenyl group (as in Figure 10.54), then the elimination strongly favors the product formed by abstraction of that β -hydrogen atom. This regiochemical preference may result from the greater acidity of that hydrogen atom.¹⁸⁴

One complication in all gas phase eliminations is uncertainty that the reaction actually occurs in the gas phase and not on the surface of the reaction vessel, because some pyrolyses appear to result from surface-mediated reactions.¹⁸⁶ For example, dissociation of an ester at the glass surface could produce a glass-stabilized carbocation that then loses a β -proton in the rate-limiting step of the reaction. Therefore, investigators sometimes add glass beads to a reaction vessel to see if product distributions are altered by the increase in surface area.¹⁸⁷

Another complication with gas phase pyrolyses is that many possible nonconcerted reaction pathways are possible. Alkyl halides undergo elimination in the gas phase,¹⁸⁸ and some compounds, such as ethyl chloride, appear to undergo unimolecular elimination.¹⁸⁹ Their unimolecular decompositions may involve transition structures with significant carbocation character.^{188,190} For example, pyrolysis of (+)-2-chlorooctane in the gas phase at 325–385°C was found to produce racemization of the starting material as well as elimination of HCl.¹⁹¹ Some compounds appear to react by radical chain mechanisms, and heterogeneous radical reactions often complicate studies that are not carried out in “well-seasoned” (i.e., coated with a layer of organic material) vessels. Furthermore, there appears to be a significant radical (but not radical chain) component to the pyrolysis of sulfoxides.¹⁹² These complications mean that many control studies are necessary to clarify the mechanism of gas phase elimination reactions.

¹⁸⁶ The investigators argued that it may be impossible to inactivate glass surfaces, so that true gas phase results can be obtained only when pyrolyses are conducted in stainless steel vessels that have carbonized interior surfaces and from which air is rigorously excluded. Wertz, D. H.; Allinger, N. L. *J. Org. Chem.* **1977**, *42*, 698.

¹⁸⁷ Dabbagh, H. A.; Davis, B. H. *J. Org. Chem.* **1990**, *55*, 2011.

¹⁸⁸ For a review, see Maccoll, A. *Chem. Rev.* **1969**, *69*, 33.

¹⁸⁹ Barton, D. H. R.; Howlett, K. E. *J. Chem. Soc.* **1949**, 165.

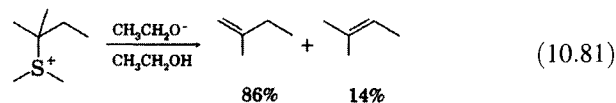
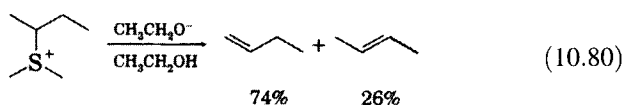
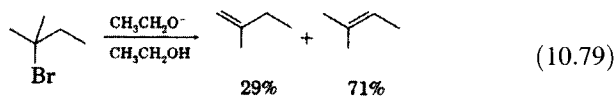
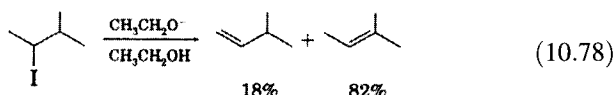
¹⁹⁰ Maccoll, A. *Adv. Phys. Org. Chem.* **1965**, *3*, 91.

¹⁹¹ Harding, C. J.; Maccoll, A.; Ross, R. A. *Chem. Commun.* **1967**, 289.

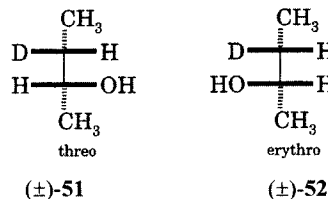
¹⁹² At lower temperatures a concerted mechanism appears to be the major pathway for reaction. Kingsbury, C. A.; Cram, D. J. *J. Am. Chem. Soc.* **1960**, *82*, 1810.

Problems

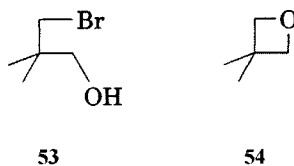
- 10.1. Ethoxide-promoted E2 elimination from 2-iodo-3-methylbutane produces 18% of the 1-alkene and 82% of the 2-alkene (equation 10.78), while elimination from 2-bromo-2-methylbutane produces 29% of the 1-alkene and 71% of the 2-alkene (equation 10.79). Similarly, E2 elimination of $(\text{CH}_3)_2\text{S}$ from dimethyl-*sec*-butylsulfonium ion produces 74% of the 1-alkene and 26% of the 2-alkenes (equation 10.80), while the bimolecular elimination of $(\text{CH}_3)_2\text{S}$ from dimethyl-*t*-amylsulfonium ion produces 86% of the 1-alkene and 14% of the 2-alkene (equation 10.81). In each case, an additional methyl substituent on the α -carbon atom leads to a greater proportion of the less substituted alkene. Explain the product distributions from all four reactions in terms of the factors that determine the distribution of products from E2 reactions.



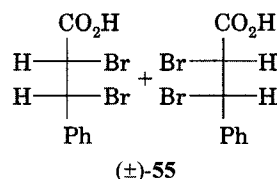
- 10.2. Construct appropriate Newman projections for **9** and **10** (page 649) to rationalize the greater reactivity of **10** than **9** in dehydrohalogenation reactions.
- 10.3. A study of the stereochemistry of the dehydration of alcohols to alkenes over metal oxide catalysts utilized the compounds (\pm)-*threo*-2-butanol-3- d_1 (**51**) and (\pm)-*erythro*-2-butanol-3- d_1 (**52**). Predict the products expected from each of these reactants for both syn and anti elimination pathways.



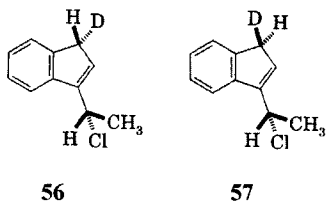
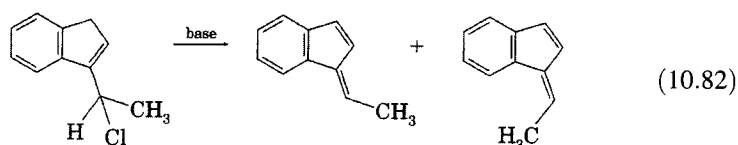
- 10.4. Reaction of 3-bromo-2,2-dimethyl-1-propanol (**53**) with KOH in aqueous solution produced a 20% yield of 2,2-dimethyltrimethylene oxide (**54**) along with isobutylene and formaldehyde. Propose a mechanism to account for the formation of these products.



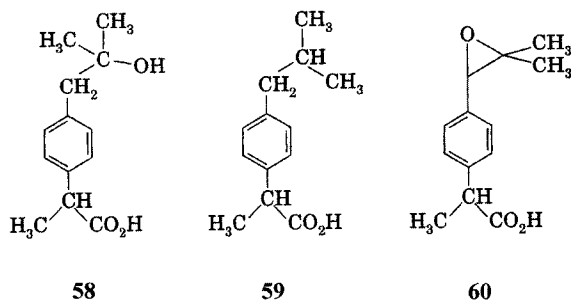
- 10.5. (\pm)-*erythro*-2,3-Dibromo-3-phenylpropanoic acid (**55**) can be decarboxylated to β -bromostyrene (1-bromo-2-phenylethene) by refluxing in water or by heating in the presence of sodium acetate in a variety of solvents. The product obtained by heating **55** in acetone in the presence of sodium acetate is the (*Z*) isomer of β -bromostyrene. In ethanol solution a mixture of (*Z*) and (*E*) isomers is formed, while in water the product is predominantly the (*E*) isomer. Propose a mechanism for the exclusive formation of the (*Z*) isomer of β -bromostyrene in acetone solution, and explain the effect of solvent on the stereoselectivity of the reaction.



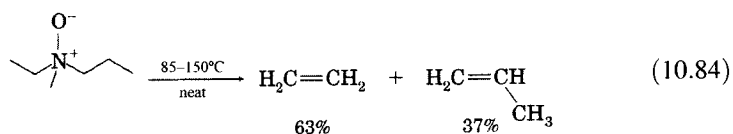
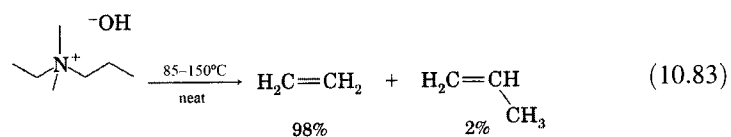
- 10.6. Base-promoted 1,4-dehydrochlorination of 3-(1-chloroethyl)indene leads to a pair of diastereomeric dienes (equation 10.82). How could compounds **56** and **57** be used to determine whether the reaction occurs by a *syn* or an *anti* pathway?



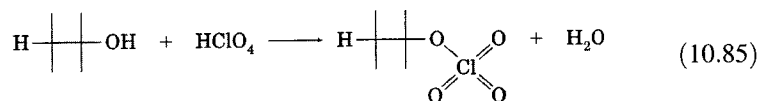
- 10.7. 2-[*p*-(2-Methyl-2-hydroxypropyl)phenyl]propionic acid (**58**) has been proposed to be a human metabolite of the analgesic ibuprofen (**59**). Propose a synthesis of **58** from **59** by a pathway involving (i) benzylic bromination with NBS, (ii) dehydrobromination, (iii) epoxidation with *m*-chloroperbenzoic acid, (iv) 1,6-eliminative cleavage of the resulting 2-[*p*-(2-methyl-1,2-epoxypropyl)phenyl]propionic acid (**60**), and (v) catalytic hydrogenation.



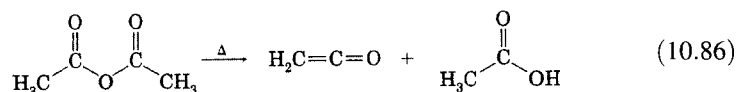
- 10.8. Reaction of 1,1-dichlorocyclohexane and of *cis*-1,2-dichlorocyclohexane with 0.1 M KOH in 4 : 1 (v : v) ethanol: water at 100°C results in the formation of a compound with the molecular formula C_6H_9Cl . Under the same conditions, however, the product of reaction of *trans*-1,2-dichlorocyclohexane has the molecular formula C_6H_8 .
- Propose a detailed mechanism to account for the formation of the products in each case, and explain why the product of the reaction of the *trans* isomer differs from the product formed by the other two isomers.
 - The relative reactivity of the three dichlorocyclohexanes under these reaction conditions is *cis*-1,2-dichlorocyclohexane (1.0), 1,1-dichlorocyclohexane (3×10^{-2}), and *trans*-1,2-dichlorocyclohexane (4.1×10^{-3}). Interpret these reactivities in terms of the mechanism proposed for each compound.
- 10.9. Concerted 1,2-eliminations occur with anti stereochemistry, and concerted 1,4-eliminations occur with predominantly syn stereochemistry. Predict the stereochemistry of concerted 1,6-, 1,8-, and 1,10-eliminations, and use a curved arrow description to illustrate the mechanism in each case.
- 10.10. Rationalize the difference in regioselectivity between the Hofmann elimination (equation 10.83) and Cope elimination (equation 10.84).



- 10.11. It has been proposed that the dehydration of alcohols catalyzed by perchloric, sulfuric, and acetic acids in methylene chloride solution could occur by a concerted elimination following formation of the alkyl ester of the inorganic acid. Show how the perchlorate ester shown in equation 10.85 could be used to carry out concerted dehydration of the alcohol in a mechanism analogous to the mechanism of the pyrolytic eliminations discussed in the section beginning on page 681, and predict whether the reaction would exhibit syn or anti stereochemistry.

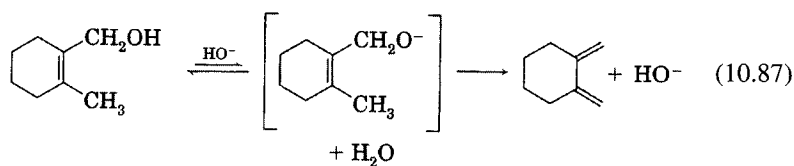


- 10.12. Ketene can be formed by pyrolysis of acetic anhydride (equation 10.86).¹⁹³ Show how cyclic transition structures similar to those drawn for other pyrolytic eliminations can explain this reaction.

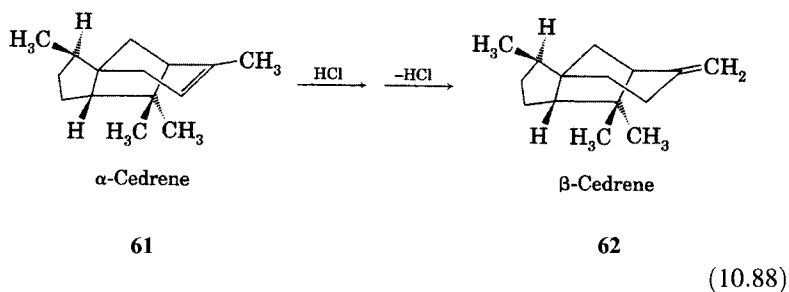


¹⁹³ Wilshire, N. T. M. *J. Chem. Soc.* **1907**, 91, 1938.

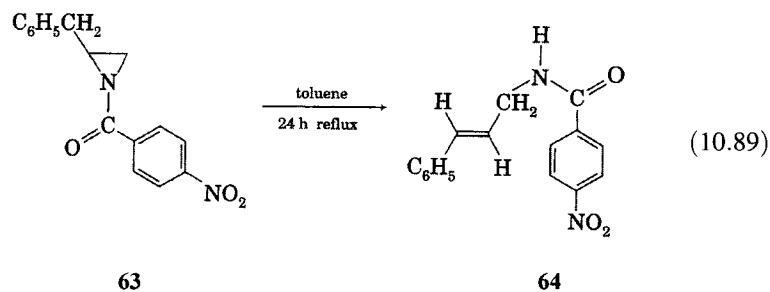
- 10.13. As noted on page 676, β,γ -unsaturated alcohols can be dehydrated to conjugated dienes with hydroxide ion. α,β -Unsaturated alcohols can also be dehydrated to conjugated dienes, as shown for the synthesis of 1,2-bis(methylene)cyclohexane in equation 10.87. Propose a mechanism for the reaction in equation 10.87 in which the second step is a concerted reaction analogous to a pyrolytic elimination reaction.



- 10.14. The hydrocarbon α -cedrene (61) has been converted to its isomer β -cedrene (62) in 52% yield by a two-step process involving first addition of HCl and then elimination of HCl (equation 10.88). Propose conditions that would optimize the formation of 62 from the intermediate alkyl halide.

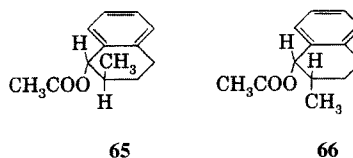


- 10.15. Rationalize the observation that $2\beta,3\alpha$ -dibromocholestane readily undergoes debromination with iodide ion, but $3\beta,4\alpha$ -dibromocholestane is unreactive under the same conditions.
- 10.16. Refluxing a solution of 1-(*p*-nitrobenzoyl)-2-benzylaziridine (63) in toluene for 24 hours produced a 91% yield of *N*-(*trans*-cinnamyl)-*p*-nitrobenzamide (64, equation 10.89). Propose a mechanism for the rearrangement.

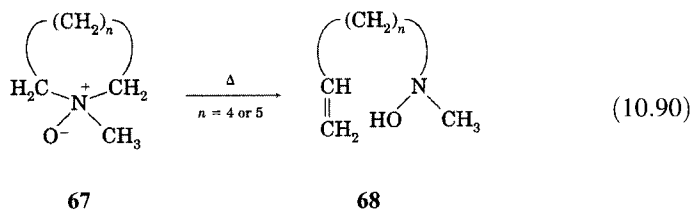


- 10.17. Treatment of *trans*-3-methoxycyclohexanecarboxylic acid with thionyl chloride produces the corresponding acid chloride. Treatment of *cis*-3-methoxycyclohexanecarboxylic acid with thionyl chloride leads to the formation of methyl *trans*-3-chlorocyclohexanecarboxylate and methyl 3-cyclohexene-1-carboxylate in a ratio of 3 : 5. Propose a mechanism to account for the formation of all of the products, and explain the difference in products observed for the *cis* and *trans* isomers.

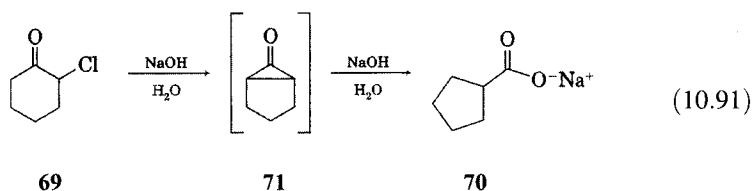
- 10.18. Propose an explanation for each of the following observations.
- Pyrolysis of the methyl xanthate of *cis*-2-phenylcyclohexanol produces nearly 100% of 3-phenylcyclohexene, but pyrolysis of the methyl xanthate of *trans*-2-phenylcyclohexanol produces about 88% of 1-phenylcyclohexene and 12% of 3-phenylcyclohexene.
 - The thermal decomposition of *trans*-2-methyl-1-tetralyl acetate (**65**) occurs at a lower temperature than does the decomposition of the *cis* isomer (**66**).



- Heating the *N*-oxides of a series of *N*-methylazacycloalkanes (**67**) does not result in reaction when *n* is 3, but under the same conditions the intramolecular Hofmann reaction to give **68** occurs when *n* is 4, and it occurs more readily when *n* is 5 (equation 10.90). Explain the dependence of the rate of the reaction on the size of the ring.



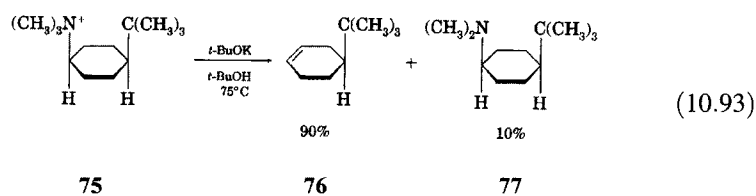
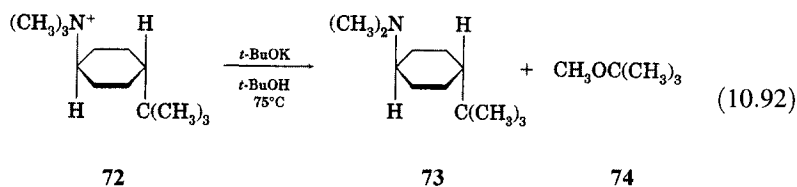
- 10.19. Treatment of 2-chlorocyclohexanone (**69**) with aqueous sodium hydroxide leads to the sodium salt of cyclopentanecarboxylic acid (**70**) in a reaction known as the Favorskii rearrangement (equation 10.91).¹⁹⁴ The ketone **71** has been proposed to be an intermediate in the reaction. Propose a mechanism for the formation of **71**.



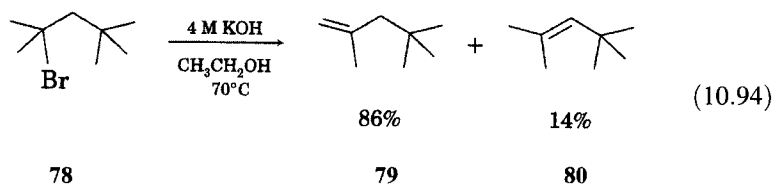
- 10.20. Reaction of *trans*-4-*t*-butylcyclohexyltrimethylammonium chloride (**72**) with *t*-BuOK in *t*-BuOH at 75°C produces *trans*-4-*t*-butylcyclohexyl-*N,N*-dimethylamine (**73**) and *t*-butyl methyl ether (**74**, equation 10.92). Reaction of *cis*-4-*t*-butylcyclohexyltrimethylammonium chloride (**75**) under the same conditions produces 90% of 4-*t*-butylcyclohexene (**76**) and 10% of *cis*-4-*t*-butylcyclohexyl-*N,N*-dimethylamine (**77**).¹⁹⁵ Considering the chair conformation(s) accessible to each isomer, propose mechanisms to account for the differing products produced by the two reactants.

¹⁹⁴ (a) Favorskii, A.; Bozhovskii, V. J. *Russ. Phys. Chem. Soc.* **1914**, 46, 1097 [*Chem. Abstr.* **1915**, 9, 1900]; (b) Lofffield, R. B. *J. Am. Chem. Soc.* **1951**, 73, 4707.

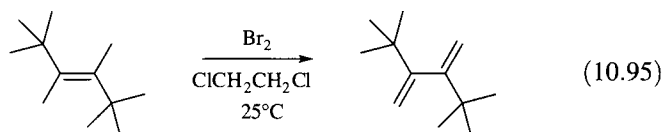
¹⁹⁵ Also formed are trimethylamine and methyl *t*-butyl ether, which are not shown in equation 10.93.



10.21. Dehydrobromination of 2-bromo-2,4,4-trimethylpentane (**78**) with 4.0 M KOH in ethanol at 70°C produces 86% of 2,4,4-trimethyl-1-pentene (**79**) and 14% of 2,4,4-trimethyl-2-pentene (**80**).⁸⁴ The heat of hydrogenation of **79** is -25.52 kcal/mol, while that of **80** is -26.79 kcal/mol.¹⁹⁶ Is this dehydrobromination an example of Saytzeff orientation or Hofmann orientation?

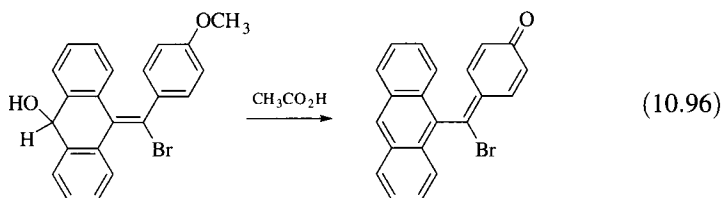


10.22. Propose a mechanism for the following reaction:



10.23. Propose a structure analogous to that shown in Figure 10.5 that could release a drug by a 1,10-elimination.

10.24. Propose a mechanism for the following transformation:

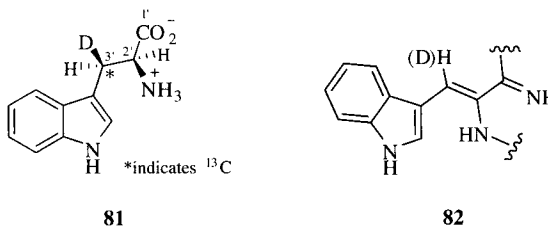


10.25. Predict the products of the following reactions:

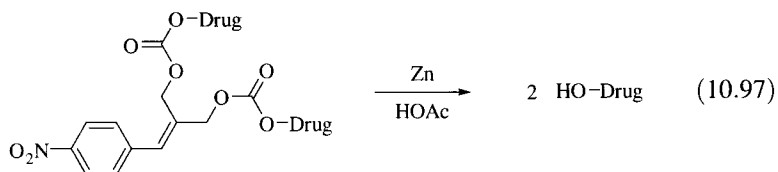
- erythro*-*N,N*-dimethyl-3-phenyl-2-butanamine oxide $\xrightarrow{\Delta}$
- threo*-*N,N*-dimethyl-3-phenyl-2-butanamine oxide $\xrightarrow{\Delta}$

¹⁹⁶ Turner, R. B.; Nettleton, D. E., Jr.; Perelman, M. J. *Am. Chem. Soc.* **1958**, *80*, 1430.

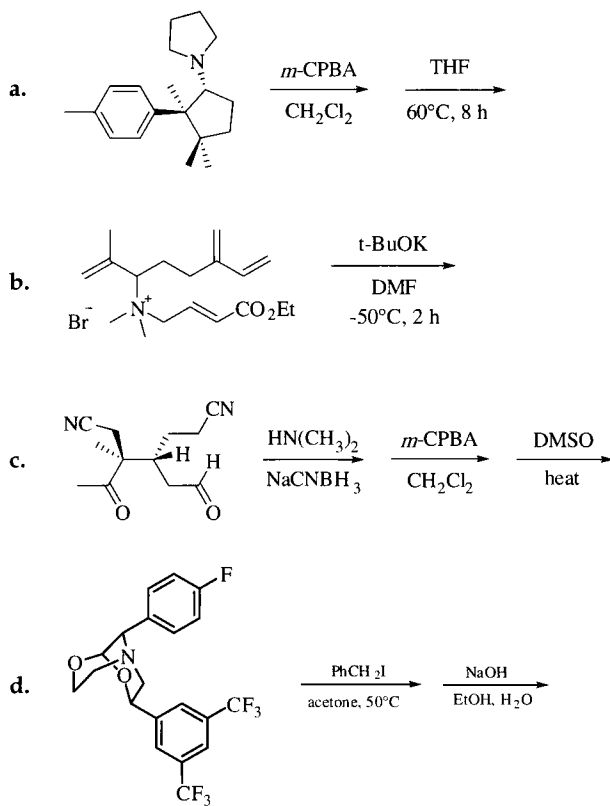
- 10.26. A microorganism fed (2'S,3'R)-[3'-²H₁, ¹³C₁]-tryptophan (**81**) produced a metabolite that incorporated the dehydrotryptophan moiety shown as **82**. The ¹³C NMR spectrum of the metabolite showed a 1: 1: 1 triplet for the C3' signal. Does the microorganism dehydrogenate the tryptophan by a syn process or by an anti process?



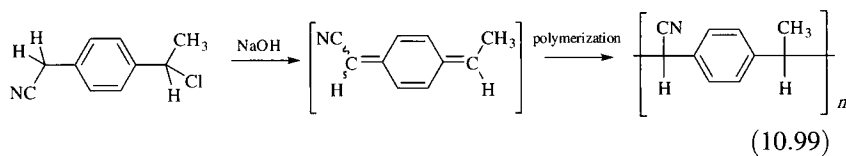
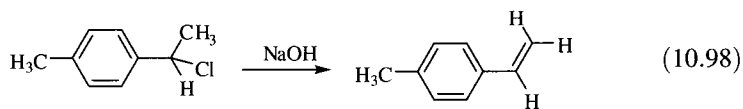
- 10.27. Propose a mechanism to explain the release of two drug molecules when the prodrug shown below reacts with Zn in acetic acid to reduce the nitro function to an amine.



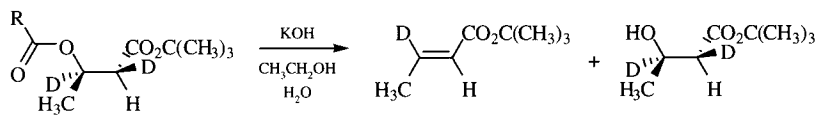
- 10.28. Predict the products of the following reactions. Where appropriate, indicate clearly the stereochemistry of the products.



- 10.29. Propose an explanation for the different elimination pathways observed in the following reactions:



- 10.30. Hydroxide-promoted elimination of acetic acid from **83** was shown to occur with about 23% net syn elimination, while that from **84** was found to occur with only about 6% net syn elimination. In both cases a by-product of the elimination results from hydrolysis of the ester. Propose an explanation for these results.



83, R=CH₃; **84**, R = C(CH₃)₃

(10.100)

Pericyclic Reactions

11.1 INTRODUCTION

The conversion of cyclobutene to 1,3-butadiene in the gas phase at 150°C is notable for two reasons. First, the activation energy for the isomerization is only 32.5 kcal/mol.¹ This is much lower than the activation energy expected for a reaction proceeding through initial homolysis of a carbon–carbon single bond as shown in Figure 11.1.² The bond strength of a typical C–C bond is about 82 kcal/mol, but the ring strain present in the cyclobutene ring and the quasi-allylic nature of the biradical intermediate **1** might be expected to lower the energy needed for bond breaking. However, thermochemical data suggest that **1** would be 47 kcal/mol higher in energy than the cyclobutene, so a reaction proceeding by the mechanism in Figure 11.1 should have an activation energy at least 15 kcal/mol higher than that which is observed for the reaction.³

Second, the corresponding reaction of substituted cyclobutenes is highly stereospecific. Thermolysis of *trans*-1,2,3,4-tetramethylcyclobutene (**2**) gave only (*E,E*)-3,4-dimethyl-2,4-hexadiene (**3**, equation 11.1). Neither the *Z,Z* diastereomer (**4**) nor the *E,Z* diastereomer (**5**) was detected.⁴ Conversely, thermolysis of *cis*-1,2,3,4-tetramethylcyclobutene (**6**) was found to give only the *E,Z* product (**5**, equation 11.2).^{5,6}

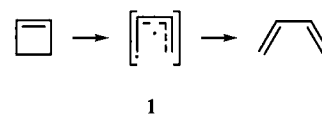


FIGURE 11.1

Hypothetical bond homolysis mechanism for conversion of cyclobutene to 1,3-butadiene.

¹ Cooper, W.; Walters, W. D. *J. Am. Chem. Soc.* **1958**, *80*, 4220.

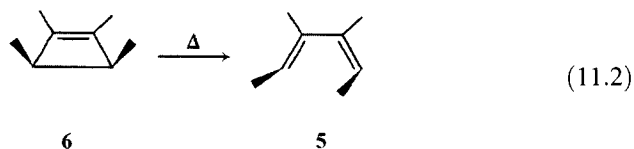
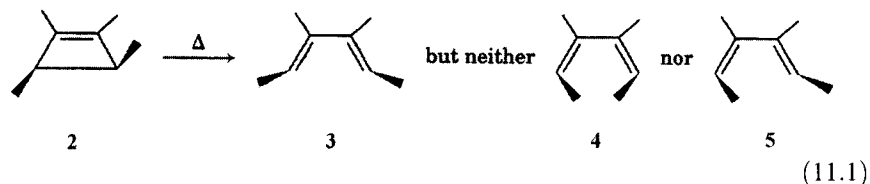
² The corresponding activation energy for the pyrolysis of cyclobutane to ethene at temperatures near 400°C is 62.5 kcal/mol. Genaux, C. T.; Kern, F.; Walters, W. D. *J. Am. Chem. Soc.* **1953**, *75*, 6196.

³ Brauman, J. I.; Archie, W. C., Jr. *J. Am. Chem. Soc.* **1972**, *94*, 4262.

⁴ Criegee, R.; Noll, K. *Liebigs Ann. Chem.* **1959**, 627, 1.

⁵ Similar results for *cis*- and *trans*-3,4-dimethylcyclobutene were reported by Winter, R. E. K. *Tetrahedron Lett.* **1965**, 1207.

⁶ Brauman and Archie (reference 3) were able to detect 0.005% of *trans,trans*-2,4-hexadiene from the reaction of *cis*-3,4-dimethylcyclobutene at 280°C.



In the reactions of 2 and 6, the stereospecificity of the opening of the cyclobutene to the 1,3-butadiene can be correlated with steric differences in the transition structures leading to the possible products.⁵ The two methyl substituents are both above the plane of the cyclobutene ring in 6 but are in the plane of the double bond in the possible products. As a result, four possible transition structures differ in the location of the two methyl groups (Figure 11.2). In path (a) both methyl groups move in a clockwise fashion as the reaction proceeds from reactant to transition structure to product 5. In path (b) both methyl groups move in a counterclockwise fashion, but the product is again the *cis,trans* isomer, 5. Path (c) involves movement of one

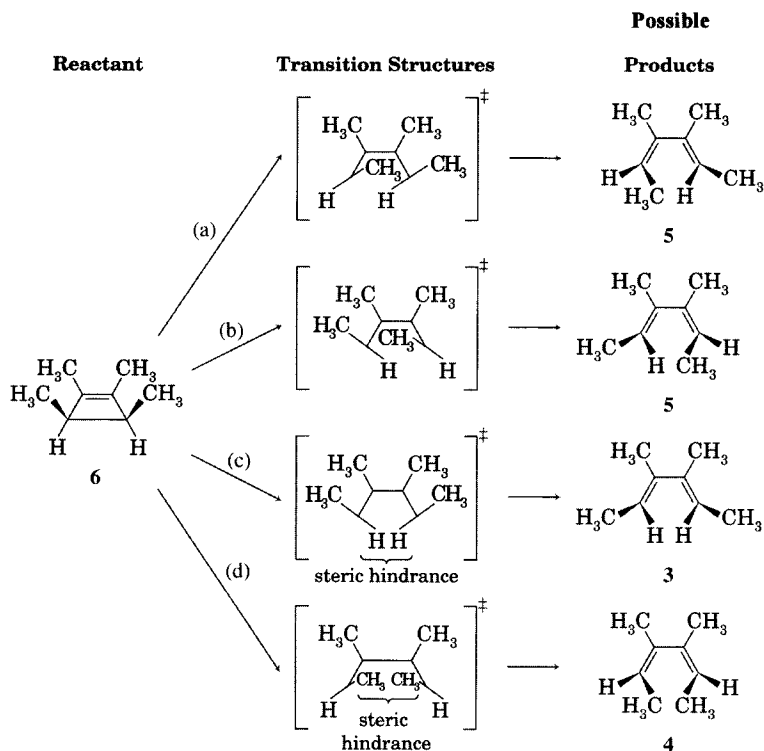
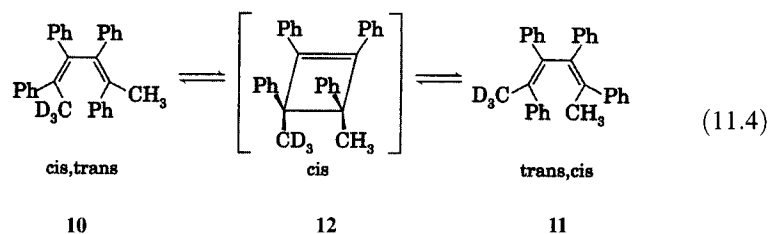
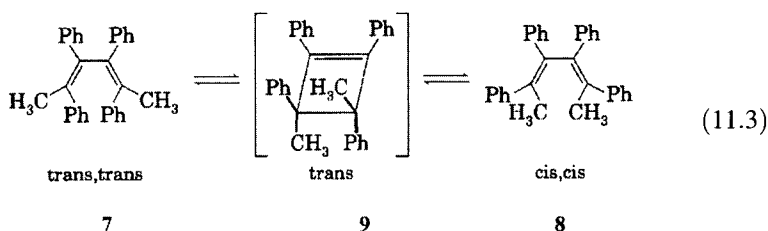


FIGURE 11.2

Possible steric effects in transition structures for thermal ring opening of *cis*-1,2,3,4-tetramethylcyclobutene (6).

methyl group counterclockwise and the other one clockwise, which suggests steric hindrance of the two hydrogen atoms in the transition structure. Path (d) also involves movement of the two methyl groups in different directions, but this pathway would produce steric hindrance of two methyl groups in the transition structure. Pathways (a) and (b) should be favored, so the steric factors correctly predict that **5** should be the major product of the reaction.

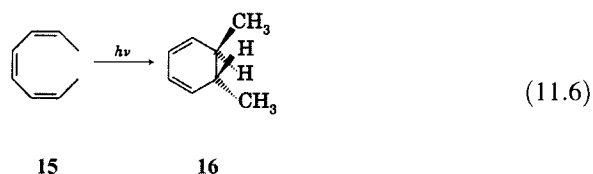
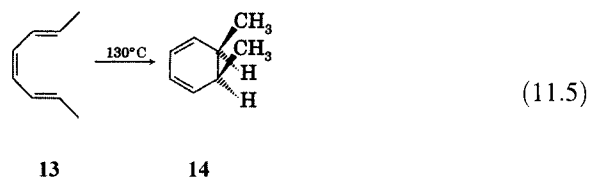
The same steric considerations should apply to the reverse process, the thermal closure of butadienes to cyclobutenes. Although the greater stability of 1,3-butadiene makes conversion to a cyclobutene endothermic, evidence that it can occur is seen in the equilibration of *trans,trans*-2,3,4,5-tetraphenyl-2,4-hexadiene (**7**) and the *cis,cis* diastereomer (**8**) through *trans*-3,4-dimethyltetraphenylcyclobutene (**9**) in pyridine solution at 110°C (equation 11.3). Similarly, at temperatures greater than 110°C, the deuterium-labeled *cis,trans*-2,3,4,5-tetraphenyl-2,4-hexadiene (**10**) equilibrates with the isomeric **11**, presumably through the *cis* cyclobutene **12** (equation 11.4). A long-term reaction of **10** revealed no evidence for isomerization to the *cis,cis* isomer, suggesting that any violations of the stereochemical preference for this reaction could occur no more than once in every 2.6×10^8 ring openings.⁷



A mechanistic model based on minimization of steric repulsion in transition structures can rationalize results of these butadiene–cyclobutene interconversions, but that explanation cannot explain the results of analogous cyclohexadiene–hexatriene reactions. As shown in equation 11.5, *trans,cis,trans*-2,4,6-octatriene (**13**) is converted only to **14**, so this process must take place through rotation of the two methyl groups in different directions (analogous to paths (c) or (d) in Figure 11.2). On the other hand,

⁷ Doorakian, G. A.; Freedman, H. H. J. *Am. Chem. Soc.* **1968**, *90*, 5310.

photochemical reaction of **15** leads to **16** by a process that involves rotation of the methyl groups in opposite directions (equation 11.6).⁸⁻¹¹



Investigators were unable to trap or detect intermediates in any of the reactions discussed here, and radical inhibitors were ineffective.¹ Therefore, the reactions appeared to be **concerted**, meaning that bond-breaking and bond-forming processes occur simultaneously rather than in stepwise fashion. A base of empirically derived knowledge enabled the products of many of these reactions to be predicted successfully, but for many years there was no satisfying theoretical explanation of the forces that determine which reactions proceed by what pathways. Thus, some concerted reactions came to be known as “no mechanism” reactions.¹² The idea that a reaction might not have a mechanism is incompatible with the fundamental assumptions of contemporary organic chemistry, but the term does suggest what was for a long time the mysterious nature of these transformations.

The period of mystery about these reactions came to an end—and a new era of theory and practice in organic chemistry began—with the publication of a series of papers by Woodward and Hoffmann on the

⁸ Vogel, E.; Grimme, W.; Dinné, E. *Tetrahedron Lett.* **1965**, 391. Also see Glass, D. S.; Watthey, J. W. H.; Winstein, S. *Tetrahedron Lett.* **1965**, 377; Marvell, E. N.; Caple, G.; Schatz, B. *Tetrahedron Lett.* **1965**, 385.

⁹ Photochemical reactions (discussed in Chapter 12) are much more complicated than will be apparent from the discussions of orbital symmetry concepts here. See, for example, van der Lugt, W. T. A. M.; Oosterhoff, L. J. J. *Am. Chem. Soc.* **1969**, *91*, 6042. For further discussion and leading references, see Bernardi, F.; Olivucci, M.; Ragazos, I. N.; Robb, M. A. J. *Am. Chem. Soc.* **1992**, *114*, 2752.

¹⁰ Fonken, G. J. *Tetrahedron Lett.* **1962**, 549.

¹¹ A time-resolved UV resonance Raman study indicated that excitation of 1,3-cyclohexadiene leads to vibrationally excited *di-s-cis*-1,3,5-hexatriene in 6 ps, which is less than the time required for vibrational cooling to the lowest vibrational level of that conformation or for relaxation to the mono-*s-cis* conformer: Reid, P. J.; Doig, S. J.; Wickham, S. D.; Mathies, R. A. J. *Am. Chem. Soc.* **1993**, *115*, 4754.

¹² For example, see the review “Rearrangements Proceeding Through ‘No Mechanism’ Pathways: The Claisen, Cope, and Related Rearrangements” by Rhoads, S. J. in de Mayo, P., Ed. *Molecular Rearrangements*, Vol. 1; Wiley-Interscience: New York, 1963; pp. 655–706.

relationship between the stereochemistry of concerted reactions and the symmetry properties of molecular orbitals.^{13–16} The interconversion of cyclobutene and 1,3-butadiene is one of many reactions Woodward and Hoffmann termed a **pericyclic reaction**—a reaction “in which concerted reorganization of bonding occurs throughout a cyclic array of continuously bonded atoms.”^{14,17}

Pericyclic reactions include a wide variety of transformations (Figure 11.3), including such well-known reactions as the Cope rearrangement and the Diels–Alder reaction. In the sections that follow, we will first discuss each of these pericyclic reactions individually. Next, we will consider the common features of these seemingly disparate reactions in terms of an inclusive theory.¹⁸ Then we will explore the use of a variety of complementary models to provide a basis for a further understanding of concerted reactions.¹⁹ Finally, we will discuss experimental results that will challenge some familiar concepts of chemical reactivity.

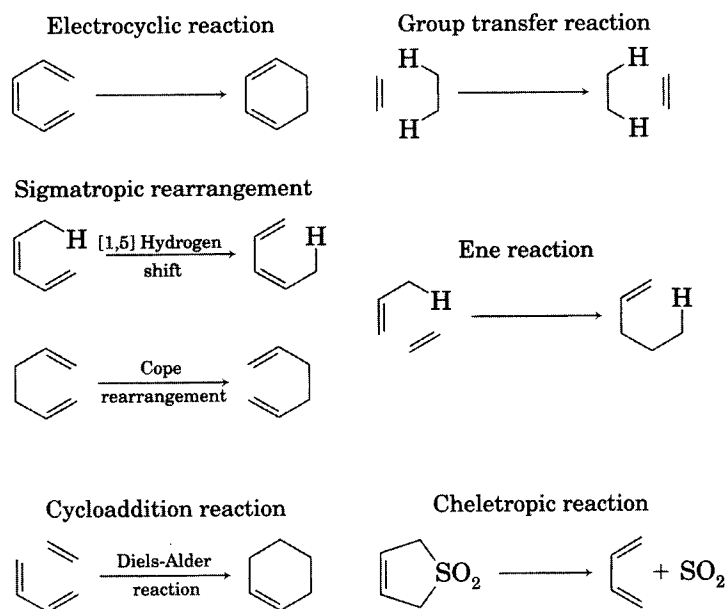


FIGURE 11.3
Examples of pericyclic reactions.

¹³ Woodward, R. B.; Hoffmann, R. J. *Am. Chem. Soc.* **1965**, *87*, 395.

¹⁴ See also Woodward, R. B.; Hoffmann, R. *The Conservation of Orbital Symmetry*; Verlag Chemie/Academic Press: Weinheim, 1971.

¹⁵ Hoffmann, R.; Woodward, R. B. *Acc. Chem. Res.* **1968**, *1*, 17.

¹⁶ The 1981 Nobel Prize in chemistry was awarded jointly to Roald Hoffmann and Kenichi Fukui (see page 756) for their studies of concerted reactions. It seems certain that R. B. Woodward would also have shared the prize (which would have been his second Nobel Prize in chemistry) if he had been living at the time of the award.

¹⁷ Constitutional isomers that are interconverted by pericyclic reactions—such as **5** and **6**—are known as *valence isomers*. Commission on Physical Organic Chemistry, IUPAC. *Pure Appl. Chem.* **1994**, *66*, 1077.

¹⁸ For a perspective on the development of theoretical models for pericyclic reactions, see Houk, K. N.; González, J.; Li, Y. *Acc. Chem. Res.* **1995**, *28*, 81.

¹⁹ For a discussion of the transition structures of pericyclic reactions, see Houk, K. N.; Li, Y.; Evansck, J. D. *Angew. Chem. Int. Ed. Engl.* **1992**, *31*, 682.

11.2 ELECTROCYCLIC TRANSFORMATIONS

Definitions and Selection Rules

Woodward and Hoffmann classified the cyclobutene–1,3-butadiene interconversion as an “**electrocyclic transformation**—the formation of a single bond between the termini of an acyclic conjugated π system containing k π -electrons or the reversal of such a reaction”^{13,14,20} (Figure 11.4, where k is an integer).

They further defined two possible pathways for such reactions

1. **Disrotatory**, in which the substituents on the two termini of the π system rotate in different directions, one turning clockwise and the other turning counterclockwise (Figure 11.5, left).
2. **Conrotatory**, in which the substituents on the termini of the π system both rotate in the same sense, either clockwise or counterclockwise, on going from reactant to product (Figure 11.5, right).

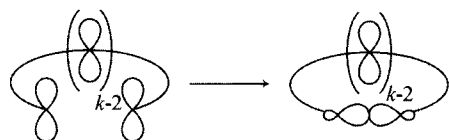
Woodward and Hoffmann observed that the products of electrocyclic transformations could be predicted on the basis of the highest occupied molecular orbital (HOMO) of the *acyclic* member of the reactant–product pair.¹³ Specifically, they suggested that the reaction pathway is associated with the formation of a bonding relationship between the termini of the π chain, so that there is either (+)–(+) or (–)–(–) overlap between the lobes of the two p orbitals that come together to form the new σ bond. An example is the interconversion of cyclobutene and 1,3-butadiene. The σ framework in the acyclic structure is assumed to be invariant throughout the reaction, so the MO analysis is only concerned with the Hückel MOs derived from the set of p orbitals in the acyclic species.²¹ The Hückel MOs of 1,3-butadiene are shown on the energy level diagram in Figure 11.6. It is not necessary to know the actual wave function for each MO. Instead, only the mathematical *sign* of the coefficient at each carbon atom in each MO is significant here. Coefficients that are positive are denoted arbitrarily by a + sign on the top lobe of the p orbital and a – sign on the bottom lobe of the p orbital at that position. Coefficients that are negative are indicated by a – sign on the top lobe and a + sign on the bottom lobe of a p orbital.

As discussed in Chapter 4, the highest occupied molecular orbital (HOMO) of 1,3-butadiene in the ground state is ψ_2 . Simultaneous rotation about both the C1–C2 bond and the C4–C3 bond in a *clockwise* fashion (as shown in Figure 11.7) would allow the two + lobes on the termini of ψ_2 to overlap in a bonding mode, so the reaction is predicted to take place by a conrotatory pathway.²² Excitation of 1,3-butadiene to its lowest excited state

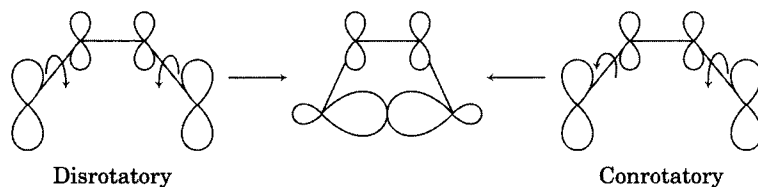
²⁰ Marvell, E. N. *Thermal Electrocyclic Reactions*; Academic Press: New York, 1980.

²¹ The new σ bond formed in the cyclic structure is described in terms of a localized σ orbital and a localized σ^* antibonding orbital formed by overlap of a pair of sp^3 hybrid orbitals that result from rotation of the two terminal p orbitals in the π system.

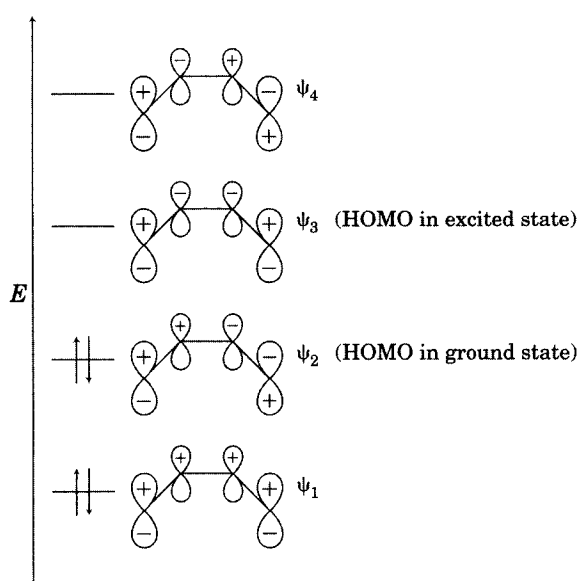
²² If the cyclobutene has an alkyl substituent at C3, both *Z* and *E* isomers are possible from the conrotatory pathway. Both steric effects and electronic effects of substituents elsewhere can influence the product distribution. See the discussion on page 757.

**FIGURE 11.4**

A general electrocyclic transformation.

**FIGURE 11.5**

Disrotatory (left) and conrotatory (right) electrocyclic conversion of 1,3-butadiene to cyclobutene.

**FIGURE 11.6**

Orbital symmetries of 1,3-butadiene orbitals. In the ground state, HOMO is ψ_2 ; in the excited state, HOMO is ψ_3 .

involves promoting one electron from ψ_2 to ψ_3 , so that ψ_3 becomes the HOMO. Now the symmetry properties of the termini of the HOMO are reversed, and the photochemical reaction should proceed by a disrotatory pathway (Figure 11.8).²³

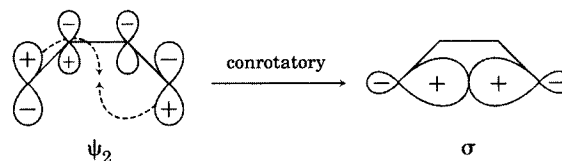
Unlike the steric explanation, this model can also rationalize the interconversion of hexatrienes and cyclohexadienes.²⁴ As shown in Figure 11.9, the ground state HOMO of 1,3,5-hexatriene is ψ_3 . Therefore, the closure of

²³ Ben-Nun and Martinez studied the photochemical opening of cyclobutene to 1,3-butadiene with ab initio molecular dynamics calculations and found that the motion leading to disrotatory ring opening is established within the first 15 fs after the electronic excitation. Ben-Nun, M.; Martinez, T. J. *J. Am. Chem. Soc.* **2000**, *122*, 6299.

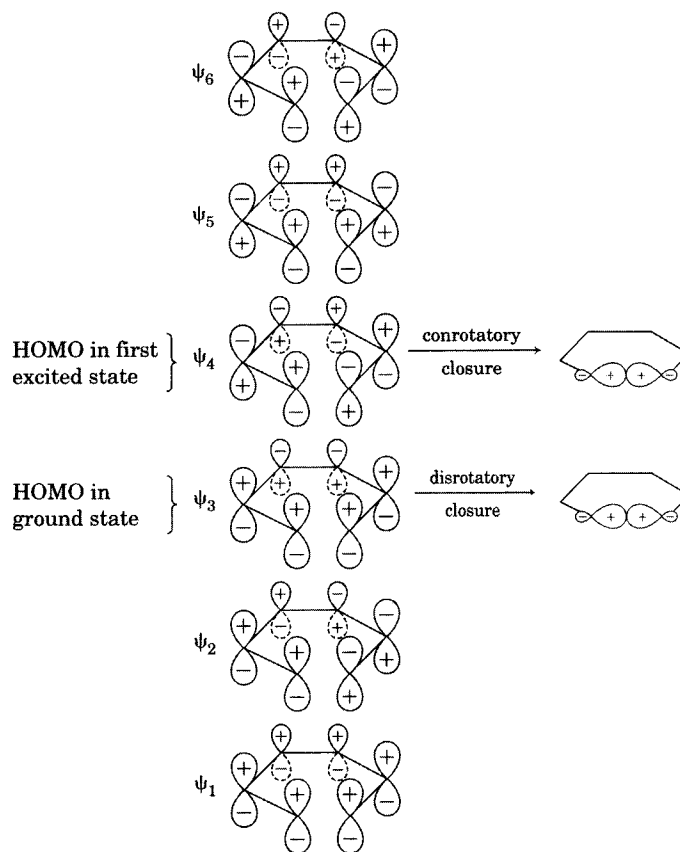
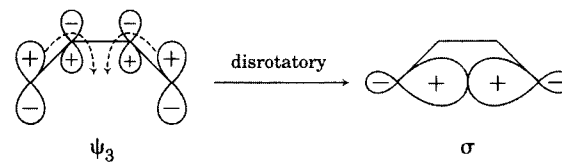
²⁴ Both **3** and **4** could be formed by conrotatory electrocyclic opening of **2**. The fact that only **3** is produced suggests a steric contribution to the barrier for the formation of **4**.

FIGURE 11.7

Formation of a σ bond by (+)-(+) overlap of p orbital lobes at the termini of ψ_2 of 1,3-butadiene through a conrotatory reaction pathway (thermal reaction).

**FIGURE 11.8**

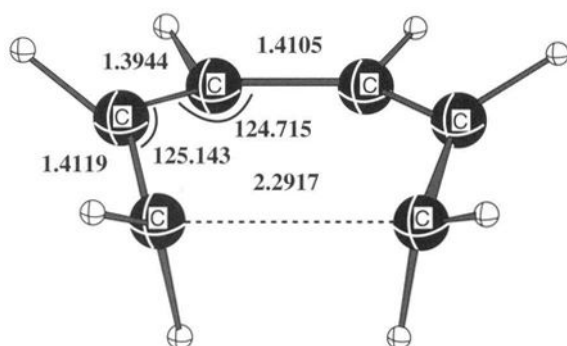
(+)-(+) Overlap of the terminal p orbital lobes of ψ_3 of photoexcited 1,3-butadiene through disrotatory closure.

**FIGURE 11.9**

Orbital symmetries for electrocyclic closure of hexatriene to 1,3-cyclohexadiene (disrotatory ground state reaction; conrotatory excited state reaction).

1,3,5-hexatriene to 1,3-cyclohexadiene should be disrotatory. Consistent with this expectation, Sakai and Takane calculated that the disrotatory pathway (Figure 11.10) for electrocyclic closure of 1,3,5-hexatriene is ca. 11 kcal/mol lower in energy than the conrotatory pathway.²⁵ In the excited state, the HOMO of 1,3,5-hexatriene is ψ_4 , so the photochemical closure of hexatriene to cyclohexadiene should be conrotatory.

²⁵ Sakai, S.; Takane, S. *J. Phys. Chem. A* **1999**, *103*, 2878.

**FIGURE 11.10**

Transition structure calculated for the disrotatory closure of 1,3,5-hexatriene to 1,3-cyclohexadiene. (Bond angles are in degrees; distances are in Å. Reproduced from reference 25.)

Because of the alternating symmetry properties of the HOMOs of linear polyene systems (see Chapter 4), Woodward and Hoffmann were able to deduce the following **selection rule for electrocyclic transformations**.²⁶

If there are $4n + 2 \pi$ electrons in a system of adjacent, parallel p orbitals undergoing an electrocyclic closure, then the reaction will be allowed thermally in the disrotatory fashion and allowed photochemically in the conrotatory fashion. If there are $4n \pi$ electrons, the reaction will be allowed thermally conrotatory and photochemically disrotatory.

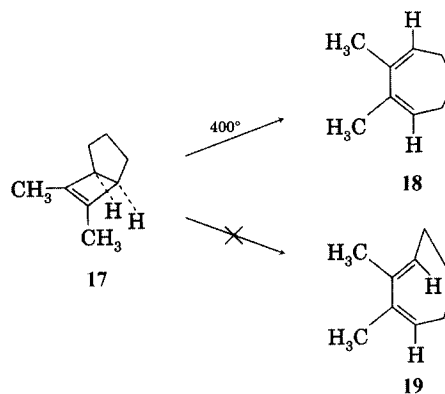
In the terminology of selection rules, the ground state disrotatory reaction involving $4n + 2 \pi$ electrons (i.e., 2, 6, 10, ... electrons) is *allowed*, while the conrotatory reaction involving $4n + 2 \pi$ electrons is *forbidden*. Conversely, the ground state conrotatory reaction involving $4n$ electrons (i.e., 4, 8, 12, ... electrons) is allowed, while the photochemical conrotatory reaction involving $4n$ electrons is forbidden.

Woodward and Hoffmann noted that the symmetry argument indicates only that one stereochemical pathway or the other is electronically favored and that the forbidden pathway might be observed if geometric constraints inhibit the allowed mechanism. As an example, they cited the disrotatory opening of the dimethylbicyclo[3.2.0]heptene (**17**) to *cis,cis*-1,3-cycloheptadiene (**18**, Figure 11.11).¹³ Here, the orbital symmetry-allowed conrotatory pathway leading to the *cis,trans* isomer **19** is precluded by the angle strain of the product, which would have a *trans* double bond in a seven-membered ring. Apparently the opening of **17** takes place by a nonconcerted process because the reaction occurs only at 400°C, much higher than the 200°C needed for the opening of *cis*-1,2,3,4-tetramethylcyclobut-1-ene (**6**, equation 11.2).²⁷

The thermal conversion of Dewar benzene (**20**, Figure 11.12) to benzene is another example of an electrocyclic reaction that has a high steric barrier for the reaction pathway allowed by orbital symmetry. The allowed conrotatory pathway would produce geometrically strained *cis,cis,trans*-1,3,5-cyclohexatriene. This isomerization was long thought to occur by the disrotatory pathway because, even though it has a higher electronic

²⁶ Adapted from reference 15.

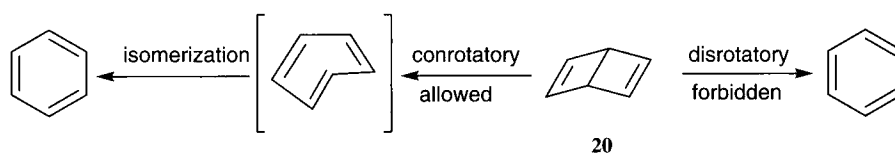
²⁷ Criegee, R.; Furrer, H. *Chem. Ber.* **1964**, *97*, 2949.

**FIGURE 11.11**

Effect of bridging on electrocyclic reactivity.

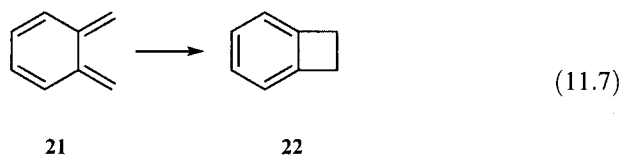
FIGURE 11.12

Allowed and forbidden pathways in isomerization of Dewar benzene (20).



barrier than the conrotatory pathway, its steric barrier would be much lower. Nevertheless, Johnson and Daoust studied the isomerization with *ab initio* calculations and identified a slightly lower energy transition state for a conrotatory process than for the disrotatory process.²⁸

Some electrocyclic reactions can be analyzed in different ways. For example, the conversion of *o*-xylylene (21) to benzocyclobutene (22) may be analyzed as either a 4-electron or an 8-electron electrocyclic process. Both analyses predict that the conrotatory pathway should be allowed, a result supported by *ab initio* calculations.²⁹

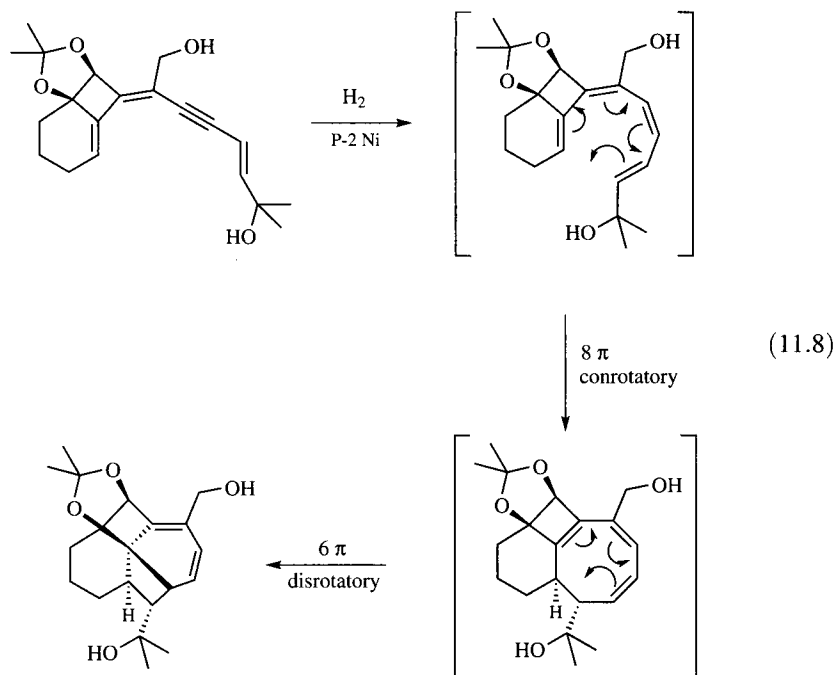


The examples presented above illustrate the fundamental principles of electrocyclic reactions with relatively simple compounds, but organic chemists have found such reactions to be useful in the synthesis of complex structures. For example, Suffert and co-workers synthesized a [4.6.4.6]fenestradiene by hydrogenating an alkyne to a *cis*-alkene, which subsequently underwent a conrotatory 8π -electrocyclization that was followed by a 6π -disrotatory electrocyclization (equation 11.8).³⁰

²⁸ Johnson, R. P.; Daoust, K. J. *J. Am. Chem. Soc.* **1996**, *118*, 7381.

²⁹ Sakai, S. J. *Phys. Chem. A* **2000**, *104*, 11615.

³⁰ Hulot, C.; Blond, G.; Suffert, J. *J. Am. Chem. Soc.* **2008**, *130*, 5046.



MO Correlation Diagrams

The HOMO “simple symmetry argument”³¹ for the stereochemistry of electrocyclic reactions was supported by extended Hückel calculations indicating that the energy of the HOMO is dominant in thermal reactions. It is not intuitively obvious, though, why the HOMO of the acyclic member of the reactant–product pair should determine the stereochemistry of the reaction in either direction. Nor is it apparent why the analysis of only one of many MOs should lead to the same result as a detailed extended Hückel calculation.³¹ Longuet-Higgins and Abrahamson augmented the initial Woodward–Hoffmann explanation for electrocyclic reactions by suggesting that the transformation should be considered as a conversion of the *entire set* of MOs of the reactant to the *entire set* of MOs of the product in such a manner that the symmetry of the molecular orbitals is retained while going from reactant through transition structure to product.³¹

As a prelude to further analysis, it is useful to review one important property of molecular orbitals. As noted in Chapter 1, symmetry-correct molecular orbitals must be either symmetric or antisymmetric with respect to the full symmetry of the basis set of atomic orbitals that are used to construct the molecular orbitals. In the analysis of orbital symmetries, we will need to consider only the number of molecular symmetry elements that are sufficient to distinguish between allowed and forbidden pathways. Also, it is not necessary to consider here the minor perturbation of molecular orbital symmetry that results from isotopic or alkyl substitution. In other words, to a first approximation the basis set orbitals of any conjugated diene are considered to be the same as those for 1,3-butadiene. Figure 11.13 shows the

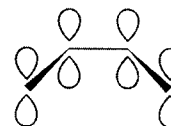


FIGURE 11.13
Basis set of atomic p orbitals of 1,3-butadiene.

³¹ Longuet-Higgins, H. C.; Abrahamson, E. W. *J. Am. Chem. Soc.* **1965**, *87*, 2045.

basis set atomic orbitals (i.e., the shapes of the p orbitals without designation of the mathematical sign of the lobes) of the π system of 1,3-butadiene superimposed on the *s-cis* conformation of its σ skeleton. This basis set has a number of symmetry elements, but a plane of symmetry bisecting the C2–C3 bond and a C_2 rotation axis perpendicular to that bond will be most important here. Each molecular orbital can be designated as either symmetric or antisymmetric (but not *asymmetric*) with respect to the symmetry elements present in the basis set of orbitals.

Figure 11.14 shows the effect of a σ reflection (top) and of a C_2 rotation (bottom) on ψ_1 of 1,3-butadiene. (The four carbon atoms of 1,3-butadiene have been labeled A, B, C, and D so that the symmetry operations will be evident.) Again, the sign of the coefficient of each atomic orbital having a positive coefficient in that wave function is indicated by labeling the top lobe of each of the p orbitals as + and the bottom lobe of each as -. The effect of the σ operation is to produce a set of orbitals that is identical in all respects to the beginning set, so ψ_1 is said to be symmetric (S) with respect to σ . A C_2 rotation on ψ_1 also puts a p orbital in the same position where there was a p orbital before the operation. Now, the sign of the lobe in each position is the negative of the sign of the lobe in that position before the symmetry operation. Thus, ψ_1 is antisymmetric (A) with respect to the C_2 operation. The symmetry operation must either change the sign of *all* of the lobes or change the sign of *none* of them. It cannot change the sign of some but not others. Otherwise, either (i) the operation is not a proper symmetry operation for that basis set or (ii) the MO under consideration is an improper MO, being asymmetric with respect to a proper symmetry operation. Figure 11.15 shows the effect of the same two operations on ψ_2 of 1,3-butadiene. This wave function is antisymmetric (A) with respect to the σ reflection, but it is symmetric (S) with respect to C_2 .

Not only must we consider the symmetry properties of 1,3-butadiene orbitals, but we must also consider the symmetry properties of both cyclobutene and the transition structure expected for the conversion of the reactant to product. The two pathways for the closure of 1,3-butadiene to cyclobutene are illustrated in Figure 11.16. The C1–C2, C2–C3, and C3–C4 σ bonds are shown as solid lines. The p orbitals of 1,3-butadiene and cyclobutene, as well as the sp^3 orbitals of the C3–C4 σ bond of cyclobutene, are represented by the shapes of the atomic p or sp^3 orbitals. This is therefore only a basis set representation, not an illustration of a particular molecular orbital. Although there are many symmetry elements present in the representations of both 1,3-butadiene and cyclobutene, in the conrotatory reaction the only symmetry element that is present *continuously* from reactant through transition structure to product is the C_2 rotation.³² Similarly, only the σ reflection is present from reactant through transition structure to product for the disrotatory pathway.

The HMO representations of electrocyclic reactions in Figure 11.16 are consistent with the results of higher level calculations. For example, C_2 symmetry is evident in the calculated transition structure shown in

³² A transition *structure* is a saddle point on a potential energy (enthalpy) surface for a reaction. A transition *state* corresponds to a free energy maximum on the path between reactant and product. The geometry of the transition structure corresponds closely to the geometry of the transition state if the barrier is relatively high and the entropy of the system does not vary rapidly near the geometry of the transition structure. If either of these conditions is not met, then the geometry of the transition structure may be very different from that of the transition state. For discussions, see references 17 and 18. Also see Bauer, S. H.; Wilcox, C. F., Jr.; *J. Chem. Educ.* **1995**, *72*, 13.

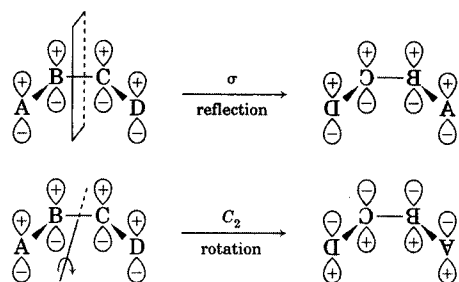


FIGURE 11.14

ψ_1 of 1,3-butadiene is symmetric with respect to σ (top) but antisymmetric with respect to C_2 (bottom). The atoms are labeled A, B, C, and D to clarify the symmetry operations.

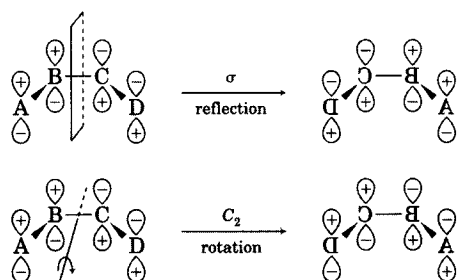


FIGURE 11.15

ψ_2 of 1,3-butadiene is antisymmetric with respect to σ (top) but symmetric with respect to C_2 (bottom).

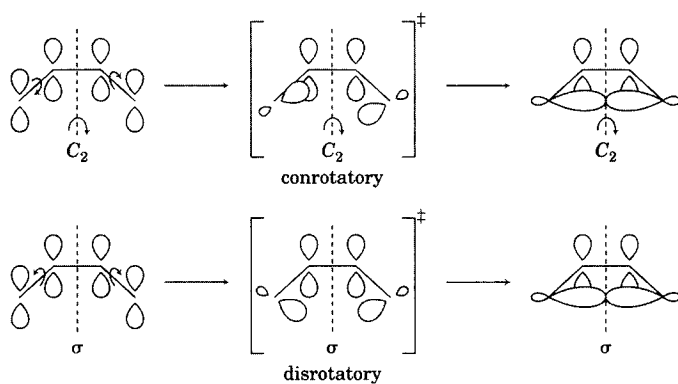


FIGURE 11.16

Symmetry elements in basis sets for electrocyclic transition structures: (a) C_2 axis in conrotatory transition structure and (b) σ in disrotatory transition structure.

Figure 11.17 for the conrotatory pathway.³³ The geometry of the transition structure is given on the left. The drawing on the right shows a different view of the transition structure with arrows representing the transition vector (indicating the relative movement of atoms along the lowest energy path from the transition structure to product) for the conversion of 1,3-butadiene to cyclobutene.³⁴

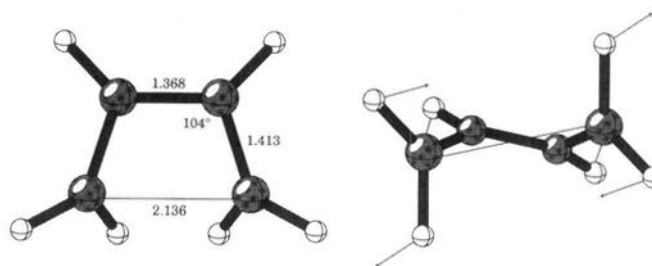
The symmetry with respect to the C_2 axis is indicated for each MO of 1,3-butadiene and for each MO of cyclobutene in a **molecular orbital**

³³ The drawings are adapted from Thomas, B. E. IV; Evanseck, J. D.; Houk, K. N. *J. Am. Chem. Soc.* **1993**, *115*, 4165.

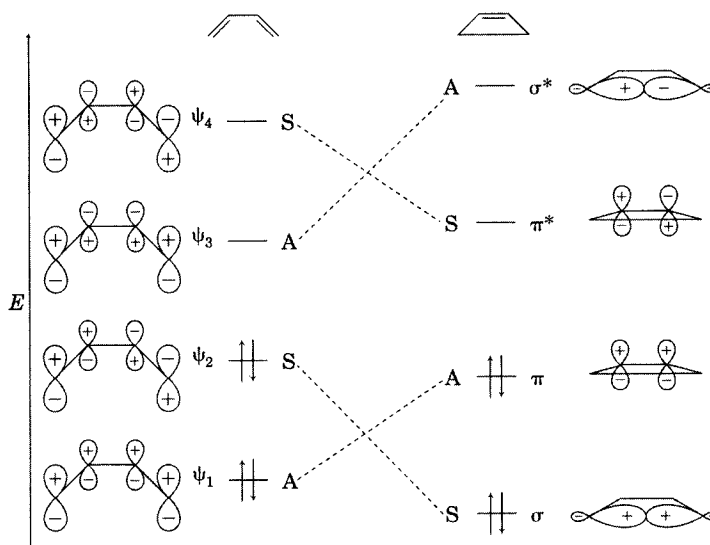
³⁴ Note that the four carbon atoms do not lie in the same plane in the calculated transition structure for the thermal conrotatory opening of cyclobutene. Lee, P. S.; Sakai, S.; Hörstermann, P.; Roth, W. R.; Kallel, E. A.; Houk, K. N. *J. Am. Chem. Soc.* **2003**, *125*, 5839 found that the energy gap between the forbidden disrotatory pathway and the allowed conrotatory pathway decreases as the transition structure for cyclobutene ring-opening becomes more planar.

FIGURE 11.17

Calculated C_2 transition structure (angle in degrees, lengths in Å) for the conrotatory interconversion of cyclobutene and 1,3-butadiene. (Reproduced from reference 33.)

**FIGURE 11.18**

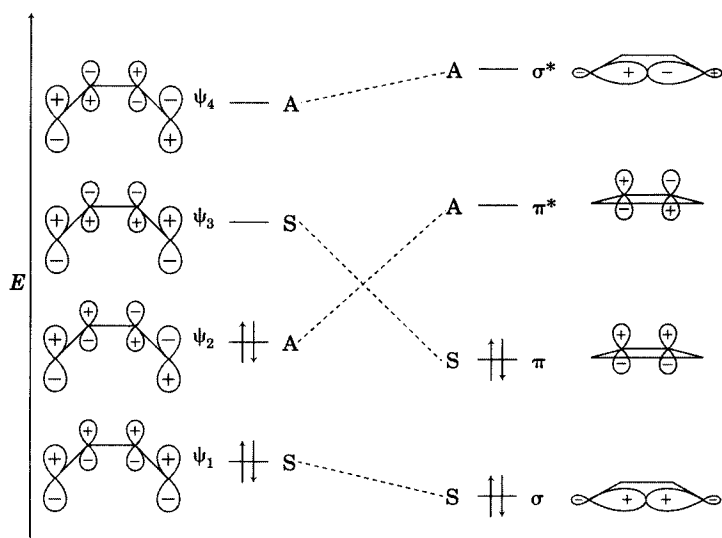
MO correlation diagram for conrotatory interconversion of 1,3-butadiene and cyclobutene (C_2 symmetry). (Adapted from reference 14.)



correlation diagram (Figure 11.18). MOs that are symmetric with respect to the C_2 rotation axis are labeled S, while orbitals that are antisymmetric with respect to C_2 are labeled A. **Correlation lines**, such as the dashed line from ψ_1 of 1,3-butadiene to π of cyclobutene, connect orbitals of reactant and product that have the same symmetry. The correlation lines are drawn by connecting the lowest energy orbital on one side of the drawing with the lowest energy orbital *with the same symmetry* (S or A) on the other side of the drawing. Then the next-lowest energy pair of orbitals with the same symmetry is connected, and so on. For example, ψ_1 of 1,3-butadiene correlates with π of cyclobutene, since both are antisymmetric with respect to C_2 . ψ_2 correlates with σ , since both are S. Similarly, ψ_3 correlates with σ^* and ψ_4 correlates with π^* .

In the electronic ground state of 1,3-butadiene there are two electrons in ψ_1 and two electrons in ψ_2 . In the electronic ground state of cyclobutene there are two electrons in σ and two electrons in π . The correlation of ψ_1 with π and ψ_2 with σ therefore means that the entire set of *bonding* orbitals of the reactant correlates with the entire set of *bonding* orbitals of the product. As a result, there should not be a large electronic barrier for the reaction. The MO correlation diagram applies to both the electrocyclic opening and closing reactions. For example, the opening of cyclobutene to 1,3-butadiene is described by viewing Figure 11.18 from right to left.

One aspect of Figure 11.18 that may not be intuitively obvious is the process by which the lowest energy orbital of cyclobutene (σ), which has electron density only on C1 and C4, is transformed into a 1,3-butadiene orbital

**FIGURE 11.19**

MO correlation diagram for disrotatory interconversion of 1,3-butadiene and cyclobutene (σ symmetry). (Adapted from reference 14.)

(ψ_2) with density on all four carbon atoms. Initially, the localized σ orbital is orthogonal to the p orbitals that comprise the double bond of cyclobutene, but the conrotatory deformation removes the orthogonality. Thus, the first movement along the reaction coordinate mixes the π and σ orbitals of cyclobutene, and the orbitals that could be calculated for all geometries intermediate between reactant and product are also mixed. When the reaction is nearly complete, the sp^3 orbitals have been almost totally converted to p orbitals and are almost completely parallel to the other p orbitals.

The MO correlation diagram for the disrotatory pathway is shown in Figure 11.19. Now ψ_1 correlates with σ , but ψ_2 correlates with π^* . Again, the ground electronic state of 1,3-butadiene has two electrons in ψ_1 and two electrons in ψ_2 . Thus, the forced conversion of the ground state of 1,3-butadiene into cyclobutene by a *disrotatory* pathway would lead to a cyclobutene molecule having two electrons in σ and two electrons in π^* . The electronic configuration $\sigma^2\pi^{*2}$ represents a *doubly excited* electronic state of cyclobutene (because it is a higher energy state than that which would be produced by promoting just one electron from π to π^*). The forced disrotatory reaction should therefore have a much higher energy barrier than the conrotatory pathway.

State Correlation Diagrams

MO correlation diagrams such as those in Figures 11.18 and 11.19 are useful tools, but they are not the final step in the analysis. We really should analyze the interconversion of molecular *states*, not orbitals, since we carry out chemical reactions on *molecules* in their various electronic states, *not on individual MOs* within molecules. The state of a molecule is determined by its configuration, which is the product of the occupied MOs that comprise it.³⁵ Thus, the ground state of cyclobutene can be described as $\sigma^2\pi^2$, while that of

³⁵ More precisely, states can be described by combinations of configurations. In the discussion here, however, each state is associated with only one configuration. For a discussion of configurations, see Turro, N. J. *Modern Molecular Photochemistry*; Benjamin/Cummings Publishing: Menlo Park, CA, 1978; pp. 17–24.

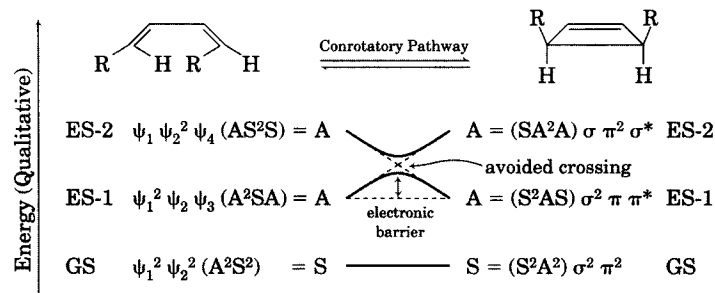
1,3-butadiene is $\psi_1^2\psi_2^2$. We can also distinguish different excited states, each formed by promotion of an electron from a bonding orbital to an antibonding orbital. Then we can represent the ground electronic state and various excited electronic states in an energy level diagram. Correlation of states on such a drawing then develops a **state correlation diagram**, which can be viewed as a reaction coordinate diagram for the electrocyclic transformation.

The correlation of states is determined by the total symmetry of each state, which is a function of the symmetry of each populated MO that characterizes that configuration. As with MOs, states that are symmetric with respect to a symmetry element are designated S, while those that are antisymmetric are labeled A.³⁶ We will use the symmetry designations in Figure 11.18 to prepare a state correlation diagram for the conrotatory conversion of cyclobutene and 1,3-butadiene. The ground state (GS) of 1,3-butadiene is $\psi_1^2\psi_2^2$, so the symmetry of that state is S^2A^2 , which mathematically is S. Similarly, the GS of cyclobutene is $\sigma^2\pi^2$, which is also S^2A^2 and is therefore also S. Assigning the state symmetries for two excited states (chosen as described below) produces a state correlation diagram that represents the diene states ranked according to energy on the left and the cyclobutene states ranked according to energy on the right (Figure 11.20). Since the GS of 1,3-butadiene has the same total symmetry as the GS of cyclobutene, the ground state of 1,3-butadiene correlates with the ground state of cyclobutene. Thus, there should not be a large electronic energy barrier for the interconversion of the two states by a conrotatory pathway, and the reaction is said to be allowed.

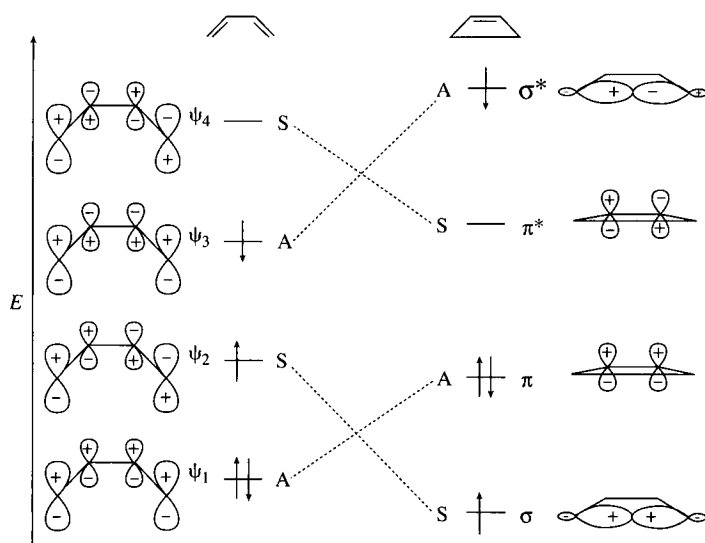
Figure 11.20 shows two electronically excited states for 1,3-butadiene and two electronically excited states for cyclobutene. In each case, the state labeled ES-1 is the excited state produced by moving one electron from the HOMO to the LUMO. For 1,3-butadiene, ES-1 has the configuration $\psi_1^2\psi_2\psi_3$. Its state symmetry is therefore the product of A^2SA , which is A. For cyclobutene ES-1 has the configuration $\sigma^2\pi\pi^*$, so its state symmetry is S^2AS , which is again A. ES-1 of 1,3-butadiene does not correlate with ES-1 of cyclobutene, however, even though the state symmetries are the same. To understand why this is so, it is necessary to follow the occupied molecular orbitals from ES-1 of 1,3-butadiene as they are converted into MOs of cyclobutene (Figure 11.21). Following the correlation line from ψ_1 leads to π ; following the correlation line from ψ_2 leads to σ ; following the correlation line from ψ_3 leads to σ^* . The

FIGURE 11.20

State correlation diagram for conrotatory interconversion of 1,3-butadiene and cyclobutene. (Adapted from reference 31.)



³⁶ The symbols S and A are used in the discussion here, but there are other ways to represent symmetric and antisymmetric wave functions and states: + or +1 can be used for S, and - or -1 can be used for A. The +1 and -1 designations may facilitate determination of the symmetry of a state, since the mathematics of multiplying signed numbers is more intuitive than the mathematics of multiplying bare signs. Thus, the symmetry of the ground state can be represented as (+1) (+1) (-1) (-1) = +1.

**FIGURE 11.21**

Correlation of the orbital populations of ES-1 of 1,3-butadiene and ES-2 of cyclobutene.

resulting state is not the lowest excited state of cyclobutene but is a higher energy state that is labeled ES-2 in Figure 11.20. ES-1 of cyclobutene would have the orbital population $\sigma^2\pi\pi^*$. Similarly, following the correlation line from σ of cyclobutene leads to ψ_2 of 1,3-butadiene; following the correlation line for π leads to ψ_1 ; following the correlation line from π^* leads to ψ_4 . The resulting configuration, $\psi_1\psi_2^2\psi_4$, is not ES-1 of 1,3-butadiene but is, instead, the configuration labeled ES-2 in Figure 11.20. It is essential to note that the state designated ES-2 is *not* necessarily the next highest energy excited state after ES-1. Rather, it is a state that is chosen to complete the diagram because its orbital population would be produced from one of the states on the other side of the diagram.

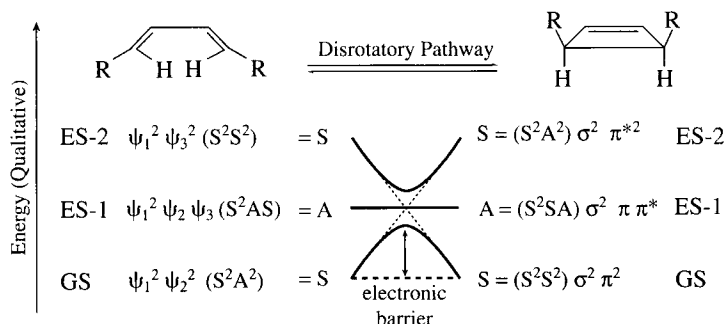
Based on the state correlation diagram for the conrotatory pathway (Figure 11.20), we say that ES-1 of 1,3-butadiene attempts to correlate with ES-2 of cyclobutene. The important term here is *attempts to correlate*, because a principle known as the **avoided crossing rule** says that configurations of the same symmetry cannot cross on an energy level diagram.³⁷ The reason is that mixing of the configurations occurs when configurations of the same symmetry come close together in energy, just as MO mixing occurs when molecular orbitals interact in perturbational MO theory (Chapter 4). In Figure 11.20 the crossing dashed lines indicate the correlations that would result if there were no configuration interaction, while the curved lines indicate the correlations that result from the avoided crossing.³¹ Even though ES-1 of 1,3-butadiene would actually be converted into ES-1 of cyclobutene, and vice versa, if the excited state of either could be forced to deform in a conrotatory fashion past the avoided crossing, the state correlation diagram indicates that there would be a high electronic energy barrier for this process. Thus, the photochemical reaction is said to be forbidden by the conrotatory pathway.

A state correlation diagram for the disrotatory pathway is shown in Figure 11.22. Now ES-1 of 1,3-butadiene does correlate with ES-1 of cyclobutene, so there should not be a high electronic barrier resulting from

³⁷ This rule is also known as the no-crossing rule. For a discussion, see Albright, T. A.; Burdett, J. K.; Whangbo, M.-H. *Orbital Interactions in Chemistry*; John Wiley & Sons: New York, 1985; pp. 52–53.

FIGURE 11.22

State correlation diagram for disrotatory interconversion of 1,3-butadiene and cyclobutene. (Adapted from reference 31.)



orbital symmetry, and the photochemical reaction is allowed. On the other hand, GS of 1,3-butadiene correlates with ES-2 of cyclobutene (and GS of cyclobutene with ES-2 of 1,3-butadiene). There is an avoided crossing between the states of S symmetry, so there should be a high electronic barrier for a process that converts GS of 1,3-butadiene to GS of cyclobutene by a pathway involving the avoided crossing. The thermal reaction is therefore forbidden by the disrotatory pathway. Similar MO and state correlation diagrams can be drawn for other electrocyclic reactions, and the results are entirely consistent with the selection rule for electrocyclic reactions on page 705.

The separation of the conrotatory and disrotatory processes into two separate diagrams here is artificial because the two reactions represent alternative pathways on the same potential energy surface. A molecule undergoing thermal activation is bent and twisted in many different directions through collisions with surfaces and with other molecules. In a sense, it can be said to "explore" the potential energy surface on which it resides. Because there is a much lower energy barrier for the conrotatory pathway than for the disrotatory pathway, a cyclobutene molecule in the electronic ground state is more likely to acquire sufficient energy to complete the conrotatory reaction than to complete the disrotatory reaction. Therefore, the difference between allowed and forbidden processes is ultimately a difference in activation energies.

It is gratifying that the pathway predicted to be allowed for the opening of cyclobutenes to butadienes is experimentally observed. The fact that the allowed concerted pathway predicts the observed product means, however, that we really do not know for certain whether the forbidden concerted pathway is higher or lower in energy than alternative, *non*concerted pathways in which some bonds break or form before others. As Stephenson and Brauman pointed out:

The ring-chain tautomerism between cyclobutene and butadiene is perhaps the most familiar example of an allowed Woodward–Hoffmann process. This transformation invariably is discussed in every attempt to rationalize or teach the Woodward–Hoffmann orbital symmetry concepts. This popularity is due in large part to the existence of a geometrically well defined (and easily visualized) alternate, forbidden, electrocyclic pathway. Thus it is exceedingly simple to set up a nonallowed strawman, the disrotatory ring opening, and show that the allowed, conrotatory path is to be preferred. . . . It has been possible to evaluate an energy difference of ~ 15 kcal/mol between an allowed conrotatory process and *some* nonallowed pathway. . . . [but] it is not possible to say with any degree of certainty whether the nonallowed path is diradical-like or a forbidden, concerted transformation (if indeed such a distinction can be made).³⁸

³⁸ Stephenson, L. M., Jr.; Brauman, J. I. *Acc. Chem. Res.* 1974, 7, 65.

11.3 SIGMATROPIC REACTIONS

Definitions and Examples

Woodward and Hoffmann termed the pericyclic rearrangement illustrated in Figure 11.23 a **sigmatropic rearrangement**: the migration of a σ bond within a molecule.

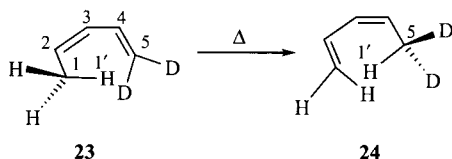


FIGURE 11.23

A [1,5] sigmatropic rearrangement in 1,3-pentadiene-1,1- d_2 .

A sigmatropic change of order $[i,j]$ is defined as^{17,39} "the migration of a σ bond, flanked by one or more π electron systems, to a new position, whose termini are atoms numbered i and j with regard to the original bonded loci (atoms 1 and 1'), in an uncatalyzed intramolecular process." The reaction in Figure 11.23 is a [1,5] sigmatropic rearrangement, specifically a [1,5] hydrogen shift, because it appears that the σ bond between atoms 1 and 1' in the reactant moves to form a new σ bond between atoms 1' and 5 in the product.⁴⁰ By convention, $i \leq j$ in the notation $[i,j]$, so this is a [1,5] sigmatropic reaction and not a [5,1] sigmatropic reaction. Also by convention, the notation for sigmatropic reactions uses square brackets for the number of *atoms* involved in the migration. As we will see later, in other pericyclic reactions the numbers in square brackets refer to the number of *electrons* in each fragment.

With only hydrogen atoms present, the reaction in Figure 11.23 would be a **degenerate rearrangement**, meaning that the product is chemically identical to the reactant.¹⁷ It is the deuterium labeling in structure 23 that allows us to determine that isomerization to 24 has occurred. On the other hand, the **Cope rearrangement** (Figure 11.24) of 25 to 26 and the **Claisen rearrangement** of 27 to 28, followed by tautomerization to 29 (Figure 11.25) are [3,3] sigmatropic reactions that have long been important synthetic tools.^{41,42}

In theory, there are two different stereochemical pathways for $[1,j]$ sigmatropic reactions, as illustrated for the [1,5] hydrogen shift in Figure 11.26. In the first, both bond breaking and bond forming take place above the plane defined by the five carbon atoms. This is known as the

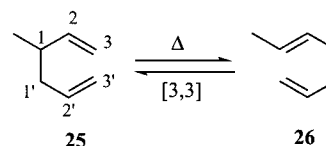


FIGURE 11.24

Cope rearrangement.

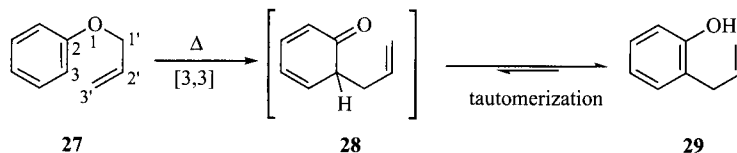


FIGURE 11.25

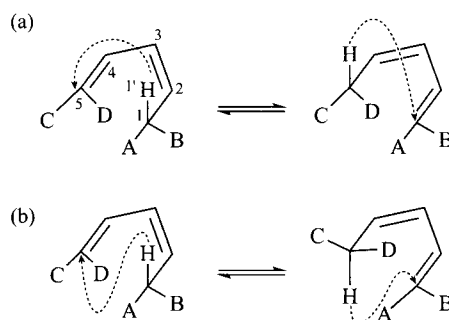
Claisen rearrangement.

³⁹ This is a restatement of the definition given by Woodward, R. B.; Hoffmann, R. J. *Am. Chem. Soc.* **1965**, *87*, 2511.

⁴⁰ Roth, W. R.; König, J. *Liebigs Ann. Chem.* **1966**, *699*, 24.

⁴¹ Rhoads, S. J.; Raulins, N. R. *Org. React.* **1975**, *22*, 1.

⁴² Ziegler, F. E. *Chem. Rev.* **1988**, *88*, 1423.

**FIGURE 11.26**

(a) Suprafacial and (b) antarafacial [1,5] hydrogen shifts. (Reproduced from reference 14.)

FIGURE 11.27

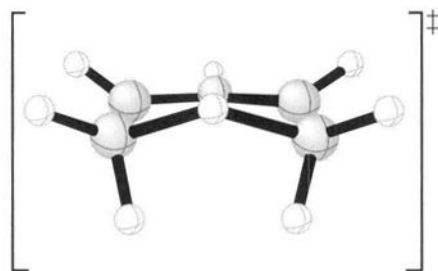
Molecular conformations suggested for suprafacial (left) and antarafacial (right) hydrogen shifts. (Adapted from reference 54a.)



suprafacial (above the face) pathway. Alternatively, the hydrogen atom might leave from above the plane of the π system and rebond below it. This process is known as the **antarafacial** (opposite face) pathway.⁴³ Both processes are drawn so as to emphasize the distinction between antarafacial and suprafacial pathways, so the dashed lines in Figure 11.26 represent overall processes, not mechanisms. The cartoon representations in Figure 11.27 indicate that both processes require proper orientation of the atoms in the π system so that the hydrogen atom can be transferred from one atom to another without having to follow an apparently sinusoidal pathway. Consistent with these simple models, Figure 11.28 shows a calculated transition structure for the suprafacial [1,5] hydrogen shift in *cis*-1,3-pentadiene,⁴⁴ and Figure 11.29 shows the transition structure calculated for the antarafacial [1,7] hydrogen shift in (3*Z*,5*Z*)-1,3,5-heptatriene.⁴⁵ The calculation of transition structures becomes increasingly complex as the size of the system undergoing sigmatropic rearrangement increases. Hess and Baldwin found one transition

FIGURE 11.28

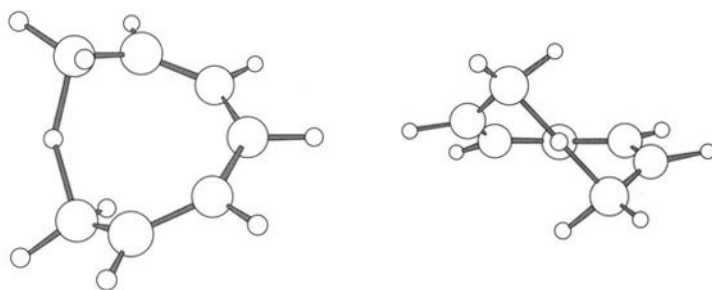
DFT transition structure for the suprafacial [1,5] hydrogen shift in *cis*-1,3-pentadiene. Note the rotation of C1 and C5 toward the migrating hydrogen atom. (Adapted from reference 44.)



⁴³ Nickon, A.; Silversmith, E. F. *Organic Chemistry, the Name Game: Modern Coined Terms and Their Origins*; Pergamon Press: New York, 1987; p. 252 indicate that *antara* is a Sanskrit word meaning "the other."

⁴⁴ Saettel, N. J.; Wiest, O. *J. Org. Chem.* **2000**, *65*, 2331.

⁴⁵ Hess, B. A., Jr.; Schaad, L. J.; Panciř, J. *J. Am. Chem. Soc.* **1985**, *107*, 149.

**FIGURE 11.29**

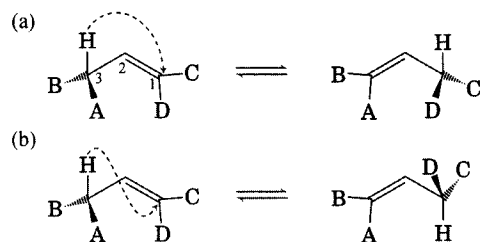
Two views of the ab initio transition structure for the antarafacial [1,7] hydrogen shift in (3Z,5Z)-1,3,5-heptatriene. Note the helical orientation of the carbon skeleton. (Adapted from reference 45.)

structure for the [1,5] hydrogen shift with 1,3-cyclohexadiene, two enantiomeric transition structures with 1,3-cycloheptadiene, and two diastereomeric transition structures with 1,3-cyclooctadiene.⁴⁶

Selection Rules for Sigmatropic Reactions

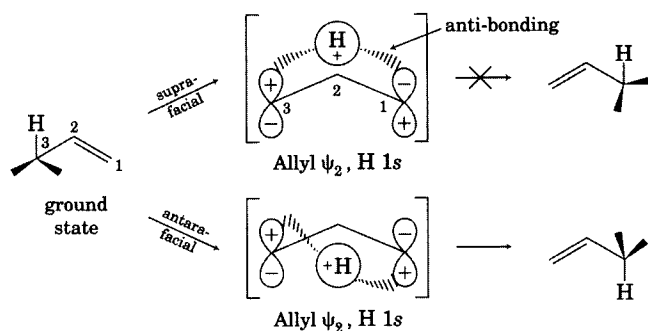
As indicated by Figures 11.28 and 11.29, sigmatropic reactions are concerted reactions in which bond breaking and bond forming take place at the same time. Nevertheless, it is useful to consider the orbital overlaps that would be possible in a mechanism that involves stretching the σ bond *almost* to the point of breaking in the transition structure. Consider first the hypothetical thermal (ground state) [1,3] hydrogen shift of a generalized propene derivative. The suprafacial pathway is illustrated in Figure 11.30(a), and the antarafacial pathway is shown in Figure 11.30(b).

We envision stretching of the C3–H bond in the reactant to the point that the chemical system resembles a hydrogen atom and an allyl radical. Now the HOMO of H is the hydrogen 1s orbital, and the HOMO of the allyl component is ψ_2 (as discussed in Chapter 4). If the transition structure represents the dissociation of a stable bond, then the sign of the overlapping lobes that were responsible for that bond must have been the same, either both plus or both minus. It is customary to represent the sign of both lobes as plus, as shown in Figure 11.31, but that choice is not essential. The allyl radical has a different sign for the coefficients of the atomic orbitals of C1 and C3. Therefore, a stable bond cannot begin to form between by overlap of the hydrogen 1s with the *top* of ψ_2 at C1 while at the same time there is a remaining bonding interaction between the hydrogen 1s and the top of ψ_2 at C1. The concerted suprafacial pathway is therefore forbidden by the principles of orbital symmetry. In the antarafacial pathway, however, there can be a bonding interaction between the bottom of the allyl ψ_2 orbital at C1 and the 1s orbital of hydrogen while

**FIGURE 11.30**

(a) Suprafacial (forbidden) and (b) antarafacial (allowed) [1,3] hydrogen shifts in propene.

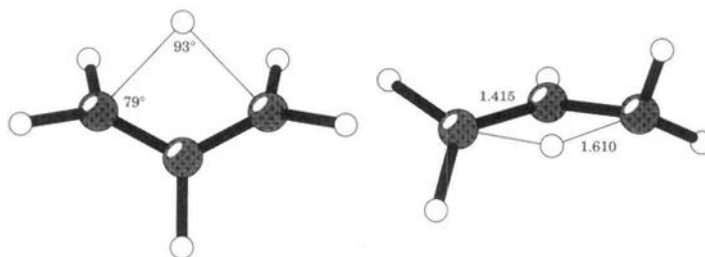
⁴⁶ Hess, B. A., Jr.; Baldwin, J. E. *J. Org. Chem.* **2002**, *67*, 6025.

**FIGURE 11.31**

Suprafacial (forbidden) and antarafacial (allowed) [1,3] hydrogen shift in ground state propene.

there is also some residual bonding between hydrogen and the top of the ψ_2 orbital at C3. Therefore, bonding can be maintained as a hydrogen atom is transferred from C3 to C1, and the antarafacial pathway is said to be allowed by the principles of orbital symmetry.

It must be emphasized that the antarafacial [1,3] hydrogen shift is allowed only by the principles of orbital symmetry. It is not necessarily compatible with the realities of bond angles and bond lengths. Indeed, the transition structure calculated for the antarafacial [1,3] hydrogen shift (Figure 11.32) is a highly contorted species calculated to have an energy similar to an allyl radical and a hydrogen atom,¹⁹ and the suprafacial [1,3] hydrogen shift is calculated to be a high energy species that resembles a trimethylene biradical. Therefore, neither process is feasible, and the thermal [1,3] hydrogen shift has not been found to occur by a concerted pathway.^{18,47}

**FIGURE 11.32**

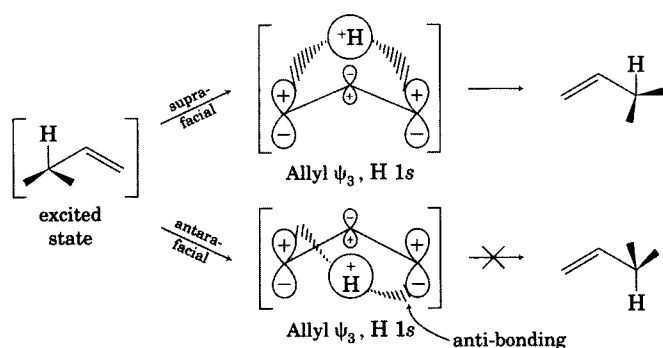
Two views of the CASSCF/6-31G* transition structure for the antarafacial [1,3] hydrogen shift. (Reproduced from reference 19.)

As was the case with electrocyclic reactions, the selection rules for sigmatropic reactions are reversed on going from ground states to excited states. If propene is photoexcited, the excitation energy is expected to reside on the allyl fragment,⁴⁸ so the HOMO of the allyl fragment is now ψ_3 . As shown in Figure 11.33, the interaction of a hydrogen 1s orbital with ψ_3 of allyl allows bonding to be maximized in the transition structure, so the *photochemical* [1,3] suprafacial rearrangement is allowed. Conversely, the photochemical antarafacial rearrangement is forbidden.

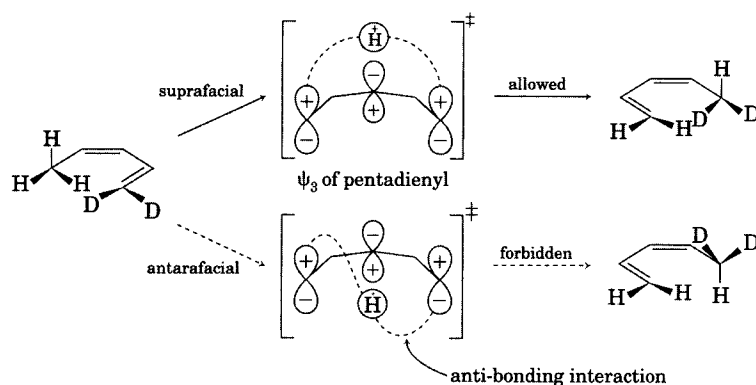
Rules for allowed and forbidden sigmatropic pathways are also reversed if the π system is extended by one carbon-carbon double bond. As

⁴⁷ Hudson, C. E.; McAdoon, D. J. *J. Org. Chem.* **2003**, *68*, 2735 used DFT calculations to locate a transition structure for an antarafacial [1,3] hydrogen shift in acetone enolate that is lower in energy than the dissociated radical species.

⁴⁸ The excitation energy of an allyl radical should be lower than that of a hydrogen atom, and the lowest energy excited state is expected to be the one from which reaction occurs (see Chapter 12).

**FIGURE 11.33**

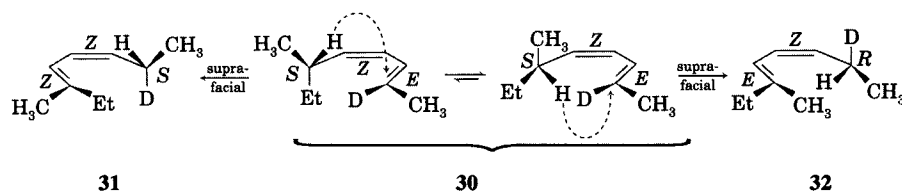
Suprafacial (allowed) and antarafacial (forbidden) [1,3] hydrogen shifts in electronically excited propene.

**FIGURE 11.34**

Suprafacial (allowed) and antarafacial (forbidden) [1,5] hydrogen shifts in ground state 1,3-pentadiene-1,1- d_2 .

Figure 11.34 illustrates, the thermal [1,5] hydrogen shift is predicted to be allowed by the suprafacial pathway but forbidden by the antarafacial pathway. On the other hand, the photochemical reaction is predicted to be allowed by the antarafacial pathway but forbidden by the suprafacial pathway. Applying the same analysis to larger π systems shows that the selection rules for the [1,7] hydrogen shift are the same as those for the [1,3] hydrogen shift, and the rules for the [1,9] hydrogen shift are the same as for the [1,5] hydrogen shift.

The suprafacial stereochemistry of the [1,5] hydrogen shift was demonstrated by Roth and co-workers, as shown in Figure 11.35.⁴⁹ The reaction of (*S*)-(2*E*,4*Z*)-6-methyl-2,4-octadiene-2-*d* (**30**) at 250°C produced a 1.5:1 ratio of (*R*)-(3*E*,5*Z*)-3-methyl-3,5-octadiene-7-*d* (**32**) to (*S*)-(3*Z*,5*Z*)-3-methyl-3,5-octadiene-7-*d* (**31**). Both are products of a suprafacial [1,5] hydrogen shift. Apparently the greater yield of **32** results from a conformational preference in **30** for the ethyl group to be oriented away from C2 of the octadiene.

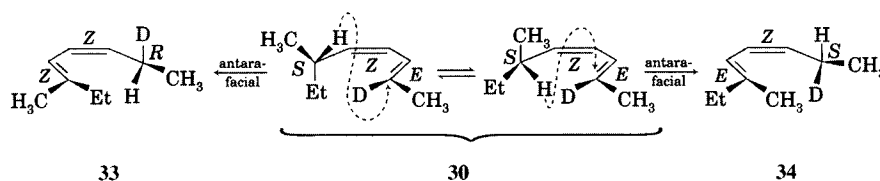
**FIGURE 11.35**

Stereochemistry of products formed by suprafacial [1,5] hydrogen shift. (Et = CH_2CH_3 .)

⁴⁹ Roth, W. R.; König, J.; Stein, K. *Chem. Ber.* **1970**, *103*, 426.

FIGURE 11.36

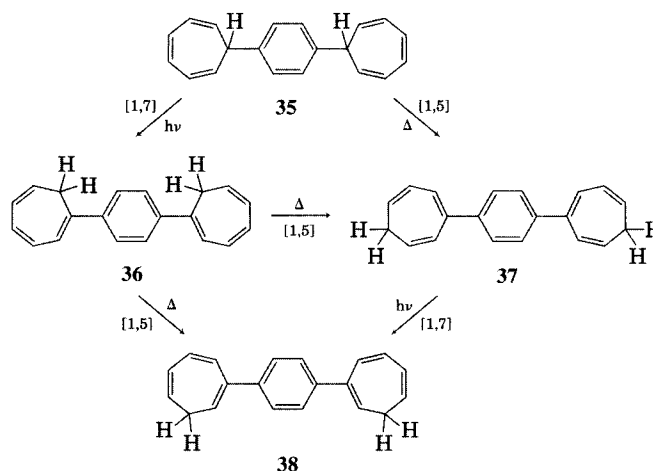
Predictions of stereochemistry of hypothetical products of antarafacial [1,5] hydrogen shift.



It is noteworthy that the products resulting from antarafacial [1,5] hydrogen shifts (structures 33 and 34 in Figure 11.36) were not observed. Roth and co-workers estimated that the energy preference for the suprafacial shift must be at least 8 kcal/mol.⁵⁰

The isomerization of 1,4-bis(7-cycloheptatrienyl)benzene (35, Figure 11.37) to 36, 37, and 38 can be rationalized as a series of thermal [1,5] and photochemical [1,7] suprafacial hydrogen shifts.^{14,51} A [1,7] hydrogen shift has also been seen in the conversion of previtamin D₃ (39) to vitamin D₃ (40, Figure 11.38). The stereochemical nature of these reactions is not apparent in the absence of labeling, but the [1,7] hydrogen shift was shown to be antarafacial in previtamin D₃ model compounds, as in the conversion of deuterium-labeled *cis*-isotachysterol 41 to 42 and 43 in Figure 11.39.⁵²⁻⁵⁴

In sigmatropic [1,*j*] hydrogen shifts, it is necessary to consider the stereochemistry of the reaction only with regard to the conjugated π system of the *j* fragment because the hydrogen radical has one electron in a

**FIGURE 11.37**

[1,5] and [1,7] Hydrogen shifts in 1,4-bis(7-cycloheptatrienyl)benzene. (Adapted from reference 14).

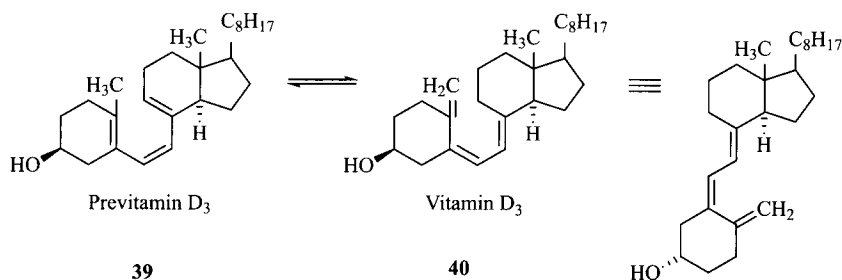
⁵⁰ For a detailed discussion of these results, see Carpenter, B. K. *Determination of Organic Reaction Mechanisms*; Wiley-Interscience: New York, 1984; pp. 180–184.

⁵¹ Murray, R. W.; Kaplan, M. L. *J. Am. Chem. Soc.* **1966**, *88*, 3527.

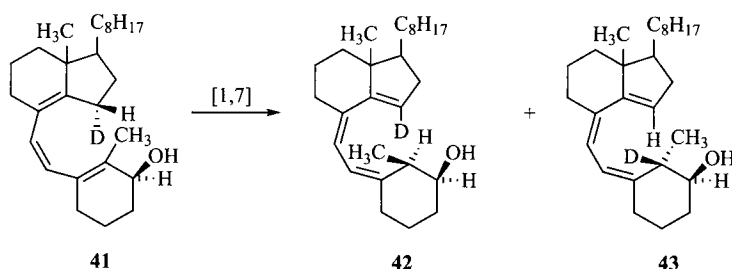
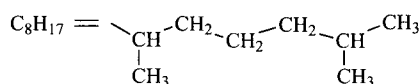
⁵² Hoeger, C. A.; Okamura, W. H. *J. Am. Chem. Soc.* **1985**, *107*, 268.

⁵³ Hoeger, C. A.; Johnston, A. D.; Okamura, W. H. *J. Am. Chem. Soc.* **1987**, *109*, 4690.

⁵⁴ (a) Spangler, C. W. *Chem. Rev.* **1976**, *76*, 187 summarized the activation parameters for many thermal [1,*j*] hydrogen shifts. For the suprafacial [1,5] hydrogen shift, typical values of ΔS^\ddagger are around -5 to -12 eu, with activation energies around 30–35 kcal/mol. For the antarafacial [1,7] hydrogen shift, the corresponding values are around -15 to -25 eu and 15–25 kcal/mol. Therefore, it appears that the [1,7] hydrogen shifts have lower activation energies but more negative activation entropies than do the [1,5] hydrogen shifts. (b) For a discussion, see Gurskii, M. E.; Gridnev, I. D.; Il'ichev, Y. V.; Ignatenko, A. V.; Bubnov, Y. N. *Angew. Chem. Int. Ed. Engl.* **1992**, *31*, 781. Also see the discussion in Burnier, J. S.; Jorgensen, W. L. *J. Org. Chem.* **1984**, *49*, 3001.

**FIGURE 11.38**

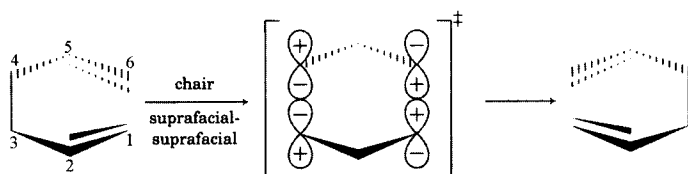
[1,7] Hydrogen shift in vitamin D₃ synthesis. (Adapted from reference 53.)

**FIGURE 11.39**

Evidence for antarafacial [1,7] hydrogen shifts in a vitamin D₃ analog. (Adapted from reference 52.)

spherically symmetric $1s$ orbital. Therefore, the hydrogen atom has only one face, and all transformations must be suprafacial with respect to it. For migration of a group other than hydrogen, however, it is necessary to consider the stereochemistry of the reaction with respect to both components. For example, the Cope rearrangement, which is a [3,3] sigmatropic reaction, can be either suprafacial or antarafacial with respect to each component.

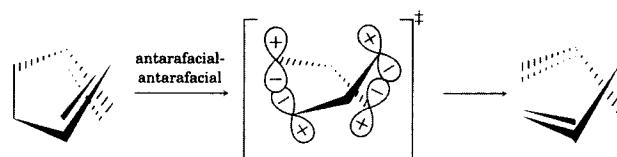
The chair transition structure shown for the Cope rearrangement in Figure 11.40 is suprafacial with respect to both components (the two allyl radicals drawn in the transition structure) because both bond breaking and bond forming take place above the plane defined by the atoms C1, C2, and C3, and both bond breaking and bond forming take place below atoms C4, C5, and C6. A transition structure that is suprafacial with respect to both components is designated as the suprafacial–suprafacial (ss) pathway. Because of the symmetry of ψ_2 of each of the allyl fragments, bonding can begin to develop between C1 and C6 as dissociation of the C3–C4 bond occurs, so the process shown is allowed by the principles of orbital symmetry.

**FIGURE 11.40**

Suprafacial–suprafacial chair transition structure for the Cope rearrangement.

FIGURE 11.41

Antarafacial–antarafacial transition structure for the Cope rearrangement.



As noted earlier, a transition structure in which a σ bond breaks from one face of a π system and a new σ bond forms to the opposite face of that π system is termed antarafacial. For example, Figure 11.41 shows a transition structure for the Cope rearrangement that is antarafacial with respect to both of the three-carbon segments. This geometry may be geometrically strained, but it is allowed by the principles of conservation of orbital symmetry because a σ bond with $(-)(-)$ orbital overlap can form while the original σ bond with $(+)(+)$ orbital overlap is breaking. A transition structure that is antarafacial with respect to both components is termed the antarafacial–antarafacial (aa) pathway.⁵⁵

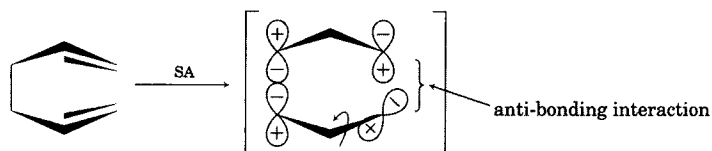
In theory, it might be possible for a Cope rearrangement to occur by a pathway that is suprafacial with respect to one component and antarafacial with respect to the other. It is difficult to visualize, but such a process would require a rotation—for example, in the C5–C6 bond—as the C3–C4 bond dissociates. Such pathways would be designated suprafacial–antarafacial (sa) or antarafacial–suprafacial (as). As shown in the example in Figure 11.42, however, such a mechanism would lead to an antibonding relationship between C6 and C1, so it is forbidden by the principle of conservation of orbital symmetry.⁵⁶

The boat transition structure shown in Figure 11.43 is also an allowed suprafacial–suprafacial pathway for the Cope rearrangement. Doering and Roth used stereochemical labels to distinguish between the suprafacial–suprafacial boat and chair transition structures for the Cope rearrangement of acyclic 1,5-dienes.⁵⁷ As shown in Figure 11.44, a chair-like transition structure for the Cope rearrangement of (\pm) -3,4-dimethyl-1,5-hexadiene should produce *trans,trans*-2,6-octadiene, but the meso diastereomer of the reactant would produce the *cis,trans* isomer of the product. On the other hand, a boat-like transition structure would result in the formation of the *trans,trans* product from the meso starting material, but the *cis,trans* product would be produced from the racemic reactant (Figure 11.45). Doering and Roth found that 90% of the product obtained from the Cope rearrangement of the racemic starting material was the *trans,trans* isomer, consistent with the chair transition structure for the reaction.⁵⁷ The boat transition structure is about 6 kcal/mol higher in energy than the chair, but boat transition structures can be equal to or lower in energy than chair transition

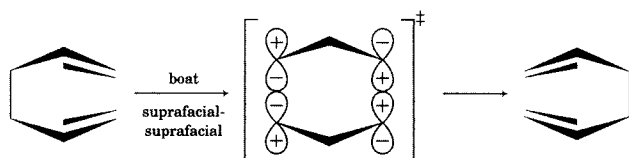
⁵⁵ An antarafacial [3,3] sigmatropic rearrangement was proposed for one reaction by Miyashi, T.; Nitta, M.; Mukai, T. *J. Am. Chem. Soc.* **1971**, *93*, 3441, but an alternative explanation for the experimental results was advanced by Baldwin, J. E.; Kaplan, M. S. *J. Am. Chem. Soc.* **1971**, *93*, 3969.

⁵⁶ Even more complicated pathways can be imagined. Hansen, H.-J.; Schmid, H. *Tetrahedron* **1974**, *1959*, considered seven possible transition structures for the Cope rearrangement, including boat and chair suprafacial–suprafacial, twist, cross, and plane antarafacial–antarafacial transition structures, and one anchor antarafacial–suprafacial transition structure.

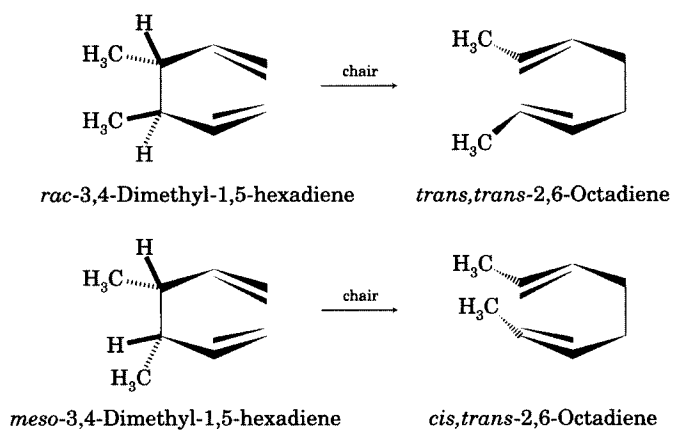
⁵⁷ Doering, W. v. E.; Roth, W. R. *Tetrahedron* **1962**, *18*, 67.

**FIGURE 11.42**

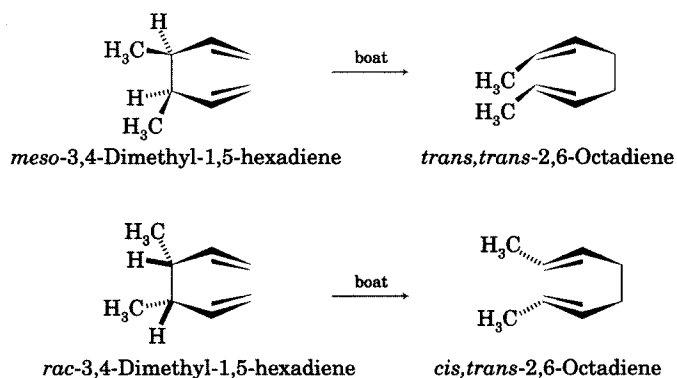
Forbidden suprafacial-antarafacial transition structure for Cope rearrangement.

**FIGURE 11.43**

Suprafacial-suprafacial boat transition structure for the Cope rearrangement.

**FIGURE 11.44**

Products of the Cope rearrangement of racemic (top) and meso (bottom) diastereomers of 3,4-dimethyl-1,5-hexadiene through chair transition structures.

**FIGURE 11.45**

Products of Cope rearrangement of racemic (top) and meso (bottom) diastereomers of 3,4-dimethyl-1,5-hexadiene through boat transition structures.

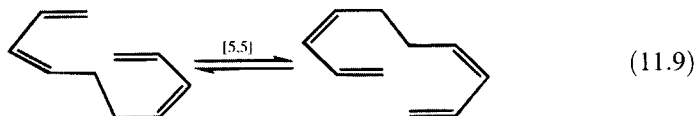
structures for Cope rearrangements of some bicyclic structures.⁵⁸ Other possible pathways appear to be much higher in energy and are not common routes for reaction.^{59–62}

As is the case for other pericyclic reactions, the selection rules for a thermal $[i,j]$ sigmatropic reaction are reversed for the photochemical reaction. If irradiation of a 1,5-hexadiene produces the electronically excited state of one and only one of the two allyl components, then the HOMO of one component is ψ_3 , and the HOMO of the other component is ψ_2 . The [3,3] suprafacial–suprafacial reaction (Figure 11.46) is forbidden (as is the antarafacial–antarafacial pathway), but the antarafacial–suprafacial and suprafacial–antarafacial pathways are allowed (Figure 11.47). Analysis of higher sigmatropic reactions shows that the selection rules also reverse with the addition of a carbon–carbon double bond to either of the π systems. Thus, the [3,5] sigmatropic reaction is thermally allowed to be suprafacial–antarafacial or antarafacial–suprafacial and photochemically allowed to be suprafacial–suprafacial or antarafacial–antarafacial. Two of these reaction modes are illustrated in Figure 11.48.

Because the symmetries of linear polyene systems alternate in a regular way as each additional carbon–carbon double bond is added to either of the fragments in the transition structures, the selection rules for sigmatropic reactions may be generalized as follows:^{14,63}

Sigmatropic reactions of order $[i,j]$ are thermally allowed to be suprafacial–suprafacial or antarafacial–antarafacial and are photochemically allowed to be antarafacial–suprafacial or suprafacial–antarafacial if $i + j = 4n + 2$. Conversely, they are thermally allowed to be antarafacial–suprafacial or suprafacial–antarafacial and photochemically allowed to be suprafacial–suprafacial or antarafacial–antarafacial if $i + j = 4n$.

The [5,5] sigmatropic rearrangement of (3Z,7Z)-1,3,7,9-decatetraene (equation 11.9) could in theory take place through either a $[5_a + 5_a]$ or a $[5_s + 5_s]$ pathway. Houk and co-workers calculated a 9 kcal/mol preference for the suprafacial–suprafacial pathway because of geometric strain in the transition structure for the antarafacial–antarafacial process.⁶⁴



⁵⁸ Tantillo, D. J.; Hoffmann, R. *J. Org. Chem.* **2002**, *67*, 1419.

⁵⁹ Shea, K. J.; Phillips, R. B. *J. Am. Chem. Soc.* **1980**, *102*, 3156.

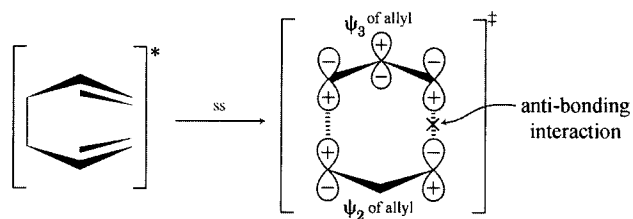
⁶⁰ Gajewski, J. J.; Benner, C. W.; Hawkins, C. M. *J. Org. Chem.* **1987**, *52*, 5198.

⁶¹ Similarly, a chair transition structure is 6.6 kcal/mol lower in energy than a boat transition structure in the Claisen rearrangement. Vance, R. L.; Rondan, N. G.; Houk, K. N.; Jensen, F.; Borden, W. T.; Komornicki, A.; Wimmer, E. *J. Am. Chem. Soc.* **1988**, *110*, 2314.

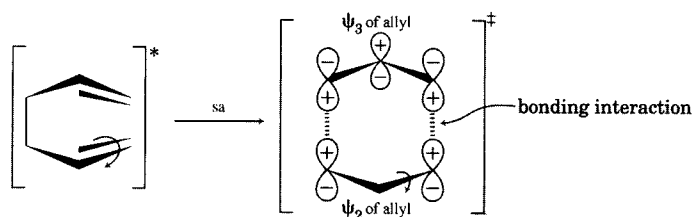
⁶² See also Shea, K. J.; Stoddard, G. J.; England, W. P.; Haffner, C. D. *J. Am. Chem. Soc.* **1992**, *114*, 2635 and references therein.

⁶³ For a further discussion of sigmatropic shifts and a method for generating qualitative potential energy surfaces to rationalize them, see Epiotis, N. D.; Shaik, S. *J. Am. Chem. Soc.* **1977**, *99*, 4936.

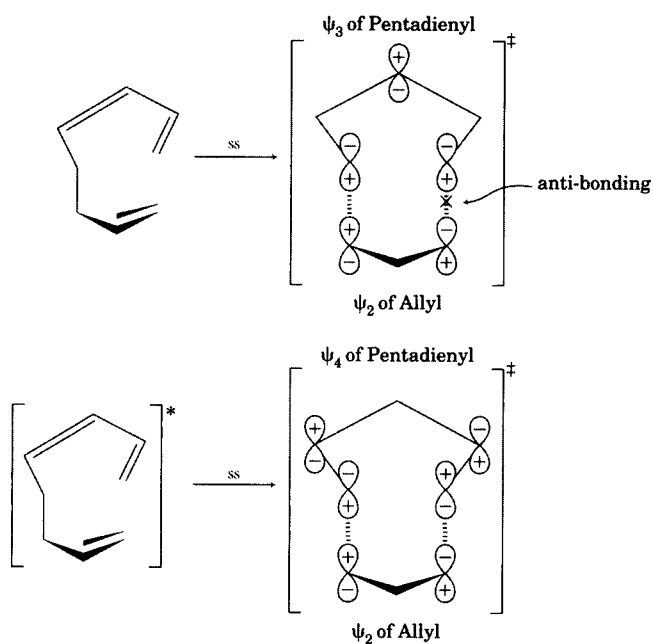
⁶⁴ Beno, B. R.; Fennen, J.; Houk, K. N.; Lindner, H. J.; Hafner, K. *J. Am. Chem. Soc.* **1998**, *120*, 10490. The calculations also revealed, however, that diradical pathways were lower in energy than the concerted pathway.

**FIGURE 11.46**

Forbidden *ss* transition structure for photochemical Cope rearrangement.

**FIGURE 11.47**

Allowed suprafacial-antarafacial transition structure for photochemical Cope rearrangement. Note the rotation about the lower portion of the structure.

**FIGURE 11.48**

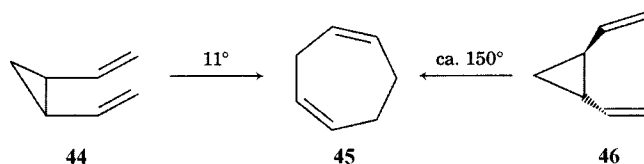
Suprafacial-suprafacial transition structures for the thermal (top) and photochemical (bottom) [3,5] sigmatropic reaction.

Further Examples of Sigmatropic Reactions

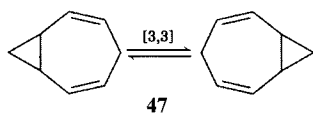
The selection rules for sigmatropic reactions are powerful predictors of thermal rearrangements.⁸ They explain how some reactions can occur stereospecifically and with surprisingly low activation energies, while others do not. For example, *cis*-1,2-divinylcyclopropane (**44**) undergoes a [3,3] sigmatropic rearrangement to *cis,cis*-1,4-cycloheptatriene (**45**) with a half-life of

FIGURE 11.49

Thermal rearrangements of *cis*- and *trans*-1,2-divinylcyclopropane.



25 min at 11°C (Figure 11.49).^{65,66} *trans*-1,2-Divinylcyclopropane (**46**) reacts to give the same product, but only upon heating to about 150°C.⁶⁷ Apparently the reaction of **44** is fast because the *cis* geometry places the two double bonds in the proper relationship for the Cope rearrangement. In the *trans* isomer, however, the termini of the two double bonds cannot overlap. Therefore, the reaction of **46** may proceed by a nonconcerted process involving breaking the cyclopropane ring to form a biradical intermediate.⁶⁸

**FIGURE 11.50**

Degenerate sigmatropic rearrangement of homotropilidene.

Both **44** and **46** are higher in energy than **45**. Sigmatropic rearrangements can also result in degenerate rearrangements of structures such as homotropilidene (**47**, Figure 11.50).⁶⁹ Perhaps the most dramatic example of a sigmatropic rearrangement is provided by tricyclo[3.3.2.0^{4,6}]deca-2,7,9-triene (**48**, Figure 11.51), more commonly known by the trivial name *bullvalene*.⁷⁰ Although there are only ten carbon atoms in the molecule, the various permutations possible through [3,3] sigmatropic rearrangements produce about 1.2 million valence isomers.^{71,72} The isomerization is so fast that the ¹H NMR spectrum is a broad peak at room temperature, and the spectrum sharpens to a single peak at 120°C. At -85°C, the isomerization slows to the point that separate peaks for vinyl, cyclopropyl, and methine protons can be seen (Figure 11.52). Analysis of the spectrum indicates that the valence isomerization occurs with a rate constant of 540 s⁻¹ at 0°C and has an activation energy of 12.8 kcal/mol.^{71,73,74}

Several reactions similar to the Cope and Claisen rearrangements have been developed for synthetic applications. A variation on the Cope

⁶⁵ Schneider, M. P.; Rebell, J. J. *Chem. Soc. Chem. Commun.* **1975**, 283. Also see (a) Brown, J. M.; Golding, B. T.; Stofko, J. J., Jr. *J. Chem. Soc. Perkin Trans. 2* **1978**, 436; (b) Gajewski, J. J.; Hawkins, C. M.; Jimenez, J. L. *J. Org. Chem.* **1990**, *55*, 674.

⁶⁶ Initial studies were reported by Vogel, E. *Angew. Chem.* **1960**, *72*, 4; Vogel, E.; Ott, K.-H.; Gajek, K. *Liebigs Ann. Chem.* **1961**, *644*, 172.

⁶⁷ For leading references, see Gajewski, J. J.; Olson, L. P.; Tupper, K. J. *J. Am. Chem. Soc.* **1993**, *115*, 4548.

⁶⁸ Arai, M.; Crawford, R. J. *Can. J. Chem.* **1972**, *50*, 2158. Reclosure of the intermediate to **44** would then allow rapid Cope rearrangement to **45**. See also the discussion in reference 67 concerning the rate-limiting step for this pathway.

⁶⁹ Doering, W. v. E.; Roth, W. R. *Tetrahedron* **1963**, *19*, 715.

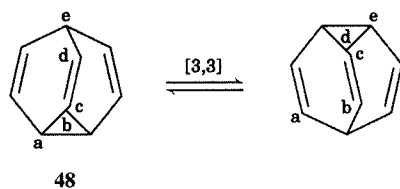
⁷⁰ See reference 43, p. 131, for an account of the origin of this name.

⁷¹ Schröder, G.; Oth, J. F. M.; Merényi, R. *Angew. Chem. Int. Ed. Engl.* **1965**, *4*, 752.

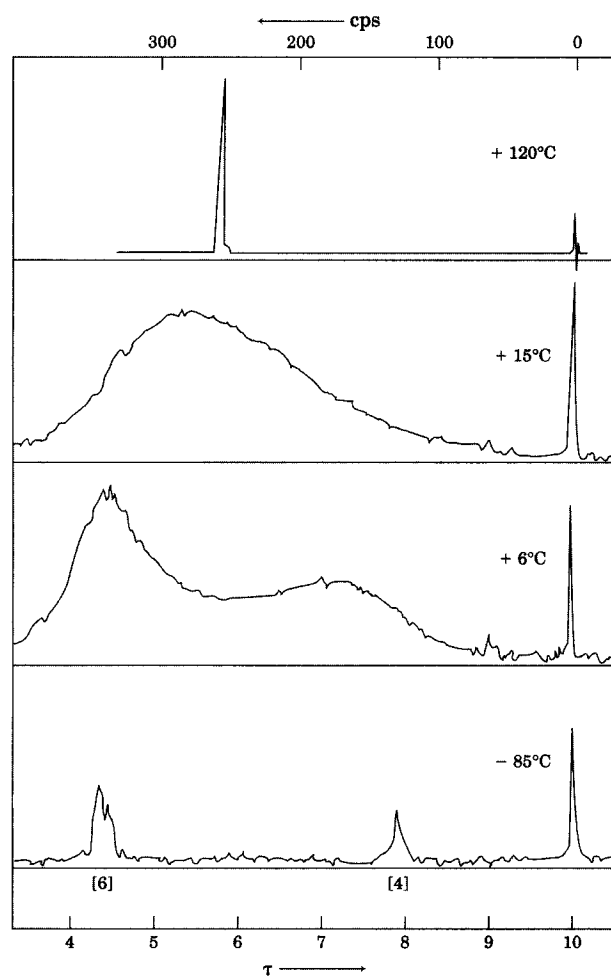
⁷² Bullvalene is said to be *fluxional*, meaning that it undergoes rapid degenerate rearrangements (reference 17).

⁷³ Analysis by deuterium NMR on a sample dissolved in a liquid crystal solvent gave a linear Arrhenius plot with a calculated rate constant of 4600 s⁻¹ at 300°C, ΔH^\ddagger of 13.3 kcal/mol, and ΔS^\ddagger of + 2.5 eu: Poupko, R.; Zimmermann, H.; Luz, Z. *J. Am. Chem. Soc.* **1984**, *106*, 5391. The value of ΔS^\ddagger for a reaction measured in a liquid crystal solvent may include a contribution from disorder introduced into the solvent as the reaction occurs.

⁷⁴ Valence tautomerization of bullvalene has also been studied both in the gas phase by Moreno, P. O.; Suarez, C.; Tafazzoli, M.; True, N. S.; LeMaster, C. B. *J. Phys. Chem.* **1992**, *96*, 10206 and in crystal form by Schlick, S.; Luz, Z.; Poupko, R.; Zimmermann, H. *J. Am. Chem. Soc.* **1992**, *114*, 4315.

**FIGURE 11.51**

Degenerate sigmatropic rearrangement in bullvalene. (Atom labels indicate the permutation arising from one [3,3] sigmatropic reaction.)

**FIGURE 11.52**

Proton NMR spectrum of bullvalene as a function of temperature. (Reproduced from reference 71. The τ scale is an older scale for NMR spectroscopy in which $\tau = 10 - \delta$.)

rearrangement is the oxy-Cope reaction.⁷⁵ As shown in Figure 11.53, a Cope rearrangement on a 3-hydroxy-1,5-hexadiene produces an enol, which can then tautomerize to the corresponding ketone or aldehyde.

An example is the conversion of 2-vinylbicyclo[2.2.2]oct-5-en-2-ol (**49**) to *cis*- $\Delta^{5,6}$ -2-octalone (**50**).^{76,77} Note that the structure in braces is intended only

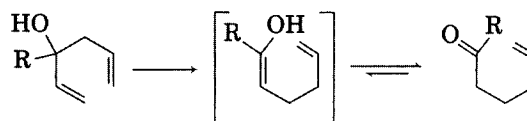
⁷⁵ Berson, J.A.; Jones, M., Jr. *J. Am. Chem. Soc.* **1964**, *86*, 5019.

⁷⁶ Berson, J. A.; Jones, M., Jr. *J. Am. Chem. Soc.* **1964**, *86*, 5017, 5019.

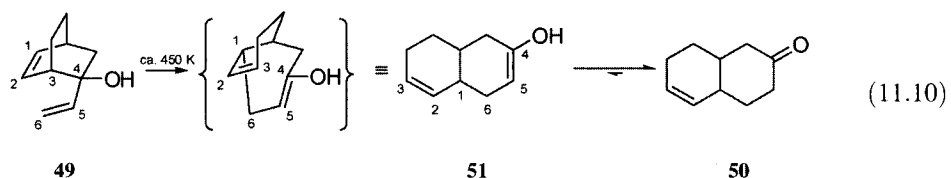
⁷⁷ For a discussion of the rate enhancement observed upon deprotonation of an OH substituent on a structure undergoing a Cope rearrangement, see (a) Wilson, S. R. *Org. React.* **1993**, *43*, 93; (b) Harris, N. J.; Gajewski, J. J. *J. Am. Chem. Soc.* **1994**, *116*, 6121.

FIGURE 11.53

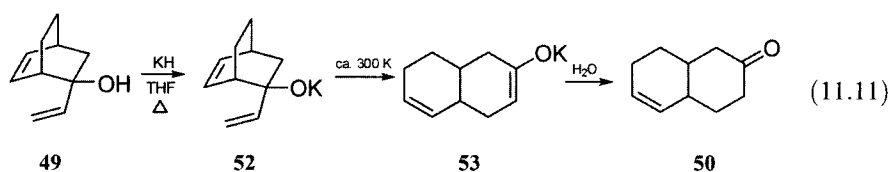
A general oxy-Cope rearrangement.



to show the bonding changes involved in the Cope rearrangement of **49** to the enol **51**.



Evans and Golob found that the rate constant for such reactions could be accelerated by factors of 10^{10} – 10^{17} by conversion to the corresponding alkoxides.⁷⁸ For example, treatment of **49** with potassium hydride produced the alkoxide **52**, which readily isomerized to **53** (equation 11.11).



The Claisen rearrangement can be catalyzed by Lewis acid catalysts (Figure 11.54), and the use of chiral Lewis catalysts provides a path to diastereoselective and enantioselective Claisen rearrangements.⁷⁹

There are many [3,3] sigmatropic rearrangements that are mechanistically similar to the Claisen rearrangement.⁸⁰ Among these is the Carroll rearrangement, which involves the conversion of an allylic β -ketoester (**54**) to the enol (**55**), which then undergoes a Cope rearrangement to yield a β -keto carboxylic acid (**56**). The rearrangement takes place only at temperatures of 130–220°C, so the β -ketoacid decarboxylates to a γ,δ -unsaturated ketone (**57**, equation 11.12).⁸¹

⁷⁸ Evans, D. A.; Golob, A. M. *J. Am. Chem. Soc.* **1975**, *97*, 4765.

⁷⁹ Nonoshita, K.; Banno, H.; Maruoka, K.; Yamamoto, H. *J. Am. Chem. Soc.* **1990**, *112*, 316; Maruoka, K.; Banno, H.; Yamamoto, H. *J. Am. Chem. Soc.* **1990**, *112*, 7791.

⁸⁰ For a review, see Castro A. M. M. *Chem. Rev.* **2004**, *104*, 2939.

⁸¹ Carroll, M. F. *J. Chem. Soc.* **1949**, 704, 1266; **1941**, 507.

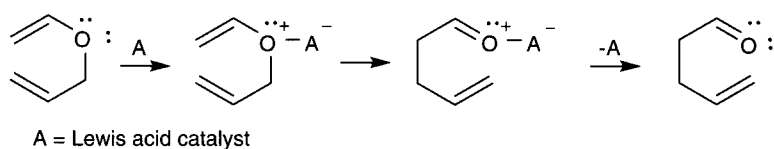
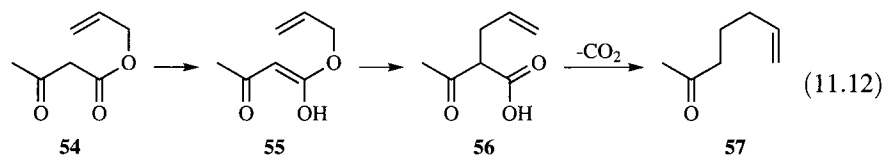
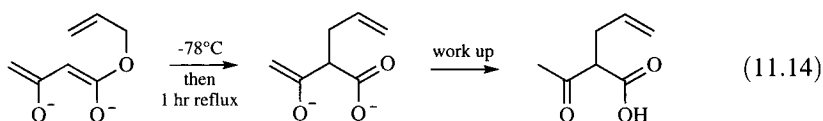
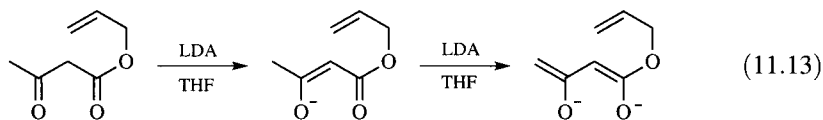


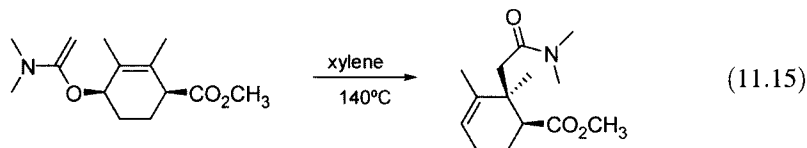
FIGURE 11.54
Lewis acid catalysis of the Cope rearrangement.



This type of reaction occurs at lower temperatures with the dianions formed from allylic acetoacetates, which can be prepared from the reaction of acetoacetates with two equivalents of lithium diisopropylamide (LDA, equations 11.13 and 11.14).



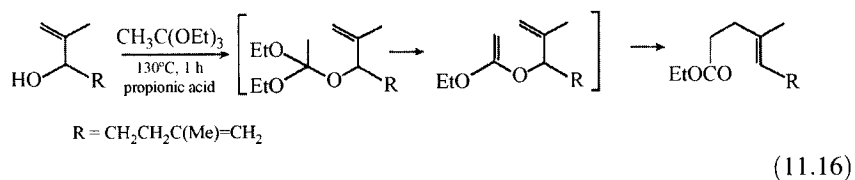
The Eschenmoser rearrangement involves the rearrangement of an *N,O*-ketene acetal to a γ,δ -unsaturated amide (equation 11.15).⁸²



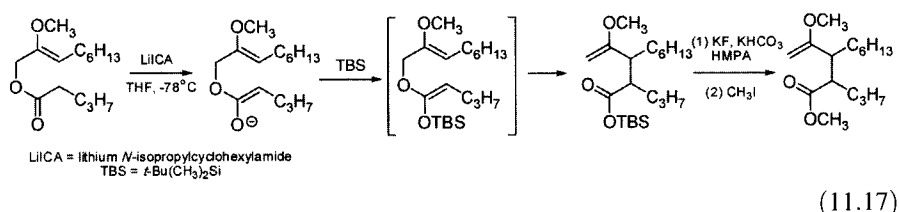
The Johnson rearrangement involves reaction of an allylic alcohol with ethyl orthoacetate to give a mixed ortho ester that loses ethanol and then undergoes

⁸² Wick, A. E.; Felix, D.; Steen, K.; Eschenmoser, A. *Helv. Chim. Acta* **1964**, *47*, 2425; Felix, D.; Gschwend-Steen, K.; Wick, A. E.; Eschenmoser, A. *Helv. Chim. Acta* **1969**, *52*, 1030.

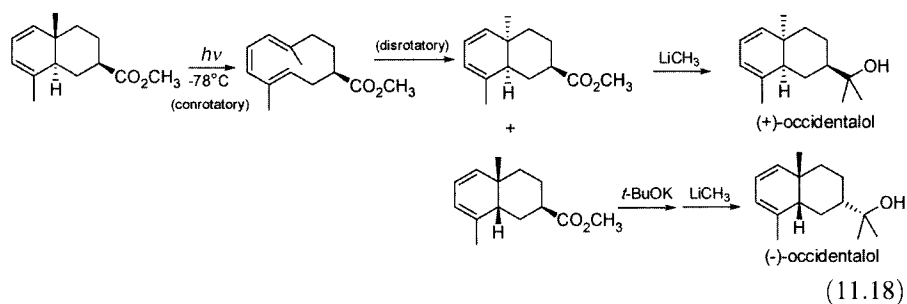
[3,3] sigmatropic rearrangement to an olefinic ester.⁸³



In the Ireland–Claisen rearrangement (equation 11.17), an allylic ester is converted to an enolate that reacts with trimethylsilyl chloride to produce an allyl trimethylsilyl ketene acetal, which then undergoes rearrangement. Depending on the reaction conditions, the product may be a γ,δ -unsaturated carboxylic acid or ester.⁸⁴



An example of the use of electrocyclizations in organic synthesis is the preparation of both (+)- and (–)-occidentalol by a path involving first a photochemical, conrotatory ring opening of a cyclohexadiene to a cyclohexatriene and then a thermal closing to a mixture of diastereomeric cyclohexadiene epimers (equation 11.18).^{85,86}



⁸³ Johnson, W. S.; Werthemann, L.; Bartlett, W. R.; Brocksom, T. J.; Li, T.; Faulkner, D. J.; Petersen, M. R. *J. Am. Chem. Soc.* **1970**, *92*, 741.

⁸⁴ Ireland, R. E.; Mueller, R. H. *J. Am. Chem. Soc.* **1972**, *94*, 5897; Ireland, R. E.; Mueller, R. H.; Willard, A. K. *J. Am. Chem. Soc.* **1976**, *98*, 2868.

⁸⁵ Hortmann, A. G.; Daniel, D. S.; Martinelli, J. E. *J. Org. Chem.* **1973**, *38*, 728.

⁸⁶ For a review of electrocyclizations in biosynthetic and biomimetic reactions, see Beaudry, C. M.; Malerich, J. P.; Trauner, D. *Chem. Rev.* **2005**, *105*, 4757.

11.4 CYCLOADDITION REACTIONS

Introduction

The pericyclic reactions discussed to this point have been unimolecular rearrangements. The principles of conservation of orbital symmetry also apply to bimolecular cycloaddition reactions such as the Diels–Alder reaction.⁸⁷ As shown in Figure 11.55(a), the Diels–Alder reaction of 1,3-butadiene with ethene produces cyclohexene. The analogous concerted cycloaddition of two ethene molecules to form cyclobutane, Figure 11.55(b), does not occur thermally, even though that reaction is calculated to be exothermic by 18 kcal/mol.⁸⁸

Ethene Dimerization

Let us analyze the hypothetical cycloaddition of two ethenes first. Figure 11.56 shows an initial arrangement of two ethene molecules in which the two σ bonds are parallel to each other and the two sets of p orbitals are also parallel to each other. We imagine that the reaction occurs through conversion of the four p orbitals into four sp^3 hybrid orbitals. Just as is the case with electrocyclic reactions, cycloaddition reactions may be characterized as antarafacial (a) or suprafacial (s) with respect to each of the π systems. The cycloaddition shown in Figure 11.56 is suprafacial with respect to each component because bonding occurs on the bottom lobes of both of the p orbitals of the upper ethene, and bonding also occurs on the top lobes of both of the p orbitals of the lower ethene.

It is customary to describe cycloaddition reactions by indicating in brackets for each component the type of orbital system involved in the reaction, the number of *electrons*, and the stereochemistry with respect to that component. Therefore, the pathway for the ethene dimerization shown in Figure 11.56 is termed a $[\pi 2_s + \pi 2_s]$ cycloaddition because each ethene reacts by way of its π system, each π bond has **two** electrons, and the stereochemistry is **suprafacial** with respect to each π system. We can see that the reaction in Figure 11.56 takes place suprafacially because the product has the same stereochemical relationships of the alkene substituents as do the reactants. That is, H is cis to H and H' is cis to H' in both the reactants and the product.

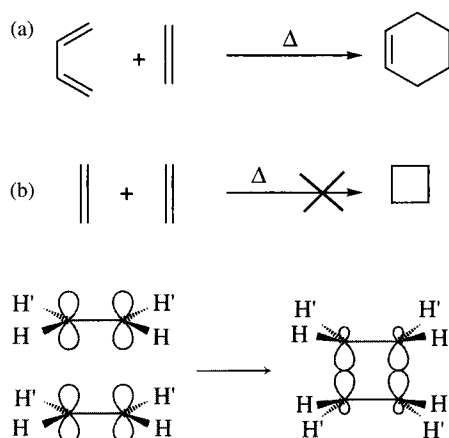


FIGURE 11.55

(a) Allowed $[4 + 2]$ and (b) forbidden $[2 + 2]$ concerted thermal cycloaddition reactions.

FIGURE 11.56

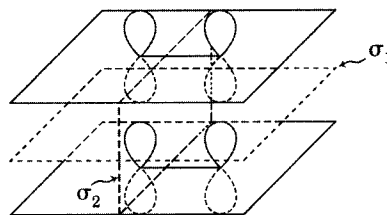
Retention of stereochemical relationships in $[\pi 2_s + \pi 2_s]$ cycloaddition.

⁸⁷ Diels, O.; Alder, K. *Liebigs Ann. Chem.* **1928**, 460, 98.

⁸⁸ Streitwieser, A., Jr. *Science* **1981**, 214, 627. The Diels–Alder reaction of ethene and 1,3-butadiene is exothermic by 40 kcal/mol.

FIGURE 11.57

Basis set of p orbitals of two ethene molecules for $[2 + 2]$ cycloaddition.



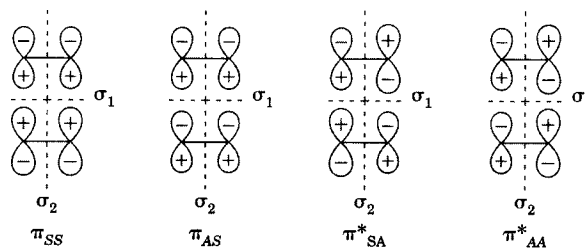
The *combined* basis set of p orbitals—all four p orbitals of the two ethene molecules taken as a group, as shown in Figure 11.57—has a number of symmetry elements. In addition to a horizontal plane of symmetry (σ_1) and a vertical plane of symmetry (σ_2), there is also a plane of symmetry bisecting the H–C–H bond angles, and there are a number of rotation axes. It is not necessary to consider all of the symmetry elements, however. We need to consider only the minimum number of symmetry elements that both (i) are present in reactant, transition structure, and product, and (ii) are needed to distinguish between allowed and forbidden pathways.

In constructing an MO correlation diagram for the $[\pi 2_s + \pi 2_s]$ reaction, it is not sufficient to consider just the MOs of each ethene molecule individually. Either of the two π bonds by itself is *asymmetric* with respect to σ_1 . That is, it does not have the full symmetry of the basis set of atomic orbitals in Figure 11.56. As noted in the discussion of PMO theory in Chapter 4, the p orbitals that comprise the π bonds will split each other strongly because they are degenerate in energy. Thus, an adequate MO description of the reactants must be symmetry correct for the *pair* of ethene units, not just for one ethene alone. Interaction of the set of four atomic p orbitals therefore produces a set of four MOs for the extended system. These reactant MOs are designated both by their bonding or antibonding characteristics and by their symmetry with respect to both of the two planes of symmetry considered in this analysis. (The symmetry designation is given first with respect to σ_1 , then with respect to σ_2 .) Thus, in Figure 11.58, π_{AS} is antisymmetric with respect to σ_1 but is symmetric with respect to σ_2 . The symmetry designations of the other three orbitals of the reactant system are also shown in Figure 11.58.

Similarly, it is necessary to consider a set of cyclobutane σ MOs that are symmetry correct with respect to the same symmetry elements. Thus, the combination of the four sp^3 atomic orbitals shown in Figure 11.59 produces two sets of σ (bonding) MOs and two sets of σ^* (antibonding) MOs. Each of these σ orbitals is characterized with respect to the two mirror planes of symmetry that are preserved throughout the reaction, σ_1 and σ_2 , in Figure 11.60.⁸⁹

FIGURE 11.58

Symmetry-correct MOs for $[2 + 2]$ cycloaddition of two ethenes. (Adapted from reference 101.)



⁸⁹ The Greek letter σ is used to designate both a σ bonding orbital and a mirror plane of symmetry.

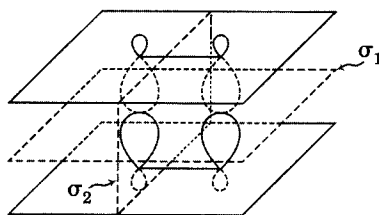


FIGURE 11.59

Basis set orbitals for cyclobutane produced by [2 + 2] cycloaddition.

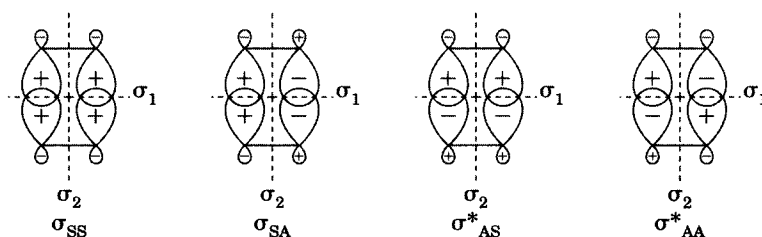


FIGURE 11.60

Symmetry-correct orbitals for σ bonds in cyclobutene. (Adapted from reference 101.)

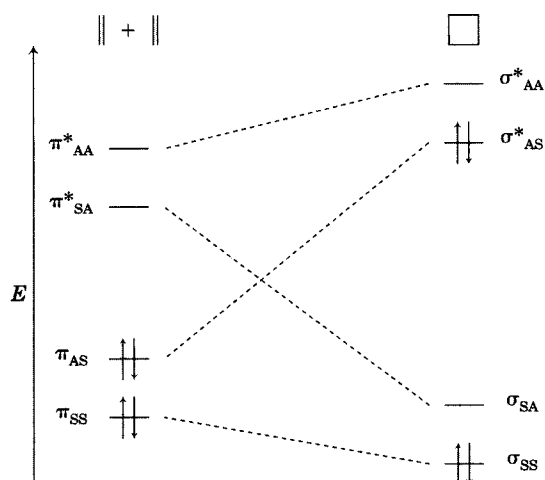


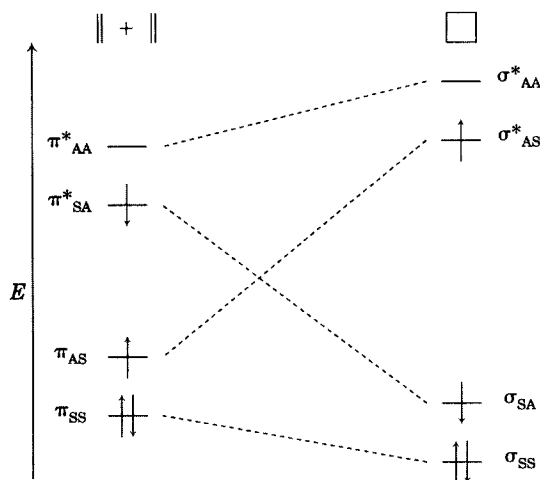
FIGURE 11.61

MO correlation diagram for thermal suprafacial-suprafacial [2 + 2] cycloaddition. (Adapted from reference 101.)

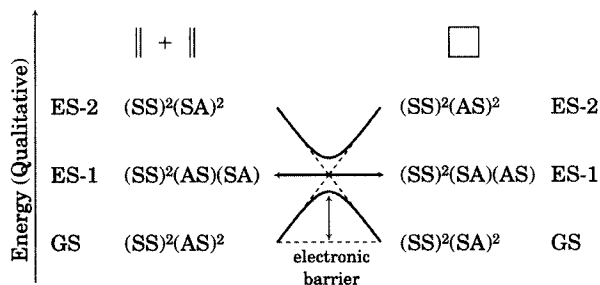
The MO correlation diagram for the cycloaddition reaction is shown in Figure 11.61. Here the artificial energy separation between the two π orbitals is introduced solely to allow clear labeling of the two orbitals and their individual symmetry properties. The same is true of the arbitrary separation between the two π^* orbitals, between the two σ orbitals, and between the two σ^* orbitals. This MO correlation diagram shows that π_{SS} correlates with σ_{SS} and π_{AS} correlates with σ_{AS}^* . Therefore, the thermal [$\pi 2_s + \pi 2_s$] cycloaddition is forbidden, since the ground state of the reactant correlates with a high energy excited state of the product. That is, a process that could force the two ethene molecules together in a suprafacial-suprafacial pathway would produce a cyclobutane molecule having the electronic configuration $\sigma^2\sigma^{*2}$ —a doubly excited electronic state. Similarly, the reverse process (**cycloreversion** of cyclobutene to two ethenes) is also forbidden. Promotion of an electron from one of the π orbitals to a π^* orbital in a photochemical reaction allows the excited state of the reactant system to correlate with the excited state of the

FIGURE 11.62

MO correlation diagram for photochemical suprafacial-suprafacial [2 + 2] cycloaddition. (Adapted from reference 101.)

**FIGURE 11.63**

State correlation diagram for suprafacial-suprafacial [2 + 2] cycloaddition.



product system (Figure 11.62), so the photochemical cycloaddition should be allowed.⁹⁰

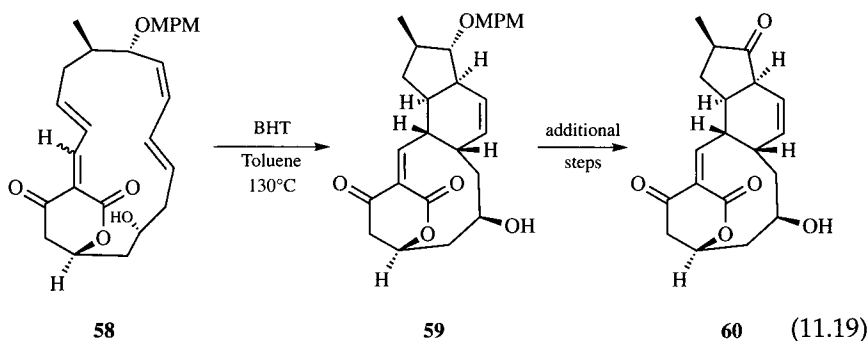
The MO correlation diagrams in Figures 11.61 and 11.62 can be used to generate a state correlation diagram (Figure 11.63). This diagram reemphasizes the conclusion that the ground state [$\pi 2_s + \pi 2_s$] cycloaddition should have a high energy barrier because of the energy needed to raise the ground state molecule to the level of the avoided crossing. Therefore, the thermal reaction is forbidden. The lowest energy excited state of the reactant correlates with the lowest energy excited state of the product, however. There should not be a large thermal energy requirement for this photochemical cycloaddition, so it is allowed by the principles of conservation of orbital symmetry.

The Diels–Alder Reaction

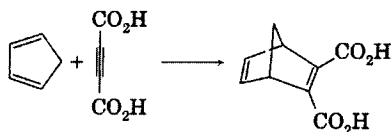
Now let us analyze the Diels–Alder reaction in the same way. Diels–Alder reactions typically involve an electron-rich diene and an electron-poor olefin called a *dienophile*. The $\pi 2$ component need not be a carbon–carbon double

⁹⁰ The first excited state of the cyclobutane, having an electron in a σ^* orbital, is much higher in energy than is the first excited state of the pair of ethenes, which has an electron in one of the π^* orbitals.

bond; other multiply bonded groups, including alkynes and allenes, may also serve as dienophiles.^{91,92} The essential features of the Diels–Alder reaction were reviewed by Sauer.⁹³ With a substituted diene and a substituted olefin, the reaction is highly stereospecific.⁹⁴ Stereochemical configuration is retained in both the olefin and diene, making the reaction very useful in organic synthesis.⁹⁵ We will analyze the reaction with very simple structures, but the principles apply as well to much more complicated reactions.⁹⁶ For example, the intramolecular cycloaddition of **58** to give **59** is a key step in the synthesis of (+)-macquarimicin A (**60**, equation 11.19).⁹⁷



⁹¹ For example, the reaction of cyclopentadiene with acetylenedicarboxylic acid was reported by Diels, O.; Alder, K.; Nienburg, H. *Liebigs Ann. Chem.* **1931**, *490*, 236:



Ketenes undergo cycloadditions with alkenes in which the stereochemistry of the alkene is retained. For a review, see Hyatt, J. A.; Reynolds, P. W. *Org. React.* **1994**, *45*, 159. Both theoretical and experimental evidence support a reaction pathway in which the alkene and the ketene are perpendicular in the transition structure: Lovas, F. J.; Suenram, R. D.; Gillies, C. W.; Gillies, J. Z.; Fowler, P. W.; Kisiel, Z. *J. Am. Chem. Soc.* **1994**, *116*, 5285. For a discussion of cycloadditions involving ketenes, alkynes, and allenes, see (a) Huntsman, W. D. in Patai, S., Ed. *The Chemistry of Ketenes, Allenes and Related Compounds*, Part 2; Wiley-Interscience: Chichester, England, 1980; pp. 521–667; (b) Bastide, J.; Henri-Rousseau, O. in Patai, S., Ed. *The Chemistry of the Carbon–Carbon Triple Bond*, Part 1; Wiley-Interscience: Chichester, England, 1978; pp. 447–522.

⁹² For a critical discussion of the mechanism of the Diels–Alder reaction, see Sauer, J.; Sustmann, R. *Angew. Chem. Int. Ed. Engl.* **1980**, *19*, 779.

⁹³ Sauer, J. *Angew. Chem. Int. Ed.* **1967**, *6*, 16.

⁹⁴ For a discussion of the stereochemistry of the Diels–Alder reaction, see Martin, J. G.; Hill, R. K. *Chem. Rev.* **1961**, *61*, 537.

⁹⁵ For a discussion of synthetic aspects of the Diels–Alder and related reactions, see (a) Kloetzel, M. C. *Org. React.* **1948**, *4*, 1; (b) Holmes, H. L. *Org. React.* **1948**, *4*, 60; (c) Fringuelli, F.; Taticchi, A. *Dienes in the Diels–Alder Reaction*; Wiley-Interscience: New York, 1990; (d) Carruthers, W. *Cycloaddition Reactions in Organic Synthesis*; Pergamon Press: Oxford, England, 1990.

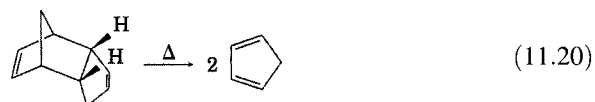
⁹⁶ For reviews, see Takao, K.; Munakata, R.; Tadano, K. *Chem. Rev.* **2005**, *105*, 4779; Brocksom, T. J.; Nakamura, J.; Ferreira, M. L.; Brocksom, U. *J. Braz. Chem. Soc.* **2001**, *12*, 597.

⁹⁷ Munakata, R.; Katakai, H.; Ueki, T.; Kurosaka, J.; Takao, K.; Tadano, K. *J. Am. Chem. Soc.* **2003**, *125*, 14722.

The *ab initio* transition structure calculated for the Diels–Alder reaction of ethene and 1,3-butadiene (Figure 11.64) suggests an initial orientation of the reactants in which the diene and the double bond of the dienophile lie in parallel planes.⁹⁸ Since both bonding changes take place on the top face of the olefin and the bottom face of the diene component, this is a $[\pi 2_s + \pi 4_s]$ cycloaddition. The minimum basis set of atomic orbitals needed to describe the reactant is a set of four *p* orbitals on the butadiene component plus a set of two *p* orbitals on the ethene component (Figure 11.65). For the product, the basis set is a set of four sp^3 hybrid orbitals (for the two σ bonds) and two *p* orbitals (for the double bond). The only symmetry element that is maintained from reactant through the transition structure to product is a plane of symmetry, so we need consider the symmetry properties of the MOs only with respect to this symmetry element. Therefore, we again need to take combinations of the σ bonding and antibonding orbitals that are either symmetric or antisymmetric with respect to the mirror plane.

Categorizing the diene and the alkene orbitals with respect to the plane of symmetry produces the designations shown on the left side of Figure 11.66. As in the case of ethene dimerization, the orbitals associated with the new σ bonds in cyclohexene must be described as symmetry-correct combinations of sp^3 hybrid orbitals (σ_S and σ_A in Figure 11.66). The MO correlation diagram indicates that each of the bonding orbitals in the reactant correlates with a bonding orbital in the product. Since the entire set of bonding MOs of the reactant correlates with the entire set of bonding MOs of the product, there should not be a large electronic barrier for the cycloaddition, and the thermal Diels–Alder reaction is allowed.

The MO correlation diagram can be used to construct a state correlation diagram for the Diels–Alder reaction (Figure 11.67). We see that the ground state of the reactant system can be converted into the ground state of the product without a large electronic barrier, so, the thermal Diels–Alder reaction is allowed. The same diagram (viewed from right to left) applies to the retro-Diels–Alder reaction, such as the cracking of dicyclopentadiene to cyclopentadiene in equation 11.20.^{99,100}

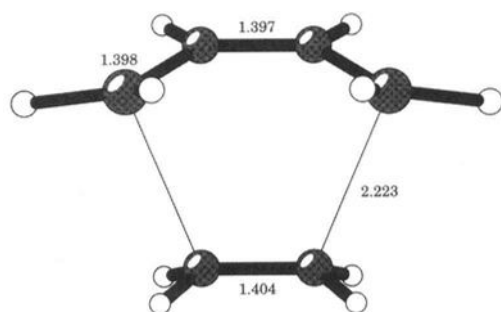


The situation is very different for the photochemical $[\pi 2_s + \pi 4_s]$ cycloaddition. The MO correlation diagram (Figure 11.68) indicates that the lowest

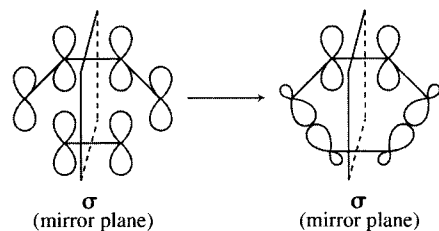
⁹⁸ Li, Y.; Houk, K. N. *J. Am. Chem. Soc.* **1993**, *115*, 7478.

⁹⁹ For leading references and a study of the effect of substituents on one retro-Diels–Alder reaction, see Chung, Y.-S.; Duerr, B. F.; Nanjappan, P.; Czarnik, A. W. *J. Org. Chem.* **1988**, *53*, 1334.

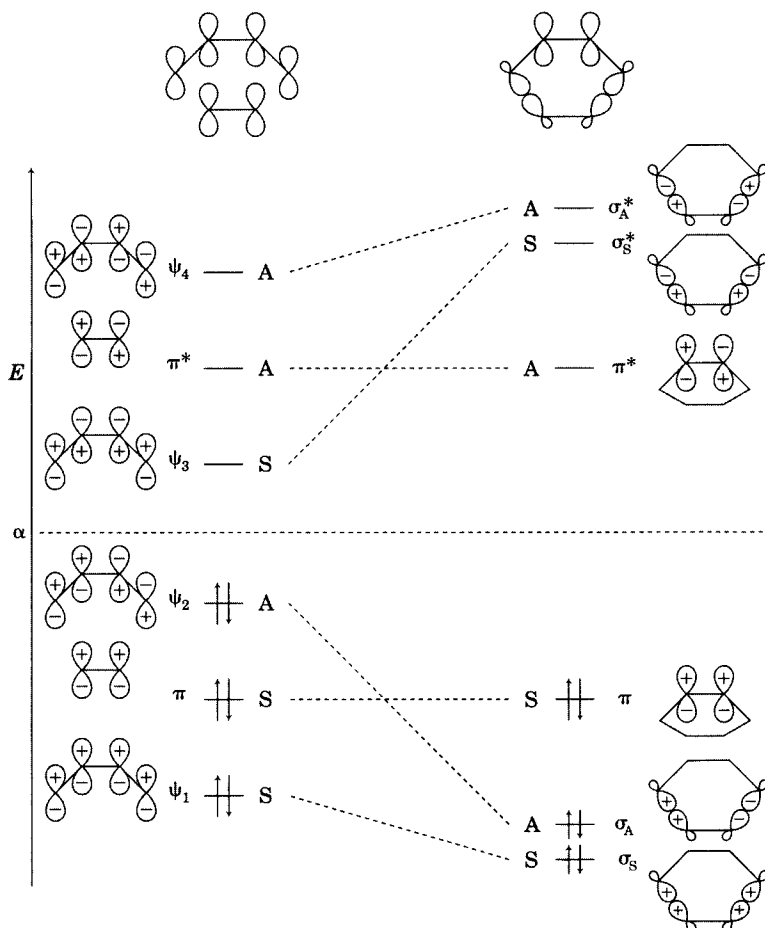
¹⁰⁰ By synthesizing a stable compound with structural features similar to the transition structure for the Diels–Alder reaction, researchers were able to produce antibodies to that analog. These antibodies were then used to catalyze the Diels–Alder reaction by binding the two reactants in the proper orientation for reaction, thus lowering their translational and rotational entropy: Braisted, A. C.; Schultz, P. G. *J. Am. Chem. Soc.* **1990**, *112*, 7430; Hilvert, D.; Hill, K. W.; Nared, K. D.; Auditor, M.-T. M. *J. Am. Chem. Soc.* **1989**, *111*, 9261. Catalytic antibodies have also been used to catalyze both the favored endo and the disfavored exo Diels–Alder adduct: Gouverneur, V. E.; Houk, K. N.; de Pascual-Teresa, B.; Benoit, B.; Janda, K. D.; Lerner, R. A. *Science* **1993**, *262*, 204.

**FIGURE 11.64**

Ab initio transition structure for the Diels–Alder reaction of 1,3-butadiene and ethene. (Adapted from reference 98; distances are in Å.)

**FIGURE 11.65**

Basis set orbitals for reactants (left) and product (right) in Diels–Alder reaction.

**FIGURE 11.66**

MO correlation diagram for a thermal $[\pi 4_s + \pi 2_s]$ cycloaddition. (Adapted from reference 101.)

FIGURE 11.67

State correlation diagram for $[\pi 4_s + \pi 2_s]$ cycloaddition.

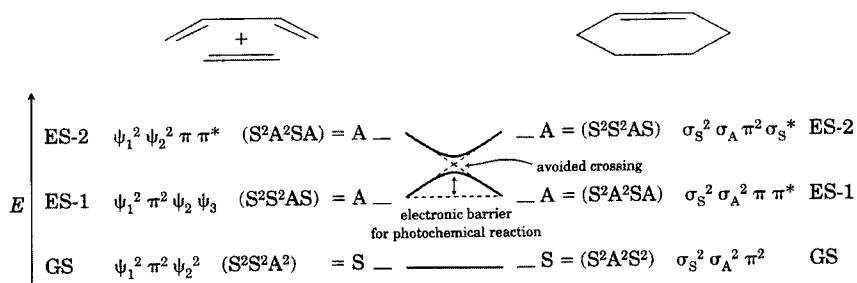
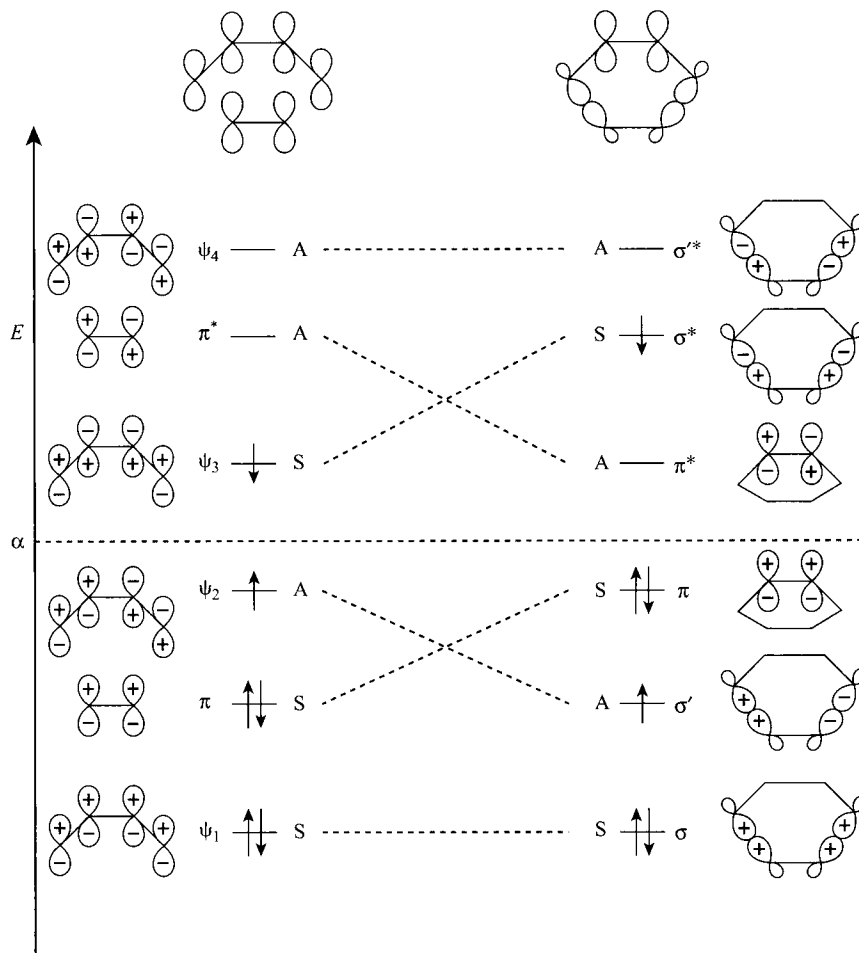


FIGURE 11.68

MO correlation diagram for a (forbidden) photochemical $[\pi 4_s + \pi 2_s]$ cycloaddition.



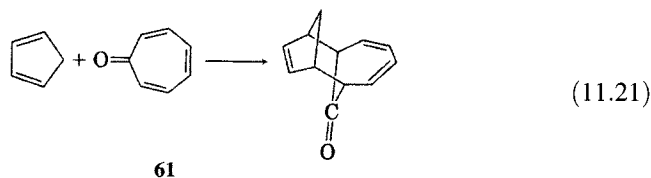
energy excited state (ES-1) of the reactants, formed by promoting an electron from ψ_2 to ψ_3 , would have the electron configuration $\psi_1^2 \pi^2 \psi_2 \psi_3$. By following the dashed MO correlation lines from reactant MOs to product MOs, we see that the suprafacial–suprafacial cycloaddition would produce cyclohexene having the electron configuration $\sigma_s^2 \sigma_A \pi^2 \sigma_s^*$. This is not the lowest energy excited state of cyclohexene, however, so this configuration is designated ES-2. We represent this conversion on the state correlation diagram (Figure 11.67) with a dashed line connecting ES-1 of the reactants with ES-2 of the products.

We may also consider the photochemical conversion of cyclohexene to 1,3-butadiene and ethene. In this case, the lowest energy excited state (ES-1) of cyclohexene would produce the electron configuration ES-1 of the product (having the configuration $\sigma_s^2\sigma_A^2\pi\pi^*$). An MO correlation diagram similar to Figure 11.68 for the reverse of the suprafacial–suprafacial cycloaddition would lead to the electron configuration $\psi_1^2\pi\psi_2^2\pi^*$, which is a higher energy excited state (ES-2) of the 1,3-butadiene–ethene system. Thus, ES-2 on the left is connected by a dashed line to ES-1 on the right in Figure 11.67. Because both ES-1 and ES-2 are antisymmetric (A) states, they do not actually cross in Figure 11.67. As the reactants begin to interact along the reaction coordinate and the energies of ES-1 and ES-2 become more similar, the states interact as described by PMO theory (Chapter 4). This leads to an avoided crossing that results in ES-1 of the reactants connecting with ES-1 of the product with an energy profile described by the solid line. The electronic energy of the system must increase considerably before the maximum occurs on the avoided crossing line, so there should be a large electronic barrier for the reaction. As a result, we say that the photochemical Diels–Alder reaction is symmetry-forbidden.

Selection Rules for Cycloaddition Reactions

From a more detailed analysis of MO and state correlation diagrams, Woodward and Hoffmann presented a set of selection rules for cycloaddition reactions, which are summarized in Table 11.1.¹⁰¹ Here p and q are the number of electrons in the two π systems undergoing the cycloaddition reaction. When the sum of p and q is a member of the $4n$ series, then the reaction is thermally allowed to be suprafacial with respect to one of the π components and antarafacial with respect to the other one. When the sum of p and q is a member of the $4n + 2$ series, then the reaction is thermally allowed when it is either suprafacial with respect to both components or antarafacial with respect to both. As usual, the selection rules are reversed for photochemical reactions.

The Diels–Alder reaction may be the best known cycloaddition, but other types of cycloaddition reactions are also synthetically important.¹⁰² Consistent with the predictions of the selection rules, the $[\pi 6_s + \pi 4_s]$ cycloaddition was seen in the reaction of cyclopentadiene with tropone (**61**):¹⁰³



¹⁰¹ Table 11.1 is adapted from Hoffmann, R.; Woodward, R. B. *J. Am. Chem. Soc.* **1965**, *87*, 2046.

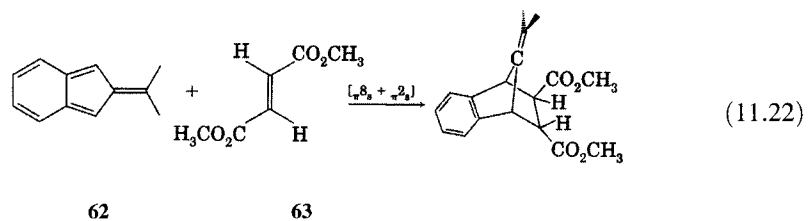
¹⁰² Cycloaddition reactions involving more than a total of six electrons in the two π systems are known as *higher order* cycloadditions. Transition metals have been found to be effective in promoting such reactions. Rigby, J. H. *Acc. Chem. Res.* **1993**, *26*, 579.

¹⁰³ Cookson, R. C.; Drake, B. V.; Hudec, J.; Morrison, A. *Chem. Commun.* **1966**, 15.

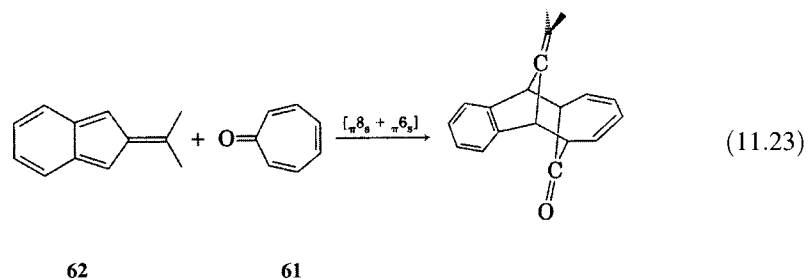
TABLE 11.1 Selection Rules for Cycloaddition Reactions

$p + q$	Thermally Allowed	Photochemically Allowed
$4n$	$p_s + q_a$ OR $p_a + q_s$	$p_s + q_s$ OR $p_a + q_a$
$4n + 2$	$p_s + q_s$ OR $p_a + q_a$	$p_s + q_a$ OR $p_a + q_s$

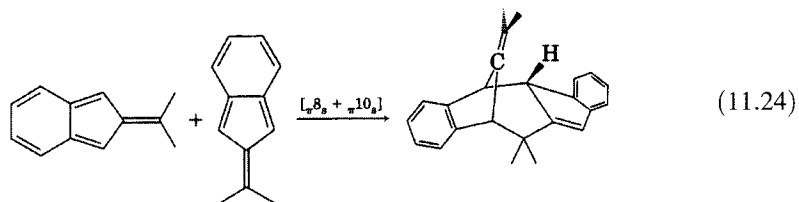
The $[\pi 8_s + \pi 2_s]$ cycloaddition was observed in the addition of 8,8-dimethylisobenzofulvene (**62**) to dimethyl fumarate (**63**).^{104,105}



The $[\pi 8_s + \pi 6_s]$ cycloaddition was seen in the addition of 8,8-dimethylisobenzofulvene to tropone:¹⁰⁶



The dimerization of 8,8-dimethylisobenzofulvene is an example of an $[\pi 8_s + \pi 10_s]$ cycloaddition:¹⁰⁷



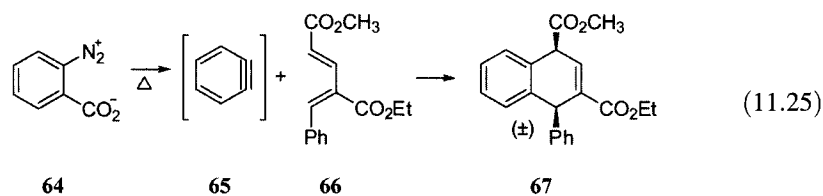
¹⁰⁴ Tanida, H.; Irie, T.; Tori, K. *Bull. Chem. Soc. Jpn.* **1972**, *45*, 1999.

¹⁰⁵ Also see Russell, R. A.; Longmore, R. W.; Warrenner, R. N. *J. Chem. Educ.* **1992**, *69*, 164.

¹⁰⁶ Paddon-Row, M. N.; Warrenner, R. N. *Tetrahedron Lett.* **1974**, 3797.

¹⁰⁷ Warrenner, R. N.; Paddon-Row, M. N.; Russell, R. A.; Watson, P. L. *Aust. J. Chem.* **1981**, *34*, 397.

Arynes may also participate in cycloaddition reactions.¹⁰⁸ As shown in equation 11.25, thermal decomposition of benzenediazonium-2-carboxylate (**64**) leads to benzyne (**65**), which undergoes the Diels-Alder reaction with the diene **66** to produce **67**.¹⁰⁹



All of the reactions shown here have been examples of suprafacial-suprafacial cycloadditions. As with sigmatropic reactions, it is reasonable to ask whether cycloaddition reactions requiring antarafacial addition to π systems are sterically feasible. Clearly, the $[p_a + q_a]$ process is possible for some values of p and q —one simply requires that the two π components be oriented at 90° with respect to each other so that a C_2 rotation axis is maintained from reactant through transition structure to product. The $[p_s + q_a]$ process is more difficult to envision, but a simple example illustrates the idea. Consider Figure 11.69(a) and Figure 11.69(b), which represent the side view and top view, respectively, of a system of two ethene units. If bonding changes occur as suggested by the double-headed curved arrows connecting lobes of the p orbitals, the cycloaddition will be suprafacial with respect to the lower component and antarafacial with respect to the top component. Twisting about the carbon-carbon bond in the upper ethene must accompany the bonding change, so substituents on the upper component that are initially *cis* to each other would become *trans* to each other in the cyclobutane product. This resulting stereochemistry is illustrated in Figure 11.70 for the hypothetical $[\pi 2_s + \pi 2_a]$ cycloaddition of two *cis*-2-butene molecules.

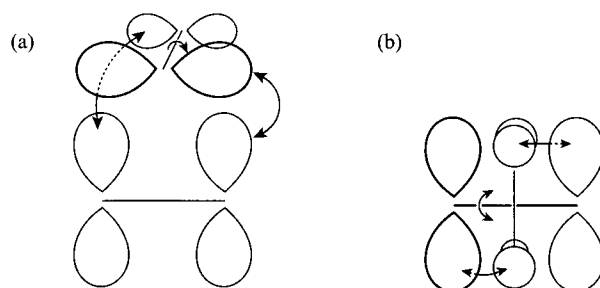


FIGURE 11.69

(a) Side and (b) top views of $[\pi 2_s + \pi 2_a]$ cycloaddition. (Adapted from reference 14.)

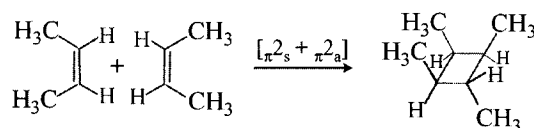


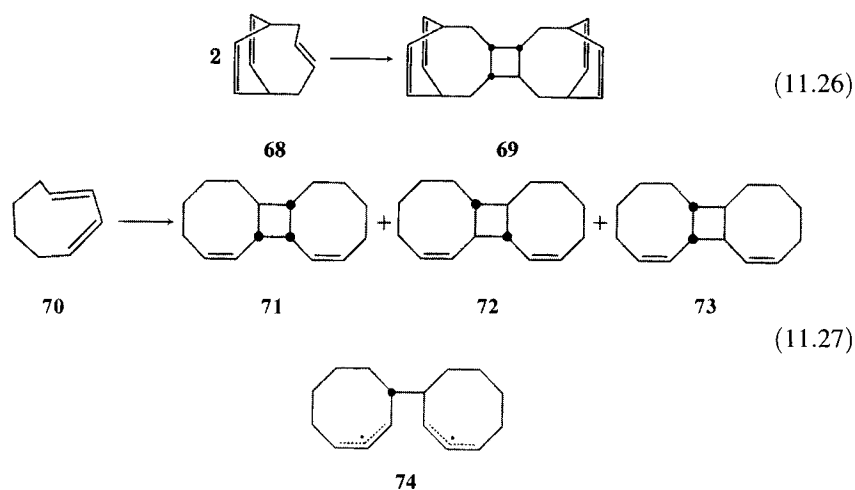
FIGURE 11.70

Hypothetical $[\pi 2_s + \pi 2_a]$ cycloaddition of *cis*-2-butene.

¹⁰⁸ Wittig, G.; Dürr, H. *Liebigs Ann. Chem.* **1964**, 672, 55.

¹⁰⁹ Dockendorff, C.; Sahli, S.; Olsen, M.; Milhau, L.; Lautens, M. *J. Am. Chem. Soc.* **2005**, 127, 15028.

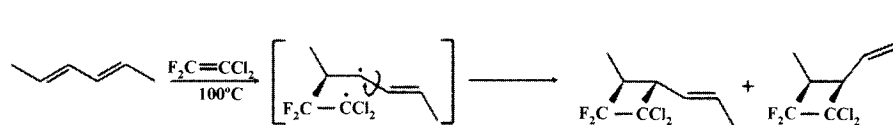
The dimerization of unstrained alkenes is not known to occur by the pathway shown in Figure 11.70, but there was a report that the dimerization of bicyclo[4.2.2]deca-*trans*-3,*cis*-7,9-triene (**68**, equation 11.26) gave as the major product **69**, in which the stereochemistry of the product is consistent with that predicted in Figure 11.70.¹¹⁰ (Two other, unidentified adducts were also formed in the reaction.) Padwa and co-workers found, however, that the thermal dimerization of *cis,trans*-1,3-cyclooctadiene (**70**) produced three dimers plus other products (equation 11.27).¹¹¹ The major dimer, **71**, was the product predicted by the $[\pi^2_s + \pi^2_a]$ pathway, but dimers **72** and **73** were also found. The results suggested that the formation of all of the dimers could be explained on the basis of closure of a biradical intermediate, **74**. Therefore, it appears that a concerted pathway is not required to explain formation of **69**, and there are no clear examples of concerted $[\pi^2_s + \pi^2_a]$ dimerization.^{111,112}



¹¹⁰ Kraft, K.; Koltzenburg, G. *Tetrahedron Lett.* **1967**, 4357.

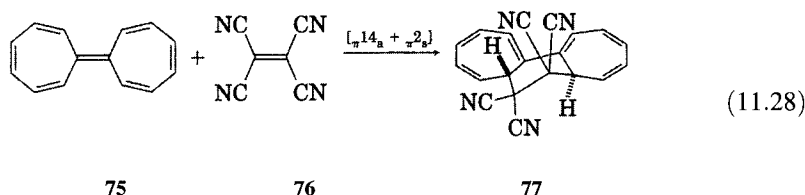
¹¹¹ Padwa, A.; Koehn, W.; Masaracchia, J.; Osborn, C. L.; Trecker, D. J. *J. Am. Chem. Soc.* **1971**, *93*, 3633.

¹¹² The formation of cyclobutanes from alkenes by radical pathways was established by the work of Bartlett and co-workers. For example, 1,1-dichloro-2,2-difluoroethene undergoes nonstereospecific cycloaddition with *trans,trans*-2,4-hexadiene at 100°C to give an 82:18 mixture of diastereomeric cyclobutanes:



Bartlett, P. D.; Montgomery, L. K.; Seidel, B. J. *Am. Chem. Soc.* **1964**, *86*, 616; Montgomery, L. K.; Schueller, K.; Bartlett, P. D. *J. Am. Chem. Soc.* **1964**, *86*, 622; Bartlett, P. D.; Montgomery, L. K. *J. Am. Chem. Soc.* **1964**, *86*, 628. Evidence for a very small amount (0.02%) of radical addition of 1,3-butadiene to ethene to form vinylcyclobutane at 175°C and 6000 psi was reported by Bartlett, P. D.; Schueller, K. E. *J. Am. Chem. Soc.* **1968**, *90*, 6071. For a review of the formation of cyclobutanes from thermal cycloaddition reactions, see Roberts, J. D.; Sharts, C. M. *Org. React.* **1962**, *12*, 1. Pedersen, S.; Herek, J. L.; Zewail, A. H. *Science* **1994**, *266*, 1359 used femtosecond spectroscopy to measure the lifetime (700 fs) of the tetramethylene diradical formed by photochemical decarbonylation of cyclopentanone. For a discussion of this work, see Berson, J. A. *Science* **1994**, *266*, 1338.

Antarafacial concerted cycloaddition may be more likely if one of the reactants has a nonplanar π system. Woodward and Hoffmann suggested that the addition of heptafulvalene (**75**) to tetracyanoethylene (**76**), reported by Doering and co-workers, could occur by a $[\pi 14_a + \pi 2_s]$ pathway. The structure of the adduct **77**, whose stereochemistry was established by X-ray crystallography, confirms the antarafacial addition to the π system of heptafulvalene.¹¹³



It is important to note that the selection rule in Table 11.1 refers to the number of *electrons* in the systems undergoing pericyclic change, not for the number of orbitals. Thus, the addition of an allyl anion to an alkene, the addition of an allyl anion to an allyl cation, and the addition of a pentadienyl cation to an alkene are all $[4 + 2]$ cycloadditions (Figure 11.71).^{14,114}

We may further extend the analysis of pericyclic reactions by considering that a single p orbital, denoted by the symbol ω , can be a participant in a pericyclic reaction. In this analysis, one lobe of the p orbital makes up the top face of a one-atom π system, while the other lobe makes up the bottom face. The participation of a single p orbital is suprafacial if both cycloaddition processes involve only one of the two lobes of the p orbital, and it is antarafacial if the cycloaddition involves both. We may thus predict that the conrotatory opening of the cyclopropyl anion to an allyl anion (Figure 11.72) should take place via an $[\omega 2_a + \sigma 2_s]$ pathway. Conversely, the opening of the cation would be a $[\omega 0_s + \sigma 2_s]$ process, giving the opposite stereochemistry in the product.¹¹⁵

An important type of cycloaddition reaction involving atoms with formal charges is known as a 1,3-dipolar cycloaddition. As illustrated by the schematic reaction in equation 11.29, a 1,3-dipole is a resonance-stabilized zwitterion that can add in a concerted fashion to an olefinic dipolarophile.

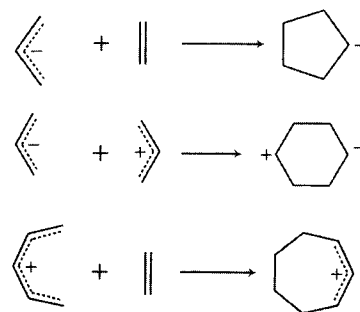


FIGURE 11.71

$[4 + 2]$ Cycloadditions. (Adapted from reference 14.)

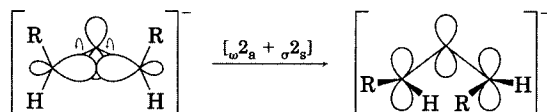


FIGURE 11.72

Pericyclic analysis of the opening of cyclopropyl anion to allyl anion.

¹¹³ Doering, W. v. E. personal communication to Woodward, R. B.; Hoffmann, R. in reference 14, p. 85.

¹¹⁴ For a discussion of cycloaddition reactions involving anions, see Staley, S. W. in Marchand, A. P.; Lehr, R. E., Eds. *Pericyclic Reactions*, Vol. I; Academic Press: New York, 1977; pp. 199–264; for a discussion of cycloaddition reactions of cations, see Sorensen, T. S.; Rauk, A. in Marchand, A. P.; Lehr, R. E., Eds. *Pericyclic Reactions*, Vol. II; Academic Press: New York, 1977; pp. 1–78.

¹¹⁵ Cycloadditions to σ bonds are described in more detail on page 753.

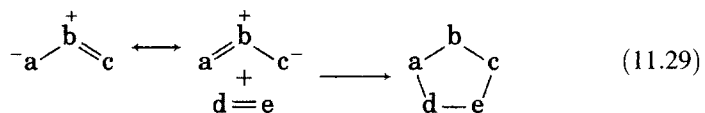
TABLE 11.2 Some 1,3-Dipoles for 1,3-Dipolar Cycloaddition Reactions^a

Diazoalkanes	$\text{N} \equiv \overset{+}{\text{N}} - \overset{-}{\text{C}}$	\longleftrightarrow	$\overset{-}{\text{N}} = \overset{+}{\text{N}} = \overset{-}{\text{C}}$
Azides	$\text{N} \equiv \overset{+}{\text{N}} - \overset{-}{\text{N}}$	\longleftrightarrow	$\overset{-}{\text{N}} = \overset{+}{\text{N}} = \overset{-}{\text{N}}$
Nitrones	$\text{C} = \overset{+}{\text{N}} - \overset{-}{\text{O}}$	\longleftrightarrow	$\overset{-}{\text{C}} - \overset{+}{\text{N}} = \overset{-}{\text{O}}$
Azoxy compounds	$\text{N} = \overset{+}{\text{N}} - \overset{-}{\text{O}}$	\longleftrightarrow	$\overset{-}{\text{N}} - \overset{+}{\text{N}} = \overset{-}{\text{O}}$
Nitro compounds	$\text{O} = \overset{+}{\text{N}} - \overset{-}{\text{O}}$	\longleftrightarrow	$\overset{-}{\text{O}} - \overset{+}{\text{N}} = \overset{-}{\text{O}}$
Carbonyl ylides	$\text{C} = \overset{+}{\text{O}} - \overset{-}{\text{C}}$	\longleftrightarrow	$\overset{-}{\text{C}} - \overset{+}{\text{O}} = \overset{-}{\text{C}}$
Carbonyl oxides	$\text{C} = \overset{+}{\text{O}} - \overset{-}{\text{O}}$	\longleftrightarrow	$\overset{-}{\text{C}} - \overset{+}{\text{O}} = \overset{-}{\text{O}}$
Nitrosimines	$\text{N} = \overset{+}{\text{O}} - \overset{-}{\text{N}}$	\longleftrightarrow	$\overset{-}{\text{N}} - \overset{+}{\text{O}} = \overset{-}{\text{N}}$
Nitrous oxide	$\overset{+}{\text{N}} \equiv \text{N} - \overset{-}{\text{O}}$	\longleftrightarrow	$\overset{-}{\text{N}} = \overset{+}{\text{N}} = \overset{-}{\text{O}}$
Ozone	$\text{O} = \overset{+}{\text{O}} - \overset{-}{\text{O}}$	\longleftrightarrow	$\overset{-}{\text{O}} - \overset{+}{\text{O}} = \overset{-}{\text{O}}$

^a Lines from atoms indicate unspecified substituents.

Source: Adapted from reference 118.

Examples of 1,3-dipoles include ozone, nitrones, and carbonyl oxides.^{95d,116,117} Table 11.2 lists some of the 1,3-dipoles that can undergo 1,3-dipolar cycloaddition.¹¹⁸



The schematic reaction in equation 11.29 is often termed a (3 + 2) cycloaddition. It is important to note that this terminology designates the number of *atoms* in each of the reactants that undergo concerted bonding changes. All of these reactions are categorized as [4 + 2] cycloadditions in the Woodward–Hoffmann formalism because the 1,3-dipole provides four π electrons and the olefin provides two π electrons. Thus, terms in *brackets* typically indicate the number of *electrons* in the cyclization, while terms in *parentheses* indicate the number of *atoms*.¹⁹ This convention is not always

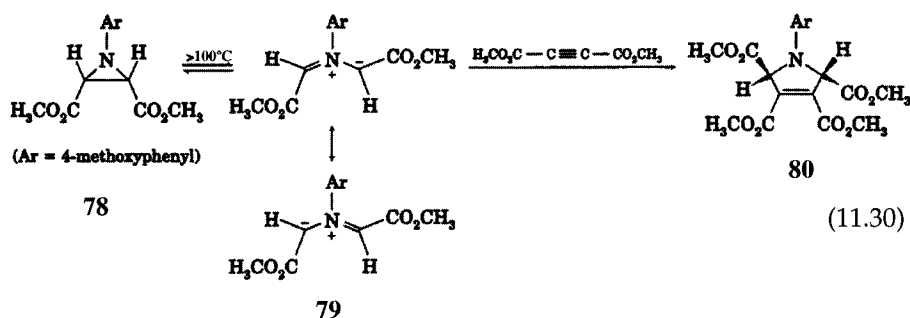
¹¹⁶ See also Padwa, A., Ed. *1,3-Dipolar Cycloaddition Chemistry*, Vols. 1 and 2; Wiley-Interscience: New York, 1984.

¹¹⁷ For a discussion of 1,3-dipolar cycloadditions to alkynes, see Rutledge, T. F. *Acetylenes and Allenes. Addition, Cyclization, and Polymerization Reactions*; Reinhold Book Corporation: New York, 1969; pp. 253–260.

¹¹⁸ Huisgen, R. *J. Org. Chem.* **1976**, *41*, 403.

observed, however, and references to [3 + 2] dipolar cycloadditions also appear in the literature.

As with the Diels–Alder reaction, the $[\pi 4 + \pi 2]$ 1,3-dipolar cycloaddition is allowed to be suprafacial with respect to both components. This pathway has been observed in the reaction shown in equation 11.30. Electrocyclic opening of dimethyl 1-(4-methoxyphenyl)aziridine-2,3-dicarboxylate (**78**) produces the azomethine ylide **79**. Dimethyl acetylenedicarboxylate traps **79** by undergoing a concerted suprafacial–suprafacial 1,3-dipolar cycloaddition to form the *trans*-tetramethyl 1-(4-methoxyphenyl)-3-pyrroline-2,3,4,5-tetracarboxylate (**80**). The stereospecificity of the reaction was confirmed by the observation that the *trans* isomer of **78** produces the *cis* isomer of **80** under the same conditions.¹¹⁹



The Criegee mechanism for the ozonolysis of alkenes (Figure 11.73) can be analyzed in terms of a series of three 1,3-dipolar cycloadditions.¹²⁰ The addition of ozone to an alkene leads first to a 1,2,3-trioxacyclopentane structure known variously as an *initial ozonide*, *primary ozonide*, or *molozone*,

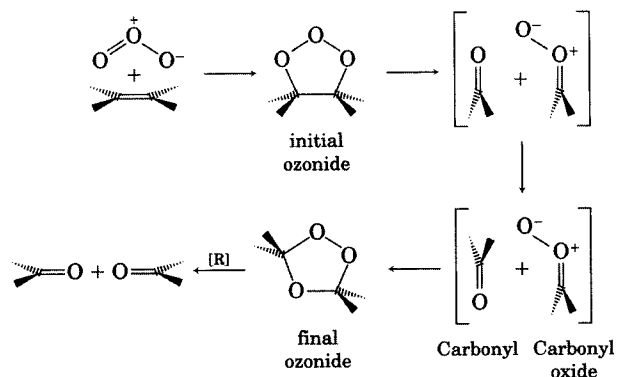
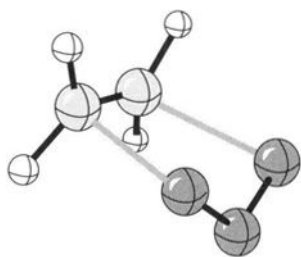


FIGURE 11.73
Criegee mechanism for ozonolysis of alkenes.

¹¹⁹ Huisgen, R.; Scheer, W.; Huber, H. *J. Am. Chem. Soc.* **1967**, *89*, 1753.

¹²⁰ Criegee, R. *Rec. Chem. Prog.* **1957**, *18*, 111.

¹²¹ Wheeler, S. E.; Ess, D. H.; Houk, K. N. *J. Phys. Chem. A* **2008**, *112*, 1798.

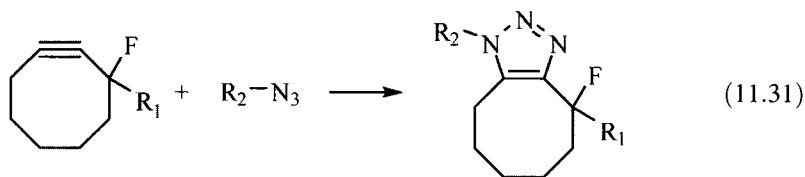
**FIGURE 11.74**

Ab initio for the concerted transition structure for the 1,3-dipolar addition of ozone to ethene. (Adapted from reference 121.)

through a $[\pi 4_s + \pi 2_s]$ cycloaddition. Figure 11.74 shows a calculated transition structure for the addition of ozone to ethene.¹²¹ Figure 11.75 shows a molecular orbital correlation diagram for the reaction in which the MOs are characterized with respect to a plane of symmetry passing through the center oxygen of ozone and through the midpoint of the carbon–carbon double bond.^{122–124}

The conversion of the initial ozonide to a carbonyl compound and a carbonyl oxide can be considered a retro-1,3-cycloaddition, and the combination of the carbonyl oxide and the carbonyl compound is another 1,3-cycloaddition (Figure 11.76). Nonconcerted mechanisms are possible for each of the three steps in the Criegee ozonolysis mechanism, but Kuczkowski has summarized evidence suggesting that the reactions are concerted.¹²⁵

1,3-Dipolar cycloadditions have been widely used in “click chemistry,” an approach to synthesis introduced by Sharpless in which small units are joined under simple reaction conditions to create larger substances in high yield and with minimal by-products.¹²⁶ For example, Bertozzi and co-workers reported that cyclooctynes add to organic azides rapidly under physiological conditions (aqueous solution and body temperature), as shown in equation 11.31.¹²⁷ With appropriate choice of substituents on the cyclooctyne and the azide, the products can be useful for labeling proteins, either in isolated form or in living cells.¹²⁸ Cyclooctyne is chosen for these reactions because the cycloaddition releases strain in the eight-membered ring. The barrier for reaction of acetylene with phenyl azide is 16.2 kcal/mol, but that for the reaction of cyclooctyne with the same azide is 8 kcal/mol.¹²⁹



¹²² Eckell, A.; Huisgen, R.; Sustmann, R.; Wallbillich, G.; Grashey, D.; Spindler, E. *Chem. Ber.* **1967**, *100*, 2192.

¹²³ Lattimer, R. P.; Kuczkowski, R. L.; Gillies, C. W. *J. Am. Chem. Soc.* **1974**, *96*, 348. This paper also discusses some alternate mechanisms proposed for the ozonolysis of alkenes.

¹²⁴ The cycloaddition can also be analyzed in terms of HOMO–LUMO interactions (see page 756), with the interaction of the LUMO of ozone and the HOMO of the alkene being dominant. For a discussion, see Kuczkowski, R. L. in Padwa, A., Ed. *1,3-Dipolar Cycloaddition Chemistry*, Vol. 2; Wiley-Interscience: New York, 1984; pp. 197–276.

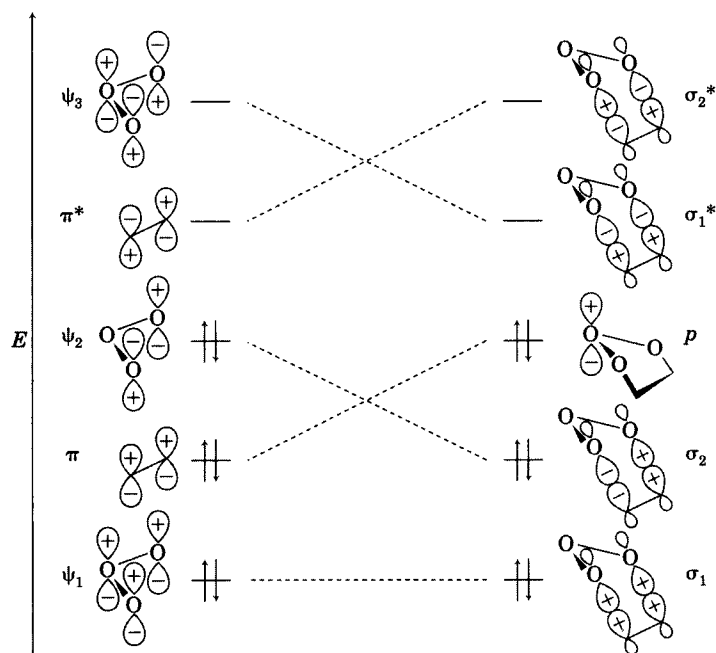
¹²⁵ Kuczkowski, R. L. *Chem. Soc. Rev.* **1992**, *21*, 79 and references therein.

¹²⁶ Kolb, H. C.; Finn, M. G.; Sharpless, K. B. *Angew. Chem. Int. Ed.* **2001**, *40*, 2004.

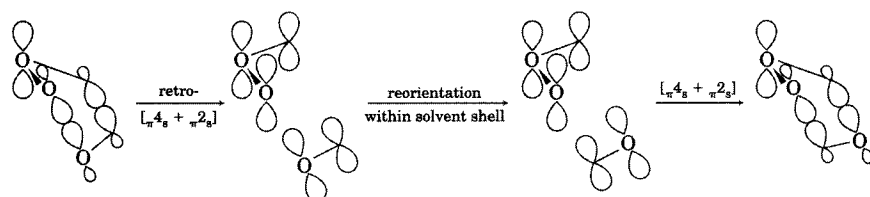
¹²⁷ Agard, N. J.; Prescher, J. A.; Bertozzi, C. R. *J. Am. Chem. Soc.* **2004**, *126*, 15046.

¹²⁸ Agard, N. J.; Baskin, J. M.; Prescher, J. A.; Lo, A.; Bertozzi, C. R. *ACS Chem. Biol.* **2006**, *1*, 644; Codelli, J. A.; Baskin, J. M.; Agard, N. J.; Bertozzi, C. R. *J. Am. Chem. Soc.* **2008**, *130*, 11486. See also Lutz, J.-F. *Angew. Chem. Int. Ed.* **2008**, *47*, 2182; Ning, X.; Guo, J.; Wolfert, M. A.; Boons, G.-J. *Angew. Chem. Int. Ed.* **2008**, *47*, 2253.

¹²⁹ Ess, D. H.; Jones, G. O.; Houk, K. N. *Org. Lett.* **2008**, *10*, 1633.

**FIGURE 11.75**

Molecular orbital correlation diagram for $[\pi 4_s + \pi 2_s]$ cycloaddition of ozone and ethene. (Adapted from reference 122.)

**FIGURE 11.76**

Retro- $[\pi 4_s + \pi 2_s]$ and $[\pi 4_s + \pi 2_s]$ reactions in the conversion of the initial ozonide to final ozonide.

11.5 OTHER CONCERTED REACTIONS

Cheletropic Reactions

The term *cheletropic* is derived from the Greek *chēlē* ("claw") and *tropos* ("turning").⁴³ Woodward and Hoffmann defined **cheletropic reactions** as those processes in which two σ bonds terminating at a single atom are made, or broken, in concert.¹⁴ Cheletropic reactions are also called *extrusion processes*, since a fragment appears to be squeezed out from a molecular system. Figure 11.77 illustrates a cheletropic reaction in which fragment Y–X–Z is extruded from a structure having m additional atoms in a ring. The reaction involves breaking two bonds, one from C1 to X and one from C m to X. Unless a redox process occurs simultaneously with the reaction, two of the electrons in these two bonds remain with the C1–C m π system and the other two depart with the group X. The extrusion leaves the fragment C1–C m as a conjugated π system with m p orbitals. Woodward and Hoffmann defined two types of pathways for such reactions—linear and nonlinear, depending on whether one of the fragments rotates during the

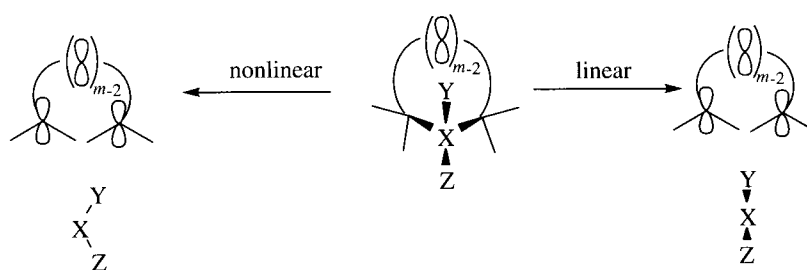


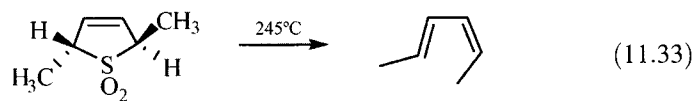
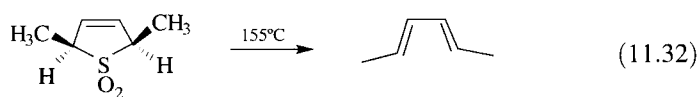
FIGURE 11.77
Nonlinear (left) and linear (right)
cheletropic reaction.

TABLE 11.3 Selection Rules for Cheletropic Reactions

m	Allowed Thermal Reactions		Allowed Photochemical Reactions	
	Linear	Nonlinear	Linear	Nonlinear
$4n$	Disrotatory	Conrotatory	Conrotatory	Disrotatory
$4n + 2$	Conrotatory	Disrotatory	Disrotatory	Conrotatory

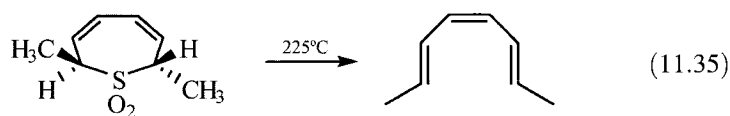
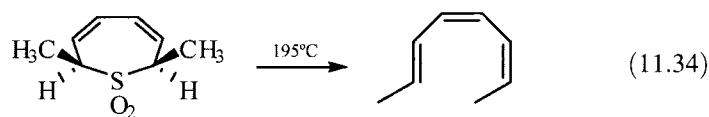
reaction.¹³⁰ In Figure 11.77 the fragment Y–X–Z rotates in the nonlinear extrusion shown on the left.

Equations 11.32 through 11.35 illustrate cheletropic reactions involving the extrusion of SO₂.¹³¹ Equations 11.32 and 11.33 show that the thermal extrusion is disrotatory with respect to the C_m fragment when $m = 4$,^{131b} while equations 11.34 and 11.35 show that the stereochemical preference is reversed when another double bond is added to the reacting system ($m = 6$).^{131c} Selection rules for cheletropic reactions are given in Table 11.3, and a more detailed discussion can be found in reference 18. The stereochemistry of the reactions in equations 11.32 through 11.35 is consistent with the linear extrusion of SO₂. It is important to note that the m in Table 11.3 refers to the number of electrons (which is also the number of p orbitals) in the conjugated fragment produced by the extrusion reaction.



¹³⁰ For a discussion, see reference 14, p. 152 ff. See also Sankararaman, S. *Pericyclic Reactions—A Textbook*; Wiley-VCH: Weinheim, 2005; pp. 308–360.

¹³¹ (a) Mock, W. L. in Marchand, A. P.; Lehr, R. E., Eds. *Pericyclic Reactions*, Vol. II; Academic Press: New York, 1977; pp. 141–179 and references therein; (b) McGregor, S. D.; Lemal, D. M. *J. Am. Chem. Soc.* **1966**, *88*, 2858; (c) Mock, W. L. *J. Am. Chem. Soc.* **1969**, *91*, 5682.



Atom Transfer Reactions

A class of reactions known as atom transfer reactions is illustrated by the transfer of two hydrogen atoms from *cis*-9,10-dihydronaphthalene (**81**) to 1,2-dimethylcyclohexene (**82**), producing naphthalene (**83**) and *cis*-1,2-dimethylcyclohexane (**84**, Figure 11.78).^{132,133}

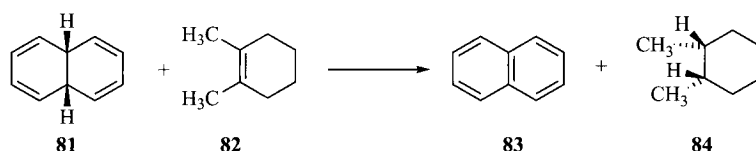
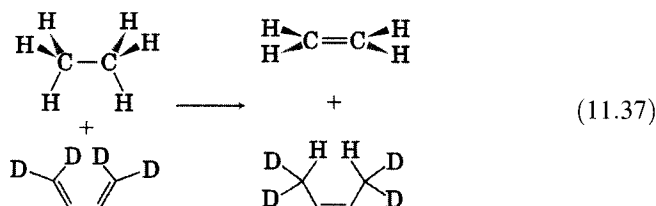
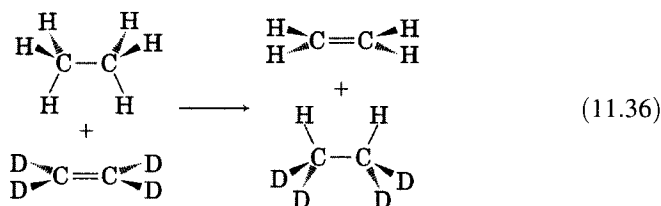


FIGURE 11.78

A synchronous suprafacial-suprafacial H₂ transfer reaction.

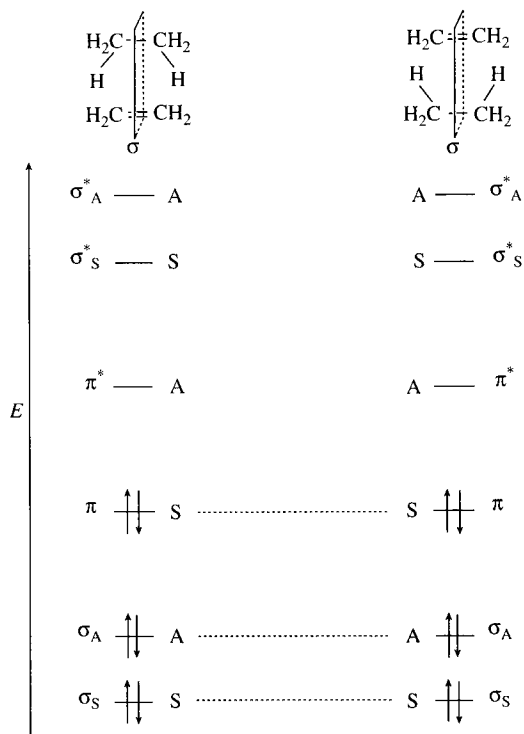
Equations 11.36 and 11.37 show two model reactions, the transfer of a pair of hydrogen (¹H) atoms from ethane to perdeuterioethene and the transfer of a pair of hydrogen atoms from ethane to 1,1,4,4-tetradeuterio-1,3-butadiene.²⁰⁸



An MO correlation diagram for the reaction in equation 11.36 is shown in Figure 11.79. As in the case of the Diels–Alder reaction (Figure 11.66), it is necessary to take combinations of the localized σ bond MOs to produce a set of MOs for the ethene component that are either symmetric or antisym-

¹³² Doering, W. v. E.; Rosenthal, J. W. *J. Am. Chem. Soc.* **1967**, *89*, 4534.

¹³³ For leading references and a theoretical study, see Frontera, A.; Suñer, G. A.; Deyà, P. M. *J. Org. Chem.* **1992**, *57*, 6731. The analogous intramolecular rearrangement is known as a **dyotropic reaction**.

**FIGURE 11.79**

Orbital correlation diagram for ethane + ethene atom transfer reaction. (Adapted from reference 14.)

metric with regard to the plane of symmetry through the basis set of orbitals. Therefore, σ_S represents a symmetric combination of two σ_{C-H} localized orbitals, while σ_A is the antisymmetric bonding combination. Since the entire set of bonding orbitals of the reactant correlates with the entire set of bonding orbitals of the product, the thermal atom transfer reaction is allowed by the principles of orbital symmetry. In the case of hydrogen atom transfer from ethane to 1,3-butadiene, however, the MO correlation diagram in Figure 11.80 indicates that the ground state of the reactants correlates with a highly excited state of the products, so the thermal reaction should be forbidden.

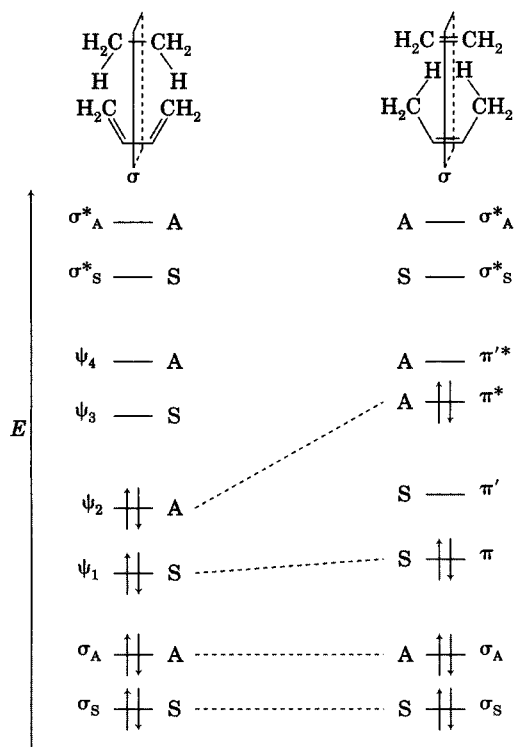
Figure 11.81 represents the general reaction for a synchronous transfer of two groups, one from each end of a system with p π centers to a group with q π centers in a suprafacial process. The selection rules for such reactions are as follows:¹³⁴

- For suprafacial–suprafacial (or antarafacial–antarafacial) double group transfers, the transfer is thermally allowed when $p + q = 4n + 2$ and photochemically allowed when $p + q = 4n$.
- For suprafacial–antarafacial double group transfers, the selection rules are reversed.

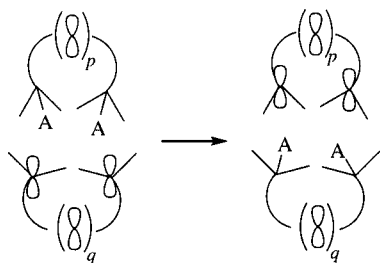
Ene Reactions

The **ene reaction** involves the addition of a compound having a double bond with an allylic hydrogen to a compound with a multiple bond in such

¹³⁴ Adapted from reference 14.

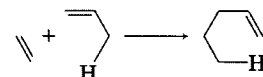
**FIGURE 11.80**

Orbital correlation diagram for ethane + 1,3-butadiene atom transfer reaction. (Adapted from reference 14.)

**FIGURE 11.81**

General synchronous double atom transfer. (Adapted from reference 14.)

a way that the allylic hydrogen is transferred from one atom to another, as shown by the general reaction in Figure 11.82.¹³⁵⁻¹³⁷ A calculated transition structure for the ene reaction of ethene and propene is shown in Figure 11.83.¹³⁸

**FIGURE 11.82**

General ene reaction.

¹³⁵ Alder, K.; Pascher, F.; Schmitz, A. *Chem. Ber.* **1943**, 76B, 27.

¹³⁶ The possibility that this reaction might proceed through a concerted mechanism or a stepwise mechanism has been considered: Berson, J. A.; Wall, R. G.; Perlmutter, H. D. *J. Am. Chem. Soc.* **1966**, 88, 187; Keung, E. C.; Alper, H. *J. Chem. Educ.* **1972**, 49, 97; Nahm, S. H.; Cheng, H. N. *J. Org. Chem.* **1986**, 51, 5093.

¹³⁷ For applications of the ene reaction in organic synthesis, see Hoffmann, H. M. R. *Angew. Chem. Int. Ed. Engl.* **1969**, 8, 556; Oppolzer, W.; Snieckus, V. *Angew. Chem.* **1978**, 90, 506. For a discussion of the ene reaction with organometallic reagents, see Dubac, J.; Laporterie, A. *Chem. Rev.* **1987**, 87, 319.

¹³⁸ Loncharich, R. J.; Houk, K. N. *J. Am. Chem. Soc.* **1987**, 109, 6947.

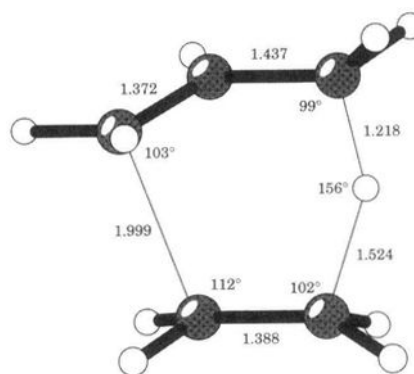
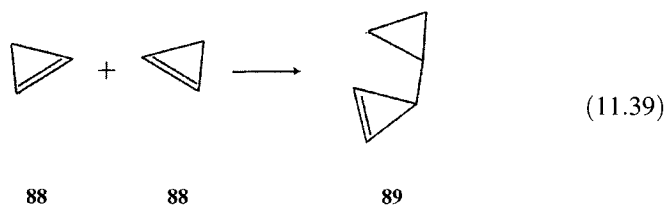
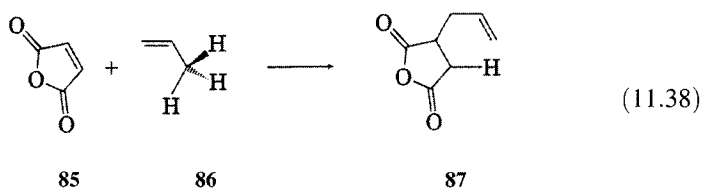


FIGURE 11.83

RHF/3-21G transition structure for the ene reaction of ethene and propene. (Distances are in angstroms, angles in degrees. Reproduced from reference 19.)

A specific example is the reaction between maleic anhydride (**85**) and propene (**86**) to give **87** (equation 11.38).¹³⁵ As in this case, the ene reaction typically involves an alkene substituted with electron-withdrawing groups.¹³⁹ Electron-withdrawing groups are not always required, however, as shown by the dimerization of cyclopropene (**88**) to give 3-cyclopropylcyclopropene (**89**, equation 11.39).¹⁴⁰



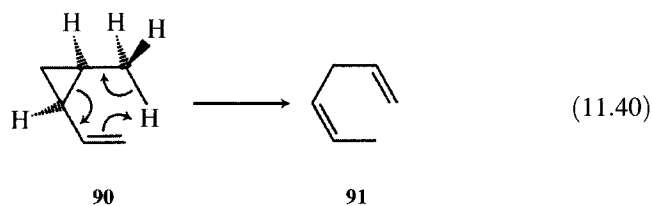
The reverse of the ene reaction is the **retroene reaction**. Equation 11.40 shows the conversion of *cis*-1-methyl-2-vinylcyclopropane (**90**) to *cis*-1,4-hexadiene (**91**) by such a process.^{141,142} This reaction can also be described as a homo-[1,5] sigmatropic shift.¹⁴

¹³⁹ The ene reaction is also promoted by Lewis acid complexation with the enophile. For a review of applications of the asymmetric ene reaction in organic synthesis, see Mikami, K.; Shimizu, M. *Chem. Rev.* **1992**, *92*, 1021.

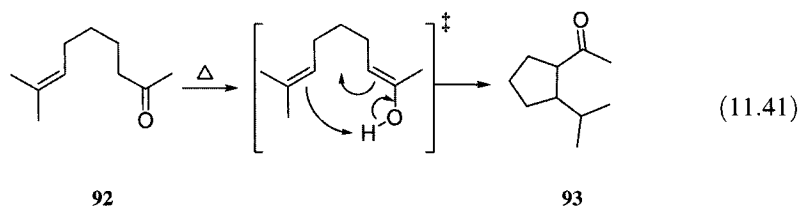
¹⁴⁰ Dowd, P.; Gold, A. *Tetrahedron Lett.* **1969**, 85. Also see Baird, M. S.; Hussain, H. H.; Clegg, W. J. *Chem. Res. (S)* **1988**, 110.

¹⁴¹ Roth, W. R.; König, J. *Liebigs Ann. Chem.* **1965**, 688, 28.

¹⁴² This reaction was characterized as one of the few thermal reactions that satisfy both kinetic and stereochemical criteria for concerted reactions: Berson, J. A. *Acc. Chem. Res.* **1972**, *5*, 406.



In the Conia-ene reaction, a carbonyl compound enolizes and then undergoes an intramolecular ene reaction.¹⁴³ The enol fragment serves as the ene component of the reaction, while the olefin fragment serves as the enophile.¹⁴⁴ An example is the reaction of 8-methyl-7-nonen-2-one (**92**), which yields 2-isopropylcyclopentyl methyl ketone (**93**, equation 11.41).¹⁴⁵



11.6 A GENERAL SELECTION RULE FOR PERICYCLIC REACTIONS

We have developed a different set of selection rules for electrocyclic, sigmatropic, cycloaddition, and other concerted reactions, but the fundamental principle—the conservation of orbital symmetry—is the same in all cases. Now we will see that all of these reactions can be considered to be variants of cycloaddition reactions. To do so, we must first note that a σ bond can participate in a cycloaddition process, just as can a π bond, with the following provisions:¹⁴

1. The participation of a σ bond is suprafacial if the cycloaddition occurs on the inside (overlapping) lobes of the two sp^3 hybrid orbitals or on their outside lobes.
2. The σ bond adds antarafacially if one cycloaddition occurs on an inside lobe and one occurs on an outside lobe.

To understand this definition, it is useful to depict cycloaddition reactions with dashed lines representing bonding interactions that will be present in the *product* of the reaction.¹⁴ The effect of the cycloaddition shown for the $[\sigma_2s + \pi_2a]$ process in Figure 11.84(a) is to pull up the inner lobe of the sp^3 hybrid orbital on C3 so that it overlaps with the upper lobe of the p orbital

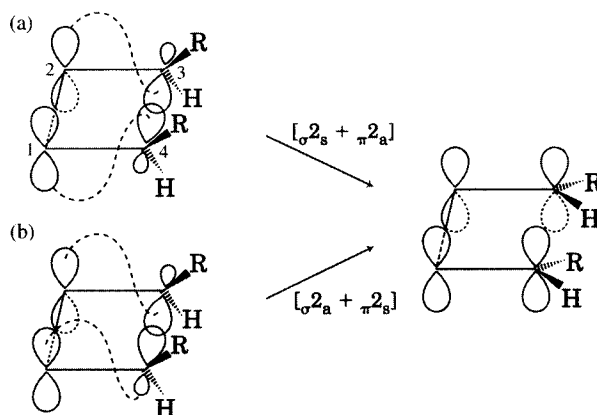
¹⁴³ Conia, J. M.; Le Perchec, P. *Synthesis* **1975**, 1.

¹⁴⁴ Moinet, G.; Brocard, J.; Conia, J. M. *Tetrahedron Lett.* **1972**, 4461.

¹⁴⁵ Fisk, J. S.; Tepe, J. J. *J. Am. Chem. Soc.* **2007**, *129*, 3058 and references therein.

FIGURE 11.84

(a) $[\sigma^2_s + \pi^2_a]$ and (b) $[\sigma^2_a + \pi^2_s]$ descriptions of cyclobutene ring opening.



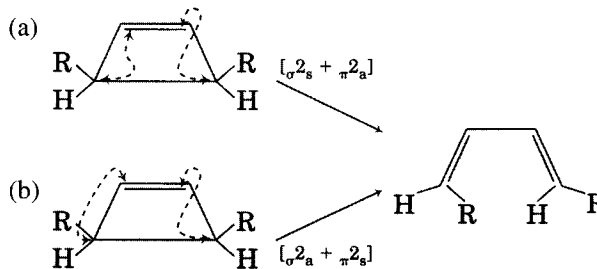
on C2 and to pull down the inner lobe of the sp^3 hybrid orbital on C4 so that it overlaps with the lower lobe of the p orbital on C1. This results in the conrotatory process that was predicted earlier for the same reaction. This reaction can also be described as a $[\sigma^2_a + \pi^2_s]$ cycloaddition, as shown in Figure 11.84(b). Both processes are thermally allowed cycloaddition reactions.

It is not necessary to draw the p and sp^3 orbital lobes to describe electrocyclic reactions as cycloadditions. Instead, we may use lines to represent bonds and then mentally picture the localized orbitals used to construct those bonds. In these cases, arrowheads on the ends of the dashed lines clarify the orbital interactions.¹⁴ Thus, Figure 11.85(a) is the equivalent of Figure 11.84(a), and Figure 11.85(b) is the equivalent of Figure 11.84(b). Similarly, a sigmatropic reaction can be described as a cycloaddition. For example, the antarafacial [1,3] hydrogen shift of propene in Figure 11.86 is seen to be equivalent to a $[\sigma^2_s + \pi^2_a]$ cycloaddition.

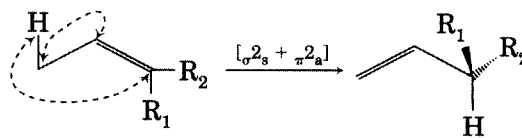
Figures 11.84 through 11.86 reemphasize the definition of pericyclic reactions (page 701), which refers to a cyclic array of continuously bonded atoms. The term *cyclic array* means that we may draw a closed curve through a reacting system of π systems (including isolated p orbitals) and σ bonds. Figure 11.87(a) is a modification of Figure 11.86 in which the closed curve is

FIGURE 11.85

Alternative representations for electrocyclic reactions considered as cycloadditions.

**FIGURE 11.86**

Antarafacial [1,3] hydrogen shift of propene classified as a $[\sigma^2_s + \pi^2_a]$ cycloaddition.



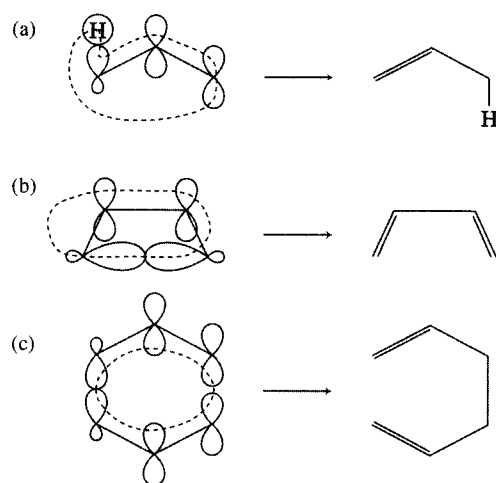
**FIGURE 11.87**

Illustration of closed curves in pericyclic reactions: (a) [1,3] hydrogen shift, (b) electrocyclic reaction, and (c) sigmatropic reaction.

indicated by a continuous dashed line. Figure 11.87(b) and Figure 11.87(c) illustrate the electrocyclic opening of cyclobutene and the sigmatropic Cope rearrangement in similar fashion.¹⁴⁶

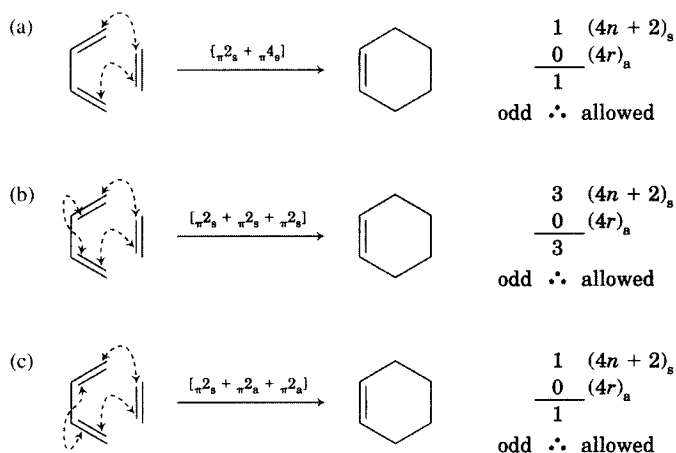
The selection rules for cycloadditions (Table 11.1) apply to pericyclic reactions described as cycloadditions, but the rules may be generalized in concise form as follows:¹⁴

A ground state pericyclic change is symmetry allowed when the total number of $(4n + 2)_s$ and $(4r)_a$ components is odd (where n and r are integers). Conversely, the photochemical reaction is forbidden. If the total number of $(4n + 2)_s$ and $(4r)_a$ components is even, then the thermal reaction is forbidden but the photochemical reaction is allowed.

Let us examine the application of this general selection rule to the various types of concerted reactions. The opening of cyclobutene to 1,3-butadiene by the conrotatory pathway (Figure 11.84) was defined to be a $[\pi 2_s + \sigma 2_a]$ cycloaddition. There is one $(4n + 2)_s$ component, because 2 is a member of the $4n + 2$ series. The number of $(4r)_a$ components is 0, because 2 is not a member of the $4n$ series. Then the total of $(4n + 2)_s + (4r)_a$ components is $1 + 0 = 1$, which is odd, so the reaction is allowed. Similarly, the hypothetical $[\pi 2_s + \pi 2_a]$ dimerization of ethene (Figure 11.57) is allowed because the number of $(4n + 2)_s$ components is 1 and the number of $(4r)_a$ components is 0, and the total is 1.

The application of the general selection rule does not require analyzing a concerted reaction in any particular way. All descriptions of a pericyclic reaction that predict the same stereochemistry in the product will lead to the same conclusion. For example, three descriptions of the Diels–Alder reaction are given in Figure 11.88. In Figure 11.88(a), the reaction is described as a $[\pi 2_s + \pi 4_s]$ cycloaddition. In this process there is one $(4n + 2)_s$ component and no $(4r)_a$ component, so the total (1) is an odd number, and the reaction is allowed. In Figure 11.88(b), each double bond of the diene is considered to be a separate unit, so the reaction is described as a $[\pi 2_s + \pi 2_s + \pi 2_s]$ process.

¹⁴⁶ Note that the path shown in Figure 11.87(b) passes through both lobes of one sp^3 orbital of the σ bond but through only one lobe of the other sp^3 orbital. As noted on page 753, this pathway is antarafacial with respect to the σ bond.

**FIGURE 11.88**

Alternative analyses of the Diels–Alder reaction as a pericyclic reaction.

That pathway has three $(4n + 2)_s$ components and no $(4r)_a$ component, so the total (3) is odd, and the reaction is allowed. Similarly, the $[\pi^2_s + \pi^2_a + \pi^2_a]$ cycloaddition in Figure 11.88(c) is also allowed.

11.7 ALTERNATIVE CONCEPTUAL MODELS FOR CONCERTED REACTIONS

In discussing concerted reactions, we first developed a set of selection rules for each type of reaction based on simple molecular orbital models. We then unified all of the reactions under one heading, pericyclic reactions, and wrote one selection rule that includes all of the cases we have studied. As a result, we have combined several simple models, each of which was intelligible by itself, into a general model that has lost much of its conceptual simplicity. It is easy to picture the rotation of orbitals of the HOMO of a system undergoing electrocyclic closure (Figure 11.20). It is more difficult to imagine the theoretical significance of the total number of $(4n + 2)_s$ and $(4r)_a$ components. The general selection rule can be shown to be correct, but it does not lend itself to an intuitive sense of the physical phenomena involved. However, additional insight into concerted reactions can be obtained from an examination of some complementary models that have been advanced to account for the same phenomena. Although all offer the same predictions, each model provides a different perspective for the basis of those predictions.

Frontier Molecular Orbital Theory

Fukui described pericyclic reactions in terms of frontier molecular orbital (FMO) theory.^{147,148} If the interaction of the HOMO of one reactant with the LUMO of the other reactant leads to bonding interactions, then the pericyclic

¹⁴⁷ Fukui, K. *Acc. Chem. Res.* **1971**, *4*, 57 and references therein.

¹⁴⁸ Salem, L. *J. Am. Chem. Soc.* **1968**, *90*, 543 and 553 presented a detailed PMO analysis of the interactions between two conjugated molecules that reaffirms the FMO predictions.

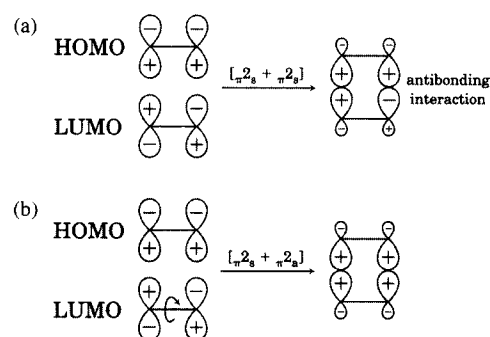


FIGURE 11.89

FMO analysis of the dimerization of two ethenes.

reaction is said to be allowed—meaning that there should be a low energy pathway for the reaction. Conversely, if the HOMO–LUMO interaction leads to an antibonding interaction between atoms that must be bonded in the product, then the reaction is forbidden.¹⁴⁹

Figure 11.89 shows an FMO analysis for two pathways for the dimerization of ethene. The HOMOs of the two molecules are degenerate, as are the LUMOs, so it does not matter which ethene's ψ_1 is used for HOMO and which ethene's ψ_2 is used as the LUMO. In Figure 11.89(a) the $[\pi^2_s + \pi^2_s]$ cycloaddition leads to an antibonding relationship between two atoms in the product. In Figure 11.89(b) the $[\pi^2_s + \pi^2_a]$ cycloaddition generates only bonding interactions in the product, so that process is allowed.

The FMO approach can be used to evaluate the two possible pathways for the opening of cyclobutene to 1,3-butadiene (Figure 11.90). Using the LUMO of the σ bond and the HOMO of the π bond, it is apparent that the conrotatory opening leads to a bonding interaction between C1 and C2 as well as to a bonding relationship between C3 and C4. The disrotatory opening leads to an antibonding relationship between two of the atoms, so the reaction is forbidden. Analysis of the reaction using the HOMO of the σ bond and the LUMO of the π bond leads to the same conclusion.¹⁵⁰

The FMO model provides insight into one aspect of electrocyclic reactions that we have not yet discussed. In the electrocyclic opening of cyclobutenes to butadienes, the tendency of a substituent at C3 of the cyclobutene to rotate inward to form a cis product (equation 11.42) or outward to form a trans product (equation 11.43) has been termed *torquoselectivity*.^{151,152} Steric effects

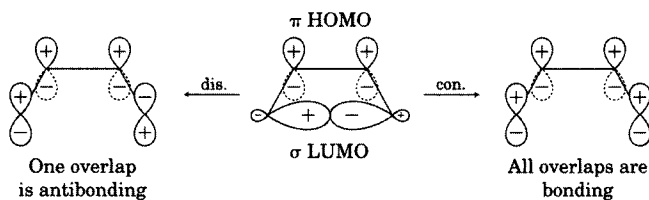


FIGURE 11.90

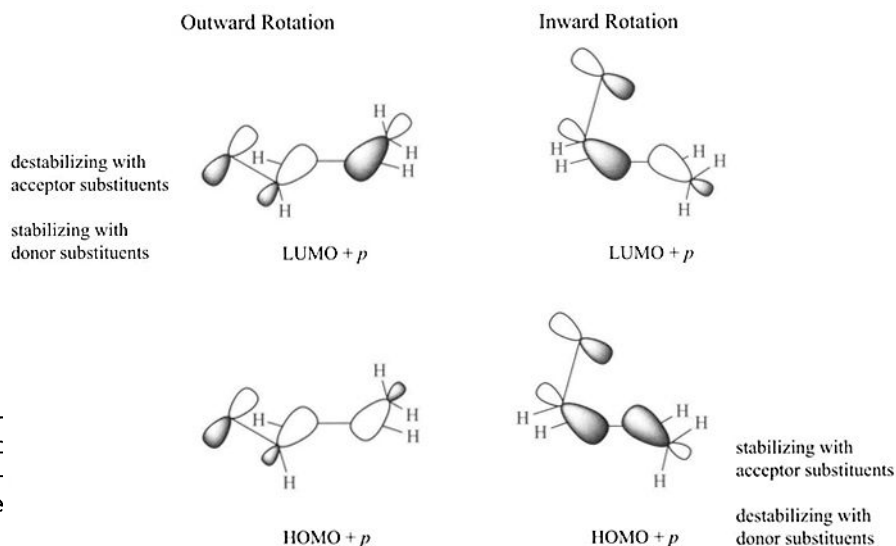
FMO analysis of the opening of cyclobutene to 1,3-butadiene by disrotatory (left) and conrotatory (right) pathways.

¹⁴⁹ For a discussion of pericyclic reactions in terms of frontier MO theory, see Houk, K. N. in Marchand, A. P.; Lehr, R. E., Eds. *Pericyclic Reactions*, Vol. II; Academic Press: New York, 1977; pp. 181–271.

¹⁵⁰ For this analysis, the σ bond and the π bond are considered to be two independent units, each with its HOMO and LUMO, even though they are in the same molecule.

¹⁵¹ Houk, K. N. in de Meijere, A.; Blechert, S., Eds., *Strain and Its Implications in Organic Chemistry*; Kluwer Academic Publishers; Dordrecht, 1989, p. 25.

¹⁵² Niwayama, S.; Kallel, E. A.; Spellmeyer, D. C.; Sheu, C.; Houk, K. N. *J. Org. Chem.* **1996**, *61*, 2813.

**FIGURE 11.91**

Orbital interactions producing torquoselectivity in the electrocyclic opening of 3-substituted cyclobutenes. (Adapted from reference 152.)

cannot account for the products of such reactions because sometimes the *cis* product is formed in greater yield. Houk and co-workers attributed the preference for inward rotation in cyclobutene-3-carboxaldehyde (**94**) to a stabilizing interaction of the formyl LUMO π^* orbital with the breaking σ bond (Figure 11.91). With electron-donating substituent groups, outward rotation was found to be favored.

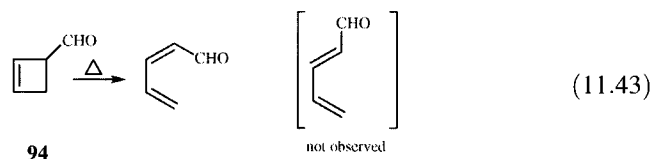
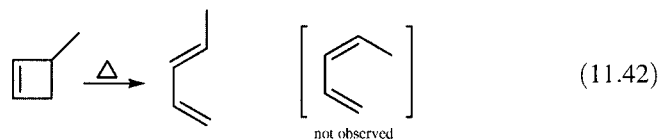
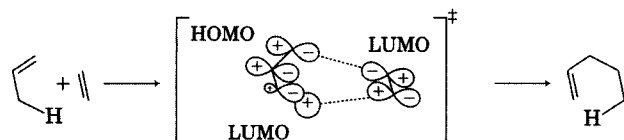
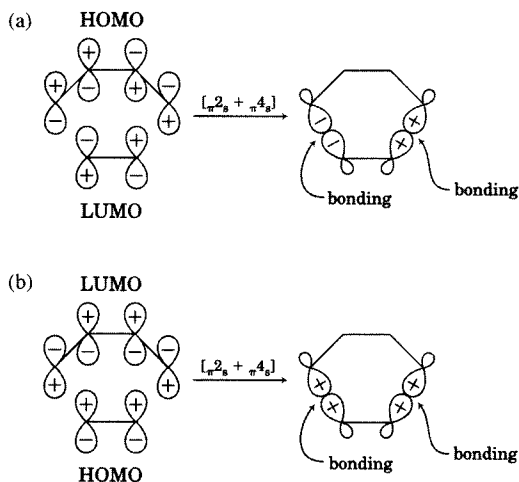


Figure 11.92 shows that the ene reaction can be described as the result of an interaction of the HOMO of the allylic double bond, the LUMO of the allylic C–H bond, and the LUMO of the enophile.¹⁵³ An FMO analysis of the Diels–Alder reaction is shown in Figure 11.93. The result is the same no matter which HOMO–LUMO combination is taken. Figure 11.93(a) shows that the combination of the HOMO of 1,3-butadiene (ψ_2) with the LUMO of ethene (π^*) leads to bonding interactions in the new σ bonds, as does the interaction of the LUMO of 1,3-butadiene (ψ_3) with the HOMO of ethene (π) in Figure 11.93(b).

¹⁵³ Inagaki, S.; Fujimoto, H.; Fukui, K. *J. Am. Chem. Soc.* **1976**, *98*, 4693.

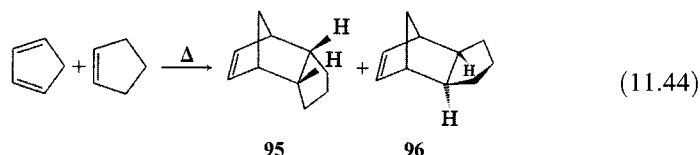
**FIGURE 11.92**

FMO analysis of the ene reaction.
(Adapted from reference 154.)

**FIGURE 11.93**

Two FMO analyses of the Diels-Alder reaction.

The product of addition of a dienophile to a cyclic diene is usually the endo product rather than the more stable exo product, although varying yields of exo product can be formed.¹⁵⁵ For example, the cycloaddition of cyclopentadiene and cyclopentene gives both the endo product (**95**) and the exo product (**96**, equation 11.44).¹⁵⁶ As shown by the data in Table 11.4, formation of the endo product is favored under conditions of lower temperature and shorter reaction time, while the exo product is formed in higher percent yield at higher temperature and longer reaction time. Thus, **95** is the product of rate (kinetic) control, meaning that ΔG^\ddagger is lower for formation of **95** than for formation of **96**. Compound **96** is the product of equilibrium (thermodynamic) control, meaning that it is lower in free energy than is **95**.⁹⁴



Woodward and Hoffmann proposed that the lower activation energies often observed for endo cycloaddition result from additional stabilization due to attractive interaction between *secondary orbitals* (i.e., lobes of *p* orbitals

¹⁵⁴ Paderes, G. D.; Jorgensen, W. L. *J. Org. Chem.* **1992**, *57*, 1904.

¹⁵⁵ Alder, K.; Stein, G. *Angew. Chem.* **1937**, *50*, 510.

¹⁵⁶ Cristol, S. J.; Seifert, W. K.; Soloway, S. B. *J. Am. Chem. Soc.* **1960**, *82*, 2351.

TABLE 11.4 Product Distribution in Diels–Alder Reaction of Cyclopentadiene with Cyclopentene

Reaction Temperature (°C)	Reaction Time (h)	% 95	% 96
198	5.3	97	3
200	11	81	9
300	5	46	50
300	40	29	72

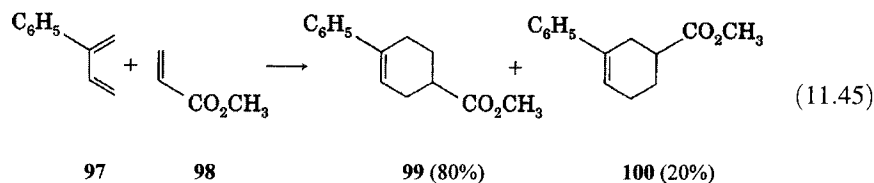
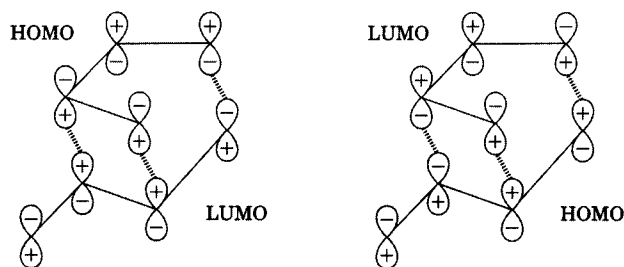
Source: Reference 156.

that are not converted to sp^3 orbitals in the reaction).¹⁵⁷ Figure 11.94 shows such an interaction for both types of HOMO–LUMO interactions in the endo transition structure for the Diels–Alder dimerization of 1,3-butadiene. HOMO–LUMO interactions cannot be the only factor favoring endo product formation in the Diels–Alder reaction, however, because cyclopentene has no p orbitals other than those in the reacting alkene. Fox and co-workers proposed that steric destabilization of the exo transition structure can account for the preferential formation of **95** in this case, and they suggested that similar effects could be important for other dienes having sterically interactive substituents.¹⁵⁸

Another aspect of the Diels–Alder reaction that can be rationalized with FMO theory is the regiochemistry observed with unsymmetric dienes or alkenes. Equation 11.45 shows the product distribution from the cycloaddition of 2-phenyl-1,3-butadiene (**97**) and methyl acrylate (**98**). The “para” product **99** (named by analogy with aromatic compounds) is the major product, but some “meta” product (**100**) is produced as well.¹⁵⁹

FIGURE 11.94

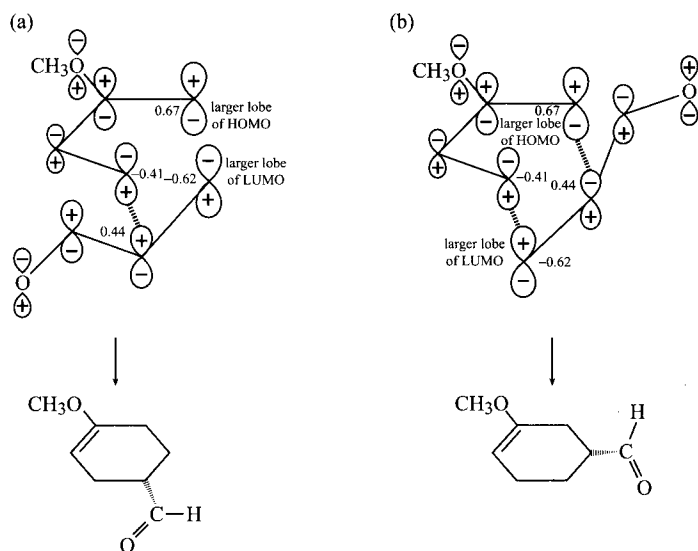
Secondary orbital overlap in the endo transition structure for the Diels–Alder dimerization of 1,3-butadiene.



¹⁵⁷ Hoffmann, R.; Woodward, R. B. *J. Am. Chem. Soc.* **1965**, *87*, 4388.

¹⁵⁸ (a) Fox, M. A.; Cardona, R.; Kiwiet, N. J. *J. Org. Chem.* **1987**, *52*, 1469. (b) Theoretical evidence for a dominant role of secondary orbital interactions in the stereochemistry of the Diels–Alder reaction of cyclopropene with a series of substituted 1,3-butadienes was reported by Apeloig, Y.; Matzner, E. *J. Am. Chem. Soc.* **1995**, *117*, 5375.

¹⁵⁹ Houk, K. N. *Acc. Chem. Res.* **1975**, *8*, 361 and references therein.

**FIGURE 11.95**

(a) Favorable interaction of larger lobe of HOMO of 2-methoxy-1,3-butadiene with larger lobe of LUMO of acrolein; (b) less favorable interaction of larger lobe of HOMO of 2-methoxy-1,3-butadiene with the smaller lobe of LUMO of acrolein.

Both products in equation 11.45 can be formed by overlap of the HOMO of the diene with the LUMO of the olefin. The product distribution is therefore predicted by the rule that the major product is formed via the transition structure in which the larger lobe of the HOMO overlaps with the larger lobe of the LUMO.¹⁶⁰ Figure 11.95(a) shows that there is bonding overlap of the larger lobe of the HOMO on C1 of 2-methoxy-1,3-butadiene with the larger lobe of the LUMO on C3 of acrolein. The orientation of reactants that leads to the minor product, shown in Figure 11.95(b), involves the less favorable overlap of the large lobe of the HOMO on C1 of the diene with a very small lobe of the LUMO on C2 of acrolein.¹⁶¹

The FMO model is also valuable in rationalizing several observations about relative reactivities in the Diels–Alder reaction. Reactivity is enhanced with electron-withdrawing groups on the olefin, as shown by the data in Table 11.5 for reaction of cyclopentadiene with cyano-substituted alkenes. Reactivity is also enhanced by any electron-donating groups on the diene, as shown by the data in Table 11.6 for the reaction of some dienes with tetracyanoethylene.

TABLE 11.5 Kinetic Data for Reaction of Cyclopentadiene with Cyanoethylenes in Dioxane at 20°C

Olefin	k_{rel}
Tetracyanoethylene	4.1×10^7
Tricyanoethylene	4.6×10^5
<i>trans</i> -1,2-Dicyanoethylene	78
Acrylonitrile	1

Source: Reference 93.

¹⁶⁰ Fleming, I. *Frontier Orbitals and Organic Chemical Reactions*; Wiley-Interscience: London, 1976; p. 121 ff.

¹⁶¹ The orbital coefficients are from an AM1 calculation carried out with Spartan '06.

TABLE 11.6 Kinetic Data for Reaction of Dienes with Tetracyanoethylene in Dioxane at 20°C

Olefin	k_{rel}
1-Methoxy-1,3-butadiene	1.1×10^3
<i>trans</i> -1-Methyl-1,3-butadiene	2.2
1,3-Butadiene	1
2-Chloro-1,3-butadiene	1.9×10^{-3}

Source: Reference 93.

Figure 11.96(a) shows that both the $\text{HOMO}_{\text{diene}}\text{-LUMO}_{\text{dienophile}}$ and the $\text{HOMO}_{\text{dienophile}}\text{-LUMO}_{\text{diene}}$ interactions are stabilizing. In a **normal electron demand** Diels–Alder reaction, the $\text{HOMO}_{\text{diene}}\text{-LUMO}_{\text{dienophile}}$ energy gap is smaller than the $\text{HOMO}_{\text{dienophile}}\text{-LUMO}_{\text{diene}}$ energy gap. This means that the $\text{HOMO}_{\text{diene}}\text{-LUMO}_{\text{dienophile}}$ energy gap is the major factor in stabilizing the transition structure, and that makes it the primary determinant of the rate constant of the reaction. Electron-donating substituents that raise the HOMO of the diene or stronger electron-withdrawing substituents that lower the LUMO of the dienophile, as shown in Figure 11.96(b), decrease the $\text{HOMO}_{\text{diene}}\text{-LUMO}_{\text{dienophile}}$ energy gap and thus enhance reactivity.¹⁶² For example, the Diels–Alder reaction is dramatically accelerated by the complexation of the dienophile with Lewis acid catalysts, which lowers the LUMO energy of the dienophile.^{163–165}

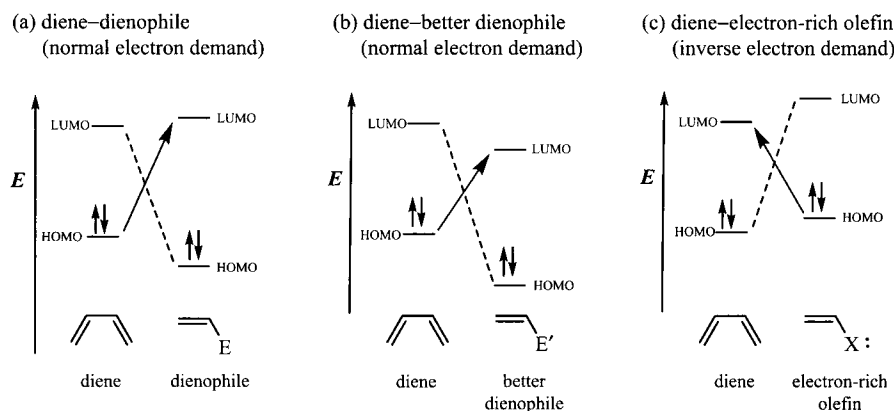
If the HOMO of the olefin is higher in energy than that of the diene and the LUMO of the diene is lower in energy than that of the olefin, the reaction is termed an **inverse electron-demand** Diels–Alder reaction. The energy relationships of these frontier orbitals are shown in Figure 11.96(c). Spino and co-workers found that the HOMO–LUMO energy gap did not correlate well with reactivity for inverse electron-demand Diels–Alder reactions.¹⁶²

¹⁶² Consistent with this expectation, Spino, C.; Rezaei, H.; Dory, Y. L. *J. Org. Chem.* **2004**, *69*, 757 found the HOMO–LUMO energy gap to be a reliable predictor of Diels–Alder reactivity for normal electron-demand reactions.

¹⁶³ (a) Yates, P.; Eaton, P. *J. Am. Chem. Soc.* **1960**, *82*, 4436. (b) For a discussion, see Guner, O. F.; Ottenbrite, R. M.; Shillady, D. D.; Alston, P. V. *J. Org. Chem.* **1987**, *52*, 391.

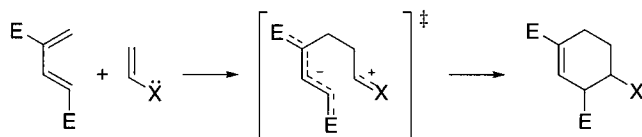
¹⁶⁴ Diels–Alder reactions are also influenced by solvent and pressure effects. For leading references, see Blake, J. F.; Jorgensen, W. L. *J. Am. Chem. Soc.* **1991**, *113*, 7430. The Diels–Alder reaction of cyclopentadiene and methyl vinyl ketone takes place nearly 300 times faster in water than in acetonitrile. In addition, use of water as a solvent favors formation of the endo product. Otto, S.; Engberts, J. B. F. N. *Pure Appl. Chem.* **2000**, *72*, 1365 and references therein. For other discussions of medium effects on the Diels–Alder reaction, see Li, C.-J.; Chen, L. *Chem. Soc. Rev.* **2006**, *35*, 68; Breslow, R. *Acc. Chem. Res.* **2004**, *37*, 471; Breslow, R. *J. Phys. Org. Chem.* **2006**, *19*, 813; Tiwari, S.; Kumar, A. *Angew. Chem. Int. Ed.* **2006**, *45*, 4824; Yoshizawa, M.; Tamura, M.; Fujita, M. *Science* **2006**, *312*, 251. Diedrich, M. K.; Hochstrate, D.; Klärner, F.-G.; Zimny, B. *Angew. Chem. Int. Ed. Engl.* **1994**, *33*, 1079 reported that (*Z*)-1,3,8-nonatriene undergoes competing intramolecular Diels–Alder reaction and a sigmatropic [1,5] hydrogen shift. At 150°C and 1 bar, the major product results from the hydrogen shift. At 7.7 bar, however, the major product is the intramolecular Diels–Alder adduct.

¹⁶⁵ Diels–Alder reactions also occur readily in chain reactions involving dienophile radical cations. Bellville, D. J.; Wirth, D. D.; Bauld, N. L. *J. Am. Chem. Soc.* **1981**, *103*, 718; Bauld, N. L. *J. Am. Chem. Soc.* **1992**, *114*, 5800. Other pericyclic reactions also occur through the intermediacy of organic radical cations. For a discussion, see Bauld, N. L.; Bellville, D. J.; Harirchian, B.; Lorenz, K. T.; Pabon, R. A., Jr.; Reynolds, D. W.; Wirth, D. D.; Chiou, H.-S.; Marsh, B. K. *Acc. Chem. Res.* **1987**, *20*, 371.

**FIGURE 11.96**

Schematic representations of frontier MO interactions in the Diels-Alder reaction. In each case, the smaller HOMO-LUMO gap is indicated with the solid arrow.

They concluded that the polarized orbitals of an electron-rich dienophile might be considered similar to those of an enolate ion. Thus, the transition structure for a Diels-Alder reaction of an electron-poor diene and an electron-rich olefin, such as a vinyl ether, would have some similarity to a Michael addition. This result suggested that the transition structure for inverse electron-demand Diels-Alder reactions is significantly nonsymmetric, with one carbon-carbon bond formation considerably more advanced than the other (Figure 11.97).

**FIGURE 11.97**

"Michael-type" transition structure proposed for an extreme inverse electron-demand Diels-Alder reaction.

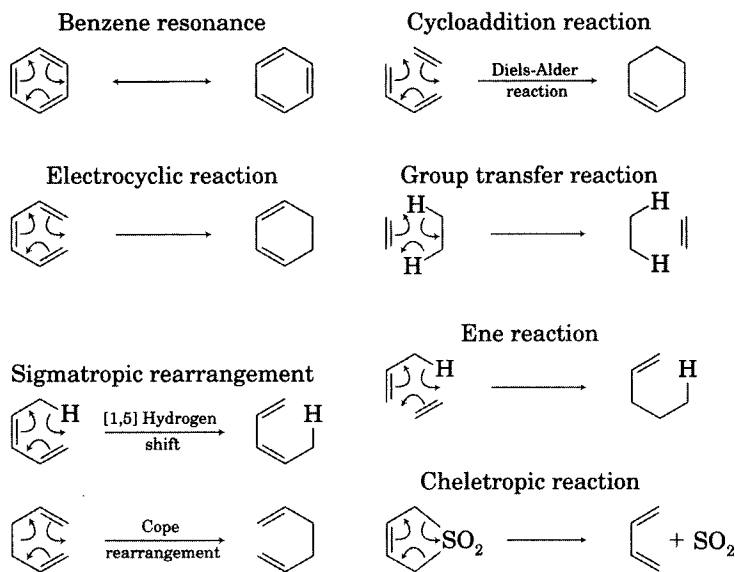
Hückel and Möbius Aromaticity of Transition Structures

Another approach to understanding concerted reactions is based on a parallel between the molecular orbitals of transition structures and the MOs of ground state species. We have seen numerous examples of selection rules that are different for $(4n + 2)$ and $(4n)$ systems, and these are the same sets of arithmetic progressions as those for aromatic and antiaromatic structures in Hückel MO theory. This observation suggests that transition structures can also be considered to be either aromatic or antiaromatic species.¹⁶⁶ In fact, the curved arrow notation for electron movement leading to the observed bonding changes for all of the allowed pericyclic reactions in Figure 11.3 resembles the curved arrow notation for conversion of one Kekulé resonance structure of benzene to the other (Figure 11.98).¹⁶⁷

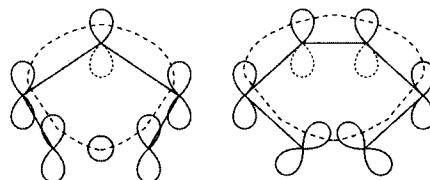
The view that the transition structures of allowed pericyclic reactions are aromatic is supported by a more detailed analysis. For example, both the suprafacial [1,5] hydrogen shift of 1,3-pentadiene and the disrotatory

¹⁶⁶ Evans, M. G.; Warhurst, E. *Trans. Faraday Soc.* **1938**, *34*, 614; Evans, M. G. *Trans. Faraday Soc.* **1939**, *35*, 824.

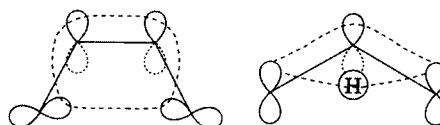
¹⁶⁷ For a discussion, see Rzepa, H. S. *J. Chem. Educ.* **2007**, *84*, 1535.

**FIGURE 11.98**

Curved arrow notation for benzene resonance and for aromatic transition structures in pericyclic reactions involving six electrons. (Adapted from reference 19.)

**FIGURE 11.99**

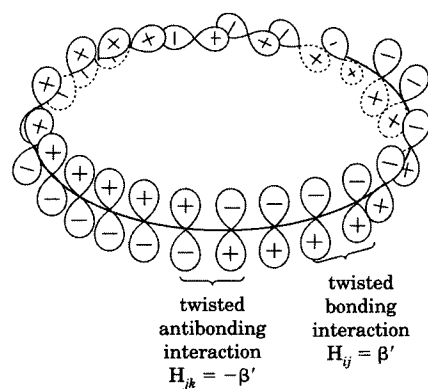
Aromatic transition structures having six electrons.

**FIGURE 11.100**

Antiaromatic transition structures having four electrons.

opening of 1,3-cyclohexadiene to 1,3,5-hexatriene (Figure 11.99) have transition structures with six electrons in a system composed of six basis set orbitals arranged in a cyclic array, just as does benzene. Thus, these are aromatic transition structures. A very different situation is found for forbidden reactions, such as the disrotatory opening of cyclobutene to 1,3-butadiene and the suprafacial [1,3] hydrogen shift in propene (Figure 11.100). In both cases the transition structures are shown with a set of four atomic orbitals arranged in a cyclic array, and there are a total of four electrons in the resulting MOs. Each system is like cyclobutadiene and therefore is an antiaromatic transition structure. Because reactions such as those in Figure 11.99 are allowed, but reactions such as those in Figure 11.100 are forbidden, Dewar proposed that systems containing $4n + 2$ electrons undergoing a pericyclic change prefer an aromatic transition state, while systems with $4n$ electrons avoid an antiaromatic transition state.¹⁶⁸ Consistent with this model,

¹⁶⁸ Dewar, M. J. S. *Tetrahedron Suppl.* 1966, 8, 75.

**FIGURE 11.101**

A hypothetical array of twisted p orbitals leading to a Möbius π system.

theoretical calculations have shown that aromaticity of transition states is a driving force in [1,5] hydrogen shifts and in Diels–Alder reactions.^{169,170}

The relationship between aromaticity and pericyclic reactions can be developed further by considering the type of orbital interactions that would be present in a novel structure proposed by Heilbronner.¹⁷¹ Imagine a large cyclic array of np orbitals arranged as shown in Figure 11.101. If each p orbital is twisted by $180^\circ/n$ with respect to the orbital adjacent to it, then after n such p orbitals the ring would be complete, but the first p orbital would have an antibonding relationship with the last. In other words, there will be one and only one (+)–(–) orbital interaction in the ring. Heilbronner noted that such a molecular system would be like a Möbius strip (Figure 11.102) in that it would have only one side.

The molecular orbitals of a Möbius system can be calculated in almost exactly the same way as can Hückel MOs. If the resonance integral for one p orbital interacting with another p orbital that is slightly twisted with respect to it is β (technically, β' , since the orbitals are not completely parallel), then the resonance integral for the first and last p orbitals is $-\beta$. Solving the secular determinant gives the energy levels of such a system as illustrated in Figure 11.103. The top part of that figure shows the basis set orbitals (a), the secular determinant from HMO theory (b), and the resulting energy levels (c) for Hückel cyclobutadiene. The bottom part of Figure 11.103 shows the corresponding representations for Möbius cyclobutadiene. (Note the antibonding overlap between the p orbitals on C1 and C2.) The secular determinant for this Möbius system has two -1 elements (for the two resonance integrals involving C1 and C2). Solving this determinant in the usual way leads to two energy levels of $\alpha + 1.414\beta$ and two energy levels of $\alpha - 1.414\beta$.

**FIGURE 11.102**

A Möbius strip.

¹⁶⁹ Alabugin, I. V.; Manoharan, M.; Breiner, B.; Lewis, F. D. *J. Am. Chem. Soc.* **2003**, *125*, 9329.

¹⁷⁰ Manoharan, M.; De Proft, F.; Geerlings, P. *J. Chem. Soc. Perkin Trans. 2* **2000**, 1767.

¹⁷¹ Heilbronner, E. *Tetrahedron Lett.* **1964**, 1923.

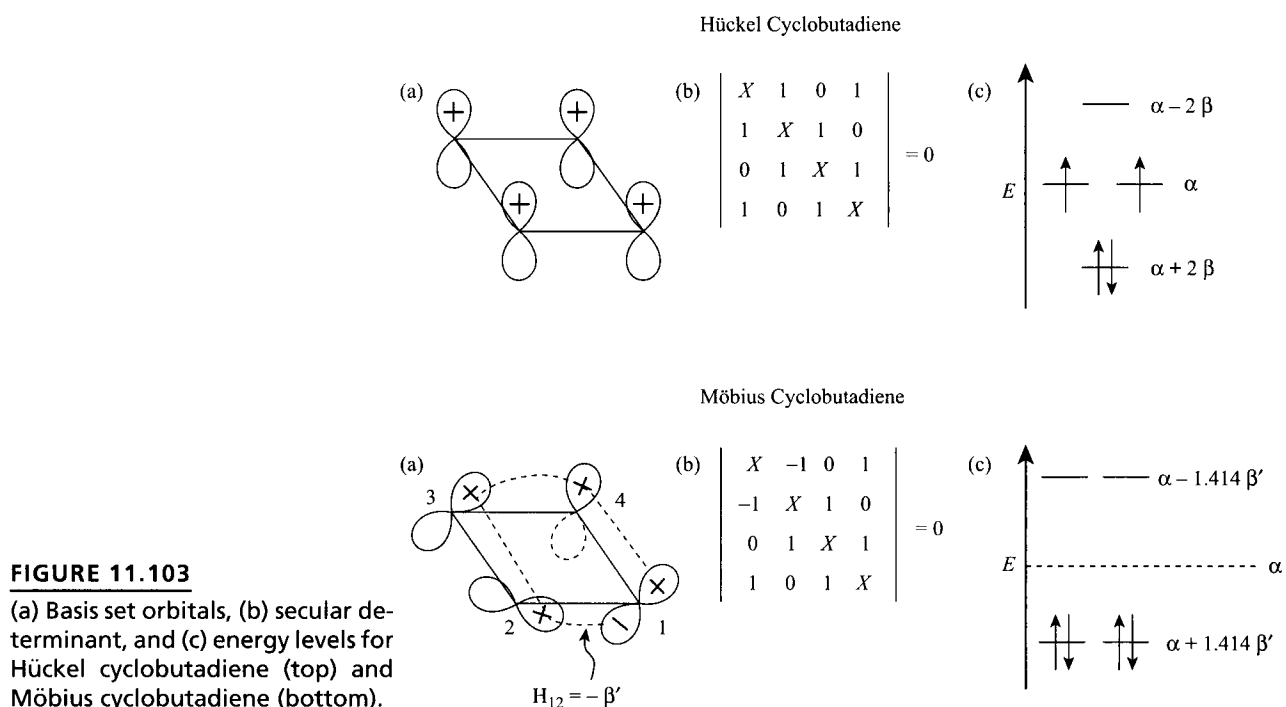


FIGURE 11.103

(a) Basis set orbitals, (b) secular determinant, and (c) energy levels for Hückel cyclobutadiene (top) and Möbius cyclobutadiene (bottom).

As is often the case with simple HMO theory, it is the energy levels of the Möbius systems and not the MOs themselves that are of primary interest. Zimmerman developed a circle mnemonic, analogous to the circle mnemonic used with HMO theory in Chapter 4, which provides a shortcut to finding the Möbius energy levels.¹⁷² For Möbius MOs, the polygon corresponding to the cyclic molecule is inscribed in the circle of radius 2β with one *side* down (not with a corner down as was done for Hückel systems).¹⁷³ This procedure is illustrated in Figure 11.104 for both (a) Hückel MOs and (b) Möbius MOs for cyclopropenyl, cyclobutadiene, and benzene.

The three structures in Figure 11.104 illustrate the contrasts between Hückel and Möbius systems.

1. In HMO theory, the cyclopropenyl cation is aromatic (i.e., it is a closed shell system with large delocalization energy), since both electrons are in the orbital with $E = \alpha + 2\beta$. The Hückel cyclopropenyl anion is antiaromatic because it is an open shell system (having one electron in each of the $E = \alpha - \beta$ orbitals) with zero delocalization energy. In contrast, the Möbius cyclopropenyl anion is aromatic, since it is a closed shell system with all four electrons in bonding orbitals, and the Möbius cyclopropenyl cation is antiaromatic.
2. Möbius cyclobutadiene has four electrons in the two lowest energy levels ($E = \alpha + 1.414\beta$), as shown in Figure 11.103. Möbius cyclobutadiene should therefore be a closed shell system with some delo-

¹⁷² (a) Zimmerman, H. E. *J. Am. Chem. Soc.* **1966**, *88*, 1564; (b) Zimmerman, H. E. *Acc. Chem. Res.* **1971**, *4*, 272; (c) Zimmerman, H. E. in Marchand, A. P.; Lehr, R. E., Eds. *Pericyclic Reactions*, Vol. 1; Academic Press: New York, 1977; pp. 53–107. See also Shen, K. *J. Chem. Educ.* **1973**, *50*, 238.

¹⁷³ This analysis assumes that the Hückel and Möbius systems have the same β value.

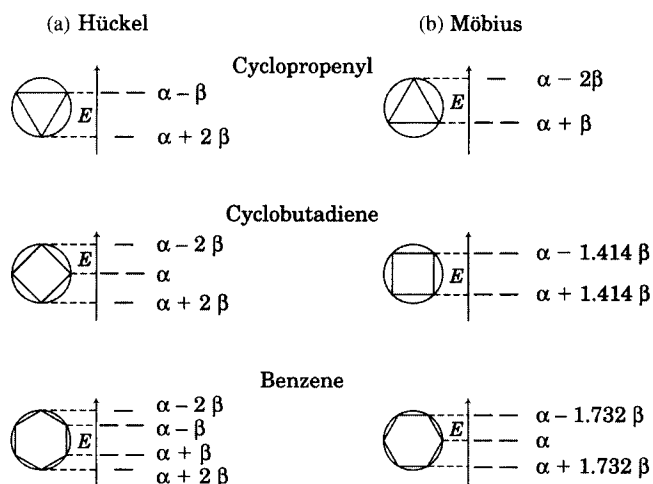


FIGURE 11.104

(a) Hückel and (b) Möbius energy levels developed for cyclopropenyl, cyclobutadiene, and benzene with the circle mnemonic. (Adapted from reference 172b.)

calization stabilization; that is, it should be aromatic (at least in comparison with a nondelocalized reference structure having a system of twisted p orbitals in a ring). Hückel cyclobutadiene is an antiaromatic, open shell species.

- Hückel benzene is aromatic. In Möbius benzene, however, the first four electrons go into orbitals with energy levels at $E = \alpha + 1.732\beta$, and the last two go separately into orbitals at $E = \alpha$. Therefore, Möbius benzene is an open shell, unstable system.

Generalizing the results from these three examples leads to the conclusion that a system with $4n$ electrons in a cyclic array of orbitals having one (+)–(–) overlap is Möbius aromatic, while a similar system with $4n + 2$ electrons is Möbius antiaromatic.

The concept of Möbius aromaticity provides additional insight into the electronic nature of the transition structures in pericyclic reactions. The four pericyclic transition structures in Figures 11.99 and 11.100 were categorized according to their Hückel aromaticity. Figure 11.105 shows an analysis of the same four transition structures as Möbius systems. The conrotatory electrocyclic interconversion of 1,3-butadiene and cyclobutene (a) is a four-electron system, so it is Möbius aromatic. The antarafacial [1,3] hydrogen shift (b) is also a four-electron system, and it too is Möbius aromatic. The antarafacial [1,5] hydrogen shift (c) is a six-electron system, so this transition structure is Möbius antiaromatic. Finally, the disrotatory electrocyclic interconversion of cyclohexadiene and hexatriene (d) is also a six-electron system, so this transition structure is also Möbius antiaromatic. The preferred pathway for the top two reactions in Figure 11.105 is Möbius aromatic, while for the bottom two reactions the preferred pathway is Hückel aromatic (Figure 11.99).

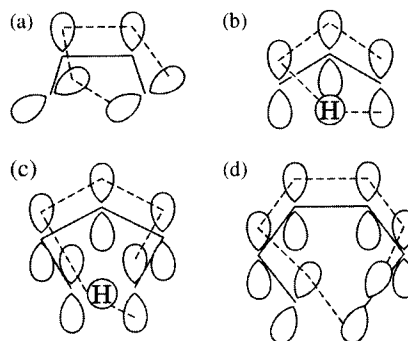
Generalizing these results leads to the following selection rule:¹⁷²

Systems containing $4n + 2$ electrons undergoing a pericyclic change prefer a Hückel aromatic transition structure, while systems with $4n$ electrons prefer a Möbius aromatic transition structure.

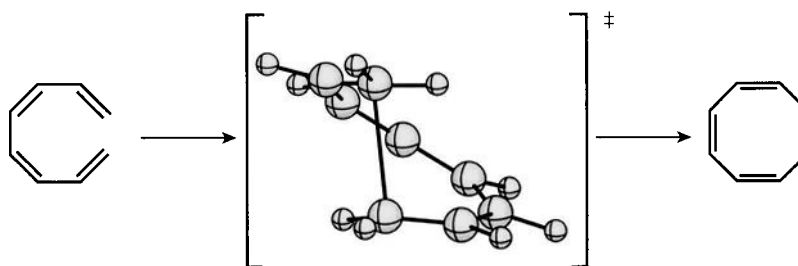
DFT calculations of the transition structure for the $[\pi 8_a]$ electrocyclic conversion of (3Z,5Z)-octa-1,3,5,7-tetraene provide support for this rule.

FIGURE 11.105

Aromatic (top) and antiaromatic (bottom) Möbius transition structures.

**FIGURE 11.106**

Calculated transition structure for the electrocyclic closure of (3Z,5Z)-octa-1,3,5,7-tetraene to cycloocta-1,3,5-triene. (Adapted from reference 174.)



As shown in Figure 11.106, the diene is coiled into a helical conformation allowing one (+)–(–) overlap in the basis set orbitals for this structure.¹⁷⁴

The distinction between the Hückel and Möbius pathways can be clarified by considering the thermal electrocyclic reaction of 1,3-butadiene to cyclobutene through both the conrotatory and disrotatory pathways. Figure 11.107 shows the energy of the various MOs, with the disrotatory transition structure and its Hückel π system drawn on the left and with the conrotatory transition structure with its Möbius π system drawn on the right. Although the drawing is not quantitative, the σ orbitals are drawn lower in energy than π orbitals, and σ^* orbitals are drawn higher than π^* orbitals.¹⁷⁵ As noted by Zimmerman, degeneracies in either the Hückel or Möbius MOs indicate MO crossings, so it is easy to follow MOs from reactant to product.¹⁷² Being able to assign energies to the MOs present in the transition structure for each pathway allows us to compare the change in energy level of each 1,3-butadiene MO as the reaction proceeds along either of the concerted pathways and also to estimate the transition state energy for each of the two pathways for the reaction.¹⁷⁶

Dewar and co-workers noted that in a pericyclic reaction there is a HOMO and a LUMO for the reactant, for the transition structure, and for

¹⁷⁴ Lecea, B.; Arrieta, A.; Cossío, F. P. *J. Org. Chem.* **2005**, *70*, 1035.

¹⁷⁵ Again, the value of β is assumed to be the same for the Hückel and Möbius systems.

¹⁷⁶ Zimmerman advocated this approach as a general tool in organic chemistry and called it *MO following*, noting that it is the molecular orbital theory counterpart to electron pushing in valence bond theory. For a discussion, see reference 172c.

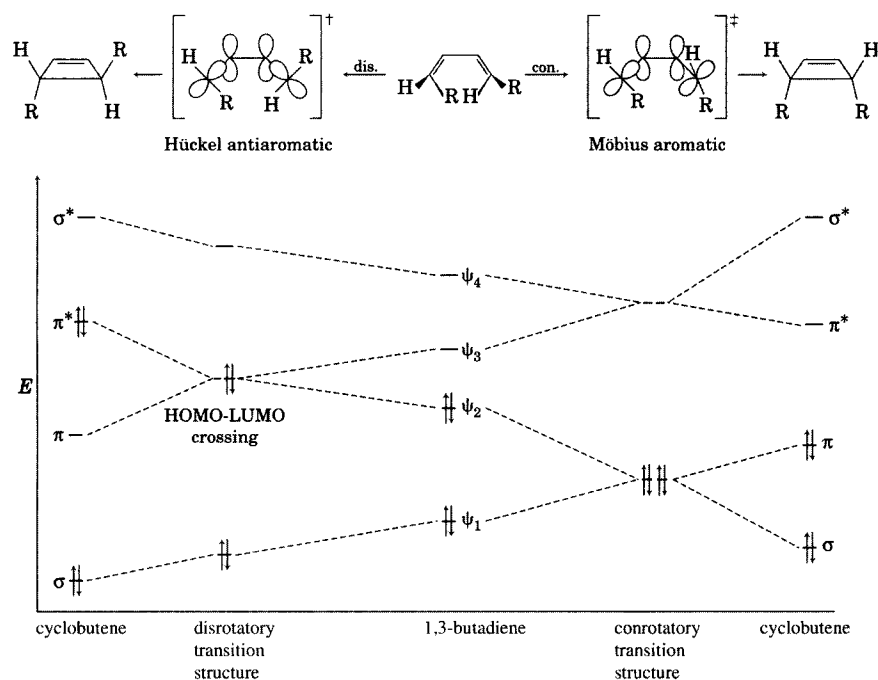


FIGURE 11.107
Hückel-Möbius MO reaction diagram for 1,3-butadiene-cyclobutene. (Adapted from reference 172b.)

the product.¹⁷⁷ For an allowed reaction, the HOMO and LUMO do not cross in energy and, in fact, the difference in their energies remains fairly constant. For a forbidden reaction, on the other hand, there is a HOMO-LUMO crossing. Therefore,

The distinction between “allowed” and “forbidden” reactions... seems to be one of topology rather than symmetry, there being a qualitative distinction between pairs of isomers that can be interconverted by a pericyclic reaction without a HOMO-LUMO crossing and pairs that cannot be so interconverted without a HOMO-LUMO crossing.¹⁷⁷

Pairs of isomers that can be interconverted without a HOMO-LUMO crossing were termed *HOMOMERS*, while those whose interconversion requires a HOMO-LUMO crossing were termed *LUMOMERS*. In contrast to the other selection rules developed above, this classification system is independent of the path by which the interconversion takes place.

The concept of Möbius aromaticity has been extended from transition structures to discussions of the stability of organic molecules. Extensive reviews of Möbius aromaticity and of Möbius structures were provided by Rzepa¹⁷⁸ and by Herges.¹⁷⁹ A computational study of the $(\text{CH})_{12}$, $(\text{CH})_{16}$, and $(\text{CH})_{20}$ annulenes found twisted Möbius structures to be energy minima, but in each case steric strain caused such structures to be higher in energy than their nontwisted Hückel counterparts.¹⁸⁰ Similar results from another study are shown in Table 11.7.¹⁸¹ In order to test the stabilizing effect of Möbius

¹⁷⁷ Dewar, M. J. S.; Kirschner, S.; Kollmar, H. W. J. *Am. Chem. Soc.* **1974**, *96*, 5240.

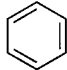

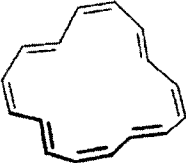

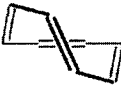
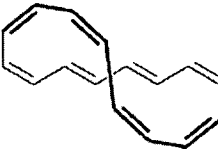
¹⁷⁸ Rzepa, H. S. *Chem. Rev.* **2005**, *105*, 3697.

¹⁷⁹ Herges, R. *Chem. Rev.* **2006**, *106*, 4820.

¹⁸⁰ Castro, C.; Isborn, C. M.; Karney, W. L.; Mauksch, M.; Schleyer, P. v. R. *Org. Lett.*, **2002**, *4*, 3431.

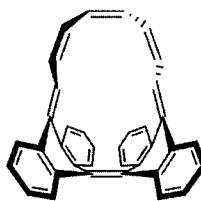
¹⁸¹ Ajami, D.; Hess, K.; Köhler, F.; Näther, C.; Oeckler, O.; Simon, A.; Yamamoto, C.; Okamoto, Y.; Herges, R. *Chem. Eur. J.* **2006**, *12*, 5434.

TABLE 11.7 Most Stable Conformations of $[n]$ Annulenes Found in DFT Calculations

	$[n]$ Annulene			
	$n=6$	$n=8$	$n=16$	$n=20$
Most stable Hückel isomer				
Most stable Möbius isomer				
Energy difference (kcal/mol)	107.0	21.3	5.1	6.2

Source: Reproduced from reference 181.

aromaticity, Herges and co-workers synthesized **101**, in which the twisted Möbius geometry of a [16]annulene core is stabilized with a bianthraquinodimethane unit.¹⁸² They reported that **101** exhibits properties expected for an aromatic system, but this conclusion was questioned by some other investigators.¹⁸³ Möbius structures based on expanded porphyrin systems have also been reported.¹⁸⁴

**101**

Synchronous and Nonsynchronous Concerted Reactions

Dewar noted that almost all analyses of concerted mechanisms implicitly assume symmetric transition structures. For example, the forbidden disrotatory interconversion of cyclobutene and 1,3-butadiene assumed a pathway in which a plane of symmetry is maintained throughout the reaction. Dewar suggested that a lower energy pathway for forbidden processes might be one in which *no* symmetry element is maintained.^{185,186} For example, in the

¹⁸² Ajami, D.; Oeckler, O.; Simon, A.; Herges, R. *Nature* **2003**, 426, 819.

¹⁸³ Castro, C.; Chen, Z.; Wannere, C. S.; Jiao, H.; Karney, W. L.; Mauksch, M.; Puchta, R.; Hommes, N. J. R. v. E.; Schleyer, P. v. R. *J. Am. Chem. Soc.* **2005**, 127, 2425.

¹⁸⁴ Sankar, J.; Mori, S.; Saito, S.; Rath, H.; Suzuki, M.; Inokuma, Y.; Shinokubo, H.; Kim, K. S.; Yoon, Z. S.; Shin, J.-Y.; Lim, J. M.; Matsuzaki, Y.; Matsushita, O.; Muranaka, A.; Kobayashi, N.; Kim, D.; Osuka, A. *J. Am. Chem. Soc.* **2008**, 130, 13568.

¹⁸⁵ Dewar, M. J. S.; Kirschner, S. *J. Am. Chem. Soc.* **1974**, 96, 5244.

¹⁸⁶ The question of symmetric transition structures in concerted reactions was also raised by McIver, J. W., Jr. *Acc. Chem. Res.* **1974**, 7, 72.

disrotatory electrocyclic closure of 1,3-butadiene, the rotation about the C1–C2 bond might occur faster than the rotation about the C3–C4 bond. Although the reaction would still be concerted (meaning that bond-breaking and bond-forming processes occur simultaneously), the reaction might not be **synchronous**, meaning that not all of the bond changes progress to the same extent along the reaction coordinate.¹⁸⁷ Furthermore, it was considered possible that nonsynchronous pathways might be lower in energy than synchronous pathways for allowed pericyclic reactions as well. Dewar and co-workers used semiempirical methods to calculate the transition structures for several pericyclic reactions, including the Diels–Alder reaction and the Claisen and Cope rearrangements.¹⁸⁸ The calculations suggested that each of these reactions takes place in a nonsynchronous way.¹⁸⁹

This report stimulated considerable discussion among theoretical chemists. Borden and co-workers reported results of ab initio calculations indicating that the Diels–Alder reaction is, in fact, a synchronous reaction. These authors indicated, however, that this result was obtained “only when a flexible basis set is used and when electron correlation is properly treated.” Otherwise, a nonsynchronous process was observed.¹⁹⁰ Bernardi and co-workers also reported ab initio evidence for a synchronous Diels–Alder reaction.¹⁹¹ Houk and co-workers reported experimental evidence that the Diels–Alder reaction is concerted and is most likely synchronous as well.¹⁹² These authors also pointed out that different computational methods have built-in biases toward different transition structures. This controversy reminds us that, as noted before, computational methods should be considered as useful tools that are developed from particular conceptual models and not as windows into reality.^{193,194}

In contrast to the Diels–Alder reaction of ethene and 1,3-butadiene, there is evidence that other pathways may be competitive with the concerted [4 + 2] cycloaddition of two 1,3-butadiene molecules to form 4-vinylcyclo-

¹⁸⁷ For an account of work in this area, see the summary by Maugh, T. H. II. *Science* **1984**, 223, 1162.

¹⁸⁸ Dewar, M. J. S.; Griffin, A. C.; Kirschner, S. J. *Am. Chem. Soc.* **1974**, 96, 6225; Dewar, M. J. S.; Wade, L. E., Jr. *J. Am. Chem. Soc.* **1977**, 99, 4417; Dewar, M. J. S.; Pierini, A. B. *J. Am. Chem. Soc.* **1984**, 106, 203; Dewar, M. J. S.; Healy, E. F. *J. Am. Chem. Soc.* **1984**, 106, 7127.

¹⁸⁹ Dewar, M. J. S. *J. Am. Chem. Soc.* **1984**, 106, 209.

¹⁹⁰ Osamura, Y.; Kato, S.; Morokuma, K.; Feller, D.; Davidson, E. R.; Borden, W. T. *J. Am. Chem. Soc.* **1984**, 106, 3362.

¹⁹¹ Bernardi, F.; Bottoni, A.; Robb, M. A.; Field, M. J.; Hillier, I. H.; Guest, M. F. *J. Chem. Soc. Chem. Commun.* **1985**, 1051.

¹⁹² Houk, K. N.; Lin, Y.-T.; Brown, F. K. *J. Am. Chem. Soc.* **1986**, 108, 554. A combination of theoretical studies and experimental data were consistent with the view that the cycloaddition of ethene and 1,3-butadiene is both concerted and synchronous: Storer, J. W.; Raimondi, L.; Houk, K. N. *J. Am. Chem. Soc.* **1994**, 116, 9675.

¹⁹³ These discussions of concerted reactions have emphasized molecular orbital theory, but valence bond theory can produce the same result. For leading references to descriptions of concerted reactions in terms of valence bond theory, see (a) Goddard, W. A. III. *J. Am. Chem. Soc.* **1972**, 94, 793; (b) Mulder, J. J. C.; Oosterhoff, L. J. *J. Chem. Soc. D Chem. Commun.* **1970**, 305, 307; (c) Silver, D. M.; Karplus, M. *J. Am. Chem. Soc.* **1975**, 97, 2645; (d) Herndon, W. C. *J. Chem. Educ.* **1981**, 58, 371; (e) Bernardi, F.; Olivucci, M.; Robb, M. A. *Acc. Chem. Res.* **1990**, 23, 405. For discussions of the relationship of valence bond theory and orbital symmetry concepts, see Berson, J. A. *Tetrahedron* **1992**, 48, 3 (especially the discussion on pp. 14–17).

¹⁹⁴ For a discussion of pericyclic reactions in terms of hardness and polarizability, see Chattaraj, P. K.; Fuentealba, P.; Gómez, B.; Contreras, R. *J. Am. Chem. Soc.* **2000**, 122, 348; De Proft, F.; Chattaraj, P. K.; Ayers, P. W.; Torrent-Sucarrat, M.; Elango, M.; Subramanian, V.; Giri, S.; Geerlings, P. *J. Chem. Theory Comput.* **2008**, 4, 595.

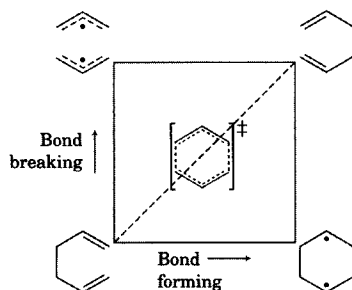


FIGURE 11.108
Reaction surface diagram for the Cope rearrangement.

hexene. Stephenson and co-workers found about a 10% loss of stereochemistry in the dimerization of *cis,cis*-1,4-dideuterio-1,3-butadiene.¹⁹⁵ Ab initio calculations by Li and Houk revealed that the concerted reaction may be only slightly lower in energy than stepwise processes involving diradical intermediates for this reaction.^{98,196} Because the allowed and forbidden pathways generalized from state correlation diagrams reveal only the energetics of concerted reactions, the possibility that alternative, nonconcerted pathways may have lower or only slightly higher energies must always be considered.

Many pericyclic reactions are clearly nonsynchronous. Studies of kinetic isotope effects on the Claisen rearrangement of allyl phenyl ether suggested that the C_α -O bond is 50–60% broken in the transition structure, while the C_γ - C_{ortho} bond is only 10–20% formed.^{197,198} The relationship between bond forming and bond breaking in the analogous Cope rearrangement is expressed graphically in Figure 11.108. A fully synchronous reaction would follow the dashed diagonal line from reactant (lower left corner) to product (upper right corner). A reaction involving complete bond breaking before any bond forming would result in a path passing through the upper left corner and the intermediacy of two allylic radicals. A reaction involving complete bond formation before any bond breaking would involve a reaction pathway passing through cyclohexane-1,4-diyl in the lower right corner.

The effect of substituents on the transition structure for the Cope rearrangement has been considered in detail by a number of workers. Ab initio and DFT calculations suggested that the synchronous pathway is followed for the Cope rearrangement of 1,5-hexadienes that do not bear radical- or ion-stabilizing substituents.^{199,200} The effect of radical-stabilizing substituents was found to depend on the position of substitution. Based on α secondary kinetic isotope effects, Gajewski and Conrad concluded that radical-stabilizing groups (such as phenyl) at C2 and C5 cause the transition structure to be more like cyclohexane-1,4-diyl (the lower right corner), but that radical-stabilizing groups at C3 cause the transition structure to resemble the diallylic species nearer the upper left corner.^{201–203} If there is more than one substituent on the 1,5-hexadiene, their effects on the reaction pathway are more complicated. Doering proposed that the transition structure could

¹⁹⁵ Stephenson, L. M.; Gemmer, R. V.; Current, S. *J. Am. Chem. Soc.* **1975**, *97*, 5909.

¹⁹⁶ Klärner, F.-G.; Krawczyk, B.; Ruster, V.; Deiters, U. K. *J. Am. Chem. Soc.* **1994**, *116*, 7646 reported that high pressure can suppress the extent of product formation by nonconcerted reaction.

¹⁹⁷ Kupczyk-Subotkowska, L.; Saunders, W. H., Jr.; Shine, H. J. *J. Am. Chem. Soc.* **1988**, *110*, 7153; Kupczyk-Subotkowska, L.; Subotkowski, W.; Saunders, W. H., Jr.; Shine, H. J. *J. Am. Chem. Soc.* **1992**, *114*, 3441. Similar results were obtained for the [3,3] rearrangement of allyl vinyl ether: Kupczyk-Subotkowska, L.; Saunders, W. H., Jr.; Shine, H. J.; Subotkowski, W. *J. Am. Chem. Soc.* **1993**, *115*, 5957.

¹⁹⁸ For a discussion of the interpretation of kinetic isotope effects, see Meyer, M. P.; DelMonte, A. J.; Singleton, D. A. *J. Am. Chem. Soc.* **1999**, *121*, 10865.

¹⁹⁹ For an ab initio study and a summary of previous theoretical investigations, see Hrovat, D. A.; Morokuma, K.; Borden, W. T. *J. Am. Chem. Soc.* **1994**, *116*, 1072.

²⁰⁰ McGuire, M. J.; Piecuch, P. *J. Am. Chem. Soc.* **2005**, *127*, 2608.

²⁰¹ Gajewski, J. J.; Conrad, N. D. *J. Am. Chem. Soc.* **1979**, *101*, 6693.

²⁰² Also see Houk, K. N.; Gustafson, S. M.; Black, K. A. *J. Am. Chem. Soc.* **1992**, *114*, 8565 and references therein.

²⁰³ The intermediates are shown here as radicals, but ions might be involved instead—especially if there is a cation-stabilizing substituent on C2 and an anion-stabilizing substituent on C5.

be either "chameleonic" or "centauric."²⁰⁴ A chameleonic transition structure was proposed for systems in which radical-stabilizing substituents contribute cooperatively in determining the transition structure. If there is a radical-stabilizing substituent on C5 as well as on C1 and C3, however, then the transition structure was said to be centauric because the C1–C2–C3 segment and the C4–C5–C6 segment changed in different ways as a result of the substituent(s) on each segment. In the case of 1,3,5-triphenylhexa-1,5-diene, Doering found the effect of substituents on the transition state energy to be intermediate between that predicted by the chameleonic and centauric models but closer to the centauric prediction. DFT calculations by Hrovat and co-workers suggested that the transition structure in the case of a 2,4-disubstituted 1,5-hexadiene seemed to be neither diallylic nor 1,4-cyclohexane-diyl-like, but neither did it appear to gain stability from the two substituents.^{205,206}

The Role of Reaction Dynamics in Rearrangements

The allowed pathway in a pericyclic reaction is lower in *electronic* energy because the symmetries of the molecular orbitals allow bonding to be maximized in the transition structure for the concerted reaction. MO and state correlation diagrams ignore any *steric* contribution to the total energies of the two pathways, however. The publications of Woodward and Hoffmann stimulated chemists to probe the extent of orbital symmetry control by studying molecules for which the allowed pathway is sterically more difficult than the forbidden reaction. For example, Berson considered whether a thermal [1,3] rearrangement could occur by a pathway that is antarafacial to the one-atom component. As noted earlier for cycloadditions, a pericyclic reaction involving a one-carbon π system has the possibility of being antarafacial with respect to the migrating atom. The antarafacial migration of a one-carbon component in a sigmatropic reaction would then require that bond breaking and bond forming occur on different lobes of the p orbital. Figure 11.109 shows that a [1,3] rearrangement, which is suprafacial with respect to the 3-component and antarafacial with respect to the 1-component, is allowed by the principles of conservation of orbital symmetry.

Note that the [1,3] carbon shift shown in Figure 11.109 takes place with inversion of a chiral center. Therefore, we may say that the migration is antarafacial (a) with respect to the one-carbon component or, equivalently, we may say that the reaction takes place with inversion (*i*). A one-carbon

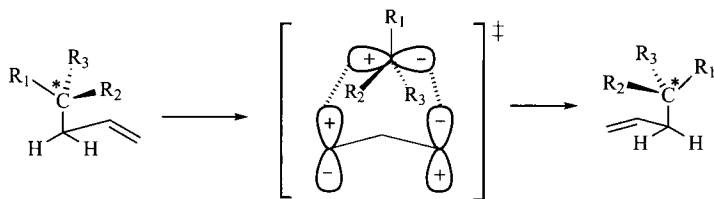


FIGURE 11.109

[1,3] Carbon shift antarafacial to the one-carbon component. (The methyl substituents are labeled to emphasize inversion of the chiral center.)

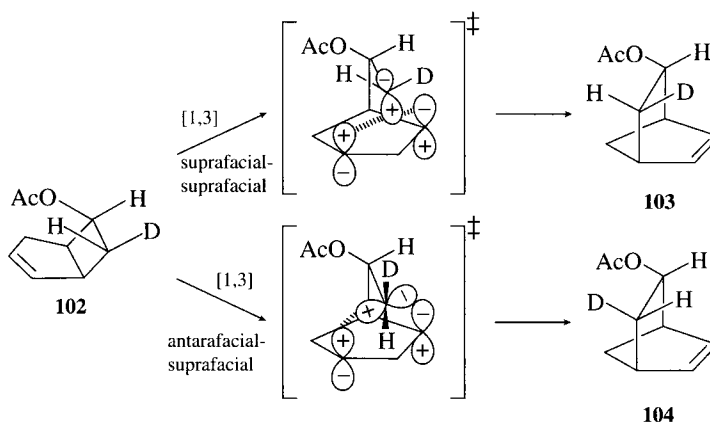
²⁰⁴ Doering, W. v. E.; Wang, Y. *J. Am. Chem. Soc.* **1999**, *121*, 10112.

²⁰⁵ Hrovat, D. A.; Beno, B. R.; Lange, H.; Yoo, H.-Y.; Houk, K. N.; Borden, W. T. *J. Am. Chem. Soc.* **1999**, *121*, 10529.

²⁰⁶ For a mathematical model of these substituent effects, see Hrovat, D. A.; Borden, W. T. *J. Chem. Theory Comput.* **2005**, *1*, 87.

FIGURE 11.110

Stereochemical labeling to investigate a possible antarafacial carbon shift.



migration with retention of configuration at the migrating carbon would require both bond forming and bond breaking to involve the same lobe of the p orbital and is suprafacial (s) with respect to that atom. The suprafacial process therefore may also be described as r (for retention).

To study whether the process shown in Figure 11.109 might be feasible, Berson and Nelson investigated the [1,3] rearrangement of *endo*-bicyclo[3.2.0]-2-hepten-6-yl acetate-*exo*-7-*d* (**102**, Figure 11.110).²⁰⁷ The top pathway is suprafacial with respect to the allyl component located in the five-membered ring and is also suprafacial with respect to the migrating carbon atom above it. The bottom pathway is suprafacial with respect to the allyl fragment but is antarafacial with respect to the migrating carbon atom. The upper pathway is forbidden by orbital symmetry, but the lower pathway is allowed. The products of the two pathways can be distinguished by ^1H NMR because the two protium atoms in the $-(\text{CHOAc}-\text{CHD})-$ bridge are *trans* to each other in **103** but they are *cis* in **104**.²⁰⁸ When the reaction was carried out, the product was found to be predominantly but perhaps not exclusively **104**, which was taken to mean that orbital symmetry conservation could be a dominant factor in determining product stereochemistry.²⁰⁹

Subsequent work by Baldwin and Belfield²¹⁰ and by Klärner and co-workers²¹¹ with deuterium-labeled structures revealed that the [1,3] carbon shift is not entirely stereospecific. As shown in equation 11.46, the rearrangement of **105** produced **106** and **107** in an 89 : 11 ratio.²¹¹ Thus, at least 11% of the rearrangement occurred through a process other than a concerted [1,3] sigmatropic rearrangement with inversion at the migrating carbon. A nonconcerted, perhaps diradical pathway was proposed as a mechanism for the formation of **107**. This conclusion raised the question as to whether some or all of **106** might also have been formed through a nonconcerted process.

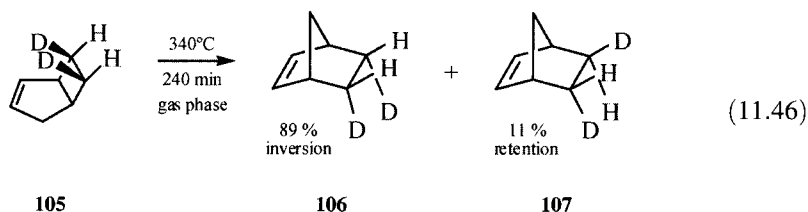
²⁰⁷ Berson, J. A.; Nelson, G. L. *J. Am. Chem. Soc.* **1967**, *89*, 5503; Berson, J. A. *Acc. Chem. Res.* **1968**, *1*, 152.

²⁰⁸ As noted in Chapter 7, the term *protium* refers specifically to the ^1H isotope of hydrogen. Commission on Physical Organic Chemistry, IUPAC. *Pure Appl. Chem.* **1988**, *60*, 1115.

²⁰⁹ The NMR spectrum indicated that a very small amount (perhaps as much as 5%) of **103** may also have been present in the product, although it could have been produced by reaction of an isomer of the starting material.

²¹⁰ Baldwin, J. E.; Belfield, K. D. *J. Am. Chem. Soc.* **1988**, *110*, 296.

²¹¹ Klärner, F.-G.; Drewes, R.; Hasselmann, D. *J. Am. Chem. Soc.* **1988**, *110*, 297.



The stereochemistry of a [1,3] carbon migration is more complex if the reaction can also be either suprafacial or antarafacial with respect to the π system. As shown in Figure 11.111, there are four different stereochemical outcomes from the [1,3] methyl shift of (1*S*,2*S*)-1-methyl-2-((*E*)-prop-1-enyl)cyclobutane (**108**) to produce a product mixture consisting of four diastereomers of 3,4-dimethylcyclohexene (**109**).^{212,213} For simplicity, the products are labeled in Figure 11.111 with the *R* or *S* designation of the chiral centers on C3 and C4. The reaction pathways are labeled as well, with the *si* pathway leading to **109SR** taking place suprafacially with respect to the three-carbon component and antarafacially with respect to the one-carbon component. Heating **108** at 275°C produced 58% of **109SR**, 5% of **109RS**, 33% of **109SS**, and 4% of **109RR**.²¹⁴ This distribution of **109** stereoisomers indicated that products arising from the two suprafacial pathways (*sr* and *si*) resulted in 91% of product, while the two antarafacial pathways (*ar* and *ai*) led to only 9% of the product. Moreover, the ratio of product formed from the pathways allowed by the conservation of orbital symmetry (*si* and *ar*) to product arising from the

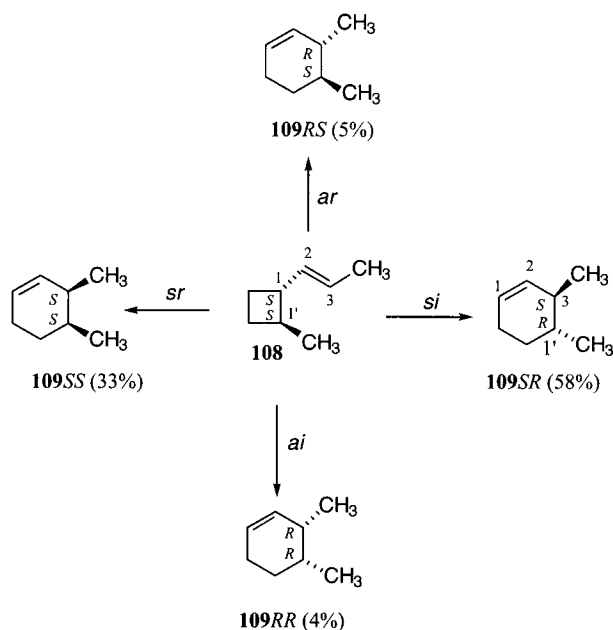


FIGURE 11.111
Possible stereochemical outcomes of [1,3] carbon shifts in **108**.

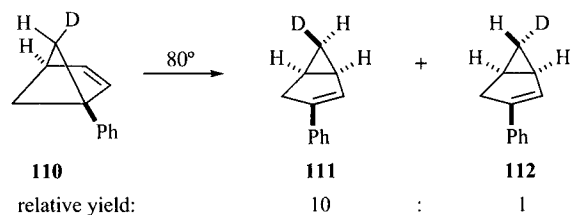
²¹² Baldwin, J. E.; Burrell, R. C. *J. Am. Chem. Soc.* **2001**, *123*, 6718.

²¹³ Leber, P. A.; Baldwin, J. E. *Acc. Chem. Res.* **2002**, *35*, 279.

²¹⁴ Other products, thought to have been formed by radical processes, accounted for 70% of the reactant.

FIGURE 11.112

Rearrangement of **110** to a 10:1 ratio of **111** to **112**. (Adapted from reference 217.)



forbidden pathways (*sr* and *ai*) was 1.7 : 1. Baldwin and co-workers therefore concluded that [1,3] sigmatropic carbon shifts are not true pericyclic reactions. Instead, they were thought to involve C–C bond cleavage to form one or more diradicals on a relatively flat potential energy surface.²¹³

Similarly, the thermal rearrangement of 1-phenylbicyclo[2.2.1]hexene-5-*d* (**110**) produced a 10 : 1 ratio of **111** to **112** (Figure 11.112). This result might suggest that **111** is formed by a concerted, symmetry-allowed antarafacial [1,3] sigmatropic pathway (*si*) but that **112** arises from a competing radical or symmetry-forbidden (*sr*) concerted pathway. Newman-Evans and Carpenter determined, however, that the product ratio of **111** to **112** is invariant over the temperature range from 80°C to 165°C, and a similar result was also observed for rearrangements of some related compounds. The investigators concluded that it is unlikely that two competing processes would be found to have identical activation energies for several different reactants. Thus, the results suggested that there is one rate-limiting step, the formation of a biradical intermediate that leads to both **111** and **112**.²¹⁵

To explain the preferential formation of **111**, Carpenter suggested that the reaction of **110** is not determined solely by the shape of the local potential energy surface at the intermediate. Rather, it was proposed that dynamic effects—the conservation of linear and angular momentum—govern nuclear motion as the molecule passes through the transition structure and then proceeds to one or the other of the products. According to this model, **111** is formed in higher yield because it results from a continuation of the nuclear motions that began with bond breaking and led to the formation of the diradical.²¹⁶ The results of semiempirical calculations of the potential energy surface for the rearrangement of **110** were consistent with this explanation.²¹⁷ Carpenter concluded that a dynamic preference for inversion in ring-opening reactions of strained-ring compounds might mean that a [1,*n*] sigmatropic shift need not be a pericyclic reaction at all.²¹⁷

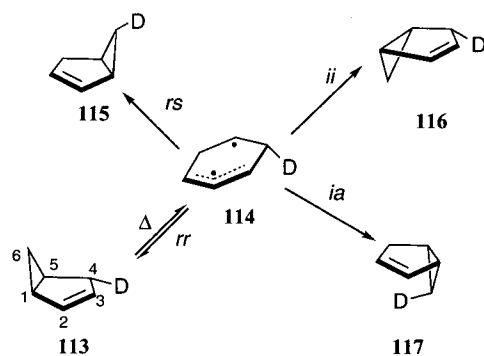
This model for the thermal rearrangement of 1-phenylbicyclo[2.2.1]hexene provides an explanation for the stereochemistry observed in the [1,3] methyl shift. More important, it also brings into question some of the common assumptions of reaction kinetics.²¹⁸ Transition state theory is based on the premise that the redistribution of internal kinetic energy is faster than is the progress of a collisionally activated reactant over a potential energy surface to a transition state and then to a product. If this assumption is not valid, then the

²¹⁵ Newman-Evans, R. H.; Carpenter, B. K. *J. Am. Chem. Soc.* **1984**, *106*, 7994.

²¹⁶ Newman-Evans, R. H.; Simon, R. J.; Carpenter, B. K. *J. Org. Chem.* **1990**, *55*, 695.

²¹⁷ Carpenter, B. K. *J. Org. Chem.* **1992**, *57*, 4645 and references therein.

²¹⁸ Carpenter, B. K. *Angew. Chem. Int. Ed.* **1998**, *37*, 3340; *Annu. Rev. Phys. Chem.* **2005**, *56*, 57; in Moss, R. A.; Platz, M. S.; Jones, M., Jr., Eds. *Reactive Intermediate Chemistry*; John Wiley & Sons, Hoboken, NJ, 2004, pp. 925–960.

**FIGURE 11.113**Rearrangement of deuterium-labeled bicyclo[3.1.0]hex-2-ene (**113**).

same mechanism can lead to different products because there are different populations of structures, characterized not by bonding differences but by different distributions of internal kinetic energy, traveling over the potential energy surface.²¹⁹

Houk and co-workers reported a theoretical study of the degenerate rearrangement of bicyclo[3.1.0]hex-2-ene labeled with deuterium in the 4-exo position (**113** in Figure 11.113) that offers additional insight into the nonstatistical dynamics model of reactivity.²²⁰ Breaking the C1–C5 bond of **113** leads to a diradical (**114**) that can reclose to **113** with retention of configuration at both C1 and C5 (the *rr* path), can close suprafacially to **115** with retention at C5 (the *rs* path), can close to **116** with inversion at both C1 and C5 (the *ii* path), or can close antarafacially to **117** with inversion at C5 (the *ia* path). Baldwin and Keliher had reported that the activation parameters for formation of **115**, **116**, and **117** are identical and that the ratio of relative rate constants $k_{rs} : k_{ii} : k_{ia}$ is 48 : 36 : 16.²²¹

Houk and co-workers calculated the potential energy surface (Figure 11.114) for the reaction and found a broad, shallow high energy plateau for the diradical intermediate. They also found four transition structures (each lying no more than 0.2 kcal/mol higher than the energy minimum) separating **114** from the products. The plateau was thus termed a **caldera** because it resembles the surface features associated with a collapsed volcanic cone. In Figure 11.114, the arrow from the transition structure nearest **113** shows the transition vector leading from **113** to the caldera. By sampling trajectories over the surface with quasiclassical direct dynamics, Houk and co-workers determined that nearly all the trajectories passed through the caldera to one of the products much more quickly than the internal kinetic energy of the atoms could be redistributed to other vibrational modes. A very simple summary of the dynamics is that most trajectories lead slightly to the left or to the right of the arrow in Figure 11.114, and that accounts for the greater yield of **115** and **116** than **117**. These results remind us that an experimental result that is consistent with a prediction based on the principles of orbital symmetry cannot by itself establish that the reaction is pericyclic. It

²¹⁹ As Carpenter (reference 218) noted, this nonstatistical dynamics model can explain how an optically active reactant could produce an optically active product even though the mechanism appears to involve an achiral intermediate.

²²⁰ Doubleday, C.; Suhrada, C. P.; Houk, K. N. *J. Am. Chem. Soc.* **2006**, *128*, 90.

²²¹ Baldwin, J. E.; Keliher, E. J. *J. Am. Chem. Soc.* **2002**, *124*, 380.

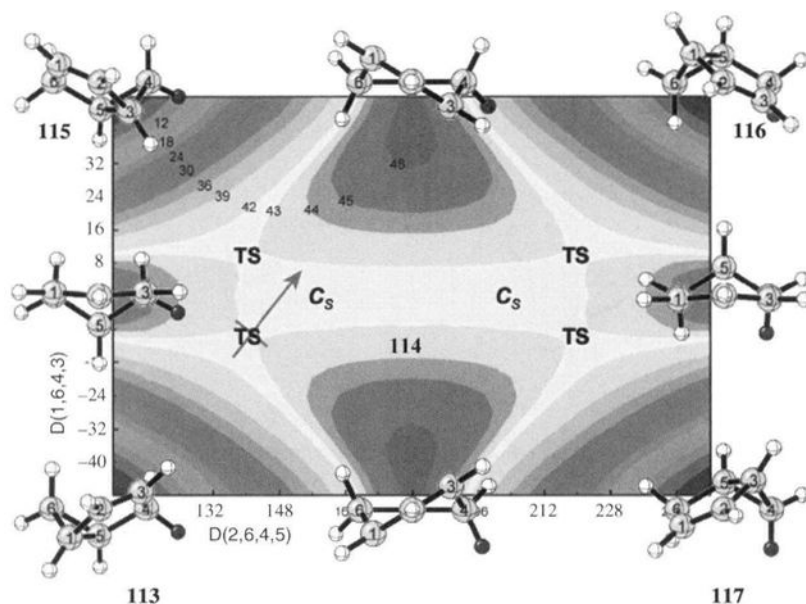
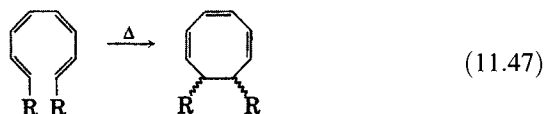


FIGURE 11.114
Contour drawing of the potential energy surface for reaction of **113**.
(Adapted from reference 220.)

must always be considered possible that other processes, perhaps unrecognized, could lead to the same product.

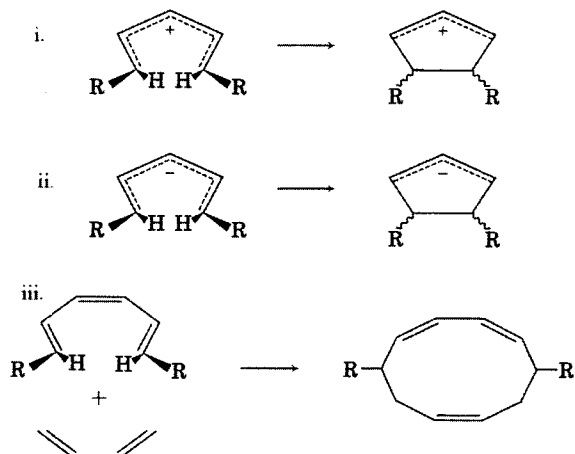
Problems

- 11.1.** Using the HOMO method given by Woodward and Hoffmann in their first communication on orbital symmetry control of chemical transformations,¹³ determine whether the thermal reaction shown in equation 11.47 should take place via a conrotatory or disrotatory pathway. Indicate the stereochemistry of the product formed by the allowed pathway. Do the same for the photochemical reaction.

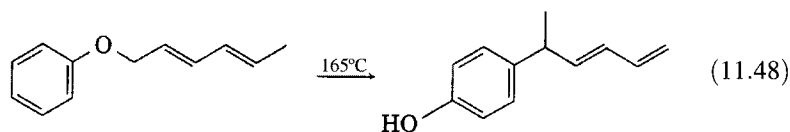


- 11.2.** Use the symmetry and nodal properties of the appropriate molecular orbitals to determine whether the thermal [1,7] and [1,9] hydrogen shifts are allowed suprafacially or antarafacially.
- 11.3.** Through the use of appropriate MO symmetry elements for reactants and products, determine whether the thermal $[\pi 2_s + \pi 6_s]$ and $[\pi 4_s + \pi 4_s]$ cycloaddition reactions are allowed or forbidden.
- 11.4.** Construct a figure similar to Figure 11.41 (page 722) to demonstrate that the photochemical antarafacial–antarafacial [3,3] sigmatropic rearrangement is forbidden by the principles of orbital symmetry.
- 11.5.** Construct a MO correlation diagram similar to Figure 11.66 (page 737) to show that the photochemical Diels–Alder reaction is forbidden by the principles of orbital symmetry.

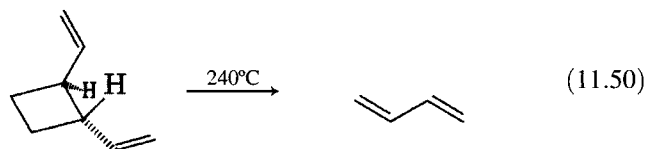
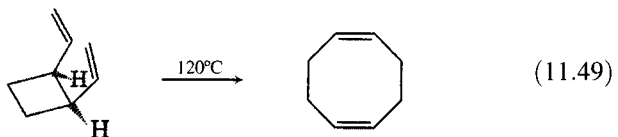
- 11.6. Use both MO and state correlation diagrams to predict the stereochemistry of the opening of the cyclopropyl anion to the allyl anion (Figure 11.72, page 743); do the same for the opening of the cyclopropyl cation to the allyl cation.
- 11.7. a. Using $-\beta$ instead of β for one p - p overlap of the type $(+)(-)$ illustrated in Figure 11.101 (page 765), calculate the energy levels of a Möbius cyclopropenyl system and verify that they are identical with those given by the circle mnemonic (Figure 11.104, page 767).
- b. Having calculated the Möbius MOs in part a, consider again the opening of cyclopropyl systems to allyl systems. Draw an MO correlation diagram (as was done for 1,3-butadiene-cyclobutene in Figure 11.107, page 769) and discuss the energetics and probable activation energies for the allowed and forbidden reactions in both cases. Discuss the diagram in terms of aromaticity of transition structures and in terms of HOMO-LUMO crossing.
- 11.8. For each of the following concerted reactions:
- Sketch one sterically feasible transition structure for a pathway that is allowed by the principles of orbital symmetry.
 - Indicate the stereochemistry of substituents in the products.
 - Classify the reaction using the usual formalism (e.g., $\pi 2_a$).
 - Use correlation arrows to indicate the bonding change(s) at each center.
 - Decide whether the reaction is thermally allowed or forbidden (stating the answer in terms of the generalized selection rule on page 755).
 - Classify the transition structure as Hückel aromatic or Möbius aromatic.



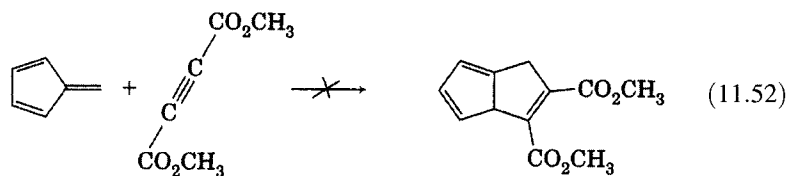
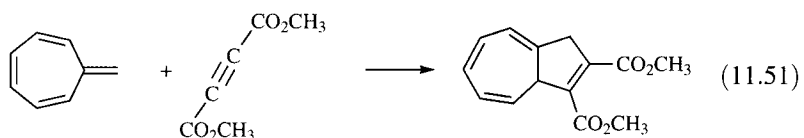
- 11.9. Classify the reaction in equation 11.48 as an allowed $[i,j]$ sigmatropic reaction, and state whether the pathway is suprafacial-suprafacial or suprafacial-antarafacial.



- 11.10. Explain the difference in reactivity between *cis*- and *trans*-1,2-divinylcyclobutane shown in equations 11.49 and 11.50.

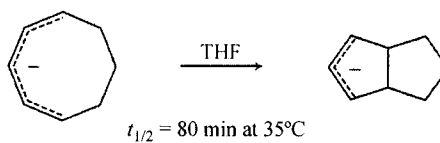


11.11. The reaction shown in equation 11.51 occurs readily, but the reaction shown in equation 11.52 does not. Explain this difference in reactivity.

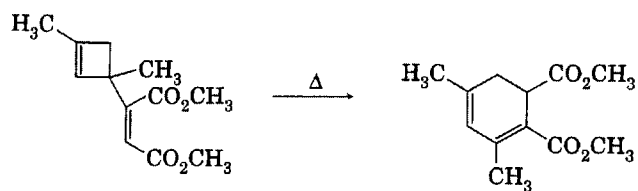


11.12. Describe each reaction below as the result of one or more allowed pericyclic reactions.

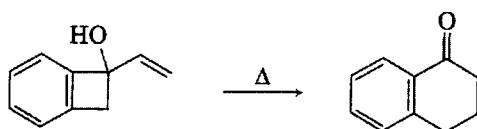
a.



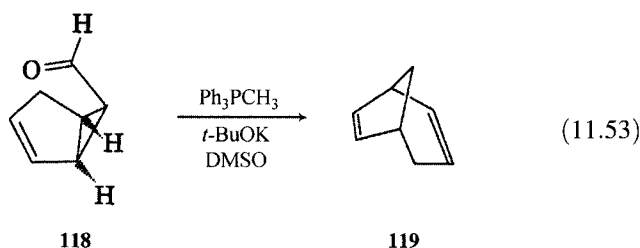
b.



c.

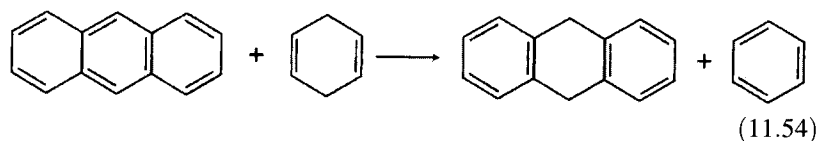


- 11.13. The reaction of bicyclo[3.1.0]hex-2-ene-*cis*-6-carboxaldehyde (**118**) with the ylide produced from a methyltriphenylphosphonium salt and potassium *t*-butoxide in DMSO produced bicyclo[3.2.1]octadiene (**119**, equation 11.53). There was evidence for an unstable initial product that rearranged with a rate constant of about 10^{-5} s^{-1} in cyclohexane solution at room temperature to produce the final product. What is the structure of the initial product, and why does it react so rapidly to produce **119**?



- 11.14. The Claisen rearrangement of allyl 2,6-dimethylphenyl ether produces both 4-allyl-2,6-dimethylphenol and 2-allyl-4,6-dimethylphenol.²²² If the reaction is interrupted before completion, some methallyl 2-allyl-6-methylphenyl ether can be isolated. Explain the formation of each of these products, and discuss the mechanism of the *para* Claisen rearrangement in view of these results.

- 11.15. Is the suprafacial-suprafacial hydrogen atom transfer reaction illustrated in equation 11.54 an allowed or forbidden reaction?

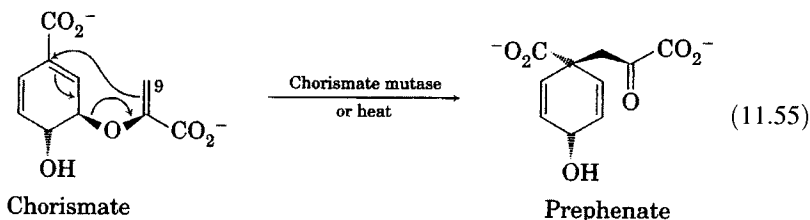


- 11.16. Benzyne can be produced by the reaction of magnesium with *o*-bromofluorobenzene in THF solution.²²³ The reaction of benzyne produced in this way with 2,5-dimethyl-2,4-hexadiene did not lead to a Diels-Alder adduct. Instead, the product isolated from the reaction mixture was 2,5-dimethyl-3-phenyl-1,4-hexadiene. Propose a mechanism for the formation of this compound.

²²² Methallyl is the 2-methyl-2-propenyl group.

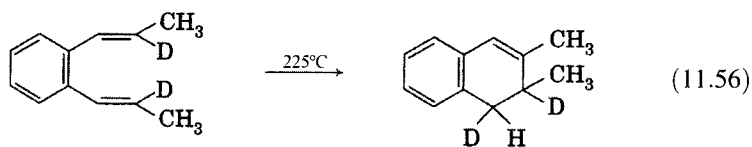
²²³ Wittig, G. *Org. Synth., Coll. Vol. 4* 1963, 964.

- 11.17. Consider the dianions chorismate and prephenate, which are shown in equation 11.55. The enzyme-catalyzed [3,3] sigmatropic shift of chorismate to prephenate is an important step in a biosynthetic pathway leading to several aromatic compounds. The reaction also occurs, although considerably more slowly, at elevated temperatures in aqueous solution. To determine whether the [3,3] sigmatropic reaction involves a chair- or boat-like transition structure, researchers prepared (*E*) and (*Z*) derivatives of chorismate by replacing one protium with tritium (represented by T or ^3H) at C9. They then followed the course of the reaction by monitoring the location of tritium in the product with the enzyme phenylpyruvate tautomerase, which preferentially releases the pro-*R* hydrogen atom of prephenate in the form of water.

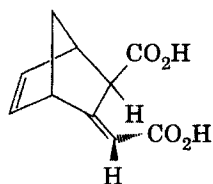


The investigators found that both the thermal and enzyme-catalyzed reactions of (*E*)-[9- ^3H]chorismate led to rapid release of tritiated water, whereas the reactions of the (*Z*) isomer did not. From this they concluded that both the enzyme-catalyzed and thermal reactions involve a chair-like transition structure.

- Show that the chorismate to prephenate reaction is a [3,3] sigmatropic rearrangement.
 - Draw the structures of the (*E*) and (*Z*) forms of [9- ^3H]chorismate.
 - Show that the (*E*) isomer leads to the (*S*) configuration of the labeled carbon atom in prephenate if the transition structure for the reaction resembles a cyclohexane boat conformation but that the (*R*) configuration results if the transition structure is similar to a cyclohexane chair conformation.
 - Show that removing the pro-*R* hydrogen (protium or tritium) atom from the labeled carbon atom of prephenate will produce tritiated water if the reaction of (*E*)-[9- ^3H]chorismate does indeed involve the chair conformation in the transition
- 11.18. The Claisen rearrangement of allyl 2,6-dimethylphenyl ether normally produces 4-allyl-2,6-dimethylphenol as the major product. When the reaction was carried out in molten maleic anhydride at 200°C, however, two products having the molecular formula $\text{C}_{15}\text{H}_{16}\text{O}_4$ were isolated in addition to 4-allyl-2,6-dimethylphenol. What are the two compounds, and what does their isolation indicate about the mechanism of the reaction?
- 11.19. Explain the following reaction in terms of two consecutive pericyclic reactions, one an electrocyclic reaction and one a sigmatropic reaction.

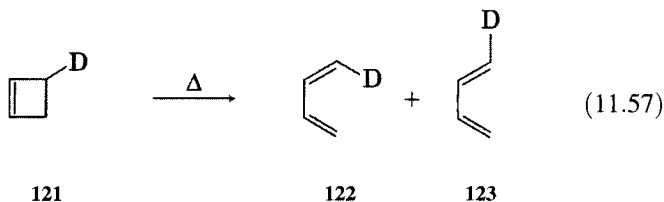


- 11.20. Both 2-acetoxy-*trans*-3-heptene and 4-acetoxy-*trans*-2-heptene were found to give a similar mixture of 1,3-heptadiene and 2,4-heptadiene upon heating at 350–360°C in the gas phase. Examination of recovered starting material revealed it to consist of a mixture of 60% of the 2-acetoxy compound and 40% of the 4-acetoxy compound, no matter which had been the reactant. Rationalize these results.
- 11.21. The Diels–Alder reaction of (–)-pentadienedioic acid ($\text{HO}_2\text{CCH}=\text{C}=\text{CH}-\text{CO}_2\text{H}$) with cyclopentadiene yields an adduct (**120**) having the absolute stereochemistry shown. What is the absolute configuration of (–)-pentadienedioic acid?



120

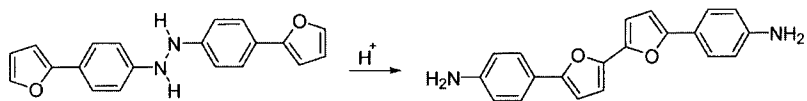
- 11.22. Upon heating, $[3\text{-}^2\text{H}]$ cyclobutene (**121**) forms products **122** and **123** in a ratio of 1.10: 1.0. The rate constant for reaction of unlabeled cyclobutene under the reaction conditions is $8.93 \times 10^{-5}\text{s}^{-1}$, while that of **121** is $8.17 \times 10^{-5}\text{s}^{-1}$.



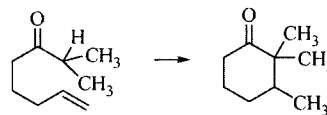
- Assume that the reaction takes place by a conrotatory pathway so that the deuterium atom can go either toward the inside to form **122** or toward the outside to form **123**. What are the individual rate constants for the formation of **122** and **123**?
- Using the results from part a, calculate the deuterium isotope effect ($k_{\text{H}}/k_{\text{D}}$) for the deuterium going inside, as well as $k_{\text{H}}/k_{\text{D}}$ for the deuterium going outside. (Remember to divide the total rate constant for reaction of the nondeuterated compound by 2 to account for the two possible modes of reaction.)
- What kind of isotope effect is this (i.e., 1° , 2° ; α , β , etc.)? Are the isotope effects normal or inverse? What does the result indicate about the degree to which an orbital from carbon to protium experiences hybridization change in the transition structure if it is inside compared to when it is outside? Discuss the significance of this result with regard to the model usually assumed for the electrocyclic reaction.

11.23. Propose a mechanism for the following reactions and characterize each as a kind of pericyclic reaction.

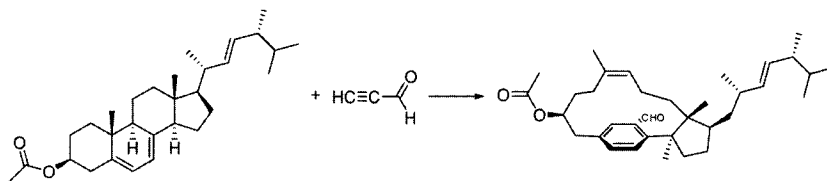
a.



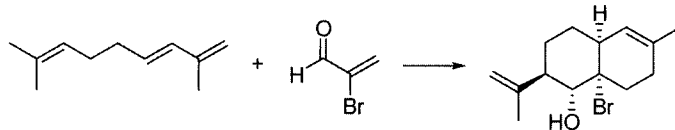
b.



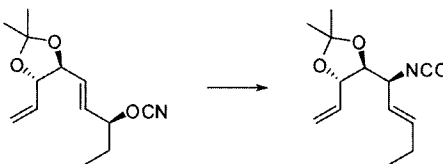
c.



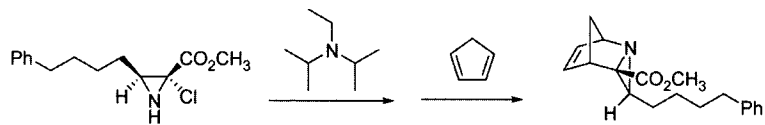
d.



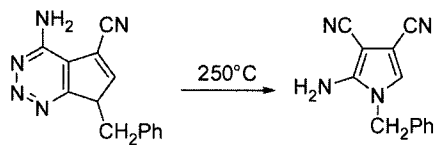
e.



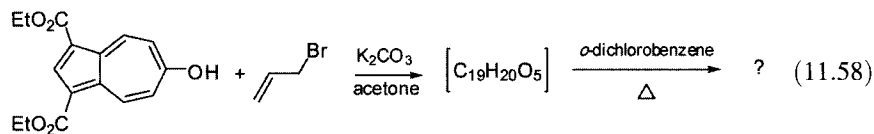
f.



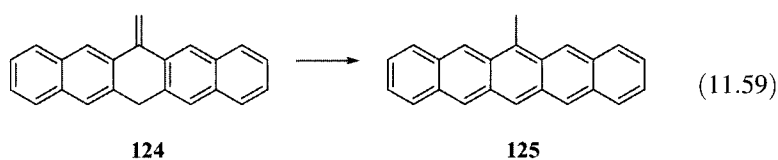
g.



11.24. The reaction in equation 11.58 produces an intermediate with molecular formula $C_{19}H_{20}O_5$ that undergoes an electrocyclic reaction to give a product that also has molecular formula $C_{19}H_{20}O_5$. What are the structures of the intermediate and the product?

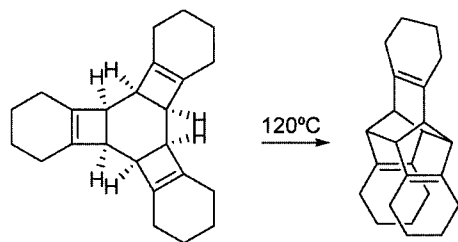


11.25. The ΔH^\ddagger for the [1,5] sigmatropic reaction of **124** to form **125** (equation 11.59) has been calculated to be 67 kcal/mol, even though the reaction is nearly thermo-neutral. Why should the activation barrier be so high?

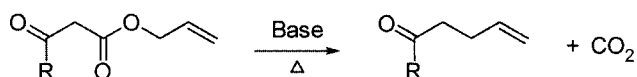


11.26. Propose a mechanism for the following transformations:

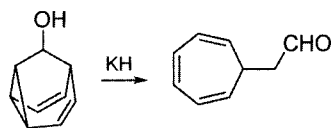
a.



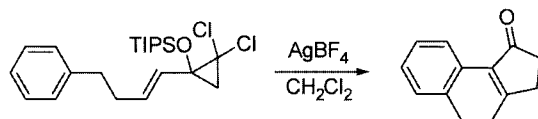
b.



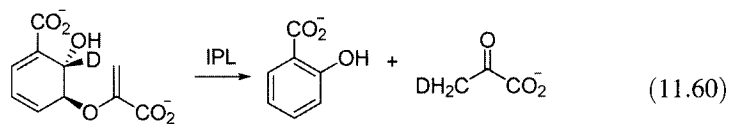
c.



d.

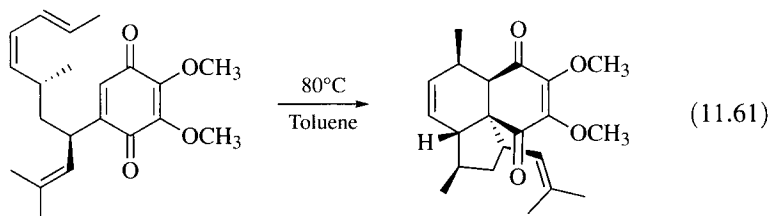


11.27. Propose a mechanism for the enzymatic reaction in equation 11.60.

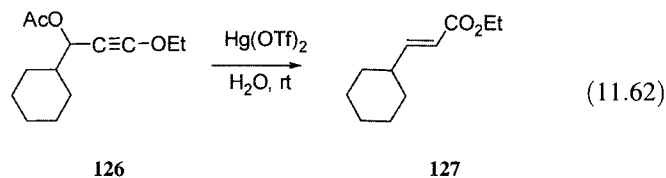


IPL = isochorismate pyruvate lyase from *pseudomonas aeruginosa*

11.28. Propose a transition structure to account for product stereochemistry in the intramolecular Diels–Alder reaction shown in equation 11.61.

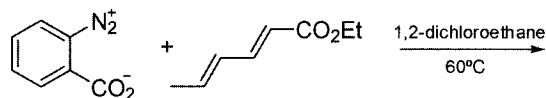


11.29. Propose a mechanism to explain how the mercuric triflate-catalyzed hydration of **126** produces **127**.

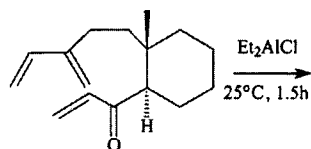


11.30. Predict the product of the following reactions:

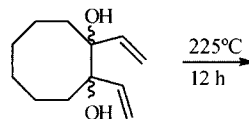
a.



b.



c.



Photochemistry

12.1 PHOTOPHYSICAL PROCESSES

Energy and Electronic States

Photochemistry is broadly defined as the study of chemical reactions caused by ultraviolet–visible (UV–vis) radiation, which is in the wavelength range from 200 to 700 nm.^{1–3} Promotion of an electron from a lower energy molecular orbital to a higher energy orbital upon absorption of UV–vis radiation produces an electronically excited state (Figure 12.1). The high energy and the altered electron distribution of the photoexcited molecule can lead to a variety of physical processes and chemical reactions. The concepts of structure and bonding, stereochemistry, reactive intermediates, and reaction type that were developed for thermal reactions also provide a foundation for the study of photochemical reactions. In particular, molecular orbital theory and valence bond theory are useful complementary models in organic photochemistry. MO theory is particularly effective in describing the spectroscopy of ground and excited states. Valence bond models provide useful depictions of electronically excited molecules in terms of the chemical properties of ground state reactive intermediates.

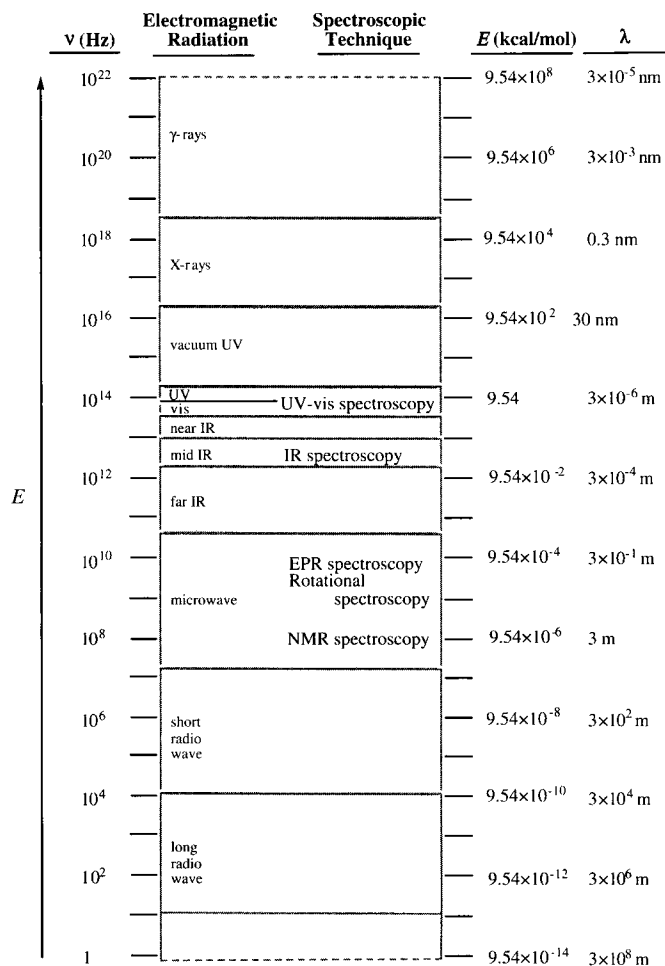
Energy levels of molecules are quantized, as shown schematically in Figure 12.2, so only certain energy values are allowed.⁴ Superimposed on each electronic state (E_0, E_1, \dots) is a set of vibrational energy levels (v_0, v_1, \dots)

¹ For a glossary of terms used in photochemistry, see (a) Pitts, J. N., Jr.; Wilkinson, F.; Hammond, G. S. *Adv. Photochem.* **1963**, *1*, 1; (b) Braslavsky, S. E. *Pure Appl. Chem.* **2007**, *79*, 293.

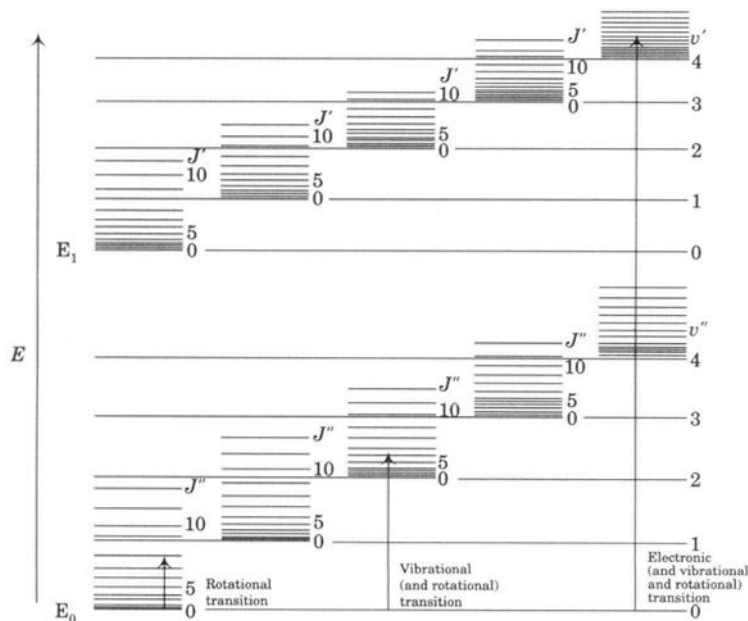
² For a summary of a wide variety of photochemical reactions of organic compounds, see Horspool, W.; Lenci, F., Eds. *CRC Handbook of Organic Photochemistry and Photobiology*, 2nd ed.; CRC Press: Boca Raton, FL, 2004.

³ Gordon, A. J.; Ford, R. A. *The Chemist's Companion*; John Wiley & Sons: New York, 1972; 166.

⁴ Moore, W. J. *Physical Chemistry*, 3rd ed.; Prentice Hall: Englewood Cliffs, NJ, 1962; p. 581 ff.

**FIGURE 12.1**

Frequencies, radiation types, spectroscopic regions, energies, and wavelengths of electromagnetic radiation of interest to chemists. (Note that the vertical scale is logarithmic. Based on data in reference 3.)

**FIGURE 12.2**

A generalized set of energy levels for an organic molecule. (Adapted from reference 4).

and, with smaller divisions still, a set of rotational energy levels (J_0, J_1, \dots).⁵ A molecule in its ground electronic state may be excited to a higher electronic, vibrational, or rotational energy level (as shown by the arrows in Figure 12.2) either by absorbing a photon of UV–vis radiation corresponding exactly to the energy difference between the initial and final states or through energy transfer from another molecule. A transition from one rotational energy level to another (within the same electronic and vibrational energy levels) needs only a small amount of energy, so the transition can be caused by microwave radiation. Changes from one vibrational level to another (within the same electronic state) involve radiation in the infrared region of the spectrum. A transition from the ground electronic state to a higher electronic state generally requires radiation in the UV–vis region, and such transitions give rise to photochemistry.

Photochemistry is inherently related to **photophysics**, the study of those radiative and nonradiative processes that convert one electronic state into another electronic state without chemical change.^{1b,6} Central to both photochemistry and photophysics is the classification of UV–vis radiation in terms of its **energy**. Because electromagnetic radiation is quantized, it has properties like those of a particle, and a mole of photons is called an **einstein**.⁶ Electromagnetic radiation also has the properties of a wave, and equation 12.1 gives the relationship between the energy of UV–vis radiation in kcal/mol and its wavelength in nm.⁷

$$E(\text{kcal/mol}) = h\nu = \frac{hc}{\lambda} = \frac{2.86 \times 10^4}{\lambda(\text{nm})} \quad (12.1)$$

In addition to units of kcal/mol, energy is often given in electron volts (eV). It is also convenient to express the energy of spectroscopic transitions in wave numbers ($\bar{\nu}$), also known as reciprocal centimeters because the units are cm^{-1} .⁸ It is important to distinguish between the **energy** of a particular wavelength of UV–vis radiation (measured in kcal or kJ per mole of photons) and the **radiant power** (measured in watts) of a particular source.⁹ A beam of low energy electromagnetic radiation with high radiant intensity (such as an infrared laser) is generally capable of causing only vibrational changes, but it

⁵ By convention in physical chemistry, vibrational levels and rotational levels of the ground electronic state are denoted with double primes, as in v'' and J'' , respectively. Vibrational levels and rotational levels of the excited electronic state are denoted with single primes, as in v' and J' . Often, however, organic photochemists omit the double prime notation for the ground electronic state. Also, the vibrational quantum levels may be denoted as v or V instead of v .

⁶ Turro, N. J. *Modern Molecular Photochemistry*; Benjamin/Cummings Publishing: Menlo Park, CA, 1978.

⁷ Organic photochemists often use units of nanometers (nm, 10^{-9} m) for wavelength, but another common unit is the angstrom (\AA , 10^{-8} cm; $1 \text{ nm} = 10 \text{ \AA}$).

⁸ These units may be interconverted by the relationship $1 \text{ eV} = 23.06 \text{ kcal/mol} = 8063 \text{ cm}^{-1}$. For a more complete discussion of units, see Gordon, A. J.; Ford, R. A. *The Chemist's Companion*; Wiley-Interscience: New York, 1972; p. 166.

⁹ One watt is equal to one J s^{-1} .

TABLE 12.1 Energy Content of Different Wavelengths of UV-vis Radiation

λ (nm)	$\bar{\nu}$ (cm ⁻¹)	ΔE (kcal/mol)	ΔE (eV)
200	50,000	143.0	6.20
250	40,000	114.4	4.96
300	33,333	95.5	4.14
350	28,571	81.7	3.54
400	25,000	71.5	3.10
450	22,222	63.6	2.76
500	20,000	57.2	2.48

can do so in a large number of molecules.¹⁰ A weak beam of high energy UV-vis radiation can cause electronic transitions, although in relatively fewer molecules.

A tabulation of UV-vis radiation energies as a function of wavelength is given in Table 12.1. UV-vis radiation with a wavelength of 300 nm has energy of ca. 96 kcal/mol, which is greater than the bond dissociation energy of many single bonds. Thus, radiation of this wavelength could be used to photodissociate organic molecules and can cause other chemical processes as well.

Designation of Spectroscopic Transitions

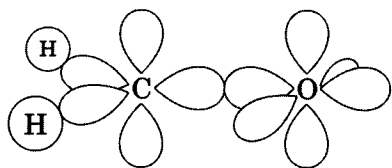
In organic photochemistry, spectroscopic transitions are often designated by terms indicating the change in electron population of molecular orbitals that is caused by the absorption of UV-vis radiation. Consider the representation of the molecular orbitals of formaldehyde proposed by Mulliken, in which the carbon atom σ bond is considered to be formed by overlap of an sp^2 hybrid orbital on carbon with a p orbital on oxygen.^{11,12} A pictorial representation of the atomic orbitals that are the basis set for the MOs is shown Figure 12.3, and the energies of the calculated set of MOs are given in Figure 12.4. The HOMO for formaldehyde is described as a nonbonding (n) orbital that is localized on oxygen and that lies in the plane of the molecule, while the LUMO is a π^*_{C-O} orbital. Thus, the lowest energy possible for an electronic transition is an $n \rightarrow \pi^*$ (pronounced “ n to π star”) transition.¹³ A higher energy transition

¹⁰ In this discussion we are ignoring the possibility of **multiphoton excitation**, in which two or more photons of lower energy light can be absorbed within a short time to produce an electronically excited state. Multiphoton infrared excitation can lead to significant photochemical reactions. See, for example, (a) Lewis, F. D.; Buechele, J. L.; Teng, P. A.; Weitz, E. *Pure Appl. Chem.* **1982**, *54*, 1683; (b) Lupo, D. W.; Quack, M. *Chem. Rev.* **1987**, *87*, 181. For a review of high intensity laser photochemistry of organic compounds, see Wilson, R. M.; Schnapp, K. A. *Chem. Rev.* **1993**, *93*, 223. Absorption of intense UV laser radiation can lead to controlled explosive decomposition of materials, a process known as *ablation*. For an introduction, see Srinivasan, R. *Science* **1986**, *234*, 559; for a specific application, see Srinivasan, R.; Ghosh, A. P. *Chem. Phys. Lett.* **1988**, *143*, 546.

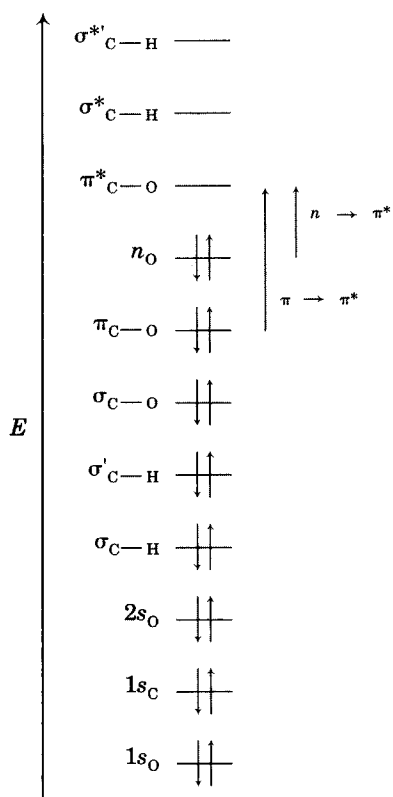
¹¹ Sidman, J. W. *Chem. Rev.* **1958**, *58*, 689. Also see the discussion in reference 6, pp. 21–22.

¹² This very simple representation of the molecular orbitals of formaldehyde provides a convenient model for describing the spectroscopy and photochemistry of carbonyl compounds, but more advanced representations may be needed in other cases. See, for example, Laing, M. J. *Chem. Educ.* **1987**, *64*, 124; Wiberg, K. B.; Marquez, M.; Castejon, H. J. *Org. Chem.* **1994**, *59*, 6817.

¹³ The notation used for these transitions is attributed to Michael Kasha (footnote 9 in reference 1a). Kasha's contributions to chemistry were summarized by Barbara, P.; Nicol, M.; El-Sayed, M. A. J. *Phys. Chem.* **1991**, *95*, 10215. See also Hochstrasser, R.; Saltiel, J. J. *Phys. Chem. A* **2003**, *107*, 3161.

**FIGURE 12.3**

Basis set atomic orbitals for MOs of formaldehyde.

**FIGURE 12.4**

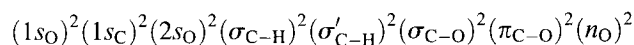
MO energy level diagram for formaldehyde showing $n \rightarrow \pi^*$ and $\pi \rightarrow \pi^*$ transitions.

is the $\pi \rightarrow \pi^*$ (pronounced “ π to π star”) transition. In principle, many other electronic transitions may be seen by irradiating the compound with UV–vis radiation having enough energy to move an electron from a lower energy bonding MO to the LUMO or from the HOMO to a higher energy antibonding orbital. In practice, however, the two transitions shown in Figure 12.4 are the ones typically responsible for the spectroscopic characteristics and photochemical reactions of carbonyl compounds.

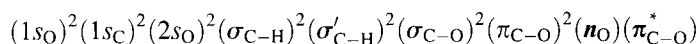
In order to give a complete description of an electronic state, it is necessary to specify fully its **configuration**—the population of electrons in each molecular orbital.¹⁴ The ground state of formaldehyde is¹⁵

¹⁴ More precisely, states can be described by combinations of configurations. In the discussion here, however, each state is associated with only one configuration. For a discussion of configurations, see reference 6.

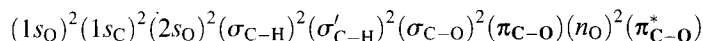
¹⁵ This term is pronounced “S zero.” In the configuration on the following line, the first term in parentheses is $1s_O$ (“one s sub oh”) meaning the $1s$ orbital on oxygen. Although they appear similar at first glance, the terms S_0 and $1s_O$ have very different meanings. The term S_0 refers to a designation of all occupied orbitals, while the term $1s_O$ indicates one particular orbital only.



The lowest energy excited state is



and the next lowest energy excited state is



In each case, the orbitals that are populated differently from the ground state are shown in bold. Such a detailed description of the electronic configuration is cumbersome, so it is useful to adopt a shorthand representation for the same information. The notation specifies the configuration of the excited state by noting the type of transition that produced it. Thus, the lower energy excited state is denoted an n, π^* state, and the higher energy excited state is called a π, π^* state.^{16,17}

One additional bit of information must be added to the description of an electronic state. In the ground electronic state of most organic molecules, all of the electrons are in doubly occupied orbitals, and two electrons in the same orbital must have their spins paired. Electrons in different MOs may either have their spins paired or unpaired. If all of the electrons are paired, the state is said to be a **singlet** state. A configuration having two electrons with the same spin is said to be a **triplet** state. States that have the same number of unpaired electrons are said to have the same **multiplicity**.¹⁸ The electronic ground state of most organic molecules has no unpaired electrons and is termed the S_0 state. The lowest energy excited singlet state is denoted S_1 , and the next lowest energy excited singlet state is called S_2 . The two lowest triplets are denoted T_1 and T_2 .¹⁹ Figure 12.5 shows the electron configurations of these states for formaldehyde.

Photophysical Processes

It is useful to represent the energies of electronic states and the processes that interconvert them with a **Jablonski diagram** (Figure 12.6).²⁰ The vertical scale represents potential energy. The horizontal scale has no particular significance; it merely allows us to separate the sets of energy levels for the singlet

¹⁶ Alternatively, these states may be denoted $n-\pi^*$ and $\pi-\pi^*$, respectively.

¹⁷ The terms used in this sentence are usually pronounced as an "n to pi* state" and a "pi to pi* state." As noted on page 790, the electronic transition leading to these states are usually written with arrows as $n \rightarrow \pi^*$ and $\pi \rightarrow \pi^*$ transitions, respectively.

¹⁸ The multiplicity (m) of a state is given by $m = 2S + 1$, where S is the total spin quantum number of the state. A species in which all the electrons are paired is called a singlet state ($m = 2 \times 0 + 1 = 1$), a radical with one unpaired electron is termed a doublet state ($m = 2 \times \frac{1}{2} + 1 = 2$), and a biradical or excited state with two unpaired electrons is called a triplet ($m = 2 \times 1 + 1 = 3$). For a discussion of the research of G. N. Lewis and the association of the triplet state with phosphorescence of organic compounds, see Kasha, M. J. *Chem. Educ.* **1984**, *61*, 204.

¹⁹ It might be argued that the state called T_1 should be called T_0 , since it is the lowest energy triplet state possible for a given molecule. Nevertheless, the subscript 0 is reserved for the ground electronic state of a molecule. In the case of structures such as diradicals for which the ground state is a triplet state, T_0 would be the ground state designation.

²⁰ For a discussion, see Wilkinson, F. Q. *Rev. Chem. Soc.* **1966**, *20*, 403.

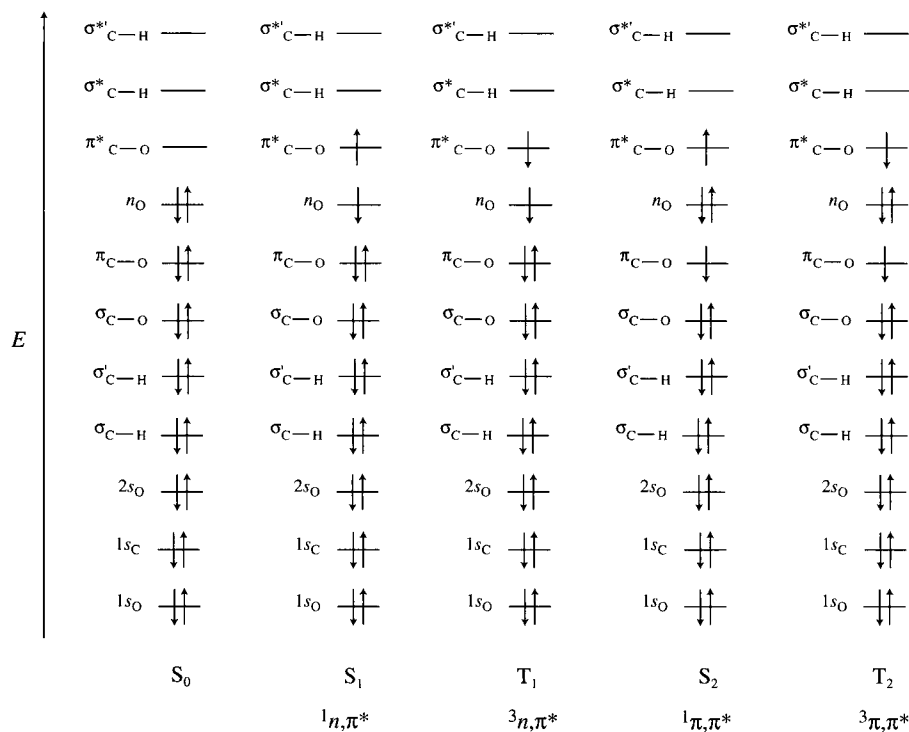


FIGURE 12.5

Electron distributions in the S_0 , S_1 , T_1 , S_2 , and T_2 states of formaldehyde.

and triplet states (known as the singlet and triplet **manifolds**) so that the excited states are more clearly distinguished. Superimposed on each electronic state is a set of vibrational energy levels. For the sake of clarity, Figure 12.6 does not show the sets of rotational energy levels superimposed on the vibrational energy levels.

There are two kinds of photophysical processes indicated in Figure 12.6. Those interconversions denoted by straight lines are **radiative processes**,

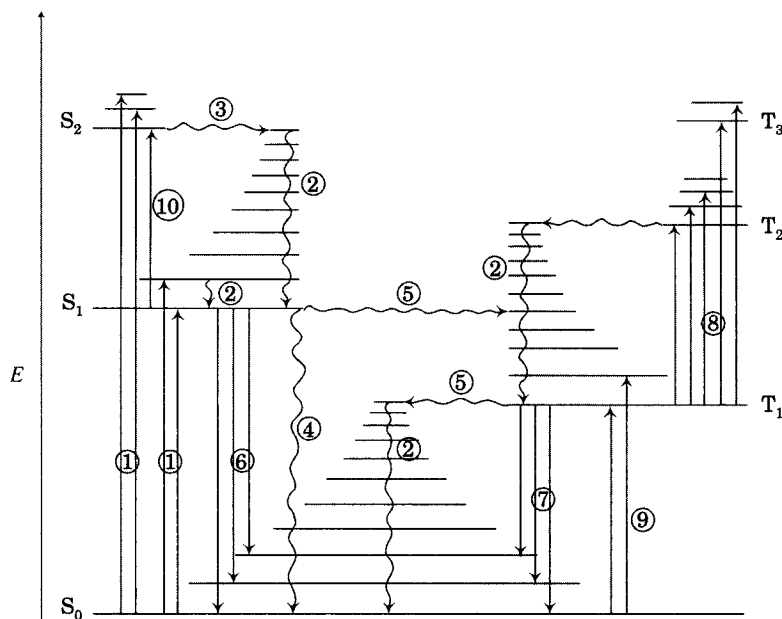


FIGURE 12.6

A Jablonski diagram. (Adapted from reference 20.)

which occur through the absorption or emission of light. Those indicated by wavy lines are **nonradiative processes**, which occur without radiation being absorbed or emitted.²¹ The numbers on the lines correspond to the following processes:

- 1. Absorption.** A ground state molecule (S_0) may absorb a photon of UV–vis radiation, thus becoming an excited singlet state. The most commonly seen transitions are $S_0 \rightarrow S_1$ or $S_0 \rightarrow S_2$, but S_0 to higher excited singlet state transitions are also possible.
- 2. Vibrational Relaxation.** The absorption from S_0 to S_n involves an energy change from the 0th vibrational level of S_0 to some vibrational level of the excited state. The $\nu'' = 0$ vibrational level is the level most populated at room temperature for the ground electronic state of a molecule, and $\nu' = 0$ also is the vibrational level of the excited electronic state that is most likely to be populated at equilibrium in condensed phases (i.e., solids or liquids). Unless the molecule dissociates before equilibrium can be obtained, rapid vibrational relaxation (with a rate constant of about 10^{12} s^{-1}) converts the higher vibrational level of the excited state to its 0th vibrational level.^{22,23}
- 3. Internal Conversion.** This is a nonradiative process that converts a higher electronic state into a lower state of the same multiplicity (i.e., a higher singlet state into a lower singlet state or a higher triplet state into a lower triplet state). The term *internal* means that the process occurs internally, that is, within the singlet manifold or within the triplet manifold. Note that the line for internal conversion is a horizontal one. This means that the 0th vibrational level of S_2 is converted into a vibrationally excited S_1 state having the same total energy. The vibrationally excited S_1 can then reach its 0th vibrational level by vibrational relaxation. The rate constants for internal conversion are fast ($>10^{10} \text{ s}^{-1}$), especially when the two states are close in energy.²¹
- 4. Radiationless Decay.** This is a process by which electronically excited states are returned to ground states (typically from S_1 to S_0) without the emission of radiation. Radiationless decay often has a relatively slow rate constant (ca. $<10^6 \text{ s}^{-1}$) because the energy gap between S_1 and S_0 is usually greater than that between S_2 and S_1 or between other pairs of excited states.
- 5. Intersystem Crossing.** This is the conversion of a singlet state into a triplet state (or vice versa) and requires a spin flip of an electron. The probability of intersystem crossing depends in part on the energy gap between the singlet and triplet states, so values of k_{isc} vary from 10^6 to 10^{10} s^{-1} . The T_n state is lower in energy than the corresponding S_n

²¹ For a discussion of nonradiative (also termed *radiationless*) processes, see Freed, K. F. *Acc. Chem. Res.* **1978**, *11*, 74.

²² Estimates for the rate constants of photochemical processes here are taken from the discussion by Porter, G. in Swanson, C. P., Ed. *An Introduction to Photobiology*; Prentice Hall: Englewood Cliffs, NJ; 1969; pp. 1–22.

²³ In the gas phase, photochemistry can occur from the upper vibrational levels of the electronic excited state, but we generally assume that vibrational relaxation occurs so rapidly in solution that most photochemical reactions in condensed phase take place from the 0th vibrational level of the electronically excited state. See, however, Manring, L. E.; Peters, K. S. *J. Am. Chem. Soc.* **1984**, *106*, 8077.

state because there is less electron repulsion between unpaired electrons than between electrons that are spin-paired.^{24,25}

Processes 2–5 above are nonradiative processes. The following are radiative processes.

6. **Fluorescence.** This is the emission of a photon accompanying a transition from an excited state to a ground state with the same multiplicity. Usually the emission is $S_1 \rightarrow S_0$, and a generalization to that effect is known as Kasha's rule.²⁶ **Anomalous fluorescence** ($S_2 \rightarrow S_0$) occurs in some compounds, among them azulene,²⁷ thiocarbonyl compounds,²⁸ and some polyenes.²⁹
7. **Phosphorescence.** This is the emission of a photon accompanying a transition from an excited state to a ground state with different multiplicity (usually from a triplet excited state to a singlet ground state). This transition involves both an electronic state change and a spin flip, so it is a relatively slow process.
8. **Triplet–Triplet Absorption.** A molecule in a triplet excited state may absorb a photon to give a higher triplet state. Triplet–triplet absorption spectroscopy can be an important technique for detecting triplet excited states.
9. **Singlet–Triplet Absorption.** Like phosphorescence, this requires that a spin flip take place at the same time the electronic transition occurs. Therefore, $S_0 \rightarrow T_n$ transitions ordinarily are not observed in UV–vis spectroscopy. These transitions can be seen under certain conditions, however, as discussed on page 801.
10. **Singlet–Singlet Absorption.** The advent of picosecond and femtosecond spectroscopy made it possible also to measure transitions from one excited singlet state to another, higher energy excited singlet state.^{30,31}

Selection Rules for Radiative Transitions

Three factors influence the probability of absorption or emission of UV–vis radiation.^{1a} One is based on symmetry considerations and the quantum mechanical formulation of transition moment integrals. If the initial and final

²⁴ For a discussion of intersystem crossing, see (a) Turro, N. J. *J. Chem. Educ.* **1969**, *46*, 2; (b) McGlynn, S. P.; Azumi, T.; Kinoshita, M. *Molecular Spectroscopy of the Triplet State*; Prentice Hall: Englewood Cliffs, NJ, 1969.

²⁵ Although intersystem crossing is usually considered to involve singlet to triplet conversion, reverse intersystem crossing from T_2 to S_1 has been observed in anthracenes: Fukumura, H.; Kikuchi, K.; Koike, K.; Kokubun, H. *J. Photochem. Photobiol. A* **1988**, *42*, 283.

²⁶ Kasha, M. *Discuss. Faraday Soc.* **1950**, *9*, 14.

²⁷ Beer, M.; Longuet-Higgins, H. C. *J. Chem. Phys.* **1955**, *23*, 1390.

²⁸ See, for example, Rao, V. P.; Ramamurthy, V. *J. Org. Chem.* **1988**, *53*, 332. For a review of thiocarbonyl photophysics, see Maciejewski, A.; Steer, R. P. *Chem. Rev.* **1993**, *93*, 67.

²⁹ Bouwman, W. G.; Jones, A. C.; Phillips, D.; Thibodeau, P.; Friel, C.; Christensen, R. L. *J. Phys. Chem.* **1990**, *94*, 7429. Both $S_1 \rightarrow S_0$ and $S_2 \rightarrow S_0$ emissions were observed from tetraenes and pentaenes in the gas phase.

³⁰ One nanosecond (ns) is 10^{-9} s. One picosecond (ps) is 10^{-12} s. One femtosecond (fs) is 10^{-15} s.

³¹ See, for example, Shank, C. V. in Zewail, A. H., Ed. *Photochemistry and Photobiology*, Vol. 1; Harwood Academic Publishers: New York, 1983; pp. 517–527; Repinec, S. T.; Sension, R. J.; Szarka, A. Z.; Hochstrasser, R. M. *J. Phys. Chem.* **1991**, *95*, 10380; Zewail, A. H. *Pure Appl. Chem.* **2000**, *72*, 2219.

electronic states differ in symmetry, then the transition is symmetry-allowed. If they do not, the transition is said to be **symmetry-forbidden**. The term *forbidden* does not necessarily mean that the transition cannot be observed, only that it is weak.

The second factor that determines the probability of a radiative electronic transition is the spin factor. Intersystem crossing, singlet–triplet absorption, and phosphorescence are said to be **spin-forbidden** processes, because an electron must undergo both an electronic transition and a spin flip during the transition. Nevertheless, singlet–triplet interconversions can be seen in many molecules because pure singlet and triplet configurations are not complete descriptions for electronically excited states. Through a process known as **spin–orbit coupling**, some triplet character is mixed into pure singlet states, and some singlet character is mixed into triplet states. The greater the mixing of singlet and triplet character, the greater will be the rate constant for the spin flipping process. The mixing of singlet and triplet configurations is thought to occur through the interaction of the magnetic moment of the spinning electron with the changing magnetic field (due to the nucleus) that the electron encounters as it moves in atomic orbitals.³² The heavier the nucleus, therefore, the greater the likelihood for a spin flip. Compounds incorporating atoms with high atomic number can exhibit a **heavy atom effect** that results in higher rate constants for intersystem crossing. In addition, greater mixing occurs when the singlet and triplet states are closer in energy. For many organic compounds the S_1 and T_1 states differ considerably in energy, so $S_1 \rightarrow T_1$ intersystem crossing is slow. For carbonyl compounds the S_1 – T_1 energy gap is often small, and $S_1 \rightarrow T_1$ intersystem crossing is much faster.

The third factor, which is often called the **Franck–Condon term**, is determined by the extent to which the nuclear coordinates are the same in the initial and final electronic states.³³ The more nearly the nuclear coordinates in the initial state are the same as those in the final state, the more probable is the transition. This can be visualized more easily by considering the electronic and vibrational energy levels of a hypothetical molecule (Figure 12.7).^{34,35} Figure 12.7(a) and (c) show the electronic and vibrational energy levels of the states S_0 and S_1 as functions of the internuclear distance r_{A-B} (where A and B are a pair of bonded atoms in the molecule). Because excitation promotes an electron from a bonding or nonbonding orbital to an antibonding orbital, the net bonding between a pair of atoms may be less in the excited state than in the ground state. The equilibrium distance of the A–B bond may be longer in the excited state than in the ground state, so the curve corresponding to the electronic energy of the excited state is shown displaced to the right of the ground state curve.

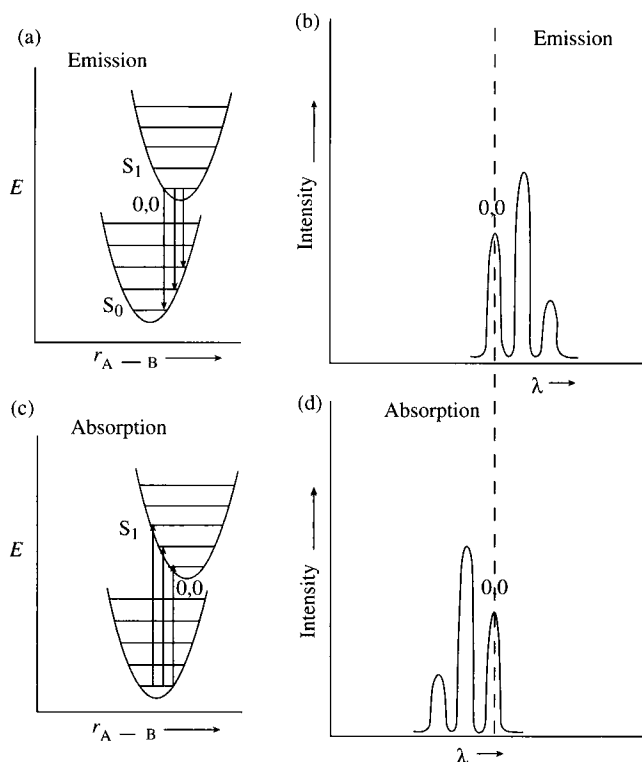
Electronic transitions are said to be *vertical*, meaning that absorption and emission of UV–vis radiation occurs with no movement of the nuclei, within the limits of the Born–Oppenheimer approximation. Since most molecules are in the 0th vibrational level of the ground electronic state, the Franck–Condon term measures the probability of the transition from the 0th vibrational level of the ground state to each vibrational level of the excited state. A transition from the 0th vibrational level of S_0 to the 0th vibrational level of S_1 is marked

³² For an introduction to spin–orbit coupling, see reference 6.

³³ Condon, E. U. *Am. J. Phys.* **1947**, *15*, 365 and references therein.

³⁴ A portion of Figure 12.7 was modified from a figure in Kohler, B. E. *Chem. Rev.* **1993**, *93*, 41.

³⁵ See also Lee, S.-Y. *J. Phys. Chem.* **1990**, *94*, 4420.

**FIGURE 12.7**

Schematic representations of the origins of fluorescence (a, b), and UV-vis absorption (c, d). (Adapted from reference 34.)

as the 0,0 transition in Figure 12.7(c). A transition from the 0th vibrational level of S_0 to the 1st vibrational level of S_1 (the 0,1 transition) requires more energy, and a 0,2 absorption requires more energy still. Therefore, the 0,1 transition occurs at shorter wavelength than the 0,0 transition, and the 0,2 transition is seen at an even shorter wavelength. A high resolution absorption spectrum showing just these three transitions would appear as indicated in Figure 12.7(d).³⁶ Organic molecules in solution usually do not exhibit sharp absorption lines in UV-vis spectra, however, because large molecules may have many closely spaced vibrational bands and because rotational transitions and collisions (especially with solvent molecules) broaden the individual vibrational bands.

Tables of absorption spectra of organic compounds usually report UV-vis spectral data in terms of the wavelength of maximum absorption (λ_{\max}) and the molar absorptivity at maximum absorption (ϵ_{\max}).³⁷ These values are characteristic for an organic compound in a particular solvent and may be used to help identify it.³⁸ For a photochemist, λ_{\max} is only part of the information available from the spectrum. Often more important is the **onset** of absorption (the longest wavelength at which absorption is evident), since that provides an upper limit for the 0,0 transition, the longest wavelength

³⁶ For a more detailed discussion, see Harris, D. C.; Bertolucci, M. D. *Symmetry and Spectroscopy*; Oxford University Press: New York, 1978; p. 330 ff.

³⁷ The Beer-Lambert law states that $\epsilon = A/bc$, where A is the absorbance of the sample, b is the path length in cm, and c is the concentration in mol L^{-1} .

³⁸ Compare Silverstein, R. M.; Bassler, G. C.; Morrill, T. C. *Spectrometric Identification of Organic Compounds*, 5th ed.; John Wiley & Sons: New York, 1991; pp. 289-314.

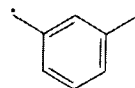
(lowest energy) absorption that can create the electronically excited state. Because vibrationally excited electronic states relax to the 0th vibrational level rapidly in condensed phases, photochemistry in solution usually occurs from the 0th vibrational level of an electronically excited state. Thus, the energy associated with the 0,0 transition can be used to determine the energy available in the photoexcited molecule to drive a photochemical reaction.

Fluorescence and Phosphorescence

For most organic molecules, fluorescence is the spontaneous emission of UV–vis radiation from the $\nu' = 0$ vibrational level of the first excited singlet state to some vibrational level ($\nu'' = 0, 1, 2, \dots$) of the (singlet) ground electronic state.³⁹ Figure 12.7(a) shows arrows representing fluorescence from the $\nu' = 0$ vibrational level of S_1 to the $\nu'' = 0, 1,$ and 2 vibrational levels of S_0 . Note that the energy of the transition from $\nu' = 0$ (S_1) to $\nu'' = 0$ (S_0) is the same as the energy for absorption from the $\nu'' = 0$ level of S_0 to the $\nu' = 0$ level of S_1 . The other two fluorescence transitions shown are lower energy emissions and should occur at longer wavelengths than 0,0 fluorescence, as shown in Figure 12.7(b). If they were plotted on the same spectrum, the fluorescence and emission spectra in this example would overlap at the 0,0 transition, providing confirmation of the 0,0 energy of the electronically excited state.

In highly conjugated molecules, the σ bonding provides a molecular framework for the planar π system, and the π bonding results from population of many bonding MOs. Therefore, promotion of one electron to an antibonding MO may not distort the molecular geometry very much. In such cases there can be a nearly mirror image relationship between the absorption and fluorescence spectra, particularly when the spectra are plotted as intensity versus wave numbers (cm^{-1}) instead of wavelength.⁴⁰ The similarity arises because the factors that make some $\nu'' = 0$ to $\nu' = x$ absorptions more probable than others also make some $\nu' = 0$ to $\nu'' = x$ emissions more probable. Figure 12.8 shows the absorption and fluorescence spectra of anthracene plotted as intensity versus wave numbers.⁴¹ There is generally a good mirror image relationship between the absorption and emission bands, although a slight difference in the 0,0 bands arises from a small difference between the geometries of the ground and excited states.⁴²

³⁹ More precisely, fluorescence is the spontaneous emission of light from a higher energy excited state resulting in the formation of a lower energy excited state with the same multiplicity. Thus, a $T_2 \rightarrow T_1$ transition is also termed fluorescence. Després, A.; Lejeune, V.; Migirdicyan, E.; Siebrand, W. *J. Phys. Chem.* **1988**, *92*, 6914, reported the fluorescence of photoexcited *m*-xylylene biradical,

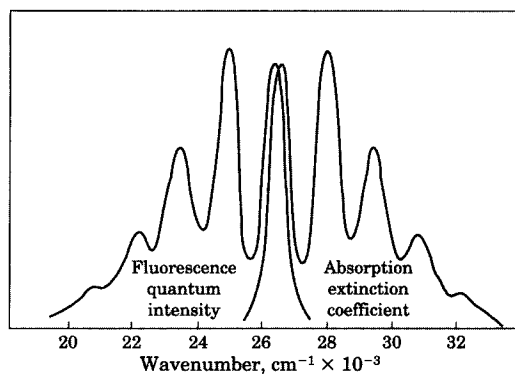


which has a triplet ground state.

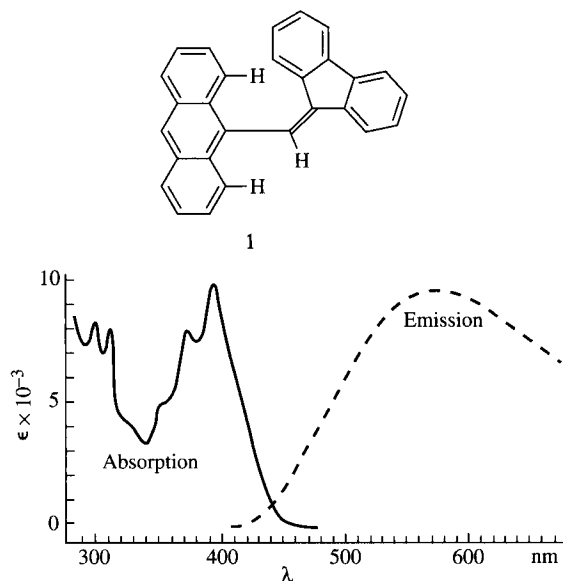
⁴⁰ For a discussion of the relationship between molecular geometry and absorption and fluorescence spectroscopy of π systems, see Berlman, I. B. *J. Phys. Chem.* **1970**, *74*, 3085.

⁴¹ Bowen, E. J. *Adv. Photochem.* **1963**, *1*, 23. In order to facilitate the comparison, the absorption and emission intensities are normalized so that the 0,0 transition has the same intensity in each.

⁴² The energy difference between the λ_{max} values for absorption and emission is called the Stokes shift.

**FIGURE 12.8**

Mirror image relationship in absorption and fluorescence spectra of anthracene. (Note that the horizontal scale is linear in wave numbers, so higher energy is to the right. Reproduced from reference 41.)

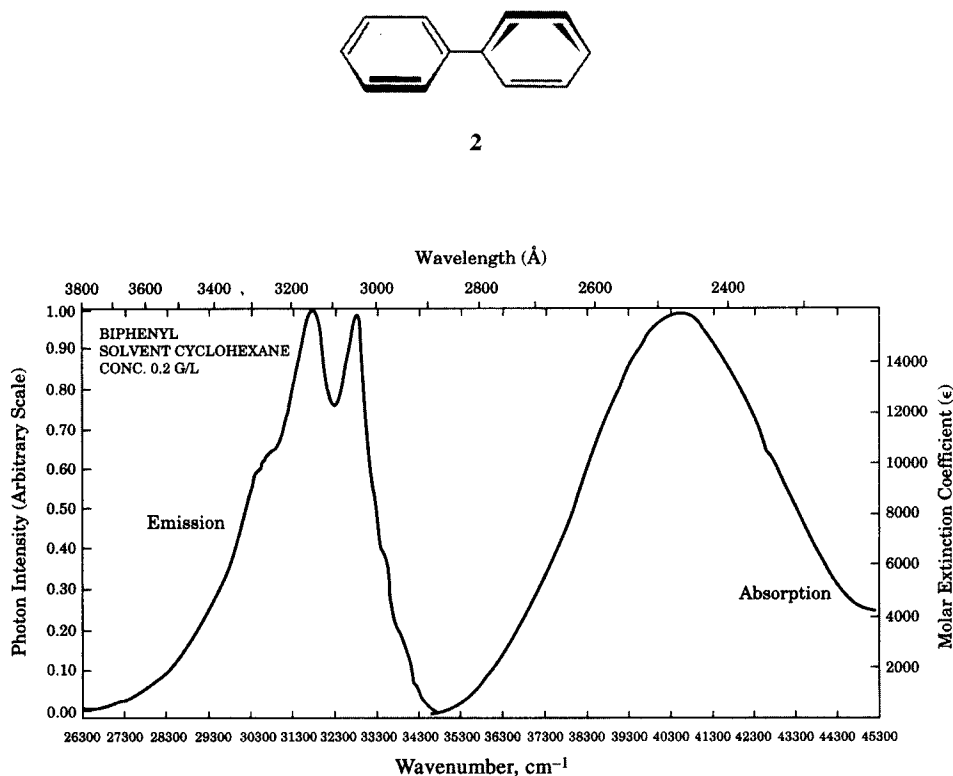
**FIGURE 12.9**

Effect of change in excited state geometry on fluorescence spectrum of 1. (The horizontal scale is linear in nm, so higher energy is to the left. Adapted from reference 43.)

The geometries of the ground and excited states may be very different for some molecules. As a result, there may be a large difference between λ_{\max} for absorption and λ_{\max} for emission, and the 0,0 band may be weak or absent. In the sterically hindered molecule fluorenylidene(9-anthryl)methane (**1**), for example, the geometry of the excited singlet state differs considerably from that of the ground state, and only a much lower energy, structureless emission is seen (Figure 12.9).⁴³ The reverse situation can also occur. The two benzene rings are not coplanar in the ground state of biphenyl (**2**), but intramolecular charge transfer produces a planar excited state with double bond character between the two rings. Thus, the absorbance of biphenyl is structureless, but the fluorescence spectrum shows some vibrational structure (Figure 12.10).⁴⁴

⁴³ Becker, H.-D.; Andersson, K. *J. Org. Chem.* **1983**, *48*, 4542.

⁴⁴ Berlman, I. B. *Handbook of Fluorescence Spectra of Aromatic Molecules*, 2nd ed.; Academic Press: New York, 1971.

**FIGURE 12.10**

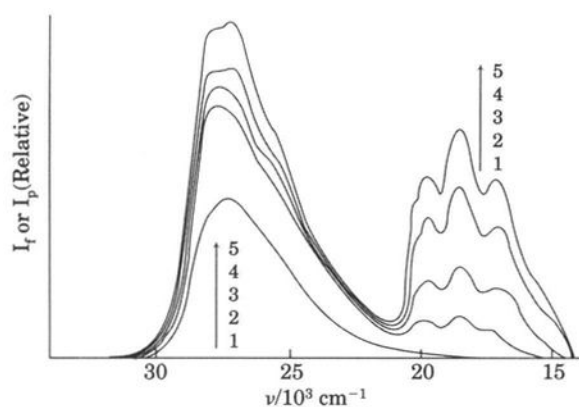
Absorption (right) and fluorescence (left) spectra of biphenyl (2). (Adapted from reference 44.)

We would expect a similar relationship between electronic state geometries and the appearance of singlet-triplet absorption and phosphorescence spectra, but this is usually difficult to observe experimentally. In fluid solution phosphorescence is reduced by diffusion-limited bimolecular interactions of the excited triplet compound and one or more ground state species known as quenchers.⁴⁵ Often phosphorescence can be observed only by irradiating the compound in environments where diffusion is quite slow, such as in an organic glass at liquid nitrogen temperature.⁴⁶ Phosphorescence can also be enhanced if photoexcited organic molecules are associated with host molecules that inhibit diffusional quenching. For example, Figure 12.11 shows a series of emission spectra of 6-bromo-2-naphthol at room temperature in aqueous solution containing varying concentrations of α -cyclodextrin.⁴⁷ In the absence of α -cyclodextrin (curve 1), only fluorescence is seen.

⁴⁵ See the discussion of quenching on page 809.

⁴⁶ A **glass** is a liquid medium that becomes extremely viscous but does not crystallize—and thus scatter light—at the temperature of the experiment. For example, an EPA glass (made by mixing ether, isopentane and ethyl alcohol in a ratio of 5:5:2) remains transparent at -196°C but is so viscous that diffusion is effectively precluded. For details, see Murov, S. L. *Handbook of Photochemistry*; Marcel Dekker: New York, 1973; pp. 90–92.

⁴⁷ A **total emission spectrum** shows both fluorescence and any phosphorescence that can be detected.

**FIGURE 12.11**

Observation of fluorescence (on the left) and phosphorescence (on the right) of 6-bromo-2-naphthol in a series of aqueous solutions at room temperature with varying concentrations of α -cyclodextrin. (Adapted from Reference 48. Note that the x-axis is linear in cm^{-1} , so higher energies are to the left.)

At an α -cyclodextrin concentration of $1 \times 10^{-2} \text{ M}$ (curve 5), appreciable phosphorescence is detected. The phosphorescence is attributed to 6-bromo-2-naphthol molecules that are encapsulated by two α -cyclodextrin molecules.⁴⁸

Singlet–triplet absorption is ordinarily difficult to detect because the transition is spin-forbidden. Heavy atom solvents and oxygen perturbation have been used to induce singlet–triplet absorption, but absorptions observed in this manner are weak, and it is important to establish that the observed absorption is not due to artifacts resulting from the solvent or additive.^{49,50} One approach is to determine the **excitation spectrum** for phosphorescence, which is a measurement of the relative efficiency of different wavelengths of UV–vis radiation in causing the phosphorescence of a compound. If the excitation spectrum for phosphorescence shows a mirror image relationship with the phosphorescence spectrum, then it seems reasonable that the excitation spectrum corresponds to the S_0 to T_1 excitation. For example, the mirror image relationship between the singlet–triplet absorption spectrum and the phosphorescence of naphthalene is shown in Figure 12.12.⁵¹

Energy Transfer and Electron Transfer

Excitation with UV–vis radiation (direct excitation) is not the only way to produce an electronically excited state.⁵² Excited states can also be created by electronic energy transfer from an electronically excited energy donor (D^*)

⁴⁸ Hamai, S. *J. Chem. Soc. Chem. Commun.* **1994**, 2243.

⁴⁹ For example, see (a) Evans, D. F. *J. Chem. Soc.* **1960**, 1735; (b) Rest, A. J.; Salisbury, K.; Sodeau, J. R. *J. Chem. Soc. Faraday Trans. 2* **1977**, 73, 1396.

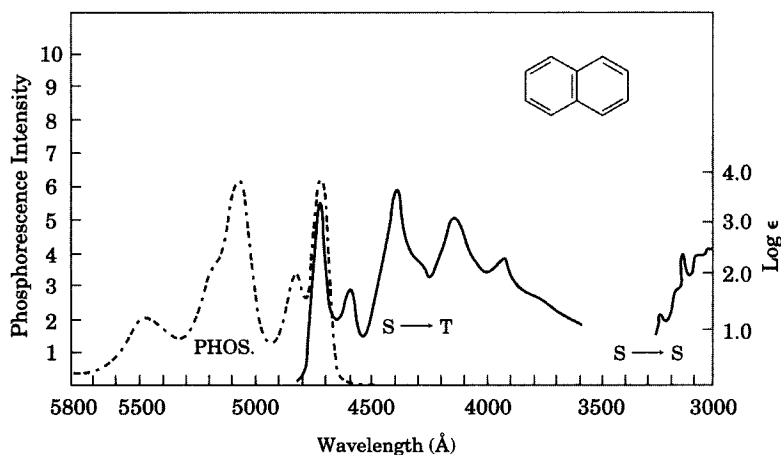
⁵⁰ Oxygen is a paramagnetic compound, so it enhances spin–orbit coupling and can enhance singlet–triplet conversions. Oxygen is a strong quencher of excited states, both singlet and triplet, but it is an especially effective quencher of triplet states due to their longer lifetimes. See the discussion of quenching beginning on page 809.

⁵¹ Marchetti, A. P.; Kearns, D. R. *J. Am. Chem. Soc.* **1967**, 89, 768.

⁵² In this section the phrase *excited state* will mean an electronically excited state unless there is a qualifying adjective, as in “vibrationally excited state.”

FIGURE 12.12

Singlet-triplet absorption spectrum and phosphorescence spectrum of naphthalene. (Reproduced from reference 51. Note that lower energy is to the left.)

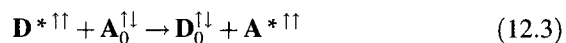


to an acceptor (**A**, equation 12.2), just as vibrationally excited states can be created by energy transfer from hot molecules or container walls.⁵³ In some cases the electronic energy is transferred by collision of the excited and ground state molecules; in other cases the energy can be transferred without direct contact.



There are at least four different kinds of energy transfer:⁶

- 1. Radiative or Trivial Energy Transfer.** In this case the donor molecule emits a photon and the acceptor molecule absorbs it.
- 2. Förster Resonance Energy Transfer.** This is a single-step, *radiationless* transfer of electronic excitation.⁵⁴ This type of energy transfer depends in part on the distance between the donor and acceptor but can take place over distances of up to 100 Å. Efficient Förster transfer also requires a good overlap of the emission spectrum of the donor and the absorption spectrum of the acceptor.
- 3. Exciton Migration.** In the solid state, an electronically excited state molecule may transfer its energy very rapidly to a nearby molecule.
- 4. Collisional Energy Transfer.** This is the process that is often of greatest interest to organic photochemists, since it allows the creation of excited triplet states that otherwise could not be produced by direct irradiation. In equation 12.3, for example, energy transfer from the triplet state of a donor molecule ($\mathbf{D}^{*\uparrow\uparrow}$) to an acceptor molecule in its \mathbf{S}_0 state produces the ground state of the donor and the triplet excited state of the acceptor. It is generally believed that collisional energy transfer occurs through exchange of electrons between the two species:



⁵³ Wilkinson, F. *Adv. Photochem.* **1964**, 3, 241.

⁵⁴ Förster, T. *Discuss. Faraday Soc.* **1959**, 27, 7.

Collisional energy transfer is frequently called **sensitization**.⁵⁵ It is an important tool in photochemistry because it provides access to excited triplet states of compounds whose singlets do not intersystem cross efficiently (such as alkenes and conjugated polyenes). It also provides access directly to the triplet states of compounds for determination of the multiplicity of the state responsible for a photochemical reaction.

Another important interaction between an electronically excited molecule and a ground state molecule is **electron transfer**.⁵⁶ Because photoexcitation of a molecule promotes an electron from a lower energy bonding or nonbonding orbital to a higher energy antibonding orbital, the excited state molecule has very different redox properties from the ground state structure. It is a better electron donor (and thus has a less positive oxidation potential) because there is an electron in a high energy orbital. The excited state is also a better electron acceptor (and therefore has a less negative reduction potential) because of the vacancy in a lower energy orbital. Photoexcited molecules can therefore undergo electron transfer processes with ground state molecules that have a lower energy LUMO, as shown in Figure 12.13(a), as well as those that have a higher HOMO, as shown in Figure 12.13(b).

The initial species formed by electron transfer may be an **exciplex** (excited complex) if it is formed from two different species or an **excimer** (excited dimer) if it is formed from two molecules of the same kind. A radical ion pair $D^{\bullet+}A^{\bullet-}$ (or $D^{\bullet-}A^{\bullet+}$) produced by this kind of electron transfer is similar to the ion pairs formed through ground state reactions in that it can be a contact or intimate ion pair, a solvent-separated ion pair, or a pair of free

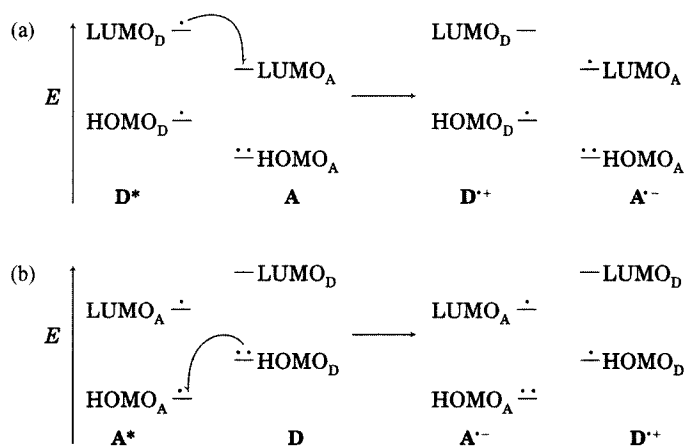


FIGURE 12.13

Creation of radical ion pairs by electron transfer: (a) from a photoexcited electron donor and (b) to a photoexcited electron acceptor. Here **A** and **D** refer to the electron acceptor and donor, respectively. Note that the curved arrows are single-barbed, denoting the movement of one electron. (Adapted from reference 58e.)

⁵⁵ The term *sensitization* was earlier used to describe the improved spectral response of silver halide crystals treated with organic dyes. See, for example, Germann, F. E. E.; Shen, D.-K. *J. Phys. Chem.* **1929**, *33*, 1583. Photochemists use the terms *sensitization* and *photosensitization* to refer simply to energy transfer. Compare reference 1.

⁵⁶ See, for example, Gould, I. R.; Farid, S. *Acc. Chem. Res.* **1996**, *29*, 522; Mataga, N.; Chosrowjan, H.; Taniguchi, S. *J. Photochem. Photobiol. C* **2005**, *6*, 37; Vauthey, E. *J. Photochem. Photobiol. A* **2006**, *179*, 1.

radical ions.⁵⁷ The radical ion pair can exist as either a singlet or as a triplet, depending on the spins of the two unpaired electrons. A radical ion pair can also be annihilated by **back electron transfer** from the radical anion to the radical cation, thus producing the electronic ground state of each species.⁵⁸ Photochemical electron transfer provides a means to investigate the mechanism of long-range electron transfer processes that may be important in the operation of many biological systems.⁵⁹ Although the energy transfer and electron transfer processes have been described in terms of bimolecular processes, the same processes can occur between two groups in the same molecule if one or the other can be photoexcited independently of the other.

12.2 FUNDAMENTALS OF PHOTOCHEMICAL KINETICS

Actinometry and Quantum Yield Determinations

The quantitative study of photochemical reactions requires knowledge of the concentrations of reactants and products as well as the number and energy of photons absorbed by the sample. The determination of the number of photons absorbed by the sample is known as **actinometry**. In some cases these measurements are made by irradiating the sample and a standard chemical reference system simultaneously. Alternatively, the measurements may be made with electronic devices.⁶⁰

A **quantum yield** (also called **quantum efficiency**) of some photochemical process is defined as the number of photochemical events of that process that occur per photon of UV–vis radiation absorbed. Consider the very simple photochemical reaction illustrated in equation 12.4:



The quantum yield of disappearance (Φ_{dis}) of reactant (A) is defined as

$$\Phi_{\text{dis}} = \frac{\text{molecules of A that disappear}}{\text{photons of light absorbed by A}} \quad (12.5)$$

⁵⁷ For discussions of photochemically generated radical ion pairs and for leading references, see Gould, I. R.; Young, R. H.; Mueller, L. J.; Farid, S. *J. Am. Chem. Soc.* **1994**, *116*, 8176; Gould, I. R.; Young, R. H.; Mueller, L. J.; Albrecht, A. C.; Farid, S. *J. Am. Chem. Soc.* **1994**, *116*, 8188; Vauthey, E.; Parker, A. W.; Nohova, B.; Phillips, D. *J. Am. Chem. Soc.* **1994**, *116*, 9182; Arnold, B. R.; Noukakis, D.; Farid, S.; Goodman, J. L.; Gould, I. R. *J. Am. Chem. Soc.* **1995**, *117*, 4399.

⁵⁸ For an introduction, see (a) Gust, D.; Moore, T. A. *Adv. Photochem.* **1991**, *16*, 1; *Top. Curr. Chem.* **1991**, *159*, 103; (b) Willner, I.; Willner, B. *Top. Curr. Chem.* **1991**, *159*, 153; (c) Lyman, S. V.; Parmon, V. N.; Zamarev, K. I. *Top. Curr. Chem.* **1991**, *159*, 1; (d) Fox, M. A. *Adv. Photochem.* **1986**, *13*, 237; *Top. Curr. Chem.* **1991**, *159*, 67; (e) Kavarnos, G. J. *Top. Curr. Chem.* **1990**, *156*, 21. For a detailed discussion of photoinduced electron transfer, see Fox, M. A.; Chanon, M., Eds. *Photoinduced Electron Transfer*, Parts A–D; Elsevier: Amsterdam, 1988.

⁵⁹ For example, see Schmidt, J. A.; McIntosh, A. R.; Weedon, A. C.; Bolton, J. R.; Connolly, J. S.; Hurley, J. K.; Wasielewski, M. R. *J. Am. Chem. Soc.* **1988**, *110*, 1733.

⁶⁰ For a review, see Kuhn, H. J.; Braslavsky, S. E.; Schmidt, R. *Pure Appl. Chem.* **2004**, *76*, 2105.

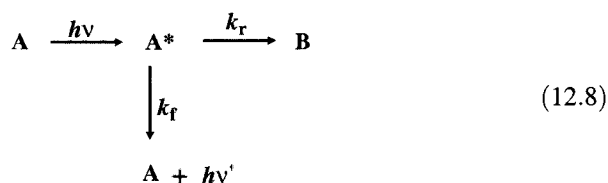
Similarly, the quantum yield of appearance (Φ_{app}) of product (**B**) is given by

$$\Phi_{\text{app}} = \frac{\text{molecules of B that are formed}}{\text{photons of light absorbed by A}} \quad (12.6)$$

More commonly, calculations are done on a molar basis, so

$$\Phi_{\text{app}} = \frac{\text{moles of B that are formed}}{\text{einsteins of light absorbed by A}} \quad (12.7)$$

Instead of the simple hypothetical reaction in equation 12.4, organic molecules normally exhibit a number of photochemical and photophysical processes that compete with each other. A minimal complication is illustrated in equation 12.8, in which the photoexcited molecule both fluoresces and forms product. The rate constant for fluorescence is k_f , and the rate constant for reaction is k_r .



Now

$$\Phi_f = \frac{\text{einsteins emitted}}{\text{einsteins absorbed}} \quad (12.9)$$

where Φ_f is the quantum yield of fluorescence. Φ_f can be determined directly by measuring the total number of photons absorbed per unit time (absorption intensity, I_a) and the number of photons emitted per unit time (fluorescence intensity, I_f).⁶¹ Φ_f can also be determined indirectly if certain rate constants are known.

Rate Constants for Unimolecular Processes

The spontaneous emission of electromagnetic radiation from an excited molecule is a unimolecular process that follows first-order kinetics. Suppose a photoexcited molecule exhibits fluorescence as its only decay pathway. If there are N_0 photoexcited molecules at time t_0 , then at a subsequent time t the number of molecules still in the excited state (N) is given by

$$N = N_0 e^{-k_f t} \quad (12.10)$$

where k_f is the rate constant for fluorescence. First-order decay processes (such as nuclear fission) are often described in terms of a half-life, but photochemists usually discuss an excited state in terms of its **lifetime**, denoted τ , which is defined as the time required for a population of excited

⁶¹ In many measurements, I_f is taken to be the magnitude of the detector (e.g., photomultiplier) response to fluorescence at a λ_{max} .

states to decay to e^{-1} of its initial value.^{62,63} Because e^{-1} equals 0.368, the lifetime of a first-order, unimolecular decay process is longer than the half-life. In the example in equation 12.10, this condition is achieved when $t = k_f^{-1}$. Thus, k_f^{-1} is defined as the **inherent fluorescence lifetime** or **inherent singlet lifetime**, τ_s^0 , which is the lifetime of the excited singlet state that would be observed if fluorescence were the only decay pathway. The inherent fluorescence lifetime of a compound can be calculated from its UV-vis absorption spectrum.⁶⁴

For most molecules fluorescence is only one of the processes that deactivate an electronically excited state. If a molecule can decay by both fluorescence (with rate constant k_f) or radiationless decay (with rate constant k_d), the time dependence of a population of excited states is given by

$$N = N_0 e^{-(k_f + k_d)t} \quad (12.11)$$

In this case,

$$\tau = \frac{1}{(k_f + k_d)} \quad (12.12)$$

In general, if there are i first-order, unimolecular decay processes that deactivate an excited singlet state, each with rate constant k_i , then the observed singlet lifetime (τ_s) is

$$\tau_s = \frac{1}{\sum_i k_i} \quad (12.13)$$

The quantum yield of fluorescence equals the rate constant for fluorescence divided by the sum of the rate constants for all decay processes:

$$\Phi_f = \frac{k_f}{\sum_i k_i} = k_f \tau_s \quad (12.14)$$

In the example described by equation 12.11,

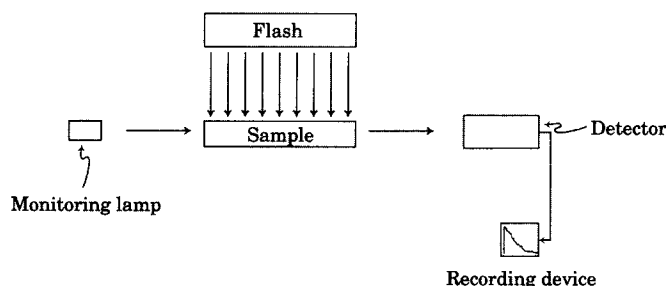
$$\Phi_f = \frac{k_f}{(k_f + k_d)} = \frac{\tau_s}{\tau_s^0} \quad (12.15)$$

where τ_s^0 is determined from the absorption spectrum and τ_s is measured experimentally.

⁶² The term *lifetime* is used by virtually all photochemists, although perhaps it is not as intuitive as another term, such as *characteristic time* might be. To be specific, authors often use the symbol τ_s for singlet lifetime or τ_f for fluorescence lifetime instead of an unsubscripted τ in order to distinguish these terms from τ_p , which is the phosphorescence lifetime. When the symbol τ is used alone, it is important to ascertain which excited state is involved.

⁶³ For the derivation of the relationship between τ and rate constants for decay, see Jaffé, H. H.; D'Agostino, J. T. *J. Chem. Educ.* **1970**, *47*, 14.

⁶⁴ For details, see Michl, J.; Bonačić-Koutecký, V. *Electronic Aspects of Organic Photochemistry*; Wiley-Interscience: New York, 1990; p. 74. In general, weak absorptions predict long inherent lifetimes, while strong absorptions are associated with high fluorescence rate constants and short inherent fluorescence lifetimes.

**FIGURE 12.14**

A schematic representation of a conventional flash spectrometer.

Transient Detection and Monitoring

Equation 12.13 describes not only the first-order decay of excited singlet states but also the decay of excited triplet states or other photochemically generated reactive species that disappear by first-order processes. If such species cannot be monitored by the emission of light, an alternative approach is to detect them through the absorption of light with a technique known as **flash spectroscopy**.⁶⁵ This method uses a short duration pulse or “flash” of UV–vis radiation to create a large population of transients that can then be monitored spectroscopically. In conventional flash spectroscopy, the flash lamp is filled with xenon or another gas that can be subjected to a several thousand volt charge between electrodes in the ends of the lamp. Discharging the lamp produces a bright flash of UV–vis radiation lasting some microseconds. Laser flash spectroscopy allows the generation of nanosecond to femtosecond flashes. When the transients are detected with a second, weaker laser pulse instead of a continuous beam of light, the method is known as the **pump-probe** technique.

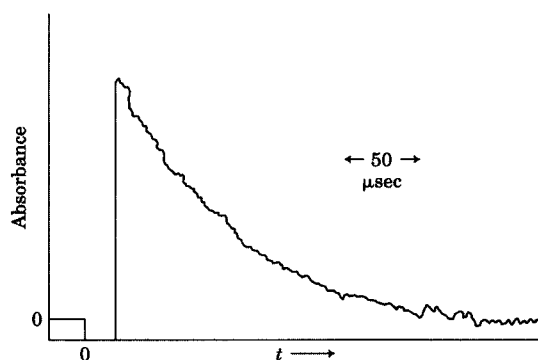
A schematic of a conventional flash spectroscopy apparatus is shown in Figure 12.14. A solution of the sample is placed in a cell made of optical material that is transparent to the wavelengths to be used in the experiment. The cell is placed in a spectrophotometer so that the absorption of monitoring light by the sample can be measured as a function of wavelength. If some ground state molecules are converted to triplet states or other species (such as radicals) by the flash, the absorption of monitoring light by the sample will be different from the absorption before the flash and will change with time as the transient species decay.

For kinetics experiments, a monochromator in the detector unit is set for one wavelength, and the photomultiplier output voltage is monitored as a function of time after the excitation flash. The schematic drawing in Figure 12.15 shows an experiment in which the monochromator is set for a wavelength at which the starting material does not absorb the monitoring UV–vis radiation. At the time of the flash, scattered radiation from the flash lamp produces an apparent decrease in absorption, and the curve drops below the signal level corresponding to zero absorption. The flash decays after a few microseconds, and the photomultiplier voltage reflects absorption

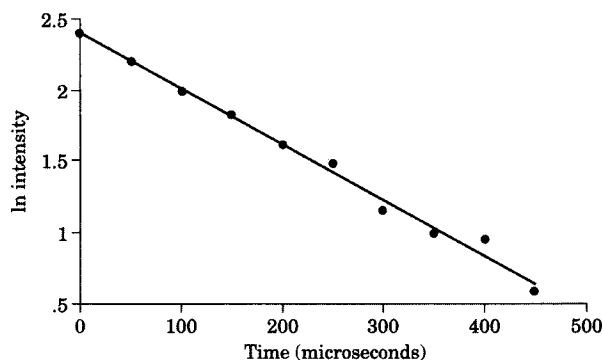
⁶⁵ Because it is used frequently to study photochemical reactions that lead to bond cleavage, this procedure is often called **flash photolysis**. The term *photolysis* literally means “breaking apart by light,” however, so technically it would not apply to the measurement of excited states that decay back to starting molecules without chemical change.

FIGURE 12.15

Transient absorption following flash excitation.

**FIGURE 12.16**

Plot of $\ln(\text{intensity})$ versus time for decay of triplet-triplet absorption, based on data in Figure 12.15.



of the monitoring light by new species in the sample.⁶⁶ If the absorption is due to a transient that decays with first-order kinetics, then the detector records a first-order decay curve. Plotting the natural logarithm of the intensity of the absorption against time ($t = 0$ arbitrarily taken as the maximum of the absorption) generates a plot such as that in Figure 12.16, which is based on the data in Figure 12.15. The value of τ is determined from the slope of a least squares analysis of the data points.

Kinetic methods such as flash spectroscopy make it possible to obtain detailed information about the unimolecular processes of electronically excited organic molecules. Table 12.2 lists some of the available data for five organic compounds.⁶⁷ Note, in particular, that the S_1 and T_1 states of benzene, naphthalene, and anthracene have differences in energy that are much greater than are the corresponding differences for acetone and benzophenone. The smaller energy gap leads to greater rate constants for intersystem crossing

⁶⁶ The ideal excitation source would provide a pulse of light that drops instantaneously from a high value to zero. Usually, however, the source has its own intensity profile, and the decay of very short-lived transients may be difficult to measure unless the effects of source decay are separated from the effects of transient absorption decay through a technique known as *deconvolution*.

⁶⁷ Data from reference 46. Energy values for S_1 and T_1 are in kcal/mol. Lifetimes are in nanoseconds for fluorescence in solution at room temperature and in seconds for phosphorescence at 77 K in an EPA glass.

TABLE 12.2 Photophysical Data for Selected Compounds

Compound	$E(S_1)$ (kcal/mol)	$E(T_1)$ (kcal/mol)	Φ_f	Φ_{isc}	Φ_p	τ_f (ns)	τ_p (s)
Benzene	110	84	0.05	0.25 ^a	0.23	29	6.3
Naphthalene	92	61	0.2	0.8	0.1	96	2.2
Anthracene	76	42	0.27	0.75		5	0.045
Acetone	88	ca. 80	ca. 10^{-3}	1.0	0.0001	2	0.04
Benzophenone	75	69	4×10^{-6}	1.0	0.74	0.005	0.006

^aData from reference 69. Φ_p is the quantum yield of phosphorescence, and τ_p is the triplet state lifetime.

Source: Reference 46.

and thus to near-unity quantum values of Φ_{isc} for benzophenone and acetone.⁶⁸

Bimolecular Decay of Excited States: Stern–Volmer Kinetics

In addition to unimolecular decay, photoexcited molecules may also exhibit bimolecular decay resulting from interactions with other (ground state) molecules. The interaction may take the form of a collisional energy transfer or sensitization process (equation 12.16) or as a quenching interaction, in which neither product is in the excited state (equation 12.17).



Suppose an excited singlet state of compound **A** can undergo fluorescence (with rate constant k_f) and radiationless decay (with rate constant k_d). In the absence of **Q**, the lifetime of A^* is the reciprocal of the sum of k_f and k_d . Adding a quencher (**Q**) introduces a bimolecular decay pathway, which is shown in equation 12.18.



Now the lifetime of A^* in the presence of **Q**, τ'_s , is given by⁷⁰

$$\tau'_s = \frac{1}{(k_f + k_d + k_q[Q])} \quad (12.19)$$

⁶⁸ Aloïse, S.; Ruckebusch, C.; Blanchet, L.; Réhault, J.; Buntinx, G.; Huvenne, J.-P. *J. Phys. Chem. A* **2008**, *112*, 224 used subpicosecond time-resolved absorption spectroscopy to study intersystem crossing in benzophenone. They identified an intermediate species (IS) in the process, and it was tentatively identified as a vibrationally excited ("hot") T_1 state. The rate constant for S_1 to IS was calculated to be $1.54 \times 10^{11} \text{ s}^{-1}$, while that for IS to T_1 was found to be $1 \times 10^{11} \text{ s}^{-1}$.

⁶⁹ Carroll, F. A.; Quina, F. H. *J. Am. Chem. Soc.* **1976**, *98*, 1.

⁷⁰ In this formulation, the lifetime of the excited singlet state in the absence of **Q** is denoted τ_s , while that in the presence of **Q** is indicated as τ'_s . Often, τ° is used to represent the lifetime of an excited state in the absence of quencher and τ to represent the lifetime of an excited state in the presence of quencher. In that case, the Stern–Volmer relationship becomes

$$\frac{\tau^\circ}{\tau} = \frac{\Phi^\circ}{\Phi} = \frac{I^\circ}{I} = 1 + k_q[Q]\tau^\circ$$

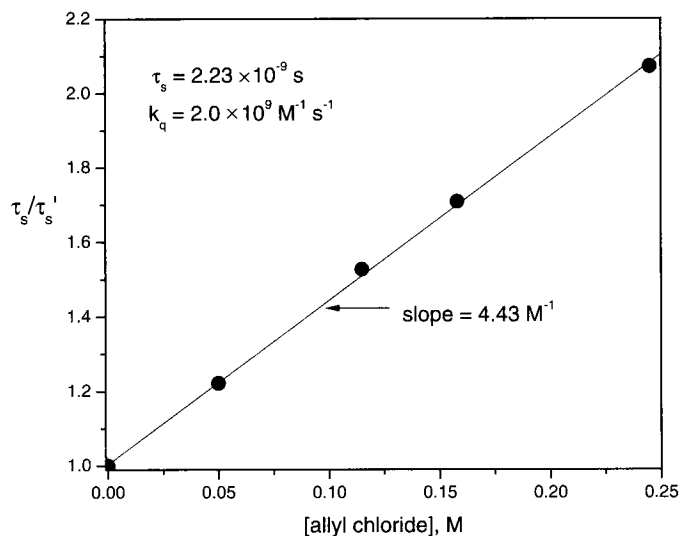


FIGURE 12.17

Stern–Volmer plot for quenching 1,4-dimethoxybenzene fluorescence by allyl chloride.

Dividing τ_s by τ'_s and rearranging terms produces the following relationships:

$$\frac{\tau_s}{\tau'_s} = \frac{\Phi_f}{\Phi'_f} = \frac{I_f}{I'_f} = \frac{1/(k_f + k_d)}{1/(k_f + k_d + k_q[Q])} = \frac{k_f + k_d + k_q[Q]}{k_f + k_d} = 1 + \frac{k_q[Q]}{k_f + k_d} \quad (12.20)$$

Since $\tau_s = 1/(k_f + k_d)$,

$$\frac{\tau_s}{\tau'_s} = \frac{\Phi_f}{\Phi'_f} = 1 + k_q[Q]\tau_s \quad (12.21)$$

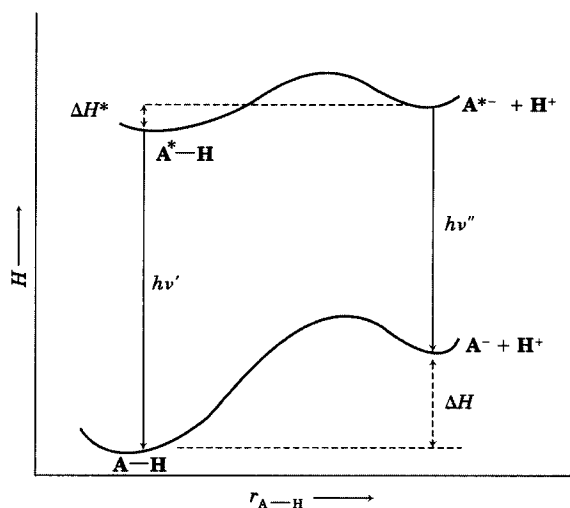
Equation 12.21 is known as the **Stern–Volmer equation**.⁷¹ Plotting the ratio of lifetimes (τ_s/τ'_s), or the ratio of fluorescence quantum yields (Φ_s/Φ'_s), or the ratio of fluorescence intensities (I_f/I'_f) versus $[Q]$ should yield a straight line with slope $k_q\tau_s$. If τ_s is known, then k_q can be determined. Figure 12.17 shows a Stern–Volmer plot for the quenching of 1,4-dimethoxybenzene fluorescence by allyl chloride in acetonitrile solution.⁷² The slope is 4.43 M^{-1} , and the lifetime of 1,4-dimethoxybenzene in the absence of quencher is 2.23 ns. Thus, the rate constant for quenching of 1,4-dimethoxybenzene singlets with allyl chloride is $2 \times 10^9 \text{ M}^{-1} \text{ s}^{-1}$.

12.3 PHYSICAL PROPERTIES OF EXCITED STATES

Electronically excited organic molecules are chemical entities, just as are ground state molecules. Even though they have short lifetimes, they have characteristic bond angles, dipole moments, bond strengths, and vibrational

⁷¹ Shetlar, M. D. *Mol. Photochem.* **1974**, *6*, 191 reported a general form of the Stern–Volmer equation for a system with multiple excited states. Green, N. J. B.; Pimblott, S. M.; Tachiya, M. *J. Phys. Chem.* **1993**, *97*, 196 presented generalizations for cases in which the quenching requires description with a time-dependent rate constant.

⁷² Unpublished data from M. C. Fitzgerald. In this experiment the solution was not degassed, so all values of τ reflect the effects of oxygen quenching.

**FIGURE 12.18**

Potential energy surfaces for dissociation of a proton from a ground state or photoexcited compound.

modes. Of course, we cannot measure the boiling point of S_1 benzene or the heat of combustion of T_1 acetone, since these are bulk properties, and typically the concentration of excited molecules at any particular time is very low. Nonetheless, spectroscopic measurements can yield useful information about the excited states and about photochemical reactions.⁷³

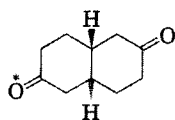
Acidity and Basicity in Excited States

Acidity and basicity are important properties of ground state molecules. If electronically excited states have lifetimes long enough for proton transfer reactions to take place, then the equilibria for such reactions can be determined. Consider the set of reaction coordinate diagrams shown in Figure 12.18. The lower curve represents a potential energy diagram for the dissociation of an acid, $A-H$, in its ground electronic state.



The molecule $A-H$ has an acidic proton as well as a π system that may absorb UV-vis radiation and remain intact after the deprotonation reaction. The

⁷³ A novel property of an electronically excited molecule can be chirality that exists only because of photoexcitation. Miesen, F. W. A. M.; Wollersheim, A. P. P.; Meskers, S. C. J.; Dekkers, H. P. J. M.; Meijer, E. W. *J. Am. Chem. Soc.* **1994**, *116*, 5129 reported the synthesis of optically pure 3-($^1n,\pi^*$)-(1*S*,6*R*)-bicyclo[4.4.0]decane-3,8-dione, which is chiral only in the excited state. The chirality was detected in the circular polarization of chemiluminescence associated with its synthesis from an optically active 1,2-dioxetane precursor.



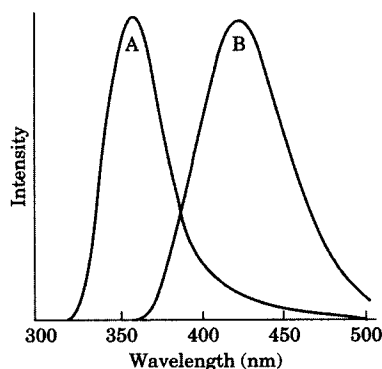
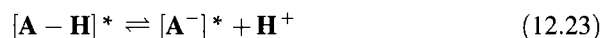


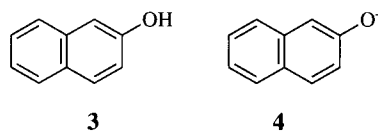
FIGURE 12.19

Fluorescence spectra of 2-naphthol in (A) 0.1 M HClO₄ and (B) 0.1 M NaOH solution. (Reproduced from reference 75.)

ionization of photoexcited $\mathbf{A}^*-\mathbf{H}$ thus occurs in such a way that the dissociation produces \mathbf{A}^{*-} , the electronically excited state of the anion. \mathbf{A}^{*-} may then fluoresce, with energy $h\nu''$. The reaction shown in equation 12.23 is said to be an **adiabatic reaction**, meaning a reaction that takes place on one potential energy surface, which—in this case—is an excited state potential energy surface. Conversely, a **nonadiabatic** process involves a change in electronic state.⁷⁴



Fluorescence from \mathbf{A}^{*-} and $\mathbf{A}^*-\mathbf{H}$ should occur at different wavelengths. Curve A in Figure 12.19 shows the fluorescence spectrum of 2-naphthol (**3**), which was recorded under acidic conditions, while curve B shows the fluorescence spectrum of the 2-naphthoate ion (**4**), which was recorded under basic conditions. At intermediate pH values, fluorescence spectra from both **3** and **4** may be seen. Figure 12.20 shows the fluorescence spectrum of 2-naphthol in a series of solutions with pH values that increase from A to G.^{75,76}

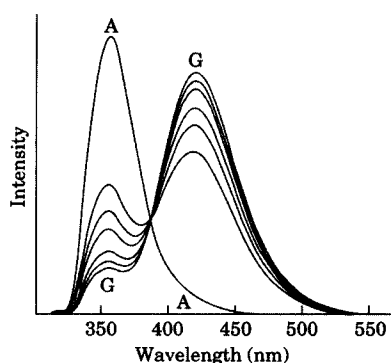


The energy difference between the ground state and excited state of $\mathbf{A}-\mathbf{H}$ can be determined from the 0,0 band of the electronic transition. Similarly, the energy difference between the ground and excited state of \mathbf{A}^- can be deter-

⁷⁴ For a more detailed definition of these terms, see reference 1; Becker, H.-D. *Pure Appl. Chem.* **1982**, *54*, 1589; Förster, T. *Pure Appl. Chem.* **1970**, *24*, 443.

⁷⁵ Lawrence, M.; Marzocco, C. J.; Morton, C.; Schwab, C.; Halpern, A. M. *J. Phys. Chem.* **1991**, *95*, 10294.

⁷⁶ See also (a) Arnaut, L. G.; Formosinho, S. J. *J. Photochem. Photobiol., A* **1993**, *75*, 1; Formosinho, S. J.; Arnaut, L. G. *J. Photochem. Photobiol., A* **1993**, *75*, 21; (b) Marciniak, B.; Kozubek, H.; Paszyc, S. *J. Chem. Educ.* **1992**, *69*, 247; (c) Shizuka, H.; Tobita, S. *Mol. Supramol. Photochem.* **2006**, *14*, 37.

**FIGURE 12.20**

Fluorescence spectra of β -naphthol solutions as a function of pH. (Adapted from reference 75.)

mined from its 0,0 band as well. The enthalpy of proton dissociation of ground state $\mathbf{A-H}$ is ΔH , while the enthalpy of proton dissociation of $\mathbf{A-H}^*$ is ΔH^* .⁷⁷ Examination of Figure 12.18 leads to equation 12.24, which can be rewritten as equation 12.25.⁷⁸

$$\Delta H^* + hv' = \Delta H + hv'' \quad (12.24)$$

$$\Delta H^* = \Delta H + (hv'' - hv') \quad (12.25)$$

If entropy changes are assumed to be approximately the same for dissociation in the ground and excited states, then equation 12.26 holds:

$$\Delta H^* - \Delta H \approx \Delta G^* - \Delta G \quad (12.26)$$

Using the relationship between ΔG values and equilibria

$$\Delta G = 2.303 RT \text{ p}K \quad (12.27)$$

produces the relationship⁷⁹

$$\text{p}K^* = \text{p}K + \frac{hv'' - hv'}{2.303RT} \quad (12.28)$$

Therefore, the $\text{p}K_a$ of the electronically excited state ($\text{p}K^*$) can be determined from the $\text{p}K_a$ of the ground state and the fluorescence energies of $\mathbf{A^*-H}$ and $\mathbf{A^{-*}}$.

Table 12.3 shows some results for $\text{p}K^*$ measurements for S_1 states of some naphthalene derivatives determined this way, as well as for $\text{p}K^*$ values for T_1 states obtained by other methods.^{80,81} The effect of electronic state on $\text{p}K_a$ values can be dramatic. For example, the S_1 state of 2-naphthol is almost one

⁷⁷ Note that ΔH^* is not related to ΔH^\ddagger , the activation enthalpy for deprotonation.

⁷⁸ This procedure is known as the Förster cycle: Förster, T. *Naturwiss.* **1949**, *36*, 186; see also Weller, A. *Prog. Reaction Kinetics* **1961**, *1*, 189.

⁷⁹ There are also other methods used to determine this difference in $\text{p}K$ values. For a more complete discussion of these relationships, see Ireland, J. F.; Wyatt, P. A. H. *Adv. Phys. Org. Chem.* **1976**, *12*, 131.

⁸⁰ Unless otherwise indicated, data are from Jackson, G.; Porter, G. *Proc. R. Soc. London* **1961**, *A260*, 13.

⁸¹ See the discussion in (a) reference 79; (b) Porter, G. in *Reactivity of the Photoexcited Organic Molecule*; Wiley-Interscience: London, 1967; pp. 79–117.

TABLE 12.3 Acidity Constants of Ground and Excited States

Compound	Reaction	pK (S ₀)	pK (S ₁)	pK (T ₁)
Naphthalene ^a	Protonation	-4.0	11.7	-2.5
2-Naphthol	Deprotonation	9.5	3.1	7.7 to 8.1
2-Naphthoic acid	Deprotonation	4.2	8.2 ^b	4.0 ^c
2-Naphthylamine	Protonation	4.1	-2.0	3.1 to 3.3

^a Data from reference 84.

^b Data from reference 85.

^c Data from reference 80.

Source: Reference 79.

million times more acidic than its ground state, while the S₁ state of protonated 2-aminoanthracene is nearly 100 million times more acidic than its ground state.^{82,83} There are also changes in the acidity of the triplet states of these molecules, but they are generally much smaller.

These acidity changes can be rationalized with Lewis structure models for ground and excited state molecules.⁸⁶ The electronically excited state is formed by promoting an electron from HOMO to LUMO. If these two MOs have different atomic coefficients, then the effect will be to shift electron density from one part of the molecule to another. In other words, a certain amount of intramolecular charge transfer accompanies the excitation. In the case of 2-naphthol, the pK_a results and other data suggest that there is charge transfer away from the oxygen and toward the aromatic ring upon excitation from S₀ to S₁. The data suggest that the 2-aminonaphthalene molecule is polarized in the same way. In the case of 2-naphthoic acid, on the other hand, intramolecular charge transfer as a result of excitation must move electron density toward the carboxylic acid group, thus reducing its acidity.

Figure 12.21 shows structures suggested by Jackson and Porter for the naphthalene derivatives described here.⁸⁰ The ground states are described as being the hybrids of predominantly type A resonance structures, with no formal charges or radicals. The excited singlet states are said to have major contributions of type B resonance structures, which have formal positive and negative charges. These charge distributions suggest acid-base properties that are consistent with the experimental results. The excited triplet states are described as having major contributions from type C structures. These resonance structures have radical character but no formal charges, so they are

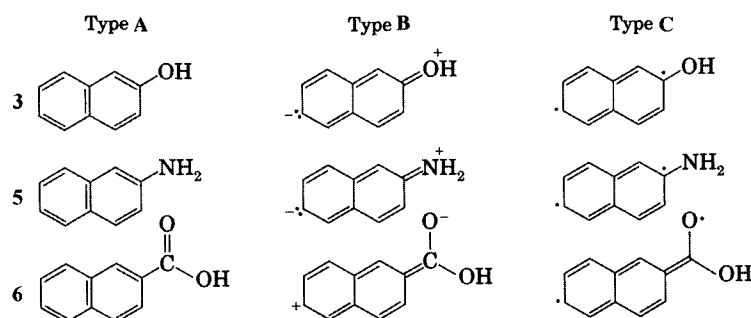
⁸² That is, the ground state amine is 10⁸ more basic than is the excited state.

⁸³ Naphthols with electron-withdrawing substituents such as cyano at C5 and C8 exhibit even more enhanced acidities in their excited singlet states and are capable of proton transfer to solvents such as alcohols in the absence of water. For example, the acidity of 5,8-dicyano-2-naphthol increases from 7.8 in the ground state to -4.5 in the excited singlet state. Tolbert, L. M.; Haubrich, J. E. *J. Am. Chem. Soc.* **1994**, *116*, 10593; Tolbert, L. M.; Solntsev, K. M. *Acc. Chem. Res.* **2002**, *35*, 19.

⁸⁴ Vander Donckt, E.; Lietaer, D.; Nasielski, J. *Bull. Soc. Chim. Belges* **1970**, *79*, 283.

⁸⁵ Kovi, P. J.; Schulman, S. G. *Anal. Chim. Acta* **1973**, *63*, 39.

⁸⁶ Craig, D. P. *Discuss. Faraday Soc.* **1950**, *9*, 5.

**FIGURE 12.21**

Resonance models for electronically excited states. (Adapted from reference 80.)

consistent with acid–base properties for triplets that are similar to the acid–base properties of the ground state molecules.⁸⁷

Bond Angles and Dipole Moments of Excited State Molecules

For small molecules such as formaldehyde, vibrational analysis of the absorption spectrum, including rotational transitions, can yield information about bond lengths and bond angles in the electronically excited state.⁸⁸ The results of such studies can offer valuable insights into photochemical reactivity. Based on the simple electronic energy diagram in Figure 12.4, the lowest energy transition in formaldehyde is predicted to be an $n \rightarrow \pi^*$ transition.⁸⁹ The spacing of the progression of vibrational lines in the $n \rightarrow \pi^*$ transition of formaldehyde indicates that the C=O stretching frequency in the S_1 state is 1182 cm^{-1} , compared to 1746 cm^{-1} in the ground state.⁹⁰ Similarly, analysis of the rotational components of the transition indicates that the S_1 state is nonplanar by 20° .⁹¹ Table 12.4 gives some experimental data for physical properties of the S_0 , S_1 (n, π^*), and T_1 (n, π^*) states of formaldehyde, and Figure 12.22 gives a valence bond representation of these states.^{92,93}

Even larger dipole moment differences between ground states and excited states can be seen. For example, the dipole moment of the n, π^* T_1 state of benzil (7, Figure 12.23) is ca. 0 D, whereas the ground state has $\mu = 3.75\text{ D}$.⁹⁴ Here the π system of the compound is much larger than in

⁸⁷ Because excited triplet states are less likely to have their unpaired electrons on the same atoms than are singlet states (see reference 24), the triplet states tend to have biradicaloid character. For a more detailed discussion of the acid–base properties of photoexcited organic molecules, including carbon acids and carbon bases, see Wan, P.; Shukla, D. *Chem. Rev.* **1993**, *93*, 571.

⁸⁸ For a discussion of the dipole moments of larger molecules in the excited state, see Liptay, W. *Excited States* **1974**, *1*, 129.

⁸⁹ Formaldehyde exhibits an $n \rightarrow \pi^*$ transition at 3.50 eV (80.7 kcal/mol), an $n \rightarrow \sigma^*$ transition at 7.09 eV (163 kcal/mol), and a $\pi \rightarrow \pi^*$ transition at 8.0 eV (184 kcal/mol): King, G. W. *Spectroscopy and Molecular Structure*; Holt, Rinehart and Winston: New York, 1964; p. 424 ff and references therein.

⁹⁰ Brand, J. C. D.; Williamson, D. G. *Adv. Phys. Org. Chem.* **1963**, *1*, 365.

⁹¹ Robinson, G. W.; DiGiorgio, V. E. *Can J. Chem.* **1954**, *36*, 31.

⁹² Turro, N. J.; Dalton, J. C.; Dawes, K.; Farrington, G.; Hautala, R.; Morton, D.; Niemczyk, M.; Schore, N. *Acc. Chem. Res.* **1972**, *5*, 92.

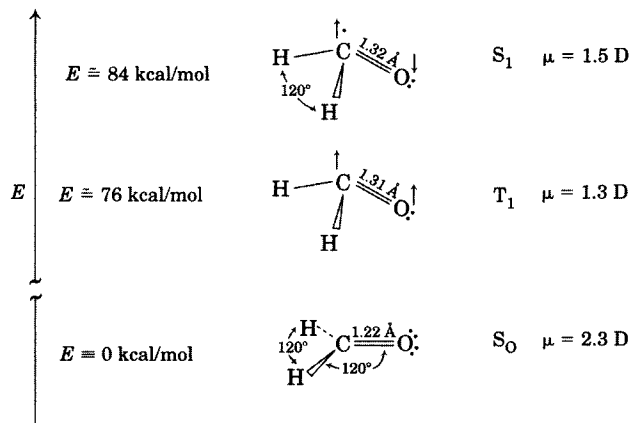
⁹³ Conformational changes can also result from photoexcitation. Tomer, J. L.; Spangler, L. H.; Pratt, D. W. *J. Am. Chem. Soc.* **1988**, *110*, 1615 reported different conformational preferences for the methyl group in S_1 and T_1 acetophenone.

⁹⁴ Fessenden, R. W.; Carton, P. M.; Shimamori, H.; Scaiano, J. C. *J. Phys. Chem.* **1982**, *86*, 3803.

TABLE 12.4 Physical Properties of Formaldehyde Excited States

Property/State	S ₀	S ₁	T ₁
Geometry	Planar	Pyramidal	Pyramidal
Δ (nonplanarity)	0°	20°	35°
C=O length	1.22 Å	1.32 Å	1.31 Å
ν C=O stretch	1746 cm ⁻¹	1182 cm ⁻¹	1251 cm ⁻¹
∠ _{HCH}	120°	122°	
Dipole moment	2.3 D	1.5 D	1.3 D

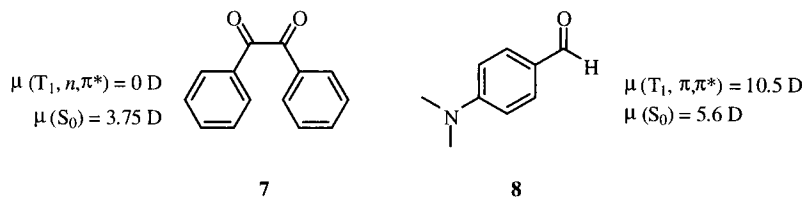
Source: Data from references 90, 91, and 92.

**FIGURE 12.22**

Representations of the electronic states of formaldehyde. (Adapted from reference 92.)

FIGURE 12.23

S₀ and T₁ dipole moments of benzil (7) and 4-(dimethylamino)benzaldehyde (8).



formaldehyde, so the electron promoted from n to π^* is removed much further from a carbonyl oxygen. The opposite effect on excited state polarity is seen for compounds with π, π^* lowest triplet states. For example, the dipole moment of ground state 4-(dimethylamino)benzaldehyde (8) is 5.6 D, but the lowest triplet, a π, π^* state, has a dipole moment of 10.5 D.⁹⁴

Because of these changes in dipole moments between ground and excited states, solvent polarity can have a pronounced effect on the absorption spectrum of some compounds. Benzophenone exhibits two broad absorption bands: a very weak absorption with λ_{max} near 325 nm (ϵ in the range 20–200) and a more intense absorption (ϵ around 20,000) at about 250 nm (Figure 12.24). The longer wavelength peak is assigned to an $n \rightarrow \pi^*$ transition and the shorter wavelength peak to a $\pi \rightarrow \pi^*$ transition. The intensities support these assignments. For the $\pi \rightarrow \pi^*$ transition there are no symmetry, spin, or Franck–Condon prohibitions. The transition is fully allowed and therefore is intense. The $n \rightarrow \pi^*$ transition is much less intense, however, because to a first approximation the n orbital and the π^* orbitals are orthogonal

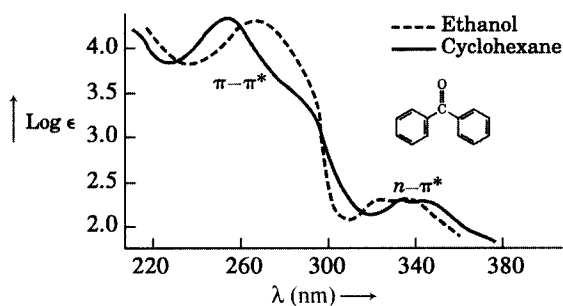


FIGURE 12.24

Solvent effect on benzophenone absorption. (Adapted from reference 6.)

to each other. Some of the orthogonality is removed by vibrational deformation of the molecule, so the transition is observed but is weak.^{95,96}

The polar ground state of a carbonyl compound is stabilized more by a polar solvent than is a less polar n,π^* excited state, so there is a greater energy gap between the two states in a more polar solvent. This means that an $n \rightarrow \pi^*$ absorption is seen at a shorter wavelength in a more polar solvent, as is seen for benzophenone in Figure 12.24. For the $\pi \rightarrow \pi^*$ transition, however, charge transfer takes place from the extended π system toward the oxygen atom, which increases the polarity of the molecule in the excited state. Therefore, the energy gap between the ground and excited states decreases, and the $\pi \rightarrow \pi^*$ ($S_0 \rightarrow S_2$) absorption occurs at longer wavelength in a more polar solvent.⁹⁷

Change in molecular polarity upon photoexcitation may also affect the partitioning of excited state molecules between environments of different polarity. Scaiano and co-workers reported laser flash spectroscopic studies of xanthone (**9**) complexed with cyclodextrins in aqueous solution. They found that photoexcited (T_1) xanthone moves from the cyclodextrin into bulk solution with a rate constant of ca. 10^7 s^{-1} .⁹⁸ This relocation was attributed to the greater polarity of the π,π^* triplet of **9**, leading to a smaller equilibrium constant for association of photoexcited xanthone with the cyclodextrin cavity as opposed to the more polar aqueous solution. Similarly, Quina and co-workers found that T_1 (π,π^*) *m*-nitroanisole (**10**) is only about one-tenth as soluble in sodium dodecyl sulfate micelles as is the ground state.⁹⁹ In this case the solubility difference was attributed to greater hydrogen bonding

⁹⁵ Pople, J. A.; Sidman, J. W. *J. Chem. Phys.* **1957**, *27*, 1270.

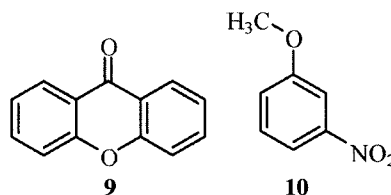
⁹⁶ Even if the molecule is excited by light sufficiently high in energy to cause a $\pi \rightarrow \pi^*$ transition, the photochemistry of many aldehydes and ketones arises from the n,π^* state because the S_2 (π,π^*) state relaxes quickly to the S_1 (n,π^*) state. Furthermore, intersystem crossing is usually very rapid in carbonyl compounds, so much of the photochemistry arises from the T_1 (n,π^*) state.

⁹⁷ In general, a shift to the red with increasing solvent polarity is characteristic of $\pi \rightarrow \pi^*$ transitions, while a blue shift is characteristic of $n \rightarrow \pi^*$ bands.⁹⁷ In spectroscopic terms, the shift of an absorption maximum to shorter wavelength is called a *hypsochromic shift* or blue shift. The shift of an absorption maximum to longer wavelength is called a *bathochromic shift* or red shift. An increase in the intensity of an absorption band is called a *hyperchromic effect*, while a decrease in the intensity of a band is called a *hypochromic effect*. The effect of solvent on $\pi \rightarrow \pi^*$ transitions is usually smaller than for $n \rightarrow \pi^*$ transitions. See, for example, Pavia, D. L.; Lampman, G. M.; Kriz, Jr., G. S. *Introduction to Spectroscopy: A Guide for Students of Organic Chemistry*; Saunders College Publishing: Philadelphia, 1979. For a theoretical study of the $\pi \rightarrow \pi^*$ blue shift of acetone, see Gao, J. *J. Am. Chem. Soc.* **1994**, *116*, 9324.

⁹⁸ Barra, M.; Bohne, C.; Scaiano, J. C. *J. Am. Chem. Soc.* **1990**, *112*, 8075.

⁹⁹ Tedesco, A. C.; Nogueira, L. C.; Bonilha, J. B. S.; Alonso, E. O.; Quina, F. H. *Química Nova* **1993**, *16*, 275.

capability of the photoexcited compound due to increased electron density on the nitro group in the excited state.¹⁰⁰



12.4 REPRESENTATIVE PHOTOCHEMICAL REACTIONS

Thermal reactions of organic molecules can be categorized according to functional groups in the reactants. In photochemical reactions the most important functional groups are the **chromophores**—the functional groups that absorb UV–vis radiation directly or that accept energy by sensitization. An excited chromophore may either undergo photochemical reaction itself or channel electronic or vibrational energy to another portion of the molecule. As was the case with thermal reactions, valence bond and molecular orbital descriptions are useful, complementary models to help us rationalize photochemical reactions.

Photochemical Reactions of Alkenes and Dienes

According to HMO theory, the HOMO of a nonconjugated alkene is a π orbital, while the LUMO is a π^* orbital (Figure 12.25). Therefore, we expect to see only a $\pi \rightarrow \pi^*$ transition in the UV–vis spectrum of an alkene. The λ_{\max} for an olefinic $\pi \rightarrow \pi^*$ transition is usually less than 200 nm, which is in a region of the spectrum known as the far UV or the vacuum UV (meaning that it is beyond the wavelength limit of spectrophotometers that operate in air).¹⁰¹ The onset of the absorption for a nonconjugated olefin is about 230 nm but is so gradual that it is difficult to determine an exact value. For that reason, alkenes are said to exhibit only **end absorption**, meaning that only the onset of the absorption can be observed, not its maximum.¹⁰²

This simple orbital model in Figure 12.25 is not entirely consistent with the available experimental data. Indeed, Kropp called the isolated carbon–carbon double bond “one of the most deceptively simple chromophores available to the organic chemist.”¹⁰³ Even though the end absorption apparently includes the π, π^* transition, there is evidence that there may also be weak absorption due to $\pi \rightarrow \sigma^*$ and Rydberg transitions. In alkenes, the Rydberg state is thought to result from promotion of an electron from the π orbital to a carbon orbital that has the characteristics of a 3s orbital in helium.

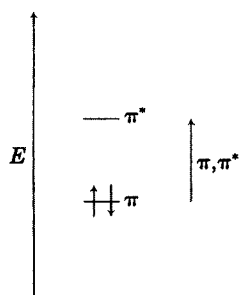


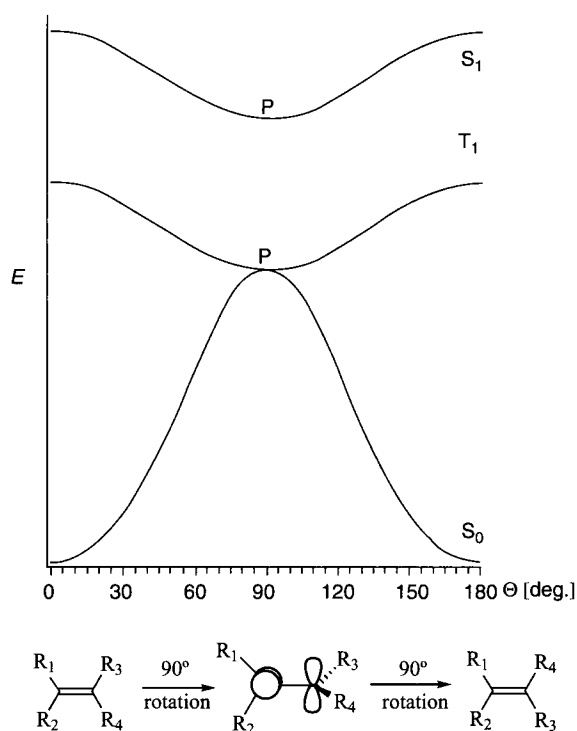
FIGURE 12.25
Origin of a π, π^* transition.

¹⁰⁰ Tedesco, A. C.; Nogueira, L. C.; Carreiro, J. C.; da Costa, A. B.; Bonilha, J. B. S.; Moreira, P. F., Jr.; Alonso, E. O.; Quina, F. H. *Langmuir*, **2000**, *16*, 134. For a model of the excited state, see Figure 12.53, page 846.

¹⁰¹ For a discussion of techniques and applications of far-UV photochemistry, see Leigh, W. J. *Chem. Rev.* **1993**, *93*, 487.

¹⁰² For a theoretical study of the excited states of ethene, see Wiberg, K. B.; Hadad, C. M.; Foresman, J. B.; Chupka, W. A. *J. Phys. Chem.* **1992**, *96*, 10756.

¹⁰³ Kropp, P. J. *Mol. Photochem.* **1978–79**, *9*, 39.

**FIGURE 12.26**

Torsional dependence of the electronic energies of the ground state and singlet and triplet π, π^* states of ethene. (Adapted from references 108a and 108b.)

The radial distribution of this orbital is large in comparison with the $2p$ orbitals that are the basis set for the π orbital. In essence, this is an orbital around the entire molecule.^{104,105} Moreover, internal conversion of the π, σ^* , Rydberg, and π, π^* states of alkenes is slow. These states may therefore exhibit their own characteristic photochemical reactions, so there can be significant wavelength effects on the distribution of photochemical products.¹⁰⁶

Figure 12.26 shows the potential energy curves for the S_0 , T_1 ($^3\pi, \pi^*$) and S_1 ($^1\pi, \pi^*$) states of an alkene as a function of rotation about the carbon–carbon double bond.^{107–109} The $^1\pi, \pi^*$ excited state created by direct excitation of an alkene is a “vertical” state (often called a **Franck–Condon state**), meaning that it has the same geometry as the ground state molecule. In the $^1\pi, \pi^*$ state the electrons in the singly occupied MOs are still spin paired, and to a first approximation the π^* orbital is antibonding to the same extent that the π orbital is bonding. Because the carbon–carbon bond order is reduced from

¹⁰⁴ Merer, A. J.; Mulliken, R. S. *Chem. Rev.* **1969**, *69*, 639.

¹⁰⁵ Evidence supporting the existence of the Rydberg state was reported by Hirayama, F.; Lipsky, S. J. *Chem. Phys.* **1975**, *62*, 576, who found weak fluorescence from a series of substituted ethenes.

¹⁰⁶ An additional complication in the photochemical reactions of alkenes in the gas phase is the possible involvement of vibrationally excited (hot) electronic ground states produced from an excited state. For a review, see Collin, G. J. *Adv. Photochem.* **1988**, *14*, 135.

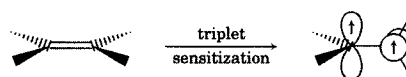
¹⁰⁷ Compare Saltiel, J.; D’Agostino, J.; Megarity, E. D.; Metts, L.; Neuberger, K. R.; Wrighton, M.; Zafiriou, O. C. *Org. Photochem.* **1973**, *3*, 1.

¹⁰⁸ (a) The curves for S_0 and T_1 are from a report by Brink, M.; Möllerstedt, H.; Ottosson, C.-H. *J. Phys. Chem. A* **2001**, *105*, 4071, and (b) the S_1 curve is modeled after that reported by Ben-Nun, M.; Quenneville, J.; Martínez, T. J. *J. Phys. Chem. A* **2000**, *104*, 5161.

¹⁰⁹ The $^1\pi, \pi^*$ designation refers to a singlet π, π^* state. Similarly, $^3\pi, \pi^*$ refers to a triplet π, π^* state. These states may also be designated as $^1(\pi, \pi^*)$ and $^3(\pi, \pi^*)$, respectively.

FIGURE 12.27

Orbital relationship in perpendicular olefinic π, π^* triplet.



two to one, excitation removes the barrier to rotation about the former double bond. The simple HMO description does not take into account the electron–electron repulsion present in the vertical excited state, however. Rotation toward a 90° (perpendicular, denoted **p** in Figure 12.26) conformation of the carbon–carbon bond makes the two *p* orbitals orthogonal, relieving some electron–electron repulsion and minimizing the energy of the system.¹¹⁰ The π, π^* singlet states of nonconjugated acyclic olefins do not fluoresce because rotation about the carbon–carbon bond is faster than fluorescence, and the perpendicular excited singlet has a negligible Franck–Condon overlap with the ground state.¹¹¹

Radiationless decay of the perpendicular excited singlet to either the cis or trans ground state can lead to isomerization of the photoexcited alkene. Furthermore, the rapid radiationless decay of the excited singlet state means that intersystem crossing from a π, π^* singlet to a triplet is extremely unlikely. Olefinic triplets can be formed by sensitization, as will be discussed later. The potential energy curve for the ${}^3\pi, \pi^*$ state is lower than that for the ${}^1\pi, \pi^*$ state at all geometries, and it also is expected to rotate toward a 90° orientation as shown in Figure 12.27.^{112,113} Intersystem crossing from the perpendicular triplet to the ground state also leads to S_0 of either the cis or trans isomer, so sensitized excitation of alkenes can lead to cis–trans isomerization.

It is not evident from Figure 12.26 how the twisted S_1 state is converted to one or the other isomer of the S_0 state. Furthermore, the figure does not take into account the distortion of molecular geometry as the planar S_0 becomes more pyramidal in the perpendicular geometries of S_1 or T_1 . A more complete model of a process involving conversion of one electronic state of an alkene to another results from consideration of two reaction coordinates, one for rotation about the olefinic C–C bond and another for change in geometry (pyramidalization) that accompanies the rotation.¹¹⁴ Including both coordinates generates a potential energy *surface* for each electronic state, as is shown for the S_0 and S_1 (${}^1\pi, \pi^*$) states of ethene in Figure 12.28. Figure 12.28(a) shows that the curves for S_0 and S_1 in Figure 12.26 are just one slice through

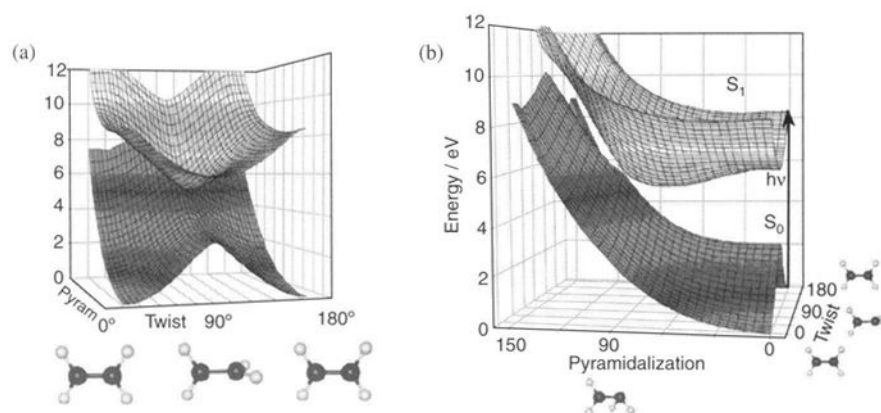
¹¹⁰ Theoretical calculations suggest that the twisted (90°) ${}^1\pi, \pi^*$ state can have considerable contribution from zwitterionic structures, particularly if the double bond has polar substituents. See, for example, Wulfman, C. E.; Kumei, S. *Science* **1971**, *172*, 1061; Salem, L. *Science* **1976**, *191*, 822; Salem, L. *Acc. Chem. Res.* **1979**, *12*, 87; Buenker, R. J.; Bonačić-Koutecký, V.; Pogliani, L. *J. Chem. Phys.* **1980**, *73*, 1836; Brooks, B. R.; Schaefer, H. F. III. *J. Am. Chem. Soc.* **1979**, *101*, 307; reference 64, pp. 206–216.

¹¹¹ Fluorescence has been observed from conjugated polyenes. See the discussion in reference 29.

¹¹² Note also that at 90° the energy of the π, π^* triplet is equal to that of the twisted ground state. Other calculations place the energy of the twisted triplet slightly lower or slightly higher than that of the twisted ground state (cf. Yamaguchi, Y.; Osamura, Y.; Schaefer, H. F. III. *J. Am. Chem. Soc.* **1983**, *105*, 7506). In any case, the two states are expected to be close in energy at that geometry.

¹¹³ For discussions of the 1,2-biradical nature of alkene triplets, see Caldwell, R. A.; Zhou, L. *J. Am. Chem. Soc.* **1994**, *116*, 2271; Caldwell, R. A.; Díaz, J. F.; Hrcncir, D. C.; Unett, D. J. *J. Am. Chem. Soc.* **1994**, *116*, 8138.

¹¹⁴ Salem, L. *Electrons in Chemical Reactions: First Principles*; Wiley-Interscience: New York, 1982.

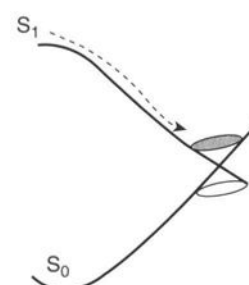
**FIGURE 12.28**

Two-dimensional representations of the S_0 and S_1 states of ethene. (Adapted from reference 108b.)

Figure 12.28 corresponding to a pyramidalization angle of 0° (i.e., with planar carbon atoms throughout the rotation). Figure 12.28(b) shows that the S_0 and S_1 potential energy surfaces just touch at one point, which is called a **conical intersection**.^{64,115–117} Now we see that an alkene excited from S_0 to S_1 would not only distort by rotation about the C–C bond but would also develop nonplanarity at the carbon atoms during the rotation. At the lowest point on the S_1 surface, the excited molecules can pass through the conical intersection (Figure 12.29) and then move over the S_0 surface toward either the planar 0° geometry or the isomerized 180° geometry.¹¹⁸

It is useful to summarize the descriptions of the isomerization of an alkene upon direct excitation in terms of the different models used in this chapter. Figure 12.30(a) shows a simple statement of the process in terms of excitation from S_0 to an upper vibrational level of S_1 , relaxation to the 0th vibrational level of S_1 , and internal conversion to an upper vibrational level of S_0 . While the drawing conveys the energy relationships, it does not indicate how the isomerization occurs. Figure 12.30(b) adds the detail that the energy of the S_0 state is a maximum at a 90° rotation and the energy of the S_1 state is a minimum at that twist angle, but the conversion of the S_1 state to the S_0 state is not indicated. Figure 12.30(c) offers a more complete—but more complex—picture of the process. Now we see that the photoisomerization involves (i) a vertical excitation, (ii) simultaneous rotation about the C–C bond and pyramidalization of the carbon atoms to achieve a minimum energy geometry on the S_1 potential energy surface, (iii) passage through the conical intersection to the S_0 potential energy surface, and (iv) relaxation of the resulting distorted S_0 structure to one or the other isomer of the olefin ground state.

The presence of substituents on the olefinic carbon atoms adds other features to the analysis. Cis isomers can be less stable than trans isomers because of van der Waals repulsion of the cis substituents. This steric interaction can distort the alkene from a perfectly planar ground state geometry, reducing the overlap of the two p orbitals. As a result, photoexcitation of the cis isomer may require shorter wavelength UV–vis radiation than

**FIGURE 12.29**

Schematic representation of the passage of a structure in an S_1 state through a conical intersection to the S_0 state. (Adapted from reference 118).

¹¹⁵ Klessinger, M.; Michl, J. *Excited States and Photochemistry of Organic Molecules*; VCH: New York, 1995.

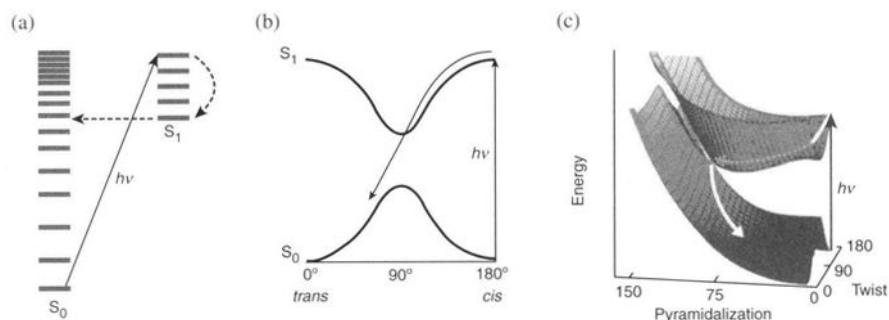
¹¹⁶ Robb, M. A.; Bernardi, F.; Olivucci, M. *Pure Appl. Chem.* **1995**, *67*, 783.

¹¹⁷ Matskia, S. *Rev. Comput. Chem.* **2007**, *23*, 83.

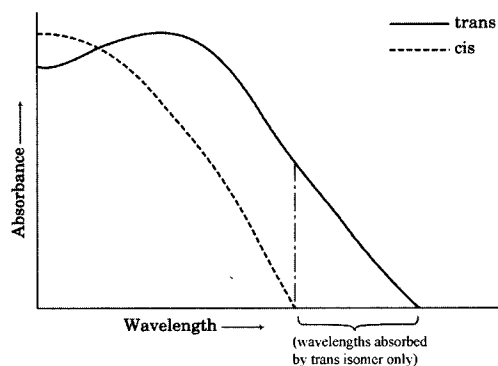
¹¹⁸ Levine, B. G.; Martínez, T. J. *Annu. Rev. Phys. Chem.* **2007**, *58*, 613.

FIGURE 12.30

Three models for the isomerization of an alkene upon direct excitation: (a) a simplified model based on an energy-state diagram, (b) a two-dimensional drawing modeled on Figure 12.26, and (c) a three-dimensional model incorporating a conical intersection. (Adapted from reference 118.)

**FIGURE 12.31**

Idealized alkene absorption spectra.



does excitation of the trans isomer, as shown by the hypothetical example in Figure 12.31. In such a case, excitation at the wavelengths indicated would excite only the trans isomer. More commonly, the absorption spectra of the cis and trans isomers overlap, so we choose a wavelength at which one isomer has a higher ϵ than the other. As an example, Figure 12.32 shows the UV absorption spectrum of the *cis*- (broken line) and *trans*- (solid line) isomers of *N,N*-dimethyl-*p*-methoxycinnamamide as a 5×10^{-5} M solution in methylene chloride.¹¹⁹

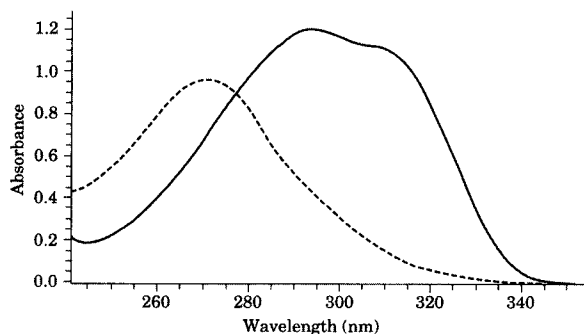
Irradiation of a mixture of *cis* and *trans* alkenes at a wavelength that is strongly absorbed by the *trans* isomer but only weakly absorbed by the *cis* isomer will allow photochemical conversion of *trans* alkene to *cis* alkene. A photoexcited *trans* molecule may relax to the perpendicular conformation, then decay either to the *cis* (C) or *trans* (T) isomer.^{120–122} If the excited state

¹¹⁹ Lewis, F. D.; Elbert, J. E.; Uptagrove, A. L.; Hale, P. D. *J. Org. Chem.* **1991**, *56*, 553.

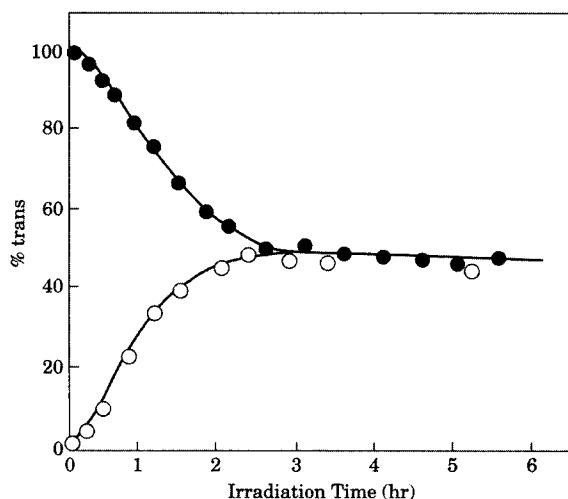
¹²⁰ This generalization of the photoisomerization of nonconjugated alkenes does not apply to one of the best-known photochemical isomerizations, the conversion of 11-*cis*-rhodopsin to the all-*trans* isomer. The speed of the isomerization (200 fs) has been related to distortion of the 11-*cis* double bond from planarity and to steric interactions in the 11-*cis* isomer that provide a force for rotation of the photoexcited *cis* isomer toward the geometry of the *trans* isomer. Wang, Q.; Schoenlein, R. W.; Peteanu, L. A.; Mathies, R. A.; Shank, C. V. *Science* **1994**, *266*, 422.

¹²¹ In some cases the rate constant for formation of the *cis* isomer (k_c) is greater than for formation of the *trans* isomer (k_t). Because the *cis* isomer is higher in energy than the *trans*, there may be better overlap of the vibrational component of the wave function of the *cis* ground state with the vibrational component of the excited state than is the case with the *trans* isomer. Thus, the Franck–Condon term for the twisted singlet to *cis* reaction could be more favorable than for the *trans*.

¹²² Some compounds exhibit “one-way” photoisomerization. For a review, see Arai, T.; Tokumaru, K. *Chem. Rev.* **1993**, *93*, 23.

**FIGURE 12.32**

UV spectra of *trans*- (solid line) and *cis*- (broken line) *N,N*-dimethyl-*p*-methoxycinnamide. (Reproduced from reference 119.)

**FIGURE 12.33**

Photochemical production of photostationary state concentrations of *cis*- (filled circles) and *trans*-cyclooctene (open circles). (Adapted from reference 123.)

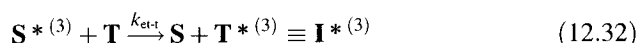
decays to the *cis* isomer, the low absorbance by that isomer means that further reaction is not very probable. If the excited state decays to the *trans* isomer, then it may be excited again later and have another chance to be converted to *cis*. Eventually, the system reaches a **photostationary state (pss)**, which is a function (equation 12.29) of the molar extinction coefficients at the irradiation wavelength and the rate constants for formation of the *cis* isomer (k_c) or for formation of the *trans* isomer (k_t) from the excited singlet state. Figure 12.33 shows results of the direct (185 nm) irradiation of cyclooctene. The percent of *trans* isomer present is plotted as a function of time for experiments beginning with pure *trans* (filled circles) or pure *cis* (open circles). The photostationary state corresponds to a 47 : 53 *trans*: *cis* mixture.¹²³

$$\frac{[\mathbf{C}]_{\text{pss}}}{[\mathbf{T}]_{\text{pss}}} = \frac{\varepsilon_{\text{trans}} k_c}{\varepsilon_{\text{cis}} k_t} \quad (12.29)$$

Even though the triplet states of simple alkenes ordinarily are not produced by direct irradiation, the $^3\pi,\pi^*$ states of alkenes can be formed

¹²³ Inoue, Y.; Takamuku, S.; Sakurai, H. *J. Phys. Chem.* 1977, 81, 7.

indirectly by sensitization.¹²⁴ If one electron of an olefin triplet excited state undergoes a spin flip, the molecule can relax to the ground state of either the cis or the trans isomer. In equations 12.30 through 12.35, **S** is a sensitizer that can be excited by direct irradiation and then undergo intersystem crossing to its triplet state. If **S***⁽³⁾ is higher in energy than **C***⁽³⁾, then energy transfer can occur (equation 12.31).¹²⁵ In these equations, the rate constants are given designations that suggest the process involved. For example, $k_{\text{et-c}}$ is the rate constant for energy transfer to the cis isomer.



Note that the intermediate triplet (**I***⁽³⁾) is assumed to be the same species, no matter whether the cis isomer or the trans isomer was sensitized.¹²⁶ Now the photostationary state is a function of the rate constants for energy transfer to the two isomers, $k_{\text{et-t}}$ and $k_{\text{et-c}}$, and the rate constants for the decay of **I***⁽³⁾ to the cis and trans isomers, k_c and k_t , respectively.¹²⁷

$$\frac{[\mathbf{C}]_{\text{pss}}}{[\mathbf{T}]_{\text{pss}}} = \frac{k_{\text{et-t}} k_c}{k_{\text{et-c}} k_t} \quad (12.35)$$

The products of photochemical reactions can arise either directly from electronically excited states or by way of reactive ground state intermediates resulting from electronic excitation. For example, irradiation of a solution of 1-methylcyclohexene (**11**) and an aromatic sensitizer such as *p*-xylene in methanol produces methyl 1-methylcyclohexyl ether (**12**) plus a small quantity of methylenecyclohexane (**13**, Figure 12.34). A plausible mechanism involves triplet-sensitized isomerization of the *cis*-1-methylcyclohexene to an unstable *trans*-cyclohexene intermediate (**14**). The highly strained **14** can rapidly add a proton from the solvent to form a 3° carbocation (**15**), which can then undergo nucleophilic addition to give **12** (major product) or elimination to give **13** (minor product).¹²⁸ This mechanism is supported by the observation of trans cycloalkenes in trapping reactions¹²⁹ and by the detection

¹²⁴ Lewis, F. D.; Bassani, D. M.; Caldwell, R. A.; Unett, D. J. *J. Am. Chem. Soc.* **1994**, *116*, 10477 found that *trans*-1-phenylpropene does not isomerize from the singlet state, but at low temperatures it undergoes intersystem crossing and then isomerizes from the triplet state. On the other hand, *cis*-1-phenylpropene undergoes isomerization primarily from the singlet state at room temperature.

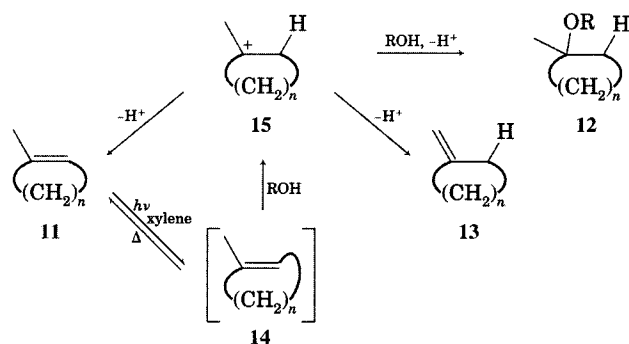
¹²⁵ Reference 6. See also Hammond, G. S. *Kagaku to Kogyō (Tokyo)* **1965**, *18*, 1464.

¹²⁶ In some cases there may be more than one minimum on an excited state potential energy surface, so this assumption may not be warranted.

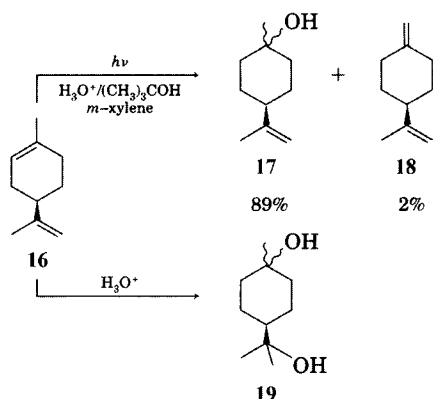
¹²⁷ For a study of sensitized isomerizations of olefins, see Snyder, J. J.; Tise, F. P.; Davis, R. D.; Kropp, P. J. *J. Org. Chem.* **1981**, *46*, 3609.

¹²⁸ Kropp, P. J. in reference 2, p. 9-1.

¹²⁹ Goodman, J. L.; Peters, K. S.; Misawa, H.; Caldwell, R. A. *J. Am. Chem. Soc.* **1986**, *108*, 6803.

**FIGURE 12.34**

Photochemical isomerization and solvent incorporation with methylcyclohexane ($n = 4$). (Adapted from reference 103.)

**FIGURE 12.35**

Photohydration of limonene. (Reproduced from reference 103.)

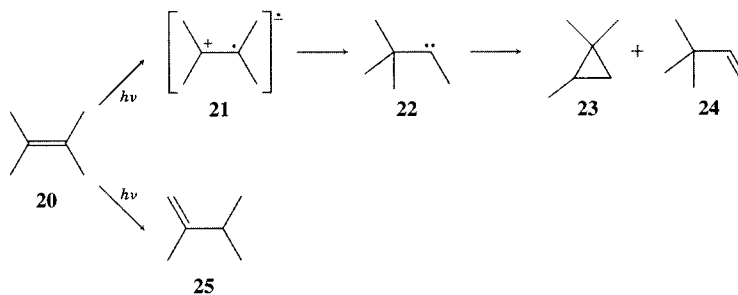
of the 1-phenylcyclohexyl cation in the flash spectroscopy of 1-phenylcyclohexene in 1,1,1,3,3,3-hexafluoroisopropyl alcohol.¹³⁰

The intermediacy of strained cycloalkenes in such reactions is further supported by the reaction of limonene. As shown in Figure 12.35, photohydration of limonene (16) produces an 89% yield of the alcohol 17 (plus a small amount of 18) as a result of hydration of the endocyclic double bond only. In contrast, acid-catalyzed hydration of 16 produces only the diol 19, in which both double bonds have been hydrated.¹⁰³

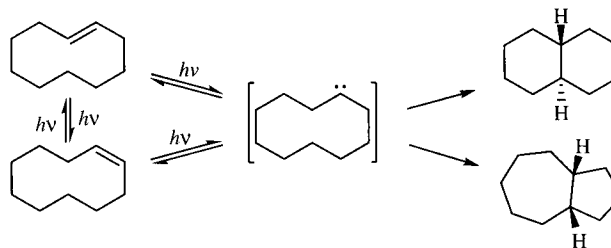
Photochemical product formation can arise from other reactive intermediates as well. Figure 12.36 shows the products from direct irradiation of 2,3-dimethylbut-2-ene (20). Excitation is thought to produce the Rydberg state 21 and then the carbene 22, which rearranges to products 23 and 24. There is apparently another mechanism responsible for the formation of the isomerization product 25, and a pathway involving a π, σ^* state has been suggested.^{103,131}

¹³⁰ Cozens, F. L.; McClelland, R. A.; Steenken, S. J. *Am. Chem. Soc.* **1993**, *115*, 5050.

¹³¹ Kropp, P. J.; Fravel, H. G., Jr.; Fields, T. R. *J. Am. Chem. Soc.* **1976**, *98*, 840. See also the discussion in (a) reference 103; (b) Cherry, W.; Chow, M.-F.; Mirbach, M. J.; Mirbach, M. F.; Ramamurthy, V.; Turro, N. J. *Mol. Photochem.* **1977**, *8*, 175; (c) Inoue, Y.; Mukai, T.; Hakushi, T. *Chem. Lett.* **1983**, 1665; Kropp, P. J. in reference 2, p. 13-1.

**FIGURE 12.36**

Products from direct irradiation of tetramethylethylene. (Adapted from reference 131b.)

**FIGURE 12.37**

Photochemical conversion of *cis*- and *trans*-cyclodecene to bicyclic products.

The intermediacy of a carbene has also been proposed to explain the formation of bicyclo[5.3.0]decane and bicyclo[4.4.0]decane from irradiation of the *cis* and *trans* isomers of cyclodecene (Figure 12.37).¹³²

Similarly, Adam and co-workers suggested that irradiation of cyclobutene (26) with 185 nm radiation produces both π, π^* and Rydberg ($\pi, 3s$) excited states. The π, π^* state is thought to lead to electrocyclic opening to 1,3-butadiene (27), while the Rydberg state leads to carbene intermediates (28 and 29) that can fragment to give ethene and acetylene or can rearrange to methylenecyclopropane (30) and 1,3-butadiene (Figure 12.38).^{133–135}

The discussion in Chapter 11 described photochemical reactions of alkenes in terms of orbital symmetry, but the possible intermediacy of multiple, independent alkene excited states complicates the analysis of photochemical reactions in terms of the Woodward–Hoffmann rules. For example, photochemical ring opening of cyclobutenes appears to be nonstereospecific.¹³⁶ Irradiation of the cyclobutene 31 with 193 nm UV radiation produced not only the allowed *cis,cis,cis*-1,3,5-cyclodecatriene 32, but also the *cis,trans,cis* isomer 33 and the *cis,cis,trans* isomer 34.¹³⁷ Among the possible explanations for the forbidden products are:

¹³² Haufe, G.; Tubergen, M. W.; Kropp, P. J. *J. Org. Chem.* **1991**, *56*, 4292.

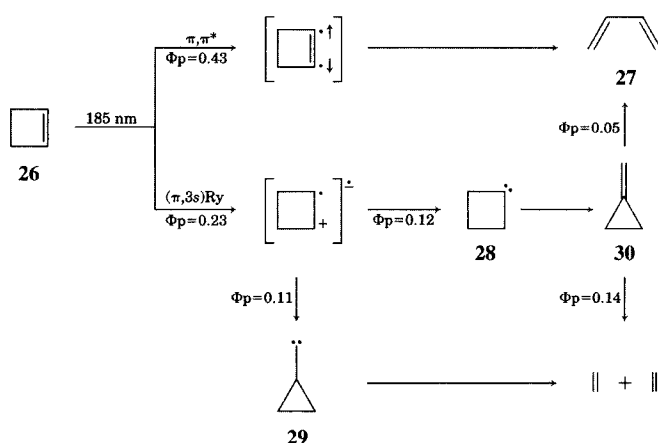
¹³³ Adam, W.; Oppenländer, T.; Zang, G. *J. Am. Chem. Soc.* **1985**, *107*, 3921.

¹³⁴ See also Leigh, W. J.; Zheng, K.; Clark, K. B. *J. Org. Chem.* **1991**, *56*, 1574; Prathapan, S.; Agosta, W. C. *Chemtracts–Org. Chem.* **1991**, *4*, 460.

¹³⁵ Leigh, W. J.; Zheng, K. *J. Am. Chem. Soc.* **1991**, *113*, 4019 reported evidence for photochemical disrotatory ring opening in one bicyclic system incorporating a cyclobutene ring, but the stereospecificity in such cases seems to depend on the structural features incorporated into the reactants. For a discussion of the relationship of orbital symmetry to the photochemistry of cyclobutene, see Leigh, W. J. *Can. J. Chem.* **1993**, *71*, 147.

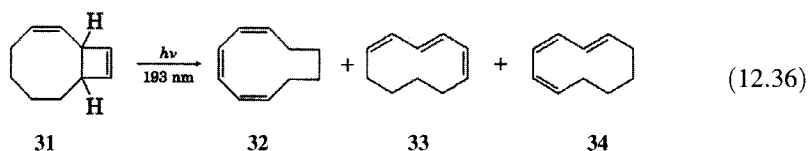
¹³⁶ Clark, K. B.; Leigh, W. J. *J. Am. Chem. Soc.* **1987**, *109*, 6086.

¹³⁷ Dauben, W. G.; Haubrich, J. E. *J. Org. Chem.* **1988**, *53*, 600.

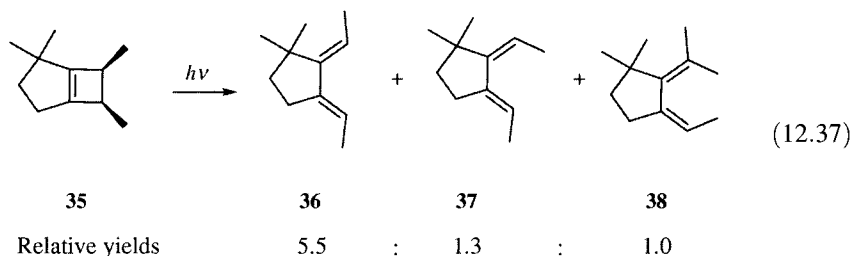
**FIGURE 12.38**

Photochemical reaction pathways in cyclobutene. (Adapted from reference 133.)

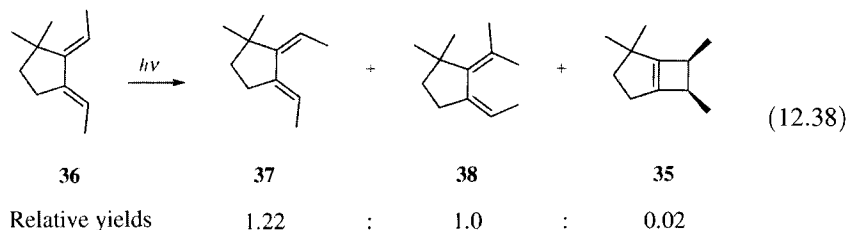
1. Thermal formation from the highly strained, photochemically allowed trans,trans,cis isomer.
2. Thermal formation from a vibrationally excited ground state formed by radiationless decay of the excited state.
3. Adiabatic opening of the cyclobutene to an electronically excited triene, which could then exhibit photochemical isomerization.
4. Reaction from some state other than a π, π^* state.



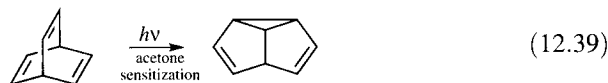
A subsequent investigation suggested that the third explanation applies for the opening of *cis*-2,2,6,7-tetramethylbicyclo[3.2.0]hept-1(5)-ene (35).¹³⁸ Irradiation of 35 led to the photochemically allowed product 36 as well as to isomers 37 and 38 (equation 12.37). In a separate reaction, irradiation of 36 produced products 37 and 38 in almost the same relative yield as when 35 was irradiated (equation 12.38). The investigators concluded that—at least in this reaction—the orbital symmetry-allowed, stereospecific, disrotatory ring opening of 35 produces 36 in an electronically excited state that then undergoes radiationless decay to 36 or photochemical *cis*–*trans* isomerization to 37 and 38.



¹³⁸ Leigh, W. J.; Postigo, J. A.; Venneri, P. C. *J. Am. Chem. Soc.* **1995**, *117*, 7826.



The preceding analysis assumed that the two double bonds in **31** are independent, and the reaction was analyzed in terms of the double bond in the cyclobutene ring. Nonconjugated double bonds may interact if they are close together. For example, the di- π -methane rearrangement (equation 12.39), first reported by Zimmerman and thus also known as the Zimmerman rearrangement, has been the subject of extensive investigation.¹³⁹⁻¹⁴¹ The exact course of the reaction and its multiplicity depend on the nature of the substituent groups attached to the double bonds. Although the process may be formally represented as a $[\sigma 2 + \pi 2]$ cycloaddition, the observation that the irradiation of the deuterium-labeled compound **39** (Figure 12.39) produced equal yields of the two products **40** and **41** suggests a mechanism involving a biradical intermediate.



1,5-, 1,6-, and 1,7-Dienes undergo sensitized intramolecular cycloaddition. The reactions can be explained in terms of stepwise addition of the triplet of one double bond to the second double bond to form a 1,4-biradical intermediate, which can then close to a cyclobutane ring through a

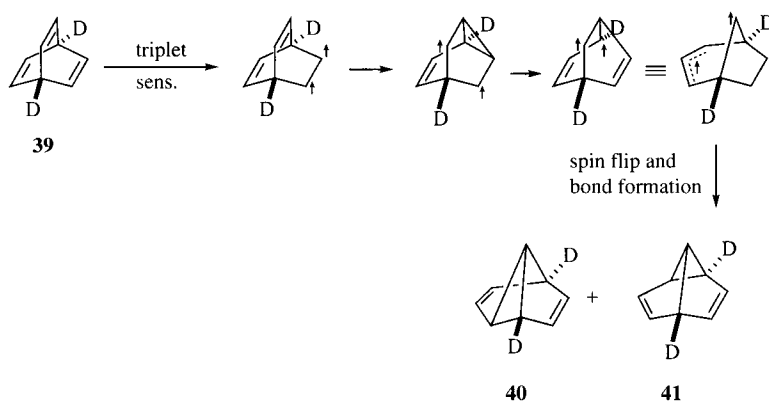


FIGURE 12.39

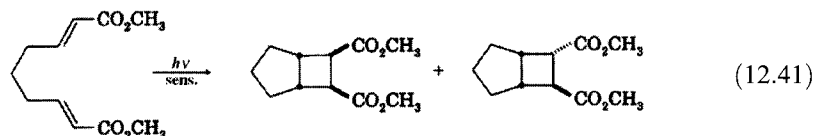
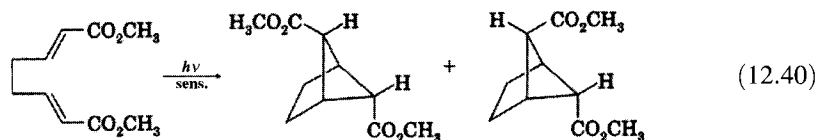
Mechanism proposed for the di- π -methane reaction. (Adapted from reference 140.)

¹³⁹ Zimmerman, H. E.; Grunewald, G. L. *J. Am. Chem. Soc.* **1966**, *88*, 183.

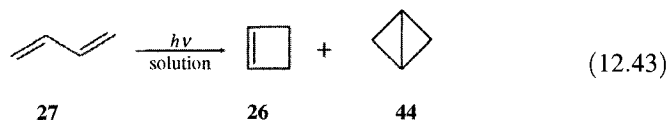
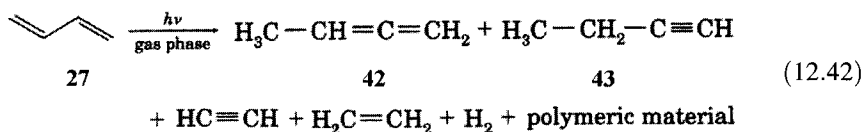
¹⁴⁰ Hixson, S. S.; Mariano, P. S.; Zimmerman, H. E. *Chem. Rev.* **1973**, *73*, 531.

¹⁴¹ Zimmerman, H. E. *Org. Photochem.* **1991**, *11*, 1.

kinetically controlled process.^{142,143} Examples are shown in equations 12.40 and 12.41.



The excited states of conjugated dienes are simpler than those of non-conjugated olefins because the smaller HOMO–LUMO gap means that the lowest energy excited singlets and triplets should be π, π^* states, not Rydberg states. The photochemistry of acyclic dienes is complicated, however, by the possibility of s-trans and s-cis conformations of the ground state molecule and the excited states. Direct irradiation of 1,3-butadiene in the vapor phase leads to 1,2-butadiene (42) and butyne (43) as well as to fragmentation and polymerization, perhaps through thermal reaction of vibrationally excited products.¹⁴⁴ In solution, direct irradiation of 1,3-butadiene results in the formation of cyclobutene and bicyclobutane (44).^{144–146}



In contrast to the photochemical ring opening of cyclobutenes to conjugated dienes, the photochemical conversion of conjugated dienes to cyclobutenes has been found to be stereospecific.¹⁰¹ The presence of substituents on the diene carbon atoms leads to the possibility of stereoisomerism, and photochemical cis–trans isomerization of such dienes is also observed. For

¹⁴² Scheffer, J. R.; Wostradowski, R. A. *J. Chem. Soc. D Chem. Commun.* **1971**, 144; Scheffer, J. R.; Wostradowski, R. A.; Dooley, K. C. *J. Chem. Soc. D Chem. Commun.* **1971**, 1217. Compounds with two functional groups capable of photochemical reaction are said to be *bichromophoric*. For a review, see De Schryver, F. C.; Boens, N.; Put, J. *Adv. Photochem.* **1977**, 10, 359.

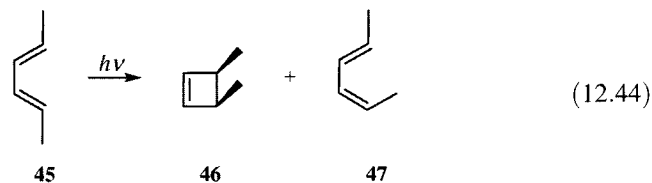
¹⁴³ For a theoretical study of photocycloaddition processes, see Bentzien, J.; Klessinger, M. *J. Org. Chem.* **1994**, 59, 4887.

¹⁴⁴ Haller, I.; Srinivasan, R. *J. Chem. Phys.* **1964**, 40, 1992.

¹⁴⁵ Fonken, G. *J. Org. Photochem.* **1967**, 1, 197.

¹⁴⁶ For a review of photochemical cycloaddition reactions of conjugated dienes and polyenes, see Dilling, W. A. *Chem. Rev.* **1969**, 69, 845.

example, irradiation of (2*E*,4*E*)-2,4-hexadiene (**45**) produced a small chemical yield of *cis*-3,4-dimethylcyclobutene (**46**) and a much larger yield of (2*E*,4*Z*)-2,4-hexadiene (**47**), among other products. The quantum yield of formation of **46** was found to be about 0.01.¹⁴⁷ The stereochemistry of **46** is consistent with its formation by the orbital symmetry allowed disrotatory closure of the excited singlet state of **45**.



The analysis of the reaction in equation 12.44 is complicated by the fact that the reactant (**45**) is shown as the *s*-*cis* conformer, even though the *s*-*trans* conformer is more stable by about 3 kcal/mol.¹⁴⁸ Most investigators had assumed that the photoproducts arose from the minor *s*-*cis* conformer, but this assumption had been questioned.¹⁴⁹ Squillacote and co-workers investigated the photoreactions of individual conjugated diene conformers using a matrix isolation technique.^{150,151} Samples of (2*E*,4*E*)-2,4-hexadiene diluted 1000 : 1 with N₂ were heated in the vapor phase to 519°C and quickly deposited onto a CsI window at 24 K. The sample was then cooled to 15 K for photochemical study. Analysis of the matrix-isolated material by IR spectroscopy showed absorptions characteristic of both conformers but with much greater amounts of the less stable *s*-*cis* conformer than would be present at room temperature. Irradiation of the sample with 254 nm UV produced rapid disappearance of IR bands for the *s*-*cis* conformer but not those corresponding to the *s*-*trans* isomer. Prolonged irradiation of the sample confirmed that the *s*-*trans* conformer was unreactive.¹⁵²

As is the case with cycloalkenes, photoisomerization of cyclic conjugated dienes can lead to strained rings and subsequent thermal reactions. For example, irradiation of cycloheptadiene (**48**) in methanol produced the bicycloheptene **49** and the methoxy ethers **50** and **51**. The products are explained by isomerization of the *cis,cis* reactant **48** to the *cis,trans* isomer **52**, which can undergo electrocyclic closure to **49**. In addition, **52** can add a proton from the solvent at either terminus of the *trans* double bond, leading to the carbocation intermediates and their ether trapping products (Figure 12.40).¹⁵³

Photochemical *cis,trans* isomerization of conjugated dienes is usually carried out through triplet sensitization, and quantitative determination of

¹⁴⁷ Srinivasan, R. *J. Am. Chem. Soc.* **1968**, *90*, 4498.

¹⁴⁸ Squillacote, M. E.; Liang, F. *J. Org. Chem.* **2005**, *70*, 6564.

¹⁴⁹ Aoyagi, M.; Osamura, Y. *J. Am. Chem. Soc.* **1989**, *111*, 470.

¹⁵⁰ Squillacote, M.; Semple, T. C. *J. Am. Chem. Soc.* **1990**, *112*, 5546.

¹⁵¹ Squillacote, M.; Semple, T.; Chen, J.; Liang, F. *Photochem. Photobiol.* **2002**, *76*, 634.

¹⁵² For an analysis of the photochemistry of *s*-*cis* conjugated dienes in terms of the excited state potential energy surface, see reference 151; Olivucci, M.; Ragazos, I. N.; Bernardi, F.; Robb, M. A. *J. Am. Chem. Soc.* **1993**, *115*, 3710; Fuß, W.; Panja, S.; Schmid, W. E.; Trushin, S. A. *Mol. Phys.* **2006**, *104*, 1133.

¹⁵³ Inoue, Y.; Hagiwara, S.; Daino, Y.; Hakushi, T. *J. Chem. Soc. Chem. Commun.* **1985**, 1307.

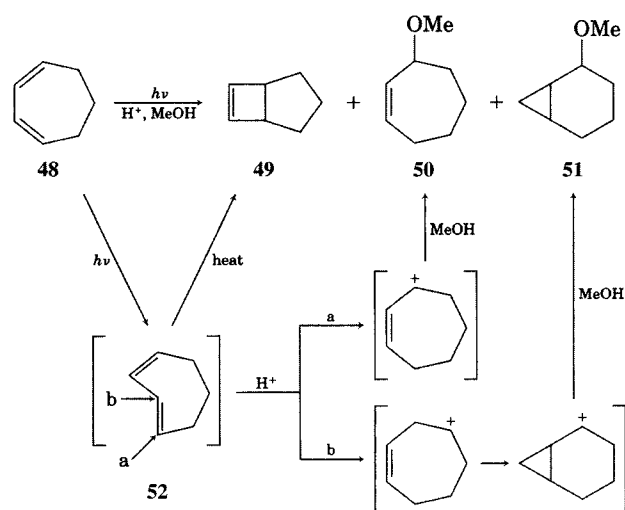


FIGURE 12.40

Photochemical reaction of 1,3-cycloheptadiene in methanol. (Reproduced from reference 153.)

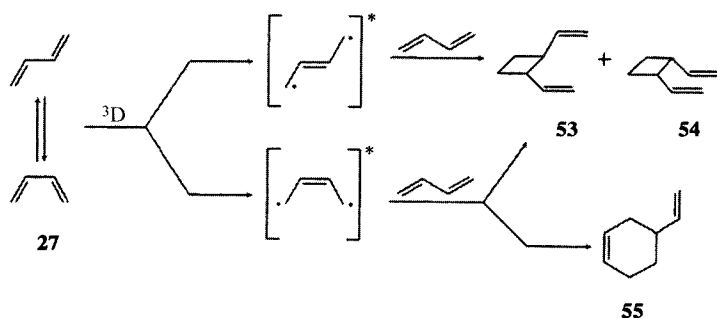
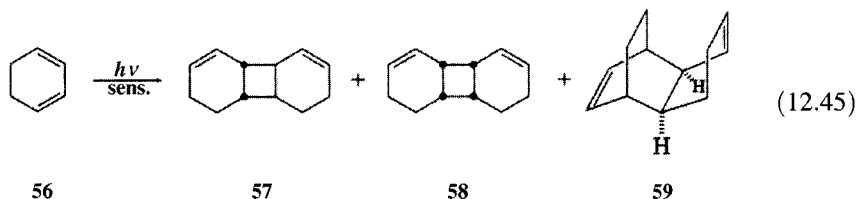


FIGURE 12.41

Pathways for triplet-sensitized reactions of 1,3-butadiene. (3D is a triplet sensitizer. Adapted from reference 107.)

cis,trans isomerization of conjugated dienes has been used to determine the quantum yield of intersystem crossing of aromatics.¹⁵⁴ At high diene concentrations, one diene triplet can undergo cycloaddition with a ground state diene before decay to the ground state occurs. Figure 12.41 shows the pathways proposed for formation of *trans*- (53) and *cis*-1,2-divinylcyclobutane (54) and 4-vinylcyclohexene (55).¹⁰⁷ Similarly, sensitized dimerization of 1,3-cyclohexadiene (56) produces the isomeric 1,2-addition products 57 and 58 and the 1,4-addition product 59 (equation 12.45).¹⁵⁵

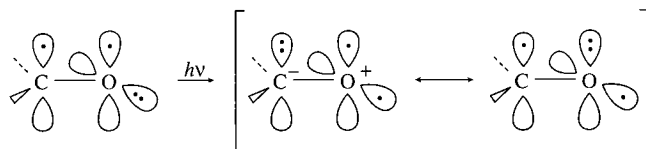


¹⁵⁴ Lamola, A. A.; Hammond, G. S. *J. Chem. Phys.* **1965**, *43*, 2129.

¹⁵⁵ Valentine, D.; Turro, N. J., Jr.; Hammond, G. S. *J. Am. Chem. Soc.* **1964**, *86*, 5202.

FIGURE 12.42

Resonance representation of a carbonyl n,π^* excited state. (Adapted from reference 92.)



Photochemical Reactions of Carbonyl Compounds

The n,π^* and π,π^* excited states of carbonyl compounds show very different patterns of chemical reactivity.¹⁵⁶ It is useful to represent the n,π^* state of carbonyl compounds as shown in Figure 12.42, in which there is appreciable radical character on both the carbon atom and the oxygen atom and in which there is charge donation from oxygen to carbon.^{92,157,158}

This simple model allows us to rationalize the major types of reactions that are characteristic of carbonyl compounds reacting from an n,π^* excited state:¹⁵⁹

1. Norrish type I cleavage (α cleavage);
2. hydrogen abstraction leading to
 - a. photoreduction,
 - b. Norrish type II cleavage (β cleavage), or
 - c. cyclobutanol formation (Yang cyclization);
3. oxetane formation (Paternò-Büchi reaction); and
4. photochemical electron transfer.

Norrish Type I Reaction (α Cleavage)

The α -cleavage reaction is the breaking of a bond α to the carbonyl group, as shown schematically in equation 12.46, where the Lewis structure in brackets emphasizes the diradical character of the n,π^* state.¹⁶⁰ Extended Hückel calculations indicate that the n orbital in formaldehyde has some density on the carbonyl hydrogen atoms, so an n to π^* excitation reduces the bonding of the carbonyl carbon to that substituent.¹⁶¹ By analogy, excitation of other aldehydes or ketones should reduce electron density between the carbonyl carbon atom and a carbon α to it, thus weakening the bond and making dissociation more likely. With ketones, the resulting acyl radical can undergo loss of CO to produce another alkyl radical (equation 12.47).

¹⁵⁶ The orbital model of formaldehyde on page 791 provides a simple basis for discussing the photochemical reactions of carbonyl compounds. For a more detailed discussion of the excited states of formaldehyde and acetaldehyde, see Hadad, C. M.; Foresman, J. B.; Wiberg, K. B. *J. Phys. Chem.* **1993**, *97*, 4293.

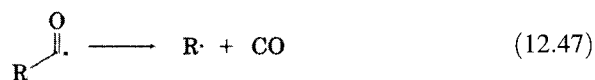
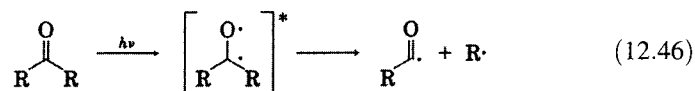
¹⁵⁷ Zimmerman, H. E. *Adv. Photochem.* **1963**, *1*, 183. Figure 12.42 is a modified form of the representation suggested in this reference.

¹⁵⁸ For another analysis of the photochemistry of carbonyl compounds, see Formosinho, S. J.; Arnaut, L. G. *Adv. Photochem.* **1991**, *16*, 67.

¹⁵⁹ These reactions are characteristic of nonconjugated carbonyl compounds; other reactions (page 841) may be observed when conjugated carbonyl systems are photoexcited.

¹⁶⁰ Bamford, C. H.; Norrish, R. G. W. *J. Chem. Soc.* **1935**, 1504 and references therein.

¹⁶¹ Jorgensen, W. L.; Salem, L. *The Organic Chemist's Book of Orbitals*; Academic Press: New York, 1973; p.84.



Equations 12.46 and 12.47 do not show the spin states of the unpaired electrons. In general, α cleavage can occur from both the singlet and triplet n,π^* states, but quantum yields are much greater for the triplet state reactions.¹¹⁵ Zewail and co-workers reported femtosecond studies and theoretical calculations of the Norrish type I reaction of acetone.¹⁶² They found a barrier of ca. 18 kcal/mol for α cleavage from the S_1 state of acetone but a barrier of only 5 kcal/mol for dissociation from the T_1 state. Thus, they concluded that the photodissociation occurs from the triplet state and that intersystem crossing from S_1 to T_1 is the rate-limiting step in the Norrish type I reaction of acetone.¹⁶³

Larger ketones may undergo further fragmentation processes after α cleavage. Consider the photochemical reactions of cyclohexanone in the gas phase (60, Figure 12.43).¹⁶⁴ Excitation produces the S_1 state, which intersystem crosses to the vibrationally excited T_1 state. In the gas phase the vibrational energy is not readily damped by collisions with other molecules, so α cleavage produces a biradical (61). Structure 61 still has sufficient vibrational energy to lose CO, resulting in 1,5-pentanediy1 (62). In turn, 62 can disproportionate to pentene (63), cyclize to cyclopentane (64), or fragment to ethene (65) and propene (66). If intramolecular disproportionation occurs before loss of CO, then 5-hexenal (67) can also be formed.

Photochemical reactions of carbonyl compounds in solution are often less complex than those in the gas phase because the excess vibrational energy

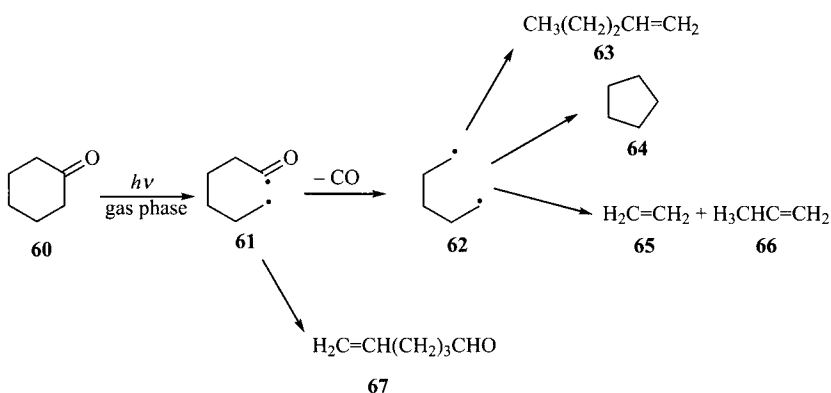


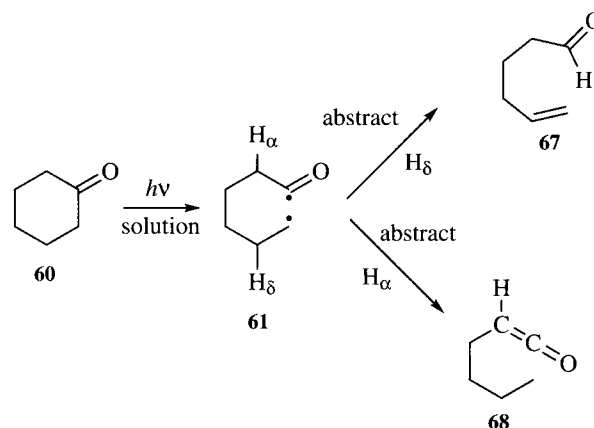
FIGURE 12.43

Photoreactions of cyclohexanone in the gas phase. (Adapted from reference 164.)

¹⁶² Diau, E. W.-G.; Kötting, C.; Zewail, A. H. *Chem. Phys. Chem.* **2001**, *2*, 273.

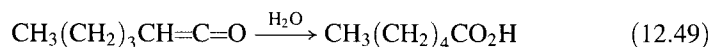
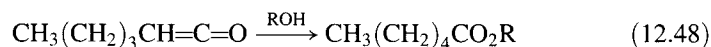
¹⁶³ See also Kim, S. K.; Pedersen, S.; Zewail, A. H. *J. Chem. Phys.* **1995**, *103*, 477; Kim, S. K.; Zewail, A. H. *Chem. Phys. Lett.* **1996**, *250*, 279; Kim, S. K.; Guo, J.; Baskin, J. S.; Zewail, A. H. *J. Phys. Chem.* **1996**, *100*, 9202; De Feyter, S.; Diau, E. W.-G.; Zewail, A. H. *Angew. Chem. Int. Ed.* **2000**, *39*, 260.

¹⁶⁴ Srinivasan, R. *Adv. Photochem.* **1963**, *1*, 83.

**FIGURE 12.44**

Photochemical reaction of cyclohexanone in solution.

is rapidly quenched by collisions with solvent molecules. Therefore, only the energy of the 0th vibrational level of T_1 is available for reaction. When **60** is irradiated in solution, for example, the biradical produced by α cleavage (**61**) does not eliminate CO. Instead, it undergoes intramolecular disproportionation by two different pathways. Abstraction of a hydrogen atom from the δ carbon atom by the radical on the acyl carbon produces the enal (**67**). If the radical centered on the ϵ carbon atom abstracts a hydrogen atom from the α carbon atom, then the reaction product is a ketene (**68**, Figure 12.44). The ketene can react with hydroxylic solvents to give addition products. For example, reaction with an alcohol produces an ester (equation 12.48), and reaction with water produces an acid (equation 12.49). The latter process can produce an appreciable pH change in the reaction medium.¹⁶⁵



Hydrogen Abstraction

The depiction of an n,π^* excited state as a biradical suggests that photoexcited carbonyl compounds might also exhibit hydrogen abstraction reactions, as shown in equation 12.50.¹⁶⁶ This behavior is exhibited in the photoreduction of benzophenone in isopropyl alcohol (equation 12.51), which was first carried out by Ciamician on the rooftops of Bologna, Italy, more than a century ago and which is one of the classic reactions of organic photochemistry.¹⁶⁷ Triplet benzophenone (**69**) reacts with 2-propanol (**70**) with a pseudo-first-order rate constant of ca. $6.7 \times 10^7 \text{ s}^{-1}$.¹⁶⁸ The products of the reaction are

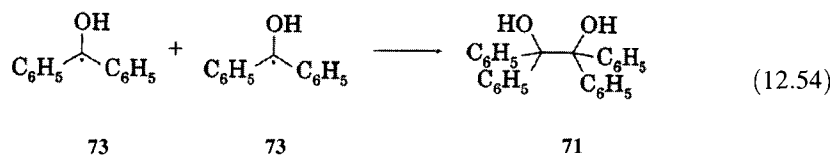
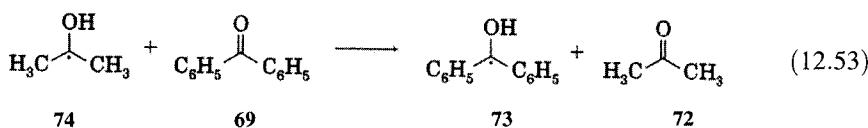
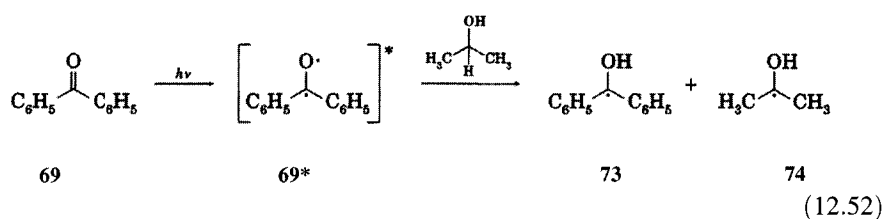
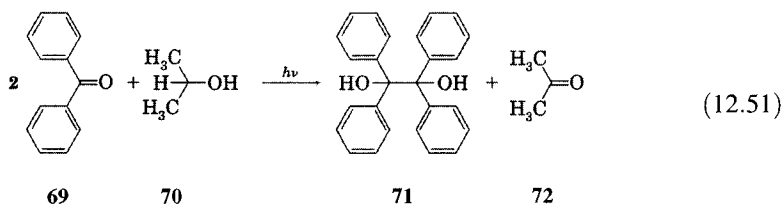
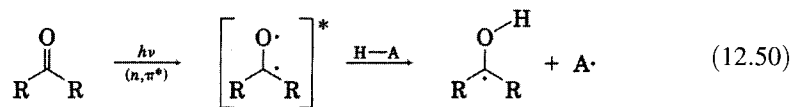
¹⁶⁵ Carroll, F. A.; Strouse, G. F.; Hain, J. M. *J. Chem. Educ.* **1987**, *64*, 84.

¹⁶⁶ For a discussion of hydrogen atom abstraction by photoexcited carbonyl compounds, see Wagner, P.; Park, B.-S. *Org. Photochem.* **1991**, *11*, 227.

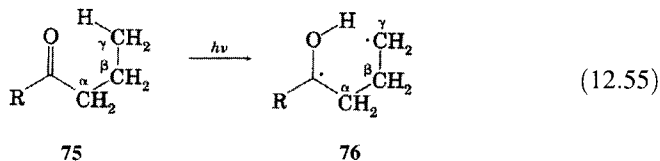
¹⁶⁷ Ciamician, G.; Silber, P. *Ber. Dtsch. Chem. Ges.* **1900**, *33*, 2911. For commentaries on the history of organic photochemistry, see Roth, H. D. *Angew. Chem. Int. Ed. Engl.* **1989**, *28*, 1193; *Pure Appl. Chem.* **2001**, *73*, 395.

¹⁶⁸ Du, Y.; Ma, C.; Kwok, W. M.; Xue, J.; Phillips, D. L. *J. Org. Chem.* **2007**, *72*, 7148.

benzpinacol (71) and acetone (72), which are generated by the reactions shown in equations 12.52 through 12.54.¹⁶⁹

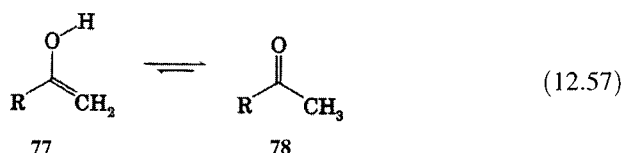
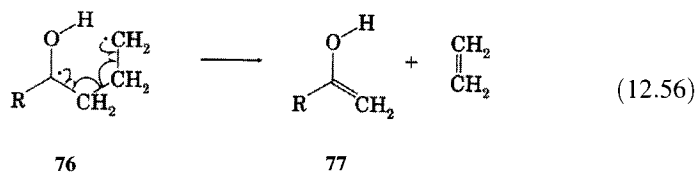


The hydrogen atom abstraction reaction can be intramolecular as well as intermolecular, provided that the molecule can achieve the conformation required for the abstraction to occur and provided that the excited state is sufficiently energetic to complete the reaction. A general example of the resulting process is shown for the alkyl propyl ketone 75. Abstraction of the γ hydrogen atom can occur from both the n,π^* singlet and n,π^* triplet excited states via a facile six-membered transition state (equation 12.55), producing the biradical 76.¹¹⁵ Zewail and co-workers found that abstraction of a γ hydrogen on the excited singlet potential energy surface occurs on a 70–90 fs time scale.¹⁶³

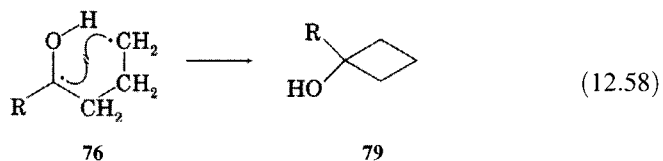


¹⁶⁹ Schönberg, A. *Preparative Organic Photochemistry*; Springer-Verlag: New York, 1968; p. 213.

A biradical such as **76** is itself a high energy species relative to stable ground state molecules, and it can further react by several competing pathways. One decay pathway is bond cleavage (equation 12.56) to produce an enol (**77**) and an alkene, and the enol tautomerizes to another ketone (**78**). The overall process is known as **β cleavage (Norrish type II cleavage)**.^{160,170} Quantum yields for the Norrish type II reaction are generally larger for triplet state than for singlet state reactions.¹¹⁵



An alternative reaction for **76** is bond formation between the two radical centers, resulting in the formation of a cyclobutanol (**79**, equation 12.58). This reaction was first reported by Yang, so the process is often called the Yang cyclization or the Norrish–Yang cyclization.^{171,172} Zewail and co-workers found that singlet biradical closure occurs 400–700 fs after excitation.¹⁶³



Alternatively, the γ carbon radical can abstract the hydrogen atom from the oxygen atom, again via a six-membered ring transition structure, to reform the starting ketone (equation 12.59). This process accomplishes no net photochemistry, so the overall effect is to convert the energy of electronic excitation into vibrational energy of the ketone and solvent. If the starting ketone was optically active due to chirality at the γ carbon atom, however, then racemization can be observed. Figure 12.45 shows the scheme described for the photochemical reaction of optically active (*S*)- γ -methylvalerophenone (**80**) by Wagner.¹⁷³ The initially-formed n, π^* singlet undergoes rapid intersystem crossing to the triplet, which can revert to the ground state or undergo hydrogen abstraction to the biradical (**81**). The rate constants for the individ-

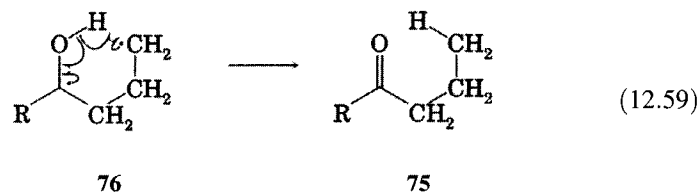
¹⁷⁰ Wagner, P. J.; Klán, P. in reference 2, p. 52-1.

¹⁷¹ Yang, N. C.; Yang, D.-D. H. *J. Am. Chem. Soc.* **1958**, *80*, 2913.

¹⁷² Wessig, P. in reference 2, p. 57-1; Wagner, P. J. in reference 2, p. 58-1.

¹⁷³ Wagner, P. J. *Acc. Chem. Res.* **1971**, *4*, 168.

ual processes can be determined from measurements of rate constants for product formation and for photophysical processes.



Steric effects can influence the paths of 1,4-biradical reactions. Moorthy and co-workers reported a kinetic study of the lifetimes of the triplet 1,4-biradicals formed in Norrish type II reactions of diastereomeric 2,3-dimethyl-1,4-diphenylbutan-1-ones.¹⁷⁴ Irradiation of the diastereomers with “syn” methyl groups (**82**) on C2 and C3 gave a 2 : 1 ratio of cyclization products to fragmentation products, while irradiation of the diastereomers with those two methyl groups anti (**83**) gave those products in a 3 : 17 ratio. Combined with quantum yield data and kinetic data from the decay of transient absorptions attributed to the 1,4-biradical intermediates, these investigators were able to calculate rate constants for cyclization (k_C), fragmentation (k_E),

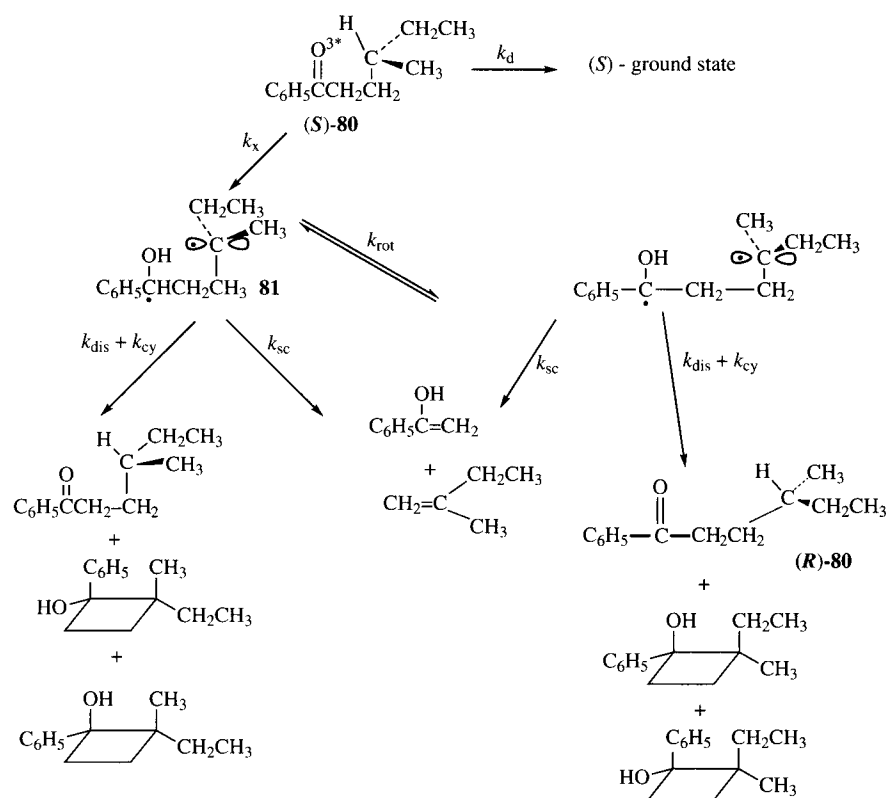
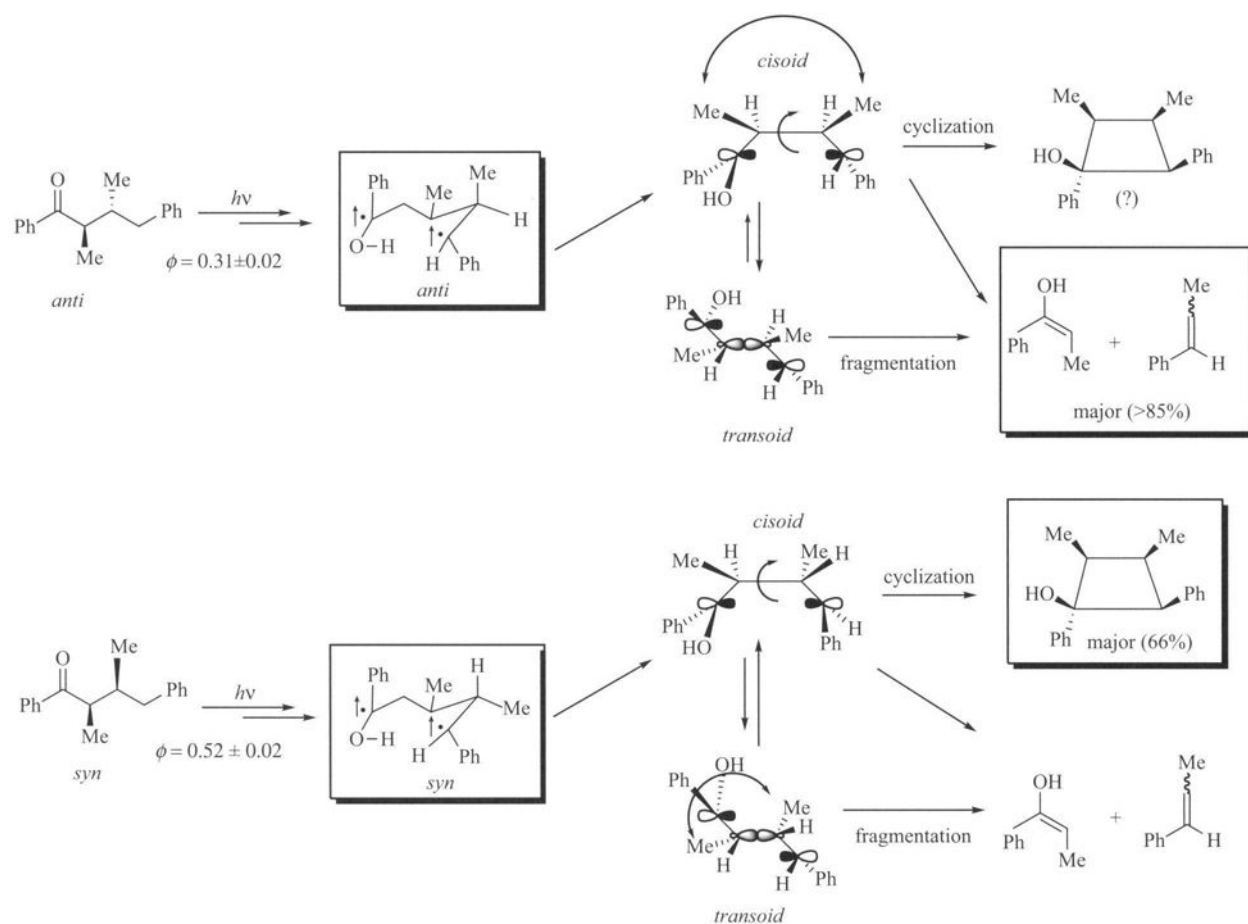


FIGURE 12.45

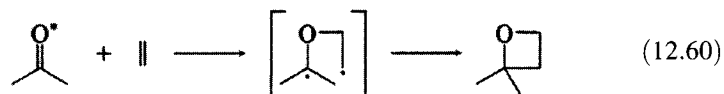
Reaction pathways in the photochemistry of γ -methylvalerophenone. (Reproduced from reference 173.)

¹⁷⁴ Moorthy, J. N.; Koner, A. L.; Samanta, S.; Singhal, N.; Nau, W. M.; Weiss, R. G. *Chem. Eur. J.* **2006**, *12*, 8744.

**FIGURE 12.46**

Detailed scheme for photochemical reactions of **82** and **83**. (Note that the biradicals are triplets. Reproduced from reference 174.)

Closure of the biradical leads to a four-membered ring containing oxygen, which is known as an oxetane. The overall 1,2-photocycloaddition reaction is often called the Paternò-Büchi reaction (equation 12.60).¹⁷⁶⁻¹⁷⁸ The Paternò-Büchi reaction provides synthetic entry into highly strained ring systems containing oxygen atoms, as exemplified by equations 12.61 and 12.62 (where Ar is 2-naphthyl).^{179,180}



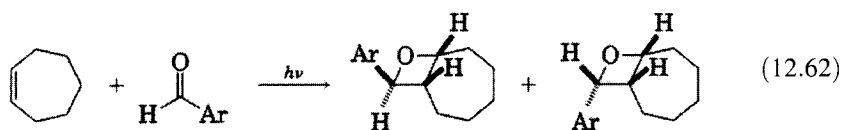
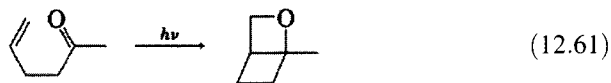
¹⁷⁶ The reaction was reported by Paternò, E.; Chieffi, G. *Gazz. Chim. Ital.* **1909**, 39, 431; Büchi, G.; Inman, C. G.; Lipinsky, E. S. *J. Am. Chem. Soc.* **1954**, 76, 4327.

¹⁷⁷ For a review, see D'Auria, M.; Emanuele, L.; Racioppi, R. *Adv. Photochem.* **2005**, 28, 81.

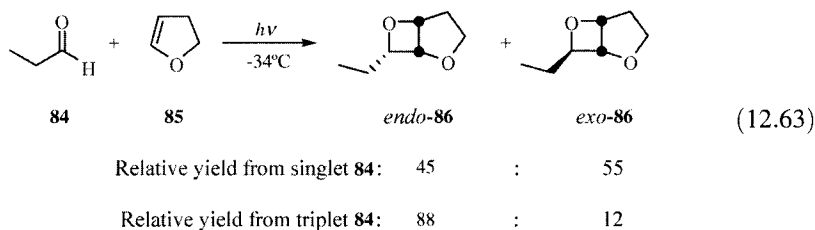
¹⁷⁸ Griesbeck, A. G.; Bondock, S. in reference 2, p. 60-1.

¹⁷⁹ Yang, N. C.; Chiang, W. *J. Am. Chem. Soc.* **1977**, 99, 3163.

¹⁸⁰ Srinivasan, R. *J. Am. Chem. Soc.* **1960**, 82, 775.



The regio- and stereochemistry of the Paternò-Büchi reaction depend on the structures of the reactants, on the electronic energy of the excited state carbonyl compound, and on the multiplicity of the excited state. With unsymmetrical alkenes, the products suggest preferential formation of the more substituted radical center in the biradical intermediate, but steric and electronic factors are also important. Stereoselectivities depend on the multiplicity of the excited state. For example, the reaction of excited singlet and triplet states of propanal (**84**) with 2,3-dihydrofuran (**85**) gave the diastereomers of 7-ethyl-2,6-dioxabicyclo[3.2.0]heptane (**86**) in different ratios (equation 12.63).¹⁸¹



The biradical model for carbonyl photoreactivity is valid only for molecules reacting from n,π^* excited states. That is the case for aliphatic ketones and is also true for some—but not all—aromatic ketones. If the carbonyl group is conjugated with a large π system or if there are conjugating substituents on an aromatic ketone, then the lowest energy state of a given multiplicity could be the π,π^* state.¹⁸² Furthermore, the lower polarity of the n,π^* triplet state relative to the π,π^* triplet state means that a polar solvent can sometimes make the π,π^* the lowest excited triplet state for some molecules. In such situations, the radical reactivity suggested by the simple Lewis structure model in Figure 12.42 is greatly diminished.⁶

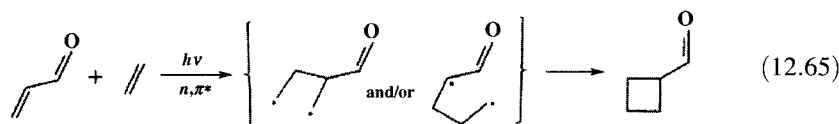
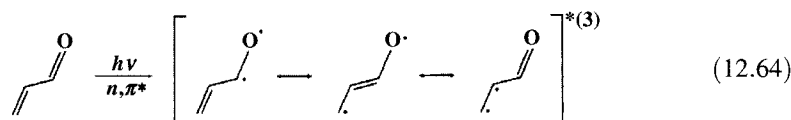
Photochemical Reactions of α,β -Unsaturated Carbonyl Compounds

Structures with a carbon-carbon double bond conjugated with a carbonyl group exhibit characteristic reactions that can be rationalized with Lewis

¹⁸¹ Griesbeck, A. G.; Abe, M.; Bondock, S. *Acc. Chem. Res.* **2004**, *37*, 919.

¹⁸² Hammond, G. S.; Leermakers, P. A. *J. Am. Chem. Soc.* **1962**, *84*, 207.

structure representations of the excited states that are combinations of those developed for the isolated carbonyl group and for the isolated carbon-carbon double bond. In most cases the lowest excited states, both singlet and triplet, are n,π^* states. Furthermore, the initially formed n,π^* singlets undergo rapid intersystem crossing, so the photochemistry of conjugated enones originates from the n,π^* triplet.¹⁸³ The π^* orbital of an α,β -unsaturated carbonyl compound has density on the olefinic carbons, primarily on the β carbon atom, as well as on the carbonyl carbon atom and the oxygen atom. Thus, the photochemistry of enones may be rationalized with the resonance structures in equation 12.64.¹⁸⁴ This model makes it easy to understand the cycloaddition of an α,β -unsaturated ketone with an olefin by the mechanism shown in equation 12.65.¹⁸⁵



The intermediacy of species with biradical character in photoaddition of enones with alkenes is supported by the observation that the reaction of cyclohexenone with isobutylene produces the mixture of products shown in equation 12.66.¹⁸⁶ α,β -Unsaturated ketones can also dimerize through the same reaction pathway. For example, cyclopentenone (**87**) gives approximately equal amounts of the head-to-head dimer **88** and the head-to-tail dimer **89** (equation 12.67).¹⁸⁷

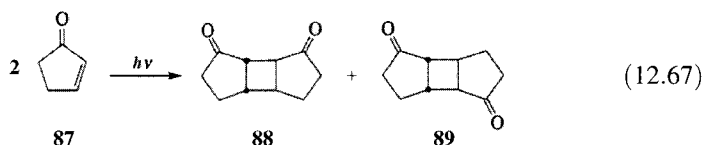
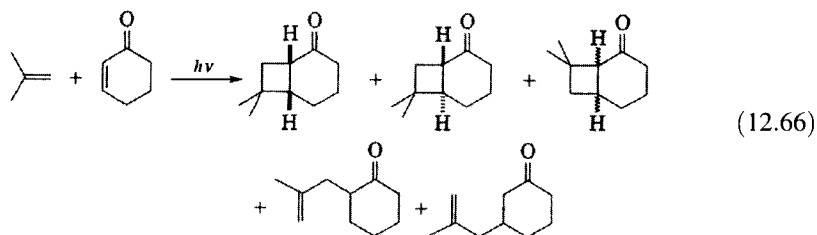
¹⁸³ For a review of the photocycloadditions of enones and alkenes, see Schuster, D. I.; Lem, G.; Kaprinidis, N. A. *Chem. Rev.* **1993**, 93, 3.

¹⁸⁴ It is not necessarily the case in such representations that all resonance structures make an equal contribution to the reactivity of the excited state.

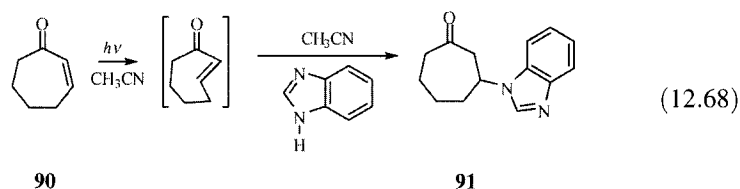
¹⁸⁵ Experimental evidence has been reported for the intermediacy of 1,4-biradicals in both intermolecular and intramolecular photocycloaddition of triplet alkenones with alkenes. For leading references, see Maradyn, D. J.; Weedon, A. C. *J. Am. Chem. Soc.* **1995**, 117, 5359. For a theoretical study of the photochemical cycloaddition of acrolein and ethene, see Erickson, J. A.; Kahn, S. D. *Tetrahedron* **1993**, 49, 9699. For a theoretical study of the regioselectivity of the photocycloaddition of triplet cyclohexenones to alkenes, see Broeker, J. L.; Eksterowicz, J. E.; Belk, A. J.; Houk, K. N. *J. Am. Chem. Soc.* **1995**, 117, 1847.

¹⁸⁶ Corey, E. J.; Bass, J. D.; LeMahieu, R.; Mitra, R. B. *J. Am. Chem. Soc.* **1964**, 86, 5570.

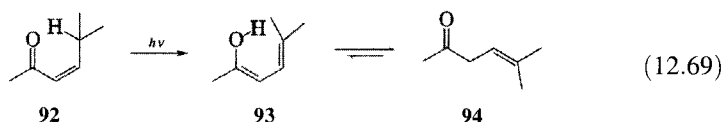
¹⁸⁷ Eaton, P. E. *J. Am. Chem. Soc.* **1962**, 84, 2344.



One of the processes available to electronically excited enones is isomerization about the carbon-carbon double bond.¹⁸⁸ Cis cycloalkenones with seven or eight atoms can undergo photoisomerization to strained trans cycloalkenones. In turn, the trans double bond can undergo addition reactions with alcohols or amines. For example, irradiation (350 nm) of cyclohept-2-enone (**90**) in acetonitrile containing benzimidazole led to a 94% conversion to 3-(1H-benzo[d]imidazol-1-yl)cycloheptanone (**91**, equation 12.68).¹⁸⁹



Irradiation of the α,β -unsaturated ketone **92** produced the dienol **93**, which tautomerized to the β,γ -unsaturated ketone **94** (equation 12.69).^{190,191} The notable aspect of this reaction is that it converts a more stable, conjugated enone to a less stable, nonconjugated enone. The reactant, being more conjugated, absorbs UV-vis radiation at longer wavelength than does the product, so the reaction can be driven by radiation that the reactant absorbs but that the product does not absorb efficiently.



¹⁸⁸ Reguero, M.; Olivucci, M.; Bernardi, F.; Robb, M. A. *J. Am. Chem. Soc.* **1994**, *116*, 2103.

¹⁸⁹ Moran, J.; Dornan, P.; Beauchemin, A. M. *Org. Lett.* **2007**, *9*, 3893.

¹⁹⁰ Yang, N. C.; Jorgenson, M. J. *Tetrahedron Lett.* **1964**, 1203.

¹⁹¹ Observation of dienol intermediates produced by the photochemical enolization of α,β -unsaturated ketones was reported by Duhaime, R. M.; Weedon, A. C. *Can. J. Chem.* **1987**, *65*, 1867.

Photochemical Reactions of Aromatic Compounds

The HMO model predicts the lowest excited state of benzene to be a π, π^* state formed by promoting a π electron from one of the degenerate HOMOs to one of the degenerate LUMOs (Figure 12.47).^{192,193} The geometry of the benzene ring is reinforced by the σ -bonded ring structure, so radiationless decay to a perpendicular state is not as fast as that for alkenes. Therefore, benzene derivatives typically exhibit fluorescence and intersystem crossing.

The larger the chromophore, the harder it is to visualize the electron redistribution accompanying the excitation in terms of simple valence bond pictures. Nevertheless, it remains helpful to use resonance structures of high energy species to model the chemical characteristics of the excited states of benzene. Bryce-Smith and Longuet-Higgins suggested the resonance structures in Figure 12.48 to explain the formation of fulvene (95) and benzvalene (96) from the $^1\pi, \pi^*$ state of benzene and the intermediates in Figure 12.49 to explain the formation of prismane (97) and Dewar benzene (98) from the triplet state of benzene.^{194,195}

Aromatic compounds also undergo photocycloaddition reactions with alkenes, leading to 1,2-, 1,3-, and (less often) 1,4-adducts, as shown for the reaction of benzene with ethene in equation 12.70.¹⁹⁶ Olefins with strongly electron-withdrawing or electron-donating substituents tend to give 1,2-photoaddition products, while olefins with alkyl substituents tend to give mostly 1,3-photoaddition.¹⁹⁷

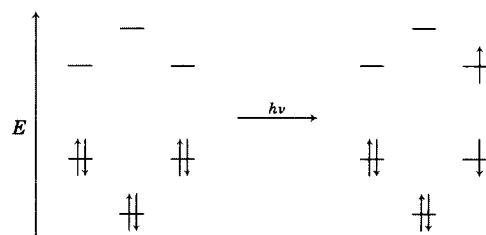
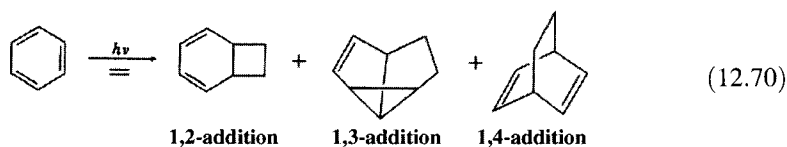


FIGURE 12.47

Schematic representation of a $\pi \rightarrow \pi^*$ transition in benzene.

¹⁹² For a more detailed discussion of spectroscopic transitions in benzene, see Gilbert, A.; Baggott, J. E. *Essentials of Molecular Photochemistry*; CRC Press: Boca Raton, FL, 1991; pp. 355–357.

¹⁹³ Rydberg states can be observed in benzene and its derivatives as well. The $3R_g$ state of benzene was reported to have a lifetime of 70 ± 20 fs and to decay to a vibrationally excited ground state: Wiesenfeld, J. M.; Greene, B. I. *Phys. Rev. Lett.* **1983**, *51*, 1745.

¹⁹⁴ Bryce-Smith, D.; Longuet-Higgins, H. C. *Chem. Commun.* **1966**, 593.

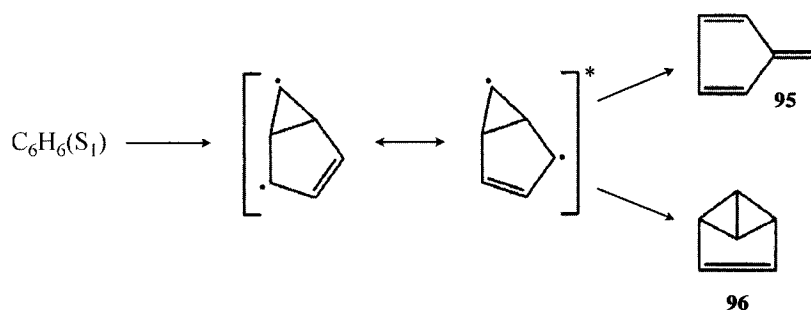
¹⁹⁵ See also the discussion by Cundall, R. B. in Burnett, G. M.; North, A. M., Eds. *Transfer and Storage of Energy by Molecules*, Vol. 1; Wiley-Interscience: London, 1969; pp. 1–66.

¹⁹⁶ Gilbert, A. in Horspool, W. M., Ed. *Synthetic Organic Photochemistry*; Plenum Press: New York, 1984; p. 1.

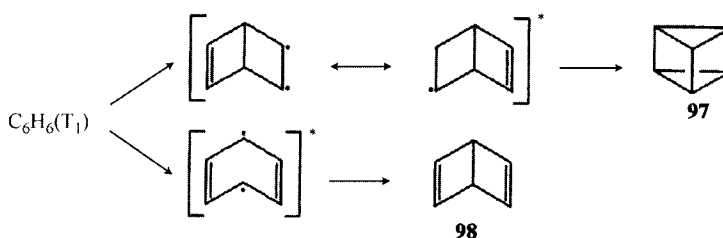
¹⁹⁷ Bryce-Smith, D.; Gilbert, A.; Orger, B.; Tyrrell, H. J. *Chem. Soc. Chem. Commun.* **1974**, 334.

FIGURE 12.48

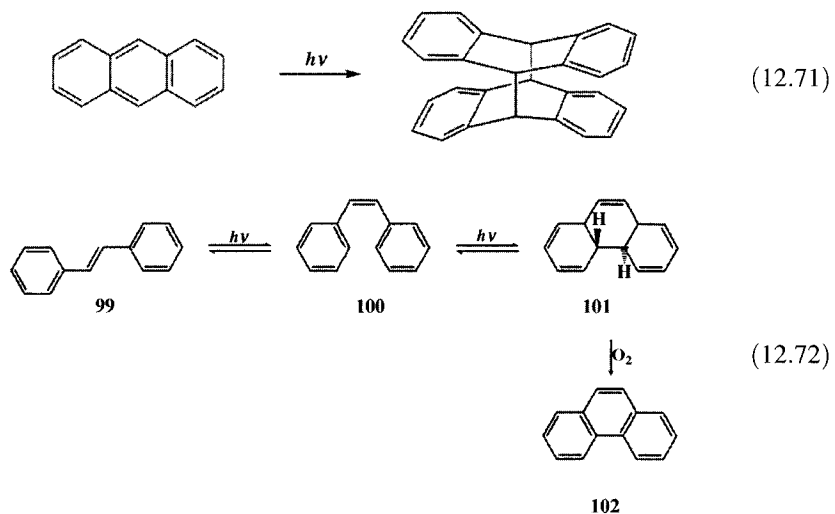
Radical resonance structures proposed for the intermediate in the formation of fulvene and benzvalene from benzene excited singlets. (Adapted from reference 195.)

**FIGURE 12.49**

Resonance structures proposed to account for the formation of prismane and Dewar benzene from benzene triplets. (Adapted from reference 195.)



The reactions of polynuclear aromatics can also be rationalized by simple models such as those shown for benzene in Figures 12.48 and 12.49. Two notable reactions are (i) the photodimerizations of anthracenes (equation 12.71)¹⁹⁸ and (ii) the photoisomerization of *trans*-stilbene (**99**) to the *cis* isomer (**100**), followed by intramolecular photocycloaddition to a dihydrophenanthrene (**101**), which can then be oxidized to phenanthrene (**102**).¹⁹⁹



¹⁹⁸ For a summary of reactions of this type, see Greene, F. D.; Misrock, S. L.; Wolfe, J. R., Jr. *J. Am. Chem. Soc.* **1955**, *77*, 3852.

¹⁹⁹ Mallory, F. B.; Wood, C. S.; Gordon, J. T.; Lindquist, L. C.; Savitz, M. L. *J. Am. Chem. Soc.* **1962**, *84*, 4361; Moore, W. M.; Morgan, D. D.; Stermitz, F. R. *J. Am. Chem. Soc.* **1963**, *85*, 829. For a review, see Mallory, F. B.; Mallory, C. W. *Org. React.* **1984**, *30*, 1.

Photosubstitution Reactions

Lewis structure models incorporating radical character are useful in the exposition of photochemical reactions of carbonyl compounds, alkenes, dienes, and aromatic compounds that are not substituted with polar groups. When heteroatoms are substituted onto an aromatic ring, considerable charge transfer character can be introduced into both the ground state and the excited state, and ionic resonance structures become more suitable as models for reactivity.^{157,200}

In nitrobenzene, for example, the nitro substituent effectively serves as an empty *p* orbital attached to the ring, so the benzyl cation provides a rough model for its MOs. Thus, the HOMO of nitrobenzene is similar to ψ_3 of the benzyl cation, and the LUMO is similar to ψ_4 of the benzyl cation (Figure 12.50). Promotion of an electron from HOMO to LUMO thus has the net effect of moving electron density from the positions meta to the nitro group to the ortho and para positions. In other words, the photoexcited nitrobenzene has even less electron density in the meta positions than does ground state nitrobenzene. This effect can be indicated with positive and negative charges in a resonance representation for the excited state (Figure 12.51).

A methoxy substituent on a benzene ring has an effect that is opposite that of a nitro substituent, so the benzyl anion is a model for the MOs of anisole. Excitation removes an electron from ψ_4 and places it in ψ_5 , which produces a charge difference suggested by the resonance representation shown in Figure 12.52. These simple models help us understand the photochemically induced solvolysis in which *m*-nitrophenyl trityl ether (**103**) does not react in the dark but does readily undergo photosolvolysis, as shown in Figure 12.53.^{201,202}

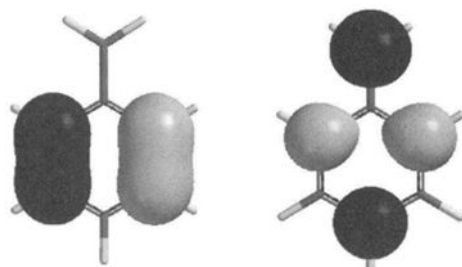


FIGURE 12.50
HOMO (left) and LUMO (right) of benzyl cation (PM3 calculation).

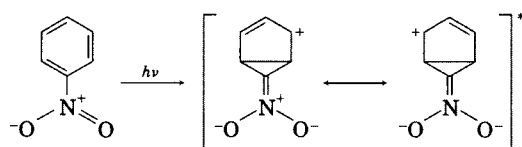


FIGURE 12.51
Resonance representation of S_1 of nitrobenzene. (Adapted from reference 200.)

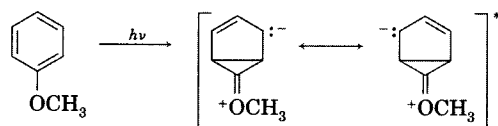


FIGURE 12.52
Valence bond representation of S_1 of anisole. (Adapted from reference 200.)

²⁰⁰ Zimmerman, H. E.; Sandel, V. R. *J. Am. Chem. Soc.* **1963**, *85*, 915.

²⁰¹ Zimmerman, H. E.; Somasekhara, S. *J. Am. Chem. Soc.* **1963**, *85*, 922.

²⁰² Radical pathways may also be involved in photosubstitution reactions. See, for example, see Bunce, N. J.; Cater, S. R.; Scaiano, J. C.; Johnston, L. J. *J. Org. Chem.* **1987**, *52*, 4214.

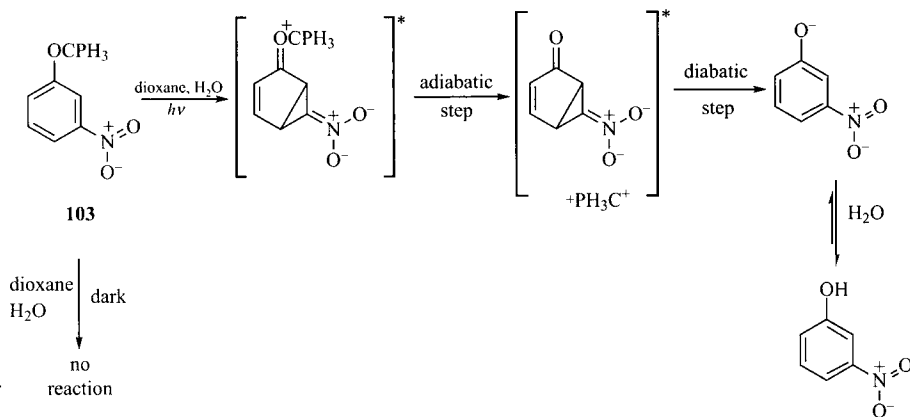


FIGURE 12.53

Photosolvolytic cleavage of *m*-nitrophenyl trityl ether. (Adapted from reference 201.)

σ Bond Photodissociation Reactions

One of the simplest photochemical reactions is the dissociation of molecular chlorine.



The absorption spectrum of molecular chlorine is shown in Figure 12.54. The λ_{max} is 330 nm with $\epsilon_{\text{max}} = 66$, but the onset of absorption is at least 478 nm. Thus, the excitation energy (60 kcal/mol) is greater than the Cl–Cl dissociation energy (58 kcal/mol). In MO terms, the excitation of an electron from a σ to a σ^* orbital creates an excited state with one electron in a bonding orbital and one electron in an antibonding orbital. With no net bonding energy, vibrational energy causes the two atoms to move apart as radicals.^{203,204} The absorption band is essentially structureless because there

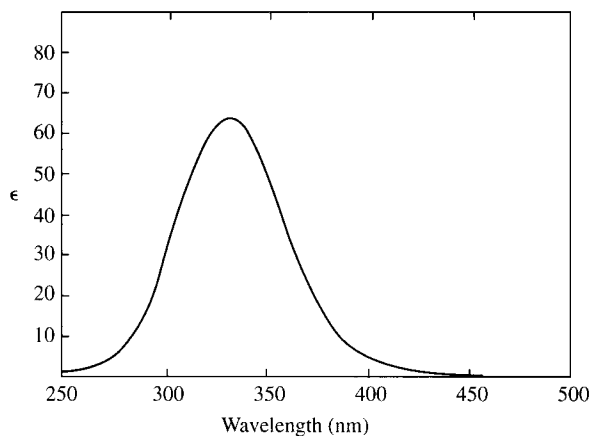


FIGURE 12.54

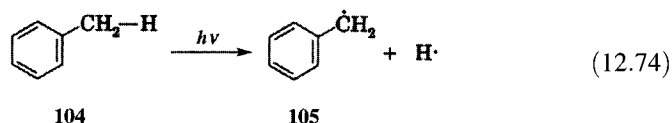
Absorption spectrum of Cl₂ in the gas phase. (Adapted from reference 204.)

²⁰³ To a first approximation there is no net bonding energy. A more detailed analysis would reveal some repulsion.

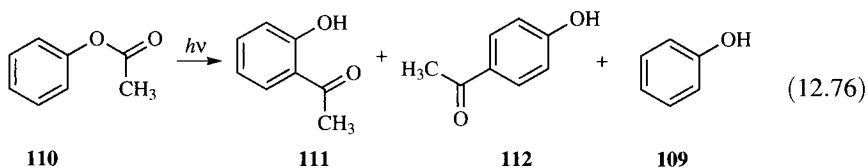
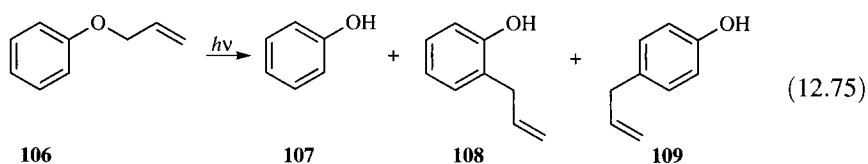
²⁰⁴ More precisely, the excitation is believed to cause a vertical transition from the ground state to an excited state with a negligible energy minimum. Calvert, J. G.; Pitts, J. N. *Photochemistry*; John Wiley & Sons: New York, 1966; pp. 184, 226.

are no longer discrete vibrational energy levels above the energy required for dissociation.

The photodissociation of toluene (**104**) to the benzyl radical (**105**) and a hydrogen atom (equation 12.74)²⁰⁵ is an example of a σ bond dissociation in an organic compound.



Two other photochemical reactions that appear to proceed through σ bond homolysis are the photo-Claisen reaction of phenyl allyl ether (**106**, equation 12.75), which produces phenol (**107**) plus *o*- (**108**) and *p*-allylphenol (**109**)²⁰⁶ and the photo-Fries reaction of phenyl acetate (**110**, equation 12.76) to produce *o*- (**111**) and *p*-hydroxyacetophenone (**112**) plus phenol. In the case of the photo-Fries reaction, both concerted and dissociative mechanisms were proposed for the formation of the acylphenols.



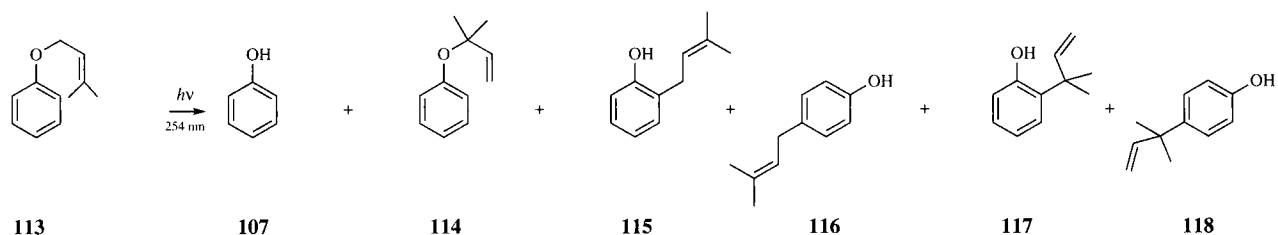
The photodissociative pathway was confirmed by Meyer and Hammond, who found that essentially no *o*- or *p*-hydroxyacetophenone was formed in the photolysis of phenyl acetate in the gas phase.²⁰⁷ Instead, all products could be rationalized by recombination of phenoxy and methyl radicals (formed from decarbonylation of acyl radicals). Similarly, a photodissociative mechanism for the photo-Claisen reaction was supported by observation of products expected from the recombination of radicals produced by photodissociation of 3-methyl-1-phenoxybut-2-ene (**113**, Table 12.6). In addition to phenol, products of the reaction are the rearranged ether **114**, the two γ,γ -dimethylallyl phenols **115** and **116**, and the two rearranged allyl phenols

²⁰⁵ Porter, G.; Strachan, E. *Trans. Faraday Soc.* **1958**, *54*, 1595.

²⁰⁶ Kelly, D. P.; Pinhey, J. T.; Rigby, R. D. G. *Aust. J. Chem.* **1969**, *22*, 977.

²⁰⁷ Meyer, J. W.; Hammond, G. S. *J. Am. Chem. Soc.* **1970**, *92*, 2187; *J. Am. Chem. Soc.* **1972**, *94*, 2219.

TABLE 12.6 Quantum Yields for Photoreactions of 2-Methyl-4-phenoxybut-2-ene



Solvent	$\Phi_{\text{app 107}}$	$\Phi_{\text{app 114}}$	$\Phi_{\text{app 115}}$	$\Phi_{\text{app 116}}$	$\Phi_{\text{app 117}}$	$\Phi_{\text{app 118}}$
Cyclohexane	0.10	0.05	0.06	0.05	0.02	0.03
2-Propanol	0.11	0.03	0.18	0.15	0.05	0.07

Source: Reference 208.

117 and 118, in ratios consistent with a reaction pathway involving radical recombination.²⁰⁸

Unlike the photodissociation of Cl_2 , direct excitation of a phenyl ether or ester to a dissociative state does not seem likely because the absorption spectrum of toluene shows some vibrational structure, and fluorescence of toluene is easily observed.²⁰⁴ Furthermore, the absorption and emission spectra of phenyl allyl ether are qualitatively similar to those of anisole. The reactions in equations 12.74 through 12.76 have therefore been explained by a process known as **predissociation**, in which internal conversion of a metastable excited state leads to a dissociative state—that is, excitation to a state with no significant energy minimum along the reaction coordinate.²⁰⁹ Figure 12.55 shows a simplified representation of the excited states of toluene as a function of the C–H bond distance.²¹⁰ The dotted lines represent an avoided crossing between the aromatic π, π^* triplet and a σ, σ^* triplet, so the lowest triplet has the energy shown by the solid line. In other words, T_1 for toluene has π, π^* character at short C–H distances but σ, σ^* character at longer C–H distances. Thus, it is a predissociative excited state, and thermal activation provides enough energy to cross the small barrier to bond homolysis.²¹¹

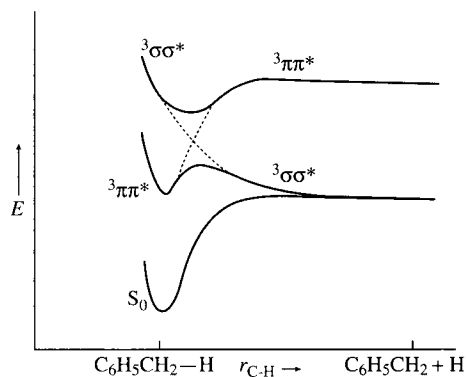
The depiction in Figure 12.55 is a very simple model of a photodissociation. As noted in Chapter 11, states of the same symmetry may not cross on a potential energy surface based on just one nuclear coordinate (the reaction coordinate). When more than one set of nuclear coordinates is included, however, then states of the same symmetry may cross.¹¹⁴ Thus, photodisso-

²⁰⁸ Carroll, F. A.; Hammond, G. S. *Israel J. Chem.* **1972**, *10*, 613.

²⁰⁹ For a discussion, see Dixon, R. N. *Acc. Chem. Res.* **1991**, *24*, 16.

²¹⁰ Michl, J. *Top. Curr. Chem.* **1974**, *46*, 1.

²¹¹ For a detailed discussion of predissociative states, see reference 89, pp. 245–247.

**FIGURE 12.55**

Predissociative model for toluene photodissociation. (Adapted from reference 210.)

ciation processes are described more completely by conical intersections such as those illustrated in Figure 12.28.²¹²

In polar solvents, α -halomethyl aromatics give rise to photochemical reactions that can be explained by both radical and ionic mechanisms. Equation 12.77 shows the results for irradiation of 1-chloromethylnaphthalene (**119**) in methanol.²¹³ The most direct pathway for formation of the methyl ether **120** is heterolytic dissociation of the C–Cl bond to give a chloride ion and a 1-naphthylmethyl carbocation, the latter then undergoing nucleophilic addition by the solvent.²¹⁴ Indeed, naphthylphenylmethyl carbocations were detected spectroscopically following laser flash photolysis of (naphthylphenylmethyl)triphenylphosphonium chlorides.²¹⁵ On the other hand, products **121**, **122**, and **123** appear to be formed via the 1-naphthylmethyl radical. Therefore, an alternative source of the carbocation leading to **120** could be electron transfer from the 1-naphthylmethyl radical instead of direct photochemical heterolysis of **119**.^{215,216} Kinetic data support the latter explanation. Peters and co-workers determined that the photolysis of diphenylmethyl chloride (**124**, equation 12.78) in cyclohexane results in homolysis of the C–Cl bond from the singlet state in ca. 230 fs, followed by electron transfer to produce the diphenylmethyl cation in ca. 5 ps. In acetonitrile solution, the radical pair and ion pair are formed in 345 fs and 833 fs, respectively.²¹⁷

²¹² See, for example, Abe, M.; Ohtsuki, Y.; Fujimura, Y.; Lan, Z.; Domcke, W. *J. Chem. Phys.* **2006**, *124*, 224316.

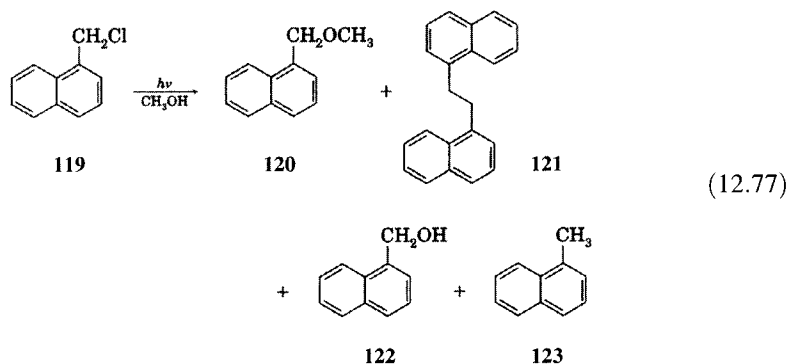
²¹³ Arnold, B.; Donald, L.; Jurgens, A.; Pincock, J. A. *Can. J. Chem.* **1985**, *63*, 3140.

²¹⁴ Sensitization and quenching studies, while not totally unambiguous, suggest that all of these products arise from the excited singlet state of **119**.

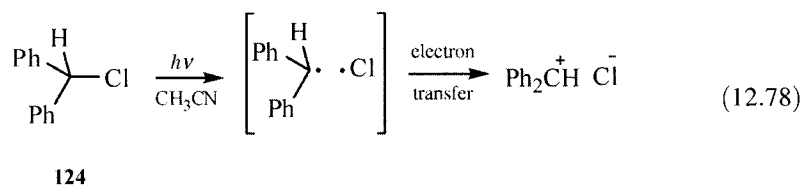
²¹⁵ Alonso, E. O.; Johnston, L. J.; Scaiano, J. C.; Toscano, V. G. *Can. J. Chem.* **1992**, *70*, 1784

²¹⁶ Pincock, J. A.; Wedge, P. J. *J. Org. Chem.* **1994**, *59*, 5587.

²¹⁷ Lipson, M.; Deniz, A. A.; Peters, K. S. *Chem. Phys. Lett.* **1998**, *288*, 781. See also Heeb, L. R.; Peters, K. S. *J. Am. Chem. Soc.* **2008**, *130*, 1711.

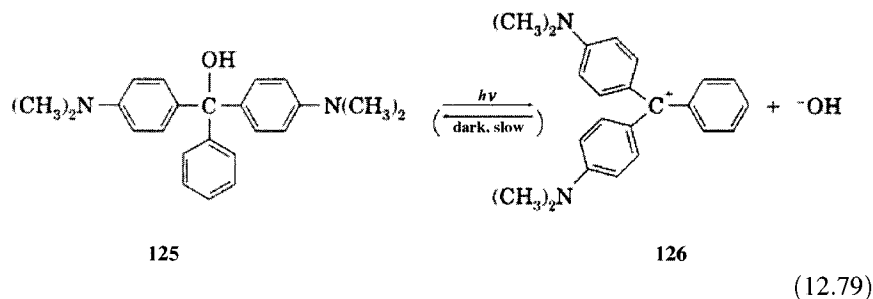


(12.77)



(12.78)

In some cases it appears that direct photodissociation to ions can occur.^{218,219} For example, irradiation of 4,4'-bis(dimethylamino)triphenylmethane leucohydroxide (**125**, 4.8×10^{-4} M) in aqueous micellar solutions led to the ejection of hydroxide ion and formation of 4,4'-bis(dimethylamino)triphenylmethyl cation (**126**, equation 12.79), which caused a pH change from 5.4 to 10.0. The pH returned to 5.4 over a period of 15 minutes as the hydroxide ion recombined with the carbocation.²²⁰



(12.79)

Similarly, a carbocation intermediate was proposed for the photochemical conversion of 9-phenylxanthen-9-ol (**127**) into the methyl ether **128** upon irradiation in methanol-water solution (equation 12.80). The investigators proposed that the reaction occurs adiabatically on the excited singlet potential energy surface, meaning that the carbocation in equation 12.80 is formed as an electronically excited singlet.²²¹

²¹⁸ For a review, see Das, P. K. *Chem. Rev.* **1993**, 93, 119.

²¹⁹ For a discussion of the photochemical production of radical, carbocation, and carbene intermediates from irradiation of alkyl halides in solution, see Kropp, P. J. *Acc. Chem. Res.* **1984**, 17, 131.

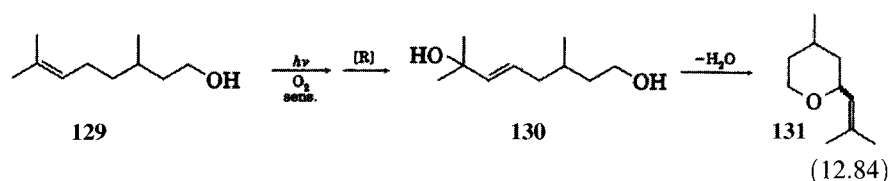
²²⁰ Irie, M. *J. Am. Chem. Soc.* **1983**, 105, 2078. The quantum yield of the process was not stated.

²²¹ Wan, P.; Yates, K.; Boyd, M. K. *J. Org. Chem.* **1985**, 50, 2881.

The second is allylic oxidation, which can also be visualized as an ene reaction.^{229–231} The resulting allyl hydroperoxide can then be reduced to an allyl alcohol.



A practical example of the use of singlet oxygen is provided by the synthesis of rose oxide (**131**) from β -citronellol (**129**, equation 12.84).²³² The sensitizer was rose bengal, a dye that can be used for singlet oxygen reactions induced by sunlight. The product of the ene reaction was reduced with Na_2SO_3 to a diol (**130**), which then underwent spontaneous cyclization to **131** in a cold, acidic solution.²³³



The use of organic compounds to sensitize formation of singlet oxygen is becoming more important in organic synthesis, and these reactions have medical applications as well. In **photodynamic therapy**, patients are first treated with dyes that are selectively taken up by tumor cells. Then percutaneous (through the skin) or endoscopic irradiation of the dye with visible light can produce cytotoxic singlet oxygen at the tumor site, minimizing the need to circulate toxic drugs throughout the patient's body.²³⁴ On the other hand, an undesirable effect of photochemistry in medicine is the development of side effects when a patient takes a drug and then is exposed to sunlight.²³⁵

²²⁹ For a review, see Gollnick, K.; Kuhn, H. J. in Wasserman, H. H.; Murray, R. W., Eds. *Singlet Oxygen*; Academic Press: New York, 1979; pp. 287–427.

²³⁰ The mechanism was characterized as a two-step process without an intermediate because two saddle points occur consecutively on the potential energy surface. Singleton, D. A.; Hang, C.; Szymanski, M. J.; Meyer, M. P.; Leach, A. G.; Kuwata, K. T.; Chen, J. S.; Greer, A.; Foote, C. S.; Houk, K. N. *J. Am. Chem. Soc.* **2003**, *125*, 1319.

²³¹ Griesbeck, A. G.; El-Idreesy, T. T.; Adam, W.; Krebs, O. in reference 2, p. 8-1.

²³² Ohloff, G.; Klein, E.; Schenck, G. O. *Angew. Chem.* **1961**, *73*, 578. See also reference 169, p. 377.

²³³ For applications of singlet oxygen in the synthesis of natural products, see Montagnon, T.; Tofi, M.; Vassilikogiannakis, G. *Acc. Chem. Res.* **2008**, *41*, 1001.

²³⁴ For examples and leading references, see (a) Ross, P., Ed. *A Comprehensive Textbook of Photodynamic Therapy: A Spectrum of Applications*; John Wiley & Sons: Hoboken, NJ, 2008; (b) Hamblin, M.; Mroz, P., Eds. *Advances in Photodynamic Therapy: Basic, Translational and Clinical*; Artech House: Norwood, MA, 2008; Wainwright, M. *Anti-Cancer Agents Med. Chem.* **2008**, *8*, 280.

²³⁵ Rubinstein, E. *Chemotherapy* **2001**, *47*, 3; Miranda, M. A. *Pure Appl. Chem.* **2001**, *73*, 481; Cosa, G. *Pure Appl. Chem.* **2004**, *76*, 263.

12.5 SOME APPLICATIONS OF ORGANIC PHOTOCHEMISTRY

Organic photochemistry has a wide range of applications in organic synthesis as well as in applied fields ranging from polymers to nanotechnology. As the examples presented above illustrate, photochemical reactions provide particularly valuable synthetic methodologies because they can produce complex or strained products and often can be carried out under mild conditions, thus enabling highly sensitive functional groups to be produced.^{236–238} Moreover, photochemical reactions allow selective activation of just one portion of a molecule (the chromophore) and may make possible reactions at selected distances from the chromophore by attaching a photoreactive group to a molecular skeleton with a tether.²³⁹ Even though the quantum efficiencies of some photochemical reactions may not be high, the chemical yields are often higher than what might be achieved in thermal reactions from easily obtained starting materials.²⁴⁰ In addition, photochemical reactions can be “greener” (from the environmental perspective) than are the thermal pathways for some syntheses.²⁴¹

The following additional examples offer a hint of the utility of organic photochemistry in synthesis.²⁴² A [2 + 2] photochemical cycloaddition was a key step in the synthesis of cubane.²⁴³ Synthesis of 2-bromocyclopenta-2,4-dienone resulted in a spontaneous Diels–Alder reaction, which produced **132**. The monoketal of the dimer (**133**) underwent intramolecular photocycloaddition to produce **134** (equation 12.85). The Favorskii reaction of **134** gave **135**, which was decarboxylated to **136** (equation 12.86). Hydrolysis of the ketal gave **137**. Subsequent Favorskii reaction to **138** and then decarboxylation produced cubane, **139**. Similarly, de Meijere and co-workers reported that the intramolecular [2 + 2] photochemical cycloaddition of **140** produced octacyclopopylcubane (**141**, equation 12.87).²⁴⁴ Maier and co-workers utilized the reaction sequence in equation 12.88 to convert the diazo compound **142** into tetra-*t*-butylcyclobutadiene (**143**) and tetra-*t*-butyltetrahydrene (**144**).²⁴⁵

²³⁶ For a discussion of this point, see Jones, S. W.; Scheinmann, F.; Wakefield, B. J.; Middlemiss, D.; Newton, R. F. *J. Chem. Soc. Chem. Commun.* **1986**, 1260.

²³⁷ Shinmyozu, T.; Nogita, R.; Akita, M.; Lim, C. in reference 2, pp. 22-1; 23-1.

²³⁸ For a review of the photochemical synthesis of polycyclic structures, see De Keukeleire, D.; He, S.-L. *Chem. Rev.* **1993**, 93, 359; De Keukeleire, D. *Aldrichimica Acta* **1994**, 27, 59.

²³⁹ Suginome, H. in reference 2, p. 102-1.

²⁴⁰ The use of chiral sensitizers or of circularly polarized light can lead to asymmetric photochemical synthesis. For a review, see Inoue, Y. *Chem. Rev.* **1992**, 92, 741. See also equation 12.99.

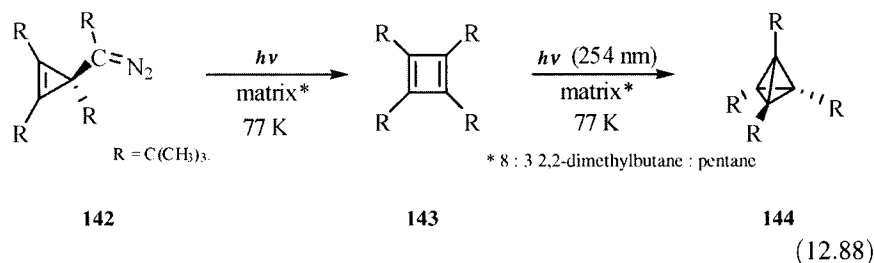
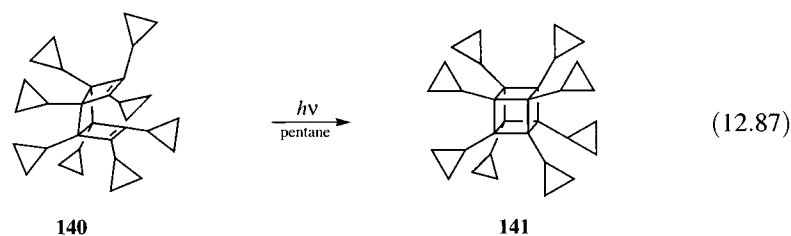
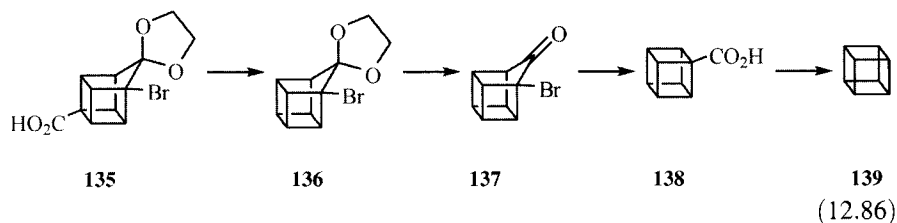
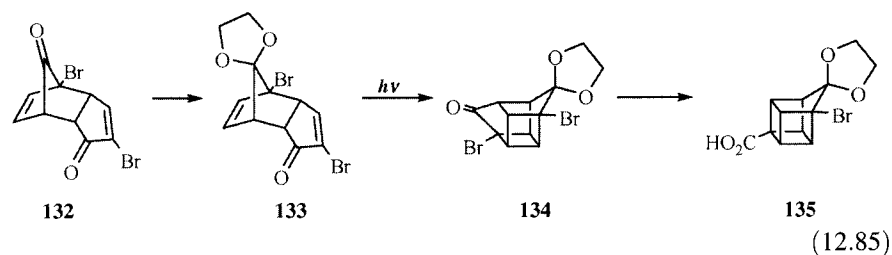
²⁴¹ Protti, S.; Dondi, D.; Fagnoni, M.; Albini, A. *Pure Appl. Chem.* **2007**, 79, 1929; Oelgemöller, M.; Jung, C.; Mattay, J. *Pure Appl. Chem.* **2007**, 79, 1939.

²⁴² For discussions of synthetic organic photochemistry, see Horspool, W. M., Ed. *Synthetic Organic Photochemistry*; Plenum Press: New York, 1984; Srinivasan, R.; Roberts, T. D., Eds. *Organic Photochemical Syntheses*, Vol. 1; Wiley-Interscience: New York, 1971; Srinivasan, R., Ed. *Organic Photochemical Syntheses*, Vol. 2; Wiley-Interscience: New York, 1976; reference 169; Ninomiya, I.; Naito, T. *Photochemical Synthesis*; Academic Press: London, 1989; Griesbeck, A. G.; Mattay, J., Eds. *Synthetic Organic Photochemistry*; CRC Press: Boca Raton, FL, 2004.

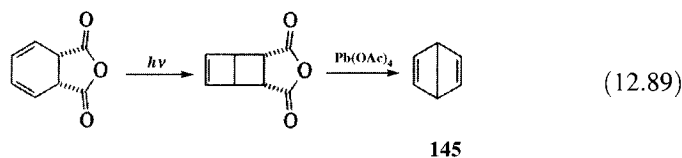
²⁴³ Eaton, P. E.; Cole, T. W., Jr. *J. Am. Chem. Soc.* **1964**, 86, 962, 3157.

²⁴⁴ de Meijere, A.; Redlich, S.; Frank, D.; Magull, J.; Hofmeister, A.; Menzel, H.; König, B.; Svoboda, J. *Angew. Chem. Int. Ed.* **2007**, 46, 4574.

²⁴⁵ Maier, G. *Pure Appl. Chem.* **1991**, 63, 275. See also Maier, G.; Wolf, R.; Kalinowski, H.-O. *Angew. Chem. Int. Ed. Engl.* **1992**, 31, 738.



Intramolecular cycloaddition also played a central role in the synthesis of Dewar benzene (**145**, equation 12.89),²⁴⁶ the bicycloheptenol **146** (equation 12.90),²⁴⁷ and the tricyclic keto ethers **147** and **148** (equation 12.91).²⁴⁸ The photochemical retro Diels–Alder reaction was also used for a synthesis of bullvalene (**149**) from cyclooctatetraene dimer (equation 12.92).²⁴⁹

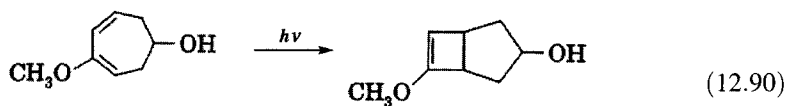


²⁴⁶ van Tamelen, E. E.; Pappas, S. P. *J. Am. Chem. Soc.* **1963**, *85*, 3297.

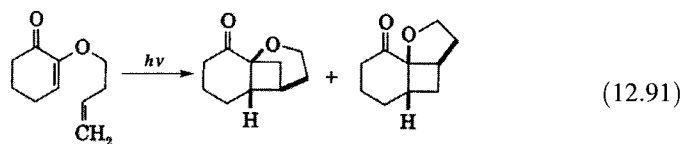
²⁴⁷ Chapman, O. L.; Pasto, D. J.; Borden, G. W.; Griswold, A. A. *J. Am. Chem. Soc.* **1962**, *84*, 1220.

²⁴⁸ Ikeda, M.; Takahashi, M.; Uchino, T.; Ohno, K.; Tamura, Y.; Kido, M. *J. Org. Chem.* **1983**, *48*, 4241.

²⁴⁹ Schröder, G. *Chem. Ber.* **1964**, *97*, 3140.

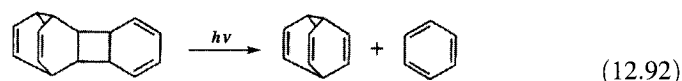


146



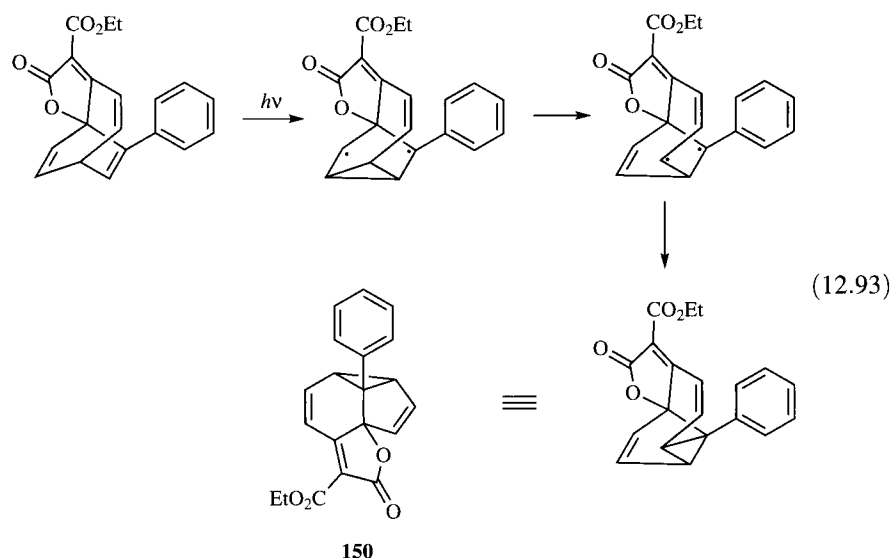
147

148



149

The di- π -methane rearrangement was a key step in the synthesis of the complex structure **150** (equation 12.93).²⁵⁰

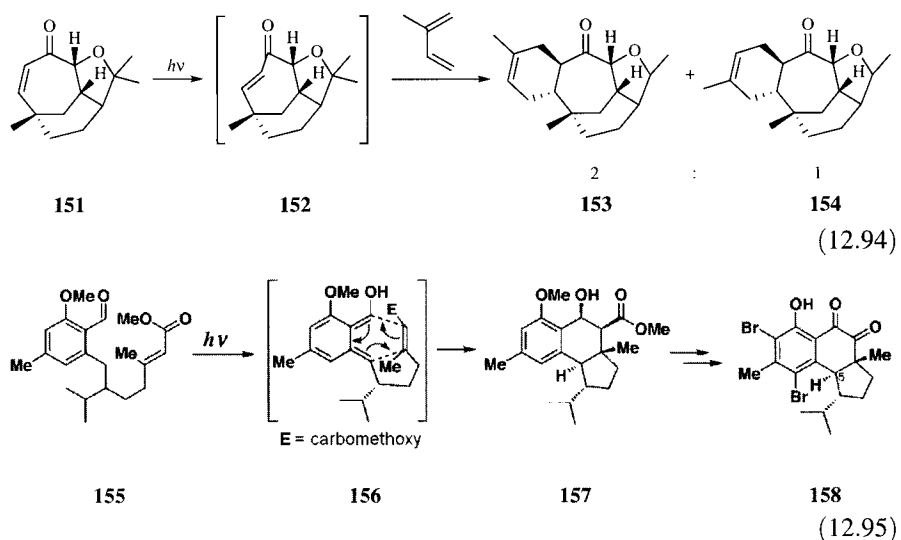


Photochemical reactions can produce highly reactive intermediates for subsequent ground state reactions. Photoisomerization of the cycloheptenone moiety in **151** led to a highly strained trans enol (**152**) that readily underwent a Diels–Alder reaction with isoprene to produce a mixture of **153** and **154**, both of which were carried forward to a structure related to a naturally occurring tricyclic diterpene, vibsandin E (equation 12.94).²⁵¹ Irradiation of the aldehyde **155** led to γ -hydrogen abstraction and formation of the transient enol (**156**),

²⁵⁰ Nair, V.; Nandakumar, M. V.; Anilkumar, G. N.; Maliakal, D.; Vairamani, M.; Prabhakar, S.; Rath, N. P. *J. Chem. Soc. Perkin Trans. 1* **2000**, 3795.

²⁵¹ Davies, H. M. L.; Loe, Ø.; Stafford, D. G. *Org. Lett.* **2005**, *7*, 5561.

which underwent an intramolecular Diels–Alder reaction to produce **157**, a precursor to 5-*epi*-4-bromohamigeran B (**158**, equation 12.95).²⁵²



Another role of photochemistry in organic synthesis is the use of UV–vis radiation to deprotect functional groups during a reaction sequence.^{253,254} In some cases, different photolabile protecting groups may be selectively removed by appropriate choice of excitation wavelength.²⁵⁵ Removal of protective groups with UV–vis radiation has applications in pharmaceutical delivery as well.²⁵⁶ For example, irradiation of the 3,5-dimethoxybenzoin ester of salicylic acid (**159**, Figure 12.56) produces aspirin (**160**) and 5,7-dimethoxy-2-phenylbenzofuran (**161**).²⁵⁷

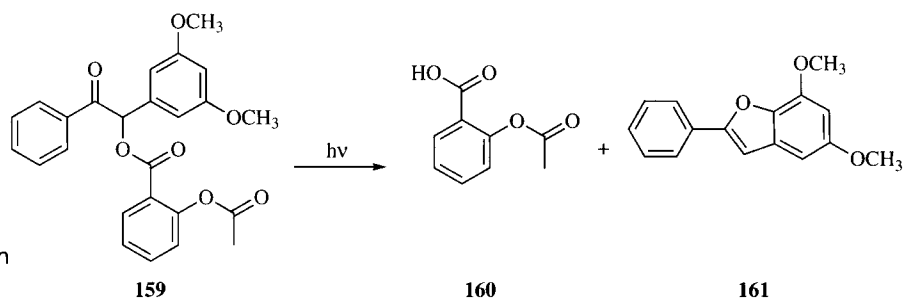


FIGURE 12.56

Photochemical release of aspirin from **159**.

²⁵² Nicolaou, K. C.; Gray, D.; Tae, J. *Angew. Chem. Int. Ed.* **2001**, *40*, 3679

²⁵³ Wuts, P. G. M.; Greene, T. W. *Greene's Protective Groups in Organic Synthesis*, 4th ed.; Wiley-Interscience: Hoboken, NJ, 2007.

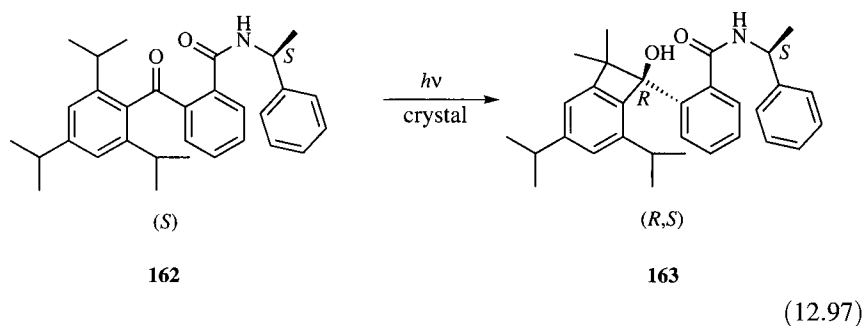
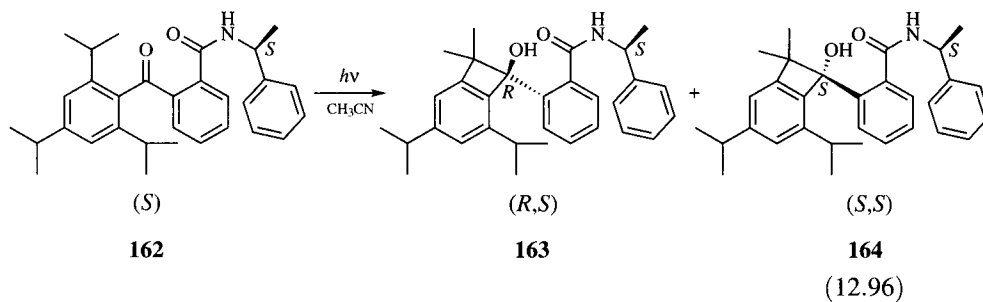
²⁵⁴ Givens, R. S.; Conrad, P. G. II.; Yousef, A. L.; Lee, J.-I. in reference 2, p. 69-1.

²⁵⁵ Kessler, M.; Glatthar, R.; Giese, B.; Bochet, C. G. *Org. Lett.* **2003**, *5*, 1179; Bochet, C. G. *Pure Appl. Chem.* **2006**, *78*, 241; Ciana, C.-L.; Bochet, C. G. *Chimia* **2007**, *61*, 650.

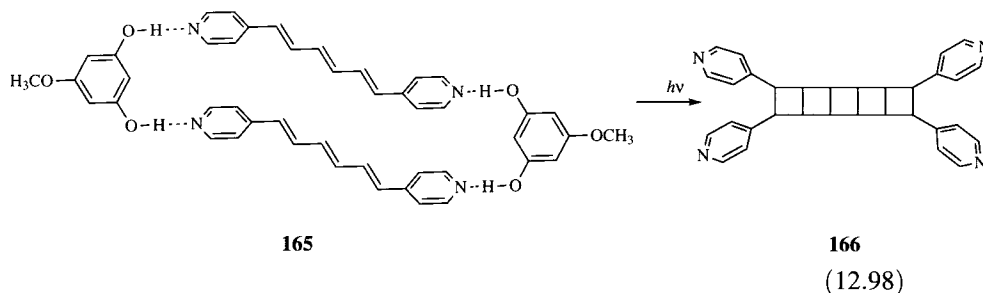
²⁵⁶ Jiang, M. Y.; Dolphin, D. J. *Am. Chem. Soc.* **2008**, *130*, 4236.

²⁵⁷ McCoy, C. P.; Rooney, C.; Edwards, C. R.; Jones, D. S.; Gorman, S. P. *J. Am. Chem. Soc.* **2007**, *129*, 9572.

Carrying out photochemical reaction in crystals offers unique synthetic possibilities, particularly for control of stereochemistry. For example, in solution the irradiation of a 2,4,6-triisopropylbenzophenone bearing the (*S*)-phenylethylamide group (**162**) gives approximately 1:1 mixture of the *R,S* (**163**) and *S,S* (**164**) diastereomers of the Norrish–Yang cyclization product (equation 12.96). However, irradiation of microcrystals of **162** led exclusively to the (*R,S*) diastereomer (equation 12.97).²⁵⁸ This stereoselectivity was attributed to steric forces present in the chiral crystal.



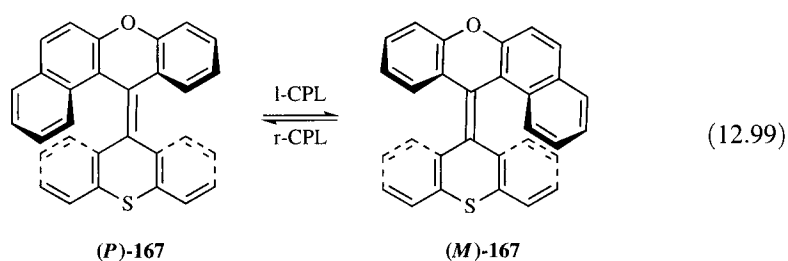
MacGillivray and co-workers utilized **165**, a co-crystal of 5-methoxyresorcinol and an all-*trans*-bis(4-pyridyl)polyene, to synthesize the “molecular ladder” **166** (equation 12.98).²⁵⁹ Here, **165** holds the carbon–carbon double bonds of the polyene in close proximity and parallel to each other. Exposure of the crystal to UV radiation led to complete conversion to the ladder structure.



²⁵⁸ Koshima, H.; Fukano, M.; Uekusa, H. *J. Org. Chem.* **2007**, *72*, 6786.

²⁵⁹ Gao, X.; Friščić, T.; MacGillivray, L. R. *Angew. Chem. Int. Ed.* **2004**, *43*, 232. See also Mascitti, V.; Corey, E. J. *Tetrahedron Lett.* **2006**, *47*, 5879.

Photochemistry plays a central role in nanotechnology and is particularly useful in the construction of molecular-scale devices that can carry out electronic or mechanical operations.²⁶⁰ Novel applications of photochemistry include the development of molecular tweezers for the photoreversible binding of metal ions²⁶¹ and the photoencapsulation of organic molecules in zeolite as an example of a molecular "ship in a bottle."²⁶² Many nanoscale devices utilize photochemically driven cis–trans isomerizations to open and close switches or to move part of a structure from one place to another.^{263,264} Feringa and co-workers described a series of chiral twisted alkenes that change helicity upon cis–trans isomerization (equation 12.99).²⁶⁵ The *P* enantiomer of **167** was converted to a slight excess of the *M* enantiomer upon irradiation with left-handed circularly polarized light (l-CPL), while the *M* enantiomer was converted to a slight excess of the *P* enantiomer with right-handed circularly polarized light (r-CPL).



There are many applications of organic photochemistry to consumer products. One is the development of a photographic system based on organic compounds rather than on silver salts.²⁶⁶ Such organic systems offer a "grain size" of molecular dimensions, much smaller than the inorganic crystals used in film based on silver halide technology. In theory at least, these organic films have a much higher resolution than does silver halide film, although at the expense of decreased spectral sensitivity and film speed.²⁶⁷ A general term for the process by which photochemical reactions lead to the formation of

²⁶⁰ Balzani, V.; Credi, A.; Venturi, M. *Pure Appl. Chem.* **2003**, *75*, 541; *ChemPhysChem* **2008**, *9*, 202; see also Yamada, M.; Kondo, M.; Mamiya, J.-I.; Yu, Y.; Kinoshita, M.; Barrett, C. J.; Ikeda, T. *Angew. Chem. Int. Ed.* **2008**, *47*, 4986.

²⁶¹ Irie, M.; Kato, M. *J. Am. Chem. Soc.* **1985**, *107*, 1024.

²⁶² Lei, X.; Doubleday, C. E., Jr.; Zimmt, M. B.; Turro, N. J. *J. Am. Chem. Soc.* **1986**, *108*, 2444.

²⁶³ Dugave, C.; Demange, L. *Chem. Rev.* **2003**, *103*, 2475; Yang, J.-S.; Huang, Y.-T.; Ho, J.-H.; Sun, W.-T.; Huang, H. H.; Lin, Y.-C.; Huang, S.-J.; Huang, S.-L.; Lu, H.-F.; Chao, I. *Org. Lett.* **2008**, *10*, 2279.

²⁶⁴ Feringa, B. L.; van Delden, R. A.; Koumura, N.; Geertsema, E. M. *Chem. Rev.* **2000**, *100*, 1789.

²⁶⁵ ter Wiel, M. K. J.; Kwit, M. G.; Meetsma, A.; Feringa, B. L. *Org. Biomol. Chem.* **2007**, *5*, 87; Feringa, B. L. *J. Org. Chem.* **2007**, *72*, 6635.

²⁶⁶ Marshall, J. L.; Telfer, S. J.; Young, M. A.; Lindholm, E. P.; Minns, R. A.; Takiff, L. *Science* **2002**, *297*, 1516.

²⁶⁷ Photochemically induced physical changes (such as a change in phase resulting from a photochemical reaction) may amplify the response of a photochemical information storage system. See, for example, (a) Tazuke, S.; Kurihara, S.; Yamaguchi, H.; Ikeda, T. *J. Phys. Chem.* **1987**, *91*, 249; (b) Zhang, M.; Schuster, G. B. *J. Am. Chem. Soc.* **1994**, *116*, 4852

²⁶⁸ For an introduction, see Laurent, H. B.; Dürr, H. *Pure Appl. Chem.* **2001**, *73*, 639.

products of a different color is **photochromism**.²⁶⁸ Photography itself is only one aspect of the more general field of imaging systems, which also includes holography and high density data storage.²⁶⁹ An advantage of some organic photochromic systems is the potential for photochemically reversible reactions so that UV–vis radiation could be used to both store and erase information.²⁷⁰ Organic photoconductive materials have been developed for use in xerography and photopolymerization.²⁷¹

Other applications of photochemistry include the development of sensitive fluorescent chemosensors for analysis of dilute solutions of inorganic cations and anions²⁷² and the study of the diffusion of individual molecules in solution at room temperature.²⁷³ Fluorescent compounds have been used as replacements for radioisotopes in the analysis of biological compounds²⁷⁴ and the study of biologically active compounds and living systems.^{275,276} Photochemical reactions also offer alternative probes for the characterization of the microenvironments in diverse solid and liquid media, including crystals,²⁷⁷ zeolites, alumina, silica and clay surfaces, semiconductor surfaces, liquid crystals and host–guest inclusion complexes,²⁷⁸ polymer films,²⁷⁹ monolayers and supported multilayers of surfactant molecules,²⁸⁰ micelles,^{281,282} and dendrimers.²⁸³

Chemiluminescence is the emission of light from electronically excited molecules produced from reactants in their ground electronic states.²⁸⁴ Luminol (**168**) is a synthetic compound that has been studied extensively. Reaction of **168** with base and oxygen is thought to generate the aminophthalate derivative **169** in an electronically excited state that can emit light or transfer the excitation energy to another species (equation 12.100).²⁸⁵

²⁶⁹ Tomlinson, W. J.; Chandross, E. A. *Adv. Photochem.* **1980**, *12*, 201. Photopolymerization of liquid crystals also offers promise for holography. Zhang, J.; Carlen, C. R.; Palmer, S.; Sponsler, M. B. *J. Am. Chem. Soc.* **1994**, *116*, 7055.

²⁷⁰ See, for example, Rieke, R. D.; Page, G. O.; Hudnall, P. M.; Arhart, R. W.; Bouldin, T. W. *J. Chem. Soc. Chem. Commun.* **1990**, 38.

²⁷¹ See, for example, (a) Monroe, B. M.; Weed, G. C. *Chem. Rev.* **1993**, *93*, 435; (b) Law, K.-Y. *Chem. Rev.* **1993**, *93*, 449.

²⁷² Czarnik, A. W. *Acc. Chem. Res.* **1994**, *27*, 302.

²⁷³ Nie, S.; Chiu, D. T.; Zare, R. N. *Science* **1994**, *266*, 1018.

²⁷⁴ Mayer, A.; Neuenhofer, S. *Angew. Chem. Int. Ed. Engl.* **1994**, *33*, 1044.

²⁷⁵ Mayer, G.; Heckel, A. *Angew. Chem. Int. Ed.* **2006**, *45*, 4900.

²⁷⁶ Neuweiler, H.; Sauer, M. *Anal. Chem.* **2005**, *77*, 178A.

²⁷⁷ Zimmerman, H. E.; Zhu, Z. *J. Am. Chem. Soc.* **1994**, *116*, 9757 and references therein.

²⁷⁸ Ramamurthy, V., Ed. *Photochemistry in Organized and Constrained Media*; VCH Publishers: New York, 1991.

²⁷⁹ Cui, C.; Weiss, R. G. *J. Am. Chem. Soc.* **1993**, *115*, 9820.

²⁸⁰ Whitten, D. G. *Acc. Chem. Res.* **1993**, *26*, 502.

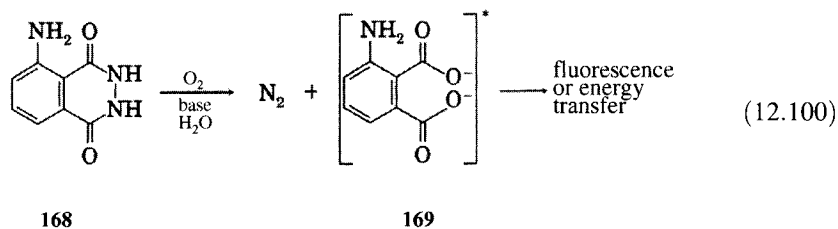
²⁸¹ Han, N.; Lei, X.; Turro, N. J. *J. Org. Chem.* **1991**, *56*, 2927.

²⁸² A general model of photochemistry in environments categorized as organized and confining media has been given by Weiss, R. G.; Ramamurthy, V.; Hammond, G. S. *Acc. Chem. Res.* **1993**, *26*, 530; see also Quina, F. H.; Lissi, E. A. *Acc. Chem. Res.* **2004**, *37*, 703.

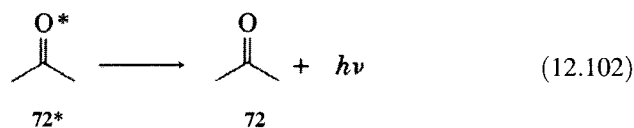
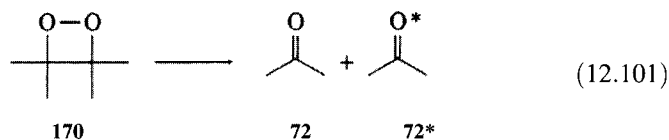
²⁸³ Kaanumalle, L. S.; Ramesh, R.; Maddipatla, V. S. N. M.; Nithyanandhan, J.; Jayaraman, N.; Ramamurthy, V. *J. Org. Chem.* **2005**, *70*, 5062.

²⁸⁴ For an introduction, see Gundermann, K.-D.; McCapra, F. *Chemiluminescence in Organic Chemistry*; Springer-Verlag: Berlin, 1987.

²⁸⁵ Merényi, G.; Lind, J.; Eriksen, T. E. *J. Biolumin. Chemilumin.* **1990**, *5*, 53.



1,2-Dioxetanes are also chemiluminescent, and tetramethyl-1,2-dioxetane (170) is reported to glow at room temperature. The data suggested that decomposition of 170 produces two molecules of acetone, one in the ground electronic state and one in an electronically excited state (equation 12.101). Most of the excited acetone molecules are triplets, so the chemiluminescence observed in the absence of oxygen is acetone phosphorescence (equation 12.102). In the presence of oxygen the acetone triplets are quenched, so the emission is acetone fluorescence that is much weaker because only 1% as many excited singlet molecules as excited triplet molecules result from the decomposition of the 1,2-dioxetane.^{286,287}



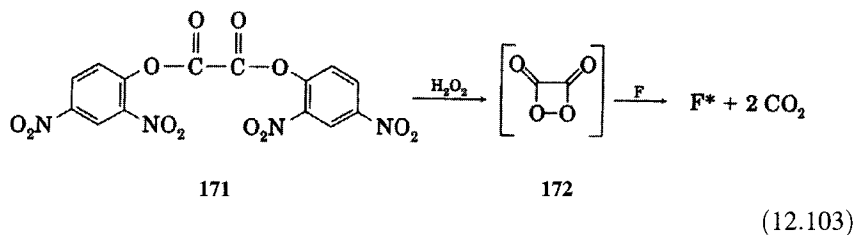
Diaryl esters of oxalic acid such as 171 can undergo reaction to form a dioxetanedione, 172, which decomposes to two molecules of CO₂, one of which is in an excited state (equation 12.103). Energy transfer to a fluorescent molecule (F) leads to the emission of light, producing chemiluminescence (equation 12.104).^{288,289}

²⁸⁶ Turro, N. J.; Lechtken, P.; Schore, N. E.; Schuster, G.; Steinmetzer, H.-C.; Yekta, A. *Acc. Chem. Res.* **1974**, *7*, 97 and references therein.

²⁸⁷ See also Turro, N. J. in Gordon, M.; Ware, W. R., Eds. *The Exciplex*; Academic Press: New York, 1975; pp. 165–186.

²⁸⁸ Rauhut, M. M.; Bollyky, L. J.; Roberts, B. G.; Loy, M.; Whitman, R. H.; Iannotta, A. V.; Semsel, A. M.; Clarke, R. A. *J. Am. Chem. Soc.* **1967**, *89*, 6515.

²⁸⁹ For a discussion, see Thrush, B. A. *J. Photochem.* **1984**, *25*, 9.



Photochemistry can be applied in novel ways in other consumer products, as in pro-fragrances that release perfumes or other aromas only when exposed to UV-vis radiation.²⁹⁰ Some photochemically generated odors are unappealing, however, such as the "skunky odor" that develops when beer is exposed to light. De Keukeleire, Forbes, and co-workers elucidated the photochemistry responsible for the formation of this "lightstruck flavor" in beer made with hops.^{291,292} The compound believed responsible for the skunky odor is 3-methylbut-2-ene-1-thiol (**174**, Figure 12.57). These investigators concluded that absorption of light by the isohumulone **173** occurs at the enolized β -triketone function (note the brackets and indications of excited state multiplicity), but endothermic intramolecular energy transfer excites the α -hydroxycarbonyl moiety. The latter excited state undergoes Norrish type I

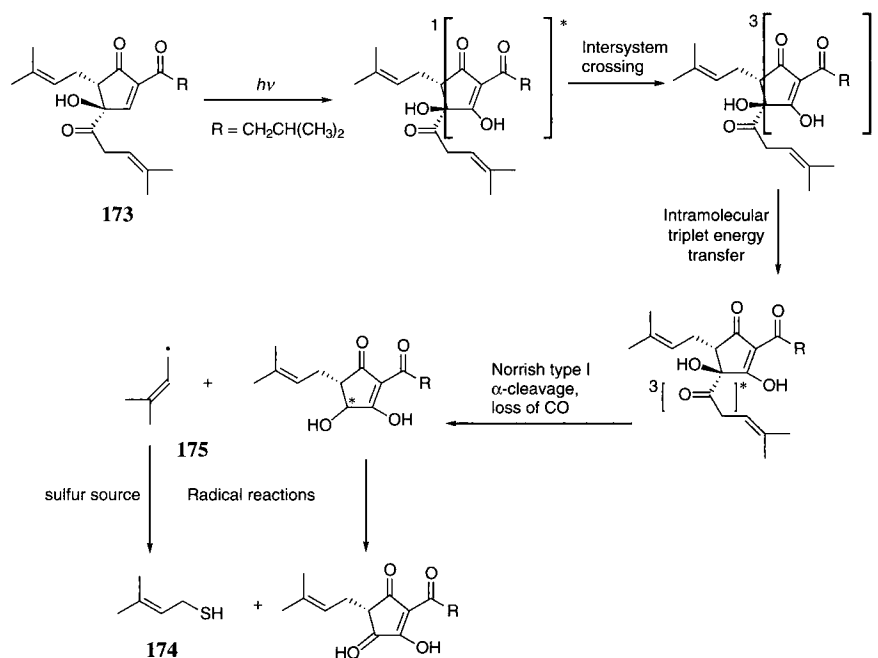


FIGURE 12.57
Photochemical formation of "light-struck flavor" in beer. (Adapted from reference 291.)

²⁹⁰ Rochat, S.; Minardi, C.; de Saint Laumer, J.-Y.; Herrmann, A. *Helv. Chim. Acta* **2000**, *83*, 1645; Herrmann, A. *Angew. Chem. Int. Ed.* **2007**, *46*, 5836.

²⁹¹ Burns, C. S.; Heyerick, A.; De Keukeleire, D.; Forbes, M. D. E. *Chem. Eur. J.* **2001**, *7*, 4553.

²⁹² Hops are dried flowers of the hop plant and are used to flavor beer.

reaction to produce an allylic radical (**175**) that can react with sulfur-containing compounds to produce **174**. This result explains why replacement of hops with borohydride-reduced hops extract allows brewers to manufacture beer that can be sold in colorless bottles.

Three additional examples illustrate some other novel applications of organic photochemistry. Cho and co-workers reported a film with a photo-switchable surface that can be varied reversibly from superhydrophobic to superhydrophilic by UV-vis radiation.²⁹³ Raghavan and co-workers found that an aqueous solution of *trans*-*o*-methoxycinnamic acid and the cationic surfactant cetyltrimethylammonium bromide (CTAB) form long micelles that increase the viscosity of the liquid. Photoisomerization of the *trans*-*o*-methoxycinnamic acid to the *cis* isomer caused a decrease in the length of the micelles. As a result, the viscosity of the solution was changed by as much as four orders of magnitude.²⁹⁴ Conversely, Kuimova and co-workers reported using a compound with a viscosity-dependent fluorescence lifetime to measure viscosity inside living cells.²⁹⁵

One of the ultimate goals of organic photochemistry is the storage of solar energy in chemical bonds, perhaps even leading to artificial photosynthesis.^{58,296} Even though photochemical electron-transport mechanisms have been developed, true artificial photosynthesis will require progress in the development of organized molecular assemblies (artificial chloroplasts) that can minimize recombination of photochemically generated charge separation.

Problems

- 12.1. Compound **A** absorbs light in the near-UV region of the spectrum. The onset of absorption is 375 nm. A dilute solution of **A** in an organic solvent exhibits fluorescence (onset = $26,900\text{ cm}^{-1}$) and phosphorescence (onset 6800 \AA). What are the energies of the S_1 and T_1 states of **A**?
- 12.2. The $S_0 \rightarrow S_1$ transitions for a series of polyacenes (Chapter 4) are seen at 370 nm for anthracene, 470 nm for tetracene, 582 nm for pentacene, and 695 nm for hexacene. What are the corresponding energy gaps in (i) eV and (ii) kcal/mol?
- 12.3. The lowest energy excited state of compound **B** exhibits photochemical reaction, fluorescence, and intersystem crossing. Measurements show that $\Phi_f = 0.3$ and $\Phi_{isc} = 0.5$. Irradiation of 100 mL of a 10^{-2} M solution of **B** with 10^{-3} einsteins (all absorbed by **B**) gives a 5.0% conversion of **B** into product **C**.
 - a. What is the quantum yield of product formation in this reaction?
 - b. Assuming that all of the product is formed from the S_1 state of **B**, what fraction of the S_1 population is *not* accounted for by fluorescence, intersystem crossing, or photochemical reaction?
- 12.4. Compound **D** exhibits triplet-triplet absorption in fluid solution at room temperature. Compound **Q** is found to quench the triplets of **D**. Table 12.7

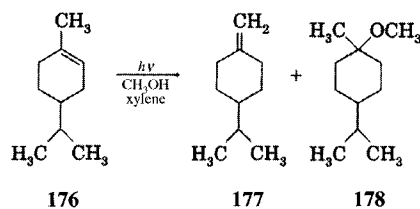
²⁹³ Lim, H. S.; Han, J. T.; Kwak, D.; Jin, M.; Cho, K. *J. Am. Chem. Soc.* **2006**, *128*, 14458.

²⁹⁴ Ketner, A. M.; Kumar, R.; Davies, T. S.; Elder, P. W.; Raghavan, S. R. *J. Am. Chem. Soc.* **2007**, *129*, 1553.

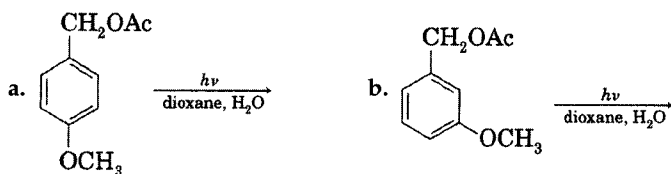
²⁹⁵ Kuimova, M. K.; Yahioglu, G.; Levitt, J. A.; Suhling, K. *J. Am. Chem. Soc.* **2008**, *130*, 6672.

²⁹⁶ Balzani, V.; Credi, A.; Venturi, M. *ChemSusChem* **2008**, *1*, 26; Barber, J. *Chem. Soc. Rev.* **2009**, *38*, 185.

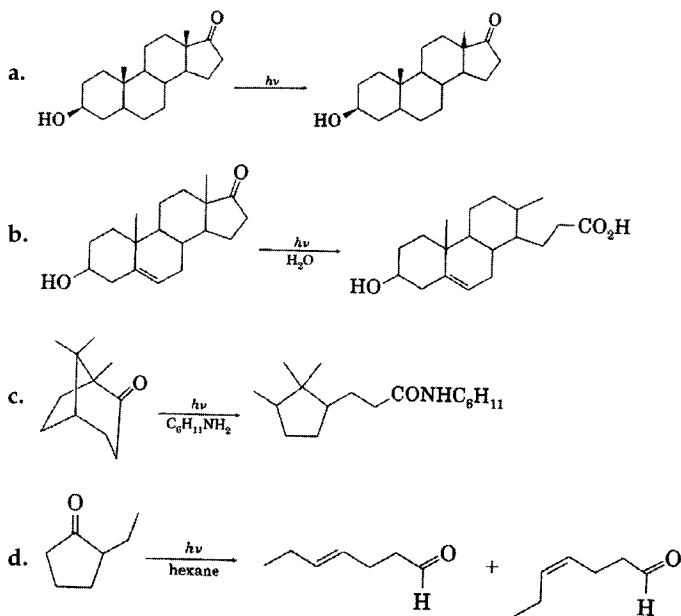
- 12.11. a. Irradiation of 176 in toluene with added methanol leads to the formation of 177 and 178. When the photochemical reaction is carried out with CH_3OD , each of the products has one deuterium atom incorporated into its structure. Where is the deuterium label found in each compound?



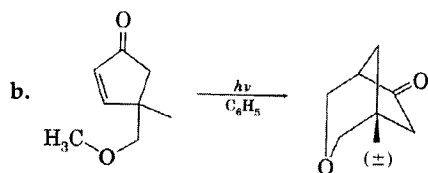
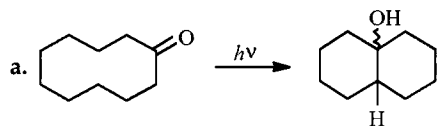
- b. Irradiation of *cis*-5-methyl-3-hexen-2-one (92, page 842) in CH_3OD produces 5-methyl-4-hexen-2-one (94, equation 12.69) in which one deuterium atom is incorporated into the structure. Where is the deuterium label located?
- 12.12. Irradiation of acetone in the presence of 2,3-dimethylbut-2-ene leads to the formation of seven photoproducts. Two products are unsaturated ethers; two are unsaturated alcohols; one is an oxetane; two are hydrocarbons. Give the structures of the products and propose mechanisms for their formation.
- 12.13. Predict the major product(s) of each of the following reactions.



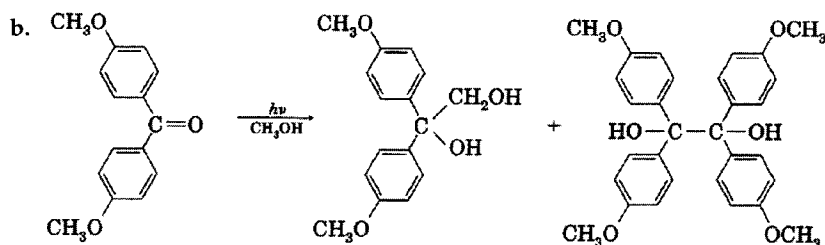
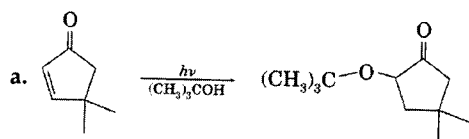
- 12.14. For each of the following reactions, propose a mechanism in which the first step is a Norrish type I reaction (α cleavage).



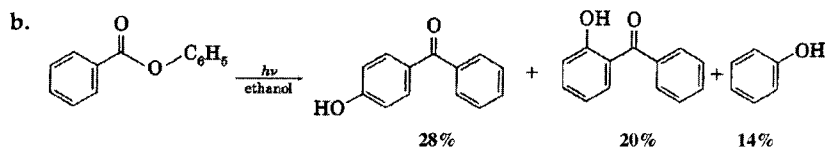
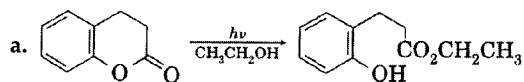
12.15. For each of the following reactions, propose a mechanism in which the first step is an intramolecular hydrogen abstraction.



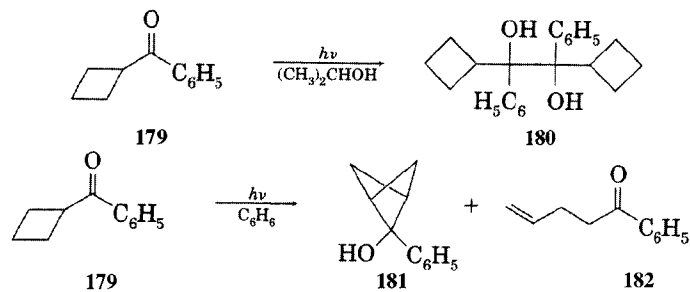
12.16. For each of the following reactions, propose a mechanism in which the first step is an intermolecular hydrogen abstraction.



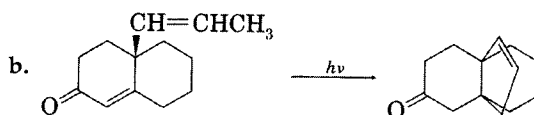
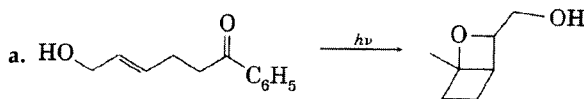
12.17. For each of the following reactions, propose a mechanism in which the first step is a σ bond photodissociation.



12.18. Irradiation of cyclobutyl phenyl ketone (179) in isopropyl alcohol leads to 180, while irradiation in benzene leads to 181 and 182. Propose mechanisms for formation of the products, and explain why different products are formed in the two solvents.

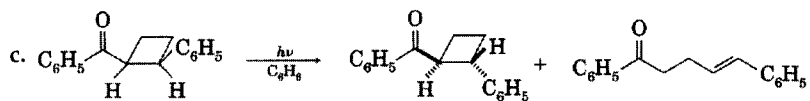
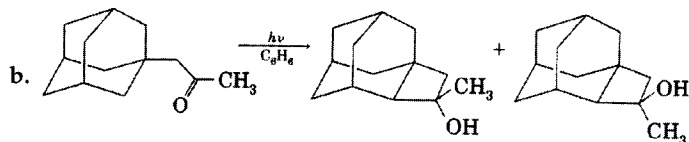
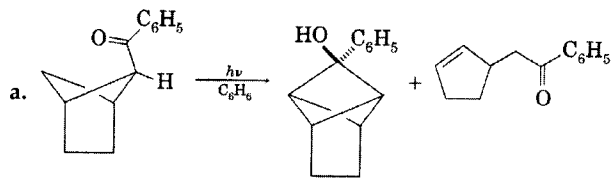


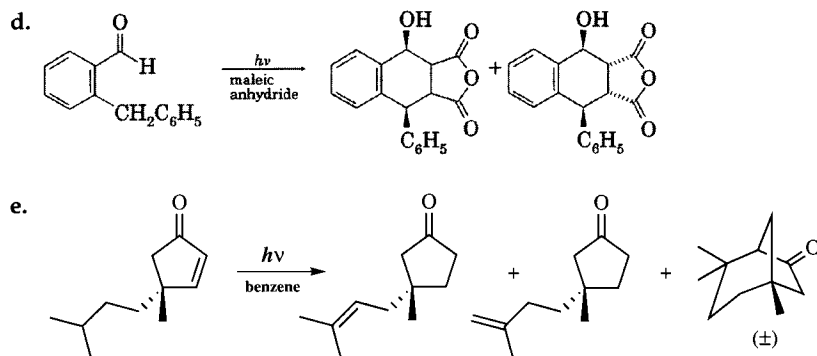
12.19. Propose a mechanism to account for the formation of the indicated product in each of the following photochemical reactions:



12.20. Irradiation of *cis*-2-propyl-4-*tert*-butylcyclohexanone in hexane produces 4-*tert*-butylcyclohexanone, but irradiation of the *trans* isomer results in photoisomerization to the *cis* isomer. Propose a mechanism for the reaction observed for each compound, and explain why the two diastereomers react differently.

12.21. Propose a mechanism for the formation of the products shown in each of the following reactions:

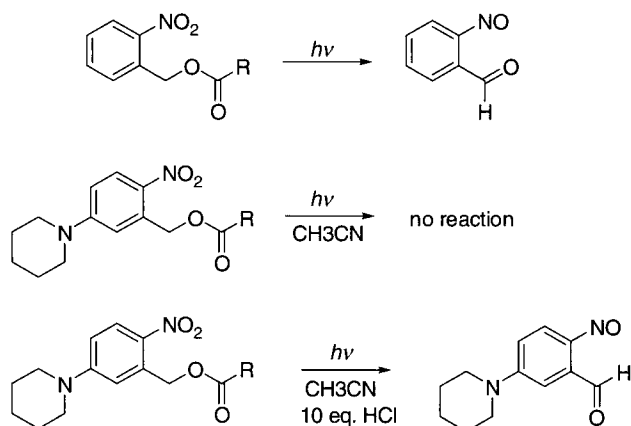




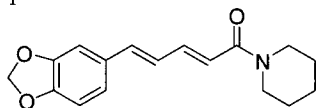
12.22. Irradiation of an equimolar mixture of benzene and 1,1-dimethoxyethene produces a 1:1 photoadduct. When the adduct is dissolved in methanol containing trace amounts of acid, 2,4,6-cyclooctatrienone is formed. Propose a structure for the 1:1 adduct and a mechanism for conversion of the adduct to the cyclooctatrienone.

12.23. The T_1 state (but not the S_1 state) of toluene sensitizes the photoisomerization of both (*E*)- and (*Z*)-2-heptene. Direct irradiation of either isomer of 1-phenyl-2-butene leads to photoisomerization. The fluorescence spectrum of 1-phenyl-2-butene is similar in shape to that of toluene but is slightly reduced in intensity. However, phosphorescence from 1-phenyl-2-butene was not detected under conditions in which phosphorescence from toluene could readily be observed. Propose an explanation for the photoisomerization of 1-phenyl-2-butene upon direct irradiation that is consistent with these observations.

12.24. Rationalize the following experimental observations:



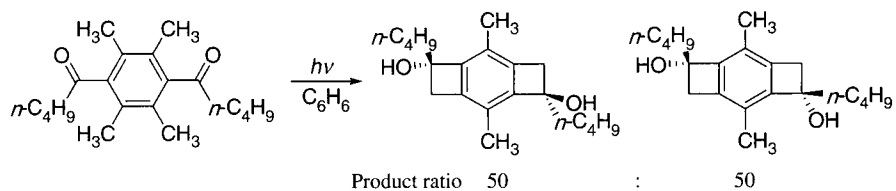
12.25. Piperine (183), reported to be the pungent component of ground black pepper,²⁹⁷ is converted to three other compounds when exposed to white fluorescent light. What are the products?



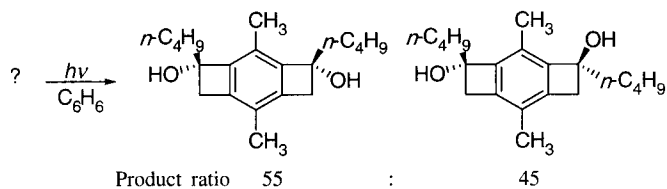
183

²⁹⁷ However, Wood, C.; Siebert, T. E.; Parker, M.; Capone, D. L.; Elsey, G. M.; Pollnitz, A. P.; Eggers, M.; Meier, M.; Vössing, T.; Widder, S.; Krammer, G.; Sefton, M. A.; Herderich, M. J. *J. Agric. Food Chem.* **2008**, *56*, 3738 identified the sesquiterpene rotundone as "the first compound found in white or black peppercorns that has a distinctive peppery aroma."

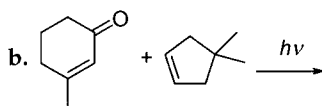
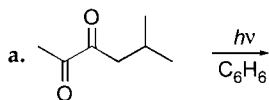
12.26. a. Propose a mechanism for the following reaction:



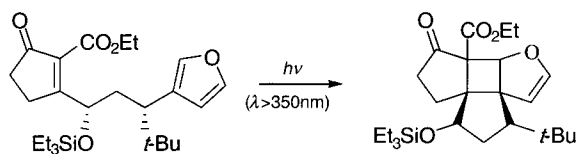
b. What reactant would lead to the following product mixture?



12.27. Predict the product(s) of the following photochemical reactions:



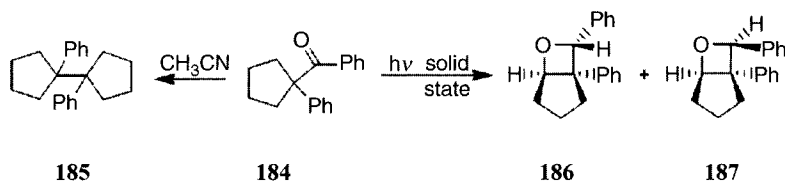
12.28. The structure shown as the product in the following reaction is incomplete. Complete the drawing with bold or hashed wedges to show all of the relevant stereochemical relationships.



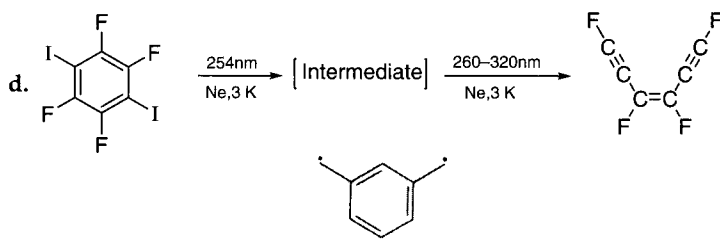
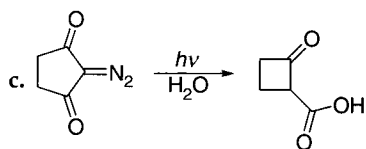
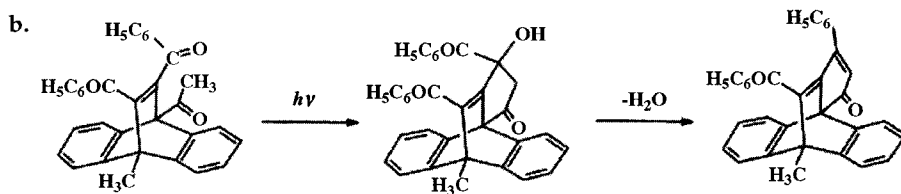
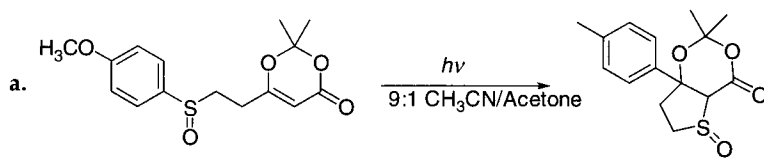
12.29. The ketone **184** forms 1,1'-diphenylbicyclopentyl (**185**) when irradiated in acetonitrile solution, but in the solid state a mixture of diastereomeric oxetanes (**186** and **187**) is formed (Figure 12.58). Explain this difference in reactivity.

FIGURE 12.58

Different photochemical reactions of **184** in solution and in the solid state.



12.30. Propose a mechanism for the following reactions:



References for Selected Problems

Chapter 1

- 1.4 Bondi, J. J. *Phys. Chem.* **1964**, *68*, 441.
- 1.5 Kiyobayashi, T.; Nagano, Y.; Sakiyama, M.; Yamamoto, K.; Cheng, P.-C.; Scott, L. T. *J. Am. Chem. Soc.* **1995**, *117*, 3270.
- 1.6 Turner, R. B.; Goebel, P.; Mallon, B. J.; Doering, W. v. E.; Coburn, J. F., Jr.; Pomerantz, M. *J. Am. Chem. Soc.* **1968**, *90*, 4315.
- 1.7 Pilcher, G.; Parchment, O. G.; Hillier, I. H.; Heatley, F.; Fletcher, D.; Ribeiro da Silva, M. A. V.; Ferrão, M. L. C. C. H.; Monte M. J. S.; Fang, J. *J. Phys. Chem.* **1993**, *97*, 243.
- 1.8 Davis, H. E.; Allinger, N. L.; Rogers, D. W. *J. Org. Chem.* **1985**, *50*, 3601.
- 1.9 a. Roux, M. V.; Temprado, M.; Jiménez, P.; Foces-Foces, C.; Notario, R.; Verevkin, S. P.; Liebman, J. F. *J. Phys. Chem. A* **2006**, *110*, 12477. b. Roux, M. V.; Temprado, M.; Jiménez, P.; Notario, R.; Chickos, J. S.; Santos, A. F. L. O. M.; Ribeiro da Silva, M. A. V. *J. Phys. Chem. A* **2007**, *111*, 11084.
- 1.10 Wiberg, K. B.; Hao, S. *J. Org. Chem.* **1991**, *56*, 5108.
- 1.11 Fang, W.; Rogers, D. W. *J. Org. Chem.* **1992**, *57*, 2294.
- 1.13 Smyth, C. P. in Weissberger, A.; Rossiter, B. W., Eds. *Physical Methods of Chemistry*, Vol. 1, Part 4; Wiley-Interscience: New York, 1972; pp. 397–429.
- 1.16 Mastryukov, V. S.; Schaefer, H. F. II; Boggs, J. E. *Acc. Chem. Res.* **1994**, *27*, 242.
- 1.17 Maksić, Z. B.; Randić, M. *J. Am. Chem. Soc.* **1970**, *92*, 424.
- 1.20 a. Newton, M. D.; Schulman, J. M.; Manus, M. M. *J. Am. Chem. Soc.* **1974**, *96*, 17; b. Muller, N.; Pritchard, D. E. *J. Chem. Phys.* **1959**, *31*, 1471.
- 1.24 Kass S. R.; Chou, P. K. *J. Am. Chem. Soc.* **1988**, *110*, 7899.

Chapter 2

- 2.2 Ramanathan, S.; Lemal, D. M. *J. Org. Chem.* **2007**, *72*, 1566.
- 2.4 j. Moore, W. R.; Anderson, H. W.; Clark, S. D.; Ozretich, T. M. *J. Am. Chem. Soc.* **1971**, *93*, 4932. k. Gerlach, H. *Helv. Chim. Acta* **1966**, *49*, 1291. l. Newman, P.; Rutkin, P.; Mislow, K. *J. Am. Chem. Soc.* **1958**, *80*, 465.
- 2.5 a. Jossang, J.; Bel-Kassaoui, H.; Jossang, A.; Seuleiman, M.; Nel, A. *J. Org. Chem.* **2008**, *73*, 412. b. Paterson, I.; Britton, R.; Delgado, O.; Wright, A. E. *Chem. Commun.* **2004**, 632. c. Chittiboyina, A. G.; Kumar, G. M.; Carvalho, P. B.; Liu, Y.; Zhou, Y.-D.; Nagle, D. G.; Avery, M. A. *J. Med. Chem.* **2007**, *50*, 6299. d. Tsuda,

- M.; Oguchi, K.; Iwamoto, R.; Okamoto, Y.; Fukushi, E.; Kawabata, J.; Ozawa, T.; Masuda, A. *J. Nat. Prod.* **2007**, *70*, 1661. e. Brimble, M. A.; Bryant, C. J. *Org. Biomol. Chem.* **2007**, *5*, 2858. f. That, Q. T.; Jossang, J.; Jossang, A.; Kim, P. P. N.; Jaureguiberry, G. *J. Org. Chem.* **2007**, *72*, 7102. g. Burks, E. A.; Johnson, W. H., Jr.; Whitman, C. P. *J. Am. Chem. Soc.* **1998**, *120*, 7665. h. McGrath, M. J.; Fletcher, M. T.; König, W. A.; Moore, C. J.; Cribb, B. W.; Allsopp, P. G.; Kitching, W. *J. Org. Chem.* **2003**, *68*, 3739. i. Stephens, P. J.; Pan, J. J.; Devlin, F. J.; Krohn, K.; Kurtán, T. *J. Org. Chem.* **2007**, *72*, 3521. j. McCann, D. M.; Stephens, P. J. *J. Org. Chem.* **2006**, *71*, 6074; k. McCann, D. M.; Stephens, P. J. *J. Org. Chem.* **2006**, *71*, 6074; l. Senanayake, C. H.; Krishnamurthy, D.; Lu, Z.-H.; Han, Z.; Gallou, I. *Aldrichchimica Acta* **2005**, *38*, 93. m. Mennucci, B.; Claps, M.; Evidente, A.; Rosini, C. *J. Org. Chem.* **2007**, *72*, 6680. n. Kuppens, T.; Vandyck, K.; Van der Eycken, J.; Herrebout, W.; van der Veken, B. J.; Bultinck, P. *J. Org. Chem.* **2005**, *70*, 9103. o. Chan, J. Y. C.; Hough, L.; Richardson, A. C. *J. Chem. Soc. Perkin Trans. 1* **1985**, 1457. p. Reddy, J. S.; Rao, B. V. *J. Org. Chem.* **2007**, *72*, 2224. q. Bonazzi, S.; Güttinger, S.; Zemp, I.; Kutay, U.; Gademann, K. *Angew. Chem. Int. Ed.* **2007**, *46*, 8707. r. Rudchenko, V. F.; Dyachenko, O. A.; Zolotoi, A. B.; Atovmyan, L. O.; Chervin, I. I.; Kostyanovsky, R. G. *Tetrahedron* **1982**, *38*, 961. s. Widjaja, T.; Fitjer, L.; Pal, A.; Schmidt, H.-G.; Noltemeyer, M.; Diedrich, C.; Grimme, S. *J. Org. Chem.* **2007**, *72*, 9264. t. Widjaja, T.; Fitjer, L.; Pal, A.; Schmidt, H.-G.; Noltemeyer, M.; Diedrich, C.; Grimme, S. *J. Org. Chem.* **2007**, *72*, 9264.
- 2.6 a. Bringmann, G.; Heubes, M.; Breuning, M.; Göbel, L.; Ochse, M.; Schöner, B.; Schupp, O. *J. Org. Chem.* **2000**, *65*, 722. b. Goel, A.; Singh, F. V.; Kumar, V.; Reichert, M.; Gulder, T. A. M.; Bringmann, G. *J. Org. Chem.* **2007**, *72*, 7765.
- 2.8 a. Yang, H.; Liebeskind, L. S. *Org. Lett.* **2007**, *9*, 2993. b. Hayashi, S.; Hirano, K.; Yorimitsu, H.; Oshima, K. *Org. Lett.* **2005**, *7*, 3577.
- 2.9 Seebach, D.; Lapierre, J.-M.; Skobridis K.; Greiveldinger, G. *Angew. Chem. Int. Ed. Engl.* **1994**, *33*, 440.
- 2.11 Dandapani, S.; Jeske, M.; Curran, D. P. *J. Org. Chem.* **2005**, *70*, 9447.
- 2.12 a. Cywin, C. L.; Webster, F. X.; Kallmerten, J. *J. Org. Chem.* **1991**, *56*, 2953. b. Ingold, K. U. *Aldrichimica Acta* **1989**, *22*, 69. c. Rychnovsky, S. D.; Griesgraber, G.; Zeller, S.; Skalitzky, D. J. *J. Org. Chem.* **1991**, *56*, 5161. d. Cianciosi, S. J.; Rangunathan, N.; Freedman, T. B.; Nafie, L. A.; Baldwin, J. E. *J. Am. Chem. Soc.* **1990**, *112*, 8204. g. Bharucha, K. N.; Marsh, R. M.; Minto, R. E.; Bergman, R. G. *J. Am. Chem. Soc.* **1992**, *114*, 3120. h. Naoshima, Y.; Munakata, Y.; Yoshida, S.; Funai, A. *J. Chem. Soc. Perkin Trans. 1* **1991**, 549. i. Walborsky, H. M.; Goedken, V. L.; Gawronski, J. K. *J. Org. Chem.* **1992**, *57*, 410. j. Rawson, D.; Meyers, A. I. *J. Chem. Soc. Chem. Commun.* **1992**, 494. k. Freedman, T. B.; Cianciosi, S. J.; Rangunathan, N.; Baldwin, J. E.; Nafie, L. A. *J. Am. Chem. Soc.* **1991**, *113*, 8298. l. Liu, C.; Coward, J. K. *J. Org. Chem.* **1991**, *56*, 2262. m. Glattfeld, J. W. E.; Chittum, J. W. *J. Am. Chem. Soc.* **1933**, *55*, 3663. n. Hammarström, L.-G.; Berg, U.; Liljefors, T. *J. Chem. Res. (S)* **1990**, 152. o. Moorthy, J. N.; Venkatesan, K. *J. Org. Chem.* **1991**, *56*, 6957.
- 2.13 a. Cavagnat, D.; Lespade, L.; Buffeteau, T. *J. Phys. Chem. A* **2007**, *111*, 7014. b. Griesbeck, A. G.; Miara, C.; Neudörfl, J. *ARKIVOC* **2007** (viii), 216. c. Gao, X.; Lin, C.-J.; Jia, Z.-J. *J. Nat. Prod.* **2007**, *70*, 830. d. Zhou, J.; Zhu, Y.; Burgess, K. *Org. Lett.* **2007**, *9*, 1391. e. Kang, B.; Britton, R. *Org. Lett.* **2007**, *9*, 5083. f. Otomaru, Y.; Tokunaga, N.; Shintani, R.; Hayashi, T. *Org. Lett.* **2005**, *7*, 307. g. Vidal-Cros, A.; Gaudry, M.; Marquet, A. *J. Org. Chem.* **1985**, *50*, 3163. h. Burton, G. W.; de la Mare, P. B. D.; Wade, M. J. *J. Chem. Soc. Perkin Trans. 2* **1974**, 591. i. Rudchenko, V.; Dyachenko, O. A.; Zolotoi, A. B.; Atovmyan, L. O.; Chervin, I. I.; Kostyanovsky, R. G. *Tetrahedron* **1982**, *38*, 961. j. Nawrath, T.; Dickshat, J. S.; Müller, R.; Jiang, J.; Cane, D. E.; Schulz, S. *J. Am. Chem. Soc.* **2008**, *130*, 430. k. Cho, E. J.; Lee, D. *Org. Lett.* **2008**, *10*, 257. l. Andersen, K. K.; Colonna, S.; Stirling, C. J. M. *J. Chem. Soc. Chem. Commun.* **1973**, 645. m. Kitching, W.; Lewis, J. A.; Perkins, M. V.; Drew, R.; Moore, C. J.; Schurig, V.; König, W. A.; Francke, W. *J. Org. Chem.* **1989**, *54*, 3893.

- n. Rao, A. V. R.; Gurjar, M. K.; Bose, D. S.; Devi, R. R. *J. Org. Chem.* **1991**, *56*, 1320.
- o. Chattopadhyay, S.; Mamdapur, V. R.; Chadha, M. S. *J. Chem. Res. (M)* **1990**, 1818.
- p. King, S. B.; Ganem, B. *J. Am. Chem. Soc.* **1994**, *116*, 562.
- 2.14 a. Coke, J. L.; Shue, R. S. *J. Org. Chem.* **1973**, *38*, 2210. b. Katsura, T.; Minamii, M. *Jpn. Kokai Tokkyo Hoho JP* 61,176,557. c,d. Floss, H. G.; Lee, S. *Acc. Chem. Res.* **1993**, *26*, 116. e. Walborsky, H. M.; Impastato, F. J.; Young, A. E. *J. Am. Chem. Soc.* **1964**, *86*, 3283. f. Skell, P. S.; Pavlis, R. R.; Lewis, D. C.; Shea, K. J. *J. Am. Chem. Soc.* **1973**, *95*, 6735. g. Wiberg, K. B. *J. Am. Chem. Soc.* **1952**, *74*, 3891. h. Abate, A.; Brenna, E.; Fuganti, C.; Gatti, F. G.; Giovenzana, T.; Malpezzi, L.; Serra, S. *J. Org. Chem.* **2005**, *70*, 1281. i. McCoull, W.; Davis, F. A. *Synthesis* **2000**, 1347.
- 2.15 Blakemore, P. R.; Kilner, C.; Milicevic, S. D. *J. Org. Chem.* **2006**, *71*, 8212.
- 2.16 Hanessian, S.; Auzzas, L. *Org. Lett.* **2008**, *10*, 261.
- 2.18 a,b. Blakemore, P. R.; Kilner, C.; Milicevic, S. D. *J. Org. Chem.* **2006**, *71*, 8212. c. Harada, N.; Saito, A.; Koumura, N.; Roe, D. C.; Jager, W. F.; Zijlstra, R. W. J.; de Lange, B.; Feringa, B. L. *J. Am. Chem. Soc.* **1997**, *119*, 7249. d. Stará, I. G.; Alexandrová, Z.; Teplý, F.; Sehnal, P.; Starý, I.; Šaman, D.; Buděšinský, M.; Cvačka, J. *Org. Lett.* **2005**, *7*, 2547. e. Cipiciani, A.; Fringuelli, F.; Mancini, V.; Piermatti, O.; Pizzo, F.; Ruzziconi, R. *J. Org. Chem.* **1997**, *62*, 3744. f,g. Baldwin, J. E.; Villarica, K. A. *J. Org. Chem.* **1995**, *60*, 186. h. Abbate, S.; Castiglioni, E.; Gangemi, F.; Gangemi, R.; Longhi, G.; Ruzziconi, R.; Spizzichino, S. *J. Phys. Chem. A* **2007**, *111*, 7031.
- 2.19 a. Eaton, P. E.; Leipzig, B. *J. Org. Chem.* **1978**, *43*, 2483. b. Halterman, R. L.; Jan, S.-T. *J. Org. Chem.* **1991**, *56*, 5253. c. Deprés, J.-P.; Morat, C. *J. Chem. Educ.* **1992**, *69*, A232. d. Wang, Y.; Stretton, A. D.; McConnell, M. C.; Wood, P. A.; Parsons, S.; Henry, J. B.; Mount, A. R.; Galow, T. H. *J. Am. Chem. Soc.* **2007**, *129*, 13193. e. Wang, Y.; Stretton, A. D.; McConnell, M. C.; Wood, P. A.; Parsons, S.; Henry, J. B.; Mount, A. R.; Galow, T. H. *J. Am. Chem. Soc.* **2007**, *129*, 13193. f. Lélias-Vanderperre, A.; Chambron, J.-C.; Espinosa, E.; Terrier, P.; Leize-Wagner, E. *Org. Lett.* **2007**, *9*, 2961.
- 2.20 Hoye, T. R.; Hanson, P. R.; Kovelesky, A. C.; Ocain, T. D.; Zhuang, Z. *J. Am. Chem. Soc.* **1991**, *113*, 9369.
- 2.21 Polniaszek, R. P.; Dillard, L. W. *Abstracts of the 203rd National Meeting of the American Chemical Society*, San Francisco, CA, April 5–10, 1992, Abstract ORGN 494.
- 2.22 Reynolds, K. A.; Fox, K. M.; Yuan, Z. M.; Lam, Y. *J. Am. Chem. Soc.* **1991**, *113*, 4339.
- 2.23 Reynolds, K. A.; Fox, K. M.; Yuan, Z.; Lam, Y. *J. Am. Chem. Soc.* **1991**, *113*, 4339.
- 2.24 Jennings, W. B. *Chem. Rev.* **1975**, *75*, 307.
- 2.27 Whitesides, G. M.; Kaplan, F.; Roberts, J. D. *J. Am. Chem. Soc.* **1963**, *85*, 2167.
- 2.29 Streitwieser, A., Jr.; Granger, M. R. *J. Org. Chem.* **1967**, *32*, 1528.
- 2.30 Hilvert, D.; Nared, K. D. *J. Am. Chem. Soc.* **1988**, *110*, 5593.
- 2.31 Xu, Z.-X.; Zhang, C.; Zheng, Q.-Y.; Chen, C.-F.; Huang, Z.-T. *Org. Lett.* **2007**, *9*, 4447.
- 2.32 LeGoff, E.; Ulrich, S. E.; Denney, D. B. *J. Am. Chem. Soc.* **1958**, *80*, 622.
- 2.33 Miyamoto, K.; Tsuchiya, S.; Ohta, H. *J. Am. Chem. Soc.* **1992**, *114*, 6256.
- 2.34 Cinquini, M.; Cozzi, F.; Sannicolò, F.; Sironi, A. *J. Am. Chem. Soc.* **1988**, *110*, 4363.
- 2.35 Jenkins, A. D. *Pure Appl. Chem.* **1981**, *53*, 733.
- 2.36 Roche, A. J.; Duan, J.-X.; Dolbier, W. R., Jr.; Abboud, K. A. *J. Org. Chem.* **2001**, *66*, 7055.

Chapter 3

- 3.1 Ōsawa, E.; Gotō, H.; Oishi, T.; Ohtsuka, Y.; Chuman, T. *Pure Appl. Chem.* **1989**, *61*, 597.

- 3.2 Allinger, N. L.; Miller, M. A. *J. Am. Chem. Soc.* **1961**, *83*, 2145; Beckett, C. W.; Pitzer, K. S.; Spitzer, R. *J. Am. Chem. Soc.* **1947**, *69*, 2488.
- 3.3 Eliel, E. L.; Allinger, N. L.; Angyal, S. J.; Morrison, G. A. *Conformational Analysis*, Wiley-Interscience: New York, 1965.
- 3.4 Booth, H.; Everett, J. R. *J. Chem. Soc. Perkin Trans. 2* **1980**, 255.
- 3.5 Juaristi, E.; Labastida, V.; Antúnez, S. *J. Org. Chem.* **1991**, *56*, 4802.
- 3.6 b. Perrin, C. L.; Fabian, M. A. *Abstracts of the 209th National Meeting of the American Chemical Society*, Anaheim, CA, April 2–6, 1995, Abstract ORGN 6. c. Jensen, F. R.; Bushweller, C. H.; Beck, B. H. *J. Am. Chem. Soc.* **1969**, *91*, 344.
- 3.7 Chupp, J. P.; Olin, J. F. *J. Org. Chem.* **1967**, *32*, 2297.
- 3.8 Huang, J.; Hedberg, K. *J. Am. Chem. Soc.* **1989**, *111*, 6909.
- 3.11 Maier, G. *Angew. Chem. Int. Ed. Engl.* **1988**, *27*, 309.
- 3.12 Turner, R. B.; Nettleton, D. E., Jr.; Perelman, M. *J. Am. Chem. Soc.* **1958**, *80*, 1430; Brown, H. C.; Berneis, H. L. *J. Am. Chem. Soc.* **1953**, *75*, 10; Saunders, W. H., Jr.; Cockerill, A. F. *Mechanisms of Elimination Reactions*; Wiley-Interscience: New York, 1973; p. 173.
- 3.13 Golan, O.; Goren, Z.; Biali, S. E. *J. Am. Chem. Soc.* **1990**, *112*, 9300; Juaristi, E.; Labastida, V.; Antúnez, S. *J. Org. Chem.* **1991**, *56*, 4802.
- 3.14 Casarini, D.; Coluccini, C.; Lunazzi, L.; Mazzanti, A. *J. Org. Chem.* **2005**, *70*, 5098.
- 3.15 Barton, D. H. R.; Cookson, R. C. Q. *Rev. Chem. Soc.* **1956**, *10*, 44; Johnson, W. S. *J. Am. Chem. Soc.* **1953**, *75*, 1498.
- 3.16 Barton, D. H. R.; Cookson, R. C. Q. *Rev. Chem. Soc.* **1956**, *10*, 44; Johnson, W. S. *J. Am. Chem. Soc.* **1953**, *75*, 1498.
- 3.17 Jensen, F. R.; Bushweller, C. H.; Beck, B. H. *J. Am. Chem. Soc.* **1969**, *91*, 344.
- 3.18 Jensen, F. R.; Bushweller, C. H.; Beck, B. H. *J. Am. Chem. Soc.* **1969**, *91*, 344.
- 3.19 Booth, H.; Everett, J. R. *J. Chem. Soc. Perkin Trans. 2* **1980**, 255.
- 3.20 Eliel, E. L.; Manoharan, M. *J. Org. Chem.* **1981**, *46*, 1959.
- 3.21 Juaristi, E.; Labastida, V.; Antúnez, S. *J. Org. Chem.* **2000**, *65*, 969.
- 3.24 Kuhn, L. P. *J. Am. Chem. Soc.* **1958**, *80*, 5950.
- 3.29 Wang, F.; Polavarapu, P. L. *J. Phys. Chem. A* **2000**, *104*, 6189.
- 3.30 Jaime, C.; Ōsawa, E.; Takeuchi, Y.; Camps, P. *J. Org. Chem.* **1983**, *48*, 4514.

Chapter 4

- 4.7 Fenet-Buchholz, J.; Boese, R.; Haumann, T.; Traetteberg, M. in Rappoport, Z., Ed. *The Chemistry of Dienes and Polyenes*, Vol. 1: John Wiley & Sons: New York, 1997, p. 25.
- 4.12 Staley, S. W.; Norden, T. D.; Taylor, W. H.; Harmony, M. D. *J. Am. Chem. Soc.* **1987**, *109*, 7641.
- 4.15 Schleyer, P. v. R. *J. Am. Chem. Soc.* **1985**, *107*, 4793.
- 4.16 Sancho-García, J. C.; Pérez-Jiménez, A. J. *J. Phys. B: At. Mol. Opt. Phys.* **2002**, *35*, 1509.
- 4.17 Binsch, G. *Top. Stereochem.* **1968**, *3*, 97.
- 4.23 a. Gutman, I.; Cyvin, S. J. *Introduction to the Theory of Benzenoid Hydrocarbons*; Springer-Verlag: Berlin, 1989. b. Gutman, I.; Gojak, S.; Furtula, B.; Radenković, S.; Vodopivec, A. *Monatsh. Chem.* **2006**, *137*, 1127.
- 4.25 Baird, N. C. *J. Chem. Educ.* **1971**, *48*, 509.
- 4.26 Iyoda, M.; Kurata, H.; Oda, M.; Okubo, C.; Nishimoto, K. *Angew. Chem. Int. Ed. Engl.* **1993**, *32*, 89.
- 4.27 Baird, N. C. *J. Chem. Educ.* **1971**, *48*, 509.

- 4.29 Allinger, N. L.; Siefert, J. H. *J. Am. Chem. Soc.* **1975**, *97*, 752.
4.30 Kitagawa, T.; Takeuchi, K. *J. Phys. Org. Chem.* **1998**, *11*, 157.
4.31 Gutman, I.; Cyvin, S. J. *Introduction to the Theory of Benzenoid Hydrocarbons*; Springer-Verlag: Berlin, 1989.

Chapter 5

- 5.1 Wentrup, C. *Reactive Molecules*; John Wiley & Sons: New York, 1984.
5.2 Ayscough, P. B. *Electron Spin Resonance in Chemistry*; Methuen & Co.: London, 1967, p. 298; Bunce, N. J. *J. Chem. Educ.* **1987**, *64*, 907.
5.3 Olah, G. A. *Carbocations and Electrophilic Reactions*; John Wiley & Sons: New York, 1974.
5.4 Olah, G. A. *Carbocations and Electrophilic Reactions*; John Wiley & Sons: New York, 1974; Olah, G. A.; White, A. M. *J. Am. Chem. Soc.* **1967**, *89*, 3591.
5.5 Olah, G. A.; Mateescu, G. D.; Wilson, L. A.; Gross, M. H. *J. Am. Chem. Soc.* **1970**, *92*, 7231.
5.6 Olah, G. A.; Prakash, G. K. S.; Williams, R. E.; Field, L. D.; Wade, K. *Hypercarbon Chemistry*; John Wiley & Sons: New York, 1987.
5.7 Olah, G. A.; Prakash, G. K. S.; Sommer, J. *Superacids*; Wiley-Interscience: New York, 1985.
5.8 Walborsky, H. M.; Periasamy, M. P. *J. Am. Chem. Soc.* **1974**, *96*, 3711.
5.9 Zimmerman, H. E.; Zweig, A. *J. Am. Chem. Soc.* **1961**, *83*, 1196
5.10 Agapito, F.; Nunes, P. M.; Costa Cabral, B. J.; Borges dos Santos, R. M.; Martinho Simões, J. A. *J. Org. Chem.* **2007**, *72*, 8770.
5.11 Fitjter, L.; Quabeck, U. *Angew. Chem. Int. Ed. Engl.* **1987**, *26*, 1023.
5.12 Oldroyd, D. M.; Fisher, G. S.; Goldblatt, L. A. *J. Am. Chem. Soc.* **1950**, *72*, 2407.
5.13 Moss, R. A.; Jones, M., Jr. in Jones, M., Jr.; Moss, R. A., Eds. *Reactive Intermediates*, Vol. 1; Wiley-Interscience: New York, 1978; pp. 67–116.
5.14 Perkins, M. J. *Adv. Phys. Org. Chem.* **1980**, *17*, 1.
5.15 Friedman, L.; Shechter, H. *J. Am. Chem. Soc.* **1960**, *82*, 1002.
5.16 Friedman, L.; Shechter, H. *J. Am. Chem. Soc.* **1961**, *83*, 3159.
5.17 Jones, R. R.; Bergman, R. G. *J. Am. Chem. Soc.* **1972**, *94*, 660.
5.18 Alabugin, I. V.; Manoharan, M. *J. Am. Chem. Soc.* **2005**, *127*, 9534; Liu, F.; Liu, K.; Yuan, X.; Li, C. *J. Org. Chem.* **2007**, *72*, 10231.
5.19 Mile, B. *Curr. Org. Chem.* **2000**, *4*, 55.
5.20 Nicolaidis, A.; Matushita, T.; Tomioka, H. *J. Org. Chem.* **1999**, *64*, 3299.
5.22 Clive, D. L. J.; Sunasee, R. *Org. Lett.* **2007**, *9*, 2677.
5.23 Coote, M. L.; Pross, A.; Radom, L. *Org. Lett.* **2003**, *5*, 4689.
5.24 Olah, G. A. *J. Org. Chem.* **2001**, *66*, 5943.
5.25 Prakash, G. K. S. *J. Org. Chem.* **2006**, *71*, 3661.
5.26 Schleyer, P. v. R.; Lam, L. K. M.; Raber, D. J.; Fry, J. L.; McKerverey, M. A.; Alford, J. R.; Cuddy, B. D.; Keizer, V. G.; Geluk, H. W.; Schlatmann, J. L. M. A. *J. Am. Chem. Soc.* **1970**, *92*, 5246.
5.28 Lossing, F. P.; Holmes, J. L. *J. Am. Chem. Soc.* **1984**, *106*, 6917.
5.29 Chandrasekhar, J.; Schleyer, P. v. R. *Tetrahedron Lett.* **1979**, 4057.
5.30 Brinker, U. H.; Weber, J. *Angew. Chem. Int. Ed. Engl.* **1997**, *36*, 1623.
5.31 Nickon, A.; Lambert, J. L. *J. Am. Chem. Soc.* **1962**, *84*, 4604.
5.32 Yoshimitsu, T.; Arano, Y.; Nagaoka, H. *J. Am. Chem. Soc.* **2005**, *127*, 11610.

Chapter 6

- 6.1 Murray, R. W. *Acc. Chem. Res.* **1968**, *1*, 313.
- 6.2 Nash, L. M.; Taylor, T. I.; Doering, W. v. E. *J. Am. Chem. Soc.* **1949**, *71*, 1516.
- 6.3 Long, F. A.; Pritchard, J. G. *J. Am. Chem. Soc.* **1956**, *78*, 2663.
- 6.8 Bartlett, P. D.; Trachtenberg, E. N. *J. Am. Chem. Soc.* **1958**, *80*, 5808.
- 6.9 Frost, A. A.; Pearson, R. G. *Kinetics and Mechanism*, 2nd ed.; John Wiley & Sons: New York, 1961.
- 6.10 Nakazawa, J.; Sakae, Y.; Aida, M.; Naruta, Y. *J. Org. Chem.* **2007**, *72*, 9448.
- 6.11 Hawkinson, D. C.; Wang, Y. *J. Org. Chem.* **2007**, *72*, 3592.
- 6.12 Harada, N.; Saito, A.; Koumura, N.; Roe, D. C.; Jager, W. F.; Zijlstra, R. W. J.; de Lange, B.; Feringa, B. L. *J. Am. Chem. Soc.* **1997**, *119*, 7249.
- 6.13 LeFevre, G. N.; Crawford, R. J. *J. Org. Chem.* **1986**, *51*, 747.
- 6.14 Kluger, R.; Brandl, M. *J. Org. Chem.* **1986**, *51*, 3964.
- 6.15 Bartlett, P. D.; Wu, C. *J. Org. Chem.* **1985**, *50*, 4087.
- 6.16 Jones, J. M.; Bender, M. L. *J. Am. Chem. Soc.* **1960**, *82*, 6322.
- 6.17 Pocker, Y. *Proc. Chem. Soc.* **1960**, 17.
- 6.18 Choe, J.-I.; Srinivasan, M.; Kuczkowski, R. L. *J. Am. Chem. Soc.* **1983**, *105*, 4703.
- 6.21 Overman, L. E.; Petty, S. T. *J. Org. Chem.* **1975**, *40*, 2779.
- 6.22 Dietze, P. E.; Underwood, G. R. *J. Org. Chem.* **1984**, *49*, 2492.
- 6.23 Whitworth, A. J.; Ayoub, R.; Rousseau, Y.; Fliszár, S. *J. Am. Chem. Soc.* **1969**, *91*, 7128.
- 6.24 Hill, R. K.; Conley, R. T.; Chortyk, O. T. *J. Am. Chem. Soc.* **1965**, *87*, 5646.
- 6.25 Maclin, K. M.; Richey, H. G., Jr. *J. Org. Chem.* **2002**, *67*, 4370.
- 6.26 Kim, S. S.; Choi, W. J.; Zhu, Y.; Kim, J. H. *J. Org. Chem.* **1998**, *63*, 1185.
- 6.27 Romero, F. A.; Hwang, I.; Boger, D. L. *J. Am. Chem. Soc.* **2006**, *128*, 14004.
- 6.28 Reddy, S. R.; Manikyamba, P. *J. Chem. Sci.* **2006**, *118*, 257.

Chapter 7

- 7.1 Barlin, G. B.; Perrin, D. D. *Q. Rev. Chem. Soc.* **1966**, *20*, 75.
- 7.2 Taft, R. W.; Bordwell, F. G. *Acc. Chem. Res.* **1988**, *21*, 463.
- 7.4 Wheeler, O. H. *J. Am. Chem. Soc.* **1957**, *79*, 4191.
- 7.6 Wiseman, J. S.; Abeles, R. H. *Biochemistry* **1979**, *18*, 427.
- 7.7 Cardwell, H. M. E.; Kilner, A. E. H. *J. Chem. Soc.* **1951**, 2430.
- 7.8 Levine, R.; Hauser, C. R. *J. Am. Chem. Soc.* **1944**, *66*, 1768.
- 7.9 Gutsche, C. D.; Redmore, D.; Buriks, R. S.; Nowotny, K.; Grassner, H.; Armbruster, C. W. *J. Am. Chem. Soc.* **1967**, *89*, 1235.
- 7.10 Smith, W. T.; McLeod, G. L. *Org. Syn. Coll. Vol. IV* **1963**, 345.
- 7.11 Stefanidis, D.; Cho, S.; Dhe-Paganon, S.; Jencks, W. P. *J. Am. Chem. Soc.* **1993**, *115*, 1650.
- 7.12 Sørensen, P. E.; Jencks, W. P. *J. Am. Chem. Soc.* **1987**, *109*, 4675.
- 7.13 Bell, R. P.; Baughan, E. C. *J. Chem. Soc.* **1937**, 1947.
- 7.14 Hurd, C. D.; Saunders, W. H., Jr. *J. Am. Chem. Soc.* **1952**, *74*, 5324.
- 7.15 Drumheller, J. D.; Andrews, L. J. *J. Am. Chem. Soc.* **1955**, *77*, 3290.
- 7.16 Bender, M. L.; Chen, M. C. *J. Am. Chem. Soc.* **1963**, *85*, 30, 37
- 7.17 Reimann, J. E.; Jencks, W. P. *J. Am. Chem. Soc.* **1966**, *88*, 3973.
- 7.18 Olson, A. R.; Youle, P. V. *J. Am. Chem. Soc.* **1951**, *73*, 2468.
- 7.19 Hoz, S.; Livneh, M.; Cohen, D. *J. Org. Chem.* **1986**, *51*, 4537.
- 7.20 Zaugg, H. E.; Papendick, V.; Michaels, R. J. *J. Am. Chem. Soc.* **1964**, *86*, 1399.

- 7.21 Hauser, C. R.; Adams, J. T. *J. Am. Chem. Soc.* **1944**, *66*, 345.
- 7.22 a. Long, F. A.; Pritchard, J. G. *J. Am. Chem. Soc.* **1956**, *78*, 2663. b. Pritchard, J. G.; Long, F. A. *J. Am. Chem. Soc.* **1956**, *78*, 2667.
- 7.23 Chang, J. A.; Chiang, Y.; Keeffe, J. R.; Kresge, A. J.; Nikolaev, V. A.; Popik, V. V. *J. Org. Chem.* **2006**, *71*, 4460.
- 7.25 García, B.; Hoyuelos, F. J.; Ibeas, S.; Leal, J. M. *J. Org. Chem.* **2006**, *71*, 3718.
- 7.26 Harrison, A. G.; Houriet, R.; Tidwell, T. T. *J. Org. Chem.* **1984**, *49*, 1302.
- 7.27 McIntyre, D.; Long, F. A. *J. Am. Chem. Soc.* **1954**, *76*, 3240.
- 7.28 Chen, X.; Walthall, D. A.; Brauman, J. I. *J. Am. Chem. Soc.* **2004**, *126*, 12614.
- 7.29 Gattin, Z.; Kovačević, B.; Maksić, Z. B. *Eur. J. Org. Chem.* **2005**, 3206.
- 7.30 Bartlett, P. D.; Woods, G. F. *J. Am. Chem. Soc.* **1940**, *62*, 2933.

Chapter 8

- 8.1 Ingold, C. K. *Structure and Mechanism in Organic Chemistry*, 2nd ed.; Cornell University Press: Ithaca, NY, 1969.
- 8.3 Magid, R. M.; Welch, J. G. *J. Am. Chem. Soc.* **1968**, *90*, 5211.
- 8.4 Smith, M. B.; Hrubiec, R. T.; Zezza, C. A. *J. Org. Chem.* **1985**, *50*, 4815.
- 8.5 Winstein, S.; Lucas, H. J. *J. Am. Chem. Soc.* **1939**, *61*, 1576.
- 8.6 McKenzie, A.; Clough, G. W. *J. Chem. Soc.* **1910**, 97, 2564.
- 8.7 Brown, R. F.; van Gulick, N. M. *J. Org. Chem.* **1956**, *21*, 1046.
- 8.8 Cram, D. J. *J. Am. Chem. Soc.* **1949**, *71*, 3863; Cram, D. J.; Davis, R. J. *J. Am. Chem. Soc.* **1949**, *71*, 3875.
- 8.10 Winstein, S.; Lucas, H. J. *J. Am. Chem. Soc.* **1939**, *61*, 1581.
- 8.11 Chapman, J. W.; Strachan, A. N. *Chem. Commun.* **1974**, 293.
- 8.12 Masci, B. *J. Org. Chem.* **1985**, *50*, 4081.
- 8.13 Brown, H. C.; Jensen, F. R. *J. Am. Chem. Soc.* **1958**, *80*, 2296.
- 8.14 Himeshima, Y.; Kobayashi, H.; Sonoda, T. *J. Am. Chem. Soc.* **1985**, *107*, 5286.
- 8.15 Grovenstein, E., Jr.; Kilby, D. C. *J. Am. Chem. Soc.* **1957**, *79*, 2972.
- 8.16 Truce, W. E.; Kreider, E. M.; Brand, W. W. *Org. React.* **1970**, *18*, 99.
- 8.17 Samuel, D. *J. Chem. Soc.* **1960**, 1318; Rosenblum, M. *J. Am. Chem. Soc.* **1960**, *82*, 3796.
- 8.18 Roberts, J. D.; Semenow, D. A.; Simmons, H. E., Jr.; Carlsmith, L. A. *J. Am. Chem. Soc.* **1956**, *78*, 601.
- 8.20 Katritzky, A. R.; Laurenzo, K. S. *J. Org. Chem.* **1986**, *51*, 5039.
- 8.21 Bunnett, J. F.; Garbisch, E. W., Jr.; Pruitt, K. M. *J. Am. Chem. Soc.* **1957**, *79*, 385.
- 8.22 Roberts, J. D.; Vaughan, C. W.; Carlsmith, L. A.; Semenow, D. A. *J. Am. Chem. Soc.* **1956**, *78*, 611.
- 8.23 Roberts, J. D.; Semenow, D. A.; Simmons, H. E., Jr.; Carlsmith, L. A. *J. Am. Chem. Soc.* **1956**, *78*, 601.
- 8.24 Makosza, M.; Winiarski, J. *J. Org. Chem.* **1984**, *49*, 1494; Makosza, M.; Ludwiczak, S. *J. Org. Chem.* **1984**, *49*, 4562; Makosza, M.; Winiarski, J. *Acc. Chem. Res.* **1987**, *20*, 282.
- 8.25 Malnar, I.; Jurić, S.; Vrček, V.; Gjuranović, Ž.; Mihalić, Z.; Kronja, O. *J. Org. Chem.* **2002**, *67*, 1490.
- 8.26 Zubkov, F. I.; Nikitina, E. V.; Kouznetsov, V. V.; Duarte, L. D. A. *Eur. J. Org. Chem.* **2004**, 5064.
- 8.27 Lovchik, M. A.; Goeke, A.; Fráter, G. *J. Org. Chem.* **2007**, *72*, 2427.

- 8.28 Pan, J.; Kampf, J. W.; Ashe, A. J. III. *Org. Lett.* **2007**, *9*, 679.
8.29 Sakamoto, Y.; Tamegai, K.; Nakata, T. *Org. Lett.* **2002**, *4*, 675.
8.30 Santiago, A. N.; Morris, D. G.; Rossi, R. A. J. *Chem. Soc. Chem. Commun.* **1988**, 220.
8.31 Galli, C.; Bunnett, J. F. *J. Am. Chem. Soc.* **1979**, *101*, 6137.

Chapter 9

- 9.1 Buckles, R. E.; Bader, J. M.; Thurmaier, R. J. *J. Org. Chem.* **1962**, *27*, 4523.
9.2 Buckles, R. E.; Forrester, J. L.; Burham, R. L.; McGee, T. W. *J. Org. Chem.* **1960**, *25*, 24.
9.3 Bellucci, G.; Bianchini, R.; Chiappe, C. *J. Org. Chem.* **1991**, *56*, 3067.
9.4 Bedoukian, P. Z. *J. Am. Chem. Soc.* **1944**, *66*, 1325.
9.5 Tarbell, D. S.; Bartlett, P. D. *J. Am. Chem. Soc.* **1937**, *59*, 407.
9.6 Rolston, J. H.; Yates, K. *J. Am. Chem. Soc.* **1969**, *91*, 1477.
9.7 van Tamelen, E. E.; Shamma, M. *J. Am. Chem. Soc.* **1954**, *76*, 2315; Butters, M.; Elliott, M. C.; Hill-Cousins, J.; Paine, J. S.; Walker, J. K. E. *Org. Lett.* **2007**, *9*, 3635.
9.8 Peterson, P. E.; Tao, E. V. P. *J. Am. Chem. Soc.* **1964**, *86*, 4503.
9.9 Fraenkel, G.; Bartlett, P. D. *J. Am. Chem. Soc.* **1959**, *81*, 5582.
9.10 Okuyama, T.; Sakagami, T.; Fueno, T. *Tetrahedron* **1973**, *29*, 1503.
9.11 Bellucci, G.; Bianchini, R.; Vecchiani, S. *J. Org. Chem.* **1987**, *52*, 3355.
9.12 Fahey, R. C.; Schneider, H.-J. *J. Am. Chem. Soc.* **1968**, *90*, 4429.
9.13 Rolston, J. H.; Yates, K. *J. Am. Chem. Soc.* **1969**, *91*, 1469.
9.14 Cabaleiro, M. C.; Johnson, M. D. *J. Chem. Soc. B* **1967**, 565.
9.15 Rozen, S.; Brand, M. *J. Org. Chem.* **1986**, *51*, 3607.
9.16 Jacobs, T. L.; Searles, S., Jr. *J. Am. Chem. Soc.* **1944**, *66*, 686.
9.17 Halpern, J.; Tinker, H. B. *J. Am. Chem. Soc.* **1967**, *89*, 6427.
9.18 Kabalka, G. W.; Newton, R. J., Jr.; Jacobus, J. *J. Org. Chem.* **1978**, *43*, 1567.
9.19 a. Brown, H. C.; Geoghegan, P., Jr. *J. Am. Chem. Soc.* **1967**, *89*, 1522. b. Brown, H. C.; Hammar, W. J. *J. Am. Chem. Soc.* **1967**, *89*, 1524.
9.20 Brown, H. C.; Kurek, J. T. *J. Am. Chem. Soc.* **1969**, *91*, 5647.
9.21 Swern, D. *J. Am. Chem. Soc.* **1947**, *69*, 1692.
9.22 Modro, A.; Schmid, G. H.; Yates, K. *J. Org. Chem.* **1977**, *42*, 3673.
9.23 Ruasse, M.-F.; Motallebi, S.; Galland, B. *J. Am. Chem. Soc.* **1991**, *113*, 3440.
9.24 Gedye, R.; Brown, R. S.; Slebocka-Tilk, H.; Buschek, J. M.; Kopecky, K. R. *J. Am. Chem. Soc.* **1984**, *106*, 4515.
9.25 Hirai, T.; Han, L.-B. *Org. Lett.* **2007**, *9*, 53.
9.26 Cui, X.-L.; Brown, R. S. *J. Org. Chem.* **2000**, *65*, 5653.
9.27 Smith, W. B. *J. Org. Chem.* **1998**, *63*, 2661.
9.28 Steinfeld, G.; Lozan, V.; Kersting, B. *Angew. Chem. Int. Ed.* **2003**, *42*, 2261.
9.29 Bach, R. D.; Glukhovtsev, M. N.; Canepa, C. *J. Am. Chem. Soc.* **1998**, *120*, 775.
9.30 Choi, H. Y.; Srisook, E.; Jang, K. S.; Chi, D. Y. *J. Org. Chem.* **2005**, *70*, 1222.

Chapter 10

- 10.1 Dhar, M. L.; Hughes, E. D.; Ingold, C. K.; Mandour, A. M. M.; Maw, G. A.; Woolf, L. I. *J. Chem. Soc.* **1948**, 2093.
10.2 Cristol, S. J.; Hause, N. L. *J. Am. Chem. Soc.* **1952**, *74*, 2193.
10.3 Kibby, C. L.; Lande, S. S.; Hall, W. K. *J. Am. Chem. Soc.* **1972**, *94*, 214.

- 10.4 Searles, S.; Gortatowski, M. J. *J. Am. Chem. Soc.* **1953**, *75*, 3030.
- 10.5 Grovenstein, E., Jr.; Lee, D. E. *J. Am. Chem. Soc.* **1953**, *75*, 2639; Cristol, S. J.; Norris, W. P. *J. Am. Chem. Soc.* **1953**, *75*, 2645.
- 10.6 Ölwegård, M.; Ahlberg, P. *J. Chem. Soc. Chem. Commun.* **1989**, 1279; **1990**, 788.
- 10.7 Kurtz, R. R.; Houser, D. J. *J. Org. Chem.* **1981**, *46*, 202.
- 10.8 Goering, H. L.; Espy, H. H. *J. Am. Chem. Soc.* **1956**, *78*, 1454.
- 10.9 Anh, N. T. *Chem. Commun.* **1968**, 1089.
- 10.10 Cope, A. C.; LeBel, N. A.; Lee, H.-H.; Moore, W. R. *J. Am. Chem. Soc.* **1957**, *79*, 4720.
- 10.11 Gandini, A.; Plesch, P. H. *J. Chem. Soc.* **1965**, 6019.
- 10.12 O'Connor, G. L.; Nace, H. R. *J. Am. Chem. Soc.* **1953**, *75*, 2118.
- 10.13 Knözinger, H. in Patai, S., Ed. *The Chemistry of the Hydroxyl Group*, Part 2; Wiley-Interscience: London, 1971.
- 10.14 Acharya, S. P.; Brown, H. C. *Chem. Commun.* **1968**, 305.
- 10.15 Barton, D. H. R.; Rosenfelder, W. J. *J. Chem. Soc.* **1951**, 1048.
- 10.16 Kashelkar, D. V.; Fanta, P. E. *J. Am. Chem. Soc.* **1960**, *82*, 4930.
- 10.17 Noyce, D. S.; Weingarten, H. I. *J. Am. Chem. Soc.* **1957**, *79*, 3093.
- 10.18 a. Alexander, E. R.; Mudrak, A. *J. Am. Chem. Soc.* **1950**, *72*, 1810. b. Alexander, E. R.; Mudrak, A. *J. Am. Chem. Soc.* **1950**, *72*, 3194. c. Cope, A. C.; LeBel, N. A. *J. Am. Chem. Soc.* **1960**, *82*, 4656.
- 10.19 Kende, A. S. *Org. React.* **1960**, *11*, 261.
- 10.20 Curtin, D. Y.; Stolow, R. D.; Maya, W. *J. Am. Chem. Soc.* **1959**, *81*, 3330.
- 10.21 Saunders, W. H., Jr.; Cockerill, A. F. *Mechanisms of Elimination Reactions*; Wiley-Interscience: New York, 1973.
- 10.22 Lenoir, D.; Chiappe, C. *Chem. Eur. J.* **2003**, *9*, 1036.
- 10.23 de Groot, F. M. H.; Loos, W. J.; Koekkoek, R.; van Berkomp, L. W. A.; Busscher, G. F.; Seelen, A. E.; Albrecht, C.; de Bruijn, P.; Scheeren, H. W. *J. Org. Chem.* **2001**, *66*, 8815.
- 10.24 Rappoport, Z.; Greenblatt, J.; Apeloig, Y. *J. Org. Chem.* **1979**, *44*, 3687.
- 10.25 Acevedo, O.; Jorgensen, W. L. *J. Am. Chem. Soc.* **2006**, *128*, 6141.
- 10.26 Amir-Heidari, B.; Mickelfield, J. *J. Org. Chem.* **2007**, *72*, 8950.
- 10.27 de Groot, F. M. H.; Albrecht, C.; Koekkoek, R.; Beusker, P. H.; Scheeren, H. W. *Angew. Chem. Int. Ed.* **2003**, *42*, 4490.
- 10.28 a. Grainger, R. S.; Patel, A. *Chem. Commun.* **2003**, 1072. b. Honda, K.; Tabuchi, M.; Kurokawa, H.; Asami, M.; Inoue, S. *J. Chem. Soc. Perkin Trans. 1* **2002**, 1387. c. Riether, D.; Mulzer, J. *Eur. J. Org. Chem.* **2003**, 30. d. Pye, P. J.; Rossen, K.; Weissman, S. A.; Maliakal, A.; Reamer, R. A.; Ball, R.; Tsou, N. N.; Volante, R. P.; Reider, P. J. *Chem. Eur. J.* **2002**, *8*, 1372.
- 10.29 Kluiber, R. W. *J. Org. Chem.* **1966**, *61*, 1298.
- 10.30 Mohrig, J. R.; Carlson, H. K.; Coughlin, J. M.; Hofmeister, G. E.; McMartin, L. A.; Rowley, E. G.; Trimmer, E. E.; Wild, A. J.; Schultz, S. C. *J. Org. Chem.* **2007**, *72*, 793.

Chapter 11

- 11.6 Longuet-Higgins, H. C.; Abrahamson, E. W. *J. Am. Chem. Soc.* **1965**, *87*, 2045
- 11.9 Fráter, G.; Schmid, H. *Helv. Chim. Acta* **1968**, *51*, 190.
- 11.10 Vogel, E. *Liebigs Ann. Chem.* **1958**, *615*, 1; Hammond, G. S.; DeBoer, C. D. *J. Am. Chem. Soc.* **1964**, *86*, 899.
- 11.11 Doering, W. v. E.; Wiley, D. W. *Tetrahedron* **1960**, *11*, 183.

- 11.12 a. Bates, R. B.; McCombs, D. A. *Tetrahedron Lett.* **1969**, 977. b. Pomerantz, M.; Wilke, R. N.; Gruber, G. W.; Roy, U. *J. Am. Chem. Soc.* **1972**, 94, 2752. c. Arnold, B. J.; Sammes, P. G. *J. Chem. Soc. Chem. Commun.* **1972**, 1034; Arnold, B. J.; Sammes, P. G.; Wallace, T. W. *J. Chem. Soc. Perkin Trans. 1* **1974**, 415.
- 11.13 Brown, J. M. *Chem. Commun.* **1965**, 226.
- 11.14 Curtin, D. Y.; Johnson, H. W., Jr. *J. Am. Chem. Soc.* **1956**, 78, 2611.
- 11.16 Arnett, E. M. *J. Org. Chem.* **1960**, 25, 324.
- 11.17 Copley, S. D.; Knowles, J. R. *J. Am. Chem. Soc.* **1985**, 107, 5306.
- 11.18 Conroy, H.; Firestone, R. A. *J. Am. Chem. Soc.* **1956**, 78, 2290.
- 11.19 Heimgartner, H.; Hansen, H.-J.; Schmid, H. *Helv. Chim. Acta* **1972**, 55, 1385.
- 11.20 Greenwood, F. L. *J. Org. Chem.* **1959**, 24, 1735.
- 11.21 Agosta, W. C. *J. Am. Chem. Soc.* **1964**, 86, 2638.
- 11.22 Baldwin, J. E.; Reddy, V. P.; Schaad, L. J.; Hess, B. A., Jr. *J. Am. Chem. Soc.* **1988**, 110, 8555.
- 11.23 a. Park, K. H.; Kang, J. S. *J. Org. Chem.* **1997**, 62, 3794. b. Moinet, G.; Brocard, J.; Conia, J. M. *Tetrahedron Lett.* **1972**, 4461. c. Schomburg, D.; Thielmann, M.; Ekkehard, W.; *Tetrahedron Lett.* **1985**, 26, 1705. d. Kraus, G. A.; Kim, J. *Org. Lett.* **2004**, 6, 3115. e. Ichikawa, Y.; Yamaoka, T.; Nakano, K.; Kotsuki, H. *Org. Lett.* **2007**, 9, 2989. f. Davis, F. A.; Deng, J. *Org. Lett.* **2007**, 9, 1707. g. Migawa, M. T.; Townsend, L. B. *Org. Lett.* **1999**, 1, 537.
- 11.24 Makosza, M.; Podraza, R. *Eur. J. Org. Chem.* **2000**, 193.
- 11.25 Norton, J. E.; Northrop, B. H.; Nuckolls, C.; Houk, K. N. *Org. Lett.* **2006**, 8, 4915.
- 11.26 a. Castro, C.; Karney, W. L.; Noey, E.; Vollhardt, K. P. C. *Org. Lett.* **2008**, 10, 1287. b. Carroll, M. F. *J. Chem. Soc.* **1940**, 704. c. Miyashi, T.; Ahmed, A.; Mukai, T. *J. Chem. Soc. Chem. Commun.* **1984**, 179. d. Grant, T. N.; West, F. G. *Org. Lett.* **2007**, 9, 3789; *J. Am. Chem. Soc.* **2006**, 128, 9348.
- 11.27 DeClue, M. S.; Baldrige, K. K.; Künzler, D. E.; Kast, P.; Hilvert, D. *J. Am. Chem. Soc.* **2005**, 127, 15002.
- 11.28 Takao, K.; Munakata, R.; Tadano, K. *Chem. Rev.* **2005**, 105, 4779.
- 11.29 Nishizawa, M.; Hirakawa, H.; Nakagawa, Y.; Yamamoto, H.; Namba, K.; Imagawa, H. *Org. Lett.* **2007**, 9, 5577.
- 11.30 a. Dockendorff, C.; Sahli, S.; Olsen, M.; Milhau, L.; Lautens, M. *J. Am. Chem. Soc.* **2005**, 127, 15028. b. Jenkins, P. R. *J. Braz. Chem. Soc.* **1996**, 7, 343. c. Marvell, E. N.; Tao, T. *Tetrahedron Lett.* **1969**, 1341.

Chapter 12

- 12.2 Houk, K. N.; Lee, P. S.; Nendel, M. *J. Org. Chem.* **2001**, 66, 5517.
- 12.5 Babu, M. K.; Rajasekaran, K.; Kannan, N.; Gnanasekaran, C. *J. Chem. Soc. Perkin Trans. 2* **1986**, 1721.
- 12.6 Pacifici, J. G.; Hyatt, J. A. *Mol. Photochem.* **1971**, 3, 271.
- 12.7 Frey, H. M.; Lister, D. H. *Mol. Photochem.* **1972**, 3, 323.
- 12.8 Tsuneishi, H.; Inoue, Y.; Hakushi, T.; Tai, A. *J. Chem. Soc. Perkin Trans. 2* **1993**, 457.
- 12.9 Alumbaugh, R. L.; Pritchard, G. O.; Rickborn, B. *J. Phys. Chem.* **1965**, 69, 3225.
- 12.10 Ohloff, G.; Klein, E.; Schenck, G. O. *Angew. Chem.* **1961**, 73, 578.
- 12.11 a. Kropp, P. J. *Mol. Photochem.* **1978-79**, 9, 39. b. Yang, N. C.; Jorgenson, M. J. *Tetrahedron Lett.* **1964**, 1203.
- 12.12 Carless, H. A. *J. Chem. Soc. Perkin Trans. 2* **1974**, 834.
- 12.13 Zimmerman, H. E.; Sandel, V. R. *J. Am. Chem. Soc.* **1963**, 85, 915.

- 12.14 a. Butenandt, A.; Poschmann, L. *Chem. Ber.* **1944**, 77B, 392. b,c. Quinkert, G. *Angew. Chem. Int. Ed. Engl.* **1962**, 1, 166. d. Medary, R. T.; Gano, J. E.; Griffin, C. E. *Mol. Photochem.* **1974**, 6, 107.
- 12.15 a. Barnard, M.; Yang, N. C. *Proc. Chem. Soc.* **1958**, 302. b. Wolff, S.; Schreiber, W. L.; Smith, A. B. III; Agosta, W. C. *J. Am. Chem. Soc.* **1972**, 94, 7797.
- 12.16 a. Agosta, W. C.; Smith, A. B. III. *J. Am. Chem. Soc.* **1971**, 93, 5513. b. Göth, H.; Cerutti, P.; Schmid, H. *Helv. Chem. Acta* **1965**, 48, 1395.
- 12.17 Anderson, J. C.; Reese, C. B. *J. Chem. Soc.* **1963**, 1781.
- 12.18 Padwa, A. *Acc. Chem. Res.* **1971**, 4, 48.
- 12.19 a. Bahurel, Y.; Descotes, G.; Pautet, F. *Compt. Rend.* **1970**, 270, 1528; Bahurel, Y.; Pautet, F.; Descotes, G. *Bull. Soc. Chim. France* **1971**, 6, 2222. b. Nobs, F.; Burger, U.; Schaffner, K. *Helv. Chim. Acta* **1977**, 60, 1607.
- 12.20 Turro, N. J.; Weiss, D. S. *J. Am. Chem. Soc.* **1968**, 90, 2185. See also Dawes, K.; Dalton, J. C.; Turro, N. J. *Mol. Photochem.* **1971**, 3, 71.
- 12.21 a. Padwa, A.; Eisenberg, W. *J. Am. Chem. Soc.* **1970**, 92, 2590. b. Gagosian, R. B.; Dalton, J. C.; Turro, N. J. *J. Am. Chem. Soc.* **1970**, 92, 4752. c. Padwa, A.; Alexander, E.; Niemczyk, M. *J. Am. Chem. Soc.* **1969**, 91, 456; see also Padwa, A. *Acc. Chem. Res.* **1971**, 4, 48. d. Arnold, B. J.; Mellows, S. M.; Sammes, P. G.; Wallace, T. W. *J. Chem. Soc. Perkin Trans. 1* **1974**, 401; see also Durst, T.; Kozma, E. C.; Charlton, J. L. *J. Org. Chem.* **1985**, 50, 4829. e. Wolff, S.; Schreiber, W. L.; Smith, A. B. III; Agosta, W. C. *J. Am. Chem. Soc.* **1972**, 94, 7797.
- 12.22 Gilbert, A.; Taylor, G. N.; bin Samsudin, M. W. *J. Chem. Soc. Perkin Trans. 1* **1980**, 869.
- 12.23 Morrison, H.; Pajak, J.; Peiffer, R. *J. Am. Chem. Soc.* **1971**, 93, 3978.
- 12.24 Riguet, E.; Bochet, C. G. *Org. Lett.* **2007**, 9, 5453.
- 12.25 Kozukue, N.; Park, M.-S.; Choi, S.-H.; Lee, S.-U.; Ohnishi-Kameyama, M.; Levin, C. E.; Friedman, M. *J. Agric. Food Chem.* **2007**, 55, 7131.
- 12.26 Moorthy, J. N.; Samanta, S. *ARKIVOC* **2007** (viii), 324.
- 12.27 a. Turro, N. J.; Lee, T.-J. *J. Am. Chem. Soc.* **1969**, 91, 5651. b. Corey, E. J.; Nozoe, S. *J. Am. Chem. Soc.* **1964**, 86, 1652.
- 12.28 Crimmins, M. T.; Pace, J. M.; Nantermet, P. G.; Kim-Meade, A. S.; Thomas, J. B.; Watterson, S. H.; Wagman, A. S. *J. Am. Chem. Soc.* **2000**, 122, 8453.
- 12.29 Kang, T.; Scheffer, J. R. *Org. Lett.* **2001**, 3, 3361.
- 12.30 a. Winkler, J. D.; Lee, E. C. Y. *J. Am. Chem. Soc.* **2006**, 128, 9040. b. Sajimon, M. C.; Ramaiah, D.; Suresh, C. H.; Adam, W.; Lewis, F. D.; George, M. V. *J. Am. Chem. Soc.* **2007**, 129, 9439. c. Chang, J. A.; Chiang, Y.; Keeffe, J. R.; Kresge, A. J.; Nikolaev, V. A.; Popik, V. V. *J. Org. Chem.* **2006**, 71, 4460. d. Klein, M.; Walenzyk, T.; König, B. *Collect. Czech. Chem. Commun.* **2004**, 59, 945.

Permissions

Chapter 1

- 8, **Figure 1.2.** Reprinted with permission from Bader, R. F. W.; Carroll, M. T.; Cheeseman, J. R.; Chang, C. J. *Am. Chem. Soc.* **1987**, *109*, 7968. Copyright © 1987 American Chemical Society.
- 31, **Figure 1.12.** Reprinted with permission from "A Novel Pictorial Approach to Teaching MO Concepts in Polyatomic Molecules," by Hoffman, D. K.; Ruedenberg, K.; Verkade, J. G. *J. Chem. Educ.* **1977**, *54*, 590–595. Copyright © 1977 American Chemical Society.
- 33, **Figure 1.15.** Reprinted from *Chemical Physics Letters*. **1968**, *1*, 613, Hamrin, K.; Johansson, G.; Gelius, U.; Fahlman, A.; Nordling, C.; Siegbahn, K., "Ionization Energies in Methane and Ethane Measured by Means of ESCA," Copyright © 1968 with permission from Elsevier Science-NL, Sara Burgerhartstraat 25, 1055 KV Amsterdam, The Netherlands.
- 34, **Figure 1.16.** Reprinted with permission from "A Novel Pictorial Approach to Teaching MO Concepts in Polyatomic Molecules," by Hoffman, D. K.; Ruedenberg, K.; Verkade, J. G. *J. Chem. Educ.* **1977**, *54*, 590–595. Copyright © 1977 American Chemical Society.
- 40, **Figure 1.22.** Reprinted with permission from Wiberg, K. B.; Hadad, C. M.; Breneman, C. M.; Laidig, K. E.; Murcko, M. A.; LePage, T. J. *Science*, **1992**, *252*, 1266. Copyright © 1992 American Association for the Advancement of Science.
- 40, **Figure 1.23.** From *Organic Reaction Mechanisms*, 2nd ed., by Breslow, R. Copyright © 1969 by W. A. Benjamin, Inc. Reprinted by permission.
- 46, **Figure 1.33** and 47, **Figure 1.34.** Reprinted with permission from "Models for the Double Bond," by Walters, E. A. *J. Chem. Educ.* **1966**, *43*, 134–137. Copyright © 1966 American Chemical Society.
- 47, **Figure 1.35.** Reprinted with permission from Hamilton, J. G.; Palke, W. E. *J. Am. Chem. Soc.* **1993**, *115*, 4159. Copyright © 1993 American Chemical Society.

Chapter 2

- 56, Figure 2.4.** Reproduced with permission from Burnett, M. N.; Johnson, C. K. *ORTEP III: Oak Ridge Thermal Ellipsoid Plot Program for Crystal Structure Illustrations*. Oak Ridge National Laboratory Report ORNL-6895, 1996.
- 61, Figure 2.11.** Reprinted with permission from "A Flow-Chart Approach to Point Group Classification," by Carter, R. L. *J. Chem. Educ.* **1968**, *45*, 44. Copyright © 1968 American Chemical Society.
- 65, Figure 2.12 and 69, Figure 2.14.** Reprinted with permission from "An Introduction to the Sequence Rule," by Cahn, R. S. *J. Chem. Educ.* **1964**, *41*, 116–125. Copyright © 1964 American Chemical Society.
- 89, Figure 2.31.** Reprinted with permission from Djerassi, C.; Wolf, H.; Bunnenberg, E. *J. Am. Chem. Soc.* **1963**, *85*, 324. Copyright © 1963 American Chemical Society.
- 99, Figure 2.45 and 100, Figure 2.46 and Table 2.3.** Reprinted with permission from Mislow, K.; Siegel, J. *J. Am. Chem. Soc.* **1984**, *106*, 3319. Copyright © 1984 American Chemical Society.
- 109, Figure 2.47.** Reprinted with permission from Hilvert, D.; Nared, K. D. *J. Am. Chem. Soc.* **1988**, *110*, 5593. Copyright © 1988 American Chemical Society.
- 110, Figure 2.48.** Reprinted with permission from Xu, Z.-S.; Zhang, C.; Zheng, Q.-Y.; Chen, C.-F.; Huang, Z.-T. *Org. Lett.*, **2007**, *9*, 4447. Copyright © 2007 American Chemical Society.

Chapter 3

- 122, Figure 3.8.** Reprinted with permission from Jorgensen, W. L.; Buckner, J. *K. J. Phys. Chem.* **1987**, *91*, 6083. Copyright © 1987 American Chemical Society.
- 136, Figure 3.14.** Reprinted with permission from "The Story Behind the Story: Why Did Adolf Baeyer Propose a Planar, Strained Cyclohexane Ring?" by Ramsay, O. B. *J. Chem. Educ.* **1977**, *54*, 563–564. Copyright © 1977 American Chemical Society.
- 127, Figure 3.17 and Figure 3.18.** Reprinted with permission from Stein, A.; Lehmann, C. W.; Luger, P. *J. Am. Chem. Soc.* **1992**, *114*, 7684. Copyright © 1992 American Chemical Society.
- 150, Figure 3.34.** Reprinted with permission from Wiberg, K. B.; Murcko, M. A.; Laidig, K. E.; MacDougall, P. J. *J. Phys. Chem.* **1990**, *94*, 6956. Copyright © 1990 American Chemical Society.

Chapter 4

- 186, Figure 4.7.** From *Molecular Orbital Calculations*, by Roberts, J. D. Copyright © 1961 by W. A. Benjamin, Inc. Reprinted by permission.
- 188, Figure 4.11 and 199, Figure 4.24.** From *Quantum Mechanics for Organic Chemists*, by Zimmerman, H. E. Copyright © 1975 by Academic Press, Inc. Reprinted by permission.
- 202, Figure 4.27.** Reprinted with permission from Cox, E. G.; Cruickshank, D. W. J.; Smith, J. A. S. *Proc. Roy. Soc. A* **1958**, *247*, 1. Copyright © 1958 Royal Society of London.

- 209, **Figure 4.36**. Reproduced from Haddon, R. C. *Acc. Chem. Res.* **2002**, *35*, 997. Copyright © 2002 American Chemical Society.
- 224, **Figure 4.51** and 226, **Figure 4.52**. From *Introduction to Computational Chemistry*, 2nd ed., by Jensen, F. John Wiley & Sons, Ltd.: Chichester, 2007. Copyright © 2007 by John Wiley & Sons, Inc. Reprinted by permission.
- 227, **Figure 4.53**. From *Valency and Bonding: A Natural Bond Orbital Donor-Acceptor Perspective*, by Weinhold, F.; Landis, C. R. Cambridge University Press: Cambridge, 2005. Copyright © 2005 by Cambridge University Press. Reprinted by permission.
- 232, **Figure 4.62**. Reprinted with permission from Schreiner, P. R. *Angew. Chem. Int. Ed. Engl.* **2002**, *41*, 3579. Copyright © 2002 VCH Publishers, Inc.
- 233, **Figure 4.63**; 234, **Figure 4.65**; and 235, **Figure 4.66**. Reproduced from Bader, R. F. W.; Carroll, M. T.; Cheeseman, J. R.; Chang, C. J. *Am. Chem. Soc.* **1987**, *109*, 7968. Copyright © 1987 American Chemical Society.
- 234, **Figure 4.64**. Reproduced from Bader, R. F. W.; Nguyen-Dang, T. T.; Tal, Y. *Rep. Prog. Phys.* **1981**, *44*, 893. Copyright © 1981 Institute of Physics and IOP Publishing Ltd.

Chapter 5

- 255, **Figure 5.2**. Reproduced from Coms, F. D.; Dougherty, D. A. *J. Am. Chem. Soc.* **1989**, *111*, 6894. Copyright © 1989 American Chemical Society.
- 256, **Figure 5.3**. Reprinted with permission from "Textbook Errors, 131: Free Energy Surfaces and Transition State Theory," by Cruickshank, F. R.; Hyde, A. J.; Pugh, D. J. *Chem. Educ.* **1977**, *54*, 288–291. Copyright © 1977 American Chemical Society.
- 260, **Figure 5.4**. Reprinted with permission from "Introduction to the Interpretation of Electron Spin Resonance Spectra of Organic Radicals," by Bunce, N. J. *J. Chem. Educ.* **1987**, *64*, 907–914. Copyright © 1987 American Chemical Society.
- 261, **Figure 5.7** and **Figure 5.8**. Reprinted with permission from Fessenden, R. W.; Schuler, R. H. *J. Chem. Phys.*, **1963**, *39*, 2147. Copyright © 1963 American Institute of Physics.
- 266, **Figure 5.18**. Reproduced from Paddon-Row, M. N.; Houk, K. N. *J. Phys. Chem.* **1985**, *89*, 3771. Copyright © 1985 American Chemical Society.
- 279, **Figure 5.27**. Reprinted with permission from Schaefer III, H. F. *Science*, **1986**, *231*, 1100. Copyright © 1986 American Association for the Advancement of Science.
- 290, **Figure 5.34**. From *Hypercarbon Chemistry*, by Olah, G. A.; Prakash, G. K. S.; Williams, R. E.; Field, L. D.; Wade, K. Copyright © 1987 by John Wiley & Sons, Inc. Reprinted by permission.
- 295, **Figure 5.42**. Reproduced from Olah, G. A. *J. Org. Chem.* **2005**, *70*, 2413. Copyright © 2005 American Chemical Society.
- 297, **Figure 5.43** and **Figure 5.44**. From Schleyer, P. v. R.; Maerker, C.; Buzek, P.; Sieber, S.; Prakash, G. K. S. in Prakash, G. K. S.; Schleyer, P. v. R., Eds., *Stable Carbocation Chemistry*; John Wiley & Sons, Inc.: New York, 1997. Copyright © 1997 by John Wiley & Sons, Inc. Reprinted by permission.

- 303, **Figure 5.52.** Reproduced from Olah, G. A.; White, A. M. *J. Am. Chem. Soc.* **1969**, *91*, 5801. Copyright © 1969 American Chemical Society.
- 306, **Figure 5.54.** Reprinted with permission from Ma, N. L.; Smith, B. J.; Pople, J. A.; Radom, L. *J. Am. Chem. Soc.* **1991**, *113*, 7903. Copyright © 1991 American Chemical Society.
- 313, **Figure 5.58.** Reproduced from Kwon, O.; Sevin, F.; McKee, M. L. *J. Phys. Chem. A* **2001**, *105*, 913. Copyright © 2001 American Chemical Society.
- 314, **Figure 5.59.** Reproduced from Walborsky, H. M.; Impastato, F. J.; Young, A. E. *J. Am. Chem. Soc.* **1964**, *86*, 3283. Copyright © 1964 American Chemical Society.

Chapter 6

- 332, **Figure 6.3** and **Figure 6.4.** Reprinted with permission from Porter, N.; Zuraw, P. *J. Chem. Soc., Chem. Commun.* **1985**, 1472. Copyright © 1985 Royal Society of Chemistry.
- 358, **Figure 6.28.** Reprinted with permission from "A New Perspective on Kinetic and Thermodynamic Control of Reactions," by Snadden, R. B. *J. Chem. Educ.* **1985**, *62*, 653–655. Copyright © 1985 American Chemical Society.
- 372, **Figure 6.49.** From *Spectroscopy and Molecular Structure*, by King, Gerald W. Copyright © 1964 by Holt, Rinehart and Winston, Inc. Renewed 1992 by Gerald W. King, reproduced by permission of the publisher.
- 372, **Figure 6.50**; 376, **Figure 6.52** and **Figure 6.54**; 377, **Figure 6.56**; and 379, **Figure 6.58** and **Figure 6.59.** Reprinted with permission from Wiberg, K. B. *Chem. Rev.* **1955**, *55*, 713. Copyright © 1955 American Chemical Society.
- 388, **Figure 6.64.** Reprinted with permission from Marriott, S.; Topsom, R. D. *J. Am. Chem. Soc.* **1985**, *107*, 2253. Copyright © 1985 American Chemical Society.
- 392, **Figure 6.67** and 396, **Figure 6.76.** Reprinted with permission from Anderson, B. M.; Jencks, W. P. *J. Am. Chem. Soc.* **1960**, *82*, 1773. Copyright © 1960 American Chemical Society.
- 396, **Figure 6.77.** Reprinted with permission from Santerre, G. M.; Hansrote, Jr., C. J.; Crowell, T. I. *J. Am. Chem. Soc.* **1958**, *80*, 1254. Copyright © 1958 American Chemical Society.

Chapter 7

- 431, **Figure 7.1.** Reprinted with permission from Jorgenson, M. J.; Hartter, D. R. *J. Am. Chem. Soc.* **1963**, *85*, 878. Copyright © 1963 American Chemical Society.
- 432, **Figure 7.2.** From *Physical Organic Chemistry: Reaction Rates, Equilibria and Mechanisms*, 2nd ed., by Hammett, L. P., p. 272. Copyright © 1970 by McGraw-Hill Book Company. Reprinted by permission.
- 442 **Figure 7.7.** Reprinted with permission from Jencks, W. P. *J. Am. Chem. Soc.* **1959**, *81*, 475. Copyright © 1959 American Chemical Society.
- 447, **Figure 7.13.** Reprinted with permission from Cordes, E. H. *Prog. Phys. Org. Chem.*, **1967**, *4*, 1. Copyright © 1967 John Wiley & Sons, Inc.
- 448, **Figure 7.14.** Reprinted with permission from Anderson, E.; Capon, B. *J. Chem. Soc. (B)* **1969**, 1033. Copyright © 1969 Royal Society of Chemistry.

- 449, Figure 7.15.** Reprinted with permission from Swain, C. G.; Brown, Jr., J. F. *J. Am. Chem. Soc.* **1952**, *74*, 2538. Copyright © 1952 American Chemical Society.
- 455, Figure 7.22.** Reprinted with permission from Bender, M. L.; Thomas, R. J. *J. Am. Chem. Soc.* **1961**, *83*, 4189. Copyright © 1961 American Chemical Society.
- 461, Figure 7.29.** Reprinted with permission from Weiner, S. J.; Singh, U. C.; Kollman, P. A. *J. Am. Chem. Soc.* **1985**, *107*, 2219. Copyright © 1985 American Chemical Society.

Chapter 8

- 480, Table 8.4.** Reprinted with permission from Ritchie, C. D. *Acc. Chem. Res.* **1972**, *5*, 348. Copyright © 1972 American Chemical Society.
- 484, Figure 8.9.** Reprinted with permission from Winstein, S.; Klinedinst, Jr., P. E.; Robinson, G. *J. Am. Chem. Soc.* **1961**, *83*, 885. Copyright © 1961 American Chemical Society.
- 485, Figure 8.11 and 486, Figure 8.12.** Reprinted with permission from Jorgensen, W. L.; Buckner, J. K.; Huston, S. E.; Rossky, P. J. *J. Am. Chem. Soc.* **1987**, *109*, 1891. Copyright © 1987 American Chemical Society.
- 498, Figure 8.31.** Reprinted with permission from Chandrasekhar, J.; Jorgensen, W. L. *J. Am. Chem. Soc.* **1985**, *107*, 2974. Copyright © 1985 American Chemical Society.
- 500, Figure 8.33.** Reprinted with permission from Gao, J. *J. Am. Chem. Soc.* **1991**, *113*, 7796. Copyright © 1991 American Chemical Society.
- 502, Figure 8.34.** Reprinted with permission from King, J. F.; Tsang, G. T. Y.; Abdel-Malik, M. M.; Payne, N. C. *J. Am. Chem. Soc.* **1985**, *107*, 2745. Copyright © 1985 American Chemical Society.
- 503, Figure 8.36.** Reprinted with permission from Bach, R. D.; Coddens, B. A.; Wolber, G. J. *J. Org. Chem.* **1986**, *51*, 1030. Copyright © 1986 American Chemical Society.
- 514, Figure 8.39.** Reprinted with permission from Pross, A.; Shaik, S. S. *Acc. Chem. Res.* **1983**, *16*, 363. Copyright © 1983 American Chemical Society.
- 516, Figure 8.41.** Reprinted with permission from Ashby, E. C.; Pham, T. N. *J. Org. Chem.* **1986**, *51*, 3598. Copyright © 1986 American Chemical Society.
- 518, Figure 8.43.** Reprinted with permission from Pross, A. *Acc. Chem. Res.* **1985**, *18*, 212. Copyright © 1985 American Chemical Society.
- 518, Figure 8.44.** Reprinted with permission from Ashby, E. C.; Park, B.; Patil, G. S.; Gadru, K.; Gurusurthy, R. *J. Org. Chem.* **1993**, *58*, 424. Copyright © 1993 American Chemical Society.
- 522, Figure 8.47.** Reprinted by permission from Stock, L. M. *Prog. Phys. Org. Chem.* **1976**, *12*, 21. Copyright © 1976 John Wiley & Sons, Inc.
- 531, Figure 8.54.** Reprinted with permission from Bacaloglu, R.; Bunton, C. A.; Cerichelli, G. *J. Am. Chem. Soc.* **1987**, *109*, 621. Copyright © 1987 American Chemical Society.
- 542, Figure 8.68.** Reprinted with permission from Kim, J. K.; Bunnett, J. F. *J. Am. Chem. Soc.* **1970**, *92*, 7463. Copyright © 1970 American Chemical Society.

Chapter 9

- 560, Figure 9.5.** Reprinted with permission from Slebocka-Tilk, H.; Zheng, C. Y.; Brown, R. S. *J. Am. Chem. Soc.* **1993**, *115*, 1347. Copyright © 1993 American Chemical Society.
- 563, Figure 9.10.** Reprinted with permission from Bellucci, G.; Chiappe, C.; Marioni, F. *J. Am. Chem. Soc.* **1987**, *109*, 515. Copyright © 1987 American Chemical Society.
- 564, Figure 9.12.** Reprinted with permission from Bellucci, G.; Bianchini, R.; Chiappe, C.; Marioni, F.; Ambrosetti, R.; Brown, R. S.; Slebocka-Tilk, H. *J. Am. Chem. Soc.* **1989**, *111*, 2640. Copyright © 1989 American Chemical Society.
- 568, Figure 9.17.** Reprinted with permission from Dubois, J.-E.; Chretien, J. R. *J. Am. Chem. Soc.* **1978**, *100*, 3560. Copyright © 1978 American Chemical Society.
- 570, Figure 9.18.** Reprinted with permission from Yates, K.; McDonald, R. S.; Shapiro, S. A. *J. Org. Chem.* **1973**, *38*, 2460. Copyright © 1973 American Chemical Society.
- 573, Figure 9.20.** Reprinted with permission from Ruasse, M.-F. *Acc. Chem. Res.* **1990**, *23*, 87. Copyright © 1990 American Chemical Society.
- 575, Table 9.3.** Reprinted with permission from Poutsma, M. L. *J. Am. Chem. Soc.* **1965**, *87*, 4285. Copyright © 1965 American Chemical Society.
- 580, Figure 9.26.** Reprinted with permission from Yamabe, S.; Minato, T.; Inagaki, S. *J. Chem. Soc., Chem. Commun.* **1988**, 532. Copyright © 1988 Royal Society of Chemistry.
- 582, Figure 9.27.** Reprinted with permission from Stavber, S.; Sotler, T.; Zupan, M.; Popovic, A. *J. Org. Chem.* **1994**, *59*, 5891. Copyright © 1994 American Chemical Society.
- 599, Figure 9.38.** Reprinted with permission from Pasto, D. J.; Gontarz, J. A. *J. Am. Chem. Soc.* **1969**, *91*, 719. Copyright © 1969 American Chemical Society.
- 608, Figure 9.45.** Reprinted from Houk, K. N.; Liu, J.; DeMello, N. C.; Condroski, K. R. *J. Am. Chem. Soc.* **1997**, *119*, 10147. Copyright © 1997 American Chemical Society.
- 610, Figure 9.47.** Reprinted with permission from Bianchini, R.; Chiappe, C.; Lo Moro, G.; Lenoir, D.; Lemmen, P.; Goldberg, N. *Chem. Eur. J.* **1999**, *5*, 1570. Copyright © 1999 Wiley-VCH, Weinheim.
- 623, Figure 9.54 and 624, Figure 9.55.** Reprinted with permission from Cram, D. J.; Kopecky, K. R. *J. Am. Chem. Soc.* **1959**, *81*, 2748. Copyright © 1959 American Chemical Society.
- 624, Figure 9.56.** Reprinted with permission from Karabatsos, G. J. *J. Am. Chem. Soc.* **1967**, *89*, 1367. Copyright © 1967 American Chemical Society.
- 625, Figure 9.58 and 626, Figure 9.60.** Reprinted with permission from Lodge, E. P.; Heathcock, C. H. *J. Am. Chem. Soc.* **1987**, *109*, 3353. Copyright © 1987 American Chemical Society.
- 626, Figure 9.61.** Reprinted with permission from Cieplak, A. S.; Tait, B. D.; Johnson, C. R. *J. Am. Chem. Soc.* **1989**, *111*, 8447. Copyright © 1989 American Chemical Society.

Chapter 10

- 646, **Figure 10.17.** Reprinted with permission from De Angelis, F.; Tarantelli, F.; Alunni, S. *J. Phys. Chem. B.* **2006**, *110*, 11014. Copyright © 2006 American Chemical Society.
- 644, **Figure 10.15 and Figure 10.16.** Reprinted with permission from Kwok, W. K.; Lee, W. G.; Miller, S. I. *J. Am. Chem. Soc.* **1969**, *91*, 468. Copyright © 1969 American Chemical Society.
- 650, **Figure 10.22.** Reprinted with permission from Dohner, B. R.; Saunders, Jr., W. H. *J. Am. Chem. Soc.* **1986**, *108*, 245. Copyright © 1986 American Chemical Society.
- 653, **Figure 10.26.** Reprinted with permission from Croft, A. P.; Bartsch, R. A. *J. Org. Chem.* **1994**, *59*, 1930. Copyright © 1994 American Chemical Society.
- 665, **Figure 10.37.** Reprinted with permission from Eubanks, J. R. I.; Sims, L. B.; Fry, A. *J. Am. Chem. Soc.* **1991**, *113*, 8821. Copyright © 1991 American Chemical Society.
- 670, **Figure 10.42.** From *Advanced Organic Chemistry*, by Fieser, L. R.; Fieser, M. Copyright © 1961 by Reinhold Publishing Company. Adapted by permission.
- 673, **Figure 10.44.** Reprinted with permission from Narayan, R; Antal, Jr., M. *J. Am. Chem. Soc.* **1990**, *112*, 1927. Copyright © 1990 American Chemical Society.
- 679, **Figure 10.48.** Reprinted with permission from Streitwieser, Jr., A.; Schaeffer, W. D. *J. Am. Chem. Soc.* **1957**, *79*, 2888. Copyright © 1957 American Chemical Society.
- 681, **Figure 10.49.** Reprinted with permission from Cram, D. J.; McCarty, J. E. *J. Am. Chem. Soc.* **1957**, *79*, 2866. Copyright © 1957 American Chemical Society.
- 686, **Figure 10.55.** Reprinted with permission from Cram, D. J.; McCarty, J. E. *J. Am. Chem. Soc.* **1954**, *76*, 5740.

Chapter 11

- 705, **Figure 11.10.** Reprinted with permission from Sakai, S.; Takane, S. *J. Phys. Chem. A* **1999**, *103*, 2878. Copyright © 1999 American Chemical Society.
- 710, **Figure 11.17.** Reprinted with permission from Thomas IV, B. E.; Evanseck, J. D.; Houk, K. N. *J. Am. Chem. Soc.* **1993**, *115*, 4165. Copyright © 1993 American Chemical Society.
- 711, **Figure 11.19 and 713, Figure 11.21.** From *The Conservation of Orbital Symmetry*, by Woodward, R. B.; Hoffmann, R. Copyright © 1970 by Verlag Chemie, GmbH, Weinheim/Bergstr. Reprinted by permission of VCH Publishers, Inc.
- 713, **Figure 11.20 and 714, Figure 11.22.** Reprinted with permission from Longuet-Higgins, H. C.; Abrahamson, E. W. *J. Am. Chem. Soc.* **1965**, *87*, 2045. Copyright © 1965 American Chemical Society.
- 717, **Figure 11.25.** From *The Conservation of Orbital Symmetry*, by Woodward, R. B.; Hoffmann, R. Copyright © 1970 by Verlag Chemie, GmbH, Weinheim/Bergstr. Reprinted by permission of VCH Publishers, Inc.

- 717, **Figure 11.27.** Reproduced from Spangler, C. W. *Chem. Rev.* **1976**, *76*, 187. Copyright © 1976 American Chemical Society.
- 717, **Figure 11.28.** Reproduced from Saettel, N. J.; Wiest, O. *J. Org. Chem.* **2000**, *65*, 2331. Copyright © 2000 American Chemical Society.
- 717, **Figure 11.29.** Reproduced from Hess, Jr., B. A.; Schaad, L. J.; Panciř, J. *J. Am. Chem. Soc.* **1985**, *107*, 149. Copyright © 1985 American Chemical Society.
- 718, **Figure 11.32.** Reprinted with permission from Houk, K. N.; Li, Y.; Evanscek, J. D. *Angew. Chem., Int. Ed. Engl.* **1992**, *31*, 682. Copyright © 1992 VCH Publishers, Inc.
- 720, **Figure 11.37.** From *The Conservation of Orbital Symmetry*, by Woodward, R. B.; Hoffmann, R. Copyright © 1970 by Verlag Chemie, GmbH, Weinheim/Bergstr. Reprinted by permission of VCH Publishers, Inc.
- 721, **Figure 11.38.** Reprinted with permission from Hoeger, C. A.; Johnston, A. D. *J. Am. Chem. Soc.* **1987**, *109*, 4690. Copyright © 1987 American Chemical Society.
- 721, **Figure 11.39.** Reprinted with permission from Hoeger, C. A.; Okamura, W. H. *J. Am. Chem. Soc.* **1985**, *107*, 268. Copyright © 1985 American Chemical Society.
- 727, **Figure 11.52.** Reprinted with permission from Schroder, G.; Oth, J. F. M.; Merenyi, R. *Angew. Chem., Int. Ed. Engl.* **1965**, *4*, 752. Copyright © 1965 VCH Publishers, Inc.
- 733, **Figure 11.58** and **Figure 11.60.** From *The Conservation of Orbital Symmetry*, by Woodward, R. B.; Hoffmann, R. Copyright © 1970 by Verlag Chemie, GmbH, Weinheim/Bergstr. Reprinted by permission of VCH Publishers, Inc.
- 733, **Figure 11.61** and **734, Figure 11.62.** Reprinted with permission from Hoffman, R.; Woodward, R. B. *J. Am. Chem. Soc.* **1965**, *87*, 2046. Copyright © 1965 American Chemical Society.
- 737, **Figure 11.64.** Reprinted with permission from Li, Y.; Houk, K. N. *J. Am. Chem. Soc.* **1993**, *115*, 7478. Copyright © 1993 American Chemical Society.
- 737, **Figure 11.66.** Reprinted with permission from Hoffman, R.; Woodward, R. B. *J. Am. Chem. Soc.* **1965**, *87*, 2046. Copyright © 1965 American Chemical Society.
- 742, **Figure 11.69** and **743, Figure 11.71.** From *The Conservation of Orbital Symmetry*, by Woodward, R. B.; Hoffmann, R. Copyright © 1970 by Verlag Chemie, GmbH, Weinheim/Bergstr. Reprinted by permission of VCH Publishers, Inc.
- 744, **Table 11.72.** Reproduced with permission from Huisgen, R. *J. Org. Chem.* **1976**, *41*, 403. Copyright © 1976 American Chemical Society.
- 746, **Figure 11.74.** Reproduced from Wheeler, S. E.; Ess, D. H.; Houk, K. N. *J. Phys. Chem. A* **2008**, *112*, 1798. Copyright © 2008 American Chemical Society.
- 747, **Figure 11.75.** With permission from Eckell, A.; Huisgen, R.; Sustmann, R.; Wallbillich, G.; Grashey, D.; Spindler, E. *Chem. Ber.* **1967**, *100*, 2192.
- 750, **Figure 11.79** and **751, Figure 11.80** and **Figure 11.81.** From *The Conservation of Orbital Symmetry*, by Woodward, R. B.; Hoffmann, R. Copyright © 1970 by Verlag Chemie, GmbH, Weinheim/Bergstr. Reprinted by permission of VCH Publishers, Inc.

- 752, **Figure 11.83** and 764, **Figure 11.98**. Reprinted with permission from Houk, K. N.; Li, Y.; Evanseck, J. D. *Angew. Chem., Int. Ed. Eng.* **1992**, *31*, 682. Copyright © 1992 VCH Publishers, Inc.
- 758, **Figure 11.91**. Reproduced from Niwayama, S.; Kallel, E. A.; Spellmeyer, D. C.; Sheu, C.; Houk, K. N. *J. Org. Chem.* **1996**, *61*, 2813. Copyright © 1996 American Chemical Society.
- 759, **Figure 11.92**. Reprinted with permission from Paderes, G. D.; Jorgensen, W. L. *J. Org. Chem.* **1992**, *57*, 1904. Copyright © 1992 American Chemical Society.
- 767, **Figure 11.104** and 769, **Figure 11.107**. Reprinted with permission from Zimmerman, H. E. *Acc. Chem. Res.* **1971**, *4*, 272. Copyright © 1971 American Chemical Society.
- 768, **Figure 11.106**. Reprinted from Lecea, B.; Arrieta, A.; Cossío, F. P. *J. Org. Chem.* **2005**, *70*, 1035. Copyright © 2005 American Chemical Society.
- 770, **Table 11.7**. Reprinted with permission from Ajami, D.; Hess, K.; Köhler, F.; Näther, C.; Oeckler, O.; Simon, A.; Yamamoto, C.; Okamoto, Y.; Herges, R. *Chem. Eur. J.* **2006**, *12*, 5434. Copyright © 2006 Wiley-VCH, Weinheim.
- 776, **Figure 11.112**. Reprinted with permission from Carpenter, B. K. *J. Org. Chem.* **1992**, *57*, 4645. Copyright © 1992 American Chemical Society.
- 778, **Figure 11.114**. Reprinted with permission from Doubleday, C.; Suhrada, C. P.; Houk, K. N. *J. Am. Chem. Soc.* **2006**, *128*, 90. Copyright © 2006 American Chemical Society.

Chapter 12

- 788, **Figure 12.2**. From *Physical Chemistry*, 3rd ed., by Moore, W. J. Copyright © 1962 by Prentice-Hall, Inc.
- 793, **Figure 12.6**. Reprinted with permission from Wilkinson, F. *Quart. Rev. Chem. Soc.* **1966**, *20*, 403. Copyright © 1966 Royal Society of Chemistry.
- 799, **Figure 12.8**. Reprinted with permission from Bowen, E. J. *Adv. Photochem.* **1963**, *1*, 23. Copyright © 1963 John Wiley & Sons, Inc.
- 797 **Figure 12.7**. Reprinted with permission from Kohler, B. E. *Chem. Rev.* **1993**, *93*, 41. Copyright © 1993 American Chemical Society.
- 799, **Figure 12.9**. Reprinted with permission from Becker H.-D.; Andersson, K. *J. Org. Chem.* **1983**, *48*, 4542. Copyright © 1983 American Chemical Society.
- 800, **Figure 12.10**. From *Handbook of Fluorescence Spectra of Aromatic Molecules*, 2nd ed., by Berlman, I. B. Copyright © 1971 Academic Press. Reprinted by permission.
- 801, **Figure 12.11**. Reprinted with permission from Hamai, S. *J. Chem. Soc., Chem. Commun.* **1994**, 2243. Copyright © 1994 Royal Society of Chemistry.
- 802, **Figure 12.12**. Reprinted with permission from Marchetti, A.P.; Kearns, D. R. *J. Am. Chem. Soc.* **1967**, *89*, 768. Copyright © 1967 American Chemical Society.
- 803, **Figure 12.13**. Reprinted from Kavarnos, G. J. *Top. Curr. Chem.* **1990**, *156*, 21. Copyright © 1990 Springer-Verlag.
- 812, **Figure 12.19** and 813, **Figure 12.20**. Reprinted with permission from Lawrence, M.; Marzacco, C. J.; Morton, C.; Schwab, C.; Halpern, A. M.

- J. Phys. Chem.* **1991**, *95*, 10294. Copyright © 1991 American Chemical Society.
- 815, Figure 12.21.** Reprinted with permission from Jackson, G.; Porter, G. *Proc. Roy. Soc. London* **1961**, *A260*, 13. Copyright © 1961 Royal Society of London.
- 816, Figure 12.22.** Reprinted with permission from Turro, N. J.; Dalton, J. C.; Dawes, K.; Farrington, G.; Hautala, R.; Morton, D.; Niemczyk, M.; Schore, N. *Acc. Chem Res.* **1972**, *5*, 92. Copyright © 1972 American Chemical Society.
- 817, Figure 12.24.** From *Modern Molecular Photochemistry*, by Turro, N. J. Copyright © 1978 by Benjamin/Cummings Publishing Co., Inc. Reprinted by permission.
- 819, Figure 12.26.** Reprinted with permission from Brink, M.; Möllerstedt, H.; Ottosson, C.-H. *J. Phys. Chem. A* **2001**, *105*, 4071. Copyright © 2001 American Chemical Society.
- 821, Figure 12.28.** Reprinted with permission from Ben-Nun, M.; Quenneville, J.; Martínez, T. J. *J. Phys. Chem. A* **2000**, *104*, 5161. Copyright © 2000 American Chemical Society.
- 821, Figure 12.29 and 822, Figure 12.30.** Reproduced with permission from Levine, B. G.; Martínez, T. J. *Annu. Rev. Phys. Chem.* **2007**, *58*, 613. Copyright © 2007 Annual Reviews.
- 823, Figure 12.32.** Reprinted with permission from Lewis, F. D.; Elbert, J. E.; Uthagrove, A. L.; Hale, P. D. *J. Org. Chem.* **1991**, *56*, 553. Copyright © 1991 American Chemical Society.
- 823, Figure 12.33.** Reprinted with permission from Inoue, Y.; Takamuku, S.; Sakurai, H. *J. Phys. Chem.* **1977**, *81*, 7. Copyright © 1977 American Chemical Society.
- 825, Figure 12.34.** Reprinted with permission from Kropp, P. J. *Mol. Photochem.* **1978–79**, *9*, 39. Copyright © 1978 Marcel Dekker, Inc.
- 826, Figure 12.36.** Reprinted with permission from Cherry, W.; Chow, M.-F.; Mirbach, J. J.; Mirbach, M. F.; Ramamurthy, V.; Turro, N. J. *Mol. Photochem.* **1977**, *8*, 175. Copyright © 1977 Marcel Dekker, Inc.
- 827, Figure 12.38.** Reprinted with permission from Adam, W.; Oppenlander, T.; Zang, G. *J. Am. Chem. Soc.* **1985**, *107*, 3921. Copyright © 1985 American Chemical Society.
- 828, Figure 12.39.** Reprinted with permission from Hixson, S. S.; Mariano, P. S.; Zimmerman, H. E. *Chem. Rev.* **1973**, *73*, 531. Copyright © 1973 American Chemical Society.
- 831, Figure 12.40.** Reprinted with permission from Inoue, Y.; Hagiwara, S.; Daino, Y.; Hakushi, T. *J. Chem. Soc., Chem. Commun.* **1985**, 1307. Copyright © 1985 Royal Society of Chemistry.
- 831, Figure 12.41.** Reprinted with permission from Saltiel, J.; D'Agostino, J.; Megarity, E. D.; Metts, L.; Neuberger, K. R.; Wrighton, M.; Zafiriou, O. C. *Org. Photochem.* **1973**, *3*, 1. Copyright © 1973 Marcel Dekker, Inc.
- 832, Figure 12.42.** Reprinted with permission from Turro, N. J.; Dalton, J. C.; Dawes, K.; Farrington, G.; Hautala, R.; Morton, D.; Niemczyk, M.; Schore, N. *Acc. Chem Res.* **1972**, *5*, 92. Copyright © 1972 American Chemical Society.
- 833, Figure 12.43.** Reprinted with permission from Srinivasan, R. *Adv. Photochem.* **1963**, *1*, 83. Copyright © 1963 John Wiley & Sons, Inc.

- 837, **Figure 12.45.** Reprinted with permission from Wagner, P. J. *Acc. Chem. Res.* **1971**, *4*, 168. Copyright © 1971 American Chemical Society.
- 839, **Figure 12.46.** Reprinted with permission from Moorthy, J. N.; Koner, A. L.; Samanta, S.; Singhal, N.; Nau, W. M.; Weiss, R. G. *Chem. Eur. J.* **2006**, *12*, 8744. Copyright © 2006 Wiley-VCH, Weinheim.
- 844, **Figure 12.48 and Figure 12.49.** From *Transfer and Storage of Energy by Molecules*, Vol. 1, Burnett, G. M.; North, A. M., Eds. Copyright © 1968 Wiley-Interscience. Reprinted by permission.
- 846, **Figure 12.51 and Figure 12.52.** Reprinted with permission from Zimmerman, H. E.; Sandel, V. R. *J. Am. Chem. Soc.* **1963**, *85*, 915. Copyright © 1963 American Chemical Society.
- 846, **Figure 12.53.** Reprinted with permission from Zimmerman, H. E.; Somasekhara, S. *J. Am. Chem. Soc.* **1963**, *85*, 922. Copyright © 1963 American Chemical Society.
- 847, **Figure 12.51.** From *Photochemistry* by Calvert, J. G.; Pitts, J. N. Copyright © 1966 by John Wiley & Sons, Inc. Reprinted by permission.
- 849, **Table 12.6.** Reprinted with permission from Carroll, F. A.; Hammond, G. S. *Israel J. Chem.* **1972**, *10*, 613. Copyright © 1972 Laser Pages Publishing Ltd.
- 849, **Figure 12.55.** Reprinted from Figure 10 in Michl, J. *Top. Curr. Chem.* **1974**, *46*, 1. Copyright © 1974 Springer-Verlag.
- 862, **Figure 12.57.** Reprinted with permission from Burns, C. S.; Heyerick, A.; De Keukeleire, D.; Forbes, M. D. E. *Chem. Eur. J.* **2001**, *7*, 4553. Copyright © 2001 Wiley-VCH, Weinheim.

Author Index

- Aarts, G. H. M., 556
Abagyan, R. A., 139
Abate, A., 873
Abbate, S., 152, 873
Abboud, J. L. M., 211, 302, 339, 500
Abboud, K. A., 873
Abd Elhafez, F. A., 623
Abdel-Malik, M. M., 502
Abe, M., 3, 840, 849
Abeles, R. H., 876
Abell, P. I., 591
Abraham, M. C., 478
Abraham, M. H., 339, 474
Abraham, R. J., 474
Abrahamson, E. W., 707, 879
Acevedo, O., 879
Acharya, S. P., 660, 879
Acree, Jr., W. E., 339
Adam, W., 826, 852, 881
Adams, D. L., 85
Adams, F. H., 310
Adams, J. T., 877
Adams, R., 492
Adcock, J. L., 159
Adcock, W., 388, 627
Addadi, L., 91
Adhikari, R. M., 207
Adlington, R. M., 274
Agapito, F., 875
Agard, N. J., 746
Agosta, W. C., 70, 161, 826, 880, 881
Ahlberg, P., 879
Ahmed, A., 880
Ahn, J.-A., 399
Aida, M., 876
Aihara, J., 207
Aizman, A., 585
Ajami, D., 769, 770
Akita, M., 853
Alabugin, I. V., 206, 231, 765, 875
Albert, A., 414
Albery, W. J., 350
Albini, A., 853
Albrecht, A. C., 804
Albrecht, C., 636, 879
Albrecht-Gary, A.-M., 350
Albridge, R. G., 32
Albright, T. A., 28, 713
Alcaraz, C., 331
Alder, K., 731, 735, 751, 759
Alder, R. W., 161
Aldoshin, S. M., 62
Aleksandrov, A., 154
Alexander, E., 881
Alexander, E. R., 879
Alexander, S. A., 242, 256
Alexandrova, Z., 873
Alford, J. R., 875
Aliev, A. E., 57
Alkorta, I., 302
Allen, A. D., 214, 215
Allen, C. R., 422
Allen, F. H., 5
Allen, L. C., 22, 23, 24, 36
Allen, R. G., 611
Allen, W. D., 364, 502
Allendoerfer, R. D., 30
Allinger, N. L., 10, 113, 121, 135–137, 151, 156, 159, 383, 496, 687, 871, 874, 875
Allred, A. L., 23
Allsopp, P. G., 872
Aloise, S., 809
Alonso, E. O., 817, 818, 849
Alonso, J. L., 223
Alper, H., 751
Alston, P. V., 762
Altmann, S. L., 204
Altona, C., 152
Alumbaugh, R. L., 880
Alunni, S., 645
Alvarado, L., 563, 668
Alvarez, M. M., 63
Alvarez, S., 6
Aman, N. I., 459
Amano, A., 583
Amarnath, K., 19
Ambidge, I. C., 598
Ambrosetti, R., 557–559, 562
Amir-Heidari, B., 879
Ammal, S. C., 395
Amrollah-Madjdabadi, A., 516
Anantakrishnan, S. V., 575
Andersen, B., 128
Andersen, K. K., 872
Anderson, B. M., 395
Anderson, E., 438, 447
Anderson, H. W., 871
Anderson, J. C., 881
Anderson, R. L., 347
Anderson, T. J., 614
Andersson, K., 799
Andersson, P. G., 652
Ando, W., 256
Andose, J. D., 12, 136
Andrade, J. G., 315
Andraos, J., 256
Andrei, H.-S., 295
Andrews, D. H., 1
Andrews, G. D., 588
Andrews, L. J., 876
Andrussow, K., 414
Anet, F. A. L., 84, 125, 131, 383
Angeles, T. S., 459
Angyal, S. J., 113, 874
Anh, N. T., 229, 626, 879
Anicich, V., 580
Anilkumar, G. N., 855
Ansems, R. B. M., 209
Antal, Jr., M. J., 673
Anthony, J. E., 207
Antúnez, S., 131, 874
Aoyagi, M., 830
Apeloig, Y., 302, 636, 760, 879
Appelman, E. H., 582
Applequist, D. E., 267, 291, 311, 314
Arad, D., 302, 429
Arai, M., 726
Arai, T., 822
Arano, Y., 875
Archie, Jr., W. C., 697
Arduengo, III, A. J., 281
Arens, J. F., 636
Arepalli, S., 378
Arganbright, R. P., 649
Argile, A., 571
Argyropoulos, J. N., 516
Arhart, R. W., 859
Ariel, S., 135
Arigoni, D., 86
Armbruster, C. W., 876
Armit, J. W., 210
Armone, M., 331
Armstrong, K. B., 151
Arnaut, L. G., 812, 832
Arnett, E. M., 18, 19, 420, 431, 880
Arnold, A., 308, 309
Arnold, B., 849

- Arnold, B. J., 880, 881
 Arnold, B. R., 214, 276, 804
 Arnold, D. R., 309
 Arnold, R. T., 685
 Arnold, S. V., 235
 Arrhenius, S., 348
 Arrieta, A., 768
 Asami, M., 879
 Asano, T., 350
 Asaoka, S., 298
 Ashby, E. C., 515–517
 Ashe, III, A. J., 878
 Asimov, I., 3
 Aso, K., 666
 Asvany, O., 290
 Atovmyan, L. O., 62, 872
 Audisio, G., 63
 Auditor, M.-T., 736
 Aue, D., 291, 423
 Auer, A. A., 128
 Auf der Heyde, T., 63
 Ault, A., 82, 96, 435
 Ausloos, P., 295
 Auzzas, L., 873
 Avakian, S., 535
 Avery, M. A., 871
 Avila, D. V., 551
 Avnir, D., 63
 Avouris, P., 3
 Axelsson, B. S., 375, 529
 Aycock, B. F., 591
 Aydin, R., 383
 Ayers, P. W., 771
 Ayoub, R., 876
 Ayres, D. C., 315
 Ayscough, P. B., 259, 875
 Ažman, A., 606
 Azoro, J., 599
 Azumi, T., 795

 Babu, M. K., 880
 Bacaloglu, R., 531
 Bach, R. D., 503, 597, 598, 608, 614, 650, 653, 878
 Bachheti, N., 209
 Bachrach, S. M., 627
 Baciocchi, E., 309, 652, 666
 Back, M. H., 348
 Bader, J. M., 878
 Bader, R. F. W., 8, 40, 233, 235, 461, 683
 Badger, G. M., 202
 Badger, R. C., 650
 Bae, S. Y., 291
 Bae, S.-K., 399
 Baerends, E. J., 232, 236, 312
 Baeyer, A., 123
 Baggott, J. E., 843
 Bahurel, Y., 881
 Bailey, W. F., 130, 319
 Baillargeon, M. M., 587
 Baird, M. S., 752
 Baird, N. C., 218, 874
 Baker, A. D., 32
 Baker, E. B., 296
 Baker, J. W., 502
 Baker, S., 2
 Bakker, M. G., 309
 Bakowies, D., 462
 Balaban, A. T., 201, 202, 211
 Balaji, V., 262
 Baldinger, L. H., 587
 Baldrige, K. K., 206, 383, 880
 Baldwin, J. E., 274, 336, 717, 722, 774, 775, 777, 872, 873, 880
 Balfe, M. P., 480
 Baliah, V., 529
 Ball, R., 879
 Ball, R. G., 556
 Ballard, R. E., 32
 Ballester, M., 258
 Ballhausen, C. J., 4
 Bally, T., 212, 213, 305
 Balogh, D. W., 162, 426
 Balzani, V., 858, 862
 Bamford W. R., 286
 Bamford, C. H., 449, 558, 832
 Bank, S., 270
 Banks, R. B., 63
 Banno, H., 728
 Banthorpe, D. V., 638, 659
 Banwell, M. G., 635
 Bar, R., 533
 Baran, Y., 388
 Barasch, W., 654
 Barbara, P. F., 4, 790
 Barber, J., 862
 Barbosa, A. G. H., 290, 526
 Barclay, L. R. C., 377
 Barczynski, P., 205
 Bard, A. J., 4
 Barden, C. J., 280
 Barić, D., 211
 Barlin, G. B., 118, 414, 876
 Barlow, S. E., 317, 423, 424
 Barnard, M., 881
 Barone, V., 335
 Barra, M., 817
 Barragán, F., 6
 Barrett, A. W., 615
 Barrett, C. J., 858
 Barrett, G. C., 118
 Barron, L. D., 63, 90, 91
 Bartell, L. S., 39, 118, 128, 136, 383
 Bartlett, P. D., 291, 300, 353, 355, 443, 444, 487, 488, 558, 578, 583, 606, 631, 742, 876–878
 Bartlett, W. R., 730
 Bartmess, J. E., 44, 401, 424, 425, 429
 Bartolotti, L. J., 236
 Barton, D. H. R., 113, 119, 128, 134, 272, 554, 667, 682, 687, 874, 879
 Bartsch, R. A., 638, 652, 663
 Bartz, Q. R., 92
 Barzagli, M., 290
 Ba-Saif, S., 458
 Basha, A., 607
 Baskin, J. M., 746
 Baskin, J. S., 833
 Bass, J. D., 841
 Bassani, D. M., 824
 Bassetti, M., 614
 Bassi, P., 611
 Bassindale, A., 65, 126
 Bassler, G. C., 797
 Bastiansen, O., 40
 Bastide, J., 735
 Bastien, I. J., 296
 Bateman, L. C., 479
 Bates, R. B., 315, 320, 880
 Bates, R. G., 414
 Batts, B. D., 385
 Bauder, A., 124
 Bauer, F., 254
 Bauer, S. H., 708
 Bauer, V. J., 124
 Baughan, E. C., 876
 Bauld, N. L., 305, 307, 310, 762
 Bauman, L. E., 128
 Baumann, W., 637
 Bawn, C. E. H., 93
 Beak, P., 337, 607
 Beauchamp, J. L., 580
 Beauchemin, A. M., 842
 Beaudry, C. M., 730
 Bebout, D. C., 291
 Becerra, R., 584
 Beck, B. H., 874
 Becke, A. D., 236, 237
 Becker, A. R., 368
 Becker, H.-D., 799, 812
 Beckett, C. W., 130, 874
 Beckhaus, H.-D., 136, 205, 268
 Beckwith, A. L. J., 273
 Becucci, M., 335
 Bedoukian, P. Z., 878
 Beebe, Jr., T. P., 4
 Beer, M., 795
 Belevskii, V. N., 306
 Belfield, K. D., 774
 Belk, A. J., 841
 Bel-Kassaoui, H., 871
 Bell, R. P., 331, 363, 372, 378, 413, 440, 876
 Bell, T. N., 255
 Bellucci, G., 556–559, 562, 573, 668, 878
 Bellville, D. J., 305, 307, 762
 Belopushkin, S. I., 306
 Beltrán, H. I., 161
 Bemis, A. G., 320
 Ben-Aim, R. I., 345
 Ben-David, I., 582
 Bender, C., 156
 Bender, C. F., 279
 Bender, C. J., 229
 Bender, M. L., 438, 451, 452, 455, 457, 458, 460, 876
 Bender, P., 134
 Bendikov, M., 207
 Benighaus, T., 237
 Benkeser, R. A., 536

- Benkovic, S. J., 455
 Benner, C. W., 724
 Bennet, A. J., 460, 461, 556, 562
 Bennett, G. M., 393
 Bennett, S. W., 669
 Ben-Nun, M., 703, 819
 Beno, B., 736
 Beno, B. R., 724, 773
 Benson, S. W., 10, 13, 16, 23, 268, 583
 Bent, H. A., xvii, 36, 37, 48
 Bentley, K. W., 118
 Bentley, T. W., 459, 477, 478
 Bentzien, J., 829
 Beranek, L., 677
 Beratan, D. N., 88
 Berg, U., 872
 Berger, R., 214
 Berger, S., 375
 Bergman, R. G., 475, 872, 875
 Bergmann, E. D., 250, 620
 Bergmann, I. E., 553
 Bergstrom, F. W., 535
 Berkovitch-Yellin, Z., 91
 Berkowitz, J., 18
 Berliner, E., 524, 529, 559
 Berlman, I. B., 798, 799
 Berman, D. W., 580
 Bernardi, F., 266, 700, 771, 821, 830, 842
 Bernasconi, C. F., 329, 331, 345, 371, 434, 533
 Berneis, H. L., 874
 Bernett, W. A., 29
 Bernstein, H. J., 121
 Berova, N., 89
 Berry, R. S., 128, 541
 Berson, J. A., 202, 356, 492, 727, 742, 751, 752, 771, 774
 Berti, G., 606
 Bertie, J. E., 213
 Bertilsson, S. K., 652
 Bertolucci, M. D., 64, 797
 Bertoncello, P., 208
 Bertozzi, C. R., 746
 Bertrán, J., 454, 500
 Bertrand, G., 278, 280, 281
 Bethell, D., 253, 289
 Betti, M. G., 207
 Beusker, P. H., 879
 Beutelman, H. P., 445
 Beveridge, D. L., 266
 Bevington, J. C., 272, 277
 Beyer, A., 154
 Bharucha, K. N., 872
 Bhattacharyya, D. N., 392
 Biale, G., 639
 Biali, S. E., 116, 132, 134, 874
 Bianchi, G., 388
 Bianchi, R., 159
 Bianchini, R., 556-559, 562, 573, 610, 668, 878
 Bianco, A., 208
 Bickart, P., 84, 86
 Bickelhaupt, F., 285
 Bickelhaupt, F. M., 205, 232, 236, 264, 311, 312, 651
 Biczysko, M., 335
 Biegler-König, F. W., 235
 Bielski, B. H. J., 343
 Bienvenüe-Goëtz, E., 575
 Bierbaum, V. M., 317, 423, 424, 512
 Bietti, M., 309
 Bigam, G., 216
 Bijvoet, J. M., 90
 Billups, W. E., 163
 bin Samsudin, M. W., 881
 Bingham, R. C., 475
 Binsch, G., 62, 96, 874
 Bittman, R., 603
 Bittner, E. W., 375
 Bjurling, P., 375
 Black, K. A., 57, 772
 Blackburn, G. M., 462
 Blackwood, J. E., 77
 Blair, L. K., 426, 428
 Blake, J. F., 512, 762
 Blakemore, P. R., 873
 Blanchard, K. R., 10, 149
 Blanchet, L., 809
 Blanco, M. A., 120, 232
 Blandino, M., 51
 Blanksby, S. J., 16, 268
 Bläser, D., 39
 Blaskó, A., 531
 Blechert, S., 757
 Blomquist, A. T., 164
 Blond, G., 706
 Blowers, P., 365
 Blumberger, J., 462
 Blunck, F. H., 683
 Boand, G., 428
 Bobko, A. A., 258
 Boche, G., 315
 Bochet, C. G., 69, 856, 881
 Bochmann, M., 294
 Bock, C. W., 12, 204
 Bock, H., 32
 Bock, M. G., 654
 Bockrath, B. C., 375
 Bodenstein, M., 345
 Bodwell, G. J., 166
 Boeckmann, J., 67
 Boekelheide, V., 168
 Boens, N., 829
 Boese, R., 39, 874
 Boga, C., 521
 Bogaard, M. P., 90
 Boger, D. L., 876
 Boggs, J. E., 871
 Böhm, S., 389, 401
 Bohme, D. K., 580
 Bohn, R. K., 232
 Bohne, C., 817
 Bökman, F., 418
 Bokser, A. D., 385
 Bollinger, J. M., 556
 Bollyky, L. J., 860
 Bolton, E., 280
 Bolton, J. R., 259, 804
 Bolton, R., 551, 553, 558
 Bonacić-Koutecký, V., 806, 820
 Bonazzi, S., 872
 Bond, D., 46
 Bondi, A., 6
 Bondi, J., 871
 Bondock, S., 839, 840
 Bonham, R. A., 39
 Bonilha, J. B. S., 817, 818
 Bonneau, R., 287, 288
 Boons, G.-J., 746
 Boord, C. E., 682
 Booth, H., 130, 874
 Booth, P., 459
 Boozer, C. E., 382
 Borden, G. W., 854
 Borden, W. T., 166, 212, 215, 724, 771, 772, 773
 Bordner, A. J., 139
 Bordwell, F. G., 309, 401, 422, 424, 438, 516, 642, 643, 644, 876
 Borges dos Santos, R. M., 19, 875
 Borman, S. A., 23, 202
 Born, M., 223, 310
 Borodkin, G. I., 302
 Borosky, G. L., 319
 Bors, D. A., 374, 421, 438
 Bosch, H. W., 86
 Boschan, R., 568
 Bose, D. S., 872
 Bottari, F., 606
 Bottoni, A., 771
 Bouchoux, G., 426
 Bouldin, T. W., 859
 Bouma, W. J., 308
 Bourn, A. J. R., 125
 Bourns, A. N., 683
 Bouwman, W. G., 795
 Bowden, K., 386, 388
 Bowen, E. J., 798
 Bowen, H. J. M., 5
 Bowen, J. P., 135
 Bowers, A., 584
 Bowers, M. T., 291, 423, 424
 Bowman, J. M., 290, 378
 Bowman, N. S., 372
 Bowman, W. R., 543
 Bowry, V. W., 275, 276
 Boyd, D. B., 135, 137, 223, 224
 Boyd, D. R., 393
 Boyd, M. K., 850
 Boyd, R. J., 23, 233, 307
 Boyle, Jr., W. J., 438
 Boys, S. F., 225
 Bozhovskii, V., 692
 Bracker, C. E., 3
 Brader, Jr., W. H., 666
 Bragin, J., 163
 Braida, B., 189
 Braisted, A. C., 736
 Brammer, L., 5

- Branch, G. E. K., 475
 Branchaud, B. P., 275
 Brand, J. C. D., 815
 Brand, M., 580, 878
 Brand, W. W., 529, 877
 Brandl, M., 876
 Brandsma, L., 164, 636
 Braslavsky, S. E., 787, 804
 Bratcher, M. S., 209
 Braton, C. M., 9
 Bratsch, S. G., 23
 Brauman, J. I., 423, 426, 428, 495, 500, 697, 714, 877
 Braun, M., 167
 Brecher, J., 56
 Bredt, J., 162
 Breen, W. H., 619
 Breiner, B., 765
 Breneman, C. M., 40
 Brenna, E., 873
 Brese, N. E., 7
 Breslow, R., 37, 201, 211, 212, 214, 762
 Breton, G. W., 587
 Brett, A. M., 12
 Brett, W. A., 39
 Brettreich, M., 209
 Breuckmann, R., 254
 Breugst, M., 509
 Breuning, M., 872
 Brewster, J. H., 84, 85, 88, 91
 Brewster, P., 92
 Brey, Jr., W. S., 282
 Bright, W. L., 393
 Brill, W. F., 332
 Brimble, M. A., 872
 Brindell, M. C., 668
 Bringmann, G., 872
 Brink, M., 819
 Brinker, U. H., 160, 285, 875
 Briody, J. M., 459
 Briscoe, H. T., 393
 Britton, R., 871, 872
 Broaddus, C. D., 315
 Brocard, J., 753, 880
 Brocksom, T. J., 730, 735
 Brocksom, U., 735
 Broeker, J. L., 841
 Bronowski, J., xi
 Brønsted, J. N., 413, 437
 Bronstein, H. E., 209
 Brooks, B. R., 117, 136, 820
 Brosch, D., 679
 Brotzel, F., 509
 Brown, D. E., 508
 Brown, F., 490, 771
 Brown, H. C., 265, 272, 391, 398, 475, 494, 569, 587, 594, 596, 597, 600, 602, 603, 616, 619, 660, 661, 662, 874, 877, 878, 879
 Brown, J. M., 726, 880
 Brown, Jr., J. F., 448, 449
 Brown, M. E., 357
 Brown, R. D., 179
 Brown, R. F., 877
 Brown, R. S., 331, 455, 460–462, 463, 556, 558, 559, 561–563, 566, 573, 608, 668, 878
 Brown, W. G., 230
 Brownlee, R. T. C., 399
 Brückner, S., 62
 Bruice, T. C., 455, 644
 Brundle, C. R., 32
 Brunton, G., 377
 Brupbacher, T., 124
 Brusse, D., 280
 Bryant, C. J., 872
 Bryce-Smith, D., 843
 Brycki, B. E., 473
 Bubnov, Y. N., 720
 Buchanan, K. J., 357
 Bucher, G., 286
 Büchi, G., 839
 Buchkremer, J., 441
 Buckels, R. E., 486, 584
 Buckingham, A. D., 90
 Buckingham, J., 62
 Buckles, R. E., 579, 584, 878
 Buckner, J. K., 121, 485
 Buda, A. B., 63
 Budavari, S., 82
 Budde, W. L., 615
 Buděšinský, M., 873
 Budzelaar, P. H. M., 163
 Budzikiewicz, H., 306
 Buechele, J. L., 790
 Buenker, R. J., 820
 Buffeteau, T., 872
 Bug, T., 509
 Bühl, M., 39
 Bultinck, P., 872
 Bumgardner, C. L., 622, 635
 Bunce, N. J., 260, 403, 845, 875
 Buncel, E., 310, 311, 313, 315, 320, 339, 371, 375, 384, 389, 399, 420, 423, 512, 531
 Bunch, J. E., 622
 Bunger, W. B., 338
 Bunker, P. R., 279
 Bunnanberg, E., 88
 Bunnnett, J. F., xvi, 344, 345, 434, 453, 504, 528–530, 541, 543, 639, 640, 663, 877, 878
 Buntinx, G., 809
 Bunton, C. A., 455, 531, 671
 Burdett, J. K., 28, 36, 713
 Bures, M. G., 525
 Burger, U., 308, 309, 881
 Burgess, K., 872
 Bürgi, H. B., 626
 Burham, R. L., 584, 878
 Buriks, R. S., 876
 Burk, P., 419
 Burke, P. J., 208
 Burkert, U., 136
 Burkitt, F. H., 193
 Burkoth, T. L., 216
 Burks, E. A., 872
 Burnett, G. M., 843
 Burnett, M. N., 56
 Burnier, J. S., 720
 Burns, C. S., 861
 Buron, C., 281
 Burrell, R. C., 775
 Burton, G. W., 375, 872
 Burton, R. D., 310
 Busca, G., 437
 Buschek, J. M., 562, 878
 Bushweller, C. H., 57, 303, 874
 Buss, J. H., 10
 Busscher, G. F., 636, 879
 Butcher, Jr., J. A., 350
 Butenandt, A., 881
 Butt, G., 388
 Butters, M., 878
 BATTERY, R. G., 285
 Buzek, P., 296, 299
 Byrman, C. P., 419
 Byun, Y.-G., 211
 Cabaleiro, M. C., 878
 Cabral, B. J. C., 19
 Cadogan, J. I. G., 669
 Cahn, R. S., 65, 68, 116
 Calado, A. R. T., 403
 Calaminici, P., 205
 Calder, I. C., 217
 Caldwell, G., 426
 Caldwell, R. A., 820, 824
 Caldwell, S. T., 277
 Callahan, J. J., 529
 Calvert, J. G., 847
 Calvin, M., 19
 Camaioni, D. M., 309
 Cameron, A. F., 118
 Camp, R. N., 329
 Campanelli, A. R., 23, 388
 Campbell, E., 462
 Campion, A., 214
 Camps, P., 874
 Canac, Y., 280
 Cañada, J., 57
 Cane, D. E., 872
 Canepa, C., 878
 Cao, A., 208
 Capellos, C., 343
 Caple, G., 700
 Caple, R., 586
 Capon, B., 435, 446, 447
 Capone, D. L., 867
 Cappel, D., 190
 Carboni, R., 386
 Carcenac, Y., 131
 Cardona, R., 760
 Cardoso, S. P., 526
 Cardwell, H. M. E., 444, 876
 Caress, E. A., 663
 Carey, F. A., 84, 163
 Cargioli, J. D., 420
 Caringi, J. J., 349
 Carlen, C. R., 859

- Carless, H. A. J., 880
 Carlsmith, L. A., 536, 539, 877
 Carlson, H. K., 879
 Carlson, R. M. K., 132
 Carmichael, I., 159
 Carmody, M. J., 215
 Carneiro, J. W. de M., 295, 303, 526, 593
 Carpenter, B. K., 214, 347, 720, 776
 Carpino, L. A., 499
 Carreiro, J. C., 818
 Carrington, A., 261
 Carriolo, J., 456, 511
 Carroll, F. A., 809, 834, 848
 Carroll, M. F., 728, 880
 Carroll, M. T., 8, 233
 Carruthers, W., 735
 Čársky, P., 419
 Carter, E. A., 47, 207
 Carter, G. E., 459
 Carter, J. V., 479
 Carter, R. E., 383
 Carter, R. L., 61
 Carton, P. M., 815
 Carvalho, P. B., 871
 Casanova, J., 163, 298
 Casarini, D., 874
 Case, D. A., 136
 Caserio, M. C., 42, 65, 617
 Casewit, C. J., 136
 Caspar, J. V., 305
 Castañer, J., 258
 Castejon, H., 130, 790
 Castiglioni, E., 873
 Castrillón, J., 85
 Castro, A. M. M., 728
 Castro, C., 216, 769, 770, 880
 Catchpole, A. G., 471
 Catellani, M., 152
 Cater, S. R., 845
 Cavagnat, D., 872
 Cavasotto, C. N., 139
 Cave, R. J., 292
 Cavicchioli, S., 83
 Cederbaum, L. S., 307
 Cedillo, A., 585
 Cee, V. J., 627
 Çelebi-Ölçüm, N., 370
 Celotta, R. J., 3
 Cerichelli, G., 531
 Cerratt, J., 239
 Cerutti, P., 881
 Cha, O. J., 684
 Chadha, M. S., 872
 Chai, J.-D., 237
 Chamberlin, T. C., xvi
 Chambers, R. D., 266
 Chambron, J.-C., 873
 Chamorro, E., 585
 Champion, W. C., 669
 Chan, B., 340
 Chan, J. Y. C., 872
 Chandler, C., 535
 Chandrasekhar, J., 497, 499, 627, 875
 Chandross, E. A., 859
 Chang, C., 8, 233
 Chang, J. A., 877, 881
 Chang, M.-K., 681
 Chanon, F., 305
 Chanon, M., 305, 543, 804
 Chao, I., 63, 858
 Chao, T. H., 265
 Chapman, D. L., 345
 Chapman, J. W., 877
 Chapman, N. B., 528
 Chapman, O. L., 125, 207, 213, 854
 Chappell, G. A., 496
 Charlton, J. C., 490
 Charlton, J. L., 881
 Charton, M., 399, 400
 Chatt, J., 595
 Chattaraj, P. K., 771
 Chattopadhyay, S., 872
 Chaudhuri, N., 285
 Chauvin, R., 7
 Cheeseman, J. R., 8, 233
 Chen, C., 241
 Chen, C.-F., 873
 Chen, J., 830, 852
 Chen, J. C., 3
 Chen, K.-H., 136
 Chen, L., 526, 762
 Chen, M. C., 451, 460, 876
 Chen, X., 624, 877
 Chen, Z., 209, 217, 770
 Cheng, H. N., 751
 Cheng, J.-P., 19, 309, 350, 424
 Cheng, L., 544
 Cheng, P.-C., 871
 Cheng, T.-C., 600
 Cheng, X., 556
 Cheng, Z., 258
 Chérest, M., 624, 626
 Chernick, C. L., 581
 Cherry, W., 266, 825
 Chervin, I. I., 872
 Chi, D. Y., 878
 Chiang, W., 839
 Chiang, Y., 298, 447, 566, 593, 877, 881
 Chiappe, C., 557, 558, 562, 573, 610, 668, 878, 879
 Chickos, J. S., 9, 871
 Chieffi, G., 839
 Chiou, H.-S., 762
 Chipman, D. M., 212
 Chirlă, C. C., 2
 Chittiboyina, A. G., 871
 Chittum, J. W., 872
 Chiu, D. T., 859
 Chloupek, F., 458
 Cho, E. J., 872
 Cho, J. K., 309
 Cho, K., 862
 Cho, S., 459, 876
 Choe, J.-I., 876
 Choe, Y. H., 636
 Choi, H. K. J., 255
 Choi, H. Y., 878
 Choi, S.-C., 274
 Choi, S.-H., 881
 Choi, W. J., 876
 Chopko, E., 166
 Chortyk, O. T., 876
 Chosrowjan, H., 803
 Chou, P. K., 319, 871
 Chow, M.-F., 825
 Chow, Y.-L., 458
 Chretián, J. R., 568
 Christensen, J. J., 429
 Christensen, R. L., 795
 Christl, M., 167
 Chu, Y. C., 509
 Chuchani, G., 683
 Chugaev, L. A., 681
 Chuman, T., 873
 Chung, A. L. H., 218
 Chung, S.-K., 517
 Chung, Y.-S., 736
 Chupka, W. A., 818
 Chupp, J. P., 118, 874
 Church, M. G., 479
 Chuvylkin, N. D., 306
 Chwang, W. K., 566
 Ciamician, G., 834
 Ciana, C.-L., 856
 Cianciosi, S. J., 872
 Cieplak, A. S., 625, 626
 Cinquini, M., 873
 Cioslowski, J., 566
 Cipiciani, A., 873
 Ciula, J. C., 421
 Clairet, F., 424
 Claps, M., 872
 Clar, E., 207, 210
 Clark, D. T., 211, 300
 Clark, J., 385
 Clark, K. B., 826
 Clark, M., 339
 Clark, S. D., 871
 Clark, T., 5, 8, 137, 140, 307, 315, 429
 Clark, W. W., 40
 Clarke, G. A., 474
 Clarke, R. A., 860
 Clegg, W., 752
 Cleland, W. W., 452, 462
 Clemmer, C. R., 4
 Cleveland, T., 29
 Clifford, P. R., 598
 Clippinger, E., 483
 Clive, D. L. J., 875
 Closs, G. L., 212
 Clough, G. W., 472, 877
 Coates, G. W., 93
 Coburn, Jr., J. F., 871
 Cockerill, A. F., 638, 874, 879
 Cocks, A. T., 267
 Coddens, B. A., 503
 Codelli, J. A., 746
 Coffey, P., 26
 Cohen, A. J., 237

- Cohen, D., 533, 876
 Cohen, I., 34
 Cohen, L. A., 399
 Cohen, M., 371
 Cohen, N., 10
 Cohen, S., 276
 Cohen, T., 314
 Coke, J. L., 872
 Cole, Jr., T. W., 162, 387, 853
 Cole, T., 261
 Collin, G. J., 819
 Collins, J. B., 124
 Collins, C. H., 588
 Collins, C. J., 330, 372, 670, 674, 681
 Collins, P. G., 208
 Collis, M. J., 578
 Colonna, S., 872
 Coluccini, C., 874
 Colwell, K. S., 136
 Comisarow, M. B., 490
 Compton, R. N., 87
 Coms, F. D., 254
 Conant, J. B., xvi, 355, 502
 Condon, E. U., 796
 Condroski, K. R., 608
 Conia, J. M., 753, 880
 Conley, R. T., 876
 Conn, J. B., 576
 Connolly, J. S., 804
 Connors, K. A., 342
 Conover, C. D., 636
 Conrad, II, P. G., 856
 Conrad, N. D., 772
 Conroy, H., 880
 Conte, V., 610
 Contreras, R., 585, 771
 Cook, D., 639
 Cook, E. R., 458
 Cook, N. C., 556, 587
 Cooke, Jr., M. P., 621
 Cooks, R. G., 424
 Cookson, R. C., 113, 134, 739, 874
 Cookson, R. F., 414
 Cooley, J. H., 271
 Cooney, R. P. J., 118
 Cooper, C. F., 227
 Cooper, D. L., 47, 205, 223, 239
 Cooper, K. A., 646
 Cooper, P. J., 604
 Cooper, W., 697
 Coote, M. L., 875
 Cope, A. C., 66, 163, 635, 656, 685, 879
 Copley, S. D., 529, 880
 Coppi, L., 559
 Coppinger, G. M., 383
 Corbin, D. R., 305
 Cordero, B., 6
 Cordes, E. H., 447
 Corey, E. J., 163, 841, 857, 881
 Corley, R. C., 277
 Corminboeuf, C., 161, 217, 237
 Cornforth, J. W., 624
 Cornforth, R. H., 624
 Coroneus, J. G., 208
 Corse, J., 490
 Corset, J., 313
 Cortés-Guzman, F., 233
 Cosa, G., 852
 Cossi, M., 566
 Cossio, F. P., 768
 Cossy, J., 269
 Costa Cabral, B. J., 875
 Cotton, F. A., 59, 96
 Cottrell, F. D., 163
 Coughlin, J. M., 879
 Coulson, C. A., 21, 26, 37, 175, 176, 189, 192, 193, 194, 204, 544
 Courtneidge, J. L., 214
 Coward, J. K., 872
 Cowdrey, W. A., 496
 Cox, E. G., 202
 Cox, H. E., 500
 Cox, R. A., 432, 433
 Cox, S. D., 3
 Cozens, F. L., 825
 Cozzi, F., 873
 Crabbé, P., 87, 90
 Crăciun, L., 40
 Craig, D. P., 814
 Craig, L. E., 215
 Craig, N. C., 190, 191
 Craig, S. L., 587
 Cram, D. J., 311, 490, 623, 648, 680, 682, 686, 687, 877
 Cramer, C. J., 151, 221, 313, 627
 Cramer, G. M., 319
 Crampton, M. R., 529
 Crawford, R. J., 315, 726, 876
 Crawford, S. D., 587, 614
 Crawford, T. H., xvii
 Crawford, T. D., 216, 225
 Creary, X., 258, 318
 Credi, A., 858, 862
 Creese, M. W., 683
 Cremades, E., 6
 Cremer, D., 124, 127, 128
 Cribb, B. W., 872
 Crich, D., 272
 Criegee, R., 404, 697, 705, 745
 Crimmins, M. T., 881
 Cristol, S. J., 504, 579, 586, 648, 649, 653, 654, 668, 759, 878, 879
 Croft, A. P., 652
 Cron, J. N., 270
 Crooks, G. P., 529
 Cross, P., 301
 Crowell, T. I., 395, 676
 Cruickshank, D. W., 202
 Cruickshank, F. R., 10, 254
 Csizmadia, I. G., 203, 227
 Csonka, G. I., 237
 Cuddy, B. D., 875
 Cuéllar Ibáñez, L., 584
 Cuevas, G., 57, 151, 232
 Cui, C., 859
 Cui, X.-L., 878
 Cundall, R. B., 843
 Cupas, C. A., 159
 Curran, D. P., 272, 872
 Curran, T. C., 459
 Current, S., 772
 Curtin, D. Y., 314, 358, 684, 879, 880
 Curtis, J., 148
 Curtiss, L. A., 226
 Custance, O., 3
 Cutting, J., 274
 Cvačka, J., 873
 Cvetković, D., 245
 Cyrański, M. K., 203
 Cyvin, S. J., 210, 874, 875
 Cywin, C. L., 77, 872
 Czarnik, A. W., 736, 859
 D'Auria, M., 839
 da Costa, A. B., 818
 Dabbagh, H. A., 683, 687
 Dagoni, R., 98
 D'Agostino, J., 819
 D'Agostino, J. T., 806
 Dahlke, G. D., 319
 Dai, H., 208
 Daino, Y., 830
 Dalton, J. C., 815, 881
 Damewood, Jr., J. R., 84
 Damrauer, R., 317, 423
 Dandapani, S., 872
 Danen, W. C., 267, 543
 Daniel, D. S., 730
 Dannenberg, J. J., 268
 Danovich, D., 309
 Dantus, M., 2
 Daoust, K. J., 164, 706
 Darby, N., 216
 Darsley, M. J., 459
 Das, P. K., 850
 Dasgupta, S., 132
 Datta, D., 151
 Dauben, W. G., 119, 625, 826
 Daudel, R., 227
 Daum, P. H., 460
 Daus, K. A., 587
 Dávalos, J. Z., 302
 Davidson, E. R., 212, 223, 224, 292, 308, 771
 Davidson, R. B., 387
 Davies, A. G., 214
 Davies, H. M. L., 855
 Davies, T. M., 544
 Davies, T. S., 862
 Davis, B. H., 677, 683, 687
 Davis, E. R., 277
 Davis, F. A., 873, 880
 Davis, H. E., 10, 871
 Davis, H. S., 555
 Davis, Jr., J. C., 26
 Davis, R., 877
 Davis, R. D., 824
 Davis, R. E., 507
 Davlieva, M. G., 330
 Dawes, K., 815, 881

- Dawson, H. M., 436, 456
 Day, L. S., 336
 De Angelis, F., 645
 de Boer, J. L., 65
 de Bruijn, P., 636, 879
 De Feyter, S., 833
 de Groot, A., 682
 de Groot, F. M. H., 636, 879
 de Jong, F., 499
 De Keukeleire, D., 853, 861
 de la Mare, P. B. D., 500, 501, 519, 551, 553, 578, 579, 872
 de Lange, B., 873, 876
 de Leeuw, F. A. A. M., 152
 De Lucia, F. C., 40
 de Mayo, P., 272, 492, 700
 de Meijere, A., 162, 237, 757, 853
 de Pascual-Teresa, B., 736
 De Proft, F., 236, 272, 765, 771
 de Queiroz, J. F., 526
 de Rossi, R. H., 543
 de Saint Laumer, J.-Y., 861
 De Schryver, F. C., 829
 De Silva, K. M. N., 159
 de Visser, S. P., 276
 De Vleeschouwer, F., 272
 de Wolf, W. H., 285
 Deardurff, L. A., 387
 DeBoer, C. D., 353, 879
 DeClue, M. S., 880
 Decouzon, M., 418
 Dedieu, A., 496
 Deeg, A., 613
 DeFellipis, J., 163
 DeFrees, D. J., 301
 Deiters, U. K., 772
 Dejaegere, A., 366
 Dekker, C., 208
 Dekkers, H. P. J. M., 811
 Del Bene, J., 34
 Del Sesto, R. E., 159
 Del Vecchio, E., 521
 Delaude, L., 524
 Delbecq, F., 241
 DeLeon, E. L., 130
 Delgado, O., 871
 Della, E. W., 512
 Dell'Erba, C., 530
 DelMonte, A. J., 772
 Demange, L., 858
 DeMeester, W. A., 621
 DeMello, N. C., 608
 DeMember, J. R., 298
 Dempsey, B., 414
 Demuth, M., 305
 Denegri, B., 513
 Denekamp, C., 118
 Deng, J., 880
 Deng, K., 314
 Deniz, A. A., 849
 Denney, D. B., 873
 Deno, N. C., 432, 520, 594
 Denot, E., 584
 Deprés, J.-P., 96, 873
 DePriest, R. N., 515, 517
 DePuy, C. H., 317, 423, 424, 512, 648, 650, 659, 681
 Dermer, O. C., 76
 Descotes, G., 881
 Deshpande, A. K., 517
 Deslongchamps, P., 151
 Després, A., 798
 Dessy, R. E., 615
 DeTar, D. F., 459
 Detert, H., 557
 Devi, R. R., 872
 Devlin, F. J., 872
 Devlin, J. P., 118
 Dewar, M. J. S., xvii, 34, 149, 195, 214, 215, 218, 223, 227, 262, 363, 564, 604, 764, 769, 770, 771
 DeWolfe, R. H., 472
 Deyà, P. M., 749
 Deyhimi, F., 160
 DeYoung, S., 559
 Deyrup, A. J., 430
 Dhar, M. L., 633, 646, 655, 878
 Dhe-Paganon, S., 459, 876
 Dhimitruka, I., 258
 Dias, J. R., 242
 Diau, E. W.-G., 833
 Díaz, J. F., 820
 Dickshat, J. S., 872
 Dickstein, J. I., 619
 Diederich, F., 63, 136
 Diedrich, C., 872
 Diedrich, M. K., 762
 Diels, O., 731, 735
 Dietrich-Buchecker, C., 67, 350
 Dietze, P. E., 671, 876
 DiGiacomo, P. M., 666
 DiGiorgio, V. E., 815
 DiLabio, G. A., 268
 Dillard, L. W., 873
 Dilling, W. A., 829
 Dillon, R. T., 554
 Dinné, E., 700
 Dinnocenzo, J. P., 305, 306, 309
 Dinur, U., 137
 Disch, R. L., 167
 DiStasio, Jr., R. A., 237
 Ditchfield, R., 12
 Diter, P., 131
 Dittmer, D. C., 508
 Dixon, R. N., 848
 Djazi, F., 426
 Djerassi, C., 88, 90, 306
 Dobosh, P. A., 266
 Dockendorff, C., 741, 880
 Dodd, J. S., 71
 Dodziuk, H., 68
 Doecke, C. W., 426
 Doering, W. v. E., 214, 285, 481, 722, 726, 743, 749, 773, 871, 876, 879
 Doetschman, D. C., 281
 Doherty, R. M., 478
 Dohner, B. R., 650
 Doi, Y., 209
 Doig, S. J., 700
 Dolbier, Jr., W. R., 266, 592, 873
 Dolbier, W. R., 551
 Dolphin, D., 856
 Domcke, W., 307, 849
 Domenicano, A., 23, 388
 Domenick, R. L., 375, 382
 Dommen, J., 124
 Donald, L., 849
 Donaruma, L. G., 410
 Dondi, D., 853
 Dong, F., 290
 Dong, Y. J., 383
 Donnadieu, B., 280
 Donnay, R. H., 561
 Donnelly, R. A., 23
 Donohue, J., 5
 Dooley, K. C., 829
 Doorakian, G. A., 699
 Dopfer, O., 295
 Dorko, E. A., 212
 Dornan, P., 842
 Dory, Y. L., 762
 Dostrovsky, I., 490, 670, 671
 Dotterer, S. K., 528
 Douberly, G. E., 294
 Doubleday, C., 777
 Doubleday, Jr., C., 329, 858
 Dougherty, C. M., 316
 Dougherty, D. A., 254
 Dougherty, R. C., 34, 227, 363
 Doughty, M. A., 480
 Dowd, P., 212, 274, 752
 Dowell, Jr., A. M., 283, 634
 Downer, E. A. W., 480
 Downes, T. M., 440
 Doyle, M. P., 53
 Dragoset, R. A., 3
 Drake, B. V., 739
 Dreger, L. H., 124
 Dresselhaus, M. S., 209
 Drew, R., 872
 Drewes, R., 774
 Drumheller, J. D., 876
 Du, Y., 834
 Duan, J.-X., 873
 Duarte, L. D. A., 877
 Dubac, J., 751
 Dubois, J.-E., 443, 557, 561, 568, 571, 575
 Duddey, J. E., 609
 Duerr, B. F., 736
 Duffey, G. H., 31
 Dugave, C., 858
 Duhaime, R. M., 842
 Dujardin, G., 3
 Duncan, M. A., 294
 Dunitz, J. D., 59, 202, 383, 626
 Dunkelblum, E., 604
 Dunkin, I. R., 213
 Dunn, T. M., 519
 Dunnavant, W. R., 318

- Dunning, Jr., T. H., 240
 Duong, H. M., 207
 Dupont, W., 274
 DuPré, D. B., 280
 Dupuis, M., 566
 Durig, J. R., 150
 Durkin, K. A., 227
 Dürr, H., 741, 858
 Durst, T., 310, 311, 313, 315, 320, 420, 423, 881
 Dust, J. M., 310
 Dux, W., 345
 Dwight, S. K., 598
 Dyachenko, O. A., 62, 872
- Eaborn, C., 669
 Earl, G. W., 544
 Eaton, H. L., 240
 Eaton, P., 762
 Eaton, P. E., 162, 166, 841, 853, 873
 Eberlin, M. N., 526
 Ebersson, L., 257, 277, 525
 Eberz, W. F., 592
 Ebrahimi, A., 151, 160
 Echenique, P., 223
 Echeverría, J., 6
 Ecke, G. G., 556, 587
 Eckell, A., 746
 Eckert-Maksić, M., 3
 Edge, R., 277
 Edgcombe, K. E., 23
 Edgell, R. G., 287
 Edgeworth, J. P., 208
 Edward, J. T., 423
 Edwards, C. R., 856
 Edwards, J. O., 404, 504, 505, 506, 507, 512
 Egger, K. W., 267
 Eggers, M., 867
 Egolf, D. A., 22
 Ehrenson, S., 399
 Eichelberger, L., 554
 Eichhorn, C., 495
 Eilers, J. E., 137
 Eisenberg, W., 881
 Eisenstein, O., 626
 Eisenthal, K. B., 278
 Ekkehard, W., 880
 Eksterowicz, J. E., 841
 El-Alaoui, M., 443
 Elango, M., 771
 Elbert, J. E., 822
 Elder, P. W., 862
 El-Idreesy, T. T., 852
 Eliel, E. L., 53, 57, 85, 86, 88, 96, 97, 113, 120, 124, 132, 231, 265, 360, 494, 503, 515, 552, 624, 874
 Elings, V. B., 3
 Ellingsen, T., 499
 Elliott, M. C., 878
 Ellison, G. B., 16, 18, 265, 268, 310, 424
 Ellzey, Jr., M. L., 241
 Elrod, J. P., 380
 El-Sayed, M. A., 790
- Elsey, G. M., 867
 Elsheimer, S., 592
 Emanuele, L., 839
 Emmel, R. H., 295
 Endo, M., 209
 Endo, Y., 120
 Engberts, J. B. F. N., 762
 Engelking, P. C., 265, 310
 Engelmann, H., 589
 Engels, B., 331
 England, W., 47
 England, W. P., 724
 Engler, E. M., 12, 136, 159
 Ensing, B., 462
 Epiotis, N. D., 240, 266, 724
 Erickson, J. A., 841
 Erickson, K. L., 164
 Eriksen, T. E., 859
 Eriksson, L. A., 307
 Erman, W. F., 315
 Ertl, P., 418
 Ervin, K. M., 424
 Esaka, M., 209
 Eschenmoser, A., 371, 607, 729
 Espenson, J. H., 342, 438
 Espinosa, E., 873
 Espy, H. H., 666, 879
 Ess, D. H., 370, 745, 746
 Esser, B., 166
 Estes, D., 316
 Esteves, P. M., 290, 291, 526
 Estiu, G., 462
 Ettayeb, R., 543
 Ettl, R., 63
 Eubanks, J. R. I., 665
 Euranto, E. K., 449, 450
 Evanochko, W. T., 212
 Evans, A. A., 480
 Evans, C. A., 277
 Evans, D. A., 608, 627, 728
 Evans, D. F., 801
 Evans, J. C., 653
 Evans, M. G., 363, 763
 Evans, T. W., 589
 Evanseck, J. D., 285, 286, 512, 702, 709
 Evenson, K. M., 279
 Everett, J. R., 130, 874
 Evidente, A., 872
 Evleth, E. M., 566
 Exner, O., 388, 389, 401, 402, 418, 419
 Eyring, H., 25, 176
- Fabian, M. A., 151, 874
 Facelli, J. C., 214
 Fager, E. W., 619
 Fagin, A. E., 500
 Fagnoni, M., 853
 Fahey, R. C., 380, 552, 569, 576, 579, 586, 588, 611, 612, 878
 Fahlman, A., 32
 Fahrenholtz, S. R., 663
 Failes, R. L., 677
- Fainberg, A. H., 477, 479, 483
 Fallah-Bagher-Shaidaei, H., 217
 Falvey, D. E., 256
 Fan, F.-R. F., 4
 Fan, W.-Q., 487
 Fang, J., 871
 Fang, W., 871
 Fanta, P. E., 879
 Fara, D. C., 338
 Fărcașiu, D., 159, 298
 Farid, S., 306, 803, 804
 Farina, M., 63, 93
 Farone, W. A., 360
 Farooq, S., 607
 Farrar, C. R., 459
 Farrell, P. G., 328
 Farrington, G., 815
 Fassberg, J., 331, 533
 Faulkner, D. J., 730
 Faulkner, T. R., 90
 Faust, R., 205
 Favorskii, A., 692
 Fawcett, F. S., 162
 Fayer, M. D., 120
 Fedorov, D. G., 229
 Fehlner, T. P., 605
 Feiring, A. E., 592
 Felder, T., 383
 Felix, D., 729
 Felkin, H., 624, 626
 Feller, D., 190, 224, 308, 771
 Fenet-Buchholz, J., 874
 Feng, X., 473
 Fennen, J., 724
 Ferguson, L. N., 40
 Feringa, B. L., 858, 873, 876
 Fernandes, P. A., 237
 Fernández, I., 294
 Fernández-Alonso, M. C., 57
 Fernández-Ramos, A., 347
 Fernández-Sánchez, J. M., 122
 Ferrão, M. L. C. C. H., 9, 871
 Ferreira, M. L., 735
 Ferreira, R., 36
 Fersht, A. R., 458
 Fessenden, R. W., 261, 266, 815
 Fevig, T. L., 272
 Field, K., 356
 Field, L. D., 290, 875
 Field, M. J., 771
 Fields, T. R., 825
 Fieser, L. F., 79, 670
 Fieser, M., 79, 670
 Fife, T. H., 438, 448, 459
 Filippi, A., 388
 Filley, J., 512
 Finn, M. G., 746
 Finston, H. L., 413
 Firestone, R. A., 880
 Fischer, A. T., 87
 Fischer, E., 92
 Fischer, H., 240, 617
 Fischer, I., 26, 331

- Fisher, G. S., 875
Fisher, W. F., 387
Fisk, J. S., 753
Fitjer, L., 132, 872, 875
Fitzgerald, P. H., 593
Fitzwater, S., 136
Flanagan, H. L., 383
Fleming, F. P., 290
Fleming, I., 197, 621, 761
Fletcher, D., 9, 871
Fletcher, J. H., 76
Fletcher, J. S., 209
Fletcher, M. T., 872
Fletcher, R. S., 475
Fliszár, S., 876
Florio, S., 531
Floris, B., 614
Floss, H. G., 654, 873
Flowers, D. L., 134
Flowers, II, R. A., 18
Flurchick, K., 236
Flurry, Jr., R. L., 34, 175
Flürscheim, B., 257
Flygare, W. H., 118
Foces-Foces, C., 871
Fokin, A. A., 162, 237
Fonken, G. J., 625, 700, 829
Font, J., 153
Foord, J. S., 287
Foote, C. S., 136, 852
Forber, C. L., 403
Forbes, G. S., 583
Forbes, M. D. E., 861
Ford, G. P., 678
Ford, R. A., 259, 343, 508, 787, 789
Ford, W. T., 639
Foresman, J. B., 818, 832
Forlani, L., 521
Forman, M. A., 166
Formosinho, S. J., 812, 832
Forni, A., 62
Forrester, A. R., 257
Forrester, J. D., 91
Forrester, J. L., 584, 878
Forsén, S., 443
Förster, T., 802, 812, 813
Forsyth, D. A., 295, 296, 317
Fossey, J., 257
Foster, J. P., 226
Foster, R., 230
Foster, T. T., 685
Fouad, F. M., 328
Fowden, L., 501
Fowler, J. S., 506
Fowler, P. W., 735
Fox, D. J., 308
Fox, K. M., 873
Fox, M. A., 241, 320, 543, 760, 804
Fox, R. B., 76
Fraenkel, G., 313, 316, 583, 878
Francisco, E., 120, 232
Francke, W., 872
Frank, D., 853
Franklin, J. L., 10, 204
Fráter, G., 877, 879
Fravel, Jr., H. G., 825
Freccero, M., 608
Freed, K. F., 794
Freedman, H. H., 699
Freedman, T. B., 90, 872
Freeman, F., 227
Freeman, P. K., 586
Freilich, S. F., 838
Freitas, M. P., 150
French, D., 582
Frenking, G., 19, 42, 189, 190, 203, 294
Freundlich, H., 489
Frey, H. M., 127, 880
Frey, T. G., 452, 619
Fridman-Marueli, G., 207
Friedl, Z., 388
Friedman, L., 287, 678, 875
Friedman, M., 881
Friel, C., 795
Frimer, A. A., 851
Fringuelli, F., 735, 873
Frisch, M. A., 124
Frisch, M. J., 449
Frišćić, T., 857
Fritsch, F. N., 40
Froemsdorf, D. H., 659, 661
Frohardt R. P., 92
Frommer, J., 3
Frontera, A., 749
Fronza, G., 85
Frost, A. A., 198, 345, 434, 876
Fry, A., 375, 603, 665
Fry, J. L., 875
Frye, S. V., 624
Fu, G. C., 608
Fu, Y., 275
Fuchs, R., 389
Fueno, T., 878
Fuentelba, P., 771
Fuganti, C., 85, 873
Fujimoto, H., 758
Fujimura, Y., 849
Fujita, M., 164, 762
Fujita, S., 100
Fujiwara, K., 159
Fukano, M., 857
Fukui, K., 553, 567, 756, 758
Fukumura, H., 795
Fukushi, E., 872
Fukuzumi, S., 558
Funai, A., 872
Furrer, H., 705
Furtula, B., 211, 874
Fusari, S. A., 92
Fusco, S., 683
Fuson, R. C., 621
Fuß, W., 830
Gabelica, V., 299
Gademann, K., 872
Gadru, K., 516
Gagosian, R. B., 881
Gajek, K., 726
Gajewski, J. J., 139, 724, 726, 727, 772
Gakh, A. A., 159
Gal, B., 555
Gal, J., 85
Gal, J.-F., 418, 424
Galabov, B., 502
Galasso, V., 159
Gall, J. S., 498
Galland, B., 561, 566, 878
Galli, C., 528, 878
Gallo, A., 166
Gallou, I., 872
Gallup, G. A., 47, 239
Galow, T. H., 873
Galván, M., 585
Gandini, A., 879
Gandolfi, R., 608
Ganellin, C. R., 66
Ganem, B., 872
Gangemi, F., 873
Gangemi, R., 873
Ganguly, S., 559
Gano, J. E., 165, 288, 881
Gao, J., 232, 500, 512, 817
Gao, X., 857, 872
Gao, Y., 305
Garbisch, Jr., E. W., 529, 877
García, B., 877
Garner, D. S., 512
Garnier, F., 557, 561
Garratt, D. G., 553
Garratt, P. J., 217
Garratt, S., 294
Garrett, B. C., 377, 378
Garst, J. F., 220
Gaspar, P. P., 278
Gasparac, R., 209
Gatti, F. G., 873
Gattin, Z., 877
Gatzke, A. L., 380
Gaudry, M., 872
Gauglhofer, J., 598
Gauld, J. W., 306
Gäumann, T., 428
Gauss, J., 124, 128, 490
Gawronski, J. K., 872
Gazit, A., 534
Geanangel, R. A., 295
Gebicki, J., 331
Geckle, M. J., 313, 316
Gedye, R., 562, 878
Geerlings, P., 236, 272, 765, 771
Geertsema, E. M., 858
Gelius, U., 32
Geluk, H. W., 875
Gemmer, R. V., 772
Genaux, C. T., 697
Geoghegan, Jr., P., 596, 878
George, M. V., 881
George, P., 12, 204

- Georges, M., 271
 Georgiadis, R., 429
 Georgian, V., 161
 Gerlach, H., 871
 Germann, F. E. E., 803
 Gerratt, J., 47, 205
 Gerson, F., 308, 309
 Geudtner, G., 205
 Ghosh, A. P., 790
 Gibian, M. J., 277
 Gielen, M., 83
 Giese, B., 272, 551, 856
 Gilbert, A., 843, 881
 Gilbert, H. F., 345
 Gilbert, J. C., 284
 Gilbert, K. E., 139
 Gilchrist, T. L., 278
 Gilkey, W. A., 535
 Gill, G., 132
 Gilles, M. K., 424
 Gillespie, R. J., 3, 36, 44
 Gillies, C. W., 735, 746
 Gillies, J. Z., 735
 Gilliom, R., 377
 Gillmore, J. G., 276
 Gilman, H., 535, 536
 Ginsburg, D., 620
 Giordano, C., 83, 559
 Giovenzana, T., 873
 Giri, S., 771
 Givens, R. S., 856
 Gjuranović, Ž., 877
 Gladstone, M. M., 589
 Gladys, C. L., 77
 Gladysz, J. A., 168
 Glaser, R., 528
 Glass, D. S., 700
 Glass, M. A., 63
 Glasson, W. A., 457
 Glattfeld, J. W. E., 872
 Glatthar, R., 856
 Gleghorn, J. T., 526
 Gleicher, G. J., 218, 291, 475
 Gleiter, R., 166, 168
 Glendening, E. D., 126
 Glenn, A. G., 275, 276
 Glick, M. D., 614
 Glukhovtsev, M. N., 161, 212, 306, 532, 608, 878
 Gnanasekaran, C., 880
 Gobbi, A., 189
 Göbel, L., 872
 Göbel, M. W., 459
 Goddard III, W. A., 47, 132, 136, 240, 298, 771
 Goebel, P., 871
 Goedken, V. L., 872
 Goeke, A., 877
 Goel, A., 872
 Goel, A. B., 515
 Goer, B., 298
 Goering, H. L., 134, 482, 591, 666, 879
 Goetz, J. M., 620
 Goh, M. C., 3
 Gojak, S., 211, 874
 Golan, O., 116, 132, 874
 Gold, A., 752
 Gold, V., 289, 385, 456, 594
 Goldberg, N., 610
 Goldblatt, L. A., 875
 Golden, D. M., 10
 Golden, R., 386
 Golding, B. T., 726
 Goldsmith, B. R., 208
 Goldsworthy, L. J., 393
 Gollnick, K., 852
 Golob, A. M., 728
 Gomberg, M., 257, 578
 Gomes, J. A. N. F., 203
 Gómez, B., 771
 Gómez, V., 6
 Gómez-Sandoval, Z., 205
 Gong, X., 526
 Gontarz, J. A., 598, 599
 Gonzales, J. M., 364
 González Moa, M. J., 235
 Gonzalez, C., 608
 Goodfriend, P. L., xvii
 Goodman, J. L., 306, 804, 824
 Goodman, J. M., 159, 160
 Goodman, L., 120, 150, 232, 568
 Goodman, M., 93
 Goosen, A., 357
 Gordon, A. J., 259, 343, 508, 787, 789
 Gordon, J. T., 844
 Gordon, M., 860
 Gordon, R. J., 378
 Goren, Z., 116, 134, 874
 Gorenstein, D. G., 528
 Gorman, S. P., 856
 Gornitzka, H., 281
 Gortatowski, M. J., 879
 Göth, H., 881
 Goto, H., 873
 Gotta, M. F., 509
 Gottlieb, L., 118
 Gould, C. W., 575
 Gould, E. S., 327, 490, 660
 Gould, I. R., 306, 803, 804
 Gould, S. A. C., 3
 Goumont, R., 531
 Gouverneur, V. E., 736
 Govind, N., 232
 Gowenlock, B. G., 349
 Goyal, R. N., 209
 Gozzi, D., 208
 Grabowski, J. J., 512
 Graeffe, A. F., 496
 Graham, G. D., 604
 Grainger, R. S., 879
 Graña, A. M., 235
 Granger, M. R., 873
 Granito, C., 531
 Grant, D. M., 148, 214
 Grant, T. N., 880
 Grashey, D., 746
 Grasley, M. H., 282
 Grasselli, P., 85
 Grassi, G., 124
 Grassner, H., 876
 Gray, H., xvii
 Gray, D., 856
 Grdinic, M., 586
 Green, J. C., 294
 Green, N. J. B., 810
 Greenberg, A., 8, 9, 51, 137, 158, 159, 163, 267, 278
 Greenblatt, J., 636, 879
 Greene, B. L., 843
 Greene, F. D., 439, 623, 648, 844
 Greene, Jr., G. H., 387
 Greene, T. W., 856
 Greenwald, R. B., 636
 Greenwood, F. L., 880
 Greenzaid, P., 440
 Greer, A., 851, 852
 Greiveldinger, G., 872
 Grev, R. S., 121
 Grice, M. E., 23
 Gridnev, I. D., 720
 Griesbeck, A. G., 839, 840, 852, 853, 872
 Griesgraber, G., 872
 Griffin, A. C., 771
 Griffin, C. E., 881
 Griffin, G. W., 162, 167
 Griffiths, J.-P., 287
 Grifoni, M., 208
 Griller, D., 267, 273, 275, 281, 287, 377
 Grimme, S., 235, 237, 872
 Grimme, W., 700
 Griswold, A. A., 854
 Griswold, P. H., 619
 Grob, C. A., 636, 637
 Groner, P., 191
 Gronert, S., 14, 269, 317, 421, 423, 424, 500, 652
 Gross, M. H., 875
 Grossi, L., 531
 Grostic, M. F., 586
 Grovenstein, Jr., E., 877, 879
 Groves, J. T., 211
 Grubbs, E. J., 387, 388
 Gruber, G. W., 880
 Grubert, L., 160
 Grunewald, G. L., 828
 Grunwald, E., 352, 477, 486, 488–490, 544, 672
 Grutzner, J. B., 313, 576
 Gschwend-Steen, K., 729
 Gu, H., 150
 Gu, Z., 208
 Guan, S., 636
 Guarnieri, F., 117
 Guénard, D., 55
 Guéritte-Voegelien, F., 55
 Guerra, C. F., 311, 312
 Guest, M. F., 771
 Guida, W. C., 147
 Gulder, T. A. M., 872

- Guldi, D. M., 208, 209
 Gundermann, K.-D., 859
 Guner, O. F., 762
 Günther, H., 383
 Guo, B.-Z., 446
 Guo, H., 455
 Guo, J., 746, 833
 Guo, Q.-X., 275, 402
 Guo, W., 350
 Gupta, K. S., 434
 Gupta, V. K., 209
 Gupta, Y. K., 434
 Gurjar, M. K., 872
 Gurskii, M. E., 720
 Gurumurthy, R., 516
 Gusev, D. V., 162
 Gust, D., 804
 Gustafson, S. M., 772
 Guthrie, J. P., 440, 453, 460
 Guthrie, R. D., 257, 450, 471, 472, 552
 Gutman, D., 18, 268
 Gutman, I., 179, 210, 211, 245, 874, 875
 Gutsche, C. D., 876
 Güttinger, S., 872
 Guzman, J., 380
 Gwaltney, S. R., 526
 Gwinn, W. D., 39

 Ha, C., 276
 Haasnoot, C. A. G., 152
 Haberfield, P., 459
 Habibi, S. M., 151
 Habibollahzadeh, D., 19
 Hadad, C. M., 40, 818, 832
 Haddon, R. C., 209, 280
 Haesler, J., 69
 Haffner, C. D., 724
 Hafner, K., 724
 Hagen, E. L., 303
 Hagen, S., 209
 Hagiwara, S., 830
 Hagler, A. T., 135, 137
 Haiduc, I., 312
 Hain, J. M., 834
 Hajee, C. A. J., 67
 Hakushi, T., 163, 825, 830, 880
 Hale, P. D., 822
 Halevi, E. A., 85, 380, 382
 Haley, M. M., 163
 Halgren, T. A., 139
 Hall, G. V., 436
 Hall, M. B., 36
 Hall, R. E., 479
 Hall, W. K., 878
 Hallé, J.-C., 531
 Haller, I., 829
 Halpern, A. M., 126, 812
 Halpern, H. J., 258
 Halpern, J., 597, 878
 Halpern, Y., 298
 Halterman, R. L., 873
 Hamai, S., 801
 Hamblin, M., 852

 Hameka, H. F., 29
 Hamill, H., 62
 Hamilton, J. G., 40
 Hamilton, T., 566
 Hamilton, T. P., 566
 Hammar, W., 596, 878
 Hammarström, L.-G., 872
 Hammer, J. D., 130
 Hammerich, O., 305
 Hammett, L. P., 360, 390, 430, 470, 481, 592
 Hammond, G. S., xvii, 278, 353, 362, 588, 787, 824, 831, 840, 847, 848, 859, 879
 Hammonds, K. D., 154
 Hamon, M. A., 280
 Hamrin, K., 32
 Han, C.-C., 423
 Han, H.-J., 399
 Han, I. S., 291
 Han, J. T., 862
 Han, L.-B., 878
 Han, N., 859
 Han, Z., 872
 Hanack, M., 115, 532, 609
 Hâncu, D., 298
 Handoo, K. L., 645
 Hanessian, S., 873
 Hang, C., 852
 Hanhart, W., 657
 Hannay, N. B., 312
 Hansch, C., 393, 400, 404
 Hansell, D. P., 512
 Hansen, D. E., 345
 Hansen, H.-J., 722, 880
 Hansen, L. D., 429
 Hansen, P. J., 242
 Hansma, P. K., 3
 Hanson, C., 486
 Hanson, K. R., 72, 96
 Hanson, P. R., 873
 Hansrote, Jr., C. J., 395
 Hanzlik, R. P., 375, 378, 607
 Hao, S., 10, 871
 Harada, N., 873, 876
 Harada, T., 320
 Harbison, K. G., 528
 Harcourt, A. V., 405
 Harding, C. J., 687
 Hargittai, I., 3, 23, 189
 Harirchian, B., 762
 Harlow, R. L., 281
 Harmony, M. D., 5, 874
 Harms, K., 315
 Harrelson, Jr., J. A., 424
 Harris, D. C., 64, 797
 Harris, H. C., 459
 Harris, H. P., 499
 Harris, J. M., 368, 478, 479, 485, 504
 Harris, K. D. M., 57
 Harris, N. J., 727
 Harris, R. L., 528
 Harrison, A. G., 424, 877
 Harrison, R. G., 638
 Hartley, R. C., 277

 Hartter, D. R., 431, 672
 Harvey, J. T., 519
 Harvey, N. G., 19
 Hase, W. L., 350, 495
 Haselbach, E., 305
 Hashizume, M., 209
 Haskell, T. H., 92
 Hassel, O., 128
 Hasselmann, D., 774
 Hati, S., 151
 Hattori, Y., 62
 Haubrich, J. E., 814, 826
 Haufe, G., 826
 Haugen, G. R., 10
 Haumann, T., 874
 Hause, N. L., 648, 649, 878
 Hauser, C. R., 318, 876, 877
 Hautala, J. A., 401
 Hautala, R., 815
 Hawkes, S. J., 414
 Hawkins, C. M., 724, 726
 Hawkins, J. M., 63
 Hawkinson, D. C., 876
 Haworth, C. A., 2
 Haworth, W. N., 113
 Hay, J. M., 257
 Hay, P. J., 240
 Hayama, T., 383
 Hayashi, S., 872
 Hayashi, T., 209, 872
 Hazzard, B. J., 20
 He, J., 551
 He, S.-L., 853
 He, X., 276
 Head, N. J., 490
 Head-Gordon, M., 237, 526
 Healy, E. F., 223, 771
 Heathcock, C. H., 85, 620, 626
 Heatley, F., 9, 871
 Hebel, D., 582
 Heckel, A., 859
 Hedberg, K., 3, 40, 128, 150, 874
 Heeb, L. R., 849
 Hegemann, I., 290
 Hehre, W. J., 12, 292, 295, 380
 Heidelberger, M., 215
 Heilbronner, E., 59, 202, 765
 Heimgartner, H., 880
 Heine, T., 161
 Heitkamp, J. J., 215
 Heitler, W., 25
 Hekkert, G. L., 86
 Heldt, W. Z., 410
 Heller, A., 672
 Heller, C., 261
 Helmchen, G., 84
 Helmreich, R. F., 653
 Hendrickson, J. B., 133
 Hengge, A. C., 335
 Henne, A. L., 588
 Henneke, H. F., 598
 Hennion, G. F., 587
 Henrichs, M., 313

- Henrichs, P. M., 459
 Henri-Rousseau, O., 395, 735
 Henry, J. B., 873
 Hepner, F. R., 598
 Herderich, M. J., 867
 Herek, J. L., 742
 Herges, R., 769, 770
 Hering, N., 509
 Hernandez, J. A., 683
 Hernandez, S. M., 164
 Hernández-Trujillo, J., 233
 Herndon, W. C., 227, 241, 242, 245, 771
 Herrebout, W., 872
 Herres, J. P., 166
 Herrmann, A., 861
 Herschbach, D. R., 46
 Hersh, W. H., 647
 Hess, Jr., B. A., 212, 218, 566, 716, 717, 880
 Hess, K., 615, 769
 Hesse, D. G., 9
 Heubes, M., 872
 Hewitt, J. M., 313
 Hey, D. H., 589
 Heyerick, A., 861
 Hiatt, R. R., 268, 353
 Hiberty, P. C., 27, 205, 240, 241, 419, 500
 Hill, B. T., 255
 Hill, K. W., 736
 Hill, R. K., 654, 735, 876
 Hill, R. R., 88
 Hill, T. L., 135
 Hill-Cousins, J., 878
 Hillier, I. H., 9, 771, 871
 Hilvert, D., 109, 736, 873, 880
 Himeshima, Y., 527, 877
 Hinckley, Jr., J. A., 589
 Hine, J., 278, 283, 311, 429, 440, 581, 634, 666
 Hinshelwood, C. N., 393
 Hippler, H., 375
 Hirai, K., 282, 287
 Hirai, T., 878
 Hirakawa, H., 880
 Hirano, K., 872
 Hirano, S., 118
 Hirayama, F., 819
 Hirota, E., 120, 279
 Hirotsu, K., 159
 Hirsch, A., 209
 Hirsch, J. A., 130, 135
 Hirschi, J., 374
 Hirschmann, H., 72
 Hixson, S. S., 828
 Ho, G.-J., 280
 Ho, J.-H., 858
 Ho, W., 3
 Hobza, P., 137
 Hochster, H. S., 257
 Hochstrasser, R., 790, 795
 Hochstrate, D., 762
 Hodakowski, L., 159
 Hodge, C. N., 300
 Hoeger, C. A., 720
 Hoegger, E. F., 649
 Hoekman, D., 400
 Hoffman, D. K., 34
 Hoffman, D. M., 607
 Hoffman, J. M., 214
 Hoffman, Jr., J. M., 214
 Hoffman, P. H., 72
 Hoffmann, A. K., 285
 Hoffmann, H. M. R., 751
 Hoffmann, R., xv, 6, 52, 53, 161, 221, 228, 240, 292, 701, 715, 724, 739, 743, 760
 Hoffmann, R. W., 116, 122, 123
 Hoffmann, U., 305
 Hofmann, A. W., 656
 Hofmeister, A., 853
 Hofmeister, G. E., 879
 Hogberg, K., 378
 Hogg, D. R., 607
 Hogg, H. J., 460
 Hogg, J. L., 385
 Hohenberg, P., 236
 Hojatti, M., 386
 Hojo, K., 216
 Hollenstein, S., 291
 Hollis, R., 275
 Holloway, F., 371
 Holmberg, B., 453
 Holmes, H. L., 735
 Holmes, J. L., 291, 875
 Holness, N. J., 130, 360
 Holt, J., 419
 Holy, N. L., 544
 Holzwarth, G., 90
 Hommes, N. J. R. v. E., 39, 312, 604, 770
 Honda, K., 879
 Hong, S., 208
 Hong, Y. J., 302
 Hopf, H., 167
 Hopkinson, A. C., 429, 580
 Hopps, H. B., 63
 Hori, M., 3
 Horner, J. H., 276
 Hornyak, F. M., 314, 322
 Horspool, W. M., 213, 843, 853
 Hörstermann, P., 709
 Hortelano, E. R., 624
 Hortmann, A. G., 730
 Hou, J. G., 3
 Houbiers, J. P. M., 86
 Hough, L., 872
 Hough, R. E., 556
 Houk, K. N., 15, 190, 207, 266, 274, 285, 286, 308, 370, 429, 500, 551, 604, 608, 701, 702, 709, 724, 736, 745, 746, 751, 757, 760, 771-773, 777, 841, 852, 880
 Houriet, R., 426, 428, 877
 House, H. O., 316, 445, 601
 Houser, D. J., 879
 Hoveyda, A. H., 608
 Howarth, O. W., 388
 Howlett, K. E., 687
 Hoye, T. R., 873
 Hoyuelos, F. J., 877
 Hoz, S., 512, 876
 Hrnčir, D. C., 820
 Hrovat, D. A., 166, 215, 772, 773
 Hrubiec, R. T., 877
 Hsu, C.-Y., 29
 Hsu, E. C., 90
 Hsü, S. K., 444
 Hu, C.-H., 331
 Hu, H., 280
 Hu, J., 566
 Hu, W.-P., 496
 Huang, B.-S., 213
 Huang, H. H., 858
 Huang, J., 150, 874
 Huang, M.-J., 214
 Huang, S.-J., 858
 Huang, S.-L., 858
 Huang, X., 290
 Huang, Y.-T., 858
 Huang, Z.-T., 873
 Hubbard, W. N., 124
 Huber, H., 745
 Hüchel, E., 175
 Hüchel, W., 662
 Hudec, J., 739
 Hudlický, M., 605
 Hudnall, P. M., 859
 Hudson, C. E., 272, 718
 Hudson, C. S., 79
 Hudson, R. F., 512
 Hug, W., 69
 Hughes, D. L., 294
 Hughes, E. D., 92, 471, 479, 490, 495, 496, 501, 502, 633, 646, 654, 655, 657, 659, 662, 878
 Hughes, L., 275
 Huheey, J. E., 292
 Hui, Y.-Z., 487
 Huisgen, R., 479, 744, 745, 746
 Huiyan, Z., 78
 Hulett, J. R., 349
 Hulot, C., 706
 Hulshof, L. A., 65, 86
 Humbel, S., 189
 Hunt, W. J., 240
 Hunter, E. P. L., 426
 Huntsman, W. D., 735
 Hurd, C. D., 683, 876
 Hurley, J. K., 804
 Huskey, W. P., 373
 Hussain, H. H., 752
 Hussey, R. E., 502
 Huston, S. E., 485
 Hutchison, Jr., C. A., 281
 Hutton, R. S., 214
 Huvenne, J.-P., 809
 Huyser, E. S., 591
 Hwang, I., 876
 Hwang, M. J., 137
 Hwang, S.-J., 512
 Hyatt, J. A., 735, 880
 Hyde, A. J., 254

- Hyde, J. L., 454
Hynes, J. T., 350, 477
- Iafe, R. G., 370
Iannotta, A. V., 860
Ibberson, R. M., 383
Ibeas, S., 877
Ibne-Rasa, K. M., 504, 512, 530
Ibrahim, P. N., 262
Ichikawa, Y., 880
Ichinose, T., 154
Iczkowski, R. P., 24
Iervolino, M., 208
Iftimie, R., 223
Ignatenko, A. V., 720
Ikeda, A., 209
Ikeda, M., 854
Ikeda, T., 858
Il'ichev, Y. V., 720
Imagawa, H., 880
Imkampe, K., 241
Impastato, F. J., 314, 873
Inagaki, S., 580, 758
Ingemann, S., 310
Ingold, C. K., 68, 92, 116, 439, 443, 444, 470, 479, 490, 496, 501, 552, 584, 633, 646, 650, 654, 655, 657, 659, 877, 878
Ingold, K. U., 69, 267, 268, 273, 275, 276, 377, 378, 551, 872
Ingraham, L. L., 487, 488
Inman, C. G., 839
Inokuma, Y., 770
Inoue, M., 644
Inoue, S., 879
Inoue, Y., 163, 823, 825, 830, 853, 880
Ioffe, A., 309, 517
Ireland, J. F., 813
Ireland, R. E., 730
Irie, M., 850, 858
Irie, T., 740
Irrgang, B., 509
Irwin, C. F., 587
Isborn, C. M., 769
Isenberg, N., 586
Islam, S. M., 562
Islas, R., 161
Isobe, H., 4
Itai, A., 154
Itkis, M. E., 280
Ito, H., 288
Ito, Y., 320
Itoh, T., 282, 287
IUPAC, 305, 337, 350, 385, 414, 450, 453, 469, 471, 551, 552, 633, 639, 681, 701, 774
Iwama, T., 258
Iwamoto, R., 872
Iwasa, Y., 207
Iyoda, M., 874
Izatt, R. M., 429
- Jackman, L. M., 313
Jackson, G., 813
Jackson, J. E., 40, 287
Jackson, R. A., 669
Jacober, S. P., 375
Jacobs, T. L., 614, 653, 878
Jacobson, R. A., 118
Jacobus, J., 878
Jaeger, F. M., 98
Jaffe, A., 214
Jaffé, H. H., 59, 390, 806
Jager, W. F., 873, 876
Jagow, R. H., 380
Jahn, H. A., 308
Jaime, C., 153, 874
Jameson, R. F., 402
Jan, S.-T., 873
Janda, K. D., 736
Jang, K. S., 878
Janker, B., 509
Janoschek, R., 161
Janousek, Z., 309
Jansen, B. J. M., 682
Janssen, M. J., 507
Janzen, E. G., 277
Jao, L. K., 448
Jarahi, E., 151
Jarowski, P. D., 15, 190
Jarret, R. M., 130
Jaruzelski, J. J., 432
Jasperse, C. P., 272
Jaureguiberry, G., 872
Jayaraman, N., 859
Jeffrey, D. A., 165
Jelinek, P., 3
Jencks, D. A., 640
Jencks, W. P., 367, 395, 434, 435, 439, 441, 450, 456, 457, 459, 460, 471, 472, 511, 552, 640, 671, 876
Jenkin, D. G., 5
Jenkins, A. D., 93, 873
Jenkins, P. R., 880
Jennings, W. B., 96, 873
Jensen, E. V., 592
Jensen, F., 225, 724
Jensen, F. R., 57, 874, 877
Jensen, P., 279
Jensen, W. B., 413
Jesinger, R. A., 255
Jeske, M., 872
Jhi, S.-H., 208
Ji, Y., 683
Jia, Y., 208
Jia, Z.-J., 872
Jiang, J., 872
Jiang, M. Y., 856
Jiang, X.-K., 487
Jiao, H., 206, 770
Jibril, A. O., 529
Jimbo, M., 168
Jimenez, J. L., 726
Jiménez, P., 871
Jiménez-Barbero, J., 57
Jiménez-Vázquez, H., 296
Jin, J., 276
Jin, M., 862
Jingyu, S., 78
Jiratova, K., 677
Jiye, F., 9
Jodhan, A., 255, 460, 461
Johannesen, R. B., 475
Johansson, G., 32
John, W. T., 347
Johnson, A. P., 68
Johnson, C. C., 275
Johnson, C. D., 390
Johnson, C. K., 56
Johnson, C. R., 626
Johnson, F., 122
Johnson, F. A., 580
Johnson, Jr., H. W., 66, 880
Johnson, Jr., W. H., 872
Johnson, L. E., 280
Johnson, L. M., 290
Johnson, M. D., 878
Johnson, R. P., 163, 164, 706
Johnson, R. R., 382, 383
Johnson, S. A., 300
Johnson, S. L., 452, 454
Johnson, W. S., 124, 730, 874
Johnston, A. D., 720
Johnston, F., 588
Johnston, J. F., 525
Johnston, L. J., 309, 845, 849
Jones, A. C., 795
Jones, B., 393
Jones, D. S., 856
Jones, G., 585, 746
Jones, H. W., 477
Jones, J. M., 876
Jones, J. P., 305, 375
Jones, Jr., M., 161, 213, 253, 255, 256, 260, 278, 284, 288, 305, 318, 727, 776, 875
Jones, M. B., 287
Jones, P. R., 604
Jones, R. A. Y., 530
Jones, R. R., 875
Jones, S. O., 592
Jones, S. W., 853
Jones, W. M., 65, 282, 399
Jordan, K. D., 314
Jorgensen, C. K., 23
Jorgensen, W. L., 34, 121, 154, 264, 485, 497, 499, 500, 512, 525, 533, 720, 759, 762, 832, 879
Jorgenson, M. J., 431, 842, 880
Jossang, A., 871, 872
Jossang, J., 871, 872
Joyner, B. L., 387
Juaristi, E., 59, 131, 137, 151, 232, 420, 874
Jubert, A., 290, 291
Judson, C. M., 378
Jug, K., 26, 192, 205
Juliá, L., 258
Juliusburger, F., 495
Jung, C., 853
Jung, M. E., 78
Jurgens, A., 849

- Jurić, S., 513, 877
 Jurs, P. C., 242
 Juveland, O. O., 591

 Kaanumalle, L. S., 859
 Kabalka, G. W., 878
 Kachanov, A. V., 62
 Kafafi, S. A., 227
 Kagramanov, N. D., 189
 Kahn, S. D., 841
 Kaiser, E. T., 305
 Kaiser, L. E., 508
 Kakiuchi, K., 168
 Kalantar, A. H., 349
 Kalasinsky, V. F., 150
 Kalinowski, H.-O., 57, 853
 Kalish, J., 409
 Kallel, E. A., 709, 757
 Kallmerten, J., 77, 872
 Kamalam, R., 402
 Kamaras, K., 280
 Kamiyama, K., 62
 Kamlet, M. J., 339, 478
 Kampf, J. W., 878
 Kanda, Y., 298
 Kane, A. A., 208
 Kane, S., 647
 Kanematsu, K., 159
 Kaner, R. B., 208
 Kanerva, L. T., 450
 Kaneti, J., 315
 Kang, B., 872
 Kang, J. S., 880
 Kang, S., 399, 605
 Kang, T., 881
 Kanjilal, A., 207
 Kannan, N., 880
 Kanno, H., 207
 Kanno, K.-i., 207
 Kao, M., 136
 Kaplan, F., 9, 76, 301, 470, 873
 Kaplan, L., 167
 Kaplan, M. L., 720
 Kaplan, M. S., 722
 Kapon, M., 118
 Kaprinidis, N. A., 841
 Kar, T., 192
 Karabatsos, G. J., 624
 Karadakov, P. B., 47
 Karelson, M., 338
 Karki, S. B., 305
 Karle, I. L., 215
 Karle, J., 3
 Karlov, S. S., 610
 Karney, W. L., 216, 769, 770, 880
 Karplus, M., 120, 136, 152, 231, 265, 366,
 462, 771
 Kartch, J. L., 578
 Karty, J. M., 419
 Karunakaran, C., 402
 Kasha, M., 792, 795, 851
 Kashelikar, D. V., 879
 Kashima, K., 207

 Kass S. R., 871
 Kass, S. R., 212, 313, 319, 654
 Kast, P., 880
 Katakai, H., 735
 Katano, S., 3
 Kates, M. R., 303, 304
 Kato, M., 858
 Kato, S., 771
 Kato, T., 291
 Katritzky, A. R., 201, 205, 310, 338, 385,
 431, 473, 877
 Katsura, T., 872
 Katz, J. J., 586
 Katz, T. J., 215
 Kaufman, M. J., 374, 421, 438
 Kaufmann, E., 312
 Kavarnos, G. J., 804
 Kawabata, J., 872
 Kawai, H., 159
 Kawai, M., 3
 Kawai, T., 154
 Kawasaki, A., 439
 Kay, P. S., 479
 Kaye, S., 588
 Ke, P. C., 209
 Kearns, D. R., 801, 851
 Keating, J. T., 482
 Kebarle, P., 426
 Keeffe, J. R., 446, 593, 877, 881
 Keehn, P. M., 168
 Keese, R., 161
 Keijzer, F., 117
 Keillor, J. W., 460
 Keizer, V. G., 875
 Keliher, E. J., 777
 Kellogg, B. A., 455
 Kellom, D. B., 684
 Kelly, C., 166
 Kelly, D. P., 847
 Kemp, J. D., 120
 Kempf, B., 509
 Kende, A. S., 76, 879
 Kendrick, R. D., 291
 Kennard, O., 5
 Kennedy, R. D., 215
 Kent IV, D. R., 298
 Kenyon, G. L., 332
 Kenyon, J., 480
 Kepler, K. D., 587
 Kepner, R. E., 472
 Kerber, R. C., 543, 544, 631
 Kern, C. W., 120, 231
 Kern, F., 697
 Kerrigan, M., 166
 Kersting, B., 878
 Kesselmayr, M. A., 331
 Kessick, M. A., 594
 Kessler, H., 57, 96
 Kessler, M., 856
 Kestner, M. M., 544
 Kestner, N. R., 438
 Ketner, A. M., 862
 Keung, E. C., 751

 Kevan, L., 305, 598
 Kevill, D. N., 460
 Key, A., 436
 Kharasch, M. S., 265, 272, 585, 586, 589,
 590, 592, 621
 Khramtsov, V. V., 258
 Kibby, C. L., 878
 Kido, M., 854
 Kikuchi, J., 209
 Kikuchi, K., 795
 Kikuchi, S., 202
 Kilby, D. C., 877
 Killion, Jr., R. B., 331, 533
 Kilner, A. E. H., 444, 876
 Kilner, C., 873
 Kilpatrick, J. E., 128
 Kim, C. J., 490
 Kim, C. K., 291
 Kim, D., 770
 Kim, G., 208
 Kim, H. J., 477
 Kim, H.-T., 399
 Kim, J., 880
 Kim, J. H., 876
 Kim, J. K., 541, 543
 Kim, J.-S., 606
 Kim, K. S., 770
 Kim, P. P. N., 872
 Kim, S., 271
 Kim, S. K., 833
 Kim, S. S., 876
 Kim, Y., 3
 Kim, Y. A., 209
 Kimball, G. E., 25, 176, 553
 Kimling, H., 164
 Kim-Meade, A. S., 881
 King, B. T., 211
 King, E. J., 415
 King, G. W., 26, 372, 815
 King, H. F., 329
 King, J. F., 502
 King, M. C., 350
 King, R. A., 216
 King, R. B., 256
 King, R. W., 681
 King, S. B., 872
 Kingsbury, C. A., 137, 687
 Kingsley, W. G., 319
 Kinoshita, M., 795, 858
 Kirby, A. J., 151, 449, 458
 Kirby, G. W., 118
 Kirmse, W., 278, 288, 298, 679
 Kirner, W. R., 502
 Kirsch, J. F., 456
 Kirschner, S., 769, 770, 771
 Kish, F. A., 594
 Kisiel, Z., 735
 Kispert, L. D., 266
 Kistiakowsky, G. B., 190, 576
 Kita, Y., 269
 Kitagawa, T., 19, 875
 Kitamura, K., 209
 Kitaura, K., 229

- Kitching, W., 872
 Kivelson, S., 207
 Kiwiet, N. J., 760
 Kiyobayashi, T., 871
 Klaine, S. J., 209
 Klán, P., 836
 Klärner, F.-G., 762, 772, 774
 Klauda, J. B., 117
 Klein, D. J., 24, 240, 241, 242, 256
 Klein, E., 852, 880
 Klein, F. M., 604
 Klein, F. S., 670, 671, 672
 Klein, J., 604
 Klein, M., 881
 Klein, M. L., 462
 Klesney, S. P., 69, 115
 Klessinger, M., 821, 829
 Kline, M., 281
 Klinedinst, Jr., P. E., 479, 483
 Klinge, S., 305
 Klippenstein, S. J., 347
 Klobukowski, M., 556, 566
 Kloetzel, M. C., 735
 Klopper, W., 295, 593
 Kloster-Jensen, E., 308
 Kluger, R., 876
 Kluiber, R. W., 879
 Klyne, W., 62, 90, 91, 115, 134
 Knaack, D. F., 579
 Knight, E. T., 22
 Knight, J. D., 623
 Knight, Jr., L. B., 308
 Knipe, A. C., 642
 Knittel, P., 593
 Knop, J. V., 242
 Knowles, J. R., 880
 Knox, L. H., 214, 291
 Knözinger, H., 669, 879
 Knutson, D., 529
 Kobayashi, H., 527, 877
 Kobayashi, M., 62
 Kobayashi, N., 770
 Kobiro, K., 168
 Koch, A. S., 379
 Koch, H. F., 379
 Koch, W., 295, 301, 303, 593
 Kochi, J. K., 201, 257, 330, 526, 558, 666
 Koehl, Jr., W. J., 314
 Koehn, W., 742
 Koekkoek, R., 636, 879
 Koelsch, C. F., 258
 Koenig, T., 636
 Koenigsberger, R., 579
 Koerner, T., 608
 Kofron, W. G., 620
 Koga, G., 68
 Koga, N., 205
 Kohen, A., 372
 Kohl, D. A., 39
 Kohler, B. E., 796
 Köhler, F., 769
 Kohli, P., 209
 Köhli, T.-P., 297
 Kohn, W., 236
 Koike, K., 795
 Kok, G. B., 388
 Kokko, B., 607
 Kokubun, H., 795
 Kol, M., 582
 Kolb, H. C., 746
 Kolb, K. E., 356
 Kollman, P. A., 135, 136, 461, 462
 Kollmar, H., 213, 317
 Kollmar, H. W., 769
 Kolos, W., 27
 Kolossváry, I., 147
 Koltzenburg, G., 742
 Komarov, I. V., 159
 Komornicki, A., 724
 Konasiewicz, A., 671
 Kondo, M., 858
 Koner, A. L., 837
 König, B., 853, 881
 König, J., 610, 715, 719, 752
 König, W. A., 872
 Konoike, T., 320
 Konrad, K. M., 164
 Kopecky, K. R., 562, 623, 878
 Kopelevich, M., 131, 383
 Köppel, H., 307
 Kornblum, N., 543, 544
 Korneev, V. A., 62
 Kortüm, G., 414
 Kos, A. J., 315, 429
 Koshima, H., 857
 Koshino, M., 4
 Koskikallio, J., 449
 Kosower, E. M., 338, 339
 Kostarelos, K., 208
 Köster, A. M., 205
 Kostyanovskii, R. G., 62
 Kostyanovsky, R. G., 62, 872
 Kotsuki, H., 880
 Kötting, C., 833
 Koubek, E., 530
 Koumura, N., 858, 873, 876
 Kouznetsov, V. V., 877
 Kovačević, B., 877
 Kovach, I. M., 380
 Kovelesky, A. C., 873
 Kovi, P. J., 814
 Kozarich, J. W., 332
 Kozhushkov, S. I., 162
 Kozima, K., 134
 Kozlowski, J. A., 621
 Kozma, E. C., 881
 Kozubek, H., 812
 Kozukue, N., 881
 Kraft, K., 742
 Kramar, V., 445
 Krammer, G., 867
 Krantz, A., 213, 331
 Krapp, A., 42, 190, 203
 Krasnoperov, L. N., 268
 Kratz, D., 168
 Kraus, G. A., 880
 Krawczyk, B., 772
 Krebs, A., 164
 Krebs, O., 852
 Kreevoy, M. M., 448
 Kreider, E. M., 529, 877
 Kresge, A. J., 298, 372, 384, 438, 446, 447, 566, 593, 877, 881
 Krisher, L. C., 46
 Krishnamurthy, D., 872
 Kriz, Jr., G. S., 817
 Kroepelin, H., 489
 Krohn, K., 872
 Krom, J. A., 421
 Kronja, O., 296, 297, 302–304, 383, 513, 877
 Kronzer, F. J., 313
 Kroposki, L. M., 320
 Kropp, P. J., 163, 587, 614, 818, 824–826, 850, 880
 Krow, G., 67
 Krug, J. P., 40, 461
 Krüger, C., 305
 Krüger, H., 331
 Kruse, L., 274
 Krygowski, T. M., 203, 389
 Kuck, V. J., 214, 279
 Kuczkowski, R. L., 746, 876
 Kuderna, B. M., 592
 Kudryavtsev, R. V., 453
 Kuehne, M. E., 84
 Kuhn, H. J., 804, 852
 Kuhn, L. P., 134, 874
 Kuhn, S. J., 296
 Kuhn, T. S., xv, 1, 251
 Kuimova, M. K., 862
 Kuivila, H. G., 271, 666
 Kula, J., 310
 Kumar, P. P., 290
 Kumar, A., 762
 Kumar, D., 276
 Kumar, G. M., 871
 Kumar, R., 862
 Kumar, V., 872
 Kumei, S., 820
 Kummli, D. S., 127
 Künzer, H., 375
 Künzler, D. E., 880
 Kupczyk-Subotkowska, L., 772
 Kuppens, T., 872
 Kurata, H., 874
 Kurek, J. T., 597, 878
 Kurihara, S., 858
 Kuroda, T., 163
 Kurokawa, H., 879
 Kurosaka, J., 735
 Kursanov, D. N., 453
 Kurtán, T., 872
 Kurtz, R. R., 879
 Kutay, U., 872
 Kutzelnigg, W., 295, 593
 Kuwajima, S., 241
 Kuwata, K. T., 852
 Kuznetsov, M. A., 162
 Kwak, D., 862

- Kwak, K., 120
 Kwan, E. E., 435
 Kwart, H., 607, 639
 Kwit, M. G., 858
 Kwok, F. C., 446
 Kwok, W. K., 643
 Kwok, W. M., 834
 Kwon, O., 312
 Kyle, R. H., 536
- Laali, K. K., 526, 610
 Laane, J., 128
 Laarhoven, W. H., 67, 117
 Labanowski, J. K., 156
 Labastida, V., 131, 874
 Lacher, J. R., 619
 Ladenheim, H., 451
 LaFemina, J. P., 227
 LaFrancois, C. J., 255
 Lafuente, P., 159
 Lahav, M., 91
 Lahtela, M., 122
 Lai, C., 462
 Laidig, K. E., 13, 40, 150
 Laidler, K. J., 342, 345, 348, 350
 Laing, J. W., 541
 Laing, M., 790
 Laiter, S., 212
 Lam, L. K. M., 875
 Lam, Y., 873
 Lambert, J. B., 62
 Lambert, J. L., 875
 Lammertsma, K., 290
 Lamola, A. A., 831
 Lampman, G. M., 817
 Lan, Z., 849
 Lande, S. S., 878
 Landis, C. R., 29, 151, 226
 Lang, T. J., 650
 Lange, H., 773
 Langenaeker, W., 236
 Langer, S. H., 503
 Langler, R. F., 227
 Langlois, D. P., 678
 Langmuir, I., xvii
 Långström, B., 375, 529
 Lankamp, H., 257
 Lanzalunga, O., 309
 Lapierre, J.-M., 872
 Laporterie, A., 751
 Lapworth, A., 443
 Larsen, D. W., 591
 Larsen, E. M., 439
 Larson, J. R., 240
 Laszlo, P., xv, 53, 524
 Lathan, W. A., 267
 Latini, A., 208
 Lattimer, R. P., 746
 Laube, T., 291, 293, 296
 Lauer, W. M., 519
 Laughlin R. G., 285
 Lauhon, L. J., 3
 Laulicht, I., 373
- Lauren, J., 213
 Laurent, H. B., 858
 Laurenzo, K. S., 877
 Lautens, M., 741, 880
 Lavallo, V., 280
 Law, K.-Y., 859
 Lawlor, J. M., 313
 Lawrence, M., 812
 le Noble, W. J., 318, 350
 Le Perchec, P., 753
 Leach, A. G., 852
 Leal, J. M., 877
 Leardini, R., 669
 LeBel, N. A., 656, 879
 Leber, P. A., 775
 Lebon, F., 152
 Lecea, B., 768
 Lechtken, P., 860
 Lectka, T., 299
 Lednicer, D., 67
 Ledwith, A., 93
 Lee, B.-S., 684
 Lee, C., 237
 Lee, C. C., 371, 384, 492
 Lee, C. S. T., 668
 Lee, C.-H., 162
 Lee, D., 872
 Lee, D. E., 879
 Lee, D.-J., 552, 611, 612
 Lee, E. C. Y., 881
 Lee, H.-H., 656, 879
 Lee, I., 684
 Lee, J.-I., 856
 Lee, J.-Y., 399
 Lee, K. A., 291
 Lee, K. Y., 298
 Lee, P. S., 207, 709, 880
 Lee, S., 873
 Lee, S.-U., 881
 Lee, S.-Y., 796
 Lee, T.-J., 881
 Lee, W. G., 643
 Leermakers, P. A., 840
 Lefebvre, R., 214
 LeFevre, G. N., 876
 Leffek, K. T., 383
 Leffler, J. E., 257, 352, 363, 402, 438, 544
 Leforestier, C., 241
 Lefort, D., 257
 Lefour, J.-M., 205, 626
 LeGoff, E., 873
 Legon, A. C., 126
 Legutke, G., 662
 Lehmann, C. W., 56, 127
 Lehn, J. M., 626
 Lehr, G. F., 350
 Lehr, R. E., 743, 748, 757, 766
 Lei, X., 858, 859
 Leicester, H. M., 585
 Leigh, W. J., 818, 826, 827
 Lein, M., 2
 Leipzig, B., 873
 Leiserowitz, L., 91
- Leize-Wagner, E., 873
 Lejeune, V., 798
 Lélias-Vanderperre, A., 873
 Lem, G., 841
 LeMahieu, R., 841
 Lemal, D. M., 748, 871
 LeMaster, C. B., 726
 Lemenovskii, D. A., 610
 Lemmen, P., 610
 Lenci, F., 213
 Lenoir, D., 165, 280, 301, 302, 557, 610, 879
 Leo, A., 393, 400, 404
 Leopold, D. G., 279
 LePage, T. J., 40
 Lepeska, B., 600
 Lerman, O., 582
 Lerner, R. A., 736
 Leroi, G. E., 120, 168
 Lespade, L., 872
 Letsinger, R. L., 314
 Leumann, C. J., 638
 Leung, C., 387
 Leung, O. M., 3
 Leutwyler, S., 127
 Levi, S., 83
 Levin, C. E., 881
 Levine, B. G., 821
 Levine, R., 876
 Levine, R. D., 6
 Levitt, J. A., 862
 Levy, A. A., 529
 Levy, G. C., 420
 Levy, J. B., 592
 Levy, M., 23
 Lewars, E. G., 165
 Lewis, A., 599
 Lewis, D. C., 873
 Lewis, E. S., xvi, 342, 344, 378, 382, 383, 389, 438
 Lewis, F. D., 765, 790, 822, 824, 881
 Lewis, G. N., 19
 Lewis, J. A., 872
 Li, A.-J., 7
 Li, C., 875
 Li, C.-J., 762
 Li, D., 208
 Li, J., 337, 683
 Li, K., 23
 Li, R.-Q., 275
 Li, S., 207, 208
 Li, T., 730
 Li, W.-K., 310
 Li, X., 208
 Li, Y., 604, 701, 702, 736
 Liang, C., 22, 67
 Liang, F., 830
 Liang, G., 215, 301
 Lias, S. G., 426
 Liberles, A., 41, 137
 Lichtenhaler, F. W., 72
 Lide, D. R., 93
 Lide, Jr., D. R., 18, 39
 Liebeskind, L. S., 872

- Liebman, J. F., 8, 9, 51, 137, 158, 159, 163, 165, 215, 267, 278, 871
 Lietaer, D., 814
 Lifson, S., 135
 Lii, J.-H., 136, 151
 Liljefors, T., 872
 Lim, C., 853
 Lim, H. S., 862
 Lim, J. M., 770
 Limbach, H.-H., 372
 Lin, C.-J., 872
 Lin, D. T., 332
 Lin, M., 232
 Lin, Y.-C., 858
 Lin, Y.-T., 771
 Linares, M., 189
 Lind, J., 859
 Lindegren, C. R., 487
 Lindeman, S. V., 330, 526
 Linden, A., 383
 Lindholm, E. P., 858
 Lindner, H. J., 724
 Lindquist, L. C., 844
 Lineberger, W. C., 265, 279, 310, 424
 Linert, W., 402
 Linn, W. S., 617
 Linstrom, P. J., 44, 425
 Liotta, C. L., 311, 387, 499
 Liotta, D., 139
 Lipinsky, E. S., 839
 Lipkowitz, K. B., 135, 137, 223, 224
 Lipp, P., 441
 Lipscomb, W. N., 118, 604
 Lipshutz, B. H., 621
 Lipsky, S., 819
 Lipson, M., 849
 Liptay, W., 815
 Lissi, E. A., 859
 Lister, D. H., 880
 Little, T. S., 150
 Liu, B., 301
 Liu, C., 872
 Liu, F., 875
 Liu, H., 314
 Liu, J., 150, 608
 Liu, K., 875
 Liu, K.-T., 587
 Liu, L., 275, 402
 Liu, L. H., 164
 Liu, M. T. H., 287, 288
 Liu, R., 159
 Liu, S., 232
 Liu, W., 280
 Liu, Y., 871
 Liu, Y.-P., 592
 Livneh, M., 876
 Llewellyn, D. R., 671
 Llewellyn, G., 478
 Llewellyn, J. A., 383
 Lloyd, D., 215
 Lloyd, D. J., 639
 Lo Moro, G., 610
 Lo, A., 746
 Lobo, A. M., 68
 Lochan, R. C., 237
 Lockyer, N. P., 209
 Lodge, E. P., 626
 Loe, Ø., 855
 Loening, K. L., 77, 385
 Lofffield, R. B., 692
 Lomas, J. S., 555, 673
 Loncharich, R. J., 751
 Long, F. A., 353, 433, 876, 877
 Long, J. W., 584
 Longhi, G., 152, 873
 Longmei, Z., 78
 Longmore, R. W., 740
 Longuet-Higgins, H. C., 193, 194, 707, 795, 843, 879
 Loo, D., 607
 Loos, R., 509
 Loos, W. J., 636, 879
 Lopez, X., 366, 462
 Lord Kelvin, 58, 84
 Lorenz, K. T., 762
 Lorusso, P., 531
 Lossing, F. P., 291, 875
 Loudon, G. M., 670
 Loupy, A., 338
 Lourderaj, U., 495
 Loutzenhiser, E., 166
 Lovas, F. J., 279, 735
 Lovchik, M. A., 877
 Lowchyj, L., 166
 Lowe, J. P., 227, 329, 650, 663
 Lowry, T. M., 347
 Lowson, W., 456
 Loy, M., 860
 Lozan, V., 878
 Lu, H.-F., 858
 Lu, X., 209
 Lu, Y., 645
 Lu, Z.-H., 872
 Lucas, H. J., 329, 485, 554, 592, 598, 877
 Lucas, J. J., 575
 Lucchini, V., 615
 Ludwiczak, S., 528, 877
 Luger, P., 56, 127, 160
 Luisi, R., 531
 Lukach, C. A., 360
 Lunazzi, L., 874
 Lund, A., 305, 307
 Lunell, S., 307
 Luo, J., 208
 Luo, Y., 207
 Luo, Y.-R., 23
 Lupo, D. W., 790
 Lupton, Jr., E. C., 399
 Luria, M., 13
 Luszytk, E., 214
 Luszytk, J., 214, 276, 298, 378, 551
 Luthra, A. K., 458
 Lutz, J.-F., 746
 Lutz, W. B., 67
 Luz, Z., 440, 726
 Lymar, S. V., 804
 Lynch, B. M., 606
 Ma, C., 834
 Ma, N. L., 306
 Maas, G., 167
 Mac Dougall, J. E., 3
 Macae, F. Z., 682
 MacArthur, C. A., 374, 421, 438
 Maccoll, A., 677, 687
 MacDougall, P. J., 150
 MacGillivray, L. R., 857
 Mach, G. W., 431
 Machiguchi, T., 213
 Macho, V., 300
 Maciejewski, A., 795
 Mackay, I. R., 67
 MacKerell, Jr., A. D., 117
 Mackie, I. D., 164
 Mackie, J. D. H., 501
 Mackor, A., 163
 MacLean, C., 257
 Maclin, K. M., 876
 MacNulty, B. J., 633, 646
 Macomber, R. S., 9, 76, 470
 MacPhail, R. A., 128
 Macpherson, J. V., 208
 Maddipatla, V. S. N. M., 859
 Maehr, H., 72, 74
 Maerker, C., 296
 Magaha, S., 459
 Maggini, M., 166
 Magid, R. M., 472, 877
 Magnus, A., 652
 Magnusson, E., 29
 Magull, J., 853
 Mahan, B. H., 344
 Mahone, L. G., 311
 Maier, G., 162, 853, 874
 Maier, W. F., 165
 Maivald, P., 3
 Majek, P., 258
 Majekova, M., 258
 Majumdar, T. K., 424
 Makosza, M., 528, 877, 880
 Maksić, Z. B., 3, 211, 871, 877
 Maksimenka, R., 331
 Maleczka, Jr., R. E., 82
 Malerich, J. P., 730
 Malhotra, R., 520
 Maliakal, A., 879
 Maliakal, D., 855
 Malinski, D. S., 310
 Mallard, W. G., 44, 425
 Mallion, R. B., 203
 Mallock, W. H., 544
 Mallon, B. J., 871
 Mallory, C. W., 844
 Mallory, F. B., 844
 Mallory, J. A., 452
 Maloney, V. M., 287
 Malpezzi, L., 873
 Malsch, K. D., 214
 Maltsev, A. K., 189

- Maltz, H., 439
 Mamantov, A., 280
 Mamdapur, V. R., 872
 Mamiya, J.-i., 858
 Mancini, P. M. E., 529
 Mancini, V., 873
 Mandado, M., 235
 Mandour, A. M. M., 633, 654, 878
 Manek, M. B., 275
 Manikyamba, P., 876
 Manly, D. G., 683
 Manoharan, M., 132, 206, 765, 874, 875
 Manor, P. C., 66
 Manring, L. E., 794
 Manthey, J. W., 544
 Manus, M. M., 871
 Maradyn, D. J., 841
 Marangos, J. P., 2
 Maraver, J. J., 454
 March, N. H., 24
 Marchand, A. P., 162, 743, 748, 757, 766
 Marchetti, A. P., 801
 Marciniak, B., 812
 Marcos, E. S., 454
 Marcus, R. A., 364
 Marcus, Y., 5, 339
 Marecic, T. C., 375
 Mareda, J., 285
 Marek, I., 316
 Margrave, J. L., 24, 124
 Maria, P.-C., 418, 424
 Mariani, C., 207
 Mariano, P. S., 305, 828
 Mariella, R. P., 529
 Marioni, F., 558, 562
 Markovnikoff, V., 585
 Markownikoff, W., 585
 Marle, E. R., 393
 Marlier, J. F., 452, 456, 462
 Marquet, A., 872
 Marquez, M., 790
 Marriott, S., 388
 Marsch, M., 315
 Marsh, B. K., 762
 Marsh, R. M., 872
 Marshall, A. G., 426
 Marshall, C., 68
 Marshall, H., 487
 Marshall, J. A., 66
 Marshall, J. L., 858
 Marshall, L., 606
 Marti, O., 3
 Martin, C. R., 209
 Martin, I., 683
 Martin, J. C., 290
 Martin, J. G., 735
 Martin, M. T., 459
 Martinelli, J. E., 730
 Martinez, A., 636
 Martinez, R. D., 529
 Martinez, T. J., 703
 Martínez, T. J., 819, 821
 Martinho Simões, J. A., 19, 875
 Martin-Polo, J., 161
 Maruoka, K., 728
 Marvel, C. S., 259
 Marvell, E. N., 700, 702, 880
 Marx, D., 290
 Marzocco, C. J., 812
 Masamune, S., 213, 216
 Masaracchia, J., 742
 Masci, B., 546, 877
 Mascitti, V., 857
 Masel, R. I., 365
 Maslak, P., 310
 Mason, S. F., 90
 Massie, J., 3
 Masterman, S., 495, 496, 646
 Mastryukov, V. S., 871
 Masuda, A., 872
 Mata, P., 68
 Mataga, N., 803
 Mateescu, G. D., 214, 296, 300, 303, 875
 Mateo-Alonso, A., 209
 Matesich, M. A., 615
 Mathai, I. M., 665, 668
 Mathew, K. K., 624
 Mathies, R. A., 700, 822
 Mathis, J. R., 477
 Matlin, A. R., 190
 Matoba, T., 209
 Matsen, F. A., xvii, 241
 Matskia, S., 821
 Matsson, O., 375, 529
 Matsubara, H., 272
 Matsugi, M., 269
 Matsui, H., 455
 Matsushita, O., 770
 Matsuura, K., 310
 Matsuzaki, Y., 770
 Matta, C. F., 233
 Mattay, J., 853
 Matteson, D. S., 29
 Matturro, M. G., 349
 Matushita, T., 875
 Matzger, A. J., 205
 Matzner, E., 760
 Maugh II, T. H., 98, 771
 Mauksch, M., 769, 770
 Maurel, F., 229
 Maw, G. A., 633, 646, 657, 878
 Maya, W., 879
 Mayer, A., 859
 Mayer, G., 859
 Mayer, J. E., 135
 Mayers, C. J., 387
 Mayo, F. R., 586, 589, 590
 Mayo, S. L., 136
 Mayr, H., 297, 473, 509, 511, 513
 Mazzanti, A., 874
 McAdoo, D. J., 272, 718
 McBride, J. M., 214, 257
 McCann, D. M., 872
 McCapra, F., 859
 McCarty, J. E., 680, 686
 McCasland, G. E., 64
 McClard, R. W., 418
 McClellan, A. L., 20
 McClelland, R. A., 452, 825
 McClung, R. E. D., 556
 McCombie, H., 500
 McCombs, D. A., 880
 McConnell, H. M., 261
 McConnell, M. C., 873
 McCoull, W., 873
 McCoy, A. B., 290
 McCoy, C. P., 856
 McCoy, J. R., 4
 McDaniel, D. H., 391
 McDonald, I. R., 154
 McDonald, R., 556
 McDonald, R. N., 617
 McDonald, R. S., 562, 565, 569, 593
 McFarlane, W., 118
 McGee, T. W., 584, 878
 McGlynn, S. P., 795
 McGrath, M. J., 872
 McGrath, M. P., 161
 McGregor, S. D., 748
 McGuire, M. J., 772
 McGuire, W. J., 503
 McIntosh, A. R., 804
 McIntosh, C. L., 213
 McIntyre, D., 877
 McIver, J. W., 329
 McIver, Jr., J. W., 770
 McIver, Jr., R. T., 424
 McKean, D. C., 191
 McKee, M. L., 164, 312, 604
 McKeever, L. D., 311
 McKellar, A. R. W., 279
 McKelvey, J., 139
 McKenzie, A., 472, 877
 McKervey, A., 288
 McKervey, M. A., 8, 62, 137, 875
 McKinley, A. J., 262
 McLennan, D. J., 382, 517, 639
 McLeod, G. L., 876
 McMahan, T. B., 426
 McManis, J., 606
 McManus, S. P., 504
 McMartin, L. A., 879
 McMillen, D. W., 576
 McMurry, J. E., 299, 300
 McNab, H., 215
 McNab, M. C., 589
 McNaught, A. D., 385
 McNelis, E., 51
 McNiven, N. L., 662
 McPherson, C. A., 586, 588
 McShane, C. M., 216
 McWeeny, R., 26
 Meador, W. R., 163
 Means, G. E., 681
 Mecca, T. G., 643
 Medary, R. T., 881
 Medawar, P., 2
 Meek, J. S., 504, 506, 648
 Meek, T. L., 23

- Meer, N., 553
 Meetsma, A., 858
 Megarity, E. D., 819
 Mehta, A. S., 635
 Mehta, G., 627
 Meier, M., 867
 Meijer, E. W., 811
 Meisels, G. G., 295
 Melander, L., 371, 383, 519
 Mele, A., 85
 Melega W. P., 215
 Mellows, S. M., 881
 Menapace, L. W., 271
 Méndez-Rojas, M. A., 161
 Meng, Q., 299
 Mengel, A., 627
 Mennucci, B., 872
 Menon, A. S., 264
 Menon, B., 313
 Menzel, H., 853
 Merényi, G., 859
 Merényi, R., 309, 726
 Merer, A. J., 819
 Merino, G., 161
 Merrall, G. T., 578
 Merrigan, S. R., 608
 Merritt, R. F., 580
 Merz, Jr., K. M., 214, 215, 237, 462
 Meskers, S. C. J., 811
 Messer, R. R., 40, 235
 Messerschmidt, M., 160
 Messmer, R. P., 46, 47, 176
 Mestdagh, J.-M., 331
 Metts, L., 819
 Meulemans, T. M., 682
 Meyer, A., 63
 Meyer, J. W., 847
 Meyer, M. P., 772, 852
 Meyers, A. I., 872
 Mezey, P. G., 58, 67, 225, 254
 Miara, C., 872
 Michaels, R., 876
 Michalak, A., 15
 Michel, R. E., 543
 Michl, J., 168, 214, 262, 806, 821, 848
 Mickelfield, J., 879
 Mickus, D. E., 81
 Middlemiss, D., 853
 Midgal, C. A., 639
 Miesen, F. W. A. M., 811
 Miesusset, J.-L., 160, 285
 Migawa, M. T., 880
 Migirdicyan, E., 798
 Mihalić, Z., 242, 877
 Mikami, K., 752
 Mikosch, J., 495
 Mile, B., 261, 875
 Miles, F. B., 672
 Milhau, L., 741, 880
 Milicevic, S. D., 873
 Miller, E., 554
 Miller, J., 527
 Miller, J. A., 347
 Miller, J. S., 159
 Miller, Jr., W. T., 619
 Miller, K. E., 212
 Miller, M. A., 135, 874
 Miller, R. J., 454
 Miller, S. I., 619, 643, 665, 668
 Mills, J. A., 91
 Mills, W. H., 206
 Mimoun, H., 606
 Minamii, M., 872
 Minardi, C., 861
 Minary, P., 223
 Minato, H., 62
 Minato, T., 580, 650
 Minegishi, S., 473
 Minieri, P. P., 409
 Minkin, V. I., 20, 221
 Minns, R. A., 858
 Minto, R. E., 872
 Mintz, C., 339
 Miranda, M. A., 852
 Mirbach, M. F., 825
 Mirbach, M. J., 825
 Mirowicz, M., 68
 Misawa, H., 824
 Mishani, E., 582
 Mishchenko, Y., 280
 Mishima, M., 395
 Mislow, K., 37, 63, 64, 66–68, 84, 86, 88, 94, 98, 871
 Mison, P., 301
 Misono, M., 298
 Misrock, S. L., 844
 Mitchell, D. J., 512
 Mitchell, R. W., 212
 Mitoraj, M., 15
 Mitra, R. B., 841
 Miura, S. S., 84
 Miyahara, I., 159
 Miyamoto, K., 873
 Miyashi, T., 722, 880
 Miyazawa, K., 209
 Miyoshi, H., 614
 Mizoguchi, N., 240, 242
 Mizuno, N., 298
 Mo, Y., 15, 46, 189, 205, 232
 Mocek, M., 380
 Mock, W. L., 748
 Modena, G., 532, 562, 615
 Modro, A., 561, 878
 Moe, H., 529
 Moffat, J. B., 315
 Moffatt, J. R., 368
 Moffatt, M. E., 296
 Moffitt, W., 90
 Mogali, S., 500
 Mohler, D. L., 205
 Mohrig, J. R., 879
 Moinet, G., 753, 880
 Moiseyev, N., 214
 Mokhtari, M., 531
 Moldoványi, L., 371
 Moldowan, J. M., 132
 Moler, J. L., 4
 Mollère, P. D., 32
 Möllerstedt, H., 819
 Moloney, M. G., 287
 Monack, L. C., 529
 Monahan, M. W., 586
 Mondal, R., 207
 Monera, O. D., 681
 Monette, M., 463
 Monguchi, K., 287
 Monroe, B. M., 851, 859
 Montagnon, T., 852
 Monte M. J. S., 871
 Monte, M. J. S., 9
 Montgomery, L. K., 742
 Moon, J. B., 378
 Moore, C. J., 872
 Moore, J., 258
 Moore, T. A., 804
 Moore, W. J., 3, 787
 Moore, W. M., 844
 Moore, W. R., 656, 871, 879
 Moorthy, J. N., 837, 872, 881
 Mootz, D., 613
 Moran, C., 166
 Moran, D., 264
 Moran, J., 842
 Morandi, C., 63
 Morat, C., 96, 873
 More O'Ferrall, R. A., 367, 384, 640
 Moreira, Jr., P. F., 818
 Moreno, P. O., 726
 Moretti, I., 62
 Morgan, C. R., 330
 Morgan, D. D., 844
 Morgan, K. M., 439, 652
 Morgan, S., 288
 Morgan, S. O., 20
 Mori, S., 770
 Mori-Sánchez, P., 237
 Morita, S., 3
 Moritani, I., 660, 662
 Morokuma, K., 257, 771, 772
 Morosi, G., 159
 Morrill, T. C., 797
 Morris, D. G., 475, 544, 878
 Morris, G. F., 650
 Morrison, A., 739
 Morrison, G. A., 113, 874
 Morrison, H., 881
 Morrissey, B. W., 344
 Morse, B. K., 490
 Mortimer, C. T., 8
 Morton, C., 812
 Morton, D., 815
 Morton, I. D., 558
 Morton, T. H., 556
 Morwick, J. J., xvii
 Moscowitz, A., 90
 Mosher, H. S., 90
 Mosley, R. B., 508
 Mosquera, R. A., 151, 235
 Moss, G. P., 78

- Moss, R. A., 213, 253, 255, 256, 260, 278,
 280, 284, 305, 318, 350, 681, 776, 875
 Moss, R. J., 635
 Mota, C. J. A., 291
 Mota, M. O., 209
 Motokawa, T., xv
 Motallebi, S., 555, 561, 878
 Motherwell, W. B., 272
 Motoc, I., 156
 Mount, A. R., 873
 Mount, A. S., 209
 Mroz, P., 852
 Mudrak, A., 879
 Mueller, L. J., 804
 Mueller, R. H., 730
 Mugnoli, A., 159
 Mujika, J. I., 462
 Mukai, T., 722, 825, 880
 Mukarakate, C., 280
 Mukhopadhyay, P., 88
 Mulder, J. J. C., 771
 Mullally, D., 329
 Mullay, J., 23
 Müller, G., 167
 Muller, N., 41, 871
 Muller, P., 94
 Müller, R., 872
 Müller, T., 211
 Müller, W. R., 242
 Müller-Dethlefs, K., 137
 Mulliken, R. S., 22, 179, 230, 307, 819
 Mulzer, J., 879
 Munakata, R., 735, 880
 Munakata, Y., 872
 Munderloh, H., 615
 Muranaka, A., 770
 Murcko, M. A., 40, 121, 150
 Murdoch, J. R., 374, 421, 438
 Murla, M., 592
 Murov, S. L., 800
 Murphy, A. R., 177
 Murphy, J. T., 374, 421, 438
 Murphy, L. R., 23
 Murphy, W. F., 121, 122
 Murray, J. S., 23
 Murray, K., 600
 Murray, K. K., 279
 Murray, R. W., 720, 852, 876
 Murrell, J. N., 229, 240
 Musci, Z., 203
 Musgrave, C. B., 237
 Musser, M. T., 544
 Musulin, B., 198
 Musumarra, G., 205
 Muto, H., 310
 Myddleton, W. W., 615
 Myers, D. R., 288
 Myers, R. J., 39
 Myhre, P. C., 291, 296, 298, 300, 588

 Nace, H. R., 681, 683, 879
 Nachbar, Jr., R. B., 137
 Nader, N.-P., 70

 Naemura, K., 63, 66
 Nafie, L. A., 90, 872
 Nagano, Y., 871
 Nagaoka, H., 875
 Nagata, C., 567
 Nagle, D. G., 871
 Nagle, J. K., 23
 Nagorski, R. W., 331, 556, 561, 563, 668
 Nahm, S. H., 751
 Nair, V., 855
 Naito, T., 853
 Nakagawa, M., 660, 661
 Nakagawa, Y., 880
 Nakai, T., 159
 Nakajima, K., 207
 Nakamura, A., 316
 Nakamura, E., 4
 Nakamura, J., 735
 Nakanishi, K., 89
 Nakano, K., 880
 Nakata, S., 298
 Nakata, T., 878
 Nakata, Y., 282
 Nakazaki, M., 66
 Nakazawa, J., 876
 Nam, H.-H., 168
 Namba, K., 880
 Nandakumar, M. V., 855
 Nanjappan, P., 736
 Nantermet, P. G., 881
 Naoshima, Y., 872
 Napper, A. D., 459
 Narang, S. C., 520
 Narayan, R., 673
 Nared, K. D., 109, 736, 873
 Naruta, Y., 876
 Narvaez, J. N., 310
 Nascimento, M. A. C., 419
 Nash, L. M., 876
 Nasielski, J., 814
 Natelson, D., 209
 Näther, C., 769
 Nau, W. M., 837
 Nauta, W. T., 257
 Navarro, J. L., 258
 Nawrath, T., 872
 Nazran, A. S., 281, 287
 Nebenzahl, L. L., 214, 420
 Neckers, D. C., 207
 Nefedov, O. M., 189
 Nel, A., 871
 Nelsen, S. F., 305, 307
 Nelson, A. F., 583
 Nelson, D. J., 604
 Nelson, G. L., 296, 774
 Nemirowski, A., 162, 282
 Nendel, M., 207, 880
 Neretin, I. S., 330
 Nesbet, R. K., 176
 Nesbitt, D. J., 290
 Nettleton, Jr., D. E., 693, 874
 Neuberger, K. R., 819
 Neudörfl, J., 872

 Neuenhofer, S., 859
 Neumann, H. C., 115
 Neuweiler, H., 859
 Nevell, T. P., 300
 Neverov, A. A., 462
 Neveu, M. C., 457, 458
 Newcomb, M., 260, 272, 273, 275, 276, 517
 Newkome, G. R., 654
 Newman, M. S., 55, 67, 119, 135, 385, 418,
 503, 556
 Newman, P., 66, 871
 Newman-Evans, R. H., 776
 Newton, Jr., R. J., 878
 Newton, M. D., 871
 Newton, R. F., 853
 Newton, T. A., 589
 Ngobo, A.-L. T. D., 521
 Nguyen, D. T., 136
 Nguyen, V., 556
 Nguyen-Dang, T. T., 233
 Niazy, O., 459
 Nibbering, N. M. M., 310
 Nichols, M. A., 313
 Nickon, A., 161, 286, 469, 716, 875
 Nicol, M., 790
 Nicolaides, A., 875
 Nicolaides, N., 377
 Nicolaou, K. C., 856
 Nie, S., 859
 Niederprüm, N., 39
 Niemczyk, M., 815, 881
 Nienburg, H., 735
 Nierengarted, J.-F., 67
 Niiranen, J. T., 268
 Nikitin, A., 208
 Nikitina, E. V., 877
 Nikolaev, V. A., 877, 881
 Nikolić, S., 242
 Nikolova, V., 502
 Nilsson, A., 208
 Nilsson, L., 136
 Nilsson, M., 443
 Nimmo, K., 435
 Ning, X., 746
 Ninomiya, I., 853
 Nishida, I., 84
 Nishiguchi, K., 209
 Nishimoto, K., 874
 Nishimura, K., 209
 Nishizawa, M., 880
 Nissfolk, F., 122
 Nithyanandhan, J., 859
 Nitta, M., 722
 Niwayama, S., 757
 Nixon, A. C., 475
 Nixon, I. G., 206
 Nobes, R. H., 310
 Nobs, F., 881
 Noe, E. A., 132
 Noey, E., 880
 Nogita, R., 853
 Nogueira, L. C., 817, 818
 Nohova, B., 804

- Nohr, R. S., 347
 Noland, W. E., 519
 Noll, K., 697
 Noller, B., 331
 Noltemeyer, M., 872
 Nonhebel, D. C., 275
 Nonoshita, K., 728
 Norbeck, J. M., 239
 Nordén, B., 402
 Norden, T. D., 874
 Nordling, C., 32
 Norris, J. R., 212
 Norris, W. P., 653, 879
 North, A. M., 843
 Northrop, B. H., 880
 Norton, J. A., 586, 590
 Norton, J. E., 880
 Notario, R., 211, 339, 500, 871
 Noukakis, D., 804
 Novak, M., 256
 Novi, M., 530
 Novoa, J. J., 159
 Nowlan, V. J., 593
 Nowotny, K., 876
 Noyce, D. S., 615, 625, 670, 672, 676, 879
 Noyes, R. M., 342
 Noyori, R., 84
 Nozaki, K., 269
 Nozoe, S., 881
 Nuckolls, C., 880
 Nudelman, N. S., 529
 Nugent, M. J., 72
 Nunes, P. M., 875
 Nunome, K., 310
 Nüsse, M., 39
 Nussim, M., 382
 Nussinov, R., 7

 O'Leary, D. J., 131
 O'Neill, J., 214
 Oakenfull, D. G., 456
 Oare, D. A., 620
 Ocain, T. D., 873
 Ochse, M., 872
 Ochterski, J., 419
 O'Connor, G. L., 681, 879
 O'Connor, P. R., 335
 O'Connor, S. F., 587
 Oda, M., 874
 O'Donnell, J. P., 433
 Oeckler, O., 769, 770
 Oelgemöller, M., 853
 Ofial, A. R., 509, 511, 513
 Ogasawara, H., 208
 Ogata, Y., 439, 606
 Ogawa, T., 209
 Ogilby, P. R., 851
 Ogilvie, J. F., 29
 Ogle, C. A., 315
 Ogliaruso, M. A., 356
 Oguchi, K., 872
 Ohanessian, G., 205, 241
 Ohloff, G., 676, 852, 880

 Ohnishi-Kameyama, M., 881
 Ohno, K., 854
 Ohnuma, Y., 316
 Ohta, B. K., 556
 Ohta, H., 873
 Ohtsuka, Y., 873
 Ohtsuki, Y., 849
 Ohwada, T., 519
 Oishi, T., 873
 Oishi, Y., 62
 Okamoto, K., 500
 Okamoto, Y., 398, 569, 594, 660, 769, 872
 Okamura, W. H., 720
 Okano, M., 614
 Okazaki, T., 610
 O'Keefe, M., 7
 Ōki, M., 66, 303
 Okubo, C., 874
 Okuhara, T., 298
 Okulik, N. B., 290, 291
 Okuyama, T., 164, 878
 Olafson, B. D., 136
 Olah, G. A., 166, 214, 215, 289, 290, 295, 296, 298–303, 472, 482, 490, 520, 526, 556, 598, 678, 875
 Olaofe, O., 677
 Olbrecht, A. J., 3
 Oldroyd, D. M., 875
 O'Leary, D. J., 383
 Olekszyk, J., 460
 Olin, J. F., 118, 874
 Olivier, S. C. J., 393
 Olivucci, M., 700, 771, 821, 830, 842
 O'Loane, J. K., 63
 Olofson, R. A., 316
 Olsen, M., 741, 880
 Olson, A. R., 454, 553, 876
 Olson, L. P., 726
 Ölwegård, M., 879
 Onderka, D. K., 654
 O'Neal, H. E., 10
 Ong, E. C., 72
 Oniciu, D. C., 201
 Onrubia, C., 258
 Oosterhoff, L. J., 700, 771
 Op't Holt, B. T., 237
 Oppenheimer, J. R., 223
 Oppenländer, T., 826
 Oppolzer, W., 751
 Orchin, M., 9, 29, 59, 76, 470
 Orendt, A. M., 214
 Orger, B., 843
 Ormsby, J. L., 211
 Orpen, A. G., 5
 Ortega, F., 531
 Ortin, J. L., 258
 Ortiz de Montellano, P. R., 276
 Ortuño, R. M., 153
 Osamura, Y., 771, 820, 830
 Ōsawa, E., 63, 124, 159, 162, 873, 874
 Osborn, C. L., 742
 Osborne, I., 2
 Oscarson, J. L., 429

 Oshima, K., 269, 872
 Osipov, O. A., 20
 Osteryoung, J., xvii
 Osuka, A., 770
 Oth, J. F. M., 726
 Otomaru, Y., 872
 Ott, K.-H., 726
 Ottavi, L., 645
 Ottenbrite, R. M., 762
 Ottensmeyer, F. P., 3
 Otto, R., 495
 Otto, S., 762
 Ottosson, C.-H., 819
 Overman, L. E., 876
 Oxgaard, J., 305
 Oyama, K., 592
 Ozawa, T., 872
 Ozretich, T. M., 871

 Pabon, Jr., R. A., 762
 Pacansky, J., 213
 Pace, J. M., 881
 Pacey, P. D., 23
 Pacifici, J. G., 439, 880
 Paddon-Row, M. N., 266, 308, 604, 740
 Paderes, G. D., 759
 Padwa, A., 742, 744, 746, 881
 Page, G. O., 859
 Page, M., 329
 Pagni, R. M., 87
 Paine, J. S., 878
 Pajak, J., 881
 Pakkanen, T. A., 122
 Pal, A., 872
 Palacios, R. E., 4
 Palacios, S. M., 544
 Pale, P., 310
 Palke, W. E., 23, 40, 46, 47
 Palmer, S., 859
 Pan, H.-Q., 551
 Pan, J., 872, 878
 Pan, J. J., 872
 Panciř, J., 716
 Pandey, B., 305
 Panja, S., 830
 Paolucci, F., 209
 Papamihail, C., 635
 Papavasileiou, M., 645
 Papendick, V., 876
 Pappas, S. P., 167, 854
 Pappo, R., 620
 Paprott, G., 592
 Paquette, L. A., 82, 162, 215, 426, 472
 Parchment, O. G., 9, 871
 Park, B., 516, 834
 Park, B. S., 165
 Park, J. D., 619
 Park, K. H., 880
 Park, M.-S., 881
 Park, N., 208
 Park, S. U., 272
 Park, S.-U., 517
 Párkányi, C., 245

- Parker, A. J., 498, 639
 Parker, A. W., 804
 Parker, D., 88
 Parker, M., 867
 Parker, R. E., 528
 Parker, V. D., 305, 645
 Parkes, A. S., 66
 Parkinson, B. A., 3
 Parmon, V. N., 804
 Parr, R. G., 23, 24, 220, 236, 237, 506
 Parsons, S., 873
 Pascal, Jr., R. A., 237
 Pascher, F., 751
 Pascual-Ahuir, J.-L., 428
 Pasquini, M., 335
 Pasteur, L., 63
 Pasto, D. J., 598, 599, 600, 604, 605, 854
 Pastor, R. W., 117
 Paszyc, S., 812
 Patai, S., 37, 65, 176, 354, 449, 553, 609, 617,
 619, 638, 640, 669, 676, 677, 735, 879
 Patel, A., 879
 Patel, R. C., 331
 Paternò, E., 839
 Paterson, I., 871
 Patil, G. S., 516
 Paton, R. S., 160
 Patz, M., 509
 Pätzelt, M., 160
 Paufler, R. M., 167
 Paukstis, E., 677
 Paul, M. A., 433
 Pauling, L., 5, 19, 21, 22, 29, 31, 35, 43, 192,
 202, 239, 266, 312
 Paulino, J. A., 168
 Paulmann, C., 160
 Pausacker, K. H., 606
 Pautet, F., 881
 Pavia, D. L., 817
 Pavlis, R. R., 583, 873
 Pavone, M., 335
 Pawar, D. M., 132
 Payne, M. T., 612
 Payne, N. C., 502
 Pazos, J. F., 439
 Pearlman, D. A., 135
 Pearson, R. G., 23, 151, 220, 345, 434,
 503–506, 512, 876
 Pedersen, S., 742, 833
 Peerdeman, A. F., 90
 Peiffer, R., 881
 Peishoff, C. E., 533
 Peleg, S., 63
 Pellerite, M. J., 423
 Pemberton, R. P., 216
 Pendás, A. M., 120, 232
 Pendri, A., 636
 Pennington, F. C., 453
 Pepper, M. J. M., 161
 Perchonock, C., 214
 Perdew, J. P., 237
 Perelman, M., 693, 874
 Perez, R., 3
 Pérez-Jiménez, A. J., 874
 Perez-Peralta, N., 161
 Periasamy, M. P., 875
 Perkins, M., 875
 Perkins, M. J., 277
 Perkins, M. V., 872
 Perlmutter, H. D., 751
 Perlmutter, P., 620
 Perrin, C., 519, 525
 Perrin, C. L., 151, 360, 383, 517, 544, 874
 Perrin, D. D., 118, 385, 414, 876
 Perry, S. S., 214
 Persico, M., 566
 Person, W. B., 557
 Persson, J., 529
 Peruchena, N. M., 290, 291
 Peteanu, L. A., 822
 Peters, K. S., 331, 794, 824, 838, 849
 Petersen, B. L., 291
 Petersen, M. R., 730
 Petersen, R. C., 403
 Peterson, A. H., 314
 Peterson, H. J., 594
 Peterson, L. I., 167
 Peterson, P. E., 459, 609, 615, 878
 Petillo, P. A., 137
 Petrarca, A. E., 77
 Petty, S. T., 876
 Peyerimhoff, S. D., 46
 Pezacki, J. P., 298
 Pfalzberger, R., 59
 Pfander, H., 638
 Pham, T. N., 515, 516, 517
 Phan, T. B., 509
 Phillips, D., 795, 804, 834
 Phillips, L., 118, 150, 581
 Phillips, R. B., 724
 Phillips, W. V., 316
 Phillips, D. C., 447
 Piani, G., 335
 Piecuch, P., 772
 Pieraccini, D., 610
 Piercy, J. E., 57
 Pierini, A. B., 544, 771
 Piermatti, O., 873
 Pierrefixe, S. C. A. H., 205
 Pierson, G. O., 439
 Pietraperzia, G., 335
 Pigman, W., 79
 Pike, R. A., 163
 Pilar, F. L., 177
 Pilcher, G., 9, 871
 Pilling, M. J., 268
 Pimblott, S. M., 810
 Pimentel, G., xvi
 Pinchas, S., 373
 Pincock, J. A., 609, 849
 Pinheiro, L. M. V., 403
 Pinhey, J. T., 847
 Pinkerton, A. A., 165
 Pinnick, H. W., 544
 Pipek, J., 225
 Pisano, D., 205
 Pittman, Jr., C. U., 211
 Pitts, Jr., J. N., 787, 847
 Pitzer, K. S., 10, 119, 120, 121, 128, 130, 874
 Pitzer, R. M., 120, 231
 Pizzo, F., 873
 Platero-Prats, A. E., 6
 Platz, M. S., 213, 255, 256, 260, 278, 280,
 284, 287, 288, 305, 776
 Plesch, P. H., 879
 Plesničar, B., 606
 Poater, J., 211
 Pocker, Y., 492, 876
 Podraza, R., 880
 Pogliani, L., 820
 Poirier, R. A., 382, 562
 Poisson, L., 331
 Polanyi, M., 363, 553
 Polavarapu, P. L., 152, 874
 Polce, M. J., 308
 Politzer, P., 19, 23
 Pollack, R. M., 672
 Pollak, A., 611
 Pollitte, J. L., 159
 Pollnitz, A. P., 867
 Polniaszek, R. P., 873
 Polyakov, A. E., 62
 Pomelli, C. S., 557
 Pomerantz, M., 871, 880
 Ponaras, A. A., 271
 Ponec, R., 300
 Pong, R. G. S., 213
 Ponomarev, D. A., 12
 Popelier, P. L. A., 40, 461
 Pophristic, V., 120, 150, 232
 Popielarz, R., 309
 Popik, V. V., 877, 881
 Pople, J. A., 12, 175, 266, 292, 294, 295, 306,
 308, 817
 Poplett, R., 480
 Popović, A., 581
 Popper, K. R., 327
 Poppinger, D., 310
 Portella, G., 211
 Porter, G., 794, 813, 847
 Porter, N., 276, 332
 Porter, N. A., 272
 Poschmann, L., 881
 Posner, G. H., 621
 Postigo, J. A., 827
 Postma, H. W. C., 208
 Potier, P., 55
 Potter, D. E., 320
 Pou, P., 3
 Poupko, R., 726
 Poutsma, M. L., 576–578
 Powell, A. L., 330
 Powell, C. E., 681
 Powell, M. F., 384, 566
 Powers, V. M., 332
 Pozzessere, A., 166
 Prabhakar, S., 855
 Prakash, G. K. S., 166, 214, 290, 296, 299,
 301, 302, 303, 305, 490, 526, 875

- Prathapan, S., 826
 Prato, M., 208, 209
 Pratt, D. A., 276
 Pratt, D. W., 308, 815
 Pratt, L. M., 313, 500
 Preda, D. V., 209
 Prelog, V., 65, 68, 83, 84, 115, 116, 128, 162
 Prescher, J. A., 746
 Presser, N., 378
 Pressman, D., 648
 Price, D. R., 216
 Prinsen, W. J. C., 67
 Prinstein, R., 301
 Pritchard, D. E., 41, 871
 Pritchard, G. O., 880
 Pritchard, H. O., 24
 Pritchard, J. G., 876, 877
 Proserpio, D. M., 6
 Proskow, S., 64
 Pross, A., 212, 365, 513, 517, 532, 875
 Protti, S., 853
 Prudent, N., 624
 Pruitt, K. M., 529, 877
 Pryor, W. A., 273, 590
 Przystas, T. J., 459
 Puchta, R., 217, 770
 Pugmire, R. J., 148
 Pullman, B., 250
 Punta, C., 276
 Punzalan, E. R., 319
 Purlee, E. L., 593
 Put, J., 829
 Puterbaugh, W. H., 556
 Pye, P. J., 879

 Qiao, R., 209
 Quabeck, U., 875
 Quack, M., 161, 790
 Quenneville, J., 819
 Quin, C., 277
 Quina, F. H., 809, 817, 818, 859
 Quinkert, G., 881
 Quinn, C. M., 224
 Quintanilla, E., 302
 Quirk, R. P., 93

 Raban, M., 88, 94
 Rabasco, J. J., 654
 Rabenstein, D. L., 216
 Raber, D. J., 479, 485, 875
 Rabitz, H., 137
 Rablen, P. R., 40
 Racah, E. J., 271
 Racela, W., 420
 Racioppi, R., 839
 Rackova, L., 258
 Radenković, S., 211, 874
 Radner, F., 525
 Radom, L., 12, 161, 264, 280, 292, 295, 306, 308, 310, 340, 532, 875
 Radziszewski, J. G., 214
 Ragazos, I. N., 700, 830
 Raghavachari, K., 122, 294, 303, 312, 593

 Raghavan, S. R., 862
 Ragsdale, J. W., 504
 Ragunathan, N., 872
 Rahman, M., 151
 Raimondi, L., 771
 Raimondi, M., 47, 205, 239
 Raines, R. T., 345
 Rains, H. C., 529
 Rajagopal, S., 256, 339
 Rajasekaran, K., 880
 Rajzmann, M., 305
 Raley, J. H., 353, 590
 Ramaiah, D., 881
 Ramakrishnan, V., 529
 Ramamurthy, V., 305, 795, 825, 859
 Ramanathan, S., 871
 Ramesh, R., 859
 Ramey, P. S., 579
 Ramondo, F., 23, 388
 Ramos, M. J., 237
 Ramsay, O. B., 125
 Randić, M., 207, 210, 211, 242, 871
 Raner, K. D., 378
 Rao, A. V. R., 872
 Rao, B. V., 872
 Rao, P. A. D. S., 92
 Rao, T. V. R., 21
 Rao, V. P., 795
 Rappé, A. K., 136
 Rappoport, Z., 316, 331, 532, 533, 534, 609, 618, 636, 642, 874, 879
 Rapson, W. S., 621
 Raske, K., 92
 Rastelli, A., 608
 Rasul, G., 166, 299, 490, 526
 Rath, H., 770
 Rath, N. P., 855
 Rathke, M. W., 316
 Ratsimandresy, B., 575
 Rauhut, M. M., 530, 860
 Rauk, A., 62, 743
 Raulins, N. R., 715
 Raunio, E. K., 619
 Rawal, V. H., 258
 Rawson, D., 872
 Rayez, M. T., 288
 Raymond, F. A., 586
 Reynolds, P. W., 735
 Read, J., 662
 Reagan, M. T., 432
 Reamer, R. A., 879
 Rebbert, R. E., 295
 Rebek, Jr., J., 606
 Rebell, J., 726
 Rector, C. L., 276
 Redding, R. W., 440
 Reddy, A. C., 309, 517
 Reddy, A. R., 207
 Reddy, J. S., 872
 Reddy, R. R., 21
 Reddy, S. R., 876
 Reddy, T. J., 258
 Reddy, V. P., 299, 880

 Redlich, B., 290
 Redlich, S., 853
 Redmore, D., 876
 Reed, A. E., 226, 312
 Reed, C. A., 291
 Reed, L. H., 177
 Rees, C. W., 278
 Reese, C. B., 881
 Reese, K. M., 202
 Reetz, M. T., 624
 Reeve, J. C., 342
 Reger, D. W., 681
 Reguero, M., 842
 Réhault, J., 809
 Rei, M.-H., 597
 Reichardt, C., 339
 Reichert, M., 872
 Reid, E. E., 592
 Reid, P. J., 700
 Reid, S. A., 280
 Reider, P. J., 879
 Reimann, J. E., 876
 Reinhardt, L. A., 462
 Reinhoudt, D. N., 499
 Reinmuth, O., 585, 592
 Reis, J. C. R., 403
 Reisenauer, H. P., 162
 Reiser, A., 627
 Reiter, R. C., 310
 Reitz, O., 444
 Remennikov, G., 509
 Ren, Y., 512
 Renaud, P., 269, 271, 272, 274, 275
 Renneberg, D., 638
 Renneboog, R., 426
 Repinec, S. T., 795
 Rest, A. J., 801
 Reuwer, Jr., J. F., 374
 Revés, M., 6
 Reynolds, C. H., 580
 Reynolds, D. W., 762
 Reynolds, K. A., 873
 Reynolds, L. J., 332
 Rezaei, H., 762
 Rhoads, S. J., 700, 715
 Ribeiro da Silva, M. A. V., 9, 871
 Richard, J. P., 438, 479
 Richards, W. G., 223
 Richardson, A. C., 872
 Richardson, W. S., 133
 Richey, Jr., H. G., 876
 Richter, R. F., 598
 Rickborn, B., 635, 652, 880
 Ricks, A. M., 294
 Ridd, J. H., 525, 677
 Riddick, J. A., 338
 Rieger, P. H., 259
 Rieke, C. A., 230
 Rieke, R. D., 859
 Riemenschneider, J. L., 300, 303
 Riera, J., 258
 Riether, D., 879
 Rigaudy, J., 69, 115

- Rigby, J. H., 739
 Rigby, R. D. G., 847
 Riguet, E., 69, 881
 Riley, K. E., 237
 Riley, T., 456
 Ritchie, C. D., 401, 479, 496
 Ritscher, J. S., 167
 Ritter, J. J., 409
 Rittner, R., 150
 Rivetti, F., 562
 Robb, M. A., 700, 771, 821, 830, 842
 Robbins, M. D., 661
 Roberts, A. P., 209
 Roberts, B. G., 860
 Roberts, I., 553
 Roberts, J. D., 42, 176, 240, 267, 291, 298, 311, 386, 492, 536, 539, 742, 873, 877
 Roberts, T. D., 853
 Robertson, J., 274
 Robertson, J. M., 67, 207
 Robertson, P. W., 555, 558, 584
 Robertson, R. E., 383
 Robie, D., 378
 Robinson, A. L., 3
 Robinson, E. A., 44
 Robinson, G. C., 479, 483
 Robinson, G. W., 815
 Robinson, J. K., 378
 Robinson, J. S., 2
 Robinson, R., 210, 621
 Robison, M. M., 453
 Roček, J., 371
 RoCHAT, S., 861
 Roche, A. J., 873
 Rodgers, A. S., 10
 Rodriguez, C. F., 429, 580
 Roe, D. C., 873, 876
 Rogers, D. W., 10, 205, 871
 Rogers, M. T., 266
 Rohde, C., 429
 Rolli, E., 426
 Rolston, J. H., 554, 570, 572, 878
 Romanenko, V., 281
 Romero, F. A., 876
 Rominger, F., 166
 Ron, A., 382
 Rondan, N. G., 429, 604, 724
 Ronzini, L., 531
 Roohi, H., 151, 160
 Rooney, C., 856
 Roos-Kozel, B. L., 525
 Root, D. M., 29
 Roothaan, C. C. J., 224
 Roschek, B., Jr., 276
 Rosenberg, R. E., 117
 Rosenblum, M., 530, 877
 Rosenfeld, S. M., 168
 Rosenfelder, W. J., 667, 879
 Rosenthal, J. W., 749
 Rosenwald, R. H., 578
 Rosini, C., 872
 Rosker, M. J., 2
 Rosokha, S. V., 201, 526
 Rosowsky, A., 578
 Ross, J., 246
 Ross, P., 852
 Ross, R. A., 687
 Ross, S. D., 528
 Rossen, K., 879
 Rossi, A. R., 262
 Rossi, R. A., 543, 544, 878
 Rossiter, B. W., 8, 20, 32, 118, 259, 871
 Rossky, P. J., 485
 Roth, H. D., 305, 834
 Roth, W. R., 254, 709, 715, 719, 722, 726, 752
 Rothstein, E., 470
 Rousseau, Y., 876
 Rouvray, D. H., 256
 Roux, M. V., 871
 Rowley, E. G., 879
 Roy, M. F., 259
 Roy, U., 880
 Royner, S. L., 54
 Rozen, S., 580, 582, 878
 Rozsondai, B., 189
 Ruasse, M. F., 555, 557, 561, 566, 571, 575, 878
 Rubinstein, E., 852
 Rüchardt, C., 136, 205, 268
 Ruckebusch, C., 809
 Rudberg, E., 207
 Rudchenko, V. F., 872
 Rudofsky, S., 202
 Rudolf, K., 636
 Ruedenberg, K., 34
 Ruhoff, J. R., 190
 Runge, W., 65
 Runtz, G. R., 40, 235
 Rush, J. E., 77
 Russell, G. A., 272, 320, 543
 Russell, R. A., 740
 Rust, F. F., 353, 589, 590
 Ruster, V., 772
 Rutkin, P., 66, 871
 Rutledge, T. F., 615, 744
 Ruzsicska, B. P., 255
 Ruzsinszky, A., 237
 Ruzziconi, R., 652, 873
 Ryan, J. P., 335
 Rychnovsky, S. D., 81, 872
 Rychtman, A., 413
 Ryckaert, J.-P., 154
 Rynard, C. M., 598
 Ryu, I., 272
 Rzepa, H. S., 202, 763, 769
 Saad, Z., 350
 Sabino, A. A., 526
 Sachs, R. K., 212
 Sadius, R. J., 153
 Saebo, S., 211
 Saegusa, T., 320
 Saettel, N. J., 305, 716
 Sager, W. F., 401
 Sahli, S., 741, 880
 Saito, A., 873, 876
 Saito, S., 120, 519, 770
 Sajimon, M. C., 881
 Sakae, Y., 876
 Sakagami, T., 878
 Sakai, S., 206, 705, 706, 709
 Sakamoto, Y., 878
 Sakano, T. K., 338
 Sakata, J., 84
 Sakiyama, M., 871
 Sakurai, H., 823
 Salama, A., 578
 Salandria, K., 166
 Salek, P., 207
 Salem, L., 34, 175, 264, 292, 756, 820, 832
 Salisbury, K., 117, 801
 Saltiel, J., 790, 819
 Saltzman, M., 161
 Saltzman, M. D., 19, 300
 Salzner, U., 151
 Šaman, D., 873
 Samanta, S., 837, 881
 Sammes, P. G., 880, 881
 Samuel, C. J., 388
 Samuel, D., 440, 530, 877
 Sancassan, F., 530
 Sanchez, M., 161
 Sanchez, R. I., 459
 Sancho-García, J. C., 874
 Sandall, J. P. B., 525
 Sandel, V. R., 313, 845, 880
 Sander, W., 164, 286
 Sanderson, R. T., 22
 Sankar, J., 770
 Sankararaman, S., 748
 Sannicolò, F., 873
 Sannigrahi, A. B., 192
 Santaballa, J. A., 447
 Santarsiero, B. D., 556
 Santerre, G. M., 395
 Santiago, A. N., 544, 878
 Santos, A. F. L. O. M., 871
 Santos, I., 426
 Santos, J. C., 585
 Sapre, R., 460
 Sardella, D. J., 241
 Sargent, G. D., 270, 300
 Sarzi-Amadè, M., 608
 Sasaki, T., 209
 Satchell, D. P. N., 459
 Sathish, M., 209
 Sato, Y., 519
 Sau, A. C., 499
 Sauer, J., 735
 Sauer, M., 859
 Sauers, R. R., 125
 Saunders, D. G., 267
 Saunders, Jr., W. H., 354, 371, 375, 445, 492, 519, 638, 643, 650, 651, 652, 659, 663, 664, 772, 874, 876, 879
 Saunders, M., 147, 214, 296, 297, 302, 303, 304, 383
 Sauriol, F., 463

- Sauvage, J.-P., 67, 350
 Savage, C., 290
 Savéant, J.-M., 543
 Savedoff, L. G., 498
 Savitz, M. L., 844
 Savoy, M. G., 586
 Sawhney, A. K., 205
 Sawyer, C. B., 456
 Sayer, T. S. B., 316
 Saytzeff, A., 655
 Scaiano, J. C., 273, 287, 815, 817, 845, 849
 Scarborough, H. A., 500
 Schaad, L. J., 212, 218, 374, 566, 716, 880
 Schadt, F. L., 477
 Schaefer III, H. F., 121, 216, 225, 254, 279, 280, 286, 331, 364, 502, 566, 820, 871
 Schaefer, A. R., 378
 Schaeffer, H. J., 674
 Schaeffer, W. D., 86, 482, 678
 Schäfer, H., 269, 371
 Schaffner, K., 881
 Schaleger, L. L., 353
 Schaller, H. F., 473
 Schalley, C. A., 383
 Schatz, B., 700
 Scheer, W., 745
 Scheeren, H. W., 636, 879
 Scheffer, J. R., 829, 881
 Scheinmann, F., 853
 Scheins, S., 160
 Schenck, G. O., 852, 880
 Schep, N. P., 309, 446
 Schiavelli, M. D., 615
 Schiccheri, N., 335
 Schiess, P. W., 636
 Schiesser, C. H., 272
 Schill, G., 67
 Schimmel, H., 509
 Schindelholz, L., 69
 Schipperijn, A. J., 212
 Schiroli, A., 666
 Schlatmann, J. L., 875
 Schlegel, H. B., 499, 517
 Schlemmer, S., 290
 Schleyer, P. v. R., 10, 12, 15, 39, 46, 124, 135, 136, 149, 151, 159, 161, 190, 202, 205, 206, 217, 237, 264, 269, 280, 290, 291, 292, 294, 295, 296, 299, 301, 302, 303, 305, 312, 315, 419, 429, 475, 477, 479, 482, 485, 490, 494, 593, 604, 678, 769, 770, 874, 875
 Schlick, S., 726
 Schlögl, K., 66
 Schlögl, R., 207
 Schlosberg, R. H., 298
 Schmalz, T. G., 211, 242
 Schmid, G. H., 553, 558, 561, 593, 609, 878
 Schmid, H., 335, 336, 722, 879, 880, 881
 Schmid, K., 335, 336
 Schmid, W. E., 830
 Schmidlin, S. P., 308
 Schmidt, E. E., 3
 Schmidt, H.-G., 872
 Schmidt, J. A., 804
 Schmidt, R., 804, 851
 Schmidt, W., 207
 Schmitz, A., 751
 Schmitz, J., 162
 Schmitz, L. R., 156
 Schnapp, K. A., 790
 Schneider, H.-J., 569, 878
 Schneider, M. P., 726
 Schneider, W. G., 296
 Schoeller, W. W., 280
 Schoenlein, R. W., 822
 Schomaker, V., 202
 Schomburg, D., 880
 Schönberg, A., 835
 Schöner, B., 872
 Schore, N., 815, 860
 Schormann, M., 294
 Schowen, R. L., 380, 384
 Schramm, C. H., 659
 Schreck, J. O., 395
 Schreiber, J., 371
 Schreiber, K. C., 490
 Schreiber, M., 663, 664
 Schreiber, W. L., 881
 Schreiner, P. R., 13, 162, 232, 237, 282
 Schriesheim, A., 432
 Schröder, G., 726, 854
 Schubert, C., 579
 Schubert, J. W., 556
 Schubert, W. M., 593
 Schuck, D. F., 533
 Schueller, K., 742
 Schug, K., 665
 Schuler, R. H., 261, 266
 Schulman, J. M., 167, 871
 Schulman, S. G., 814
 Schultz, B. G., 439
 Schultz, N. E., 237
 Schultz, P. A., 46, 47, 176
 Schultz, P. G., 736
 Schultz, S. C., 879
 Schulz, S., 872
 Schupp, O., 872
 Schurig, V., 872
 Schurman, I., 682
 Schuster, D. I., 841
 Schuster, G. B., 858, 860
 Schuster, P., 154
 Schutt, C., 137
 Schwab, C., 812
 Schwab, P. A., 617
 Schwabe, T., 237
 Schwarz, J. C. P., 79
 Schweitzer, C., 851
 Schlove, D. B., 439
 Scott, A. D., 496, 633
 Scott, A. P., 280
 Scott, C. B., 504, 508
 Scott, L. T., 161, 209, 272, 871
 Scribner, J. D., 678
 Scuseria, G., 566
 Seager, J. H., 615
 Seakins, P. W., 268
 Searle, C. E., 480
 Searles, Jr., S., 614, 878
 Searles, S., 879
 Sears, T. J., 279
 Sebastian, J. F., 428
 Seburg, R. A., 255
 Seebach, D., 83, 84, 872
 Seelen, A. E., 636, 879
 Seeles, H., 441
 Seeman, J. I., 360
 Sefton, M. A., 867
 Sehmi, P., 385
 Sehna, P., 873
 Seibl, J., 607
 Seidel, B., 742
 Seidl, E. T., 254
 Seidner, T., 216
 Seifert, W. K., 759
 Seltzer, R. J., 202
 Seltzer, S., 381
 Selwood, P. W., 259
 Semenow, D., 678
 Semenow, D. A., 536, 539, 877
 Sementsov, A., 202
 Semple, T., 830
 Semple, T. C., 830
 Semsel, A. M., 860
 Sen, K. D., 22, 23
 Senanayake, C. H., 872
 Senderowitz, H., 117
 Sendra, J. M., 258
 Sension, R. J., 795
 Sentandreu, E., 258
 Senthilnathan, V. P., 288
 Seppelt, K., 592
 Serjeant, E. P., 414
 Serra, S., 873
 Servis, K. L., 375, 382
 Seuleiman, M., 871
 Sevin, F., 312
 Sgobba, V., 208
 Shafer, S. G., 368
 Shah, B. K., 207
 Shaik, S. S., 19, 27, 205, 238, 240, 266, 276, 309, 365, 479, 499, 500, 503, 513, 517, 533, 724
 Shallenberger, R. S., 63
 Sham, L. J., 236
 Shamma, M., 878
 Shandala, M. Y., 483
 Shank, C. V., 795, 822
 Shapiro, R. H., 286
 Shapiro, S. A., 562, 569
 Sharma, P. K., 276
 Sharp, R. L., 603
 Sharpless, K. B., 746
 Sharrah, M. L., 619
 Sharts, C. M., 586, 742
 Shavitt, I., 161
 Shaw, R., 10
 Shea, K. J., 606, 724, 873
 Shearer, G. O., 607

- Sheats, J. E., 528
 Shechter, H., 287, 875
 Shefter, E., 626
 Shen, C. C., 374, 421, 438
 Shen, D.-K., 803
 Shen, K., 766
 Sheppard, W. A., 330, 586
 Sheridan, R. S., 125, 331
 Sherman, J., 239
 Sherrill, C. D., 254
 Sherrod, S. A., 475
 Shetlar, M. D., 810
 Sheu, C., 757
 Shevlin, P. B., 164, 255
 Shi, B., 683
 Shida, T., 305
 Shieh, T.-C., 581
 Shih, C.-H., 678
 Shilav, R., 118
 Shillady, D. D., 762
 Shima, M., 392
 Shimamori, H., 815
 Shimizu, M., 752
 Shin, J.-Y., 770
 Shine, H. J., 772
 Shiner, Jr., V. J., 262, 383
 Shingu, H., 567
 Shinmyozu, T., 853
 Shinokubo, H., 770
 Shintani, R., 872
 Shiotani, M., 305, 307
 Shizuka, H., 812
 Shoemaker, D. P., 66
 Shoppee, C. W., 134, 492
 Shorter, J., 358, 389, 400
 Shu, Q., 163, 208
 Shubin, V. G., 250, 302
 Shudo, K., 519
 Shue, R. S., 872
 Shukla, D., 298, 815
 Shum, K., 636
 Shurki, A., 238
 Shustov, G. V., 62
 Sibi, M. P., 269, 271, 272, 274, 275
 Siddhanta, A. K., 446
 Sidman, J. W., 790, 817
 Sieber, S., 296, 302, 490
 Siebert, T. E., 867
 Siebrand, W., 798
 Sieck, L. W., 295
 Siefert, J. H., 875
 Siegbahn, K., 32
 Siegel, J., 84, 98
 Siegel, J. S., 206, 209, 383
 Siegel, S., 496
 Siehl, H.-U., 302, 304
 Siggel, M. R., 418
 Siggel, M. R. F., 418, 428
 Silber, P., 834
 Silberman, L., 274
 Silla, E., 428
 Silva, C. O., 419
 Silver, D. M., 771
 Silversmith, E. F., 161, 469, 533, 716
 Silverstein, R.M., 797
 Sime, J. G., 67
 Simmons, H. E., 283
 Simmons, Jr., H. E., 536, 877
 Simms, J. A., 619
 Simões, J. A. M., 267
 Simon, A., 769, 770
 Simon, E., 63
 Simon, J. D., 331
 Simon, R. J., 776
 Simonetta, M., 159, 290
 Simons, J., 35, 224
 Simonson, T., 154
 Sims, L. B., 375, 665
 Singer, L., 85
 Singer, S. R., 336
 Singh, F. V., 872
 Singh, U. C., 461
 Singhal, N., 837
 Singleton, D. A., 309, 374, 608, 772, 852
 Singleton, D. M., 666
 Sinke, G. C., 10, 156
 Sirois, S., 429
 Sironi, A., 873
 Sironi, M., 205
 Siskin, M., 298
 Sjöqvist, L., 307
 Skalitzy, D. J., 872
 Skell, P. S., 482, 583, 611, 873
 Skiff, W. M., 136
 Skinner, K. J., 257
 Skobridis K., 872
 Slater, J. C., 25, 29
 Slauch, L. H., 379
 Slayden, S. W., 215
 Slebocka-Tilk, H., 460-463, 556, 558, 559,
 562, 563, 573, 608, 668, 878
 Slocum, D. W., 79
 Slutsky, J., 159
 Smat, R. J., 650
 Smid, J., 392
 Smiles, S., 529
 Smissman, E. E., 683
 Smith, B. J., 306
 Smith, D., 533
 Smith, E. A., 576
 Smith, F. F. P., 500
 Smith, G. F., 505
 Smith, G. G., 685
 Smith, H. A., 190
 Smith, H. G., 584
 Smith, III, A. B., 881
 Smith, J. A. S., 202
 Smith, J. C., 136
 Smith, J. F., 490
 Smith, J. S., 650
 Smith, K., 524
 Smith, M. B., 877
 Smith, R. A., 2, 586
 Smith, R. D., 283
 Smith, S., 498
 Smith, S. F., 497
 Smith, W. B., 227, 526, 878
 Smith, W. T., 876
 Smolinsky, G., 685
 Smyth, C. P., 20, 118, 312, 871
 Snadden, R. B., 357
 Snatzke, G., 90
 Sneen, R. A., 479
 Snieckus, V., 751
 Snirc, V., 258
 Snow, D. H., 544
 Snyder, J. J., 824
 Soanes, P. W., 528
 Sobel, H., 505
 Sodeau, J. R., 801
 Solà, M., 211, 311, 500
 Solcà, N., 295
 Solin, N., 4
 Soltsev, K. M., 814
 Solomons, T. W. G., 357
 Soloway, S. B., 759
 Soltanov, R. I., 677
 Somasekhara, S., 845
 Sommer, J., 296, 875
 Sondheimer, F., 217
 Song, B. D., 460
 Song, L., 232
 Songstad, J., 505
 Sonoda, T., 527, 877
 Sorba, J., 257
 Sørensen, P. E., 439, 876
 Sorensen, T. S., 299, 304, 743
 Sotler, T., 581
 Soundararajan, N., 287
 Sousa, S. F., 237
 Souto-Bachiller, F. A., 213
 Sovers, O. J., 120, 231
 Spangler, C. W., 720
 Spangler, L. H., 815
 Sparrapan, R., 526
 Spatcher, D. N., 455
 Spellmeyer, D. C., 274, 757
 Spencer, C. F., 163
 Speranza, M., 388
 Spiesecke, H., 296
 Spindler, E., 746
 Spino, C., 762
 Spitzer, R., 128, 130, 874
 Spitznagel, G. W., 315, 429
 Spizzichino, S., 873
 Sponsler, M. B., 859
 Sprecher, R. F., 267
 Spreer, L. O., 347
 Squillacote, M., 125, 131, 163, 830
 Squires, R. R., 168, 255
 Srinivasan, M., 876
 Srinivasan, R., 790, 829, 830, 833, 839, 853
 Srisook, E., 878
 Stacey, F. W., 591
 Staemmler, V., 213
 Stafford, D. G., 855
 Stahl, F., 206
 Stairs, J., 166
 Staley, S. W., 215, 319, 743, 874

- Standard, J. M., 356
 Stang, P. J., 135, 532, 609
 Stanger, A., 16, 205, 217, 269
 Stanton, J. F., 216
 Stará, I. G., 873
 Staral, J. S., 215
 Starcher, P. S., 607
 Starikov, E. B., 402
 Starkey, K., 207
 Starý, I., 873
 Stauffer, C. H., 443
 Stavber, S., 581
 Steadman, J., 308
 Steen, K., 729
 Steenken, S., 825
 Steer, R. P., 795
 Stefanidis, D., 457, 459, 876
 Stefek, M., 258
 Steigman, J., 470, 481
 Stein, A., 56, 127
 Stein, G., 759
 Stein, K., 719
 Stein, R., 520
 Steinfeld, G., 878
 Steinmetzer, H.-C., 860
 Stepanov, A. G., 677
 Stephens, P. J., 872
 Stephenson, Jr., L. M., 714
 Stephenson, L. M., 772, 851
 Stermitz, F. R., 579, 844
 Stern, P. S., 135
 Sternberg, R. J., xvi
 Stevens, B., 459
 Stevens, I. D. R., 498, 639
 Stevens, J. B., 431
 Stevens, P. G., 682
 Stevens, T. S., 286
 Stevenson, G. R., 310
 Stewart, E. T., 37, 176
 Stewart, J. J. P., 214, 223
 Stewart, R., 42, 214, 380, 415, 433, 593
 Stiasny, H. C., 275
 Stiles, P. J., 96
 Still, W. C., 117
 Stille, J. K., 617
 Stimson, V. R., 677
 Stirling, C. J. M., 472, 512, 872
 Stivers, E. C., 374
 Stock, L. M., 386–388, 523
 Stockfisch, T. P., 137
 Stoddard, G. J., 724
 Stoddard, J. F., 8, 137
 Stofko, Jr., J. J., 304, 726
 Stoll, S., 94
 Stolow, R. D., 879
 Stolte, S., 117
 Storer, J. W., 771
 Stork, G. A., 682
 Stowell, J. C., 315
 Strachan, A. N., 877
 Strachan, E., 847
 Stranges, A. N., 19
 Strating, J., 556
 Strausz, O. P., 255
 Strazzari, S., 531
 Streiter, A., 513
 Streitwieser, Jr., A., 86, 175, 204,
 214, 240, 291, 311, 374, 380,
 382, 418–421, 438, 482, 502, 603,
 678, 731, 873
 Stretton, A. D., 873
 Stroschio, J. A., 3
 Strouse, G. F., 834
 Strub, H., 214
 Strunk, R. J., 666
 Stuchal, F. W., 544
 Stucky, G. D., 3
 Stull, D. R., 10, 156
 Sturtevant, J. M., 8
 Su, B. M., 313
 Su, P., 500
 Su, W.-Y., 517
 Suarez, C., 726
 Subba Rao, B. C., 600
 Subotkowski, W., 772
 Subrahmanyam, S. V., 57
 Subramanian, L. R., 532, 609
 Subramanian, V., 771
 Suenaga, K., 4
 Suenram, R. D., 735
 Suffert, J., 706
 Sugarman, D., 79
 Sugasawara, R., 459
 Sugimoto, Y., 3
 Suhling, K., 862
 Suhrada, C. P., 777
 Sullivan, D. F., 316
 Sullivan, J. M., 586
 Sullivan, T. F., 644
 Sulzbach, H. M., 280
 Sumner, F. H., 24
 Sun, F., 304
 Sun, W.-T., 858
 Sun, X.-J., 517
 Sunasee, R., 875
 Sundberg, K. R., 604
 Suñer, G. A., 749
 Sunko, D. E., xvii, 296, 299, 301, 380
 Suresh, C. H., 205, 881
 Susnow, R., 137
 Sustmann, R., 735, 746
 Sutton, H. C., 440
 Suzuki, M., 770
 Suzuki, S., 380
 Suzuki, T., 159
 Svoboda, J., 853
 Swain, C. G., 330, 374, 399, 448, 449, 470,
 488, 504, 508, 528
 Swanson, C. P., 794
 Swedlund, B. E., 555
 Swern, D., 605, 878
 Swiger, R. T., 544
 Symons, M. C. R., 261, 262
 Szabo, A., 553
 Szafran, M., 205
 Szarka, A. Z., 795
 Szeimies, G., 160
 Szilagy, S., 566
 Szulejko, J. E., 426
 Szwarc, M., 392, 485
 Szymanski, K., 242
 Szymanski, M. J., 852
 Taber, R. L., 669
 Tabet, J.-C., 424
 Tabuchi, M., 879
 Tabushi, I., 606
 Tachiya, M., 810
 Tadano, K., 735, 880
 Tae, J., 856
 Tafazzoli, M., 726
 Taft, R. W., 339, 385, 393, 399, 400, 418, 422,
 474, 478, 576, 592, 593, 876
 Tahara, K., 166
 Taher, N. A., 479
 Tai, A., 880
 Tai, J. C., 496
 Tait, B. D., 626
 Takada, Y., 62
 Takahashi, J., 639
 Takahashi, M., 854
 Takahashi, T., 168, 207
 Takamuku, S., 823
 Takane, S., 705
 Takao, K., 735, 880
 Takeda, M., 154
 Takeda, T., 159
 Takemura, A., 168
 Takenobu, T., 207
 Takeuchi, K., 19, 875
 Takeuchi, Y., 874
 Takeya, J., 207
 Takeya, T., 209
 Takhistov, V. V., 12
 Takiff, L., 858
 Tal, Y., 233, 235
 Talaty, E. R., 19
 Talbot, R. J. E., 449
 Talkowski, C. J., 681
 Tallman, K. A., 276
 Tamegai, K., 878
 Tamiri, T., 118
 Tamm, K., 338
 Tamm, T., 338
 Tamura, K., 159
 Tamura, M., 762
 Tamura, Y., 854
 Tanaka, K., 159, 268
 Tanaka, R., 619
 Tanaka, T., 4
 Tang, T.-H., 235
 Tang, W. C., 208
 Tang, Y., 132
 Tangsheng, P., 78
 Tani, H., 316
 Tanida, H., 740
 Taniguchi, S., 803
 Tantillo, D. J., 300, 302, 724
 Tao, C., 280

- Tao, E. V. P., 878
 Tao, T., 880
 Tao, Y.-T., 651
 Tappe, W., 662
 Tarantelli, F., 645
 Tarbell, D. S., 334, 558, 631, 878
 Tárnoky, A. L., 480
 Tarrant, P., 619
 Tasevski, M., 606
 Taticchi, A., 735
 Tavernier, D., 84
 Tawney, P. O., 621
 Taylor, G. N., 881
 Taylor, R., 5, 310, 522
 Taylor, R. J. K., 310
 Taylor, T. I., 876
 Taylor, W. H., 874
 Tazuke, S., 858
 Tchoubar, B., 338
 Tedder, J. M., 309, 378, 590
 Tedesco, A. C., 817, 818
 Teepen, T., 208
 Teets, D. E., 1
 Telfer, S. J., 858
 Teller, E., 308
 Templeton, D. H., 91
 Temprado, M., 871
 Tendil, J., 611
 Teng, H., 2
 Teng, P. A., 790
 Tenud, L., 607
 Tepe, J. J., 753
 Teplý, F., 873
 ter Wiel, M. K. J., 858
 Ternansky, R. J., 162
 Terrier, F., 527, 531
 Terrier, P., 873
 Terry, E. M., 554
 Tewfik, R., 328
 Texier, F., 395
 That, Q. T., 872
 Thatcher, G. R. J., 151
 Théron, F., 533
 Thibblin, A., 299
 Thibodeau, P., 795
 Thiébauld, A., 543
 Thiele, G., 421
 Thielecke, W., 159
 Thielmann, M., 880
 Thilgen, C., 63
 Thomas IV, B. E., 709
 Thomas, J. B., 881
 Thomas, J. M., 677
 Thomas, R. C., 274
 Thomas, R. J., 455
 Thomas, T. D., 418, 428
 Thomassen, L. M., 499
 Thompson, J. D., 313
 Thompson, M., 32
 Thomson, R. H., 257
 Thouet, H., 162
 Thrush, B. A., 860
 Thummel, 652
 Thurmaier, R. J., 878
 Thyagarajan, B. S., 85, 619
 Tichý, M., 63
 Ticknor, B. W., 294
 Tidwell, T. T., 214, 215, 257, 592, 593, 598, 612, 877
 Tieman, C. H., 654
 Tiernan, T. O., 295
 Tierney, J., 585
 Timmermans, P. J. J. A., 163
 Timmons, C. J., 118
 Timmons, R. B., 380
 Tinker, H. B., 597, 878
 Tinsley, S. W., 607
 Tipper, C. F. H., 449, 558
 Tipton, T. J., 267
 Tirado-Rives, J., 154
 Tisch, J. W. G., 2
 Tise, F. P., 824
 Tishkov, A. A., 473
 Titmas, R. C., 459
 Tiwari, S., 762
 Tobe, Y., 166, 168
 Tobey, S. W., 455
 Tobia, D., 635
 Tobita, S., 812
 Toda, F., 118, 159
 Todd, D., 68
 Todd, W. P., 306
 Tofi, M., 852
 Tokitoh, N., 256
 Tokumaru, K., 822
 Tokunaga, N., 872
 Tolbert, L. M., 517, 814
 Tolgyesi, W. S., 296
 Tomasi, J., 566
 Tomer, J. L., 815
 Tomioka, H., 282, 284, 287, 875
 Tomioka, K., 316
 Tomioka, N., 154
 Tomlinson, W. J., 859
 Tommila, E., 393
 Tonellato, U., 562, 611
 Topley, B., 495
 Topsom, R. D., 385, 388, 400
 Tordeux, M., 131
 Tori, K., 740
 Torossian, G., 526
 Torre, G., 62
 Torrent-Sucarrat, M., 771
 Toscano, V. G., 849
 Toullec, J., 443
 Towle, P. H., 685
 Townsend, L. B., 880
 Toy, P. H., 276
 Toyonaga, B., 558
 Toyota, S., 118
 Tozzi, S., 521
 Trachtenberg, E. N., 876
 Trachtman, M., 12, 204
 Traetteberg, M., 874
 Trager, W. F., 375
 Trần Huu Dâu, M.-E., 626
 Trattner, R. B., 459
 Trauner, D., 730
 Traynham, J. G., 289
 Trecker, D. J., 742
 Tremmel, J., 189
 Trenary, M., 3
 Trifan, D. S., 583
 Trifunac, A. D., 309
 Trimmer, E. E., 879
 Trinajstić, N., 24, 240, 242, 245
 Trippel, S., 495
 Troe, J., 375
 Trofin, L., 209
 Troisi, L., 531
 Trout, N. A., 388, 627
 Truce, W. E., 529, 619, 877
 True, N. S., 726
 Truhlar, D. G., 237, 313, 347, 350, 377, 378, 496
 Trumbull, E. R., 685
 Trushin, S. A., 830
 Tsang, G. T. Y., 502
 Tse, J. E., 455
 Tseng, J., 164
 Tsoglin, A., 118
 Tsou, N. N., 879
 Tsubomura, H., 230
 Tsuchiya, S., 873
 Tsuda, M., 871
 Tsukada, T., 209
 Tsuneishi, H., 880
 Tsuno, Y., 399
 Tubergen, M. W., 587, 826
 Tucker, S. P., 79
 Tuckerman, M. E., 223
 Tüllmann, S., 190
 Tuñón, I., 428
 Tupper, K. J., 726
 Turkenburg, L. A. M., 285
 Turner, R. B., 163, 693, 871, 874
 Turnquest, B. W., 457
 Turro, N. J., 4, 278, 350, 711, 789, 795, 815, 825, 831, 858–860, 881
 Tuttle, Jr., T. R., 726
 Tyminski, I. J., 135
 Tyrrell, H., 843
 Uchino, T., 854
 Ueki, T., 735
 Uekusa, H., 857
 Uemura, S., 614
 Ueoka, T., 163
 Ugelstad, J., 499
 Uggerud, E., 505
 Ulrich, S. E., 873
 Um, I.-H., 399, 512
 Underhill, L. K., 345
 Underwood, G. R., 876
 Unett, D. J., 820, 824
 Unwin, P. R., 208
 Upthagrove, A. L., 822
 Urry, W. H., 272, 591, 592
 Usui, M., 307

- Utimoto, K., 269
 Vaidyanathan, S., 209
 Vairamani, M., 855
 Vajda, E., 189
 Valdes, T. A., 319
 Valentine, D., 831
 Van Auken, T. V., 66
 van Bekkum, H., 400
 van Berkomp, L. W. A., 636, 879
 van Bommel, A. J., 90
 van Boom, J. H., 636
 van Delden, R. A., 858
 Van der Eycken, J., 872
 van der Lugt, W. T. A. M., 700
 van der Veken, B. J., 872
 van Dijk, B., 65
 Van Doren, J. M., 423
 Van Doren, M., 544
 Van Eldik, R., 350
 van Gulick, N. M., 877
 van Lenthe, J. H., 163
 Van Sickle, D. E., 382
 Van Speybroeck, V., 272
 van Tamelen, E. E., 167, 216, 854, 878
 Van-Catledge, F. A., 135
 Vance, R. L., 724
 Vančik, H., 299, 301
 Vander Donckt, E., 814
 Vandyck, K., 872
 Vardhan, H. B., 597
 Varick, T. R., 275, 276
 Variyar, J. E., 128
 Varnerin, R. E., 380
 Vasilyev, A. V., 526
 Vassilikogiannakis, G., 852
 Vaughan, C. W., 539, 877
 Vaughan, W. E., 20, 190, 353, 589, 590
 Vauthey, E., 803, 804
 Vayner, G., 500
 Vecchiani, S., 559, 878
 Veillard, A., 496
 Vela, A., 161
 Venable, R. M., 117
 Venepalli, B. R., 161
 Venkataraman, R., 575
 Venkatesan, K., 872
 Venneri, P. C., 827
 Venturi, M., 858, 862
 Verbeek, J., 163
 Verbit, L., 603
 Verevkin, S. P., 205, 871
 Verkade, J. G., 34
 Verkade, P. E., 400
 Verkruijsse, H. D., 164
 Verma, A. L., 121
 Vermeij, R. J., 166
 Verney, M., 611
 Vernon, C. A., 447
 Vessiere, R., 611
 Vestling, M. M., 642
 Vickerman, J. C., 209
 Vidal-Cros, A., 872
 Vidrine, D. W., 459
 Viehe, H. G., 309
 Vila, A., 151, 235
 Villa, M., 83
 Villarica, K. A., 873
 Vincent, J. R., 444
 Viossat, V., 345
 Vipond, P. W., 607
 Vishwakarma, L. C., 603
 Viskolcz, B., 203
 Viswanath, R., 21
 Vlahov, G., 388
 Vodopivec, A., 211, 874
 Voge, H. H., 553
 Vogel, E., 700, 726, 879
 Vogel, P., 310
 Vogel, W., 414
 Vogt, R. R., 587
 Volante, R. P., 879
 Vollhardt, K. P. C., 205, 880
 von Niessen, W., 307
 Vorachek, J. H., 295
 Vössing, T., 867
 Voter, A. F., 240
 Vottero, L. R., 529
 Vrček, I. V., 304
 Vrček, V., 302, 304, 877
 Vreven, T., 257
 Waack, R., 311
 Wade, Jr., L. E., 771
 Wade, Jr., L. G., 68
 Wade, K., 290, 875
 Wade, M., 872
 Wade, P. A., 544
 Wagman, A. S., 881
 Wagner, A. F., 378
 Wagner, P., 834, 836
 Wahl, Jr., G. H., 63
 Waight, E. S., 483
 Wainwright, M., 852
 Wakefield, B. J., 621, 853
 Wakselman, C., 131
 Walborsky, H. M., 63, 314, 322, 872, 873, 875
 Walbrick, J. M., 65
 Walden, P., 494
 Walenzyk, T., 881
 Walker, F. H., 160
 Walker, G. E., 304
 Walker, J. K. E., 878
 Walkup, R. E., 3
 Wall, R. G., 751
 Wallace, T. W., 880, 881
 Wallbillich, G., 746
 Waller, F. J., 459
 Walling, C., 256, 271, 272, 302, 591
 Wallis, E. S., 310
 Walsh, A. D., 37
 Walsh, R., 10
 Walsingham, R. W., 669
 Walter, J., 25, 176
 Walters, E. A., 46
 Walters, W., 697
 Walthall, D. A., 877
 Walton, A., 1
 Walton, J. C., 267
 Wan, P., 815, 850
 Wang, C., 387
 Wang, F., 152, 874
 Wang, H., 287
 Wang, K., 3, 208
 Wang, Q., 822
 Wang, X., 23, 604
 Wang, Y., 382, 773, 873, 876
 Wang, Z., 208
 Wann, S. R., 448
 Wannere, C. S., 15, 190, 217, 770
 Ward, A. M., 503
 Ware, W. R., 860
 Warhurst, E., 763
 Warkentin, J., 298
 Warner, P. M., 163
 Waroquier, M., 272
 Warren, R. N., 740
 Warzecha, K.-D., 305
 Washburn, W. N., 458
 Wasielewski, M. R., 804
 Wasserman, E., 214, 279
 Wasserman, H. H., 852
 Watanabe, M., 159
 Watanabe, W., 371
 Waters, W. A., 589
 Waters, W. L., 65, 617
 Watson, D. G., 5
 Watson, H. B., 443
 Watson, P. L., 740
 Wattenbach, C., 165
 Watterson, S. H., 881
 Watthey, J. W. H., 700
 Waugh, J. S., 96
 Waymouth, R. M., 93
 Wayner, D. D. M., 309
 Weber, A. P., 393
 Weber, J., 875
 Weber, J. Q., 668
 Weber, M., 462
 Webster, F. X., 77, 872
 Wedge, P. J., 849
 Weed, G. C., 859
 Weedon, A. C., 804, 841, 842
 Wei, J., 208
 Weidemüller, M., 495
 Weigang, Jr., O. E., 72
 Weil, J. A., 259
 Weiner, S. J., 136, 461
 Weingarten, H. I., 879
 Weinhold, F., 120, 151, 226, 231, 232
 Weininger, D., 54
 Weinstock, J., 644
 Weinstock, M., 483
 Weisberg, M., xi, 52
 Weisenhorn, A. L., 3
 Weiser, J., 132
 Weisman, G. R., 257
 Weiss, D. S., 881

- Weiss, G. A., 208
 Weiss, H. M., 612
 Weiss, J., 495
 Weiss, R. G., 837, 859
 Weiss, S., 120
 Weissberger, A., 8, 20, 32, 118, 259, 578, 871
 Weissbuch, I., 91
 Weissman, S. A., 879
 Weissman, S. I., 261
 Weitz, E., 790
 Welch, J. G., 877
 Welch, S. C., 319
 Weller, A., 813
 Wells, P. R., 504
 Wenderoth, B., 515
 Wenthold, P. G., 168
 Wentrup, C., 875
 Wepster, B. M., 400
 Werst, D. W., 309
 Werthemann, L., 730
 Wertz, D. H., 687
 Wesdemiotis, C., 308
 Wessig, P., 836
 West, F. G., 880
 Westaway, K. C., 382
 Wester, R., 495
 Westheimer, F. H., 135, 371, 372, 377, 519
 Westrum, Jr., E. F., 10, 156
 Wettach, R. H., 288
 Whalley, E., 350
 Whangbo, M.-H., 28, 227, 622, 713
 Whatley, B. G., 88
 Wheatley P. J., 5
 Wheeler, O. H., 441, 660, 876
 Wheeler, S. E., 370, 745
 Wheland, G. W., 189, 192, 239, 240, 241, 262, 520
 Whetten, R. L., 63
 Whiffen, D. H., 5
 Whitaker, D., 253
 White, A. M., 303, 875
 White, E. H., 677
 White, E. P., 584
 White, J. C., 292
 White, J. H., xvi
 White, R. L., 215
 White, W., 287
 Whitehurst, D. D., 617
 Whiteside, R. A., 294
 Whitesides, G. M., 311, 873
 Whitlock, H. W., xv
 Whitman, C. P., 332, 872
 Whitman, L. J., 3
 Whitman, R. H., 860
 Whitmore, F. C., 289, 556, 587, 588, 678
 Whitten, D. G., 859
 Whitworth, A. J., 876
 Wiberg, K. B., 8, 10, 36, 40, 117, 121, 130, 150, 160, 175, 212, 349, 371, 372, 379, 419, 439, 449, 790, 818, 832, 871, 873
 Wick, A. E., 729
 Wickham, S. D., 700
 Widder, S., 867
 Widjaja, T., 872
 Wiene, W. J., 63
 Wieringa, J. H., 556
 Wierlacher, S., 286
 Wiesenfeld, J. M., 843
 Wiest, O., 305, 716
 Wilby, J., 662
 Wilcox, C. F., 387
 Wilcox, Jr., C. F., 161, 245, 708
 Wild, A. J., 879
 Wilen, S. H., 53, 85, 87, 120, 231, 360
 Wiley, D. W., 879
 Wilhelm, R. S., 621
 Wilk, K. A., 639
 Wilke, J. J., 502
 Wilke, R. N., 880
 Wilkins, C. L., 215
 Wilkinson, F., 787, 792, 802
 Willard, A. K., 730
 Wille, U., 272
 Williams, A., 458, 459
 Williams, C. R., 387
 Williams, D. H., 306
 Williams, E. A., 296
 Williams, E. G., 393
 Williams, F. V., 503
 Williams, I. H., 348, 383
 Williams, J. E., 10, 135, 149
 Williams, K. B., 438
 Williams, L. F., 267
 Williams, R. A., 659
 Williams, R. E., 290, 875
 Williams, W. G., 276
 Williamson, D. G., 815
 Williard, P. G., 313
 Willis, C. J., 28
 Willner, B., 804
 Willner, I., 804
 Willstätter, R., 215
 Wilsmore, N. T. M., 690
 Wilson, B., 429
 Wilson, C. A., 516
 Wilson, C. L., 300, 443, 444
 Wilson, E. B., 5
 Wilson, H., 389
 Wilson, J. C., 375
 Wilson, L. A., 875
 Wilson, M. A., 552
 Wilson, R. M., 9, 76, 470, 790
 Wilson, S. R., 727
 Wilson, V. P., 587
 Wilzbach, K. E., 167
 Wimmer, E., 724
 Winiarski, J., 528, 877
 Winkler, H. J. S., 66
 Winkler, J. D., 881
 Winstanley, Jr., J., 164
 Winstein, S., 130, 329, 360, 472, 477, 479, 482, 483, 485-490, 492, 494, 498, 554, 568, 598, 639, 648, 700, 877
 Winter, R. A. E., 163
 Winter, R. E. K., 697
 Wintner, C. E., 42
 Wipf, P., 88
 Wipff, G., 626
 Wirth, D. D., 762
 Wirz, J., 447
 Wise, W. S., 3
 Wiseman, F., 438
 Wiseman, J. S., 876
 Wiskott, E., 159
 Wiswesser, W. J., 202
 Witanowski, M., 311
 Wittig, G., 741, 781
 Wodrich, M. D., 15, 190, 237, 269
 Wolak, R., 606
 Wolber, G. J., 503
 Wolf, H., 88
 Wolf, R., 853
 Wolf, S. A., 559
 Wolf, V., 610
 Wolfe, Jr., J. R., 86, 844
 Wolfe, S., 150, 499, 512, 517, 659
 Wolfert, M. A., 746
 Wolff, L., 288
 Wolff, M. A., 604
 Wolff, S., 205, 881
 Wolfsberg, M., 214, 383
 Wolinsky, J., 164
 Wollersheim, A. P. P., 811
 Wolniewicz, L., 27
 Wong, M. W., 449
 Woning, J., 117
 Wood, C., 867
 Wood, C. S., 844
 Wood, D. E., 262, 267
 Wood, G. P. F., 264
 Wood, P. A., 873
 Woodard, R. A., 614
 Woodcock, D. J., 677
 Woods, C., 159
 Woods, G. F., 877
 Woods, K. W., 607
 Woodward, R. B., 90, 701, 715, 739, 743, 760
 Woody, R. W., 89
 Woolf, L. I., 633, 657, 878
 Workentin, M. S., 309
 Wostradowski, R. A., 829
 Wotiz, J. H., 202
 Wray, V., 150, 581
 Wright, A. E., 871
 Wright, P. G., 422
 Wright, R. E., 535
 Wrighton, M., 819
 Wu, A., 128
 Wu, C., 420, 876
 Wu, D., 208
 Wu, F. T., 496
 Wu, W., 232, 500
 Wu, Y.-D., 604
 Wu, Y.-T., 209, 383
 Wu, Z., 528
 Wudl, F., 207
 Wulfman, C. E., 820
 Wuts, P. G. M., 856

- Wyatt, P. A. H., 813
Wynberg, H., 65, 86, 556
- Xia, X., 500
Xiao, H., 526
Xiao, J., 526
Xidos, J. D., 313
Xie, D., 455
Xie, J., 120
Xie, L., 445
Xiong, Y., 462
Xu, D., 455
Xu, L., 370
Xu, Z.-X., 873
Xue, D., 23
Xue, J., 834
- Yager, W. A., 279
Yahioğlu, G., 862
Yamabe, S., 580, 650
Yamada, C., 279
Yamada, K., 316
Yamada, M., 858
Yamaguchi, H., 858
Yamaguchi, Y., 820
Yamamoto, C., 769
Yamamoto, H., 728, 880
Yamamoto, K., 66, 871
Yamaoka, T., 880
Yamataka, H., 316, 395, 512
Yamauchi, M., 316
Yan, L., 78
Yang, D.-D. H., 836
Yang, H., 338, 872
Yang, J.-R., 317
Yang, J.-S., 858
Yang, N. C., 581, 836, 839, 842, 880, 881
Yang, W., 24, 237
Yannoni, C. S., 291, 296, 300
Yao, T., 166
Yao, Z., 208
Yasuda, H., 316
Yates B. F., 121
Yates, B. F., 308
Yates, B. L., 685
Yates, K., 200, 380, 431–433, 451, 452, 554, 561, 562, 565, 569, 570, 572, 609, 850, 878
Yates, P., 762
Yato, M., 519
Yau, C.-C., 316
Ye, T., 288
Yee, K. C., 438, 642
Yekta, A., 860
Yen, S.-F., 208
Yeston, J., 2
Yin, J., 284
- Ying, F., 500
Yogo, K., 209
Yonemitsu, O., 63, 162
Yonezawa, T., 567
Yoo, H.-Y., 773
Yoon, J.-Y., 271
Yoon, Z. S., 770
Yorimitsu, H., 269, 872
York, K. A., 385
Yoshida, S., 872
Yoshimitsu, T., 875
Yoshino, T., 134
Yoshizawa, M., 762
Youle, P. V., 454, 876
Young, A. E., 314, 873
Young, M. A., 858
Young, R. H., 804
Young, W. G., 472, 482, 554, 648, 678
Yousef, A. L., 856
Youssef, A. K., 356
Yu, H., 166
Yu, L., 258
Yu, L. H., 209
Yu, Y., 858
Yu, Z., 208
Yuan, H. C., 23
Yuan, X., 875
Yuan, Z., 873
Yuan, Z. M., 873
Yue, P. L., 677
Yuh, Y. H., 136, 137
Yukawa, Y., 399
Yurchenko, E. N., 677
Yuzhakov, G., 300
- Zabalov, M. V., 610
Zabicky, J., 439, 443
Zabrodsky, H., 63
Zafriou, O. C., 819
Zahler, R. E., 528
Zahradnik, R., 137
Zaitseva, G. S., 610
Zalewski, R. I., 389
Zalkin, A., 91
Zamaraev, K. I., 677
Zamarev, K. I., 804
Zandler, M. E., 19
Zang, G., 826
Zare, R. N., 859
Zaugg, H. E., 876
Závada, J., 638
Zefirov, N. S., 360
Zeidan, T. A., 231
Zeiss, H. H., 481
Zeller, S., 872
Zellmer, V., 298
Zemp, I., 872
Zewail, A., 2
- Zewail, A. H., 2, 742, 795, 833
Zeza, C. A., 877
Zhan, C.-G., 462
Zhang, B.-L., 561
Zhang, C., 873
Zhang, G., 208, 237
Zhang, J., 859
Zhang, J. X., 495
Zhang, J.-Y., 350
Zhang, M., 858
Zhang, Q., 232
Zhang, X.-M., 309
Zhang, Z., 208
Zhao, B., 280
Zhao, H., 636
Zhao, Y., 237, 645
Zhdanov, Y. A., 20
Zheng, C. Y., 559, 563, 668
Zheng, J., 120
Zheng, K., 826
Zheng, Q.-Y., 873
Zhou, J., 872
Zhou, L., 820
Zhou, X., 159
Zhou, Y., 455
Zhou, Y.-D., 871
Zhou, Z., 220
Zhu, H., 15
Zhu, X.-Q., 350
Zhu, Y., 872, 876
Zhu, Z., 859
Zhuang, D., 208
Zhuang, Z., 873
Ziegler, F. E., 715
Ziegler, T., 15, 264
Zijlstra, R. W. J., 873, 876
Zimmer, H., 9, 76, 470
Zimmerman, H. E., 85, 167, 175, 766, 828, 832, 845, 859, 875, 880
Zimmermann, H., 726
Zimmt, M. B., 858
Zimny, B., 762
Zipse, H., 272, 551
Živković, T. P., 241
Zoebisch, E. G., 223
Zollinger, H., 519
Zolotoi, A. B., 872
Zuber, G., 88
Zubkov, F. I., 877
Zucco, C., 446, 531
Zuckerman, J. J., 312
Zuman, P., 331
Zupan, M., 581, 611
Zuraw, P., 332
Zweier, J. L., 258
Zweifel, G., 600, 602, 616
Zweig, A., 875

Subject Index

- a*
activity, 415
conformational descriptor, 116
hyperfine coupling constant, 260
- A*
equatorial preference, 130
in Edwards equation, 507
overall solute hydrogen bond acidity, 339
preexponential factor, 349
A value in conformational analysis, 131, 135, 151, 169
*A*₁ mechanism, 447
A^(1,2) strain, 122
*A*₂ mechanism, 447
A^(1,3) strain, 122
*A*_{Ac}1 mechanism, 450, 451
*A*_{Ac}2 mechanism, 450–452
*A*_{Al}1 mechanism, 450–452
*A*_{Al}2 mechanism, 450
Ab initio calculation, 223
acidity, 419
amide hydrolysis, 461
bromonium ion, 566
carbene rearrangement, 286
carbocation, 593
carboxylate stability, 418
chloronium ion, 580
computational resources, 223
computational time, 136
Cope rearrangement, 772
Diels–Alder reaction, 736
electrophilic addition, 557
epoxidation, 606
ethyl cation, 294
formic acid, 429
gas phase acidity, 428
hydration of alkene, 593
hydroboration, 604
in chirality determination, 91
in conformational studies, 150
methyl anion, 315
nucleophilic addition to
 carbonyl, 626
 nucleophilic vinylic substitution, 532
 ozonolysis, 747
 pericyclic reaction, 706, 771
 *S*_N2 reaction, 496, 502
Ab initio theory, 223
- Ablation, 790
Abnormal addition, 589
Absolute configuration, 68, 91
Absolute electronegativity, 23
Absolute hardness and aromaticity, 220
Absolute hardness, η , 220, 506
Absolute softness, σ , 506
Absorption of UV-vis radiation, 787, 794
 by CT complex, 557
 + *ac*, 115
 – *ac*, 115
Acceptable representations of stereochemistry, 56
Acenaphthylene, syn addition of chlorine, 579
Acene, 206
Acetal hydrolysis, 447
Acetic acid
 acidity, 418
 acidity and thermodynamic values, 429
 acidity in gas phase and in solution, 428
Acetolysis, 481, 485, 488–491
Acetone
 as solvent for nucleophilic substitution, 498
 basicity, 421
 gas phase acidity, 425
 gas phase basicity, 427
 hydration, 441
 photochemical reaction, 833
 photophysical data, 808, 809
 reaction with hydroxylamine, 441
 solvent parameters, 340
Acetylenic carbanion hybridization, 311
Achiral structure, 64
Achirotopic, 98
Acid
 Brønsted, 413, 414
 hydron, 414
 Lewis, 413
 proton, 414
 triton, 414
Acid catalysis
 Brønsted catalysis law, 437
 buffer ratio, 437
 general, 435
 in alcohol dehydration, 670
 in alkene hydration, 592, 594
 in alkyne hydration, 614
 significance of Brønsted α , 437, 438
 specific, 434
Acidity
 and bent bond description of double bonds, 45
 and Hammett equation, 415
 and hybridization, 41, 44
 and ion pairing, 415
 and *J*_{13C-H}, 41
 and photochemical reaction, 834
 and Taft equation, 418
 and σ, π description of double bonds, 44
 ΔG_{acid} , 424
 ΔH_{acid} , 424
 ΔS_{acid} , 424
 ethane, 44
 ethene, 44
 ethyne, 44
 formic acid, 419
 gas phase data for selected compounds, 425
 importance of ΔS in solution, 429
 in aqueous solution, 416
 in cyclohexylamine solution, 421
 in DMSO solution, 422
 in gas phase, 422, 423
 in nonaqueous solvents, 420
 in THF solution, 421
 *K*_a, 414
 *K*_a^T, 415
 *K*_i, 415
 kinetic, 41
 leveling effect, 422
 leveling effect of solvent, 430
 of electronically excited states, 812, 813
 *pK*_a, 414
 *pK*_{CSCHA}, 421
 radical cation, 309
 solvation effects, 428
 trends of alcohols in gas phase and in solution, 426
Acidity constant, 414
Acidity function
 excess acidity, 433
 H^{'''}, 431
 *H*_A, 431
 *H*_C, 432
 *H*_R, 432
 other, 432

- Actinometry, 804
 Activated complex, 350
 Activation energy, 348
 negative value of E_a , 350
 Activation enthalpy, ΔH^\ddagger , 350
 Activation entropy, ΔS^\ddagger , 350
 and mechanism, 353
 Activation free energy, ΔG^\ddagger , 350
 Activation volume, ΔV^\ddagger , 448
 Activity (a), 415
 Activity coefficient (γ), 415
 Acylium ion
 in A_{AC} mechanism, 451
 in acyl substitution, 460
 in Friedel–Crafts acylation, 330
 Ad mechanism label, 552
 Adamantene, 669
 1-Adamantyl radical, 267
 1,4-Addition, 285, 553, 620
 1,6-Addition, 553
 Addition, 551
 anti, 552
 anti-Markovnikov orientation, 568
 chemoselectivity, 567
 IUPAC terminology, 552
 kinetics, 558
 Markovnikov orientation, 567
 of Br_2 to alkene, 553
 photochemical, 841
 regiochemistry, 568
 solvent effects, 561
 stereochemistry, 552, 554
 syn, 552
 Taft equation, 555
 to carbonyl group, 439
 Ad_E2 mechanism, 552, 586, 613
 denoted as ($A_E + A_N$), 552
 Ad_E2M mechanism, 586
 Ad_E3 mechanism, 586, 610, 611, 613
 Ad_E4 mechanism, 611
 Ad_EC1 mechanism, 557
 Ad_EC2 mechanism, 557
 Adiabatic process, 812, 827, 850
 Adjacent exchange integral, 239
 $A_E + A_N$ mechanism, 552
 AFM, 3
 $A_h + A_N + A_hD_h + D_N + D_h$
 mechanism, 450
 $A_h + D_N + A_N + D_h$ mechanism, 450
 AIBN, 271
 AIM, 232
 Alcohol acidity in gas phase and in
 solution, 426
 Aldol reaction, 318, 621
 acid and base catalysis, 446
 reverse aldol reaction, 638
 Alkane acidity, 44
 Alkaplane, 161
 Alkene
 acidity, 44
 addition of Br_2 , 331, 342, 553
 addition of Br_2 by radical pathway,
 576
 addition of Cl_2 , 575
 addition of F_2 , 580
 addition of HX , 585
 addition of mixed halogens, 584
 anti-Markovnikov addition of HBr , 589
 as dipolarophile in 1,3-dipolar
 cycloaddition, 743
 di- π -methane rearrangement, 828
 electronically excited states, 818
 epoxidation, 605
 hydration, 592
 hydroboration, 600
 oxymercuration, 595
 ozonolysis, 404, 745
 photochemical carbocation formation
 from cycloalkene, 824
 photocycloaddition, 828
 photohydration of cyclic alkene, 825
 photoisomerization, 820
 radical addition of HBr , 271
 reaction with carbene, 284
 reaction with XeF_2 , 581
 solvomercuration, 596
 UV-vis absorption, 818
 Alkoxymercuration, 596
 1,2-Alkyl shift, 272
 Alkyne
 acidity, 44
 addition of Br_2 , 609
 addition of HX , 612, 614
 and angle strain, 164
 electrophilic addition, 609
 hydration, 614, 615
 hydroboration, 616
 oxymercuration, 615
 radical addition of HBr , 611
 reaction with peroxyacids, 616
 Allen electronegativity, 23
 Allowed pericyclic reaction, 705
 Allowed process, 274, 705, 796
 Allowed spectroscopic transition, 816
 Allyl anion
 DE_{π} , 188
 in cycloaddition, 743
 q_i , 192
 resonance structures, 189
 ρ_i , 192
 Allyl cation, 482
 DE_{π} , 188
 HMO calculation, 188
 in cycloaddition, 743
 q_i , 192
 resonance structures, 189
 ρ_i , 192
 Allyl radical
 DE_{π} , 188
 HMO calculation, 188
 q_i , 192
 resonance structures, 189
 ρ_i , 192
 Allyl system
 HMO calculation, 182
 NBMO, 196
 α
 in Brønsted catalysis law, 437
 in Edwards equation, 507
 in HMO theory, 179
 in Leffler equation, 363
 in Taft–Topsom equation, 400
 solvent parameter, 339
 stereochemical descriptor, 79
 α effect in nucleophilicity, 512
 α secondary kinetic isotope effect, 380, 772
 $[\alpha]$ (specific rotation), 86
 α,β -unsaturated carbonyl compound
 and conjugate addition, 620
 photochemical deconjugation, 842
 photochemistry, 841
 α,β -elimination, 635
 α -cleavage, Norrish type I reaction, 832
 α -cyclodextrin, and phosphorescence, 801
 α -diazoketone, in Wolff
 rearrangement, 288
 α -elimination, 634
 and carbene generation, 283
 Alternant structure, 194, 195
 even alternant, 195
 odd alternant, 195, 243
 AM1 method, 223
 AMBER force field, 136
 Amide hydrolysis, 460
 Amine
 basicity, 421
 basicity in solution, 420
 deamination, 677
 gas phase basicity, 427
 Aminolysis, 459
 $A_N + D_N$ mechanism, 528
 A_ND_N mechanism, 471
 3/1/ A_ND_N mechanism, 472
 $A_N + D_N + A_{xh}D_h$ mechanism, 453
 A_N mechanism label, 471
 3/ A_N mechanism label, 471
 Anchimeric assistance, 485, 487–489, 553,
 562, 674, 683
 Angle strain, 137
 and carbocations, 291
 and carbonyl hydrate formation, 441
 and cycloalkanes, 124
 Baeyer strain, 123
 calculation, 123
 in hemiketal formation, 441
 in molecular mechanics, 138
 in planar annulenes, 216
 in ΔH_f calculation, 13
 Angstrochemistry, 3
 Anh–Eisenstein model, 626
 Anisochronous groups, 96
 Anisotropic hyperfine coupling, 261
 Annulene, 215–217, 769, 770
 [4 n]Annulene, 218
 [4 n + 2]Annulene, 218
 [8]Annulene, 216
 [10]Annulene, 216
 [12]Annulene, 769
 [16]Annulene, 769, 770

- [18]Annulene, 217
 [20]Annulene, 769
 Anomalous fluorescence, 795
 Anomeric effect, 151
 Anomers, 79, 81
 Antara, 716
 Antarafacial pathway, 716, 717, 719, 721, 731, 739, 741, 743, 754, 767, 773, 774
 Antarafacial-antarafacial pathway, 722
 Antarafacial-suprafacial pathway, 722
 Anthracene
 calculation of resonance energy, 239
 DRE, 219
 Kekulé structures, 238
 Kekulé structure count (KSC), 242
 number of Kekulé structures, 242
 photodimerization, 844
 photophysical data, 809
 resonance energy, 206, 238
 SRT resonance energy, 244
 UV-vis absorption and fluorescence, 798
 VB calculation, 239
 Anti, 77
 Anti addition, 552, 583, 617, 619
 in oxymercuration of alkenes, 598
 in oxymercuration of alkynes, 614
 of Br₂ to alkene, 566
 of Br₂ to alkyne, 610
 of Cl₂ to alkene, 577
 of HBr to alkyne, 611
 of HCl to cyclohexene, 586
 Anti conformation, 114, 115
 Anti elimination, 633, 648–651, 667, 668
 Antiaromatic destabilization, 212
 Antiaromatic structure, 201
 DRE value, 219
 NCIS value, 217
 η value, 220
 Antiaromatic transition state, 764
 Antiaromatic transition structure, 763
 Antibonding orbital, 42, 150, 180, 182, 231, 712, 791
 H₂, 28
 Anti-Bredt compound, 162
 Anti-clinal conformation, 115, 647, 649
 + Anti-clinal conformation, 115
 – Anti-clinal conformation, 115
 Anti-coplanar conformation, 647
 Anti-coplanar orientation, in
 dehalogenation of vicinal
 dihalide, 667
 Anti-Hammond effect, 365
 Anti-Markovnikov addition, 271, 567, 568, 588–590, 600
 Anti-Markovnikov orientation, 590
 Anti-Michael orientation, 622
 Anti-periplanar, 115, 358, 623, 647, 651
 + Anti-periplanar, 115
 Antisymmetric molecular orbital, 33, 707, 708, 712, 732, 739, 750
 Aprotic solvent, 131, 498, 512, 562, 574, 666
 aR, 70, 72
 Aracemic, 85
 Aromatic structure, 201
 Aromatic transition state, 764
 Aromatic transition structure, 763, 764
 Aromaticity, 201
 4*n* + 2 rule, 201
 and delocalization energy, 218
 Clar notation, 210
 Möbius, 767
 of transition structures in pericyclic
 reactions, 763
 Arrhenius equation, 348
 Arrhenius plot, 350
 Artificial photosynthesis, 862
 Aryne, 168, 541, 542
 in cycloaddition reactions, 741
 aS, 70, 72
 A_{SE}2 mechanism, 593
 A-S_E2 mechanism, 593
 Association process, 450
 Asym-methylethylethylene, 592
 Asymmetric induction, 623
 Asymmetric structure, 62
 Atactic polymer, 93
 Atom transfer reaction, 378, 749
 selection rules, 750
 Atom type in molecular mechanics, 140
 Atomic carbon, 255
 Atomic force microscopy (AFM), 3
 Atomic radius in QTAIM, 235
 Atomic surface area, 6
 Atomic volume, 6
 calculated, 7
 in QTAIM, 235
 Atoms in molecules, 232
 Atropisomers, 66
 Attached atoms list, 139
 Attachment step, 533, 590
 Aufbau principle, 187
 Autocatalytic reaction, 442
 Average bond dissociation energy, 16
 Avoided crossing, 514, 713, 734, 739, 848
 Avoided crossing rule, 713
 A_w (activity of water), 432
 A_{xh} mechanism descriptor, 639
 A_{xh}D_H + D_N mechanism, 639
 A_{xh}D_H + D_N[‡] mechanism, 644
 A_{xh}D_H⁺D_N[‡] mechanism, 644
 A_{xh}D_H[‡] + D_N mechanism, 644
 A_{xh}D_H[‡]+D_N mechanism, 644
 A_{xh}D_HD_N mechanism, 639
 Axial chirality, 70
 Axial substituent, 128, 626, 665
 Azobisisobutyronitrile, 271
 Azulene, 195, 244, 432, 795
 B
 in Edwards equation, 507
 overall solute hydrogen bond
 basicity, 339
 B3LYP functional, 237
 B-A_{Ac}3 mechanism, 450
 B_{Ac}1 mechanism, 453
 B_{Ac}2 mechanism, 453–456
 Back electron transfer, 306, 804
 Back-side attack in S_N2 reaction, 495
 Baeyer strain, 123, 148
 B_{Al}1 mechanism, 456
 B_{Al}2 mechanism, 453
 Baldwin's rules, 274
 Bamford–Stevens reaction, 286
 Banana bond, 42, 46
 Barrelene, 108, 167
 Base
 Brønsted, 413, 414
 Lewis, 413
 Base catalysis, 437
 alcohol dehydration, 676
 α-halogenation of carbonyl
 compounds, 444
 and carbonyl hydration, 439
 Brønsted catalysis law, 437
 enolate formation, 446
 ester hydrolysis, 457
 Base-promoted reaction, 449
 Basicity
 equilibrium concept, 504
 gas phase basicity, 426
 in aqueous solution, 420, 421
 proton affinity, 426
 selected gas phase data, 426
 Basicity function, 433
 Basis set, 224, 771
 in DFT, 236
 in HMO theory, 175
 Basis set function, 224
 Basketane, 163, 170
 Bathochromic shift, 817
 Beckmann rearrangement, 409
 Beer and photochemistry, 861
 Bell–Evans–Polanyi (BEP) principle, 363
 Beltene, 166
 Bema Hapothle, 363
 Benson electronegativity, 23
 Bent bond, 46, 47
 and acidity, 45
 and bond length, 44
 and conformation of propene, 46
 and LMO, 225
 and Pauling, Linus, 43
 and theoretical calculations, 46
 as starting point, 47
 banana bond, 42
 description of double bond, 42
 τ bond, 42
 Bent bond line representation of glycosidic
 linkage, 81
 Benzene
 DE_π, 190, 201
 DRE, 219
 electron diffraction, 202
 heat of hydrogenation, 190, 203
 HMO energy levels, 198
 Hückel MOs, 186
 isomer counting, 4
 Kekulé structures, 238
 Möbius molecular orbitals, 766

- Benzene (*Continued*)
 photochemistry, 843
 photophysical data, 809
 resonance energy, 190, 203, 238, 239
 SRT resonance energy, 245
 valence bond calculation, 238
- Benzene hexachloride, 648
- Benzil dipole moment in T1 state, 815
- Benzophenone
 DRE, 219
 photophysical data, 809
 photoreduction, 834
- Benzvalene, 167, 843
- Benzyl NBMO, 196
- Benzyl radical
 EPR spectrum, 197
 from toluene photodissociation, 847
- Benzyne, 168, 532, 536, 539, 541
 in cycloaddition reactions, 741
- m*-Benzyne, 168
- o*-Benzyne, 168
- p*-Benzyne, 168
- Benzyne mechanism, 537, 540, 549
- BEP principle, 363
- β
 in Edwards equation, 507
 in HMO theory, 179, 190
 isokinetic temperature, 402
 solvent parameter, 339
 stereochemical descriptor, 79
- β 2° kinetic isotope effect, 382
- β' in Möbius MO theory, 765
- β -bromovinyl cation, 610
- β -cleavage, 832, 836
- β_e (Bohr magneton), 259
- β -elimination, 633
- Bichromophoric structure, 829
- Bicyclo[1.1.0]butane, 108
 radical cation, 308
- Bicyclo[2.2.2]octane, 387
- Bicyclobutonium ion, 300
- In*-bicyclo[4.4.4]-1-tetradecene, 299
- Bifunctional catalysis, 448, 458
- Bifurcated potential energy surface, 370
- Biphenyl
 DRE, 219
 SRT resonance energy, 245
- Biradical, 308, 541, 697, 718, 726, 742, 776, 792, 798, 828, 833, 836–838
 as model for n, π^* state, 834
- Bishomocyclopropenyl structure, 494
- Bisulfite addition to carbonyl, 439
- Blue shift, 817
- Boat conformation, 124, 132, 782
- Boat transition structure
 for Claisen rearrangement, 724
 for Cope rearrangement, 722
- Boat-like transition structure, 782
- Bodenstein approximation, 345
- Bohr magneton (β_e), 259
- Bold wedge stereochemical descriptor, 55
- Boltzmann constant, 351
- Boltzmann distribution, 152, 157, 259
- Bond critical point, 235
- Bond curvature, 128
- Bond dipole moment calculation, 20
- Bond dissociation energy, 16
- Bond increment calculation, 10
- Bond order, 160, 192, 820
 in HMO theory, 193
 in QTAIM, 235
- Bond path, 234
- Bond stretch strain, 137
- Bonding orbital
 allyl, 182
 ethene π orbital, 180
 ethene π orbital from EHT calculation, 223
- H₂, 28
- Born–Oppenheimer approximation, 223, 796
- Bowsprit hydrogen, 125
- Boys method, 225
- Br₃[−] in electrophilic addition, 556, 558, 559, 562
- Brackets in pericyclic reaction
 designation, 744
- Bredt's rule, 162
- Bridgehead carbanion, 311
- Bridgehead carbocation, 475
- Bridgehead double bond, 162
- Bridgehead proton acidity, 51
- Bridgehead radical, 267
- Bridging in carbocations, 295
- Bridging power, 583
- Broken bold line in Maehr convention, 75
- Broken wedge in Maehr convention, 74
- Bromohydrin, 578
- Bromonium ion, 488, 553, 556, 598
 resonance structures, 564
- Brønsted acid, 413, 414
- Brønsted α , 438
- Brønsted base, 413, 414
- Brønsted β , 457
- Brønsted catalysis law, 437
- Brønsted correlation, 505
- Brønsted superacid, 296
- Brønsted–Lowry acid, 339, 413
- Buffer ratio, r , 437
- Bullvalene, 726, 854
- Bu₃SnH, 271
- 1,3-Butadiene
 C2–C3 rotational barrier, 190
 DE_{π} , 201
 Diels–Alder reaction, 731
 electrocyclic reaction, 702
 \mathcal{F}_i , 193
 HMO calculation, 184
 P_{ij} , 193
- Butane
 distribution of conformations, 121
 molecular mechanics calculation, 139
 radical cation, 307
- Butanoic acid acidity in gas phase and in solution, 428
- Butterfly mechanism, 606
- sec*-Butyl carbocation, 297, 298
 rearrangement, 304
- t*-Butyl alcohol gas phase acidity, 426, 428
- t*-Butyl carbocation
 ESCA, 321
 geometry, 291, 293
 reaction with nucleophile, 678
 rearrangement, 321
- t*-Butyl radical geometry, 267
- t*-Butylcyclohexane conformation, 132
- 1-Butyne gas phase acidity, 428
- c*
 conformational descriptor, 117
s-cis, 117
 stereochemical descriptor, 76
- 3c–2e bond, 290
- C₂H₅⁺, 294
- C₆₀, 209
- C₇₆, 63
- C₇₈, 63
- Cahn–Ingold–Prelog (CIP) system, 67
- Caldera, 777
- Calorimetry, 8
- Canonical MO, 225
- Carbanion
 racemization, 314
 rearrangement, 319
 stability, 317
- Carbene, 278
 cycloaddition with alkene, 284
 insertion, 285
 rearrangement, 286
- Carbenium ion, 289
- Carbenoid, 283
- Carbinolamine, 441
- Carbocation, 289
 and ion pairing, 298
 conformationally equilibrated, 594
 hydrogen-bridged, 299
 lifetime, 594
 rearrangement, 298, 302, 577, 674
 stability, 291, 302
- Carbonium ion, 289, 300
- Carbonyl hydrate dissociation
 constant, 439
- Carbonyl oxide in 1,3-dipolar
 cycloaddition, 744
- Carbyne, 255
- Carroll rearrangement, 728
- CASSCF, 225
- Catalytic antibody, 459
- Catenane, 67
- Cation radical, 305, 309. *See also* Radical cation
- CCSD(T), 225
- CD (circular dichroism), 89
- Centauric transition structure, 773
- Center of inversion (*i*), 60
- CH₂Cl₂
 and variable hybridization, 39
 geometry, 39
 isomer counting, 4

- CH₃Br geometry, 5
CH₃Cl
 and variable hybridization, 37
 and VSEPR theory, 36
 gas phase acidity, 429
 geometry, 5, 36, 38
 isomer counting, 4
CH₃F
 gas phase acidity, 429
 geometry, 5
CH₃I geometry, 5
Chain reaction, 542, 543, 592
Chair conformation, 80, 124, 128, 148, 383
Chair transition structure
 for Claisen rearrangement, 724
 for Cope rearrangement, 721
Chair-like transition structure, 782
Chameleonic transition structure, 773
Charge density (q_i), 192
Charge-transfer complex, 66, 229, 560. *See also* CT complex; CTC
 in electrophilic addition, 557
 in S_NAr reaction, 528
 spectroscopic detection, 520
CHARMM force field, 136
Cheletropic, 747
Cheletropic reaction, 747
 selection rules, 748
Chemical potential (μ), 23
Chemiluminescence, 859
Chemoselectivity, 567
 χ in Taft-Topsom equation, 400
 χ_a (Nagle electronegativity), 23
 χ_M (Mulliken electronegativity), 22
 χ_P (Pauling electronegativity), 21
 χ_{spec} (Allen electronegativity), 23
Chiral center, 68
Chiral plane, 72
Chirality, 58
 molecular designation, 86
Chirality about a plane, 66
Chirality about an axis, 64
Chirality center, 68
Chirotopic atoms and spaces, 98
Chirotopicity, 98
Chlorine substituent and acidity, 429
2-Chlorobutane representations, 55, 56
Chlorocarbene, 280
1-Chloroethyl carbocation, 580
Chlorohydrin, 578
Chloronium ion, 488, 556, 575, 577, 578, 580, 598
m-Chloroperbenzoic acid, 605
Chlorophenylcarbene, 287
Cholesterol, 54
 ent-cholesterol, 81
 specific rotation, 87
Chromophore, 87, 818, 843, 853
Chugaev reaction, 681, 683
CI (configuration interaction), 225
Cine substitution, 530
CIP (Cahn-Ingold-Prelog), 67
CIP system priority rules, 68
 in conformational designation, 116
 in *E* or *Z* designation, 76
Circle in Clar notation, 210
Circle mnemonic
 and Möbius molecular orbitals, 766
 in HMO theory, 198
Circle representation of aromaticity, 210
Circular birefringence, 88
Circular dichroism (CD), 89
Circular polarization of light, 88
Circumanthracene, 208
Cis addition, 552. *See also* Syn addition
Cis elimination, 663. *See also* Syn elimination
Cis,trans isomers, 58, 116
Claisen rearrangement, 333, 335, 715, 772
 kinetic isotope effect, 772
 Lewis acid catalysis, 728
Clar notation of aromaticity, 210
Classical carbocation, 290
Click chemistry, 746
Clinal conformation, 115
Closed shell configuration, 201
C_n
 chirality and point group, 62, 63
 proper rotation axis, 60
 symmetry operation, 59
Collisional energy transfer, 802
Combination of radicals, 276
Common ion effect, 338, 474
Competent intermediate, 332
Complex reaction, 342
Concerted process, 329
Concerted reaction, 700
 ab initio calculation, 771
 alternative models, 756
 orbital topology, 769
 synchronous and nonsynchronous pathways, 770, 773
Configuration, 67
 designation as *R* or *S*, 68
Configuration interaction (CI), 26, 225, 713
Conformation, 55, 113
 origin of the term, 113
Conformational analysis, 119
Conformationally equilibrated carbocation, 594
Conformer, 113
Conia-ene reaction, 753
Conical intersection, 821, 849
Conjugate addition, 620, 621
Connected atoms list, 139
Conrotatory pathway, 702, 703, 705, 708, 711-714, 754, 755, 767
Conservation of orbital symmetry, 707, 753
Constitution, 53
Constitutional isomers, 57
Constitutionally heterotopic substituents, 94
Contact ion pair, 313, 421, 485, 803
Conventional flash spectroscopy, 331, 807
Cope elimination, 685
Cope rearrangement, 353, 701, 715, 721, 726, 755, 772
 ab initio calculation, 772
 boat transition structure, 722
 chair transition structure, 721
Coplanar conformation, 647
Corannulene, 209
Cornforth model, 624
Coronene, 208
Correlation diagram
 MO, 707
 state, 712
Correlation line, 710
COT (cyclooctatetraene), 215
Cotton effect, 88
Coulomb integral, 177
Coulombic interaction, 120, 231
Covalent bond with ionic character, 21
Covalent radius, 5
Covalent radius (r_c), 6
*m*CPBA, 605
Cracking of dicyclopentadiene, 736
Cram's rule, 623
Criegee mechanism, 404, 745, 746
Crossover experiment, 333
12-Crown-4, 499
18-Crown-6, 499
Crown ether, 499
CS in molecular mechanics, 137
CT complex, 557, 560, 574
CTC, 560
Cubane, 108, 162, 170, 387, 853
Cubene, 166
Cubic stretching constant, 137
Cumulene
 addition of Br₂, 618
 chirality, 65
 electrophilic addition, 609, 617
 oxymercuration, 618
Cuneane, 163
Curtin-Hammett principle, 358, 360, 624, 651, 680
Curved bond, 128, 266
Cyanohydrin formation, 439
Cyclacene, 166
Cyclizable radical probe, 515
Cycloaddition, 731
 dimerization of ethene, 731, 755
 examples, 741
 FMO theory, 757
 higher order, 739
 participation of a σ bond, 753
 photochemical, 828, 831, 839, 841, 843, 853, 854
 selection rules, 739
 terminology, 731
 with singlet oxygen, 851
1,2-Cycloalkadiene, 164
Cycloalkyne, 164
Cyclobutadiene
 and resonance theory, 240
 DE_{cr}, 201
 DRE, 219

- Cyclobutadiene (*Continued*)
 geometry, 213, 214
 HMO energy levels, 198, 212
 matrix isolation study, 213
 Möbius molecular orbitals, 765
 tunneling, 214
- Cyclobutane
 conformation, 126
 electron density, 127
 strain energy, 158
 X-ray crystal structure, 127
- Cyclobutanol formation, 836
- Cyclobutene electrocyclic reaction, 702
- Cyclocumulene, 164
- Cyclodecapentaene, 216
 DRE, 219
- Cyclo- $D_E D_N A_n$ mechanism, 681
- Cycloheptatrienyl anion HMO calculation, 214
- Cycloheptatrienyl cation HMO calculation, 214
- trans*-Cycloheptene, 163
- Cycloheptyne, 164
- 1,3-Cyclohexadiene heat of hydrogenation, 203
- Cyclohexane
 conformation, 128
 steric isotope effect, 383
- Cyclohexene
 conformation, 134
 heat of hydrogenation, 203
- trans*-Cyclohexene, 163
- Cyclohexyne, 164
- Cyclooctatetraene (COT)
 DRE, 219
 HMO calculation, 215
- trans*-Cyclooctene, 163
 chirality, 66, 71
 configuration of (–) enantiomer, 66
 geometry, 66
- Cyclooctyne, 164
- Cyclopentadiene dimerization, 353
- Cyclopentadienyl anion
 acidity of cyclopentadiene, 214
 HMO calculation, 214
- Cyclopentadienyl cation, 214
- Cyclopentane conformation, 128
- Cyclopentyl carbocation, 297
 rearrangement, 302
- Cyclophane, 72, 168
- Cyclopropane
 angle strain, 123
 geometry, 40
- Cyclopropanone hydrate, 440, 464
- Cyclopropene dimerization, 752
- Cyclopropenyl anion, 212
- Cyclopropenyl cation
 HMO calculation, 211
 synthesis, 211
- Cyclopropenyl HMO energy levels, 198
- Cyclopropenyl radical, 211
- Cyclopropenylidene, 280
- Cyclopropyl carbanion and retention of configuration, 314
- Cyclopropyl radical and racemization, 314
- Cyclopropylmethyl cation, 299
- Cycloreversion, 733
- D mechanism label, 472
- σ stereochemical descriptor, 78
- Deamination of amines, 677
- cis*-Decalin, 171
- trans*-Decalin, 171
- Deconvolution, 808
- Degenerate energy levels, 200
- Degenerate molecular orbitals, 186
- Degenerate rearrangement, 715, 726
- Dehalogenation of vicinal dihalide, 665
 kinetics, 666
- Dehydration
 in gas phase, 676
 kinetic isotope effect, 380
 mechanism, 670
 of alcohols, 669
- 1,2-Dehydrocubane, 166
- Dehydronation, 414
- Delocalization energy (DE_π), 188
 and molecular orbital theory, 189
 and radical combination, 268
- Delocalized molecular orbital, 33
- $\delta\Delta G^\ddagger$, 354
- $\Delta\Delta G^\ddagger$, 354
- $\delta\Delta H^\ddagger$, 402
- $\Delta\Delta H^\ddagger$, 402
- $\delta\Delta S^\ddagger$, 402
- $\Delta\Delta S^\ddagger$, 402
- δ -elimination, 635
- ΔG_{acid} , 424
- ΔG^\ddagger (activation free energy), 350
- ΔG^\ddagger_{int} in Marcus theory, 364
- $^1\Delta_g O_2$, singlet oxygen, 851
- ΔH^\ddagger
 activation enthalpy, 350
 role of solvent, 354
- ΔH_{acid} , 424
- ΔH°_{acid} in gas phase, 423
- ΔS^\ddagger
 activation entropy, 350
 and reaction mechanism, 353, 448, 646
 and transition state, 488
 for pericyclic reaction, 720
 relationship to Arrhenius A , 353
 role of solvent, 354
- ΔS_{acid} , 424
- ΔV^\ddagger , 448
- Demercuration, 595
 stereochemistry, 599
- Density functional theory (DFT), 236
- DE_π , 188
- Deprotection, 856
- Deprotonation, 414
- Detachment step, 533
- Determination of product
 in mechanism study, 327
- Deuteron ($^2H^+$), 414
- Dewar benzene, 167, 705, 843, 854
- Dewar resonance energy (DRE), 219
- Dextrorotatory, 86
- DFT (density functional theory), 236
- DFT calculation
 acidity, 419
 Cope rearrangement, 773
 electrophilic addition, 557
 epoxidation, 608
 Markovnikov's rule, 585
 transfer hydrogenation, 341
- DH° , 16
- Diadamantylcarbene, 288
- Diamagnetic anisotropy, 217
- Diastereomers, 58
- Diastereotopic substituents, 94, 96
- 1,3-Diaxial interaction, 130, 665
- Diazoalkane and carbene generation, 282
- Diazonium ion, 527, 678
- Diborane, 600
- Dichlorocarbene, 280, 283, 285, 634
- Dicyclohexano-18-crown-6, 499
- Dicyclopentadiene cracking, 736
- Dielectric constant (ϵ), 20, 415, 477
 as measure of solvent polarity, 338
- Diels–Alder reaction, 701, 731, 734, 736, 755, 853, 855, 856
 aromaticity of transition state, 765
 endo product, 759
 exo product, 759
 FMO theory, 758, 761
 inverse electron demand, 762
 kinetic control of product
 distribution, 759
 Lewis acid catalysis, 762
 normal electron demand, 762
 regiochemistry, 760
 secondary orbital interactions, 759
 stereochemistry, 759
 thermodynamic control of product
 distribution, 759
 with benzyne, 741
- Dienophile, 734
- Differential rate equation, 343
- Diffusion-controlled reaction, 337
- Diffusion-limited process, 565, 800, 801
- 1,2-Difluoroethane conformation, 150
- Dig (in Baldwin's rules), 274
- Dihedral angle, 113
- 1,4-Dioxane radical cation, 308
- 1,2-Dioxetane chemiluminescence, 860
- Diphenylcarbene, 281, 287
- 1,3-Dipolar cycloaddition, 743
- Dipolarophile, 743
- Dipole moment (μ), 20, 477
- Disproportionation
 of biradical, 834
 of radicals, 276
- Disrotatory pathway, 702–704, 711
- Dissociation constant (K_d)
 of carbonyl hydrate, 439
 of hemiketals, 441

- Dissociation process, 450
 Dissociative state, 848
 Dissymmetric structure and point group, 63
 Dissymmetry, 63
 Distonic radical ion, 308
 Di-*t*-butylcarbene, 280, 288
 Di- π -methane rearrangement, 828, 855
 dm, 87
 1/D_N mechanism label, 471
 1/D_N + 3/A_N mechanism, 471
 D_N + A_N + A_{xh}D_H mechanism, 453
 D_N + A_N mechanism, 471
 D_N*A_N mechanism, 471
 D_N + A_{xh}D_H mechanism, 639
 D_N + D + A_N mechanism, 472
 D_N + D_E mechanism, 639
 D_N mechanism label, 471
 DNA, 4
 Dodecahedrane, 162
 Doering-Zeiss intermediate, 482
 Doering-Zeiss mechanism, 482
 Dot stereochemical descriptor, 58
 Dotted line in Maehr convention, 75
 Doublet state, 792
 DPPH, 258
 DRE, 219
 Dual attraction, 503
 Dynamic effects, 776
 Dyotropic reaction, 749
- E*, 77
 identity symmetry operator, 61
 in Mayr equation, 509
 solute excess molar refraction, 339
- E_a*, 348
E_{act}, 348
E(d) in molecular mechanics, 137, 139
 E1_(anion) mechanism, 642
 Early transition state, 362, 375, 457, 590, 595, 602, 605, 624, 625, 651, 662, 680
 and kinetic isotope effect, 375
 in diazonium ion decomposition, 680
- E2C mechanism, 639
 E1cb mechanism, 639, 650
 E1cb_(anion) mechanism, 642
 E1cb_I mechanism, 644
 E1cb_{ip} mechanism, 643
 E1cb_R mechanism, 643
 Eclipsed conformation, 114, 115
 E2 competition with S_N2, 646
 Edwards equation, 507
E_f in Mayr equation, 513
 E2H mechanism, 639
 EHT (extended Hückel theory), 221, 223
 EHT calculation
 electrocyclic reaction, 707
 ethene, 221
 ethyl anion, 317
 ethyl cation, 293
 ethyl radical, 263
 formaldehyde, 832
- E_{HOMO}*, 220
 E2_{ip} mechanism, 643
 E_i mechanism, 683
 E1 mechanism, 633, 639, 670
 E mechanism label, 471
 E2 mechanism, 633, 639
 and dehydration of 1° alcohol, 673
 Einstein, 789
 Electrocyclic reaction, 702
 and FMO theory, 757
 as cycloaddition reaction, 754
 cyclobutene-butadiene
 interconversion, 697, 702, 708, 710, 713, 714, 755, 757, 767, 768, 770
 cyclohexadiene-hexatriene
 interconversion, 699
 cyclopropyl-allyl interconversion, 743
 Möbius aromaticity, 767
 photochemical, 826, 829
 selection rules, 705
- Electrofuge, 450, 469, 513, 543
 Electron affinity, 18
 and absolute hardness, 506
 and charge transfer complex, 229
 and Mulliken electronegativity, 22
 in gas phase acidity determination, 424
 relationship to *E_{LUMO}*, 220
 Electron configuration, 26, 225, 711, 713, 733
 of formaldehyde electronic states, 791
 Electron correlation, 223
 Electron density
 and basis sets, 224
 and QTAIM, 233
 in DFT, 236
 in HMO theory, 191
 Kohn-Sham theory, 236
 Electron density contour, 127
 Electron donor-acceptor complex, 229
 Electron paramagnetic resonance (EPR), 259
 Electron pushing and MO following, 768
 Electron spin resonance (ESR), 259
 Electron transfer, photoinduced, 803
 Electronegativity, 21, 626
 absolute, 23
 Allen, 23
 and acidity, 386, 429
 and benzyne formation, 538
 and benzyne reaction, 541
 and bond curvature, 150
 and substituent effect, 400
 and variable hybridization, 37
 and VSEPR, 36
 Benson, 23
 comparison, 23
 group, 23
 Mulliken, 22
 Nagle, 23
 Pauling, 21
 Electronic chemical potential (μ), 23
- Electronic energy transfer, 802
 collisional, 802
 Förster, 802
 radiative, 802
 trivial, 802
 Electron-rich alkene, 555
 Electrophile, 469
 Electrophilic addition, 206, 575
 chemoselectivity, 567
 epoxidation, 605
 hydroboration, 600
 Markovnikov's rule, 585
 oxymercuration, 596
 regiochemistry, 568
 reversibility, 563
 solvent effects, 561
 solvent participation, 561
 solvomercuration, 596
 surface-mediated, 587
 Electrophilicity parameter, 509
 Electrostatic effect, 386
 Element effect, 529, 533, 642
 Elementary reaction, 328, 350, 363
 molecularity, 342
 Elimination, 633
 heterogeneous, 652
 1,1-Elimination, 634, 653
 1,2-Elimination, 633, 638
 1/2/Elimination, 633
 1,3-Elimination, 635
 1,4-Elimination, 635
 stereochemistry, 654
 1,6-Elimination, 636
 1,8-Elimination, 636
 1,10-Elimination, 636
E_{LUMO}, 220
E_n
 electronic energy level, 787
 in Edwards equation, 507
 Enantiomer, 57
 and optical activity, 86
 physical properties, 92
 Enantiomeric excess, 88
 Enantiomerically enriched, 85
 Enantiomerically pure, 85
 Enantiopure, 85
 Enantiotopic substituents, 94
 magnetic equivalence, 95
 Encounter complex, 520
 Encounter-controlled reaction, 337
 End absorption, 818
 Endo, 78
 Endo closure in Baldwin's rules, 274
 Endocyclic restriction test, 337, 607
 Endoscopic irradiation, 852
 Endothermic step and Hammond postulate, 362
 Ene reaction, 750
 FMO theory, 758
 Energy minimization, 141
 Energy of UV-vis radiation, 789
 Energy surface, 820

- Enol, 443
 in Conia-ene reaction, 753
 in oxy-Cope reaction, 727
 intermediate in Norrish type II reaction, 836
 photochemical generation, 446
 regiochemistry, 444
- Enolate, 443
 as model for dienophile, 763
 conjugate addition, 621
 in α -halogenation, 443
 nucleophilic addition, 318
 oxidative coupling, 320
 regiochemistry, 444
- Enolization, 442
- Ent- (stereochemical descriptor), 81
- Entgegen, 77
- Enthalpy-controlled reaction, 570
- Enthalpy-entropy compensation, 402
- Entropy units, 351
- Entropy-controlled reaction, 570
- Envelope conformation, 128
- EPA glass, 800
- $E(\Phi)$ in molecular mechanics, 137, 139
- Epi-, 82
- E_π
 allyl anion, 188
 allyl cation, 188
 allyl radical, 188
 energy of the π system, 188
 in HMO theory, 188
- Epimer, 81
- Epimeric center, 81
- Epoxidation of alkenes, 605
- EPR, 259
- ϵ
 dielectric constant, 20, 338
 extinction coefficient, 466
- ϵ_{\max} , 797
- Equatorial preference (*A* value), 130
- Equatorial substituent, 128
- Equilibrium control of product distribution, 357, 759
- Equilibrium isotope effect, 382
 and acidity, 382
 and conformation, 383
- Equilibrium substituent effect, 390
- E2 reaction and Curtin-Hammett principle, 358
- $E(r)$ in molecular mechanics, 137
- Erythro, 83, 571
- Erythrose, 83
- E_s in Taft equation, 401
- E_{SB} in molecular mechanics, 138
- ESCA, 32
 2-norbornyl carbocation, 300
 cyclopentyl cation, 303
- Eschenmoser rearrangement, 729
- ESR (electron spin resonance), 259
- Ester
 acid-catalyzed hydrolysis, 449
 alkaline hydrolysis, 452
 aminolysis, 459
- $E_T(30)$ scale of solvent polarity, 339
- η (absolute hardness), 506
- Ethane
 acidity, 44
 conformational energy, 119
 gas phase acidity, 317
 gas phase basicity, 427
 origin of rotational barrier, 120, 231
 VSEPR description, 36
- Ethanol
 acidity, 386, 419
 gas phase acidity, 426, 428
 80% Ethanol, 646
- Ethanolysis, 476
- Ethene
 acidity, 44
 bent-bond description, 42
 dimerization, 731, 755, 757
 EHT calculation, 221
 electron density, 233
 gas phase acidity, 425
 gas phase basicity, 427
 geometry, 42
 HMO calculation, 176
 LMOs, 225
 natural bond orbitals, 226
 photochemical reaction with benzene, 843
 radical cation, 307
 π, π^* state, 819, 820
 σ, π description, 42
- $E(\theta)$ in molecular mechanics, 137
- Ethyl anion
 EHT calculation, 317
 HOMO, 317
 inversion barrier, 315
- Ethyl cation
 ab initio calculation, 294
 bridged structure, 294
 EHT calculation, 293
 formation in gas phase, 678
 geometry, 294
 hyperconjugation, 292
 LUMO, 293
 PMO analysis, 292
 rearrangement, 298
- Ethyl radical
 dimerization, 268
 EHT calculation, 263
 EPR spectrum, 261
 hyperconjugation, 262, 268
 PMO description, 264
 pyramidalization, 266
 SOMO, 263
- Ethyne
 acidity, 44
 bent-bond description, 44
 gas phase acidity, 425, 428
 gas phase basicity, 427
 σ, π description, 44
- eu, 351
- Even alternant structure, 195
- Excess acidity, 433
- Exchange-correlation functional, 237
- Excimer, 803
- Exciplex, 803
- Excitation spectrum, 801
- Excited state kinetics, 805
- Exciton migration, 802
- Exo, 78
- Exo closure in Baldwin's rules, 274
- Exothermic reaction
 and kinetic isotope effect, 376
 and Marcus theory, 365
- Exothermic step and Hammond postulate, 362
- Extended Hückel theory (EHT), 221
- Extent of reaction, 254
- Extrusion reaction, 747
- Eyring plot, 351
- F*
 in Swain-Lupton equation, 399
 in Taft-Topsom equation, 400
- f* in Swain-Lupton equation, 399
- f^Z , 522
- F1 fragmentation, 637
- F1cb fragmentation, 637
- F2 addition to alkene, 580
- F2 fragmentation, 637
- FA (flowing afterglow), 317, 423
- FA-SIFT, 423
- Fast reaction techniques, 331
- Favorskii rearrangement, 692, 853
- Felkin model, 624
- Femtosecond, 331
- Fenestrane, 161, 170
 [4.4.4]Fenestrane, 161
- \mathcal{F}_i (free valence index), 193
- Field effect, 386
 and substituent effect, 400
- Field effect constant, 399
- First-order decay process, 805
- Fischer projection, 72
 allowed operations, 73
 forbidden operations, 73
- Fischer-Tollens projection, 72
- Flagpole hydrogen, 124
- Flash photolysis, 807
- Flash spectroscopy, 807
 conventional, 807
 laser, 807
 pump-probe technique, 807
- Flowing afterglow (FA or FA-SIFT), 317, 423
- Fluorescence, 795, 798
 and excited state geometry, 799
- Fluorescence lifetime, 806
- Fluorescent chemosensor, 859
- Fluorine substituent
 and acidity, 386, 429
 as a bridging atom, 580
 as a leaving group, 663
 effect on radical geometry, 265, 311
- 2-Fluoroethanol acidity, 386
- Fluorohydrin, 578

- Fluoronium ion, 556
 Fluxional structure, 726
 FMO (frontier molecular orbital), 229
 FMO theory, 229
 and pericyclic reactions, 756
 and torquoselectivity, 757
 charge-transfer complex formation, 229
 Diels–Alder reaction, 758, 760, 761
 dimerization of ethene, 757
 electrocyclic reaction, 757
 ene reaction, 759
 stereochemistry of addition reactions, 553
 Forbidden pericyclic reaction, 705
 Forbidden process, 274, 796
 Forbidden transition, 796
 Force field, 135
 Force field method, 135
 Formaldehyde
 molecular orbitals, 790
 physical properties of excited states, 815
 Formic acid
 acidity, 419
 acidity and thermodynamic values, 429
 Formolysis, 480
 Förster cycle, 813
 Förster energy transfer, 802
 Fractional ionic character, 312
 Fragmentation reaction, 636
 Franck–Condon overlap, 820
 Franck–Condon state, 819
 Franck–Condon term, 796
 Free radical, 256
 Free rotation, 120
 Free valence index (\mathcal{F}_i), 193
 Frontier molecular orbital, 229
 fs (femtosecond), 331
 Fullerene, 209
 Fulvene, 167, 843
 Function, 236
 Functional, 236
 Functional group isomers, 57
 Furan resonance energy, 206
 Furanose, 80

 G (Gauss), 261
 g (spectroscopic splitting factor), 259
 g^+ conformational descriptor, 116
 g^- conformational descriptor, 116
 γ (activity coefficient), 415
 Γ_1 in structure-resonance theory, 243
 Γ_2 in structure-resonance theory, 243
 γ -elimination, 635
 γ -hydrogen abstraction
 photochemical, 835, 855
 Gas constant (R), 349
 Gas phase basicity (GB), 426
 Gauche conformation, 114, 115
 Gauche effect, 581
 and curved bonds, 150
 Gauche interaction, 12
 as 1,3-diaxial interaction, 130
 Gaussian type orbital (GTO), 224

 GB (gas phase basicity), 426
 General acid catalysis, 435, 437, 439, 447, 593
 Brønsted catalysis law, 437
 General base catalysis, 435, 437, 439, 447, 462
 Brønsted catalysis law, 437
 in ester hydrolysis, 456
 Geometric isomers, 58
 Gibbs diagram, 255
 Glass, 800
 Global minimum, 147, 294, 580
 Glucopyranose, 80
 Graph theory, 242
 Graphene, 207
 Graphene nanoribbon, 207
 Grob fragmentation, 636
 Group electronegativity, 23
 Group increment calculation, 10, 12
 Grunwald–Winstein equation, 477
 C^{θ} and Gibbs diagram, 255
 GTO (Gaussian type orbital), 224
 GVB calculation, 46, 240

 h (Planck's constant), 351
 H (nucleophile basicity), 507
 $^2\text{H}^+$ (deuteron), 414
 $^3\text{H}^+$ (triton), 414
 H_- basicity function, 433
 H' acidity function, 431
 H''' acidity function, 431
 H_0
 acidity function, 430, 431
 external magnetic field, 259
 H_0' acidity function, 431
 H_A acidity function, 431
 Half-life and first-order decay, 805
 Haloform reaction, 444
 Halohydrin
 dehydrohalogenation, 605
 synthesis and reaction, 578
 Hammett correlation, 392, 448, 529, 572, 594, 603, 605, 609, 650, 659, 672
 and ΔS^\ddagger , 402
 bent downward, 395
 bent upward, 395
 curved, 573
 nonlinear, 395, 399
 pK_a values, 415
 with maximum, 395
 Hammett equation, 390, 477
 Hammett ρ interpretation, 448
 Hammond postulate, 362, 524, 655
 and kinetic isotope effect, 375
 and S_N1 reaction, 474
 anti-Hammond effect, 365
 Hammond–Leffler postulate, 363
 Hard base, 505
 Hard-soft acid-base theory, 505
 Hartree–Fock limit, 225
 Hartree–Fock theory, 223, 226
 Hashed line stereochemical descriptor, 55

 Hashed wedge stereochemical descriptor, 55
 Haworth representation, 80
 H_{Az} acidity function, 432
 H_B acidity function, 432
 H_C acidity function, 432
 Head-to-head dimer, 841
 Head-to-tail dimer, 841
 Heat of combustion, 8, 148
 Heat of formation, 8
 Heat of fusion, 9
 Heat of hydrogenation, 190
 Heat of sublimation, 9
 Heat of vaporization, 9
 Heavy atom effect, 796, 801
 Helical chirality, 66
 Hemiacetal, 441
 carbohydrate anomers, 79
 formation, 439
 hydrolysis, 448
 Hemiketal, 439, 441
 Heptacene, 207
 Hermitian, 177
 Hess' law, 18
 Heterogeneous catalysis
 alcohol dehydration, 677
 electrophilic addition, 614
 Heterogeneous reaction, 687
 syn elimination, 652
 Heterotopic substituents, 94
 Hexaasterane, 163
 Hexacene, 207
 Hexahelicene, 66
 chirality, 71
 Hexaphenylethane, 257
 Hexaplane, 161
 1,3,5-Hexatriene
 DE_{π} , 201
 Hückel MOs, 185
 HF (Hartree-Fock), 223
 H_1 acidity function, 432
 $HIA(R^+)$, 291
 High pressure mass spectrometry (HPMS), 317, 423
 Higher order cycloaddition, 739
 Highest occupied molecular orbital, 229
 H_m acidity function, 432
 HMO theory, 175
 Hofmann elimination, 656, 662
 Hofmann product, 657
 Hofmann rule, 656
 HOMO, 220, 229
 and Diels–Alder regiochemistry, 761
 1,3-butadiene, 702
 in electrocyclic reaction, 702
 in FMO theory, 756
 in hydroboration, 604
 of alkene, 818
 of ethene, 222
 of formaldehyde, 790
 of 1,3,5-hexatriene, 705
 of methanol, 306
 of nitrobenzene, 845

- Homoallylic structure, 494
 Homoaromaticity, 493
 Homochiral, 84
 Homoconjugation, 493
 Homodesmotic reaction, 12
 HOMO-LUMO crossing, 769
 HOMO-LUMO gap, 220, 506, 762
 and excitation wavelength, 829
 HOMOMERS, 769
 Homo-[1,5] sigmatropic rearrangement, 752
 Homotopic substituents, 94, 96
 Homotropilidene, 726
 Horizontal plane of symmetry (σ_h), 60
 HPMS, 317, 423
 H_R , 96
 H_R acidity function, 432
 H_S , 97
 Hückel $4n + 2$ rule, 201
 Hückel cyclobutadiene, 765
 Hückel molecular orbital theory, 175, 702
 Hund's rule, 278
 Hybrid orbitals
 energies, 29
 shapes, 30
 Hybridization, 3, 29, 31
 and electronegativity, 37
 and geometry, 38
 Hybridization index, 37
 Hybridization parameter, 37
 Hydration
 of alkene, 592
 of alkyne, 614
 of carbonyl compound, 439
 Hydride ion affinity, 291
 Hydride shift, 301
 1,2-Hydride shift, 303, 304
 1,3-Hydride shift, 304
 1,4-Hydride shift, 304
 Hydroboration, 600
 regioselectivity, 600
 stereochemistry, 601
 Hydrogen abstraction, 834
 Hydrogen shift, 719, 720
 [1,3], 717, 718, 754, 764, 767
 [1,5], 715, 719, 763, 767
 [1,7], 719, 720
 [1,9], 719
 Hydrolysis
 nucleophilic catalysis, 457
 of acetals, 447, 448
 of amides, 460
 of esters, 449, 452
 of hemiacetals, 448
 of mesitoate esters, 451
 Hydron, 414
 Hydration, 414
 Hydroperoxide (HOO^-)
 nucleophilicity, 511
 Hydroxymethyl radical, 264
 Hyperchromic effect, 817
 Hyperconjugation, 151, 230
 and EPR spectra, 262
 and ethane torsional barrier, 231
 and kinetic isotope effect, 383
 ethyl radical, 264
 in carbene, 280, 282
 in carbocation, 292
 in radical cation, 307
 Hypercoordinate structure, 290, 320
 Hyperfine coupling
 anisotropic, 261
 in EPR, 260
 isotropic, 261
 Hyperfine coupling constant (a), 260
 in methyl radical, 265
 Hypersurface, 253
 Hypochromic effect, 817
 Hypsochromic shift, 817
- i*
 center of inversion, 60
 symmetry operation, 59
 +I inductive effect, 385
 -I inductive effect, 385
 Ibuprofen, 689
 Iceane, 159
 ICR (ion cyclotron resonance), 423
 Identity reaction, 366
 Identity symmetry operator (E), 61
 I_f (fluorescence intensity), 805
 IIP (intimate ion pair), 560
 Improper rotation axis (S_n), 60, 99
 InChI, 54
 Induction, 280
 and acidity, 419
 and Hofmann orientation, 659
 structural representation, 386
 substituent effect, 385
 Inert radical, 258
 Inherent fluorescence lifetime, 806
 Inherent singlet lifetime, 806
 Inherent strain, 156
 Initial ozonide, 745
 Initiation step in chain reaction, 270, 271, 589
In silico experiment, 339
 Integrated rate equation, 343
 1,3-Interaction, 269
 Internal conversion, 794
 Internal return, 482
 Internally compensated structure, 82
 International Chemical Identifier (InChI), 54
 Internuclear bond angle, 39
 Interorbital angle and hybridization, 38, 39
 Intersystem crossing, 794
 and heavy atom effect, 796
 of carbonyl n, π^* singlets, 841
 Intimate ion pair (IIP), 482, 483, 560, 804
 Intramolecular charge transfer in
 electronic excitation, 799, 814, 817, 845
- Intrinsic barrier ($\Delta G_{\text{int}}^\ddagger$) in Marcus theory, 364
 Inverse electron-demand in Diels-Alder reaction, 762
 Inverse secondary kinetic isotope effect, 381
 Inversion of configuration, 92
 in hydrolysis of β -butyrolactone, 453
 in pericyclic reaction, 773
 in S_N2 reaction, 337
 Inverted region in Marcus theory, 364
 Iodine addition to alkene, 583
 Iodinium ion, 556
 Iodoform reaction, 444
 Iodohydrin, 578
 Ion pairing, 298
 and acidity, 415
 in solvolysis, 482
 Ionic radius (r_i), 5
 Ionization potential, 479
 and absolute hardness, 506
 and charge transfer complex formation, 229, 557
 and gas phase acidity determination, 424
 in EHT theory, 223
 in Mulliken electronegativity, 22
 in reaction of alkenes with XeF_2 , 581
 of alkyl anions, 423
 relationship to E_{HOMO} , 220
 Ionization potential, 18
 Ionizing power of a solvent, 477
 Ipso substitution, 519
 Ireland-Claisen rearrangement, 730
 Irreversible reaction, 344, 354
 Isoaromatic structure, 167
 Isobenzene, 167
 Isobutane gas phase acidity, 317
 Isochronous groups, 96
 Isodensity surface, 233
 Isodesmic reaction, 12, 264
 Isoequilibrium relationship, 403
 Isoergonic reaction, 364
 Isokinetic relationship, 403
 Isokinetic temperature, 403
 Isologous structures, 12
 Isomers, 56
 constitutional, 57
 functional group, 57
 positional, 57
 stereoisomers, 57
 Isopropyl cation, 297
 rearrangement, 303
 Isotactic polymer, 93
 Isotopic dilution, 330
 Isotopic exchange
 in ester hydrolysis, 455
 in ketones, 443
 Isotopic fractionation factor, 384
 Isotopic labeling, 304, 335, 453, 454, 495, 586, 774
 in alcohol dehydration, 674
 in alkaline hydrolysis of esters, 455

- in amide hydrolysis, 460
 in amine deamination, 679
 in benzyne reaction, 537
 in carbocation rearrangement, 302
 in elimination, 634
 in ester hydrolysis, 457
 in ester pyrolysis, 684
 in hydrolysis of ethyl propionate, 453
 in hydrolysis of methyl mesitoate, 451
 in pericyclic reaction, 699, 719, 749, 772, 774, 777
 in von Richter reaction, 530
 Isotopologue, 94
 Isotopomer, 94
 Isotropic hyperfine coupling, 261

 $J_{13\text{C-H}}$
 and hybridization parameter, 41
 and kinetic acidity, 41
 Jablonski diagram, 792
 Jackson–Meisenheimer complex, 316, 529
 Jahn–Teller effect and geometry of methyl radical cation, 308
 J_n (rotational energy level), 789
 Johnson rearrangement, 729

 K_a , 414
 k_{app} , 344
 Karplus equation, 152
 Kasha's rule, 795
 K_a^T , 415
 K_b , 420
 K_{BH^+} , 420
 κ in transition state theory, 351
 k_d , 809
 Kekulé molecular models, 125
 Kekulé structure, 48, 53, 202, 210, 238
 counting, 241
 k_f (fluorescence rate constant), 805
 K_i , 415
 Kinetic acidity, 41, 421
 Kinetic control of product
 distribution, 356, 357, 581, 670, 759
 Kinetic isotope effect, 370, 371
 and temperature, 379
 and tunneling, 378
 in aryldiazonium reaction, 527
 in bromine addition to alkene, 559
 in Chugaev reaction, 683
 in Claisen rearrangement, 772
 in elimination, 642–644, 673
 in Hofmann elimination, 665
 in hydroboration, 605
 in hydrolysis of formamide, 462
 in hydrolysis of methyl formate, 452, 456
 in pyrolysis, 684
 in $S_{\text{E}}\text{Ar}$ reaction, 519
 intramolecular, 378
 usual range, 377
 1° Kinetic isotope effect, 371
 2° Kinetic isotope effect, 371, 380
 Kinetically stable radical, 258

 Kinetics and mechanism
 determination, 341
 K_{ion} , 420
 Koelsch radical, 258
 Kohn–Sham theory, 236
 Koopmans' theorem, 32
 Kosower Z scale of solvent polarity, 339
 k_{Ψ} , 344
 K_{SC} , 244

 l (like), 84
 l (sensitivity to solvent nucleophilicity), 478
 L (stereochemical descriptor), 78
 Ladenburg benzene, 21, 163
 λ
 hybridization parameter, 37
 weighting parameter for ionic character, 21
 λ_{max} , 797
 Lapworth mechanisms, 443
 Laser flash spectroscopy, 331, 807
 Late transition state, 362, 376, 452, 680
 and kinetic isotope effect, 375
 Law of definite proportions, 2
 LCAO (linear combination of atomic orbitals), 175
 L-CPL, 858
 Left-handed helix, 71
 Leveling effect of solvent, 422, 430
 Levorotatory, 86
 Lewis acid, 413
 Lewis acid catalysis
 Claisen rearrangement, 728
 Diels–Alder reaction, 762
 Friedel–Crafts reaction, 330
 Lewis base, 413, 504
 Lewis cubical bonding model, 19
 Lewis structure, 226, 524, 564, 814
 representation of electronically excited state, 814, 832, 840, 841, 845
 LFER, 389
 Lifetime
 of 1,4-biradical, 837
 of bromonium ion, 564
 of carbene, 288
 of carbocation, 298, 674
 of excited state, 805, 809, 810, 862
 of intermediate, 254, 320, 533, 555, 565, 571, 594
 of singlet oxygen, 851
 relationship to half-life, 806
 Lightstruck flavor of beer, 861
 Limonene
 deprotonation, 315
 photohydration, 825
 Line formula conventions, 54
 Linear cheletropic reaction, 747
 Linear free energy relationship (LFER), 389, 477, 507
 and gas phase acidity, 423
 Hammett equation, 390
 Linear Hammett correlation, 392

 lk (like), 84
 LMO, 33, 225
 Local minimum, 147
 and reactive intermediate, 254
 Localized molecular orbital, 33, 225
 London dispersion forces, 139
 Lowest unoccupied molecular orbital, 229
 Luminol, 859
 LUMO, 220, 229
 and conjugate addition, 621
 and Diels–Alder regiochemistry, 761
 in FMO theory, 756
 of alkene, 818
 of ethyl cation, 293
 of formaldehyde, 790
 of nitrobenzene, 845
 LUMOMERS, 769
 Lyate ion, 435
 Lyonium ion, 434

 M chirality descriptor, 71, 72
 m in Grunwald–Winstein equation, 477
 $-M$ mesomeric effect, 385
 $+M$ mesomeric effect, 385
 M05-2X functional, 237
 Maehr convention for stereochemical drawings, 74
 Magic acid, 296
 Magnetic susceptibility and triphenylmethyl radical, 258
 Manifold, 793
 singlet, 793
 triplet, 793
 Marcus equation, 364
 Markovnikov orientation, 567, 592, 595, 597, 603
 Markovnikov spelling, 585
 Markovnikov's rule, 405, 585, 631
 Mass law effect, 474
 Matrix isolation study, 213, 307, 308, 320, 331, 830
 benzyne, 541
 MC (Monte Carlo statistical mechanics), 154
 MD (molecular dynamics), 153
 Mechanism of a reaction, 327
 * Mechanism descriptor, 644
 ‡ Mechanism descriptor, 644
 Menschutkin reaction, 500
 Menschutkin reaction, 500
 Mercurinium ion, 598, 614, 615, 617
 Mercuronium ion, 598
 Meso
 alternative definition, 82
 stereochemical descriptor, 82
 Meso structure, 82
 and stereogenicity, 98
 physical properties, 93
 with internal plane of symmetry, 82
 without internal plane of symmetry, 82
 Mesomeric effect, 385
 Metal ion catalysis, 458

- Methane
 gas phase acidity, 317, 429
 heterolysis in gas phase, 423
 homolytic dissociation in gas phase, 423
 PES spectrum, 32
 radical cation, 307
 VSEPR description, 36
- Methanol
 acidity, 417
 gas phase acidity, 426
 radical cation, 306
 reaction with singlet carbene, 287
- Methanolysis, 480, 481
- '657 Method' and geometry, 51
- Methonium ion (CH_5^+), 290
- Methyl anion
 ab initio calculation, 315
 from gas phase heterolysis of methane, 423
 geometry, 310
 inversion barrier, 315
- Methyl radical, 256, 260
 EPR spectrum, 261
 geometry, 264, 265
 hyperfine coupling constant, 265
- Methylcyclohexane
 conformation, 129
 Newman projection, 129
- Methylene
 electronic energy levels, 279
 electronic states, 278
 geometry, 279
- Metropolis sampling, 154
- Michael addition, 620
- Microenvironment characterization, 859
- Microwave spectroscopy, 5, 118
- Mills–Nixon effect, 206
- Minimized geometry, 141
- Mixed halogen
 addition to alkenes, 584
 addition to alkynes, 611
- MM1, 136
 MM2, 136
 MM2(77), 136
 MM3, 136
 MM4, 136
 MMX, 139
- MO correlation diagram, 709
 atom transfer reaction, 749, 750
 Diels–Alder reaction, 736
 electrocyclic reaction, 710
 ethene dimerization, 732, 733
 ozonolysis, 745
 photo-Diels–Alder reaction, 736
- MO following, 848
- Möbius antiaromaticity, 767
- Möbius aromaticity, 763, 767, 769
- Möbius cyclobutadiene, 765
- Möbius molecular orbitals, 765
- Möbius π system, 765
- Möbius strip, 765
- Molecular dimensions, 3, 5, 154, 858
- Molecular dipole moment (μ), 20
 as measure of solvent polarity, 338
- Molecular dynamics, 153
- Molecular graph in QTAIM, 235
- Molecular ladder, 857
- Molecular mechanics, 135
 computational time, 136
- Molecular orbital symmetry, 707
 and basis set symmetry, 33
- Molecular orbital theory (MO theory), 24, 25, 175
 and delocalization energy, 189
- Molecular 'ship in a bottle', 858
- Molecular simulation, 153
- Molecular surface area, 6
- Molecular tweezers, 858
- Molecular volume, 6, 233
 calculated, 7
- Molecularity, 342
 and Ingold designation, 470, 471
 in IUPAC mechanism label, 552
- Molozonide, 745
- Monochiral, 85
- Monochloroborane, 605
- Monte Carlo statistical mechanics, 154
- More O'Ferrall–Jencks diagram, 367, 472, 639
- MP2, 225
 MP3, 225
- m_s (spin quantum number), 259
- mT (millitesla), 261
- μ
 chemical potential, 23
 dipole moment, 338, 477
- μ -hydridobridged cation, 299, 304
- Mulliken electronegativity, 22
- Mulliken relationship
 charge-transfer complex absorption, 229
- Multiphoton excitation, 790
- Multiplicity of electronic state, 284, 792
- Mustard gas, 488
- n
 hybridization index, 37
 in Swain–Scott equation, 507
 nonbonding MO, 790
- N (solvent nucleophilicity), 478
- $4n + 2$ rule, 201
- n, π^* state, 792
- $^1n, \pi^*$ state, 793
- $^3n, \pi^*$ state, 793
- $n \rightarrow \pi^*$ transition, 790
 in benzophenone, 816
 solvent effect, 817
- N_+ in Ritchie equation, 479
- Nagle electronegativity, 23
- Nanosecond, 331
- Naphthalene
 Clar notation, 211
 DRE, 219
 electrophilic aromatic substitution, 206
 Kekulé structures, 238
 photophysical data, 809
 resonance energy, 206, 238
 SRT resonance energy, 245
- 2-Naphthol excited state acidity, 813
- 1-Naphthylmethyl radical, 849
- Natural bond orbital, 226
- NBMO (nonbonding molecular orbital), 183, 243
- NBO (natural bond orbital), 226, 232, 302
- Neat reagent, 576
- Negative activation energy, 557
- Negative electron affinity, 310
- Negative kinetic temperature effect, 350
- Neighboring group participation, 487, 568
- Newman projection, 55
 and dihedral angle, 113
- N_i in Mayr equation, 513
- NICS, 217
- m*-Nitroanisole, solubility of T_1 state, 817
- Nitrone in 1,3-dipolar cycloaddition, 744
- No-crossing rule, 713
- Node, 182
- 'No mechanism' rearrangement, 700
- Nonadiabatic process, 812
- Nonalternant structure, 194
- Nonaromatic structure, 215
- Nonbonding molecular orbital (NBMO), 183
 designated as n , 790
 in odd alternant system, 195
- Nonclassical carbocation, 290, 294, 300, 491
- Nonconcerted pathway for electrocyclic reaction, 714
- Nondissymmetric structure
 and point group, 64
- Non-Kekulé structure, 238
- Nonlinear cheletropic reaction, 747
- Nonlinear Hammett correlation, 395, 399
- Nonobservables, 40, 48, 120, 149, 203, 236, 388, 471
- Nonradiative process, 794
- Nonstereogenic atom, 98
- Nonsynchronous reaction, 770, 771, 772
- 2-Norbornyl cation, 300, 301
- 7-Norbornyl radical, 267
- Norbornyne, 284
- Norcarane, 285
- Normal addition, 589
- Normal E2 mechanism, 639
- Normal electron demand Diels–Alder reaction, 762
- Normal salt effect, 479
- Normal secondary kinetic isotope effect, 380
- Normalization integral, 177
- Normalized wave function, 181
- Norrish type I reaction, 832, 862
- Norrish type II reaction, 447, 836
- Norrish–Yang cyclization, 836, 857
- Not acceptable representations of stereochemistry, 56, 80

- N_{OTs} , 478
n-radical cation, 306
ns (nanosecond), 331
Nucleofugality, 512
Nucleofuge, 469
Nucleofugic detachment (D_N), 471
Nucleophile, 469
 as Lewis base, 504
Nucleophilic attachment (A_N), 471
Nucleophilic catalysis
 in ester hydrolysis, 457
 intermolecular, 457
 intramolecular, 457
Nucleophilic susceptibility, 567, 615
Nucleophilic vinylic substitution, 532
Nucleophilicity
 kinetic concept, 504
 of halide ions, 504
 trends, 504
Nucleus-independent chemical shift (NICS), 217
- Observables, 1, 19, 40, 48, 120, 236, 471
Octacyclopropylcubane, 853
Octahedrane, 162
Octant rule, 90
Odd alternant structure, 195, 243
Off-diagonal overlap integral, 221
Oligomeric species, 312
 ω
 component in pericyclic reaction, 743
 interaction energy in Mulliken relationship, 230
'onium compound, 657
Onset of UV-vis absorption and photochemistry, 797
 Cl_2 , 846
Open shell configuration, 201
Optical activity, 86
(*d*) Optical activity descriptor, 86
(*l*) Optical activity descriptor, 86
(-) Optical activity descriptor, 86
(+) Optical activity descriptor, 86
Optical purity, 87
Optical rotary dispersion (ORD), 88
ORD, 88
Order of a reaction, 342
'Organic thinking', 48
ORTEP plot, 56
Orthogonal orbitals, 120, 189, 231, 541, 711, 816, 820
Orthogonene, 165
Ovalene, 208
 SRT resonance energy, 245
Overall order of a reaction, 342
Overlap integral, 177, 179
Oxetane formation, 839
Oxibase scale, 507
Oxirene, 617
Oxonium ion, 434
Oxy-Cope reaction, 727
Oxygen perturbation of singlet-triplet transitions, 801
- Oxymercuration, 595
 stereochemistry, 599
Ozone pericyclic reaction, 744
Ozonolysis, 404
 Criegee mechanism, 745
- P*
 chirality descriptor, 71, 72
 polarizability in Edwards equation, 507
PA (proton affinity), 426
Paclitaxel, 55
Pagodane, 163
 dication, 305
[2.2]Paracyclophane, 168
[6]Paracyclophane, 66, 168
Paradigm, xv, 212, 251, 279
Parallel orbitals, 42, 175, 215, 297, 648, 705, 711
Parameterization
 in semiempirical molecular MO calculations, 223
 of a force field, 135
Parentheses in 1,3-dipolar cycloaddition designation, 744
Parf, 84
Partial charge, 20
Partial rate factor, 522
Partially bridged intermediate, 565
Paternò-Büchi reaction, 839
 regiochemistry, 840
 stereochemistry, 840
Pauli exchange principle, 260
Pauli exclusion principle, 120, 231
PCMODEL, 139
Pentacene, 207
Pentadienyl MOs, 185
Pentaprismane, 163
1-Pentene radical cation, 307
2-Pentene radical cation, 307
Peracid, 605
Percent ionic character, 312
Percutaneous irradiation, 852
Pericyclic reaction, 701, 754
 aromaticity of transition structure, 763
 atom transfer, 749
 cheletropic, 747
 classification as cycloaddition, 753
 cycloaddition, 731
 electrocyclic, 702
 ene reaction, 750
 FMO theory, 756
 general selection rule, 755
 hydrogen shift, 715
 nonsynchronous, 772
 ozonolysis, 745
 participation of *p* orbital, 743
 photochemical, 703, 705, 719, 724, 733, 739, 750, 755
 semiempirical MO calculation, 771
 sigmatropic rearrangement, 715
 terminology, 731
Periplanar conformation, 115
Peristylane, 163
- Peroxidation reaction, 616
Peroxide effect, 589
Peroxy acid, 605
Perpendicular excited state, 820
Perpendicular orbitals, 189
Persistent radical, 258
Perturbational molecular orbital (PMO) theory, 226
PES of methane, 32
PET (photoinduced electron transfer), 306
Phenanthrene
 Clar notation, 211
 DRE, 219
 electrophilic addition, 206
 Kekulé structures, 238
 resonance energy, 206, 238, 239
 SRT resonance energy, 245
 VB calculation, 239
Phenonium ion, 490, 674
Phenyl radical, 256
1-Phenylethyl carbocation, 571
 Φ (quantum yield), 804
Phlogiston, xvi
Phosphorescence, 795, 800
Photochemical hydrogen abstraction, 834, 855
Photochemical oxetane formation, 839
Photochemical pericyclic reaction, 703, 705, 719, 724, 755
Photochemical pH change, 834
Photochemistry, 787
Photochromism, 858
Photo-Claisen reaction, 335, 847
Photoconductive materials, 859
Photocycloaddition, 828, 831, 839, 841, 843, 853, 854
Photodeconjugation, 842
Photodeprotection, 856
Photodimerization, 844
Photodissociation, 833, 847-850
Photodynamic therapy, 852
Photoelectron spectroscopy (PES), 32
Photo-Fries reaction, 847
Photography, 858
Photohydration, 447, 825
Photoinduced electron transfer (PET), 306, 543, 803, 804
Photoisomerization, 820, 821, 824, 830, 842, 844, 855, 862, 863
Photolysis, 807
Photophysical process, 793, 805, 837
Photophysics, 789
Photopolymerization, 859
Photoracemization, 836
Photoreduction, 834
Photosolvolysis, 845
Photostationary state, 823, 824
Photosubstitution, 845
pH-rate constant curve, 441
 π bond order (P_{ij}), 192
 π bonding orbital, 180
 π complex, 557, 603, 610

- π -electron deficient carbene, 280
 π electron density (ρ_i), 191
 π molecular orbital, 175
 π -nucleophile, 509
 π, π^* state, 792
 $^1\pi, \pi^*$ state, 793, 819
 $^3\pi, \pi^*$ state, 793, 819
 π -radical cation, 306
 π system in pericyclic reaction, 702
 π^*
 antibonding orbital, 180
 solvent dipolarity/polarizability index, 338
 π^*_{azo} solvent parameter, 339
 $\pi \rightarrow \pi^*$ transition
 and solvent effect, 817
 in alkene, 818
 in benzene, 843
 in benzophenone, 816
 Picosecond (ps), 331
 Pilot atom, 72
 Pipek–Mezey method, 225
 Piperine, 867
 pK_a , 414
 of electronically excited state, 813
 $PK_{\text{C}_5\text{CHA}}$, 421
 PKIE, 371
 Plain curve, 88
 Planar carbon atom, 161
 Planar chirality, 70
 Planck's constant (h), 351
 Plane of chirality, 66
 Plane polarized light, 86
 Platonic solid, 161
 PM3, 223
 PM6, 223
 PMO calculation
 carbocation, 230, 292
 conformation of ethane, 231
 ethyl radical, 263, 264
 pericyclic reaction, 756
 torsional barrier in ethane, 231
 PMO theory, 226
 Point group, 61
 and chirality, 62, 63, 65
 and nondissymmetry, 64
 classification scheme, 61
 Polar Felkin–Anh model, 627
 Polarizability
 and acidity, 429
 and base softness, 505
 and nucleophilicity, 504, 507
 and pericyclic reaction, 771
 and substituent effect, 400
 Polarized light
 circularly polarized, 88
 plane polarized, 86
 Polyacene, 206
 Polymerization, 271
 Ponderal effect, 501
 Positional isomers, 57
 Positive Cotton effect, 88
 Post-Hartree–Fock method, 225
 Potential energy surface, 147, 216, 253,
 366, 370, 472, 566, 640, 645, 714, 777,
 812, 821, 848, 850
 acid-base reaction, 418
 and electrocyclic reaction, 714
 and kinetic isotope effect, 373
 and syn elimination, 651
 bifurcated, 370
 bromonium ion, 566
 for electronically excited state, 820
 pR , 70, 72
 Preassociation mechanism, 595
 Predissociation, 848
 Predissociative state, 848
 Preexponential factor (A), 349
 and kinetic isotope effect, 374
 Pref, 84
 Preferred representations of
 stereochemistry, 56, 81
 Previtamin D₃, 720
 Principle of microscopic reversibility, 344
 Prismane, 163, 170, 843
 (Pro)^p-chirality, 99
 Pro-(*R*) descriptor, 96, 97
 Pro-(*S*) descriptor, 97
 Prochiral structure, 96
 Prodrug, 636
 Product development control, 625
 Product distribution and $\delta\Delta G^\ddagger$, 354
 Pro-fragrance, 861
 Progress of reaction, 253, 361, 641
 Propagation step in chain reaction, 270,
 271, 543, 583, 589
 Propane gas phase acidity, 317
 2-Propanol
 acidity, 418
 gas phase acidity, 426, 428
 [1.1.1]Propellane, 160, 168
 Propene conformations
 and bonding models, 46
 Proper rotation axis (C_n), 60, 99
 Propionic acid acidity, 428
 1-Propyl cation, ab initio calculation, 298
 1-Propyl radical, 270
 hyperfine coupling, 262
 Propyne gas phase acidity, 428
 Protium (^1H), 516, 774
 Protobranching, 15
 Proton ($^1\text{H}^+$), 414
 Proton affinity (PA), 426
 Proton inventory, 385
 Protonation, 414
 pS , 70, 72
 ps (picosecond), 331
 Pseudoasymmetric atom, 98
 Pseudoaxial substituent, 135
 Pseudoequatorial substituent, 135
 Pseudo-first-order kinetics, 344, 452, 474
 Pseudorotation, 128
 pss, 823
 PTOC ester, 272
 Puckered conformation, 126
 Pulsed ion cyclotron resonance (ICR)
 spectrometry, 423
 Push-pull carbene, 281
 Push-push carbene, 281
 Pyramidal carbon atom, 160
 Pyramidalization
 alkene distortion, 166
 in excited state, 820, 821
 Pyramidane, 163
 Pyrene SRT resonance energy, 245
 Pyridine reaction with singlet
 carbene, 287
 Pyridine-2-thione-*N*-oxycarbonyl
 ester, 272
 2-Pyridone-2-hydroxypyridine
 tautomerization, 449
 Pyridyne, 168
 Pyrolytic elimination, 681

 Q_i (charge density), 192
 QTAIM, 233
 methonium ion, 290
 Quantitative conformational analysis, 135
 Quantum Chemistry Program
 Exchange, 137
 Quantum efficiency, 804
 Quantum theory of atoms in
 molecules, 233
 Quantum yield, 804
 Quasi-steady-state approximation, 345
 Quencher, 800
 of electronically excited state, 809

 R
 gas constant, 349
 in Swain–Lupton equation, 399
 in Taft–Topsom equation, 400
 in Yukawa–Tsuno equation, 399
 stereochemical descriptor, 67, 68, 76
 + R resonance effect, 385
 – R resonance effect, 385
 R^* , 76
 R_a , 70
Rac- (stereochemical descriptor), 87
 Racemate, 87
 physical properties, 93
 Racemic mixture, 87
 Racemic modification, 87
 Racemization, 135
 and A1 mechanism, 447
 and carbanion, 314, 333
 and carbocation, 291
 and radicals, 314
 and SET mechanism, 517
 and S_N1 mechanism, 480
 of chiral ketones, 443
 [4]Radialene, 167
 Radiant intensity, 789

- Radiant power, 789
Radiationless decay, 794, 820
Radiationless process, 794
Radiationless transfer of electronic excitation, 802
Radiative process, 793
Radical
 bromine-bridged, 591
 inert, 258
 kinetically stable, 258
 origin of the term, 256
 persistent, 258
 stability, 268
 trapping, 270
Radical anion, 270, 310, 543
 and photoinduced electron transfer, 804
 EPR spectrum, 261
 generation, 310
 in SET reaction, 515
 reactions, 310
Radical cation, 270, 305
 acidity, 309, 422
 and photoinduced electron transfer, 804
 classification, 306
 distonic, 308
 generation, 305
 in nitration of benzene, 526
 reactions, 309
Radical clock, 275
Radical combination, 276
Radical cyclization, 273
Radical disproportionation, 276
Radical intermediate, 341
Radical ion pair, 803
Radical stabilization energy (RSE), 264
Radical trap, 515, 542
Rapidly equilibrating classical carbocations, 300, 494
Rate control of product distribution, 357
Rate equation, 342
 differential, 343
 integrated, 343
Rate expression, 342
Rate-limiting step (RLS), 336, 348, 443, 444
 and ‡ mechanism descriptor, 644
 and acid catalysis, 434
 and anchimeric assistance, 486
 and categories of elimination reactions, 644
 and ΔS^\ddagger , 353
 and Hammett correlation, 394
 and kinetic isotope effect, 370
 and molecularity of reaction, 342
 and pH, 441
 and preassociation mechanism, 595
 and reaction dynamics, 776
 and solvent isotope effect, 385
 and surface effects, 687
 in addition of Br₂ to alkene, 559, 561
 in alcohol dehydration, 670, 673
 in amide hydrolysis, 460, 463
 in benzyne formation, 538
 in dehalogenation reaction, 668
 in electrophilic aromatic substitution, 519, 520
 in ester hydrolysis, 449, 450, 452, 454, 456, 457
 in hydration of alkene, 594
 in nucleophilic acyl substitution, 459
 in nucleophilic aromatic substitution, 527
 in nucleophilic vinylic substitution, 533
 in oxymercuration, 597
 in photochemical process, 833
 in pyrolytic elimination, 683
 in reaction of XeF₂ with alkene, 581
 in S_N1 reaction, 473
r_c (covalent radius), 5
R-CPL, 858
Re face, 98
Reaction constant in Hammett equation, 390
Reaction coordinate, 253, 254, 367
 and excited states, 820
 and kinetic isotope effect, 376
 and VBCM, 514
 E1 reaction, 642
 Gibbs diagram, 255
 Marcus theory, 363
 pericyclic reaction, 711, 739
 photodissociation, 848
 S_N2 reaction, 361
Reaction coordinate diagram, 253
 acetal hydrolysis, 447
 and excited state acidity, 811
 and Hammond postulate, 362
 and product distribution, 357
 and reactive intermediate, 254
 and substituent effect, 390
 E1 reaction, 641
 E1c_BR reaction, 643
 E2 reaction, 641
 elementary reaction, 348
 Gibbs diagram, 328
 Hofmann orientation, 658
 Saytzeff orientation, 655
 S_EAr reaction, 519
 S_N2 reaction, 361
 solvolysis, 485
Reaction mechanism, 327
Reaction velocity, 342
Reactive intermediate, 253, 254
 and Hammond postulate, 362
 detection, 531
 energy requirement, 329
 isolation, 329, 330
 lifetime, 254
 photochemical generation, 824, 842, 855
 spectroscopic detection, 330
 trapping, 331, 483
Rectus, 67
Red shift, 817
Regiochemistry, 621
 and Markovnikov's rule, 585
 in addition of HBr to alkene, 589
 in addition of HCl to alkyne, 612
 in benzyne reaction, 537
 in electrophilic addition, 568, 574, 582, 584
 in elimination, 654
 in hydration of alkene, 593
 in hydroboration of alkene, 596, 602
 in hydroboration of terminal alkyne, 616
 in nucleophilic addition, 620
 in oxymercuration of alkene, 597
 in oxymercuration of alkyne, 614
 in α -halogenation of ketones, 444
 of Cope elimination, 686
 of Diels-Alder reaction, 760
 of enol formation, 444
 of enolate formation, 444
Regioselective reaction, 86
Regioselectivity, 567, 584, 597, 603, 605, 661
Regiospecific reaction, 86
Rel, 76
Relative configuration, 74–76, 91, 92
Relative hardness and aromaticity, 220
Relative static permittivity, 338
Resolution of a racemate, 87
Resolve (a racemate), 87
Resonance, 189, 192, 197, 198, 239
 and acidity of carboxylic acids, 418
 and benzyne reaction, 541
 and substituent effect, 400
 bromonium ion, 564
 carbanion stabilization, 311
 carbene stabilization, 280
 carbocation stabilization, 292
 description of carbanion, 312
 nucleophilic aromatic substitution, 529
 substituent effect, 385
Resonance effect constant, 399
Resonance energy, 204
 and aromaticity, 206
 and heat of formation, 218
 and number of resonance structures, 238
 and SRT method, 241, 244
 and valence bond theory, 189
 annulenes, 218
 benzene, 190, 203–205, 238, 239
 Dewar resonance energy, 218
 furan, 206
 naphthalene, 206
 phenanthrene, 206
 thiophene, 206
Resonance hybrid, 189
Resonance integral
 HMO theory, 177
 in Möbius π systems, 765
Resonance structure, 189, 197, 238
 and electrophilic aromatic substitution, 524
 and hyperconjugation, 230, 262
 and representation of electronically excited state, 814, 832, 841, 843, 845

- Retention of configuration, 92
 in ester hydrolysis, 453, 456
- Retro-1,3-cycloaddition, 746
- Retro-Diels–Alder reaction, 736, 854
- Retro-ene reaction, 683, 752
- Reverse aldol reaction, 638
- Reverse Michael addition, 638
- ρ
 in Hammett equation, 390, 400
 interpretation, 392
 negative value, 392
 positive value, 392
 reaction constant, 391
- ρ , (electron density), 191
- $\rho(r)$ in QTAIM, 233
- ρ^* in Taft equation, 401
- 11-*cis*-Rhodopsin
 photoisomerization, 822
- r_i , 5
- Ring current, 203
- Ritchie equation, 479, 511
- RLS (rate limiting step), 336
- Robinson annulation, 621
- Rose bengal, 852
- Rose oxide, 852
- Rotamer, 113
- [3]Rotane, 163
- Rotational energy level notation, 789
- Rotational isomer, 113. *See also* Rotamer
- Rotundone, 867
- Rp, 70
- RS (stereochemical descriptor), 87
- RSE (radical stabilization energy), 264
- Rule of steric control of asymmetric induction, 623
- r_{vdw} (van der Waals radius), 5
- Rydberg state, 818, 819, 825, 826, 829, 843
- Rydberg transition, 818
- S
 in Taft equation, 401
 solute dipolarity/polarizability parameter, 339
 stereochemical descriptor, 67, 68
- s in Swain–Scott equation, 507
- S^+ , 76
- S_0 state, 792
- S_1 state, 792
- Sa, 70
- Saddle point, 641, 852
 and potential energy surface, 366
 and transition structure, 708
- Salt effect, 338
 normal, 479
 special, 483
- Sawhorse representation, 55
- Saytzeff orientation, 655, 662
- Saytzeff product, 657
- Saytzeff rule, 654, 656
- SC (structure count), 241
 +sc, 115
 -sc, 115
- Scalemic, 85
- Scanning tunneling microscopy (STM), 3
- SCF, 224, 225, 244
- Schrödinger equation, 25, 176
- s-cis* conformational descriptor, 117
- s*-(E), 117
- s_E in Mayr equation, 510
- S_E mechanism label, 593
- S_EAr reaction
 and single-electron transfer, 525
 electrophilic aromatic substitution, 518
- Secondary kinetic isotope effect, 371, 380, 673
- Secondary orbital interactions, 759
- Secondary solvent kinetic isotope effect, 384
- Secular determinant, 178
- Selection rules
 and number of electrons, 743
 atom transfer reactions, 750
 cheletropic reactions, 748
 cycloaddition, 739
 electrocyclic reactions, 705
 pericyclic reactions in general, 755
 sigmatropic reaction, 717, 724
 transition state aromaticity, 767
- Self-consistent field (SCF), 224
- Semiempirical method, 223
- Semiempirical MO calculation, 223, 226
 computational resources, 223
 pericyclic reaction, 771
- Sensitization, 283, 809, 818, 820, 824, 830, 851
 electronic energy transfer, 803
 origin of the term, 803
- Sensitizer, 283
- SET, 513, 517
- S_f in Mayr equation, 513
- SF in molecular mechanics, 138
- Si face, 98
- σ
 absolute softness, 506
 in Hammett equation, 390, 400
 substituent constant, 391
 symmetry operation, 59
- σ bond
 heterolytic dissociation, 19
 photodissociation, 847
- σ complex, 520, 553
- σ^- substituent constant, 399
- σ^+ in Taft equation, 400, 401
- σ, π description of double bond, 42
 and acidity, 44
- σ^+ substituent constant, 398
- σ^0 substituent constant, 400
- σ -complex, 526
- σ -electron rich carbene, 280
- $^1\Sigma_g^+$ O_2 (electronic state of O_2), 851
- $^3\Sigma_g^-$ state of O_2 , 851
- σ_h (horizontal plane of symmetry), 60
- σ_I substituent constant, 400
- σ_m in Hammett equation, 395
- σ'' substituent constant, 400
- σ_p in Hammett equation, 395
- σ_R substituent constant, 400
- σ_R^- substituent constant, 400
- σ_R^+ substituent constant, 400
- σ -radical cation, 307
- σ_v (vertical plane of symmetry), 59
- Sigmatropic reaction, 715, 725
 as cycloaddition reaction, 754
 Möbius aromaticity, 767
 selection rules, 717, 724
- Simmons–Smith reaction, 283
- Single electron shift, 513, 515
- Single electron transfer (SET), 269, 513, 517, 525, 531, 581
- Single-molecule
 spectroelectrochemistry, 4
- Singlet lifetime, 806
- Singlet manifold, 793, 794
- Singlet oxygen, 851
 lifetime, 851
 photodynamic therapy, 852
- Singlet state, 792
 of carbene, 288
 of methylene, 278
- Singlet-singlet absorption, 795
- Singlet-triplet absorption, 795
- Single-walled nanotube, 208
- Singly-occupied molecular orbital, 262
- Sinister, 67
- Skew conformation, 114
- Slater type orbital (STO), 224
- SMILES notation, 54
- Smiles rearrangement, 529
- S_n
 chirality and point group, 63
 symmetry operation, 59
- s_N in Mayr equation, 509
- $S_N(EA)$ mechanism, 536
- S_N1 mechanism label
 meaning intended by Ingold, 471
- S_N1 reaction, 470
 anchimeric assistance, 485
 and salt effect, 479
 and solvent polarity, 477
 and steady-state approximation, 473
 and steric effects, 474
 designated as ($D_N + A_N$), 471
 kinetic isotope effect, 382
 nonclassical carbocations, 491
 potential energy surface, 472
 racemization, 337, 480
 rate equation, 470
 reactivity and carbocation stability, 362, 474, 475
- S_N1' mechanism designated as ($1/D_N + 3/A_N$), 471
- S_N2 mechanism label meaning intended by Ingold, 471
- S_N2 reaction, 337, 361, 381, 470, 494
 and 18-crown-6, 499
 and back-side attack, 496
 and B_{A12} mechanism, 453
 and Hammett ρ , 393, 394
 and radical intermediate, 515

- and single-electron shift, 515
back-side displacement, 495
competition with E2, 646
designated as ($A_N D_N$), 471
effect of leaving group, 512
effect of solvent, 496
inversion of configuration, 337
nucleophilicity of nucleophile, 506
of diazonium ion, 679
ponderal effect, 501
steric effect, 501
transition structure, 502
- S_N2' mechanism designated as ($3/1/A_N D_N$), 472
- S_NAr reaction
and single-electron transfer, 531
first-order reaction, 527
nucleophilic aromatic substitution, 527
second-order reaction, 528
- S_Ni mechanism designated as ($D_N + D + A_N$), 472
- Snoutane, 163
Soft base, 505
Solar energy storage, 862
Solid bold line in Maehr convention, 75
Solid dot stereochemical descriptor, 58
Solid wedge in Maehr convention, 74
Solvatochromism, 339
Solvent cage, 335, 515–517, 526, 599, 613
Solvent dipolarity/polarizability index (π^*), 338
Solvent effect on Hammett ρ , 393
Solvent isotope effect, 384, 594
1° Solvent kinetic isotope effect, 384
2° Solvent kinetic isotope effect, 384
Solvent kinetic isotope effect, 448, 559, 562, 615
in amide hydrolysis, 460
Solvent polarity and mechanism determination, 338
Solvent reorientation time, 595
Solvent-separated ion pair, 313, 421, 483, 485, 560, 804
Solvent viscosity
and encounter-controlled reactions, 337
and reaction in solvent cage, 517
in mechanism determination, 338
- Solvolysis, 477, 478
anchimeric assistance, 485
and carbocation stability, 475
and elimination, 645
and nonclassical carbocations, 300
and nonplanar carbocations, 475
and solvent polarity, 477
Grunwald–Winstein equation, 477
internal return, 482
ion pair intermediate, 485
kinetics, 344
LFER, 398
2-norbornyl system, 493
pseudo-first-order kinetics, 474
salt effect, 479
stereochemistry, 480
- Solvomercuration, 596, 614
SOMO, 262
sp, 115
+ *sp*, 115
– *sp*, 115
Sp, 70
Special salt effect, 483
Specific acid catalysis, 434, 437, 670, 673
Specific acid, general base catalysis, 436
Specific base catalysis, 435, 437, 456
Specific base, general acid catalysis
in ester hydrolysis, 456
Specific hydroxide ion catalysis, 435
Specific lyate ion catalysis, 435
Specific lyonium ion catalysis, 434
Specific oxonium ion catalysis, 434, 435
Specific rotation, 86
conventions, 87
Spin adduct, 277
Spin-forbidden process, 796
Spin-forbidden transition, 801
Spin-orbit coupling, 796, 801
Spin polarization, 260
Spin quantum number, m_s , 259
Spin trap, 277
Spin trapping, 277
Spiro transition structure, 608
Spirocyclopentadiene, 163
sR, 70
SR (stereochemical descriptor), 87
 $S_{RN}1$ mechanism, 543
 $S_{RN}1$ reaction, 544
designated as ($T + D_N + A_N$), 543
SRT (structure resonance theory), 241
counting Kekulé structures, 241
resonance energy, 244
types of electron permutations, 243
SSIP, 560
Staggered conformation, 114
Standard heterolytic bond dissociation energy, 18
Standard homolytic bond dissociation enthalpy, 16
Stark effect, 20
State correlation diagram, 712, 734
Diels–Alder reaction, 736
Steady-state approximation, 345–348, 473, 642
Step-wise process, 329
Stereocenter, 75, 98
(\pm) Stereochemical descriptor, 87
Stereochemistry, 53
acceptable representations, 56
not acceptable representations, 56, 81
preferred representations, 56, 81
Stereochemical effect, 151
Stereogenic atom, 98
Stereogenicity, 98
and meso structure, 98
Stereochemical substituents, 94
Stereoisomers, 57
cis,trans, 58
configuration, 67
- diastereomers, 58
geometric, 58
Stereoselective reaction, 85, 122
Stereospecific reaction, 85, 533, 569, 668, 669, 697, 735, 745
Stereotopicity, 94
Steric acceleration in solvolysis, 494
Steric energy, 136, 155
Steric interaction, 120, 231
Steric isotope effect, 383
Stern–Volmer equation, 809, 810
Stern–Volmer plot, 810
Stilbene
DRE, 219
SRT resonance energy, 245
STM, 3
STO (Slater type orbital), 224
STO-3G basis set, 224
Stokes shift, 798
Strain energy, 155
Strained molecule, 155
Strained π bond, 164
Strainless bond enthalpy, 157
s-trans conformational descriptor, 117
Stretch-bend term in molecular mechanics, 138
Structural isomers, 57
Structure-resonance theory (SRT), 241
Styrene
DRE, 219
SRT resonance energy, 245
Substituent constant
in Hammett equation, 390
selected values, 401
Substituent effects on reactions, 385
Substituent topicity
constitutionally heterotopic, 94
diastereotopic, 94
enantiotopic, 94
heterotopic, 94
homotopic, 94
stereoheterotopic, 94
Substitution, 469
Ingold notation, 470
IUPAC notation, 471
solvolysis, 474
Superacid media, 296, 298, 320
Suprafacial-antarafacial pathway, 722
Suprafacial pathway, 715, 717–721, 731, 739, 741, 743, 750, 777
Suprafacial-suprafacial pathway, 721
Surface effect, 681
Surface-mediated reaction, 587, 614, 687
Swain–Schaad equation, 374
Swain–Scott equation, 507, 508, 511
SWNT, 208
Symmetric molecular orbital, 33, 707, 708, 712, 732
Symmetry element, 59, 708, 736
Symmetry operation, 59, 708
and MO symmetry, 708
and substituent topicity, 99
Symmetry operation of the first kind, 99

- Symmetry point group, 61
 classification scheme, 61
- Symmetry-allowed transition, 796
- Symmetry-correct molecular orbital, 33, 707, 732
- Symmetry-forbidden process, 776
- Symmetry-forbidden reaction, 739
- Symmetry-forbidden transition, 796
- Syn, 77
- Syn addition, 552, 571, 581, 582, 586, 601, 602, 614
 in hydroboration, 600, 616
 of Cl₂ to acenaphthylene, 579
 of F₂ to alkene, 580
 of HCl to alkyne, 612
- Syn conformation, 114
- Syn elimination, 634, 649, 669, 682–685, 695
 and E1cb character, 650
 in β-elimination, 649
 in pyrolytic elimination, 681
 potential energy surface, 651
- Synchronous reaction, 459, 472, 513, 608, 664, 750, 770–773
- Syn-clinal conformation, 115, 647
 + Syn-clinal conformation, 115
 –Syn-clinal conformation, 115
- Syn-coplanar conformation, 647
- Syndiotactic polymer, 93
- Syn-pentane interaction, 122
- Syn-periplanar, 115, 647
 –Syn-periplanar conformation, 115
 + Syn-periplanar conformation, 115
- s*-(Z), 117
- t*
 conformational descriptor, 116, 117
 stereochemical descriptor, 76
s-trans, 117
- T mechanism label, 543
- T (³H), 782
- T + D_N + A_N mechanism, 543
- T₁ state, 792
- Taft equation, 401
- Taft E_s, 401
- Taft ρ*, 401
- Taft S, 401
- Taft σ*, 400
 and E2 reaction, 664
 and electrophilic addition, 555, 575
 and pK_a, 418
- τ
 excited state lifetime, 805
 lifetime of carbocation, 594
 NMR scale, 727
- τ bond, 42
- Tau bond, 42
- τ_p (phosphorescence lifetime), 809
- τ_s (singlet lifetime), 806
- τ_s⁰ (inherent singlet lifetime), 806
- Tele substitution, 530
- Termination step in chain reaction, 270, 276, 543, 589
- Tesla, 261
- Tet (in Baldwin's rules), 274
- Tetracene, 207, 427
- Tetrahedrane, 161, 170
- Tetramethyl-1,2-dioxetane
 chemiluminescence, 860
- Tetra-*t*-butylcyclobutadiene, 853
- Tetra-*t*-butylethylene, 165
- Tetra-*t*-butyltetrahedrane, 162, 168, 853
- Thermochemical cycle in gas phase acidity
 determination, 424
- Thermodynamic acidity constant, 415
- Thermodynamic control of product
 distribution, 356, 357, 581, 670
- Thermolysis, 349
- Thermoneutral reaction
 and Hammond postulate, 362
 and kinetic isotope effect, 377
 nature of transition state, 375
 reaction coordinate diagram, 363
- THF, 421
- Thiophene resonance energy, 206
- Threo, 83, 571
- Threose, 83
- Toluene
 bromination, 523
 fluorescence, 848
 gas phase basicity, 427
 intramolecular PKIE in radical
 halogenation, 378
 nitration, 520
 photodissociation, 847
 pK_{HA} value in DMSO, 309
- Toluene radical cation, pK_{HA*+}
 value, 309
- Topic relationship classification
 scheme, 99
- Topicity, 94, 97, 99
- Topology and pericyclic reactions, 769
- Torquoselectivity, 757
- Torsion angle in radical cation, 307
- Torsional barrier, 120
 and hyperconjugation, 231
 and nucleophilic addition, 625
- Torsional strain, 119, 137
 and syn elimination, 649
- Total bond order, 193
- Total emission spectrum, 801
- Trans addition, 552
- Trans elimination, 633. *See also* Anti
 elimination
- Transfer hydrogenation, 340
- 0,0 Transition, 797, 812
- 0,1 Transition, 797
- Transition state, 350
 and Brønsted α, 438
 and free energy surface, 708
 and Gibbs diagram, 255
 and Hammond postulate, 362
 and kinetic isotope effect, 375
 antiaromatic, 764
 aromatic, 764
- Transition state theory, 350, 776
- Transition structure, 254, 328
 and acid-catalyzed hydrolysis of
 acetals, 447
 and biases of computational
 methods, 771
 and ΔS[‡], 353
 and Hammett ρ, 392
 and kinetic isotope effect, 375
 and orbital symmetry, 708
 and potential energy surface, 708
 antiaromatic, 763
 aromatic, 763
 centauric, 772
 chameleonic, 772
 saddle point on potential energy
 surface, 366
 symmetry, 770
- Transition structure, 348
- Transmission coefficient in transition state
 theory, 351
- Trapping reactive intermediate, 163, 270, 277, 331, 341, 483, 515, 542, 555, 700, 824, 830
 in pericyclic reaction, 745
- Trefoil knot, 67
- Triethylborane and radical
 generation, 269
- Trifluoromethyl radical geometry, 266
- Trig (in Baldwin's rules), 274
- Trimethylene diradical, 336
- Tri-*n*-butyltin hydride (Bu₃SnH), 271
- Triphenylene Clar notation, 211
- Triphenylmethyl cation, 475
- Triphenylmethyl radical, 256, 257
 and magnetic susceptibility, 258
- Triplet manifold, 793, 794
- Triplet state, 278, 792
 of methylene, 278
- Triplet-triplet absorption, 795
- Tritium (³H), 782
- Triton (³H⁺), 414
- Trityl, 475. *See also* Triphenylmethyl
- Twist boat
 cyclohexane, 124
cis-1,4-di-*t*-butylcyclohexane, 132
- Twist conformation of cyclopentane, 128
- Twistane, 163, 170
- Twisted alkene, 165
 and chirality, 858
- Twisted excited state, 820
- Twisted π system and Möbius MO
 theory, 765
- u* (unlike), 84
- ul* (unlike), 84
- Unichiral, 85
- Unimolecular process, 255, 805
- Unimolecular reaction, 309, 318, 343, 372, 450, 472, 683, 731
- Unnormal addition, 589
- UV-vis region of the electromagnetic
 spectrum, 787

- ν (vibrational energy level), 787, 798
 V (characteristic volume), 339
Vacuum UV, 818
Valence bond configuration mixing (VBCM), 513
Valence bond (VB) theory, 24, 35, 240
 and resonance, 189
 and resonance energy, 237, 240
Valence isomerization, 726
Valence isomers, 167, 701, 726
Valence shell electron pair repulsion theory (VSEPR), 36
Valley-ridge inflection point (VRI), 370
van der Waals radius, 5, 6
 and non-bonded interactions, 6
 of deuterium relative to hydrogen, 383
van der Waals strain, 121, 139
 and $A^{(1,2)}$ strain, 122
 and $A^{(1,3)}$ strain, 122
 and annulenes, 217
 and axial substituent, 129
 and butane gauche conformation, 150
 and limits to molecular stability, 160
 and *syn*-pentane interaction, 122
 and UV-vis absorption, 821
van der Waals surface area (A_w), 7
van der Waals volume (V_w), 7
Variable hybridization
 and acidity, 45
 and carbanion stability, 45
 and electronegativity, 37
 and geometry, 37, 39
 and f_{13c-H} , 41
 and p character, 37
 and s character, 37
 CH_2Cl_2 , 39
 CH_3Cl , 40
 CH_3F , 40
 cyclopropane, 40
 hybridization index, 37
 hybridization parameter, 37
Variable transition state theory in
 elimination reactions, 664
Variational principle, 176–178, 236, 239
VB theory, 24, 25
VBCM, 513
Velocity of a reaction, 342
Vertical excitation, 821
Vertical excited state, 819, 820
Vertical plane of symmetry (σ_v), 59
Vertical transition, 796, 847
Vibrational energy level, 372, 787
 and electronic states, 793
Vibrational relaxation, 794
Vicarious nucleophilic aromatic
 substitution, 530
Vicinal dihalide dehalogenation, 665
Vinyl alcohol acidity, 419
Vinyl carbanion, 212
 hybridization, 311
 reactive intermediate, 653
Vinyl cation, 532, 609, 612, 613, 615
Vinyl halide
 dehydrohalogenation, 653
 electrophilic addition, 585
 nucleophilic vinylic substitution, 533
Vinyl radical, 256
 in addition of HBr to propyne, 611
Virtual experiment, 339
Vitamin D₃, 720, 721
Vitamin E, 69
Von Richter reaction, 530
VRI, 370
VSEPR theory, 36
 and electronegativity, 36
 and variable hybridization, 37
 methylene, 279
 V_x (Benson electronegativity), 23
Wagner–Meerwein rearrangement, 492
Wagner–Meerwein–Whitmore
 rearrangement, 492
Walden cycle, 495
Walden inversion, 337, 494, 671
Wavelength
 and energy of light, 789
 and specific rotation, 87
Wavy line stereochemical descriptor,
 58
Wedge outline in Maehr convention,
 75
Westheimer method, 135
Wheland intermediate, 330, 520
Winstein–Holness equation, 360
Wolff rearrangement, 288
Woodward–Hoffmann rules
 atom transfer reaction, 750
 chelotropic reaction, 749
 cycloaddition, 739
 electrocyclic reaction, 705
 general selection rule, 755
 pericyclic reaction, 755
 sigmatropic reaction, 718, 724
X (excess acidity function), 433
Xanthate ester pyrolysis, 682
Xanthone, polarity of electronically
 excited states, 817
 XeF_2 , 581, 611
Xi-bond, 58
 ξ -bond, 58
m-Xylylene, 798
Y in Grunwald–Winstein equation, 477
Yang cyclization, 836
Ylide elimination mechanism, 635
 Y_{OTs} scale of solvent ionizing power, 477
Yukawa–Tsuno equation, 399
Z, 76
Z scale of solvent polarity, 339
Zero point energy (ZPE), 373, 382
Zig-zag conformation, 154, 234
Zimmerman rearrangement, 828
ZPE, 373
Zusammen, 76
Zwitterionic structures and electronically
 excited states, 820

WILEY END USER LICENSE AGREEMENT

Go to www.wiley.com/go/eula to access Wiley's ebook EULA.